RECENT ADVANCES IN HETEROATOMIC-HECK REACTIONS TOWARDS THE SYNTHESIS OF UNSATURATED SILANES AND BORONIC ESTERS

by

William Blackburn Reid

A dissertation submitted to the Faculty of the University of Delaware in partial fulfillment of the requirements for the degree of Doctor of Philosophy in Chemistry & Biochemistry.

Spring 2018

RECENT ADVANCES IN HETEROATOMIC-HECK REACTIONS TOWARDS THE SYNTHESIS OF UNSATURATED SILANES AND BORONIC ESTERS

by

William Blackburn Reid

Approved: _____
Brian J. Bahnson, Ph.D.
Chair of the Department of Chemistry & Biochemistry

Approved: _____
George H. Watson, Ph.D.
Dean of the College of Arts and Sciences

Approved: _____
Ann L. Ardis, Ph.D.
Senior Vice Provost for Graduate and Professional Education

I certify that I have read this dissertation and that in my opinion it meets the academic and professional standard required by the University as a dissertation for the degree of Doctor of Philosophy.

Signed: _____

Donald A. Watson, Ph.D.
Professor in charge of dissertation

I certify that I have read this dissertation and that in my opinion it meets the academic and professional standard required by the University as a dissertation for the degree of Doctor of Philosophy.

Signed: _____

Mary P. Watson, Ph.D.
Member of dissertation committee

I certify that I have read this dissertation and that in my opinion it meets the academic and professional standard required by the University as a dissertation for the degree of Doctor of Philosophy.

Signed: _____

Klaus H. Theopold, Ph.D.
Member of dissertation committee

I certify that I have read this dissertation and that in my opinion it meets the academic and professional standard required by the University as a dissertation for the degree of Doctor of Philosophy.

Signed: _____

Olga Dmytrenko, Ph.D.
Member of dissertation committee

ACKNOWLEDGMENTS

I would like to thank professor Donald A. Watson for the opportunity to conduct my Ph.D. studies in his research lab. He has always challenged me as a student and pushed me to become a better scholar. I would also like to thank my dissertation committee members Mary Watson, Klaus Theopold, and Olga Dmytrenko helping to guide me through my Ph.D.

The University of Delaware, in particular the Department of Chemistry and Biochemistry (CHBC), has provided above par facilities and equipment with which I could conduct my research. The staff in this department have been invaluable in my progress and I would like to thank Susan Cheadle, Sue James, Brenda Carboni, Lori Nesnow, and all of the department secretaries for their assistance with all of my questions about the department. The department facility directors and staff including Steve Bai, PapaNii Asare-Okai, Glenn Yap, Pat McMahon, and Rick Bernard have aided me many times with my research which would not have been possible without their reliable assistance. I would like to personally thank John Famiglietti, Jim Draper, Moicell Robinson, Mark Schrader, Doug Nixon, Brandon Calitree and Gary Lance for their assistance over the years with instruments, machines, broken glassware and general laboratory repairs. I feel that I have learned as much from them as I have in my Ph.D. studies.

I would like to extent my undying gratitude to both past and current lab mates. In particular, graduate students Jesse McAtee, Sara Martin, Andrew Cinderella, and Sarah Krause who have personally assisted me with my work pertaining to silicon and

boron. Post-docs in our lab including Luis Mori-Quiorz, Guoyin Yin, and Bojan Vulovic have been very supportive both academically and morally and were crucial to my continued persistence towards my Ph.D. I consider everyone I have had the pleasure of working with a friend and hope to stay in touch into the future.

Lastly, I would like to thank my family and friends who have supported me all the way through this endeavor without a clue as to what I do. Their continued love and support has kept me going for these 5 years. To all of them and everyone else I have known and met through this process, Thank You!

TABLE OF CONTENTS

LIST OF TABLES

LIST OF FIGURES

ABSTRACT

Unsaturated heteroatomic compounds are an important class of molecules in many disciplines of chemistry. In particular, organosilanes and boronic esters serve as valued reagents and intermediates in the synthesis of complicated organic materials. Because of their high synthetic value, much interest has been payed towards the synthesis of these unique reagents. This thesis details my endeavors towards discovering new synthetic routes to unsaturated organo silanes and boronic esters. I assisted in the development of a nickel catalyzed methods for the silylation of aromatic alkenes with various different electrophilic silyl-triflate reagents. My studies of the intramolecular silyl-Heck reaction resulted in several new discoveries including the first examples of silylation of disubstituted alkenes. Computational investigation into the mechanism of the silyl-Heck reaction led to a better and more complete understanding of the inter- and intramolecular reaction pathways. My work involving boron electrophiles in Heck reactions resulted in the first boryl-Heck reaction published in the Journal of the American Chemical Society. Follow up studies increased the reactivity of the catalytic system allowing for the synthesis of trisubstituted alkenyl boronic esters from disubstituted and internal alkenes. During these studies, several new and related reactions were discovered and are detailed in the appendix of this thesis, some of which are currently being investigated.

Chapter 1

DEVELOPMENT OF A NICKEL CATALYZED SILYL-HECK REACTION

1.1 Introduction and Overview

Unsaturated organosilanes are potent nucleophiles and highly useful intermediates in organic synthesis.[1] Based on the precedence from Tanaka,[2] our lab has developed a direct and efficient route to synthesize vinyl silanes directly from terminal styrene derivatives.[3] These methods, however, are limited to the cross-coupling of silyl iodides. When silyl triflates are utilized in the reaction, an iodide additive is required for reactivity.[3b] We recognized that silyl triflates are more mild and more commercially abundant and wanted to utilize them directly in our silyl-Heck reactions.

Herein, we describe the first examples of a nickel-catalyzed silyl-Heck reaction. We show that, unlike in palladium-catalyzed reactions, these nickel-catalyzed reactions are able to utilize silyl triflate electrophiles without the need for iodide additives. Using this system, a variety of styrene derivatives, and related terminal alkenes lacking allylic hydrogen atoms, can be successfully transformed into *E*-vinyl silanes. As significantly, for the first time, this catalytic system allows for the direct preparation of vinyl trialkyl silanes from trialkylsilyl electrophiles larger than trimethylsilane. We believe that this new catalytic system not only provides promise for developing general base-metal catalysts for this class of reaction, but also greatly expands the types of unsaturated organosilanes that can be accessed using the silyl-Heck reaction.

1.2 Applications and Synthesis of Vinyl Silanes

Vinyl silanes are important compounds in organic synthesis due to their wide array of diverse reactivity. They can undergo cross coupling reactions such as the Hiyama and Hiyama-Denmark reactions[1h, 4] to form new carbon-carbon bonds as well as electrophilic halogenation reactions for forge new carbon-halogen bonds.[5] Additionally, vinyl silanes can be oxidized *via* a Tamao-Fleming oxidation[1c, 6] to give access to carboxylic acids, aldehydes or ketones as well as carbonylation reactions to give rise to α- and β-silylesters.[7]

Because of high utility and demand for functionalized vinyl silanes, many routes to synthesize them have been developed over the years. The simplest approach is the hydrosilylation of terminal alkynes (Figure 1.1).[8] In most cases the *syn*-hydrosilylation product (**1.1**) is formed following the Chalk-Harrod mechanism. This can be done with a variety of metal catalysts including rhodium, platinum and cobalt. The *trans*-hydrosilylation is possible using ruthenium catalysts.[9]

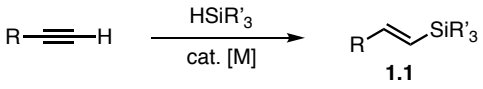

Figure 1.1 Hydrosilylation of Alkynes

A few methods exist for the direct conversion of terminal alkenes to vinyl silanes. Among these, metathesis and dehydrogenative silylation are both effective but each has its own drawbacks. Metathesis can be very sensitive to the substitution of the silane and dehydrogenative silylation often results in accompanied reduction to the alkyl silane producing difficult to separate mixtures.

Recently, we have established the silyl-Heck reaction as a novel route to access both allyl and vinyl silanes.[3, 10,2, 11] This general method allows for the direct silylation of terminal alkenes using silyl halides and transition metal catalysts, in a reaction that we believe is analogous to classical Heck arylation (Figure 1.2).[12]

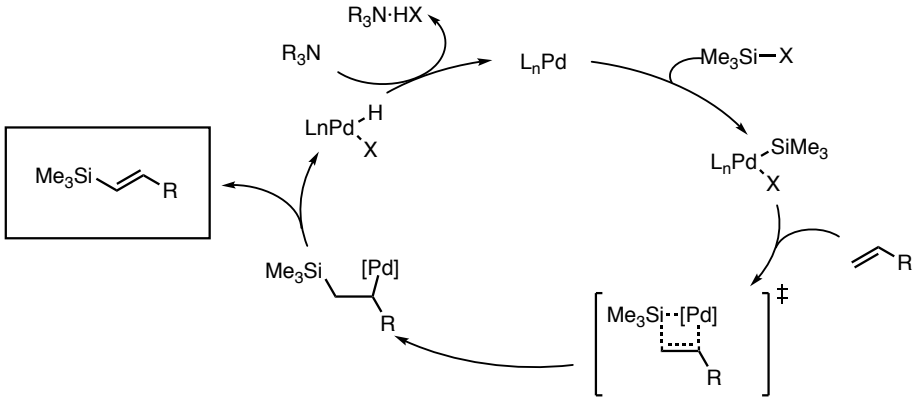

Figure 1.2 General Mechanism of the Silyl-Heck Reaction

In the continuous development of this chemistry, we have designed new ligands and catalysts for this reaction.[13] These improved catalytic conditions allow for more mild reaction conditions as well as improve yields and selectivities. This work has also been expanded the synthesis of vinyl silyl ethers and disiloxanes (Figure 1.3).[3b] Using silyl ditriflates with an iodide additive under palladium catalysis, a variety of silyl ethers and disiloxanes were synthesized.

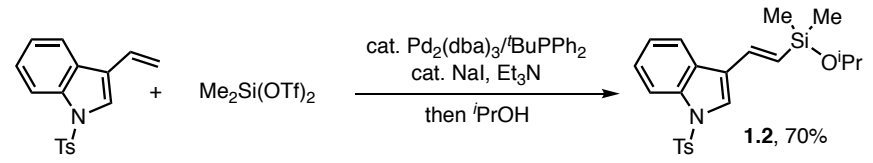

Figure 1.3 Synthesis of Vinyl Silyl Ethers *via* the Silyl-Heck Reaction

1.3 Hypothesis and Proposal

Our previous work has focused exclusively on the use of palladium-based catalysts in this transformation.[3] In these processes, we have found that the use of iodosilanes is required. These can either be used directly or prepared *in situ* from silyl chlorides, bromides, or triflates and simple iodide salts (Figure 1.4).[14]

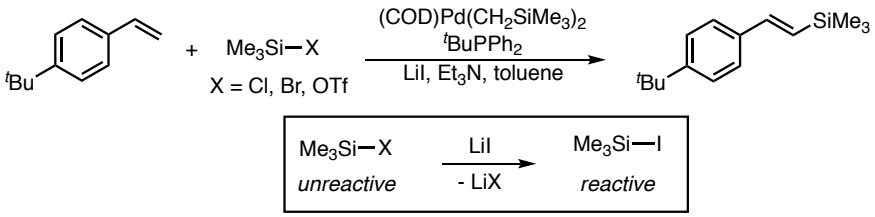

Figure 1.4 *In Situ* Silicon-Halogen Exchange

An active interest in our group is developing a catalyst capable of engaging alternative silyl halides other than iodosilanes in silyl-Heck type reactions. This interest is fueled by the recognition that iodosilanes are potent Lewis acids, and thus have attenuated functional group compatibility. In addition, access to silyl iodides is limited, with only trimethylsilyl iodide being commercially available. In contrast, a much wider variety of silyl chlorides and triflates can be purchased, making methods that can directly utilize these reagents attractive to develop.[15]

In an effort to expand the silicon scope of this reaction, we turned to investigating the use of silyl triflate reagents as electrophilic cross-coupling partners. Unfortunately, even the most reactive silyl triflate, trimethylsilyl triflate, fails to undergo reaction under palladium-catalyzed conditions without added iodide. Therefore, we sought to find a catalytic system that could activate and efficiently cross-couple silyl triflates with alkenes. Silicon-oxygen bonds are known to be very strong, and while the bond dissociation energy (BDE) of a silicon triflate bond is not known, we hypothesize that it should be lower than a Si-OMe bond but stronger than a Si-I BDE. With analogous carbon electrophiles, aryl triflates generally have similar reactivity to aryl bromides.[16] Table 1.1 depicts known bond dissociation energies of trimethylsilyl halide and methoxy bonds. We attribute the lack of reactivity with silyl triflates to the reluctance of palladium to insert into the strong Si-OTf bond.[17]

Table 1.1 Silicon Halide and Oxygen Bond Dissociation Energies

entry	bond	BDE (kcal/mol)
1	$Me_3Si–I$	77
2	$Me_3Si–Br$	96
3	$Me_3Si–Cl$	113
4	$Me_3Si–OMe$	123

In cross-coupling chemistry of carbon electrophiles, nickel catalysts have proven adept at the activation of strong carbon-heteroatom bonds (such as aryl ethers and carboxylates), particularly in comparison to palladium catalysts.[18] Seminal studies from the Wenkert[19] and Chatani[20] demonstrated that a simple phosphine supported nickel catalyst is capable of activating C-O bonds in Kumada and Suzuki reactions respectively (Figure 1.5).

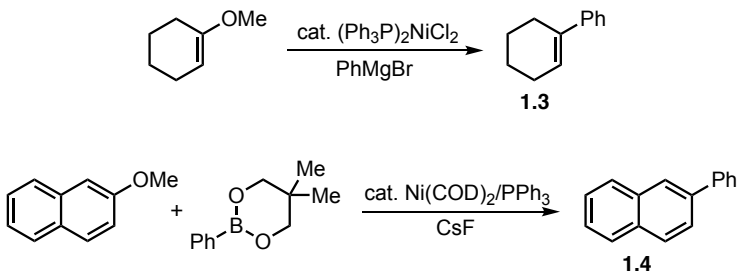

Figure 1.5 Nickel Catalyzed Activation of Strong Carbon-Oxygen Bonds

Despite the fact that silyl bromides and iodides been shown to oxidatively add to a variety of late transition metals complexes, to our knowledge such reactions involving nickel compounds have not been described.[2, 11a-d, 21] Based upon the precedent with strong C–X bonds, we decided to investigate silyl-Heck type reactions with nickel-based catalysts.[22]

1.4 Reaction Optimization

To begin our investigation of nickel-catalyzed silyl-Heck reactions, we studied the reaction of 4-*tert*-butyl styrene with trimethylsilyl triflate (Me_3SiOTf) without iodide additives (Table 1.2). Consistent with our previous observations, palladium-based catalysts provided only trace yield of desired vinyl silane **1.5** (entry 1). In our hands, this outcome is not improved by variation of either palladium pre-catalyst, nature of phosphine ligand, metal:ligand ratio, solvent, or temperature (not shown). In contrast, a modest screen of catalysts derived from $Ni(COD)_2$ and phosphine ligands revealed a significantly different outcome. Whereas catalysts employing triaryl phosphines (entries 2 and 3) or mixed aryl-alkyl phosphines (entries 4 and 5) were ineffective, moderately bulky trialkyl phosphines provided highly active catalysts (entries 6–10). Interestingly, however, there seems to be a steric limit regarding ligand size; the very bulky $^tBu_3P$ was

ineffective (entry 11). Further optimization revealed that a highly effective catalyst was obtained using ^{t}BuPCy$_2$ and Ni(COD)$_2$ when a 1.5:1 ligand:metal ratio was employed (entry 13).

Table 1.2 Identification of Nickel-Based Catalyst

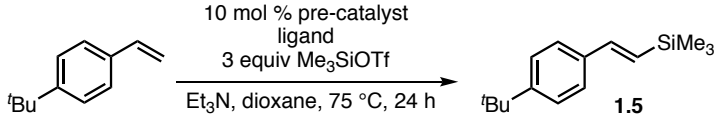

entry	pre-catalyst	ligand (mol %)	yield (**1.5**)
1	(COD)Pd(CH_2SiMe_3)$_2$	^{t}BuPPh$_2$ (30)	0%
2	Ni(COD)$_2$	PPh$_3$ (30)	0%
3	Ni(COD)$_2$	P(*o*-tol)$_3$ (30)	0%
4	Ni(COD)$_2$	^{t}BuPPh$_2$ (30)	12%
5	Ni(COD)$_2$	Cy$_2$PPh (30)	11%
6	Ni(COD)$_2$	^{n}Bu$_3$P (30)	69%
7	Ni(COD)$_2$	PCy$_3$ (30)	57%
8	Ni(COD)$_2$	PCyp$_3$ (30)	65%
9	Ni(COD)$_2$	^{t}BuPCy$_2$ (30)	71%
10	Ni(COD)$_2$	^{t}Bu$_2$PCy (30)	55%
11	Ni(COD)$_2$	^{t}Bu$_3$P (30)	7%
12	Ni(COD)$_2$	^{t}BuPCy$_2$ (20)	85%
13	Ni(COD)$_2$	^{t}BuPCy$_2$ (15)	90%

1.5 Scope of Nickel Catalyzed Silyl-Heck Reaction

1.5.1 Styrene Scope

Using these optimized conditions, we studied the scope of the nickel-catalyzed silyl-Heck reaction (Figure 1.6). A variety of styrenyl alkenes participate in the reaction. On preparative scale (1 mmol), vinyl silane **1.5** was isolated in 82% yield. Likewise, unsubstituted styrene could be silylated in 89% isolated yield under these conditions (**1.6**). A variety of ethereal substrates were also tolerated, including those

with both electron-donating *para*-methoxy (**1.7**) and electron-withdrawing *meta*-methoxy groups (**1.8**) in good yield (71% and 76%, respectively). Silyl ethers (**1.9**) and dioxoles (**1.10**) were also well tolerated. Aromatic fluorides proved amenable to the reaction conditions; fluorinated vinyl styrene **1.11** was isolated in 66% yield. Unfortunately, larger aromatic halogens were not compatible with the silylation conditions. For example, the use of 4-chlorostyrene as substrate led to a complex mixture of products without detectable formation of desired vinyl styrene **1.12**. Also problematic were highly electron-deficient or electron-rich styrenes. For example, the formation of ester **1.13** was not observed, and dimethylamino product **1.14** was formed in low yield. Strained rings, such as benzocyclobutane (**1.15**), and steric bulk on the aromatic group *ortho* to the alkene (**1.16**), however, were well tolerated. Some heterocyclic substrates could also be silylated using this protocol. For example, silylation of *N*-vinyl carbazole led to vinyl silane **1.17** in high yield. In this case, as well as all others reported herein, no more than trace product was observed in reactions conducted without catalyst. However, in other cases, such as in the formation of benzofuran **1.18**, yields proved to be suboptimal. Finally, more complex vinyl silanes, such as pinacol borane **1.19** and estradiol-derived **1.20**, could also be accessed using the nickel-catalyzed protocol. In the case of **1.19**, tricyclopentyl phosphine (Cyp_3P) proved to be a slightly more effective ligand than $^{t}BuPCy_2$, demonstrating that some ligand optimization might prove necessary to maximize vinyl silane yield. Silylation of terminal alkenes bearing allylic hydrogen atoms, such as 1-decene, were also investigated. However, with these substrates only trace desired product was observed; alkene isomerization predominated. Overall, while these yields are slightly lower and scope is somewhat more limited than our previously reported palladium-catalyzed silyl-

Heck protocol involving Me_3SiI, we believe that this reaction enjoys sufficient substrate scope to make it a synthetically viable alternative, particularly given the advantages of using a nonprecious metal, nickel-based catalyst, and a silyl triflate as the silylating reagent.

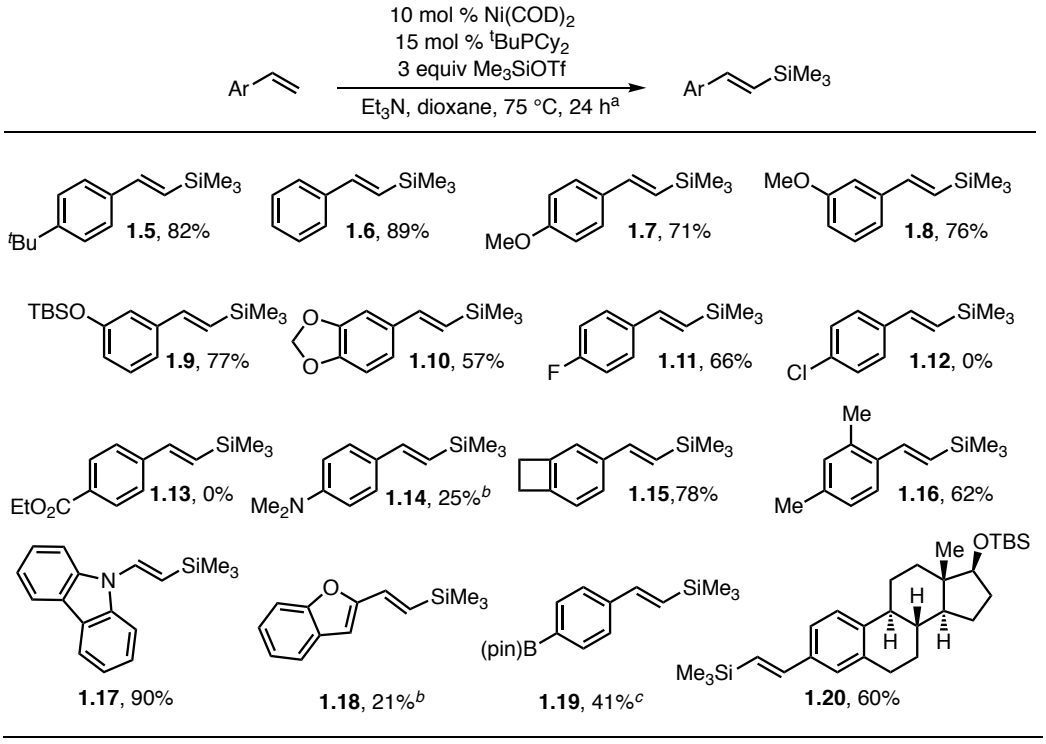

[a] Isolated yields. All reactions run at 0.5 M concentration. [b] Yields determined by NMR.
[c] 30 mol % Cyp_3P used in place of $^tBuPCy_2$.

Figure 1.6 Scope with Respect to Styrene Derivatives

1.5.2 Scope of Silyl-Triflate Electrophiles

As mentioned above, silyl triflates are much more abundant than silyl iodides. We therefore wanted to investigate the scope of the transformation with respect to the silyl triflate. Initial investigations using $^tBuPCy_2$ and the above-optimized conditions

revealed that silyl triflates larger than trimethylsilyl triflate do participate in the reaction. However, we rapidly identified the use of Cy_3P with a ligand:metal ratio of 3:1 as an alternative catalyst that provided generally higher yields with larger silanes.

Scope studies using 4-*tert*-butyl styrene and this latter catalyst system are outlined in Figure 1.7. Dimethylsilyl triflates containing one primary alkyl group, such as $^{n}BuMe_2SiOTf$ or $BnMe_2SiOTf$ participate well under these conditions (**1.21** and **1.22**), providing similar yields to Me_3SiOTf. One secondary substituent, such as in $^{i}PrMe_2SiOTf$, can also be tolerated without loss of yield (**1.23**). However, a tertiary silyl substituent proved to be beyond the steric limit under these conditions; using Cy_3P as ligand, none of desired vinyl silane **1.24** was observed using $^{t}BuMe_2SiOTf$ (TBSOTf). However, switching to the smaller ligand $^{n}Bu_3P$ and using elevated temperatures did allow for the formation of **1.24**. Despite the modest yield, this transformation is remarkable as it presumably involves oxidative addition at a silicon center that bears a fully substituted adjacent center (akin to a neopentylic carbon center). Silyl triflates bearing aromatic groups are also good substrates for the nickel-catalyzed silyl-Heck reaction. Both phenyldimethyl and diphenylmethyl vinyl silanes can be prepared in good yield in this way (**1.25** and **1.26**). Finally, triethylsilyl triflate also participates in the reaction; **1.27** was prepared in 65% yield. However, triisopropylsilyl triflate appears to be too large (even under forcing conditions). As the previously developed palladium-catalyzed reaction only tolerates Me_3SiI (used directly or generated in situ), these results greatly expand the types of electrophilic trialkylsilanes that can participate in the silyl-Heck reaction.

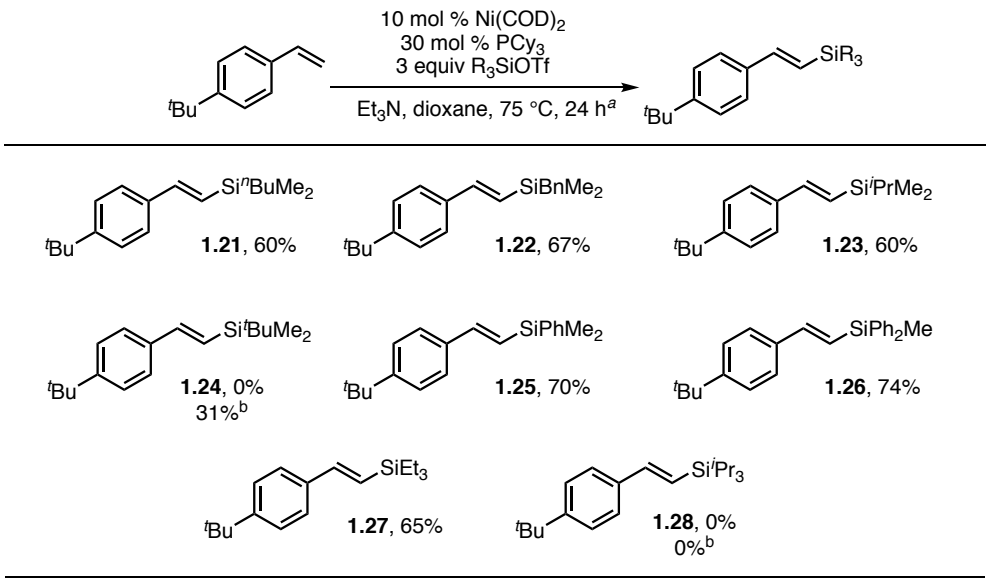

[a] Isolated yields. Unless otherwise noted, all reactions run at 0.5 M concentration.
[b] 40% $^{n}Bu_3P$ in place of PCy_3,105 °C, 1.0 M concentration.

Figure 1.7 Scope with Respect to Silyl-Triflate

1.6 Dimerization Byproduct

In the case of reactions using larger silyl triflates (Table 1.7), the major byproduct is alkene **1.32** (Figure 1.8). We hypothesize that this styrene dimer arises *via* a metal hydride-mediated Heck-type pathway.[23] Palladium hydride **1.29**, formed as a catalytic intermediate in the desired pathway, can react with an equivalent of alkene to form **1.30**. Migratory insertion of another alkene leads to **1.32** which can undergo β-hydride elimination to for dimer **1.32** and regenerate **1.29**.

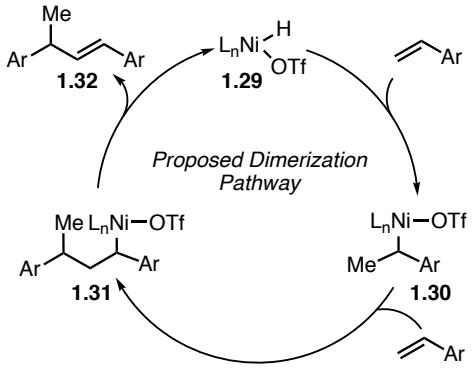

Figure 1.8 Proposed Dimerization Catalytic Cycle

Minor amounts of similar dimers are also observed as byproducts in reactions using Me_3SiOTf (Figure 1.6); however, formation of these dimers is less significant. These results suggest that the dimerization pathway becomes more competitive with increasing steric bulk of the silyl triflate, likely due to the difficulty of oxidative addition.

1.7 Summary

For the first time, we have demonstrated a nickel-catalyzed silyl-Heck reaction, the first demonstration of a first-row transition metal catalyst in this type of reaction. We have shown that simple phosphine-supported nickel-based catalysts are not only capable of silylating styrene derivatives, but are also capable of promoting the reaction with silyl triflate reagents without the need for *in situ* generation of silyl iodides. Moreover, good substrate scope with respect to the alkene has been observed. More importantly, for the first time electrophilic trialkylsilanes bearing alkyl groups larger than methyl have been shown to participate in Heck-like reactions. These results

provide promising leads for the further development of silyl-Heck reactions using inexpensive catalysts and silylating reagents.

This work was communicated in 2014 in *Tetrahedron* as an invited article honoring Professor Sarah Reisman as recipient of the 2014 Tetrahedron Young Investigator Award.[24]

1.8 Experimental Details

1.8.1 General Experimental Details

Dioxane, tetrahydrofuran, and dichloromethane were dried on alumina according to published procedures.[25] Triethylamine was distilled from CaH_2 and then sparged with nitrogen. 2-Dimethylaminoethanol was distilled under vacuum from anhydrous potassium carbonate and sparged with nitrogen. Trifluoromethanesulfonic acid (TfOH) was distilled under vacuum and stored under nitrogen in a teflon-sealed vessel. Trimethylsilyl-, triethylsilyl-, (Oakwood Chemical), *tert*-butyldimethylsilyl- (Combi-Blocks) and tri-*iso*-propylsilyl- (Gelest) trifluoromethanesulfonate were distilled under vacuum and degassed prior to use. All hot glassware was oven dried for a minimum of four hours or flame-dried under vacuum prior to use. All other substrates and reagents were purchased in highest analytical purity from commercial suppliers. Liquid substrates were sparged with nitrogen before use, and all others were used as received. Column chromatography was performed with 5-20 μm or 40-63 μm silica gel (Silicycle) with the eluent reported in parentheses. Analytical thin-layer chromatography (TLC) was performed on precoated glass plates and visualized by UV or by staining with $KMnO_4$.

1.8.2 Instrumentation and Chromatography

NMR spectra were obtained on a Bruker AV400 MHz FT-NMR spectrometer equipped with a Bruker CryoPlatform (400 MHz ^{1}H, 101 MHz ^{13}C, and 376 MHz ^{19}F) or on a Bruker AVIII 600 MHz FT-NMR spectrometer (600 MHz ^{1}H, 151 MHz ^{13}C), in the indicated deutero-solvent and were recorded at ambient temperatures. Chemical shifts are reported in ppm. ^{1}H NMR were calibrated using the residual protio-solvent as a standard. ^{13}C NMR spectra are calibrated using the deutero-solvent as a standard and were recorded using the attached proton test.[26] ^{19}F spectra are referenced to an external $FCCl_3$ sample. IR spectra were recorded on a Nicolet Magna 560 FTIR spectrometer as thin films. GCMS data was collected using an Agilent 6850 series GC and 5973 MS detector. High resolution MS was attained on a Waters GCT Premier spectrometer using electron impact ionization (EI).

1.8.3 Reactions of Alkenes with Trimethylsilyl Trifluoromethanesulfonate

1.8.3.1 General Procedure A

In a glovebox (N_2 atmosphere), dicyclohexyl-*tert*-butylphosphine (15 mol %) and $Ni(COD)_2$ (10 mol %) were added to a 2-dram vial equipped with a stirbar. Solid alkenes were also added at this time. Dioxane and triethylamine (5 equiv) were then added sequentially, followed by liquid alkene (1 equiv) if applicable. The vial was sealed with a Teflon-lined septum cap and removed from the glovebox. The reaction mixture was stirred at room temperature until homogeneous. Trimethylsilyl trifluoromethanesulfonate (3 equiv) was then added *via* syringe at room temperature with stirring. The vessel was then heated in an oil bath at 75 °C with stirring for 24 h. The reaction was removed from the oil bath and cooled to room temperature. The reaction vessel was then opened to air, and brine and diethyl ether or hexanes were

added. The brine layer was removed, and the organic layer was washed twice with brine. The combined aqueous layers were back-extracted twice with diethyl ether or hexanes. The combined organic layers were dried over $MgSO_4$ and concentrated *in vacuo*. The product was purified using flash silica chromatography, eluting with the indicated solvent noted in parenthesis.

1.8.3.2 Characterization Data

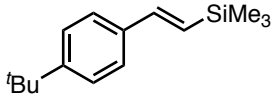

(**1.5**) According to general procedure A, 1-*tert*-butyl-4-vinylbenzene (183 µL, 1 mmol), $^{t}BuPCy_2$ (38 mg, 0.15 mmol), $Ni(COD)_2$ (27.5 mg, 0.1 mmol), Et_3N (700 µL, 5 mmol), and Me_3SiOTf (540 µL, 3 mmol) were reacted in dioxane (2 mL) at 75 °C for 24 h. The product was purified by flash chromatography on silica gel (petroleum ether) and concentrated *in vacuo* to yield of **1.5** as a colorless oil (190 mg, 82%): ^1H NMR (400 MHz, $CDCl_3$) δ 7.38 (d, J = 8.7 Hz, 2H), 7.35 (d, J = 8.7 Hz, 2H), 6.85 (d, J = 19.1 Hz, 1H), 6.42 (d, J = 19.1 Hz, 1H), 1.31 (s, 9H), 0.14 (s, 9H); ^{13}C NMR (101 MHz, $CDCl_3$) δ 151.2, 143.4, 135.8, 128.6, 126.2, 125.6, 34.7, 31.4, -1.0; FTIR (cm^{-1}): 2957, 1248, 986, 868, 838. HRMS (EI) m/z, calcd for [$C_{15}H_{24}Si$]: 232.1647; found: 232.1668.

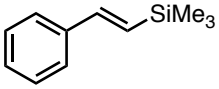

(**1.6**) According to general procedure A, styrene (115 µL, 1 mmol), $^{t}BuPCy_2$ (38 mg, 0.15 mmol), $Ni(COD)_2$ (27.5 mg, 0.1 mmol), Et_3N (700 µL, 5 mmol), and Me_3SiOTf (540 µL, 3 mmol) were reacted in dioxane (2 mL) at 75 °C for 24 h. The product was purified by flash chromatography on silica gel (petroleum ether) and concentrated *in vacuo* to yield of **1.6** as a colorless oil (158 mg, 89%): ^1H NMR (400 MHz, $CDCl_3$) δ 7.44 (d, J = 7.0 Hz, 2H), 7.33 (t, J = 7.4 Hz, 2H), 7.25 (t, J = 7.2 Hz, 1H), 6.88 (d, J = 19.2 Hz, 1H), 6.48 (d, J = 19.1 Hz, 4H), 0.16 (s,

9H); ^{13}C NMR (101 MHz, $CDCl_3$) δ 143.7, 138.5, 129.7, 128.7, 128.1, 126.5, -1.1; FTIR (cm^{-1}) 2955, 1247, 988, 866, 843. HRMS (EI) m/z, calcd for [$C_{11}H_{16}Si$]: 176.1021; found: 176.1048.

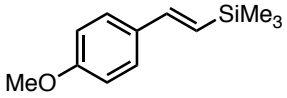

(**1.7**) According to general procedure A, 4-vinyl-anisole (134 µL, 1 mmol), ^{t}BuPCy$_2$ (38 mg, 0.15 mmol), Ni(COD)$_2$ (27.5 mg, 0.1 mmol), Et_3N (700 µL, 5 mmol), and Me_3SiOTf (540 µL, 3 mmol) were reacted in dioxane (2 mL) at 75 °C for 24 h. The product was purified by flash chromatography on silica gel (petroleum ether) and concentrated *in vacuo* to yield **1.7** as a white solid (146 mg, 71%): ^{1}H NMR (400 MHz, $CDCl_3$) δ 7.38 (d, J = 8.8 Hz, 2H), 6.91 – 6.75 (m, 3H), 6.31 (d, J = 19.1 Hz, 1H), 3.81 (s, 3H), 0.14 (s, 9H); ^{13}C NMR (101 MHz, $CDCl_3$) δ 159.6, 143.1, 131.5, 127.7, 126.8, 114.0, 55.5, -1.0; FTIR (cm^{-1}) 2958, 1608, 1510, 1251, 1033, 993, 835, 798. HRMS (EI) m/z, calcd for [$C_{12}H_{18}OSi$]: 206.1127; found: 206.1140.

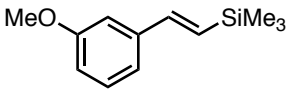

(**1.8**) According to general procedure A, 3-vinyl-anisole (139 µL, 1 mmol), ^{t}BuPCy$_2$ (38 mg, 0.15 mmol), Ni(COD)$_2$ (27.5 mg, 0.1 mmol), Et_3N (700 µL, 5 mmol), and Me_3SiOTf (540 µL, 3 mmol) were reacted in dioxane (2 mL) at 75 °C for 24 h. The product was purified by flash chromatography on silica gel (5 : 95 Et_2O : hexanes) and concentrated *in vacuo* to yield **1.8** as a colorless oil (159 mg, 77%): ^{1}H NMR (400 MHz, $CDCl_3$) δ 7.27 (t, J = 7.8 Hz, 1H), 7.06 (d, J = 7.7 Hz, 1H), 7.01 (t, J = 2.0 Hz, 1H), 6.87 (d, J = 19.2 Hz, 1H), 6.83 (dd, J = 2.7, 0.8 Hz, 1H), 6.50 (d, J = 19.1 Hz, 1H), 3.86 (s, 3H), 0.18 (s, 9H); ^{13}C NMR (101 MHz, $CDCl_3$) δ 159.9, 143.5, 139.9, 130.0, 129.6, 119.2, 114.0, 111.3, 55.5, -1.1; FTIR (cm^{-1})

2954, 1263, 865, 838. HRMS (EI) m/z, calcd for [$C_{12}H_{18}OSi$]: 206.1127; found: 206.1148.

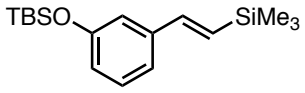

(**1.9**) According to general procedure A, *tert*-butyldimethyl(3-vinylphenoxy)silane[27] (234 mg, 1 mmol), ^{t}BuPCy$_2$ (38 mg, 0.15 mmol), Ni(COD)$_2$ (27.5 mg, 0.1 mmol), Et_3N (700 µL, 5 mmol), and Me_3SiOTf (540 µL, 3 mmol) were reacted in dioxane (2 mL) at 75 °C for 24 h. The product was purified by flash chromatography on silica gel (petroleum ether) and concentrated *in vacuo* to yield **1.9** as a colorless oil (236 mg, 77%): ^{1}H NMR (400 MHz, $CDCl_3$) δ 7.18 (t, J = 7.8 Hz, 1H), 7.04 (d, J = 7.7 Hz, 1H), 6.91 (t, J = 2.1 Hz, 6H), 6.80 (d, J = 19.1 Hz, 1H), 6.73 (dd, J = 8.0, 2.3 Hz, 1H), 6.43 (d, J = 19.1 Hz, 1H), 0.99 (s, 9H), 0.20 (s, 6H), 0.15 (s, 9H); ^{13}C NMR (101 MHz, $CDCl_3$) δ 156.0, 143.5, 140.0, 129.7, 129.5, 119.9, 119.8, 118.0, 25.9, 18.4, -1.1, -4.2; FTIR (cm^{-1}) 2956, 2859, 1575, 1280, 985, 838. HRMS (EI) m/z, calcd for [$C_{17}H_{30}OSi_2$]: 306.1835; found: 306.1819.

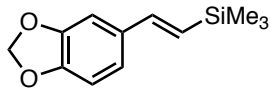

(**1.10**) According to general procedure A, 5-vinylbenzo[*d*][1,3]dioxole[27] (148 mg, 1 mmol), ^{t}BuPCy$_2$ (38 mg, 0.15 mmol), Ni(COD)$_2$ (27.5 mg, 0.1 mmol), Et_3N (700 µL, 5 mmol), and Me_3SiOTf (540 µL, 3 mmol) were reacted in dioxane (2 mL) at 75 °C for 24 h. The product was purified by flash chromatography on silica gel (hexanes) and concentrated *in vacuo* to yield **1.10** as a colorless oil (127 mg, 57%): ^{1}H NMR (600 MHz, $CDCl_3$) δ 7.00 (d, J = 1.8 Hz, 1H), 6.86 (dd, J = 8.0, 1.7 Hz, 1H), 6.80 – 6.74 (m, 2H), 6.27 (d, J = 19.1 Hz, 1H), 5.95 (s, 2H), 0.14 (s, 9H); ^{13}C NMR (151 MHz, $CDCl_3$) δ 148.2, 147.6,

143.1, 133.4, 127.4, 121.5, 108.3, 105.6, 101.2, -1.0; FTIR (cm^{-1}) 2954, 2895, 1489, 1248, 866, 839. HRMS (EI) m/z, calcd for [$C_{12}H_{16}O_2Si$]: 220.0920; found: 220.0933.

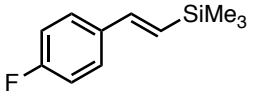

(**1.11**) According to general procedure A, 4-fluorostyrene (119 μL, 1 mmol), ^{t}BuPCy$_2$ (38 mg, 0.15 mmol), Ni(COD)$_2$ (27.5 mg, 0.1 mmol), Et_3N (700 μL, 5 mmol), and Me_3SiOTf (540 μL, 3 mmol) were reacted in dioxane (2 mL) at 75 °C for 24 h. The product was purified by flash chromatography on silica gel (hexanes) and concentrated *in vacuo* to yield **1.11** as a colorless oil (128 mg, 66%): ^{1}H NMR (400 MHz, $CDCl_3$) δ 7.40 (ddt, J = 8.3, 5.4, 2.5 Hz, 2H), 7.01 (app tt, J = 8.5, 1.9 Hz, 2H), 6.82 (d, J = 19.1 Hz, 1H), 6.38 (d, J = 19.1 Hz, 1H), 0.15 (s, 9H); ^{13}C NMR (101 MHz, $CDCl_3$) δ 162.7 (d, J = 247.3 Hz), 142.4 (s), 134.7 (s), 129.4 (d, J = 2.2 Hz), 128.0 (d, J = 8.0 Hz), 115.5 (d, J = 21.5 Hz), -1.1 (s); ^{19}F NMR (376 MHz, $CDCl_3$) δ -114.2; FTIR (cm^{-1}) 2956, 1507, 1248, 836. HRMS (EI) m/z, calcd for [$C_{11}H_{15}FSi$]: 194.0927; found: 194.0945.

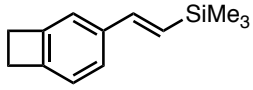

(**1.15**) According to general procedure A, 4-vinylbenzocyclobutene (130 mg, 1 mmol), ^{t}BuPCy$_2$ (38 mg, 0.15 mmol), Ni(COD)$_2$ (27.5 mg, 0.1 mmol), Et_3N (700 μL, 5 mmol), and Me_3SiOTf (540 μL, 3 mmol) were reacted in dioxane (2 mL) at 75 °C for 24 h. The product was purified by flash chromatography on silica gel (petroleum ether) and concentrated *in vacuo* to yield **1.15** as a colorless oil (157 mg, 78%): ^{1}H NMR (400 MHz, $CDCl_3$) δ 7.24 (d, J = 10.1 Hz, 1H), 7.18 (s, 1H), 7.00 (d, J = 7.5 Hz, 1H), 6.85 (d, J = 19.1 Hz, 1H), 6.38 (d, J = 19.1 Hz, 1H), 3.16 (s, 4H), 0.14 (s, 9H); ^{13}C NMR (101 MHz, $CDCl_3$) δ 146.2, 146.1, 144.7, 137.5, 127.8, 126.1, 122.7, 120.0, 29.6, 29.4, -1.0; FTIR (cm^{-1})

2955, 2930, 1247, 985, 866, 837. HRMS (EI) m/z, calcd for [$C_{13}H_{18}Si$]: 202.1178; found: 202.1194.

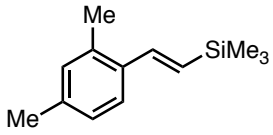

(**1.16**) According to general procedure A, 2,4-dimethystyrene (146 μL, 1 mmol), ^{t}BuPCy$_2$ (38 mg, 0.15 mmol), Ni(COD)$_2$ (27.5 mg, 0.1 mmol), Et$_3$N (700 μL, 5 mmol), and Me$_3$SiOTf (540 μL, 3 mmol) were reacted in dioxane (2 mL) at 75 °C for 24 h. The product was purified by flash chromatography on silica gel (hexanes) and concentrated *in vacuo* to yield **1.16** as a colorless oil (126 mg, 62%): ^{1}H NMR (400 MHz, $CDCl_3$) δ 7.43 (d, J = 7.9 Hz, 1H), 7.10 (d, J = 19.0 Hz, 1H), 6.99 (d, J = 8.4 Hz, 1H), 6.96 (s, 1H), 6.33 (d, J = 19.0 Hz, 1H), 2.35 (s, 3H), 2.31 (s, 3H), 0.16 (s, 9H); ^{13}C NMR (101 MHz, $CDCl_3$) δ 141.2, 137.6, 135.3, 134.9, 131.2, 130.2, 127.0, 125.3, 21.3, 19.7, -1.0; FTIR (cm^{-1}) 2954, 1247, 987, 868, 842. HRMS (EI) m/z, calcd for [$C_{13}H_{20}Si$]: 204.1334; found: 204.1350.

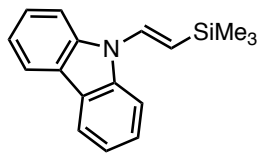

(**1.17**) According to general procedure A, *N*-vinyl carbazole (193 mg, 1 mmol), ^{t}BuPCy$_2$ (38 mg, 0.15 mmol), Ni(COD)$_2$ (27.5 mg, 0.1 mmol), Et$_3$N (700 μL, 5 mmol), and Me$_3$SiOTf (540 μL, 3 mmol) were reacted in dioxane (2 mL) at 75 °C for 24 h. The product was purified by flash chromatography on silica gel (petroleum ether) and concentrated *in vacuo* to yield **1.17** as a white solid (248 mg, 93%): ^{1}H NMR (400 MHz, $CDCl_3$) δ 8.07 (d, J = 7.8 Hz, 2H), 7.72 (d, J = 8.3 Hz, 2H), 7.48 (ddd, J = 8.3, 7.2, 1.3 Hz, 2H), 7.38 – 7.27 (m, 3H), 6.04 (d, J = 17.2 Hz, 1H), 0.27 (s, 9H); ^{13}C NMR (101 MHz, $CDCl_3$) δ 139.4, 133.6,

126.3, 124.2, 120.8, 120.4, 113.5, 110.9, 77.2, -0.6; FTIR (cm^{-1}) 2953, 1610, 1447, 834, 751, 721. HRMS (EI) m/z, calcd for [$C_{17}H_{19}NSi$]: 265.1287; found: 265.1262.

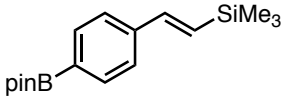

(**1.19**) Using a modification of general procedure A, 4-pinacolatoboryl styrene[28] (230 mg, 1 mmol), tricyclopentylphosphine (72 mg, 0.3 mmol), $Ni(COD)_2$ (27.5 mg, 0.1 mmol), Et_3N (700 µL, 5 mmol), and Me_3SiOTf (540 µL, 3 mmol) were reacted in dioxane (2 mL) at 75 °C for 24 h. The product was purified by flash chromatography on silica gel (15 : 85 CH_2Cl_2 : hexanes) and concentrated *in vacuo* to yield **1.19** as a white solid (123 mg, 41%): ^{1}H NMR (600 MHz, $CDCl_3$) δ 7.76 (d, J = 8.0 Hz, 2H), 7.43 (d, J = 8.0 Hz, 2H), 6.88 (d, J = 19.1 Hz, 1H), 6.55 (d, J = 19.1 Hz, 1H), 1.35 (s, 12H), 0.16 (s, 9H); ^{13}C NMR (151 MHz, $CDCl_3$) δ 143.7, 141.1, 135.2, 131.1, 125.8, 83.9, 25.0, -1.1 (the carbon attached to boron was not observed); FTIR (cm^{-1}) 2953, 1607, 1358, 1141, 1090, 869. HRMS (EI) m/z, calcd for [$C_{17}H_{27}BO_2Si$]: 302.1873; found: 302.1893.

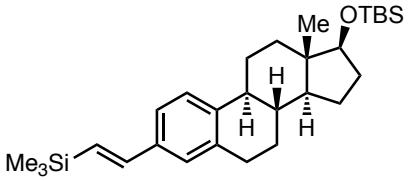

(**1.20**) According to general procedure A, *tert*-butyldimethyl(((8*R*,9*S*,13*S*,14*S*,17*S*)-13-methyl-3-vinyl-7,8,9,11,12,13,14,15,16,17-decahydro-6*H*-cyclopenta[*a*]phenanthren-17-yl)oxy)silane[3b] (396 mg, 1 mmol), ^{t}BuPCy$_2$ (38 mg, 0.15 mmol), $Ni(COD)_2$ (27.5 mg, 0.1 mmol), Et_3N (700 µL, 5 mmol), and Me_3SiOTf (540 µL, 3 mmol) were reacted in dioxane (2 mL) at 75 °C for 24 h. The product was purified by flash chromatography on silica gel (petroleum ether) and concentrated *in vacuo* to yield **1.20** as a white foam (283 mg, 60%): ^{1}H NMR (400 MHz, $CDCl_3$) δ 7.25 – 7.18 (m, 2H), 7.15 (s, 1H), 6.82 (d, J = 19.1 Hz, 1H), 6.40 (d, J = 19.2 Hz, 1H), 3.64

(t, J = 8.2 Hz, 1H), 2.98 – 2.73 (m, 2H), 2.30 (dt, J = 12.8, 3.0 Hz, 1H), 2.21 (td, J = 11.5, 11.0, 3.9 Hz, 1H), 2.08 – 1.79 (m, 3H), 1.76 – 1.59 (m, 1H), 1.59 – 1.09 (m, 7H), 0.89 (s, 9H), 0.74 (s, 3H), 0.14 (s, 9H), 0.04 (s, 3H), 0.03 (s, 3H); ^{13}C NMR (101 MHz, $CDCl_3$) δ 143.6, 140.7, 137.0, 135.9, 128.5, 127.0, 125.7, 123.7, 81.9, 49.9, 44.7, 43.7, 38.8, 37.3, 31.1, 29.7, 27.4, 26.4, 26.0, 23.4, 18.3, 11.5, -1.0, -4.3, -4.6; FTIR (cm^{-1}) 2926, 1248, 1095, 866, 836. HRMS (EI) m/z, calcd for [$C_{29}H_{48}OSi_2$]: 468.3244; found: 468.3259.

1.8.4 Reactions of Larger Silyl Triflates

1.8.4.1 General Procedure B

In a glovebox (N_2 atmosphere), tricyclohexylphosphine (30 mol %) and $Ni(COD)_2$ (10 mol %) were added to a 2-dram vial equipped with a stirbar. Dioxane, triethylamine (5 equiv), and 1-*tert*-butyl-4-vinylbenzene (1 equiv) were then added, sequentially. The vial was sealed with a Teflon-lined septum cap and removed from the glovebox. The reaction mixture was stirred at room temperature until homogeneous. The appropriate silyl trifluoromethanesulfonate reagent (3 equiv) was then added *via* syringe at room temperature with stirring. The vessel was then heated in an oil bath at 75 °C with stirring for 24 h, after which time *N*,*N*-dimethyl ethanolamine (3 equiv) was added *via* syringe with stirring at 75 °C. The vessel was stirred at 75 °C for approximately 1 minute before stirring at room temperature for approximately 15 minutes. The reaction vessel was then opened to air, and hexanes and HCl (1 M aqueous) were added. The HCl layer was removed, and the organic layer was washed twice with HCl (1 M aqueous). The combined aqueous layers were back-extracted with hexanes. The combined organic layers were dried over $MgSO_4$ and concentrated *in*

vacuo. The product was purified using flash silica chromatography, eluting with the indicated solvent noted in parenthesis.

1.8.4.2 Characterization Data

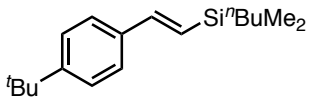

(**1.21**) According to general procedure B, 1-*tert*-butyl-4-vinylbenzene (183 μL, 1 mmol), Cy_3P (84 mg, 0.3 mmol), $Ni(COD)_2$ (27.5 mg, 0.1 mmol), Et_3N (700 μL, 5 mmol), and *n*-butyldimethylsilyl trifluoromethanesulfonate[15b] (790 mg, 3 mmol) were reacted in dioxane (2 mL) at 75 °C for 24 h. *N*,*N*-dimethyl ethanolamine (300 μL, 3 mmol) was added after reaction. The product was purified by flash chromatography on silica gel (petroleum ether) and concentrated *in vacuo* to yield **1.21** as a colorless oil (165 mg, 60%): ^{1}H NMR (600 MHz, $CDCl_3$) δ 7.38 (d, J = 8.4 Hz, 2H), 7.35 (d, J = 8.5 Hz, 2H), 6.85 (d, J = 19.2 Hz, 1H), 6.41 (d, J = 19.1 Hz, 1H), 1.35 – 1.28 (m, 13H), 0.88 (t, J = 6.8 Hz, 3H), 0.64 – 0.59 (m, 2H), 0.12 (s, 6H); ^{13}C NMR (151 MHz, $CDCl_3$) δ 151.2, 143.8, 135.9, 127.8, 126.2, 125.6, 34.8, 31.5, 26.7, 26.3, 15.6, 14.0, -2.8; FTIR (cm^{-1}) 2956, 1982, 986, 837. HRMS (EI) m/z, calcd for [$C_{18}H_{30}Si$]: 274.2117; found: 274.2092.

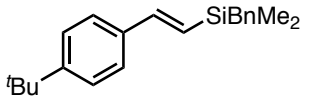

(**1.22**) According to general procedure B, 1-*tert*-butyl-4-vinylbenzene (183 μL, 1 mmol), Cy_3P (84 mg, 0.3 mmol), $Ni(COD)_2$ (27.5 mg, 0.1 mmol), Et_3N (700 μL, 5 mmol), and benzyldimethylsilyl trifluoromethanesulfonate[15a] (895 mg, 3 mmol) were reacted in dioxane (2 mL) at 75 °C for 24 h. *N*,*N*-dimethyl ethanolamine (300 μL, 3 mmol) was added after reaction. The product was purified by flash chromatography on silica gel (5 : 95 CH_2Cl_2 : hexanes) and concentrated *in vacuo* to yield **1.22** as a colorless oil (206 mg, 67%): ^{1}H NMR (400 MHz, $CDCl_3$) δ 7.36 (app s, 4H), 7.22 (t, J = 7.6 Hz, 2H), 7.08 (t, J = 7.4

Hz, 1H), 7.03 (app d, J = 7.3 Hz, 2H), 6.84 (d, J = 19.2 Hz, 1H), 6.38 (d, J = 19.2 Hz, 1H), 2.21 (s, 2H), 1.33 (s, 9H), 0.13 (s, 6H); ^{13}C NMR (101 MHz, $CDCl_3$) δ 151.4, 144.6, 140.1, 135.7, 128.4, 128.3, 126.4, 126.2, 125.6, 124.1, 34.8, 31.4, 26.3, -3.2; FTIR (cm^{-1}) 2961, 1493, 832, 698. HRMS (EI) m/z, calcd for [$C_{21}H_{28}Si$]: 308.1960; found: 308.1950.

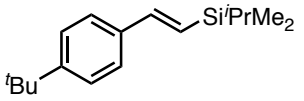

(**1.23**) According to general procedure B, 1-*tert*-butyl-4-vinylbenzene (183 µL, 1 mmol), Cy_3P (84 mg, 0.3 mmol), $Ni(COD)_2$ (27.5 mg, 0.1 mmol), Et_3N (700 µL, 5 mmol), and isopropyldimethylsilyl trifluoromethanesulfonate[15a] (750 mg, 3 mmol) were reacted in dioxane (2 mL) at 75 °C for 24 h. *N*,*N*-dimethyl ethanolamine (300 µL, 3 mmol) was added after reaction. The product was purified by flash chromatography on silica gel (petroleum ether) and concentrated *in vacuo* to yield **1.23** as a colorless oil (157 mg, 60%): ^{1}H NMR (400 MHz, $CDCl_3$) δ 7.39 (d, J = 8.6 Hz, 2H), 7.36 (d, J = 8.4 Hz, 2H), 6.86 (d, J = 19.2 Hz, 1H), 6.41 (d, J = 19.2 Hz, 1H), 1.32 (s, 9H), 0.98 (d, J = 7.1 Hz, 6H), 0.93 – 0.80 (m, 1H), 0.10 (s, 6H); ^{13}C NMR (101 MHz, $CDCl_3$) δ 151.2, 144.4, 135.9, 126.4, 126.2, 125.6, 34.7, 31.4, 17.8, 14.0, -5.1; FTIR (cm^{-1}) 2955, 2863, 1267, 987, 839. HRMS (EI) m/z, calcd for [$C_{17}H_{28}Si$]: 260.1960; found: 260.1968.

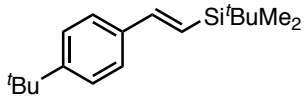

(**1.24**) Using a modification of general procedure B, 1-*tert*-butyl-4-vinylbenzene (183 µL, 1 mmol), ^{n}Bu$_3$P (81 mg, 0.4 mmol), $Ni(COD)_2$ (27.5 mg, 0.1 mmol), Et_3N (700 µL, 5 mmol), and *tert*-butyldimethylsilyl trifluoromethanesulfonate (690 µL, 3 mmol) were reacted in dioxane (1 mL) at 110 °C for 24 h. *N*,*N*-dimethyl ethanolamine (300 µL, 3 mmol) was added

after reaction. The product was purified by flash chromatography on silica gel (hexanes) and concentrated *in vacuo* to yield **1.24** as a colorless oil (86 mg, 31%): ^{1}H NMR (400 MHz, $CDCl_3$) δ 7.39 (d, J = 8.6 Hz, 2H), 7.36 (d, J = 8.5 Hz, 2H), 6.87 (d, J = 19.2 Hz, 1H), 6.43 (d, J = 19.1 Hz, 1H), 1.32 (s, 9H), 0.91 (s, 9H), 0.11 (s, 6H); ^{13}C NMR (101 MHz, $CDCl_3$) δ 151.2, 144.7, 135.9, 126.2, 125.8, 125.6, 34.8, 31.4, 26.6, 17.0, -5.9; FTIR (cm^{-1}) 2954, 2856, 1247, 987, 828. HRMS (EI) m/z, calcd for [$C_{18}H_{30}Si$]: 274.2117; found: 274.2103.

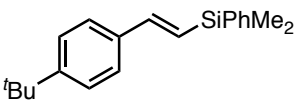

(**1.25**) According to general procedure B, 1-*tert*-butyl-4-vinylbenzene (183 µL, 1 mmol), Cy_3P (84 mg, 0.3 mmol), $Ni(COD)_2$ (27.5 mg, 0.1 mmol), Et_3N (700 µL, 5 mmol), and phenyldimethylsilyl trifluoromethanesulfonate[15c] (850 mg, 3 mmol) were reacted in dioxane (2 mL) at 75 °C for 24 h. *N*,*N*-dimethyl ethanolamine (300 µL, 3 mmol) was added after reaction. The product was purified by flash chromatography on silica gel (petroleum ether) and concentrated *in vacuo* to yield **1.25** as a colorless oil (205 mg, 70%): ^{1}H NMR (600 MHz, $CDCl_3$) δ 7.58 – 7.55 (m, 2H), 7.39 (d, J = 8.4 Hz, 4H), 7.37 – 7.33 (m, 5H), 6.93 (d, J = 19.1 Hz, 1H), 6.54 (d, J = 19.2 Hz, 1H), 1.32 (s, 9H), 0.42 (s, 6H); ^{13}C NMR (151 MHz, $CDCl_3$) δ 151.5, 145.3, 138.9, 135.6, 134.1, 129.1, 127.9, 126.4, 126.2, 125.6, 34.8, 31.4, -2.3; FTIR (cm^{-1}) 2960, 1247, 1112, 841, 821, 729, 698. HRMS (EI) m/z, calcd for [$C_{20}H_{26}Si$]: 294.1804; found: 294.1788.

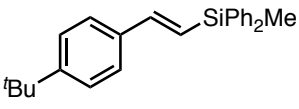

(**1.26**) According to general procedure B, 1-*tert*-butyl-4-vinylbenzene (137 µL, 0.75 mmol), Cy_3P (63 mg, 0.225 mmol), $Ni(COD)_2$ (20.6 mg, 0.075 mmol), Et_3N (529 µL, 3.75 mmol), and

diphenylmethylsilyl trifluoromethanesulfonate[15c] (780 mg, 2.25 mmol) were reacted in dioxane (1.5 mL) at 75 °C for 24 h. *N*,*N*-dimethyl ethanolamine (225 μL, 2.25 mmol) was added after reaction. The product was purified by flash chromatography on silica gel (10 : 90 CH_2Cl_2 : hexanes) and concentrated *in vacuo* to yield **1.26** as a colorless oil (198 mg, 74%): ^{1}H NMR (400 MHz, $CDCl_3$) δ 7.59 (dd, J = 7.5, 1.8 Hz, 4H), 7.47 – 7.33 (m, 10H), 6.97 (d, J = 19.1 Hz, 1H), 6.73 (d, J = 19.0 Hz, 1H), 1.33 (s, 9H), 0.72 (s, 3H); ^{13}C NMR (101 MHz, $CDCl_3$) δ 151.7, 147.1, 136.7, 135.5, 135.1, 129.4, 128.0, 126.5, 125.6, 123.9, 34.8, 31.4, -3.5; FTIR (cm^{-1}) 2961, 1427, 1111, 800, 699. HRMS (EI) m/z, calcd for [$C_{25}H_{28}Si$]: 356.1960; found: 356.1955.

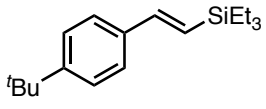

(**1.27**) According to general procedure B, 1-*tert*-butyl-4-vinylbenzene (183 μL, 1 mmol), Cy_3P (84 mg, 0.3 mmol), $Ni(COD)_2$ (27.5 mg, 0.1 mmol), Et_3N (700 μL, 5 mmol), and triethylsilyl trifluoromethanesulfonate (680 μL, 3 mmol) were reacted in dioxane (2 mL) at 75 °C for 24 h. *N*,*N*-dimethyl ethanolamine (300 μL, 3 mmol) was added after reaction. The product was purified by flash chromatography on silica gel (petroleum ether) and concentrated *in vacuo* to yield **1.27** as a colorless oil (178 mg, 65%): ^{1}H NMR (400 MHz, $CDCl_3$) δ 7.40 (d, J = 8.6 Hz, 2H), 7.36 (d, J = 8.6 Hz, 2H), 6.88 (d, J = 19.3 Hz, 1H), 6.38 (d, J = 19.3 Hz, 1H), 1.32 (s, 9H), 0.98 (t, J = 7.9 Hz, 9H), 0.65 (q, J = 7.9 Hz, 6H); ^{13}C NMR (101 MHz, $CDCl_3$) δ 151.2, 144.7, 135.9, 126.1, 125.6, 125.0, 34.7, 31.4, 7.6, 3.7; FTIR (cm^{-1}) 2954, 2874, 987, 788, 731. HRMS (EI) m/z, calcd for [$C_{18}H_{30}Si$]: 274.2117; found: 274.2093.

REFERENCES

(1) (a) Hosomi, A.; Endo, M.; Sakurai, H., *Chem. Lett.* **1976,** *5*, 941; (b) Masse, C. E.; Panek, J. S., *Chem. Rev.* **1995,** *95*, 1293; (c) Fleming, I.; Barbero, A.; Walter, D., *Chem. Rev.* **1997,** *97*, 2063; (d) Brook, M. A., *Silicon in Organic, Organometallic, and Polymer Chemistry*. Wiley: Chichester, 2000; (e) Denmark, S. E.; Fu, J., *Chem. Rev.* **2003,** *103*, 2763; (f) Fleming, I.; Dunoguès, J.; Smithers, R., The Electrophilic Substitution of Allylsilanes and Vinylsilanes. In *Organic Reactions*, John Wiley & Sons, Inc.: New York, 2004; pp 57; (g) Denmark, S. E.; Liu, J. H. C., *Angew. Chem., Int. Ed.* **2010,** *49*, 2978; (h) Nakao, Y.; Hiyama, T., *Chem. Soc. Rev.* **2011,** *40*, 4893.
(2) Yamashita, H.; Kobayashi, T.; Hayashi, T.; Tanaka, M., *Chem. Lett.* **1991,** *20*, 761.
(3) (a) McAtee, J. R.; Martin, S. E. S.; Ahneman, D. T.; Johnson, K. A.; Watson, D. A., *Angew. Chem., Int. Ed.* **2012,** *51*, 3663; (b) Martin, S. E. S.; Watson, D. A., *J. Am. Chem. Soc.* **2013,** *135*, 13330.
(4) (a) Hatanaka, Y.; Hiyama, T., *Synlett* **1991,** *1991*, 845; (b) Hiyama, T.; Hatanaka, Y., *Pure Appl. Chem.* **1994,** *66*, 1471; (c) Denmark, S. E.; Sweis, R. F., *Acc. Chem. Res.* **2002,** *35*, 835; (d) Hiyama, T., *J. Organomet. Chem.* **2002,** *653*, 58; (e) Handy, C. J.; Manoso, A. S.; McElroy, W. T.; Seganish, W. M.; DeShong, P., *Tetrahedron* **2005,** *61*, 12201; (f) Denmark, S. E.; Baird, J. D., *Chem. - Eur. J.* **2006,** *12*, 4954; (g) Denmark, S. E.; Regens, C. S., *Acc. Chem. Res.* **2008,** *41*, 1486; (h) Sore, H. F.; Galloway, W. R. J. D.; Spring, D. R., *Chem. Soc. Rev.* **2012,** *41*, 1845; (i) Komiyama, T.; Minami, Y.; Hiyama, T., *ACS Catal.* **2017,** *7*, 631.
(5) (a) Jarvie, A. W. P.; Holt, A.; Thompson, J., *Journal of the Chemical Society B: Physical Organic* **1969,** 852; (b) Miller, R. B.; McGarvey, G., *J. Org. Chem.* **1978,** *43*, 4424; (c) Miller, R. B.; McGarvey, G., *Synth. Commun.* **1978,** *8*, 291; (d) Chan, T. H.; Koumaglo, K., *Tetrahedron Lett.* **1986,** *27*, 883; (e) Tamao, K.; Akita, M.; Maeda, K.; Kumada, M., *J. Org. Chem.* **1987,** *52*, 1100; (f) Chou, S. S. P.; Kuo, H. L.; Wang, C. J.; Tsai, C. Y.; Sun, C. M., *J. Org. Chem.* **1989,** *54*, 868; (g) Brook, M. A.; Neuy, A., *J. Org. Chem.* **1990,** *55*, 3609; (h) Stamos, D. P.; Taylor, A. G.; Kishi, Y., *Tetrahedron Lett.* **1996,** *37*, 8647.
(6) Jones, G. R.; Landais, Y., *Tetrahedron* **1996,** *52*, 7599.
(7) (a) Tamao, K.; Kakui, T.; Kumada, M., *Tetrahedron Lett.* **1979,** *20*, 619; (b) Hatanaka, Y.; Fukushima, S.; Hiyama, T., *Tetrahedron* **1992,** *48*, 2113; (c) Takeuchi, R.; Ishii, N.; Sugiura, M.; Sato, N., *J. Org. Chem.* **1992,** *57*, 4189; (d) Yamane, M.; Uera, K.; Narasaka, K., *Bull. Chem. Soc. Jpn.* **2005,** *78*, 477; (e) Pawluć, P.; Szudkowska, J.; Hreczycho, G.; Marciniec, B., *J. Org. Chem.* **2011,** *76*, 6438.
(8) (a) Marciniec, B.; Guliński, J., *J. Organomet. Chem.* **1993,** *446*, 15; (b) Roy, A. K., *Adv. Organomet. Chem.* **2007,** *55*, 1; (c) Nakajima, Y.; Shimada, S., *RSC Advances*

2015, *5*, 20603; (d) Sun, J.; Deng, L., *ACS Catal.* **2016,** *6*, 290; (e) Zaranek, M.; Marciniec, B.; Pawluc, P., *Organic Chemistry Frontiers* **2016,** *3*, 1337.
(9) Trost, B. M.; Ball, Z. T., *J. Am. Chem. Soc.* **2005,** *127*, 17644.
(10) Martin, S. E. S.; Watson, D. A., *Synlett* **2013,** *24*, 2177.
(11) (a) Yamashita, H.; Hayashi, T.; Kobayashi, T.; Tanaka, M.; Goto, M., *J. Am. Chem. Soc.* **1988,** *110*, 4417; (b) Chatani, N.; Amishiro, N.; Murai, S., *J. Am. Chem. Soc.* **1991,** *113*, 7778; (c) Chatani, N.; Amishiro, N.; Morii, T.; Yamashita, T.; Murai, S., *J. Org. Chem.* **1995,** *60*, 1834; (d) Yamashita, H.; Tanaka, M.; Goto, M., *Organometallics* **1997,** *16*, 4696; (e) Terao, J.; Jin, Y.; Torii, K.; Kambe, N., *Tetrahedron* **2004,** *60*, 1301; (f) Terao, J.; Torii, K.; Saito, K.; Kambe, N.; Baba, A.; Sonoda, N., *Angew. Chem., Int. Ed.* **1998,** *37*, 2653.
(12) Oestreich, M., *The Mizoroki-Heck Reaction*. John Wiley & Sons: Chichester, U.K., 2008.
(13) (a) McAtee, J. R.; Krause, S. B.; Watson, D. A., *Adv. Synth. Catal.* **2015,** *357*, 2317; (b) Krause, S. B.; McAtee, J. R.; Yap, G. P. A.; Watson, D. A., *Org. Lett.* **2017,** *19*, 5641; (c) McAtee, J. R.; Yap, G. P. A.; Watson, D. A., *J. Am. Chem. Soc.* **2014,** *136*, 10166.
(14) Olah, G. A.; Narang, S. C.; Gupta, B. G. B.; Malhotra, R., *J. Org. Chem.* **1979,** *44*, 1247.
(15) (a) Aizpurua, J. M.; Palomo, C., *Tetrahedron Lett.* **1985,** *26*, 6113; (b) Coppi, L.; Ricci, A.; Taddei, M., *Tetrahedron Lett.* **1987,** *28*, 965; (c) Uhlig, W., *J. Organomet. Chem.* **1993,** *452*, 29.
(16) Fu, G. C., *Acc. Chem. Res.* **2008,** *41*, 1555.
(17) Walsh, R., *Acc. Chem. Res.* **1981,** *14*, 246.
(18) (a) Li, B.-J.; Yu, D.-G.; Sun, C.-L.; Shi, Z.-J., *Chem. - Eur. J.* **2011,** *17*, 1728; (b) Rosen, B. M.; Quasdorf, K. W.; Wilson, D. A.; Zhang, N.; Resmerita, A.-M.; Garg, N. K.; Percec, V., *Chem. Rev.* **2011,** *111*, 1346.
(19) Wenkert, E.; Michelotti, E. L.; Swindell, C. S., *J. Am. Chem. Soc.* **1979,** *101*, 2246.
(20) Tobisu, M.; Shimasaki, T.; Chatani, N., *Angew. Chem., Int. Ed.* **2008,** *47*, 4866.
(21) (a) Kuyper, J., *Inorg. Chem.* **1978,** *17*, 77; (b) Usón, R.; Oro, L.; Fernandez, M., *J. Organomet. Chem.* **1980,** *193*, 127; (c) Yamashita, H.; Kobayashi, T.; Hayashi, T.; Tanaka, M., *Chem. Lett.* **1989,** *18*, 471; (d) Zlota, A. A.; Frolow, F.; Milstein, D., *J. Chem. Soc., Chem. Commun.* **1989,** 1826; (e) Yamashita, H.; Kawamoto, A.; Tanaka, M.; Goto, M., *Chem. Lett.* **1990,** *19*, 2107; (f) Yamashita, H.; Kobayashi, T.; Hayashi, T.; Tanaka, M., *Chem. Lett.* **1990,** *19*, 1447; (g) Kirss, R. U., *Inorg. Chem.* **1992,** *31*, 3451; (h) Levy, C. J.; Puddephatt, R. J.; Vittal, J. J., *Organometallics* **1994,** *13*, 1559; (i) Levy, C. J.; Vittal, J. J.; Puddephatt, R. J., *Organometallics* **1996,** *15*, 2108; (j) Gatard, S.; Chen, C.-H.; Foxman, B. M.; Ozerov, O. V., *Organometallics* **2008,** *27*, 6257; (k) Esposito, O.; Roberts, D. E.; Cloke, F. G. N.; Caddick, S.; Green, J. C.; Hazari, N.; Hitchcock, P. B., *Eur. J. Inorg. Chem.* **2009,** *2009*, 1844; (l) Mitton, S. J.; McDonald, R.; Turculet, L., *Organometallics* **2009,** *28*, 5122.
(22) Ng, S.-S.; Ho, C.-Y.; Jamison, T. F., *J. Am. Chem. Soc.* **2006,** *128*, 11513.

(23) Choi, J. H.; Kwon, J. K.; RajanBabu, T. V.; Lim, H. J., *Adv. Synth. Catal.* **2013,** *355*, 3633.
(24) McAtee, J. R.; Martin, S. E. S.; Cinderella, A. P.; Reid, W. B.; Johnson, K. A.; Watson, D. A., *Tetrahedron* **2014,** *70*, 4250.
(25) Pangborn, A. B.; Giardello, M. A.; Grubbs, R. H.; Rosen, R. K.; Timmers, F. J., *Organometallics* **1996,** *15*, 1518.
(26) Patt, S. L.; Shoolery, J. N., *J. Magn. Reson.* **1982,** *46*, 535.
(27) Faler, C. A.; Joullié, M. M., *Org. Lett.* **2007,** *9*, 1987.
(28) Cambre, J. N.; Roy, D.; Gondi, S. R.; Sumerlin, B. S., *J. Am. Chem. Soc.* **2007,** *129*, 10348.

Chapter 2

DEVELOPMENT OF THE INTRAMOLECULAR SILYL-HECK REACTION

2.1 Introduction and Overview

Unsaturated silanes have widespread applications in various fields of chemistry.[1] In 2012, our group published a palladium-catalyzed method for the synthesis of allyl- and vinyl-silanes directly from unfunctionalized alkenes and trimethylsilyliodide (TMSI).[2] To this point, our studies have focused on bimolecular cross-coupling reactions yielding linear silicon containing products.[3] We sought to develop an analogous intramolecular variant by tethering pendant alkenes to an electrophilic silane. An intramolecular cyclization would give access to a new class of cyclic unsaturated silicon containing heterocycles which are inaccessible with our previous methods.[4] In addition, we suspect that internal alkenes, which have proven to be unreactive substrates in bimolecular reactions, may show reactivity in an intramolecular system. We also saw this as an opportunity to further explore the silyl-Heck mechanism. By examining the endo versus exo selectivities, we hoped to gain insight into the factors that affect the migratory insertion of the alkene and ultimately promote internal alkene participation in a bimolecular reaction.

Herein, I report the reactivity of multiple silicon scaffolds, alkenyl chain lengths and alkene substitutions in an intramolecular silyl-Heck reaction. This method works well for the synthesis of 5- and 6-membered unsaturated silacycles. We found that endo cyclization is preferred for most terminal alkenes, however, substitution on the alkene has a pronounced effect on reaction efficiency, cyclization pattern, and product ring

size. Additionally, many of the products formed were vinyl silanes, which contrasts earlier bimolecular studies where formation of the allylic isomer is preferred when possible. Lastly, for the first time, we demonstrate that internal and disubstituted alkenes participate in this silyl-Heck reaction with interesting selectivity.

2.2 Applications of Cyclic Silanes

Many researchers have explored the synthesis and applications of cyclic silanes in organic synthesis. These unique compounds find use in many fields of chemistry from medicines, to materials, to synthetic intermediates. The carbon to silicon switch, which has had great success in the discovery of new drugs and bioactive molecules,[5] can have much more drastic results when incorporated into a cyclic system. The longer C-Si bond lengths and change in bond polarization can cause silicon containing rings to adopt new and unique conformations. Many reviews have been written discussing the ample utilizations of silicon containing heterocycles.[1, 6]

2.2.1 Applications in Drugs and Medicine

Silacycles are common motifs in silicon derivatives of drugs known as siladrugs.[6a, 7] When silicon is introduced into an organic compound, the change in chemical and physical properties can introduce new and unique properties. The larger covalent radius and increased lipophilicity makes silicon containing molecules important bioisosteres for pharmacological and medicinal purposes. The carbon to silicon switch can be useful in the fine tuning of optimized functionality of nuclear receptor ligands and can serve in mechanistic probes as transition state analogs. The electropositive silicon atom (compared to C, N, O, etc.) can reverse bond polarization, enhance hydrogen-bonding abilities and effect the metabolic pathways. Lastly, there is

no known element specific toxicity associated with silicon, making it optimal for drug and medicinal applications.[6a]

Silicon analogs of bexarotene have been investigated because the longer Si-C bond length was expected to give different ring conformations (Figure 2.1, top).[8] An X-ray crystal structure of each compound confirmed the change in conformation and the disila-bexarotene was shown to be an excellent and highly potent retinoid X receptor (RXR) agonist. Silicon-analogs of many related compound were also synthesized and examined *in vitro*. All of them showed equipotent or superior pharmacological potency when compared to their carbon analogs.[8a, 8b]

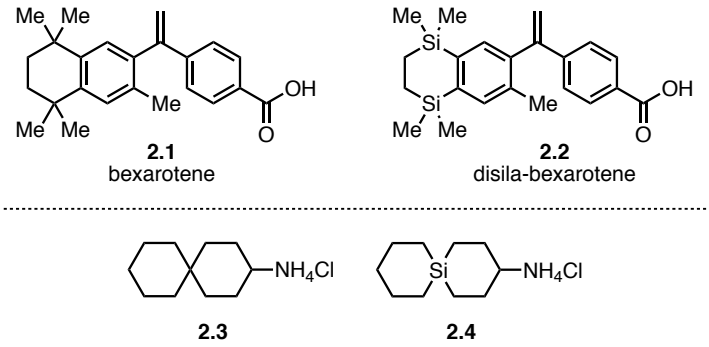

Figure 2.1 Carbon to Silicon Switch in Bioactive Materials

In another example, when examining silaspirane amines, DeGrado found that **2.4** demonstrated enhance potency as inhibitors against a drug resistant A/M2-V27A mutant (Figure 2.1, bottom).[9] The silicon-analog (**2.4**) showed a 2.7-fold increase in activity when compared to the carbon-analog (**2.3**).

2.2.2 Precursors for Polymers

Unsaturated cyclic silanes have also proven very useful in the development of silicon based polymers.[10] Polycarbosilanes have been the subject of much interest and study over the past several decades. They can have unique and novel characteristics when compared to polysiloxane and hydrocarbon polymers. Applications of polycarbosilanes include optical materials, organic semi-conductors, ceramic precursors and heat-resistant materials.[10b, 11]

Using a molybdenum catalyst, Gibson demonstrated the ring-opening metathesis polymerization (ROMP) of simple cyclic silanes (Figure 2.2).[10a] The degree of polymerization (monomer, dimer, polymer, etc.) could be controlled with varying reaction conditions. When the reaction is run with benzene as a solvent, 10-membered cyclo-dimers are the major product formed (**2.5**). These dienes arise *via* secondary metathesis in which the active alkylidene prefers to bend back on the polymer chain rather than add a new fragment, thus limiting the size of the polymers. On the other hand, in the absence of solvent, **2.6** is readily polymerized to low molecular weight oligomeric materials with sizes ranging from 40-100 kDa (**2.7**). On average, **2.7** polymers contain between 55-75% *trans*-alkene.

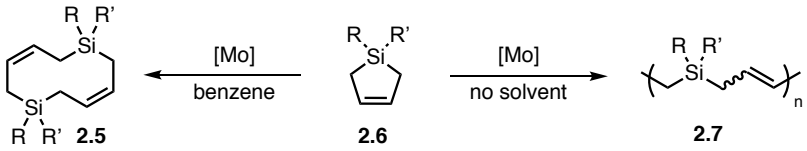

Figure 2.2 Ring-Opening Metathesis Polymerization of Unsaturated Cyclic Silane

2.2.3 Synthetic Intermediates

Silacycles are also important as synthetic intermediates and have been utilized in many total syntheses.[12] They are often employed as temporary silicon tethers for intramolecular reactions to help control selectivity and yield.[6b, 6c, 13] After the cyclization reaction, the silicon is usually cleaved *via* hydrolysis or oxidation. However, the wide synthetic potential of organosilicon groups can also be applied to obtain highly complex compounds in a few steps. Most commonly, silicon containing rings are oxidized to form complex alcohols.[12, 14] Recently, Steel utilized a cyclic allylic silane **2.8** in his synthesis of prelactone B (Figure 2.3).[12b]

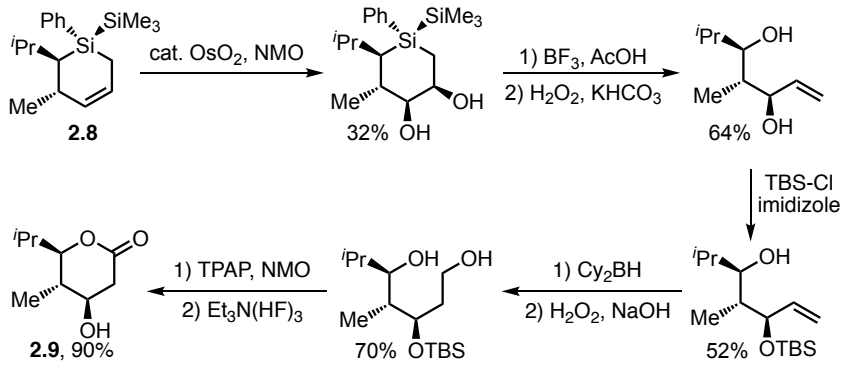

Figure 2.3 Steel's Synthesis of Prelactone B (**2.9**)

In addition to oxidation, cyclic silanes have also been used in other silicon related reactions. Denmark demonstrated that Hiyama-Denmark cross-coupling reactions with cyclic vinyl silane ethers could give rise to stereodefined trisubstituted olefins (Figure 2.4, top).[15] The reaction with cyclic vinyl silane **2.10** and 3-iodopyridine under palladium catalysis produced **2.12** in 73% yield. In a separate reaction, Oshima

and Utimoto successfully demonstrated an allylation reaction with a cyclic allyl siloxane (Figure 2.4, bottom).[16]

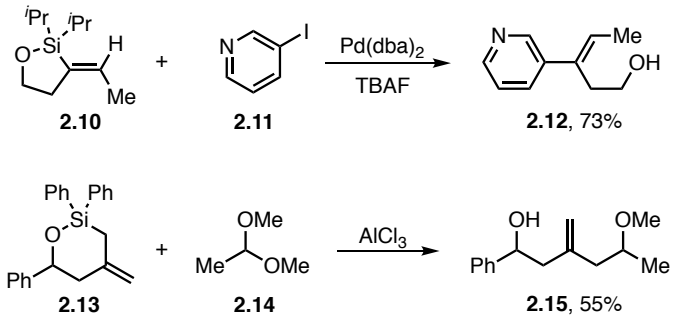

Figure 2.4 Other Cross-Coupling Reactions of Cyclic Silyl Ethers

2.3 Synthesis of Cyclic Allyl and Vinyl Silanes

Over the past several decades, there have been numerous procedures reported for the synthesis of cyclic organic silanes. However, many of these methods, especially earlier ones, only produce trace amounts of silacycles as byproducts or as complex mixtures of product isomers. For the sake of this thesis, I will only discuss synthetically useful methods to prepare unsaturated silicon containing heterocycles. Additionally, I will focus on the synthesis of 5- and 6-membered rings.

2.3.1 Barbier and Grignard Reactions

Unsaturated cyclic silanes can be synthesized in a variety of ways. The earliest synthesis of a cyclic organosilane is an intramolecular Barbier cyclization of an open chain organochlorosilanes (Figure 2.5).[17] Quenching the resulting chlorosilane with phenyl lithium gives **2.18** in a moderate yield. This method has also been use to synthesize 5-membered[18] and 4-membered[16] rings. Similarly, the formation of

organodimetallic reagents such as **2.20** can be mixed with methylphenylsilylchloride ($MePhSiCl_2$) to form **2.21** (Figure 2.5, bottom). This method avoids the synthesis of complex and reactive silyl chlorides and allows for easy modification of the substitution on silicon by changing the dichlorosilane used. However, both tactics require the formation of highly reactive and sensitive reagents.

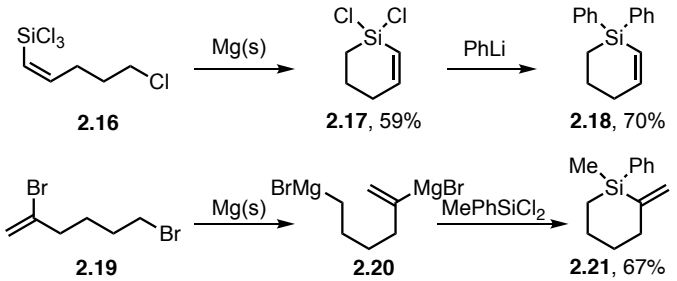

Figure 2.5 Early Synthesis of Cyclic Organosilanes Using Organometallic Reagents

2.3.2 Cycloadditions

Classically, silacycles can be synthesized from cycloadditions of reactive silenes or silylenes with dienes (Figure 2.6).[4] Silylenes (**2.23**) and silenes (**2.25**) can both react with dienes (**2.22**) to give unsaturated silicon containing heterocycles **2.24** and **2.26** respectively. These reactive intermediates are typically formed *via* flash vacuum pyrolysis (FVP) which requires extreme temperatures and pressures,[4] however, milder synthetic approaches have also been applied.[19] While these cycloaddition reactions have been exploited for the synthesis of heterocycles they were originally conducted for the indirect observation of these reactive intermediates.[20]

Figure 2.6 Cycloaddition Reactions of Reactive Silylenes and Silenes with Dienes

Pyrolysis of an excess of di- or trisilanes in a vacuum has been a common method for the synthesis of reactive silylenes (Figure 2.7). In one example, Gasper heated 1,2-dimethoxytetramethyldisilane (**2.27**) to 460 °C and found that one equivalent of added diene (**2.30** or **2.32**) gives moderate yield of silacycles **2.31** and **2.33** respectively.[21]

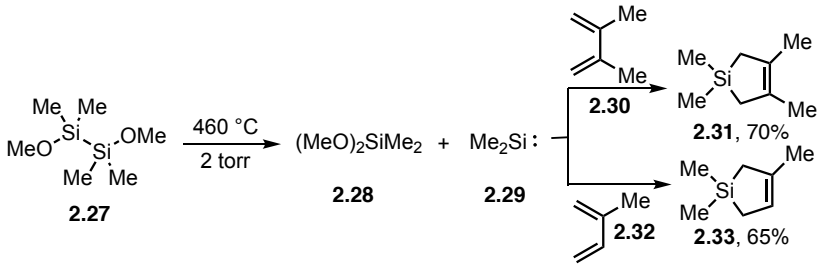

Figure 2.7 Synthesis of Silacycles *via* Silylene Cycloaddition

Under similar conditions, Conlin reported FVP of silacyclobutenes in the presence of alkenes (Figure 2.8).[22] Under these extreme conditions, silacyclobutenes undergoes a electrocyclic ring opening to form silene **2.35**. Since **2.35** is a conjugated compound, alkenes were added to quench the reactive intermediate. When *trans*-2-butene was added, **2.37** and **2.38** were isolated in a 1:1 ratio. Both products were

determined to have a *trans*-geometry between the methyl groups which supports a concerted cycloaddition mechanism. Similarly, when *cis*-2-butene was added, **2.39** and **2.40** were formed both with a *cis*-orientation of the methyl groups. Interestingly, both reactions provide equimolar vinyl and allyl products. The vinyl product is likely the result of a direct Diels-Alder cycloaddition of intermediate diene **2.35** with the alkene. However, the allyl product is thought to go through a different mechanistic pathway (Figure 2.8, bottom). Conlin proposed an initial [2+2] cycloaddition between the alkene and the double bond of the silene to form intermediate **2.41**. A stereoretentive 1,3-silyl shift to the terminal methylene produces the allyl silane **2.42**.

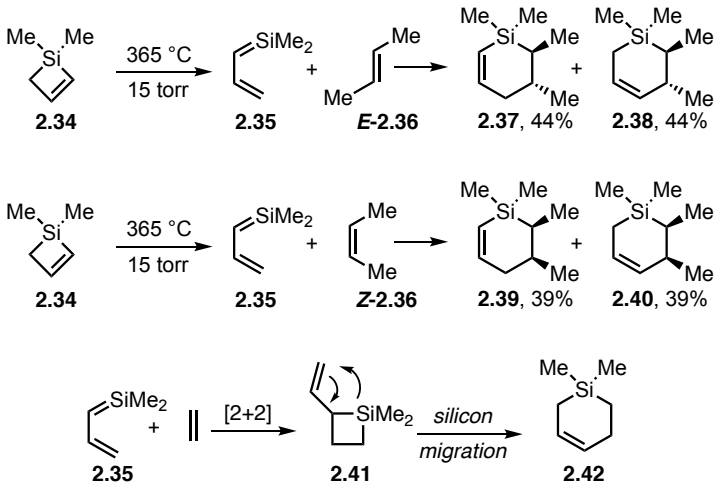

Figure 2.8 Stereospecific Cycloadditions of Reactive Silene Intermediates

The excessive temperatures required to form these reactive intermediates limit the practicality of this method for the synthesis of silacycles. In addition, these extreme conditions promote the formation of multiple products due to competing cycloaddition

and rearrangement pathways. As such, new and more mild methods for the generation of these reactive silene intermediate were developed.

One approach, a modified Peterson-type reaction, can form silenes from nucleophilic silicon reagents and simple ketones (Figure 2.9).[19] Nucleophilic addition to a carbonyl followed by a base promoted elimination of trimethylsilanolate form silenes at room temperature (**2.45**). With few exceptions,[19d, 19i] silenes are still highly unstable and reactive intermediates. Therefore, they must still be quenched with dienes to form silicon containing heterocycles (**2.46**).[19b]

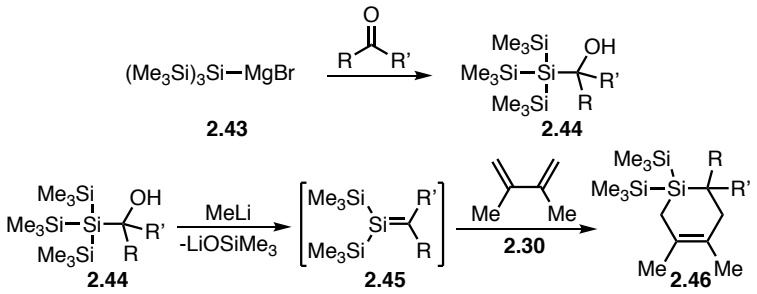

Figure 2.9 Peterson Modification for the Formation of Silene Intermediates

2.3.3 Ring Expansions

In 1975, Sakurai and Imai reported the palladium catalyzed reaction of 1,1-dimethyl silacyclobutane (**2.47**) and acetylene **2.48** (Figure 2.10, top).[23] This reaction proceeds with an excellent yield of the cyclic vinyl silane **2.49**. Unfortunately, substitution on the silacyclobutane ring or unsymmetrical alkynes produce multiple isomeric products.[23-24] Tanaka later discovered that reacting silacyclobutanes with acid chlorides can form cyclic silyl enol ethers (**2.51**) in good yields.[25] Furthermore,

Woerpel ascertained that using silacyclopropanes and alkynes 5-membered silacycles can be formed (**2.54**).[26]

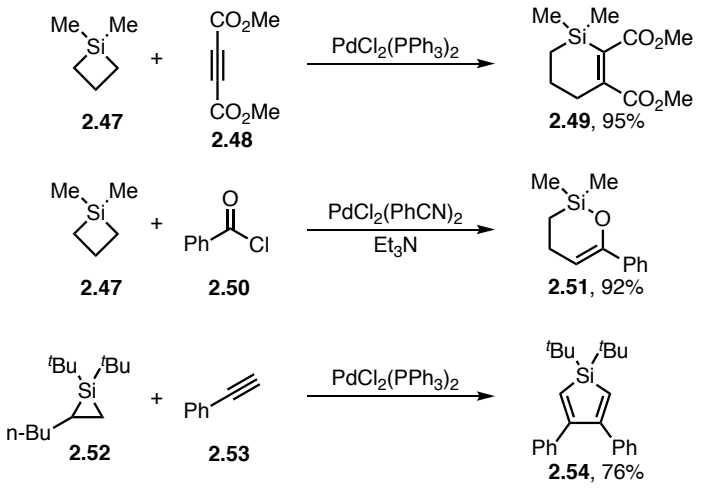

Figure 2.10 Bimolecular Palladium Catalyzed Ring Expansions of Small Silacycles

This reaction is thought to proceed through palladium activation of the strained Si-C bond of **2.47** forming a 5-membered palladacycle. Migratory insertion of the unsaturated fragment into the Si-Pd bond followed by reductive elimination gives rise to the observed products.

This strategy has been applied to the enantioselective synthesis of complex silicon containing heterocycle fragments. In 2011, Hayashi and Shintani demonstrated the palladium-catalyzed desymmetrization of silacyclobutanes for the construction of silacycles possessing a chiral tetraorganosilicon stereocenter (Figure 2.11).[27] Using a chiral phosphoramidite ligand, the ring expansion of silacyclobutane **2.55** proceeds with excellent yields and enantioselectivities. This intramolecular cyclization follows the

same mechanism as the bimolecular reactions, however, regioselectivity is not an issue due to the geometric constraints of the starting material.

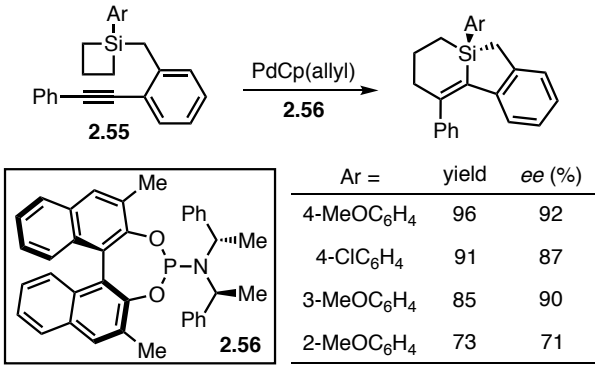

Ar =	yield	*ee* (%)
4-$MeOC_6H_4$	96	92
4-ClC_6H_4	91	87
3-$MeOC_6H_4$	85	90
2-$MeOC_6H_4$	73	71

Figure 2.11 Asymmetric Ring Expansion of Alkyne Tethered Silacyclobutanes

2.3.4 Intramolecular Hydrosilylation

More recently, intramolecular hydrosilylation has become a common method for the synthesis of various unsaturated silacycles. Speier's catalyst (H_2PtCl_6) is commonly used and gives a strong preference for exo-cyclizations (Figure 2.12).[28]

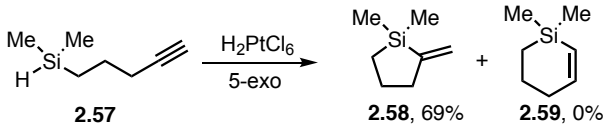

Figure 2.12 Exo-Selective Intramolecular Hydrosilylation

Tamao and Ito explored the use of Speier's catalyst in the intramolecular hydrosilylation of homopropargylic alcohol derivatives (Figure 2.13).[28c] These reactions proceeded with the same preference for exo ring closure as the carbon analogs. In

addition, the oxidation (**2.62**) and halogenation (**2.63**) of **2.61** was demonstrated, displaying the utility of these cyclic siloxane intermediates.

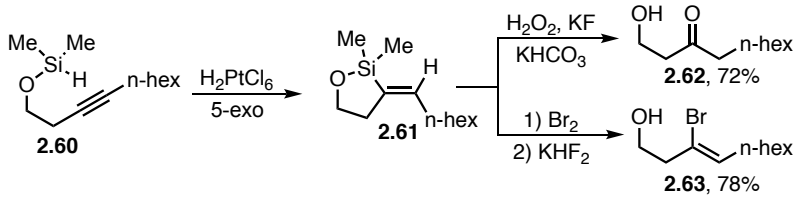

Figure 2.13 Tamao's and Ito's Intramolecular Hydrosilylation of Homopropargylic Alcohol Derivatives

Following the Chalk-Harrod mechanism,[29] oxidative addition into the Si-H bond and coordination of the tethered alkyne leads to **2.65** (Figure 2.14). In a bimolecular scenario, platinum would be added to the terminal position driven by steric repulsion. However, the *syn*-addition of platinum to the terminal position would lead to intermediate **2.69**. Not only is **2.69** disfavored because it is a 7-membered ring with a *trans*-alkene, but the reductive elimination forming the C-Si bond would also form a 6-membered ring with a *trans*-alkene. This distortion overrides the preference for terminal silylation and thus proceeds through the lower energy, exo-pathway (**2.67**). After reductive elimination of **2.67**, **2.68** is formed as a stereodefined alkene.

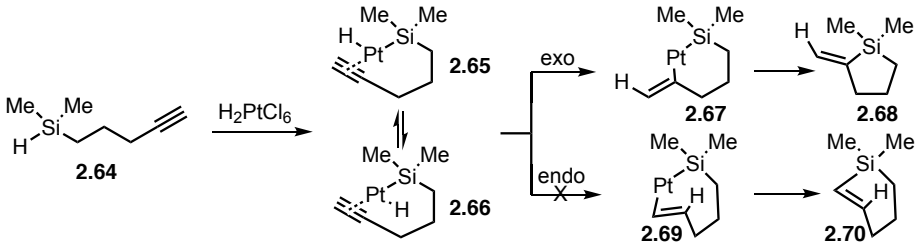

Figure 2.14 Rational for the Exo-Selectivity of Intramolecular Hydrosilylation

Sashida has also demonstrated a 6-exo cyclization *via* intramolecular hydrosilylation (Figure 2.15).[28f] As predicted by the mechanism, the exo-alkene is formed as a single stereoisomer reflecting the *syn*-addition of the silicon and hydrogen across the initial alkyne (**2.72**).

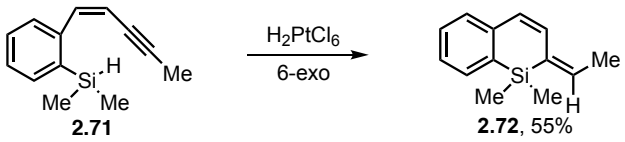

Figure 2.15 Sashida's 6-Exo Intramolecular Hydrosilation Reaction

Although exo-cyclization is preferred, few methods exist for the endo-cyclization of pendant alkynes. By its very nature, this requires a net *trans*-addition of silicon and hydrogen across the alkyne. Yamamoto reported a Lewis acid catalyzed intramolecular *trans*-hydrosilylation of unactivated alkynes.[30] Catalyzed by aluminum trichloride, Yamamoto was able to synthesize the 6-membered vinyl silacycle **2.59** in 70% yield (Figure 2.16).

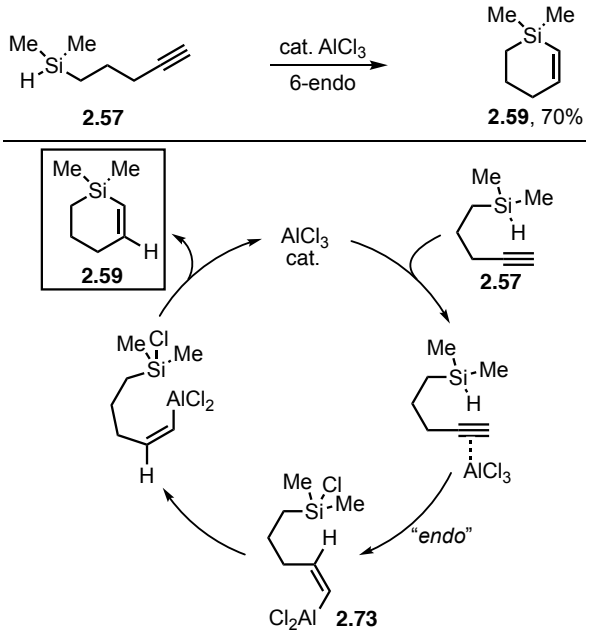

Figure 2.16 Yamamoto's Lewis Acid Catalyzed Intramolecular *Trans*-Hydrosilylation Reaction

Yamamoto proposes initial bimolecular coordination of the tethered alkyne to aluminum trichloride ($AlCl_3$). Intramolecular hydride transfer leads to the formal *trans*-hydroalumination intermediate **2.73**. The nucleophilic vinyl aluminum fragment can attack the silicon in an intramolecular fashion leading to the product (**2.59**). This method was also used to synthesize 5-, 7-, and 8-membered rings with similar cyclization patterns.

Trost demonstrated an alternative approach to intramolecular endo-hydrosilylation reaction using a ruthenium catalyst typically used for *trans*-hydrosilylation reactions (Figure 2.17).[31] The mechanism of this transformation is not known, however, Trost suggests the *trans*-hydrosilylation could be facilitated by a dinuclear rhodium intermediate.

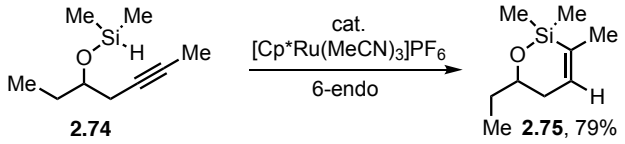

Figure 2.17 Trost's Intramolecular *trans*-Hydrosilylation Reaction

2.3.5 Summary and Outlook

Many of the early methods to access these multifunctional silacycles require extremely harsh reaction conditions. The use of reactive organometallic reagents or FVP severely limits the functional group tolerance as well as the products that can be synthesized. In addition, many of these methods proceed with poor regioselectivity resulting in many isomeric byproducts with also drastically limits the synthetic utility of the method. Intramolecular hydrosilylation is a promising solution to these limitations, however, the incorporation of tethered alkynes into the substrate framework can be difficult and more expensive to achieve than the analogous alkenes.

We envisioned that an intramolecular silyl-Heck reaction could provide an alternative approach for the synthesis of many of these silicon-containing heterocycles and were motivated to investigate such a reaction. This approach would allow for much milder conditions than many of the current methods used. In addition, tethered alkenes could be utilized as opposed to the more expensive alkynes.

2.4 Intramolecular Heck Cyclization

Since its discovery, the Heck reaction has become a popular method for C-C bond formation between a carbon electrophile and an alkene. The intramolecular variant of the Heck reaction has emerged as a reliable method for the synthesis of small, medium, and large rings (Figure 2.18).

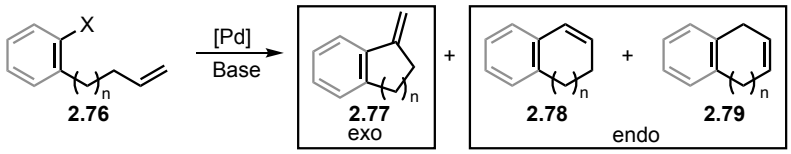

Figure 2.18 General Scheme of the Intramolecular Heck Reaction

This reaction was first reported by Mori[32] and Heck,[33] and originally used for the synthesis of indoles and similar nitrogen containing heterocycles. Since then, this reaction has been well studied and utilized in many total syntheses.[3a, 3b, 3d, 3e] Overman,[34] Shibasaki,[35] Grigg[36] and others have done tremendous work exploring and diastereoselectivity of this reaction and have even been able to induce enantioselectivity. The continuous study of this reaction has led to a significant understanding of the mechanism and general factors that affect ring closure selectivities.

2.4.1 Mechanism and Selectivity

The mechanism of the intramolecular Heck reaction proceeds *via* the same core steps as the bimolecular reaction (Figure 2.19). Oxidative addition of palladium into the aryl- or vinyl-halide bond forms the bis-ligated intermediate **2.80**. The reaction rate of this step is heavily dependent on the identity of the halide, where X = I > Br >> Cl. Loss of a neutral ligand followed by coordination and migratory insertion of the tethered alkene can occur in two possible ways. In one scenario, palladium is added to the terminal position (or farther from the tether) placing the arene on the closer side of the alkene (**2.81**). Since the palladium ends up outside of the newly formed ring, this mode of ring closure is called "exo". Subsequent β-hydride elimination leads to the exo-product **2.82**, with the alkene outside of the ring. Another possibility is the addition of the arene to the terminal (outside) position of the pendant alkene (**2.83**). This places

palladium directly attached to the newly formed ring and is described as an "endo" cyclization. After β-hydride elimination, the new alkene is inside the newly formed ring (**2.84**).

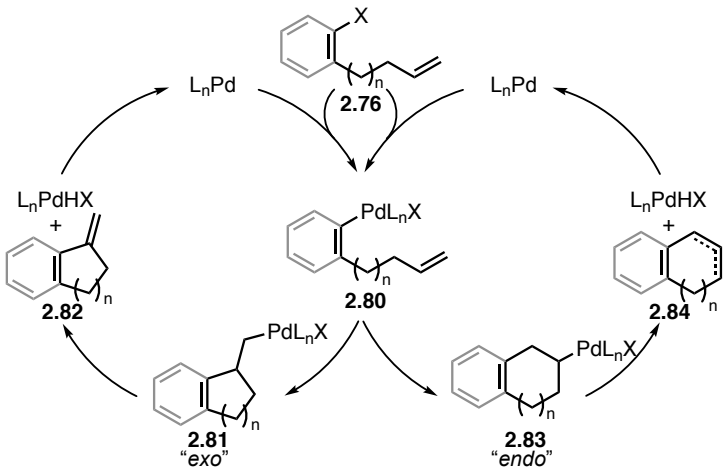

Figure 2.19 Mechanism for Exo and Endo Intramolecular Heck Reactions

As drawn above, during the course of this reaction pathway, the charge on palladium balanced therefore this is considered the "neutral" pathway. If the leaving group "X" is a highly stabilized anion such as a triflate or a nonaflate, then it is not bound to palladium during the entire reaction and is considered a "cationic" pathway. This pathway can have several advantages over the neutral method. Since the palladium is cationic, the alkene can bind without loss of ligand. As such, this is usually combined with asymmetric ligands and used for the desymmetrization of the migratory insertion. Asymmetric ligands have been used with neutral conditions but products typically result with lower enantiomeric excess.

Alkenes are known to undergo suprafacial insertion into palladium carbon bonds. There are two possible geometries in which this can occur (Figure 2.20). The eclipsed geometry, in which the palladium-carbon bond overlaps with the inserting alkene, and the twisted geometry, where the palladium-carbon bond is out of plane with the incoming alkene. Overman probed this distinction with a diastereoselective reaction towards synthesizing amaryllidaceae alkaloids.[37]

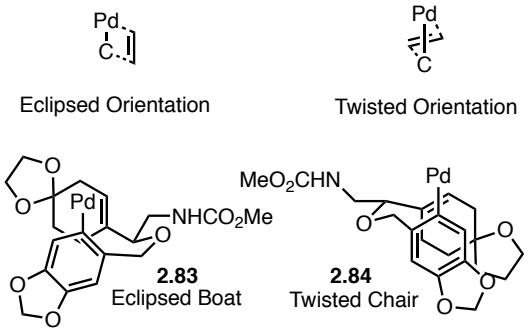

Figure 2.20 Two Possible Orientations for Migratory Insertion

Considering that both migratory insertion conformations have the pendant carbamate group in the more favored equatorial position, Overman examined the product ratio of this reaction. He found that the diastereomer derived from the eclipsed boat conformation is favored by more than 20:1. This demonstrates that the migratory insertion occurs *via* an eclipsed trajectory.

2.4.2 Exo Cyclizations

Generally, the intramolecular Heck reaction has a strong preference for exo ring closures. Both 5- and 6-exo ring closures are very common among various substrates (Figure 2.21). In one example, Overman demonstrated the formation of a quaternary

center with the synthesis of spirooxindole **2.86** *via* 5-exo ring closure (Figure 2.21, top).[38] The formation of quaternary centers can be a difficult task to achieve even in modern organic chemistry. However, it has become commonplace with the intramolecular Heck reaction. More recently, quaternary centers have been formed asymmetrically using chiral phosphine ligands.[3b, 3d, 39] In a second example, Danishefsky was able to synthesize a variety of congeners of FR 900482 (Figure 2.21, bottom).[40] The key step in the synthesis of these congeners is the 6-exo intramolecular Heck cyclization that proceeds with an excellent yield and stereoselectivity.

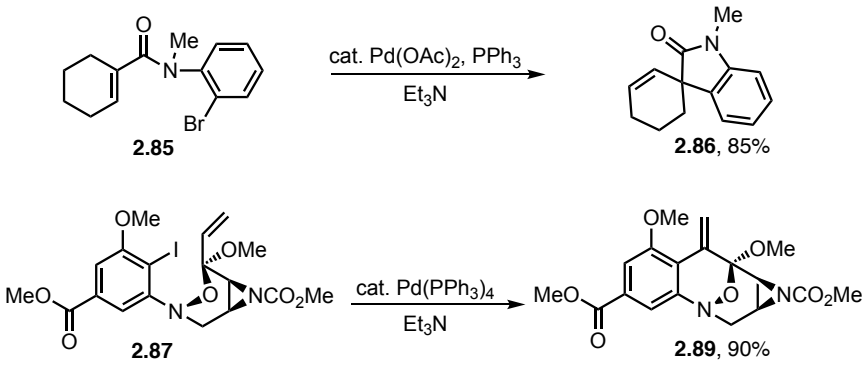

Figure 2.21 Selected Examples of 5- and 6-exo Intramolecular Heck Reactions

While the majority of intramolecular Heck reactions are designed to proceed through a 5- or 6-exo cyclization, syntheses of other ring sizes have also been demonstrated. Typically, 5-endo cyclizations are preferred over 4-exo due to the high strain associated with the formation of a 4-membered ring. However, 4-exo cyclizations have been established,[41] validating the strong preference for exo cyclization. In 1999, Brase demonstrated an unprecedented 4-exo cyclization *via* an intramolecular Heck

reaction (Figure 2.22). Nonaflate **2.90** undergoes palladium catalyzed cyclization to form diene **2.91** in a moderate yield.

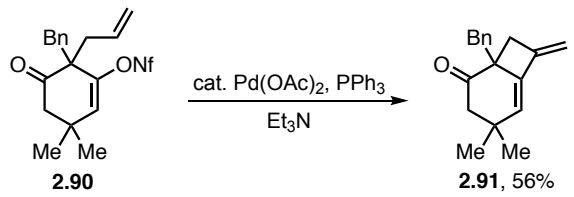

Figure 2.22 Brase's 4-exo-trig Cyclization

Larger rings have also been synthesized *via* exo cyclizations forming 7- and 8-membered rings. Tietze has utilized a 7-exo cyclization as a key step in his synthesis of cephalotaxine.[42]

2.4.3 Endo Cyclizations

At a certain point, the tethered alkene chain length becomes so large that the system behaves like a bimolecular system.[43] An early report by Ziegler demonstrated this principle with a macrocyclic ring closure (Figure 2.23).[44] Compound **2.93**, a 16-membered macrocycle was synthesized *via* an intramolecular Heck reaction and gave complete endo selectivity. This cyclization served as a model system for the aglycone of carbomycin B.

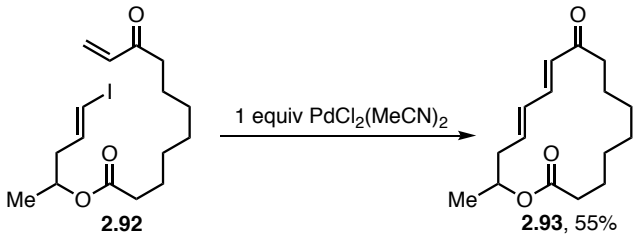

Figure 2.23 Selected Example of Macrocyclic Cyclization

Some medium sized rings can be formed *via* 7- and 8-endo cyclizations.[45] However, these reactions are often titled "uncommon" or "unusual" and generally have electronic or steric factors that influence the migratory insertion step. Additionally, many examples form mixtures of exo and endo products.[45h, 46] In 1997, Gibson investigated the reaction of conformationally constrained phenylalanine analogues (Figure 2.24, top).[45a] She found that 7-, 8-, and 9-membered rings could be formed selectively using an intramolecular Heck reaction with various chain lengths of **2.94**.

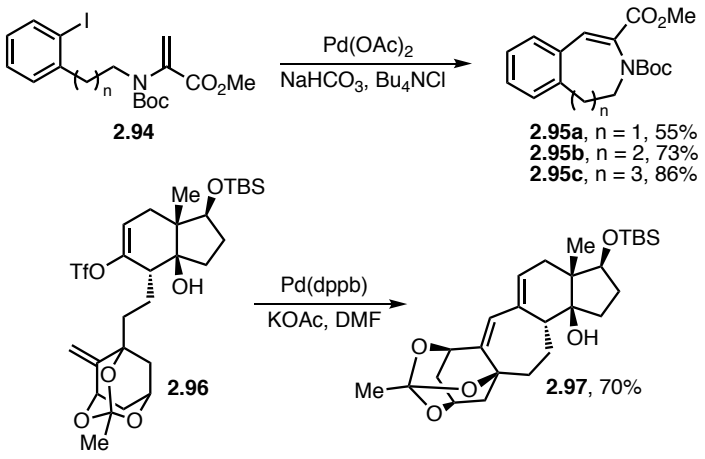

Figure 2.24 Selected Examples of Endo-Heck Cyclizations

In 2006, Overman reported the 7-endo cyclization of compound **2.96**.[45d] They expected a 6-exo/3-exo cascade cyclization however only observed the 7-endo product. This can be explained by examining the insertion topographies and they realized that the 7-endo cyclization had less steric encumbrance. Other reports of endo cyclizations have been determined to proceed through a radical pathway.[47]

In some cases where endo products are observed, it proceeds through a 6-exo insertion and rearrangement to form the 7-endo product (Figure 2.25).[33, 45h, 48] In an example from Rawal, he expected a 6-exo cyclization of **2.98**, but only observed the 7-endo product **2.100**.[48b] He proposes that after an initial 6-exo cyclization, coordination of the palladium with the carbamate prevents β-hydride elimination. Intermediate **2.101** can undergo a 3-exo cyclization to form cyclopropane intermediate **2.102** which can β-carbo eliminate to form **2.103**. β-hydride elimination from **2.103** leads to the formal 7-endo product **2.100**. This rearrangement, originally discovered by Negishi, is usually observed when β-hydride elimination is not possible.[48a, 48c, 48d]

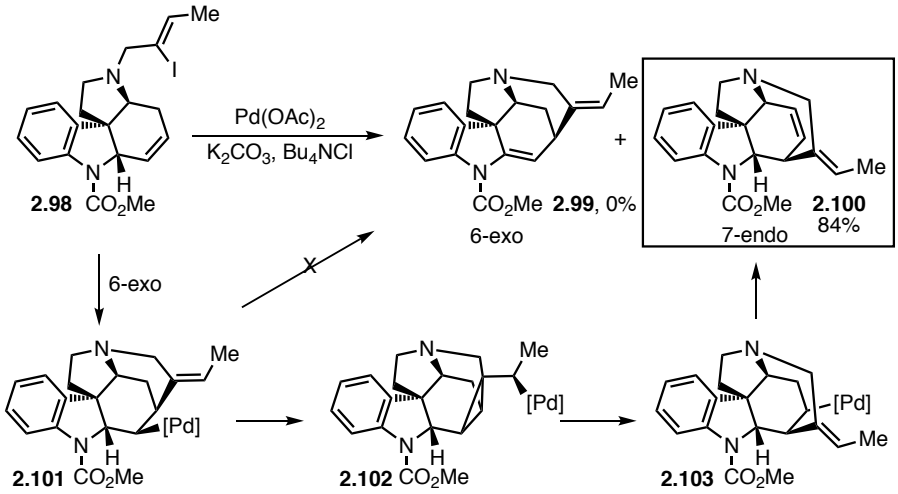

Figure 2.25 Rawal's 6-exo/3-exo Cascade Cyclization

Since the initial discovery of the intramolecular Heck reaction, it has become a common route for the synthesis of various 5-membered nitrogen and oxygen containing rings. These reactions typically form the 5-endo product over the 4-exo. This selectivity was originally thought to arise from the strain associated with the formation of a 4-membered ring. However, Baldwin concluded that 5-endo-trig cyclizations are disfavored and another mechanism must be in place.[49] In 2000, Grigg proposed an alternative mechanism that rationalizes the observed selectivity (Figure 2.26).[50]

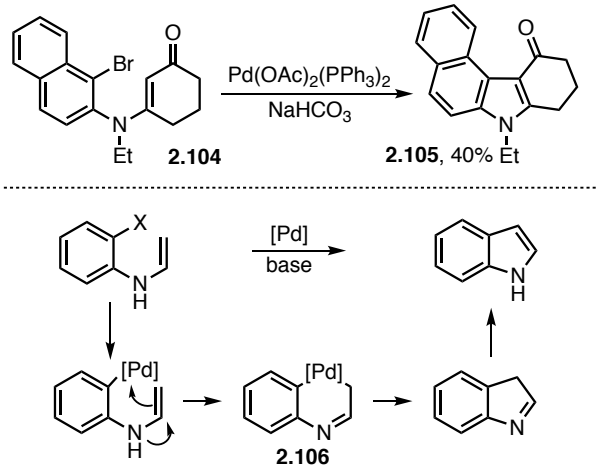

Figure 2.26 Alternative Mechanism for the 5-Endo Cyclization of Enamines

Typically, condensation of a carbonyl with a haloaniline form the cyclization precursor. The electron rich nature of these indole precursors allows for an unconventional mechanism to explain the observed products. After oxidative addition, the 5-endo-trig cyclization is disfavored; however, coordination of the electron rich enamine to palladium occurs forming a 6-membered palladacycle (**2.106**). Direct reductive elimination and tautomerization results in the observed product. This

mechanism circumvents the disfavored 5-endo-trig cyclization through the formation of the 6-membered palladacycle and is specific to this class of substrates.

2.4.4 Highly Substituted Alkenes

The reaction of tri- and tetrasubstituted alkenes is a very difficult task to achieve with the bimolecular Heck reaction.[51] We notice a similar trend with the silyl-Heck reaction, where we observe no reactivity with and internal or disubstituted alkenyl substrates. However, the reaction of tri- and tetrasubstituted alkenes has become common practice with the intramolecular Heck reaction (Figure 2.27).

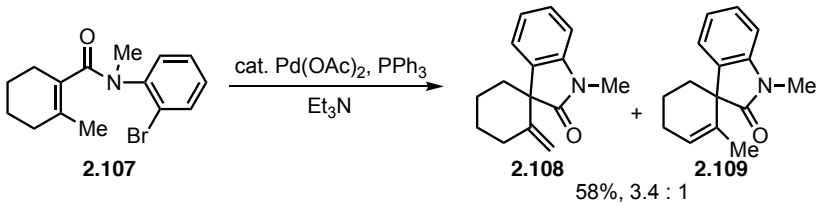

Figure 2.27 Intramolecular Migratory Insertion of a Tetrasubstituted Alkene

In 1987, Overman demonstrated the intramolecular migratory insertion of a tetrasubstituted alkene.[38] This reaction proceeded with complete 5-exo selectivity in a moderate yield to form a new fully substituted quaternary center. This example demonstrates the strong entropic contribution gained by tethering the alkene to the electrophile.

2.5 Development of General Conditions

We wanted to investigate the plausibility of an intramolecular silyl-Heck reaction for several reasons. In addition to devising a new and efficient route to

unsaturated silacycles, we saw this as a chance to further investigate our proposed silyl-Heck mechanism and better understand the limitations. The majority of our previous silyl-Heck procedures require the use of silyl iodides with a palladium catalyst. However, silyl triflates and chlorides can be utilized, provided there is an iodide additive to form the active silyl iodide *in situ*. In our early studies of the silyl-Heck reaction, we identified $^{t}BuPPh_2$ as an effective ligand for this transformation (Figure 2.28).[2, 52] With these catalytic conditions both allylic and vinylic silanes are accessible in moderate to good yields. However, after enormous amounts of additional optimization and ligand fine-tuning, **JessePhos** was determined to be the most effective ligand to date.[53] Further studies involving this catalytic system reveled various air, moisture and thermally stable single component precatalysts containing both palladium and **JessePhos** in differing ligand to metal ratios and oxidation states (Figure 2.28, bottom).[54]

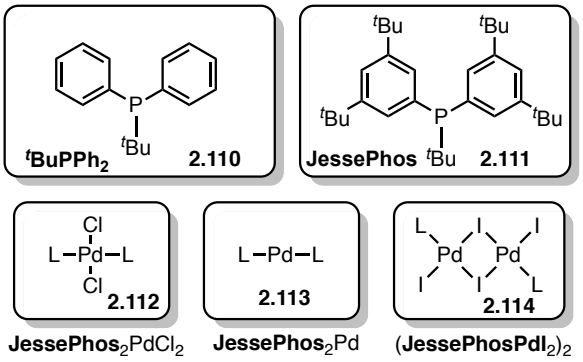

Figure 2.28 Optimal Ligands and Catalysts for the Bimolecular Silyl-Heck Reaction

2.5.1 Investigation of Silyl Iodides

For the initial exploration of an intramolecular silyl-Heck reaction, we sought to design a substrate that closely resembles our bimolecular reactions, which utilize trimethylsilyl iodide and a simple terminal alkene. To this end, 4-pentenyldimethyl iodosilane (**2.116**) was identified as an ideal substrate due to minimal steric and electronic bias. However, due to the harsh nature of the silyl iodide synthesis,[55] compound **2.116** was synthesized in only 80% purity (the remainder being inseparable internal alkene isomers).

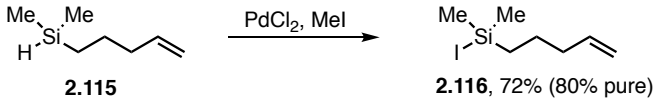

2.115 **2.116**, 72% (80% pure)

Figure 2.29 Synthesis of Silyl Iodide Substrate

Compound **2.116** can undergo either a 6-endo (**2.117** or **2.118**) or 5-exo (**2.119**) cyclization (Figure 2.30, top); however, based on the intramolecular Heck precedence, the 5-exo product **2.119** was expected to predominate since there is no significant electronic contribution from the tethered alkene. Under modified silyl-Heck reaction conditions[53b] (Pd_2dba_3/**JessePhos**), compound **2.116** underwent cyclization in 61% yield forming exclusively the 6-endo products **2.117** and **2.118** in a 1:1 ratio. Surprisingly, no 5-exo product (**2.119**) was detected.

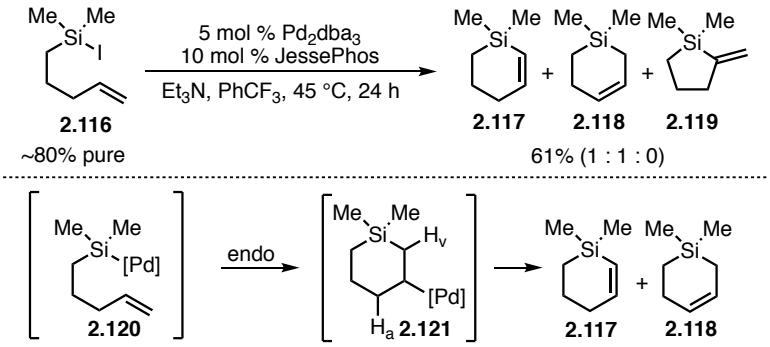

Figure 2.30 First Example of a 6-Endo Intramolecular Silyl-Heck Reaction

The mechanism of this reaction likely proceeds *via* our proposed mechanism for the intermolecular silyl-Heck reaction. After oxidative addition of the palladium (0) complex to compound 2.116, exclusive endo cyclization occurs to form intermediate **2.121**, followed by β-hydride elimination. The mixture of vinyl and allyl products can be explained from β-hydride elimination with both H_v or H_a. In contrast, the bimolecular reaction has a large preference for formation of allyl silanes in all cases where it is possible.[2, 53a, 56]

In all reported examples of silyl-Heck and related reactions,[57] silicon exclusively prefers silylation at the terminal carbon of the alkene. The exclusive endo cyclization observed with **2.116** is likely due to this inherent preference for silylation of the terminal position. This selectivity likely stems from the disfavored steric interaction between the large groups on the silicon atom and the substitution of the alkene. The strong preference for terminal silylation overrides the geometric alignment that typically favors 5-exo cyclizations in the intramolecular Heck reaction.[37, 39c]

Due to the volatility of the products derived from **2.116**, as well as their similar structure, purification of the geometrical isomers required preparatory gas

chromatography, leading to greatly reduced isolated yields of **2.117** and **2.118** (ca 12% and 9% respectively). To facilitate the investigation of the intramolecular silyl-Heck reaction, silyl electrophiles with groups larger than dimethyl were desired. Unfortunately, the synthesis of diphenyl silyl iodide did not proceed without significant alkene isomerization (Figure 2.31) and therefore, other silicon electrophiles were considered.

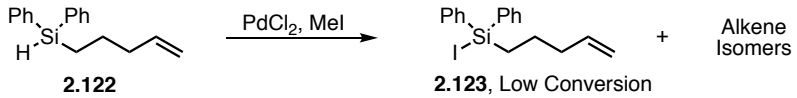

Figure 2.31 Low Conversion of Diphenylsilanes

2.5.2 Investigation of Silyl Triflates

We have previously shown that with the use of silyl-triflates, groups larger than methyl can be tolerated on silicon in the bimolecular reaction (see Chapter 1).[58] We saw this as an opportunity to both change the electrophilic silane as well as modify the silicon scaffold. We proposed that compound **2.124** would have the right combination of stability and reactivity to be a model system. Additionally, we were interested the effect different substitution on silicon would have on the cyclization pattern.

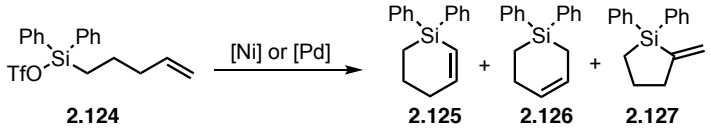

Figure 2.32 Proposed Silyl-Triflate Substrate for the Intramolecular Silyl-Heck Reaction

I began by finding a practical way to synthesize the compound **2.124**. The simplest method we envisioned was the slow addition silanol **2.128** to a cooled solution of trifluoromethanesulfonic (triflic) anhydride (Figure 2.33, top). This is a common method for the synthesis of aryl triflates from phenols.[59] Unfortunately, none of the desired **2.124** was detected. However, we observed full conversion to the disiloxane **2.129**, presumably through rapid attack of free silanol **2.128** to the newly formed silyl-triflate (**2.124**). Silyl-triflates are significantly more electrophilic than the analogous aryl or alkyl triflates thus making this a difficult route for the formation of **2.124**.

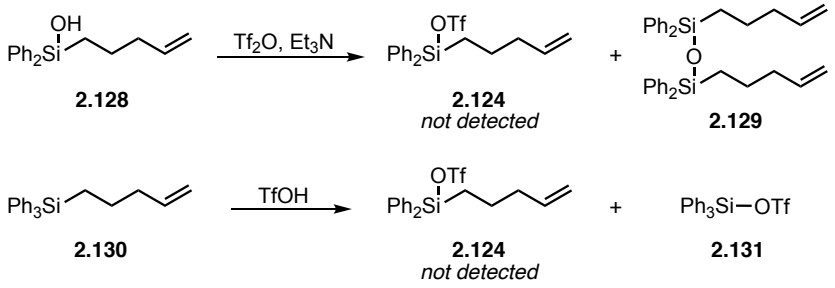

Figure 2.33 Early Attempts to Synthesize Silyl-Triflate Substrate

Many of the non-commercial silyl triflates, used as substrates in our nickel catalyzed reaction, were synthesize *via* protodearylation of phenyl silanes (Figure 2.33, bottom).[60] Subjecting **2.130** to 1.0 equivalents of triflic acid only resulted in dealkylation of the pendant alkene to form triphenyl silyl triflate (**2.131**). This demonstrates the higher reactivity of alkenes over arenes in the presence of a strong acid such as triflic acid.

Allyl silanes have been shown to undergo deallylation in the presence of triflic acid,[61] and are considered to be more reactive that phenylsilanes.[60b, 62] Additionally,

since allyl silanes are considered to be more nucleophilic then carbon analogs, we hypothesized that the desired deallylation should be compatible in the presence of the tethered alkene. Unfortunately, when the reaction is run at room temperature with 1.0 equivalents of triflic acid mixtures of products are obtained (Figure 2.34). While the majority of the product mixture is the desired product (**2.124**), about 30% of the dealkylation product (**2.133**) was formed. Cooling the reaction down resulted in incomplete conversion of **2.132**, however, 1.5 equivalents of triflic acid at –78 °C resulted in full conversion to the desired product **2.124**.

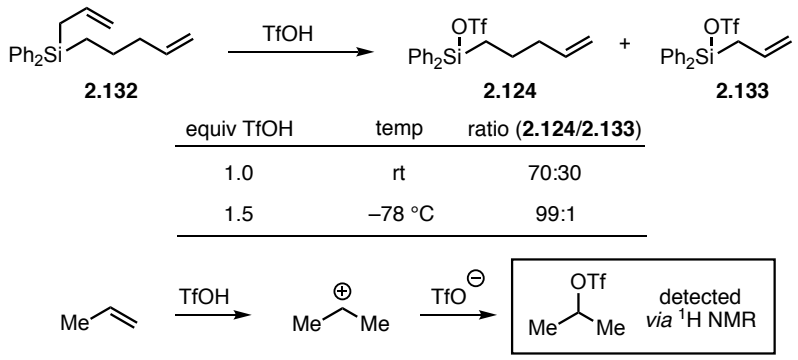

Figure 2.34 Optimal Synthesis of Diphenyl Silyl-Triflate Substrate **2.124**

Upon a more thorough examination of the crude reaction mixture, isopropyl triflate was detected in the solution before the removal of solvent. At cooler temperatures, the propene generated from the deallylation reaction remains in solution. After protonation with triflic acid the resulting carbocation is trapped with the triflate anion to form isopropyl triflate. Unfortunately, this side reaction consumes varying amounts of triflic acid making this a very sensitive and irreproducible reaction.

Nonetheless, with **2.124** in hand, we were able to explore the reactivity of silyl triflates in this intramolecular reaction.

With clean substrate in hand, I was able to begin investigating the use of silyl triflates for this transformation. Initially, substrate **2.124** was subjected to the nickel catalyzed conditions shown to be superior for triflate coupling (Figure 2.35, top).[58] Similar to the cyclization of silyl iodide **2.116**, only 6-endo products were observed by ^{1}H NMR spectroscopy as a 1:1 ratio. Unfortunately, **2.125** and **2.126** were only formed in a combined 16%. The remaining mass balance consisted of various internal alkene isomers of the starting material. While these conditions were optimal for styrene derivatives, alkenes with allylic protons are problematic due to this undesired isomerization pathway.

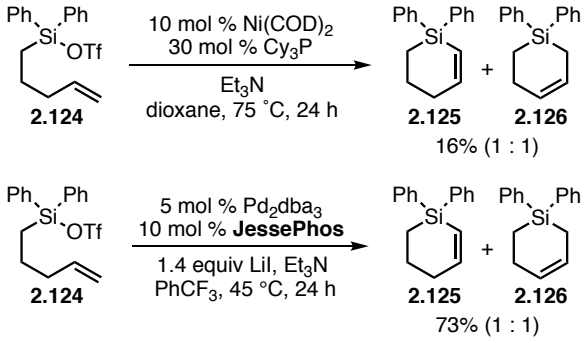

Figure 2.35 Determining Catalytic Conditions for the Cyclization of Silyl-Triflate **2.124**

I sought to investigate the use of palladium in this reaction, because palladium in combination with **JessePhos** results in no isomerization of aliphatic alkenes. However, to date, there are no examples of silicon-triflate bond activation using palladium, therefore an *in situ* formation of a silyl iodide is necessary for the reaction to proceed.

Switching to a palladium catalysis with stoichiometric lithium iodide (LiI), moderate yields of **2.125** and **2.126** can be obtained. Again, these products are formed as an equal molar ratio of allylic and vinylic isomers. Products **2.125** and **2.126** were isolated in a combined 73% yield and analytically separated using silver nitrate ($AgNO_3$) impregnated silica gel. Once separated, the tentatively assigned structures were confirmed. As further conformation, a portion of the isolated mixture of **2.125** and **2.126** was hydrogenated to demonstrate convergence to a single reduced product **2.134** (Figure 2.36).[63]

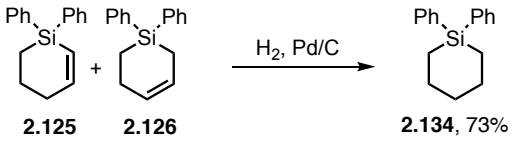

Figure 2.36 Hydrogenation of Product Mixture to a Single Saturated Product

Moving forward, we wanted to synthesize multiple tether lengths and internal alkene isomers to explore the reactivity and selectivity of this reaction. For a rigorous investigation, clean and isomerically pure alkenes are required. However, these substrates are quite labile and difficult to handle and purify. As mentioned above, I had to optimize specific conditions to form silyl triflate **2.124**. Even with these conditions, the formation of **2.124** was inconsistent due to varying concentrations of propene mopping up the triflic acid generated in the reaction. Moreover, when switching to other substrate precursors, especially ones containing internal alkenes, which are slightly more electron rich, results in alkene isomerization and decomposition. A thorough study

of this reaction would require a facile, mild, and general method for the synthesis of a variety of intramolecular substrates.

2.5.3 Investigation of Silyl Chlorides

We recognized that silyl chlorides provide an alternative class of silyl electrophiles capable of forming silyl iodides *in situ*.[64] Additionally, silyl chlorides can be formed under much milder reaction conditions, allowing for higher yields and purity of starting material. Using 2.0 equivalents $CuCl_2$ and catalytic CuI, silanes can be converted in to chlorosilanes under mild conditions (Figure 2.37).[65] Because of the ease of synthesis, both diphenyl (**2.135**) and methylphenyl (**2.137**) chlorosilanes were synthesized and examined.

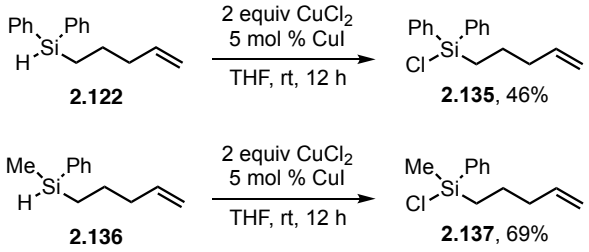

Figure 2.37 Synthesis of Silyl Chloride Substrates

Both **2.135** and **2.137** were subjected to similar reaction conditions to those discussed earlier. We found that the addition of super stoichiometric LiI (1.4 equiv), as an iodide source for silicon halogen exchange, is still required for the reaction to proceed (Figure 2.38).[52, 64]

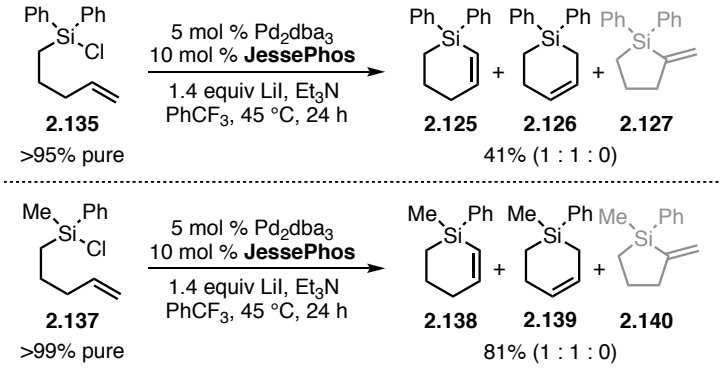

Figure 2.38 Cyclization of Silyl Chloride Substrates

Both compounds cyclized in an analogous manner to **2.116** and **2.124**, resulting in exclusively endo ring closure with a 1:1 ratio of vinylic and allylic isomers. Silyl chloride **2.135** provided a combined 41% yield of products **2.125** and **2.126**. However, compound **2.137** was much more reactive and yielded **2.138** and **2.139** in 81% combined yield. In both cases, no exo-product (**2.127** or **2.140**) was observed. These results suggest that while steric bulk of the silicon group can affect overall rate, the selectivity for cyclization and β-hydride elimination is not influenced.

We have reported the use of single-component pre-ligated palladium precatalysts with JessePhos.[66] Use of these precatalysts both simplify reaction setup and, on average, lead to higher and more reproducible yields. Using the single component catalyst (**JessePhos**)$_2$PdCl$_2$, methyl(phenyl)silane **2.137** cyclized to yield products **2.138** and **2.139** in 88% combined yield. Therefore, the methyl(phenyl)silyl chloride scaffold in combination with catalytic (**JessePhos**)$_2$PdCl$_2$ was chosen to further explore the scope of the intermolecular silyl-Heck reaction.

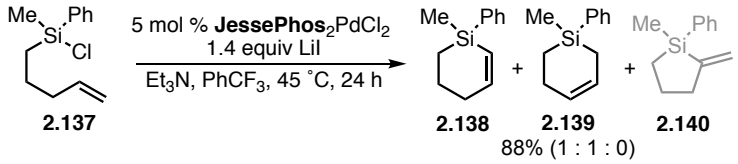

Figure 2.39 Intramolecular Cyclization with Single-Component Precatalyst

2.6 Scope and Reactivity of the Intramolecular Silyl-Heck Reaction

After establishing a general and mild route for the synthesis of silyl chlorides, I sought to explore the effects of alkyl chain length and alkene substitution. We wanted to determine if the exclusive endo-ring closure was limited to the pentenyl tether we have explored so far or if it is general to different ring sizes and alkene substitutions. Various chlorosilanes were synthesized using a simple two-step procedure (Figure 2.40). Using commercially available methylphenylchlorosilane and the corresponding Grignard reagent in conjunction with Kunai's chlorination reaction, rapid access to all desired chlorosilane alkene isomers is possible with good yields and purities.[65]

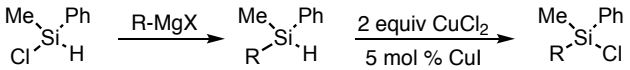

Figure 2.40 General Synthetic Route to Chlorosilane Reagents

2.6.1 Exploring the Chain Length

First, we examined a one-carbon shorter analog under the same reaction conditions (Figure 2.41). The butenyl substrate **2.141** provided a comparable yield of 5-endo products **2.142** and **2.143**. Similarly, in this case, both allyl and vinyl isomers were obtained and no exo product (**2.144**) was observed. Baldwin suggested that 5-endo trig cyclizations are disfavored due to the distortion required for orbital overlap.[49] However,

5-endo products have been observed in Heck reactions[50, 67] to form indoles and related compounds, although they are thought to react through 6-membered palladacycles intermediates.[50, 68]

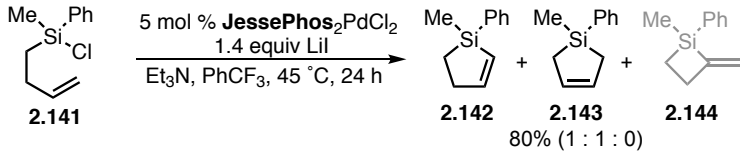

Figure 2.41 5-Endo Cyclization of **2.141**

No 4-exo product was observed presumably because the formation of siletane is highly disfavored due to ring strain. Attempting to favor siletane formation as the endo product, allyl(methylphenyl)chlorosilane provided no cyclized product, with only unreacted or isomerized starting material remaining even at elevated temperatures (Figure 2.42).

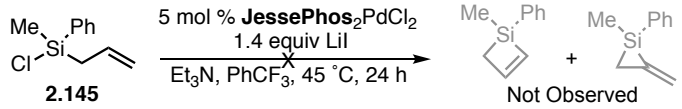

Figure 2.42 Limited Reactivity of Allyl(methylphenyl)chlorosilane (**2.145**)

We next sought to examine longer alkene tether lengths. When **2.146** was subjected to the reaction conditions, products **2.148** and **2.149** were obtained in 31% combined yield as a 3:1 mixture.

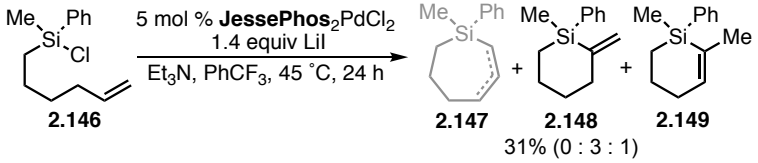

Figure 2.43 6-Exo Cyclization of **2.146**

Both products are formed *via* a 6-exo cyclization and no 7-endo products (**2.147**) were detected. The direct product of this reaction (**2.148**) can slowly isomerize to the more stable trisubstituted alkene product **2.149** throughout the reaction. This is the first example of an exo-cyclization *via* a silyl-Heck reaction and more significantly, this is the first example of the internal silylation of an alkene using this method. The low yield and reversed selectivity demonstrates the difficulty associated with forming 7-membered rings *via* this method. Interestingly, 7-endo Heck-cyclizations are common and can be favored over 6-exo under certain reaction conditions,[45b, 69] though most examples are influenced electronically[45a, 45f, 46b] or sterically.[45d, 45h]

Unfortunately, attempting to drive larger ring cyclization with the 7-carbon alkene tether failed to react, providing no observable quantities of 7- or 8-membered silacycles (Figure 2.45).

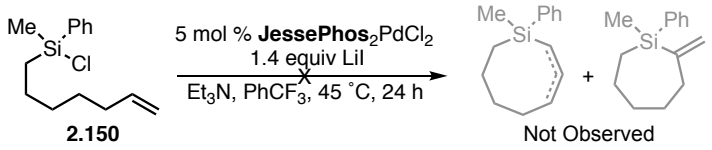

Figure 2.44 Limited Reactivity of **2.150**

2.6.2 Reaction of 1,1-Disubstitued Alkenes

After determining the range of reactive chain lengths, we next turned our attention to studying the effects of substitution on the tethered alkene. Even simple disubstituted alkenes have never participated in the bimolecular silyl-Heck reaction and are poor substrates for dehydrogenative silylation.[70] This is presumably due to the disfavored steric interaction between the silicon and the extra substitution on the alkene. A similar limitation is observed in the Heck reaction wherein rates of reactivity decrease with increasing olefin substitution.[51] The intramolecular Heck reaction; however, can easily tolerate tri- and even tetrasubstituted alkenes with good yields, excellent diastereoselectivity,[34] and enantioselectivity.[39a, 39b]

A silyl-Heck reaction with disubstituted alkenes would be of great value because it would give access to more complex silicon containing products, greatly expanding this methods utility. Considering the precedent of intramolecular Heck reactions, we saw the intramolecular silyl-Heck reaction as an opportunity to examine the possibility of internal alkene silylation. We began with the simple 1,1-disubstituted terminal alkene **2.151** (Figure 2.45). While this is still a terminal alkene, we have seen no reactivity with *gem*-disubstituted olefins in any bimolecular reactions.

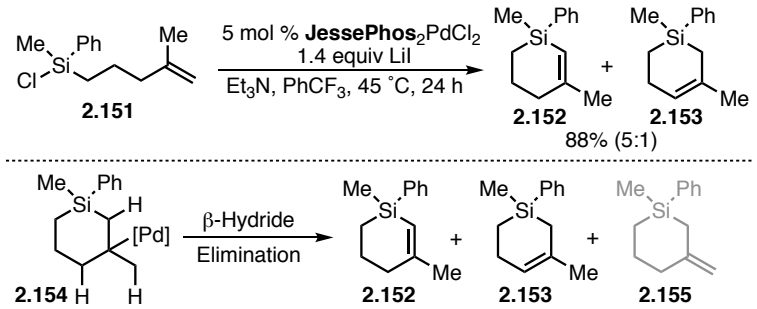

Figure 2.45 Intramolecular Cyclization of a 1,1-Disubstituted Tethered Alkene

Subjecting alkene **2.151** to the reaction conditions gave rise to products **2.152** and **2.153** in a combined 88% yield as a 5:1 vinyl to allyl ratio. This is the first example of the silylation of a disubstituted alkene using a silyl-Heck reaction. Consistent with the previous intramolecular cases, the reaction proceeds with exclusive 6-endo selectivity over 5-exo. However, contrary to the previous cases, there is a preference for the vinyl isomer over the allyl isomers. Intermediate **2.154** contains three accessible hydrogen atoms for which β-hydride elimination could proceed but only the vinyl product is favored. The preference for vinyl silane in this case is interesting because there is no preference in the absence of the exocyclic methyl and in the bimolecular case there is a strong empirical preference for formation of the allylic product isomer.

2.6.3 Reaction of *E*-Alkene

Next, we investigated the reactivity of internal alkenes (Figure 2.46). We began with the methyl-substituted *E*-alkene **2.156**. We were particularly interested in the reactivity of this substrate because an endo cyclization should result in selective allyl silane formation (**2.158**). Under the same mechanistic hypothesis, a *syn*-migratory insertion would lead to intermediate **2.157**. With restricted bond rotation due to the geometry constraints of the ring, the vinylic proton cannot properly align with palladium for β-hydride elimination. Furthermore, if **2.156** undergoes a 5-exo cyclization, a single isomer of **2.161** should be formed.

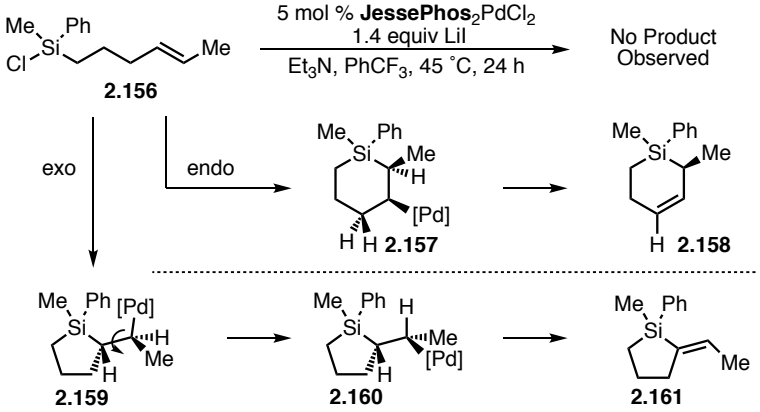

Figure 2.46 Limited Reactivity of *E*-Methyl Tethered Alkene **2.156**

Unfortunately, compound **2.156** failed to yield more than trace product, even under elevated temperatures and reaction times. We attribute the lack of reactivity due to steric congestion during the migratory insertion between the groups on silicon and the methyl group of the *E*-alkene.

2.6.4 Reaction of *Z*-Alkenes

Lastly, we investigated the reactivity of tethered *Z*-alkenes beginning with the methyl-substituted **2.162**. When subjected to the reaction conditions, compound **2.162** cyclized to form product **2.163** in 18 % yield.

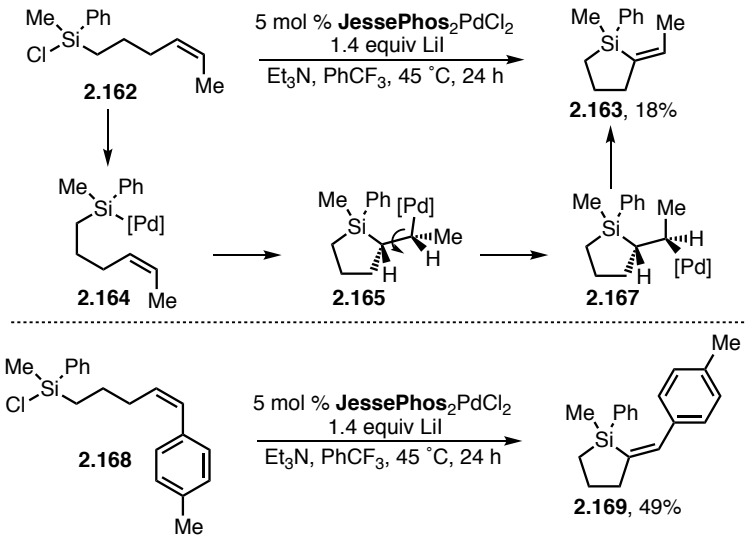

Figure 2.47 Intramolecular Cyclization of *Z*-Substituted Tethered Alkenes

While this yield is low, this result is significant because it demonstrates for the first time, internal alkenes participating in the silyl-Heck reaction. Additionally, only a single alkene regioisomer results with high control of alkene stereochemistry. In the absence of a terminal carbon to silylate, both ends of the alkene have similar steric demands, therefore the conformational considerations dominate the transition state, an effect commonly observed in the intramolecular Heck reaction of 5- and 6-membered rings.[3a]

The selective formation of the *Z*-alkene product can be explained *via* oxidative addition into the Si-X bond (**2.164**), followed by *syn*-facial 5-exo migratory insertion (**2.165**) and rotation about the C-C bond (**2.167**). A *syn*-periplanar β-hydride elimination would then result in the observed *Z*-product **2.163**. Similarly, using the tethered *Z*-styrene derivative **2.168**, the product **2.169** was obtained in 49% yield as a single *Z*-

isomer. These results suggest that there is no alkene isomerization with these substrates which is contrary to the previous examples.

2.7 Conclusion

In conclusion, the intramolecular silyl-Heck reaction is an effective way to synthesize 5- and 6-membered unsaturated silicon containing rings. In nearly all cases, terminal alkenes exclusively cyclize with endo selectivity presumably driven by the strong steric preference for silicon to go to the less hindered terminal position. Interestingly, with no terminal position to silylate, a tethered *Z*-olefin prefers exo cyclization forming a stereodefined exocyclic alkene. For the first time, both 1,1 and 1,2-disubstituted alkenes have shown reactivity in this reaction and cyclic, trisubstituted vinyl silanes can be synthesized from disubstituted olefins.

2.8 Experimental Details

2.8.1 General Experimental Details

Diethyl ether (Et_2O), tetrahydrofuran (THF), hexanes, and dichloromethane (DCM) were dried on alumina according to published procedures.[71] Trifluorotoluene ($PhCF_3$) was purchased from Sigma Aldrich in an anhydrous septum sealed bottle, transferred to a Straus flask by cannula and sparged with nitrogen for 15 minutes. Magnesium turnings (Mg), copper (II) chloride ($CuCl_2$), copper (I) iodide (CuI), 2,6-di-tert-butyl-4-methylpyridine, and iodomethane, were purchased from commercial suppliers and used as received. Dimethylchlorosilane, diphenylchlorosilane, methylphenylchlorosilane and allyldiphenylchlorosilane were purchased from Gelest and used as received. Trifluoromethanesulfonic acid (TfOH) was distilled under vacuum and stored under nitrogen in a high-pressure reaction vessel. Non-commercial

alkyl bromides were prepared from the corresponding alcohols using a 2-step published procedure.[72] Tris(dibenzylideneacetone)dipalladium(0) [$Pd_2(dba)_3$] was purchased from Aldrich or Strem and used as received. Bis(3,5-di-*tert*-butylphenyl)(*tert*-butyl)phosphine (JessePhos)[53a] and the single component catalyst $(JessePhos)_2PdCl_2$[66] were prepared according to published procedures. Vials used in the glovebox were dried in a gravity oven at 140 °C for a minimum of 12 h, transferred into the glovebox hot, and then stored at rt in the glovebox prior to use. All other glassware was flame-dried under vacuum prior to use. All reactions (0.25 - 1.0 mmol) were run in a nitrogen-filled glovebox and heated using an aluminum block on a magnetic stir plate. All yields were determined using ^1H NMR using 1,3,5-trimethoxybenzene as an internal standard and isolated to confirm yield.

2.8.2 Instrumentation and Chromatography

400 MHz ^1H, 101 MHz ^{13}C and 376 MHz ^{19}F spectra were obtained on a 400 MHz FT-NMR spectrometer equipped with a Bruker CryoPlatform. 600 MHz ^1H, 151 MHz ^{13}C, and 193 MHz ^{11}B spectra were obtained on a 600 MHz FT-NMR spectrometer equipped with a Bruker SMART probe. All samples were analyzed in the indicated deutero-solvent and were recorded at ambient temperatures. All chemical shifts are reported in ppm. ^1H NMR spectra were calibrated using the residual protio-signal in deutero-solvents as a standard. ^{13}C NMR spectra were calibrated using the deutero-solvent as a standard. IR spectra were recorded on a Nicolet Magma-IR 560 FT-IR spectrometer as thin films on KBr plates. High resolution MS data was obtained on a Thermo Q-Exactive Orbitrap using electrospray ionization (ESI), or a Waters GCT Premier spectrometer using chemical ionization (CI) or liquid injection field desorption ionization (LIFDI). Column chromatography was performed with 40-63 μm silica gel

with the eluent reported in parentheses. Analytical thin-layer chromatography (TLC) was performed on pre-coated glass plates and visualized by UV or by staining $KMnO_4$.

2.8.3 Synthesis of Silane Precursors

2.8.3.1 General Procedure A

To an oven dried 3-neck flask fitted with a condenser, magnesium turnings (1.2-1.4 equiv) were added, placed under vacuum while hot, and allowed to cool under vacuum. Once the glassware was at rt, the vessel was backfilled with nitrogen and the minimum amount of anhydrous diethyl ether needed to cover the magnesium turnings was added, followed by roughly 5% of the corresponding alkyl bromide. If the Grignard formation failed to initiate after a couple of minutes, a catalytic amount (ca. 3 μL) of 1,2-dibromoethane was added. Once the solution began to self-reflux the remaining diethyl ether and alkyl bromide were slowly added as needed to maintain a gentle reflux. The reaction was refluxed for 1 hour (45 °C). The chlorosilane (1.0 equiv) in anhydrous diethyl ether (1 M) was added *via* syringe to a separate flame-dried round bottom flask with septum and stir bar under nitrogen at rt. The Grignard was transferred to the round bottom flask containing the silyl chloride *via* syringe using a dropwise addition, and the reaction was stirred at rt overnight. The reaction was cooled with an ice/water bath and slowly quenched with water. The mixture was extracted with diethyl ether three times and the combined organic layers were rinsed with brine. The organic extract was dried over $MgSO_4$, filtered, concentrated to a crude residue and purified by distillation or flash silica gel chromatography to give the silane product.

2.8.3.2 Characterization Data

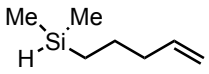

(**S2.1**) According to general procedure A, the Grignard formed from 5-bromopent-1-ene (16 mL of a 1.5 M solution in Et_2O, 24.0 mmol) was reacted with dimethylchlorosilane (3.2 mL, 28.8 mmol) to give 2.23 g (73%) of **S2.1** as a clear oil after distillation (80 °C/220 mtorr). ^{1}H NMR (400 MHz, $CDCl_3$) δ 5.80 (ddt, *J* = 16.9, 10.1, 6.7 Hz, 1H), 5.13 – 4.77 (m, 2H), 3.84 (dt, *J* = 7.1, 3.5 Hz, 1H), 2.16 – 1.91 (m, 2H), 1.51 – 1.35 (m, 2H), 0.69 – 0.50 (m, 2H), 0.06 (d, *J* = 3.7 Hz, 6H); ^{13}C NMR (101 MHz, $CDCl_3$) δ 139.04, 114.65, 37.38, 23.98, 13.84, -4.31; FTIR (cm^{-1}) 2925, 1256, 1063, 845, 800. HRMS (LIFDI) m/z, calcd for [$C_7H_{16}Si$]: 128.1021; found: 128.0997.

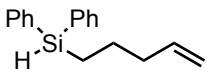

(**S2.2**) According to general procedure A, the Grignard formed from 5-bromo-1-pentene (16.2 mL of a 2 M solution in Et_2O, 32.4 mmol), was reacted with diphenylchlorosilane (5.0 mL, 27 mmol) in 30 mL Et_2O to give 5.8 g (85%) of **S2.2** as a clear oil after distillation (120 °C/150 mtorr). ^{1}H NMR (400 MHz, $CDCl_3$) δ 7.58 – 7.53 (m, 4H), 7.41 – 7.34 (m, 6H), 5.77 (ddt, *J* = 17.0, 10.2, 6.7 Hz, 1H), 5.04 – 4.91 (m, 2H), 4.86 (t, *J* = 3.7 Hz, 1H), 2.19 – 2.04 (m, 2H), 1.63 – 1.50 (m, 2H), 1.21 – 1.10 (m, 2H); ^{13}C NMR (101 MHz, $CDCl_3$) δ 138.6, 135.3, 134.6, 129.7, 128.1, 115.0, 37.3, 23.9, 11.8; FTIR (cm^{-1}) 3068, 2924, 2117, 1428, 1117, 808, 699. HRMS (EI) m/z, calcd for [$C_{17}H_{20}Si$]: 252.1334; found: 252.1349.

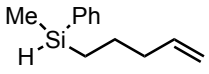

(**S2.3**) According to general procedure A, the Grignard formed from 5-bromo-1-pentene (30 ml of a 2 M solution in Et_2O, 60 mmol) was reacted with methylphenylchlorosilane (7.8 g, 50 mmol) in 50 mL Et_2O to give 7.4 g (92%) of **S2.3** as a clear oil after distillation (77 °C/1.8 torr). ^{1}H NMR (600 MHz,

$CDCl_3$) δ 7.63 – 7.48 (m, 2H), 7.48 – 7.30 (m, 3H), 5.78 (ddt, *J* = 17.0, 10.2, 6.7 Hz, 1H), 5.07 – 4.85 (m, 2H), 4.36 (q, *J* = 3.6 Hz, 1H), 2.25 – 1.96 (m, 2H), 1.55 – 1.40 (m, 2H), 0.86 (dtd, *J* = 13.6, 8.2, 3.4 Hz, 2H), 0.34 (d, *J* = 3.8 Hz, 3H); ^{13}C NMR (151 MHz, $CDCl_3$) δ 138.7, 136.6, 134.3, 129.2, 127.9, 114.7, 37.2, 23.8, 12.9, -5.7; FTIR (cm^{-1}) 3069, 2922, 2114, 1428, 1251, 1115, 878, 700. HRMS (EI) m/z, calcd for [$C_{12}H_{18}Si$]: 190.1178; found: 190.1201.

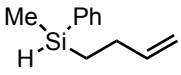

(**S2.4**) According to general procedure A, the Grignard formed from 4-bromo-1-butene (16.8 mL of a 2.5 M solution in Et_2O, 42 mmol) was reacted with methylphenylchlorosilane (4.8 g, 30 mmol) to give 3.7 g (68%) of **S2.4** as a clear oil after distillation (80 °C/2 torr). ^{1}H NMR (400 MHz, $CDCl_3$) δ 7.60 – 7.49 (m, 2H), 7.43 – 7.32 (m, 3H), 5.88 (ddt, *J* = 16.5, 10.1, 6.3 Hz, 1H), 5.07 – 4.84 (m, 2H), 4.38 (q, *J* = 3.6 Hz, 1H), 2.22 – 2.06 (m, 2H), 1.08 – 0.84 (m, 2H), 0.36 (d, *J* = 3.8 Hz, 3H); ^{13}C NMR (101 MHz, $CDCl_3$) δ 140.9, 136.3, 134.4, 129.3, 127.9, 113.2, 28.4, 12.5, -5.7; FTIR (cm^{-1}) 3069, 2915, 2117, 1639, 1428, 1252, 1116, 833. HRMS (EI) m/z, calcd for [$C_{11}H_{16}Si$]: 176.1021; found: 176.1013.

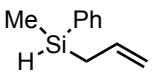

(**S2.5**) Using a modification of general procedure A, the commercial allyl magnesium bromide (23 mL of a 1.7 M solution in Et_2O), was reacted with methylphenylchlorosilane (5.0 g, 32 mmol) to give 4.4 g (85%) of **S2.5** as a clear oil after distillation (68 °C/2 torr). ^{1}H NMR (400 MHz, $CDCl_3$) δ 7.62 – 7.52 (m, 2H), 7.46 – 7.33 (m, 3H), 5.82 (ddt, *J* = 16.9, 10.1, 8.0 Hz, 1H), 4.97 – 4.84 (m, 2H), 4.36 (q, *J* = 3.5 Hz, 1H), 1.93 – 1.76 (m, 2H), 0.37 (d, *J* = 3.7 Hz, 3H); ^{13}C NMR (101 MHz, $CDCl_3$) δ 135.6, 134.4, 134.2, 129.5, 127.9, 114.1, 21.1, -6.2; FTIR (cm^{-1}) 3070, 2122,

1630, 1428, 1116, 879, 709. HRMS (EI) m/z, calcd for [$C_{10}H_{14}Si$]: 162.0865; found: 162.0882.

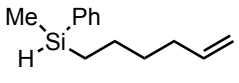

(**S2.6**) According to general procedure A, the Grignard formed from 6-bromo-1-hexene (21.5 mL of a 1.5 M solution in Et_2O, 32.3 mmol) was reacted with methylphenylchlorosilane (3.5 g, 23 mmol) to give 4.1 g (89%) of **S2.6** as a clear oil after distillation (80 °C/1.4 torr). ^{1}H NMR (400 MHz, $CDCl_3$) δ 7.58 – 7.51 (m, 2H), 7.40 – 7.32 (m, 3H), 5.79 (ddt, *J* = 16.9, 10.2, 6.7 Hz, 1H), 5.05 – 4.86 (m, 2H), 4.34 (q, *J* = 3.6 Hz, 1H), 2.13 – 1.95 (m, 2H), 1.51 – 1.34 (m, 4H), 1.01 – 0.72 (m, 2H), 0.33 (d, *J* = 3.8 Hz, 3H); ^{13}C NMR (101 MHz, $CDCl_3$) δ 139.1, 136.8, 134.4, 129.3, 128.0, 114.4, 33.6, 32.5, 24.0, 13.3, -5.5; FTIR (cm^{-1}) 2924, 2115, 878, 700. HRMS (EI) m/z, calcd for [$C_{13}H_{20}Si$]: 204.1334; found: 204.1351.

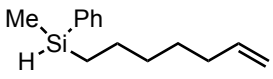

(**S2.7**) According to general procedure A, the Grignard formed from 7-Bromo-1-heptene (12 mL of a 1.5 M solution in Et_2O) was reacted with methylphenylchlorosilane (2.3 g, 15 mmol) to give 2.3 g (69%) of **S2.7** as a clear oil after distillation (60 °C/150 mtorr). ^{1}H NMR (600 MHz, $CDCl_3$) δ 7.72 – 7.44 (m, 2H), 7.44 – 7.31 (m, 3H), 5.80 (ddt, *J* = 17.0, 10.2, 6.7 Hz, 1H), 5.01 – 4.89 (m, 2H), 4.34 (q, *J* = 3.6 Hz, 1H), 2.07 – 1.97 (m, 2H), 1.45 – 1.31 (m, 6H), 0.93 – 0.75 (m, 2H), 0.33 (d, *J* = 3.8 Hz, 3H); ^{13}C NMR (151 MHz, $CDCl_3$) δ 139.3, 136.9, 134.4, 129.3, 128.0, 114.3, 33.8, 32.8, 28.7, 24.3, 13.5, -5.5; FTIR (cm^{-1}) 2924, 2114, 1115, 878, 700. HRMS (EI) m/z, calcd for [$C_{14}H_{22}Si$]: 218.1491; found: 218.1507.

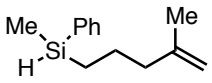

(**S2.8**) According to general procedure A, the Grignard formed from

5-bromo-2-methylpent-1-ene (16 mL of a 1.5 M solution in Et_2O, 24 mmol) was reacted with methylphenylchlorosilane (3.0 g, 20 mmol) to give 1.8 g (60%) of **S2.8** as a clear oil after distillation (50 °C/200 mtorr). ^{1}H NMR (600 MHz, $CDCl_3$) δ 7.57 – 7.49 (m, 2H), 7.42 – 7.31 (m, 3H), 4.76 – 4.58 (m, 2H), 4.36 (q, *J* = 3.6 Hz, 1H), 2.05 (t, *J* = 7.5 Hz, 2H), 1.68 (s, 3H), 1.56 – 1.49 (m, 2H), 0.87 – 0.77 (m, 2H), 0.34 (d, *J* = 3.8 Hz, 3H); ^{13}C NMR (151 MHz, $CDCl_3$) δ 145.8, 136.7, 134.4, 129.3, 128.0, 110.3, 41.3, 22.5, 22.4, 13.1, -5.5; FTIR (cm^{-1}) 3070, 2929, 2115, 1116, 879, 700. HRMS (EI) m/z, calcd for [$C_{13}H_{20}Si$]: 204.1334; found: 204.1338.

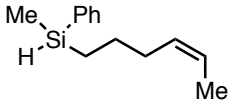

(**S2.9**) According to general procedure A, the Grignard from using (*Z*)-6-iodohex-2-ene (40 mL of a 1.5 M solution in Et_2O, 60 mmol, 1.2 equiv) was reacted with methylphenylchlorosilane (7.8 g, 50 mmol) to give 8.9 g (87%) of **S2.9** as a clear oil after distillation (80 °C/1.5 torr). ^{1}H NMR (400 MHz, $CDCl_3$) δ 7.58 – 7.49 (m, 2H), 7.40 – 7.34 (m, 3H), 5.53 – 5.41 (m, 1H), 5.41 – 5.29 (m, 1H), 4.35 (q, *J* = 3.6 Hz, 1H), 2.13 – 1.99 (m, 2H), 1.59 (d, *J* = 6.7 Hz, 3H), 1.51 – 1.35 (m, 2H), 0.98 – 0.75 (m, 2H), 0.34 (d, *J* = 3.7 Hz, 3H); ^{13}C NMR (101 MHz, $CDCl_3$) δ 136.70, 134.43, 130.45, 129.32, 127.96, 124.27, 30.33, 24.43, 13.19, 13.02, -5.53; FTIR (cm^{-1}) 2921, 2114, 1115, 878, 849, 699. HRMS (EI) m/z, calcd for [$C_{13}H_{20}Si$]: 204.1334; found: 204.1350.

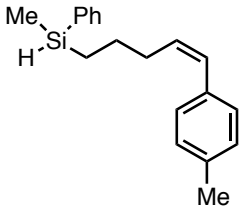

(**S2.10**) According to general procedure A, the Grignard formed from (*Z*)-1-(5-bromopent-1-enyl)-4-methylbenzene, 18 mL of a 1.5 M solution in Et_2O, 27 mmol) reacted with methylphenylchlorosilane (3.0 g, 20 mmol) to give 2.1 g (69%) of

S2.10 as a clear oil after distillation (120 °C/200 mtorr). ^{1}H NMR (600 MHz, $CDCl_3$) δ 7.55 – 7.45 (m, 2H), 7.43 – 7.31 (m, 3H), 7.15 (q, *J* = 7.9 Hz, 4H), 6.38 (d, *J* = 11.7 Hz, 1H), 5.63 – 5.48 (m, 1H), 4.38 – 4.24 (m, 1H), 2.41 – 2.33 (m, 2H), 2.33 (s, 3H), 1.61 – 1.45 (m, 2H), 0.95 – 0.79 (m, 2H), 0.33 (d, *J* = 3.8 Hz, 3H); ^{13}C NMR (151 MHz, $CDCl_3$) δ 136.6, 136.3, 135.0, 134.5, 132.1, 129.4, 129.1, 129.0, 128.8, 128.0, 32.2, 25.0, 21.3, 13.4, -5.5; FTIR (cm^{-1}) 2921, 2113, 1512, 1428, 1115, 878, 838, 701. HRMS (EI) m/z, calcd for [$C_{19}H_{24}Si$]: 280.1647; found: 280.1675.

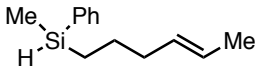

(**S2.11**) According to general procedure A, the Grignard formed from (*E*)-1-Bromo-2-hexene (7 mL of a 1 M solution in Et_2O, 7.0 mmol) was reacted with methylphenylchlorosilane (1.1 g, 7.0 mmol) to give 4.7 g (85%) of **S2.11** as a clear oil after distillation (85 °C/1.7 torr). ^{1}H NMR (400 MHz, $CDCl_3$) δ 7.59 – 7.44 (m, 2H), 7.43 – 7.31 (m, 3H), 5.55 – 5.23 (m, 2H), 4.34 (q, *J* = 3.6 Hz, 1H), 2.09 – 1.92 (m, 2H), 1.64 (dd, *J* = 3.5, 1.3 Hz, 3H), 1.49 – 1.29 (m, 2H), 0.95 – 0.64 (m, 2H), 0.33 (d, *J* = 3.8 Hz, 3H); ^{13}C NMR (101 MHz, $CDCl_3$) δ 136.8, 134.5, 131.3, 129.3, 128.0, 125.3, 36.2, 24.5, 18.1, 13.1, -5.5; FTIR (cm^{-1}) 2920, 2114, 1428, 1251, 1116, 965, 877, 848, 700. HRMS (EI) m/z, calcd for [$C_{13}H_{20}$Si-H]: 203.1256; found: 203.1239.

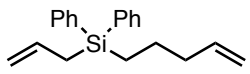

(**S2.12**) According to general procedure A, the Grignard formed from 5-bromo-1-pentene (4.5 mL of a 2 M solution in Et_2O, 9 mmol) was reacted with allyldiphenylchlorosilane (2.0 g, 7.7 mmol) to give 1.9 g (84%) of **S2.12** as a clear oil after flash chromatography (100% petroleum ether). ^{1}H NMR (400 MHz, $CDCl_3$) δ 7.53 – 7.45 (m, 4H), 7.40 – 7.30 (m, 6H), 5.86 – 5.68 (m, 2H),

5.05 – 4.82 (m, 4H), 2.15 – 2.03 (m, 4H), 1.54 – 1.41 (m, 2H), 1.16 – 1.06 (m, 2H); ^{13}C NMR (101 MHz, $CDCl_3$) δ 138.7, 135.6, 135.0, 134.2, 129.4, 127.9, 115.0, 114.5, 37.7, 23.1, 20.6, 11.7; FTIR (cm^{-1}) 3070, 2924, 1428, 1111, 699. HRMS (EI) m/z, calcd for [$C_{20}H_{24}Si$]: 292.1647; found: 292.1667.

2.8.4 Synthesis of Silyl-Iodides and Silyl-Triflates

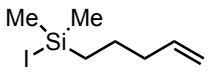

(**2.116**) Following a modified procedure,[55] a flame-dried round bottom flask was fitted with a condenser, septum and stir bar and charged with silane **S2.1** (700 mg, 5.5 mmol, 1.0 equiv), iodomethane (690 μL, 11 mmol, 2.0 equiv), and palladium chloride (29.1 mg, 165 μmol, 1 mol %) the solution was immediately cooled to 0 °C under positive nitrogen pressure, venting a slow stream of gas out of the top of the condenser through an oil bubbler. The reaction was stirred for 15 minutes at 0 °C then at rt for 1-3 h. The release of methane gas was observed by bubble formation around the palladium. The product was then directly distilled under partial vacuum into a flame-dried flask with Teflon screw cap containing copper beads to yield 1.0 g (72%) of **2.116** as a clear oil after distillation (78 °C, 20 torr). The resulting product was determined by ^{1}H NMR to contain 80% of the desired terminal alkene geometry. ^{1}H NMR (400 MHz, C_6D_6) δ = 5.67 (ddt, *J*=17.1, 10.3, 6.9, 1H), 5.04 – 4.93 (m, 2H), 1.92 (q, *J*=6.8, 2H), 1.34 (dt, *J*=15.8, 7.5, 2H), 0.79 – 0.69 (m, 2H), 0.47 (s, 6H); ^{13}C NMR (101 MHz, C_6D_6) δ = 138.4, 115.3, 36.8, 23.9, 19.7, 3.5; HRMS (LIFDI) m/z, calcd for [$C_7H_{15}SiI$]: 253.9988; found: 254.0000.

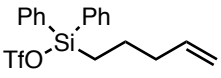

(**2.124**) Following a modified procedure,[61b] allyl silane **S2.12** (292 mg, 1 mmol, 1.0 equiv) and anhydrous dichloromethane (4 mL) were added to a flame dried 25 mL schlenk flask with a stir bar. The mixture was cooled to –

78 °C and trifluoromethansulfonic acid (1.5 mmol, 132 μL, 1.5 equiv) was added dropwise from a glass syringe. The reaction was allowed to stir at –78 °C for 30 minutes. Using a base trap (a ground glass frit adapter filled with solid potassium hydroxide, placed in-between the flask and vacuum manifold), the DCM and excess acid was removed *in vacuo*. Silyl triflate **2.124** was immediately used without further purification. ^{1}H NMR (600 MHz, $CDCl_3$) δ = 7.65 – 7.61 (m, 4H), 7.55 (tt, *J*=7.5, 1.8, 2H), 7.46 (t, *J*=7.6, 4H), 5.74 (ddt, *J*=17.1, 10.3, 6.8, 1H), 5.03 – 4.97 (m, 2H), 2.17 – 2.11 (m, 2H), 1.63 – 1.56 (m, 2H), 1.50 – 1.47 (m, 2H); ^{13}C NMR (151 MHz, $CDCl_3$) δ 137.7, 134.9, 132.0, 129.4, 128.6, 115.8, 36.9, 21.7, 13.3; ^{19}F NMR (565 MHz, $CDCl_3$) δ = -76.53.

2.8.5 Synthesis of Silyl-Chlorides

The chlorosilanes used for this study we all synthesize *via* a method from Kunai.[55] **Note:** Due to moisture sensitivity of the silyl chlorides only ^{1}H and ^{13}C NMR were used for characterization.

2.8.5.1 General Procedure B

In a nitrogen filled glovebox, $CuCl_2$ (2.0 equiv), CuI (0.05 equiv), and THF (0.3-0.5M) were added to a schlenk flask with stir bar and sealed with a rubber septum. The vessel was removed from the glovebox and placed under positive nitrogen pressure and stirred. The silane (1.0 equiv) was added *via* syringe in one portion. The color of the salts changed from brown to light brown/white within 30 min. The reaction was allowed to stir under positive nitrogen pressure overnight. The THF was removed *in vacuo* with a base trap (a ground glass frit adapter filled with solid potassium hydroxide and placed in-between the vacuum and flask). Anhydrous hexanes was added to the

remaining salts and the organic solution was cannula filtered into another schlenk flask. The salts were rinsed twice more with anhydrous hexanes and cannula filtered into the same 100 mL flask. The volitile organics were removed *in vacuo* and the product was distilled into a flame-dried high-pressure vessel with a Teflon screw cap.

2.8.5.2 Characterization Data

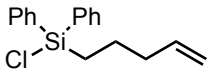

(**2.135**) According to general procedure B, silane **S2.2** (3.0 g, 11.9 mmol), $CuCl_2$ (3.2 g, 23.7 mmol), and CuI (100 mg, 1 mmol) were reacted in THF (25 mL) to give 1.6 g (47%) of **2.135** as a clear, viscous oil after distillation (125 °C/200 mtorr). ^{1}H NMR (600 MHz, $CDCl_3$) δ = 7.63 (dd, *J*=7.9, 1.3, 4H), 7.45 (tt, *J*=7.4, 1.8, 2H), 7.41 (t, *J*=7.2, 4H), 5.76 (ddt, *J*=17.0, 10.3, 6.7, 1H), 5.03 – 4.93 (m, 2H), 2.13 (q, *J*=7.1, 2H), 1.61 (dt, *J*=16.5, 7.5, 2H), 1.39 – 1.33 (m, 2H); ^{13}C NMR (151 MHz, $CDCl_3$) δ = 138.3, 134.5, 133.8, 130.7, 128.3, 115.3, 37.0, 22.5, 16.1.

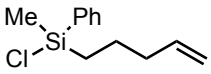

(**2.137**) According to general procedure B, silane **S2.3** (4.0 g, 21 mmol), $CuCl_2$ (5.65 g, 42 mmol), and CuI (190 mg, 1 mmol) were reacted in THF (40 mL) to give 3.27 g (69%) of **2.137** as a clear, viscous oil after distillation (80 °C/700 mtorr). ^{1}H NMR (400 MHz, $CDCl_3$) δ = 7.62 (dd, *J*=7.6, 1.8, 2H), 7.45 – 7.38 (m, 3H), 5.77 (ddt, *J*=17.0, 10.2, 6.7, 1H), 5.03 – 4.95 (m, 2H), 2.11 (q, *J*=7.1, 2H), 1.61 – 1.48 (m, 2H), 1.12 – 1.03 (m, 2H), 0.66 (s, 3H); ^{13}C NMR (101 MHz, $CDCl_3$) δ 138.4, 135.5, 133.5, 130.5, 128.2, 115.3, 37.0, 22.5, 17.6, 0.5.

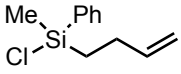

(**2.141**) According to general procedure B, silane **S2.4** (2.0 g, 11.2 mmol), $CuCl_2$ (3.04 g, 22.4 mmol), and CuI (190 mg, 1 mmol) were reacted in THF (20 mL) to give 1.34 g (57%) of **2.141** as a clear, viscous oil after

distillation (55 °C/150 mtorr). ^{1}H NMR (600 MHz, $CDCl_3$) δ = 7.68 – 7.58 (m, 2H), 7.48 – 7.37 (m, 3H), 5.88 (ddt, *J*=16.5, 10.1, 6.2, 1H), 5.02 (dq, *J*=17.0, 1.7, 1H), 4.93 (dq, *J*=10.1, 1.6, 1H), 2.24 – 2.18 (m, 2H), 1.25 – 1.10 (m, 2H), 0.68 (s, 3H); ^{13}C NMR (151 MHz, $CDCl_3$) δ 140.3, 135.4, 133.5, 130.5, 128.3, 113.8, 27.2, 17.3, 0.6.

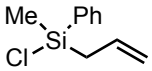

(**2.145**) According to general procedure B, silane **S2.5** (4.0 g, 24.6 mmol), $CuCl_2$ (6.62 g, 49.3 mmol), and CuI (190 mg, 1 mmol) were reacted in THF (60 mL) to give 2.04 g (42%) of **2.145** as a clear, viscous oil after distillation (40 °C/200 mtorr). ^{1}H NMR (400 MHz, $CDCl_3$) δ = 7.65 – 7.60 (m, 2H), 7.46 – 7.39 (m, 3H), 5.79 (ddt, *J*=17.5, 9.6, 7.9, 1H), 5.02 – 4.96 (m, 2H), 2.12 – 2.01 (m, 2H), 0.68 (s, 3H); ^{13}C NMR (101 MHz, $CDCl_3$) δ 134.8, 133.6, 131.8, 130.6, 128.2, 116.1, 25.7, -0.3.

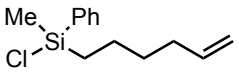

(**2.146**) According to general procedure B, silane **S2.6** (3.0 g, 15 mmol), $CuCl_2$ (4.0 g, 30 mmol), and CuI (190 mg, 1 mmol) were reacted in THF (40 mL) to give 2.76 g (77%) of **2.146** as a clear, viscous oil after distillation (65 °C/300 mtorr). ^{1}H NMR (400 MHz, $CDCl_3$) δ = 7.62 (dd, *J*=7.6, 1.8, 2H), 7.45 – 7.38 (m, 3H), 5.78 (ddt, *J*=16.9, 10.2, 6.7, 1H), 5.00 (dq, *J*=17.1, 1.6, 1H), 4.93 (ddt, *J*=10.1, 2.2, 1.2, 1H), 2.09 – 2.01 (m, 2H), 1.50 – 1.40 (m, 4H), 1.12 – 1.02 (m, 2H), 0.66 (s, 3H); ^{13}C NMR (101 MHz, $CDCl_3$) δ 138.9, 135.6, 133.5, 130.4, 128.2, 114.6, 33.5, 32.3, 22.6, 18.0, 0.5.

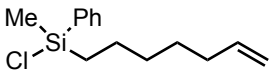

(**2.150**) According to general procedure B, silane **S2.7** (2.0 g, 9 mmol), $CuCl_2$ (2.46 g, 18 mmol), and CuI (190 mg, 1 mmol) were reacted in THF (20 mL) to give 1.18 g (51%) of **2.150** as a clear, viscous oil after

distillation (85 °C/200 mtorr). ^{1}H NMR (400 MHz, $CDCl_3$) δ 7.69 – 7.58 (m, 2H), 7.49 – 7.36 (m, 3H), 5.79 (tdd, *J* = 10.0, 6.0, 2.4 Hz, 1H), 5.06 – 4.84 (m, 2H), 2.02 (d, *J* = 6.9 Hz, 2H), 1.51 – 1.40 (m, 2H), 1.40 – 1.32 (m, 4H), 1.13 – 1.00 (m, 2H), 0.66 (s, 3H); ^{13}C NMR (101 MHz, $CDCl_3$) δ 139.15, 135.65, 133.47, 130.41, 128.20, 114.42, 33.77, 32.57, 28.57, 22.96, 18.10, 0.47.

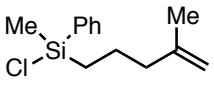

(**2.151**) Using a modified version of general procedure B, 2,6-di-tert-butyl-4-methylpyridine (2.5 g, 12 mmol), silane **S2.8** (2.0 g, 10.0 mmol), $CuCl_2$ (2.6 g, 20 mmol), and CuI (100 mg, 1 mmol) were reacted in THF (20 mL) to give 1.38 g (58%) of **2.151** as a yellow, viscous oil after distillation (90 °C/1.5 mtorr). ^{1}H NMR (600 MHz, $CDCl_3$) δ = 7.65 (dd, *J*=7.7, 1.4, 2H), 7.47 – 7.41 (m, 3H), 4.75 (s, 1H), 4.69 (s, 1H), 2.10 (t, *J*=7.4, 2H), 1.70 (s, 3H), 1.62 (dq, *J*=9.0, 7.4, 2H), 1.08 (td, *J*=7.7, 5.5, 2H), 0.69 (s, 3H); ^{13}C NMR (151 MHz, $CDCl_3$) δ 145.3, 135.6, 133.5, 130.4, 128.2, 110.7, 41.0, 22.3, 21.1, 17.6, -0.5.

Note: 2,6-di-tert-butyl-4-methylpyridine was used to prevent the acid catalyzed alkene isomerization to the internal alkene isomer during the course of the reaction.

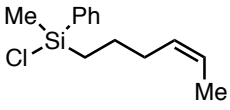

(**2.162**) According to general procedure B, silane **S2.9** (2.34 g, 11.4 mmol), $CuCl_2$ (3.08 g, 23 mmol), and CuI (190 mg, 1 mmol) were reacted in THF (25 mL) to give 1.3 g (51%) of **2.162** as a clear, viscous oil after distillation (58 °C/150 mtorr). ^{1}H NMR (600 MHz, $CDCl_3$) δ = 7.63 (dd, *J*=7.8, 1.4, 2H), 7.46 – 7.39 (m, 3H), 5.48 (dqt, *J*=10.8, 6.8, 1.5, 1H), 5.36 (dtq, *J*=10.6, 7.2, 1.6, 1H), 2.11 (q, *J*=7.2, 2H), 1.60 (dd, *J*=6.7, 0.6, 3H), 1.52 (dq, *J*=9.8, 7.1, 1H), 1.09 (td,

J=7.6, 3.9, 2H), 0.67 (s, 3H); ^{13}C NMR (151 MHz, $CDCl_3$) δ 135.6, 133.5, 130.4, 130.1, 128.2, 124.7, 30.1, 23.1, 17.8, 13.0, 0.5.

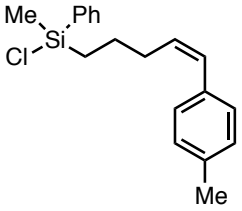

(**2.168**) According to general procedure B, silane **S2.10** (2.1 g, 7.5 mmol), $CuCl_2$ (2.0 g, 15 mmol), and CuI (190 mg, 1 mmol) were reacted in THF (15 mL) to give 884 mg (37%) of **2.168** as a clear, viscous oil after distillation (130 °C/250 mtorr). ^{1}H NMR (600 MHz, $CDCl_3$) δ = 7.61 – 7.59 (m, 2H), 7.41 (m, 3H), 7.15 (d, *J*=8.3, 2H), 7.13 (d, *J*=8.2, 2H), 6.40 (d, *J*=11.6, 1H), 5.57 (dt, *J*=11.5, 7.2, 1H), 2.39 (qd, *J*=7.2, 1.8, 2H), 2.34 (s, 3H), 1.61 (h, *J*=7.4, 6.9, 2H), 1.16 – 1.04 (m, 2H), 0.65 (s, 3H); ^{13}C NMR (151 MHz, $CDCl_3$) δ 136.2, 135.4, 134.8, 133.3, 131.5, 130.3, 129.3, 128.8, 128.6, 128.1, 31.7, 23.4, 21.1, 17.8, 0.3.

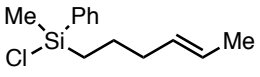

(**2.156**) According to general procedure B, silane **S2.11** (4.74 g, 23 mmol), $CuCl_2$ (6.25 g, 46 mmol), and CuI (190 mg, 1 mmol) were reacted in THF (50 mL) to give 3.25 g (59%) of **2.156** as a clear, viscous oil after distillation (60 °C/300 mtorr). ^{1}H NMR (600 MHz, $CDCl_3$) δ = 7.62 (dd, *J*=7.8, 1.4, 2H), 7.45 – 7.38 (m, 3H), 5.46 – 5.34 (m, 2H), 2.03 (q, *J*=7.1, 6.4, 2H), 1.64 (d, *J*=4.8, 3H), 1.50 (dq, *J*=9.8, 7.0, 2H), 1.06 (td, *J*=7.6, 5.8, 2H), 0.66 (s, 3H); ^{13}C NMR (151 MHz, $CDCl_3$) δ = 135.7, 133.5, 130.9, 130.4, 128.2, 125.7, 35.9, 23.2, 18.0, 17.8, 0.5.

2.8.6 Intramolecular Silyl-Heck Procedure

2.8.6.1 General Procedure C

In a nitrogen filled glovebox, $(JessePhos)_2PdCl_2$ (13.9 mg, 0.125 mmol, 5 mol %), LiI (47 mg, 0.35 mmol, 1.4 equiv), Et_3N (175 μL, 1.25 mmol, 5.0 equiv) and $PhCF_3$ (500 μL, 0.5M) were added to a 1-dram vial with a magnetic stir bar. The silyl chloride, (0.25 mmol, 1.0 equiv) was added in one portion *via* micropipette. The vial was then sealed, and stirred at 45 °C for 24 h. The reaction was removed from heat, allowed to cool to rt, and 1,3,5-trimethoxy benzene (28 mg, 2/3 equiv) was added under air. A small aliquot was taken for NMR without concentration, the sample was returned to the crude mixture, filtered thru celite with Et_2O and concentrated before purification. The crude oil was purified by flash silica chromatography with the indicated solvent in parenthesis.

2.8.6.2 Characterization Data

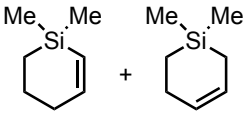

(**2.117** and **2.118**) In a nitrogen filled glovebox, trisdibenzyladinedipalladium (Pd_2dba_3, 11 mg), bis(3,5-ditertbutyl-C_5H_3)-*tert*butylphosphine (JessePhos, 12 mg), Et_3N (175 μL) and $PhCF_3$ (500 μL) were added to a 1-dram vial with a magnetic stir bar. The vial was capped, heated at 45 °C and stirred for 5 min. The vial was removed from heat and silyliodide **2.116** (64 mg), was added in one portion without cooling. The vial was then resealed, and stirred at 45 °C for 24 h. The reaction was removed from heat, allowed to cool to rt, and mesitylene (35 μL) was added and a small aliquot was taken for NMR without concentration. The volitiles (including products) of the crude were vacuum transferred to separate them from the catalyst and ligand, and an analytical amount of the two isomeric products were purified to ≥70% purity by preparatory gas chromatography.

(**2.117**, vinylsilane): ^{1}H NMR (400 MHz, C_6D_6) δ = 6.72 (dt, *J*=14.2, 4.0, 1H), 5.79 (d, *J*=14.1, 1H), 2.02 – 1.94 (m, 2H), 1.72 (dq, *J*=7.0, 5.9, 2H), 0.66 – 0.62 (m, 2H), 0.08 (s, 6H); ^{13}C NMR (101 MHz, C_6D_6) δ = 149.1, 127.1, 31.2, 21.5, 12.3, -1.6. HRMS (LIFDI) calcd for [$C_7H_{14}Si$]: 126.0865, found: 126.0847. (**2.118**, allylsilane): ^{1}H NMR (400 MHz, C_6D_6) δ = 5.86 (dtt, *J*=10.1, 4.9, 1.8, 1H), 5.72 (dtt, *J*=10.7, 4.4, 1.9, 1H), 2.21 (tdt, *J*=6.4, 3.8, 1.9, 2H), 1.17 (dq, *J*=4.0, 1.9, 2H), 0.63 (t, *J*=6.9, 2H), 0.00 (s, 6H); ^{13}C NMR (101 MHz, $CDCl_3$) δ = 130.5, 126.2, 23.2, 13.3, 10.3, -2.5. HRMS (LIFDI) calcd for [$C_7H_{14}Si$]: 126.0865, found: 126.0835.

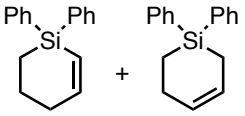

(**2.125** and **2.126**) In a nitrogen filled glovebox, trisdibenzyladinedipalladium (Pd_2dba_3, 45.6 mg), bis(3,5-ditertbutyl-C_5H_3)-*tert*butylphosphine (JessePhos, 46.4 mg), Et_3N (700 μL) and $PhCF_3$ (2 mL) were added to a 1-dram vial with a magnetic stir bar. The vial was capped, heated at 45 °C and stirred for 5 min. The vial was removed from heat and silyl triflate **2.124**, was added in one portion without cooling. The vial was then resealed, and stirred at 45 °C for 24 h. The reaction was removed from heat, allowed to cool to rt, quenched by the addition of water (ca. 2 mL) and extracted with diethyl ether (2 times ca. 1 mL ea.). The organic layer was separated, dried with $MgSO_4$, filtered, and concentrated to a crude oil that was purified by flash silica chromatography (pentane) to give 183 mg (73%) of a 1:1 mixture of vinyl and allylsilane **2.125** and **2.126**, respectively. (**2.125**, vinylsilane): ^{1}H NMR (600 MHz, $CDCl_3$) δ 7.61 – 7.50 (m, 4H), 7.44 – 7.30 (m, 6H), 7.03 (dt, *J* = 14.1, 4.0 Hz, 1H), 6.07 (dt, *J* = 14.2, 2.0 Hz, 1H), 2.32 – 2.24 (m, 2H), 1.98 – 1.85 (m, 2H), 1.23 – 1.17 (m, 2H). (**2.126**, allylsilane): ^{1}H NMR (600 MHz, $CDCl_3$) δ 7.58 – 7.52 (m, 4H), 7.42 – 7.32 (m, 6H), 5.96 – 5.90 (m, 1H), 5.78 – 5.69 (m, 1H), 2.39 –

2.32 (m, 2H), 1.81 – 1.76 (m, 2H), 1.25 (t, J = 6.9 Hz, 2H). (**2.125** and **2.126**, mixture): ^{13}C NMR (151 MHz, $CDCl_3$) δ 152.0, 136.9, 136.6, 135.0, 134.7, 131.0, 129.5, 129.4, 128.0, 128.0, 125.6, 122.6, 31.1, 22.9, 21.0, 11.0, 10.3, 8.1; FTIR (cm^{-1}) 2908, 1427, 1112. HRMS (EI) m/z, calcd for [$C_{13}H_{20}Si$]: 250.1178; found: 250.1205.

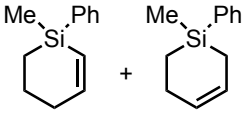

(**2.138** and **2.139**) According to general procedure C, silyl chloride **2.137** (56 mg, 0.25 mmol), $(JessePhos)_2PdCl_2$ (13.9 mg, 0.125 mmol, 5 mol %), LiI (47 mg, 0.35 mmol, 1.4 equiv), Et_3N (175 μL, 1.25 mmol, 5.0 equiv) and $PhCF_3$ (500 μL, 0.5M) were stirred at 45 °C for 24 h. Analysis of the crude reaction mixture *via* ^{1}H NMR revealed an 88% yield. The crude material was purified *via* silica gel chromatography (hexanes) to afford a mixture of **2.138** and **2.139** as a colorless oil (38 mg, 81%): (**2.138**, vinylsilane): ^{1}H NMR (600 MHz, $CDCl_3$) δ 7.59 – 7.51 (m, 2H), 7.39 – 7.32 (m, 3H), 6.91 (dt, J = 14.1, 4.0 Hz, 1H), 5.91 – 5.79 (m, 1H), 2.25 – 2.18 (m, 2H), 1.90 – 1.80 (m, 2H), 1.03 – 0.80 (m, 2H), 0.35 (s, 3H). (**2.139**, allylsilane): ^{1}H NMR (600 MHz, $CDCl_3$) δ 7.61 – 7.51 (m, 2H), 7.40 – 7.32 (m, 3H), 5.91 – 5.80 (m, 1H), 5.78 – 5.66 (m, 1H), 2.36 – 2.27 (m, 2H), 1.63 – 1.36 (m, 2H), 1.04 – 0.80 (m, 2H), 0.33 (s, 3H). (**2.138** and **2.139**, mixture): ^{13}C NMR (151 MHz, $CDCl_3$) δ 150.8, 139.0, 138.9, 134.2, 133.8, 130.7, 129.2, 129.1, 128.0, 127.9, 125.9, 124.7, 31.1, 23.0, 21.2, 12.1, 11.6, 9.4, -3.0, -3.8; FTIR (cm^{-1}) 2907, 1590, 1427, 1251, 1111, 809, 699. HRMS (CI) m/z, calcd for [$C_{12}H_{16}Si$]: 188.1021; found: 188.1012.

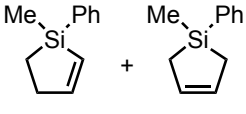

(**2.142** and **2.143**) According to general procedure C, silyl chloride **2.141** (53 mg, 0.25 mmol), $(JessePhos)_2PdCl_2$ (13.9 mg, 0.125 mmol, 5 mol %), LiI (47 mg, 0.35 mmol, 1.4 equiv), Et_3N (175 μL, 1.25 mmol, 5.0

equiv) and $PhCF_3$ (500 µL, 0.5M) were stirred at 45 °C for 24 h. Analysis of the crude reaction mixture *via* ^1H NMR revealed an 80% yield. The crude material was purified *via* silica gel chromatography (pentane) to afford a mixture of **2.142** and **2.143** as a colorless oil (31 mg, 71%): (**2.142**, vinylsilane): ^1H NMR (600 MHz, $CDCl_3$) δ 7.55 – 7.48 (m, 2H), 7.42 – 7.32 (m, 3H), 7.00 (dt, *J* = 10.1, 2.7 Hz, 1H), 6.07 (dt, *J* = 10.1, 2.3 Hz, 1H), 2.70 – 2.51 (m, 2H), 1.06 – 0.82 (m, 2H), 0.48 (s, 3H). (**2.143**, allylsilane): ^1H NMR (600 MHz, $CDCl_3$) δ 7.61 – 7.55 (m, 2H), 7.43 – 7.31 (m, 3H), 5.97 (s, 2H), 1.69 – 1.43 (m, 4H), 0.48 (s, 3H). (**2.142** and **2.143**, mixture): ^{13}C NMR (101 MHz, $CDCl_3$) δ 155.2, 138.9, 138.3, 134.0, 133.8, 131.2, 129.4, 129.2, 128.7, 128.0, 127.9, 32.4, 17.7, 8.8, -3.0, -3.7; FTIR (cm^{-1}) 3019, 2905, 1114. HRMS (CI) m/z, calcd for [$C_{11}H_{14}Si$]: 174.0865; found: 174.0858.

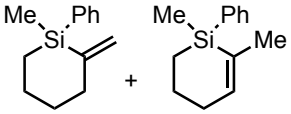

(**2.148** and **2.149**) According to general procedure C, silyl chloride **2.146** (240 mg, 1.0 mmol), $(JessePhos)_2PdCl_2$ (56 mg, 0.5 mmol, 5 mol %), LiI (188 mg, 1.4 mmol, 1.4 equiv), Et_3N (700 µL, 5.0 mmol, 5.0 equiv) and $PhCF_3$ (2 mL, 0.5M) were stirred at 45 °C for 24 h. Analysis of the crude reaction mixture *via* ^1H NMR revealed a 31% yield. The crude material was purified *via* silica gel chromatography (hexanes) to afford a mixture of **2.148** and **2.149** as a colorless oil (23 mg, 12%): (**2.148**, exo): ^1H NMR (400 MHz, $CDCl_3$) δ 7.59 – 7.51 (m, 3H), 7.40 – 7.33 (m, 3H), 5.60 (dd, *J* = 3.3, 1.6 Hz, 1H), 5.19 (dt, *J* = 3.6, 1.2 Hz, 1H), 2.49 – 2.27 (m, 2H), 1.96 – 1.83 (m, 1H), 1.70 – 1.60 (m, 1H), 1.54 – 1.39 (m, 1H), 1.20 – 1.09 (m, 1H), 0.86 – 0.72 (m, 1H), 0.34 (s, 3H). (**2.149**, endo): ^1H NMR (400 MHz, $CDCl_3$) δ 7.61 – 7.49 (m, 2H), 7.43 – 7.30 (m, 3H), 6.49 (dq, *J* = 4.2, 1.8 Hz, 1H), 2.23 – 2.12 (m, 2H), 1.84 – 1.76 (m, 2H), 1.71 (q, *J* = 2.0 Hz, 3H), 1.00 – 0.89 (m,

1H), 0.86 – 0.71 (m, 1H), 0.37 (s, 3H). (**2.148** and **2.149**, mixture): ^{13}C NMR (101 MHz, $CDCl_3$) δ 150.8, 143.9, 138.2, 137.0, 134.4, 134.3, 131.9, 129.2, 129.1, 127.9, 127.9, 123.5, 40.0, 31.0, 30.6, 24.5, 21.9, 21.4, 13.7, 11.9, -4.3, -4.9; FTIR (cm^{-1}) 2921, 2852, 1653. HRMS (CI) m/z, calcd for [$C_{13}H_{18}Si$]: 202.1178; found: 202.1176.

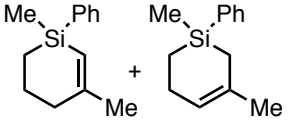

(**2.152** and **2.153**) According to general procedure C, silyl chloride **2.151** (60 mg, 0.25 mmol), $(JessePhos)_2PdCl_2$ (13.9 mg, 0.125 mmol, 5 mol %), LiI (47 mg, 0.35 mmol, 1.4 equiv), Et_3N (175 μL, 1.25 mmol, 5.0 equiv) and $PhCF_3$ (500 μL, 0.5M) were stirred at 45 °C for 24 h. Analysis of the crude reaction mixture *via* ^{1}H NMR revealed an 88% yield. The crude material was purified *via* silica gel chromatography (pentane) to afford a mixture of **2.152** and **2.153** as a colorless oil (42 mg, 82%): (**2.152**, vinylsilane): ^{1}H NMR (400 MHz, $CDCl_3$) δ 7.61 – 7.50 (m, 2H), 7.41 – 7.31 (m, 3H), 5.51 (s, 1H), 2.11 (t, 2H), 1.89 (d, 3H), 1.88 – 1.79 (m, 2H), 0.94 – 0.69 (m, 2H), 0.31 (s, 3H). (**2.153**, allylsilane): ^{1}H NMR (400 MHz, $CDCl_3$) δ 7.60 – 7.49 (m, 2H), 7.41 – 7.31 (m, 3H), 5.51 (s, 1H), 2.29 – 2.21 (m, 2H), 1.79 (d, J = 1.8 Hz, 3H), 1.53 – 1.29 (m, 2H), 0.97 – 0.68 (m, 2H), 0.31 (s, 3H). (**2.152** and **2.153**, mixture): ^{13}C NMR (101 MHz, $CDCl_3$) δ 159.0, 139.6, 134.2, 133.8, 129.1, 128.9, 127.9, 127.8, 124.3, 118.4, 100.1, 35.3, 29.5, 28.5, 22.8, 21.6, 17.4, 10.7, 9.0, -2.8; FTIR (cm^{-1}) 2924, 1608, 1427, 1250, 1111, 815, 731, 698. HRMS (CI) m/z, calcd for [$C_{13}H_{20}Si$]: 202.1178; found: 202.1174.

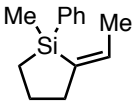

(**2.163**) According to general procedure C, silyl chloride **2.162** (240 mg, 1.0 mmol), $(JessePhos)_2PdCl_2$ (56 mg, 0.5 mmol, 5 mol %), LiI (188 mg, 1.4 mmol, 1.4 equiv), Et_3N (700 μL, 5.0 mmol, 5.0 equiv) and $PhCF_3$ (2 mL, 0.5M)

were stirred at 45 °C for 24 h. Analysis of the crude reaction mixture *via* ^{1}H NMR revealed a 18% yield. The crude material was purified *via* silica gel chromatography (pentane) to afford **2.163** as a colorless oil (36 mg, 17%): (**2.163**, single isomer): ^{1}H NMR (600 MHz, $CDCl_3$) δ 7.61 – 7.52 (m, 2H), 7.40 – 7.30 (m, 3H), 6.29 (qt, *J* = 6.6, 2.0 Hz, 1H), 2.39 – 2.33 (m, 2H), 1.85 – 1.69 (m, 2H), 1.64 (dt, *J* = 6.7, 1.9 Hz, 3H), 0.98 – 0.81 (m, 2H), 0.50 (s, 3H); ^{13}C NMR (151 MHz, $CDCl_3$) δ 142.5, 138.1, 134.3, 133.8, 129.1, 127.9, 39.2, 25.5, 19.8, 15.0, -3.9; FTIR (cm^{-1}) 2916, 1428, 1250, 1112, 732, 698. HRMS (CI) m/z, calcd for [$C_{13}H_{16}Si$]: 202.1178; found: 202.1177.

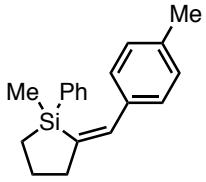

(**2.169**) According to general procedure C, silyl chloride **2.168** (158 mg, 0.5 mmol), $(JessePhos)_2PdCl_2$ (28 mg, 0.25 mmol, 5 mol %), LiI (94 mg, 0.7 mmol, 1.4 equiv), Et_3N (350 μL, 2.5 mmol, 5.0 equiv) and $PhCF_3$ (1.0 mL, 0.5M) were stirred at 45 °C for 24 h. Analysis of the crude reaction mixture *via* ^{1}H NMR revealed a 49% yield. The crude material was purified *via* silica gel chromatography (hexanes) to afford **2.169** as a colorless oil (57 mg, 41%): ^{1}H NMR (400 MHz, $CDCl_3$) δ 7.58 – 7.52 (m, 2H), 7.37 – 7.31 (m, 3H), 7.26 (s, 1H), 7.08 (d, *J* = 8.1 Hz, 2H), 6.94 (d, *J* = 7.8 Hz, 2H), 2.66 – 2.58 (m, 2H), 2.25 (s, 3H), 1.98 – 1.85 (m, 1H), 1.76 – 1.63 (m, 1H), 0.97 (dd, *J* = 7.8, 6.6 Hz, 2H), 0.38 (s, 3H); ^{1}H NMR (400 MHz, C_6D_6) δ 7.62 – 7.53 (m, 2H), 7.35 (s, 1H), 7.26 – 7.21 (m, 2H), 7.22 – 7.17 (m, 3H), 6.79 (d, *J* = 7.8 Hz, 2H), 2.66 – 2.52 (m, 2H), 1.98 (s, 3H), 1.94 – 1.79 (m, 1H), 1.71 – 1.57 (m, 1H), 0.99 – 0.84 (m, 2H), 0.41 (s, 3H); ^{13}C NMR (101 MHz, $CDCl_3$) δ 144.0, 139.1, 138.4, 136.6, 136.6, 134.2, 129.2, 128.8, 128.0, 127.9, 42.8, 24.8, 21.3, 15.8, -5.0; ^{13}C NMR (101 MHz, C_6D_6) δ 143.6, 140.0, 138.6, 137.1, 136.8, 134.5,

129.5, 129.1, 128.3, 43.0, 25.1, 21.1, 16.1, -4.9; FTIR (cm^{-1}) 2920, 1510, 1428, 1110, 809, 699. HRMS (CI) m/z, calcd for [$C_{19}H_{22}Si$]: 278.1491; found: 278.1493.

REFERENCES

(1) Komiyama, T.; Minami, Y.; Hiyama, T., *ACS Catal.* **2017,** *7*, 631.
(2) McAtee, J. R.; Martin, S. E. S.; Ahneman, D. T.; Johnson, K. A.; Watson, D. A., *Angew. Chem., Int. Ed.* **2012,** *51*, 3663.
(3) (a) Gibson, S. E.; Middleton, R. J., *Contemporary Organic Synthesis* **1996,** *3*, 447; (b) Shibasaki, M.; Boden, C. D. J.; Kojima, A., *Tetrahedron* **1997,** *53*, 7371; (c) Beletskaya, I. P.; Cheprakov, A. V., *Chem. Rev.* **2000,** *100*, 3009; (d) Link, J. T., The IntramolecularHeck Reaction. In *Organic Reactions*, John Wiley & Sons, Inc.: 2002; pp 157; (e) Dounay, A. B.; Overman, L. E., *Chem. Rev.* **2003,** *103*, 2945; (f) Zeni, G.; Larock, R. C., *Chem. Rev.* **2006,** *106*, 4644; (g) Geoghegan, K., Regioselectivity in the Heck (Mizoroki-Heck) Reaction. In *Selectivity in the Synthesis of Cyclic Sulfonamides: Application in the Synthesis of Natural Products*, Springer International Publishing: Cham, 2014; pp 17.
(4) (a) Hermanns, J.; Schmidt, B., *J. Chem. Soc., Perkin Trans. 1* **1998,** 2209; (b) Ottosson, H.; Steel, P. G., *Chem. - Eur. J.* **2006,** *12*, 1576.
(5) Tacke, R.; Dörrich, S., Drug Design Based on the Carbon/Silicon Switch Strategy. In *Atypical Elements in Drug Design*, Schwarz, J., Ed. Springer International Publishing: Cham, 2014; pp 29.
(6) (a) Franz, A. K.; Wilson, S. O., *J. Med. Chem.* **2013,** *56*, 388; (b) Fensterbank, L.; Malacria, M.; Sieburth, S. M. N., *Synthesis* **1997,** *1997*, 813; (c) Bols, M.; Skrydstrup, T., *Chem. Rev.* **1995,** *95*, 1253; (d) Jones, G. R.; Landais, Y., *Tetrahedron* **1996,** *52*, 7599.
(7) (a) Díez-González, S.; Paugam, R.; Blanco, L., *Eur. J. Org. Chem.* **2008,** *2008*, 3298; (b) Ramesh, R.; Reddy, D. S., *Org. Biomol. Chem.* **2014,** *12*, 4093; (c) Igawa, K.; Yoshihiro, D.; Abe, Y.; Tomooka, K., *Angew. Chem., Int. Ed.* **2016,** *55*, 5814.
(8) (a) Bauer, J. B.; Lippert, W. P.; Dörrich, S.; Tebbe, D.; Burschka, C.; Christie, V. B.; Tams, D. M.; Henderson, A. P.; Murray, B. A.; Marder, T. B.; Przyborski, S. A.; Tacke, R., *ChemMedChem* **2011,** *6*, 1509; (b) Tacke, R.; Müller, V.; Büttner, M. W.; Lippert, W. P.; Bertermann, R.; Daiß, J. O.; Khanwalkar, H.; Furst, A.; Gaudon, C.; Gronemeyer, H., *ChemMedChem* **2009,** *4*, 1797; (c) Daiss, J. O.; Burschka, C.; Mills, J. S.; Montana, J. G.; Showell, G. A.; Fleming, I.; Gaudon, C.; Ivanova, D.; Gronemeyer, H.; Tacke, R., *Organometallics* **2005,** *24*, 3192.
(9) Wang, J.; Ma, C.; Wu, Y.; Lamb, R. A.; Pinto, L. H.; DeGrado, W. F., *J. Am. Chem. Soc.* **2011,** *133*, 13844.
(10) (a) Anhaus, J. T.; Clegg, W.; Collingwood, S. P.; Gibson, V. C., *J. Chem. Soc., Chem. Commun.* **1991,** 1720; (b) Birot, M.; Pillot, J.-P.; Dunogues, J., *Chem. Rev.* **1995,**

95, 1443; (c) Matsumoto, K.; Shimazu, H.; Deguchi, M.; Yamaoka, H., *Journal of Polymer Science Part A: Polymer Chemistry* **1997,** *35*, 3207.
(11) (a) Hiroshi, Y.; Masato, T., *Bull. Chem. Soc. Jpn.* **1995,** *68*, 403; (b) Comstock, M. J., Silicon-Based Polymer Science, Copyright, Advances in Chemistry Series, FOREWORD, ABOUT THE EDITORS. In *Silicon-Based Polymer Science*, Comstock, M. J., Ed. American Chemical Society: 1989; Vol. 224, pp i.
(12) (a) Brummond, K. M.; Sill, P. C.; Chen, H., *Org. Lett.* **2004,** *6*, 149; (b) Sellars, J. D.; Steel, P. G., *Tetrahedron* **2009,** *65*, 5588.
(13) Bracegirdle, S.; Anderson, E. A., *Chem. Soc. Rev.* **2010,** *39*, 4114.
(14) (a) Brummond, K. M.; Sill, P. C.; Rickards, B.; Geib, S. J., *Tetrahedron Lett.* **2002,** *43*, 3735; (b) Kuznetsov, A.; Gevorgyan, V., *Org. Lett.* **2012,** *14*, 914.
(15) Denmark, S. E.; Pan, W., *Org. Lett.* **2001,** *3*, 61.
(16) Okada, K.; Matsumoto, K.; Oshima, K.; Utimoto, K., *Tetrahedron Lett.* **1995,** *36*, 8067.
(17) Benkeser, R.; Cunico, R. F., *J. Organomet. Chem.* **1965,** *4*, 284.
(18) (a) Benkeser, R. A.; Nagai, Y.; Noe, J. L.; Cunico, R. F.; Gund, P. H., *J. Am. Chem. Soc.* **1964,** *86*, 2446; (b) Benkeser, R. A.; Noe, J. L.; Nagai, Y., *J. Org. Chem.* **1965,** *30*, 378; (c) Dunogues, J.; Calas, R.; Dedier, J.; Pisciotti, F.; Lapouyade, P., *J. Organomet. Chem.* **1970,** *25*, 51.
(19) (a) Bravo-Zhivotovskii, D.; Braude, V.; Stanger, A.; Kapon, M.; Apeloig, Y., *Organometallics* **1992,** *11*, 2326; (b) Krempner, C.; Reinke, H.; Oehme, H., *Chem. Ber.* **1995,** *128*, 143; (c) Krempner, C.; Reinke, H.; Oehme, H., *Chem. Ber.* **1995,** *128*, 1083; (d) Apeloig, Y.; Bendikov, M.; Yuzefovich, M.; Nakash, M.; Bravo-Zhivotovskii, D.; Bläser, D.; Boese, R., *J. Am. Chem. Soc.* **1996,** *118*, 12228; (e) Hoffmann, D.; Reinke, H.; Oehme, H., *J. Organomet. Chem.* **1996,** *526*, 185; (f) Luderer, F.; Reinke, H.; Oehme, H., *Chem. Ber.* **1996,** *129*, 15; (g) Luderer, F.; Reinke, H.; Oehme, H., *J. Organomet. Chem.* **1996,** *510*, 181; (h) Wendler, C.; Oehme, H., *Z. Anorg. Allg. Chem.* **1996,** *622*, 801; (i) Sakamoto, K.; Ogasawara, J.; Sakurai, H.; Kira, M., *J. Am. Chem. Soc.* **1997,** *119*, 3405.
(20) Gusel'nikov, L. E.; Nametkin, N. S., *Chem. Rev.* **1979,** *79*, 529.
(21) Lei, D.; Hwang, R.-J.; Caspar, P. P., *J. Organomet. Chem.* **1984,** *271*, 1.
(22) Conlin, R. T.; Namavari, M., *J. Am. Chem. Soc.* **1988,** *110*, 3689.
(23) Sakurai, H.; Imai, T., *Chem. Lett.* **1975,** *4*, 891.
(24) Takeyama, Y.; Nozaki, K.; Matsumoto, K.; Oshima, K.; Utimoto, K., *Bull. Chem. Soc. Jpn.* **1991,** *64*, 1461.
(25) Tanaka, Y.; Yamashita, H.; Tanaka, M., *Organometallics* **1996,** *15*, 1524.
(26) (a) Palmer, W. S.; Woerpel, K. A., *Organometallics* **1997,** *16*, 1097; (b) Palmer, W. S.; Woerpel, K. A., *Organometallics* **1997,** *16*, 4824.
(27) Shintani, R.; Moriya, K.; Hayashi, T., *J. Am. Chem. Soc.* **2011,** *133*, 16440.
(28) (a) Fessenden, R. J.; Kray, W. D., *J. Org. Chem.* **1973,** *38*, 87; (b) Swisher, J. V.; Chen, H.-H., *J. Organomet. Chem.* **1974,** *69*, 83; (c) Tamao, K.; Maeda, K.; Tanaka, T.; Ito, Y., *Tetrahedron Lett.* **1988,** *29*, 6955; (d) Steinmetz, M. G.; Udayakumar, B. S., *J.*

Organomet. Chem. **1989,** *378*, 1; (e) Ito, Y.; Suginome, M.; Murakami, M., *J. Org. Chem.* **1991,** *56*, 1948; (f) Sashida, H.; Kudoda, A., *Synthesis* **1999,** *1999*, 921.
(29) Chalk, A. J.; Harrod, J. F., *J. Am. Chem. Soc.* **1965,** *87*, 16.
(30) Sudo, T.; Asao, N.; Yamamoto, Y., *J. Org. Chem.* **2000,** *65*, 8919.
(31) Trost, B. M.; Ball, Z. T., *J. Am. Chem. Soc.* **2003,** *125*, 30.
(32) Mori, M.; Chiba, K.; Ban, Y., *Tetrahedron Lett.* **1977,** *18*, 1037.
(33) Terpko, M. O.; Heck, R. F., *J. Am. Chem. Soc.* **1979,** *101*, 5281.
(34) (a) Earley, W. G.; Oh, T.; Overman, L. E., *Tetrahedron Lett.* **1988,** *29*, 3785; (b) Madin, A.; Overman, L. E., *Tetrahedron Lett.* **1992,** *33*, 4859.
(35) (a) Sato, Y.; Sodeoka, M.; Shibasaki, M., *J. Org. Chem.* **1989,** *54*, 4738; (b) Sato, Y.; Sodeoka, M.; Shibasaki, M., *Chem. Lett.* **1990,** *19*, 1953.
(36) (a) Grigg, R.; Dorrity, M. J. R.; Malone, J. F.; Mongkolaussavaratana, T.; Norbert, W. D. J. A.; Sridharan, V., *Tetrahedron Lett.* **1990,** *31*, 3075; (b) Grigg, R.; Sridharan, V.; Stevenson, P.; Sukirthalingam, S.; Worakun, T., *Tetrahedron* **1990,** *46*, 4003.
(37) Abelman, M. M.; Overman, L. E.; Tran, V. D., *J. Am. Chem. Soc.* **1990,** *112*, 6959.
(38) Abelman, M. M.; Oh, T.; Overman, L. E., *J. Org. Chem.* **1987,** *52*, 4130.
(39) (a) Ashimori, A.; Overman, L. E., *J. Org. Chem.* **1992,** *57*, 4571; (b) Ashimori, A.; Matsuura, T.; Overman, L. E.; Poon, D. J., *J. Org. Chem.* **1993,** *58*, 6949; (c) Overman, L. E., Application of intramolecular Heck reactions for forming congested quaternary carbon centers in complex molecule total synthesis. In *Pure Appl. Chem.*, 1994; Vol. 66, p 1423.
(40) McClure, K. F.; Danishefsky, S. J., *J. Am. Chem. Soc.* **1993,** *115*, 6094.
(41) (a) Bräse, S., *Synlett* **1999,** *1999*, 1654; (b) Yoshito, T.; Tetsuya, S.; Masahiro, M.; Masakatsu, N., *Bull. Chem. Soc. Jpn.* **1999,** *72*, 2345; (c) Innitzer, A.; Brecker, L.; Mulzer, J., *Org. Lett.* **2007,** *9*, 4431.
(42) (a) Tietze, L. F.; Schirok, H., *Angew. Chem., Int. Ed.* **1997,** *36*, 1124; (b) Tietze, L. F.; Schirok, H., *J. Am. Chem. Soc.* **1999,** *121*, 10264; (c) Tietze, L. F.; Schirok, H.; Wöhrmann, M., *Chem. - Eur. J.* **2000,** *6*, 510.
(43) Stocks, M. J.; Harrison, R. P.; Teague, S. J., *Tetrahedron Lett.* **1995,** *36*, 6555.
(44) Ziegler, F. E.; Chakraborty, U. R.; Weisenfeld, R. B., *Tetrahedron* **1981,** *37*, 4035.
(45) (a) E. Gibson, S.; Guillo, N.; J. Middleton, R.; Thuilliez, A.; J. Tozer, M., *J. Chem. Soc., Perkin Trans. 1* **1997,** 447; (b) Kotoku, N.; Sumii, Y.; Kobayashi, M., *Org. Lett.* **2011,** *13*, 3514; (c) Klein, J. E. M. N.; Műller-Bunz, H.; Ortin, Y.; Evans, P., *Tetrahedron Lett.* **2008,** *49*, 7187; (d) Iimura, S.; Overman, L. E.; Paulini, R.; Zakarian, A., *J. Am. Chem. Soc.* **2006,** *128*, 13095; (e) Hegedus, L. S.; Sestrick, M. R.; Michaelson, E. T.; Harrington, P. J., *J. Org. Chem.* **1989,** *54*, 4141; (f) Gao, P.; Cook, S. P., *Org. Lett.* **2012,** *14*, 3340; (g) Dankwardt, J. W.; Flippin, L. A., *J. Org. Chem.* **1995,** *60*, 2312; (h) Naoyuki Kotoku, Y. S., Takeshi Hayashi, and Motomasa Kobayashi*, *Heterocycles* **2011,** *83*, 1535.
(46) (a) Grigg, R.; Stevenson, P.; Worakun, T., *J. Chem. Soc., Chem. Commun.* **1984,** 1073; (b) Gibson, S. E.; Middleton, R. J., *J. Chem. Soc., Chem. Commun.* **1995,** 1743.

(47) (a) Parasram, M.; Iaroshenko, V. O.; Gevorgyan, V., *J. Am. Chem. Soc.* **2014,** *136*, 17926; (b) Dong, X.; Han, Y.; Yan, F.; Liu, Q.; Wang, P.; Chen, K.; Li, Y.; Zhao, Z.; Dong, Y.; Liu, H., *Org. Lett.* **2016,** *18*, 3774.
(48) (a) Owczarczyk, Z.; Lamaty, F.; Vawter, E. J.; Negishi, E., *J. Am. Chem. Soc.* **1992,** *114*, 10091; (b) Rawal, V. H.; Michoud, C., *J. Org. Chem.* **1993,** *58*, 5583; (c) Albéniz, A. C.; Espinet, P.; Lin, Y.-S., *J. Am. Chem. Soc.* **1996,** *118*, 7145; (d) Grigg, R.; Sridharan, V.; Sukirthalingam, S., *Tetrahedron Lett.* **1991,** *32*, 3855.
(49) (a) Baldwin, J. E., *J. Chem. Soc., Chem. Commun.* **1976,** 734; (b) Baldwin, J. E.; Cutting, J.; Dupont, W.; Kruse, L.; Silberman, L.; Thomas, R. C., *J. Chem. Soc., Chem. Commun.* **1976,** 736; (c) Baldwin, J. E.; Thomas, R. C.; Kruse, L. I.; Silberman, L., *J. Org. Chem.* **1977,** *42*, 3846.
(50) Grigg, R.; Savic, V., *Chem. Commun.* **2000,** 873.
(51) Heck, R. F., Palladium-Catalyzed Vinylation of Organic Halides. In *Organic Reactions*, John Wiley & Sons, Inc.: 1982.
(52) Martin, S. E. S.; Watson, D. A., *J. Am. Chem. Soc.* **2013,** *135*, 13330.
(53) (a) McAtee, J. R.; Yap, G. P. A.; Watson, D. A., *J. Am. Chem. Soc.* **2014,** *136*, 10166; (b) McAtee, J. R.; Krause, S. B.; Watson, D. A., *Adv. Synth. Catal.* **2015,** *357*, 2317.
(54) Krause, S. B.; McAtee, J. R.; Yap, G. P. A.; Watson, D. A., *Org. Lett.* **2017,** *19*, 5641.
(55) Kunai, A.; Ohshita, J., *J. Organomet. Chem.* **2003,** *686*, 3.
(56) Vulovic, B.; Watson, D. A., *Eur. J. Org. Chem.* **2017,** *2017*, 4996.
(57) (a) Chatani, N.; Amishiro, N.; Murai, S., *J. Am. Chem. Soc.* **1991,** *113*, 7778; (b) Hiroshi, Y.; Toshi-aki, K.; Teruyuki, H.; Masato, T., *Chem. Lett.* **1991,** *20*, 761; (c) Chatani, N.; Amishiro, N.; Morii, T.; Yamashita, T.; Murai, S., *J. Org. Chem.* **1995,** *60*, 1834.
(58) McAtee, J. R.; Martin, S. E. S.; Cinderella, A. P.; Reid, W. B.; Johnson, K. A.; Watson, D. A., *Tetrahedron* **2014,** *70*, 4250.
(59) Stang, P. J.; Hanack, M.; Subramanian, L. R., *Synthesis* **1982,** *1982*, 85.
(60) (a) Matyjaszewski, K.; Chen, Y. L., *J. Organomet. Chem.* **1988,** *340*, 7; (b) Uhlig, W., *Chem. Ber.* **1996,** *129*, 733.
(61) (a) Brook, M. A.; Crowe, G. D.; Hiemstra, H., *Can. J. Chem.* **1994,** *72*, 264; (b) Suslova, E. N.; Albanov, A. I.; Shainyan, B. A., *J. Organomet. Chem.* **2009,** *694*, 420.
(62) Levin, Vitalij V.; Dilman, Alexander D.; Belyakov, Pavel A.; Korlyukov, Alexander A.; Struchkova, Marina I.; Tartakovsky, Vladimir A., *Eur. J. Org. Chem.* **2004,** *2004*, 5141.
(63) Negishi, E.-i.; Zhang, Y.; O'Connor, B., *Tetrahedron Lett.* **1988,** *29*, 2915.
(64) (a) Olah, G. A.; Narang, S. C.; Gupta, B. G. B.; Malhotra, R., *J. Org. Chem.* **1979,** *44*, 1247; (b) Lissel, M.; Drechsler, K., *Synthesis* **1983,** *1983*, 459.
(65) Kunai, A.; Kawakami, T.; Toyoda, E.; Ishikawa, M., *Organometallics* **1992,** *11*, 2708.
(66) Reid, W. B.; Spillane, J. J.; Krause, S. B.; Watson, D. A., *J. Am. Chem. Soc.* **2016,** *138*, 5539.

(67) (a) Iida, H.; Yuasa, Y.; Kibayashi, C., *J. Org. Chem.* **1980,** *45*, 2938; (b) Shaw, K. J.; Luly, J. R.; Rapoport, H., *J. Org. Chem.* **1985,** *50*, 4515; (c) Sakamoto, T.; Nagano, T.; Kondo, Y.; Yamanaka, H., *Synthesis* **1990,** *1990*, 215; (d) Michael, J. P.; Chang, S.-F.; Wilson, C., *Tetrahedron Lett.* **1993,** *34*, 8365; (e) Koerber-Plé, K.; Massiot, G., *Synlett* **1994,** *1994*, 759; (f) Chen, L.-C.; Yang, S.-C.; Wang, H.-M., *Synthesis* **1995,** *1995*, 385; (g) Chen, C.-y.; Lieberman, D. R.; Larsen, R. D.; Verhoeven, T. R.; Reider, P. J., *J. Org. Chem.* **1997,** *62*, 2676; (h) Henke, B. R.; Aquino, C. J.; Birkemo, L. S.; Croom, D. K.; Dougherty, R. W.; Ervin, G. N.; Grizzle, M. K.; Hirst, G. C.; James, M. K.; Johnson, M. F.; Queen, K. L.; Sherrill, R. G.; Sugg, E. E.; Suh, E. M.; Szewczyk, J. W.; Unwalla, R. J.; Yingling, J.; Willson, T. M., *J. Med. Chem.* **1997,** *40*, 2706; (i) Yamazaki, K.; Kondo, Y., *Chem. Commun.* **2002,** 210; (j) Ackermann, L.; Kaspar, L. T.; Gschrei, C. J., *Chem. Commun.* **2004,** 2824; (k) Watanabe, T.; Arai, S.; Nishida, A., *Synlett* **2004,** *2004*, 0907.
(68) Ichikawa, J.; Sakoda, K.; Mihara, J.; Ito, N., *J. Fluorine Chem.* **2006,** *127*, 489.
(69) Rigby, J. H.; Hughes, R. C.; Heeg, M. J., *J. Am. Chem. Soc.* **1995,** *117*, 7834.
(70) Mazzacano, T. J.; Mankad, N. P., *ACS Catal.* **2017,** *7*, 146.
(71) Pangborn, A. B.; Giardello, M. A.; Grubbs, R. H.; Rosen, R. K.; Timmers, F. J., *Organometallics* **1996,** *15*, 1518.
(72) (a) Becker, D.; Nagler, M.; Sahali, Y.; Haddad, N., *J. Org. Chem.* **1991,** *56*, 4537; (b) Clive, D. L. J.; Hisaindee, S., *J. Org. Chem.* **2000,** *65*, 4923.

Chapter 3

DISCOVERY AND DEVELOPMENT OF THE BORYL-HECK REACTION

3.1 Introduction and Overview

Unsaturated boronic esters are extremely valuable in organic synthesis and as materials; therefore, an efficient route to synthesize them is highly desirable. We have recently developed a palladium-catalyzed direct silylation of alkenes using electrophilic silanes (silyl-Heck reactions).[1] This work inspired us to reinvestigate the analogous boryl-Heck transformation. A boryl-Heck reaction would provide a direct route to alkenyl or allyl boronic esters directly from unfunctionalized alkenes (Figure 3.1).

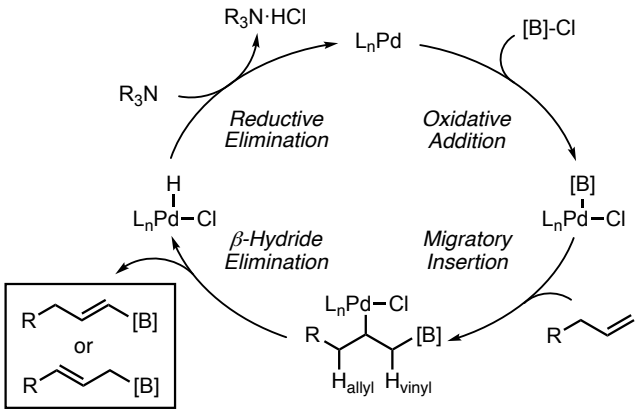

Figure 3.1 Proposed Boryl-Heck Reaction

Herein, I describe the successful palladium-catalyzed borylation of alkenes using readily available B-chlorocatechol borane (catBCl) as an electrophilic boron

source. This transformation converts a wide range of terminal mono-substituted alkenes into terminal *trans*-alkenyl boronic esters with excellent regio- and stereoselectivity. The labile catechol group of the initial products allows facile transesterification to a variety of boronic acid derivatives. This reaction avoids problematic reduction and overborylation products, utilizes an inexpensive boron source, and most importantly, demonstrates for the first time that electrophilic borylation reagents are compatible with a Heck-like catalytic cycle.

3.2 Applications of Alkenyl Boronic Esters

Organoboron compounds are among the most versatile reagents in synthetic chemistry.[2] The hydroboration of unsaturated bonds has made boronic acids and esters readily available and inexpensive. Easy access to these versatile reagents resulted in an explosion of novel C-C and C-Het bond forming reaction in the 1970's. These reactions have since revolutionized organic synthesis and led to countless scientific breakthroughs that have impacted the world today. The major utility of this class of compounds is use as cross-coupling reagents in organic synthesis. Alkenyl boronic esters, in particular, have gained great interest in recent years, as they participate in a variety of transformations, including Suzuki-Miyaura cross-couplings[2] and Petasis reactions.[3] The Suzuki-Miyaura reaction is commonly employed in industrial syntheses of pharmaceutical and fine chemicals because, it is cost efficient and scalable. These reagents can also be used to forge C-O, C-N, C-F, C-Br and C-I bonds.[4] In addition to being invaluable synthetic reagents, organoboronic acids have recently been introduced in to pharmaceutical frameworks being incorporated into drugs and other therapeutic applications including as anti-cancer, viral, fungal and bacterial agents.[5]

3.2.1 Suzuki-Miyaura Cross-Coupling

The Suzuki-Miyaura cross-coupling reaction was first reported by Akira Suzuki and Norio Miyaura in 1979.[6] They originally reported the coupling of alkenyl boronic esters, formed from hydroboration of alkynes, with aryl and alkenyl halides. This reaction has since evolved into one of the most commonly applied reactions in modern organic synthesis.[2, 7] The recognition of the potential of this reaction led to a Nobel prize, awarded to Suzuki, Negishi and Heck for their contributions to the development of cross-coupling chemistry.

The Suzuki reaction is a commonly utilized method for the formation of new C-C bonds in both academia and industry. The low toxicity associate with boron makes it an ideal reagent for large scale reactions. Additionally, organoboronic acids and esters are relatively stable when compared to other cross-coupling nucleophiles such as organolithium, organomagnesium, and organozinc reagents. The general utility of this reaction has been displayed again and again over the years demonstrating that virtually any boronic acid derivative can be coupled with any electrophile to form a new carbon-carbon bond (Figure 3.2).[2]

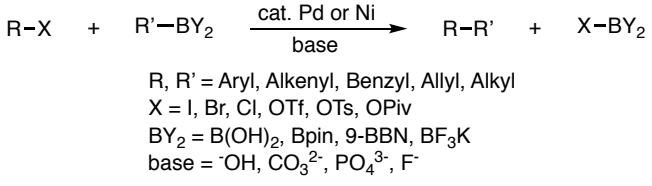

Figure 3.2 General Scheme of the Suzuki Reaction

The generally accepted mechanism for the Suzuki-Miyaura reaction is displayed in Figure 3.3. Oxidative addition of palladium into a carbon-halide bond, results in

formation of intermediate **3.3**. Transmetallation of the R' group from boron to palladium forms intermediate **3.6** which can reductively eliminate to forge the new C-C bond and regenerate the active palladium catalyst (**3.1**).

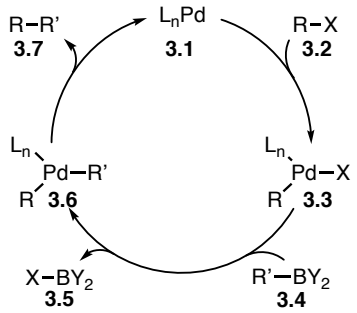

Figure 3.3 General Mechanism of the Suzuki Reaction

In the majority of cases, with trivalent boron, a stoichiometric excess of base is required for transmetallation. The base coordinates to the vacant *p*-orbital on boron forming a borate complex *in situ*. The high electron density on the borate, caused by the negative charge, makes the carbon ligand on boron significantly more nucleophilic and facilitates its transmetallation to palladium.

The hydroboration of alkynes creates rapid access to various functionalized alkenyl boronic ester derivatives. This makes for very accessible cross-coupling partners and has resulting in the synthesis of a wide range of natural products using a Suzuki reaction.[8] In one example, a leukotriene B_4 precursor was synthesized on a multi-gram scale (Figure 3.4).[9] Using a Suzuki reaction between **3.9** and **3.10**, Sato was able to make 1.2 grams of compound **3.11** in 70% yield.

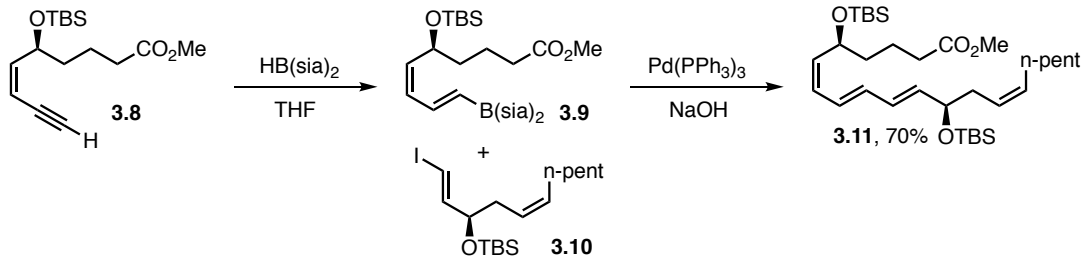

Figure 3.4 Multigram Synthesis of Leukotriene B_4 Precursor

Organotrifluoroborates are much more stable and easier to handle than boronic acids or esters. They are generally white crystalline solids and indefinitely stable to air. Additionally, they can be easily prepared with the addition of potassium bifluoride (KHF_2) to a variety of boronic acid derivatives. Work form the Molander group has popularized the synthesis and applications of alkenyltrifluoroborates in many organic reactions including the Suzuki reaction (Figure 3.5).[10] This reaction displays high functional group tolerance with a variety of terminal and internal alkenyl trifluorborate substrates.

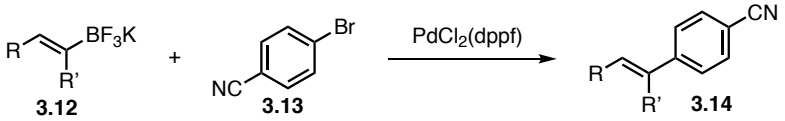

entry	R =	R' =	product	yield
1	n-oct	H	**3.14a**	87%
2	H	Me	**3.14b**	70%
3	H	H	**3.14c**	76%
4	Ph	H	**3.14d**	80%
5	$Cl(CH_2)_3$	H	**3.14e**	52%
6	Et	Et	**3.14f**	70%

Figure 3.5 Molander's Suzuki Reaction of Alkenyl Trifluoroborates

3.2.2 Petasis Reaction

Functionalized amines are routinely found in biological, pharmaceutical, and natural compounds. In addition, amines can serve as ligands for transition metal catalysis or as catalysts themselves in organocatalysis. They also serve as instrumental precursors in the preparation of many polymers and materials. One general method for the preparation of these versatile chemicals is the organometallic addition to an unsaturated C-N bond (imines, nitriles, etc.). Many of these organometallic nucleophiles are considered harsh reagents and are sensitive to air and moisture, which can limit the functional group tolerance of the reaction.

Organoboranes, on the other hand, are considered much milder organometallic reagents. They are generally air and moisture stable, relatively functional group tolerant, and have a significantly lower toxicity associates with them. The Petasis reaction is the three-component coupling reaction of aldehydes, amines, and organoboronic esters (Figure 3.6).[2-3] When alkenyl boronic esters are utilized, allylic amines can be synthesized with great diversity (Figure 3.6, bottom).

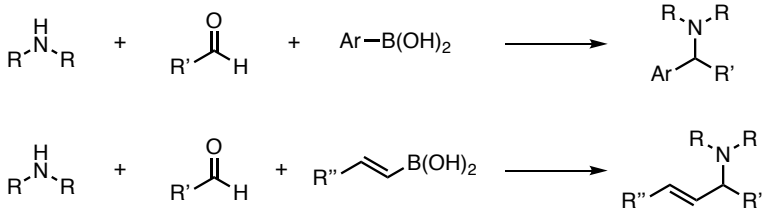

Figure 3.6 General Scheme of the Borono-Mannich (Petasis) Reaction

This operationally simple reaction was first reported by Petasis and Akritopoulou in 1993.[11] Anhydrous and degassed solvents are not required and the

reaction byproducts generally have low toxicity. The mechanism of this transformation involves the condensation of an amine with an aldehyde to form an iminium ion or hemi-aminal (Figure 3.7). Transfer of the carbon group from boron to the iminium forms a new C-C bond attached to an amine.

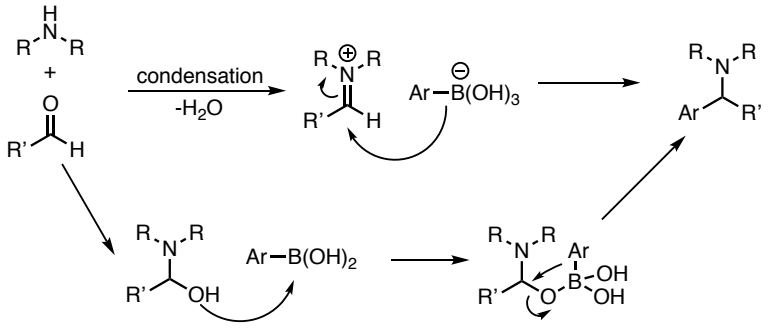

Figure 3.7 Mechanism of the Petasis Reaction

This reaction is highly stereospecific with respect to the geometry of the alkenyl boronic ester and proceeds with excellent diastereoselectivity.[12] Using a chiral biaryl phenol catalyst, enantioenriched allylic amines can be synthesized with good yields and high enantiomeric excess.[13]

3.2.3 Heteroatomic Functional Group Conversions

The Suzuki and Petasis reactions are essentially functional group conversions from boron to carbon. However, the versatility of boronic esters is not limited to forging new C-C bonds. These reagents can also be used to forge new C-O, C-N, C-S, C-F, C-Br and C-I bonds. The Chan-Lam-Evans cross-coupling reaction readily converts C-B bonds into C-N, C-O, or C-S bonds using stoichiometric or catalytic copper salts.

Alkenyl boronic esters can also be converted in to stereodefined alkenyl halides which switches the polarity of the compound from a nucleophile to an electrophile.

3.2.3.1 Chan-Lam-Evans Reaction

Nitrogen and oxygen containing compounds are very useful as drugs, pharmaceuticals, polymers, and materials. The formation of a new C-N or C-O bond is therefore a very desirable task. These bonds can be formed in a variety of ways including non-catalyzed reactions such as substitution reactions and transition metal catalyzed Buchwald-Hartwig amination. Both of these involve carbon electrophiles, such as halides or other activated leaving groups and free alcohols or amines. In 1998, three groups reported the copper promoted cross-coupling between heteroatomic nucleophiles and aryl boronic esters.[14] This reaction became known as the Chan-Lam-Evans reaction and has revolutionized the synthesis of aryl ethers, amines, and thioethers (Figure 3.8).[2, 15]

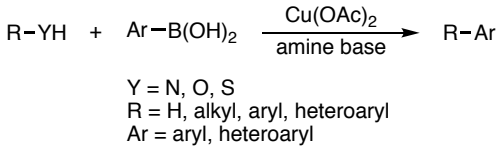

Figure 3.8 General Scheme of the Chan-Lam-Evans Reactions

The reaction mechanism of this reaction is not well understood; however, some general trends and observations have been reported over the years. Electronic effects were studied on the coupling of phthalimides and aryl boronic acids.[2] Electron rich phthalimides performed better than electron deficient ones, however, electronics on the

boronic acid partner had little effect on rate. The addition of radical trap 1,1-diphenylethylene has no effect on the reaction. This suggests that the reaction does not proceed *via* a free radical pathway. However, the reaction can be catalyzed by copper if oxygen is added to turn over the catalytic cycle.[16]

N- and O-vinyl functional groups can be used as protecting groups and easily cleaved using ozonolysis or acidic hydrolysis. Thus, a Chan-Lam coupling reaction between alkenyl boronic esters and amines and alcohols would be of great value to the synthetic community. In 2003, Lam reported a copper promoted C-N and C-O bond cross coupling with alkenyl boronic esters (Figure 3.9).[17] Using a $Cu(OAc)_2$, the cross-coupling of alkenyl boronic esters with variety of heterocyclic nucleophiles proceeded with excellent yields.

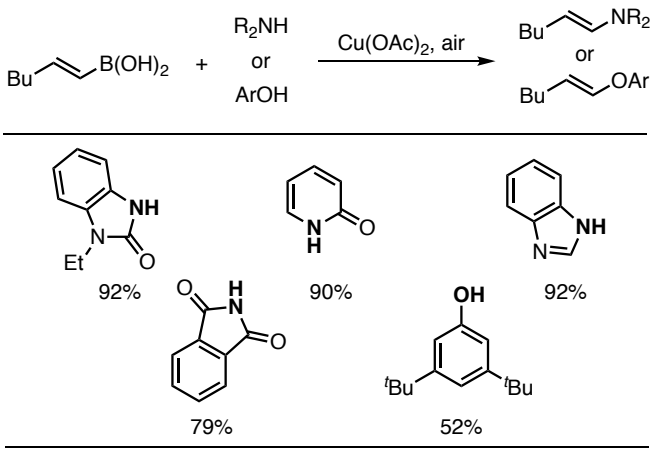

Figure 3.9 Chan-Lam-Evans Coupling of Alkenyl Boronic Esters

Since Lam's seminal report with alkenyl boronic esters, several other groups have investigated their use in copper promoted cross-coupling reactions. In 2008, Batey

reported the synthesis of a variety of enamides via a copper catalyzed cross-coupling of free amides and alkenyl trifluoroborates.[18] Merlic discovered conditions for the coupling of alkenyl pinacol boronic esters with aliphatic alcohols and silanols further expanding the utility of the Chan-Lam-Evans reaction.[4b, 19]

3.2.3.2 Halogenation of Alkenyl Boronic Esters

One of the oldest applications of alkenyl boronic esters is the halogenation to form alkenyl halides. The earliest reports of deboronohalogenation describe a stereospecific synthesis of alkenyl bromides and iodides from alkenyl boronic esters.[4a, 20] Interestingly, bromination of alkenyl boronic esters proceeds with inversion of alkene geometry while iodination proceeds with retention. The accepted mechanisms for bromination and iodination, and thus origin of stereoselectivity, were determined by Matteson[20a] and Brown[20b] respectively (Figure 3.10).

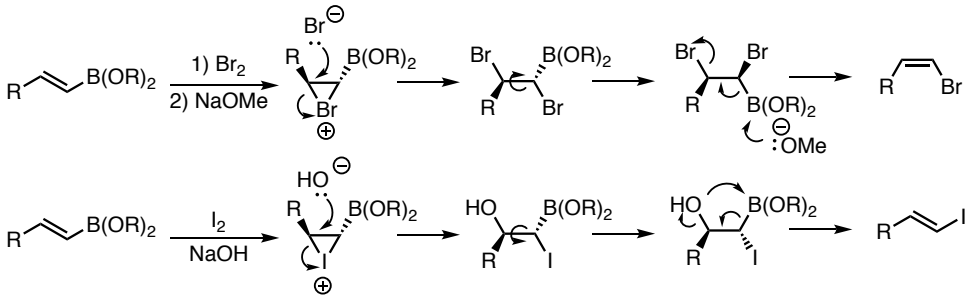

Figure 3.10 Stereochemical Model for Deboronohalogenation

More recently, the fluorination of aryl and alkenyl boronic esters has been made possible.[4c, 21] While this field has been mostly focused on the fluorination of aryl boronic esters due to their prevalence in pharmaceuticals, these methods have been

shown to be effective with alkenyl boronic esters as well. Ritter showed that silver could mediate the regioselective fluorination of aryl and alkenyl boronic acids (Figure 3.11). Combining **3.15** with AgOTf and NaOH undergoes transmetallation of silver to form **3.16**, which can be isolated. Subsequent fluorination with SelectFluor leads to vinyl fluoride **3.17**.

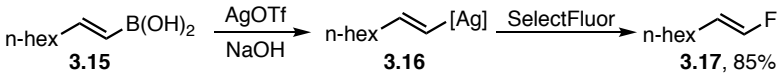

3.15 **3.16** **3.17**, 85%

Figure 3.11 Silver Promoted Fluorination of Alkenyl Boronic Esters

Sanford and Scott have discovered a rapid way to incorporate ^{18}F in the fluorination of boronic acids for the development of PET radiotracers.[21c] In a related transformation, the Buchwald group has reported an iron catalyzed method for the trifluoromethylation of alkenyl trifluorobornates.[22] The trifluoromethyl group has had a significant impact on the discovery and development of biologically active molecules.

3.2.3.3 Oxidation to Carbonyls

In addition to the Chan-Lam coupling, the C-B bond can be converted into a C-O bond *via* oxidation of alkenyl boronic esters. In this case, however, the direct product is a labile boron enolate which rapidly decomposes and tautomerizes to the more stable carbonyl (Figure 3.12). Since it was first reported by Brown,[23] many oxidants have been used to oxidize alkenyl boronic esters.[24]

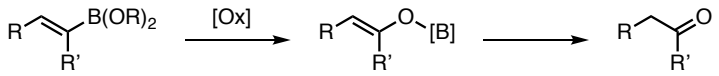

Figure 3.12 Oxidation of Alkenyl Boronic Esters to Carbonyls

The oxidation of terminal alkenyl boronic esters into aldehydes has become a common practice in the total synthesis of many natural products. Hydroboration of terminal alkynes can be followed with oxidation to get the aldehyde group (Figure 3.13, top).[23] Dansishefsky developed a two-step process for the conversion of terminal alkene to an aldehyde using cross-metathesis followed by oxidation (Figure 3.13, bottom).[25] This sequence typically uses trimethylamine N-oxide (Me_3NO) as the oxidant and has been utilized in many total syntheses.[24, 26]

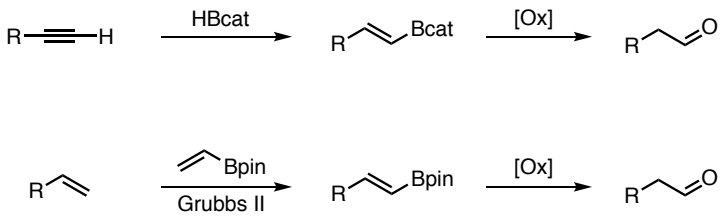

Figure 3.13 Two-Step Sequence to form Aldehyde from Alkynes or Alkenes

3.2.4 Biological Applications

Boron has long been considered biologically inert due to the lack of C-B bonds found in natural products. However, the vacant *p*-orbital gives boron very unique properties in biological environments. Additionally, the lack of toxicity associated with boron makes it an ideal candidate for incorporation into biologically relevant molecules and drugs. Many recent reviews have been written on the utility of varying boron

containing fragments from single molecules,[5f, 27] to polymers,[5a, 5e] to boron neutron capture therapy.[5d]

In fact, in 2003, the first boron containing drug was approved by the FDA. Bortezomib was approved as a proteasome inhibitor for treatment of multiple myeloma and other cancers (Figure 3.14).[28]

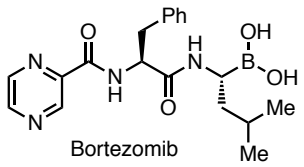

Figure 3.14 Structure of Bortezomib; The First FDA Approved Boron Containing Drug

Since then there has been an explosion of boron containing compounds examined for biological activity with many compounds in varying stages of approval.[5b, 5c, 5f, 29] Boron containing organic compounds have also seen new applications in diagnosis and theroputics.[5c, 30] Boron is typically incorporated *via* attachment to sugars, carbohydrates, or peptides.[31] However, benzoboroxoles have become an interesting class of compounds.[30, 32]

3.3 Known Synthesis of Alkenyl Boronic Esters

Due to the high synthetic utility of alkenyl boronic esters, a variety of methods for their synthesis have been developed. Most commonly used, alkyne hydroboration is a simple way to access these versatile compounds. This method however required the higher oxidation state of the alkyne to be reduced to the product. Starting from the alkene oxidation state, several methods have been developed and utilized over the years.

Miyaura borylation is a popular method coupling nucleophilic boron reagents with sp^2-electrophiles. On the other hand, organometallic nucleophiles can be added to electrophilic borates or chloroboranes to form new C-B bonds. These methods required prefunctionalized alkenes, some of which are very reactive and difficult to handle. The most optimal route to alkenyl boronic esters would be directly from unfunctionalized alkenes. Cross-metathesis and dehydrogenative borylation have become popular for this direct approach however each has some drawbacks. Both of these methods produce product in moderate yields, however, regioselectivity and dimerization can create undesired side products which cannot be separated. Each of these approaches along with advantages and disadvantages will be discussed below.

3.3.1 Hydroboration

Alkyne hydroboration is perhaps the most common method for the synthesis of alkenyl boronic esters.[33] This approach is high yielding and highly regioselective with terminal alkynes. The mechanism of the uncatalyzed alkyne hydroboration involves the concerted *syn*-addition of the boron and hydrogen atoms across a carbon-carbon triple bond (Figure 3.15, top). In all uncatalyzed reactions, this leads to the *trans*-product due to the *syn*-facial addition of the borane and hydrogen atoms, however, several catalysts exist for synthesis of the *cis*-product. The uncatalyzed reaction goes through a four-membered transition state which explains the observed regioselectivity.

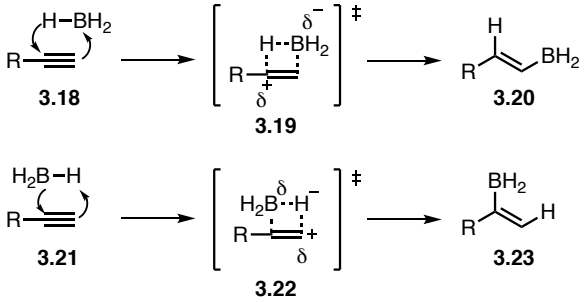

Figure 3.15 Mechanism of Alkyne Hydroboration

The borane adds in an *anti*-Markovnikov fashion adding the boron atom to the less substituted carbon of the alkyne. The π-electrons of the alkyne coordinate to the electro positive boron leaving a partial positive charge at either the internal or terminal carbon (**3.19** and **3.22** respectively). The internal carbon can better stabilize a positive charge, therefore transition **3.19** is lower in energy leading to the observed product.

3.3.1.1 Early Reports of Uncatalyzed Hydroboration

In 1972, Brown reported the use of catecholborane (catBH) as a hydroboration reagent for this mild synthesis of alkenyl catechol boronic esters (Figure 3.16, top).[23, 34] Unfortunately, the catechol ester is air and moisture sensitive, making it difficult to purify, often leading to complex mixtures of products. Upon examining other hydroboration reagents, pinacolborane (pinBH) was found to be an advantageous alternative with good reactivity, excellent selectivity and stable isolable products (Figure 3.16, Bottom).[35]

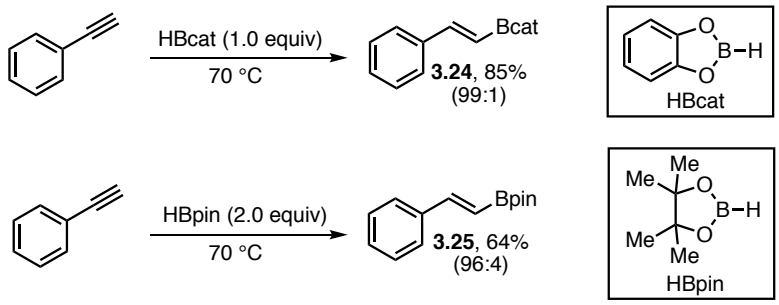

Figure 3.16 Early Examples of Uncatalyzed Alkyne Hydroboration

3.3.1.2 Metal Catalyzed Alkyne Hydroboration

Although the uncatalyzed reaction can give high yields and good selectivity, catalyzed reactions can offer several advantages including lower temperatures, different regioselectivity, and better functional group tolerance. In 1995, Srebnik reported the zirconium catalyzed hydroboration of alkynes with pinacolborane (Figure 3.17).[36]

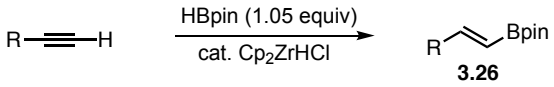

R =	product	yield	ratio of **3.26**/ other isomers
n-hex	**3.26a**	93%	98:2
$Cl(CH_2)_3$	**3.26b**	94%	97:3
Me_3Si	**3.26c**	87%	90:10
Cyp	**3.26d**	94%	98:2
Ph	**3.26e**	75%	97:3
$Ph(CH_2)_3$	**3.26f**	87%	98:2

Figure 3.17 Zirconium Catalyzed Hydroboration

Using 5 mol % of Schwartz's reagent, this method allows for the formation of alkenyl boronic esters at 25 °C with only 1.05 equivalents of pinacolborane. This

method shows good yields and selectivities as well as improved functional group tolerance. More recently, this approach has been used in the synthesis of macrocyclic dienes[37] and has been applied in many total synthesis.[38]

Soon after his initial publication, Srebnik reported the rhodium catalyzed hydroboration of alkynes using Wilkinson's catalyst.[39] While this reaction gave excellent yields, the regioselectivity dropped to 50-70%. However, altering the precatalyst by replacing one of the triphenylphosphine ligands with carbon monoxide, excellent yields and selectivities (>99:1) can be obtained (Figure 3.18).

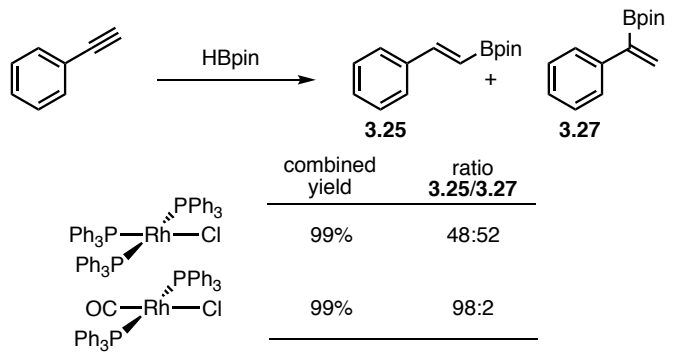

Figure 3.18 Selectivity of Rhodium Catalyzed Alkyne Hydroboration

The *trans*-selective synthesis of alkenyl boronic esters was made possible with a rhodium/triisopropylphosphine catalyst and triethylamine.[40] Using a deuterated alkyne, Miyaura found that that product contained the deuterium atom *trans* to the added catechol borane, suggesting that a 1,2-shift occurs. This result led Miyaura to propose an alternative mechanism for the formation of the *Z*-alkenyl boronic esters. Miyaura's originally proposed mechanism was reexamined using density functional theory (DFT)

calculations and a slightly modified and more complete view of the mechanism was proposed (Figure 3.19).[41]

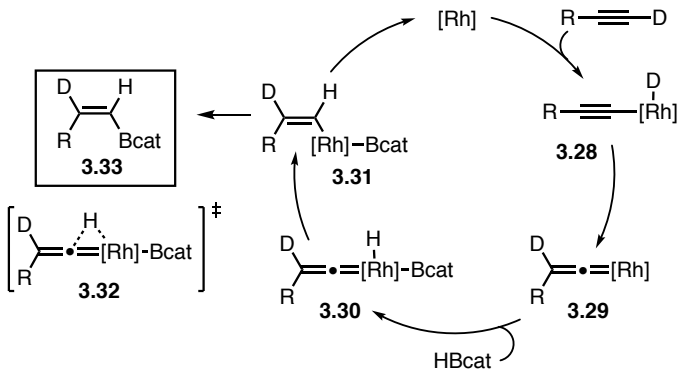

Figure 3.19 Mechanism of *Trans*-Hydroboration of Terminal Alkynes

Oxidative addition of rhodium into the carbon hydrogen bond leads to intermediate **3.28** which can isomerize to a vinylidene complex **3.29**. This step accounts for the 1,2-shift of the deuterium from the terminal position to the internal position. The rhodium carbine **3.29** can oxidatively add into a B-H bond of catechol borane and undergo a 1,2-migration of the metal hydride to form intermediate **3.31**. Carbo and Fernandez postulate that the *cis*-geometry of **3.31** is caused by the irreversible 1,2-migration of the metal-hydride to carbon (**3.32**). Reductive elimination of **3.31** leads to **3.35** which is the deuterated product as observed by Miyaura.

Bispinacol boronate, which is more stable and easier to handle than pinacol borane, can be used with stoichiometric copper to convert alkynes into alkenyl boronic esters. In 2001, Miyaura reported a copper promoted Cu-B addition to terminal alkynes (Figure 3.20).[42] Due to the mild conditions and experimentally simple setup, this has become a popular and well-studied method for the synthesis of alkenyl boronic esters.[43]

The mechanism is thought to be the addition of an *in situ* formed Cu-B complex (**3.34**) across an alkyne to form intermediate **3.35**. Protonation with water or methanol results in the formal hydroboration product **3.25**.

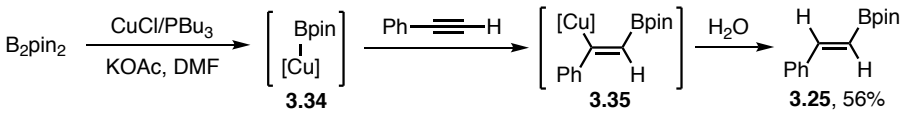

Figure 3.20 Miyaura's Copper Promoted Formal Hydroboration of Alkynes

3.3.2 Miyaura Borylation

With the advent of modern cross-coupling reactions, an endless supply of sp^2-hybridized electrophiles have become widely available. In 1995, Miyaura discovered a novel method for the direct borylation of these organic electrophiles converting them into nucleophilic boronic esters (Figure 3.21).[44]

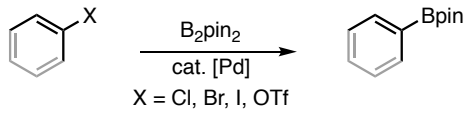

Figure 3.21 Miyaura Borylation of Organic Electrophiles

Nucleophilic addition of alkenyl organometallic reagents to boron electrophiles is a common method for the synthesis of simple alkenyl boronic esters, however, with more complicated substrates, it is often difficult to retain stereochemistry and the harsh nature of the organometallic reagents limits the functional group tolerance. Miyaura borylation provides a much milder route to similar and new products.[2] Additionally, all

the components of a typical reaction are stable and easily handled greatly simplifying the reaction. While aryl electrophiles are commonly employed as substrates in this reaction, the use of alkenyl halides results in the formation alkenyl boronic esters. This reaction proceeds with complete retention of stereochemistry and is compatible with a variety of functional groups.[45]

The mechanism of this transformation is similar to the Suzuki reaction except a boron group undergoes transmetallation to the transition metal center rather than a carbon group (Figure 3.22). Oxidative addition of palladium into a carbon-halide bond, results in formation of intermediate **3.36**. Transmetallation of one of the two boron groups from B_2pin_2 to palladium forms intermediate **3.37** which can reductively eliminate to forge the new C-C bond and regenerate the active palladium catalyst. Similar to the Suzuki reaction, a base is also needed to activate the diboron reagent for transmetallation.

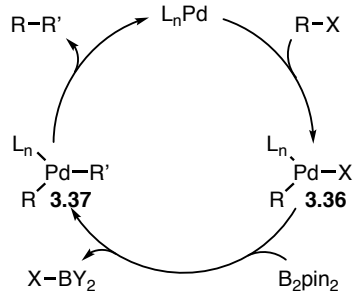

Figure 3.22 Mechanism of the Miyaura Borylation

3.3.3 Syntheses from Other Prefunctionalized Alkenes

Alkenyl boronic esters can also be synthesized from nucleophilic addition of organometallic reagents to electrophilic boron reagents (Figure 3.23). Typically, this

requires formation of a reactive organometallic reagent such as a Grignard or lithium reagent and slow addition to a cooled solution of the boron electrophile. While Grignard reagents are the most common, many other organometallic nucleophiles have also been utilized in this reaction.

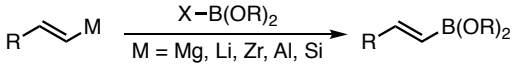

Figure 3.23 Alkenyl Boronic Ester Synthesis *via* Nucleophilic Addition of an Organometallic Reagent

The nucleophile addition of Grignard reagents to boronic electrophiles such as trialkylborates dates to 1926.[46] Gilman was able to synthesize phenyl boronic acid from phenylmagnesium bromide and trimethylborate observing benzene and methanol as byproducts. For the synthesis of alkenyl boronic esters, alkenyl nucleophiles are required (Figure 3.24). In 1966, Hunter reported the synthesis of vinyl boronic ester **3.39** using vinyl magnesium chloride and borate **3.38** (Figure 3.24, top). This reaction must be carried out at very low temperatures (–70 °C) to obtain a useful yield, when run at –10 °C there was only 40% yield of **3.39**.

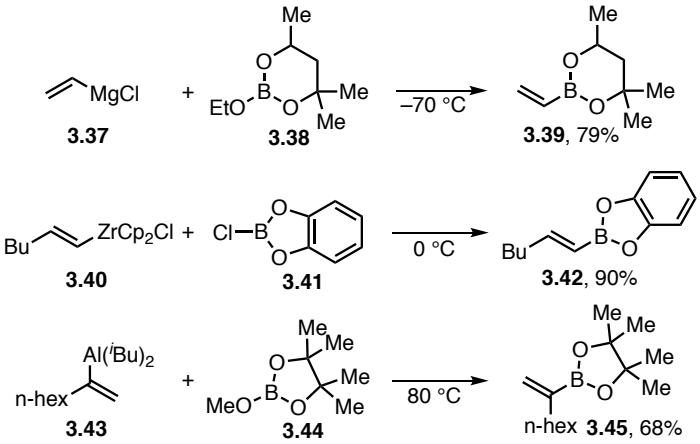

Figure 3.24 Addition of Alkenyl Nucleophiles to Boron Electrophiles

In 1991, Cole reported the transmetallation of organozirconium reagents to boron (Figure 3.24, middle). Using catBCl (**3.41**), alkenyl boronic esters can be formed under much more mild reaction conditions. Additionally, nucleophilic zirconium reagents (**3.40**) can be easily synthesized from the hydroziconation of terminal alkynes with Schwartz's reagent.[47] More recently, Hoveyda reported a unique method to synthesize internal alkenyl boronic esters (Figure 3.24, bottom).[48] The key to this approach is a nickel-catalyzed Markovnikov hydroalumination of terminal alkynes. This reaction provides a facile and selective route to internal alkenyl aluminum reagents (**3.43**) and nucleophile addition to borate **3.44** gives moderate yields of alkenyl boronic esters (**3.45**).

Alkenyl boronic esters can also be synthesized from milder organometallic reagents such as a vinyl silanes. The conversion of aryl silanes into aryl boronic esters with the use of boron trichloride (BCl_3) has been known since the late 1980's.[49] In 1995, Naso was the first to apply this principle to the synthesis of alkenyl boronic esters

(Figure 3.25).[50] While this method utilizes milder organometallic reagents and results in good yields, the use of BCl_3 hinders the method's functional group tolerance.

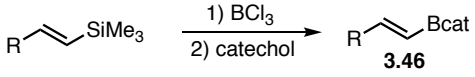

3.46

R =	product	yield
Ph	**3.46a**	79%
4-MeC_6H_4	**3.46b**	88%
n-Bu	**3.46c**	89%

Figure 3.25 Conversion of Vinyl Silanes to Alkenyl Boronic Esters

These methods, including Miyaura borylation, require prefunctionalized alkenes as starting materials. The organometallic reagents are typically synthesized from alkenyl halides or alkynes, which themselves can require multiple steps to prepare. In addition, several of these methods required the use of harsh and reactive organometallic reagents which can be difficult to prepare and handle. This reduces the functional group tolerance permitted with these reactions and limits the practicality of their use. Methods to synthesize alkenyl boronic esters directly from alkenes would be very advantageous to the synthetic community.

3.3.4 Alkene Cross Metathesis

Over the past several decades, alkene cross-metathesis has become a widely developed method for the synthesis of a diverse range of substituted alkenes.[51] This strategy has been applied to many total syntheses[52] and has become so commonplace that even general rules for predicting selectivity have been developed.[53] The widely

accepted mechanism was first proposed by Hérisson and Chauvin in 1971 (Figure 3.26).[54]

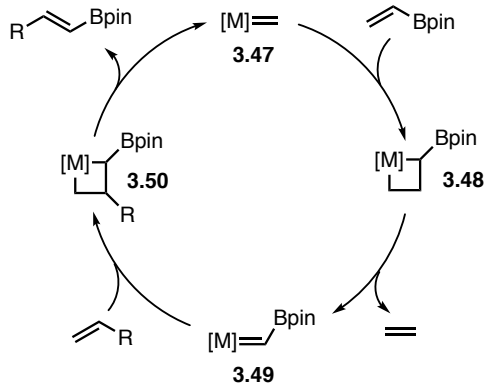

Figure 3.26 Chauvin Mechanism for Cross-Metathesis

This mechanism involves the formation of a metallacyclobutane (**3.48**) from the [2+2] addition of an alkene and a metal alkylidene. Normally, a [2+2] cycloaddition is symmetry forbidden, resulting from a very high activation barrier, however, the interaction of the alkene with the d-orbitals of the metal alkylidene lowers the energy enough to react at modest temperatures. After the formation of **3.48**, a cycloreversion expelling ethylene results in the formation of a different alkylidene (**3.49**). An alkene can then react with **3.49** in a similar fashion to form metallacyclobutane **3.50** which can form product and regenerate the active metal alkylidene **3.47**.

Using simple vinyl boronic esters, alkene metathesis can provide one route to substituted alkenyl boronic esters directly from unactivated alkenes. Despite this seemingly simple approach, few reports on the synthesis of alkenyl boronic esters *via* cross-metathesis exist in the literature.

3.3.4.1 General Cross-Metathesis

In 1998, Renaud reported the first example of a cross-metathesis reaction involving an alkenyl boronic ester.[55] This report demonstrates the ring-closing metathesis of alkenyl boronic esters tethered to pendant alkenes to form cyclic alkenyl boronic esters (Figure 3.27). Using Grubbs 1st generation catalyst with boronic acids, yields were limited to about 50%, however, using the more stable pinacol boronic ester, five-, six-, and seven-membered carbo- and heterocyclic rings were formed in good to excellent yields.

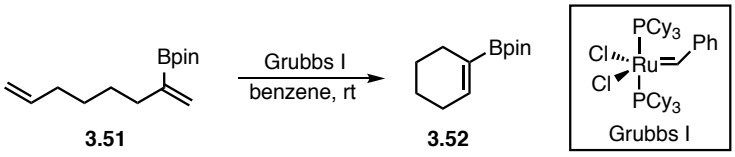

3.51 **3.52**

Figure 3.27 Renaud's Intramolecular Ring Closing Metathesis

Grubbs reported the first example of a bimolecular cross-metathesis reaction to form a linear alkenyl boronic ester with a single example in 2000.[56] Subsequent studies exploring the scope and generality of this method revealed that the use of ruthenium based catalysts generally results in selective *E*-vinyl boronic ester formation (Figure 3.28).[4a, 57] Formation of disubstituted alkenyl boronic esters (**3.53**) proceeds in moderate to excellent yields (55-99%),[4a] however, the synthesis of trisubstituted products gave severely reduced yields (30-59%) (**3.54**).[57b]

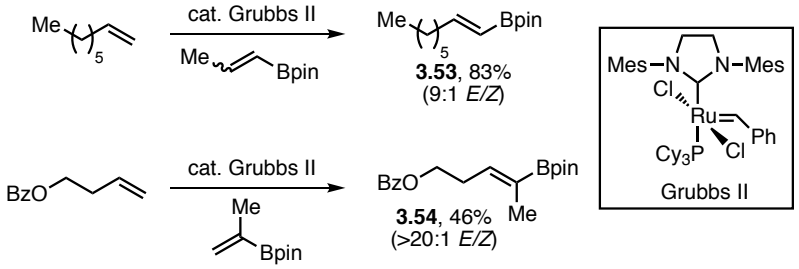

Figure 3.28 Bimolecular Cross-Metathesis to Form Alkenyl Boronic Esters

The *Z*-selective formation of linear alkenyl boronic esters *via* cross-metathesis was made possible with a Mo-based monoaryloxide pyrrolide (MAP) complex.[58] A variety of alkenyl boronic esters were synthesized with excellent yields and *Z*-selectivities (Figure 3.29).

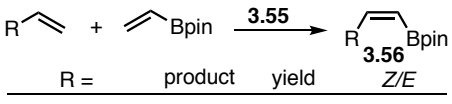

R =	product	yield	*Z/E*
n-oct	**3.56a**	68%	90:10
Cy	**3.56b**	51%	93:7
CH_2OTBS	**3.56c**	70%	96:4
CH_2phthal	**3.56d**	71%	93:7
O*n*Bu	**3.56e**	80%	93:7
CH_2Bpin	**3.56f**	60%	97:3

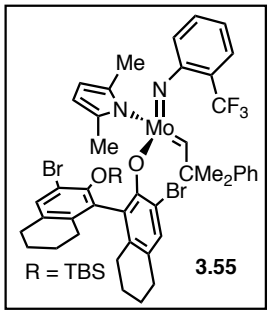

Figure 3.29 *Z*-Selective Cross-Metathesis to Form Alkenyl Boronic Esters

Cross-metathesis of alkenyl boronic esters has also been applied in the total synthesis of a few molecules.[25, 59] Danishefsky used this strategy to set-up for an intramolecular Suzuki reaction to form Epothilone 490, a 16-membered macrocycle (Figure 3.30).[25]

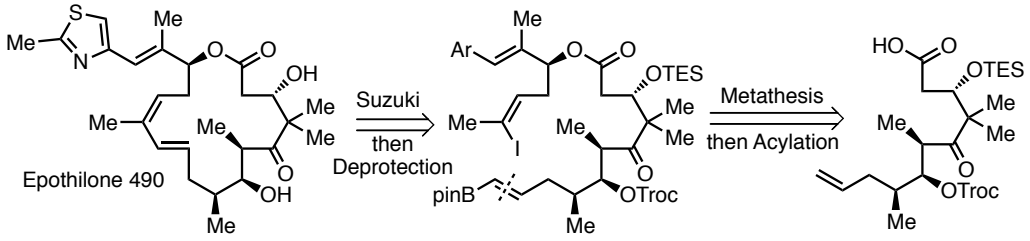

Figure 3.30 Danishefsky's Synthesis of Epothilone 490

3.3.4.2 Condensation Cross-Metathesis

Another approach to the synthesis of *Z*-alkenyl boronic esters is an intramolecular ring closing metathesis (RCM) to form cyclic alkenyl boronic half acids (Figure 3.31, top).[60]

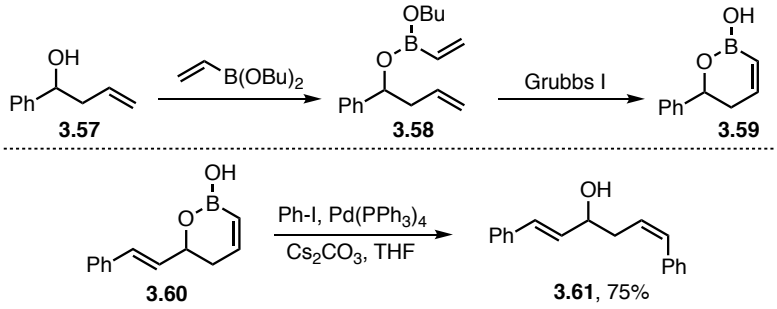

Figure 3.31 Transesterification and Ring Closing Metathesis

This reaction is distinct from the original work from Renaud in that the tethered alkene is linked via a B-O bond. The transesterification of an unsaturated boronic ester with a homoallylic alcohol (**3.57**) provides a transient, mixed organoboronic ester (**3.58**) which can be trapped using RCM with Grubbs 1st generation catalyst. Products from this RCM such as **3.60** can be further manipulated in a stereoretentive fashion to form compound **3.61** in a single step. This RCM has also been applied asymmetrically for the

desymmetrization of symmetric achiral allylic alcohols to form optically active unsaturated cyclic boronic esters.[61]

3.3.4.3 Trans-Borylation

In a related reaction, Marciniec has reported the cross-coupling of non-isomerizing olefins with vinyl substituted boronic esters (Figure 3.32, top).[62]

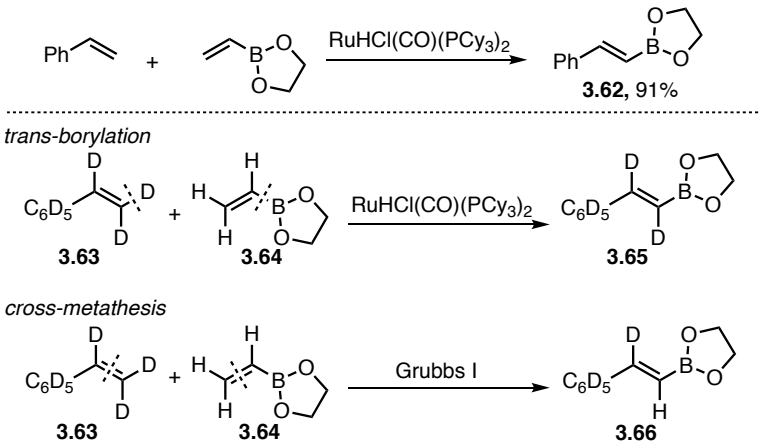

Figure 3.32 Marciniec's Trans-Borylation Reaction and Deuterium Labeling Studies

Using a ruthenium hydride complex [$RuHCl(CO)(PCy_3)_2$], instead of the ruthenium carbine (Grubbs catalyst) used in traditional olefin metathesis, Marciniec has shown that this reaction proceeds *via* a C-H cleavage rather than C-C cleavage (Figure 3.32, bottom).[62a] Deuterium labeling studies with styrene-d_8 (**3.63**) indicated that the carbon-boron bond of the vinyl substituted boronic ester (**3.64**) is cleaved presumably forming a ruthenium boron complex which reacts with styrene to form product. Conversely, the same labeling study with Grubbs 1st generation catalyst, indicates the carbon-carbon double bond is cleaved, as expected for classical cross-metathesis (*vide*

supra). These results combined with a series of stoichiometric experiments[62a] led Marciniec to propose the following mechanism (Figure 3.33).

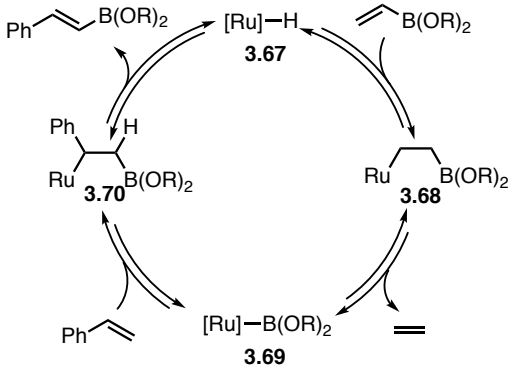

Figure 3.33 Mechanism of Marciniec's *trans*-Borylation Reaction

The mechanism begins with migratory insertion of the vinyl boronic ester into the ruthenium hydride bond to form an alkyl ruthenium complex **3.68**. β-boryl elimination results in the expulsion of ethylene and the formation of a ruthenium boron complex (**3.69**). Migratory insertion of a styrene forms a second alkyl ruthenium complex (**3.70**) which can undergo β-hydride elimination to form product and regenerate the active ruthenium hydride **3.67**. DFT calculations from the Marder group support this proposed mechanism.[63]

3.3.4.4 Synthesis of Starting Materials

While these approaches allow for the synthesis of a variety of alkenyl boronic esters with good yields and selectivity for *E*- or *Z*-products, there are still some inherent drawbacks to this approach. This method requires preformed vinyl or propenyl boronic esters as coupling partners. These substrates require multiple steps to form and are

therefore expensive to purchase or time consuming to prepare. These reagents are typically prepared from a step intensive nucleophilic addition of an alkenyl group to BCl_3 or $B(OMe)_3$ (Figure 3.34).

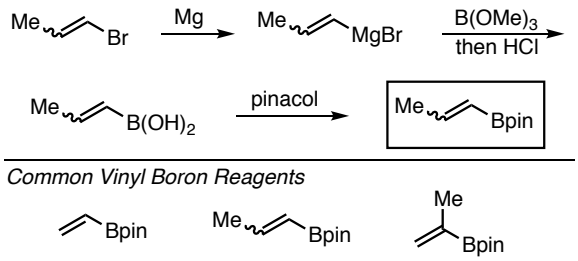

Figure 3.34 Synthesis of Common Vinyl Boronate Reagents

3.3.5 Heck Reactions

Using the same vinyl boronic esters as cross-coupling partners, one could imagine a Heck reaction, to add substitution, rather than olefin metathesis. Unfortunately, the Suzuki reaction uses nearly identical reagents and conditions which makes selecting for one reaction over the other a very difficult task. In the early '90s, Whiting studied the reaction of B-vinyl pinacolborane with these cross-coupling conditions (Figure 3.35).[64]

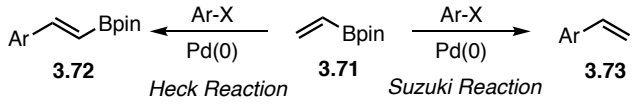

Figure 3.35 Heck vs. Suzuki Reaction of Pinacol Vinyl Boronic Ester

Compound **3.71** can potentially react *via* a Heck or Suzuki reaction to form vinyl boronate **3.72** or styrene **3.73** respectively. With this train of thought **3.71** can be considered a *trans*-vinyl dianion equivalent since the Heck coupling would lead to a functionalized vinyl boronic ester which can undergo further cross-coupling. Particularly, Whiting was interested in exploring how various sets of reaction conditions effected the selectivity of one reaction verse the other.

3.3.5.1 Deciphering Between Heck and Suzuki Pathways

From his initial studies,[64a] Whiting made several general observations. First, there was no general trend among the reactivity of aryl halides. Various reaction conditions were screened against each aryl halide to find the best conditions for both reaction pathways. Second, it was found that reactions conducted at lower temperatures tended to favor the Heck product over the Suzuki product, suggesting that the Heck product may be kinetically favored. Lastly, upon examining a variety of palladium precatalysts, there was no inherent preference for one palladium source over another. However, he found that phenanthroline, as a ligand, tended to favor the Heck product.

Originally this reaction was thought to go through a classic Heck reaction (Figure 3.36, top), with arylation of the terminal position of the vinyl boronic ester **3.71**. However, after further mechanistic investigation, Whiting discovered some inconsistencies with his original proposal.[64b] At 80 °C, after 3 hours, the reaction showed approximately 20% conversion of the aryl halide to only the Suzuki product (**3.73**). Conversely, after 9 hours, the same reaction had gone to completion yielding only the Heck product (**3.72**) (Figure 3.36, bottom).

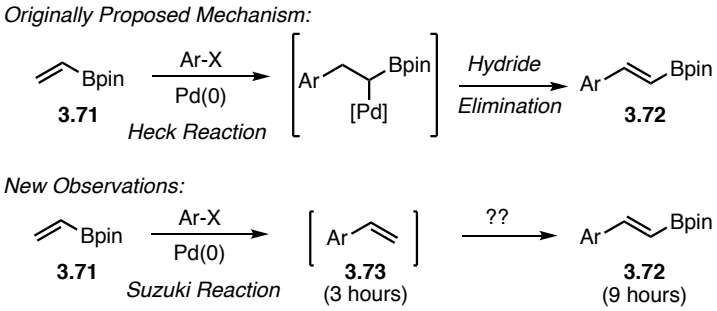

Figure 3.36 Proposed Mechanism of Heck Reaction

Whiting proposes that **3.71** initially undergoes a Suzuki reaction to form **3.73** as observed at shorter times. Balancing the reaction suggests the formation of a haloborane (**3.74**) which is presumably in an equilibrium with the ammonium adduct **3.75**. The boryl-halogenation of **3.73** with **3.74** forms **3.76** which can undergo an E2 elimination to form the observed "Heck product" (Figure 3.37, bottom).

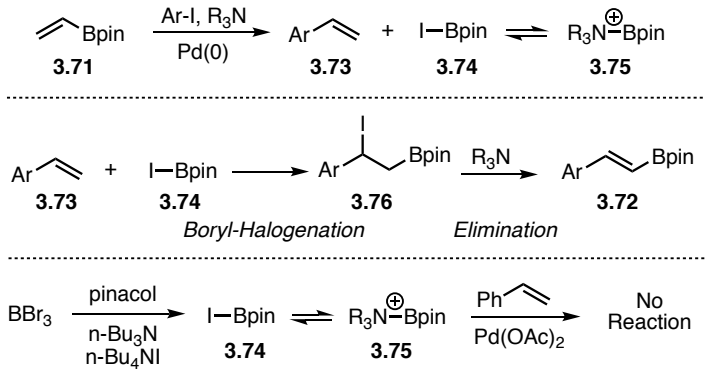

Figure 3.37 Mechanistic Studies on Heck Reaction of Pinacol Vinyl Boronic Ester

Testing this mechanistic theory, boron tribromide (BBr_3) and pinacol were premixed and added to styrene with palladium and ligand but no product was observed

(Figure 3.37, bottom). As of now, the mechanism of this transformation is still unclear but nonetheless this reaction has found use in the synthesis of polyenes, natural products and material.

3.3.5.2 Applications of Vinyl Boronic Ester Heck Coupling Reactions

Once general conditions for the selective Heck coupling of **C.1** with aryl halides was established, Whiting moved to exploring the reactivity with alkenyl halides.[65] The product from this reaction is a fully conjugated polyene. The key to using alkenyl halides was the use of silver or thalium salts in the reaction medium.[65a] This approach to polyene synthesis has been applied to many total syntheses[66] such as Viridenomycin (Figure 3.38).

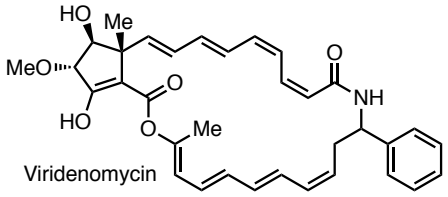

Figure 3.38 Structure of Viridenomycin

This approach has also been applied to the synthesis of multi-substituted conjugated olefins such as triarylethylene units and larger.[67] using this strategy in an iterative process allows for rapid access to large molecular weight dendrimers.[67b] These dendrimers have various applications including electroactive, light emitting stilbenoids and dyes in OLED devices (Figure 3.39).

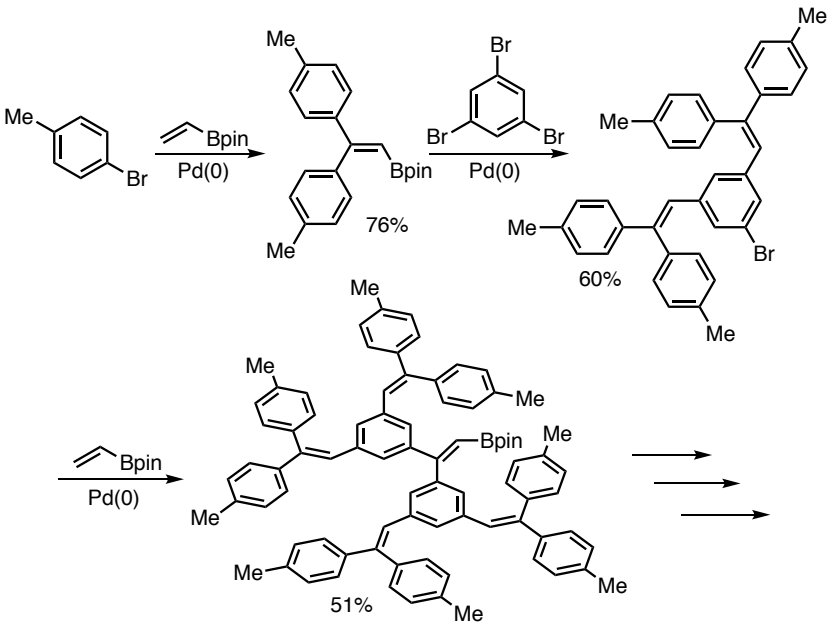

Figure 3.39 Iterative Synthesis of Stilbenoid Dendrimers

More recently, similar procedures have been reported in which the vinyl boronate is the electrophile in the Heck-type cross-coupling reaction. Using a bisfunctionalized alkenyl fragment containing both a halide and MIDA boronate as the electrophile, the formation of various dienes and polyenes was accomplished.[8, 68] (Figure 3.40)

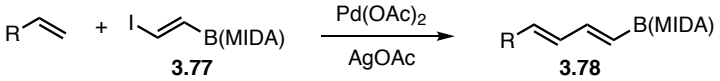

R =	product	yield	L/B
$CH(OMe)_2$	**3.78a**	75%	85:15
CH_2OH	**3.78b**	58%	88:12
$CH_2OTBDPS$	**3.78c**	74%	90:10
4-pyr	**3.78d**	75%	95:5
$SiMe_3$	**3.78e**	89%	80:20
Bpin	**3.78f**	90%	90:10

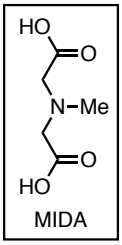

Figure 3.40 Synthesis of MIDA Protected Dienes

3.3.6 Dehydrogenative Borylation

The dehydrogenative borylation of alkenes has become a common method for the direct borylation of terminal alkenes. Generally, the conditions include pinacol borane or B_2pin_2 with a transition metal catalyst and an alkene (Figure 3.41).

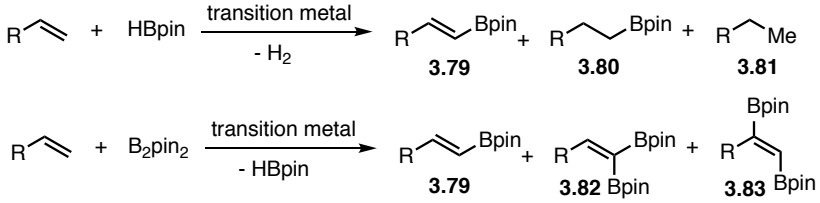

Figure 3.41 General Scheme of Dehydrogenative Borylation

Yields and selectivities with pinacol borane for **3.79** are generally good, but can become complicated by inseparable reduction products (**3.80** and **3.81**). However, these side products can be limited with extra equivalents of alkene or external sacrificial alkenes to absorb the generated hydrogen. Using B_2pin_2 also limits reduction byproducts by eliminating the formation of stoichiometric hydrogen (Figure 3.41,

bottom). However, these conditions often result in over borylation, forming mixtures of mono- and di-borylated products (**3.82** and **3.83**).

3.3.6.1 Sacrificial Alkenes

The first examples of dehydrogenative borylation were reported in the 1980's by Sneddon and coworkers.[69] In his initial report, Sneddon described the reaction of pentaborane (B_5H_9) with simple terminal olefins such as propane and butane in the presence of catalytic palladium bromide ($PdBr_2$) to form various isomers of alkenyl boron containing products. In addition, an equimolar ratio of reduced alkene (propane, butane, etc.) was observed in these reactions, thus limiting the reaction yield to a maximum of 50% (Figure 3.42).

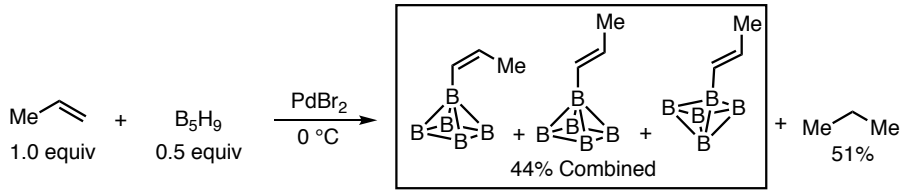

Figure 3.42 Sneddon's Dehydrogenative Borylation with Pentaborane

In 1992, Brown and Lloyd-Jones demonstrated the dehydrogenative borylation of a few styrenes with oxazaborolidene catalyzed by a rhodium dimer (Figure 3.43).[70]

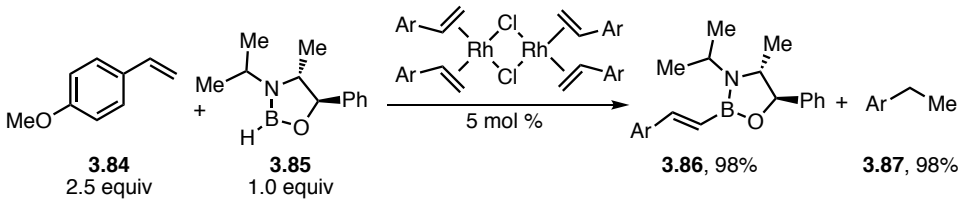

Figure 3.43 Brown and Lloyd-Jones' Dehydrogenative Borylation

These reactions also resulted in a 1:1 ratio of alkenyl boronic ester product and reduced starting material, however excellent yields of **3.86** can be obtained when considering the borane (**3.85**) as the limiting reagent. A series of detailed mechanistic studies led Brown and Lloyd-Jones to propose the following mechanism (Figure 3.44).[70-71]

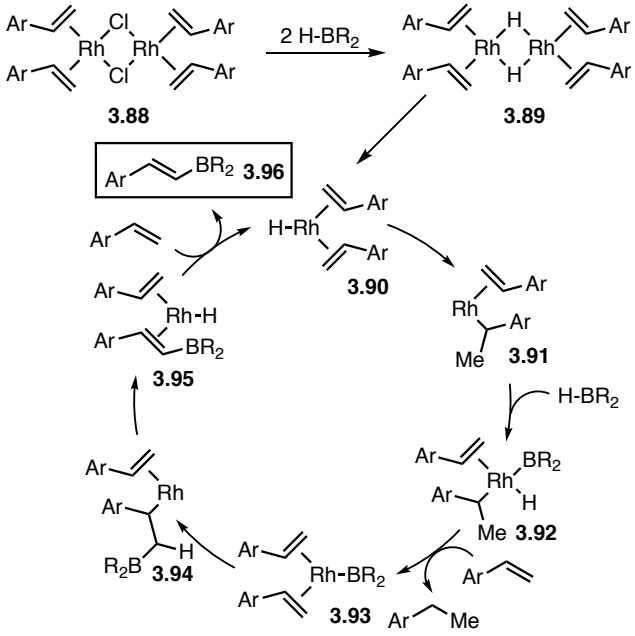

Figure 3.44 Mechanism of Dehydrogenative Borylation with Sacrificial Alkenes

The first step is the formation of catalytically active rhodium hydride dimer **3.89** from the rhodium precatalyst **3.88**. Migratory insertion an alkene into the rhodium-hydride bond forms intermediate **3.91**. Then oxidative addition of **3.91** to an oxazaborolidene B-H bond leads to intermediate **3.92**. Reductive elimination of the alkane and coordination of another styrene gives borylated rhodium bis-alkene complex **3.93**. This ligand exchange on rhodium reflects the reduction of one equivalent of styrene as observed in this reaction. Migratory insertion of another styrene into the rhodium-boron bond and subsequent β-hydride elimination leads to intermediate **3.95** which consists of the borylated product coordinated to rhodium. Ligand exchange with a new styrene releases one equivalent of alkenyl boronate **3.95** and restarts the catalytic cycle. Each catalytic cycle requires two equivalents of styrene and produces one equivalent of reduced alkane and one equivalent of borylated product (**3.96**).

Many other research groups have explored the dehydrogenative borylation reactions with alkenes utilizing different boron sources such as catecholborane,[72] pinacolborane,[73] azaborine,[74] and napthalene-1,8-diaminatoborane.[75] In all cases, regardless of the boryl hydride used, 50% of the starting alkene acts as a hydrogen acceptor and is reduced to the corresponding alkane. Additionally, only styrene derived substrates are viable in these reactions (Figure 3.45). The reaction of 1-hexene under identical conditions resulted in nearly selective hydroboration (**3.100**) over dehydrogenative borylation (**3.101**)[73b]

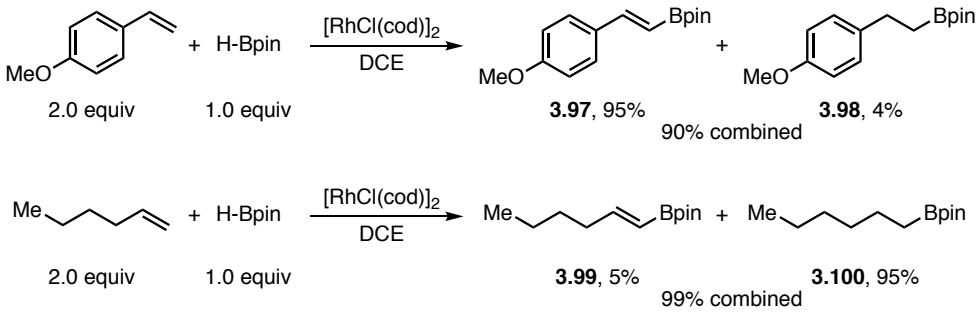

Figure 3.45 Dehydrogenative Borylation of 1-Hexene

To overcome this limitation, Murata and Masuda found that with the addition of a "sacrificial" alkene, slightly increased yields can be obtained.[73b] This was the first example of using an external alkene as the hydrogen acceptor in place of the precious alkene of interest. Murakami has expanded upon this principle and developed, for the first time, general conditions for the dehydrogenative borylation of aliphatic alkenes.[76] He found that using 2.3 equivalents of norbornene (nbe) in conjunction with pinacol borane and catalytic rhodium(I), a variety of terminal alkenes can be converted into the corresponding alkenyl boronic esters. This reaction proceeds with moderate yields, chemo- and regioselectivity for the linear alkenyl boronic ester (Figure 3.46).

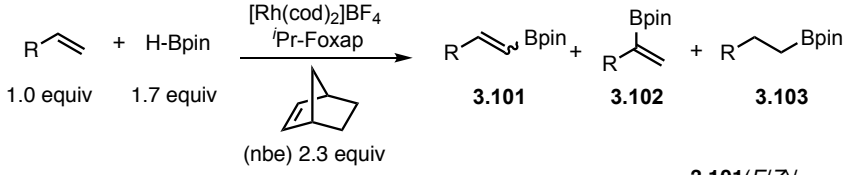

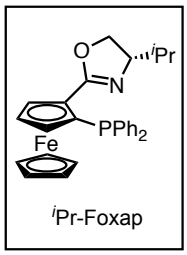

R =	product	combined yield	**3.101**(*E*/*Z*)/ **3.102**/**3.103**
n-hex	**3.101a**	75%	91(91/9):3:6
CH_2Ph	**3.101b**	78%	89(88/12):0:11
CH_2Cyp	**3.101c**	71%	92(91/9):2:6
$TBSO(CH_2)_4$	**3.101d**	80%	89(91/9):3:8
$Cl(CH_2)_4$	**3.101e**	74%	90(86/14):3:7
4-OMe-C_6H_4	**3.101f**	78%	96(95/5):0:4

Figure 3.46 Selected Scope of Murakami's Borylation Reaction

While this was the first general method for the direct borylation of terminal, non-aromatic alkenes, the yields are moderate and the isolated products are contaminated with ~10% inseparable byproducts.

3.3.6.2 No Sacrificial Alkenes

Whether half the starting alkene or an external "sacrificial" alkene, the above methods all required a hydrogen acceptor to absorb the stoichiometric H_2 produced during the reaction. To overcome this inherent limitation, Marder and his colleagues discovered that using *trans*-[$RhCl(CO)(PPh_3)_2$] in combination with diboron reagents such as B_2pin_2 and B_2neop_2, allows for the dehydrogenative borylation of aromatic alkenes without significant hydrogenation or hydroboration.[77]

The ruthenium catalyzed reaction of B_2pin_2 with 4-vinyl anisole in solvents such as toluene, tetrahydrofuran and 1,4-dioxane gave complicated mixtures of products containing dehydrogenative borylation, diboration, hydroboration, hydrogenation and more.[77b] However, they found that in acetonitrile, the reactions were much cleaner but

with significantly slower rates. By using a combination of benzene and acetonitrile as a solvent 93% of the styrene derived product was obtained with ~7% hydroboration.

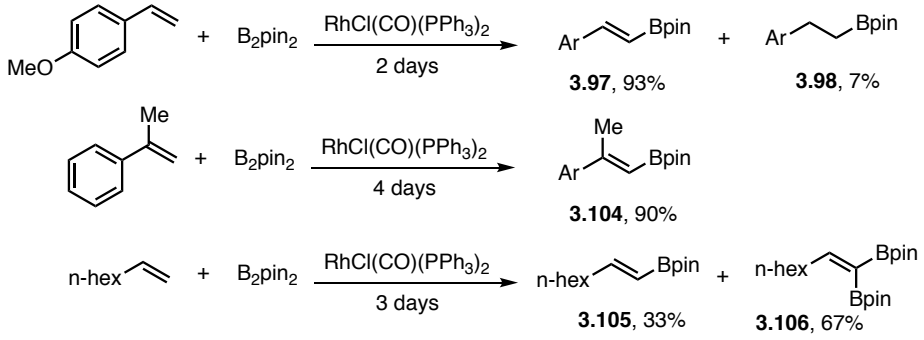

Figure 3.47 Marder's Borylation Without Sacrificial Alkenes

Examining other substrates showed that each alkene must be individually optimized to obtain a high and selective yields. 1,1-Disubstituted alkenes such as α-methylstyrene and α-phenylstyrene showed good reactivity with both B_2pin_2 and B_2neop_2 (Figure 3.47, middle). However, when a non-aromatic alkene such as 1-octene, is subjected to the reaction conditions, only mixtures of vinyl boronic ester (**3.105**) and vinyl bis-boronic ester (**3.106**) are obtained (Figure 3.47, bottom), demonstrating that this is not a viable method for synthesis of non-conjugated alkenyl boronic esters. Additionally, reaction times with conventional heating ranged from 2-6 days to observe full conversion, however, using microwave irradiation reaction times could be as low as 30 min.

The key to this approach is encased in the proposed catalytic cycle. The mechanisms put forth in the previous section, produce rhodium hydride intermediates which reduce other alkenes to turn over the catalytic cycle. The B_2pin_2, used here, is

reduced to pinacol borane, which reacts poorly under these catalytic conditions.[77b] The proposed mechanism for this transformation closely resembles a Heck-like pathway (Figure 3.48).

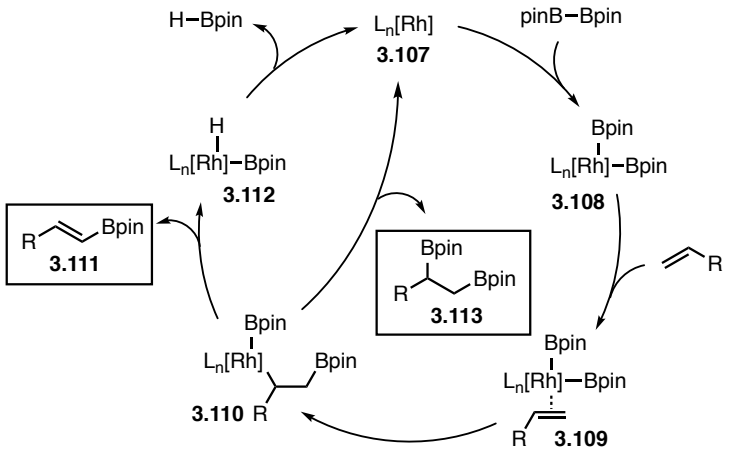

Figure 3.48 Mechanism of Dehydrogenative Borylation with B_2pin_2

The active rhodium complex (**3.107**) undergoes oxidative addition into the B-B bond of B_2pin_2 to form **3.108**. An alkene can then coordinate to rhodium, replacing a ligand or solvent molecule and then migratory insert into a rhodium-boron bond to form complex **3.110**. Intermediate **3.110** can either directly reductively eliminate to form diboronic ester **3.113** and regenerate **3.107** or β-hydride eliminate to release product **3.111**. In the latter case, rhodium hydride **3.112** is also formed which can reductively eliminate to form pinacolborane and regenerate the active rhodium complex **3.107**.

Palladium catalyzed dehydrogenative borylation had remained untouched since Sneddon's seminal results.[69] This is perhaps because palladium is not efficient at cleaving sp^2 C-H bonds under such reducing conditions as such with diboronic esters

and boryl hydrides. However, Szabo[78] and Iwasawa[79] have both independently reported the palladium catalyzed dehydrogenative borylation of alkenes to form alkenyl boronic esters (Figure 3.49). Both methods use elaborate palladium pincer complexes (**3.114** and **3.116**) and are sensitive to equivalents of B_2pin_2 often resulting in over borylation. However, with extra equivalents of alkene, overborylation can be suppressed (Figure 3.49, bottom).

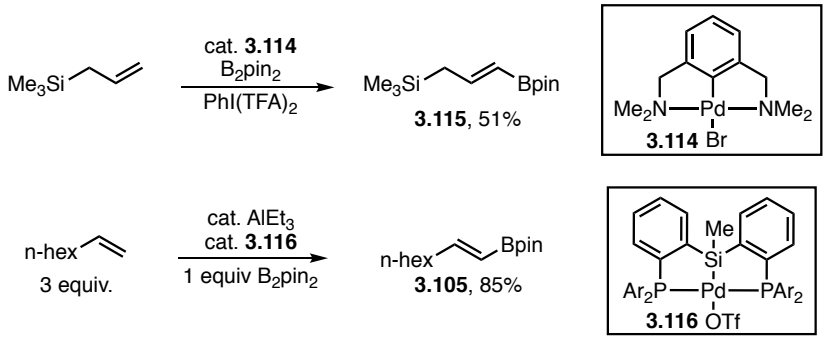

Figure 3.49 Palladium Pincer Catalyzed Dehydrogenative Borylation

In addition to rhodium and palladium, iron[80] and copper[81] have also been shown to catalyze dehydrogenative borylation with styrene derived alkenes (Figure 3.50).

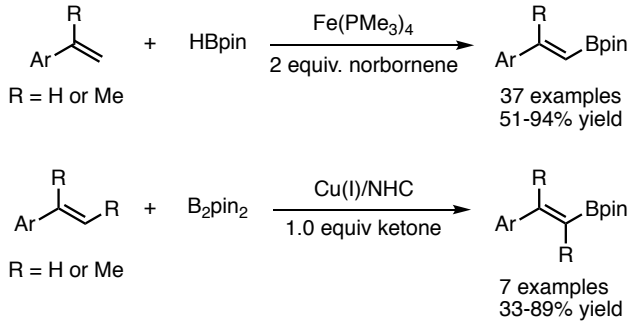

Figure 3.50 Iron and Copper Catalyzed Dehydrogenative Borylation Reactions

3.3.7 Summary and Outlook

While there are several methods for the synthesis of alkenyl boronic esters, there are inherent drawbacks to each of these. Hydroboration,[33d] requires access to the appropriate alkynes, and Miyaura borylation,[82] requires prefunctionalized alkenes. Both classes of starting materials are significantly more expensive and less commercially abundant than the corresponding alkenes. Alkene cross-metathesis and Heck reactions on vinyl boronic esters work well, however, they require vinyl boronic esters to make vinyl boronic esters, eliminating the carbon-boron bond formation step. Dehydrogenative borylation is by far the most modern method for the direct borylation of alkenes. Unfortunately, the developed methods are typically limited in scope (particularly with respect to linear α-olefins) and frequently suffer from competitive over-borylation, or alkene reduction/hydroboration. Many of these problems stem from the use of highly reduced boron reagents. In addition, although some are commercially available, diboranes require several synthetic steps to access and thus are relatively expensive.[83]

3.4 Hypothesis and Background

We envisioned an alternative approach towards the synthesis of alkenyl boronic esters which involves the palladium-catalyzed borylation of alkenes using chloroborane reagents *via* a Heck-like reaction (Figure 3.1). Such a boryl-Heck process would be advantageous, as the use of a more highly oxidized reagent would eliminate problematic reduction byproducts. In addition, the required chloroboranes can be prepared directly from inexpensive boron trichloride and diols.

3.4.1 Preliminary Studies

The first step of this proposed mechanism would be the oxidative addition of palladium into the B-X bond. While the oxidative addition of various transition metals into B-X bonds has been demonstrated[84] we were more interested in the use of d^{10} metals. The oxidative addition of platinum into B-F,[85] B-Cl,[86] B-Br,[87] and B-I[88] has been well established over the past several decades (Figure 3.51).

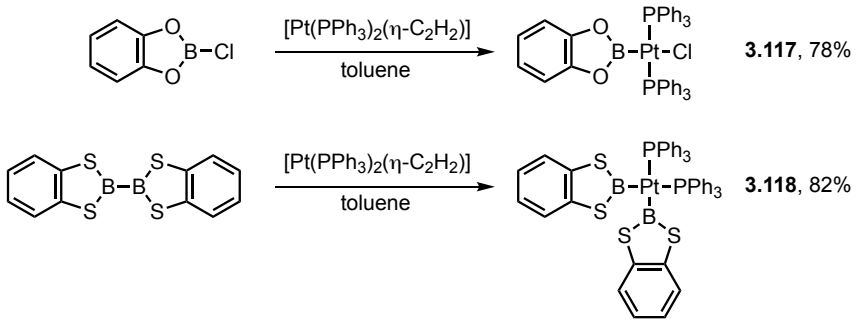

Figure 3.51 Oxidative Addition of Platinum into B-Cl and B-B Bonds

Accompanied by two phosphine ligands, dozens of crystal structures exist showing the oxidative addition product with haloboranes. In every case, the boron and

the halide have a trans-configuration about the platinum center.[87c] This contrasts the cis-configuration observed with oxidative addition of platinum into B-B bonds,[86a] and compliments the observed oxidative addition into Si-X bonds.[1d, 89]

Tanaka has established that the oxidative addition of palladium into B-Cl bonds and subsequent migratory insertion of alkynes is a feasible process (Figure 3.52).[90]

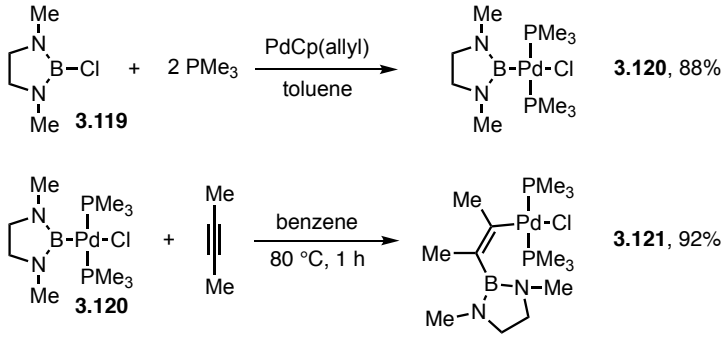

Figure 3.52 Oxidative Addition of Palladium into a B-Cl Bond and Migratory Insertion of 2-Butyne

The oxidative addition complex of PdCp(allyl) into a B-Cl bond (**3.120**) was formed and isolated by Tanaka. Mixing **3.120** with 2-butyne in benzene resulted in the formation of **3.121**. While this discovery is not synthetically useful, it demonstrates that our proposed catalytic cycle is feasible.

3.4.2 Related Carboboration Reactions

Suginome was the first to recognize the synthetic utility of these fundamental steps.[91] In 2005, he reported that chloroboryl homopropargylic ethers can undergo *trans*-alkynylborylation using nickel catalysis and alkynyl tin reagents.[92] This reaction is thought to proceed through activation of the boron chlorine bond by nickel catalysis

followed by transmetallation of an organic group from an organotin reagent (Figure 3.53).

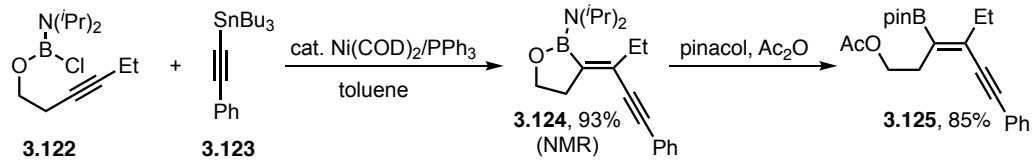

Figure 3.53 Suginome's Nickel Catalyzed Carboboration Reaction

The immediate products are unstable towards moisture and therefore were treated with pinacol and acetic anhydride to aid in isolation. Interestingly, only *trans*-carboboration of the tethered alkyne was observed. Mechanistically, this contradicts traditional metal catalyzed addition to alkynes which usually proceed in a *cis*-fashion.[33a, 33d] A crystal structure was obtained of the intermediate before transmetallation of the organotin reagent and displays the *trans*-addition configuration (Figure 3.54).

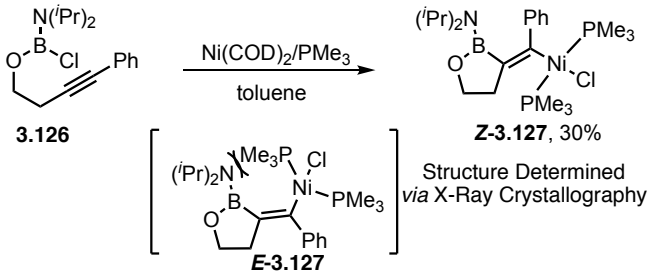

Figure 3.54 Model for Vinyl-Nickel Isomerization

The observed *trans*-addition of the metalloboron intermediate is thought to arise from the isomerization of intermediate ***E*-3.127** to the lower energy isomer ***Z*-3.127**. This result, in conjunction with the stereochemistry of the products led to the following proposed mechanism (Figure 3.55).

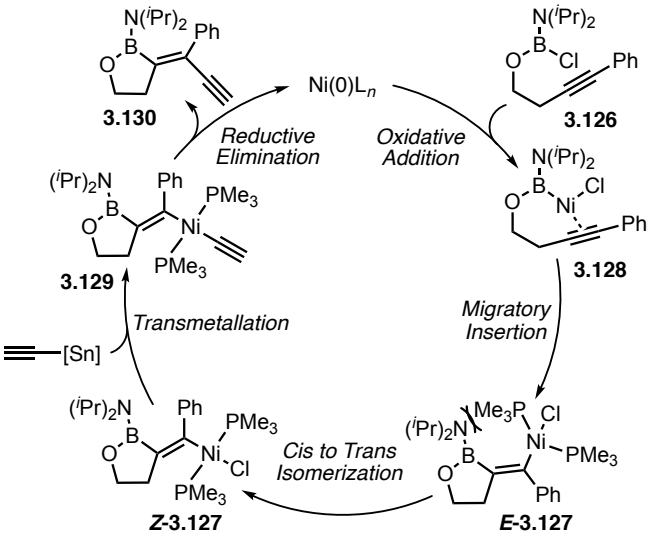

Figure 3.55 Mechanism of Suginome's Nickel Catalyzed Carboboration Reaction

Suginome's proposed mechanism begins with the oxidative addition of nickel (0) into the B-Cl bond of **3.126**. Subsequent coordination and migratory insertion of the tethered alkyne results in intermediate ***E*-3.127**, which is thought to be unstable due to the disfavored steric interaction of the ligands on boron and nickel. *Cis*- to *trans*-isomerization about the C-C double bond occurs leading to ***Z*-3.127** which is an isolated intermediate. Transmetallation and reductive elimination of the alkynyl group forms **3.13**, which can be quenched with pinacol and isolated.

Switching to a palladium catalyst and an organo-zirconium transmetallating reagent, Suginome found that both *trans*- and *cis*- carboboration are possible in a controlled manner with a similar chloroboryl homopropargylic ether substrate.[93] Using bulky trialkyl phosphines such as $P(^tBu)_3$ and $P(Cy)_3$, the previously observed *trans*-carboboration product was observed with moderate yields and excellent stereocontol (Figure 3.56).

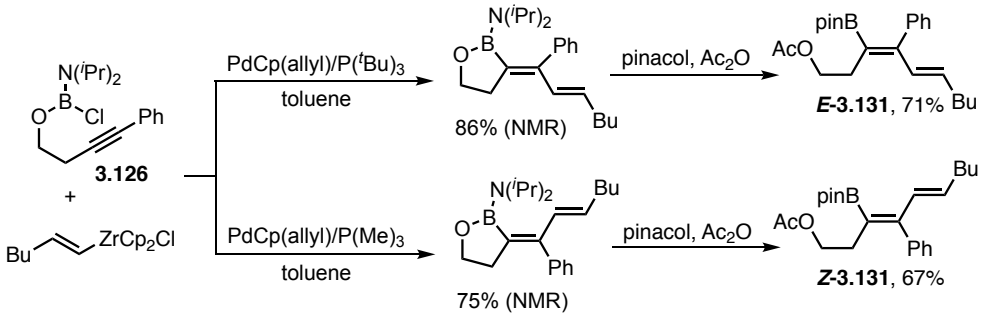

Figure 3.56 Ligand Controlled Stereoselective Carboboration Reactions

However, switching the ligand to $P(Me)_3$ the *cis*-carboboration product was observed. Isolating a crystal of the migratory insertion intermediate clearly shows that with PMe_3 the *cis*-carbopalladation occurs. In this scenario, with palladium, they show that stereoselective and the steric demand of the phosphine ligand are directly correlated. They propose that the isomerization pathway can be driven by large steric repulsion between the isopropyl group on nitrogen and the bulky phosphine ligands on palladium.

In the previous scenarios, the chloroboranes were tethered to the alkyne in which the intramolecular cyclizations were trapped with organometallic reagents. While

intramolecular cyclizations facilitate the reaction, they can also limit the scope and utility of this reaction. Using a palladium catalysis, Suginome also demonstrated a three-component coupling reaction of bis(diamino)chloroboranes, alkynes and organozirconium reagents (Figure 3.57).[94]

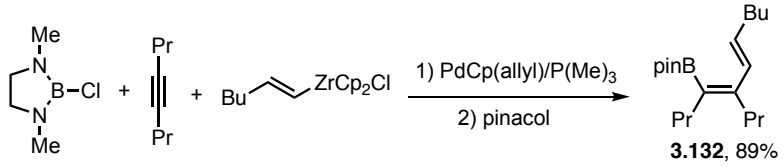

Figure 3.57 Suginome's 3-Componant Carboboration

Using $P(Me)_3$, on the *cis*-carboboration product was observed in moderate to excellent yields after a pinacol quench. Both alkenyl and aryl zirconium reagents were successful in this reaction giving access to acyclic tri- and tetrasubstituted alkenyl boronic esters. These conditions are nearly identical to the seminal work by Tanaka[90a] with the exception of the organozirconium nucleophile added to turn over the reaction.

Since Tanaka's original publication on the oxidative addition of palladium into boryl chloride bonds, Suginome has expanded the utility of this B-Cl activation by exploring the migratory insertion of various alkynes and transmetallation of various organometallic reagents. In the context of our proposed boryl-Heck reaction, we were more interested in the bimolecular migratory insertion of an alkene and termination *via* hydride elimination rather than transmetallation and reductive elimination.

Suginome has also shown that both mechanistic steps are feasible under similar conditions. In 2011, Suginome reported the intramolecular cyclization of chloroboryl

ethers derived from homoallylic alcohols in a similar fashion to the homopropargylic alcohols (Figure 3.58).

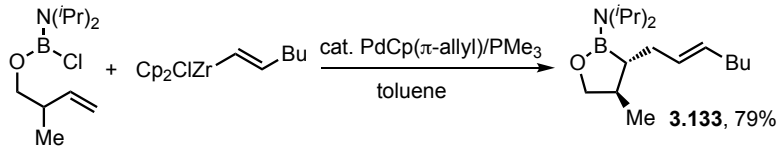

Figure 3.58 Suginome's Carboboration of Alkenes

Under a similar mechanistic regime, this reaction gives rise to selective 5-exo cyclization products with high stereoselectivity with substitutions on the alkyl tether. The high degree of diastereoselectivity can be rationalized by examining the chair like migratory insertion transition states (Figure 3.59).

Figure 3.59 Stereochemical Model for Observed Diastereoselectivity

The substitutions on the tether prefer equatorial positions over axial. More importantly, this shows that the migratory insertion of alkenes is possible under catalytic conditions.

Lastly, Suginome has demonstrated that alkenes such as styrenes and acrylates can serve as nucleophiles in the intramolecular cyclization of homopropargylic alkynes (Figure 3.60).[95]

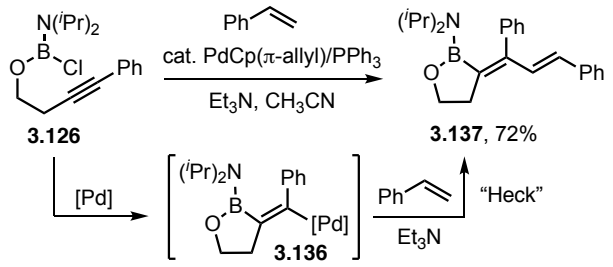

Figure 3.60 Suginome's Intramolecular Reaction Terminated *via* a Heck Reaction

These reactions follow the same mechanistic hypothesis as the rest of his work except rather than terminating with transmetallation of an organic nucleophile, the catalytic cycle is terminated with a bimolecular Heck reaction. This is perhaps the most encouraging of Suginome's results because it demonstrates that amines are compatible with similar reaction conditions.

3.5 Discovery and Development of the Boryl-Heck Reaction

Suginome has demonstrated that all of the proposed fundamental steps are plausible, however, a complete boryl-Heck reaction that converts an alkene to an unsaturated boronic ester using an electrophilic borane had not yet been demonstrated.[95] In fact, Marder has previously suggested a boryl-Heck reaction may be possible.[96] However, his preliminary studies showed that catecholchloroborane (catBCl) and triethyl amine (Et_3N, a common base in Heck reactions) form highly stable amine-borane adduct **3.138** (Figure 3.61), which presumably prevents oxidative addition.

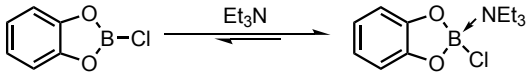

3.138

Figure 3.61 Equilibrium of catBCl and Et_3N

He also showed that phosphines can both coordinate, deactivate and decompose catBCl. Marder's results, along with Suginome's use of less electrophilic aminoboranes, illustrate the inherent difficulty of developing a boryl-Heck reaction to deliver a simple alkenyl boronic ester. Such a reaction requires both Lewis acidic chloroboronic esters and an effective base to turn over the catalytic cycle.

I envisioned using catBCl as the boron electrophile, as it is commercially available and readily synthesized from BCl_3 and catechol (both are abundant and inexpensive on-scale).[97,98] I initially explored borylation of 1-decene using conditions similar to our silyl-Heck protocol (20 mol % Cy_3P, 10 mol % [(COD)Pd(CH_2SiMe_3)$_2$], Et_3N, $PhCF_3$, 80 °C).[1a] Unfortunately, I observed no borylated product but only starting alkene by ^1H NMR spectrometry and GCMS. However, when examining the ^{11}B NMR spectrum to determine the fate of the catBCl under these conditions, I observed the quantitative formation of amine-borane adduct **3.138** (~13 ppm) previously reported by Marder (Figure 3.62).[96]

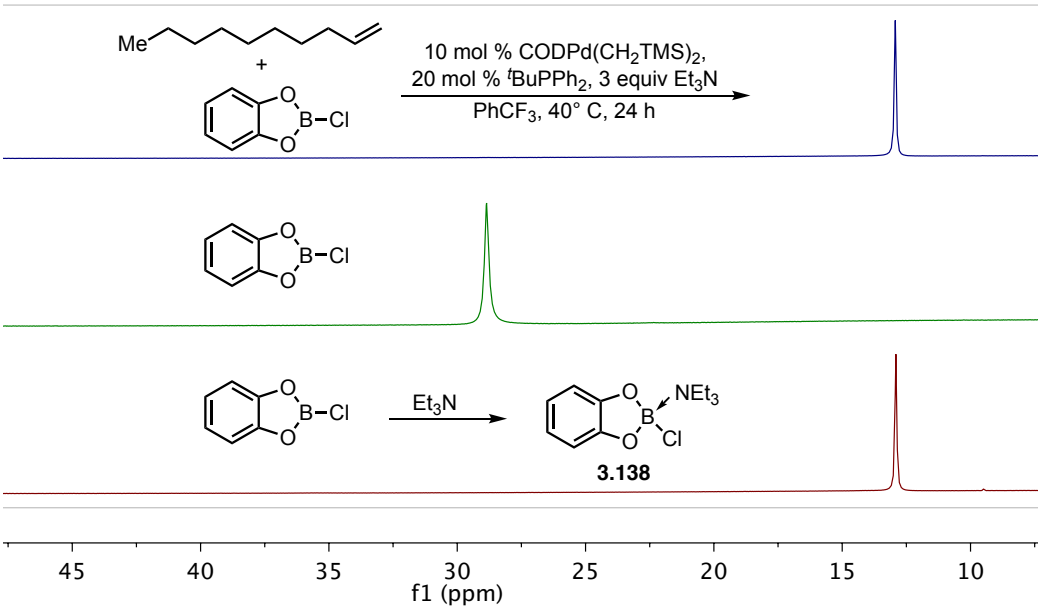

Figure 3.62 ^{11}B NMR of Crude Reaction

3.5.1 Base Optimization

We hypothesized that formation of amine-borane adducts could be disrupted by use of a different class of base or by a larger amine that might form a less stable adduct. This would shift the equilibrium away from **3.138**, resulting in a higher concentration of free catBCl in solution to enter the catalytic cycle. As mentioned above Et_3N resulted in no conversion of starting material (Table 3.1, entry 1).

Table 3.1 Identification of an Effective Base

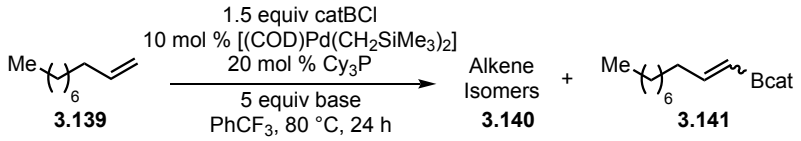

entry	base	**3.139** (%)	**3.140** (%)	**3.141** (%)	*E*/*Z* of **3.141**
1	Et_3N	100	0	0	–
2	none	3	97	0	–
3	K_2CO_3	4	96	0	–
4	pyridine	91	9	0	–
5	2,6-lutidine	70	30	0	–
6	$^{i}Pr_2NEt$	52	33	15	~90:10
7	Cy_2NMe	65	9	26	~90:10

Without base or with inorganic bases such as potassium carbonate, nearly full isomerization of the starting material to internal alkene isomers **3.140** was observed (entries 2 and 3). Weaker organic bases, such as pyridine or 2,6-lutidine, suppressed isomerization but did not lead to **3.141** (entries 4 and 5). In contrast, with the larger trialkylamine Hünig's base, 15% of *trans*-alkenyl boronic ester **3.141** was observed (entry 6). With *N*,*N*-dicyclohexylmethylamine (Cy_2NMe) even more of **3.141** (26%) was formed along with less starting material isomerization (entry 7). Importantly, in both entries 6 and 7, **3.141** was the only organoboron product; no internal alkenyl- or allyl-boronic esters were detected. In both cases, **3.141** was formed with high *E*/*Z* selectivity (ca. 90:10).

3.5.2 Catalyst Optimization

To optimize the reaction further, we turned our attention to the nature of the catalyst. In the absence of palladium and ligand, no product was observed (Table 3.2, entry 1).

Table 3.2 Optimization of Catalytic Conditions

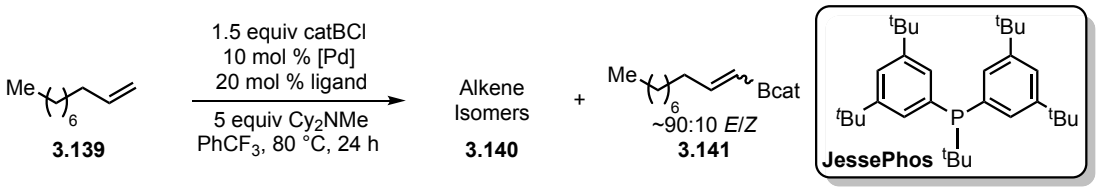

entry	catalyst (mol %)	ligand (mol %)	**3.141** (%)	**3.140** (%)	**3.141** (%)
1	none	none	100	0	0
2	Pd_2dba_3 (5 mol %)	Cy_3P (20 mol %)	53	15	32
3	Pd_2dba_3 (5 mol %)	none	0	35	65
4	Pd_2dba_3 (5 mol %)	Ph_3P (20 mol %)	65	10	25
5	Pd_2dba_3 (5 mol %)	$^tBu_3P$ (20 mol %)	0	>99	0
6	Pd_2dba_3 (5 mol %)	dppe (10 mol %)	>99	0	0
7	Pd_2dba_3 (5 mol %)	dppp (10 mol %)	96	0	4
8	Pd_2dba_3 (5 mol %)	SPhos (10 mol %)	0	56	44
9	Pd_2dba_3 (5 mol %)	^{t}BuXPhos (10 mol %)	0	68	32
10	Pd_2dba_3 (5 mol %)	$^tBuPPh_2$ (20 mol %)	19	19	62
11	Pd_2dba_3 (5 mol %)	**JessePhos** (20 mol %)	2	16	82
12	Pd_2dba_3 (2.5 mol %)	**JessePhos** (10 mol %)	0	18	82

Using Cy_3P as ligand, various palladium precatalysts provided similar yields of **1.141**; however, Pd_2dba_3 was selected for further study (entry 2). Interestingly, Pd_2dba_3 without added phosphine yielded a significant quantity of **1.141** (65%, entry 3). Mono- and bidentate phosphines as well as Buchwald ligands all prove inferior to entry 3 (entries 4-9).[99] In contrast, the use of $^tBuPPh_2$ led to less alkene isomerization, albeit in similar yield as entry 3 (entry 10). We next examined **JessePhos**, a ligand designed in our group for silyl-Heck reactions.[1d] Somewhat unexpectedly, this ligand provided a notable increase in the production of **1.141** (82%, entry 11), even with only 5 mol % Pd (entry 12), and has proven to be the most effective to date. We suspect that **JessePhos** has the correct balance of electron donor ability to support a highly active palladium catalyst, but is sterically hindered enough to prevent decomposition or deactivation of the boron reagent *in situ*.

3.5.3 Suppression of Starting Material Isomerization

Even with **JessePhos**, alkene isomerization of the starting material continued to erode the yield. Jesse Spillane, an undergraduate working with me, investigated the use of additives and found that the addition of 1.5 equivalents of lithium trifluoromethanesulfonate (LiOTf) fully suppressed starting material isomerization (Table 3.3). With no competing isomerization, an increase in temperature was permissible (90 °C), and a quantitative yield was achieved (entry 2).

Table 3.3 Additive Screen

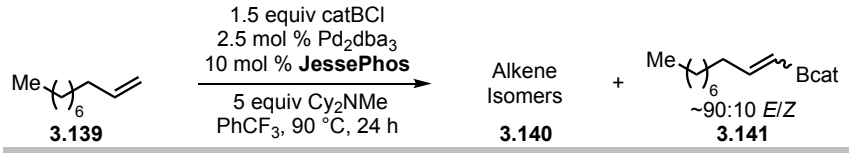

entry	additive (1.5 equiv)	**3.139** (%)	**3.140** (%)	**3.141** (%)
1	none	0	18	82
2	LiOTf	0	0	>99

We do not fully understand the role of LiOTf in suppressing alkene isomerization, but suspect that the limited solubility of LiCl in $PhCF_3$ might be important in controlling unfavorable palladium hydride equilibria in the reaction (Figure 3.63).

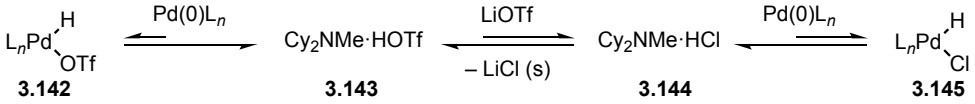

Figure 3.63 Palladium Hydride Equilibrium with Triflate and Chloride Anions

We suspect that the starting alkene isomerization is catalyzed by a palladium hydride complex formed during this reaction. Migratory insertion of the alkene into the palladium hydride bond forming an alkyl palladium which can β-hydride eliminate to form the more stable and unreactive internal alkene isomer. Stoichiometric triflate anions can exchange with chloride anions from the ammonium chloride formed. This exchange is driven by limited solubility of LiCl in $PhCF_3$ and produces the ammonium triflate which is less prone to form a palladium hydride complex (**3.142**).

3.5.4 Single Component Catalyst

During the optimization process, we found that isolated products were contaminated with ~5% of a yellow solid. Sarah Krause, a colleague of mine identified this impurity as the phosphine-ligated palladium complex (**JessePhos**)$_2$PdCl$_2$. Sarah also found that using a palladium scavenger (ammonium pyrrolidine-dithiocarbamate),[100] this impurity could easily be removed resulting in pure products. Interested in this palladium complex, she was able to independently synthesize (**JessePhos**)$_2$PdCl$_2$ and sought to further simplify the setup of this reaction using this single component precatalyst. With this air and moisture stable complex, a quantitative yield of **3.141** was observed as a 90:10 mixture of *E*/*Z* alkenyl boronate isomers with only 2.5 mol % catalyst (Figure 3.64). Further studies also revealed that the single component catalyst provided more consistent results on preparative scale.

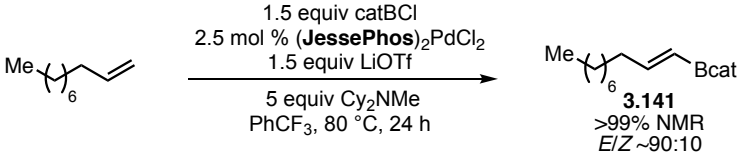

Figure 3.64 Boryl-Heck Reaction with Single Component Catalyst

3.6 Substrate Scopes

Next, we sought to examined the scope of this reaction. Catechol boronic esters are known to be air and moisture sensitive and prone to oxidation and hydrolysis. To facilitate isolation, pinacol (3 equiv) was added at the end of each reaction, resulting in rapid, quantitative conversion of the products to more easily isolated pinacol boronic esters (Figure 3.65).

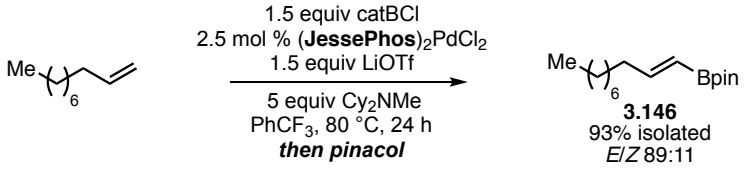

Figure 3.65 Pinacol Quench for Isolation

Even as the pinacol ester, boronic esters are known to partially decompose during purification on silica gel. However, boric acid impregnated silica has been shown to decrease this decomposition resulting in increased isolated yields.[101] In our hands, use of commercial, untreated silica gel resulted in yields ~5-10 % lower than with boric acid impregnated silica gel (see Experimental Details).

3.6.1 Reactions with α-Olefins

Under these conditions, the product from 1-decene (**3.146**) was isolated in 93% yield with an *E*/*Z* ratio of 89:11 (Figure 3.66). Other aliphatic alkenes were converted to alkenyl boronic esters with good yields and *E*/*Z* selectivities (**3.147**-**3.148**). Using 3 equivalents of catBCl, 1,7-octadiene was bisborylated in 83% yield (**3.149**). A variety of functional groups were well tolerated, including silyl-protected alcohols (**3.150**), ethers (**3.151**), alkyl chlorides (**3.152**), silanes (**3.153**), and alkyl pinacol boronic esters

(**3.154**). Although enolizable carbonyls interfered with the reaction (**3.155**-**3.156**, presumably due to competitive formation of boron enolates), non-enolizable carbonyls (**3.157**-**3.158**) did not. When allylbenzene was used as substrate, boronate **3.159** was observed as a mixture of alkene isomers. This is the only case where an allyl boronic ester was observed, which we attribute to the stability of a conjugated aromatic group.

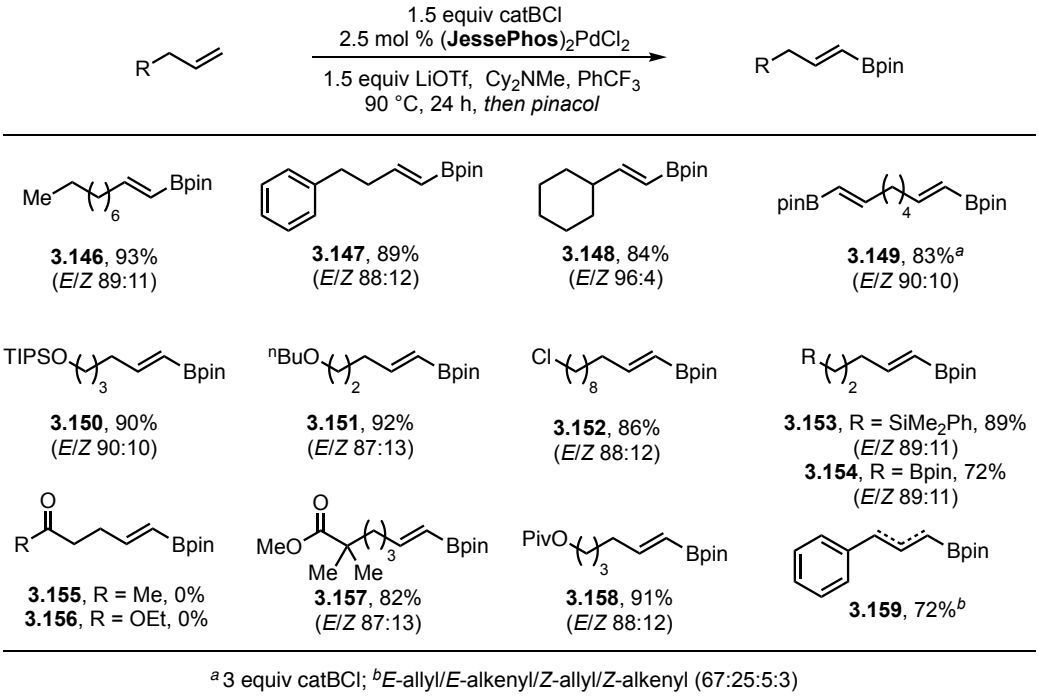

[a] 3 equiv catBCl; [b] *E*-allyl/*E*-alkenyl/*Z*-allyl/*Z*-alkenyl (67:25:5:3)

Figure 3.66 Scope of Linear α-Olefin Substrates

3.6.2 Reactions with Styrene Derivatives

Substituted styrenes were also investigated (Figure 3.67). Since starting material isomerization is not possible, LiOTf is not required. Jesse Spillane examined other additives and found that 5 mol % LiI accelerated the rate of these reactions, allowed for lower reaction temperature (70 °C), and led to improved yields. However, added LiI

increases starting material isomerization with non-styrenyl substrates. In the case of styrenyl substrates (except for **3.170**), only *E*-alkenyl boronic esters were observed. 4-*tert*-Butylstyrene was converted to **3.160** in 92% yield. Sterically hindered (**3.161**), electron-rich (**3.162**-**3.163**), and electron-poor substrates (**3.164**-**3.165**) all gave good to excellent yields. Aryl fluorides (**3.166**) and chlorides (**3.167**) were well tolerated. Heterocyclic alkenes, such as indoles (**3.168**) and dioxolanes (**3.169**), were also excellent substrates. Significantly, α-methylstyrene was also borylated in good yield and with excellent *E*/*Z* selectivity (**3.170**).[77] This product cannot be synthesized *via* hydroboration, and it demonstrates that increased substitution on the alkene may be accessible in future work.

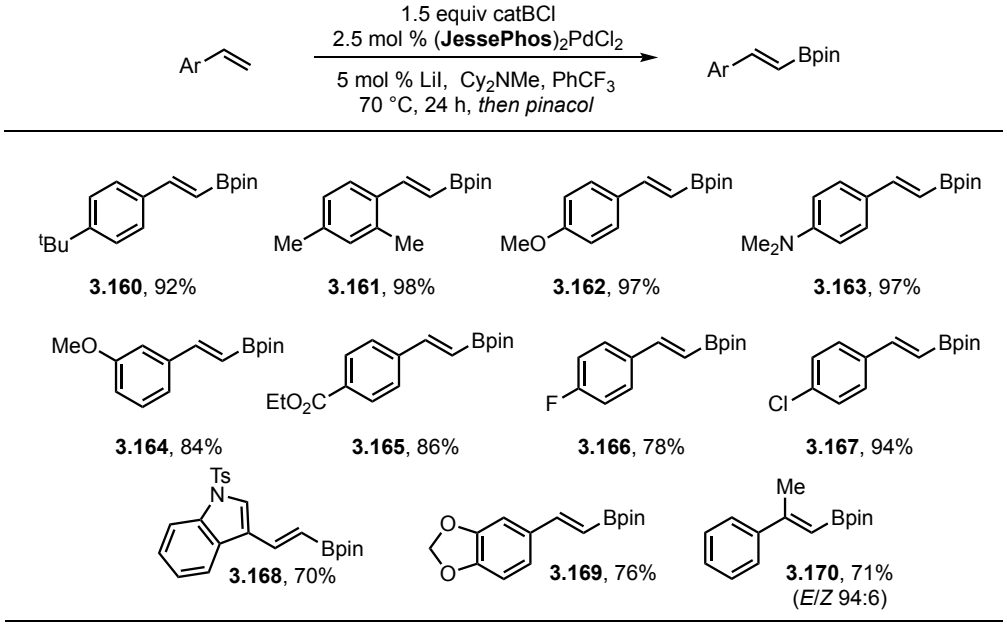

Figure 3.67 Scope of Styrenyl Substrates

3.6.3 Formation of Different Boronic Acid Derivatives

Different boronic esters provide different and sometimes orthogonal reactivity in a variety of chemical transformations.[2] This boryl-Heck reaction is readily adapted to produce diverse boronate derivatives by simply changing the nucleophile added after the reaction, delivering various boronic esters (Figure 3.68, **3.171**-**3.173**), amides (**3.174**), and trifluoroborates (**3.175**). We believe that this is a significant advantage over other reported methods, which have traditionally required different reaction conditions and boron containing precursors to access different alkenyl boronic esters.

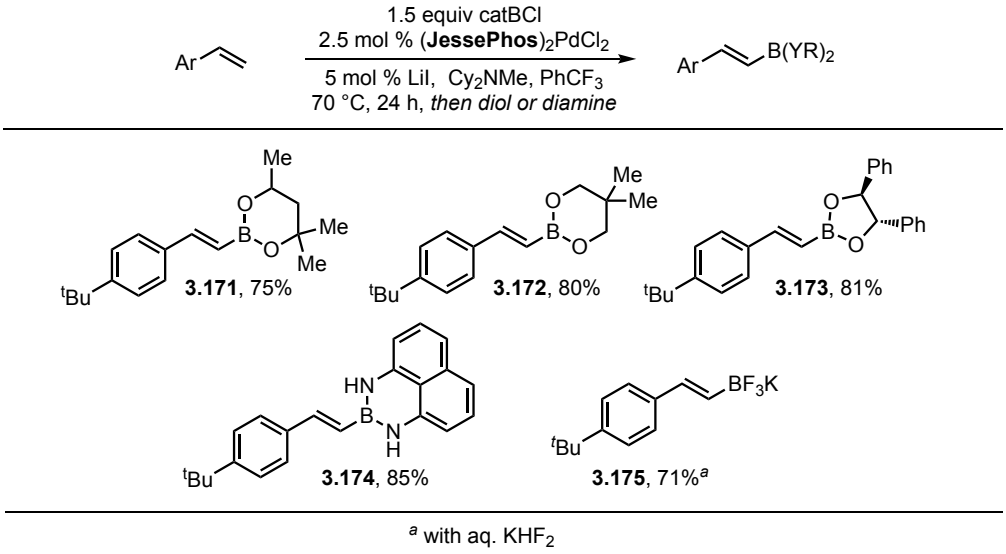

Figure 3.68 Synthesis of Alternative Boronic Acid Derivatives

3.6.4 *In Situ* Suzuki Reaction

While some applications exist, boronic ester themselves are not particularly interesting in biomedical or material uses. However, due to their non-toxicity, stability, and high reactivity, alkenyl boronic esters serve as optimal intermediates in the synthesis of countless medicines and materials.

The high degree of regio- and stereoselectivity of this reaction provides the potential for further cross coupling with the same selectivity. A two step, one pot sequence of boryl-Heck then Suzuki reaction with an aryl halide would give rapid access to stereo defined functionalized alkenes in a single step. The addition of iodobenzene and Cs_2CO_3 to the crude reaction mixture (**3.176**) gave stilbene **3.177** in 98% yield as a single *E*-isomer (Figure 3.69). No catalyst exchange or addition was necessary, showing that (**JessePhos**)$_2PdCl_2$ is a competent precatalyst for both reactions under the same conditions.

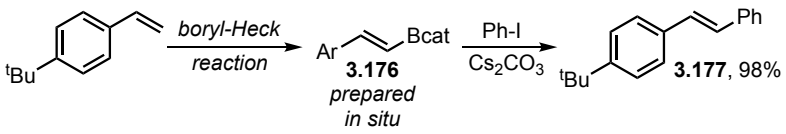

Figure 3.69 One Pot Boryl-Heck/Suzuki Sequence

3.7 Mechanistic Studies

On-going studies are aimed at elucidating the mechanism. At present, we favor the Heck-like pathway outlined in Figure 3.1. While we do not yet have a complete understanding of the mechanism, preliminary studies have revealed some key observations and insights.

3.7.1 Formation of Amine-Borane Adduct

First, we decided to investigate the role of the Cy_2NMe in this reaction and its effectiveness when compared to Et_3N. To probe this, Jesse Spillane used ^{11}B NMR to monitor the formation of relevant amine-borane adducts. Although the combination of catBCl and Cy_2NMe (in $CDCl_3$) does reveal formation of an amine-borane adduct by

^{11}B NMR spectroscopy (Figure 3.70, **3.178**), it is distinct from that formed with Et_3N (**3.138**). The Cy_2NMe derived complex has a broader peak and is shifted more downfield, both of which indicate a less tightly bound boron atom. Furthermore, the addition of 1 equiv of Et_3N to **3.178** results in complete conversion to **3.138**, providing additional evidence for a less stable Cy_2NMe complex. This data supports the notion that a greater concentration of free catBCl is available with the use of a larger base and explains our success when compared to earlier reports.

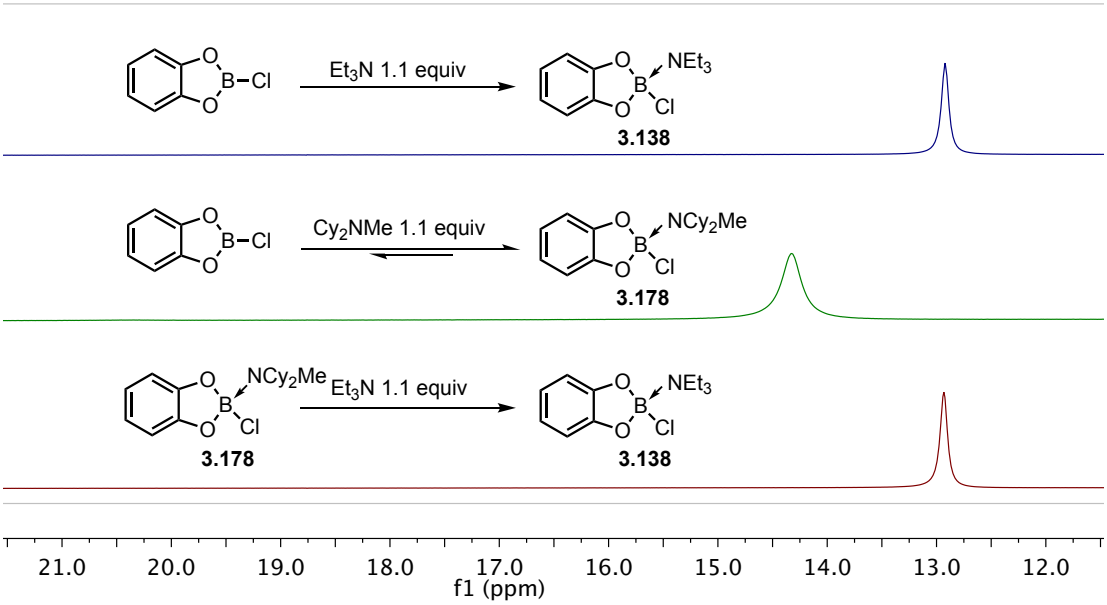

Figure 3.70 ^{11}B NMR Spectra of Amine-Borane Coordination Complexes.

Density functional theory calculations (B3LYP/6-31++G(d,p)) modeling this coordination also suggest that Cy_2NMe coordinates more reversibly with catBCl (Figure 3.71). Examination of the ΔH of the coordination complexes compared to the free amine and catBCl show –7.2 kcal/mol with triethylamine but only –3.2 kcal/mol with

Cy_2NMe. The stability of catBCl·Et_3N sequesters the catBCl, preventing it from entering the catalytic cycle.

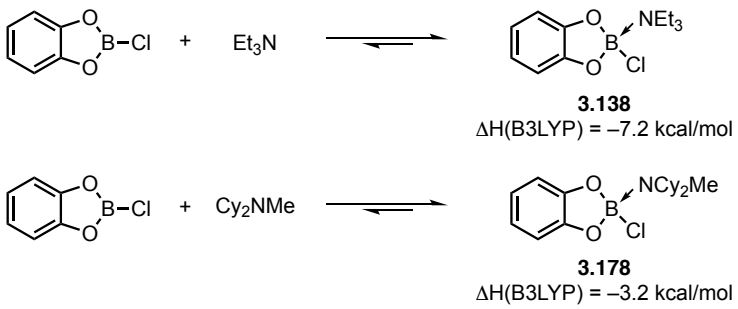

Figure 3.71 DFT Calculations of Coordination Amine Coordination Complex

3.7.2 Isomerization Studies

Second, I wanted to better understand the origin of vinyl/allyl selectivity in the boryl-Heck reaction. When given an opportunity to select between vinyl or allyl alkenyl boronic ester, the boryl-Heck exclusively prefers to form the vinyl product. The analogous bimolecular silyl-Heck reaction has a high selectivity for allyl silanes over vinyl (Figure 3.72).

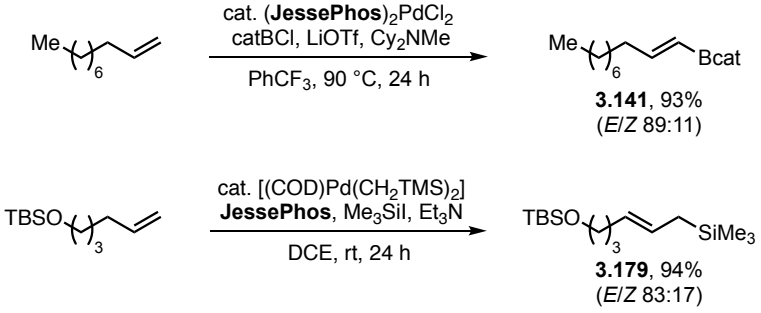

Figure 3.72 Vinyl vs. Allyl Selectivity for Boryl- and Silyl-Heck Reactions

The observed *E*/*Z* ratio is similar to that of earlier rhodium-catalyzed processes,[76] which suggest a thermodynamic distribution of products. Experimental evidence for thermodynamic control was gained by spiking isomerically pure (*E*)-hexenylborane **3.180** into the boryl-Heck reaction of 4-phenylbutene (Figure 3.73). Boronate **3.147** was formed with the expected *E*/*Z* selectivity, however **3.181** was detected with only a 93:7 *E*/*Z* ratio. This isomerization is not due to transesterification as erosion of alkene geometry is not seen without catalyst. These results show that under our exact catalytic conditions, isomerization of product can and does occur demonstrating that the vinyl/allyl and *E*/*Z* selectivity we observe in thermodynamically derived. Future studies will be aimed at elucidating the kinetic product.

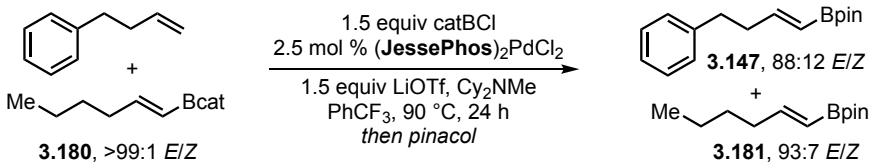

Figure 3.73 Isomerization Study

We sought to compare some of the experimental *E*/*Z* ratios to calculated DFT energies for several substrates. All of the following calculations (B3LYP/6-31++G(d,p)) were performed at 90 °C. Ground state calculations for each of the four possible butene product isomers were performed to determine the relative ΔH. The products of 1-butene were chosen because they should be representative of all larger α-olefins. The computed and experimentally measured *E*-alkenyl, *Z*-alkenyl, *E*-allyl, and *Z*-allyl products correlate very well supporting the notion that the observed ratio is thermodynamic (Figure 3.74).

Compound	Structure	Relative Energy ΔH B3LYP	Theoretical Distribution	Experimental Distribution
3.182	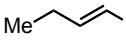	0.0 kcal/mol	92%	93%
3.183	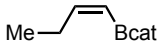	1.9 kcal/mol	6%	7%
3.184	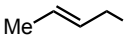	2.8 kcal/mol	2%	0%
3.185	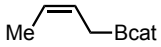	4.3 kcal/mol	0%	0%

Figure 3.74 Comparison of Theoretical and Experimental Product Distributions of 1-Butene

The products from allylbenzene and styrene were also examined and show similar correlations (Figures 3.75 and 3.76).

Compound	Structure	Relative Energy ΔH B3LYP	Theoretical Distribution	Experimental Distribution
3.186	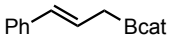	0.0 kcal/mol	56%	67%
3.187	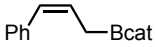	2.9 kcal/mol	1%	5%
3.188	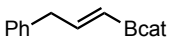	0.2 kcal/mol	40%	25%
3.189	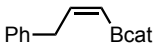	2.1 kcal/mol	3%	3%

Figure 3.75 Comparison of Theoretical and Experimental Product Distributions of Allylbenzene

Compound	Structure	Relative Energy ΔH B3LYP	Theoretical Distribution	Experimental Distribution
3.190	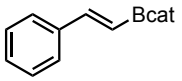	0.0 kcal/mol	>99%	>99%
3.191	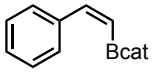	4.2 kcal/mol	0%	0%

Figure 3.76 Comparison of Theoretical and Experimental Product Distributions of Styrene

3.8 Conclusion

In conclusion, we have demonstrated the first example of a boryl-Heck reaction using an electrophilic boron reagent. This transformation converts terminal alkenes to alkenyl boronic esters and their derivatives in high yield and with good functional group tolerance. The reaction is compatible with both linear α-olefin and styrenyl substrates and provides products with excellent *E*/*Z* ratios. The utility of this reaction was demonstrated with a tandem boryl-Heck/Suzuki reaction to synthesize a non-symmetric stilbene product. This work demonstrates that identification of a bulky amine base, in combination with appropriate catalyst and additives, overcomes the previously observed incompatibility of chloroboranes with conditions that enable β-hydride elimination. Both experimental and computation studies indicate that the high level of selectivity is derived from a thermodynamic equilibrium of the lowest energy isomers. By harnessing a Heck mechanism, this method enables use of an inexpensive, readily available borylation reagent and avoids formation of byproducts, two significant advantages over existing methods to deliver these valuable versatile synthetic intermediates.

This work was communicated in 2016 in *The Journal of the American Chemical Society*.[99]

3.9 Experimental Details

3.9.1 General Experimental Details

Diethyl ether, tetrahydrofuran and dichloromethane were dried on alumina according to published procedures.[102] Catechol was purchased from Alfa Aesar and recrystallized from hot toluene prior to use. Boron trichloride was purchased from Acros as a 1 M solution in hexanes and used as received. N,N-Dicyclohexylmethylamine was purchased from TCI, distilled from calcium hydride (80 °C, 150 mtorr) and stored at rt on the bench in a nitrogen-filled Strauss flask. Trifluorotoluene was purchased from Sigma Aldrich in an anhydrous septum sealed bottle, transferred to a Straus flask by cannula transfer and sparged with nitrogen for 15 minutes. Lithium trifluoromethanesulfonate was purchased from Oakwood and stored in a nitrogen-filled glovebox or in a desiccator under air. Bis(trimethylsilylmethyl)-(cycloocta-1,5-diene) palladium(II) [(COD)Pd(CH_2SiMe_3)$_2$] was prepared according to a published procedure.[1a] Tris(dibenzylideneacetone)dipalladium(0) [$Pd_2(dba)_3$] was purchased from Aldrich or Strem and used as received. Bis(3,5-di-*tert*-butylphenyl)(*tert*-butyl)phosphine (L1) was prepared according to a published procedure.[1d] Substrates ethyl 4-vinylbenzoate,[1b] 5-vinylbenzo-1,3-dioxole[103] and 1-(toluene-4-sulfonyl)-2-vinyl-1*H*-indole[104] were prepared according to published literature procedures. All other substrates and reagents were purchased in highest analytical purity from commercial suppliers and used as received. Vials used in the glovebox were dried in a gravity oven at 140 °C for a minimum of 12 h, transferred into the glovebox hot, and then stored at rt in the glovebox prior to use. All other glassware was flame-dried under vacuum prior to use. “Double manifold” refers to a standard Schlenk-line gas manifold equipped with nitrogen and vacuum (ca. 100 mtorr). All

optimization reactions (0.25 mmol) were run in a nitrogen-filled glovebox and heated using an aluminum block on a magnetic stir plate. All yields in optimization reactions were determined using ^{1}H NMR using 1,3,5-trimethoxybenzene or ferrocene as an internal standard and *E/Z* ratios were determined using ^{1}H NMR of unpurified products. All other reactions were set up using standard Schlenk technique and heated with stirring in temperature controlled oil baths. Any product yields listed in the main text that do not match those listed in the supporting information are the average of multiple isolated yields. The *E/Z* ratio of the isolated products may differ from the crude mixture due to enrichment during purification. Only the *E*-isomer is reported for the ^{1}H and ^{13}C NMR spectral data. The ^{13}C NMR spectra may contain extra, unassigned peaks, which we attribute to the minor *Z*-isomer. Note: The ^{13}C NMR signal for carbons attached to boron did not appear in the collected spectra due to the quadruple splitting of ^{11}B.[105] NMR data for some compounds may be reported in two different solvents to resolve overlapped ^{13}C peaks.

3.9.2 Instrumentation and Chromatography

400 MHz ^{1}H, 101 MHz ^{13}C and 376 MHz ^{19}F spectra were obtained on a 400 MHz FT-NMR spectrometer equipped with a Bruker CryoPlatform. 600 MHz ^{1}H, 151 MHz ^{13}C, and 193 MHz ^{11}B spectra were obtained on a 600 MHz FT-NMR spectrometer equipped with a Bruker SMART probe. All samples were analyzed in the indicated deutero-solvent and were recorded at ambient temperatures. All chemical shifts are reported in ppm. ^{1}H NMR spectra were calibrated using the residual protio-signal in deutero-solvents as a standard. ^{13}C NMR spectra were calibrated using the deutero-solvent as a standard. IR spectra were recorded on a Nicolet Magma-IR 560 FT-IR spectrometer as thin films on KBr plates. High resolution MS data was obtained

on a Thermo Q-Exactive Orbitrap using electrospray ionization (ESI), or a Waters GCT Premier spectrometer using chemical ionization (CI) or liquid injection field desorption ionization (LIFDI). Column chromatography was performed with boric acid impregnated 40-63 μm silica gel[101] with the eluent reported in parentheses. Analytical thin-layer chromatography (TLC) was performed on pre-coated glass plates and visualized by UV or by staining with iodine or $KMnO_4$.

3.9.3 Synthesis of Non-commercial Starting Materials and Reagents

3.9.3.1 Alkenes Substrates

(**S3.1**) A 500 mL round bottom flask equipped with a magnetic stir bar and rubber septum was charged with 4-dimethylaminopyridine (305 mg, 0.1 equiv), triethylamine (100 mL), dichloromethane (100 mL), and 5-hexenol (3.0 mL, 25 mmol, 1.0 equiv) and sealed under air. Triisopropylchlorosilane (6.7 mL, 31.3 mmol, 1.25 equiv) was then added dropwise *via* syringe and the reaction was stirred for 72 h. The reaction was opened to air, quenched with water (100 mL), and extracted with diethyl ether (3 x 100 mL). The combined organic layers were washed with 1M hydrochloric acid (100 mL), dried with $MgSO_4$, filtered through Celite, and concentrated *in vacuo*. The crude oil was purified by flash silica gel chromatography (hexanes) to afforded **S3.1** as a colorless oil (5.32 g, 83%): ^{1}H NMR (400 MHz, $CDCl_3$) δ 5.82 (ddt, *J* = 16.9, 10.2, 6.6 Hz, 1H), 5.01 (dd, *J* = 17.1, 1.7 Hz, 1H), 4.94 (d, *J* = 10.2 Hz, 1H), 3.69 (t, *J* = 6.4 Hz, 2H), 2.08 (q, *J* = 7.1 Hz, 2H), 1.62 – 1.52 (m, 2H), 1.51 – 1.41 (m, 2H), 1.14 – 0.96 (m, 21H); ^{13}C NMR (101 MHz, $CDCl_3$) δ 139.1, 114.5, 63.4, 33.8, 32.6, 25.3, 18.2, 12.2; FTIR (cm^{-1}): 2942,

2892, 2866, 1463, 1106, 1070, 1013, 994, 910, 882, 680, 658. HRMS (CI) m/z, calcd for $[C_{15}H_{33}OSi]^+$: 257.2301; found: 257.2296.[106]

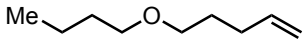

(**S3.2**) A 500 mL round bottom flask equipped with a magnetic stir bar and a rubber septum was flame dried under vacuum, cooled to rt and refilled with nitrogen. The flask was briefly opened to air, and quickly charged with sodium hydride 60% dispersion in mineral oil (3.5 g, 87.5 mmol, 1.5 equiv), and the flask was resealed. Anhydrous tetrahydrofuran (250 mL) was then added *via* syringe. The stirred suspension was cooled to 0 °C and 4-pentenol (6 mL, 58.1 mmol, 1.0 equiv) was added dropwise *via* syringe (*caution: vigorous gas evolution*). The cooling bath was removed, and the reaction was allowed to stir for 3 h at rt. The mixture was then recooled to 0° C and 1-bromobutane (12.5 mL, 116.2 mmol, 2 equiv) was added dropwise *via* syringe. The cooling bath was removed, and the mixture was stirred overnight at rt. The reaction was opened to air and quenched with saturated ammonium chloride (50 mL), adding the first few mL dropwise. This mixture was diluted with 200 mL diethyl ether, and the organic layer was separated, dried with $MgSO_4$, filtered through Celite and concentrated *in vacuo*. The crude oil was purified by flash silica gel chromatography (5 : 95 ethyl acetate : hexanes) affording **S3.2** as a colorless oil (70%): ^{1}H NMR (400 MHz, $CDCl_3$) δ 5.82 (ddt, *J* = 16.9, 10.2, 6.6 Hz, 1H), 5.02 (dd, *J* = 17.1, 1.9 Hz, 1H), 4.95 (dd, *J* = 10.2, 2.0 Hz, 1H), 3.40 (td, *J* = 6.6, 2.8 Hz, 4H), 2.11 (q, *J* = 6.9 Hz, 2H), 1.75 – 1.62 (m, 2H), 1.59 – 1.49 (m, 2H), 1.43 – 1.31 (m, 2H), 0.91 (t, *J* = 7.4 Hz, 3H); ^{13}C NMR (101 MHz, $CDCl_3$) δ 138.5, 114.8, 70.8, 70.3, 32.0, 30.5, 29.1, 19.5, 14.1; FTIR (cm^{-1}): 2954, 2924, 2854, 1457, 1377. HRMS (CI) m/z, calcd for $[C_9H_{19}O]^+$: 143.1436; found: 143.1425.

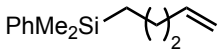

(**S3.3**) A 250 mL 3-neck round bottom flask equipped with a magnetic stir bar and a water condenser was charged with magnesium turnings (1.4 equiv), sealed with 3 rubber septa, flame dried under vacuum, cooled to rt and refilled with nitrogen. Anhydrous diethyl ether (5 mL) was added to cover the magnesium turnings and 5-bromopentene (1.2 equiv) was added dropwise *via* syringe. After the solution began to self-reflux the remaining diethyl ether (95 mL) and 5-bromopentene were slowly added as needed to maintain a gentle reflux. After all of the bromide was added, the reaction was heated to 40 °C to reflux for 1 h. A separate oven dried round bottom flask equipped with a magnetic stir bar and rubber septum was cooled under vacuum, refilled with nitrogen, charged with dimethylphenylchlorosilane (2.5 mL, 15 mmol, 1.0 equiv), diluted with anhydrous diethyl ether (15 mL, 1 M) and cooled to 0 °C. The Grignard reagent, prepared above, was added dropwise *via* syringe to the solution of dimethylphenylchlorosilane at 0 °C. After the addition was complete, catalytic $ZnCl_2$ (0.5 mL, 1 M in diethyl ether, 0.03 equiv) was added *via* syringe and the reaction was stirred for 72 h at rt under nitrogen. The reaction was cooled to 0 °C, opened to air, diluted with diethyl ether (10 mL) then slowly quenched with water (15 mL). The mixture was extracted with diethyl ether (3 x 10 mL) and the combined organic layers were washed with brine, dried with $MgSO_4$, filtered through Celite, and concentrated *in vacuo*. The crude oil was purified *via* flash silica gel chromatography (hexanes) to give **S3.3** as a clear oil (2.09 g, 68%): ^{1}H NMR (400 MHz, $CDCl_3$) δ 7.56 – 7.49 (m, 2H), 7.41 – 7.33 (m, 3H), 5.79 (ddt, J = 17.0, 10.2, 6.7 Hz, 1H), 5.06 – 4.91 (m, 2H), 2.08 (q, J = 7.1 Hz, 2H), 1.51 – 1.36 (m, 2H), 0.85 – 0.73 (m, 2H), 0.28 (s, 6H); ^{13}C NMR (101 MHz, $CDCl_3$) δ 139.6, 139.0, 133.7, 128.9, 127.9, 114.7, 37.8,

23.5, 15.4, -2.9; FTIR (cm^{-1}): 3069, 2955, 2922, 1427, 1248, 1114, 910, 834, 811, 771, 728, 699, 469. HRMS (CI) m/z, calcd for $[C_{13}H_{21}Si]^+$: 205.1413; found: 205.1429.[107]

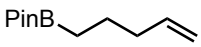

(**S3.4**) A 100 mL round bottom flask equipped with a magnetic stir bar was charged with 4-pentenyl-1-boronic acid (1.65 g, 14.5 mmol, 1.0 equiv), pinacol (1.75 g, 14.5 mmol, 1.0 equiv), $MgSO_4$ (8.7 g, 5 equiv) and diluted with diethyl ether (15 mL, 1 M) under air. The reaction vessel was sealed with a rubber septum and stirred at rt overnight. The crude reaction mixture was filtered through Celite and concentrated *in vacuo*. The crude oil was purified *via* flash silica gel chromatography (5 : 95 ethyl acetate : hexanes) to give **S3.4** as a colorless oil (2.10 g, 75%): ^{1}H NMR (600 MHz, $CDCl_3$) δ 5.80 (ddt, *J* = 17.0, 10.2, 6.7 Hz, 1H), 4.99 (dd, 1H), 4.93 (d, 1H), 2.05 (q, *J* = 7.0 Hz, 2H), 1.51 (p, *J* = 7.7 Hz, 2H), 1.24 (s, 12H), 0.79 (t, *J* = 7.9 Hz, 2H). ^{13}C NMR (151 MHz, $CDCl_3$) δ 139.1, 114.6, 83.0, 36.5, 25.0, 23.6; ^{11}B NMR (193 MHz, $CDCl_3$) δ 34.1; FTIR (cm^{-1}): 2979, 2931, 1407, 1378, 1318, 1146, 969, 910. HRMS (CI) m/z, calcd for $[C_{11}H_{22}BO_2]^+$: 197.1713; found: 197.1701.[108]

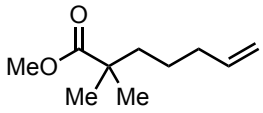

(**S3.5**) A 100 mL round bottom flask equipped with a magnetic stir bar and a rubber septum was flame dried under vacuum, cooled to rt and refilled with nitrogen. Diisopropylamine (3.08 mL, 24 mmol, 1.2 equiv) and anhydrous tetrahydrofuran (10 mL) were added *via* syringe and the mixture was cooled to -78 °C under a positive pressure of nitrogen. A solution of n-butyllithium (9.2 mL, 2.6 M in hexanes, 1.95 equiv) was added dropwise *via* syringe and the solution was stirred for 1 h at -78 °C. A solution of methyl isobutyrate (2.3 mL, 20 mmol, 1.0 equiv) in anhydrous tetrahydrofuran (10 mL, 2 M) was added dropwise *via* syringe and the

reaction was stirred for 2 h at -78 °C. 5-Bromopentene (2.86 mL, 24 mmol, 1.2 equiv) was added *via* syringe then the cooling bath was removed and the reaction was stirred at rt for 24 h. The reaction was then cooled to 0 °C, opened to air and quenched with saturated aqueous ammonium chloride (20 mL). The mixture was extracted with diethyl ether (3 x 10 mL) and the combined organic layers were washed with brine, dried with $MgSO_4$, filtered through Celite, and concentrated *in vacuo*. The crude oil was purified *via* flash silica gel chromatography (5 : 95 ethyl acetate : hexanes) to give **S3.5** as a colorless oil (1.62 g, 48%): ^{1}H NMR (600 MHz, $CDCl_3$) δ 5.78 (ddt, J = 16.9, 10.2, 6.6 Hz, 1H), 4.99 (dd, J = 17.1 Hz, 1H), 4.94 (d, J = 10.9 Hz, 1H), 3.65 (s, 3H), 2.02 (q, J = 7.3 Hz, 2H), 1.55 – 1.47 (m, 2H), 1.39 – 1.27 (m, 2H), 1.16 (s, 6H); ^{13}C NMR (151 MHz, $CDCl_3$) δ 178.6, 138.7, 114.7, 51.8, 42.4, 40.4, 34.2, 25.3, 24.4; FTIR (cm^{-1}): 2978, 2946, 1734, 1474, 1268, 1195, 1150, 911. HRMS (CI) m/z, calcd for $[C_{10}H_{19}O_2]^+$: 171.1385; found: 171.1365.[109]

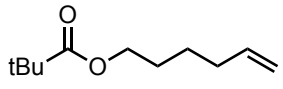

(**S3.6**) A 500 mL round bottom flask equipped with a magnetic stir bar and a rubber septum, was flame dried under vacuum, cooled to rt, and refilled with nitrogen. Anhydrous dichloromethane (200 mL), 5-hexenol (4.8 mL, 40 mmol, 1.0 equiv), pivaloyl chloride (5.9 mL, 48 mmol, 1.2 equiv) and triethylamine (6.7 mL, 48 mmol, 1.2 equiv) were each added sequentially *via* syringe. The reaction was stirred at rt for 20 h. The reaction was then opened to air and quenched with 3M aqueous ammonium hydroxide (60 mL). The organic layer was separated then washed with an additional 3 M ammonium hydroxide (1 x 60 mL) then with brine (1 x 60 mL). The combined aqueous layers were extracted with dichloromethane (1 x 60 mL). The combined organic layers were dried with $MgSO_4$,

filtered through Celite, and concentrated *in vacuo*. The crude liquid was purified *via* flash silica gel chromatography (5 : 95 diethyl ether : hexanes) to give **S3.6** as a colorless liquid (6.57g, 89%): ^{1}H NMR (400 MHz, $CDCl_3$) δ 5.79 (ddt, *J* = 16.9, 10.2, 6.7 Hz, 1H), 5.01 (dd, *J* = 17.1, 1.6 Hz, 1H), 4.96 (dd, *J* = 10.2, 3.1, 1.2 Hz, 1H), 4.05 (t, *J* = 6.6 Hz, 2H), 2.08 (q, *J* = 7.2 Hz, 2H), 1.74 – 1.57 (m, 2H), 1.54 – 1.37 (m, 2H), 1.19 (s, 9H); ^{13}C NMR (101 MHz, $CDCl_3$) δ 178.8, 138.6, 114.9, 64.4, 38.9, 33.4, 28.2, 27.3, 25.3; FTIR (cm^{-1}): 2975, 2936, 1730, 1481, 1285, 1156, 911. HRMS (CI) m/z, calcd for $[C_{11}H_{21}O_2]^+$: 185.1542; found: 185.1525.

3.9.3.2 Single Component Precatalyst (JessePhos$_2$PdCl$_2$)

(**JessePhos$_2$PdCl$_2$**) Bis(acetonitrile)dichloropalladium(II) (311 mg, 1.2 mmol, 1.0 equiv) and bis(3,5-di-*tert*-butylphenyl)(*tert*-butyl)phosphine (1.12 g, 2.4 mmol, 2.0 equiv) was added to a 50 mL round bottom flask equipped with a magnetic stir bar and a rubber septum. The atmosphere in the flask was replaced with nitrogen, and anhydrous dichloromethane (20 mL) was added *via* syringe. The reaction was stirred for 30 minutes at rt. The flask was then briefly opened to air and the solvent was removed in *vacuo* (~200 mtorr). The resulting solid was recrystallized from anhydrous diethyl ether (15 mL) under a nitrogen atmosphere at 0 °C for 24 h to give (JessePhos)$_2$PdCl$_2$ as an air stable, fine yellow solid (1.23 g, 92% yield): ^{1}H NMR (400 MHz, C_6D_6) δ 8.08 (t, *J* = 5.1 Hz, 8H), 7.60 (s, 4H), 1.76 (t, *J* = 7.3 Hz, 18H), 1.33 (s, 72H); ^{13}C NMR (101 MHz, C_6D_6) δ 149.6 (t, *J* = 4.7 Hz), 131.0 (t, *J* = 5.8 Hz), 130.5 (t, *J* = 40.1 Hz), 123.8, 36.6 (t, *J* = 10.6 Hz), 35.2, 31.6, 31.1 (t, *J* = 2.6 Hz); ^{31}P NMR (162 MHz, C_6D_6) δ 41.9; FTIR (cm^{-1}): 2962, 2903, 2868, 1477, 1419, 1362, 1248, 1135, 708; mp = 261 °C (dec.). HRMS (LIFDI) m/z, calcd for $[C_{64}H_{102}Cl_2P_2Pd]$: 1108.5885; found: 1108.5583. Anal.

Calcd for $C_{64}H_{102}Cl_2P_2Pd$: C, 69.20; H, 9.26; Cl, 6.38. Found: C, 69.04; H, 9.38; Cl, 6.23.

A small portion of $(JessePhos)_2PdCl_2$ was dissolved in dichloromethane under air and recrystallized *via* slow evaporation at rt to give an X-ray quality crystal (Figure 3.77, see below for full crystallographic details).

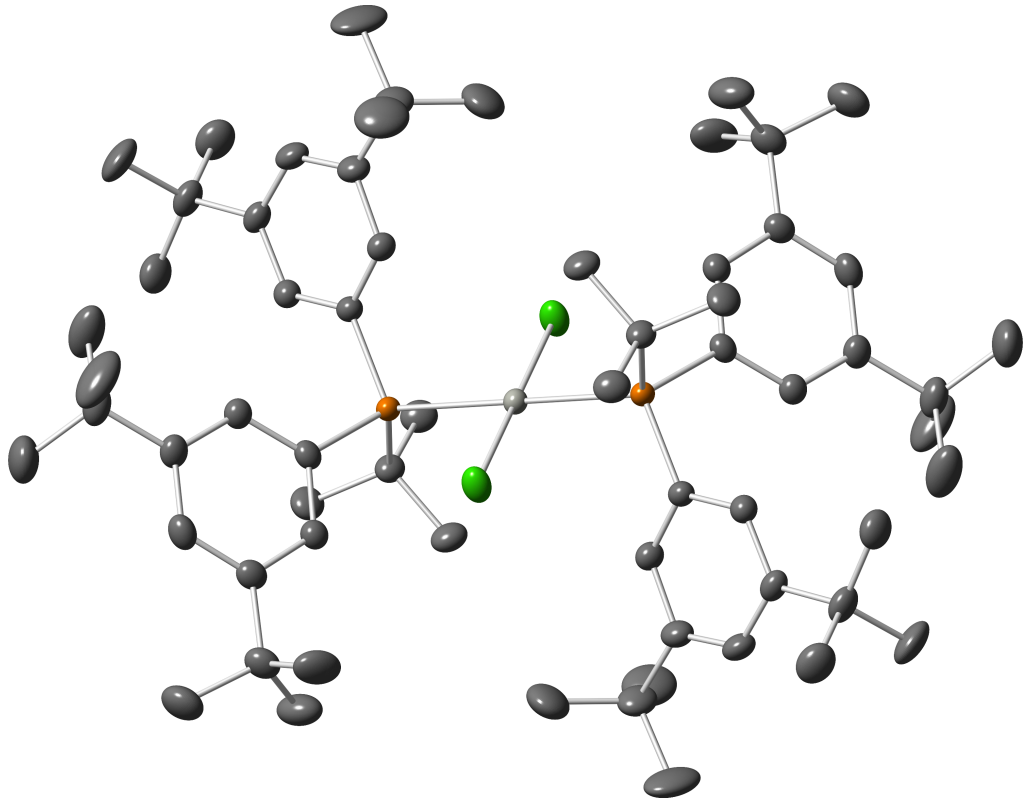

Figure 3.77 Crystal Structure of (**JessePhos**)$_2$PdCl$_2$ (hydrogen atoms omitted for clarity).

3.9.3.3 Catecholchloroborane (catBCl)

Note: Although catecholchloroborane is commercially available, for this communication we prepared it using a modification of literature procedures.[110]

Caution: This reaction generates 2 equivalents of anhydrous hydrogen chloride gas. The addition rate of boron trichloride must be controlled to prevent over-pressurization of the reaction vessel. All gas leaving the reaction should be scrubbed by base to prevent harm to people or equipment.

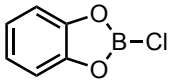

(**catBCl**) A flame dried 500 mL Schlenk flask equipped with a magnetic stir bar and a rubber septum was cooled to rt under vacuum and refilled with nitrogen. The flask was briefly opened and quickly charged with catechol (10.46 g, 95 mmol, 0.95 equiv) then resealed. The flask was then evacuated and refilled with nitrogen 3 times. Anhydrous hexanes (200 mL) was added *via* canula transfer. With a positive flow of nitrogen, the septum was removed and the Schlenk flask was equipped with an oven dried 100 mL pressure-equalizing addition funnel equipped with a rubber septum. The apparatus was fitted with a vent tube attached to a gas scrubber filled with aqueous NaOH (250 mL, ~10 M, 0 °C). The catechol solution was cooled to 0 °C with stirring (~1 h). Boron trichloride (100 mL, 1.0 M in hexane, 1.0 equiv) was cannula transferred into the addition funnel (stopcock closed). The stopcock was opened slightly to add boron trichloride dropwise to the solution of catechol with rapid stirring. Once the addition of boron trichloride was complete, the reaction was allowed to warm to rt and stir overnight (8-12 h) with a slow, constant flow of nitrogen entering the Schlenk flask through the side arm, and exiting the addition funnel through the vent tube leading to the gas scrubber. After 8-12 h, when the solution has become homogeneous, the slow addition funnel was quickly replaced with a glass stopper and the hexanes was removed *in vacuo* (~200 mtorr) through a solid NaOH trap to quench any residual hydrogen chloride gas. Once dried, the flask was sealed under vacuum, brought into a dry

glovebox and scraped into vials. The catecholchloroborane was used without further purification, but it can be sublimed (70 °C, 20 torr) to give a white solid (13.77 g, 94%): ^{1}H NMR (400 MHz, $CDCl_3$) δ 7.18 – 7.12 (m, 2H), 7.07 – 7.00 (m, 2H); ^{13}C NMR (101 MHz, $CDCl_3$) δ 148.2, 123.6, 112.9; ^{11}B NMR (128 MHz, $CDCl_3$) δ 28.9.

3.9.3.4 Comments and Preparation of Boric Acid Impregnated Silica

Note: Many boronic esters are known to partially decompose during purification on silica gel. However, boric acid impregnated silica has been shown to decrease this decomposition resulting in increased isolated yields.[101] In our hands, use of commercial, untreated silica gel resulted in yields ~5-10 % lower than with boric acid impregnated silica gel (prepared according to the procedure below). Importantly, while boric acid impregnated silica gel is not necessary for this method, the use of it for purification did result in more consistent isolated yields.

Boric Acid Impregnated Silica: A 1000 mL round bottom flask equipped with a thick stir bar was charged with silica gel (300 mL), boric acid (28 g) and ethanol (550 mL) under air. The suspension was stirred at rt for 2 h at which time the ethanol and excess boric acid were removed by filtration through a fine glass frit. The impregnated silica was washed with ethanol (3 x 200 mL) and left to dry on the frit under constant suction for 16 h then placed in a 140 °C gravity oven to dry for an additional 48 h. Once dried, the boric acid impregnated silica was stored at rt in a desiccator until used.

3.9.4 Procedure for the α-Olefin Boryl-Heck Reaction

Note: All reactions in this section were performed on a 3 mmol scale.

3.9.4.1 General Procedure A (α-Olefins)

In a nitrogen-filled glovebox, catecholchloroborane (1.5 equiv), lithium trifluoromethanesulfonate (1.5 equiv) and $(JessePhos)_2PdCl_2$ (2.5 mol %), were added to a flame-dried or oven-dried 25 mL Schlenk flask equipped with a stir bar. The flask was sealed with a rubber septum, removed from the glovebox and attached to a nitrogen manifold *via* the sidearm. 3 mL of trifluorotoluene (1 mL per mmol) was added *via* syringe with stirring. N,N-dicyclohexylmethylamine (5.0 equiv) was added *via* syringe and then the sides of the flask were rinsed with 3 mL of additional trifluorotoluene (1 mL per mmol). The solution was stirred in an oil bath at 90 °C for 15 minutes, at which time the alkene substrate (1.0 equiv) was added in one portion *via* syringe. The reaction was allowed to stir at 90 °C for 24 h. After 24 h, the reaction was removed from the oil bath and opened to air. Pinacol (3 equiv) was added in one portion and the reaction was removed from heat and stirred for 1 h at rt. At that time, and with the reactor now cooled to rt, the reaction was diluted with 20 mL of diethyl ether. The reaction was stirred for 10 min, filtered through Celite and concentrated *in vacuo* to remove solvents, including trifluorotoluene. The crude oil was diluted with diethyl ether (30 mL) and washed with 1 M hydrochloric acid (3 x 20 mL) to remove excess amine. The organic layer was stirred with ammonium pyrrolidine-dithiocarbamate (palladium scavenger, 6 equiv to palladium)[100] for 1 h, then dried with $MgSO_4$, filtered through Celite and concentrated *in vacuo*. A small aliquot of the crude reaction mixture (~20 μL) was analyzed by ^1H NMR to determine the *E*/*Z* ratio. The crude material was purified *via* silica column chromatography on boric acid impregnated silica gel (as prepared above) in the indicated solvent combination.

Note: Only the *E* isomer is reported for the ^{1}H and ^{13}C NMR spectral data. The ^{13}C NMR spectra may contain extra, unassigned peaks, which are attributed to the minor *Z* isomer.

3.9.4.2 Characterization Data

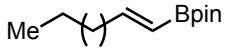

(**3.146**) According to general procedure A, catecholchloroborane (694 mg, 4.5 mmol), $(JessePhos)_2PdCl_2$ (83 mg, 0.075 mmol), lithium trifluoromethanesulfonate (702 mg, 4.5 mmol), N,N-dicyclohexylmethylamine (3.2 mL, 5.0 mmol), trifluorotoluene (6.0 mL, 0.5 M), and 1-decene (443 mg, 3.0 mmol) were combined under N_2 and stirred at 90 °C for 24 h. The reaction was worked up according to general procedure A. Analysis of the crude reaction mixture *via* ^{1}H NMR revealed an 88:12 *E*/*Z* ratio. The product was purified on boric acid impregnated silica gel chromatography (5 : 95 dichloromethane : hexanes) to afford **3.146** as a colorless oil (747 mg, 94%): ^{1}H NMR (600 MHz, $CDCl_3$) δ 6.64 (dt, *J* = 17.9, 6.5 Hz, 1H), 5.42 (dd, *J* = 17.9, 1.9 Hz, 1H), 2.20 – 2.08 (m, 2H), 1.45 – 1.36 (m, 2H), 1.30 – 1.22 (m, 22H), 0.87 (t, 3H); ^{1}H NMR (400 MHz, C_6D_6) δ 7.00 (dt, *J* = 17.8, 6.5 Hz, 1H), 5.82 (dt, *J* = 17.8, 1.5 Hz, 1H), 2.07 (q, 2H), 1.42 – 1.13 (m, 12H), 1.10 (s, 12H), 0.92 – 0.83 (m, 3H); ^{13}C NMR (151 MHz, $CDCl_3$) δ 155.0, 83.1, 36.0, 32.0, 29.6, 29.4, 28.4, 24.9, 22.8, 14.3; ^{13}C NMR (101 MHz, C_6D_6) δ 155.1, 82.9, 36.3, 32.3, 29.9, 29.7, 29.6, 28.8, 25.0, 23.1, 14.4; ^{11}B NMR (193 MHz, $CDCl_3$) δ 29.9; ^{11}B NMR (128 MHz, C_6D_6) δ 30.0; FTIR (cm^{-1}): 2978, 2926, 2855, 1639, 1362, 1320, 1146. HRMS (CI) m/z, calcd for $[C_{16}H_{32}BO_2]^+$: 267.2495; found: 267.2484.

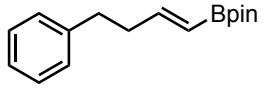

(**3.147**) According to general procedure A, catecholchloroborane (694 mg, 4.5 mmol), $(JessePhos)_2PdCl_2$ (83 mg, 0.075 mmol),

lithium trifluoromethanesulfonate (702 mg, 4.5 mmol), N,N-dicyclohexylmethylamine (3.2 mL, 5.0 mmol), trifluorotoluene (6.0 mL, 0.5 M), and 4-phenyl-1-butene (397 mg, 3.0 mmol) were combined under N_2 and stirred at 90 °C for 24 h. The reaction was worked up according to general procedure A. Analysis of the crude reaction mixture *via* ^{1}H NMR revealed an 88:12 *E*/*Z* ratio. The product was purified on boric acid impregnated silica gel chromatography (3 : 7 dichloromethane : hexanes) to afford **3.147** as a colorless oil (687 mg, 89%): ^{1}H NMR (600 MHz, $CDCl_3$) δ 7.30 – 7.27 (m, 2H), 7.20 – 7.16 (m, 3H), 6.70 (dt, *J* = 18.0, 6.2 Hz, 1H), 5.50 (d, *J* = 18.0 Hz, 1H), 2.79 – 2.68 (m, 2H), 2.53 – 2.39 (m, 2H), 1.27 (s, 12H); ^{1}H NMR (400 MHz, C_6D_6) δ 7.18 – 6.90 (m, 6H), 5.78 (d, *J* = 17.9 Hz, 1H), 2.57 – 2.48 (m, 2H), 2.37 – 2.25 (m, 2H), 1.09 (s, 12H); ^{13}C NMR (101 MHz, $CDCl_3$) δ 153.6, 141.9, 128.5, 126.0, 83.2, 37.7, 34.7, 24.9; ^{13}C NMR (101 MHz, C_6D_6) δ 153.8, 141.9, 128.7, 128.6, 126.1, 83.0, 37.9, 35.0, 25.0; ^{11}B NMR (193 MHz, $CDCl_3$) δ 29.7; ^{11}B NMR (128 MHz, C_6D_6) δ 29.8; FTIR (cm^{-1}): 2977, 2929, 1637, 1361, 1320, 1144. HRMS (CI) m/z, calcd for $[C_{16}H_{24}BO_2]^+$: 259.1869; found: 259.1867.

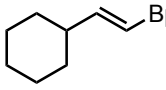

(**3.148**) According to general procedure A, catecholchloroborane (694 mg, 4.5 mmol), $(JessePhos)_2PdCl_2$ (83 mg, 0.075 mmol), lithium trifluoromethanesulfonate (702 mg, 4.5 mmol), N,N-dicyclohexylmethylamine (3.2 mL, 5.0 mmol), trifluorotoluene (6.0 mL, 0.5 M), and vinylcyclohexane (341 mg, 3.0 mmol) were combined under N_2 and stirred at 90 °C for 24 h. The reaction was worked up according to general procedure A. Analysis of the crude reaction mixture *via* ^{1}H NMR revealed a 96:4 *E*/*Z* ratio. The product was purified on boric acid impregnated silica gel chromatography (1 : 9 dichloromethane : hexanes) to afford **3.148** as a pale yellow oil

(595 mg, 84%): ^{1}H NMR (600 MHz, $CDCl_3$) δ 6.58 (dd, *J* = 18.2, 6.2 Hz, 1H), 5.38 (d, *J* = 18.2, 1H), 2.07 – 1.94 (m, 1H), 1.80 – 1.67 (m, 4H), 1.67 – 1.60 (m, 2H), 1.27 (s, 12H), 1.20 – 1.00 (m, 4H); ^{13}C NMR (151 MHz, $CDCl_3$) δ 160.0, 83.1, 43.4, 32.1, 26.3, 26.1, 24.9; ^{11}B NMR (193 MHz, $CDCl_3$) δ 30.1; FTIR (cm^{-1}): 2978, 2925, 2852, 1636, 1371, 1349, 1321, 1147. HRMS (CI) m/z, calcd for $[C_{14}H_{26}BO_2]^+$: 237.2026; found: 237.2041.

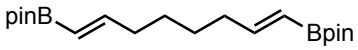

(**3.149**) According to general procedure A, catecholchloroborane (694 mg, 4.5 mmol), $(JessePhos)_2PdCl_2$ (83 mg, 0.075 mmol), lithium trifluoromethanesulfonate (702 mg, 4.5 mmol), N,N-dicyclohexylmethylamine (3.2 mL, 5.0 mmol), trifluorotoluene (6.0 mL, 0.5 M), and 1,7-octadiene (165 mg, 1.5 mmol) were combined under N_2 and stirred at 90 °C for 24 h. The reaction was worked up according to general procedure A. Analysis of the crude reaction mixture *via* ^{1}H NMR revealed a 90:10 *E*/*Z* ratio. The product was purified on boric acid impregnated silica gel chromatography (1 : 1 dichloromethane : hexanes) to afford **3.149** as a white solid (450 mg, 83%): ^{1}H NMR (600 MHz, $CDCl_3$) δ 6.61 (dt, *J* = 17.9, 6.5 Hz, 2H), 5.42 (d, *J* = 17.9 Hz, 2H), 2.20 – 2.07 (m, 4H), 1.43 (p, *J* = 3.5 Hz, 4H), 1.26 (s, 24H); ^{13}C NMR (151 MHz, $CDCl_3$) δ 154.6, 83.0, 35.8, 27.9, 24.9; ^{11}B NMR (193 MHz, $CDCl_3$) δ 29.9; FTIR (cm^{-1}): 2978, 2929, 1638, 1362, 1320, 1146; mp = 53 °C. HRMS (CI) m/z, calcd for $[C_{20}H_{37}B_2O_4]^+$: 363.2878; found: 363.2879.

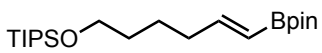

(**3.150**) According to general procedure A, catecholchloroborane (694 mg, 4.5 mmol), $(JessePhos)_2PdCl_2$ (83 mg, 0.075 mmol), lithium trifluoromethanesulfonate (702 mg,

4.5 mmol), N,N-dicyclohexylmethylamine (3.2 mL, 5.0 mmol), trifluorotoluene (6.0 mL, 0.5 M), and triisopropylsiloxy-5-hexene (770 mg, 3.0 mmol) were combined under N_2 and stirred at 90 °C for 24 h. The reaction was worked up according to general procedure A. Analysis of the crude reaction mixture *via* ^{1}H NMR revealed a 90:10 *E*/*Z* ratio. The product was purified on boric acid impregnated silica gel chromatography (3 : 7 dichloromethane : hexanes) to afford **3.150** as a colorless oil (1.02 g, 90%): ^{1}H NMR (600 MHz, $CDCl_3$) δ 6.63 (dt, *J* = 17.9, 6.4 Hz, 1H), 5.43 (d, *J* = 17.9 Hz, 1H), 3.67 (t, *J* = 6.3 Hz, 2H), 2.17 (q, 2H), 1.67 – 1.43 (m, 4H), 1.26 (s, 12H), 1.05 (s, 21H); ^{13}C NMR (151 MHz, $CDCl_3$) δ 154.7, 83.1, 63.3, 35.8, 32.7, 24.9, 24.7, 18.2, 12.2; ^{11}B NMR (193 MHz, $CDCl_3$) δ 29.8; FTIR (cm^{-1}): 2941, 2866, 1638, 1363, 1320, 1147, 1108. HRMS (CI) m/z, calcd for $[C_{21}H_{44}BO_3Si]^+$: 383.3153; found: 383.3134.

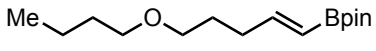

(**3.151**) According to general procedure A, catecholchloroborane (694 mg, 4.5 mmol), $(JessePhos)_2PdCl_2$ (83 mg, 0.075 mmol), lithium trifluoromethanesulfonate (702 mg, 4.5 mmol), N,N-dicyclohexylmethylamine (3.2 mL, 5.0 mmol), trifluorotoluene (6.0 mL, 0.5 M), and 5-butoxy-pent-1-ene (426 mg, 3.0 mmol) were combined under N_2 and stirred at 90 °C for 24 h. The reaction was worked up according to general procedure A. Analysis of the crude reaction mixture *via* ^{1}H NMR revealed an 87:13 *E*/*Z* ratio. The product was purified on boric acid impregnated silica gel chromatography (1 : 9 dichloromethane : hexanes) to afford **3.151** as a colorless oil (741 mg, 92%): ^{1}H NMR (600 MHz, $CDCl_3$) δ 6.63 (dt, *J* = 17.9, 6.4 Hz, 1H), 5.45 (d, *J* = 18.0 Hz, 1H), 3.50 – 3.30 (m, 4H), 2.28 – 2.13 (m, 2H), 1.75 – 1.63 (m, 2H), 1.54 (ddd, *J* = 14.6, 11.2, 4.9 Hz, 2H), 1.42 – 1.31 (m, 2H), 1.26 (s, 12H), 0.91 (t, *J* = 7.4 Hz, 3H); ^{13}C NMR (151

MHz, $CDCl_3$) δ 154.0, 83.2, 70.8, 70.3, 32.5, 32.0, 28.4, 24.9, 19.5, 14.1; ^{11}B NMR (193 MHz, $CDCl_3$) δ 29.8; FTIR (cm^{-1}): 2977, 2934, 2862, 1639, 1364, 1321, 1146. HRMS (CI) m/z, calcd for $[C_{15}H_{30}BO_3]^+$: 269.2288; found: 269.2274.

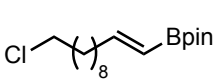

(**3.152**) According to general procedure A, catecholchloroborane (694 mg, 4.5 mmol), $(JessePhos)_2PdCl_2$ (83 mg, 0.075 mmol), lithium trifluoromethanesulfonate (702 mg, 4.5 mmol), N,N-dicyclohexylmethylamine (3.2 mL, 5.0 mmol), trifluorotoluene (6.0 mL, 0.5 M), and 11-chloro-1-undecene (584 mg, 3.0 mmol) were combined under N_2 and stirred at 90 °C for 24 h. The reaction was worked up according to general procedure A. Analysis of the crude reaction mixture *via* ^1H NMR revealed an 88:12 *E*/*Z* ratio. The product was purified on boric acid impregnated silica gel chromatography (1 : 4 dichloromethane : hexanes) to afford **3.152** as a colorless oil (830 mg, 88%): ^1H NMR (600 MHz, $CDCl_3$) δ 6.63 (dt, *J* = 18.0, 6.4 Hz, 1H), 5.42 (d, *J* = 18.0, 1H), 3.53 (t, *J* = 6.8 Hz, 2H), 2.19 – 2.03 (m, 2H), 1.76 (p, 2H), 1.46 – 1.36 (m, 4H), 1.28 (s, 8H), 1.26 (s, 12H); ^1H NMR (400 MHz, C_6D_6) δ 7.01 (dt, *J* = 17.8, 6.5 Hz, 1H), 5.83 (d, *J* = 17.8 Hz, 1H), 3.12 (t, *J* = 6.7 Hz, 2H), 2.09 (q, *J* = 6.6 Hz, 2H), 1.56 – 1.23 (m, 6H), 1.21 – 0.97 (m, 20H); ^{13}C NMR (151 MHz, $CDCl_3$) δ 154.9, 83.1, 45.3, 36.0, 32.8, 29.5, 29.3, 29.0, 28.3, 27.0, 25.0; ^{13}C NMR (101 MHz, C_6D_6) δ 154.9, 83.0, 45.0, 36.2, 32.9, 29.71, 29.65, 29.5, 29.1, 28.8, 27.1, 25.0; ^{11}B NMR (193 MHz, $CDCl_3$) δ 30.0; ^{11}B NMR (128 MHz, C_6D_6) δ 29.3; FTIR (cm^{-1}): 2978, 2928, 2855, 1639, 1362, 1330, 1146. HRMS (CI) m/z, calcd for $[C_{17}H_{33}BO_2Cl]^+$: 315.2262; found: 315.2263.

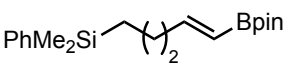

(**3.153**) According to general procedure A,

catecholchloroborane (694 mg, 4.5 mmol), $(JessePhos)_2PdCl_2$ (83 mg, 0.075 mmol), lithium trifluoromethanesulfonate (702 mg, 4.5 mmol), N,N-dicyclohexylmethylamine (3.2 mL, 5.0 mmol), trifluorotoluene (6.0 mL, 0.5 M), and (dimethyl)pent-4-enyl(phenyl)silane (613 mg, 3.0 mmol) were combined under N_2 and stirred at 90 °C for 24 h. The reaction was worked up according to general procedure A. Analysis of the crude reaction mixture *via* ^{1}H NMR revealed an 89:11 *E*/*Z* ratio. The product was purified on boric acid impregnated silica gel chromatography (1 : 9 dichloromethane : hexanes) to afford **3.153** as a yellow oil (881 mg, 89%): ^{1}H NMR (400 MHz, $CDCl_3$) δ 7.59 – 7.44 (m, 2H), 7.40 – 7.31 (m, 3H), 6.60 (dt, *J* = 17.9, 6.5 Hz, 1H), 5.46 – 5.37 (m, 1H), 2.24 – 2.09 (m, 2H), 1.54 – 1.36 (m, 2H), 1.26 (s, 12H), 0.82 – 0.71 (m, 2H), 0.25 (s, 6H); ^{13}C NMR (101 MHz, $CDCl_3$) δ 154.6, 139.5, 133.7, 128.9, 127.8, 83.1, 39.8, 24.9, 22.9, 15.6, -2.9; ^{11}B NMR (193 MHz, $CDCl_3$) δ 29.8; FTIR (cm^{-1}): 2978, 2924, 1638, 1427, 1398, 1389, 1362, 1320, 1249, 1214, 1146, 972, 850, 835, 812, 729, 700. HRMS (CI) m/z, calcd for $[C_{19}H_{32}BO_2Si]^+$: 331.2265; found: 331.2245.

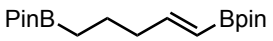

(**3.154**) According to general procedure A, catecholchloroborane (694 mg, 4.5 mmol), $(JessePhos)_2PdCl_2$ (83 mg, 0.075 mmol), lithium trifluoromethanesulfonate (702 mg, 4.5 mmol), N,N-dicyclohexylmethylamine (3.2 mL, 5.0 mmol), trifluorotoluene (6.0 mL, 0.5 M), and pent-4-enyl-pinicolborane (570 mg, 2.9 mmol) were combined under N_2 and stirred at 90 °C for 24 h. The reaction was worked up according to general procedure A. Analysis of the crude reaction mixture *via* ^{1}H NMR revealed an 89:11 *E*/*Z* ratio. The product was purified on boric acid impregnated silica gel chromatography (1 : 9 dichloromethane : hexanes) to afford **3.154** as a yellow oil (677 mg, 72%): ^{1}H NMR (400 MHz, $CDCl_3$) δ 6.59 (dt, *J* = 17.9,

6.5 Hz, 1H), 5.39 (d, J = 17.9 Hz, 1H), 2.25 – 2.01 (m, 2H), 1.68 – 1.38 (m, 2H), 1.23 (s, 12H), 1.21 (s, 12H), 0.76 (t, J = 7.9 Hz, 2H); ^{1}H NMR (400 MHz, CD_3CN) δ 6.52 (dt, J = 17.9, 6.6 Hz, 1H), 5.35 (dt, J = 17.9, 1.5 Hz, 1H), 2.15 – 2.09 (m, 2H), 1.47 (p, J = 7.6 Hz, 2H), 1.21 (s, 12H), 1.20 (s, 12H), 0.70 (t, J = 7.7 Hz, 2H); ^{13}C NMR (101 MHz, $CDCl_3$) δ 154.7, 83.1, 83.0, 38.5, 25.0, 22.9; ^{13}C NMR (101 MHz, CD_3CN) δ 155.2, 83.8, 83.7, 38.8, 25.12, 25.07, 23.6; ^{11}B NMR (193 MHz, $CDCl_3$) δ 34.1, 29.9; ^{11}B NMR (128 MHz, CD_3CN) δ 35.5, 31.2; FTIR (cm^{-1}): 2978, 2931, 1631, 1371, 1362, 1319, 1267, 1239, 1214, 1146, 969, 849; HRMS (CI) m/z, calcd for $[C_{17}H_{33}B_2O_4]^+$: 323.2565; found: 323.2576.

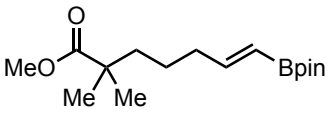

(**3.157**) According to general procedure A, catecholchloroborane (694 mg, 4.5 mmol), $(JessePhos)_2PdCl_2$ (83 mg, 0.075 mmol), lithium trifluoromethanesulfonate (702 mg, 4.5 mmol), N,N-dicyclohexylmethylamine (3.2 mL, 5.0 mmol), trifluorotoluene (6.0 mL, 0.5 M), and methyl 2,2-dimethylhept-6-enoate (511 mg, 3.0 mmol) were combined under N_2 and stirred at 90 °C for 24 h. The reaction was worked up according to general procedure A. Analysis of the crude reaction mixture *via* ^{1}H NMR revealed an 87:13 *E*/*Z* ratio. The product was purified on boric acid impregnated silica gel chromatography (7 : 3 dichloromethane : hexanes) to afford **3.157** as a yellow oil (732 mg, 82%): ^{1}H NMR (400 MHz, $CDCl_3$) δ 6.60 (dt, J = 18.0, 6.4 Hz, 1H), 5.42 (dt, J = 18.0, 1.6 Hz, 1H), 3.65 (s, 3H), 2.17 – 1.99 (m, 2H), 1.55 – 1.46 (m, 2H), 1.34 (tdd, J = 8.9, 7.1, 4.5 Hz, 2H), 1.26 (s, 12H), 1.15 (s, 6H); ^{13}C NMR (101 MHz, $CDCl_3$) δ 178.6, 154.2, 83.2, 51.8, 42.4, 40.5, 36.3, 25.3, 24.9, 23.8; ^{11}B NMR (193 MHz, $CDCl_3$) δ 30.2; FTIR (cm^{-}

^{1}): 2978, 2944, 1733, 1639, 1362, 1320, 1146. HRMS (CI) m/z, calcd for $[C_{16}H_{30}BO_4]^+$: 297.2237; found: 297.2240.

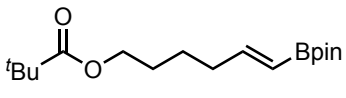

(**3.158**) According to general procedure A, catecholchloroborane (694 mg, 4.5 mmol), $(JessePhos)_2PdCl_2$ (83 mg, 0.075 mmol), lithium trifluoromethanesulfonate (702 mg, 4.5 mmol), N,N-dicyclohexylmethylamine (3.2 mL, 5.0 mmol), trifluorotoluene (6.0 mL, 0.5 M), and hex-5-enyl pivalate (553 mg, 3.0 mmol) were combined under N_2 and stirred at 90 °C for 24 h. The reaction was worked up according to general procedure A. Analysis of the crude reaction mixture *via* ^{1}H NMR revealed an 88:12 *E*/*Z* ratio. The product was purified on boric acid impregnated silica gel chromatography (3 : 7 dichloromethane : hexanes) to afford **3.158** as a yellow oil (847 mg, 91%): ^{1}H NMR (600 MHz, $CDCl_3$) δ 6.61 (dt, *J* = 18.0, 6.4 Hz, 1H), 5.44 (d, *J* = 18.0 Hz, 1H), 4.04 (t, *J* = 6.5 Hz, 2H), 2.19 (tdd, *J* = 7.7, 6.3, 1.5 Hz, 2H), 1.68 – 1.59 (m, 2H), 1.53 – 1.44 (m, 2H), 1.26 (s, 12H), 1.19 (s, 9H); ^{13}C NMR (101 MHz, $CDCl_3$) δ 178.8, 154.0, 83.2, 64.3, 38.9, 35.4, 28.3, 27.3, 24.9, 24.7; ^{11}B NMR (193 MHz, $CDCl_3$) δ 29.8; FTIR (cm^{-1}): 2978, 2935, 1730, 1269, 1363, 1147. HRMS (CI) m/z, calcd for $[C_{17}H_{32}BO_4]^+$: 311.2394; found: 311.2379.

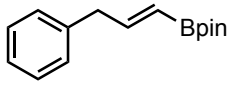

(**3.159**) According to general procedure A, catecholchloroborane (694 mg, 4.5 mmol), $(JessePhos)_2PdCl_2$ (83 mg, 0.075 mmol), lithium trifluoromethanesulfonate (702 mg, 4.5 mmol), N,N-dicyclohexylmethylamine (3.2 mL, 5.0 mmol), trifluorotoluene (6.0 mL, 0.5 M), and allylbenzene (356 mg, 3.0 mmol) were combined under N_2 and stirred at 90 °C for 24 h. The reaction was worked

up according to general procedure A. The product was purified on boric acid impregnated silica gel chromatography (3 : 7 dichloromethane : hexanes) to afford four isomers of **3.159** as a yellow oil (527 mg, 72%): ^{1}H NMR (400 MHz, $CDCl_3$) *E*-allyl product: δ 7.35 – 7.14 (m, 5H), 6.38 (d, *J* = 15.8 Hz, 1H), 6.30 (m, 1H), 1.88 (d, *J* = 7.0 Hz, 2H), 1.26 (s, 12H), ^{11}B NMR (128 MHz, $CDCl_3$) δ 33.6; *E*-alkenyl product: δ 7.35 – 7.14 (m, 5H), 6.76 (dt, *J* = 17.8, 6.3 Hz, 1H), 5.45 (dt, *J* = 17.9, 1.6 Hz, 1H), 3.48 (dd, *J* = 6.3, 1.4 Hz, 2H), 1.25 (s, 12H); ^{11}B NMR (128 MHz, $CDCl_3$) δ 30.4; FTIR (cm^{-1}): 3026, 2978, 2931, 1637, 1496, 1449, 1361, 1325, 1271, 1214, 1167, 1144, 1109, 998, 967, 887, 851, 745, 695, 673. HRMS (CI) m/z, calcd for $[C_{15}H_{22}BO_2]^+$: 245.1713; found: 245.1722.

3.9.5 Procedure for the Styrene Boryl-Heck Reaction

Note: All reactions in this section were performed on a 3 mmol scale.

3.9.5.1 General Procedure B (Styrenes)

In a nitrogen-filled glovebox, catecholchloroborane (1.5 equiv) was added to a dry 25 mL Schlenk flask equipped with a stir bar. The flask was sealed with a rubber septum, removed from the glovebox and attached to a nitrogen manifold *via* the sidearm. The flask was briefly opened and lithium iodide (5 mol %) and $(JessePhos)_2PdCl_2$ (2.5 mol %) were added and the flask was resealed, then evacuated and refilled with nitrogen 3 times. 3 mL of trifluorotoluene (1 mL per mmol) was added *via* syringe with stirring. N,N-dicyclohexylmethylamine (5.0 equiv) was added *via* syringe and then the sides of the flask were rinsed with 3 mL of additional trifluorotoluene (1 mL per mmol). The solution was stirred in an oil bath at 70 °C for 15 minutes, at which time the alkene substrate (1.0 equiv) was added in one portion *via*

syringe. The reaction was allowed to stir at 70 °C for 24 h. After 24 h, the reaction was removed from the oil bath and opened to air. Pinacol (3 equiv) was added in one portion and the reaction was removed from heat and stirred for 1 h at rt. At that time, and with the reactor now cooled to rt, the reaction was diluted with 20 mL of diethyl ether. The reaction was stirred for 10 min, filtered through Celite and concentrated *in vacuo* to remove solvents, including trifluorotoluene. The crude oil was diluted with diethyl ether (30 mL) and washed with 1 M hydrochloric acid (3 x 20 mL) to remove excess amine. The organic layer was stirred with ammonium pyrrolidine-dithiocarbamate (palladium scavenger, 6 equiv to palladium)[100] for 1 h, then dried with $MgSO_4$, filtered through Celite and concentrated *in vacuo*. The crude material was purified *via* silica column chromatography on boric acid impregnated silica gel (as prepared above) in the indicated solvent combination.

3.9.5.2 Characterization Data

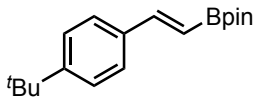

(**3.160**) According to general procedure B, catecholchloroborane (694 mg, 4.5 mmol), $(JessePhos)_2PdCl_2$ (83 mg, 0.075 mmol), lithium iodide (20 mg, 0.15 mmol), N,N-dicyclohexylmethylamine (3.2 mL, 5.0 mmol), trifluorotoluene (6.0 mL, 0.5 M), and 4-*tert*-butylstyrene (481 mg, 3.0 mmol) were combined under N_2 and stirred at 70 °C for 24 h. The reaction was worked up according to general procedure B and purified on boric acid impregnated silica gel chromatography (3 : 7 dichloromethane : hexanes) to afford **3.160** as a white solid (814 mg, 95%): ^{1}H NMR (600 MHz, $CDCl_3$) δ 7.43 (d, J = 8.3 Hz, 2H), 7.41 – 7.33 (m, 3H), 6.12 (d, J = 18.4 Hz, 1H), 1.31 (s, 21H); ^{13}C NMR (151 MHz, $CDCl_3$) δ 152.3, 149.5, 134.9, 127.0, 125.7, 83.4, 34.9, 31.4, 25.0; ^{11}B NMR (193 MHz, $CDCl_3$) δ 30.6; FTIR

(cm^{-1}): 2966, 1625, 1346, 1329, 1141; mp = 89-90 °C. HRMS (CI) m/z, calcd for $[C_{18}H_{28}BO_2]^+$: 287.2182; found: 287.2191.

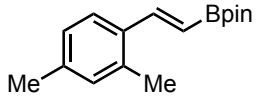

(**3.161**) According to general procedure B, catecholchloroborane (694 mg, 4.5 mmol), $(JessePhos)_2PdCl_2$ (83 mg, 0.075 mmol), lithium iodide (20 mg, 0.15 mmol), N,N-dicyclohexylmethylamine (3.2 mL, 5.0 mmol), trifluorotoluene (6.0 mL, 0.5 M), and N,N-dimethylamino-4-vinylbenzene (442 mg, 3.0 mmol) were combined under N_2 and stirred at 70 °C for 24 h. The reaction was worked up according to general procedure B and purified on boric acid impregnated silica gel chromatography (1 : 9 dichloromethane : hexanes) to afford **3.161** as a pale yellow solid (766 mg, 94%): ^{1}H NMR (400 MHz, $CDCl_3$) δ 7.40 (d, *J* = 8.8 Hz, 2H), 7.33 (d, *J* = 18.4 Hz, 1H), 6.66 (d, *J* = 8.8 Hz, 2H), 5.92 (d, *J* = 18.3 Hz, 1H), 2.98 (s, 6H), 1.30 (s, 12H); ^{13}C NMR (151 MHz, $CDCl_3$) δ 151.1, 149.9, 128.5, 126.1, 112.1, 83.2, 40.5, 25.0; ^{11}B NMR (193 MHz, $CDCl_3$) δ 29.8; FTIR (cm^{-1}): 2977, 1604, 1522, 1430, 1388, 1351, 1319, 1227, 1197, 1182, 1166, 1143, 807; mp = 83-87 °C. HRMS (ESI) m/z, calcd for $[C_{16}H_{25}BNO_2]^+$: 274.1973; found: 274.1984.

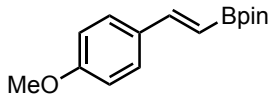

(**3.162**) According to general procedure B, catecholchloroborane (694 mg, 4.5 mmol), $(JessePhos)_2PdCl_2$ (83 mg, 0.075 mmol), lithium iodide (20 mg, 0.15 mmol), N,N-dicyclohexylmethylamine (3.2 mL, 5.0 mmol), trifluorotoluene (6.0 mL, 0.5 M), and 2,4-dimethylstyrene (408 mg, 3.0 mmol) were combined under N_2 and stirred at 70 °C for 24 h. The reaction was worked up according to general procedure B and purified on boric acid impregnated silica gel chromatography (7 : 13 dichloromethane : hexanes) to afford **3.162** as a pale yellow oil

(742 mg, 99%): ^{1}H NMR (600 MHz, $CDCl_3$) δ 7.62 (d, *J* = 18.3 Hz, 1H), 7.47 (d, *J* = 7.9 Hz, 1H), 6.99 (d, *J* = 8.0 Hz, 1H), 6.97 (s, 1H), 6.04 (d, *J* = 18.3 Hz, 1H), 2.39 (s, 3H), 2.30 (s, 3H), 1.31 (s, 12H); ^{13}C NMR (151 MHz, $CDCl_3$) δ 147.1, 138.7, 136.4, 134.0, 131.3, 127.0, 125.9, 83.4, 25.0, 21.3, 19.9; ^{11}B NMR (193 MHz, $CDCl_3$) δ 29.6; FTIR (cm^{-1}): 2978, 1622, 1348, 1323, 1145. HRMS (CI) m/z, calcd for $[C_{16}H_{24}BO_2]^+$: 259.1869; found: 259.1876.

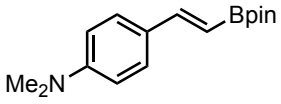

(**3.163**) According to general procedure B, catecholchloroborane (694 mg, 4.5 mmol), $(JessePhos)_2PdCl_2$ (83 mg, 0.075 mmol), lithium iodide (20 mg, 0.15 mmol), N,N-dicyclohexylmethylamine (3.2 mL, 5.0 mmol), trifluorotoluene (6.0 mL, 0.5 M), and 4-vinylanisole (403 mg, 3.0 mmol) were combined under N_2 and stirred at 70 °C for 24 h. The reaction was worked up according to general procedure B and purified on boric acid impregnated silica gel chromatography (1 : 1 dichloromethane : hexanes) to afford **3.163** as a yellow solid (765 mg, 98%): ^{1}H NMR (600 MHz, $CDCl_3$) δ 7.44 (d, *J* = 8.6 Hz, 2H), 7.35 (d, *J* = 18.4 Hz, 1H), 6.87 (d, *J* = 8.7 Hz, 2H), 6.01 (d, *J* = 18.4 Hz, 1H), 3.81 (s, 3H), 1.31 (s, 12H); ^{13}C NMR (151 MHz, $CDCl_3$) δ 160.4, 149.2, 130.6, 128.6, 114.1, 83.4, 55.4, 25.0; ^{11}B NMR (193 MHz, $CDCl_3$) δ 30.3; FTIR (cm^{-1}): 2978, 1626, 1605, 1511, 1355, 1254, 1144; mp = 55 °C. HRMS (CI) m/z, calcd for $[C_{15}H_{22}BO_3]^+$: 261.1662; found: 261.1652.

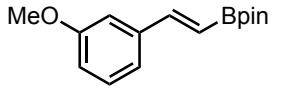

(**3.164**) According to general procedure B, catecholchloroborane (694 mg, 4.5 mmol), $(JessePhos)_2PdCl_2$ (83 mg, 0.075 mmol), lithium iodide (20 mg, 0.15 mmol), N,N-dicyclohexylmethylamine (3.2 mL, 5.0 mmol),

trifluorotoluene (6.0 mL, 0.5 M), and 3-vinylanisole (403 mg, 3.0 mmol) were combined under N_2 and stirred at 70 °C for 24 h. The reaction was worked up according to general procedure B and purified on boric acid impregnated silica gel chromatography (2 : 98 ethyl acetate : hexanes) to afford **3.164** as a yellow oil (657 mg, 84%): ^{1}H NMR (600 MHz, $CDCl_3$) δ 7.37 (d, *J* = 18.4 Hz, 1H), 7.28 – 7.22 (m, 1H), 7.08 (d, *J* = 7.6 Hz, 1H), 7.03 (s, 1H), 6.85 (dd, *J* = 8.2, 2.6 Hz, 1H), 6.16 (d, *J* = 18.4 Hz, 1H), 3.81 (s, 3H), 1.31 (s, 12H); ^{13}C NMR (151 MHz, $CDCl_3$) δ 159.9, 149.5, 139.1, 129.7, 120.0, 115.0, 112.1, 83.5, 55.3, 25.0; ^{11}B NMR (193 MHz, $CDCl_3$) δ 30.3; FTIR (cm^{-1}): 2977, 1625, 1350, 1260, 1145. HRMS (CI) m/z, calcd for $[C_{15}H_{22}BO_3]^+$: 261.1662; found: 261.1644.

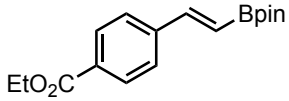

(**3.165**) According to general procedure B, catecholchloroborane (694 mg, 4.5 mmol), $(JessePhos)_2PdCl_2$ (83 mg, 0.075 mmol), lithium iodide (20 mg, 0.15 mmol), N,N-dicyclohexylmethylamine (3.2 mL, 5.0 mmol), trifluorotoluene (6.0 mL, 0.5 M), and ethyl 4-vinylbenzoate (529 mg, 3.0 mmol) were combined under N_2 and stirred at 70 °C for 24 h. The reaction was worked up according to general procedure B and purified on boric acid impregnated silica gel chromatography (1 : 1 dichloromethane : hexanes) to afford **3.165** as a pale yellow solid (778 mg, 86%): ^{1}H NMR (600 MHz, $CDCl_3$) δ 8.01 (d, *J* = 8.3 Hz, 2H), 7.53 (d, *J* = 8.2 Hz, 2H), 7.41 (d, *J* = 18.4 Hz, 1H), 6.27 (d, *J* = 18.4 Hz, 1H), 4.37 (q, *J* = 7.1 Hz, 2H), 1.39 (t, *J* = 7.1 Hz, 3H), 1.32 (s, 12H); ^{13}C NMR (151 MHz, $CDCl_3$) δ 166.4, 148.3, 141.8, 130.7, 130.0, 127.0, 83.7, 61.1, 25.0, 14.5; ^{11}B NMR (193 MHz, $CDCl_3$) δ 30.2; FTIR (cm^{-1}): 2979, 1717, 1624, 1414, 1381, 1370,

1350, 1327, 1273, 1213, 1176, 1144, 1106, 970, 850, 764; mp = 79-80 °C. HRMS (CI) m/z, calcd for $[C_{17}H_{24}BO_4]^+$: 303.1768; found: 303.1771.

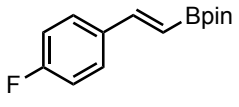

(**3.166**) According to general procedure B, catecholchloroborane (694 mg, 4.5 mmol), $(JessePhos)_2PdCl_2$ (83 mg, 0.075 mmol), lithium iodide (20 mg, 0.15 mmol), N,N-dicyclohexylmethylamine (3.2 mL, 5.0 mmol), trifluorotoluene (6.0 mL, 0.5 M), and 4-fluorostyrene (386 mg, 3.0 mmol) were combined under N_2 and stirred at 70 °C for 24 h. The reaction was worked up according to general procedure B and purified on boric acid impregnated silica gel chromatography (1 : 4 dichloromethane : hexanes) to afford **3.166** as a white solid (582 mg, 78%): ^{1}H NMR (600 MHz, $CDCl_3$) δ 7.51 – 7.42 (m, 2H), 7.35 (d, *J* = 18.4 Hz, 1H), 7.02 (t, *J* = 8.6 Hz, 2H), 6.07 (d, *J* = 18.4 Hz, 1H), 1.31 (s, 12H); ^{13}C NMR (101 MHz, $CDCl_3$) δ 163.3 (d, *J* = 250 Hz), 148.3, 133.8 (d, *J* = 3 Hz), 128.8 (d, *J* = 8 Hz), 115.7 (d, *J* = 22 Hz), 83.5, 25.0; ^{11}B NMR (193 MHz, $CDCl_3$) δ 30.3; ^{19}F NMR (565 MHz, $CDCl_3$) δ -112.4; FTIR (cm^{-1}): 2978, 1508, 1350, 1326, 1144; mp = 62-63 °C. HRMS (CI) m/z, calcd for $[C_{14}H_{19}BO_2F]^+$: 249.1462; found: 249.1470.

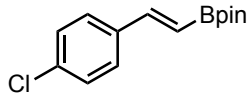

(**3.167**) According to general procedure B, catecholchloroborane (694 mg, 4.5 mmol), $(JessePhos)_2PdCl_2$ (83 mg, 0.075 mmol), lithium iodide (20 mg, 0.15 mmol), N,N-dicyclohexylmethylamine (3.2 mL, 5.0 mmol), trifluorotoluene (6.0 mL, 0.5 M), and 4-chlorostyrene (416 mg, 3.0 mmol) were combined under N_2 and stirred at 70 °C for 24 h. The reaction was worked up according to general procedure B and purified on boric acid impregnated silica gel chromatography (3 : 7 dichloromethane : hexanes) to afford **3.167** as a white solid (745

mg, 94%): ^{1}H NMR (600 MHz, $CDCl_3$) δ 7.41 (d, 2H), 7.33 (d, J = 18.5 Hz, 1H), 7.30 (d, 2H), 6.13 (d, J = 18.4 Hz, 1H), 1.31 (s, 12H); ^{13}C NMR (151 MHz, $CDCl_3$) δ 148.2, 136.1, 134.8, 129.0, 128.4, 83.6, 25.0; ^{11}B NMR (193 MHz, $CDCl_3$) δ 30.2; FTIR (cm^{-1}): 2974, 1627, 1492, 1411, 1380, 1372, 1356, 1323, 1212, 1166, 1146, 1089, 993, 803, 640, 491; mp = 84-85 °C. HRMS (CI) m/z, calcd for $[C_{14}H_{19}BO_2Cl]^+$: 265.1167; found: 265.1170.

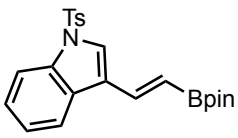

(**3.168**) According to general procedure B, catecholchloroborane (694 mg, 4.5 mmol), $(JessePhos)_2PdCl_2$ (83 mg, 0.075 mmol), lithium iodide (20 mg, 0.15 mmol), N,N-dicyclohexylmethylamine (3.2 mL, 5.0 mmol), trifluorotoluene (6.0 mL, 0.5 M), and 1-(toluene-4-sulfonyl)-2-vinyl-1*H*-pyrrole (893 mg, 3.0 mmol) were combined under N_2 and stirred at 70 °C for 24 h. The reaction was worked up according to general procedure B and purified on boric acid impregnated silica gel chromatography (3 : 2 dichloromethane : hexanes) to afford **3.168** as a white solid (906 mg, 71%): ^{1}H NMR (600 MHz, $CDCl_3$) δ 7.98 (d, J = 8.5 Hz, 1H), 7.86 (d, J = 8.1 Hz, 1H), 7.75 (d, J = 8.5 Hz, 2H), 7.69 (s, 1H), 7.46 (d, J = 18.7 Hz, 1H), 7.37 – 7.30 (m, 1H), 7.26 (s, 1H), 7.21 (d, J = 8.2 Hz, 2H), 6.20 (d, J = 18.7 Hz, 1H), 2.33 (s, 3H), 1.32 (s, 12H); ^{13}C NMR (101 MHz, $CDCl_3$) δ 145.3, 140.4, 135.8, 135.0, 130.1, 128.9, 127.0, 126.4, 125.2, 123.9, 121.6, 121.0, 113.8, 83.6, 25.0, 21.7; ^{11}B NMR (193 MHz, $CDCl_3$) δ 29.2; FTIR (cm^{-1}): 2977, 1627, 1372, 1348, 1175, 1142, 972; mp = 69 °C. HRMS (ESI) m/z, calcd for $[C_{23}H_{27}BNO_2S]^+$: 424.1748; found: 424.1765.

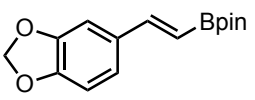

(**3.169**) According to general procedure B, catecholchloroborane

(694 mg, 4.5 mmol), $(JessePhos)_2PdCl_2$ (83 mg, 0.075 mmol), lithium iodide (20 mg, 0.15 mmol), N,N-dicyclohexylmethylamine (3.2 mL, 5.0 mmol), trifluorotoluene (6.0 mL, 0.5 M), and ethenyl-1,3-benzodioxole (445 mg, 3.0 mmol) were combined under N_2 and stirred at 70 °C for 24 h. The reaction was worked up according to general procedure B and purified on boric acid impregnated silica gel chromatography (2 : 3 dichloromethane : hexanes) to afford **3.169** as a yellow solid (616 mg, 76%): ^{1}H NMR (600 MHz, $CDCl_3$) δ 7.30 (d, J = 18.3 Hz, 1H), 7.03 (s, 1H), 6.94 (d, J = 9.3 Hz, 1H), 6.77 (d, J = 8.0 Hz, 1H), 5.99 – 5.93 (m, 3H), 1.31 (s, 12H); ^{13}C NMR (151 MHz, $CDCl_3$) δ 149.2, 148.5, 148.2, 132.4, 122.8, 108.4, 106.0, 101.3, 83.4, 25.0; ^{11}B NMR (193 MHz, $CDCl_3$) δ 30.4; FTIR (cm^{-1}): 2978, 1506, 1446, 1330, 1250, 1144, 1040; mp = 83 °C. HRMS (CI) m/z, calcd for $[C_{15}H_{20}BO_4]^+$: 275.1455; found: 275.1456.

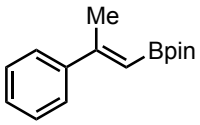

(**3.170**) According to general procedure B, catecholchloroborane (694 mg, 4.5 mmol), $(JessePhos)_2PdCl_2$ (83 mg, 0.075 mmol), lithium iodide (20 mg, 0.15 mmol), N,N-dicyclohexylmethylamine (3.2 mL, 5.0 mmol), trifluorotoluene (6.0 mL, 0.5 M), and α-methylstyrene (354 mg, 3.0 mmol) were combined under N_2 and stirred at 70 °C for 24 h. The reaction was worked up according to general procedure B and purified on boric acid impregnated silica gel chromatography (7 : 13 dichloromethane : hexanes) to afford **3.170** as a light orange oil (517 mg, 71%): ^{1}H NMR (600 MHz, $CDCl_3$) δ 7.50 (d, 2H), 7.32 (t, J = 7.4 Hz, 2H), 7.28 (d, 1H), 5.76 (s, 1H), 2.41 (s, 3H), 1.32 (s, 12H); ^{13}C NMR (151 MHz, $CDCl_3$) δ 157.9, 144.0, 128.3, 128.1, 126.0, 83.1, 25.1, 20.2; ^{11}B NMR (193 MHz, $CDCl_3$) δ 30.0; FTIR (cm^{-1}): 2978, 1621, 1355, 1145. HRMS (CI) m/z, calcd for $[C_{15}H_{22}BO_2]^+$: 245.1713; found: 245.1710.

3.9.6 Preparation of Non-Pinacol Containing Boronic Esters

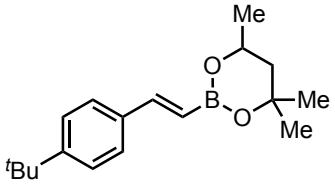

(**3.171**) Using a modification of general procedure B, catecholchloroborane (694 mg, 4.5 mmol), $(JessePhos)_2PdCl_2$ (83 mg, 0.075 mmol), lithium iodide (20 mg, 0.15 mmol), N,N-dicyclohexylmethylamine (3.2 mL, 5.0 mmol), trifluorotoluene (6.0 mL, 0.5 M), and 4-*tert*-butylstyrene (481 mg, 3.0 mmol) were combined under N_2 and stirred at 70 °C for 24 h. After 24 h, the reaction was removed from the oil bath and opened to air. 2-Methyl-2,4-pentanediol (1.2 mL, 9.0 mmol) was added in one portion and the reaction was allowed to cool to rt with stirring. Once at rt, the reaction was diluted with 20 mL of diethyl ether. The reaction was stirred for 10 min, filtered through Celite and concentrated *in vacuo* to remove solvents including trifluorotoluene. The crude oil was diluted with diethyl ether (30 mL) and washed with 1 M hydrochloric acid (3 x 20 mL) to remove excess amine. The organic layer was dried with $MgSO_4$, filtered through Celite and concentrated *in vacuo*. The crude material was purified by boric acid impregnated silica gel chromatography (3 : 7 dichloromethane : hexanes) to afford **3.171** as a slight red solid (620 mg, 75%): ^{1}H NMR (400 MHz, $CDCl_3$) δ 7.42 (d, J = 8.3 Hz, 2H), 7.36 – 7.30 (m, 3H), 6.06 (d, J = 18.2 Hz, 1H), 4.27 (ddt, J = 12.0, 5.9, 3.0 Hz, 1H), 1.82 (dd, J = 13.9, 3.0 Hz, 1H), 1.56 (t, J = 14.0, 11.4 Hz, 1H), 1.35 (m, J = 2.6 Hz, 6H), 1.33 (s, 3H), 1.31 (s, 9H); ^{13}C NMR (101 MHz, $CDCl_3$) δ 151.5, 146.5, 135.4, 126.8, 125.5, 71.0, 64.9, 46.1, 34.8, 31.4, 28.3, 23.4; ^{11}B NMR (128 MHz, C_6D6) δ 25.6; mp = 70-73 °C; FTIR (cm^{-1}): 2970, 1623, 1411, 1391, 1331, 1307, 1267, 1218, 996, 815; HRMS (LIFDI) m/z, calcd for $[C_{18}H_{27}BO_2]^+$: 286.2104; found: 286.2111.

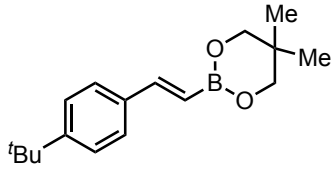

(**3.172**) Using a modification of general procedure B, catecholchloroborane (694 mg, 4.5 mmol),

(JessePhos)$_2$PdCl$_2$ (83 mg, 0.075 mmol), lithium iodide (20 mg, 0.15 mmol), N,N-dicyclohexylmethylamine (3.2 mL, 5.0 mmol), trifluorotoluene (6.0 mL, 0.5 M), and 4-*tert*-butylstyrene (481 mg, 3.0 mmol) were combined under N_2 and stirred at 70 °C for 24 h. After 24 h, the reaction was removed from the oil bath and opened to air. 2,2-Dimethyl-1,3-propanediol (937 mg, 9.0 mmol) was added in one portion and the reaction was allowed to cool to rt with stirring. Once at rt, the reaction was diluted with 20 mL of diethyl ether. The reaction was stirred for 10 min, filtered through Celite and concentrated *in vacuo* to remove solvents including trifluorotoluene. The crude oil was diluted with diethyl ether (30 mL) and washed with 1 M hydrochloric acid (3 x 20 mL) to remove excess amine. The organic layer was dried with $MgSO_4$, filtered through Celite and concentrated *in vacuo*. The crude material was purified by boric acid impregnated silica gel chromatography (1 : 9 ethyl acetate : hexanes) to afford **3.172** as a white solid (655 mg, 80%): ^{1}H NMR (600 MHz, $CDCl_3$) δ 7.43 (d, *J* = 8.3 Hz, 2H), 7.35 (d, *J* = 8.3 Hz, 2H), 7.31 (d, *J* = 18.3 Hz, 1H), 6.06 (d, *J* = 18.3 Hz), 3.70 (s, 4H), 1.31 (s, 9H), 1.01 (s, 6H); ^{13}C NMR (151 MHz, $CDCl_3$) δ 151.9, 147.1, 135.2, 126.9, 125.6, 72.4, 34.8, 32.0, 31.4, 22.1; ^{11}B NMR (193 MHz, $CDCl_3$) δ 26.3; FTIR (cm^{-1}): 2962, 2872, 1622, 1513, 1476, 1313, 1256, 996, 815; mp = 79-81 °C. HRMS (CI) m/z, calcd for $[C_{17}H_{26}BO_2]^+$: 273.2026; found: 273.2026.

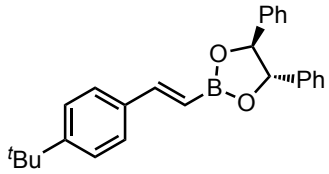

(**3.173**) Using a modification of general procedure B, catecholchloroborane (694 mg, 4.5 mmol), (JessePhos)$_2$PdCl$_2$ (83 mg, 0.075 mmol), lithium iodide (20 mg, 0.15 mmol), N,N-dicyclohexylmethylamine (3.2 mL, 5.0 mmol), trifluorotoluene (6.0 mL, 0.5 M), and 4-*tert*-butylstyrene (481 mg, 3.0 mmol) were combined under N_2

and stirred at 70 °C for 24 h. After 24 h, the reaction was removed from the oil bath and opened to air. (1R,2R)-1,2-diphenyl-1,2-ethanediol (1.93 g, 9.0 mmol) was added in one portion and the reaction was allowed to cool to rt with stirring. Once at rt, the reaction was diluted with 20 mL of diethyl ether. The reaction was stirred for 10 min, filtered through Celite and concentrated *in vacuo* to remove solvents including trifluorotoluene. The crude oil was diluted with diethyl ether (30 mL) and washed with 1 M hydrochloric acid (3 x 20 mL) to remove excess amine. The organic layer was stirred with ammonium pyrrolidine-dithiocarbamate (palladium scavenger, 6 equiv to palladium)[100] for 1 h, then dried with $MgSO_4$, filtered through Celite and concentrated *in vacuo* The crude material was purified by boric acid impregnated silica gel chromatography (1 : 4 ethyl acetate : hexanes) to afford **3.173** as a thick yellow oil (929 mg, 81%): ^{1}H NMR (600 MHz, $CDCl_3$) δ 7.61 (d, J = 18.4 Hz, 1H), 7.50 (d, J = 8.3 Hz, 2H), 7.43 – 7.39 (m, 6H), 7.38 – 7.33 (m, 6H), 6.32 (d, J = 18.4 Hz, 1H), 5.25 (s, 2H), 1.34 (s, 9H); ^{13}C NMR (101 MHz, $CDCl_3$) δ 152.7, 151.1, 140.4, 134.7, 129.0, 128.5, 127.2, 126.0, 125.8, 86.7, 34.9, 31.4; ^{11}B NMR (193 MHz, $CDCl_3$) δ 30.8; FTIR (cm^{-1}): 2963, 1622, 1344, 1319, 1175, 999, 815, 761, 698. HRMS (CI) m/z, calcd for $[C_{26}H_{28}BO_2]^+$: 383.2182; found: 383.2178.

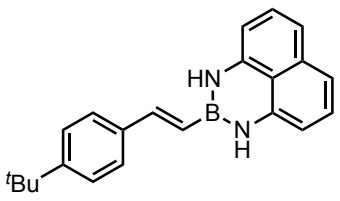

(**3.174**) Using a modification of general procedure B, catecholchloroborane (694 mg, 4.5 mmol), $(JessePhos)_2PdCl_2$ (83 mg, 0.075 mmol), lithium iodide (20 mg, 0.15 mmol), N,N-dicyclohexylmethylamine (3.2 mL, 5.0 mmol), trifluorotoluene (6.0 mL, 0.5 M), and 4-*tert*-butylstyrene (481 mg, 3.0 mmol) were combined under N_2 and stirred at 70 °C for 24 h. After 24 h, the reaction

was removed from the oil bath and opened to air. 1,8-Diaminonapthalene (1.42 g, 9.0 mmol) was added in one portion and the reaction was allowed to cool to rt with stirring. Once at rt, the reaction was diluted with 20 mL of diethyl ether. The reaction was stirred for 10 min, filtered through Celite and concentrated *in vacuo* to remove solvents including trifluorotoluene. The crude material was purified by boric acid impregnated silica gel chromatography (3 : 7 dichloromethane : hexanes) to afford **3.174** as a yellow solid (664 mg, 85%): ^{1}H NMR (400 MHz, $CDCl_3$) δ 7.46 (d, *J* = 8.4 Hz, 2H), 7.41 (d, *J* = 8.4 Hz, 2H), 7.15 (d, *J* = 10.5 Hz, 1H), 7.11 (d, *J* = 7.5 Hz, 2H), 7.02 (d, *J* = 8.1 Hz, 2H), 6.37 (d, *J* = 7.3 Hz, 2H), 6.29 (d, *J* = 18.6 Hz, 1H), 5.86 (s, 2H), 1.34 (s, 9H); ^{13}C NMR (101 MHz, $CDCl_3$) δ 152.1, 143.7, 141.3, 136.5, 134.9, 127.7, 126.7, 125.8, 120.0, 117.7, 105.9, 34.9, 31.4; ^{11}B NMR (193 MHz, $CDCl_3$) δ 28.9; FTIR (cm^{-1}): 2962, 1600, 1513, 1413, 818, 762; mp = 135-136 °C. HRMS (ESI) m/z, calcd for $[C_{22}H_{24}BN_2]^+$: 327.2027; found: 327.2041.

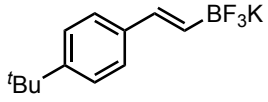

(**3.175**) Using a modification of general procedure B, catecholchloroborane (694 mg, 4.5 mmol), $(JessePhos)_2PdCl_2$ (83 mg, 0.075 mmol), lithium iodide (20 mg, 0.15 mmol), N,N-dicyclohexylmethylamine (3.2 mL, 5.0 mmol), trifluorotoluene (6.0 mL, 0.5 M), and 4-*tert*-butylstyrene (481 mg, 3.0 mmol) were combined under N_2 and stirred at 70 °C for 24 h. After 24 h, the reaction was removed from the oil bath and allowed to cool to rt with stirring. Once at rt, the reaction was diluted with 20 mL of diethyl ether. The reaction was stirred for 10 min, filtered through Celite and concentrated *in vacuo* to remove solvents including trifluorotoluene. The crude oil was diluted with diethyl ether (30 mL) and washed with 1 M hydrochloric acid (3 x 20 mL) to remove excess amine.

The organic layer was dried with $MgSO_4$, filtered through Celite and concentrated *in vacuo*. The crude solid was diluted with diethyl ether (10 mL) and cooled 0 °C in an ice bath. Once at 0 °C, potassium bifluoride (1.41 g, 18.0 mmol) was added with stirring. Deionized water (3 mL) was then added dropwise over 30 minutes, at which time the ice bath was removed and the reaction was allowed to warm to rt with stirring. Once at rt, the solvent was removed *in vacuo*. The crude solid was dissolved in acetone (20 ml), filtered through Celite and concentrated *in vacuo*. The crude material was purified by dissolving in hot acetone (10 mL) and precipitating with diethyl ether (20 mL) to afford **3.175** as a white solid (564 mg, 71%): ^{1}H NMR (600 MHz, acetone-d6) δ 7.27 (s, 4H), 6.62 (d, J = 18.2 Hz, 1H), 6.29 (d, J = 18.0 Hz, 1H), 1.28 (s, 9H); ^{13}C NMR (101 MHz, Acetone-d6) δ 149.1, 139.2, 134.3 (q), 126.2, 125.7, 34.8, 31.7; ^{11}B NMR (193 MHz, Acetone-d6) δ 3.0; ^{19}F NMR (376 MHz, Acetone-d6) δ -141.6; FTIR (cm^{-1}): 3647, 2966, 2869, 1705, 1627, 1563, 1464, 1412, 1393, 1364, 1296, 1098, 966, 855, 754, 560, 514; mp = 263-267°C (dec.). HRMS (LIFDI) m/z, calcd for [$C_{12}H_{15}BF_3K$]: 266.0856; found: 266.0872.

3.9.7 Computational Methods

All DFT calculations were performed with the Gaussian 09 software package.[111] Optimizations of the geometries of the minima were conducted with the B3LYP[112] method. The 6-31++G(d,p) basis set was applied to all atoms. Vibrational frequencies were computed at the same level of theory for each calculation to verify that the structure is an energy minimum and to evaluate the thermochemical properties. Solvent effects were computed based upon the gas-phase optimized structures using the same level of theory with the default polarized continuum solvation model (PCM) in Gaussian.[113] 1,2-Dichloroethane (ε = 10.13) was used instead of trifluorotoluene (ε =

9.18) because the Gaussian 09 program does not contain default solvent parameters for trifluorotoluene.[114] In this section, all the energies are discussed in terms of enthalpy.

3.9.8 Crystallographic Details

X-ray Structural Analysis for (**JessePhos**)$_2$PdCl$_2$. The crystal was mounted using viscous oil onto a plastic mesh and cooled to the data collection temperature (200 K). Data were collected on a Bruker-AXS APEX Duo CCD diffractometer. Unit cell parameters were obtained from 36 data frames, 0.3º ω, from three different sections of the Ewald sphere. No symmetry higher than triclinic was observed and the centrosymmetric space group option yielded chemically reasonable and computationally stable results of refinement. The data-set was treated with absorption corrections based on redundant multiscan data. The structure was solved using direct methods and refined with full-matrix, least-squares procedures on F^2.[115] The molecule is located at the inversion center.

All non-hydrogen atoms were refined with anisotropic displacement parameters. All hydrogen atoms were treated as idealized contributions. Scattering factors are contained in the SHELXTL 6.12 program library.[115] The CIF has been deposited under CCDC 1463772.

REFERENCES

(1) (a) McAtee, J. R.; Martin, S. E. S.; Ahneman, D. T.; Johnson, K. A.; Watson, D. A., *Angew. Chem., Int. Ed.* **2012,** *51*, 3663; (b) Martin, S. E. S.; Watson, D. A., *J. Am. Chem. Soc.* **2013,** *135*, 13330; (c) McAtee, J. R.; Martin, S. E. S.; Cinderella, A. P.; Reid, W. B.; Johnson, K. A.; Watson, D. A., *Tetrahedron* **2014,** *70*, 4250; (d) McAtee, J. R.; Yap, G. P. A.; Watson, D. A., *J. Am. Chem. Soc.* **2014,** *136*, 10166; (e) McAtee, J. R.; Krause, S. B.; Watson, D. A., *Adv. Synth. Catal.* **2015,** *357*, 2317.
(2) Hall, D. G., *Boronic Acids*. Wiley-VCH: Weinheim, 2011.
(3) Candeias, N. R.; Montalbano, F.; Cal, P. M. S. D.; Gois, P. M. P., *Chem. Rev.* **2010,** *110*, 6169.
(4) (a) Morrill, C.; Grubbs, R. H., *J. Org. Chem.* **2003,** *68*, 6031; (b) Shade, R. E.; Hyde, A. M.; Olsen, J.-C.; Merlic, C. A., *J. Am. Chem. Soc.* **2010,** *132*, 1202; (c) Furuya, T.; Ritter, T., *Org. Lett.* **2009,** *11*, 2860; (d) Tao, C.-Z.; Cui, X.; Li, J.; Liu, A.-X.; Liu, L.; Guo, Q.-X., *Tetrahedron Lett.* **2007,** *48*, 3525.
(5) (a) Cambre, J. N.; Sumerlin, B. S., *Polymer* **2011,** *52*, 4631; (b) Ciani, L.; Ristori, S., *Expert Opinion on Drug Discovery* **2012,** *7*, 1017; (c) Das, B. C.; Thapa, P.; Karki, R.; Schinke, C.; Das, S.; Kambhampati, S.; Banerjee, S. K.; Van Veldhuizen, P.; Verma, A.; Weiss, L. M.; Evans, T., *Future Med. Chem.* **2013,** *5*, 653; (d) Moss, R. L., *Appl. Radiat. Isot.* **2014,** *88*, 2; (e) Brooks, W. L. A.; Sumerlin, B. S., *Chem. Rev.* **2016,** *116*, 1375; (f) Diaz, D. B.; Yudin, A. K., *Nature Chem.* **2017,** *9*, 731.
(6) (a) Miyaura, N.; Suzuki, A., *J. Chem. Soc., Chem. Commun.* **1979,** 866; (b) Miyaura, N.; Yamada, K.; Suzuki, A., *Tetrahedron Lett.* **1979,** *20*, 3437.
(7) (a) Miyaura, N.; Suzuki, A., *Chem. Rev.* **1995,** *95*, 2457; (b) Suzuki, A., *J. Organomet. Chem.* **1999,** *576*, 147.
(8) Lee, S. J.; Gray, K. C.; Paek, J. S.; Burke, M. D., *J. Am. Chem. Soc.* **2008,** *130*, 466.
(9) Kobayashi, Y.; Shimazaki, T.; Sato, F., *Tetrahedron Lett.* **1987,** *28*, 5849.
(10) Molander, G. A.; Bernardi, C. R., *J. Org. Chem.* **2002,** *67*, 8424.
(11) Petasis, N. A.; Akritopoulou, I., *Tetrahedron Lett.* **1993,** *34*, 583.
(12) (a) Southwood, T. J.; Curry, M. C.; Hutton, C. A., *Tetrahedron* **2006,** *62*, 236; (b) Churches Quentin, I.; Stewart Helen, E.; Cohen Scott, B.; Shröder, A.; Turner, P.; Hutton Craig, A., Stereoselectivity of the Petasis reaction with various chiral amines and styrenylboronic acids. In *Pure Appl. Chem.*, 2008; Vol. 80, p 687.
(13) Lou, S.; Schaus, S. E., *J. Am. Chem. Soc.* **2008,** *130*, 6922.
(14) (a) Lam, P. Y. S.; Clark, C. G.; Saubern, S.; Adams, J.; Winters, M. P.; Chan, D. M. T.; Combs, A., *Tetrahedron Lett.* **1998,** *39*, 2941; (b) Evans, D. A.; Katz, J. L.; West, T. R., *Tetrahedron Lett.* **1998,** *39*, 2937; (c) Chan, D. M. T.; Monaco, K. L.; Wang, R.-P.; Winters, M. P., *Tetrahedron Lett.* **1998,** *39*, 2933.

(15) (a) Sanjeeva Rao, K.; Wu, T.-S., *Tetrahedron* **2012,** *68*, 7735; (b) Ley, S. V.; Thomas, A. W., *Angew. Chem., Int. Ed.* **2003,** *42*, 5400.
(16) King, A. E.; Brunold, T. C.; Stahl, S. S., *J. Am. Chem. Soc.* **2009,** *131*, 5044.
(17) Lam, P. Y. S.; Vincent, G.; Bonne, D.; Clark, C. G., *Tetrahedron Lett.* **2003,** *44*, 4927.
(18) Bolshan, Y.; Batey, R. A., *Angew. Chem., Int. Ed.* **2008,** *47*, 2109.
(19) Chan, D. G.; Winternheimer, D. J.; Merlic, C. A., *Org. Lett.* **2011,** *13*, 2778
(20) (a) Matteson, D. S.; Liedtke, J. D., *J. Am. Chem. Soc.* **1965,** *87*, 1526; (b) Brown, H. C.; Hamaoka, T.; Ravindran, N., *J. Am. Chem. Soc.* **1973,** *95*, 6456; (c) Brown, H. C.; Hamaoka, T.; Ravindran, N., *J. Am. Chem. Soc.* **1973,** *95*, 5786; (d) Brown, H. C.; Somayaji, V., *Synthesis* **1984,** *1984*, 919.
(21) (a) Mazzotti, A. R.; Campbell, M. G.; Tang, P.; Murphy, J. M.; Ritter, T., *J. Am. Chem. Soc.* **2013,** *135*, 14012; (b) Ye, Y.; Schimler, S. D.; Hanley, P. S.; Sanford, M. S., *J. Am. Chem. Soc.* **2013,** *135*, 16292; (c) Mossine, A. V.; Brooks, A. F.; Makaravage, K. J.; Miller, J. M.; Ichiishi, N.; Sanford, M. S.; Scott, P. J. H., *Org. Lett.* **2015,** *17*, 5780.
(22) Parsons, A. T.; Senecal, T. D.; Buchwald, S. L., *Angew. Chem., Int. Ed.* **2012,** *51*, 2947.
(23) Brown, H. C.; Gupta, S. K., *J. Am. Chem. Soc.* **1972,** *94*, 4370.
(24) (a) Duroure, L.; Jousseaume, T.; Araoz, R.; Barre, E.; Retailleau, P.; Chabaud, L.; Molgo, J.; Guillou, C., *Org. Biomol. Chem.* **2011,** *9*, 8112 ; (b) Enquist Jr, J. A.; Virgil, S. C.; Stoltz, B. M., *Chem. - Eur. J.* **2011,** *17*, 9957
(25) Njardarson, J. T.; Biswas, K.; Danishefsky, S. J., *Chem. Commun.* **2002,** 2759
(26) (a) Nicolaou; Li, A.; Edmonds, D. J., *Angew. Chem., Int. Ed.* **2006,** *45*, 7086 ; (b) Nicolaou; Lister, T.; Denton, R. M.; Montero, A.; Edmonds, D. J., *Angew. Chem., Int. Ed.* **2007,** *46*, 4712 ; (c) Nicolaou; Tang, Y.; Wang, J.; Stepan, A. F.; Li, A.; Montera, A., *J. Am. Chem. Soc.* **2007,** *129*, 14850 ; (d) Nicolaou, K. C.; Stepan, A. F.; Lister, T.; Li, A.; Montero, A.; et al., *J. Am. Chem. Soc.* **2008,** *130*, 13110 ; (e) Nicolaou; Li, A.; Edmonds, D. J.; Tria, G. S.; Ellery, S. P., *J. Am. Chem. Soc.* **2009,** *131*, 16905 ; (f) Nicolaou; Tria, G. S.; Edmonds, D. J.; Kar, M., *J. Am. Chem. Soc.* **2009,** *131*, 15909 ; (g) Jousseaume, T.; Retailleau, P.; Chabaud, L.; Guillou, C., *Tetrahedron Lett.* **2012,** *53*, 1370
(27) Baker, S. J.; Tomsho, J. W.; Benkovic, S. J., *Chem. Soc. Rev.* **2011,** *40*, 4279.
(28) (a) Richardson, P. G.; Hideshima, T.; Anderson, K. C., *Cancer Control* **2003,** *10*, 361; (b) Adams, J.; Kauffman, M., *Cancer Investigation* **2004,** *22*, 304.
(29) Leśnikowski, Z. J., *Expert Opinion on Drug Discovery* **2016,** *11*, 569.
(30) Liu, C. T.; Tomsho, J. W.; Benkovic, S. J., *Bioorg. Med. Chem.* **2014,** *22*, 4462.
(31) (a) Kim, B. J.; Zhang, J.; Tan, S.; Matteson, D. S.; Prusoff, W. H.; Cheng, Y.-C., *Org. Biomol. Chem.* **2012,** *10*, 9349; (b) *Future Med. Chem.* **2013,** *5*, 693; (c) Imperio, D.; Del Grosso, E.; Fallarini, S.; Lombardi, G.; Panza, L., *Org. Lett.* **2017,** *19*, 1678.
(32) Alam, M. A.; Arora, K.; Gurrapu, S.; Jonnalagadda, S. K.; Nelson, G. L.; Kiprof, P.; Jonnalagadda, S. C.; Mereddy, V. R., *Tetrahedron* **2016,** *72*, 3795.

(33) (a) Beletskaya, I.; Pelter, A., *Tetrahedron* **1997,** *53*, 4957; (b) Christopher, M. V.; Stephen, A. W., *Curr. Org. Chem.* **2005,** *9*, 687; (c) Trost, B. M.; Ball, Z. T., *Synthesis* **2005,** 853; (d) Barbeyron, R.; Benedetti, E.; Cossy, J.; Vasseur, J.-J.; Arseniyadis, S.; Smietana, M., *Tetrahedron* **2014,** *70*, 8431.
(34) Brown, H. C.; Gupta, S. K., *J. Am. Chem. Soc.* **1975,** *97*, 5249.
(35) Tucker, C. E.; Davidson, J.; Knochel, P., *J. Org. Chem.* **1992,** *57*, 3482.
(36) Pereira, S.; Srebnik, M., *Organometallics* **1995,** *14*, 3127.
(37) Iafe, R. G.; Chan, D. G.; Kuo, J. L.; Boon, B. A.; Faizi, D. J.; Saga, T.; Turner, J. W.; Merlic, C. A., *Org. Lett.* **2012,** *14*, 4282.
(38) (a) Bandur, N. G.; Brückner, D.; Hoffmann, R. W.; Koert, U., *Org. Lett.* **2006,** *8*, 3829; (b) Reddy Iska, V. B.; Verdolino, V.; Wiest, O.; Helquist, P., *J. Org. Chem.* **2010,** *75*, 1325.
(39) Pereira, S.; Srebnik, M., *Tetrahedron Lett.* **1996,** *37*, 3283.
(40) Ohmura, T.; Yamamoto, Y.; Miyaura, N., *J. Am. Chem. Soc.* **2000,** *122*, 4990.
(41) Cid, J.; Carbó, J. J.; Fernández, E., *Chem. - Eur. J.* **2012,** *18*, 1512.
(42) Takahashi, K.; Ishiyama, T.; Miyaura, N., *J. Organomet. Chem.* **2001,** *625*, 47.
(43) Yun, J., *Asian J. Org. Chem.* **2013,** *2*, 1016.
(44) Ishiyama, T.; Murata, M.; Miyaura, N., *J. Org. Chem.* **1995,** *60*, 7508.
(45) (a) Kou, T.; Jun, T.; Tatsuo, I.; Norio, M., *Chem. Lett.* **2000,** *29*, 126; (b) Takagi, J.; Takahashi, K.; Ishiyama, T.; Miyaura, N., *J. Am. Chem. Soc.* **2002,** *124*, 8001.
(46) Gilman, H.; Vernon, C. C., *J. Am. Chem. Soc.* **1926,** *48*, 1063.
(47) Stephen L. Buchwald, S. J. L., Ralph B. Nielsen, Brett T. Watson, and Susan M. King, *Organic Synthesis* **1993,** *71*, 77.
(48) Gao, F.; Hoveyda, A. H., *J. Am. Chem. Soc.* **2010,** *132*, 10961.
(49) (a) Haubold, W.; Herdtle, J.; Gollinger, W.; Einholz, W., *J. Organomet. Chem.* **1986,** *315*, 1; (b) Kaufmann, D., *Chem. Ber.* **1987,** *120*, 901; (c) Kaufmann, D., *Chem. Ber.* **1987,** *120*, 853.
(50) Farinola, G. M.; Fiandanese, V.; Mazzone, L.; Naso, F., *J. Chem. Soc., Chem. Commun.* **1995,** 2523.
(51) (a) Schuster, M.; Blechert, S., *Angew. Chem., Int. Ed.* **1997,** *36*, 2036; (b) Grubbs, R. H.; Chang, S., *Tetrahedron* **1998,** *54*, 4413; (c) Fürstner, A., *Angew. Chem., Int. Ed.* **2000,** *39*, 3012; (d) Connon, S. J.; Blechert, S., *Angew. Chem., Int. Ed.* **2003,** *42*, 1900; (e) Schrock, R. R.; Hoveyda, A. H., *Angew. Chem., Int. Ed.* **2003,** *42*, 4592; (f) Grubbs, R. H., *Tetrahedron* **2004,** *60*, 7117; (g) Hoveyda, A. H.; Zhugralin, A. R., *Nature* **2007,** *450*, 243.
(52) Nicolaou, K. C.; Bulger, P. G.; Sarlah, D., *Angew. Chem., Int. Ed.* **2005,** *44*, 4490.
(53) Chatterjee, A. K.; Choi, T.-L.; Sanders, D. P.; Grubbs, R. H., *J. Am. Chem. Soc.* **2003,** *125*, 11360.
(54) Jean-Louis Hérisson, P.; Chauvin, Y., *Die Makromolekulare Chemie* **1971,** *141*, 161.
(55) Renaud, J.; Ouellet, S. G., *J. Am. Chem. Soc.* **1998,** *120*, 7995.
(56) Blackwell, H. E.; O'Leary, D. J.; Chatterjee, A. K.; Washenfelder, R. A.; Bussmann, D. A.; Grubbs, R. H., *J. Am. Chem. Soc.* **2000,** *122*, 58.

(57) (a) Hemelaere, R.; Carreaux, F.; Carboni, B., *J. Org. Chem.* **2013,** *78*, 6786; (b) Morrill, C.; Funk, T. W.; Grubbs, R. H., *Tetrahedron Lett.* **2004,** *45*, 7733.
(58) Kiesewetter, E. T.; O'Brien, R. V.; Yu, E. C.; Meek, S. J.; Schrock, R. R.; Hoveyda, A. H., *J. Am. Chem. Soc.* **2013,** *135*, 6026.
(59) (a) Jacobsen, M. F.; Moses, J. E.; Adlington, R. M.; Baldwin, J. E., *Org. Lett.* **2005,** *7*, 641; (b) Ghidu, V. P.; Wang, J.; Wu, B.; Liu, Q.; Jacobs, A.; Marnett, L. J.; Sulikowski, G. A., *J. Org. Chem.* **2008,** *73*, 4949; (c) Rahn, N.; Kalesse, M., *Angew. Chem., Int. Ed.* **2008,** *47*, 597.
(60) (a) Micalizio, G. C.; Schreiber, S. L., *Angew. Chem., Int. Ed.* **2002,** *41*, 3272; (b) McNulty, L.; Kohlbacher, K.; Borin, K.; Dodd, B.; Bishop, J.; Fuller, L.; Wright, Z., *J. Org. Chem.* **2010,** *75*, 6001.
(61) Jernelius, J. A.; Schrock, R. R.; Hoveyda, A. H., *Tetrahedron* **2004,** *60*, 7345.
(62) (a) Marciniec, B.; Jankowska, M.; Pietraszuk, C., *Chem. Commun.* **2005,** 663; (b) Jankowska, M.; Pietraszuk, C.; Marciniec, B.; Zaidlewicz, M., *Synlett* **2006,** *2006*, 1695; (c) Żak, P.; Dudziec, B.; Kubicki, M.; Marciniec, B., *Chem. - Eur. J.* **2014,** *20*, 9387.
(63) Lam, K. C.; Lin, Z.; Marder, T. B., *Organometallics* **2007,** *26*, 3149.
(64) (a) Hunt, A. R.; Stewart, S. K.; Whiting, A., *Tetrahedron Lett.* **1993,** *34*, 3599; (b) Stewart, S. K.; Whiting, A., *J. Organomet. Chem.* **1994,** *482*, 293.
(65) (a) Stewart, S. K.; Whiting, A., *Tetrahedron Lett.* **1995,** *36*, 3925; (b) Lightfoot, A. P.; Maw, G.; Thirsk, C.; Twiddle, S. J. R.; Whiting, A., *Tetrahedron Lett.* **2003,** *44*, 7645; (c) Lightfoot, A. P.; Twiddle, S. J. R.; Whiting, A., *Org. Biomol. Chem.* **2005,** *3*, 3167.
(66) (a) Hénaff, N.; Whiting, A., *Org. Lett.* **1999,** *1*, 1137; (b) Hénaff, N.; Whiting, A., *Tetrahedron* **2000,** *56*, 5193; (c) Batsanov, A. S.; Knowles, J. P.; Whiting, A., *J. Org. Chem.* **2007,** *72*, 2525; (d) Xue, C.; Kung, S.-H.; Wu, J.-Z.; Luo, F.-T., *Tetrahedron* **2008,** *64*, 248.
(67) (a) Itami, K.; Tonogaki, K.; Ohashi, Y.; Yoshida, J.-i., *Org. Lett.* **2004,** *6*, 4093; (b) Itami, K.; Tonogaki, K.; Nokami, T.; Ohashi, Y.; Yoshida, J.-i., *Angew. Chem., Int. Ed.* **2006,** *45*, 2404; (c) Khanizeman, R. N.; Barde, E.; Bates, R. W.; Guérinot, A.; Cossy, J., *Org. Lett.* **2017,** *19*, 5046.
(68) Cornil, J.; Echeverria, P.-G.; Phansavath, P.; Ratovelomanana-Vidal, V.; Guérinot, A.; Cossy, J., *Org. Lett.* **2015,** *17*, 948.
(69) (a) Davan, T.; Corcoran, E. W.; Sneddon, L. G., *Organometallics* **1983,** *2*, 1693; (b) Llynch, A. T.; Sneddon, L. G., *J. Am. Chem. Soc.* **1989,** *111*, 6201.
(70) Brown, J. M.; Lloyd-Jones, G. C., *J. Chem. Soc., Chem. Commun.* **1992,** 710.
(71) Brown, J. M.; Lloyd-Jones, G. C., *J. Am. Chem. Soc.* **1994,** *116*, 866.
(72) Westcott, S. A.; Marder, T. B.; Baker, R. T., *Organometallics* **1993,** *12*, 975.
(73) (a) Murata, M.; Watanabe, S.; Masuda, Y., *Tetrahedron Lett.* **1999,** *40*, 2585; (b) Murata, M.; Kawakita, K.; Asana, T.; Watanabe, S.; Masuda, Y., *Bull. Chem. Soc. Jpn.* **2002,** *75*, 825.
(74) Brown, A. N.; Zakharov, L. N.; Mikulas, T.; Dixon, D. A.; Liu, S.-Y., *Org. Lett.* **2014,** *16*, 3340.

(75) Iwadate, N.; Suginome, M., *Chem. Lett.* **2010,** *39*, 558.
(76) Morimoto, M.; Miura, T.; Murakami, M., *Angew. Chem., Int. Ed.* **2015,** *54*, 12659.
(77) (a) Coapes, R. B.; Souza, F. E. S.; Thomas, R. L.; Hall, J. J.; Marder, T. B., *Chem. Commun.* **2003,** 614; (b) Mkhalid, I. A. I.; Coapes, R. B.; Edes, S. N.; Coventry, D. N.; Souza, F. E. S.; Thomas, R. L.; Hall, J. J.; Bi, S.-W.; Lin, Z.; Marder, T. B., *Dalton Trans.* **2008,** 1055.
(78) Selander, N.; Willy, B.; Szabó, K. J., *Angew. Chem., Int. Ed.* **2010,** *49*, 4051.
(79) (a) Takaya, J.; Kirai, N.; Iwasawa, N., *J. Am. Chem. Soc.* **2011,** *133*, 12980; (b) Kirai, N.; Iguchi, S.; Ito, T.; Takaya, J.; Iwasawa, N., *Bull. Chem. Soc. Jpn.* **2013,** *86*, 784.
(80) Wang, C.; Wu, C.; Ge, S., *ACS Catal.* **2016,** *6*, 7585.
(81) Mazzacano, T. J.; Mankad, N. P., *ACS Catal.* **2017,** *7*, 146.
(82) Ishiyama, T.; Miyaura, N., *The Chemical Record* **2004,** *3*, 271.
(83) Anastasi, N. R.; Waltz, K. M.; Weerakoon, W. L.; Hartwig, J. F., *Organometallics* **2003,** *22*, 365.
(84) (a) Knorr, J. R.; Merola, J. S., *Organometallics* **1990,** *9*, 3008; (b) Schlecht, S.; Hartwig, J. F., *J. Am. Chem. Soc.* **2000,** *122*, 9435; (c) Braunschweig, H.; Colling, M., *Coord. Chem. Rev.* **2001,** *223*, 1; (d) Aldridge, S.; Coombs, D. L., *Coord. Chem. Rev.* **2004,** *248*, 535; (e) Souza, F. E. S.; Nguyen, P.; Marder, T. B.; Scott, A. J.; Clegg, W., *Inorg. Chim. Acta* **2005,** *358*, 1501; (f) Esteruelas, M. A.; Fernández, I.; López, A. M.; Mora, M.; Oñate, E., *Organometallics* **2012,** *31*, 4646; (g) Frank, R.; Howell, J.; Campos, J.; Tirfoin, R.; Phillips, N.; Zahn, S.; Mingos, D. M. P.; Aldridge, S., *Angew. Chem., Int. Ed.* **2015,** *54*, 9586.
(85) Bauer, J.; Braunschweig, H.; Kraft, K.; Radacki, K., *Angew. Chem., Int. Ed.* **2011,** *50*, 10457.
(86) (a) Clegg, W.; Lawlor, F. J.; Lesley, G.; Marder, T. B.; Norman, N. C.; Orpen, A. G.; Quayle, M. J.; Rice, C. R.; Scott, A. J.; Souza, F. E. S., *J. Organomet. Chem.* **1998,** *550*, 183; (b) Charmant, J. P. H.; Fan, C.; Norman, N. C.; Pringle, P. G., *Dalton Trans.* **2007,** 114; (c) Braunschweig, H.; Fuß, M.; Radacki, K.; Uttinger, K., *Z. Anorg. Allg. Chem.* **2009,** *635*, 208.
(87) (a) Braunschweig, H.; Radacki, K.; Rais, D.; Seeler, F., *Organometallics* **2004,** *23*, 5545; (b) Braunschweig, H.; Radacki, K.; Rais, D.; Uttinger, K., *Angew. Chem., Int. Ed.* **2006,** *45*, 162; (c) Braunschweig, H.; Brenner, P.; Müller, A.; Radacki, K.; Rais, D.; Uttinger, K., *Chem. - Eur. J.* **2007,** *13*, 7171; (d) Braunschweig, H.; Radacki, K.; Uttinger, K., *Angew. Chem., Int. Ed.* **2007,** *46*, 3979; (e) Braunschweig, H.; Green, H.; Radacki, K.; Uttinger, K., *Dalton Trans.* **2008,** 3531; (f) Braunschweig, H.; Kupfer, T.; Radacki, K.; Schneider, A.; Seeler, F.; Uttinger, K.; Wu, H., *J. Am. Chem. Soc.* **2008,** *130*, 7974; (g) Braunschweig, H.; Radacki, K.; Uttinger, K., *Organometallics* **2008,** *27*, 6005; (h) Braunschweig, H.; Radacki, K.; Schneider, A., *Science* **2010,** *328*, 345.
(88) Braunschweig, H.; Radacki, K.; Uttinger, K., *Inorg. Chem.* **2007,** *46*, 8796.
(89) Esposito, O.; Roberts, D. E.; Cloke, F. G. N.; Caddick, S.; Green, J. C.; Hazari, N.; Hitchcock, P. B., *Eur. J. Inorg. Chem.* **2009,** *2009*, 1844.

(90) (a) Onozawa, S.-y.; Tanaka, M., *Organometallics* **2001,** *20*, 2956; (b) Braunschweig, H.; Gruss, K.; Radacki, K.; Uttinger, K., *Eur. J. Inorg. Chem.* **2008,** *2008*, 1462.
(91) Suginome, M., *The Chemical Record* **2010,** *10*, 348.
(92) Yamamoto, A.; Suginome, M., *J. Am. Chem. Soc.* **2005,** *127*, 15706.
(93) Daini, M.; Yamamoto, A.; Suginome, M., *J. Am. Chem. Soc.* **2008,** *130*, 2918.
(94) Daini, M.; Suginome, M., *Chem. Commun.* **2008,** 5224.
(95) Nakada, K.; Daini, M.; Suginome, M., *Chem. Lett.* **2013,** *42*, 538.
(96) Coapes, R. B.; Souza, F. E. S.; Fox, M. A.; Batsanov, A. S.; Goeta, A. E.; Yufit, D. S.; Leech, M. A.; Howard, J. A. K.; Scott, A. J.; Clegg, W.; Marder, T. B., *Journal of the Chemical Society, Dalton Transactions* **2001,** 1201.
(97) Gerrard, W.; Lappert, M. F.; Mountfield, B. A., *Journal of the Chemical Society* **1959,** 1529.
(98) (a) Hirner, J. J.; Faizi, D. J.; Blum, S. A., *J. Am. Chem. Soc.* **2014,** *136*, 4740; (b) Faizi, D. J.; Issaian, A.; Davis, A. J.; Blum, S. A., *J. Am. Chem. Soc.* **2016,** *138*, 2126.
(99) Reid, W. B.; Spillane, J. J.; Krause, S. B.; Watson, D. A., *J. Am. Chem. Soc.* **2016,** *138*, 5539.
(100) Gallagher, W. P.; Vo, A., *Org. Process Res. Dev.* **2015,** *19*, 1369.
(101) Hitosugi, S.; Tanimoto, D.; Nakanishi, W.; Isobe, H., *Chem. Lett.* **2012,** *41*, 972.
(102) Pangborn, A. B.; Giardello, M. A.; Grubbs, R. H.; Rosen, R. K.; Timmers, F. J., *Organometallics* **1996,** *15*, 1518.
(103) Aslam, S. N.; Stevenson, P. C.; Phythian, S. J.; Veitch, N. C.; Hall, D. R., *Tetrahedron* **2006,** *62*, 4214.
(104) Waser, J.; Gaspar, B.; Nambu, H.; Carreira, E. M., *J. Am. Chem. Soc.* **2006,** *128*, 11693.
(105) Wrackmeyer, B., *Prog. Nucl. Magn. Reson. Spectrosc.* **1979,** *12*, 227.
(106) Doi, T.; Fukuyama, T.; Minamino, S.; Husson, G.; Ryu, I., *Chem. Commun.* **2006,** 1875.
(107) Peñafiel, I.; Pastor, I. M.; Yus, M., *Tetrahedron* **2010,** *66*, 2928.
(108) Nakamura, M.; Hara, K.; Hatakeyama, T.; Nakamura, E., *Org. Lett.* **2001,** *3*, 3137.
(109) Itoh, T.; Matsueda, T.; Shimizu, Y.; Kanai, M., *Chem. - Eur. J.* **2015,** *21*, 15955.
(110) (a) He, X.; Hartwig, J. F., *Organometallics* **1996,** *15*, 400; (b) Bettinger, H. F.; Filthaus, M.; Bornemann, H.; Oppel, I. M., *Angew. Chem., Int. Ed.* **2008,** *47*, 4744.
(111) Frisch, M. J.; Trucks, G. W.; Schlegel, H. B.; Scuseria, G. E.; Robb, M. A.; Cheeseman, J. R.; Scalmani, G.; Barone, V.; Mennucci, B.; Petersson, G. A.; Nakatsuji, H.; Caricato, M.; Li, X.; Hratchian, H. P.; Izmaylov, A. F.; Bloino, J.; Zheng, G.; Sonnenberg, J. L.; Hada, M.; Ehara, M.; Toyota, K.; Fukuda, R.; Hasegawa, J.; Ishida, M.; Nakajima, T.; Honda, Y.; Kitao, O.; Nakai, H.; Vreven, T.; Montgomery Jr., J. A.; Peralta, J. E.; Ogliaro, F.; Bearpark, M. J.; Heyd, J.; Brothers, E. N.; Kudin, K. N.; Staroverov, V. N.; Kobayashi, R.; Normand, J.; Raghavachari, K.; Rendell, A. P.; Burant, J. C.; Iyengar, S. S.; Tomasi, J.; Cossi, M.; Rega, N.; Millam, N. J.; Klene, M.; Knox, J. E.; Cross, J. B.; Bakken, V.; Adamo, C.; Jaramillo, J.; Gomperts, R.;

Stratmann, R. E.; Yazyev, O.; Austin, A. J.; Cammi, R.; Pomelli, C.; Ochterski, J. W.; Martin, R. L.; Morokuma, K.; Zakrzewski, V. G.; Voth, G. A.; Salvador, P.; Dannenberg, J. J.; Dapprich, S.; Daniels, A. D.; Farkas, Ö.; Foresman, J. B.; Ortiz, J. V.; Cioslowski, J.; Fox, D. J. *Gaussian 09*, Gaussian, Inc.: Wallingford, CT, USA, 2009.
(112) (a) Becke, A. D., *Phys. Rev. A* **1988,** *38*, 3098; (b) Lee, C.; Yang, W.; Parr, R. G., *Physical Review B* **1988,** *37*, 785; (c) Becke, A. D., *The Journal of Chemical Physics* **1993,** *98*, 5648.
(113) Cossi, M.; Rega, N.; Scalmani, G.; Barone, V., *J. Comput. Chem.* **2003,** *24*, 669.
(114) Belding, L.; Chemler, S. R.; Dudding, T., *J. Org. Chem.* **2013,** *78*, 10288.
(115) Sheldrick, G., *Acta Crystallographica Section A* **2008,** *64*, 112.

Chapter 4

DEVELOPMENT OF A SECOND-GENERATION BORYL-HECK REACTION

4.1 Introduction and Overview

As discussed in Chapter 3, alkenyl boronic esters are important and versatile synthons in organic synthesis. The first-generation boryl-Heck approach proved to be an excellent route to synthesize *trans*-1,2-disubstituted alkenyl boronic esters.[1] The conditions presented in Chapter 3 are efficient in the coupling of B-chlorocatecholborane (catBCl) with a variety of terminal olefins with excellent yields and moderate functional group tolerance. We had even demonstrated that α-methyl styrene, a 1,1-disubstituted alkene, was an adequate coupling partner yielding a stereodefined trisubstituted alkenyl boronic ester in a moderate yield (Figure 4.1).

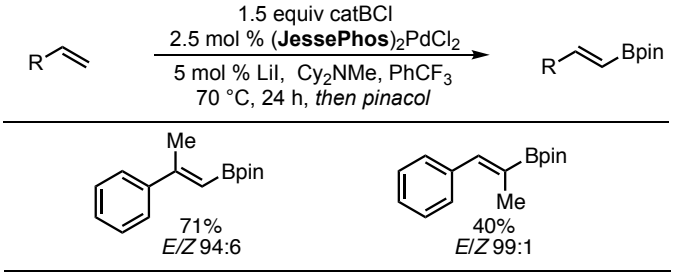

Figure 4.1 First Generation Synthesis of Disubstituted Styrene Derivatives

This was a very encouraging result because it demonstrated that higher substitution on the alkene substrate was feasible, and if general, would allow for the

synthesis of significantly more diverse alkenyl boronic esters using this method. Unfortunately, other disubstituted alkenes proved to be poor substrates under the original reaction conditions. For example, β-methyl styrene, a simple 1,2-disubstituted alkene, only gave 40% yield. Other 1,1-disubstituted alkenes, such as non-conjugated olefins, produce nothing more than trace yields, even under our most forcing conditions (Figure 4.2).

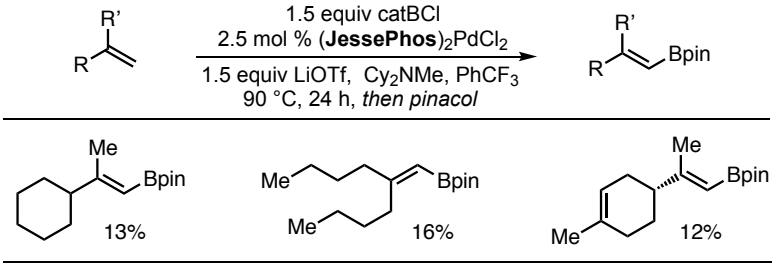

Figure 4.2 Limited Reactivity of Non-Conjugated 1,1-Disubstituted Alkenes Using 1st Generation Boryl-Heck Reaction Conditions

Herein, I report the development and utility of second-generation boryl-Heck conditions. These modified conditions allow for the direct borylation of a variety of 1,1- and 1,2-disubstituted alkenes to synthesize stereodefined trisubstituted alkenyl boronic esters. A tandem boryl-Heck/Suzuki reaction gives rise to a trisubstituted alkene in excellent yield in a stereodefined manner. The stereospecificity of this reaction supports our hypothesis of a Heck-like mechanism. Additionally, I found that formation of allyl boronic esters is kinetically disfavored with these conditions and does not form during the course of the reaction even as an intermediate.

4.2 Applications of Highly Substituted Alkenyl Boronic Esters

Access to highly substituted alkenyl boronic esters would vastly increase the utility of the boryl-Heck reaction as the products would have several advantages over the mono-substituted analogs. In addition to the applications discussed in Chapter 3, highly substituted alkenyl boronic esters have several more synthetic utilities. They are perhaps most commonly used for the synthesis tri- and tetrasubstituted alkenes *via* the Suzuki reaction,[2] expanding their use in the total synthesis of natural products and drugs.[3] In addition, tri- and tetrasubstituted alkenyl boronic esters also have many synthetic applications that are not possible with lower substitution. Those methods and other applications will be discussed below.

4.2.1 Asymmetric Hydrogenation of Alkenyl Boronic Esters

One very useful application of highly substituted alkenyl boronic esters is the reductive hydrogenation of the alkenyl bond to form the corresponding alkyl boronic ester. Hydrogenation of simple alkenyl boronic esters would lead to linear alkyl boronic esters. However, the reduction of tri- and tetrasubstituted alkenyl boronic esters creates a new stereocenter, allowing for the possibility of desymmetrization. This provides a straightforward route to access to enantioenriched alkyl boronic esters.

In 2002, Knochel reported the diastereoselective hydrogenation of alkenyl boronic esters (Figure 4.3).[4] This directed reduction results in excellent diastereoselectivity allowing for excellent control of three adjacent stereocenters as shown in **4.1**. Surprisingly, this reaction proceeds under simple palladium catalyzed hydrogenation conditions (H_2 with Pd/C).

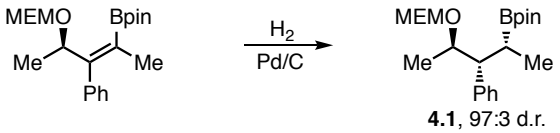

Figure 4.3 Knochel's Diastereoselective Hydrogenation of Alkenyl Boronic Esters

Miyaura was the first to report the asymmetric hydrogenation of a 1-alkenyl boron compound.[5] While this was an important seminal result, only one substrate (1-phenylethenylboronic acid and its esters) was examined and the enantiomeric excess obtained was considerable low, ranging from 16-80%. Morken followed up on this work by demonstrating that, with proper rhodium precatalyst and chiral phosphine ligand, excellent yields with high enantiomeric excess can be obtained for this class of prochiral alkenyl boronic ester substrates (Figure 4.4).[6] Morken also explored the asymmetric hydrogenation of 1,2-diboronic esters which can be synthesized from the diboration of terminal alkynes.[7]

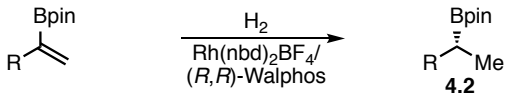

R =	product	yield	ee
Cy	**4.2a**	>95%	97%
n-hex	**4.2b**	>95%	81%
$TBSO(CH_2)_2$	**4.2c**	>95%	90%
$PivO(CH_2)_2$	**4.2d**	>95%	90%
$PhCH_2$	**4.2e**	>95%	88%

Figure 4.4 Scope of Morken's Rhodium Catalyzed Asymmetric Hydrogenation Reaction

Soon after, the use of catalytic iridium for this transformation became the state of the art (Figure 4.5).[8] In general, the iridium catalyzed reaction provides higher enantiomeric excess and better functional group tolerance. Additionally, 1,2-disubstituted alkenyl boronic esters are well tolerated, opening up a new class of products accessible *via* this strategy.

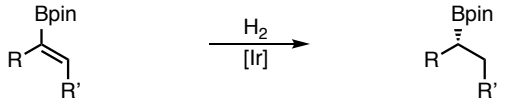

Figure 4.5 Iridium Catalyzed Asymmetric Hydrogenation of Alkenyl Boronic Esters

4.2.2 Synthesis of Acylboronates *via* Ozonolysis

Acylboron compounds have gained increased interest due to their unique reactivity.[9] Most notably, these reagents are used in amide coupling reactions due to their high chemoselectivity. In 2017, Bode and Ito reported a relatively unique procedure to synthesize acylboronate reagents from internal alkenyl boronic esters (Figure 4.6).[10] The ozonolysis of alkenyl MIDA boronates (**4.3**) provides a concise route to acyl MIDA boronates (**4.4**), which can be further converted into the analogous acyl trifluoroborates (**4.5**) with potassium bifluoride. This reaction exhibits excellent functional group tolerance and gives access to acylboron reagents which were previously inaccessible.

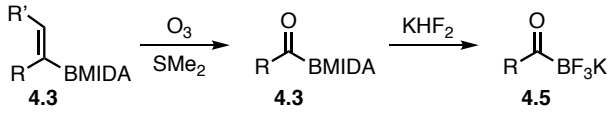

R =	R' =	product	yield
n-Bu	Ph	**4.5a**	87%
Cy	Ph	**4.5b**	84%
Ph	Ph	**4.5c**	90%
$Cl(CH_2)_3$	Ph	**4.5d**	94%
$AcOCH_2$	H	**4.5e**	85%
$BnOCH_2$	H	**4.5f**	80%
$TIPSOCH_2$	H	**4.5g**	66%
$(phth)NCH_2$	TMS	**4.5h**	90%
$BocHNCH_2$	H	**4.5i**	91%
$FmocHNCH_2$	H	**4.5j**	65%

Figure 4.6 Selected Scope of Acylboronate Synthesis *via* Ozonolysis

4.2.3 Synthesis of Polyene Fragments

As briefly discussed in Chapter 3, highly conjugated organic materials have unique and useful applications. They can function as light emitters, charge transporters, or both. The properties of these organic light-emitting diodes (OLEDs) has attracted much attention towards the synthesis and diversification of these frameworks.[11] A common route for synthesizing these large compounds is through a Suzuki reaction of two highly conjugated fragments. This can require highly conjugated tri- and tetrasubstituted alkenyl boronic esters. For example, Shu and Diau used this strategy to synthesize novel distyrylcarbazole derivatives for use as simultaneously hole-transporting and light-emitting layers in blue light-emitting diodes (Figure 4.7).[12] Through a bis-Suzuki reaction, **4.6** was coupled with two equivalents of **4.7** to form the highly conjugated **4.8** distyrylcarbazole. With access to **4.8**, they were able to study the photophysical properties, thermos properties, electrochemistry, and electroluminescence properties.

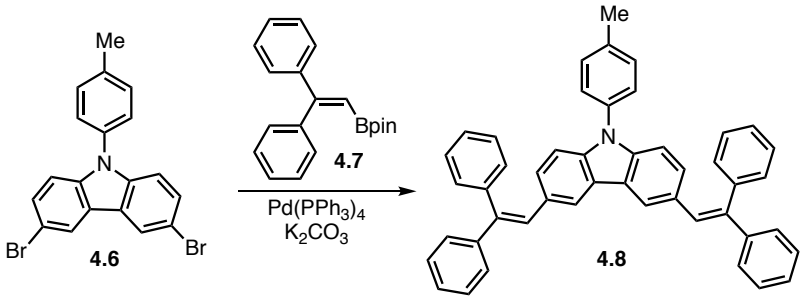

Figure 4.7 Synthesis of Distyrylcarbazole Derivatives

4.3 Typical Synthesis of Highly Substituted Alkenyl Boronic Esters

Trisubstituted alkenyl boronic esters are especially valuable reagents in organic synthesis. However, far fewer methods for the synthesis of trisubstituted alkenyl boronic esters exist than for disubstituted analogs. In particular, synthesizing these compounds in a stereodefined manner is a difficult task to achieve. Many of the methods discussed in Chapter 3 can also be applied for the synthesis of trisubstituted alkenyl boronic esters, however, several new and distinct strategies have been recently realized.

4.3.1 Hydroboration of Unsaturated Carbon-Carbon Bonds

Similar to Chapter 3, Section 3.3.1, hydroboration is a common route to synthesize trisubstituted alkenyl boronic esters. Although, similar in principle to the hydroboration of terminal alkynes, internal alkyne hydroboration suffers from poor regioselectivity and significantly reduced reactivity.[13] Additionally, due to the inherent mechanism, this is not viable for the synthesis of 1,1-disububstituted alkenyl boronic esters. However, many methods have been developed for the synthesis of 1,2-disubstituted alkenyl boronic esters *via* the hydroboration of internal alkynes.

4.3.1.1 Uncatalyzed Hydroboration of Internal Alkynes

The uncatalyzed direct hydroboration of internal alkynes is not as simple as for the terminal substrates. The direct hydroboration of internal alkynes follows the same hydroboration mechanism leading to the *cis*-product derived from a *syn*-addition of the boron and hydrogen atoms (Figure 4.8, top). Unfortunately, in non-symmetric cases, this reaction generally does not proceed with good regioselectivity (Figure 4.8, bottom). The regioselectivity observed with terminal alkynes is thought to arise from an electronic preference that occurs during the transition state of the addition. However, in the case of internal alkynes, there is less of an electronic bias, and in addition, added steric effects can drastically influence the regioselectivity.

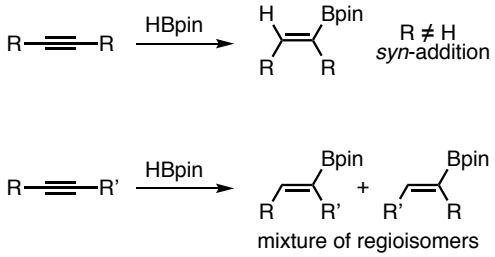

Figure 4.8 Hydroboration of Symmetric and Non-Symmetric Internal Alkynes

Many borohydride reagents have been examined over the years and all show poor to moderate regioselectivity.[13] Even with an electronically and sterically biased system (phenylpropyne), poor regioselectivity is observed across the board (Figure 4.9). Additionally, the hydroboration of more functionalized alkynes, such as acetylenic esters[14] or diphenyl acetylene,[15] does not occur even after prolonged reaction times.

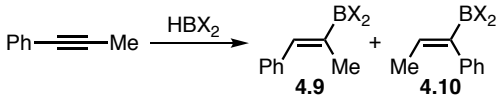

hydroborating reagent	**4.9/4.10**
$HBBr_2{\cdot}SMe_2$	64/36
9-BBN	65/35
$HB(Sia)_2$	19/81
HBpin	15/85

Figure 4.9 Selectivities of Uncatalyzed Hydroboration of Phenylpropyne

4.3.1.2 Copper Catalyzed Hydroboration of Internal Alkynes

To overcome this severe limitation of hydroboration, copper catalysis has recently become a popular approach to synthesize alkenyl boronic esters from internal alkynes. Lipshutz and Aue found that the hydroboration of acetylenic esters is possible with pinacol borane in the presence of catalytic copper hydride (Figure 4.10).[14] The reactive copper hydride can be formed *in situ* from CuCl, 1,2-bis(diphenylphosphino)benzene, and sodium *tert*-butoxide or a commercial copper hydride reagent such as Stryker's reagent can be used. Excellent stereochemistry was observed in all products giving nearly selective formation of the *Z*-product as a single regioisomer (**4.11**). Using this method, various α-carboalkoxyalkenyl boronic esters could be synthesized with good yields and excellent stereoselectivities.

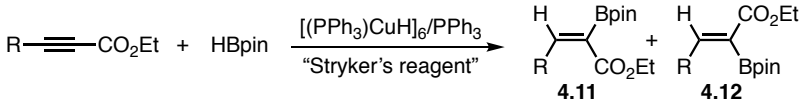

R =	product	yield	**4.11/4.12**
Et	**4.11a**	80%	14:1
n-Pr	**4.11b**	85%	>25:1
Cy	**4.11c**	87%	>25:1
Ph	**4.11d**	95%	10:1
$SiMe_3$	**4.11e**	81%	>99:1

Figure 4.10 Lipshutz's Copper Catalyzed Hydroboration of Acetylenic Esters

Contrasting the uncatalyzed hydroboration mechanism, the boron and hydride are not added simultaneously to the alkyne (Figure 4.11). However, the formal *syn*-addition suggests a 1,2-addition to form carbon bound copper intermediate (**4.14**). Additionally, the high level of stereoselectivity suggests that the carbon bound intermediate does not isomerize to the oxygen bound complex (**4.16**) even though the Cu-C bonds are considerably weaker than Cu-O bonds. Using *ab initio* calculations, Lipshutz and Aue found that complex (**4.14**) is significantly more stable than (**4.16**). Furthermore, they calculated the transition state **4.13** which forms from a weakly bound π-complex between the copper hydride (**4.12**) and the alkyne.

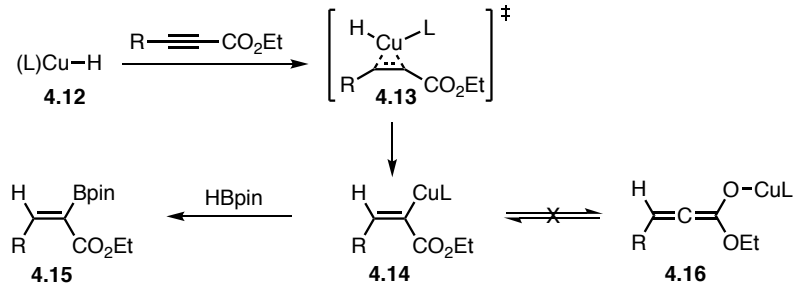

Figure 4.11 Mechanism of Copper Catalyzed Hydroboration of Acetylenic Esters

In 2008, Yun reported the stereoselective, formal hydroboration, of acetylenic esters to form β-boryl-α,β-ethylenic esters.[16] Using copper catalysis combined with B_2pin_2 and methanol, the formal hydroboration of acetylenic esters could be performed. Interestingly, this method shows complete selectivity for the opposite regioisomer as demonstrated above (Figure 4.12).

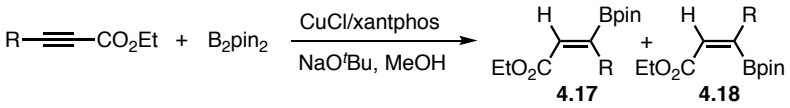

R =	product	yield	**4.17/4.18**
n-hex	**4.17a**	93%	>99:1
Cy	**4.17b**	99%	>99:1
$CyCH_2$	**4.17c**	88%	>99:1
^{t}Bu	**4.17d**	71%	34:66
H	**4.17e**	65%	>99:1

Figure 4.12 Yun's Formal Hydroboration of Acetylenic Esters with Copper and B_2pin_2

This reaction proceeds with good to excellent yields and perfect regioselectivity (except for the *tert*-butyl substituted alkyne (**4.17d**). The switch in regioselectivity from the copper hydride conditions can be explained by an alternative mechanism (Figure 4.13). Rather than a copper hydride adding across the alkyne, the phosphine ligated copper boryl complex (**4.20**), formed from Cu-X and B_2pin_2, adds across the alkyne to form copper enolate **4.21**. Quenching with methanol, protonates the enolate to form the product as well as an alkoxy copper species (**4.18/4.19**) which can react with B_2pin_2 to regenerate **4.20**.

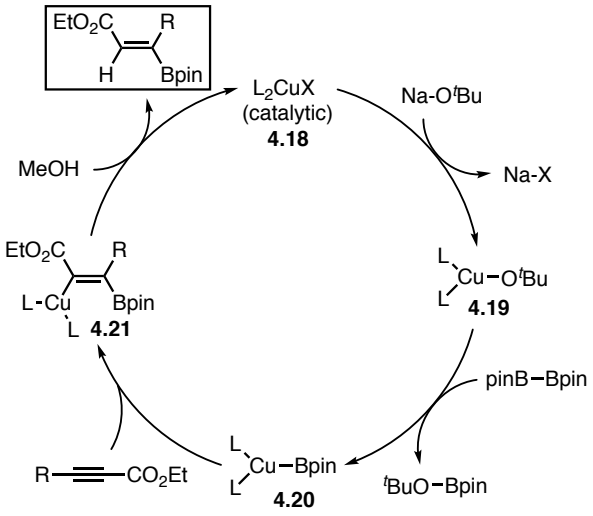

Figure 4.13 Mechanism of the Hydroboration of Acetylenic Esters with Copper and B_2pin_2

A one-pot procedure has also been developed for an *in situ* asymmetric reduction to the chiral alkyl borane with excellent enantiomeric excess (Figure 4.14).[17] As mentioned above, the synthesis of enantiopure alkyl boronic esters is a highly desired task to accomplish. Asymmetric copper hydride addition to alkenyl boronic ester **4.22** and resulting protonation can give access to enantiopure products (**4.23**). Using (*R*,*S*)-Josiphos, polymethylhydrosilane (PMHS) and *tert*-butanol, chiral alkyl pinacol boronic esters can by formed with excellent yields and enantiomeric excess. This can be done from either the isolated alkenyl boronic esters (Figure 4.14, top) or generated *in situ* (Figure 4.14, bottom).

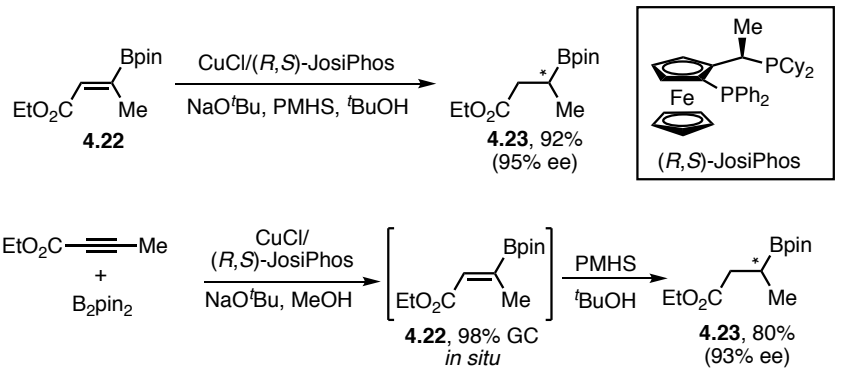

Figure 4.14 Asymmetric Reduction of Alkenyl Boronic Esters

While these catalytic conditions worked well for acetylenic esters and terminal alkynes, they were inefficient at the hydroboration of internal aryl alkynes. In 2010, Yun and Son discovered that strong σ-donating NHC ligands with copper catalysis are effective in the regioselective hydroboration of internal aryl methyl alkynes (Figure 4.15, **4.25a**).[18]

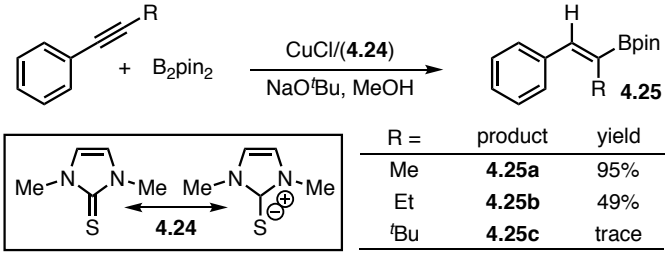

R =	product	yield
Me	**4.25a**	95%
Et	**4.25b**	49%
^{t}Bu	**4.25c**	trace

Figure 4.15 Yun's Copper/NHC Catalyzed Hydroboration of Internal Aryl Alkynes

This reaction generally proceeds with excellent regioselectivity, however, switching to alkyl substitution larger than methyl such as ethyl (**4.25b**) or *tert*-butyl (**4.25c**) significantly reduces the yield. Improved reaction conditions, by replacing the

NHC ligand with P(p-tol)$_3$ gave excellent yields with a broader substrate scope.[19] Larger substitution patterns, including β-branching substituents, were well tolerated with good yields under these new reaction conditions (Figure 4.16). Unfortunately, isopropyl- and cyclohexyl- substitutions proceeded with diminished regioselectivity, only about 80% for β-borylation.

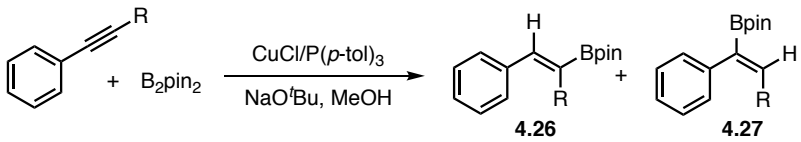

4.26 **4.27**

R =	product	yield	**4.26/4.27**
Et	**4.26a**	90%	100:1
Cy	**4.26b**	88%	86:14
^{i}Pr	**4.26c**	82%	80:20

Figure 4.16 Yun's Hydroboration of Larger Aryl-Alkyl Alkynes

Interestingly, when *tert*-butyl substituted substrates were subjected to these conditions a complete switch in selectivity is observed (Figure 4.17). Selective α-borylation occurs with these substrates in great yields. Furthermore, only the *anti*-addition product (**4.28**) was detected. The switch in selectivity is likely due to increased steric repulsion between the pinacol boronate and the *tert*-butyl group.

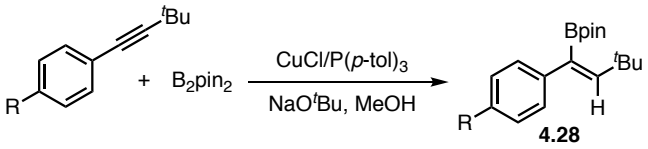

R =	product	yield
H	**4.28a**	91%
CF_3	**4.28b**	92%
CN	**4.28c**	92%

Figure 4.17 Reversed Selectivity of *tert*-Butyl Substituted Aryl Alkynes

For the regioselective hydroboration of dialkyl alkynes, two research groups have independently applied a directing group approach. Using propargylic-functionalized internal alkynes in combination with copper catalysis, Carretero demonstrated that selective β-borylation was possible with moderate to good yields.[20] A wide variety of Lewis basic functional groups were applicable to this approach, showing good to excellent regioselectivities (Figure 4.18).

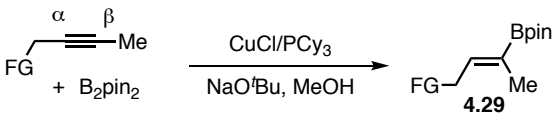

FG	product	yield	β/α ratio
S(2-Py)	**4.29a**	82%	>98:2
OH	**4.29b**	69%	>98:2
OBn	**4.29c**	78%	>98:2
OTIPS	**4.29d**	82%	>98:2
OAc	**4.29e**	76%	90:10
NHTs	**4.29f**	89%	>98:2
CH_2OBn	**4.29g**	72%	88:12

Figure 4.18 Selected Scope of Carretero's Directed Internal Alkyne Hydroboration

This reaction is thought to proceed through a mechanism similar to Figure 4.13. However, DFT calculations suggest that the regioselectivity is a result of orbital control rather than steric or coordination effects.[20]

The McQuade group showed that the regioselectivity of hydroboration with propargylic alcohols can be controlled using copper catalysis with different NHC ligands (Figure 4.19).[21] Using protected alcohols with complex **4.31**, excellent α-selectivities and yields could be obtained (**4.32**). In contrast, using free alcohols with complex **4.33**, the L.5 was major product with excellent yields (**4.34**). The McQuade group has since applied this directed approach to the synthesis of methyl axenoside and methyl 3-*epi*-axenoside.[22]

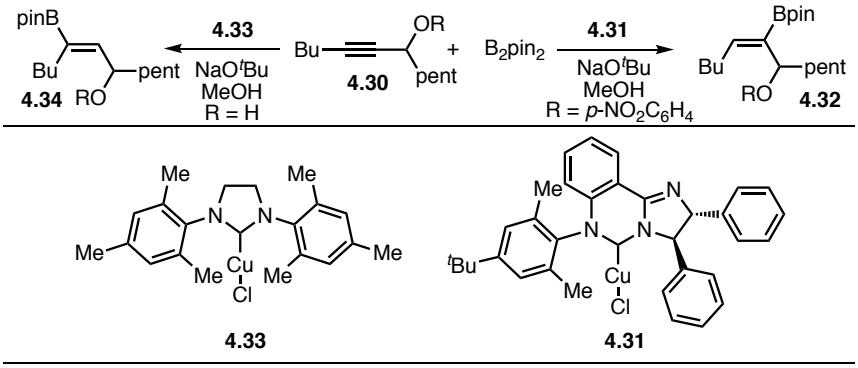

Figure 4.19 McQuade's Regioselective Hydroboration of Propargylic Internal Alkynes

4.3.1.3 Non-Copper Catalyzed Hydroboration of Alkynes

Silver,[23] aluminum,[24] palladium,[25] Lewis acids,[26] and even carboxylic acids[27] have all been used to promote the *syn*-hydroboration of internal alkynes. However, the second most common metal for the hydroboration of internal alkynes by far, is iron. Cheap, widely abundant and non-toxic, many researchers have explored the use of

various iron sources in the hydroboration of alkynes. Iron is very effective for the selective hydroboration of terminal alkynes using HBpin or B_2pin_2 and has recently been applied to internal alkynes for the synthesis of 1,2-disubstitued alkenyl boronic esters (Figure 4.20). Unfortunately, so far, the scope has been limited to simple alkynes such as diphenyl acetylene and 4-octyne but generally show good yields for the mono-borylation with a variety of iron precatalysts.[15, 28]

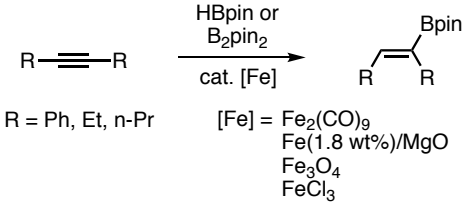

Figure 4.20 Iron Catalyzed Hydroboration of Internal Alkynes

All of the catalysts discussed so far involve the *syn*-addition of the boron and hydrogen atoms across the alkyne forming the *cis*-product. On the other hand, the *trans*-hydroboration of internal alkynes remains a much more difficult task to achieve and significantly fewer reports exist. In 2013, Früstner reported a ruthenium catalyst that could achieve the selective *trans*-hydroboration of internal alkynes (Figure 4.21).[29] This method demonstrated excellent yields, selectivities, and functional group tolerance. Even macrocyclic alkynes could be *trans*-borylated to form compounds such as **4.36** with excellent yields.

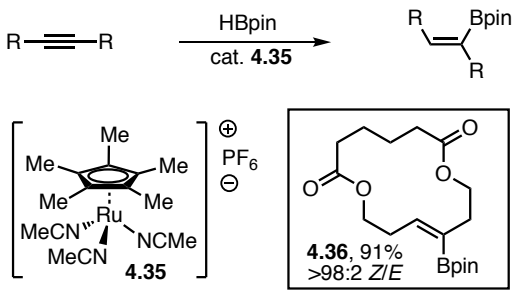

Figure 4.21 Früstner's Ruthenium Catalyzed *Trans*-Hydroboration of Internal Alkynes

4.3.1.4 Hydroboration of Allenes

In a similar fashion to the copper catalyzed hydroboration of alkynes, the hydroboration of allenes can result in the same class of products. Unfortunately, this also has the potential to give rise to a mixture of products (Figure 4.22). An early study by Miyaura found that with a phosphine supported platinum catalysis, **4.38** is the major product in as mixture with up to 50% **4.37**.[30] Interestingly, the other potential isomers (**4.39** and **4.40**) were not observed.

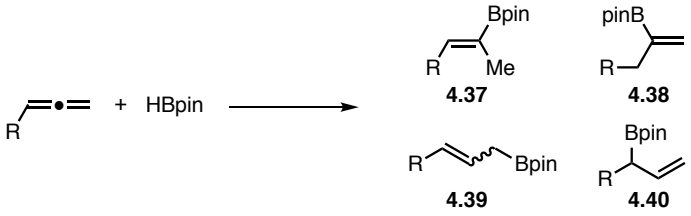

Figure 4.22 Potential Products of the Hydroboration of Allenes

More than a decade later, this reaction was reinvestigated with different catalysts to examine their effect on reactivity and selectivity.[31] Ma developed a ligand controlled highly selective copper-catalyzed borylmetalation of aryl allenes (Figure 4.23).[31b] Using

copper (I) chloride and bidentate ligand **4.41**, good yields of **4.42** can be obtained, all with >95:5 selectivity. Under nearly identical conditions except with mono phosphine ligand **4.43** instead, **4.44** can be obtained with good yields as a single regioisomer.

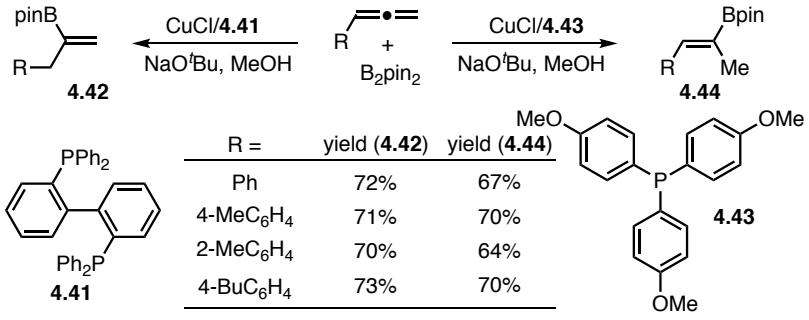

R =	yield (**4.42**)	yield (**4.44**)
Ph	72%	67%
4-MeC_6H_4	71%	70%
2-MeC_6H_4	70%	64%
4-BuC_6H_4	73%	70%

Figure 4.23 Ma's Ligand Controlled Regioselective Hydroboration of Allenes

4.3.2 Carboboration of Unsaturated Carbon-Carbon Bonds

While many hydroboration procedures have been developed for the synthesis of trisubstituted alkenyl boronic esters, due to the inherent mechanism, these methods are limited to the synthesis of 1,2-(α,β)-carbosubstituted products. New methods were required for the synthesis of α,α-disubstituted and fully substituted alkenyl boronic esters. Recently, carboboration had become a common approach to solve this problem. Rather than adding a boron and a hydrogen atom across a triple bond, carboboration adds a boron and carbon atom resulting in a α,α-disubstituted configuration (Figure 4.24). Additionally, with internal alkenes this would give rise to fully substituted alkenyl boronic esters. Recently a comprehensive review on this topic has been published.[32]

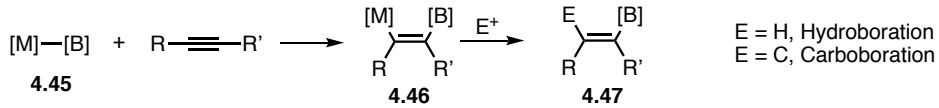

Figure 4.24 General Scheme of Carboboration of an Alkyne

Generally, this process includes the formation of a metalloborane **4.45** (usually with copper) either isolated or made *in situ*. Combination of **4.45** with an alkyne result in the borylmetalation of the alkyne usually in a stereospecific manner which can be affected by steric interactions, electronic characteristics, or directing groups. Intermediate **4.46** can react with a carbon electrophile (E^+) to form product (**4.47**). In the case of hydroboration, the electrophile is a proton usually from added water or methanol. However, E^+ can also be an alkyl halide, aldehyde, conjugate acceptor, etc., forming a new carbon-carbon bond in a formal carboboration reaction. Typically, these methods involve the formation of highly nucleophilic boron reagents or intermediates (**4.45** or **4.46**) and are limited to the formation of 1,1-disubstituted and fully substituted alkenyl boronic esters.

The earliest example of this approach using a nucleophilic boron reagent used a stoichiometric boryllithium nucleophile and copper (I) to add across extremely electron deficient alkynes and quenched with an electrophile (Figure 4.25).[33] The stereochemistry of the alkenyl product can directly be affected by the temperature at which the reaction was run. The *syn*-product (**4.50**) is favored at lower temperatures and the *anti*-product (**4.51**) is favored at room temperature. Presumably, the higher temperatures allow for alkene isomerization to the more thermodynamically stable **4.51**.

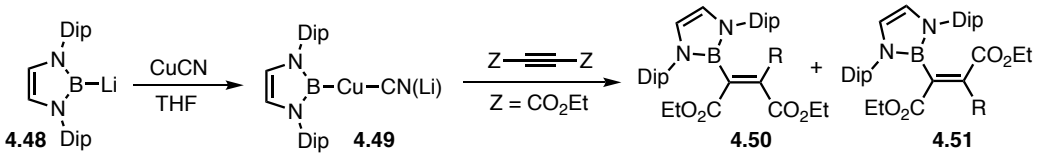

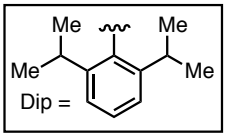

electrophile	temperature	yield	**4.50/4.51**
PhCOCl	–78 °C	80%	60/40
PhCOCl	rt	71%	1/99
allylBr	–78 °C	93%	99/1
allylBr	rt	96%	38/62

Figure 4.25 Yamashita's and Nozaki's Carboboration of an Electron-Deficient Alkyne

4.3.2.1 Copper-Catalyzed Carboboration of Alkynes

The most common method for carboboration is the copper catalyzed addition of B_2pin_2 and a carbon electrophile across a triple bond. This reaction follows nearly an identical pathway as copper catalyzed hydroboration of alkynes (Figure 4.26). Tortosa was the first to recognize the vinyl copper intermediate (**4.52**) in the proposed copper catalyzed hydroboration mechanism could be coupled with more than just a proton. Using an alkyl electrophile and stoichiometric sodium *tert*-butoxide to make the active copper species, the carboboration of alkynes was made possible.

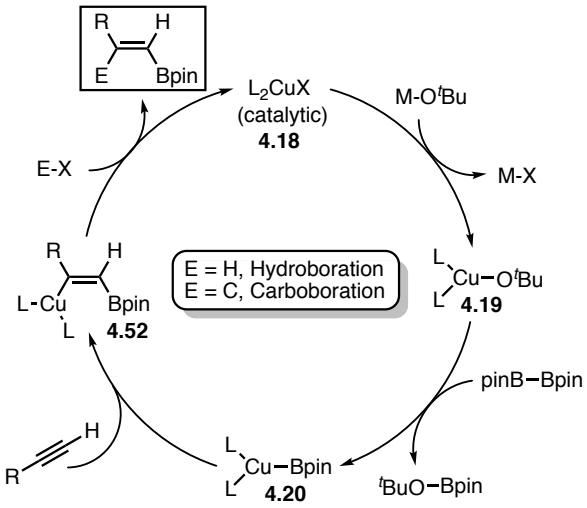

Figure 4.26 Mechanism of Copper Catalyzed Hydro- and Carboboration of Alkynes

The catalytic cycle begins with activation of copper with an alkoxide base to form **4.19**. Transmetallation with B_2pin_2 results in the nucleophilic metalloborane intermediate **4.20**. Addition of **4.20** across the alkyne results in vinyl copper species **4.52** which can be quenched with a carbon electrophile to form product.

In Tortosa's seminal publication, methyl iodide shown to be a competent electrophile in this reaction (Figure 4.27).[34] While the majority of reactions used methyl iodide to form *cis*-branched methyl alkenyl boronic esters, allyl iodide and benzyl bromide proceeded but were less effective electrophiles.

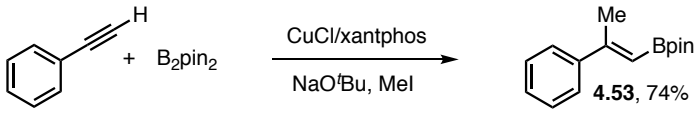

Figure 4.27 Tortosa's Carboboration with Methyl Iodide

Following this initial report, an explosion of chemistry using this strategy has been explored. Varying the phosphine or NHC ligand used, various allyl, benzyl and alkyl electrophiles including halides,[35] phosphates,[36] carbonates,[37] and sulfonates[35d] can be used to synthesize a variety of α,α-disubstituted and fully substituted alkenyl boronic esters.

Other non-traditional electrophiles are also effective in this reaction. Hou found that using an NHC copper complex the boracarboxylation of various alkynes could be achieved (Figure 4.28, top).[38] This method is useful for the formation of multi-functionalized alkenes using cheap and abundant copper and carbon dioxide. Brown was the first to utilize sp^2 electrophiles and demonstrated the carboboration to form borylated styrene products such as **4.55.**

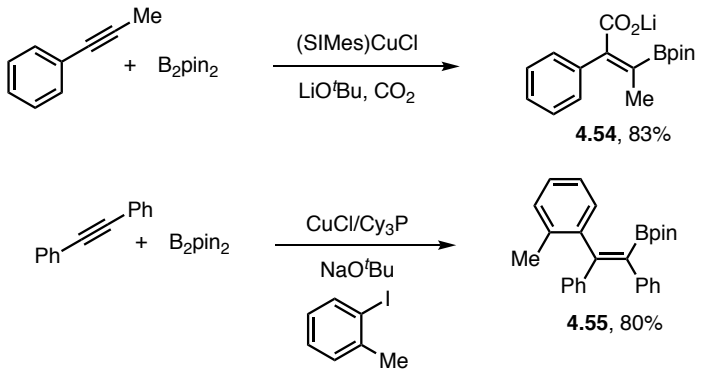

Figure 4.28 Carboboration with Non-Traditional Electrophiles

Ito has applied this strategy to a cyclization carboboration reaction in an intramolecular alkylboration of propargylic ethers and amines (Figure 4.29).[39] This provides an efficient route to alkenyl boronic esters bearing heterocyclic moieties

(**4.57**). These products can be further modified *via* a Suzuki reaction to give elaborate, stereodefined tri- and tetrasubstituted alkenes (**4.58**).

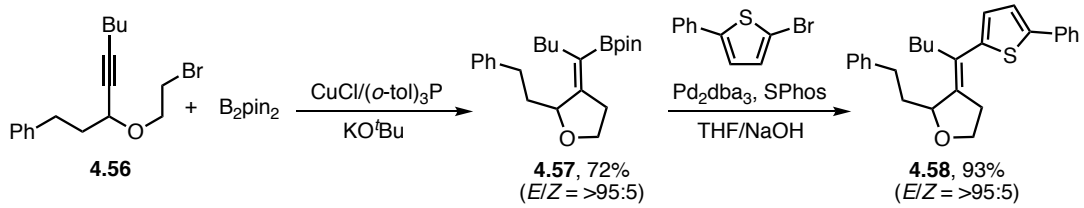

Figure 4.29 Ito's Intramolecular Carboboration Reaction

In all cases mentioned so far, the boryl-metalation occurs so that boron is positioned on the less hindered carbon. Although, some DFT calculations have suggested that selectively is actually electronic in nature.[39] Recently, Fu and Xiao reported a ligand controlled, regiodivergent carboboration of unactivated terminal alkynes.[40] Both Markovnikov and *anti*-Markovnikov products can be selectively obtained by switching ligand and boron source (Figure 4.30). Using the bidentate phosphine ligand dppbz with B_2pin_2, normal Markovnikov regioselectivity is observed (**4.59**). However, using B_2pai_2 and DMAP as a ligand, internal borylation is possible, favoring **4.60**. This reaction provides an efficient new route to alkenyl boronic esters from readily available terminal alkynes and *bis*-boron reagents.

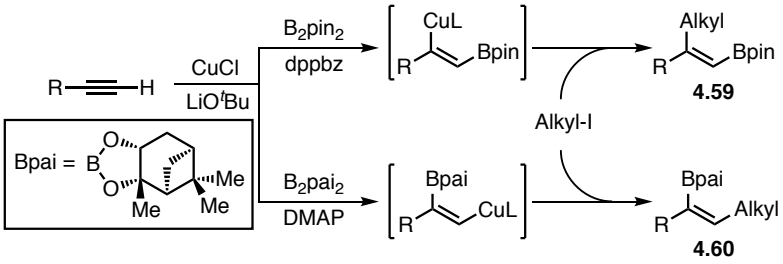

Figure 4.30 Fu's and Xiao's Regiodivergent Carboboration of Unactivated Terminal Alkynes

4.3.2.2 Carboboration of Allenes

Akin to copper catalyzed hydroboration, the carboboration of allenes also provides a route to substituted alkenyl boronic esters (Figure 4.31). **4.63** can be synthesized from allene **4.61** and allyl phosphate **4.62** using copper/NHC catalysis.[41] The initial boryl cupperation forms allyl cupperate **4.64** which reacts with **4.62** to form **4.63** through a S_N2'-like reaction (**4.64**).

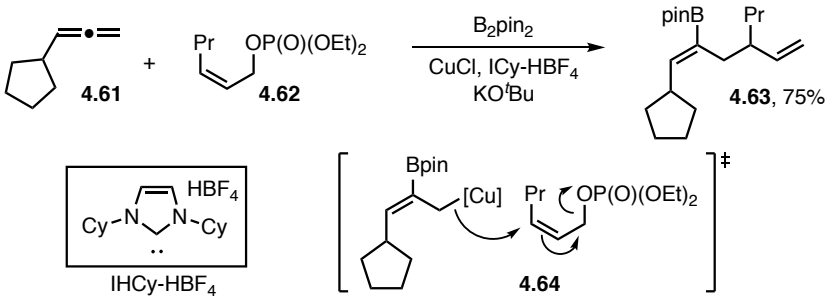

Figure 4.31 Carboboration of Allenes with Allyl Phosphates

4.3.3 1,2-Borylmetallation of Unsaturated Carbon-Carbon Bonds

At the core, the copper catalyzed hydroboration and carboboration reactions are just a 1,2-borylcupperation of alkynes or allenes. Quenching the intermediate vinyl

copper species with an electrophile produces isolable products. In a broader sense, this is just the 1,2-borylmetallation of unsaturated carbon-carbon bonds (Figure 4.32). Fundamentally, this involves the addition of a metalloborane reagent across an unsaturated bond (**4.46**) followed by cross coupling with some carbon or heteroatomic electrophile (**4.47**).

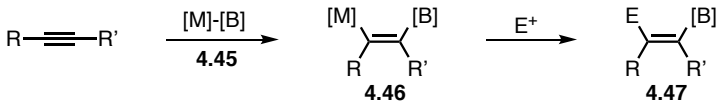

Figure 4.32 General Scheme for the Borylmetalation of Alkynes

Adding non-transition metal boron complexes across unsaturated bonds would give rise to similar yet more stable **4.46** complexes. For example, if M = B, Si, or Sn, then intermediate **4.46** may be able to be isolated. Additionally, as different compounds can have orthogonal reactivity, this significantly increases the diversity of post-modification procedures.

4.3.3.1 Diboration of Alkynes

Perhaps the most obvious example of the 1,2-borylmetallation of C-C unsaturated bonds is the diboration of terminal or internal alkynes. Suzuki and Miyaura were the first to report the platinum(0) catalyzed diboration of alkynes in 1993 (Figure 4.33, top).[42] They demonstrated that this method works for both terminal and internal alkynes with good yields. In one example, the diboron compound **4.65b** was cross-coupled with iodobenzene to replace both boronic esters with phenyl rings to form **4.66** (Figure 4.33, bottom).

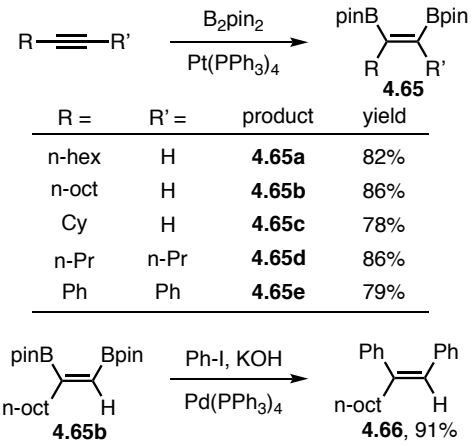

Figure 4.33 Platinum Catalyzed Diboration of Terminal and Internal Alkynes

Soon after their initial report, Miyaura demonstrated the mono-arylation of 1,2-diborylalkenes (Figure 4.34, top).[43] The key to the mono-arylation is the use of a slight excess of **4.67** (1.1 equiv) to the electrophile (1.0 equiv). The reaction proceeds in a regioselective manner, presumably derived from the different steric environments around each of the two different boronic esters. Furthermore, when triborylated alkenes (**4.69**) are subjected to similar conditions the same selectivity is observed for **4.70** (Figure 4.34, bottom).[44]

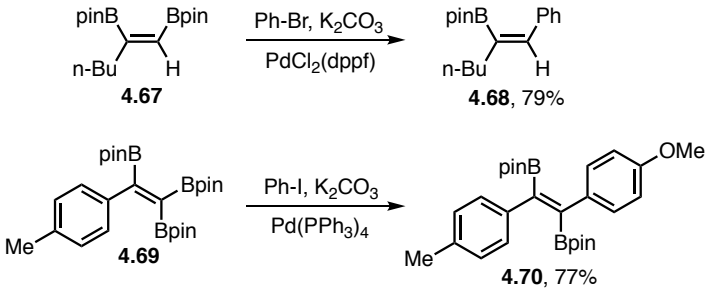

Figure 4.34 Regioselective Mono-Arylation of Di- and Triborylalkenes

While this method works well, the inherent selectivity of the Suzuki reaction limits the utility of this to the synthesis of 1,2-disubstitued alkenyl boronic esters. Suginome developed a modified procedure using a non-symmetric diboron reagent **4.71** (Figure 4.35). Using either platinum or iridium catalysis, Suginome demonstrated the synthesis of various diboronic esters containing both a pinacolborane and a 1,8-diaminonapthalene (Bdan) boron handle.[45] The significance of this discovery is embedded in the regioselectivity of the diboration step. The Bdan group ends up at the *trans*-position relative to the initial substitution on the alkyne, placing the pinacolborane group at the internal position. Subsequent cross-coupling reacts selectively with the pinacolborane group (Figure 4.35, bottom). This results in the formation of 1,1-disubstituted alkenyl boronic esters (**4.73**) with excellent yields and selectivities.

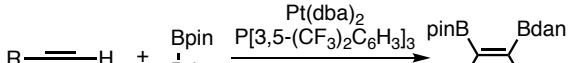

		Pt		Ir	
R =	product	yield	ratio	yield	ratio
Ph	**4.72a**	69%	96:4	85%	99:1
4-MeC_6H_4	**4.72b**	67%	93:7	67%	93:7
4-$MeOC_6H_4$	**4.72c**	90%	93:7	57%	85:15
2-thiophene	**4.72d**	61%	89:11	64%	99:1
n-hex	**4.72e**	73%	93:7	74%	93:7

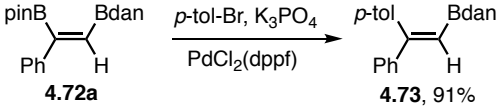

Figure 4.35 Suginome's Differentially Protected Diboration of Alkynes

4.3.3.2 Diboration of Allenes

The diboration of allenes can also give rise to disubstituted alkenyl boronic esters (Figure 4.36).[46] In the platinum catalyzed reaction, the addition has a strong tendency to occur at the internal position of the allene (**4.75**).[46a] However, steric factors can erode reaction selectivity as seen in **4.75d** and **4.75e**.

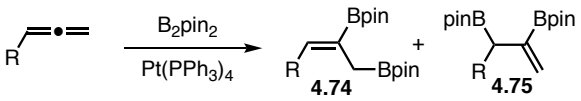

R =	product	yield	**4.74/4.75**
H	**4.75a**	99%	--
Bu	**4.75b**	97%	6:94
CH_2CO_2Et	**4.75c**	90%	7:93
Ph	**4.75d**	94%	27:71
Cy	**4.75e**	96%	50:50

Figure 4.36 Selectivity of Platinum Catalyzed Diboration of Allenes

The formation of **4.75** also generates a new stereocenter. This allows the potential for desymmetrization of this reaction. In 2005, Morken reported a sequential asymmetric allene diboration/allylation reaction (Figure 4.37).[47] The product from the diboration reaction (**4.79**) can act as both an allyl and an alkenyl boronic ester fragment. An asymmetric allylation reaction and sequential oxidation provides a route to synthesize enantioenriched β-hydroxyl ketones (**4.80**). This two-step process proceeds with good yields with high enantiomeric excess for differentially substituted allenes and aldehydes.

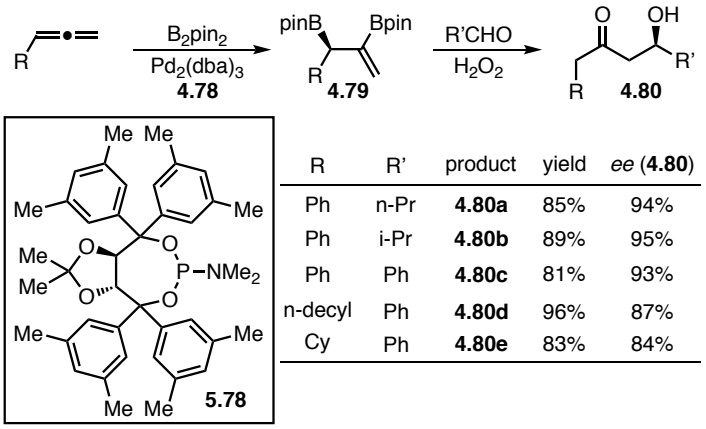

R	R'	product	yield	*ee* (**4.80**)
Ph	n-Pr	**4.80a**	85%	94%
Ph	i-Pr	**4.80b**	89%	95%
Ph	Ph	**4.80c**	81%	93%
n-decyl	Ph	**4.80d**	96%	87%
Cy	Ph	**4.80e**	83%	84%

Figure 4.37 Morken's Asymmetric Diboration of Allenes and Subsequent Allylation Reaction

Allyl boronate **4.81** can also react with imines directly or aldehydes with added ammonium salts to form β-aminoketones after acylation (**4.82** and **4.83**).[48] These alkenyl boronic esters can be further functionalized *via* protodeboronation or a Suzuki reaction to form **4.84** or **4.85** respectively, each with excellent enantiomeric excess.

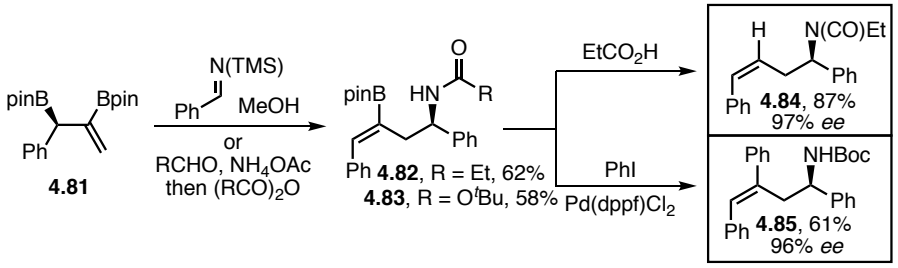

Figure 4.38 Morken's Allylation of Imines and Downstream Functionalization

4.3.3.3 Silylboration of Alkynes

The silylboration of alkynes demonstrates similar reactivity and generates similar products to those of the diboration reaction. Ito found that with catalytic

palladium and silylborane **4.86**, a variety of terminal and internal alkynes can undergo silylboration (Figure 4.39).[49] And although two different group are being added across the alkyne, this reaction generally proceeds with excellent regioselectivity, placing the boron at the terminal position in the reaction with terminal alkynes. The internal alkynes Ito examined were symmetric therefore there are not issues with regioselectivity (**4.87e** and **4.87f**).

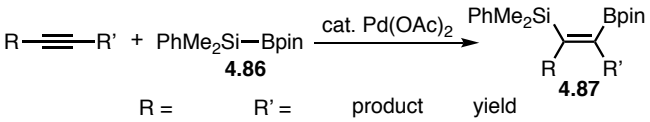

R =	R' =	product	yield
Ph	H	**4.87a**	82%
$THPO(CH_2)_2$	H	**4.87b**	88%
Cy	H	**4.87c**	82%
Me_3Si	H	**4.87d**	73%
Ph	Ph	**4.87e**	74%
Bu	Bu	**4.87f**	24%

Figure 4.39 Ito's Palladium Catalyzed Silylboration of Alkynes

All d-10 metals are effective at catalyzing the silylboration of alkynes, however, palladium and platinum were found to prefer to yield monomer products similar to **4.87,** while nickel tends to for dimer products (Figure 4.40).[50] This reaction proceeds in a regio- and stereospecific manner resulting in the *cis*,*cis*-1-silyl-4-boryl diene products (**4.88**).

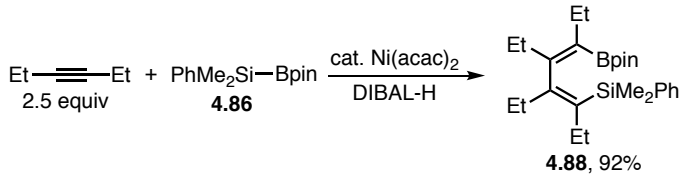

Figure 4.40 Nickel Catalyzed Silylborative Dimerization of Alkynes

While silylborane **4.86** is the most commonly used reagent, other silylborane have been utilized in similar reactions.[32, 51] All of which give the same regioselectivity across a terminal alkyne. These products are useful as bis-nucleophilic fragments. However, the more reactive boron handle is generally cross-coupled first with Suzuki reaction conditions leaving a highly substituted vinyl silane.[49, 52]

4.3.3.4 Silylboration of Allenes

In a similar fashion to the diboration of allenes, the silylboration of allenes is also possible. These reactions proceed with excellent regio- and chemoselectivity forming the alkenyl boronic ester and allyl silane simultaneously (Figure 4.41, top).[53] Reagents such as **4.89** are very useful in the synthesis of highly substituted alkenes. A Lewis acid promoted Sakurai reaction with **4.90** yields **4.91** in an excellent yield and stereochemistry.[54]

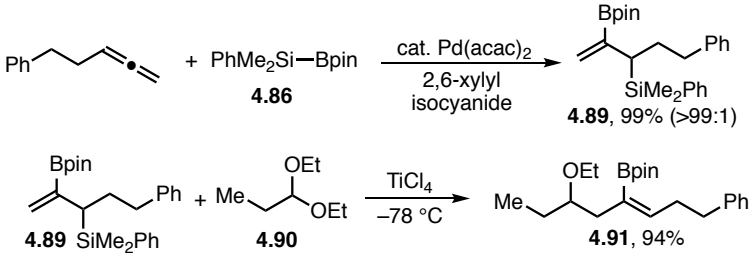

Figure 4.41 Formation of Alkenyl Boronic Esters *via* a Sakurai Reaction

This reaction can also be desymmetrized using a chiral silylborane with a chiral palladium catalysis (Figure 4.42).[55] With these conditions, a variety of alkenyl boronic esters can be synthesized with high diastereoselectivity. These products can also be utilized in an enantiospecific Sakurai reaction.

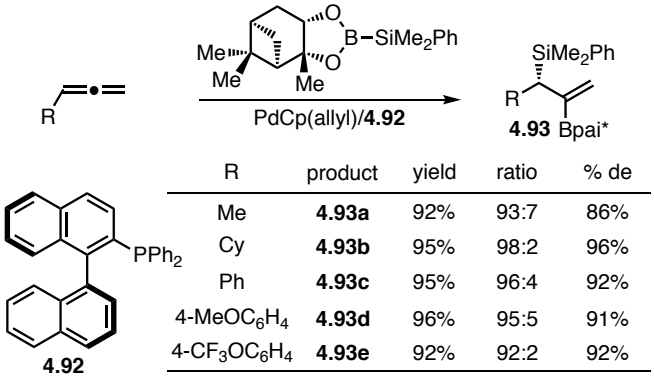

R	product	yield	ratio	% de
Me	**4.93a**	92%	93:7	86%
Cy	**4.93b**	95%	98:2	96%
Ph	**4.93c**	95%	96:4	92%
4-$MeOC_6H_4$	**4.93d**	96%	95:5	91%
4-$CF_3OC_6H_4$	**4.93e**	92%	92:2	92%

Figure 4.42 Suginome's and Murakami's Asymmetric Silylboration of Allenes

4.3.3.5 Borylstannylation of Alkynes

Another common approach for the synthesis of highly substituted alkenyl boronic esters is the borylstannylation of alkynes and subsequent Stille coupling. Typical borylstannylation reactions involve reagent **4.94** and proceed under transition-metal catalysis (Figure 4.43).[56]

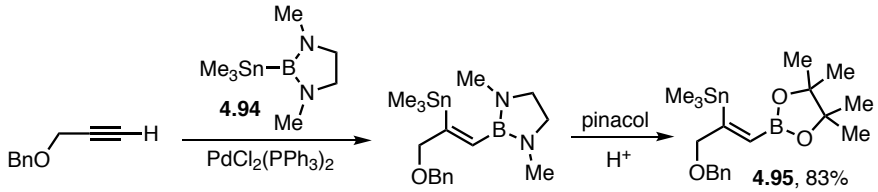

Figure 4.43 Palladium Catalyzed Borylstannylation of Alkynes

Recently, Yoshida reported with copper catalyzed borylstannylation of alkyne using B_2pin_2 and tributyltin fluoride.[57] Additionally, the other regioisomer is accessible with pinB-Bban and tributyltin methoxide forming the 1,8-diaminonapthyl boronic amide.[58] Takaki and Yoshida have demonstrated the borylstannylation, followed by Stille and Suzuki reactions in a 3-step synthesis of the tetrasubstituted, breast cancer treatment drug (*Z*)-tamoxifen (Figure 4.44, **4.99**).[59]

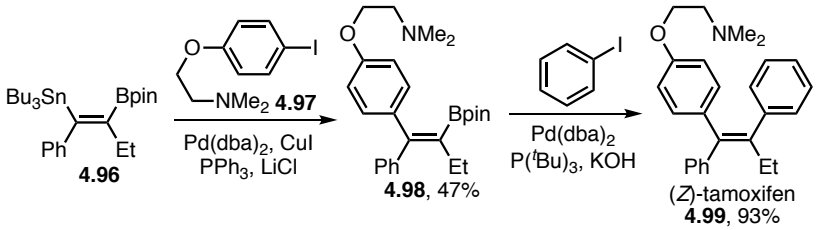

Figure 4.44 Takaki's and Yoshida's Synthesis of (*Z*)-Tamoxifen

4.3.4 Tandem Haloboration/Negishi Reactions

In 1964, Lappert reported the first example of the haloboration of alkynes.[60] This reaction is thermodynamically favored due to the high electronegativity of boron and the preference to be carbon-bound over halogen-bound. The products from this reaction have at least two functional handles that can be further functionalized. Suzuki was the first to recognize this bis-functionality with a tandem Negishi/Suzuki Reaction (Figure 4.45).[61] The haloboration of a terminal alkyne with BBr_3 forms compound **4.100**. **4.100** was then subjected to Negishi cross-coupling conditions (**4.101**) followed by the addition of base and an aryl halide to form and isolate **4.102**.

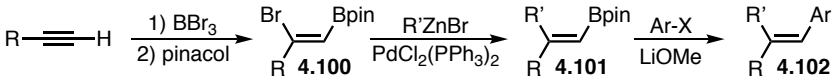

Figure 4.45 Haloboration with Tandem Negishi/Suzuki Reaction

4.3.4.1 Haloboration of Alkynes

Wang followed up on these initial findings and explored the Negishi cross-coupling of intermediate **4.100** with alkynyl zinc reagents.[62] The boronic esters synthesized from this method were converted to the vinyl iodides and again coupled with Negishi cross-coupling conditions. While the work from Wang was limited to alkynyl zinc reagents, it serves as a rapid and efficient method for the synthesis of elaborate enyne fragments.

Negishi discovered general conditions for the haloboration of propyne.[63] With the same sequence of steps, Negishi was able to synthesize methyl substituted (*Z*)-trisubstitued alkenes (Figure 4.46). These fragments are very prevalent in terpenoids and can be difficult to synthesize in a stereodefined manner.

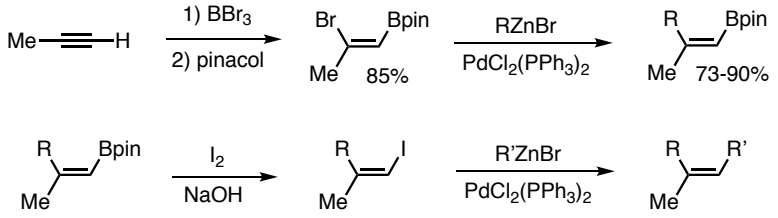

Figure 4.46 Negishi's Haloboration and Negishi Cross-Coupling of Propyne

4.3.4.2 Reactions of 1,1-Haloborylalkenes

A related approach involves the hydroboration of 1-halo-alkynes and subsequent Negishi cross-coupling.[64] This is an effective method for the synthesis of stereodefined

1,2-disubstituted alkenyl boronic esters. This method also demonstrates a wide functional group tolerance. Alkyl, aryl, vinyl and alkynyl zinc reagents were all tolerated with moderate to good yields (Figure 4.47).

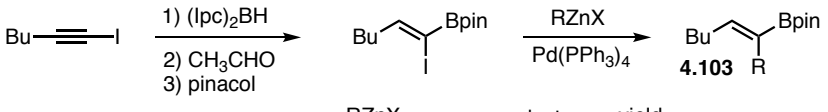

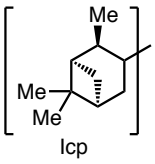

RZnX	product	yield
$PhCH_2ZnBr$	**4.103a**	62%
Me_3SiCH_2ZnI	**4.103b**	85%
PhZnCl	**4.103c**	87%
$Me_2C{=}CHZnCl$	**4.103d**	40%
$BuC{\equiv}CZnCl$	**4.103e**	67%

Figure 4.47 Scope of Zinc Reagents for the Formation of 1,2-Disubstituted Alkenyl Boronic Esters

In a related process, both Brown[65] and Suzuki[66] independently reported that alkyl lithium and Grignard reagents can directly react with α-halo-alkenyl boronic esters (Figure 4.48). Interestingly, this reaction results in inversion of the sp^2 center resulting in a *trans*-configuration for **4.104** which is complimentary to the above strategy. Intermediate **4.105** is thought to undergo a 1,2-shift of R' group expelling the bromide and causing the inversion. While this reaction is limited by the functional group tolerance of harsh organometallic reagents, the yields and selectivities are generally high.

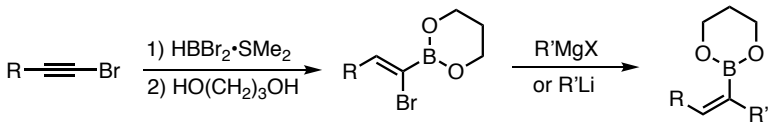

R	R'MgX or R'Li	product	yield
n-Bu	n-BuLi	**4.104a**	87%
n-hex	n-BuLi	**4.104b**	83%
Cy	MeLi	**4.104c**	77%
$Cl(CH_2)_3$	i-PrMgCl	**4.104d**	80%
n-Bu	EtMgBr	**4.104e**	79%
i-Pr	MeLi	**4.104f**	74%

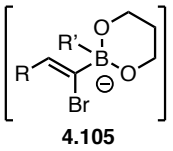

Figure 4.48 Nucleophilic Substitution on α-Halo-Alkenyl Boronic Esters

4.3.5 1,1-Borylmetallation of Alkynes

The above methods typically add a boron reagent across an unsaturated C-C bond. Due to the *syn*-nature of the addition this process tends to add boron in a *trans*-conformation to the original groups attached to the alkyne. On the contrary, if boron is already attached to the alkyne, then addition across it will result in a *cis*-conformation of boron and the other pre-attached group. Several groups have explored the hydrometallation of alkynyl boronic esters giving access to new and unique chemical compound entities.

4.3.5.1 Transition Metal Boron Complexes

In 1994, Srebnik reported the synthesis of the first stable 1,1-bismetalloalkene with boron and zirconium (Figure 4.49).[67] Using a method developed by Brown,[68] the 1-alkynyldioxaboralane (**4.106**) could be synthesized from mixing *tert*-butyl acetylene with *n*-butyl lithium and quenching with isopropoxypinacol borane. Hydrozirconation of **4.106** with Schwartz's reagent produces **4.107** in 82% isolated yield. X-ray analysis was used to confirm the structure and the *cis*-configuration of the zirconium and hydrogen atoms in complex **4.107**.

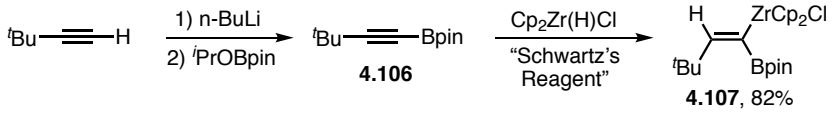

Figure 4.49 Srebnik's Synthesis of **4.107**

To demonstrate the versatility of this reagent, compound **4.107** was reacted with various electrophiles (Figure 4.50). A copper promoted conjugate addition of **4.107** with an enone provides **4.108** in 73% yield. Similarly, the reaction with acyl chlorides produces α-boryl enones **4.109** and **4.110** in good yields. Skipped diene **4.111** was synthesized from the reaction of **4.107** with allyl bromide in 87% yield. Additionally, when N-halosuccinimides are combined with **4.107** a variety of 1,1-haloboranes (**4.112a-c**) can be synthesize in excellent yields.

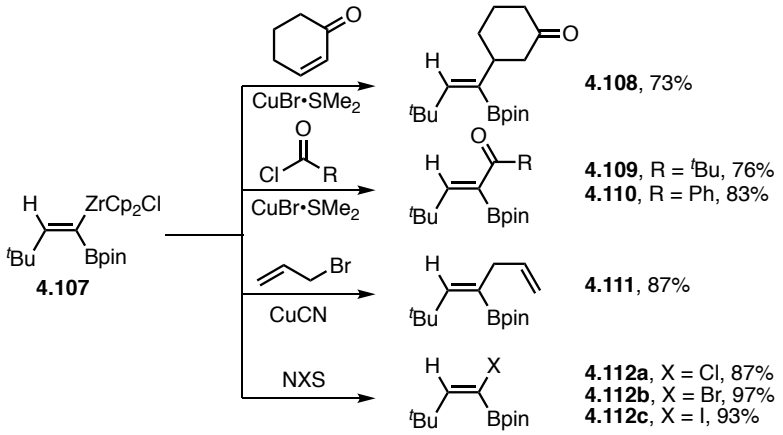

Figure 4.50 Reactivity of Srebnik's 1,1-Borylzirconium Reagent

While this method shows good reactivity and functional group tolerance, the use of stoichiometric Schwartz reagent would be impractical and prohibitively expensive on

a large scale. To circumvent this, Walsh explored the synthesis and reactivity of related reagents (Figure 4.51).[69] **4.115** can be synthesized by the hydroboration of 1-alkynyldioxaboralane **4.113** with dicyclohexylborane to form bis-borane **4.114**. Transmetallation with dimethyl zinc produces **4.115** with excellent stereoretention. The high stereochemistry is derived from the transmetallation rate difference between dialkyl borane and pinacol boronic esters. The transmetallation of dialkyl boranes proceeds even at very low temperatures,[70] however, boronic acid derivatives require high temperatures and prolonged reaction times (60 °C, 12 h) for transmetallation.[71] Furthermore, Walsh demonstrated the utility of this class of reagents by reacting **4.115** with many electrophiles including aldehydes and imines to get **4.116** and **4.117** respectively in good to excellent yields.[69a, 69c, 69f]

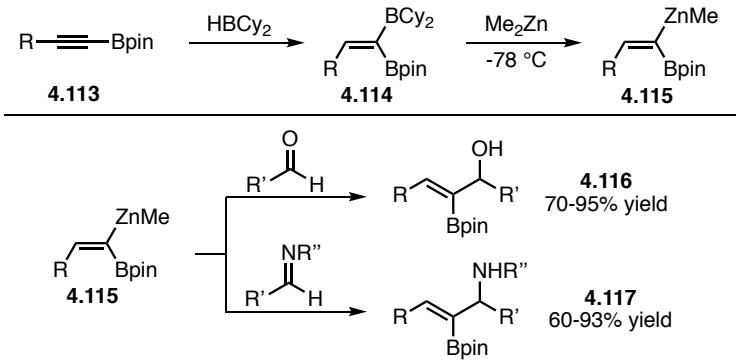

Figure 4.51 Synthesis and Reactivity of **4.115**

4.3.5.2 Diboronic Esters

Alternatively, symmetric alkenyl-1,1-diboronic esters, which can be synthesized in a variety of ways, can undergo a mono-Suzuki reaction to give rise to trisubstituted alkenyl boronic esters such as **4.118** (Figure 4.52).

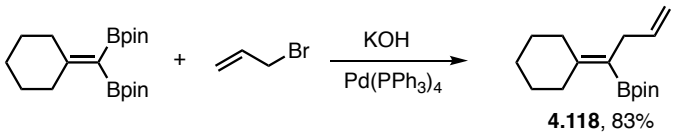

Figure 4.52 Mono-Cross-Coupling of 1,1-Bisboronic Esters

Chirk developed a cobalt catalyst (**4.119**) capable of converting terminal alkynes into differentially substituted 1,1-diboranes such as **4.120**.[72] The difference in reactivity between the two boron groups allows for a selective Suzuki reaction resulting in *Z*-disubstituted alkenyl boronic ester **4.121**. This two-step procedure represents a formal 1,1-carboboration of 1-heptyne.

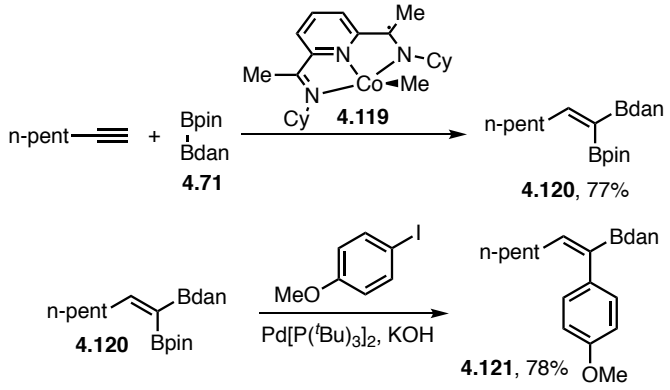

Figure 4.53 Chirk's Cobalt Catalyzed 1,1-Diboration of Terminal Alkynes

4.3.6 Alkene Cross-Metathesis

As discussed in Chapter 3, Section 3.3.4, metathesis provides a simple route to alkenyl boronic esters directly from alkenes. This approach works well for the synthesis of disubstituted alkenyl boronic esters, however, metathesis reactions show a significant decrease in yield when synthesizing trisubstituted alkenyl boronic esters (Figure 4.54).

Yields and selectivities drop even more when cross-coupling more functionalized alkenyl boronic esters (Figure 4.54, bottom). Additionally, an excess of the boronic ester coupling partner are required for even modest yields. While this method can be applied to the synthesis of trisubstituted products, this is not a synthetically reasonable approach.

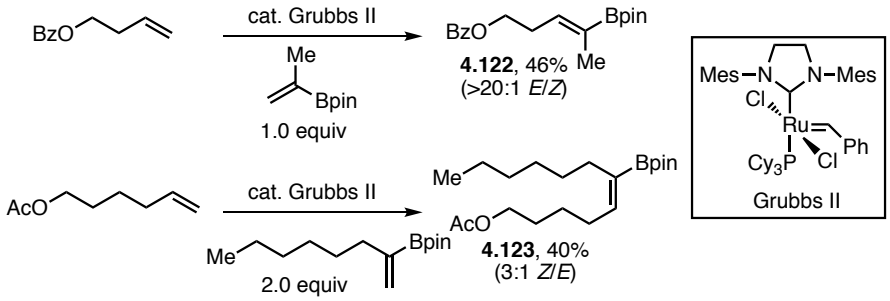

Figure 4.54 Synthesis of Trisubstituted Alkenyl Boronic Esters *via* Metathesis

4.3.7 Dehydrogenative Alkene Borylation

In many of the dehydrogenative borylation reactions discussed in Chapter 3, Section 3.3.5, examples of 1,1- and/or 1,2-disubstituted alkenes were shown to be viable substrates.[73] However, Marder[73a, 73b] demonstrated only four disubstituted alkene substrates in his reports and Iwasawa[73c, 73d] only reported five. Furthermore, both groups only demonstrated the simplest of disubstituted alkenes. For example, Marder only examined hydrocarbon and mostly symmetric 1,1-disubstituted alkenes (Figure 4.55). While this is a big step forward for this chemistry, a more general and functional group tolerant method is desired.

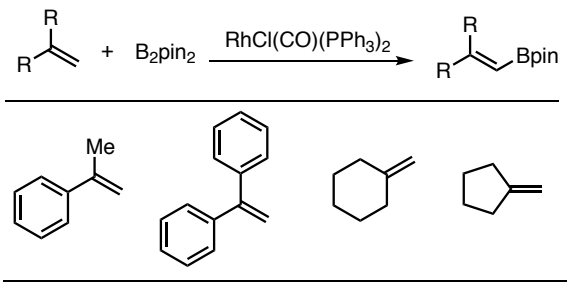

Figure 4.55 Marder's Limited Scope of Disubstituted Alkene Substrates

Recently, Ge reported an iron catalyzed borylation of vinyl arenes (Figure 4.56).[74] This method tolerates a variety of functionalized arenes but is strictly limited to α-substituted vinyl arenes and is not general among other alkenes.

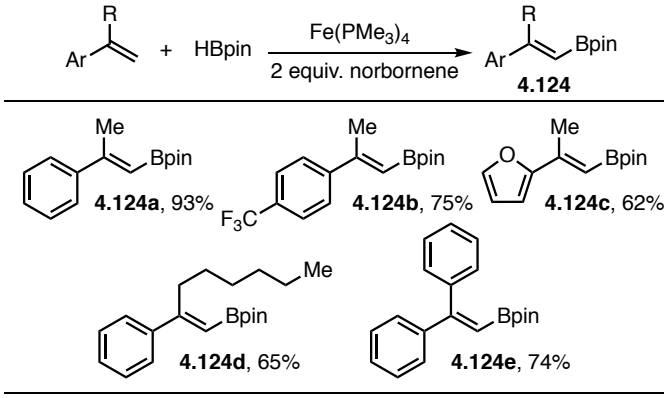

Figure 4.56 Selected Scope from Ge's Iron Catalyzed Dehydrogenative Borylation of α-Substituted Vinyl Arenes

4.3.8 Summary and Outlook

The majority of methods designed to synthesize highly substituted alkenyl boronic esters require prefunctionalized alkenes or alkynes are precursors which limit the utility of their approach. Additionally, many of these strategies require multiple

steps to add all the substituents in a stereodefined manner and require the use of harsh and reactive vinyl-metallic intermediates. The methods to synthesize trisubstituted alkenyl boronic esters directly from alkenes also suffer from poor reactivity, generality, and functional group tolerance.

4.4 Hypothesis and Development of Reaction Conditions

We thought that if we could extend our boryl-Heck reaction to tolerate more substitution on the alkene, then this could become a synthetically valuable method for the synthesis of highly substituted alkenyl bononic esters directly from alkenes. Additionally, we hoped to develop general set of conditions for synthesis of both 1,1- and 1,2-disubstituted alkenyl boronic esters from their respective alkene precursors.

Under the previous reaction conditions, terminal alkenes were well tolerated with excellent yields, regioselectivity and geometric selectivity. Vinyl cyclohexane reacted to from **4.125** in 84% isolated yield with a 96:4 *E*/*Z* ratio (Figure 4.57). Unfortunately, simply replacing one hydrogen atom with a methyl group at the α-position gave nothing more than trace yield (**4.126**).

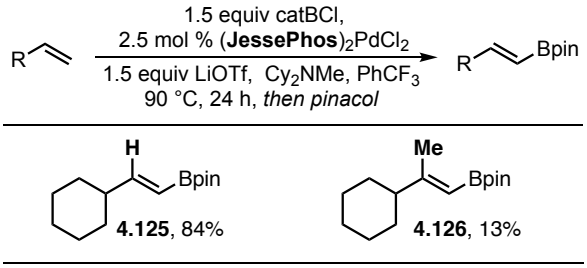

Figure 4.57 Reactivity Difference Mono- and Disubstituted Alkenes

To explain this limitation towards both 1,1- and 1,2-disubstituted alkenes, we hypothesize that the steric repulsion from the added groups on the alkene and the ligands on palladium strongly disfavors the migratory insertion transition state (Figure 4.58). A similar trend is observed in the Heck reaction, where reactivity drops off with increase alkenes substitution.[75] This issue may be overcome with an intramolecular cyclization similar to Suginome's work, however, we wanted to develop a more general bimolecular reaction. We hypothesized that lowering the coordination number on palladium by either lowering ligand to metal ratio or using a less coordinating X-type group from the boron electrophile, may allow for a more facile migratory insertion.

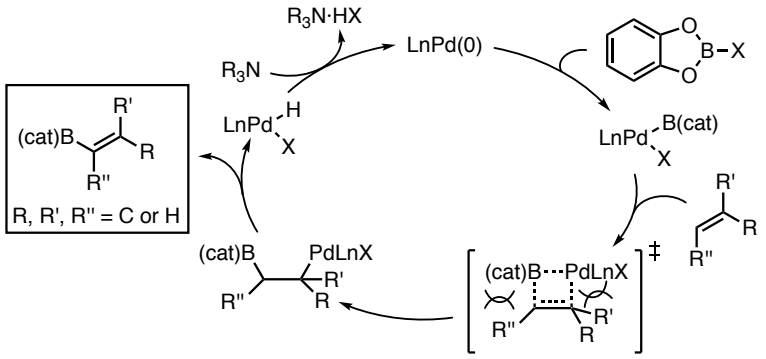

Figure 4.58 Proposed Boryl-Heck Reaction Pathway

4.4.1 Reaction Optimization

I decided to reinvestigated the reaction of **4.126** under modified reaction conditions. I began by exploring more mild and simple conditions than the first generation boryl-Heck (70 °C in the absence of LiOTf), and only observed 3% yield by ^{1}H NMR spectroscopy (Table 4.1, entry 1). Switching to the commercially available catBBr (entry 2), showed a significant increase in yield to 63% is observed with

minimal isomerization of **4.126**. In the absence of palladium there is no reactivity, ruling out the possibility of Lewis acid driven reaction (entry 3).

Table 4.1: Optimization of Reaction Conditions

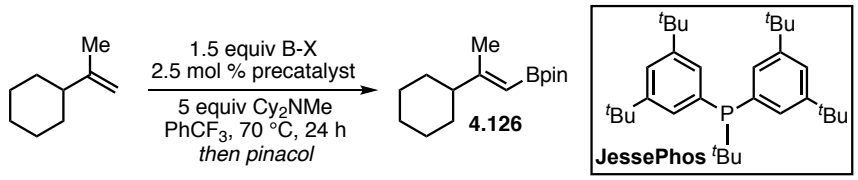

entry	B-X (equiv)	precatalyst	time (h)	isom. SM	**4.126**
1	catBCl (1.5)	(**JessePhos**)$_2$PdCl$_2$	24	0%	3%
2	catBBr (1.5)	(**JessePhos**)$_2$PdCl$_2$	24	2%	63%
3	catBBr (1.5)	none	24	0%	0%
4	catBBr (1.5)	(**JessePhos** PdI$_2$)$_2$	24	2%	95%
5	catBCl (1.5)	(**JessePhos** PdI$_2$)$_2$	24	12%	33%

Next, I examined a different single component catalyst which also contains palladium and **JessePhos**. Originally discovered as a possible intermediate in the silyl-Heck catalytic cycle,[76] complex (**JessePhos**PdI$_2$)$_2$ was used and 95% yield was observed with minimal starting material isomerization (entry 4). This dimer catalyst has an inherent ligand to metal ratio of 1:1. Comparing that to (**JessePhos**)$_2$PdCl$_2$ which has a ligand to metal ratio of 2:1, the lower ligand to metal ratio may result in a lower coordination number on palladium during that catalytic cycle. This may help to lower the transition state barrier for the migratory insertion step of the catalytic cycle. However, this catalyst did not produce reasonable yields in combination with catBCl (entry 5) which suggests a synergistic effect of both using a more electrophilic boron source and a lower ligand to metal ratio.

By slightly increasing the equivalents of catBBr, excellent yields were obtained with no starting material isomerization (Figure 4.59). Additionally, adding catBBr as a

solution in toluene (~2 M) allowed for the entire reaction set-up to be performed without the use of a glovebox.

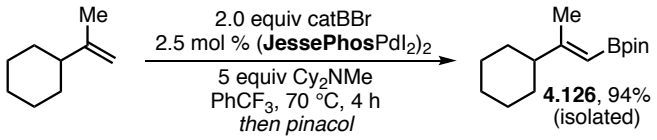

Figure 4.59 Optimal Conditions for the Boryl-Heck Reaction of 1,1-Disubstituted Alkenes

4.5 Exploration of Reaction Scope

With optimal conditions determined, I sought to explore the generality of these conditions by examining the functional group tolerance and limits. Additionally, to be more synthetically useful, this set of conditions is general for both 1,1- and 1,2-disubstituted alkenes.

4.5.1 1,1-Disubstituted Alkenyl Boronic Esters

First, I subjected a variety of 1,1-disubstituted alkenes to these reaction conditions to explore the generality of this reaction (Figure 4.60).

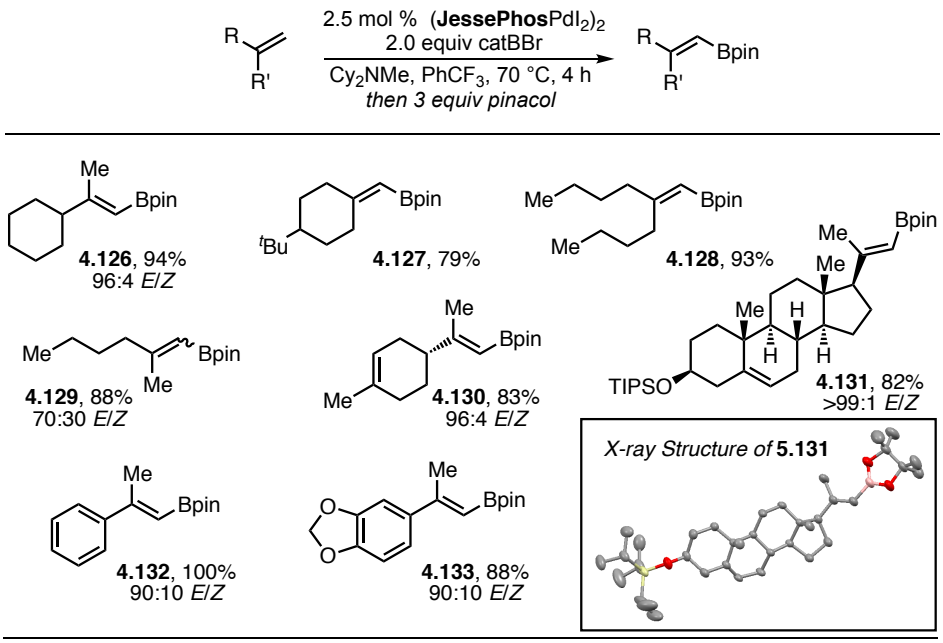

Figure 4.60 Scope of 1,1-Disubstituted Alkene Substrates

Compound **4.126** was isolated in 94% yield as the *E*-stereoisomer. Both exo-cyclic and acyclic symmetric alkenes gave excellent yields of single vinyl products **4.127** and **4.128** respectively. Non-symmetric alkenes such as 2-methylhexene provided an excellent yield but unfortunately proceeded with poor *E*/*Z* selectivity (**4.129**, ca. 2:1). Naturally derived products such as limonene (**4.130**) and a pregnenolone derivative (**4.131**) can be borylated with good yields and excellent *E*/*Z* selectivities demonstrating that these feedstock chemicals could be used as starting materials in total syntheses. Furthermore, an X-ray structure was obtained of **4.131** confirming the proposed *E*-alkene geometry. Under the first-generation conditions (Chapter 3), **4.132** was formed in only 70% yield. With the second-generation conditions, a quantitative yield of **4.132** can be obtained demonstrating the increased reactivity of these second-generation

conditions. Other styrene derived products such as heterocycle **4.133** gave and excellent yield and moderate *E*/*Z* selectivity.

4.5.2 1,2-Disubstituted Alkenyl Boronic Esters

Next, I examined several 1,2-disubstituted alkenes under the identical reaction conditions determined to be optimal for the 1,1-disubstituted alkenes and found that they are just as effective. Additionally, this presented the opportunity to further explore the functional group tolerance of this reaction (Figure 4.61).

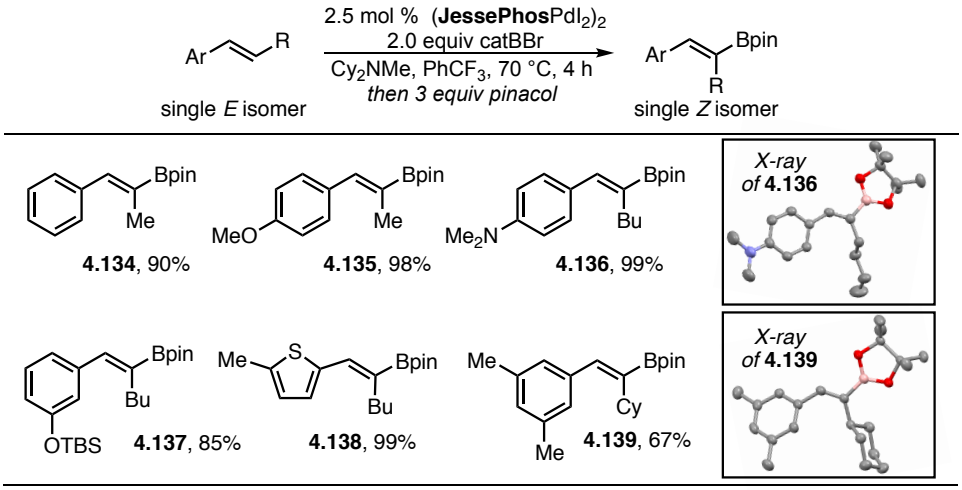

Figure 4.61 Scope of 1,2-Disubstituted Alkene Substrates

β-Methyl styrene can be isolated in 90% yield as a single *Z*-alkene isomer (**4.134**) which is a significant improvement over the 40% obtained with the first-generation conditions. Electron rich functional groups including anisoles (**4.135**) and anilines (**4.136**) gave quantitative yields. Electron withdrawing groups such as *meta*-silyl protected ether are also well tolerated with 85% yield (**4.137**). Thiophene

heterocycles are excellent substrates for this reaction providing a quantitative yield of **4.138**. In addition to the displayed functional group tolerance, β-substitution with methyl (**4.134**-**4.135**), butyl (**4.136**-**4.137**), and even cyclohexyl (**4.139**) groups is well tolerated all with good yields. In the case of **4.139**, the remaining mass balance was unreacted and non-isomerized starting material. Additionally, in every case, a single *Z*-isomer product is obtained from a single *E*-isomer of starting alkene.

Unfortunately, when 1,2-dialiphatic alkenes such as *trans*-2-octene were employed, numerous products were formed as an inseparable mixture (Figure 4.62). Gas chromatography analysis of the crude reaction mixture revealed more than 4 products with the mass of the intended product. Further optimization of this reaction, including a more selective catalyst, will be the subject of future investigations.

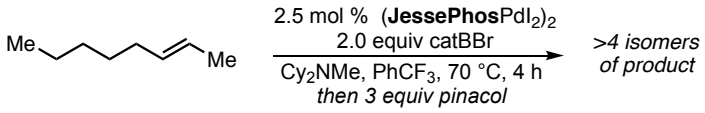

Figure 4.62 Borylation of 2-Butene

4.5.3 Tandem Boryl-Heck and Other Product Utilities

Alkenyl boronic esters are excellent substrates for the Suzuki reaction which converts C-B bonds into C-C bonds. As demonstrated in Chapter 3, the tandem boryl-Heck/Suzuki reaction provides a rapid and efficient route to stereodefined highly substituted alkenes. Now with access to disubstituted alkenyl boronic esters, this tandem reaction has the potential to synthesize stereodefined trisubstituted alkenes (Figure 4.63). Subjecting racemic limonene to the second-generation boryl-Heck reaction generates **4.140** *in situ*. The addition of 4-methoxyiodobenzene and $CsCO_3$

leads to trisubstituted alkene **4.141** in 92% isolate yield in 94% isomeric purity. Furthermore, the addition of trimethylamine N-oxide to the crude reaction mixture directly oxidizes **4.140** to **4.142** in 71% yield as a mixture of diastereomers.

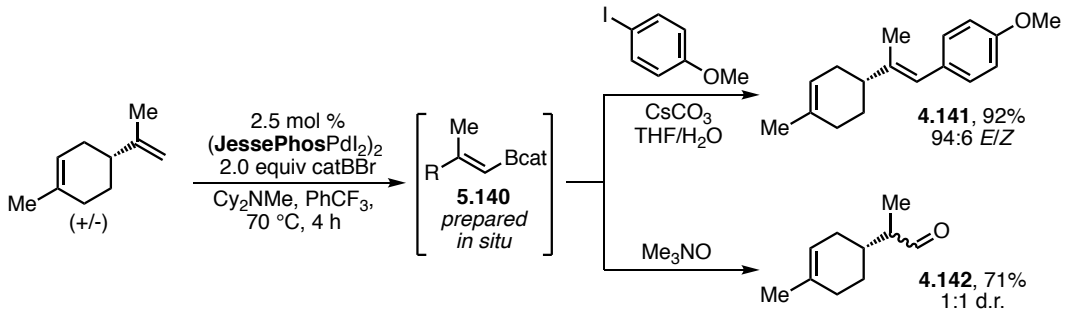

Figure 4.63 Tandem Boryl-Heck/Suzuki Reaction and Boryl-Heck/Oxidation

The stereodefined formation of C-O and C-X bonds is a difficult talk in organic chemistry. In addition to one-pot reactions demonstrated above, several 2-step procedures using the isolated products from this reaction can lead to new heteroatomic-carbon bonds with excellent stereochemistry (Figure 4.64).

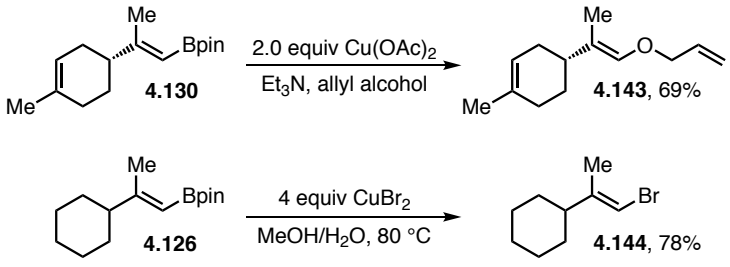

Figure 4.64 Synthetic Applications of Isolated Trisubstituted Alkenyl Boronic Esters

Using a procedure developed by Merlic,[77] allyl vinyl ether **4.143** was synthesized as a single stereoisomer in 69% yield. Compound **4.144** was synthesized in 78% yield using $CuBr_2$ as a brominating reagent.

4.6 Mechanistic Investigations

After exploring the scope and utility of this second-generation boryl-Heck reaction, I sought to further probe the mechanism by which it operates. We initially proposed a Heck-like mechanism but could not rule out other reaction pathways such as a C-H activation pathway. The observed inversion in alkene geometry when examining β-substituted alkenes is supportive of a Heck-like mechanism but not definitive. I carried out a series of mechanistic experiments to better understand the reaction mechanism.

4.6.1 Study of Alkene Geometry

To further probe this inversion of alkene geometry I examined the reaction of stilbene under these reaction conditions (Figure 4.65). When *trans*-stilbene was subjected to these reaction conditions the *Z*-isomer is the major product (**4.145**). This is consistent with all the other β-substituted styrenes and is indicative of a Heck-like reaction pathway. Both migratory insertion (**4.146**) and β-hydride elimination (**4.147**) are suprafacial processes (Figure 4.65, middle). Therefore, the borylpalladation, C-C bond rotation and β-hydride elimination should result in the *Z*-product **4.148**. By the same mechanistic hypothesis, *cis*-stilbene should result in the *E*-product **4.149**. When *cis*-stilbene is subjected to the same reaction conditions a 4:1 *E*/*Z* ratio is observed (Figure 4.65, bottom).

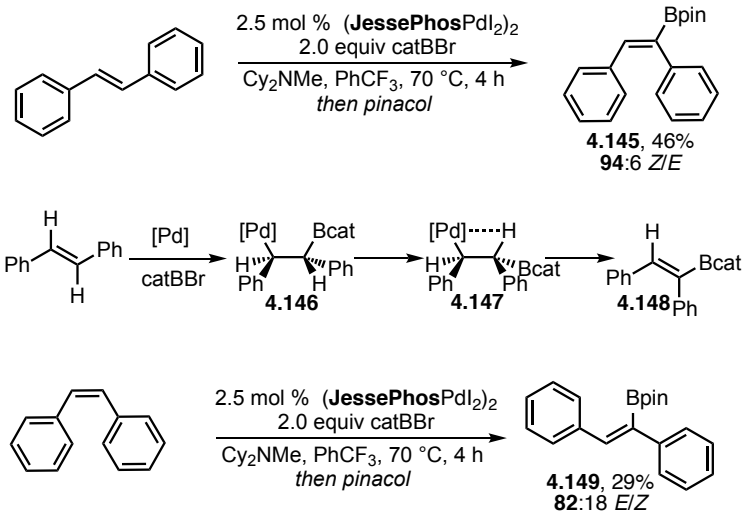

Figure 4.65 Inversion of Alkene Geometry During Reaction

Both results are supportive of a Heck-type mechanism and oppose a C-H activation pathway, which would result in opposite products. while these substrates are obligated to give vinyl product we next turned our attention to a system where the allyl product is possible.

4.6.2 Selectivity of Cyclohexene Reaction

Next, I chose to examine the borylation of cyclohexene *via* the boryl-Heck reaction (Figure 4.66). Cyclohexene is a particularly unique substrate. Both allyl and vinyl products exist (**4.150** and **4.151**), however, through our proposed mechanism, only the allyl product (**4.150**) should be formed. The migratory insertion of cyclohexene into the palladium-boron bond would result in intermediate **4.152**. Due to the geometric restrictions from the ring, H_v and palladium cannot properly align with a *syn*-periplanar geometry for β-hydride elimination. The palladium can only align with $H_{a'}$ for β-hydride elimination leading to the allylic product. However, non-traditional β-hydride

eliminations or post isomerization may result formation of the more stable vinyl product **4.151**.[73d, 78]

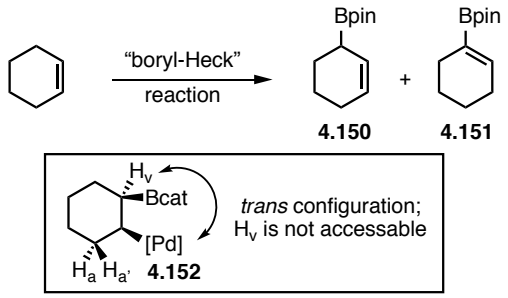

Figure 4.66 Geometric Constraints Associated with the Boryl-Heck Reaction of Cyclohexene

When we subjected cyclohexene to slightly modified boryl-Heck reaction conditions (100 °C) we observed almost exclusive formation of the allyl product **4.150** (Figure 4.67). The hydroboration product was formed in 8% (**4.152**) and only trace (4%) vinyl product was detected (**4.151**). The low yield is most likely a result of the high temperature required, leaving some unreacted cyclohexene in the vapor phase inside the reactor. Nonetheless, this result further supports our proposed Heck-type mechanism. More interestingly, this demonstrates that significant product isomerization does not occur, even at elevated reaction temperatures, which is contrary to our first-generation conditions.

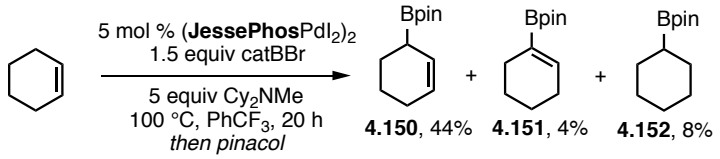

Figure 4.67 Boryl-Heck Reaction of Cyclohexene

This also demonstrates the second example of a rigged substrate leading to allylic products (the first being allyl benzene).[1] In the future, we hope to better harness this reaction to select for the allylic products.

4.6.3 Kinetic Nature of β-Hydride Elimination

With our first-generation conditions, we showed that the selective vinyl product formation is due to a thermodynamic equilibrium of product isomers funneling to the more stable vinyl boronic ester. similar to the first-generation conditions, we still only observe alkenyl product (except with cyclohexene). Therefore, we wanted to determine if the allylic product is kinetically accessible under normal reaction conditions.

Subjecting enantiopure limonene to these conditions, we hypothesized that the proposed alkyl palladium intermediate **4.153** could eliminate to give the vinyl product directly (**4.155**) or eliminate from one of the allylic protons (**4.154**) then funnel to the thermodynamic alkenyl product **4.155.** In the latter case, then we would expect observe racemization of the stereocenter in the isolated product.

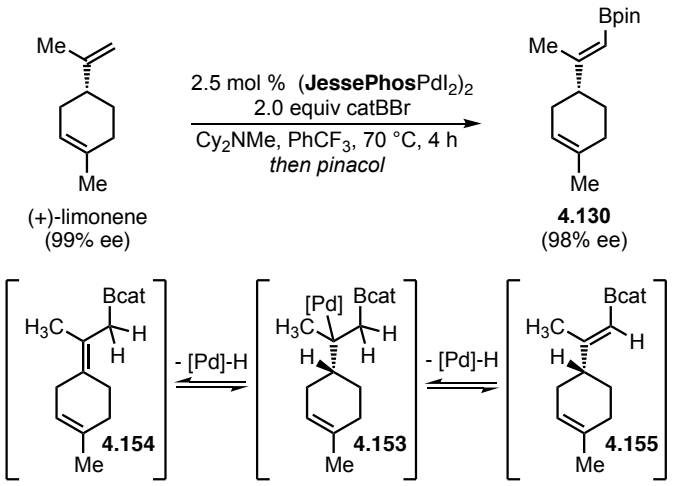

Figure 4.68 Retention of α-Stereocenter During Boryl-Heck Reaction

Upon examining the enantiomeric excess of **4.130**, no racemization of the allylic stereocenter occurred. This shows that intermediate **4.153** has a strong kinetic preference for β-hydride elimination of the vinylic proton. Therefore, formation of the alkenyl product is both thermodynamically and kinetically favored under our current reaction conditions.

4.7 Conclusion

In conclusion, I have developed new reaction conditions for the direct borylation of various disubstituted alkenes. Both 1,1- and 1,2-disubstituted alkenes are excellent substrates for these second-generation boryl-Heck conditions, proceeding with excellent yields and *E*/*Z* selectivities. The utility of these improved reaction conditions has been demonstrated with a tandem boryl-Heck/Suzuki reaction leading to a stereodefined trisubstituted olefin. Mechanistic studies have revealed that this reaction is stereospecific with respect to starting material and product alkene geometry which rules out a C-H activation mechanism and is highly suggestive of a Heck-like pathway.

Further support for a Heck-like mechanism was acquired from the near selective allyl boronic ester formation from cyclohexene. Subjecting enantiopure limonene to these reaction conditions revealed that β-hydride elimination of the vinylic hydrogen atom is kinetically preferred over the allylic hydrogen atom.

4.8 Experimental Details

4.8.1 General Experimental Details

Diethyl ether, tetrahydrofuran, toluene and dichloromethane were dried on alumina according to published procedures.[79] B-bromocatecholborane (catBBr) was purchased from TCI and either stored as a toluene solution in a nitrogen filled Strauss flask on the bench or stored as a solid in a nitrogen filled glovebox at -35 °C. N,N-Dicyclohexylmethylamine was purchased from TCI, distilled from calcium hydride (80 °C, 150 mtorr) and stored at rt on the bench in a nitrogen-filled Strauss flask. Trifluorotoluene was purchased from Sigma Aldrich in an anhydrous septum sealed bottle, transferred to a Straus flask by cannula transfer and sparged with nitrogen for 15 minutes. Bis(3,5-di-*tert*-butylphenyl)(*tert*-butyl)phosphine (JessePhos),[80] $(JessePhos)_2PdCl_2$,[1] and $[(JessePhos)PdI_2]_2$[76] were all prepared according to published procedures. All other substrates and reagents were purchased in highest analytical purity from commercial suppliers and used as received. Vials used in the glovebox were dried in a gravity oven at 140 °C for a minimum of 12 h, transferred into the glovebox hot, and then stored at rt in the glovebox prior to use. All other glassware was flame-dried under vacuum prior to use. "Double manifold" refers to a standard Schlenk-line gas manifold equipped with nitrogen and vacuum (ca. 100 mtorr). All optimization reactions (0.25 mmol) were run in a nitrogen-filled glovebox and heated using an

aluminum block on a magnetic stir plate. All yields in optimization reactions were determined using ^{1}H NMR using 1,3,5-trimethoxybenzene as an internal standard and *E*/*Z* ratios were determined using ^{1}H NMR of purified products and geometry was confirmed with nOe experiments. All other reactions were set up using standard Schlenk technique and heated with stirring in temperature controlled oil baths. Any product yields listed in the main text that do not match those listed in the supporting information are the average of multiple isolated yields. In most cases, only the major isomer is reported for the ^{1}H and ^{13}C NMR spectral data. The ^{13}C NMR spectra may contain extra, unassigned peaks, which we attribute to the minor isomer. **Note:** The ^{13}C NMR signal for carbons attached to boron did not appear in the collected spectra due to the quadruple splitting of ^{11}B.[81] NMR data for some compounds may be reported in two different solvents to resolve overlapped ^{13}C peaks.

4.8.2 Instrumentation and Chromatography

400 MHz ^{1}H, 101 MHz ^{13}C and 376 MHz ^{19}F spectra were obtained on a 400 MHz FT-NMR spectrometer equipped with a Bruker CryoPlatform. 600 MHz ^{1}H, 151 MHz ^{13}C, and 193 MHz ^{11}B spectra were obtained on a 600 MHz FT-NMR spectrometer equipped with a Bruker SMART probe. All samples were analyzed in the indicated deutero-solvent and were recorded at ambient temperatures. All chemical shifts are reported in ppm. ^{1}H NMR spectra were calibrated using the residual protio-signal in deutero-solvents as a standard. ^{13}C NMR spectra were calibrated using the deutero-solvent as a standard. IR spectra were recorded on a Nicolet Magma-IR 560 FT-IR spectrometer as thin films on KBr plates. High resolution MS data was obtained on a Thermo Q-Exactive Orbitrap using electrospray ionization (ESI), or a Waters GCT Premier spectrometer using chemical ionization (CI) or liquid injection field desorption

ionization (LIFDI). Column chromatography was performed with boric acid impregnated 40-63 μm silica gel[82] with the eluent reported in parentheses. Analytical thin-layer chromatography (TLC) was performed on pre-coated glass plates and visualized by UV or by staining with iodine or $KMnO_4$.

4.8.3 Synthesis of Non-Commercial Alkene Substrates

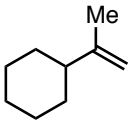

(**S4.1**) Under nitrogen atmosphere, methyl triphenylphosphonium bromide (21.87 g, 60 mmol, 2.0 equiv) and anhydrous THF (60 mL) were added to a 200 mL round bottom flask with stir bar, and the contents of the flask were sparged with a stream of N_2 for 10 minutes. The suspension was cooled to 0 °C, followed by anhydrous addition of t-BuOK (6.7 g, 60 mmol, 2.0 equiv) in one portion by quickly removing and replacing the septum. The resulting orange solution was allowed to stir at 0 °C for 1 hour, and then cyclohexylmethyl ketone (4.35 mL, 30 mmol, 1.0 equiv) was added in dropwise *via* syringe. The resulting yellow suspension was stirred for 16 hours, slowly warming to room temperature. TLC showed full conversion of starting material, so the reaction was poured into a 1 M HCl solution (20 mL), and extracted with diethyl ether (3 X 30 mL). The organic layer was dried with $MgSO_4$, filtered through Celite and concentrated *in vacuo*. The crude material was purified *via* silica column chromatography (pentane) to afford **S4.1** as a colorless liquid (2.53 g, 68%): ^{1}H NMR (600 MHz, $CDCl_3$) δ 4.66 (s, 2H), 1.86 (tt, *J* = 11.6, 3.2 Hz, 1H), 1.79 – 1.72 (m, 4H), 1.71 (s, 3H), 1.67 (d, *J* = 12.8 Hz, 1H), 1.27 (qt, *J* = 13.5, 3.6 Hz, 2H), 1.21 – 1.10 (m, 3H); ^{13}C NMR (101 MHz, $CDCl_3$) δ 151.5, 107.9, 45.7, 32.1, 26.8, 26.5, 21.1; FTIR (cm^{-1}): 2928, 2853, 1644, 1449, 1374, 885. HRMS (CI) m/z, calcd for $[C_9H_{17}]^+$: 125.1330; found: 125.1338.

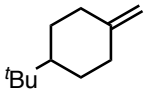

(**S4.2**) Under nitrogen atmosphere, methyl triphenylphosphonium bromide (16.4 g, 45 mmol, 1.5 equiv) and anhydrous diethyl ether (120 mL) were added to a 250 mL round bottom flask with stir bar, and the contents of the flask were sparged with a stream of N_2 for 10 minutes. The suspension was cooled to 0 °C, followed by anhydrous addition of t-BuOK (5.1 g, 45 mmol, 1.5 equiv) in one portion by quickly removing and replacing the septum. The resulting orange solution was allowed to stir at 0 °C for 15 min, and then 4-*tert*-butyl cyclohexanone (4.67 g, 30 mmol, 1.0 equiv) was added in one portion via syringe. The resulting yellow suspension was refluxed for 2.5 hours. TLC showed full conversion of starting material, so the reaction was poured into a water (100 mL), and extracted with diethyl ether (3 X 50 mL). The organic layer was dried with $MgSO_4$, filtered through Celite and concentrated *in vacuo*. The crude material was purified *via* distillation (56 °C, 8 torr) to afford **S4.2** as a colorless liquid (3.86 g, 84%): ^{1}H NMR (600 MHz, $CDCl_3$) δ 4.58 (t, J = 1.8 Hz, 2H), 2.33 (dp, J = 13.7, 1.9 Hz, 2H), 2.06 – 1.95 (m, 2H), 1.91 – 1.81 (m, 2H), 1.15 (tt, J = 11.8, 2.9 Hz, 1H), 1.10 – 1.00 (m, 2H), 0.86 (s, 9H); ^{13}C NMR (151 MHz, $CDCl_3$) δ 150.4, 106.2, 48.1, 35.5, 32.6, 29.1, 27.8; FTIR (cm^{-1}): 2943, 2867, 2838, 1651, 1365, 886. HRMS (CI) m/z, calcd for $[C_{11}H_{21}]^+$: 153.1643; found: 153.1647.

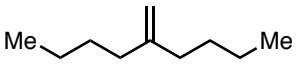

(**S4.3**) Under nitrogen atmosphere, methyl triphenylphosphonium bromide (12.7 g, 35.5 mmol, 1.2 equiv) and anhydrous THF (250 mL) were added to a 500 mL round bottom flask with stir bar, and the contents of the flask were sparged with a stream of N_2 for 10 minutes. The suspension was cooled to 0 °C, followed by addition of n-BuLi (12.0 mL, 2.72 M, 32.5 mmol, 1.1 equiv) in one portion *via* syringe. The resulting orange solution was allowed

to stir at 0 °C for 30 min, and then 5-nonanone (5 mL, 29.6 mmol, 1 equiv) was added dropwise *via* syringe. The resulting yellow suspension was stirred for 16 hours, slowly warming to room temperature. TLC showed full conversion of starting material, so the reaction was poured into a water (100 mL), and extracted with diethyl ether (3 X 50 mL). The organic layer was dried with $MgSO_4$, filtered through Celite and concentrated *in vacuo*. The crude material was purified *via* distillation (65 °C, 20 torr) to afford **S4.3** as a colorless liquid (1.11 g, 27%): ^{1}H NMR (600 MHz, $CDCl_3$) δ 4.66 (s, 2H), 2.03 – 1.92 (m, 4H), 1.42 – 1.34 (m, 4H), 1.33 – 1.20 (m, 4H), 0.88 (t, J = 7.3 Hz, 6H); ^{13}C NMR (151 MHz, $CDCl_3$) δ 150.9, 108.5, 35.9, 30.2, 22.7, 14.2; FTIR (cm^{-1}): 2959, 2930, 2873, 1644, 1467, 1379, 887. HRMS (CI) m/z, calcd for $[C_{10}H_{21}]^+$: 141.1643; found: 141.1642.

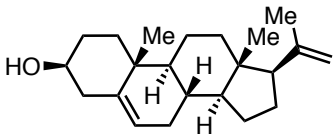

(S4.4) Under nitrogen atmosphere, methyl triphenylphosphonium bromide (35.72 g, 100 mmol, 2.5 equiv) and anhydrous THF (80 mL) were added to a 250 mL round bottom flask with stir bar, and the contents of the flask were sparged with a stream of N_2 for 10 minutes. The suspension was cooled to 0 °C, followed by anhydrous addition of t-BuOK (10.77 g, 96 mmol, 2.4 equiv) in one portion by quickly removing and replacing the septum. The resulting orange solution was allowed to stir at 0 °C for 1 hour, and then pregenolone (12.66 g, 40 mmol, 1.0 equiv) was dissolved in anhydrous THF and added dropwise *via* syringe. The resulting yellow suspension was stirred for 16 hours, slowly warming to room temperature. TLC showed full conversion of starting material, so the reaction was poured into a water (100 mL), and extracted with diethyl ether (3 X 30 mL). The organic layer was dried with $MgSO_4$, filtered through Celite and

concentrated *in vacuo*. The crude material was purified *via* silica column chromatography (1 : 4 ethyl acetate : hexanes) to afford **S4.4** as a white solid (12.14 g, 97%): ^{1}H NMR (400 MHz, $CDCl_3$) δ 5.41 – 5.30 (m, 1H), 4.82 (s, 1H), 4.69 (s, 1H), 3.62 – 3.41 (m, 1H), 2.40 – 2.15 (m, 2H), 2.07 – 1.92 (m, 2H), 1.91 – 1.76 (m, 4H), 1.74 (d, *J* = 1.6 Hz, 3H), 1.71 – 1.62 (m, 2H), 1.60 – 1.38 (m, 6H), 1.29 – 1.02 (m, 4H), 0.99 (s, 3H), 0.97 – 0.90 (m, 1H), 0.56 (s, 3H); ^{13}C NMR (101 MHz, $CDCl_3$) δ 145.8, 140.9, 121.8, 110.8, 71.9, 57.4, 56.6, 50.4, 43.2, 42.4, 38.8, 37.4, 36.7, 32.3, 32.0, 31.8, 25.5, 24.8, 24.4, 21.3, 19.6, 12.8; FTIR (cm^{-1}): 2933, 1062, 886, 668; mp = 133-135 °C. HRMS (ESI) m/z, calcd for $[C_{22}H_{33}]^{+}$: 297.2577; found: 297.2566. (M – OH)

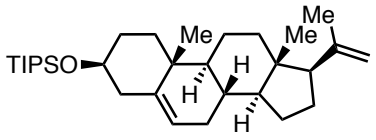

(**S4.5**) A 100 mL round bottom flask equipped with a magnetic stir bar and rubber septum was charged with imidizole (2.7 g, 40 mmol, 2.0 equiv), dichloromethane (20 mL), DMF (20 mL), and **S4.4** (6.22 g, 20 mmol, 1.0 equiv) and sealed under air. Triisopropylchlorosilane (5.5 mL, 25 mmol, 1.3 equiv) was then added dropwise *via* syringe and the reaction was stirred for 48 h at room temperature. The reaction was opened, quenched with water (20 mL), and extracted with dichloromethane (3 x 20 mL). The combined organic layers were washed with sat. $NaHCO_3$ (10 mL), water (10 mL), and brine (10 mL), then dried with $MgSO_4$, filtered through Celite, and concentrated *in vacuo*. The crude solid was recrystallized from hot *iso*-propanol to afforded **S4.5** as white solid (7.92 g, 85%): ^{1}H NMR (400 MHz, $CDCl_3$) δ 5.29 (d, *J* = 4.6 Hz, 1H), 4.82 (s, 1H), 4.69 (s, 1H), 3.63 – 3.43 (m, 1H), 2.35 – 2.17 (m, 2H), 2.09 – 1.91 (m, 2H), 1.91 – 1.75 (m, 4H), 1.73 (s, 3H), 1.66 (ddt, *J* = 11.5, 6.5, 3.7 Hz, 2H), 1.61 – 1.37 (m, 5H), 1.25 – 1.13 (m, 2H), 1.13 – 1.00 (m, 23H), 0.99 (s, 3H), 0.92 (ddd,

J = 12.2, 10.7, 4.9 Hz, 1H), 0.56 (s, 3H); ^{13}C NMR (101 MHz, $CDCl_3$) δ 145.9, 141.8, 121.1, 110.8, 72.6, 57.4, 56.7, 50.5, 43.2, 38.8, 37.6, 36.8, 32.5, 32.4, 32.0, 25.5, 24.8, 24.4, 21.3, 19.7, 18.3, 12.8, 12.5; FTIR (cm^{-1}): 2940, 1384, 1105, 884; mp = 96-98 °C. HRMS (ESI) m/z, calcd for $[C_{31}H_{55}SiO]^+$: 471.4017; found: 471.4001.

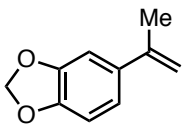

(**S4.6**) Under nitrogen atmosphere, 3′,4′-(Methylenedioxy)acetophenone (5.02 g, 30 mmol, 1.0 equiv) and anhydrous THF (30 mL) were added to a 100 mL round bottom flask with stir bar. The solution was cooled to 0 °C, followed by dropwise addition of MeMgCl (12 mL, 3.0 M, 36 mmol, 1.2 equiv). The suspension was stirred for 16 hours, slowly warming to room temperature. The solution was again cooled to 0 °C slowly quenched with sat. aqueous NH_4Cl (10 mL) and washed with 1M HCl (10 mL). The organic layer was dried with $MgSO_4$, filtered through Celite and concentrated *in vacuo*. The crude material dissolved in anhydrous diethyl ether (30 mL) and dry HCl (30 mL, 2 M in diethyl ether) was added and the reaction was stirred for 15 minutes at room temperature. The solution was cooled to 0 °C, slowly quenched with sat. aqueous $NaHCO_3$ (10 mL) and extracted with diethyl ether (3 X 30 mL). The organic layer was dried with $MgSO_4$, filtered through Celite and concentrated *in vacuo*. The crude material was purified *via* silica column chromatography (1 : 49 ethyl acetate : hexanes) to afford **S4.6** as a colorless oil (2.4 g, 49%): ^{1}H NMR (600 MHz, $CDCl_3$) δ 6.96 (d, J = 1.8 Hz, 1H), 6.92 (dd, J = 8.1, 1.8 Hz, 1H), 6.75 (d, J = 8.1 Hz, 1H), 5.93 (s, 2H), 5.23 (s, 1H), 5.03 – 4.91 (m, 1H), 2.09 (s, 3H); ^{13}C NMR (151 MHz, $CDCl_3$) δ 147.9, 147.2, 142.9, 135.9, 119.3, 111.4, 108.0, 106.3, 101.1, 22.2; FTIR (cm^{-1}): 1503, 1491, 1444,

1230, 1040, 935, 886, 812. HRMS (CI) m/z, calcd for $[C_{10}H_{10}O]$: 162.0681; found: 162.0680.

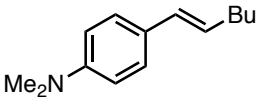

(**S4.7**) Under nitrogen atmosphere, 4-bromo-dimethylaniline (1.0 g, 5.0 mmol, 1.0 equiv), $(JessePhos)_2PdCl_2$ (270 mg, 5 mol %) and $CsCO_3$ (4.07 g, 12.5 mmol, 2.5 equiv) were added to a dry 50 mL Schlenk flask equipped with a magnetic stir bar. The flask was sealed with a rubber septum and evacuated and refilled with nitrogen 3 times. A mixture of THF:water (10:1, 20 mL) was added *via* syringe. (*E*)-1-hexenyl-catecholborane (2.0 g, 10 mmol, 2.0 equiv) was added *via* syringe and the solution was stirred in an oil bath at 70 °C for 2 h. At that time, the reaction was diluted with diethyl ether (20 mL), stirred for 10 min, and filtered through Celite. The crude solution was washed with water (10 mL) and brine (10 mL). The organic layer was dried with $MgSO_4$, filtered through Celite and concentrated *in vacuo*. The crude material was purified via silica column chromatography (1 : 9 dichloromethane : hexanes) to afford **S4.7** as a yellow oil (1.01 g, 100%): ^{1}H NMR (600 MHz, $CDCl_3$) δ 7.31 (d, 2H), 6.76 (d, 2H), 6.37 (d, J = 15.8 Hz, 1H), 6.10 (dt, J = 15.7, 6.9 Hz, 1H), 3.01 (s, 6H), 2.25 (q, 2H), 1.55 – 1.47 (m, 2H), 1.47 – 1.40 (m, 2H), 0.99 (t, J = 7.2 Hz, 3H); ^{13}C NMR (151 MHz, $CDCl_3$) δ 149.9, 129.6, 127.2, 127.0, 126.9, 112.9, 40.8, 32.9, 32.0, 22.4, 14.1; FTIR (cm^{-1}): 2955, 2924, 1611, 1521, 1350, 1164, 962, 803. HRMS (CI) m/z, calcd for $[C_{14}H_{22}N]^+$: 204.1752; found: 204.1749.

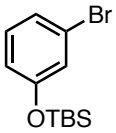

(**S4.8**) A 100 mL round bottom flask equipped with a magnetic stir bar and rubber septum was charged with imidizole (1.5 mg, 22 mmol, 1.1 equiv), dichloromethane (40 mL), and 3-bromophenol (3.46 g, 25 mmol, 1.0 equiv)

and sealed under air. A solution of *tert*-butyldimethylchlorosilane (3.31 g, 22 mmol, 1.1 equiv) in dichloromethane was then added dropwise *via* syringe and the reaction was stirred for 24 h at room temperature. The reaction was opened, quenched with water (10 mL), and extracted with dichloromethane (2 x 20 mL). The combined organic layers were washed with water (10 mL) and brine (10 mL), then dried with $MgSO_4$, filtered through Celite, and concentrated *in vacuo*. The crude oil was purified by flash silica gel chromatography (2 : 98 ethyl acetate : hexanes) to afforded **S4.8** as a colorless oil (5.67 g, 99%): ^{1}H NMR (400 MHz, $CDCl_3$) δ 7.09 – 7.05 (m, 2H), 7.00 – 6.96 (m, 1H), 6.78 – 6.70 (m, 1H), 0.96 (s, 9H), 0.18 (s, 6H); ^{13}C NMR (101 MHz, $CDCl_3$) δ 156.6, 130.6, 124.6, 123.6, 122.6, 119.0, 25.7, 18.3, -4.3; FTIR (cm^{-1}): 2930, 2859, 1590, 1474, 1270, 1239, 932, 827, 782, 682. HRMS (CI) m/z, calcd for $[C_{12}H_{20}OSiBr]^+$: 287.0467; found: 287.0464.

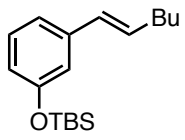

(**S4.9**) Under nitrogen atmosphere, $(JessePhos)_2PdCl_2$ (250 mg, 2.5 mol %) and $CsCO_3$ (8.14 g, 25 mmol, 2.5 equiv) were added to a dry 100 mL Schlenk flask equipped with a magnetic stir bar. The flask was sealed with a rubber septum and evacuated and refilled with nitrogen 3 times. A mixture of THF:water (10:1, 66 mL) was added via syringe followed by **S4.8** (2.87 g, 10 mmol, 1.0 equiv). (*E*)-1-hexenyl-catecholborane (4.04 mL, 20 mmol, 2.0 equiv) was added *via* syringe and the solution was stirred in an oil bath at 70 °C for 2 h. At that time, the reaction was diluted with diethyl ether (30 mL), stirred for 10 min, and filtered through Celite. The crude solution was washed with water (10 mL) and brine (10 mL). The organic layer was dried with $MgSO_4$, filtered through Celite and concentrated *in vacuo*. The crude material was purified *via* silica column chromatography (hexanes) to afford

S4.9 as a colorless oil (2.77 g, 96%): ^{1}H NMR (400 MHz, $CDCl_3$) δ 7.12 (t, *J* = 7.8 Hz, 1H), 6.92 (d, *J* = 7.7 Hz, 1H), 6.79 (t, *J* = 2.0 Hz, 1H), 6.65 (ddd, *J* = 8.1, 2.4, 1.0 Hz, 1H), 6.29 (dt, *J* = 15.7, 1.3 Hz, 1H), 6.17 (dt, *J* = 15.7, 6.8 Hz, 1H), 2.17 (q, 2H), 1.51 – 1.39 (m, 2H), 1.38 – 1.28 (m, 2H), 0.97 (s, 9H), 0.90 (t, *J* = 7.2 Hz, 3H), 0.18 (s, 6H); ^{13}C NMR (101 MHz, $CDCl_3$) δ 155.9, 139.6, 131.4, 129.6, 129.4, 119.2, 118.6, 117.6, 32.9, 31.6, 25.9, 22.4, 18.4, 14.1, -4.2; FTIR (cm^{-1}): 2957, 2929, 2858, 1598, 1579, 1279, 1157, 967, 854, 781. HRMS (CI) m/z, calcd for $[C_{18}H_{31}OSi]^+$: 291.2144; found: 291.2132.

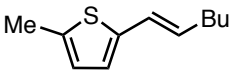

(**S4.10**) Under nitrogen atmosphere, $(JessePhos)_2PdCl_2$ (250 mg, 2.5 mol %) and $CsCO_3$ (8.14 g, 25 mmol, 2.5 equiv) were added to a dry 100 mL Schlenk flask equipped with a magnetic stir bar. The flask was sealed with a rubber septum and evacuated and refilled with nitrogen 3 times. A mixture of THF:water (10:1, 66 mL) was added via syringe followed by 2-iodo-5-methyl thiophene (1.2 mL, 10 mmol, 1.0 equiv). (*E*)-1-hexenyl-catecholborane (4.04 mL, 20 mmol, 2.0 equiv) was added *via* syringe and the solution was stirred in an oil bath at 70 °C for 2 h. At that time, the reaction was diluted with diethyl ether (30 mL), stirred for 10 min, and filtered through Celite. The crude solution was washed with water (10 mL) and brine (10 mL). The organic layer was dried with $MgSO_4$, filtered through Celite and concentrated *in vacuo*. The crude material was purified via silica column chromatography (hexanes) to afford **S4.10** as a colorless oil (1.40 g, 78%): ^{1}H NMR (400 MHz, $CDCl_3$) δ 6.60 (d, *J* = 3.4 Hz, 1H), 6.54 (dq, *J* = 3.5, 1.1 Hz, 1H), 6.39 (dt, *J* = 15.6, 1.6 Hz, 1H), 5.90 (dt, *J* = 15.6, 7.0 Hz, 1H), 2.41 (s, 3H), 2.12 (qd, *J* = 7.1, 1.5 Hz, 2H), 1.48 – 1.27 (m, 4H), 0.89 (t, *J* = 7.2 Hz, 3H); ^{13}C NMR (101 MHz, $CDCl_3$) δ

141.3, 137.8, 130.1, 125.3, 124.3, 123.4, 32.6, 31.6, 22.4, 15.7, 14.1; FTIR (cm^{-1}): 2924, 1384, 952, 792. HRMS (CI) m/z, calcd for $[C_{11}H_{17}S]^+$: 181.1051; found: 181.1047.

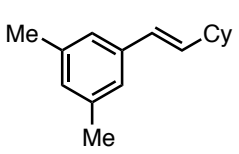

(**S4.11**) Under nitrogen atmosphere, $(JessePhos)_2PdCl_2$ (250 mg, 2.5 mol %) and $CsCO_3$ (7.17 g, 22 mmol, 2.5 equiv) were added to a dry 100 mL Schlenk flask equipped with a magnetic stir bar. The flask was sealed with a rubber septum and evacuated and refilled with nitrogen 3 times. A mixture of THF:water (10:1, 66 mL) was added via syringe followed by 5-bromo-*meta*-xylenes (1.64 g, 8.8 mmol, 1.0 equiv). (*E*)-1-vinyl-2-cyclohexyl-catecholborane (4.25 mL, 18.6 mmol, 2.1 equiv) was added *via* syringe and the solution was stirred in an oil bath at 70 °C for 3 h. At that time, the reaction was diluted with diethyl ether (30 mL), stirred for 10 min, and filtered through Celite. The crude solution was washed with water (10 mL) and brine (10 mL). The organic layer was dried with $MgSO_4$, filtered through Celite and concentrated *in vacuo*. The crude material was purified via silica column chromatography (hexanes) to afford **S4.11** as a pale yellow oil (818 mg, 44%): ^1H NMR (600 MHz, $CDCl_3$) δ 6.95 (s, 2H), 6.81 (s, 1H), 6.26 (d, 1H), 6.12 (dd, *J* = 15.9, 7.0 Hz, 1H), 2.27 (s, 6H), 2.16 – 2.03 (m, 1H), 1.82 – 1.69 (m, 4H), 1.68 – 1.59 (m, 1H), 1.29 (dddd, *J* = 16.1, 12.7, 8.2, 3.4 Hz, 2H), 1.22 – 1.09 (m, 3H); ^{13}C NMR (151 MHz, $CDCl_3$) δ 138.1, 138.0, 136.6, 128.6, 127.4, 124.0, 41.3, 33.2, 26.4, 26.2, 21.4; FTIR (cm^{-1}): 2923, 2850, 1601, 1448, 964. HRMS (CI) m/z, calcd for $[C_{15}H_{19}]^+$: 214.1722; found: 214.1724.

4.8.4 Preparation and Titration of CatBBr Solution

Preparation: Under nitrogen atmosphere, B-bromocatecholborane (5.96 g, 30 mmol) was quickly added to a dry 50 mL Schlenk flask equipped with a magnetic stir

bar. The flask was sealed with a rubber septum and evacuated and refilled with nitrogen 3 times. Anhydrous toluene (10-15 mL) was added *via* syringe and the solution was stirred under a nitrogen atmosphere until all of the catBBr was dissolved. The solution was transferred into a nitrogen-filled 15 mL Strauss flask by cannula transfer and stored at room temperature under a nitrogen atmosphere.

Titration: Under a nitrogen atmosphere trimethoxybenzene (28 mg) was weighed into a 1-dram vial and dissolved in ~2 mL anhydrous $CDCl_3$. A solution of catBBr in toluene (prepared above, 250 µL) and Cy_2NMe (250 µL) were added *via* syringe. The solution was mixed and directly examined by ^1H NMR in a septum sealed NMR tube. The direct ratio of either catechol peak (6.95 and 6.86 ppm) to the $C(sp^2)$-H peak of trimethoxybenzene (6.15 ppm) is the effective concentration of catBBr in toluene (Figure 4.69).

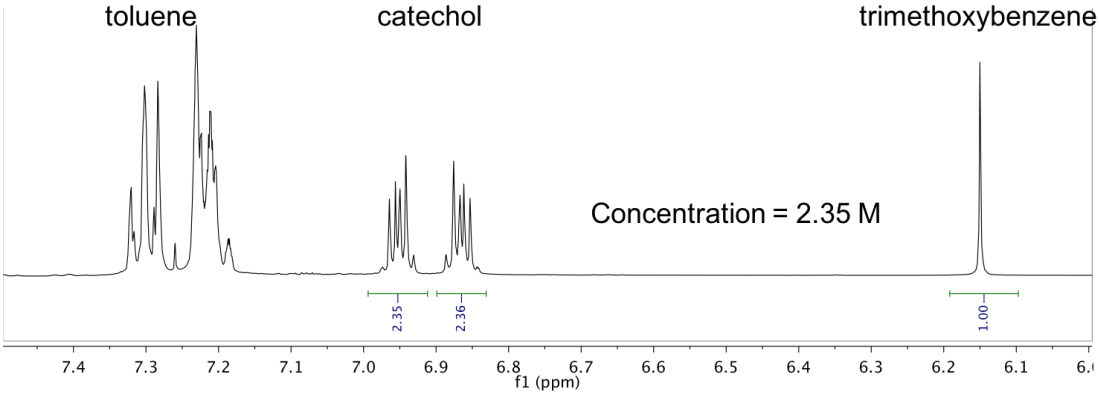

Figure 4.69 Sample NMR of Used to Calculate Concentration

4.8.5 Procedure for the Boryl-Heck Reaction

Note: All reactions in this section were performed on a 1 mmol scale using double manifold technique.

4.8.5.1 General Procedure

[(JessePhos)PdI_2]$_2$ (41 mg, 5 mol %) was added to a dry 10 mL Schlenk flask equipped with a magnetic stir bar. The flask was sealed with a rubber septum and evacuated and refilled with nitrogen 3 times. Trifluorotoluene (2 mL/mmol) was added *via* syringe followed by N,N-dicyclohexylmethylamine (1.1 mL, 5.0 equiv). B-bromocatecholborane (1.1 mL, ~2 M, 2.0 equiv) was added quickly *via* syringe and the solution was stirred in an oil bath at 70 °C for 5 minutes. Alkene (1.0 equiv) was added in one portion *via* syringe and the reaction was stirred at 70 °C for 4 h. After 4 h, the reaction was removed from the oil bath and opened to air. Pinacol (350 mg, 3 equiv) was added in one portion and the reaction was removed from heat and stirred for 30 min at rt. At that time, the reaction was diluted with 5 mL of diethyl ether, stirred for 10 min, and filtered through Celite. Ammonium pyrrolidine-dithiocarbamate (palladium scavenger, 6 equiv to palladium)[83] was added to this crude mixture and stirred for 30 min at rt. This mixture was filtered through Celite again and concentrated *in vacuo* to remove solvents, including trifluorotoluene. The crude oil was diluted with diethyl ether (10 mL) and washed with 1 M hydrochloric acid (3 x 10 mL) to remove excess amine. This solution was dried with $MgSO_4$, filtered through Celite and concentrated *in vacuo*. The crude material was purified via silica column chromatography on boric acid impregnated silica gel in the indicated solvent combination.

Note: Only the *E* isomer is reported for the ^{1}H and ^{13}C NMR spectral data. The ^{13}C NMR spectra may contain extra, unassigned peaks, which are attributed to the minor *Z* isomer.

4.8.5.2 Characterization Data

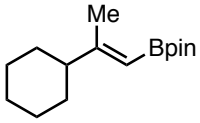

(**4.126**) According to the general procedure, $[(JessePhos)PdI_2]_2$ (41 mg, 0.05 mmol), trifluorotoluene (3.0 mL, 0.5 M), N,N-dicyclohexylmethylamine (1.1 mL, 5.0 mmol), catBBr (1.1 mL, 2.0 mmol), and **S4.1** (124 mg, 1.0 mmol) were combined under N_2 and stirred at 70 °C for 4 h. The reaction was worked up according to the general procedure. The product was purified on boric acid impregnated silica gel chromatography (3 : 7 dichloromethane : hexanes) to afford **4.126** as a colorless oil (236 mg, 94%): ^{1}H NMR (600 MHz, $CDCl_3$) δ 5.10 (p, *J* = 1.0 Hz, 1H), 1.97 (d, *J* = 1.0 Hz, 3H), 1.94 – 1.87 (m, 1H), 1.79 – 1.69 (m, 4H), 1.69 – 1.62 (m, 1H), 1.27 (s, 12H), 1.26 – 1.09 (m, 5H); ^{13}C NMR (151 MHz, $CDCl_3$) δ 168.0, 82.7, 49.6, 32.0, 26.9, 26.5, 25.0, 19.9; ^{11}B NMR (193 MHz, $CDCl_3$) δ 29.9; FTIR (cm^{-1}): 2978, 2926, 2853, 1653, 1319, 1260, 1145, 968, 850; mp = 27-28 °C. HRMS (CI) m/z, calcd for $[C_{15}H_{28}BO_2]^+$: 251.2182; found: 251.2183.

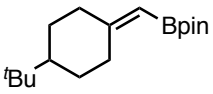

(**4.127**) According to the general procedure, $[(JessePhos)PdI_2]_2$ (41 mg, 0.05 mmol), trifluorotoluene (3.0 mL, 0.5 M), N,N-dicyclohexylmethylamine (1.1 mL, 5.0 mmol), catBBr (1.1 mL, 2.0 mmol), and **S4.2** (457 mg, 1.0 mmol) were combined under N_2 and stirred at 70 °C for 4 h. The reaction was worked up according to the general procedure. The product was purified on boric acid impregnated silica gel chromatography (3 : 7 dichloromethane : hexanes) to afford **4.127** as a colorless oil (687 mg, 82%): ^{1}H NMR (600 MHz, $CDCl_3$) δ 5.01 (s, 1H), 3.28 – 3.14 (m, 1H), 2.32 (dq, *J* = 13.1, 2.9 Hz, 1H), 2.21 – 2.09 (m, 1H), 1.96 – 1.81 (m, 3H), 1.26 (s, 12H), 1.22 – 1.04 (m, 3H), 0.85 (s, 9H); ^{13}C NMR (101 MHz, $CDCl_3$) δ 167.2, 82.7, 48.0, 40.1, 33.1, 32.6, 29.4, 29.2, 27.8, 25.0, 24.9; ^{11}B NMR (193 MHz,

$CDCl_3$) δ 29.5; FTIR (cm^{-1}): 2942, 1642, 1384, 1036, 852. HRMS (CI) m/z, calcd for $[C_{17}H_{32}BO_2]^+$: 279.2495; found: 279.2485.

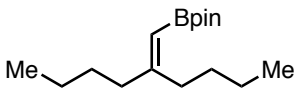

(**4.128**) According to the general procedure, $[(JessePhos)PdI_2]_2$ (41 mg, 0.05 mmol), trifluorotoluene (3.0 mL, 0.5 M), N,N-dicyclohexylmethylamine (1.1 mL, 5.0 mmol), catBBr (1.1 mL, 2.0 mmol), and **S4.3** (420 mg, 1.0 mmol) were combined under N_2 and stirred at 70 °C for 4 h. The reaction was worked up according to the general procedure. The product was purified on boric acid impregnated silica gel chromatography (2 : 8 dichloromethane : hexanes) to afford **4.128** as a colorless oil (742 mg, 93%): ^{1}H NMR (600 MHz, $CDCl_3$) δ 5.03 (d, J = 1.3 Hz, 1H), 2.39 – 2.26 (m, 2H), 2.09 – 1.97 (m, 2H), 1.38 – 1.28 (m, 4H), 1.28 – 1.20 (m, 4H), 1.19 (s, 12H), 0.83 (dt, J = 11.3, 7.3 Hz, 6H); ^{13}C NMR (151 MHz, $CDCl_3$) δ 167.8, 82.5, 38.8, 34.5, 31.8, 30.1, 24.8, 22.7, 22.5, 14.17, 14.14; ^{11}B NMR (193 MHz, $CDCl_3$) δ 30.0; FTIR (cm^{-1}): 2958, 1634, 1317, 1263, 1145. HRMS (CI) m/z, calcd for $[C_{16}H_{32}BO_2]^+$: 267.2495; found: 267.2482.

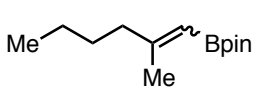

(**4.129**) According to the general procedure, $[(JessePhos)PdI_2]_2$ (41 mg, 0.05 mmol), trifluorotoluene (3.0 mL, 0.5 M), N,N-dicyclohexylmethylamine (1.1 mL, 5.0 mmol), catBBr (1.1 mL, 2.0 mmol), and 2-methylhexene (98 mg, 1.0 mmol) were combined under N_2 and stirred at 70 °C for 4 h. The reaction was worked up according to the general procedure. The product was purified on boric acid impregnated silica gel chromatography (1 : 9 dichloromethane : hexanes) to afford **4.129** as a colorless oil (196 mg, 88%): ^{1}H NMR (600 MHz, $CDCl_3$) *E*-**4.129**: δ 5.11 (s, 1H), 2.09 (t, 2H), 2.02 (s, 3H), 1.48 – 1.37 (m, 2H), 1.34 – 1.27 (m,

2H), 1.26 (s, 12H), 0.89 (t, J = 12.6 Hz, 3H); *Z*-**4.129**: δ 5.11 (s, 1H), 2.40 (dd, J = 8.4, 6.9 Hz, 2H), 1.85 (d, J = 1.3 Hz, 3H), 1.48 – 1.37 (m, 2H), 1.34 – 1.27 (m, 2H), 1.25 (s, 12H), 0.91 (t, J = 7.3 Hz, 3H); ^{13}C NMR (151 MHz, $CDCl_3$) mixture: δ 163.9, 163.4, 82.7, 82.6, 42.0, 35.9, 31.3, 30.0, 25.03, 24.98, 22.59, 22.56, 21.3, 14.1; ^{11}B NMR (193 MHz, $CDCl_3$) mixture: δ 29.8; FTIR (cm^{-1}): 2929, 1640, 1317, 1264, 1144, 1053, 852. HRMS (CI) m/z, calcd for $[C_{13}H_{26}BO_2]^+$: 225.2026; found: 225.2023.

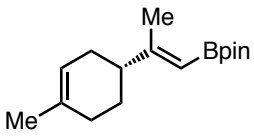

(**4.130**) According to the general procedure, $[(JessePhos)PdI_2]_2$ (41 mg, 0.05 mmol), trifluorotoluene (3.0 mL, 0.5 M), N,N-dicyclohexylmethylamine (1.1 mL, 5.0 mmol), catBBr (1.1 mL, 2.0 mmol), and (+)-limonene (480 mg, 1.0 mmol) were combined under N_2 and stirred at 70 °C for 4 h. The reaction was worked up according to the general procedure. The product was purified on boric acid impregnated silica gel chromatography (2 : 8 dichloromethane : hexanes) to afford **4.130** as a colorless oil (617 mg, 78%): ^{1}H NMR (600 MHz, $CDCl_3$) δ 5.44 – 5.33 (m, 1H), 5.15 (s, 1H), 2.19 – 2.10 (m, 1H), 2.10 – 2.00 (m, 2H), 1.99 (d, J = 0.9 Hz, 3H), 1.97 – 1.88 (m, 2H), 1.83 – 1.76 (m, 1H), 1.64 (s, 3H), 1.48 (qd, J = 11.9, 5.5 Hz, 1H), 1.27 (s, 12H); ^{13}C NMR (151 MHz, $CDCl_3$) δ 167.0, 133.8, 120.8, 82.8, 45.2, 30.9, 30.9, 28.0, 25.0, 23.6, 19.7; ^{11}B NMR (193 MHz, $CDCl_3$) δ 30.2; FTIR (cm^{-1}): 2977, 2930, 1717, 1635, 1438, 1145, 970, 851, 673. HRMS (CI) m/z, calcd for $[C_{16}H_{28}BO_2]^+$: 263.2182; found: 263.2187.

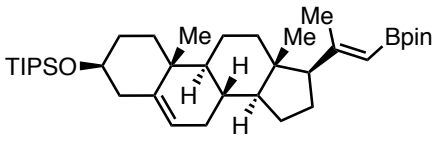

(**4.131**) According to the general procedure, $[(JessePhos)PdI_2]_2$ (41 mg, 0.05 mmol), trifluorotoluene (3.0 mL, 0.5 M), N,N-

dicyclohexylmethylamine (1.1 mL, 5.0 mmol), catBBr (1.1 mL, 2.0 mmol), and **S4.5** (1.41 g, 1.0 mmol) were combined under N_2 and stirred at 70 °C for 4 h. The reaction was worked up according to the general procedure. The product was purified on boric acid impregnated silica gel chromatography (3 : 7 dichloromethane : hexanes) to afford **4.131** as a white solid (1.47 g, 82%): ^{1}H NMR (600 MHz, $CDCl_3$) δ 5.31 (dt, *J* = 4.8, 2.1 Hz, 1H), 5.16 (s, 1H), 3.55 (tt, *J* = 10.4, 4.8 Hz, 1H), 2.33 – 2.18 (m, 2H), 2.13 (t, *J* = 9.3 Hz, 1H), 2.01 (s, 4H), 1.92 – 1.76 (m, 4H), 1.66 (tt, *J* = 8.6, 2.6 Hz, 2H), 1.60 – 1.50 (m, 3H), 1.43 (pd, *J* = 13.2, 11.8, 4.5 Hz, 2H), 1.27 (s, 12H), 1.24 – 1.14 (m, 2H), 1.05 (d, *J* = 2.4 Hz, 22H), 1.00 (s, 3H), 0.94 (td, *J* = 11.8, 4.8 Hz, 1H), 0.57 (s, 3H); ^{13}C NMR (151 MHz, $CDCl_3$) δ 162.5, 141.9, 121.1, 82.7, 72.6, 61.1, 56.9, 50.5, 43.9, 43.3, 38.8, 37.6, 36.8, 32.5, 32.4, 32.0, 25.6, 25.1, 25.0, 24.5, 23.5, 21.2, 19.6, 18.3, 13.0, 12.5.; ^{11}B NMR (193 MHz, $CDCl_3$) δ 30.8; FTIR (cm^{-1}): 2940, 2866, 1629, 1326, 1145, 1104; mp = 137-140 °C. HRMS (ESI) m/z, calcd for $[C_{37}H_{66}O_4BSi]^+$: 597.4869; found: 597.4848.

A small sample was recrystallized from ethyl acetate layered with methanol to afford an X-ray quality crystal to confirm alkene geometry (see details below).

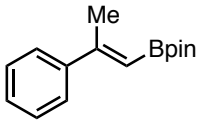

(**4.132**) According to the general procedure, $[(JessePhos)PdI_2]_2$ (41 mg, 0.05 mmol), trifluorotoluene (3.0 mL, 0.5 M), N,N-dicyclohexylmethylamine (1.1 mL, 5.0 mmol), catBBr (1.1 mL, 2.0 mmol), and α-methylstyrene (130 mg, 1.0 mmol) were combined under N_2 and stirred at 70 °C for 4 h. The reaction was worked up according to the general procedure. The product was purified on boric acid impregnated silica gel chromatography (2 : 10 dichloromethane : hexanes) to afford **4.132** as a colorless oil (245 mg, 100%): ^{1}H NMR

(600 MHz, $CDCl_3$) δ 7.53 – 7.47 (m, 2H), 7.35 – 7.30 (m, 2H), 7.30 – 7.27 (m, 1H), 5.76 (d, *J* = 1.0 Hz, 1H), 2.41 (d, *J* = 0.9 Hz, 3H), 1.32 (s, 13H); ^{13}C NMR (151 MHz, $CDCl_3$) δ 157.9, 144.0, 128.3, 128.0, 126.0, 83.1, 25.1, 20.2; ^{11}B NMR (193 MHz, $CDCl_3$) δ 30.2; FTIR (cm^{-1}): 2978, 2361, 1621, 1384, 1355, 1144, 1035, 760. HRMS (CI) m/z, calcd for $[C_{15}H_{22}BO_2]^+$: 245.1713; found: 245.1703.

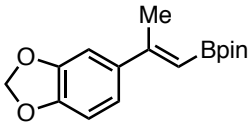

(**4.133**) According to the general procedure, $[(JessePhos)PdI_2]_2$ (10.1 mg, 2.5 mol %), catBBr (100 mg, 0.5 mmol), trifluorotoluene (500 μL, 0.5 M), N,N-dicyclohexylmethylamine (265 μL, 1.25 mmol), and **S4.6** (36 mg, 0.25 mmol) were combined under N_2 and stirred at 70 °C for 4 h. The reaction was worked up according to the general procedure. The product was purified on boric acid impregnated silica gel chromatography (3 : 7 dichloromethane : hexanes) to afford **4.133** as a white solid (66 mg, 88%): ^1H NMR (600 MHz, $CDCl_3$) δ 7.04 – 6.98 (m, 2H), 6.79 – 6.75 (m, 1H), 5.95 (s, 2H), 5.66 (q, *J* = 0.9 Hz, 1H), 2.36 (d, *J* = 0.9 Hz, 3H), 1.31 (s, 12H); ^{13}C NMR (151 MHz, $CDCl_3$) δ 157.1, 147.8, 138.3, 119.9, 107.9, 106.5, 101.2, 83.1, 31.6, 25.0, 20.4; ^{11}B NMR (193 MHz, $CDCl_3$) δ 30.2; FTIR (cm^{-1}): 1384, 1321, 1236, 1038; mp = 50-53 °C. HRMS (CI) m/z, calcd for $[C_{16}H_{22}BO_4]^+$: 289.1611; found: 289.1605.

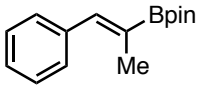

(**4.134**) According to the general procedure, $[(JessePhos)PdI_2]_2$ (41 mg, 0.05 mmol), trifluorotoluene (3.0 mL, 0.5 M), N,N-dicyclohexylmethylamine (1.1 mL, 5.0 mmol), catBBr (1.1 mL, 2.0 mmol), and *trans*-β-Methylstyrene (118 mg, 1.0 mmol) were combined under N_2 and stirred at 70 °C for 4 h. The reaction was worked up according to the general procedure. The product was

purified on boric acid impregnated silica gel chromatography (3 : 7 dichloromethane : hexanes) to afford **4.134** as a colorless oil (196 mg, 90%): ^{1}H NMR (600 MHz, $CDCl_3$) δ 7.41 – 7.37 (m, 2H), 7.34 (t, *J* = 7.7 Hz, 2H), 7.26 – 7.21 (m, 2H), 1.99 (d, *J* = 1.8 Hz, 3H), 1.32 (s, 12H); ^{13}C NMR (151 MHz, $CDCl_3$) δ 142.5, 138.1, 129.6, 128.2, 127.2, 83.7, 25.0, 16.0; ^{11}B NMR (193 MHz, $CDCl_3$) δ 30.8; FTIR (cm^{-1}): 2977, 1616, 1384, 1369, 1310, 1145, 1035, 865, 752, 699, 668. HRMS (CI) m/z, calcd for $[C_{15}H_{22}BO_2]^+$: 245.1713; found: 245.1718.

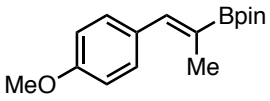

(**4.135**) According to the general procedure, $[(JessePhos)PdI_2]_2$ (41 mg, 0.05 mmol), trifluorotoluene (3.0 mL, 0.5 M), N,N-dicyclohexylmethylamine (1.1 mL, 5.0 mmol), catBBr (1.1 mL, 2.0 mmol), and *trans*-anethole (449 mg, 1.0 mmol) were combined under N_2 and stirred at 70 °C for 4 h. The reaction was worked up according to the general procedure. The product was purified on boric acid impregnated silica gel chromatography (5 : 95 dichloromethane : hexanes) to afford **4.135** as a pale yellow oil (804 mg, 98%): ^{1}H NMR (600 MHz, $CDCl_3$) δ 7.42 – 7.36 (m, 2H), 7.20 (d, *J* = 1.8 Hz, 1H), 6.93 – 6.88 (m, 2H), 3.84 (s, 3H), 2.02 (d, *J* = 1.8 Hz, 3H), 1.33 (s, 12H); ^{13}C NMR (151 MHz, $CDCl_3$) δ 158.7, 141.9, 130.9, 130.8, 113.5, 83.4, 55.2, 24.9, 15.9; ^{11}B NMR (193 MHz, $CDCl_3$) δ 30.9; FTIR (cm^{-1}): 2977, 1605, 1510, 1250, 1146, 1099, 668. HRMS (CI) m/z, calcd for $[C_{16}H_{24}BO_3]^+$: 275.1819; found: 275.1823.

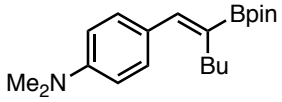

(**4.136**) According to the general procedure, $[(JessePhos)PdI_2]_2$ (41 mg, 0.05 mmol), trifluorotoluene (3.0 mL, 0.5 M), N,N-dicyclohexylmethylamine (1.1 mL, 5.0 mmol), catBBr (1.1 mL, 2.0 mmol), and **S4.7**

(203 mg, 1.0 mmol) were combined under N_2 and stirred at 70 °C for 4 h. The reaction was worked up according to the general procedure. The product was purified on boric acid impregnated silica gel chromatography (1 : 99 ethyl acetate : hexanes) to afford **4.136** as a red solid (322 mg, 99%): ^{1}H NMR (600 MHz, $CDCl_3$) δ 7.30 (d, *J* = 8.7 Hz, 2H), 7.10 (s, 1H), 6.72 – 6.66 (m, 2H), 2.97 (s, 6H), 2.47 – 2.39 (m, 2H), 1.52 – 1.44 (m, 2H), 1.44 – 1.33 (m, 2H), 1.29 (s, 12H), 0.92 (t, *J* = 7.3 Hz, 3H); ^{13}C NMR (151 MHz, $CDCl_3$) δ 149.7, 142.0, 130.7, 126.6, 112.0, 83.2, 40.5, 32.4, 29.5, 25.0, 23.1, 14.3; ^{11}B NMR (193 MHz, $CDCl_3$) δ 31.1; FTIR (cm^{-1}): 1602, 1519, 1384, 1349, 1037; mp = 79-81 °C. HRMS (CI) m/z, calcd for $[C_{20}H_{33}BNO_2]^+$: 330.2604; found: 330.2598. A small sample was recrystallized by slow evaporation of methanol to afford an X-ray quality crystal to confirm alkene geometry (see details below).

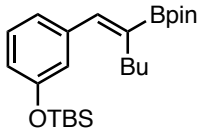

(**4.137**) According to the general procedure, $[(JessePhos)PdI_2]_2$ (41 mg, 0.05 mmol), trifluorotoluene (3.0 mL, 0.5 M), N,N-dicyclohexylmethylamine (1.1 mL, 5.0 mmol), catBBr (1.1 mL, 2.0 mmol), and **S4.9** (871 mg, 1.0 mmol) were combined under N_2 and stirred at 70 °C for 4 h. The reaction was worked up according to the general procedure. The product was purified on boric acid impregnated silica gel chromatography (3 : 7 dichloromethane : hexanes) to afford **4.137** as a colorless oil (905 mg, 72%): ^{1}H NMR (600 MHz, $CDCl_3$) δ 6.99 (t, *J* = 7.9 Hz, 1H), 6.95 (s, 1H), 6.72 (ddt, *J* = 7.6, 1.6, 0.8 Hz, 1H), 6.63 (t, *J* = 2.0 Hz, 1H), 6.53 (ddd, *J* = 8.1, 2.5, 1.0 Hz, 1H), 2.23 – 2.14 (m, 2H), 1.30 – 1.21 (m, 2H), 1.21 – 1.13 (m, 2H), 1.12 (s, 12H), 0.79 (s, 9H), 0.69 (t, *J* = 7.3 Hz, 3H), 0.00 (s, 6H); ^{13}C NMR (151 MHz, $CDCl_3$) δ 155.3, 141.5, 139.4, 128.9, 122.3, 120.6, 118.9, 83.4, 32.3, 29.3, 25.7, 24.8, 22.9, 14.1, -4.4; ^{11}B NMR (193 MHz, $CDCl_3$) δ 31.2; FTIR

(cm^{-1}): 2957, 2930, 2859, 1596, 1575, 1378, 1279, 1147, 1131, 838, 781, 689. HRMS (CI) m/z, calcd for $[C_{24}H_{42}BO_3Si]^+$: 417.2996; found: 417.3016.

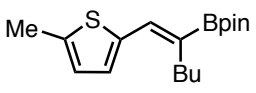

(**4.138**) According to the general procedure, $[(JessePhos)PdI_2]_2$ (41 mg, 0.05 mmol), trifluorotoluene (3.0 mL, 0.5 M), N,N-dicyclohexylmethylamine (1.1 mL, 5.0 mmol), catBBr (1.1 mL, 2.0 mmol), and **S4.10** (180 mg, 1.0 mmol) were combined under N_2 and stirred at 70 °C for 4 h. The reaction was worked up according to the general procedure. The product was purified on boric acid impregnated silica gel chromatography (1 : 9 dichloromethane : hexanes) to afford **4.138** as a colorless oil (304 mg, 99%): ^{1}H NMR (600 MHz, $CDCl_3$) δ 7.22 (s, 1H), 6.91 (d, J = 3.5 Hz, 1H), 6.73 – 6.60 (m, 1H), 2.54 – 2.45 (m, 5H), 1.49 – 1.38 (m, 4H), 1.28 (s, 12H), 0.94 (t, J = 7.0 Hz, 3H); ^{13}C NMR (151 MHz, $CDCl_3$) δ 141.8, 139.1, 134.5, 130.1, 125.1, 83.4, 31.8, 30.1, 24.9, 23.2, 15.6, 14.3; ^{11}B NMR (193 MHz, $CDCl_3$) δ 31.0; FTIR (cm^{-1}): 2976, 1603, 1361, 1304, 1215, 1146. HRMS (CI) m/z, calcd for $[C_{17}H_{28}BO_2S]^+$: 307.1903; found: 307.1903.

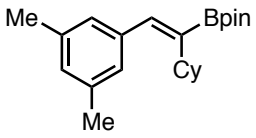

(**4.139**) According to the general procedure, $[(JessePhos)PdI_2]_2$ (41 mg, 0.05 mmol), trifluorotoluene (3.0 mL, 0.5 M), N,N-dicyclohexylmethylamine (1.1 mL, 5.0 mmol), catBBr (1.1 mL, 2.0 mmol), and **S4.11** (214 mg, 1.0 mmol) were combined under N_2 and stirred at 70 °C for 4 h. The reaction was worked up according the general procedure. The product was purified on boric acid impregnated silica gel chromatography (2 : 8 dichloromethane : hexanes) to afford **4.139** as a white solid (227 mg, 67%): ^{1}H NMR (600 MHz, $CDCl_3$) δ 7.00 (s, 1H), 6.83 (s, 2H), 6.81 (s, 1H), 2.60 (tt, J = 11.7, 3.5 Hz, 1H), 2.23 (s, 6H), 1.67

– 1.53 (m, 5H), 1.50 – 1.41 (m, 2H), 1.22 (s, 12H), 1.17 – 1.08 (m, 3H); ^{13}C NMR (151 MHz, $CDCl_3$) δ 140.5, 138.3, 137.5, 128.6, 126.9, 83.1, 39.7, 32.2, 26.5, 26.2, 24.9, 21.5; ^{11}B NMR (193 MHz, $CDCl_3$) δ 31.1; FTIR (cm^{-1}): 3853, 2924, 2361, 2337, 1653, 1559, 1441; mp = 83-85 °C. HRMS (CI) m/z, calcd for $[C_{21}H_{30}BO_2]^+$: 325.2339; found: 325.2328. (M - CH_3)

A small sample was recrystallized by slow evaporation of methanol to afford an X-ray quality crystal to confirm alkene geometry (see details below).

4.8.6 Downstream Functionalization Reactions

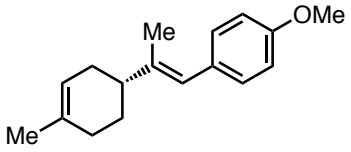

(**4.141**) In a nitrogen-filled glovebox, to a 1-dram vial with a stir bar, was added $[(JessePhos)PdI_2]_2$ (10.1 mg, 2.5 mol %), catBBr (100 mg, 0.5 mmol), trifluorotoluene (500 μL, 0.5 M), N,N-dicyclohexylmethylamine (265 μL, 1.25 mmol), and (+/-)-limonene (41 μL, 0.25 mmol). The vial was capped and stirred at 70 °C for 4 h. The reaction was removed heat, opened to air and diluted with a mixture of THF:water (10:1, 500 μL). $CsCO_3$ (250 mg, 0.75 mmol, 3.0 equiv) and 4-iodoanisole (146 mg, 0.625 mmol, 2.5 equiv) were added and the vial was resealed and stirred at 60 °C for 16 h. At that time, the reaction was diluted with diethyl ether (500 μL), stirred for 10 min, and filtered through Celite and concentrated *in vacuo*. The crude material was purified *via* silica column chromatography (5 : 95 dichloromethane : hexanes) to afford **4.141** as a colorless oil (56 mg, 92%): ^{1}H NMR (600 MHz, $CDCl_3$) δ 7.22 – 7.13 (m, 2H), 6.91 – 6.80 (m, 2H), 6.24 (s, 1H), 5.44 (s, 1H), 3.81 (s, 3H), 2.29 – 2.20 (m, 1H), 2.16 – 1.96 (m, 4H), 1.87 – 1.80 (m, 4H), 1.68 (s, 3H), 1.63 – 1.55 (m, 1H); ^{13}C NMR (151 MHz, $CDCl_3$) δ 157.8, 141.9, 133.9, 131.5, 130.2, 123.0, 120.9, 113.6, 55.4, 43.9, 31.0, 30.9,

28.1, 23.7, 16.0; FTIR (cm^{-1}): 2918, 1608, 1510, 1441, 1249, 1177, 1038, 862, 821. HRMS (EI) m/z, calcd for $[C_{17}H_{22}O]^+$: 242.1671; found: 242.1661.

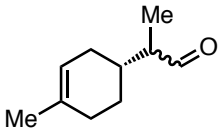

(**4.142**) In a nitrogen-filled glovebox, to a 1-dram vial with a stir bar, was added $[(JessePhos)PdI_2]_2$ (10.1 mg, 2.5 mol %), catBBr (100 mg, 0.5 mmol), trifluorotoluene (500 μL, 0.5 M), N,N-dicyclohexylmethylamine (265 μL, 1.25 mmol), and (+/-)-limonene (41 μL, 0.25 mmol). The vial was capped and stirred at 70 °C for 4 h. The reaction was removed heat, opened to air and trimethylamine N-oxide (112 mg, 1.5 mmol) was added. The vial was resealed and stirred at 70 °C for 18 h. The reaction was removed heat, opened to air, diluted with 1 mL diethyl ether, filtered thru Celite and concentrated. The crude oil was diluted with diethyl ether (1 mL) and washed with 1 M hydrochloric acid (3 x 1 mL) to remove excess amine. This solution was dried with $MgSO_4$, filtered through Celite and concentrated *in vacuo*. The crude material was purified via silica column chromatography (1 : 1 dichloromethane : pentane) to afford **4.142** as a colorless oil (27 mg, 71%): ^{1}H NMR (400 MHz, $CDCl_3$) δ 9.66 (dd, J = 5.5, 2.5 Hz, 1H), 5.36 (dtt, J = 5.9, 3.2, 1.6 Hz, 1H), 2.37 – 2.21 (m, 1H), 2.10 – 1.66 (m, 6H), 1.64 (s, 3H), 1.45 – 1.29 (m, 1H), 1.07 (dd, J = 7.0, 5.2 Hz, 3H); ^{13}C NMR (101 MHz, $CDCl_3$) δ 205.8, 205.7, 134.3, 134.2, 120.1, 120.0, 100.1, 51.2, 50.8, 34.43, 34.37, 30.3, 30.1, 29.8, 28.2, 27.5, 25.6, 23.6, 10.5, 10.4; FTIR (cm^{-1}): 2916, 2702, 1723, 1439, 1377, 799.

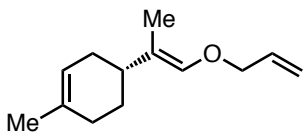

(**4.143**) According to a modified literature procedure,[77] a 1-dram vial equipped with a magnetic stir bar was charged with alkenyl boronic ester **4.130** (69 mg, 0.25 mmol, 1.0 equiv), copper acetate (91 mg, 0.50 mmol, 2.0 equiv), triethylamine (140 μL, 0.25 mmol, 1.0

equiv), and allyl alcohol (500 μL) and sealed under air. The reaction was stirred for 20 h at room temperature. The reaction was opened, quenched with water (1 mL), and extracted with diethyl ether (3 x 500 μL). The combined organic layers were dried with $MgSO_4$, filtered through Celite, and concentrated *in vacuo*. The crude oil was purified by flash silica gel chromatography (1 : 9 dichloromethane : hexanes) to afforded **4.143** as a colorless oil (33 mg, 69%): ^{1}H NMR (400 MHz, $CDCl_3$) δ 6.00 – 5.85 (m, 2H), 5.43 – 5.34 (m, 1H), 5.30 (dq, *J* = 17.2, 1.7 Hz, 1H), 5.19 (dq, *J* = 10.5, 1.4 Hz, 1H), 4.21 (dt, *J* = 5.4, 1.5 Hz, 2H), 2.10 – 1.97 (m, 2H), 1.97 – 1.88 (m, 3H), 1.72 – 1.63 (m, 4H), 1.60 (d, *J* = 1.4 Hz, 3H), 1.57 – 1.42 (m, 1H); ^{13}C NMR (101 MHz, $CDCl_3$) δ 139.7, 134.5, 133.8, 120.9, 118.8, 117.1, 72.5, 38.1, 30.9, 30.7, 28.1, 23.7, 10.9; FTIR (cm^{-1}): 2918, 1680, 1437, 1278, 1154, 923. HRMS (EI) m/z, calcd for $[C_{13}H_{30}O]^+$: 192.1514; found: 192.1510.

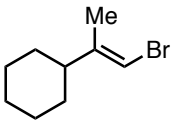

(**4.144**) According to a modified literature procedure,[72] a 2-dram vial equipped with a magnetic stir bar was charged with alkenyl boronic ester **4.126** (63 mg, 0.25 mmol, 1.0 equiv), copper (II) bromide (224 mg, 1.0 mmol, 4.0 equiv), methanol (1.5 mL), and water (1.5 mL) and sealed under air. The reaction was stirred for 22 h at 80 °C. The reaction was cooled to room temperature, diluted with diethylether (1 mL), and extracted with diethyl ether (3 x 500 μL). The combined organic layers were dried with $MgSO_4$, filtered through Celite, and concentrated *in vacuo*. The crude oil was purified by flash silica gel chromatography (pentane) to afforded **4.144** as a colorless oil (40 mg, 78%): ^{1}H NMR (600 MHz, $CDCl_3$) δ 5.92 (t, *J* = 1.2 Hz, 1H), 2.02 (tt, *J* = 11.3, 3.3 Hz, 1H), 1.81 – 1.74 (m, 5H), 1.69 (dddd, *J* = 17.2, 12.0, 3.6, 1.7 Hz, 3H), 1.29 – 1.12 (m, 5H); ^{13}C NMR (151 MHz,

$CDCl_3$) δ 146.9, 101.1, 47.1, 31.7, 26.6, 26.3, 17.8; FTIR (cm^{-1}): 2927, 2853, 1624, 1448, 1307, 1166, 774. HRMS (EI) m/z, calcd for $[C_9H_{15}Br]^+$: 202.0357; found: 202.0362.

4.8.7 Additional Optimization Data

During optimization, some additives were examined that were not included in the communication. The results from those experiments are shown below (Table 4.2). **Note:** All reactions in this section were performed on 0.25 mmol in a nitrogen-filled glovebox.

Table 4.2 Additional Optimization Data

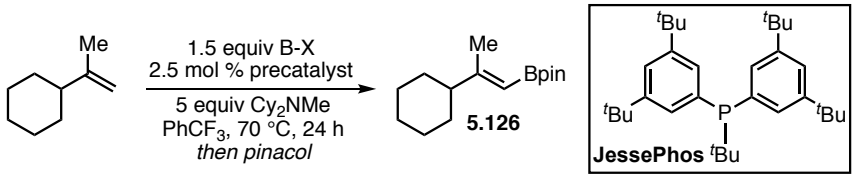

entry	B-X (equiv)	precatalyst	additives	**Isom. SM**	**4.126**
1	catBCl (1.5)	(**JessePhos**)$_2$PdCl$_2$	none	0%	3%
2	catBBr (1.5)	(**JessePhos**)$_2$PdCl$_2$	none	2%	63%
3	catBBr (1.5)	none	none	0%	0%
4	catBBr (1.5)	(**JessePhos**PdI$_2$)$_2$	none	2%	95%
5	catBBr (1.5)	(**JessePhos**PdI$_2$)$_2$	2.5 mol % **JessePhos**	2%	90%
6	catBBr (1.5)	(**JessePhos**PdI$_2$)$_2$	cat. $Cy_2NMeHCl$	2%	91%

7	catBBr (1.5)	(**JessePhos**)$_2$PdCl$_2$	cat. LiI	6%	81%
8	catBCl (1.5)	(**JessePhos**)$_2$PdCl$_2$	cat. LiI	22%	59%
9	catBCl (1.5)	(**JessePhos**PdI$_2$)$_2$	none	12%	33%
10	catBBr (2.0)	(**JessePhos**PdI$_2$)$_2$	none	0%	94%

4.8.8 Chiral GC Trace of 4.130

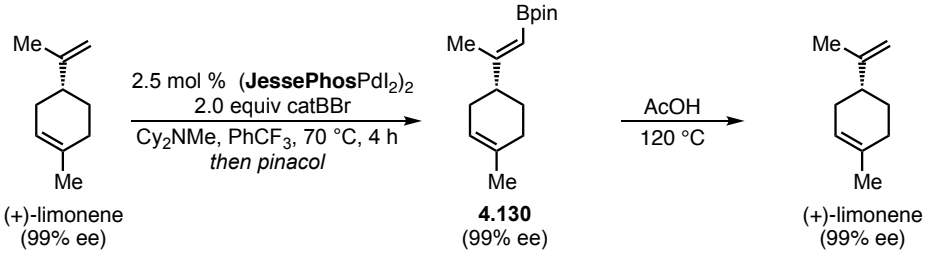

Figure 4.70 Enantiomeric Excess and Protodeboronation of **4.130**

The enantiomeric excess of **4.130** was determined to be 99% by chiral GC analysis (CYCLOSIL-B, 30m X 0.25mm, ramp 5 °C/min from 40 °C to 230 °C); t_R(major) = 37.440 min, t_R(minor) = 37.320 min. To rule out inversion of the stereocenter during the boryl-Heck reaction, isolated **4.130** was subjected to protodeboronation conditions. Refluxing **4.130** in acetic acid provided (+)-limonene in 22% yield as a single enantiomer. This verifies that no epimerization or inversion occurs during the reaction.

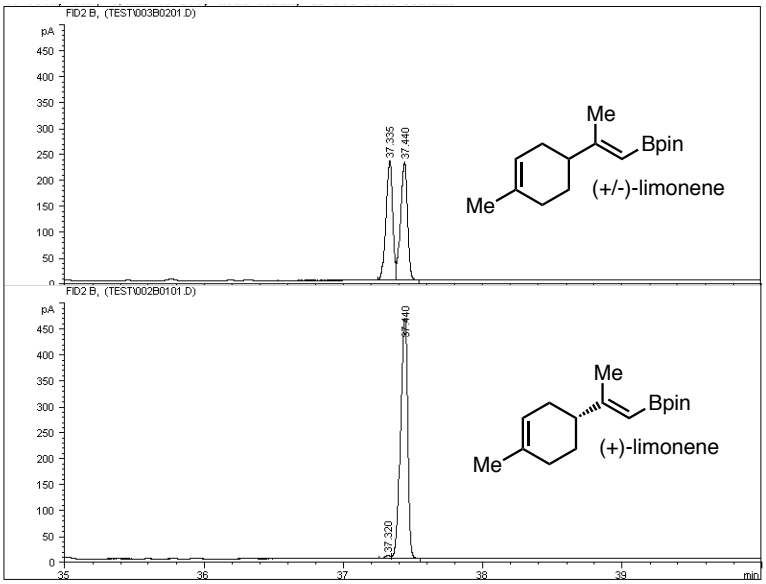


```
================================================================
                    Area Percent Report
================================================================

Sorted By             :      Signal
Multiplier            :      1.0000
Dilution              :      1.0000
Use Multiplier & Dilution Factor with ISTDs


Signal 1: FID2 B,

Peak RetTime Type  Width     Area      Height     Area
  #   [min]        [min]   [pA*s]      [pA]         %
----|-------|----|-------|----------|----------|--------|
   1  37.320 BV    0.0443   18.45809    6.35974  1.09631
   2  37.440 VB    0.0563 1665.19263  463.30499 98.90369
```

4.8.9 Crystallographic Details

X-ray structural analysis for **4.131**, **4.136**, and **4.139**: Crystals were mounted using viscous oil onto a plastic mesh and cooled to the data collection temperature. Data were collected on a Bruker-AXS APEX II DUO CCD diffractometer with Cu-Kα radiation (λ = 1.54178 Å) focused with Goebel mirrors. Unit cell parameters were obtained from 36 data frames, 0.5 º ω, from three different sections of the Ewald sphere. The unit cell parameters, and systematic absences in the diffraction data are consistent with $P2_1$ (4) and $P2_1/m$ (11) for **4.131**; and, uniquely, with $P2_1/c$ (14) for **4.136** and **4.139**. The occupancy and absence of a molecular mirror or inversion for **4.131** is consistent with the non-centrosymmetric space group option that yielded chemically reasonable and computationally stable results of refinement. For **4.131**, refinement of the absolute

structure parameter to nil indicates the true hand of the data has been determined. For **4.139**, two symmetry unique, but chemically identical compound molecules were found in the asymmetric unit. The data were treated with multi-scan absorption corrections.[84] The structure was solved using intrinsic phasing methods and refined with full-matrix, least-squares procedures on F^2.[85] All non-hydrogen atoms were refined with anisotropic displacement parameters. Hydrogen atoms were treated as idealized contributions with geometrically calculated positions and with U_{iso} equal to 1.2 (or 1.5 for methyl) U_{eq} of the attached atom. Atomic scattering factors are contained in the SHELXTL program library.[85]

REFERENCES

(1) Reid, W. B.; Spillane, J. J.; Krause, S. B.; Watson, D. A., *J. Am. Chem. Soc.* **2016,** *138*, 5539.
(2) Flynn, A. B.; Ogilvie, W. W., *Chem. Rev.* **2007,** *107*, 4698.
(3) Nicolaou, K. C.; Bulger, P. G.; Sarlah, D., *Angew. Chem., Int. Ed.* **2005,** *44*, 4442.
(4) Hupe, E.; Marek, I.; Knochel, P., *Org. Lett.* **2002,** *4*, 2861.
(5) Ueda, M.; Saitoh, A.; Miyaura, N., *J. Organomet. Chem.* **2002,** *642*, 145.
(6) Moran, W. J.; Morken, J. P., *Org. Lett.* **2006,** *8*, 2413.
(7) Morgan, J. B.; Morken, J. P., *J. Am. Chem. Soc.* **2004,** *126*, 15338.
(8) (a) Paptchikhine, A.; Cheruku, P.; Engman, M.; Andersson, P. G., *Chem. Commun.* **2009,** 5996 ; (b) Mazuela, J.; Norrby, P.-O.; Andersson, P. G.; Pamies, O.; Dieguez, M., *J. Am. Chem. Soc.* **2011,** *133*, 13634 ; (c) Ganic, A.; Pfaltz, A., *Chem. - Eur. J.* **2012,** *18*, 6724 ; (d) Ganic, A.; Rageot, D.; Troendlin, L.; Pfaltz, A., *Chimia* **2012,** *66*, 187 ; (e) Gazia?smilovia, I.; Casas-Arce, E.; Roseblade, S. J.; Nettekoven, U.; Zanotti-Gerosa, A.; Kovac?evic, M.; C?asar, Z., *Angew. Chem., Int. Ed.* **2012,** *51*, 1014 ; (f) Coll, M.; Pamies, O.; Dieguez, M., *Adv. Synth. Catal.* **2013,** *355*, 143 ; (g) Mazuela, J.; Pamies, O.; Dieguez, M., *Adv. Synth. Catal.* **2013,** *355*, 2569 ; (h) Margalef, J. s.; Caldentey, X.; Karlsson, E. A.; Coll, M.; Mazuela, J.; P?mies, O.; Di?guez, M.; Peric?s, M. A., *Chem. - Eur. J.* **2014,** *20*, 12201 ; (i) Biosca, M.; Paptchikhine, A.; Pa mies, O.; Andersson, P. G.; DiA?guez, M., *Chem. - Eur. J.* **2015,** *21*, 3455 ; (j) Borr?s, C.; Biosca, M.; P?mies, O.; Di?guez, M., *Organometallics* **2015,** *34*, 5321 ; (k) Biosca, M.; Coll, M.; Lagarde, F.; Br?mond, E.; Routaboul, L.; Manoury, E.; P?mies, O.; Poli, R.; Di?guez, M., *Tetrahedron* **2016,** *72*, 2623 ; (l) Biosca, M.; Magre, M.; Coll, M.; P?mies, O.; Di?guez, M., *Adv. Synth. Catal.* **2017,** *359*, 2801
(9) (a) Noda, H.; Bode, J. W., *Org. Biomol. Chem.* **2016,** *14*, 16; (b) Scharnagl, F. K.; Bose, S. K.; Marder, T. B., *Org. Biomol. Chem.* **2017,** *15*, 1738.
(10) Taguchi, J.; Ikeda, T.; Takahashi, R.; Sasaki, I.; Ogasawara, Y.; Dairi, T.; Kato, N.; Yamamoto, Y.; Bode, J. W.; Ito, H., *Angew. Chem., Int. Ed.* **2017,** *56*, 13847.
(11) (a) Chen, C. H.; Shi, J., *Coord. Chem. Rev.* **1998,** *171*, 161; (b) Mitschke, U.; Bauerle, P., *J. Mater. Chem.* **2000,** *10*, 1471.
(12) Wu, F.-I.; Shih, P.-I.; Yuan, M.-C.; Dixit, A. K.; Shu, C.-F.; Chung, Z.-M.; Diau, E. W.-G., *J. Mater. Chem.* **2005,** *15*, 4753
(13) (a) Brown, H. C.; Scouten, C. G.; Liotta, R., *J. Am. Chem. Soc.* **1979,** *101*, 96; (b) Brown, H. C.; Campbell, J. B., *J. Org. Chem.* **1980,** *45*, 389; (c) Tucker, C. E.; Davidson, J.; Knochel, P., *J. Org. Chem.* **1992,** *57*, 3482.
(14) Lipshutz, B. H.; Bošković, Ž. V.; Aue, D. H., *Angew. Chem., Int. Ed.* **2008,** *47*, 10183.

(15) Haberberger, M.; Enthaler, S., *Chem. - Asian J.* **2013,** *8*, 50.
(16) Lee, J.-E.; Kwon, J.; Yun, J., *Chem. Commun.* **2008,** 733.
(17) Jung, H.-Y.; Feng, X.; Kim, H.; Yun, J., *Tetrahedron* **2012,** *68*, 3444
(18) Kim, H. R.; Jung, I. G.; Yoo, K.; Jang, K.; Lee, E. S.; Yun, J.; Son, S. U., *Chem. Commun.* **2010,** *46*, 758
(19) Kim, H. R.; Yun, J., *Chem. Commun.* **2011,** *47*, 2943.
(20) Moure, A. L.; Gómez Arrayás, R.; Cárdenas, D. J.; Alonso, I.; Carretero, J. C., *J. Am. Chem. Soc.* **2012,** *134*, 7219.
(21) Park, J. K.; Ondrusek, B. A.; McQuade, D. T., *Org. Lett.* **2012,** *14*, 4790.
(22) Ondrusek, B. A.; McQuade, D. T., *Synlett* **2014,** *25*, 1547
(23) Yoshida, H.; Kageyuki, I.; Takaki, K., *Org. Lett.* **2014,** *16*, 3512
(24) Bismuto, A.; Thomas, S. P.; Cowley, M. J., *Angew. Chem., Int. Ed.* **2016,** *55*, 15356
(25) Ojha, D. P.; Prabhu, K. R., *Org. Lett.* **2016,** *18*, 432
(26) (a) Fleige, M.; M?bus, J.; Vom Stein, T.; Glorius, F.; Stephan, D. W., *Chem. Commun.* **2016,** *52*, 10830 ; (b) Lawson, J. R.; Wilkins, L. C.; Melen, R. L., *Chem. - Eur. J.* **2017,** *23*, 10997
(27) Ho, H. E.; Asao, N.; Yamamoto, Y.; Jin, T., *Org. Lett.* **2014,** *16*, 4670.
(28) (a) Khan, A.; Asiri, A. M.; Kosa, S. A.; Garcia, H.; Grirrane, A., *J. Catal.* **2015,** *329*, 401 ; (b) Tseng, K.-N. T.; Kampf, J. W.; Szymczak, N. K., *ACS Catal.* **2015,** *5*, 411 ; (c) Rawat, V. S.; Sreedhar, B., *Synlett* **2014,** *25*, 1132 ; (d) Nakajima, K.; Kato, T.; Nishibayashi, Y., *Org. Lett.* **2017,** *19*, 4323 ; (e) Greenhalgh, M. D.; Thomas, S. P., *Chem. Commun.* **2013,** *49*, 11230; (f) Espinal-Viguri, M.; Woof, C. R.; Webster, R. L., *Chem. - Eur. J.* **2016,** *22*, 11605
(29) Sundararaju, B.; Fürstner, A., *Angew. Chem., Int. Ed.* **2013,** *52*, 14050.
(30) Yamamoto, Y.; Fujikawa, R.; Yamada, A.; Miyaura, N., *Chem. Lett.* **1999,** 1069
(31) (a) Thorpe, S. B.; Guo, X.; Santos, W. L., *Chem. Commun.* **2011,** *47*, 424 ; (b) Yuan, W.; Ma, S., *Adv. Synth. Catal.* **2012,** *354*, 1867; (c) Meng, F.; Jung, B.; Haeffner, F.; Hoveyda, A. H., *Org. Lett.* **2013,** *15*, 1414 ; (d) Semba, K.; Fujihara, T.; Terao, J.; Tsuji, Y., *Angew. Chem., Int. Ed.* **2013,** *52*, 12400 ; (e) Semba, K.; Shinomiya, M.; Fujihara, T.; Terao, J.; Tsuji, Y., *Chem. - Eur. J.* **2013,** *19*, 7125; (f) Yuan, W.; Zhang, X.; Yu, Y.; Ma, S., *Chem. - Eur. J.* **2013,** *19*, 7193
(32) Yoshida, H., *ACS Catal.* **2016,** *6*, 1799.
(33) Okuno, Y.; Yamashita, M.; Nozaki, K., *Angew. Chem., Int. Ed.* **2011,** *50*, 920.
(34) Alfaro, R.; Parra, A.; Aleman, J.; Garcia Ruano, J. L.; Tortosa, M., *J. Am. Chem. Soc.* **2012,** *134*, 15165
(35) (a) Tai, C.-C.; Yu, M.-S.; Chen, Y.-L.; Chuang, W.-H.; Lin, T.-H.; Yap, G. P. A.; Ong, T.-G., *Chem. Commun.* **2014,** *50*, 4344 ; (b) Yoshida, H.; Kageyuki, I.; Takaki, K., *Org. Lett.* **2013,** *15*, 952; (c) Itoh, T.; Shimizu, Y.; Kanai, M., *J. Am. Chem. Soc.* **2016,** *138*, 7528 ; (d) Jing, H.; Feng, X.; Guo, M.; Zhou, S.; Li, Y.; Zhang, J.; Zhao, W.; Tang, X.; Wang, G., *Asian J. Org. Chem.* **2017,** *6*, 1375
(36) Bin, H.-Y.; Wei, X.; Zi, J.; Zuo, Y.-J.; Wang, T.-C.; Zhong, C.-M., *ACS Catal.* **2015,** *5*, 6670

(37) Mateos, J.; Rivera-Chao, E.; Fa?an?s-Mastral, M. n., *ACS Catal.* **2017,** *7*, 5340
(38) Zhang, L.; Cheng, J.; Carry, B.; Hou, Z., *J. Am. Chem. Soc.* **2012,** *134*, 14314.
(39) Iwamoto, H.; Ozawa, Y.; Kubota, K.; Ito, H., *J. Org. Chem.* **2017,** *82*, 10563.
(40) Su, W.; Gong, T.-J.; Zhang, Q.; Zhang, Q.; Xiao, B.; Fu, Y., *ACS Catal.* **2016,** *6*, 6417
(41) Semba, K.; Bessho, N.; Fujihara, T.; Terao, J.; Tsuji, Y., *Angew. Chem., Int. Ed.* **2014,** *53*, 9007
(42) Ishiyama, T.; Matsuda, N.; Miyaura, N.; Suzuki, A., *J. Am. Chem. Soc.* **1993,** *115*, 11018
(43) Ishiyama, T.; Yamamoto, M.; Miyaura, N., *Chem. Lett.* **1996,** 1117
(44) Lee, C.-I.; Shih, W.-C.; Zhou, J.; Reibenspies, J. H.; Ozerov, O. V., *Angew. Chem., Int. Ed.* **2015,** *54*, 14003
(45) Iwadate, N.; Suginome, M., *J. Am. Chem. Soc.* **2010,** *132*, 2548
(46) (a) Ishiyama, T.; Kitano, T.; Miyaura, N., *Tetrahedron Lett.* **1998,** *39*, 2357; (b) Yang, F.-Y.; Cheng, C.-H., *J. Am. Chem. Soc.* **2001,** *123*, 761; (c) Bonet, A.; Pubill-Ulldemolins, C.; Bo, C.; Gulyas, H.; Fernandez, E., *Angew. Chem., Int. Ed.* **2011,** *50*, 7158
(47) Woodward, A. R.; Burks, H. E.; Chan, L. M.; Morken, J. P., *Org. Lett.* **2005,** *7*, 5505
(48) Sleber, J. D.; Morken, J. P., *J. Am. Chem. Soc.* **2006,** *128*, 74
(49) Suginome, M.; Nakamura, H.; Ito, Y., *Chem. Commun.* **1996,** 2777
(50) Suginome, M.; Matsuda, T.; Ito, Y., *Organometallics* **1998,** *17*, 5233
(51) (a) Suginome, M.; Ito, Y., *J. Organomet. Chem.* **2003,** *680*, 43 ; (b) Ohmura, T.; Suginome, M., *Bull. Chem. Soc. Jpn.* **2009,** *82*, 29
(52) (a) Suginome, M.; Matsuda, T.; Nakamura, H.; Ito, Y., *Tetrahedron* **1999,** *55*, 8787; (b) Morita, R.; Shirakawa, E.; Tsnchimoto, T.; Kawakami, Y., *Org. Biomol. Chem.* **2005,** *3*, 1263 ; (c) Ohmura, T.; Oshima, K.; Suginome, M., *Chem. Commun.* **2008,** 1416 ; (d) Zhou, H.; Moberg, C., *J. Am. Chem. Soc.* **2012,** *134*, 15992; (e) Ohmura, T.; Oshima, K.; Suginome, M., *Organometallics* **2013,** *32*, 2870 ; (f) Saito, N.; Saito, K.; Sato, H.; Sato, Y., *Adv. Synth. Catal.* **2013,** *355*, 853
(53) Suginome, M.; Ohmori, Y.; Ito, Y., *Synlett* **1999,** 1567
(54) Suginome; Ohmori; Ito, *J. Am. Chem. Soc.* **2001,** *123*, 4601
(55) Suginome, M.; Ohmura, T.; Miyake, Y.; Mitani, S. i.; Ito, Y.; Murakami, M., *J. Am. Chem. Soc.* **2003,** *125*, 11174.
(56) (a) Onozawa, S.-y.; Hatanaka, Y.; Sakakura, T.; Shimada, S.; Tanaka, M., *Organometallics* **1996,** *15*, 5450; (b) Murakami, M.; Ashida, S.; Matsuda, T., *J. Am. Chem. Soc.* **2004,** *126*, 10838 ; (c) Singidi, R. R.; Rajanbabu, *Org. Lett.* **2010,** *12*, 2622
(57) Yoshida, H.; Kimura, M.; Osaka, I.; Takaki, K., *Organometallics* **2017,** *36*, 1345
(58) Yoshida; Takemoto; Takaki, *Chem. Commun.* **2015,** *51*, 6297
(59) Takemoto, Y.; Yoshida, H.; Takaki, K., *Chem. - Eur. J.* **2012,** *18*, 14841.
(60) Lappert, M. F.; Prokai, B., *J. Organomet. Chem.* **1964,** *1*, 384.
(61) Satoh, Y.; Serizawa, H.; Miyaura, N.; Hara, S.; Suzuki, A., *Tetrahedron Lett.* **1988,** *29*, 1811.

(62) (a) Wang, K. K.; Wang, Z., *Tetrahedron Lett.* **1994,** *35*, 1829; (b) Wang, K. K.; Wang, Z.; Tarli, A.; Gannett, P., *J. Am. Chem. Soc.* **1996,** *118*, 10783; (c) Tarli, A.; Wang, K. K., *J. Org. Chem.* **1997,** *62*, 8841.
(63) Wang, C.; Tobrman, T.; Xu, Z.; Negishi, E.-I., *Org. Lett.* **2009,** *11*, 4092
(64) Moriya, T.; Miyaura, N.; Suzuki, A., *Chem. Lett.* **1993,** 1429
(65) (a) Brown, H. C.; Imai, T., *Organometallics* **1984,** *3*, 1392 ; (b) Brown, H. C.; Imai, T.; Bhat, N. G., *J. Org. Chem.* **1986,** *51*, 5277.
(66) Makoto, S.; Norio, M.; Akira, S., *Chem. Lett.* **1986,** *15*, 1329.
(67) Deloux, L.; Skrzypczak-Jankun, E.; Cheesman, B. V.; Srebnik, M.; Sabat, M., *J. Am. Chem. Soc.* **1994,** *116*, 10302
(68) Srebnik, M.; Bhat, N. G.; Brown, H. C., *Tetrahedron Lett.* **1988,** *29*, 2635.
(69) (a) Li, H.; Carroll, P. J.; Walsh, P. J., *J. Am. Chem. Soc.* **2008,** *130*, 3521 ; (b) Hussain, M. M.; Li, H.; Hussain, N.; Urena, M.; Carroll, P. J.; Walsh, P. J., *J. Am. Chem. Soc.* **2009,** *131*, 6516 ; (c) Hussain, M. M.; Walsh, P. J., *Angew. Chem., Int. Ed.* **2010,** *49*, 1834 ; (d) Hernandez-Toribio, J.; Hussain, M. M.; Cheng, K.; Carroll, P. J.; Walsh, P. J., *Org. Lett.* **2011,** *13*, 6094 ; (e) Hussain, M. M.; Hernandez Toribio, J.; Carroll, P. J.; Walsh, P. J., *Angew. Chem., Int. Ed.* **2011,** *50*, 6337 ; (f) Hussain, N.; Hussain, M. M.; Ziauddin, M.; Triyawatanyu, P.; Walsh, P. J., *Org. Lett.* **2011,** *13*, 6464 ; (g) Hussain, N.; Hussain, M. M.; Carroll, P. J.; Walsh, P. J., *Chem. Sci.* **2013,** *4*, 3946 ; (h) Kim, B.-S.; Hussain, M. M.; Hussain, N.; Walsh, P. J., *Chem. - Eur. J.* **2014,** *20*, 11726
(70) Srebnik, M., *Tetrahedron Lett.* **1991,** *32*, 2449.
(71) Rudolph, J.; Schmidt, F.; Bolm, C., *Synthesis* **2005,** *2005*, 840.
(72) Krautwald, S.; Bezdek, M. t. J.; Chirik, P. J., *J. Am. Chem. Soc.* **2017,** *139*, 3868
(73) (a) Coapes, R. B.; Souza, F. E. S.; Thomas, R. L.; Hall, J. J.; Marder, T. B., *Chem. Commun.* **2003,** 614; (b) Mkhalid, I. A. I.; Coapes, R. B.; Edes, S. N.; Coventry, D. N.; Souza, F. E. S.; Thomas, R. L.; Hall, J. J.; Bi, S.-W.; Lin, Z.; Marder, T. B., *Dalton Trans.* **2008,** 1055; (c) Takaya, J.; Kirai, N.; Iwasawa, N., *J. Am. Chem. Soc.* **2011,** *133*, 12980; (d) Kirai, N.; Iguchi, S.; Ito, T.; Takaya, J.; Iwasawa, N., *Bull. Chem. Soc. Jpn.* **2013,** *86*, 784.
(74) Wang, C.; Wu, C.; Ge, S., *ACS Catal.* **2016,** *6*, 7585.
(75) Heck, R. F., Palladium-Catalyzed Vinylation of Organic Halides. In *Organic Reactions*, John Wiley & Sons, Inc.: 2004.
(76) Krause, S. B.; McAtee, J. R.; Yap, G. P. A.; Watson, D. A., *Org. Lett.* **2017,** *19*, 5641.
(77) Shade, R. E.; Hyde, A. M.; Olsen, J.-C.; Merlic, C. A., *J. Am. Chem. Soc.* **2010,** *132*, 1202.
(78) (a) Olsson, V. J.; Szabó, K. J., *Angew. Chem., Int. Ed.* **2007,** *46*, 6891; (b) Olsson, V. J.; Szabó, K. J., *J. Org. Chem.* **2009,** *74*, 7715; (c) Kondoh, A.; Jamison, T. F., *Chem. Commun.* **2010,** *46*, 907; (d) Selander, N.; Willy, B.; Szabó, K. J., *Angew. Chem., Int. Ed.* **2010,** *49*, 4051.
(79) Pangborn, A. B.; Giardello, M. A.; Grubbs, R. H.; Rosen, R. K.; Timmers, F. J., *Organometallics* **1996,** *15*, 1518.

(80) McAtee, J. R.; Yap, G. P. A.; Watson, D. A., *J. Am. Chem. Soc.* **2014,** *136*, 10166.
(81) Wrackmeyer, B., *Prog. Nucl. Magn. Reson. Spectrosc.* **1979,** *12*, 227.
(82) Hitosugi, S.; Tanimoto, D.; Nakanishi, W.; Isobe, H., *Chem. Lett.* **2012,** *41*, 972.
(83) Gallagher, W. P.; Vo, A., *Org. Process Res. Dev.* **2015,** *19*, 1369.
(84) *Apex3 software suite*, Bruker AXS, Inc.: Madison, WI, 2015.
(85) Sheldrick, G., *Acta Crystallographica Section C* **2015,** *71*, 3.

Appendix A

Permission for Published Work

Title: The first example of nickel-catalyzed silyl-Heck reactions: direct activation of silyl triflates without iodide additives

Author: Jesse R. McAtee,Sara E.S. Martin,Andrew P. Cinderella,William B. Reid,Keywan A. Johnson,Donald A. Watson

Publication: Tetrahedron

Publisher: Elsevier

Date: 8 July 2014

Order Completed

Thank you for your order.

This Agreement between University of Delaware -- William Reid ("You") and Elsevier ("Elsevier") consists of your license details and the terms and conditions provided by Elsevier and Copyright Clearance Center.

Your confirmation email will contain your order number for future reference.

printable details

License Number	4330220456418
License date	Apr 15, 2018
Licensed Content Publisher	Elsevier
Licensed Content Publication	Tetrahedron
Licensed Content Title	The first example of nickel-catalyzed silyl-Heck reactions: direct activation of silyl triflates without iodide additives
Licensed Content Author	Jesse R. McAtee,Sara E.S. Martin,Andrew P. Cinderella,William B. Reid,Keywan A. Johnson,Donald A. Watson
Licensed Content Date	Jul 8, 2014
Licensed Content Volume	70
Licensed Content Issue	27-28
Licensed Content Pages	7
Type of Use	reuse in a thesis/dissertation
Portion	full article
Format	electronic
Are you the author of this Elsevier article?	No
Will you be translating?	No
Title of your thesis/dissertation	Recent Advances in Heteroatomic-Heck Reactions Towards the Synthesis of Unsaturated Silanes and Boronic Esters
Expected completion date	Apr 2018

Estimated size (number of pages)	500
Attachment	
Requestor Location	University of Delaware 104 Brown Lab NEWARK, DE 19711 United States Attn: University of Delaware
Publisher Tax ID	98-0397604
Total	0.00 USD

ORDER MORE **CLOSE WINDOW**

Title: Direct Synthesis of Alkenyl Boronic Esters from Unfunctionalized Alkenes: A Boryl-Heck Reaction

Author: William B. Reid, Jesse J. Spillane, Sarah B. Krause, et al

Publication: Journal of the American Chemical Society

Publisher: American Chemical Society

Date: May 1, 2016

PERMISSION/LICENSE IS GRANTED FOR YOUR ORDER AT NO CHARGE

This type of permission/license, instead of the standard Terms & Conditions, is sent to you because no fee is being charged for your order. Please note the following:

- Permission is granted for your request in both print and electronic formats, and translations.
- If figures and/or tables were requested, they may be adapted or used in part.
- Please print this page for your records and send a copy of it to your publisher/graduate school.
- Appropriate credit for the requested material should be given as follows: "Reprinted (adapted) with permission from (COMPLETE REFERENCE CITATION). Copyright (YEAR) American Chemical Society." Insert appropriate information in place of the capitalized words.
- One-time permission is granted only for the use specified in your request. No additional uses are granted (such as derivative works or other editions). For any other uses, please submit a new request.

Appendix B

Spectral Data for Chapter 1

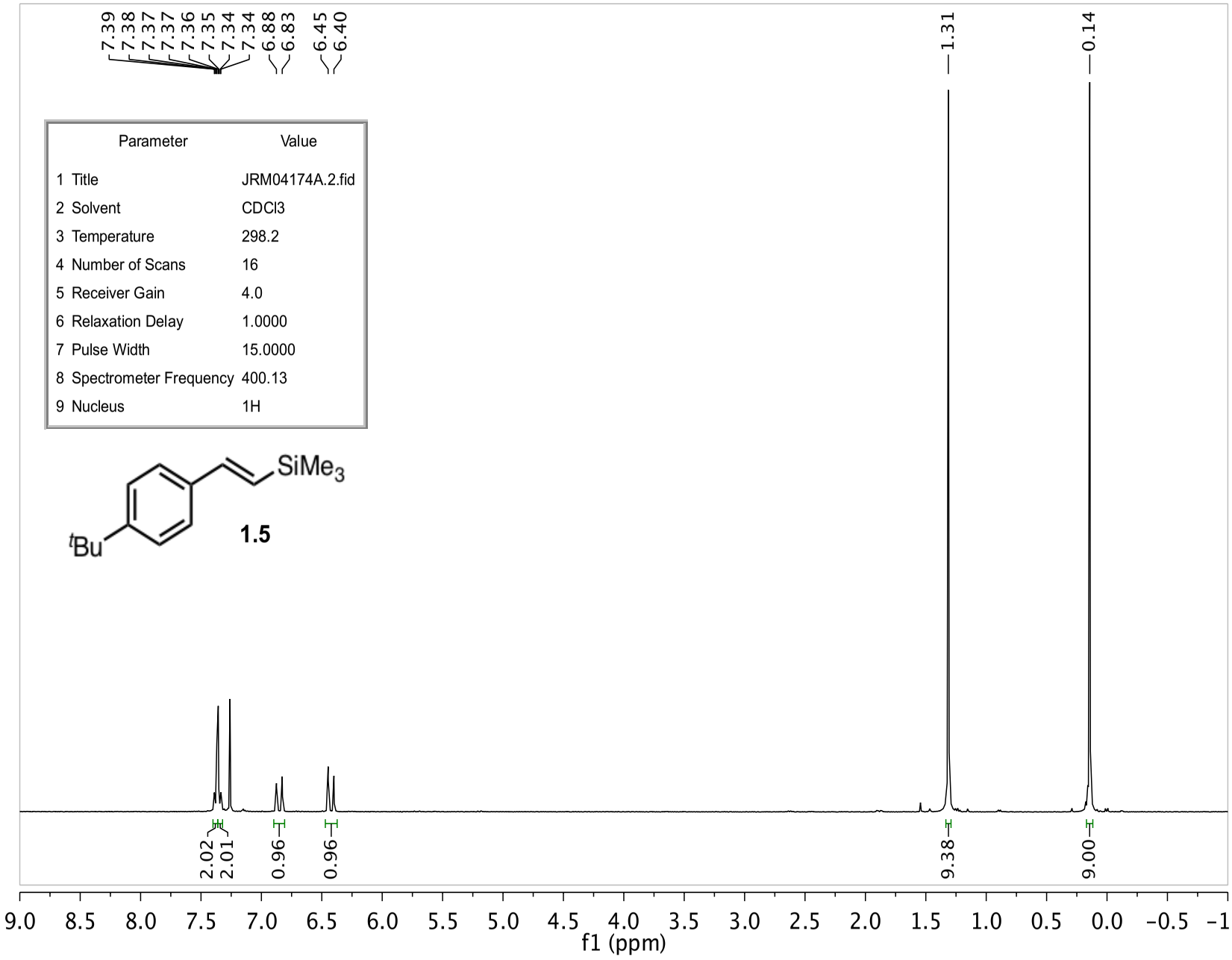
7.39
7.38
7.37
7.37
7.36
7.35
7.34
7.34
6.88
6.83
6.45
6.40
1.31
0.14
Parameter Value
1 Title JRM04174A.2.fid
2 Solvent CDCl3
3 Temperature 298.2
4 Number of Scans 16
5 Receiver Gain 4.0
6 Relaxation Delay 1.0000
7 Pulse Width 15.0000
8 Spectrometer Frequency 400.13
9 Nucleus 1H
SiMe3
tBu
1.5
2.02
2.01
0.96
0.96
9.38
9.00
9.0 8.5 8.0 7.5 7.0 6.5 6.0 5.5 5.0 4.5 4.0 3.5 3.0 2.5 2.0 1.5 1.0 0.5 0.0 -0.5 -1.0
f1 (ppm)

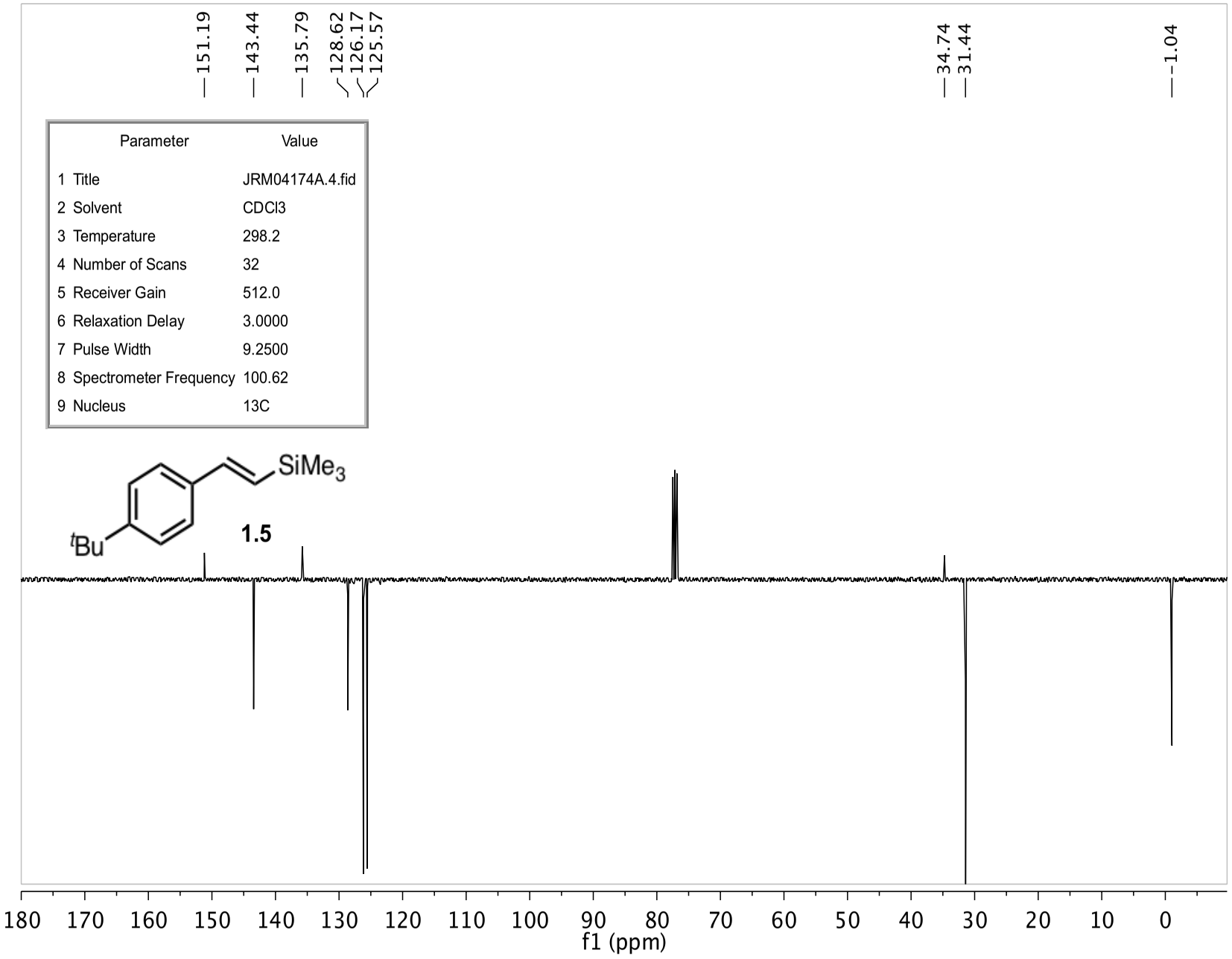
151.19
143.44
135.79
128.62
126.17
125.57
34.74
31.44
-1.04
Parameter Value
1 Title JRM04174A.4.fid
2 Solvent CDCl3
3 Temperature 298.2
4 Number of Scans 32
5 Receiver Gain 512.0
6 Relaxation Delay 3.0000
7 Pulse Width 9.2500
8 Spectrometer Frequency 100.62
9 Nucleus 13C
SiMe3
tBu
1.5
180 170 160 150 140 130 120 110 100 90 80 70 60 50 40 30 20 10 0
f1 (ppm)

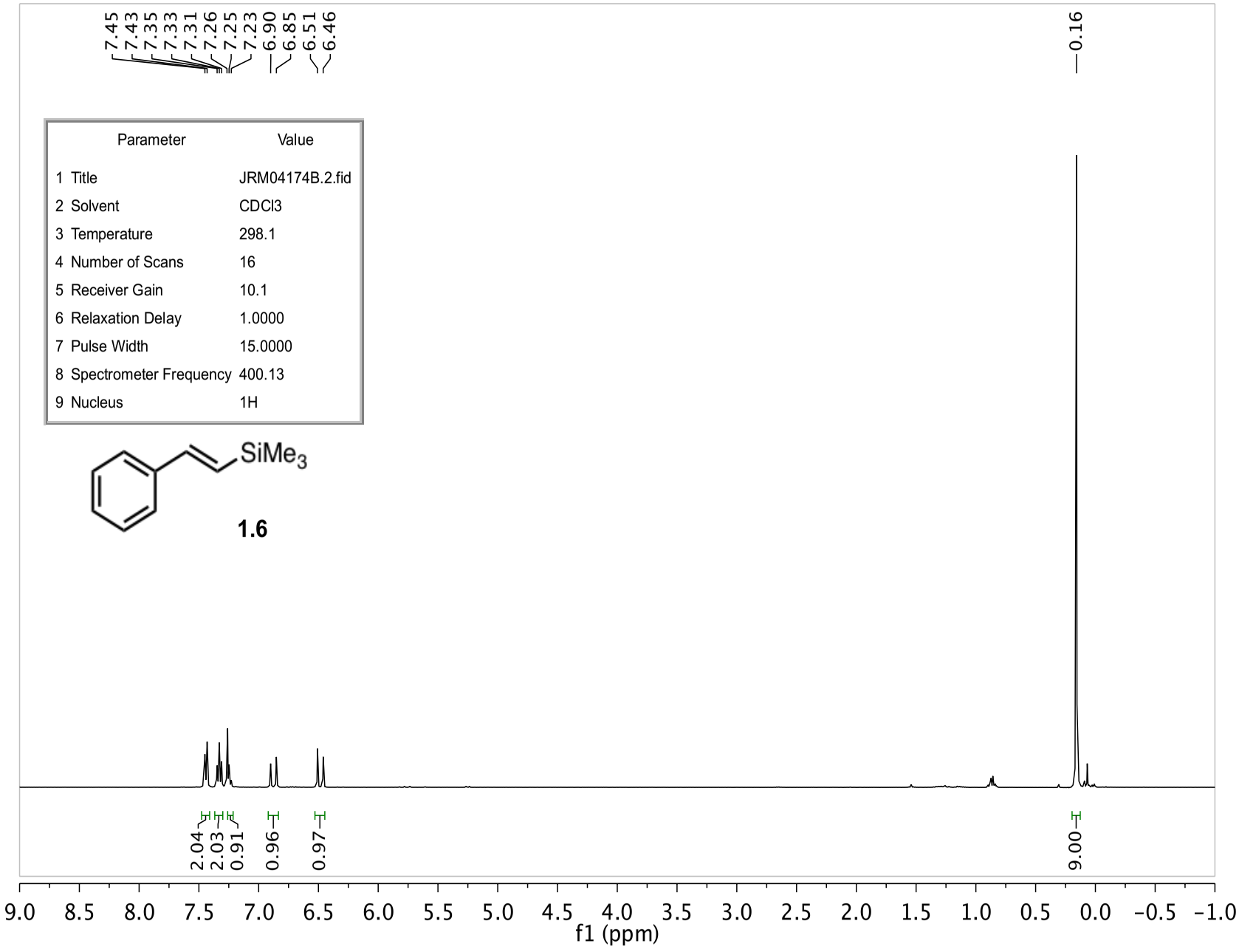
7.45
7.43
7.35
7.33
7.31
7.26
7.25
7.23
6.90
6.85
6.51
6.46
0.16
Parameter Value
1 Title JRM04174B.2.fid
2 Solvent CDCl3
3 Temperature 298.1
4 Number of Scans 16
5 Receiver Gain 10.1
6 Relaxation Delay 1.0000
7 Pulse Width 15.0000
8 Spectrometer Frequency 400.13
9 Nucleus 1H
SiMe3
1.6
2.04
2.03
0.91
0.96
0.97
9.00
9.0 8.5 8.0 7.5 7.0 6.5 6.0 5.5 5.0 4.5 4.0 3.5 3.0 2.5 2.0 1.5 1.0 0.5 0.0 -0.5 -1.0
f1 (ppm)

1.

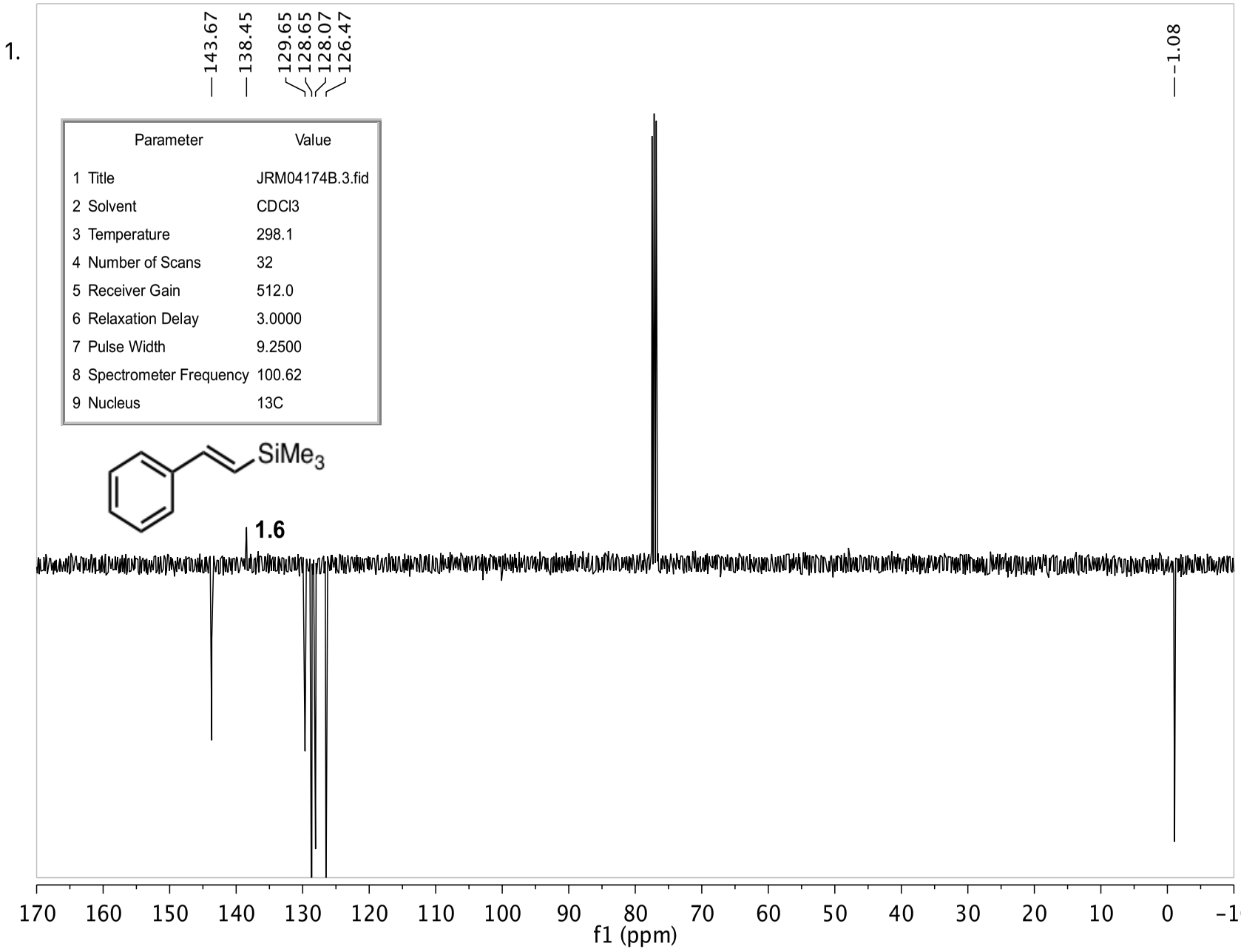
1.
143.67
138.45
129.65
128.65
128.07
126.47
-1.08
Parameter Value
1 Title JRM04174B.3.fid
2 Solvent CDCl3
3 Temperature 298.1
4 Number of Scans 32
5 Receiver Gain 512.0
6 Relaxation Delay 3.0000
7 Pulse Width 9.2500
8 Spectrometer Frequency 100.62
9 Nucleus 13C
SiMe3
1.6
170 160 150 140 130 120 110 100 90 80 70 60 50 40 30 20 10 0 -10
f1 (ppm)

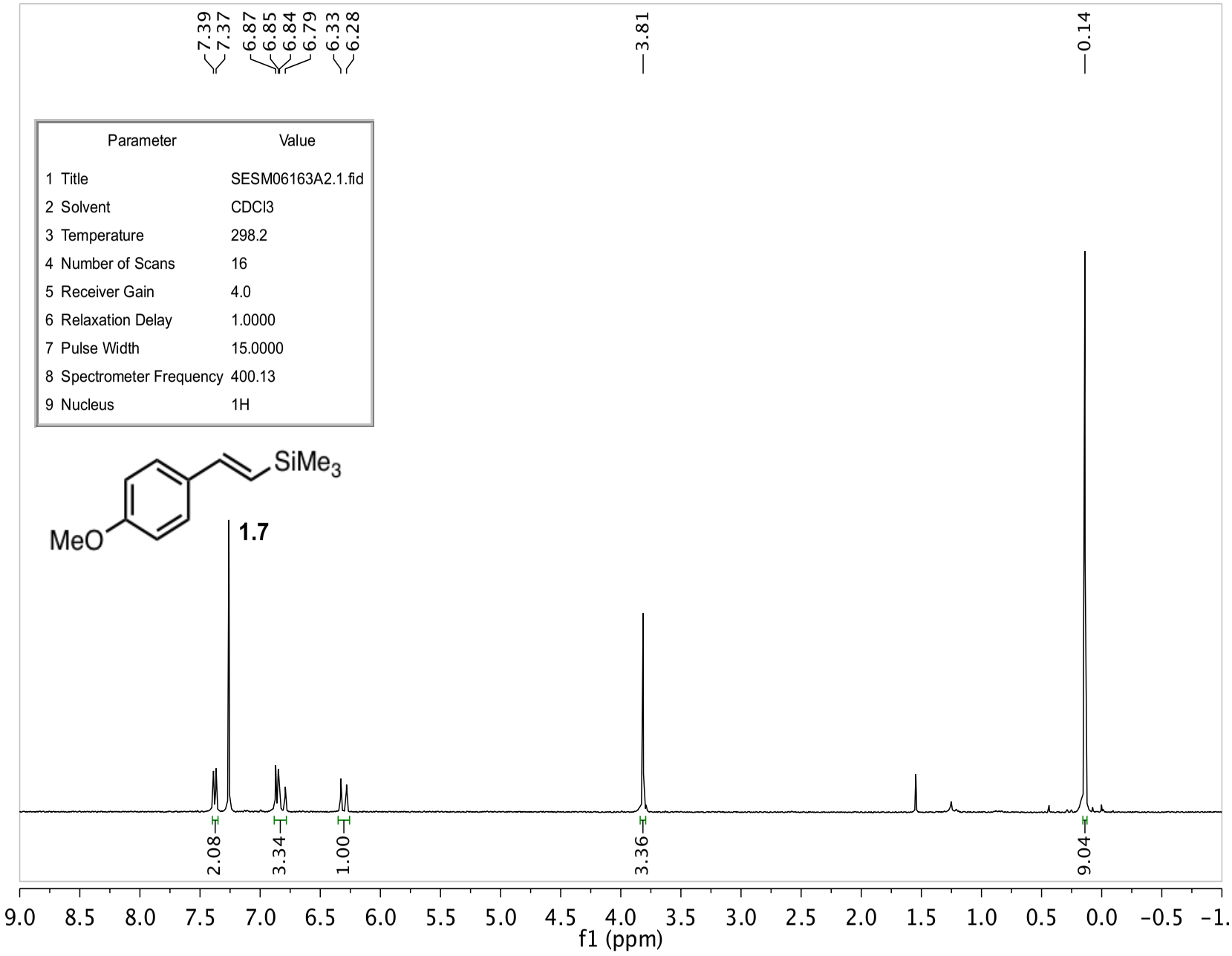
7.39
7.37
6.87
6.85
6.84
6.79
6.33
6.28
3.81
0.14
Parameter Value
1 Title SESM06163A2.1.fid
2 Solvent CDCl3
3 Temperature 298.2
4 Number of Scans 16
5 Receiver Gain 4.0
6 Relaxation Delay 1.0000
7 Pulse Width 15.0000
8 Spectrometer Frequency 400.13
9 Nucleus 1H
SiMe3
MeO
1.7
2.08
3.34
1.00
3.36
9.04
9.0 8.5 8.0 7.5 7.0 6.5 6.0 5.5 5.0 4.5 4.0 3.5 3.0 2.5 2.0 1.5 1.0 0.5 0.0 -0.5 -1.0
f1 (ppm)

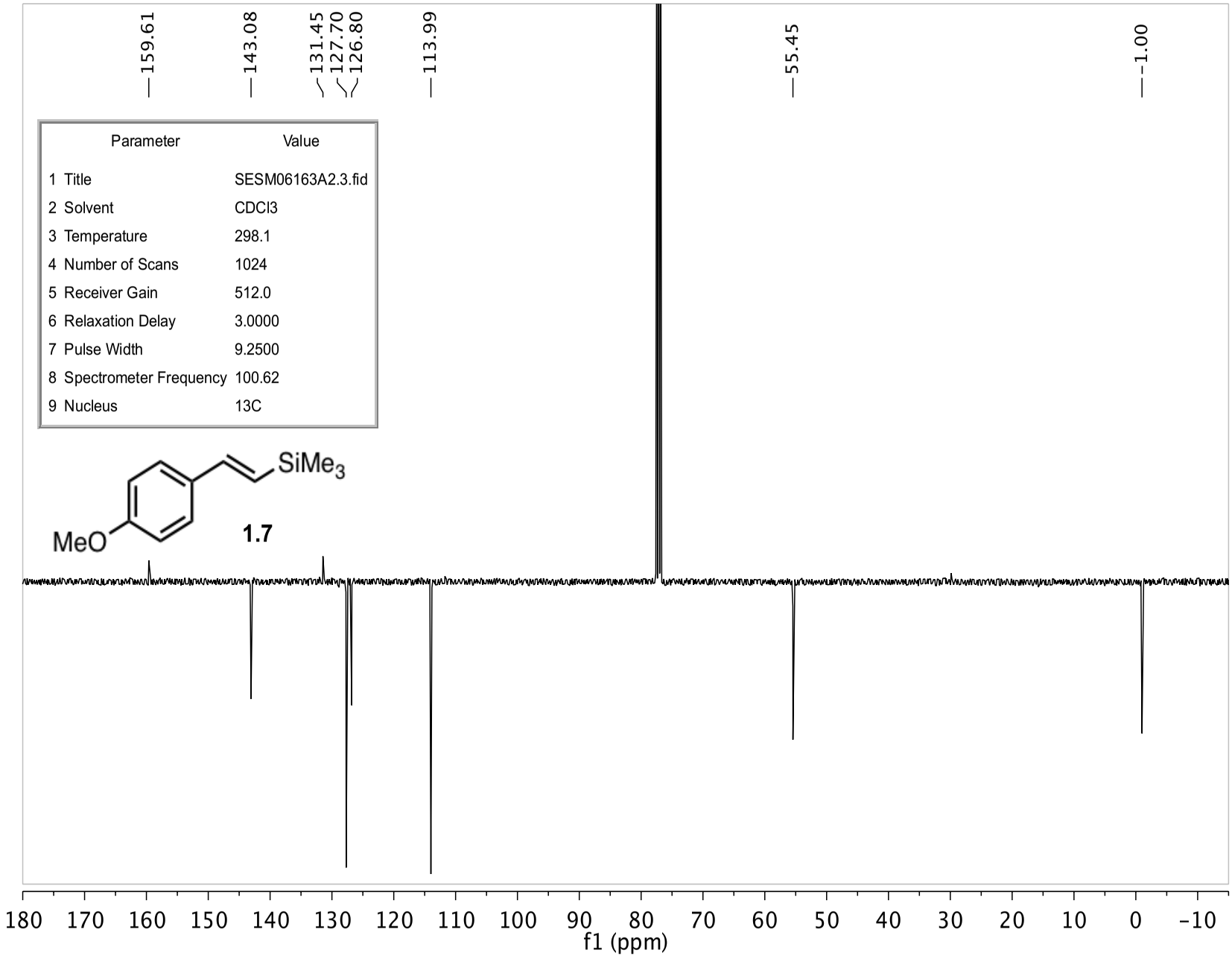
159.61
143.08
131.45
127.70
126.80
113.99
55.45
1.00
Parameter Value
1 Title SESM06163A2.3.fid
2 Solvent CDCl3
3 Temperature 298.1
4 Number of Scans 1024
5 Receiver Gain 512.0
6 Relaxation Delay 3.0000
7 Pulse Width 9.2500
8 Spectrometer Frequency 100.62
9 Nucleus 13C
SiMe3
MeO
1.7
180 170 160 150 140 130 120 110 100 90 80 70 60 50 40 30 20 10 0 -10
f1 (ppm)

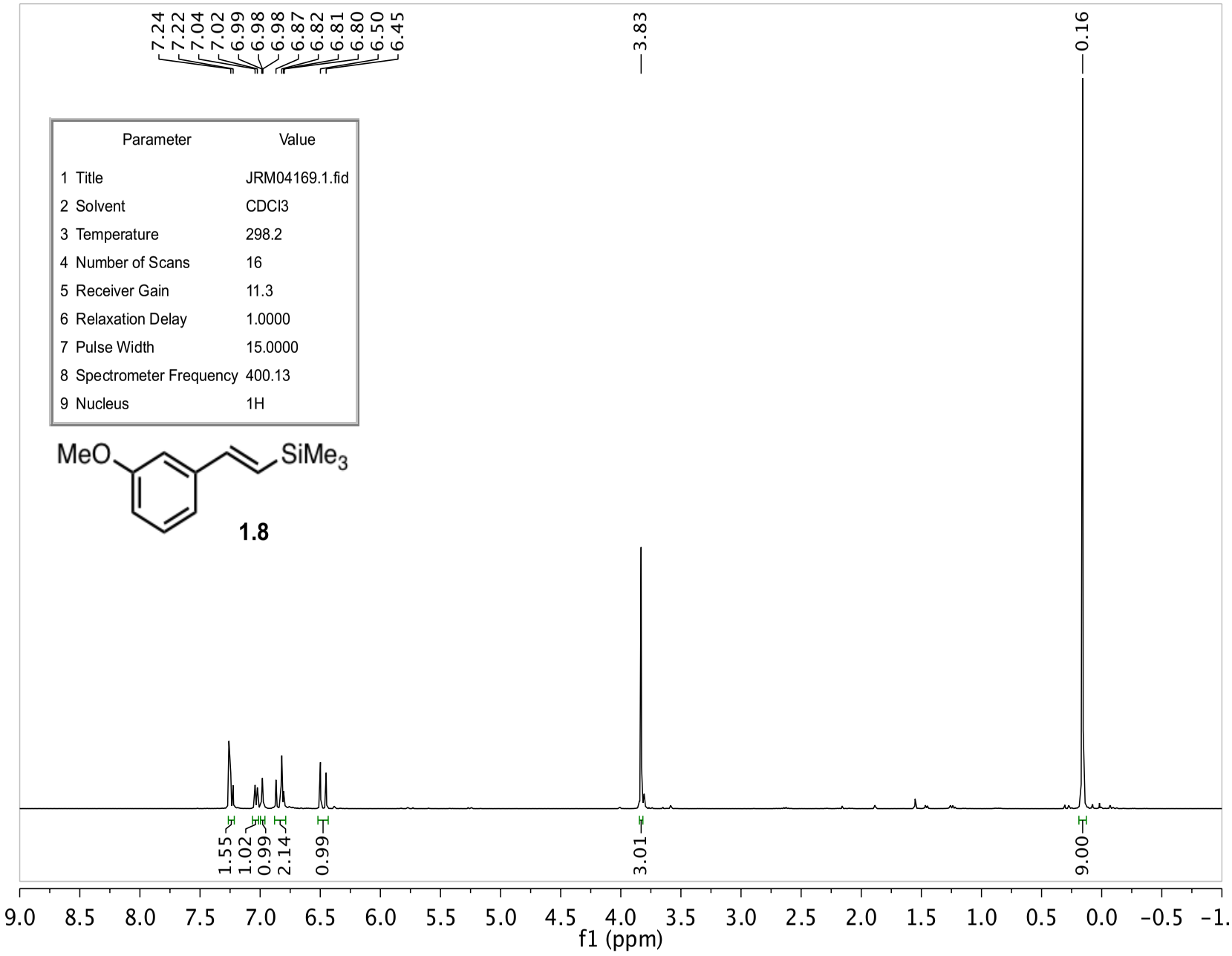
7.24
7.22
7.04
7.02
6.99
6.98
6.98
6.87
6.82
6.81
6.80
6.50
6.45
3.83
0.16
Parameter Value
1 Title JRM04169.1.fid
2 Solvent CDCl3
3 Temperature 298.2
4 Number of Scans 16
5 Receiver Gain 11.3
6 Relaxation Delay 1.0000
7 Pulse Width 15.0000
8 Spectrometer Frequency 400.13
9 Nucleus 1H
MeO
SiMe3
1.8
1.55
1.02
0.99
2.14
0.99
3.01
9.00
9.0 8.5 8.0 7.5 7.0 6.5 6.0 5.5 5.0 4.5 4.0 3.5 3.0 2.5 2.0 1.5 1.0 0.5 0.0 -0.5 -1.0
f1 (ppm)

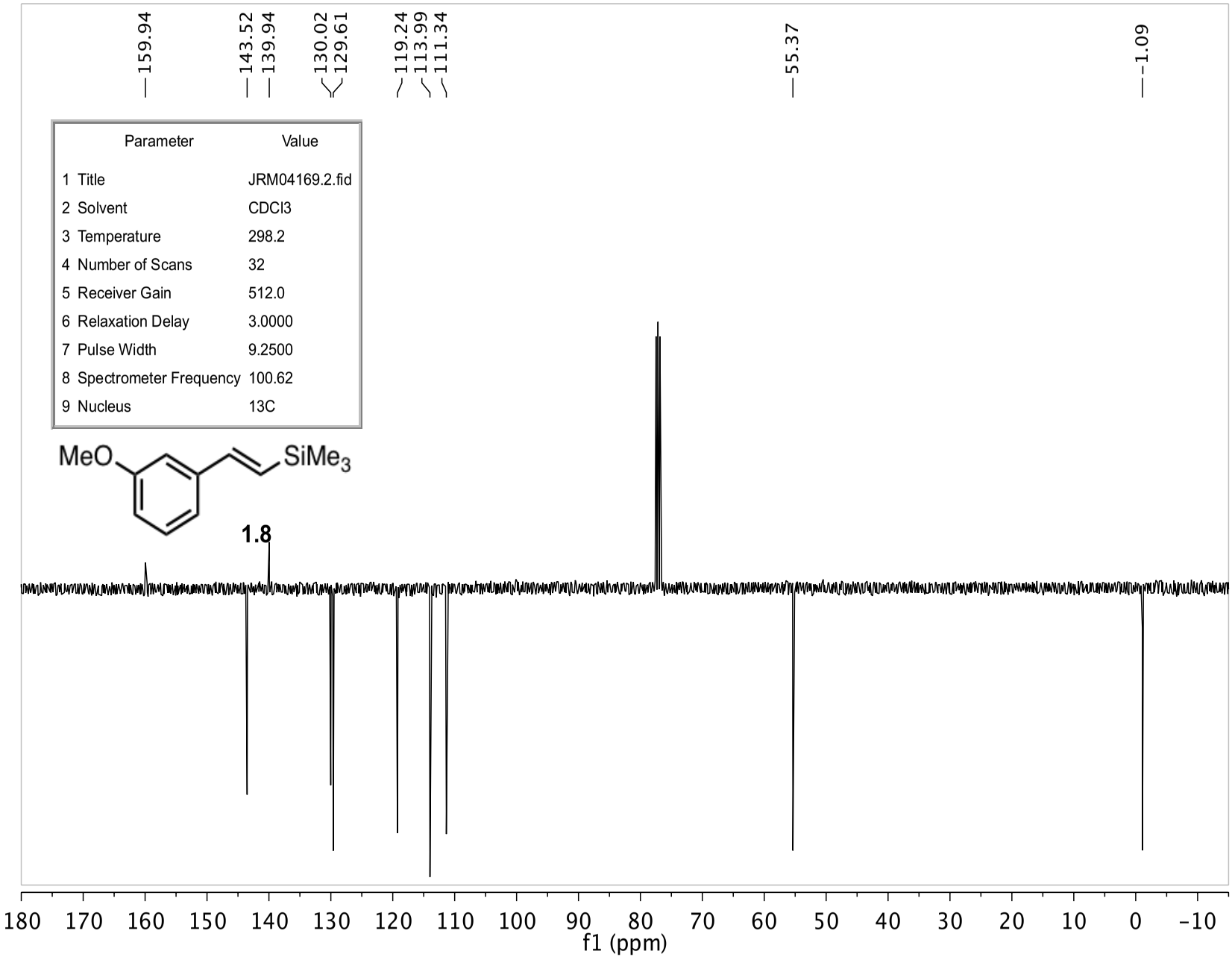
159.94
143.52
139.94
130.02
129.61
119.24
113.99
111.34
55.37
1.09
Parameter Value
1 Title JRM04169.2.fid
2 Solvent CDCl3
3 Temperature 298.2
4 Number of Scans 32
5 Receiver Gain 512.0
6 Relaxation Delay 3.0000
7 Pulse Width 9.2500
8 Spectrometer Frequency 100.62
9 Nucleus 13C
MeO
SiMe3
1.8
180 170 160 150 140 130 120 110 100 90 80 70 60 50 40 30 20 10 0 -10
f1 (ppm)

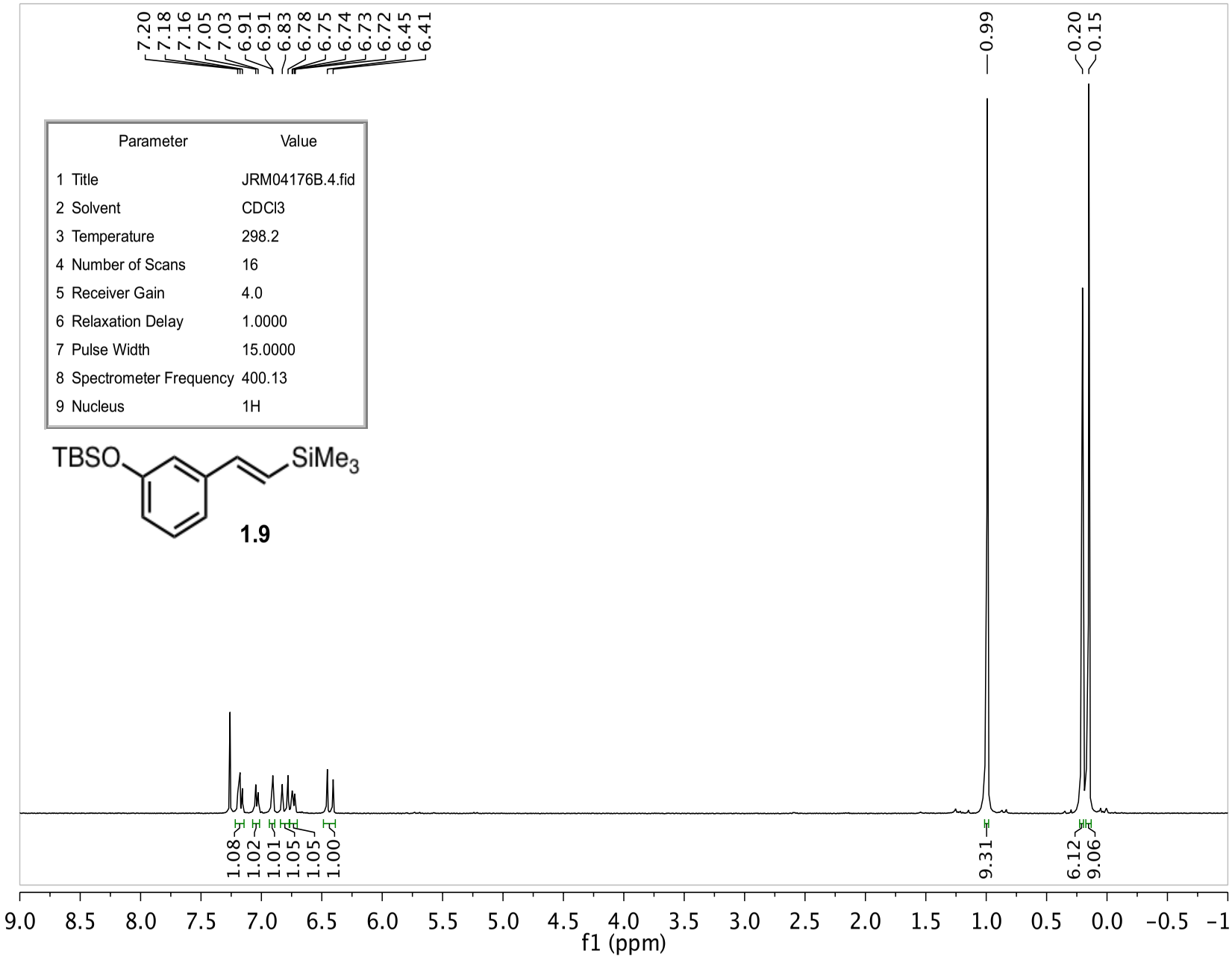
7.20
7.18
7.16
7.05
7.03
6.91
6.91
6.83
6.78
6.75
6.74
6.73
6.72
6.45
6.41
0.99
0.20
0.15
Parameter Value
1 Title JRM04176B.4.fid
2 Solvent CDCl3
3 Temperature 298.2
4 Number of Scans 16
5 Receiver Gain 4.0
6 Relaxation Delay 1.0000
7 Pulse Width 15.0000
8 Spectrometer Frequency 400.13
9 Nucleus 1H
TBSO
SiMe3
1.9
1.08
1.02
1.01
1.05
1.05
1.00
9.31
6.12
9.06
9.0 8.5 8.0 7.5 7.0 6.5 6.0 5.5 5.0 4.5 4.0 3.5 3.0 2.5 2.0 1.5 1.0 0.5 0.0 -0.5 -1.0
f1 (ppm)

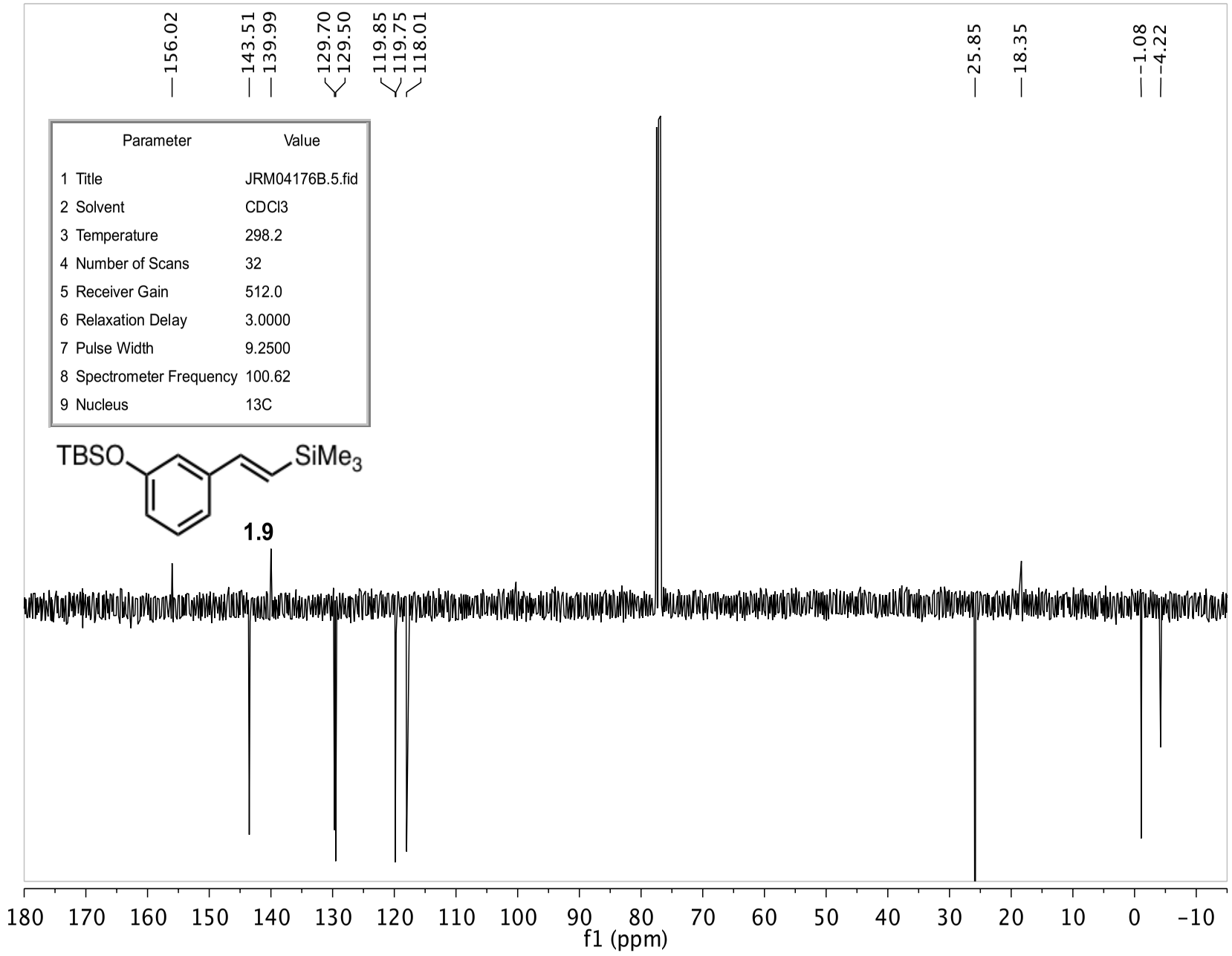
156.02
143.51
139.99
129.70
129.50
119.85
119.75
118.01
25.85
18.35
-1.08
-4.22
Parameter Value
1 Title JRM04176B.5.fid
2 Solvent CDCl3
3 Temperature 298.2
4 Number of Scans 32
5 Receiver Gain 512.0
6 Relaxation Delay 3.0000
7 Pulse Width 9.2500
8 Spectrometer Frequency 100.62
9 Nucleus 13C
TBSO
SiMe3
1.9
180 170 160 150 140 130 120 110 100 90 80 70 60 50 40 30 20 10 0 -10
f1 (ppm)

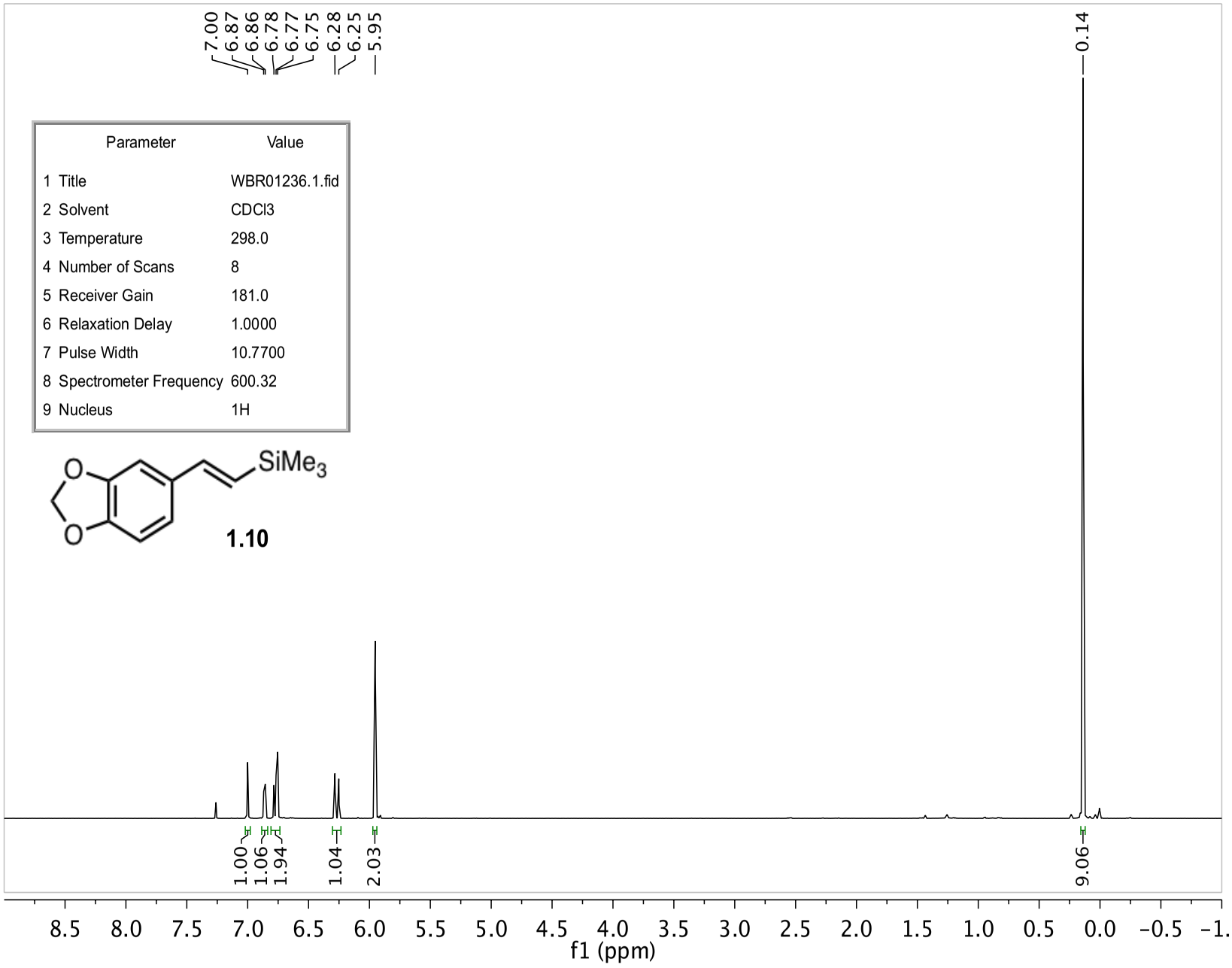
7.00
6.87
6.86
6.78
6.77
6.75
6.28
6.25
5.95
0.14
Parameter Value
1 Title WBR01236.1.fid
2 Solvent CDCl3
3 Temperature 298.0
4 Number of Scans 8
5 Receiver Gain 181.0
6 Relaxation Delay 1.0000
7 Pulse Width 10.7700
8 Spectrometer Frequency 600.32
9 Nucleus 1H
SiMe3
1.10
1.00
1.06
1.94
1.04
2.03
9.06
8.5 8.0 7.5 7.0 6.5 6.0 5.5 5.0 4.5 4.0 3.5 3.0 2.5 2.0 1.5 1.0 0.5 0.0 -0.5 -1.0
f1 (ppm)

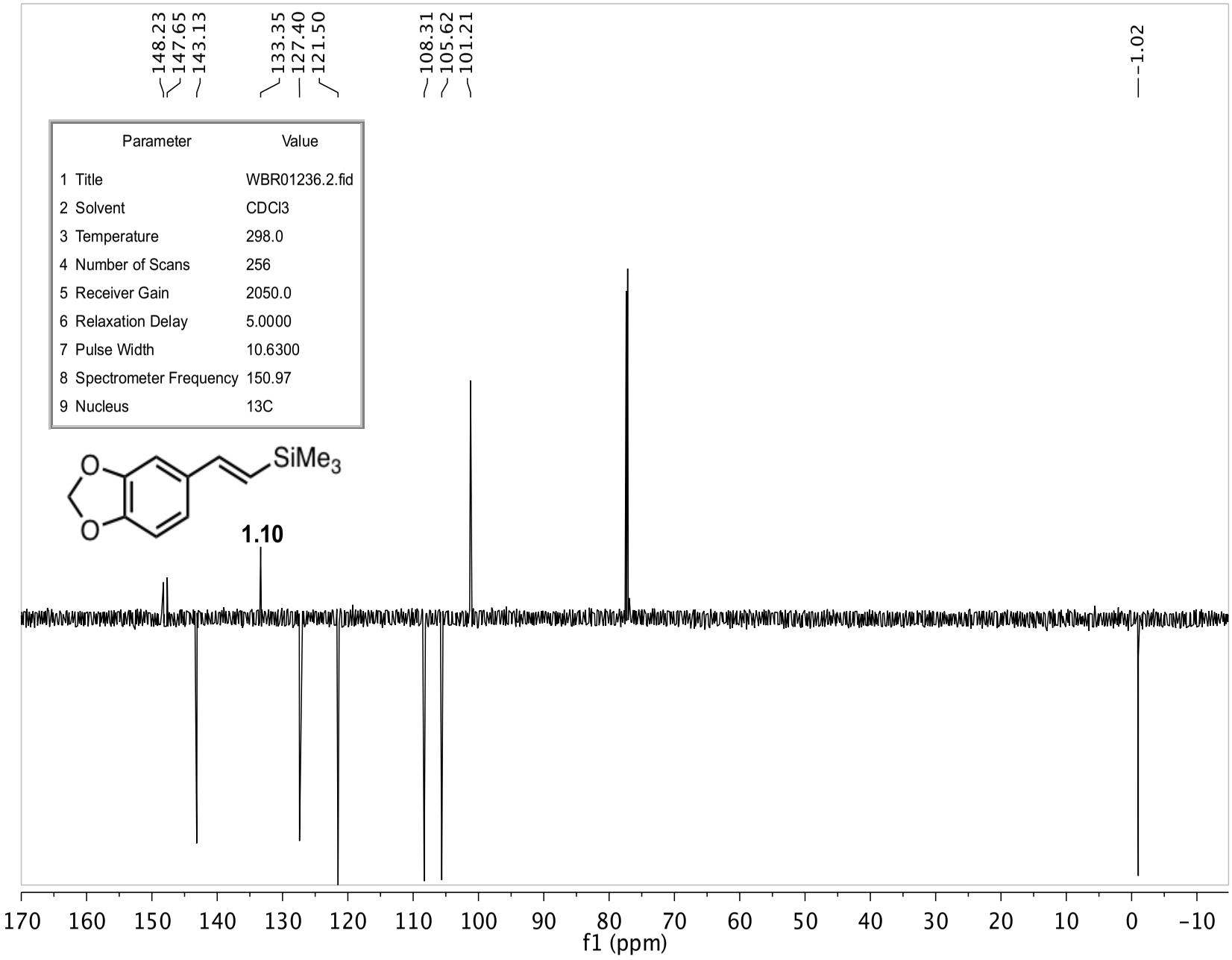
148.23
147.65
143.13
133.35
127.40
121.50
108.31
105.62
101.21
1.02
Parameter Value
1 Title WBR01236.2.fid
2 Solvent CDCl3
3 Temperature 298.0
4 Number of Scans 256
5 Receiver Gain 2050.0
6 Relaxation Delay 5.0000
7 Pulse Width 10.6300
8 Spectrometer Frequency 150.97
9 Nucleus 13C
SiMe3
O
O
1.10
170 160 150 140 130 120 110 100 90 80 70 60 50 40 30 20 10 0 -10
f1 (ppm)

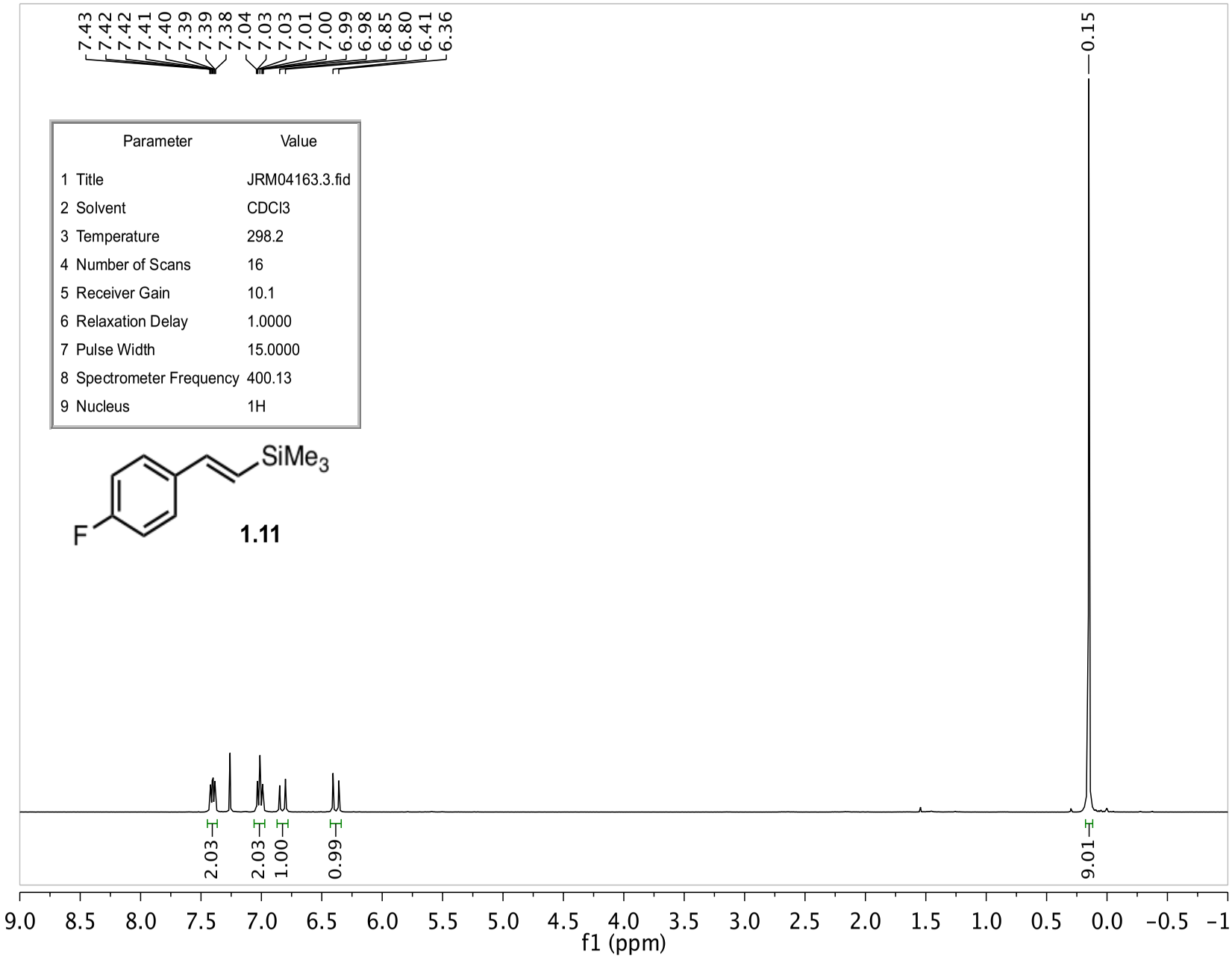
7.43
7.42
7.42
7.41
7.40
7.39
7.39
7.38
7.04
7.03
7.03
7.01
7.00
6.99
6.98
6.85
6.80
6.41
6.36
0.15
Parameter Value
1 Title JRM04163.3.fid
2 Solvent CDCl3
3 Temperature 298.2
4 Number of Scans 16
5 Receiver Gain 10.1
6 Relaxation Delay 1.0000
7 Pulse Width 15.0000
8 Spectrometer Frequency 400.13
9 Nucleus 1H
SiMe3
F
1.11
2.03
2.03
1.00
0.99
9.01
9.0 8.5 8.0 7.5 7.0 6.5 6.0 5.5 5.0 4.5 4.0 3.5 3.0 2.5 2.0 1.5 1.0 0.5 0.0 -0.5 -1.0
f1 (ppm)

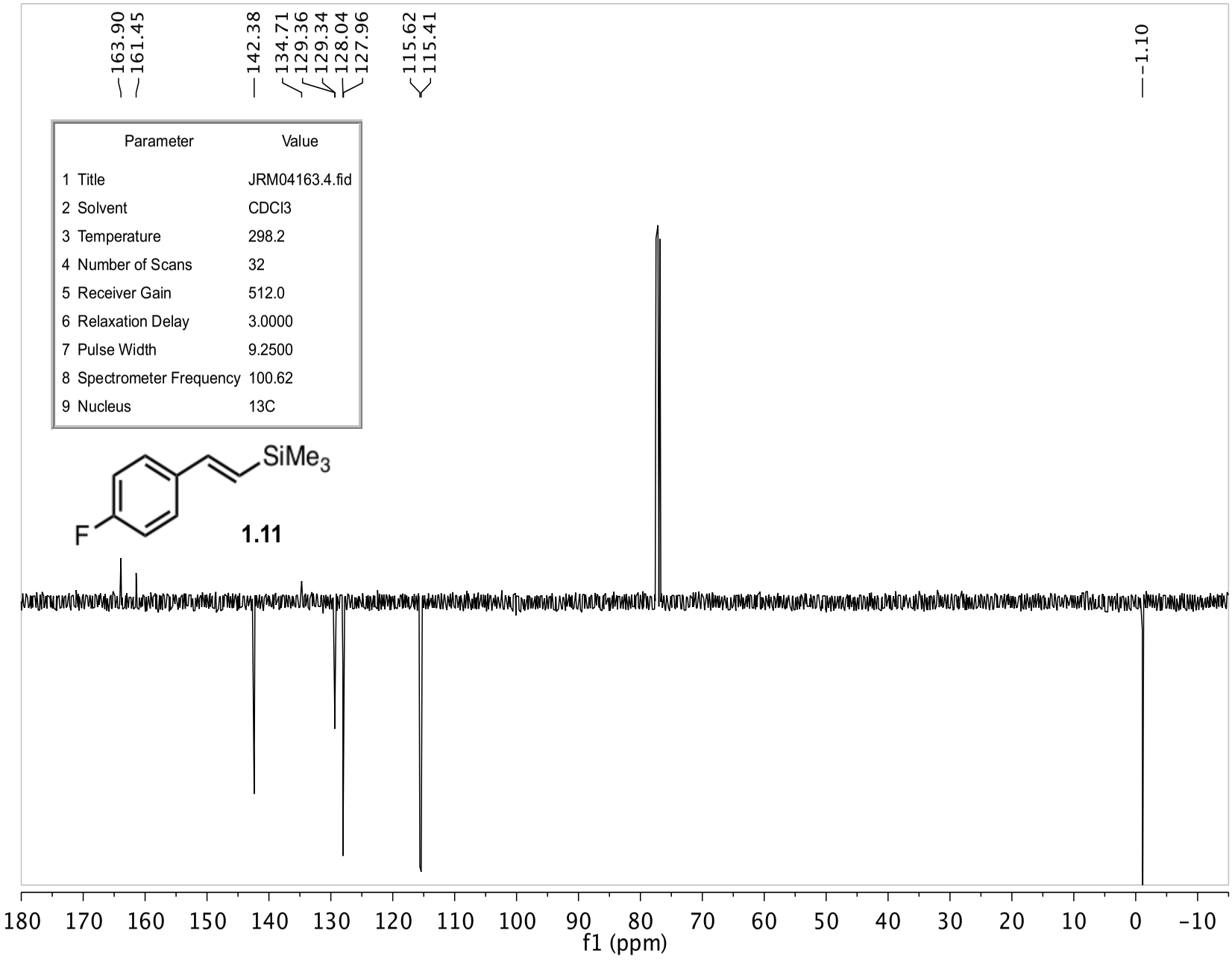
163.90
161.45
142.38
134.71
129.36
129.34
128.04
127.96
115.62
115.41
1.10
Parameter Value
1 Title JRM04163.4.fid
2 Solvent CDCl3
3 Temperature 298.2
4 Number of Scans 32
5 Receiver Gain 512.0
6 Relaxation Delay 3.0000
7 Pulse Width 9.2500
8 Spectrometer Frequency 100.62
9 Nucleus 13C
SiMe3
F
1.11
180 170 160 150 140 130 120 110 100 90 80 70 60 50 40 30 20 10 0 -10
f1 (ppm)

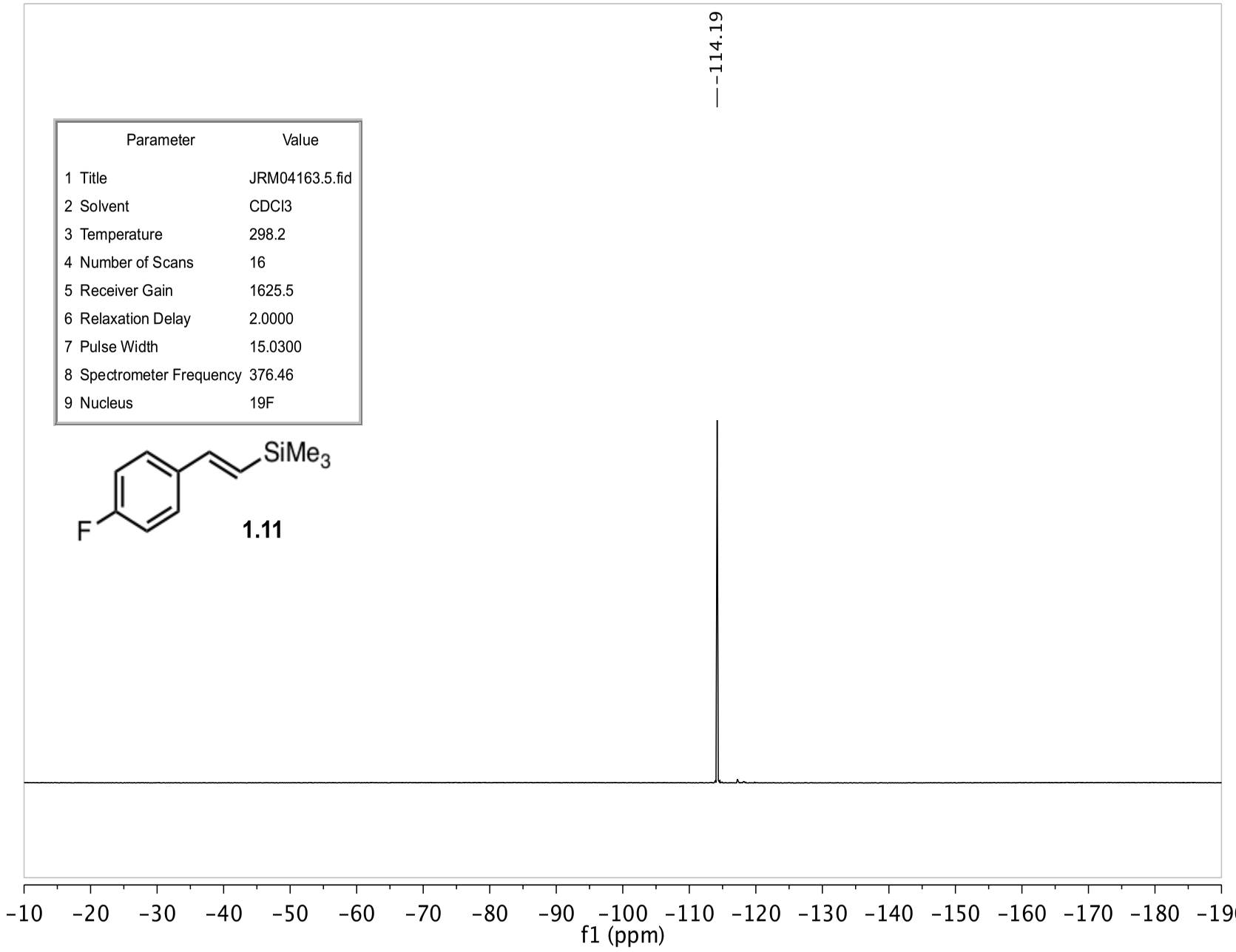
-114.19
Parameter Value
1 Title JRM04163.5.fid
2 Solvent CDCl3
3 Temperature 298.2
4 Number of Scans 16
5 Receiver Gain 1625.5
6 Relaxation Delay 2.0000
7 Pulse Width 15.0300
8 Spectrometer Frequency 376.46
9 Nucleus 19F
SiMe3
F
1.11
-10 -20 -30 -40 -50 -60 -70 -80 -90 -100 -110 -120 -130 -140 -150 -160 -170 -180 -190
f1 (ppm)

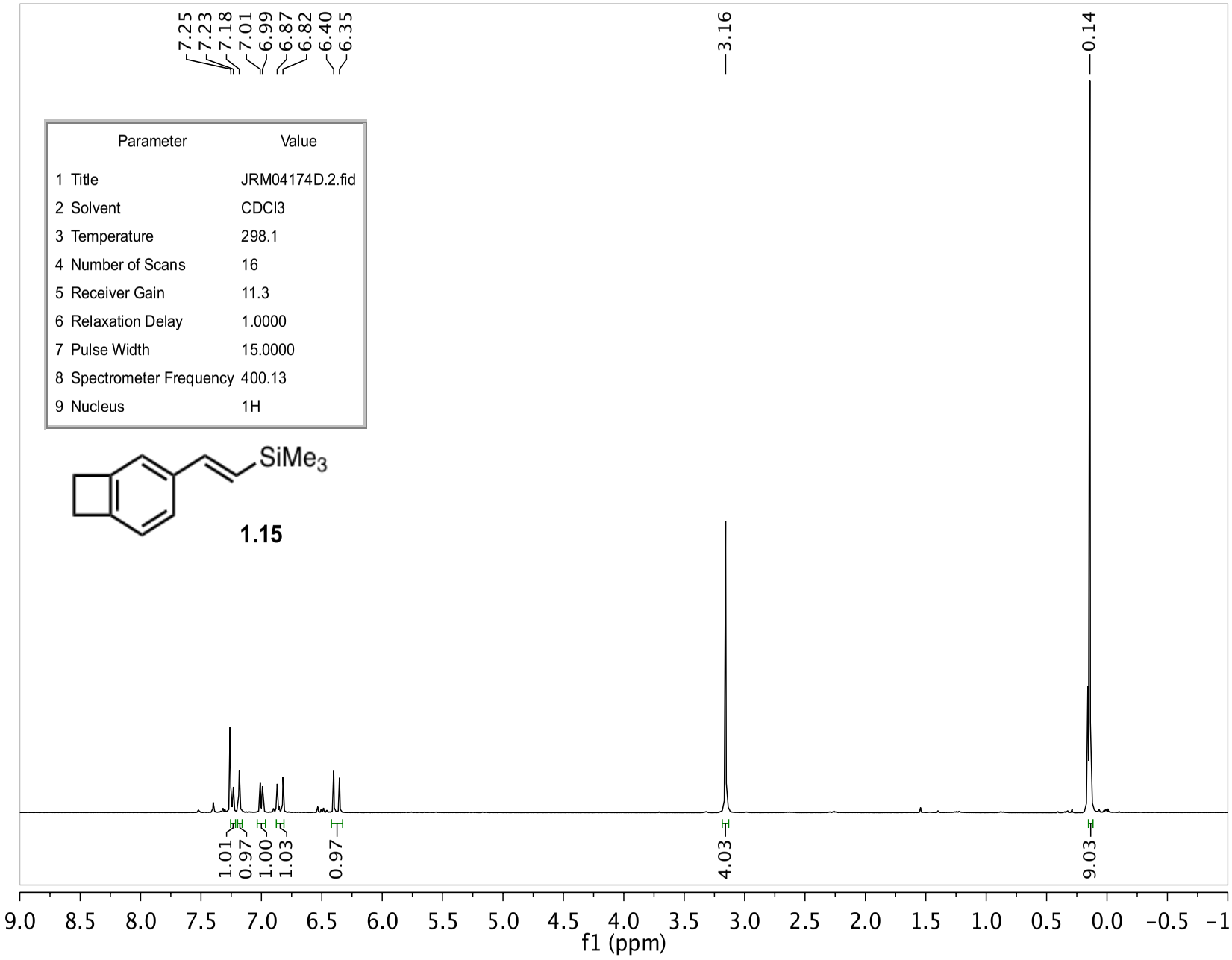
7.25
7.23
7.18
7.01
6.99
6.87
6.82
6.40
6.35
3.16
0.14
Parameter Value
1 Title JRM04174D.2.fid
2 Solvent CDCl3
3 Temperature 298.1
4 Number of Scans 16
5 Receiver Gain 11.3
6 Relaxation Delay 1.0000
7 Pulse Width 15.0000
8 Spectrometer Frequency 400.13
9 Nucleus 1H
SiMe3
1.15
1.01
0.97
1.00
1.03
0.97
4.03
9.03
9.0 8.5 8.0 7.5 7.0 6.5 6.0 5.5 5.0 4.5 4.0 3.5 3.0 2.5 2.0 1.5 1.0 0.5 0.0 -0.5 -1.0
f1 (ppm)

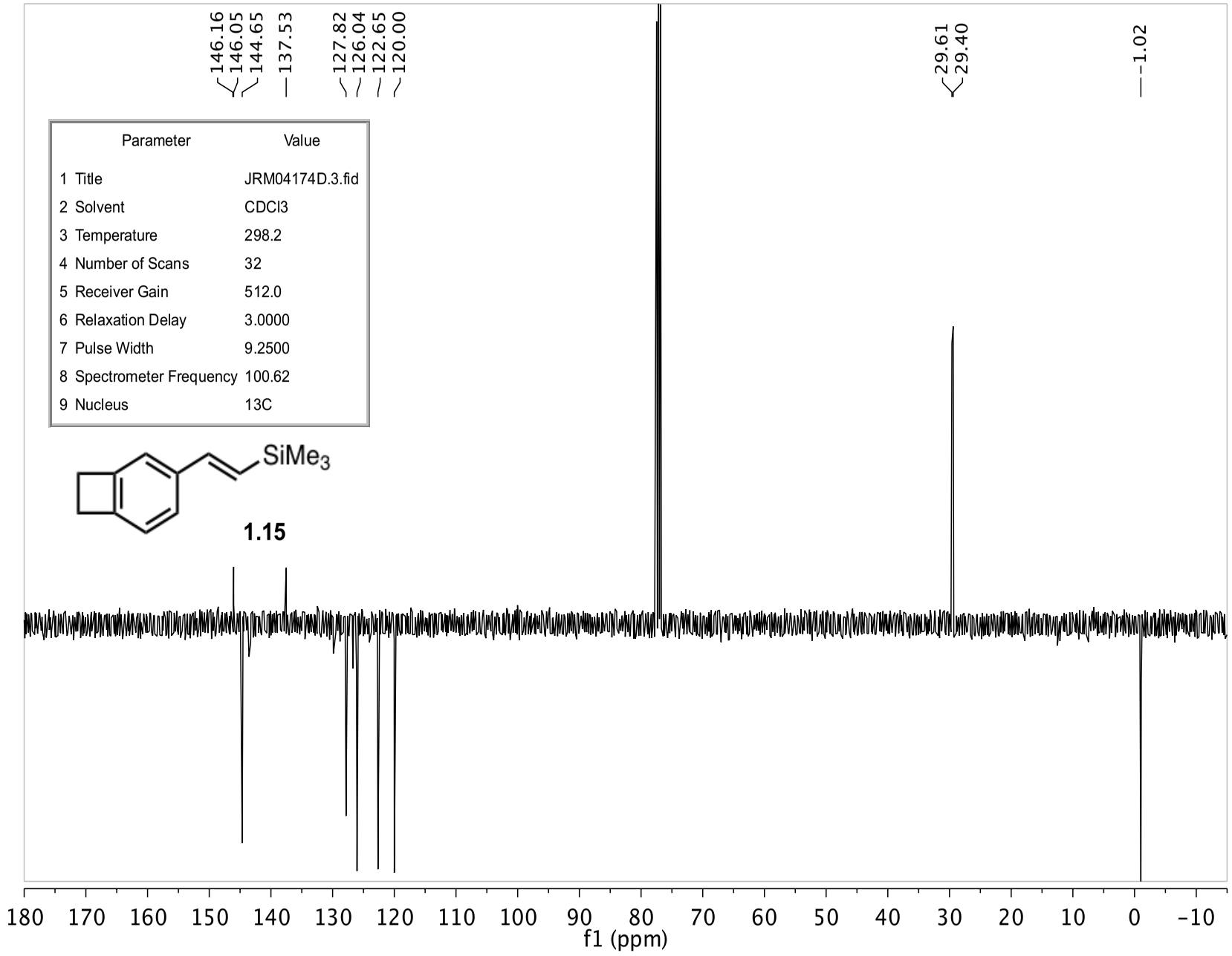
146.16
146.05
144.65
137.53
127.82
126.04
122.65
120.00
29.61
29.40
-1.02
Parameter Value
1 Title JRM04174D.3.fid
2 Solvent CDCl3
3 Temperature 298.2
4 Number of Scans 32
5 Receiver Gain 512.0
6 Relaxation Delay 3.0000
7 Pulse Width 9.2500
8 Spectrometer Frequency 100.62
9 Nucleus 13C
SiMe3
1.15
180 170 160 150 140 130 120 110 100 90 80 70 60 50 40 30 20 10 0 -10
f1 (ppm)

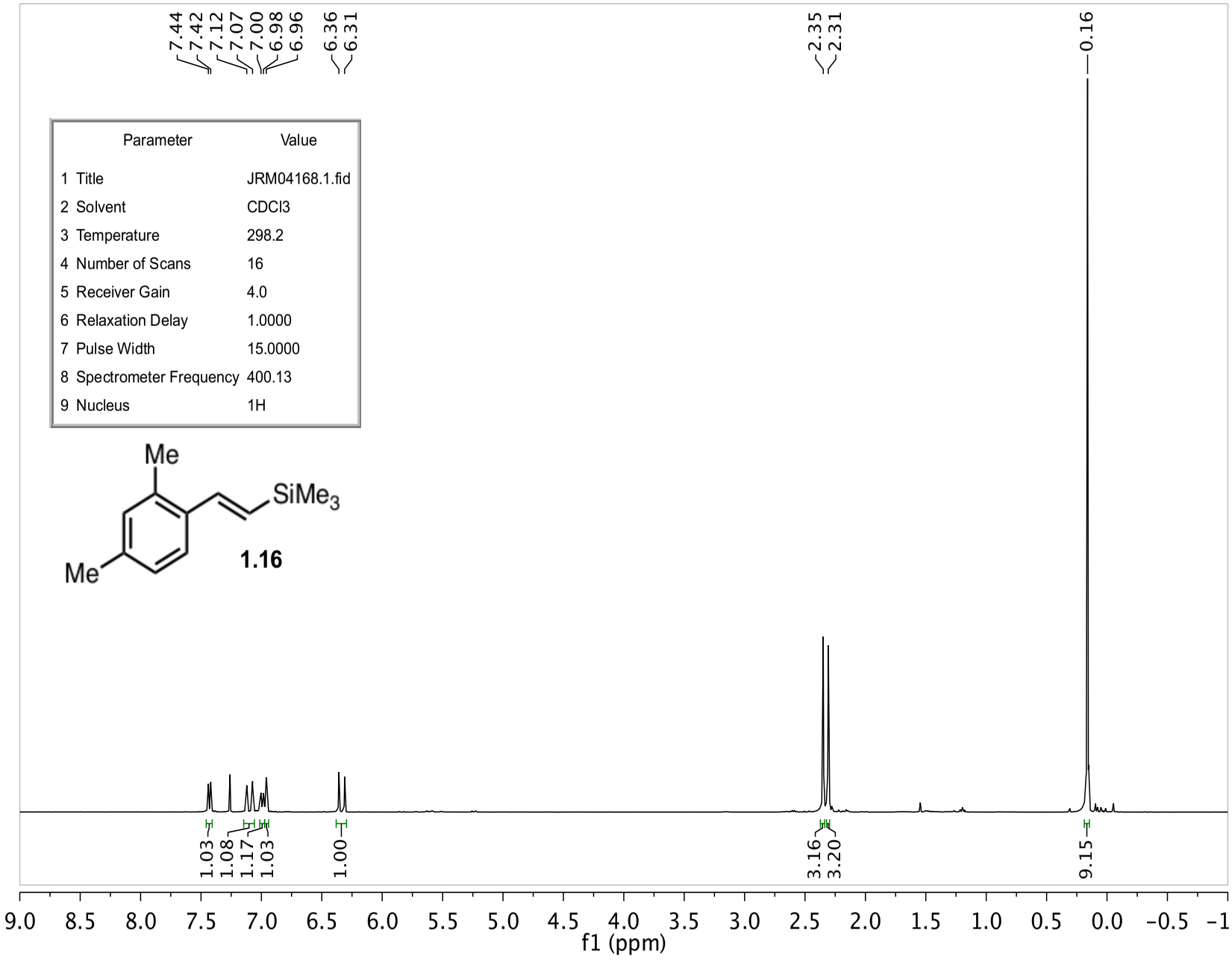
7.44
7.42
7.12
7.07
7.00
6.98
6.96
6.36
6.31
2.35
2.31
0.16
Parameter Value
1 Title JRM04168.1.fid
2 Solvent CDCl3
3 Temperature 298.2
4 Number of Scans 16
5 Receiver Gain 4.0
6 Relaxation Delay 1.0000
7 Pulse Width 15.0000
8 Spectrometer Frequency 400.13
9 Nucleus 1H
Me
SiMe3
Me
1.16
1.03
1.08
1.17
1.03
1.00
3.16
3.20
9.15
9.0 8.5 8.0 7.5 7.0 6.5 6.0 5.5 5.0 4.5 4.0 3.5 3.0 2.5 2.0 1.5 1.0 0.5 0.0 -0.5 -1.0
f1 (ppm)

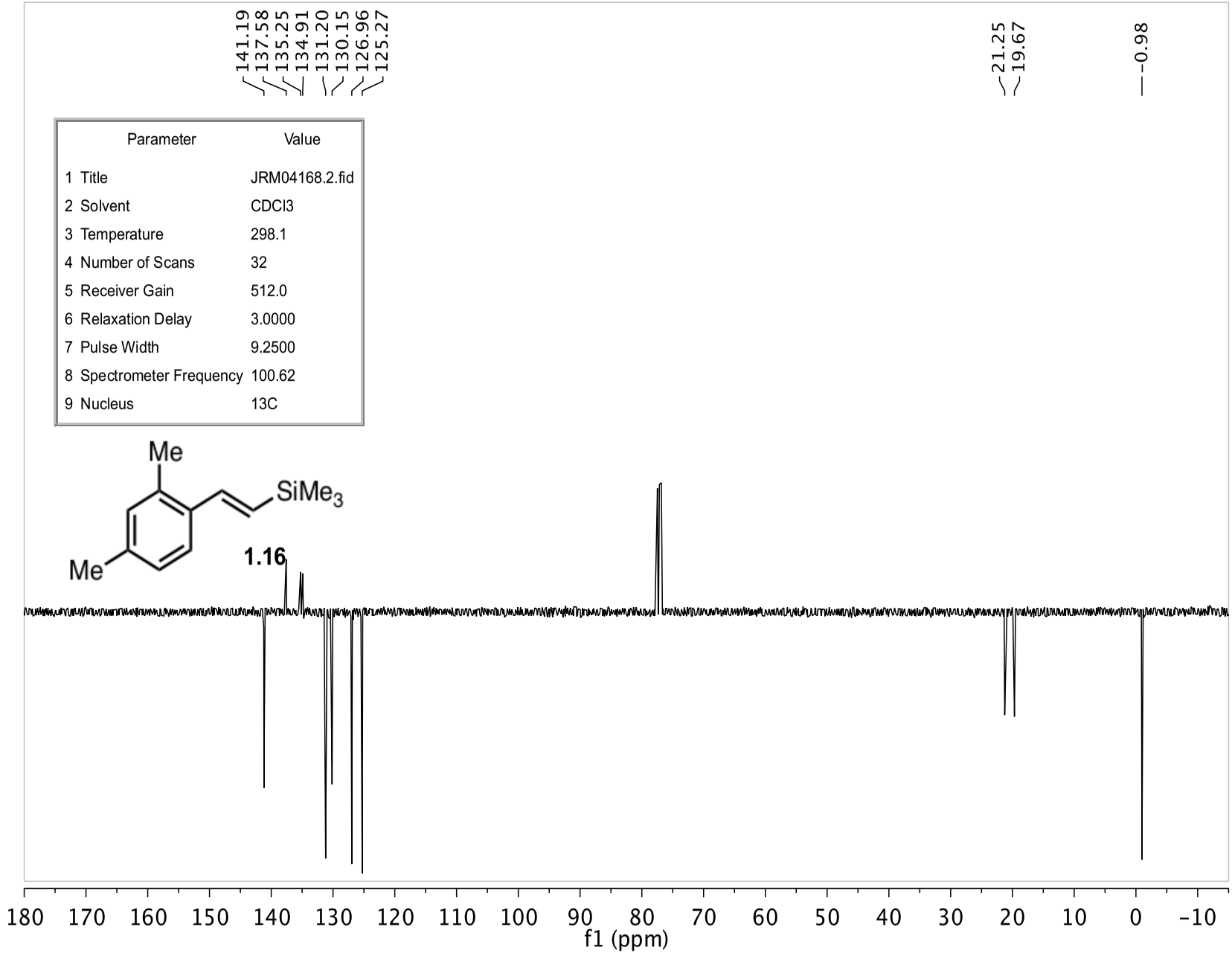
141.19
137.58
135.25
134.91
131.20
130.15
126.96
125.27
21.25
19.67
-0.98
Parameter Value
1 Title JRM04168.2.fid
2 Solvent CDCl3
3 Temperature 298.1
4 Number of Scans 32
5 Receiver Gain 512.0
6 Relaxation Delay 3.0000
7 Pulse Width 9.2500
8 Spectrometer Frequency 100.62
9 Nucleus 13C
Me
SiMe3
Me
1.16
180 170 160 150 140 130 120 110 100 90 80 70 60 50 40 30 20 10 0 -10
f1 (ppm)

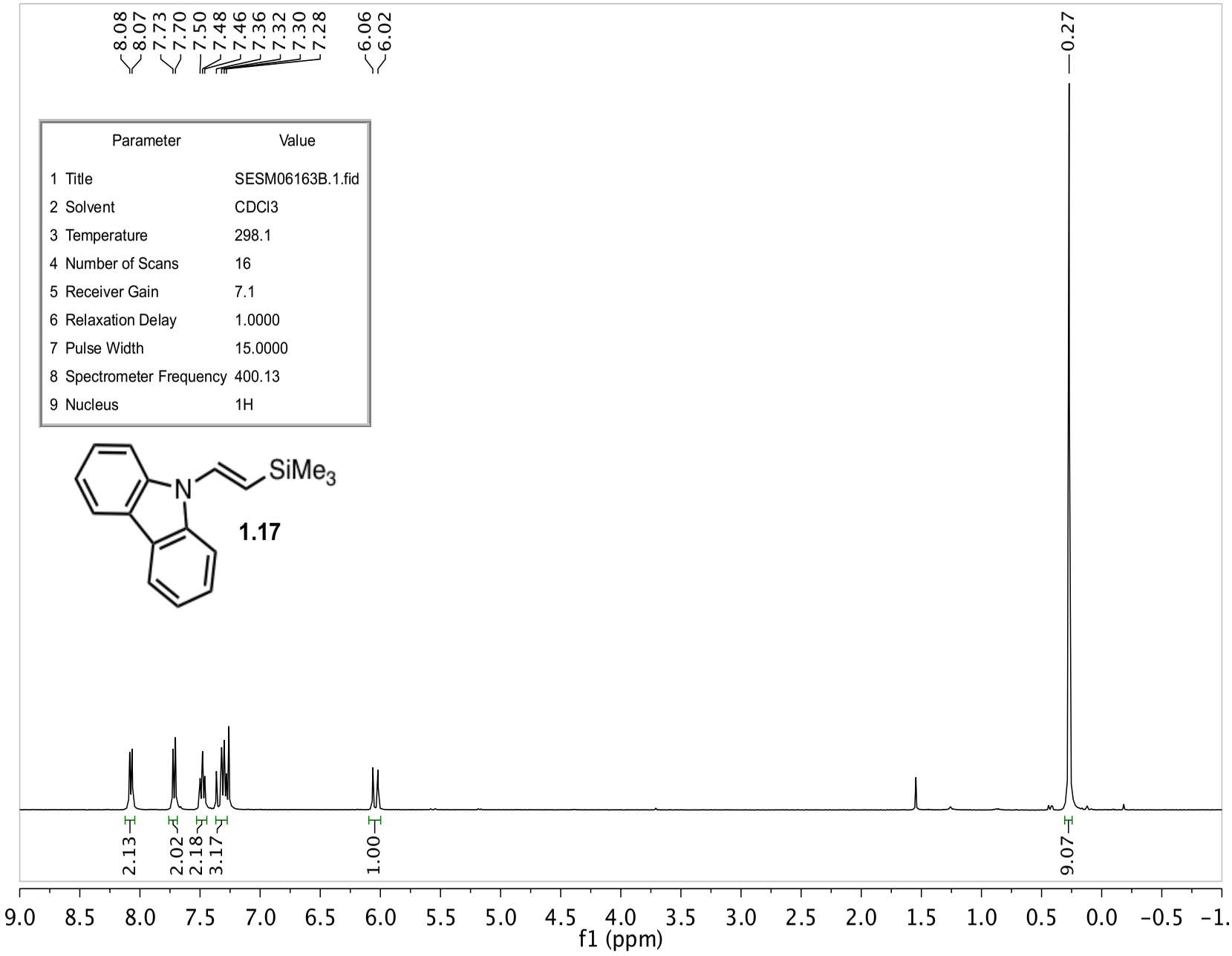
8.08
8.07
7.73
7.70
7.50
7.48
7.46
7.36
7.32
7.30
7.28
6.06
6.02
0.27
Parameter Value
1 Title SESM06163B.1.fid
2 Solvent CDCl3
3 Temperature 298.1
4 Number of Scans 16
5 Receiver Gain 7.1
6 Relaxation Delay 1.0000
7 Pulse Width 15.0000
8 Spectrometer Frequency 400.13
9 Nucleus 1H
N
SiMe3
1.17
2.13
2.02
2.18
3.17
1.00
9.07
9.0 8.5 8.0 7.5 7.0 6.5 6.0 5.5 5.0 4.5 4.0 3.5 3.0 2.5 2.0 1.5 1.0 0.5 0.0 -0.5 -1.0
f1 (ppm)

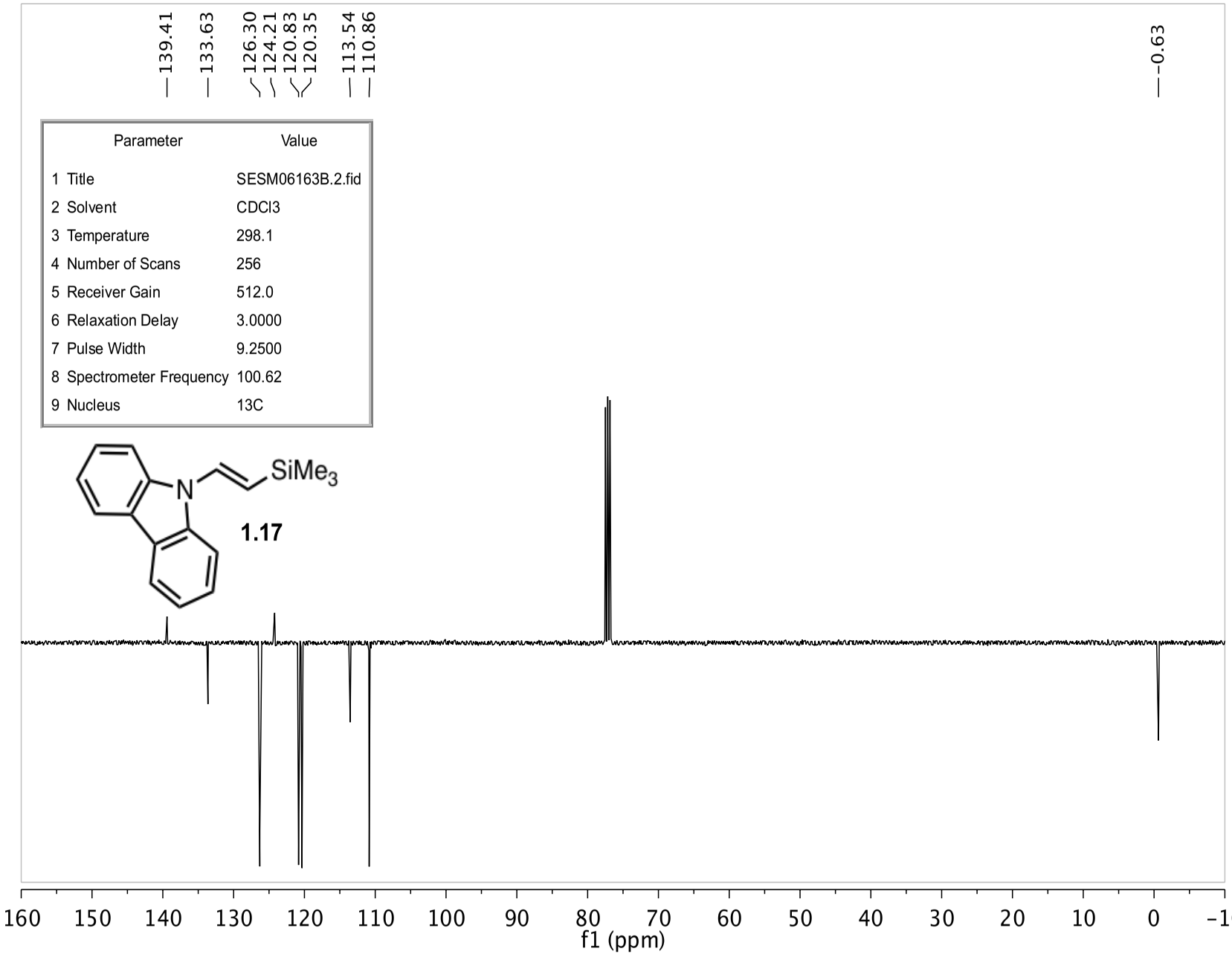
139.41
133.63
126.30
124.21
120.83
120.35
113.54
110.86
-0.63
Parameter Value
1 Title SESM06163B.2.fid
2 Solvent CDCl3
3 Temperature 298.1
4 Number of Scans 256
5 Receiver Gain 512.0
6 Relaxation Delay 3.0000
7 Pulse Width 9.2500
8 Spectrometer Frequency 100.62
9 Nucleus 13C
N
SiMe3
1.17
160 150 140 130 120 110 100 90 80 70 60 50 40 30 20 10 0 -10
f1 (ppm)

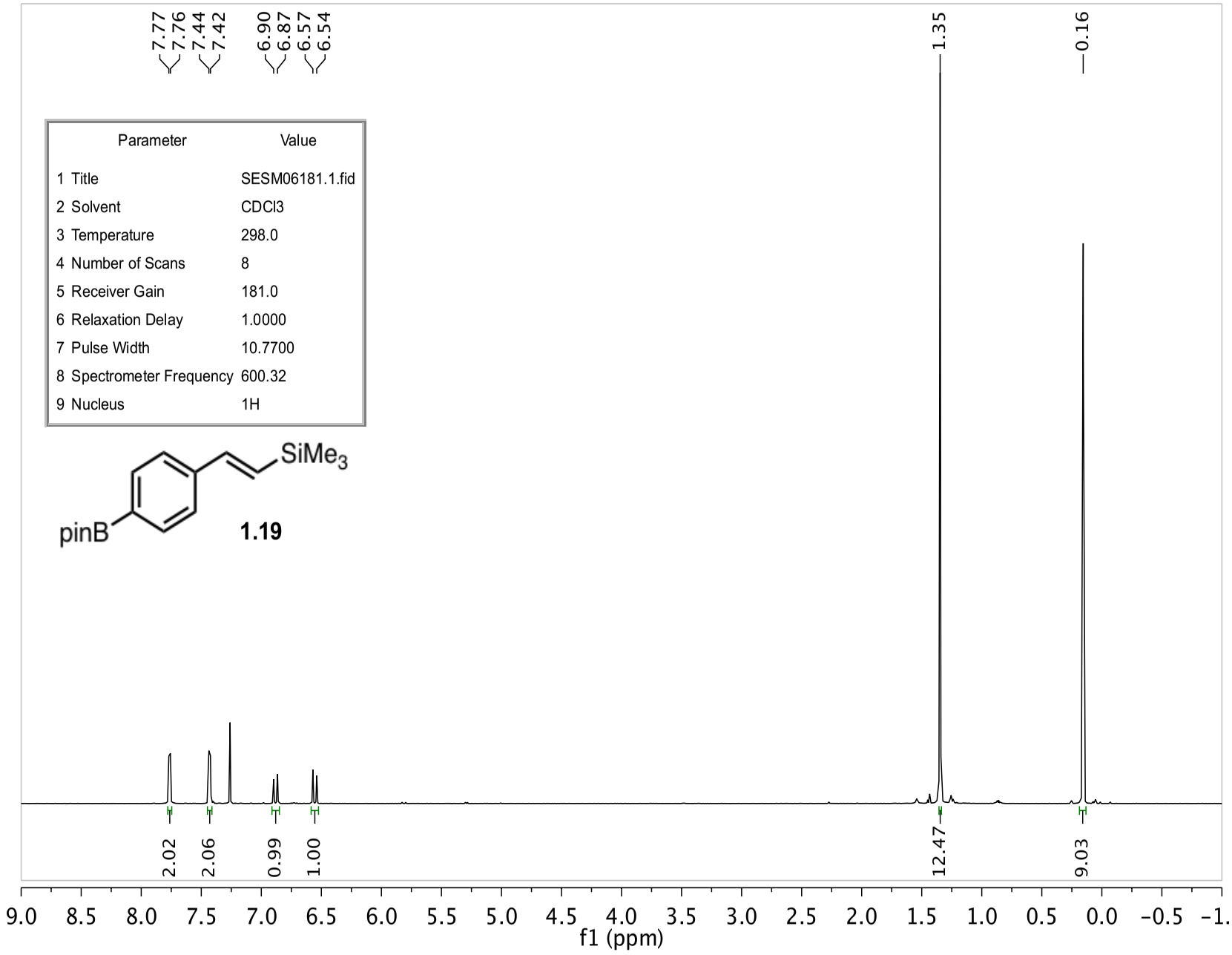
7.77
7.76
7.44
7.42
6.90
6.87
6.57
6.54
1.35
0.16
Parameter Value
1 Title SESM06181.1.fid
2 Solvent CDCl3
3 Temperature 298.0
4 Number of Scans 8
5 Receiver Gain 181.0
6 Relaxation Delay 1.0000
7 Pulse Width 10.7700
8 Spectrometer Frequency 600.32
9 Nucleus 1H
SiMe3
pinB
1.19
2.02
2.06
0.99
1.00
12.47
9.03
9.0 8.5 8.0 7.5 7.0 6.5 6.0 5.5 5.0 4.5 4.0 3.5 3.0 2.5 2.0 1.5 1.0 0.5 0.0 -0.5 -1.0
f1 (ppm)

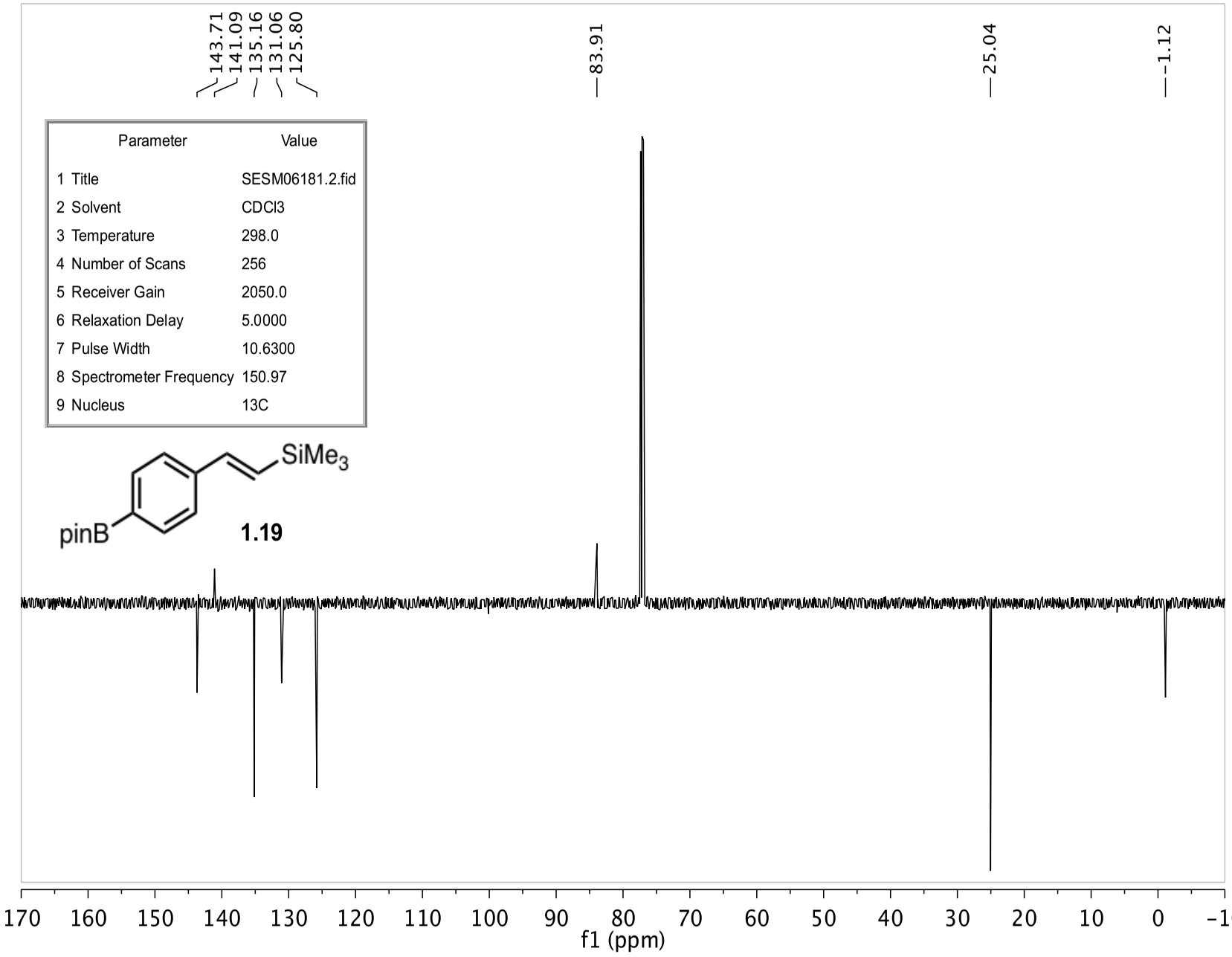
143.71
141.09
135.16
131.06
125.80
83.91
25.04
-1.12
Parameter Value
1 Title SESM06181.2.fid
2 Solvent CDCl3
3 Temperature 298.0
4 Number of Scans 256
5 Receiver Gain 2050.0
6 Relaxation Delay 5.0000
7 Pulse Width 10.6300
8 Spectrometer Frequency 150.97
9 Nucleus 13C
SiMe3
pinB
1.19
170 160 150 140 130 120 110 100 90 80 70 60 50 40 30 20 10 0 -10
f1 (ppm)

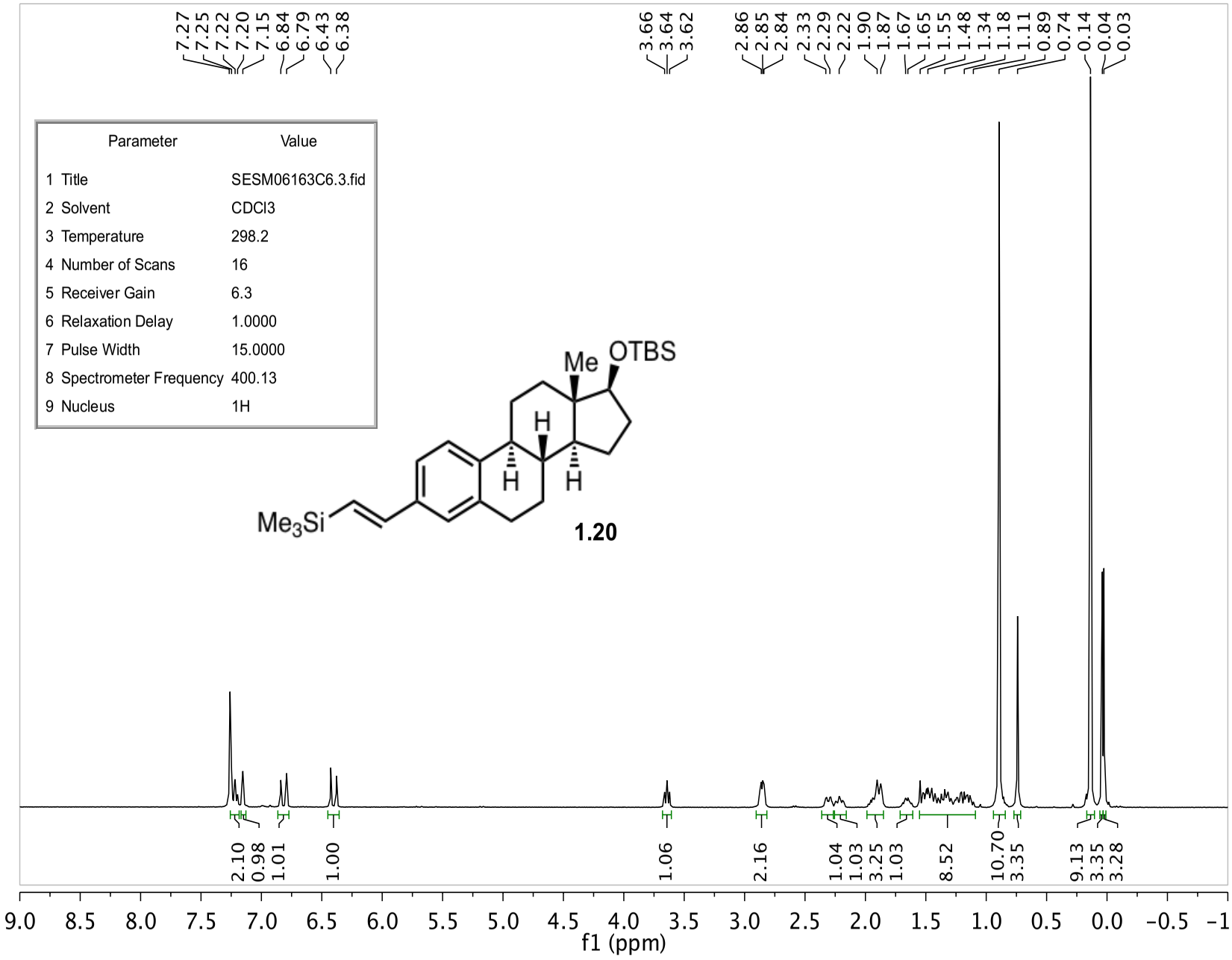
7.27
7.25
7.22
7.20
7.15
6.84
6.79
6.43
6.38
3.66
3.64
3.62
2.86
2.85
2.84
2.33
2.29
2.22
1.90
1.87
1.67
1.65
1.55
1.48
1.34
1.18
1.11
0.89
0.74
0.14
0.04
0.03
Parameter Value
1 Title SESM06163C6.3.fid
2 Solvent CDCl3
3 Temperature 298.2
4 Number of Scans 16
5 Receiver Gain 6.3
6 Relaxation Delay 1.0000
7 Pulse Width 15.0000
8 Spectrometer Frequency 400.13
9 Nucleus 1H
Me
OTBS
H
H
H
Me3Si
1.20
2.10
0.98
1.01
1.00
1.06
2.16
1.04
1.03
3.25
1.03
8.52
10.70
3.35
9.13
3.35
3.28
9.0 8.5 8.0 7.5 7.0 6.5 6.0 5.5 5.0 4.5 4.0 3.5 3.0 2.5 2.0 1.5 1.0 0.5 0.0 -0.5 -1.0
f1 (ppm)

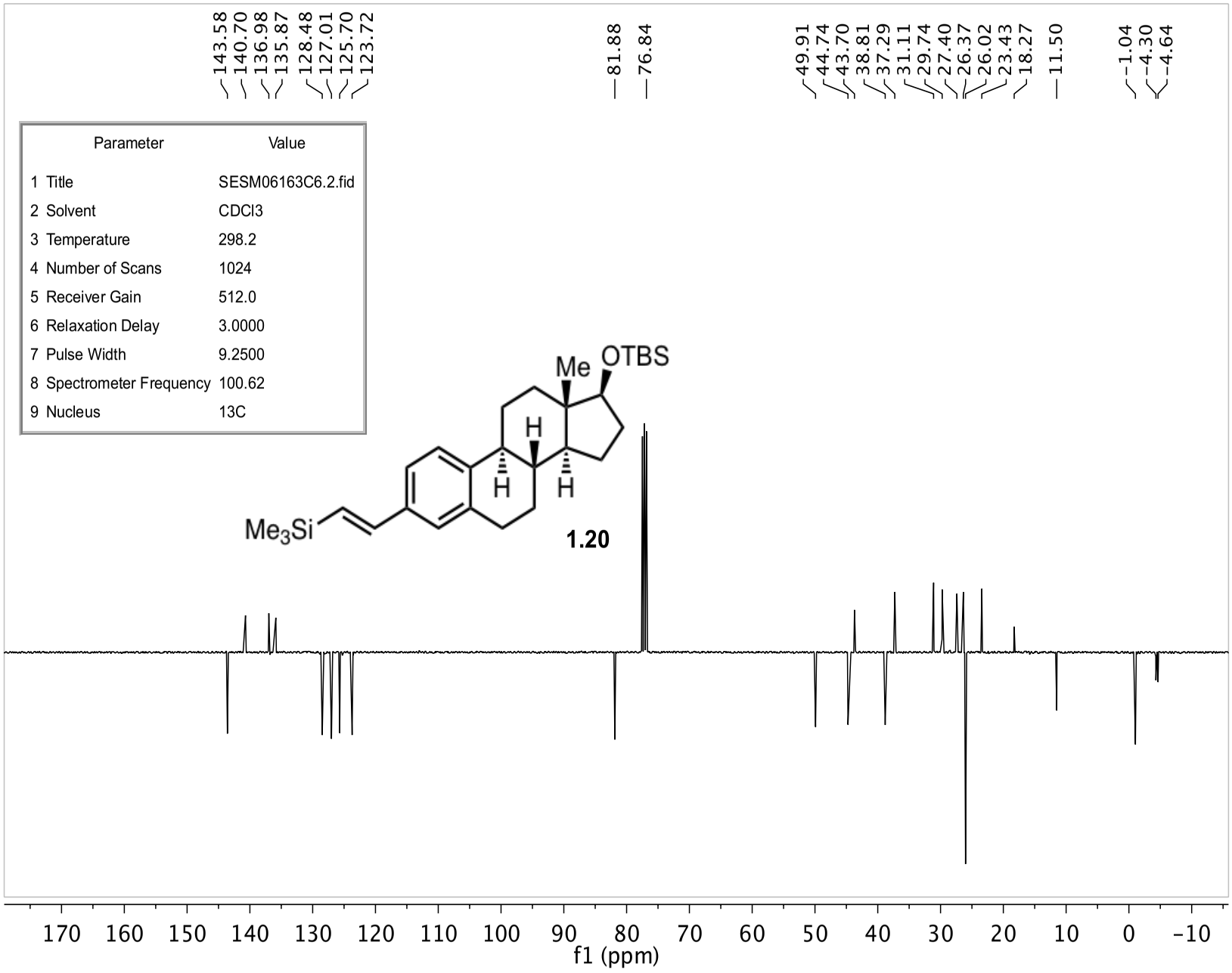
143.58
140.70
136.98
135.87
128.48
127.01
125.70
123.72
81.88
76.84
49.91
44.74
43.70
38.81
37.29
31.11
29.74
27.40
26.37
26.02
23.43
18.27
11.50
-1.04
-4.30
-4.64
Parameter Value
1 Title SESM06163C6.2.fid
2 Solvent CDCl3
3 Temperature 298.2
4 Number of Scans 1024
5 Receiver Gain 512.0
6 Relaxation Delay 3.0000
7 Pulse Width 9.2500
8 Spectrometer Frequency 100.62
9 Nucleus 13C
Me
OTBS
H
H
H
Me3Si
1.20
170 160 150 140 130 120 110 100 90 80 70 60 50 40 30 20 10 0 -10
f1 (ppm)

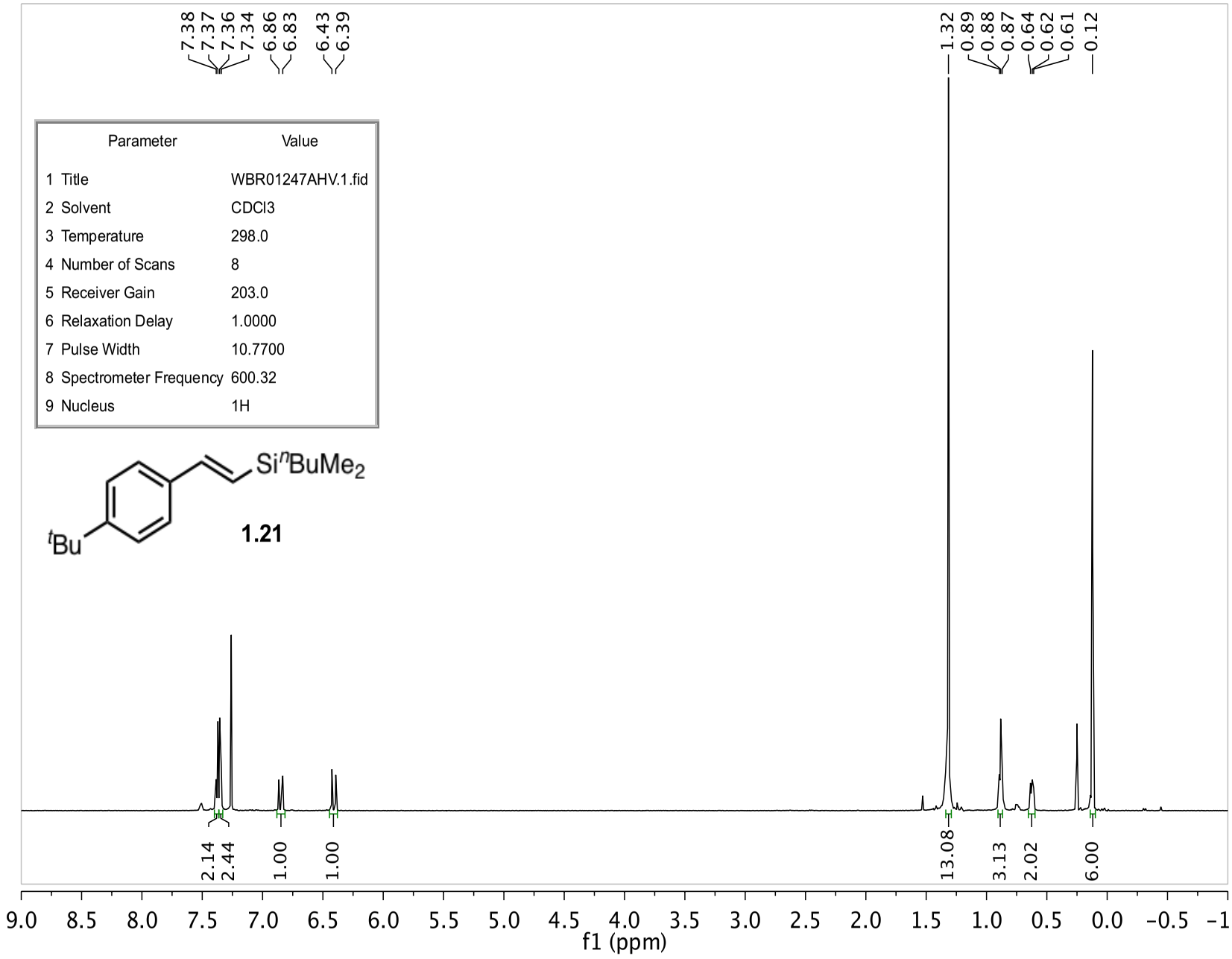
7.38
7.37
7.36
7.34
6.86
6.83
6.43
6.39
1.32
0.89
0.88
0.87
0.64
0.62
0.61
0.12
Parameter Value
1 Title WBR01247AHV.1.fid
2 Solvent CDCl3
3 Temperature 298.0
4 Number of Scans 8
5 Receiver Gain 203.0
6 Relaxation Delay 1.0000
7 Pulse Width 10.7700
8 Spectrometer Frequency 600.32
9 Nucleus 1H
Si^{n}BuMe$_2$
^{t}Bu
1.21
2.14
2.44
1.00
1.00
13.08
3.13
2.02
6.00
9.0 8.5 8.0 7.5 7.0 6.5 6.0 5.5 5.0 4.5 4.0 3.5 3.0 2.5 2.0 1.5 1.0 0.5 0.0 -0.5 -1.0
f1 (ppm)

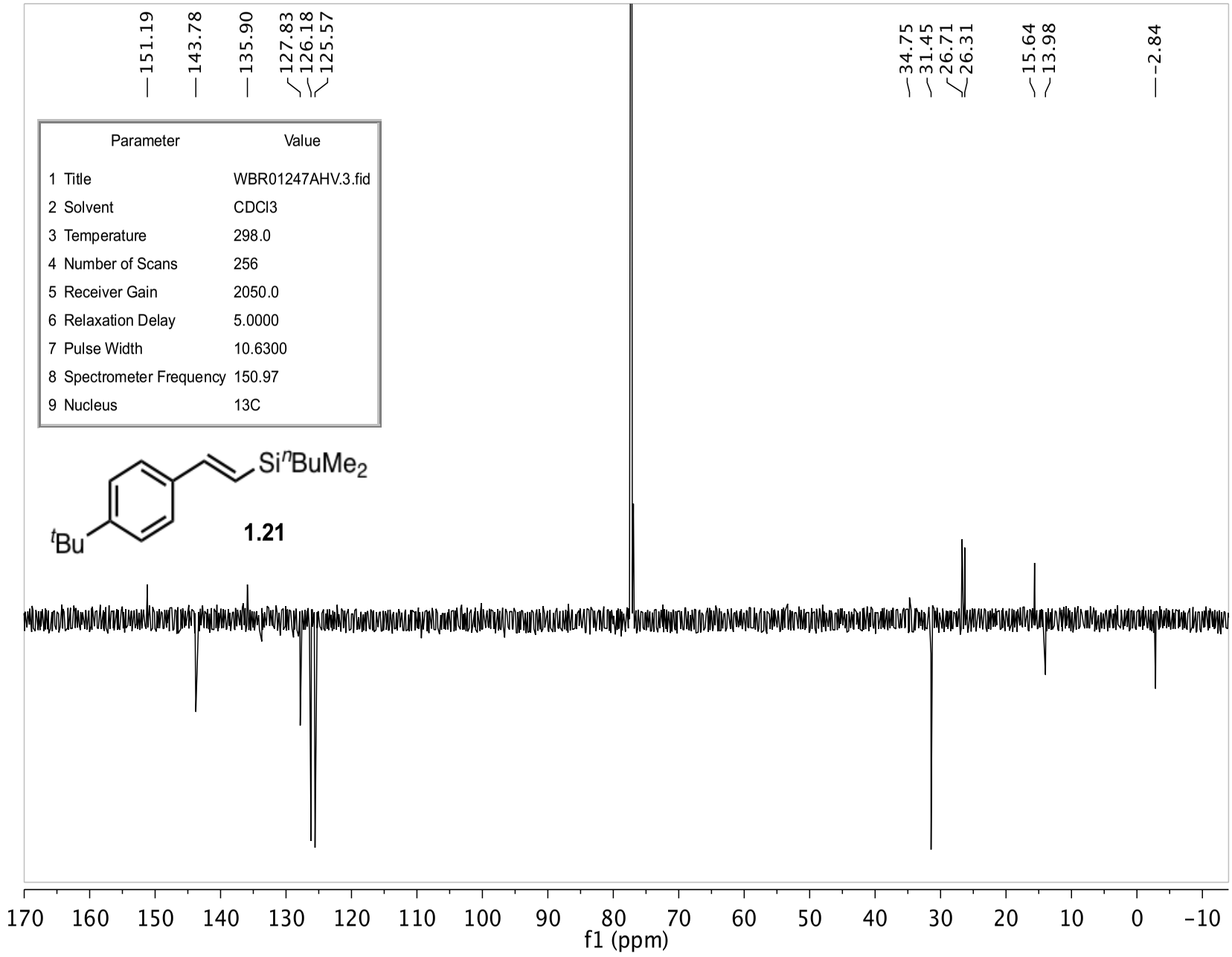
151.19
143.78
135.90
127.83
126.18
125.57
34.75
31.45
26.71
26.31
15.64
13.98
-2.84
Parameter Value
1 Title WBR01247AHV.3.fid
2 Solvent CDCl3
3 Temperature 298.0
4 Number of Scans 256
5 Receiver Gain 2050.0
6 Relaxation Delay 5.0000
7 Pulse Width 10.6300
8 Spectrometer Frequency 150.97
9 Nucleus 13C
Si^{n}BuMe$_2$
^{t}Bu
1.21
170 160 150 140 130 120 110 100 90 80 70 60 50 40 30 20 10 0 -10
f1 (ppm)

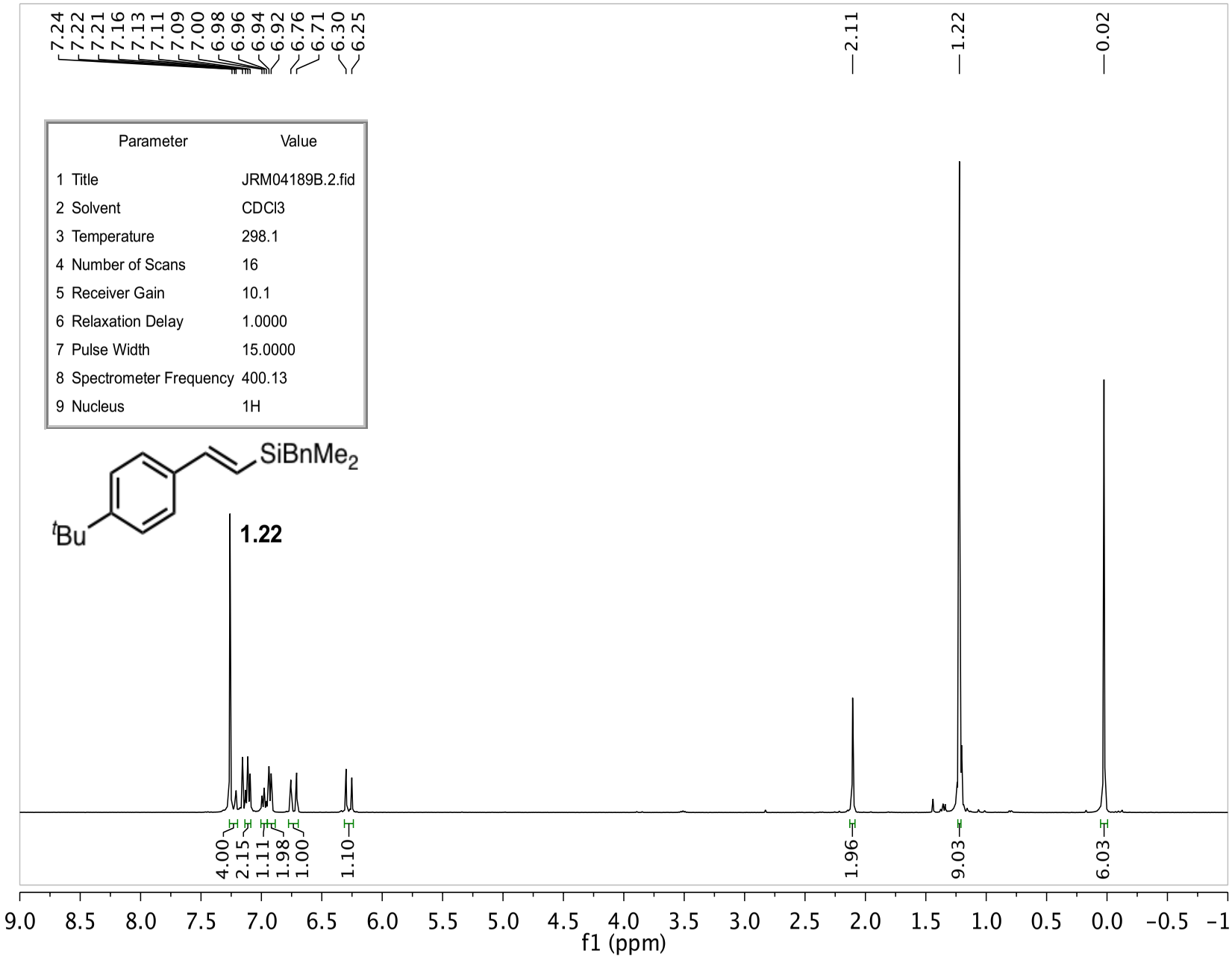
7.24
7.22
7.21
7.16
7.13
7.11
7.09
7.00
6.98
6.96
6.94
6.92
6.76
6.71
6.30
6.25
2.11
1.22
0.02
Parameter Value
1 Title JRM04189B.2.fid
2 Solvent CDCl3
3 Temperature 298.1
4 Number of Scans 16
5 Receiver Gain 10.1
6 Relaxation Delay 1.0000
7 Pulse Width 15.0000
8 Spectrometer Frequency 400.13
9 Nucleus 1H
SiBnMe2
tBu
1.22
4.00
2.15
1.11
1.98
1.00
1.10
1.96
9.03
6.03
9.0 8.5 8.0 7.5 7.0 6.5 6.0 5.5 5.0 4.5 4.0 3.5 3.0 2.5 2.0 1.5 1.0 0.5 0.0 -0.5 -1.0
f1 (ppm)

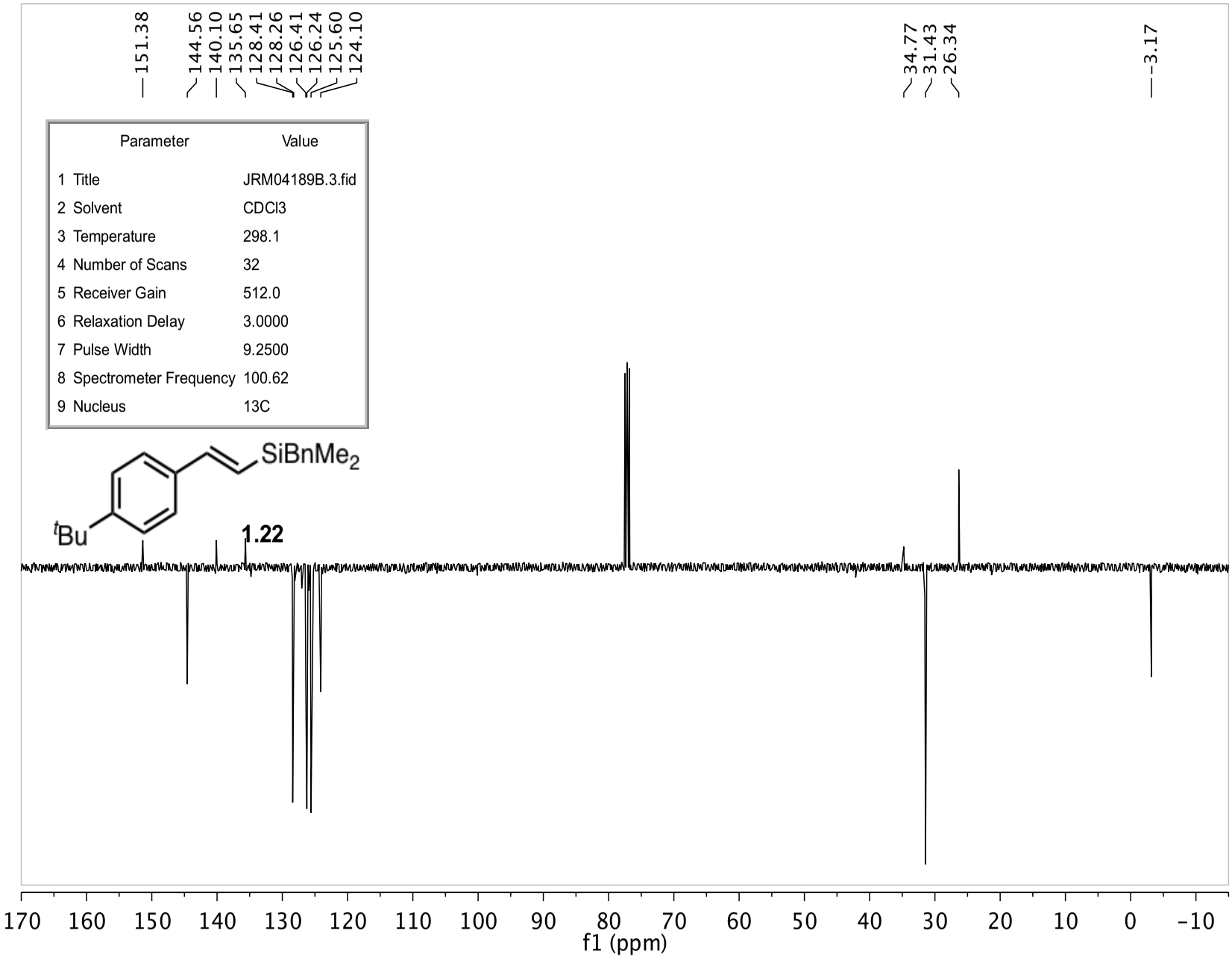
151.38
144.56
140.10
135.65
128.41
128.26
126.41
126.24
125.60
124.10
34.77
31.43
26.34
-3.17
Parameter Value
1 Title JRM04189B.3.fid
2 Solvent CDCl3
3 Temperature 298.1
4 Number of Scans 32
5 Receiver Gain 512.0
6 Relaxation Delay 3.0000
7 Pulse Width 9.2500
8 Spectrometer Frequency 100.62
9 Nucleus 13C
SiBnMe2
tBu
1.22
170 160 150 140 130 120 110 100 90 80 70 60 50 40 30 20 10 0 -10
f1 (ppm)

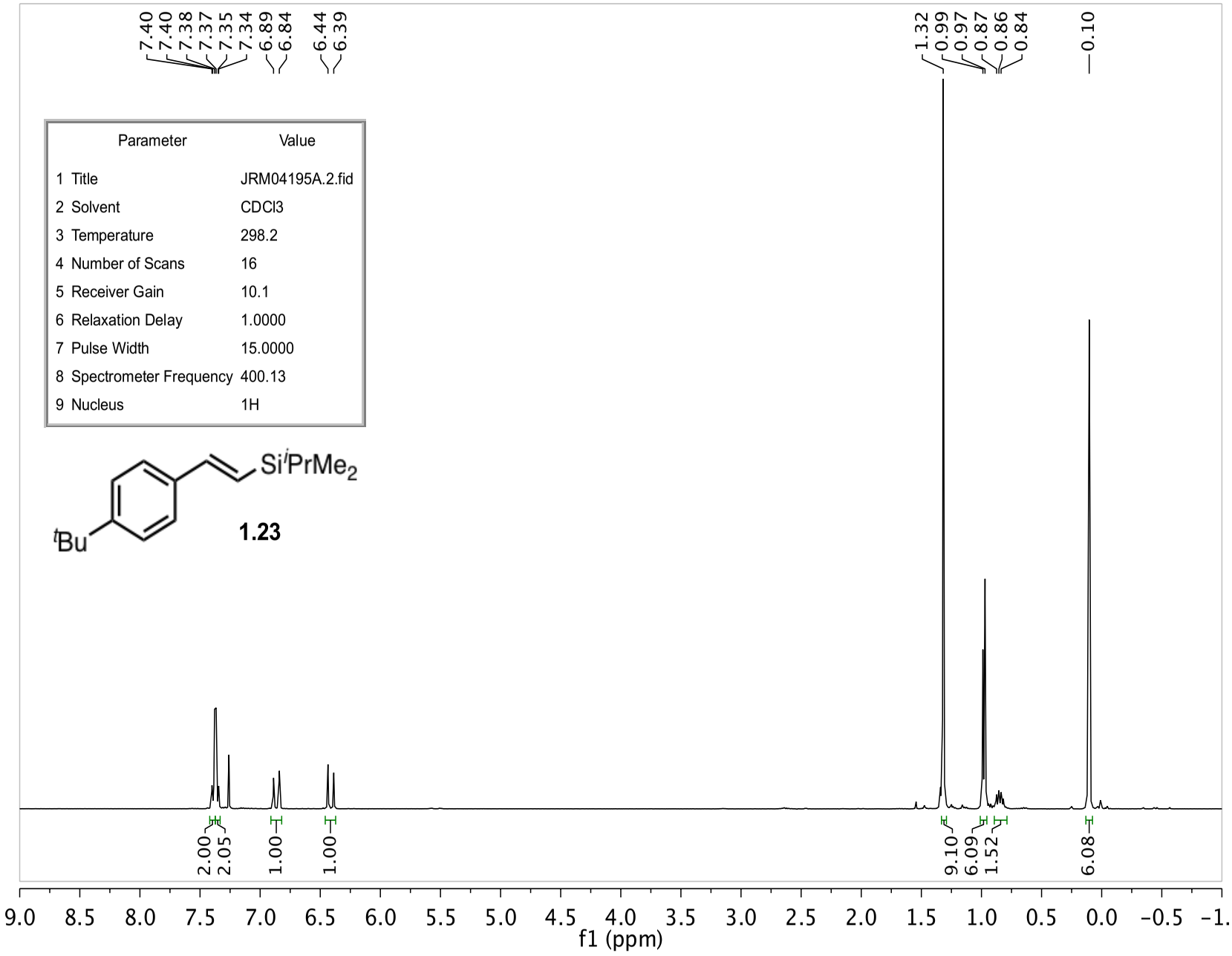
7.40
7.40
7.38
7.37
7.35
7.34
6.89
6.84
6.44
6.39
1.32
0.99
0.97
0.87
0.86
0.84
0.10
Parameter Value
1 Title JRM04195A.2.fid
2 Solvent CDCl3
3 Temperature 298.2
4 Number of Scans 16
5 Receiver Gain 10.1
6 Relaxation Delay 1.0000
7 Pulse Width 15.0000
8 Spectrometer Frequency 400.13
9 Nucleus 1H
Si^{i}PrMe$_2$
^{t}Bu
1.23
2.00
2.05
1.00
1.00
9.10
6.09
1.52
6.08
9.0 8.5 8.0 7.5 7.0 6.5 6.0 5.5 5.0 4.5 4.0 3.5 3.0 2.5 2.0 1.5 1.0 0.5 0.0 -0.5 -1.0
f1 (ppm)

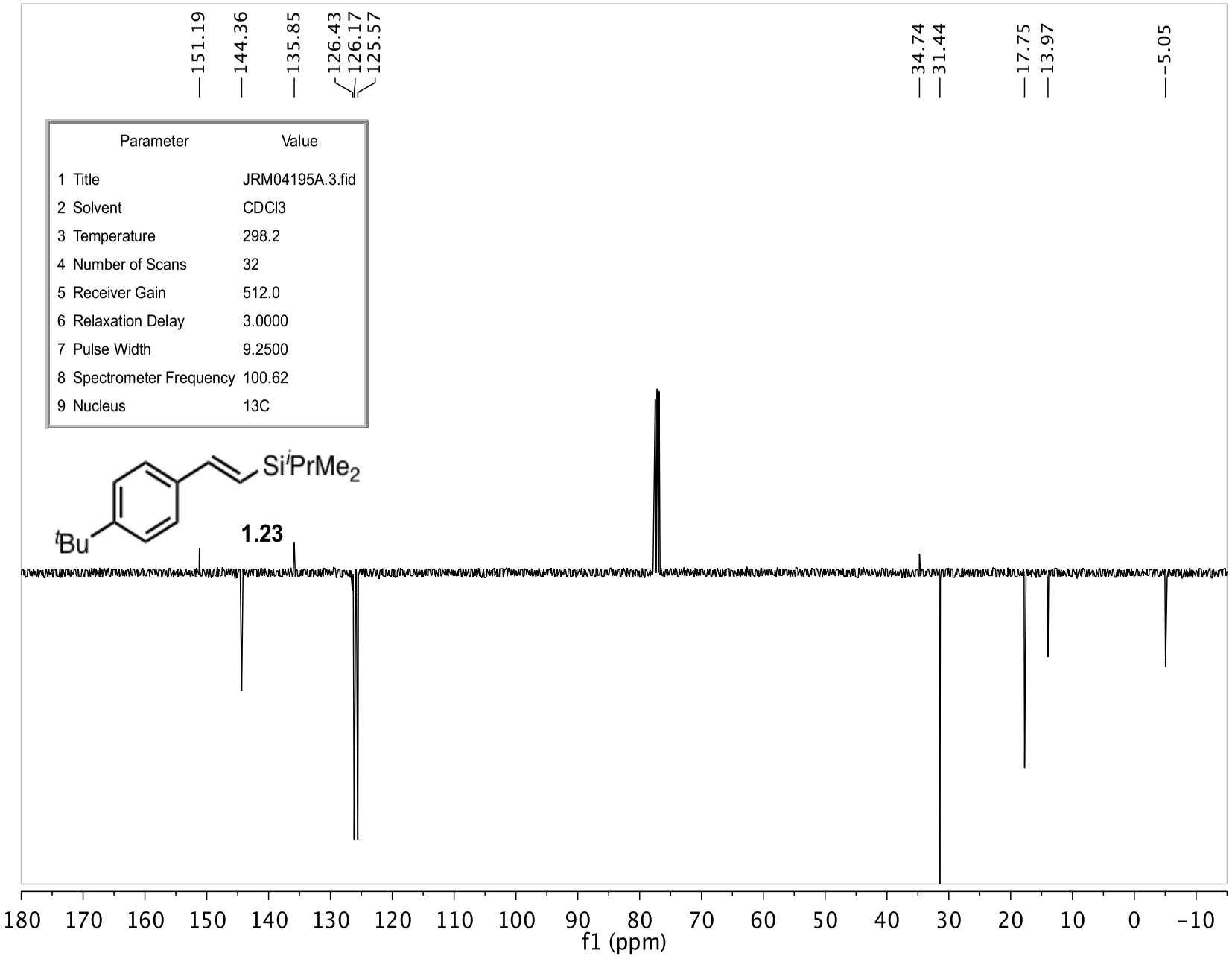
151.19
144.36
135.85
126.43
126.17
125.57
34.74
31.44
17.75
13.97
-5.05
Parameter Value
1 Title JRM04195A.3.fid
2 Solvent CDCl3
3 Temperature 298.2
4 Number of Scans 32
5 Receiver Gain 512.0
6 Relaxation Delay 3.0000
7 Pulse Width 9.2500
8 Spectrometer Frequency 100.62
9 Nucleus 13C
Si^{i}PrMe$_2$
^{t}Bu
1.23
180 170 160 150 140 130 120 110 100 90 80 70 60 50 40 30 20 10 0 -10
f1 (ppm)

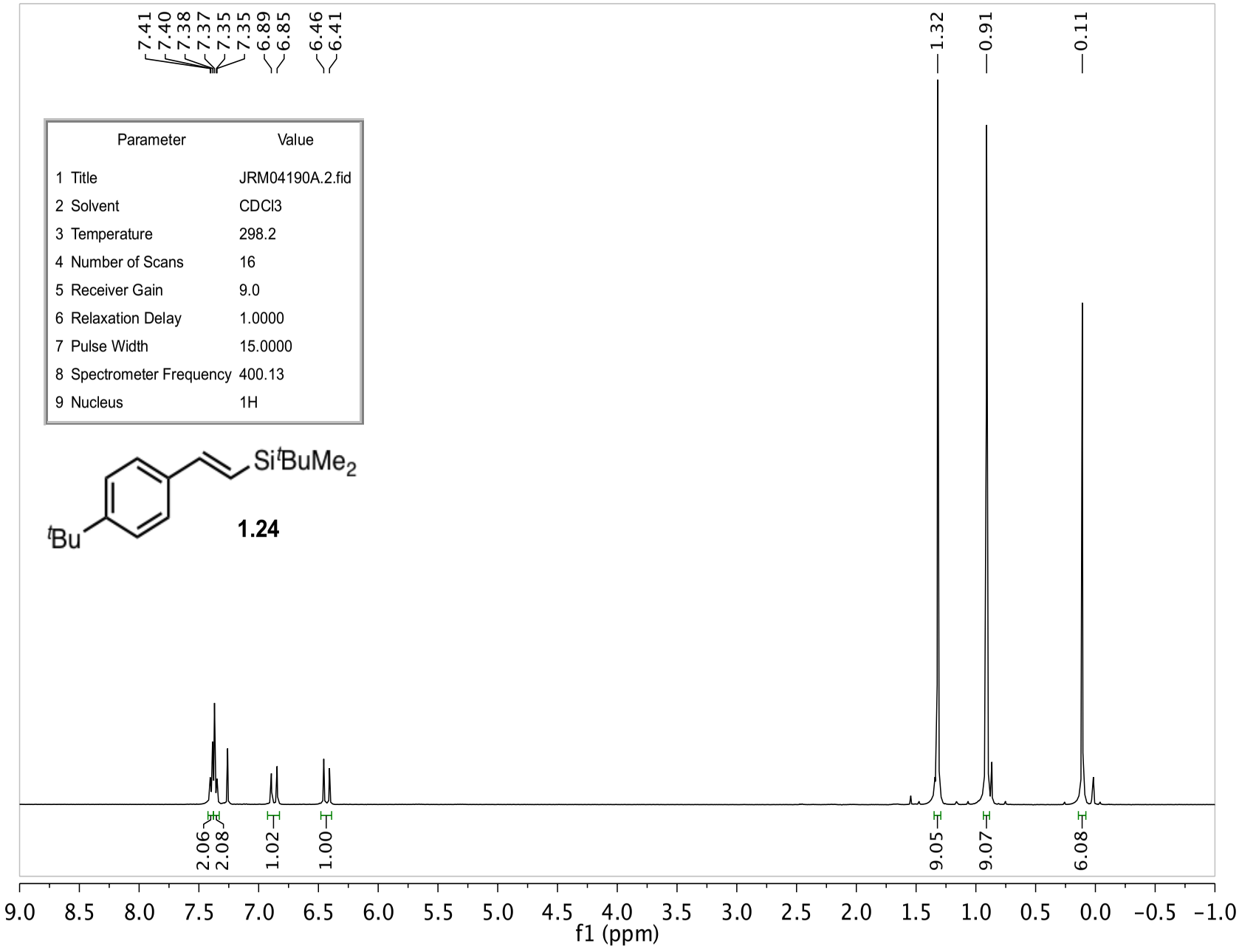
7.41
7.40
7.38
7.37
7.35
7.35
6.89
6.85
6.46
6.41
1.32
0.91
0.11
Parameter Value
1 Title JRM04190A.2.fid
2 Solvent CDCl3
3 Temperature 298.2
4 Number of Scans 16
5 Receiver Gain 9.0
6 Relaxation Delay 1.0000
7 Pulse Width 15.0000
8 Spectrometer Frequency 400.13
9 Nucleus 1H
SitBuMe2
tBu
1.24
2.06
2.08
1.02
1.00
9.05
9.07
6.08
9.0 8.5 8.0 7.5 7.0 6.5 6.0 5.5 5.0 4.5 4.0 3.5 3.0 2.5 2.0 1.5 1.0 0.5 0.0 -0.5 -1.0
f1 (ppm)

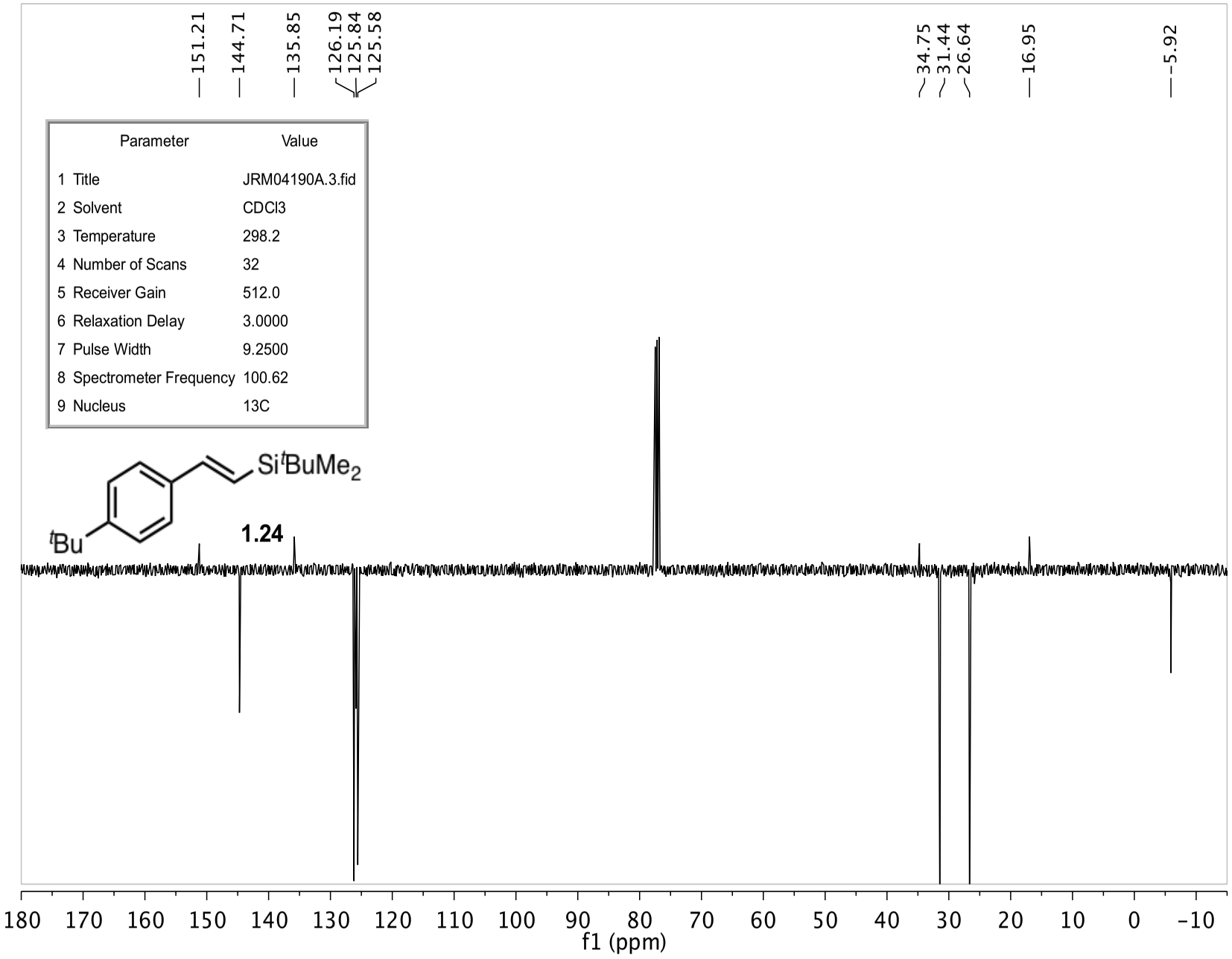
151.21
144.71
135.85
126.19
125.84
125.58
34.75
31.44
26.64
16.95
-5.92
Parameter Value
1 Title JRM04190A.3.fid
2 Solvent CDCl3
3 Temperature 298.2
4 Number of Scans 32
5 Receiver Gain 512.0
6 Relaxation Delay 3.0000
7 Pulse Width 9.2500
8 Spectrometer Frequency 100.62
9 Nucleus 13C
SitBuMe2
tBu
1.24
180 170 160 150 140 130 120 110 100 90 80 70 60 50 40 30 20 10 0 -10
f1 (ppm)

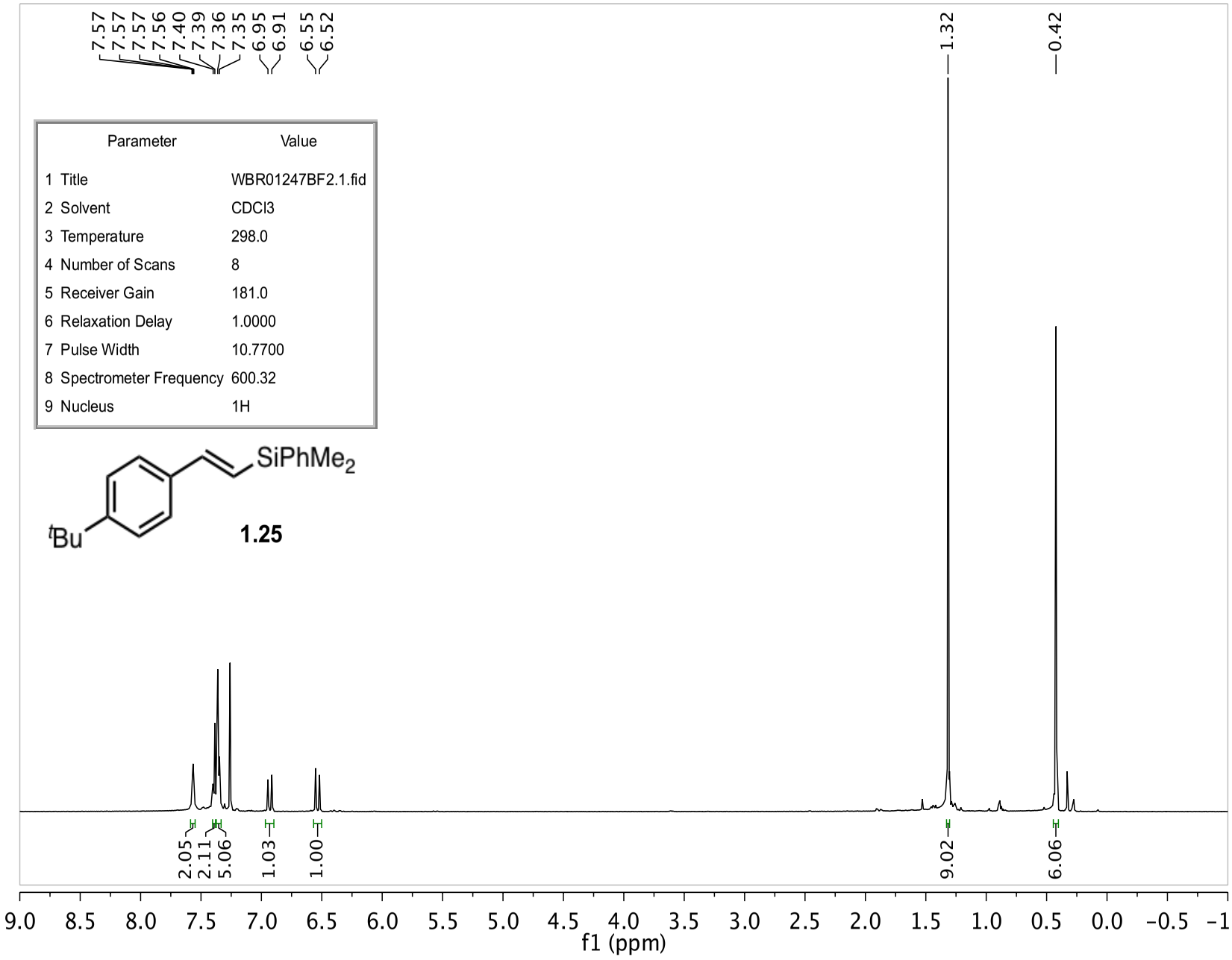
7.57
7.57
7.57
7.56
7.40
7.39
7.36
7.35
6.95
6.91
6.55
6.52
1.32
0.42
Parameter Value
1 Title WBR01247BF2.1.fid
2 Solvent CDCl3
3 Temperature 298.0
4 Number of Scans 8
5 Receiver Gain 181.0
6 Relaxation Delay 1.0000
7 Pulse Width 10.7700
8 Spectrometer Frequency 600.32
9 Nucleus 1H
SiPhMe2
tBu
1.25
2.05
2.11
5.06
1.03
1.00
9.02
6.06
9.0 8.5 8.0 7.5 7.0 6.5 6.0 5.5 5.0 4.5 4.0 3.5 3.0 2.5 2.0 1.5 1.0 0.5 0.0 -0.5 -1.0
f1 (ppm)

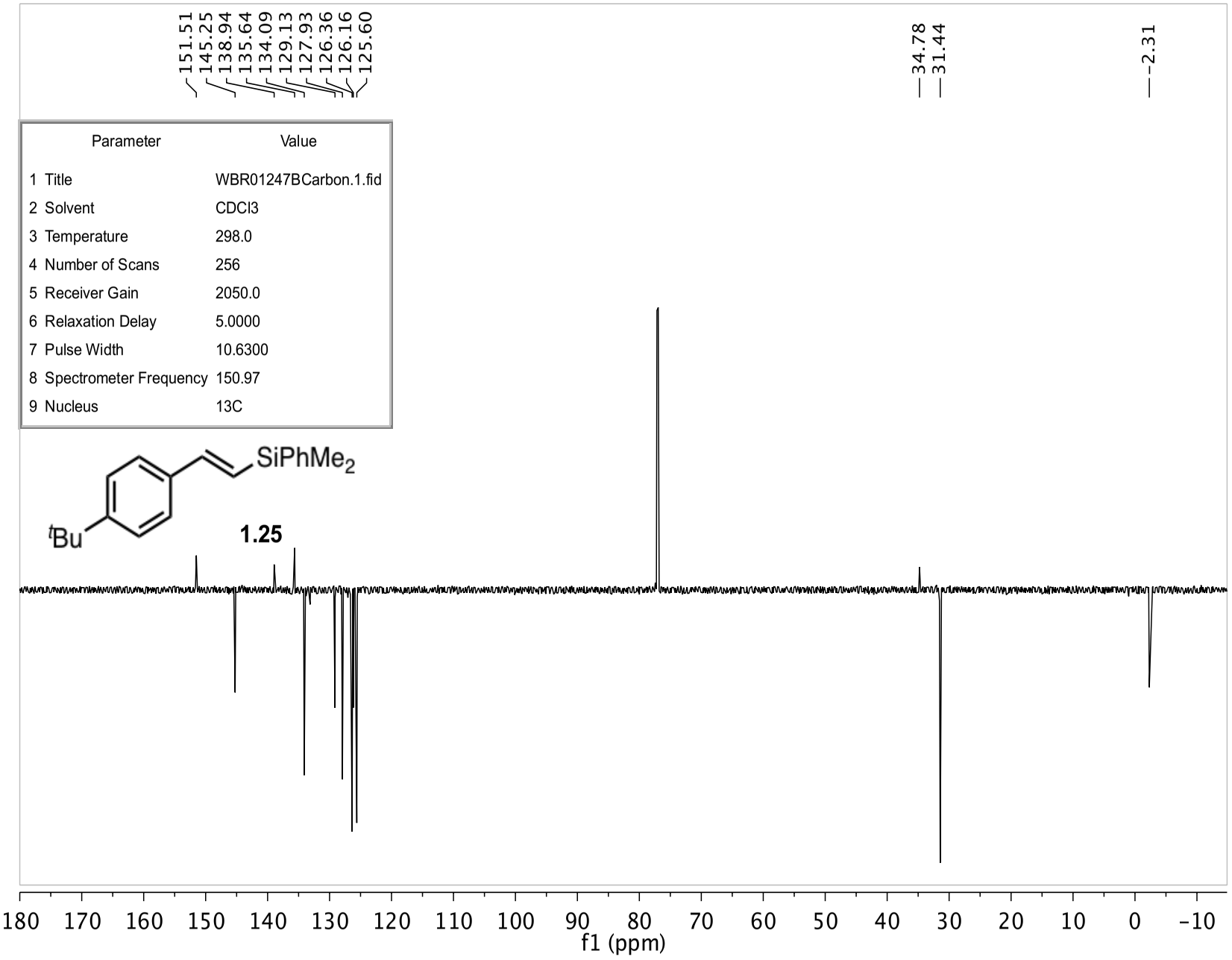
151.51
145.25
138.94
135.64
134.09
129.13
127.93
126.36
126.16
125.60
34.78
31.44
-2.31
Parameter Value
1 Title WBR01247BCarbon.1.fid
2 Solvent CDCl3
3 Temperature 298.0
4 Number of Scans 256
5 Receiver Gain 2050.0
6 Relaxation Delay 5.0000
7 Pulse Width 10.6300
8 Spectrometer Frequency 150.97
9 Nucleus 13C
SiPhMe2
tBu
1.25
180 170 160 150 140 130 120 110 100 90 80 70 60 50 40 30 20 10 0 -10
f1 (ppm)

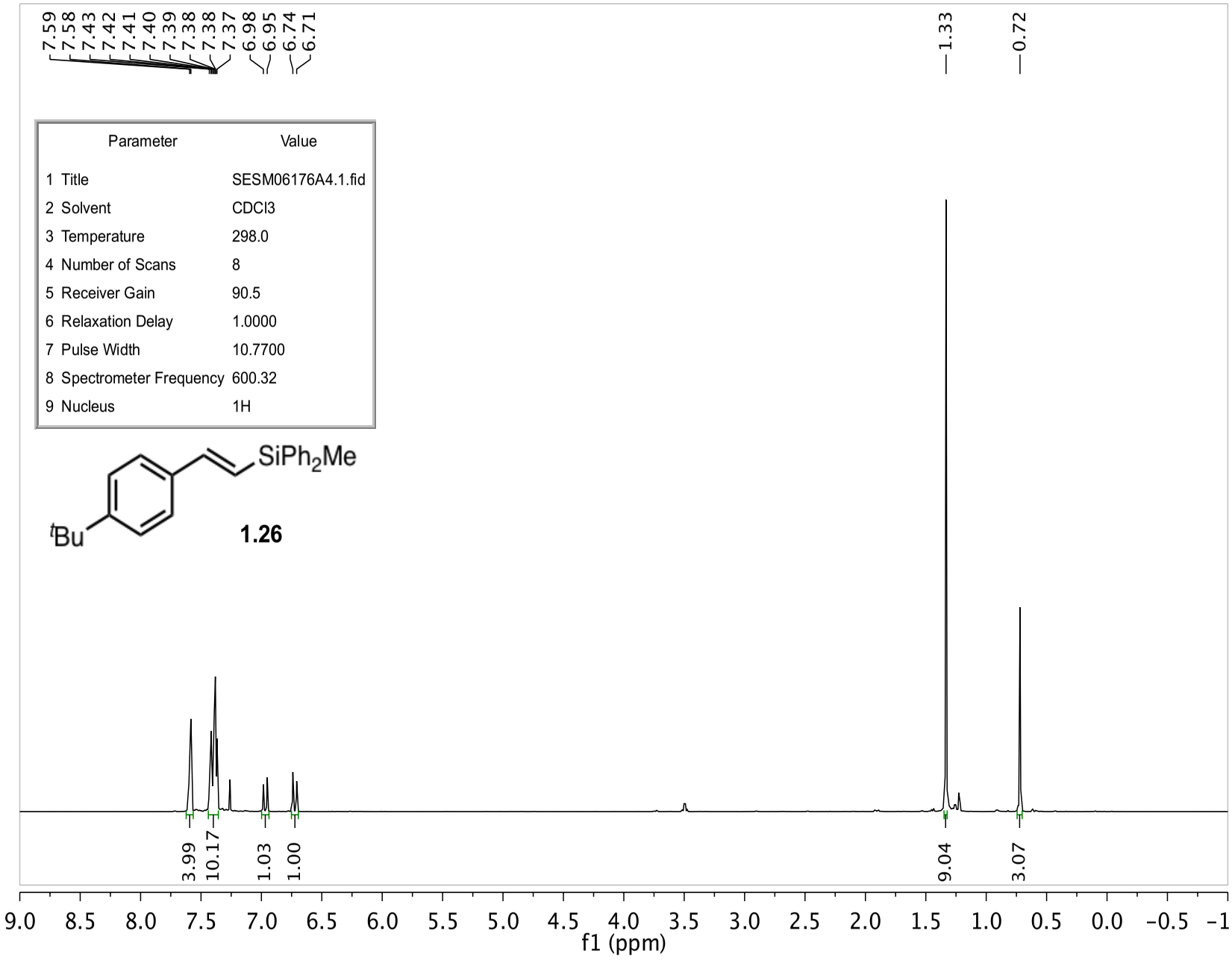
7.59
7.58
7.43
7.42
7.41
7.40
7.39
7.38
7.38
7.37
6.98
6.95
6.74
6.71
1.33
0.72
Parameter Value
1 Title SESM06176A4.1.fid
2 Solvent CDCl3
3 Temperature 298.0
4 Number of Scans 8
5 Receiver Gain 90.5
6 Relaxation Delay 1.0000
7 Pulse Width 10.7700
8 Spectrometer Frequency 600.32
9 Nucleus 1H
SiPh2Me
tBu
1.26
3.99
10.17
1.03
1.00
9.04
3.07
9.0 8.5 8.0 7.5 7.0 6.5 6.0 5.5 5.0 4.5 4.0 3.5 3.0 2.5 2.0 1.5 1.0 0.5 0.0 -0.5 -1.0
f1 (ppm)

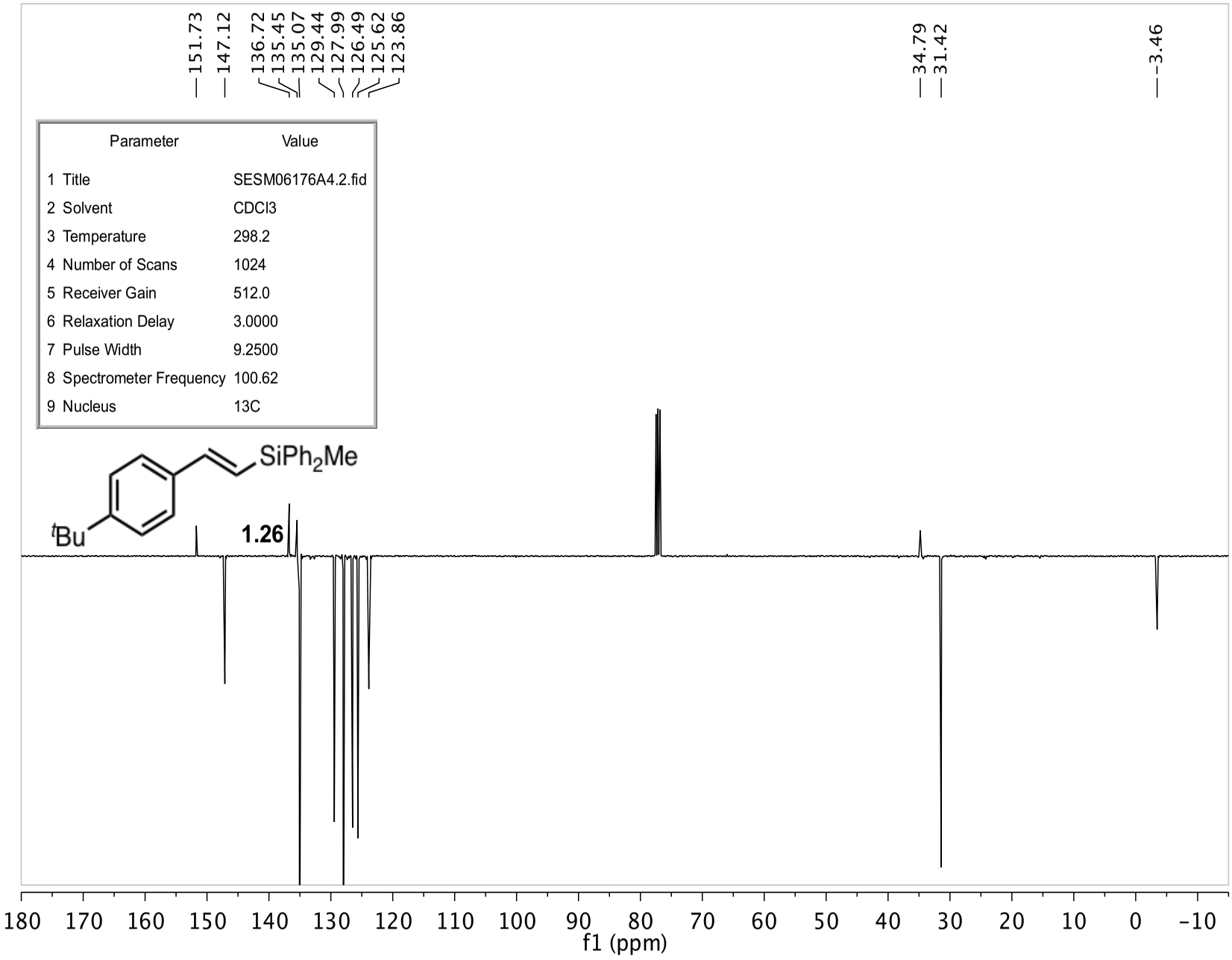
151.73
147.12
136.72
135.45
135.07
129.44
127.99
126.49
125.62
123.86
34.79
31.42
-3.46
Parameter Value
1 Title SESM06176A4.2.fid
2 Solvent CDCl3
3 Temperature 298.2
4 Number of Scans 1024
5 Receiver Gain 512.0
6 Relaxation Delay 3.0000
7 Pulse Width 9.2500
8 Spectrometer Frequency 100.62
9 Nucleus 13C
SiPh2Me
tBu
1.26
180 170 160 150 140 130 120 110 100 90 80 70 60 50 40 30 20 10 0 -10
f1 (ppm)

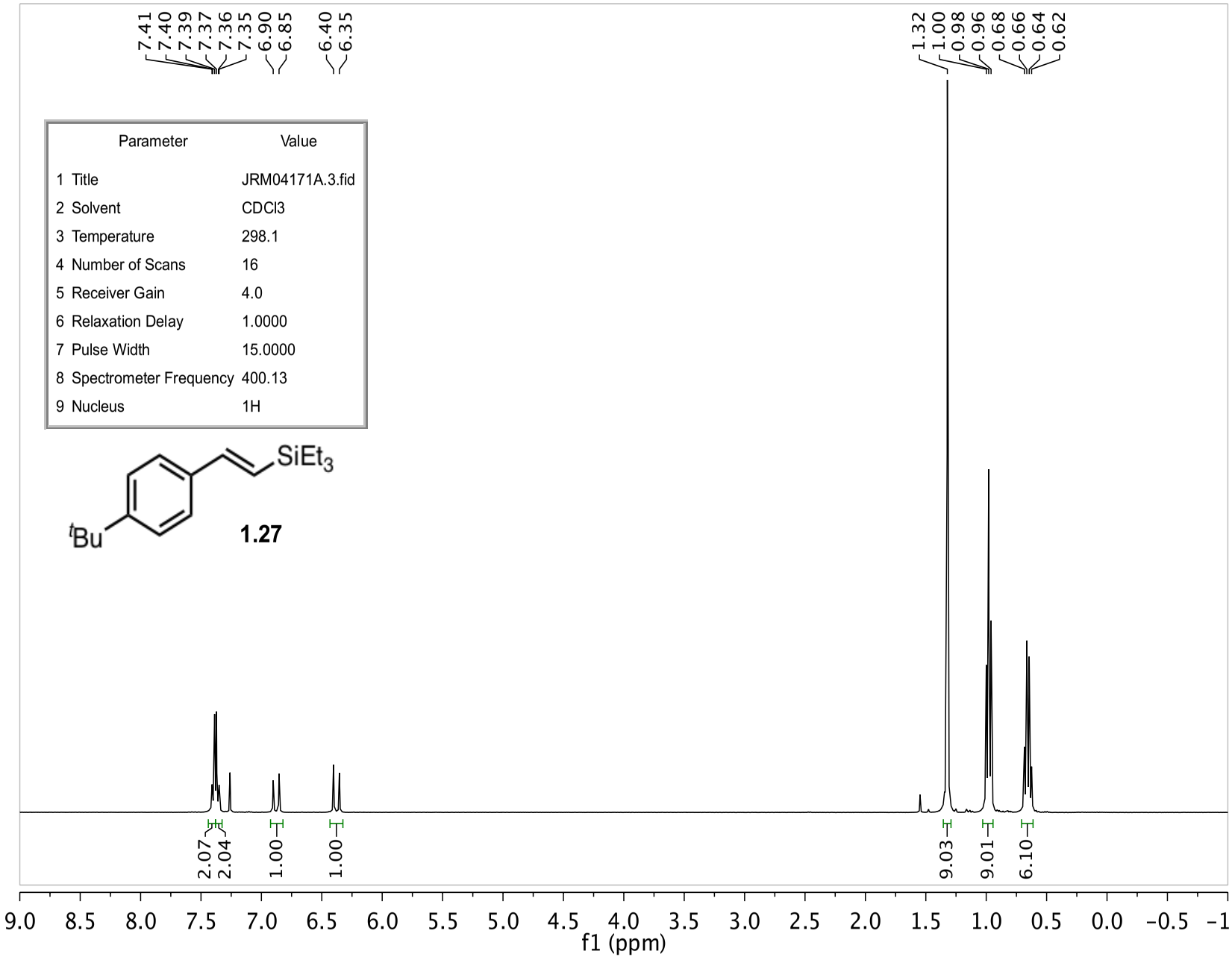
7.41
7.40
7.39
7.37
7.36
7.35
6.90
6.85
6.40
6.35
1.32
1.00
0.98
0.96
0.68
0.66
0.64
0.62
Parameter Value
1 Title JRM04171A.3.fid
2 Solvent CDCl3
3 Temperature 298.1
4 Number of Scans 16
5 Receiver Gain 4.0
6 Relaxation Delay 1.0000
7 Pulse Width 15.0000
8 Spectrometer Frequency 400.13
9 Nucleus 1H
SiEt3
tBu
1.27
2.07
2.04
1.00
1.00
9.03
9.01
6.10
9.0 8.5 8.0 7.5 7.0 6.5 6.0 5.5 5.0 4.5 4.0 3.5 3.0 2.5 2.0 1.5 1.0 0.5 0.0 -0.5 -1.0
f1 (ppm)

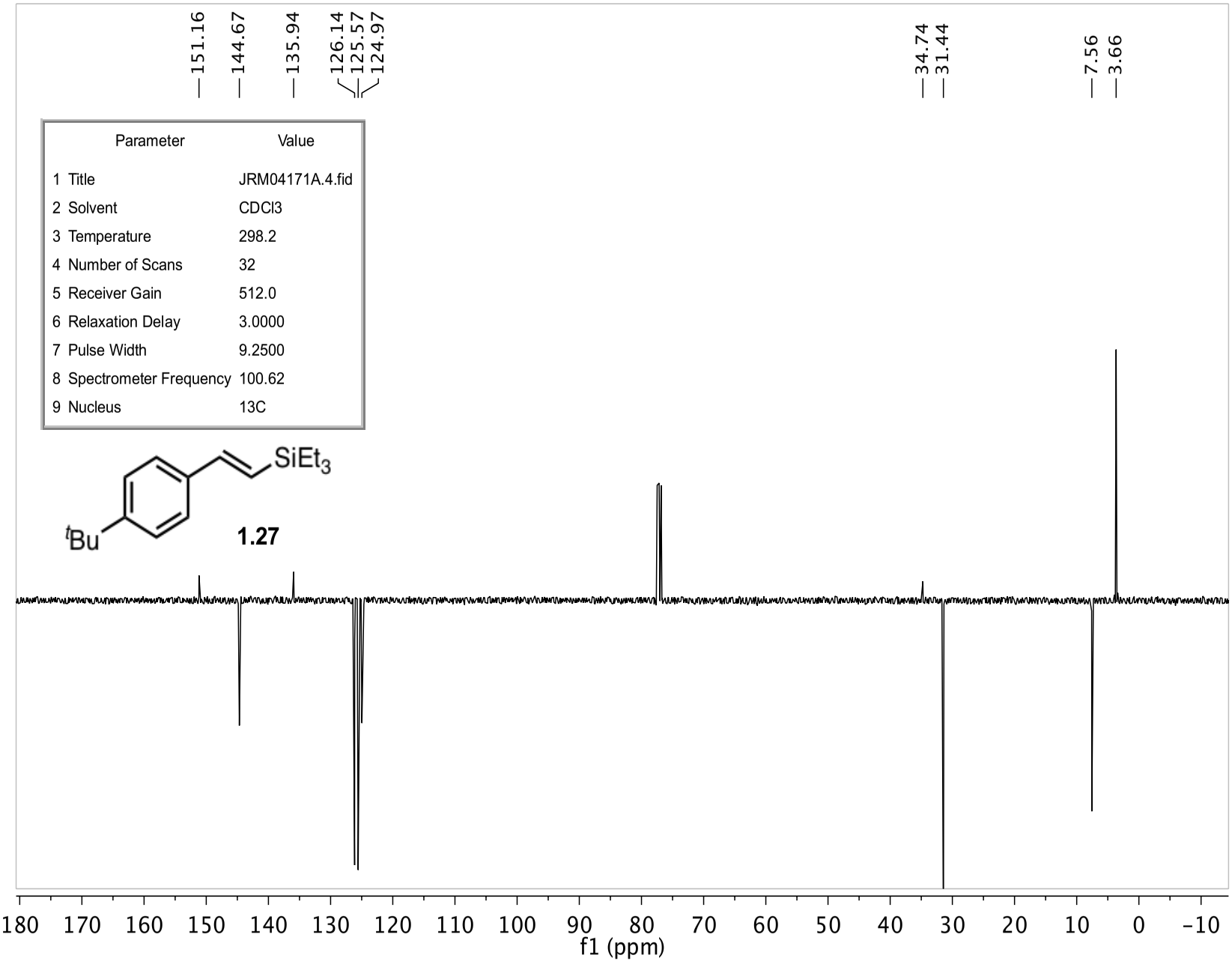
151.16
144.67
135.94
126.14
125.57
124.97
34.74
31.44
7.56
3.66
Parameter Value
1 Title JRM04171A.4.fid
2 Solvent CDCl3
3 Temperature 298.2
4 Number of Scans 32
5 Receiver Gain 512.0
6 Relaxation Delay 3.0000
7 Pulse Width 9.2500
8 Spectrometer Frequency 100.62
9 Nucleus 13C
SiEt3
tBu
1.27
180 170 160 150 140 130 120 110 100 90 80 70 60 50 40 30 20 10 0 -10
f1 (ppm)

Appendix C

Spectral Data for Chapter 2

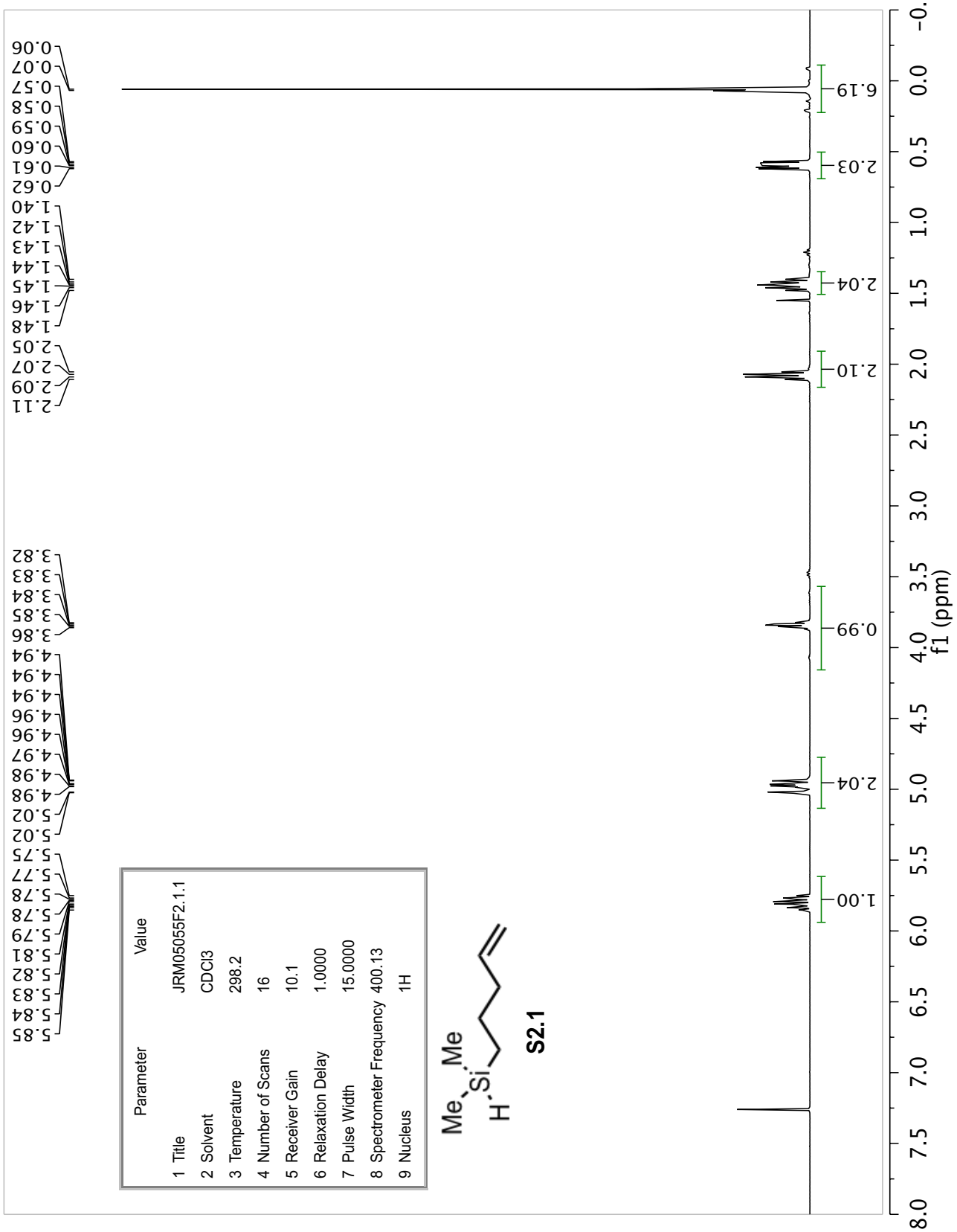
Parameter Value
1 Title JRM05055F2.1.1
2 Solvent CDCl3
3 Temperature 298.2
4 Number of Scans 16
5 Receiver Gain 10.1
6 Relaxation Delay 1.0000
7 Pulse Width 15.0000
8 Spectrometer Frequency 400.13
9 Nucleus 1H
Me
Me
Si
H
S2.1
1.00
2.04
0.99
2.04
2.10
2.03
6.19
f1 (ppm)

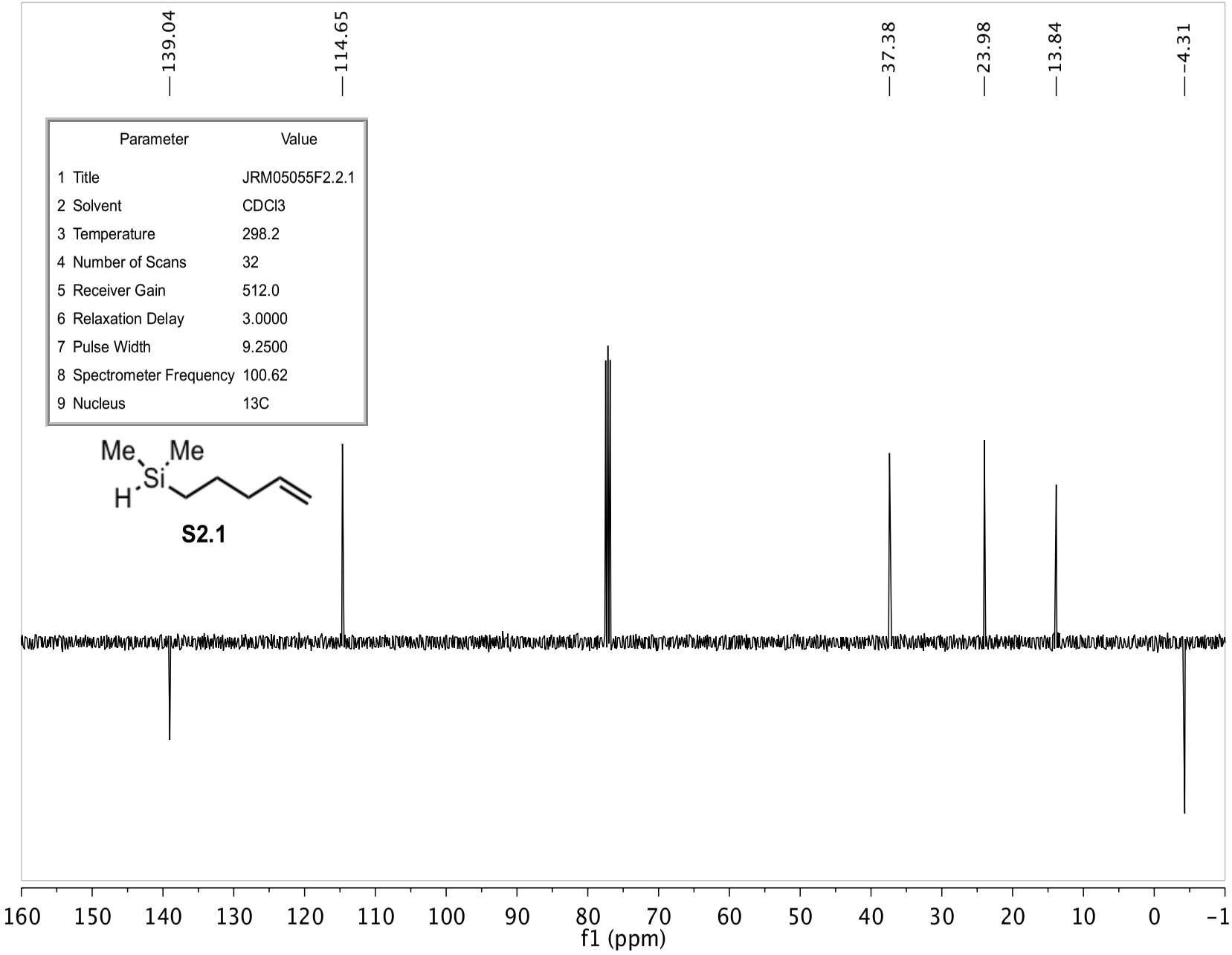
139.04
114.65
37.38
23.98
13.84
-4.31
Parameter Value
1 Title JRM05055F2.2.1
2 Solvent CDCl3
3 Temperature 298.2
4 Number of Scans 32
5 Receiver Gain 512.0
6 Relaxation Delay 3.0000
7 Pulse Width 9.2500
8 Spectrometer Frequency 100.62
9 Nucleus 13C
Me
Me
Si
H
S2.1
160 150 140 130 120 110 100 90 80 70 60 50 40 30 20 10 0 -10
f1 (ppm)

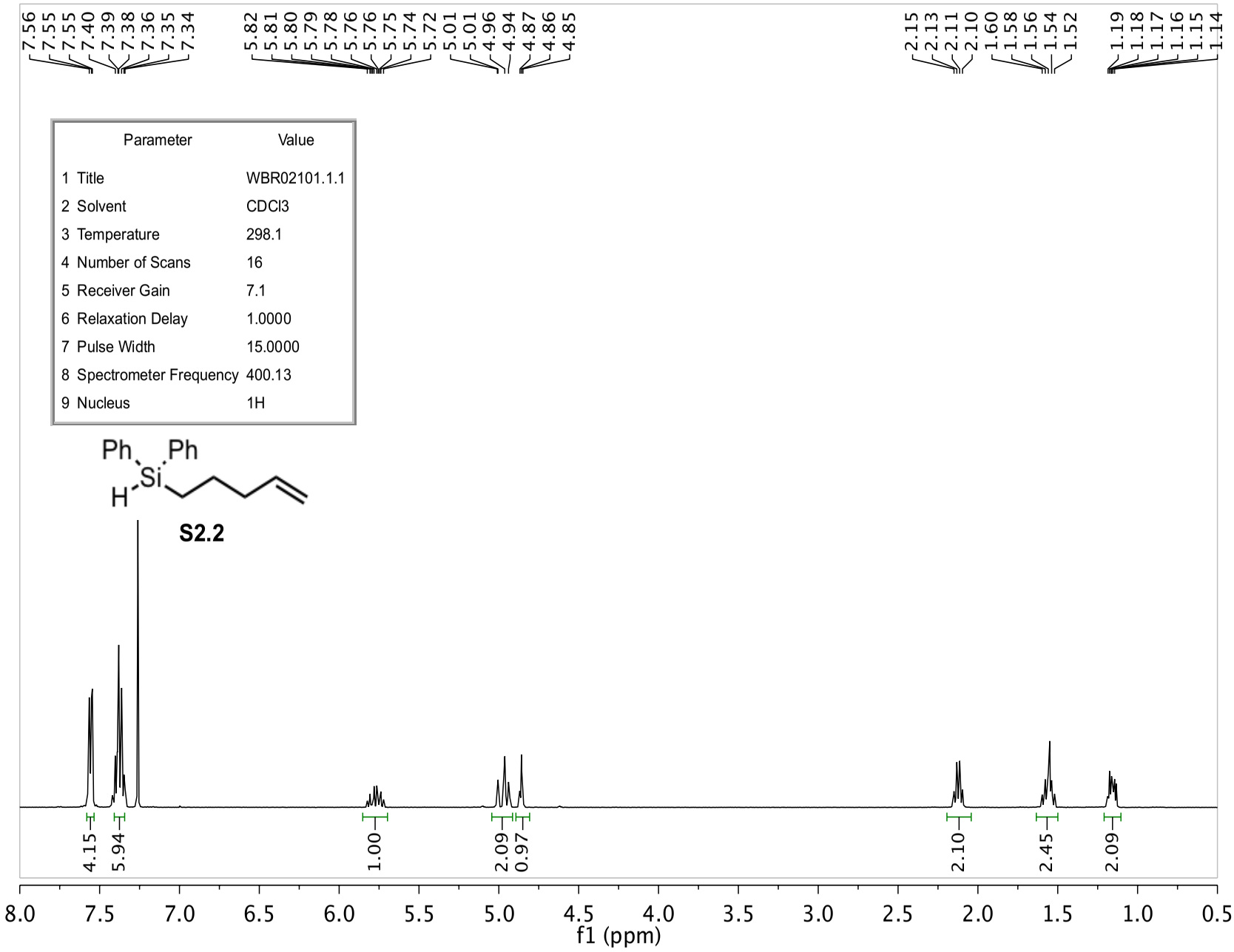
7.56 7.55 7.55 7.40 7.39 7.38 7.36 7.35 7.34
5.82 5.81 5.80 5.79 5.78 5.76 5.76 5.75 5.74 5.72
5.01 5.01 4.96 4.94 4.87 4.86 4.85
2.15 2.13 2.11 2.10 1.60 1.58 1.56 1.54 1.52
1.19 1.18 1.17 1.16 1.15 1.14
Parameter Value
1 Title WBR02101.1.1
2 Solvent CDCl3
3 Temperature 298.1
4 Number of Scans 16
5 Receiver Gain 7.1
6 Relaxation Delay 1.0000
7 Pulse Width 15.0000
8 Spectrometer Frequency 400.13
9 Nucleus 1H
Ph Ph
Si
H
S2.2
4.15 5.94 1.00 2.09 0.97 2.10 2.45 2.09
8.0 7.5 7.0 6.5 6.0 5.5 5.0 4.5 4.0 3.5 3.0 2.5 2.0 1.5 1.0 0.5
f1 (ppm)

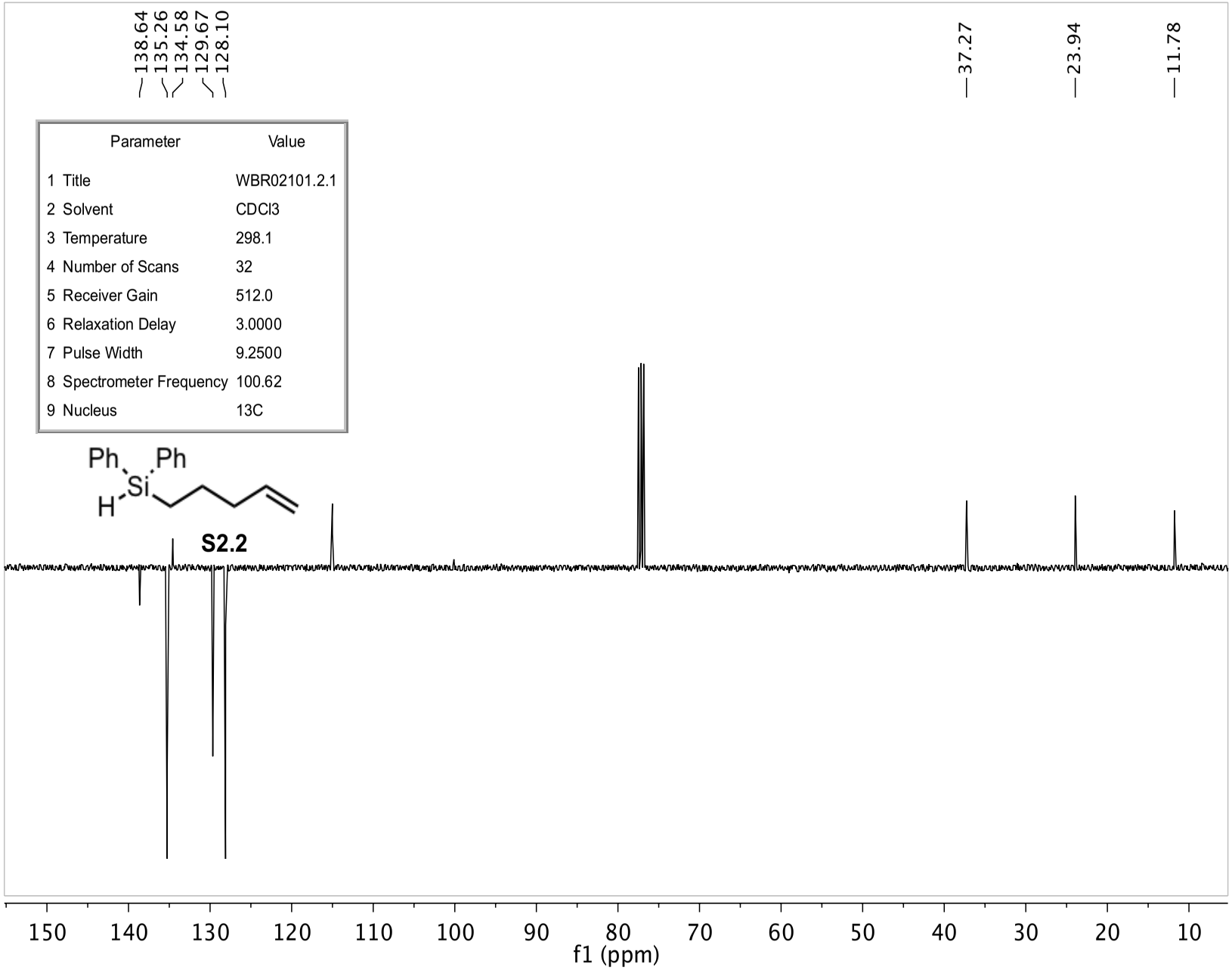
138.64
135.26
134.58
129.67
128.10
37.27
23.94
11.78
Parameter Value
1 Title WBR02101.2.1
2 Solvent CDCl3
3 Temperature 298.1
4 Number of Scans 32
5 Receiver Gain 512.0
6 Relaxation Delay 3.0000
7 Pulse Width 9.2500
8 Spectrometer Frequency 100.62
9 Nucleus 13C
Ph
Ph
Si
H
S2.2
150 140 130 120 110 100 90 80 70 60 50 40 30 20 10
f1 (ppm)

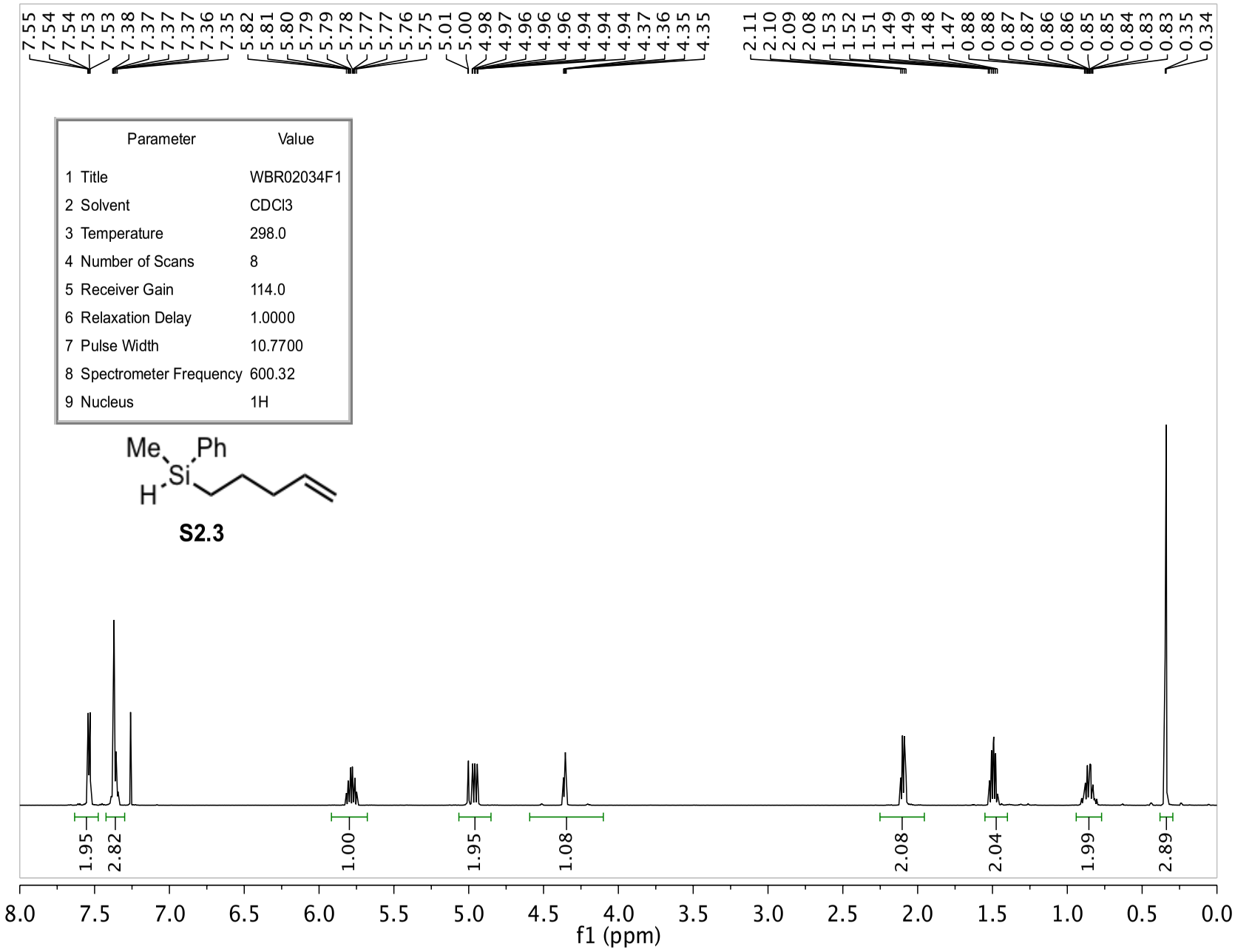
7.55 7.54 7.54 7.53 7.53 7.38 7.37 7.37 7.37 7.36 7.35 5.82 5.81 5.80 5.79 5.79 5.78 5.77 5.77 5.76 5.75 5.01 5.00 4.98 4.97 4.96 4.96 4.96 4.94 4.94 4.94 4.37 4.36 4.35 4.35 2.11 2.10 2.09 2.08 1.53 1.52 1.51 1.49 1.49 1.48 1.47 0.88 0.88 0.87 0.87 0.86 0.86 0.85 0.85 0.84 0.83 0.83 0.35 0.34
Parameter Value
1 Title WBR02034F1
2 Solvent CDCl3
3 Temperature 298.0
4 Number of Scans 8
5 Receiver Gain 114.0
6 Relaxation Delay 1.0000
7 Pulse Width 10.7700
8 Spectrometer Frequency 600.32
9 Nucleus 1H
Me
Ph
Si
H
S2.3
1.95 2.82 1.00 1.95 1.08 2.08 2.04 1.99 2.89
8.0 7.5 7.0 6.5 6.0 5.5 5.0 4.5 4.0 3.5 3.0 2.5 2.0 1.5 1.0 0.5 0.0
f1 (ppm)

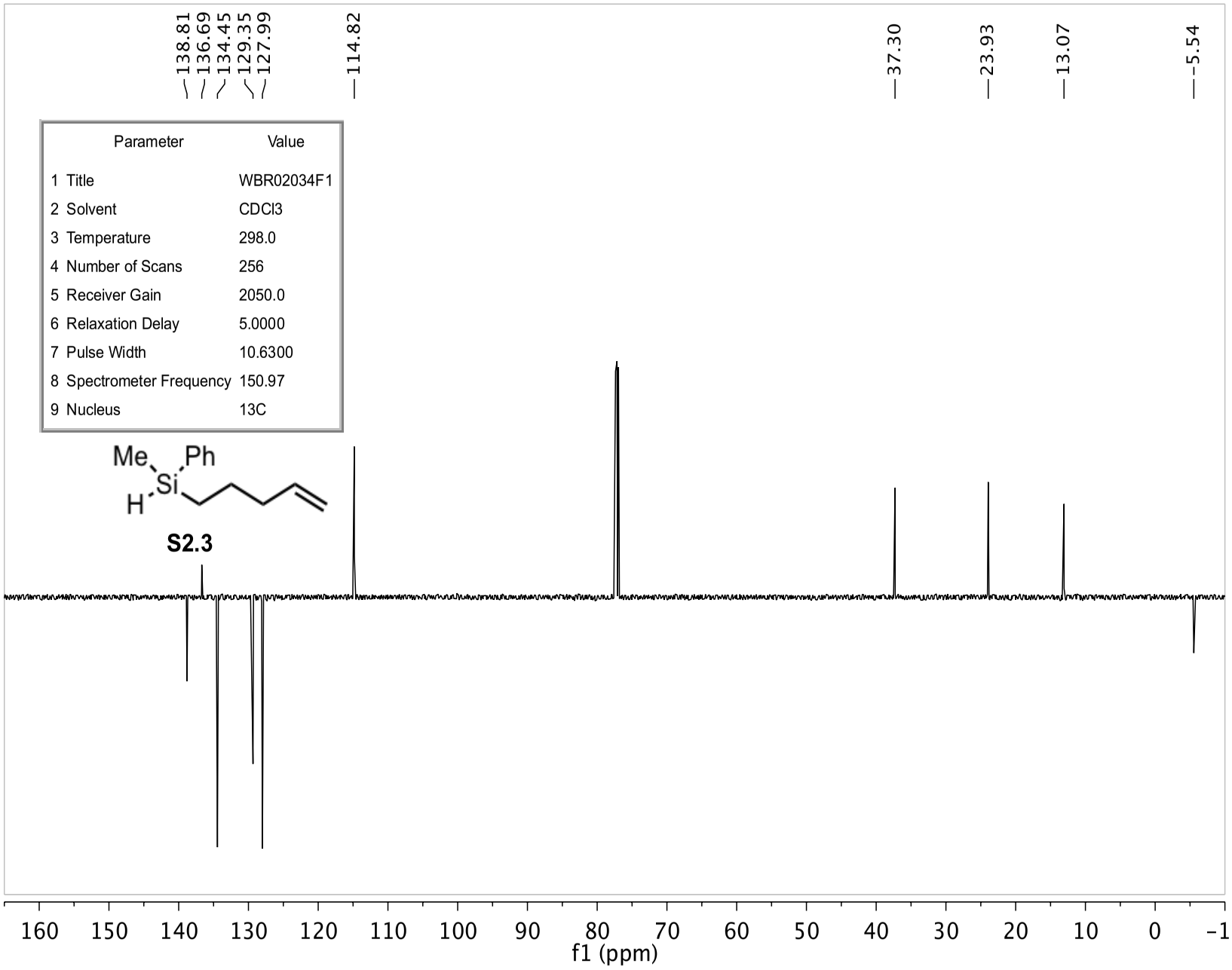
138.81
136.69
134.45
129.35
127.99
114.82
37.30
23.93
13.07
-5.54
Parameter Value
1 Title WBR02034F1
2 Solvent CDCl3
3 Temperature 298.0
4 Number of Scans 256
5 Receiver Gain 2050.0
6 Relaxation Delay 5.0000
7 Pulse Width 10.6300
8 Spectrometer Frequency 150.97
9 Nucleus 13C
Me
Ph
Si
H
S2.3
160 150 140 130 120 110 100 90 80 70 60 50 40 30 20 10 0 -10
f1 (ppm)

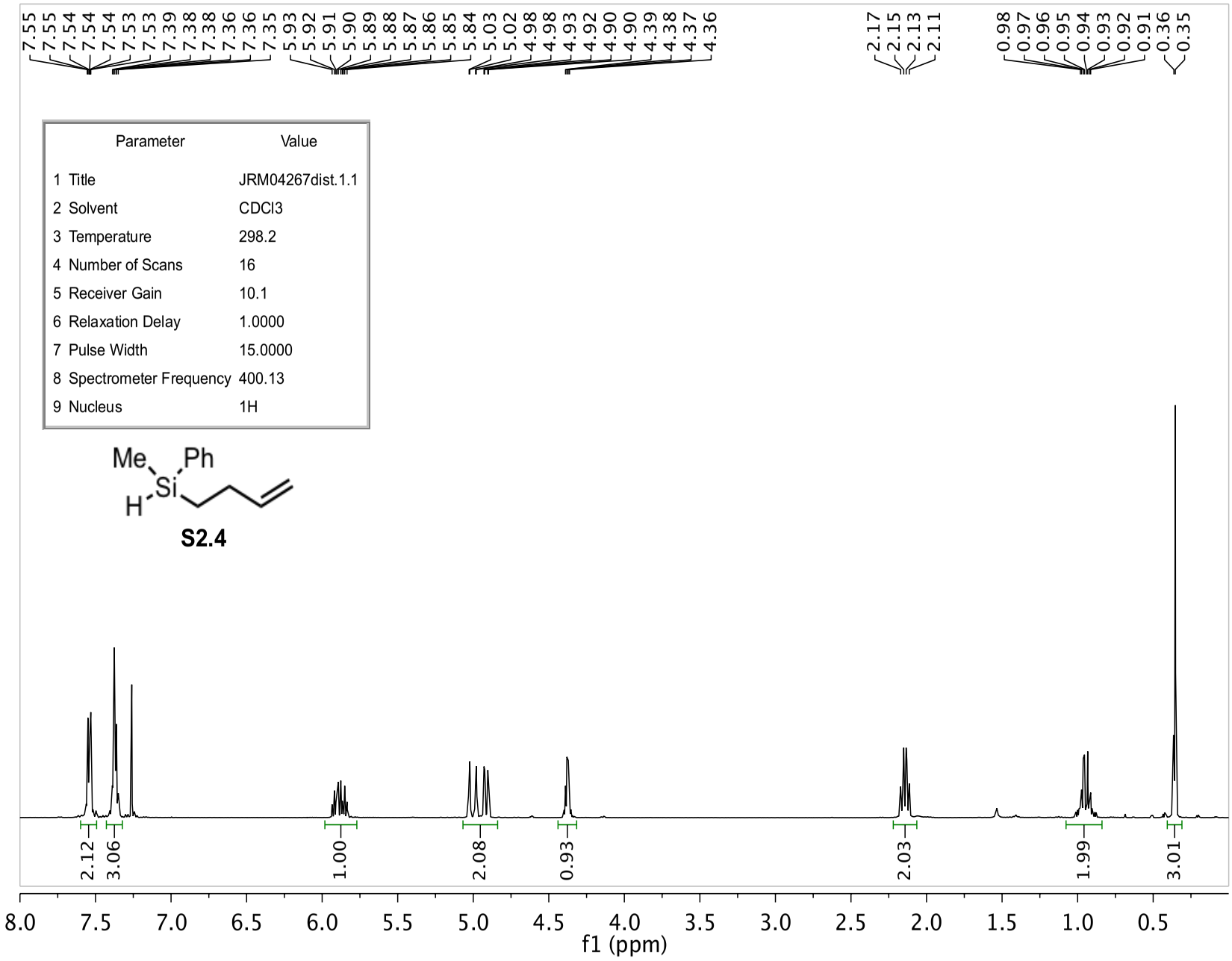
7.55 7.55 7.54 7.54 7.54 7.53 7.53 7.39 7.38 7.38 7.36 7.36 7.35
5.93 5.92 5.91 5.90 5.89 5.88 5.87 5.86 5.85 5.84 5.03 5.02 4.98 4.98 4.93 4.92 4.90 4.90 4.39 4.38 4.37 4.36
2.17 2.15 2.13 2.11
0.98 0.97 0.96 0.95 0.94 0.93 0.92 0.91 0.36 0.35
Parameter Value
1 Title JRM04267dist.1.1
2 Solvent CDCl3
3 Temperature 298.2
4 Number of Scans 16
5 Receiver Gain 10.1
6 Relaxation Delay 1.0000
7 Pulse Width 15.0000
8 Spectrometer Frequency 400.13
9 Nucleus 1H
Me
Ph
Si
H
S2.4
2.12
3.06
1.00
2.08
0.93
2.03
1.99
3.01
8.0 7.5 7.0 6.5 6.0 5.5 5.0 4.5 4.0 3.5 3.0 2.5 2.0 1.5 1.0 0.5
f1 (ppm)

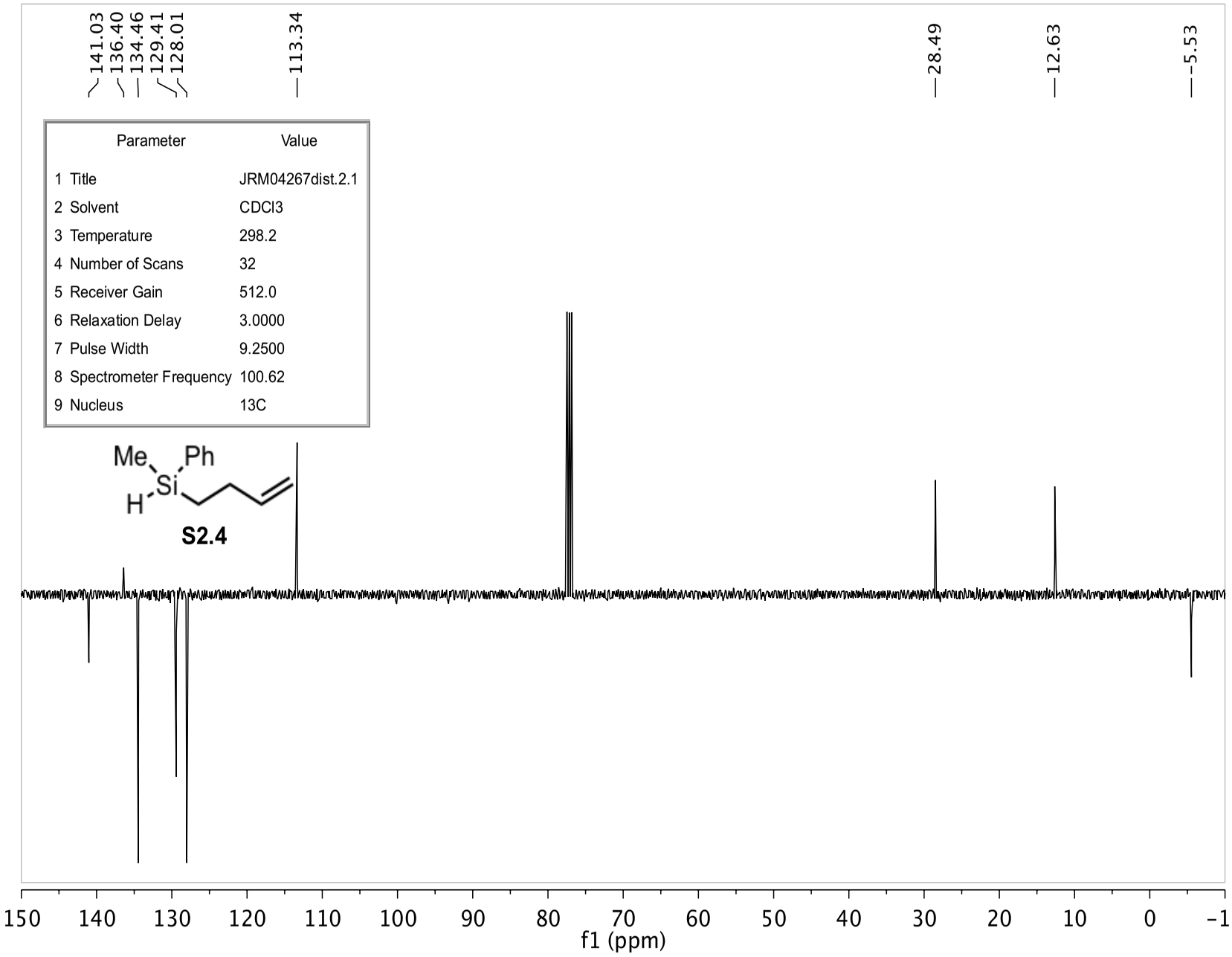
141.03
136.40
134.46
129.41
128.01
113.34
28.49
12.63
-5.53
Parameter Value
1 Title JRM04267dist.2.1
2 Solvent CDCl3
3 Temperature 298.2
4 Number of Scans 32
5 Receiver Gain 512.0
6 Relaxation Delay 3.0000
7 Pulse Width 9.2500
8 Spectrometer Frequency 100.62
9 Nucleus 13C
Me
Ph
Si
H
S2.4
150 140 130 120 110 100 90 80 70 60 50 40 30 20 10 0 -10
f1 (ppm)

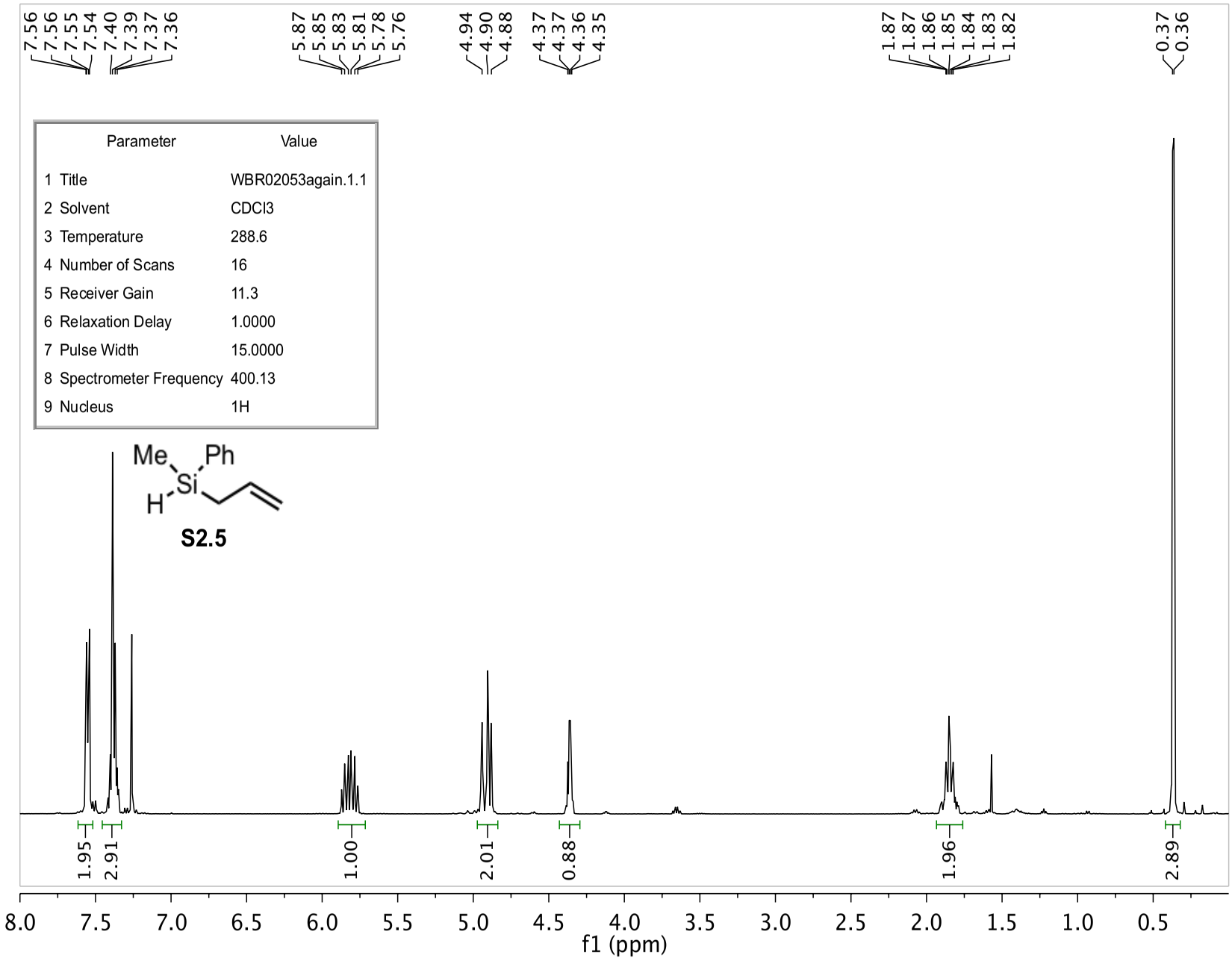
7.56
7.56
7.55
7.54
7.40
7.39
7.37
7.36
5.87
5.85
5.83
5.81
5.78
5.76
4.94
4.90
4.88
4.37
4.37
4.36
4.35
1.87
1.87
1.86
1.85
1.84
1.83
1.82
0.37
0.36
Parameter Value
1 Title WBR02053again.1.1
2 Solvent CDCl3
3 Temperature 288.6
4 Number of Scans 16
5 Receiver Gain 11.3
6 Relaxation Delay 1.0000
7 Pulse Width 15.0000
8 Spectrometer Frequency 400.13
9 Nucleus 1H
Me
Ph
Si
H
S2.5
1.95
2.91
1.00
2.01
0.88
1.96
2.89
8.0
7.5
7.0
6.5
6.0
5.5
5.0
4.5
4.0
3.5
3.0
2.5
2.0
1.5
1.0
0.5
f1 (ppm)

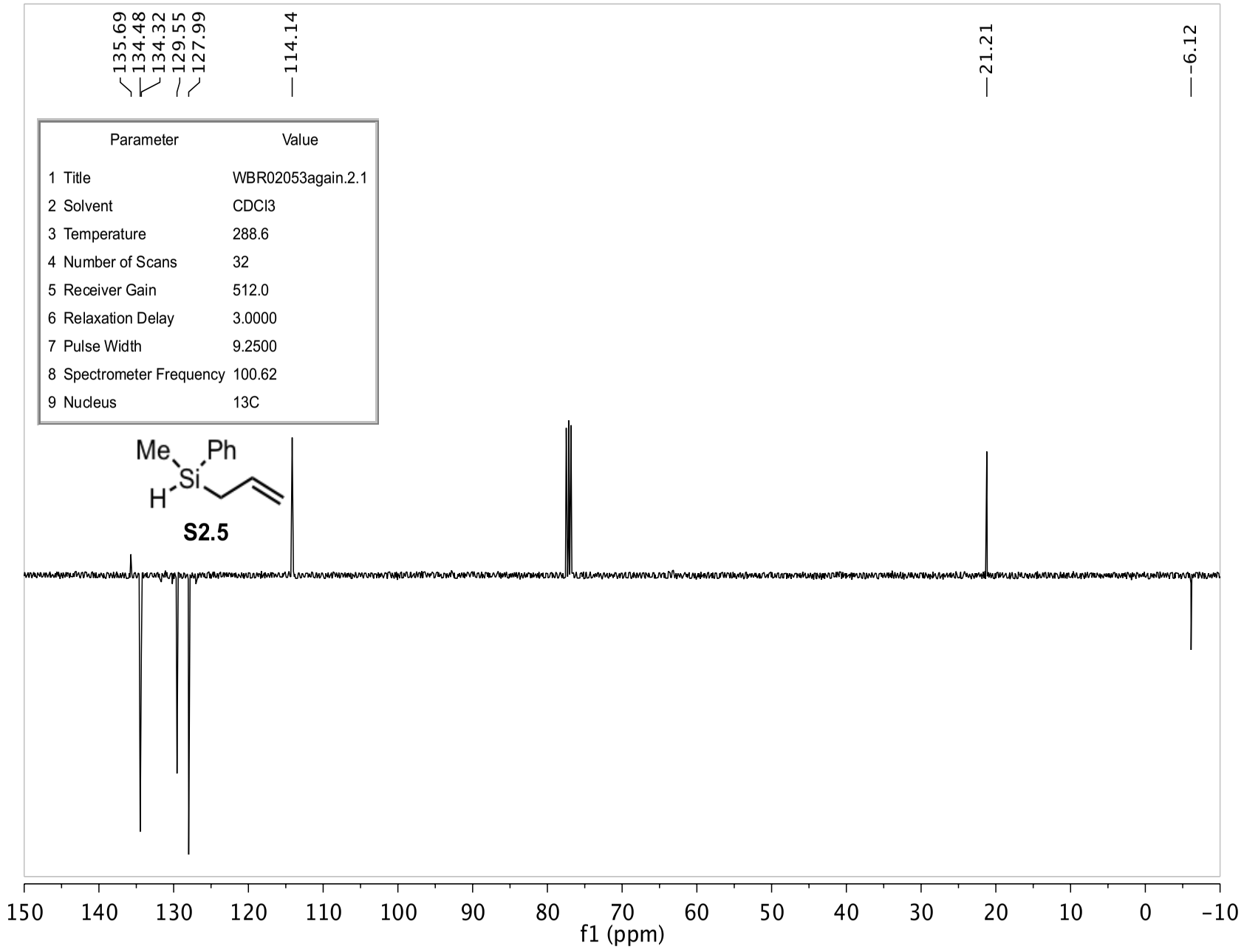
135.69
134.48
134.32
129.55
127.99
114.14
21.21
-6.12
Parameter Value
1 Title WBR02053again.2.1
2 Solvent CDCl3
3 Temperature 288.6
4 Number of Scans 32
5 Receiver Gain 512.0
6 Relaxation Delay 3.0000
7 Pulse Width 9.2500
8 Spectrometer Frequency 100.62
9 Nucleus 13C
Me
Ph
Si
H
S2.5
150 140 130 120 110 100 90 80 70 60 50 40 30 20 10 0 -10
f1 (ppm)

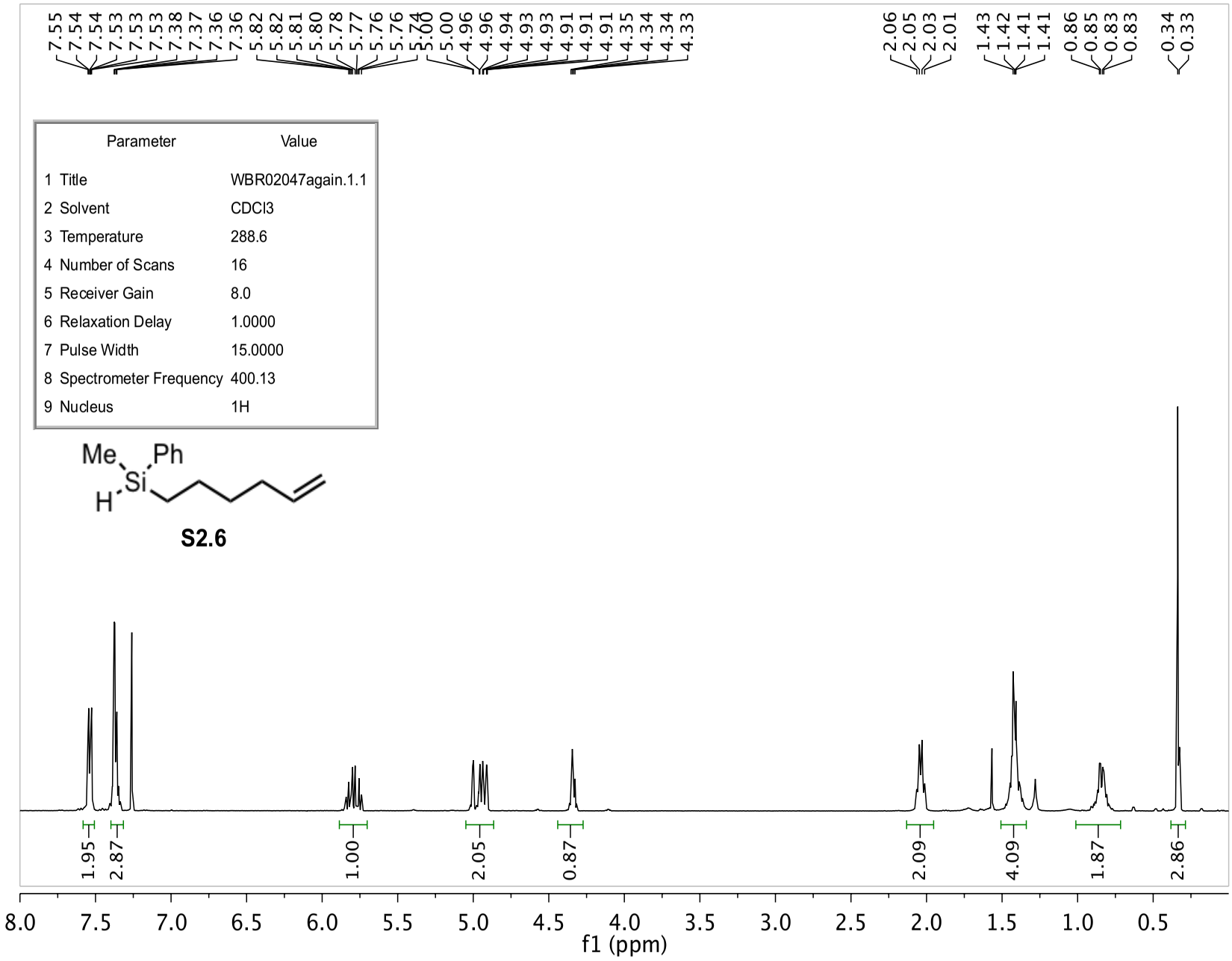
7.55 7.54 7.54 7.53 7.53 7.53 7.38 7.37 7.36 7.36
5.82 5.82 5.81 5.80 5.78 5.77 5.76 5.76 5.74 5.00
4.96 4.96 4.94 4.93 4.93 4.91 4.91 4.91 4.35 4.34 4.34 4.33
2.06 2.05 2.03 2.01
1.43 1.42 1.41 1.41
0.86 0.85 0.83 0.83
0.34 0.33
Parameter Value
1 Title WBR02047again.1.1
2 Solvent CDCl3
3 Temperature 288.6
4 Number of Scans 16
5 Receiver Gain 8.0
6 Relaxation Delay 1.0000
7 Pulse Width 15.0000
8 Spectrometer Frequency 400.13
9 Nucleus 1H
Me
Ph
Si
H
S2.6
1.95
2.87
1.00
2.05
0.87
2.09
4.09
1.87
2.86
8.0 7.5 7.0 6.5 6.0 5.5 5.0 4.5 4.0 3.5 3.0 2.5 2.0 1.5 1.0 0.5
f1 (ppm)

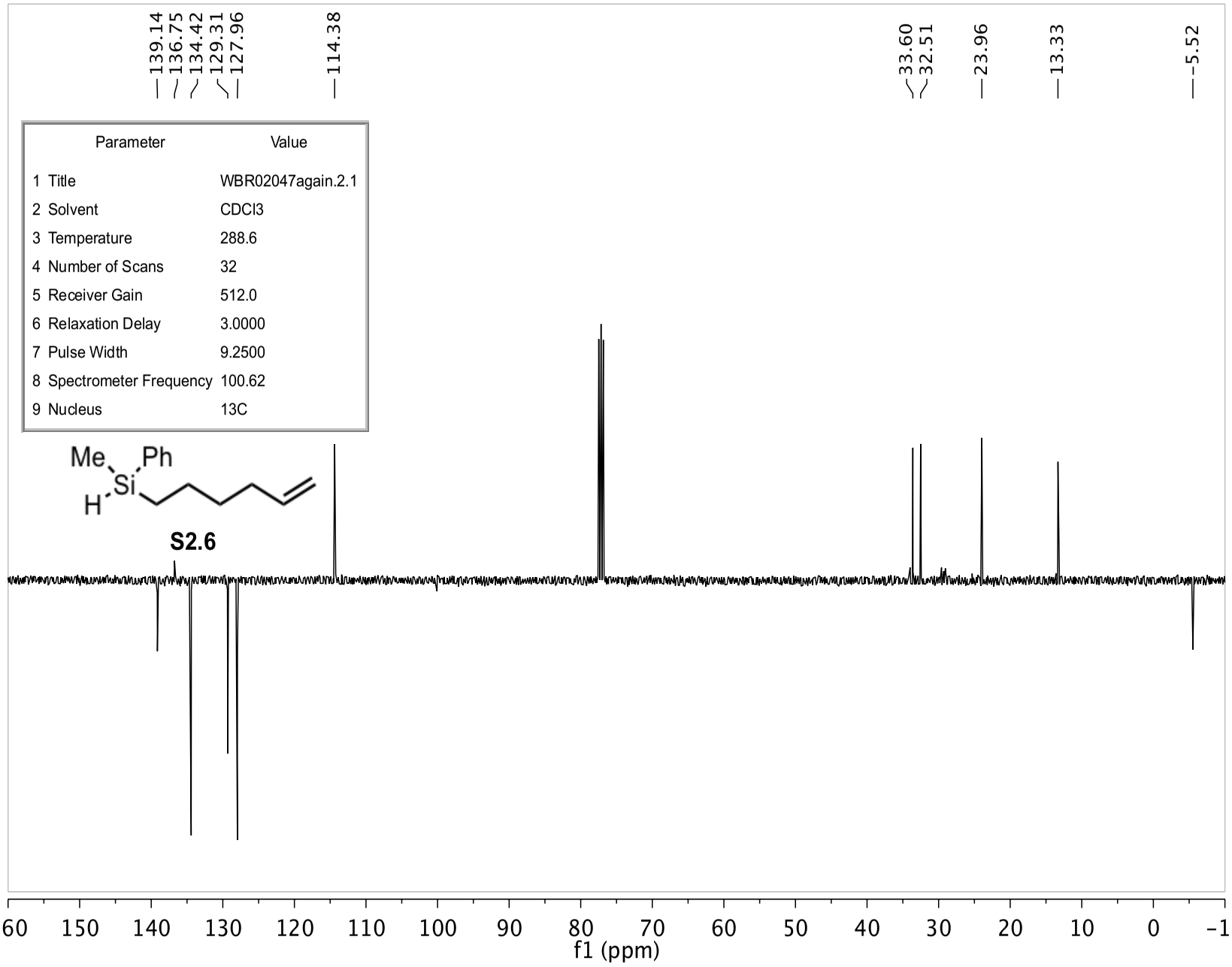
139.14
136.75
134.42
129.31
127.96
114.38
33.60
32.51
23.96
13.33
-5.52
Parameter Value
1 Title WBR02047again.2.1
2 Solvent CDCl3
3 Temperature 288.6
4 Number of Scans 32
5 Receiver Gain 512.0
6 Relaxation Delay 3.0000
7 Pulse Width 9.2500
8 Spectrometer Frequency 100.62
9 Nucleus 13C
Me
Ph
Si
H
S2.6
160 150 140 130 120 110 100 90 80 70 60 50 40 30 20 10 0 -10
f1 (ppm)

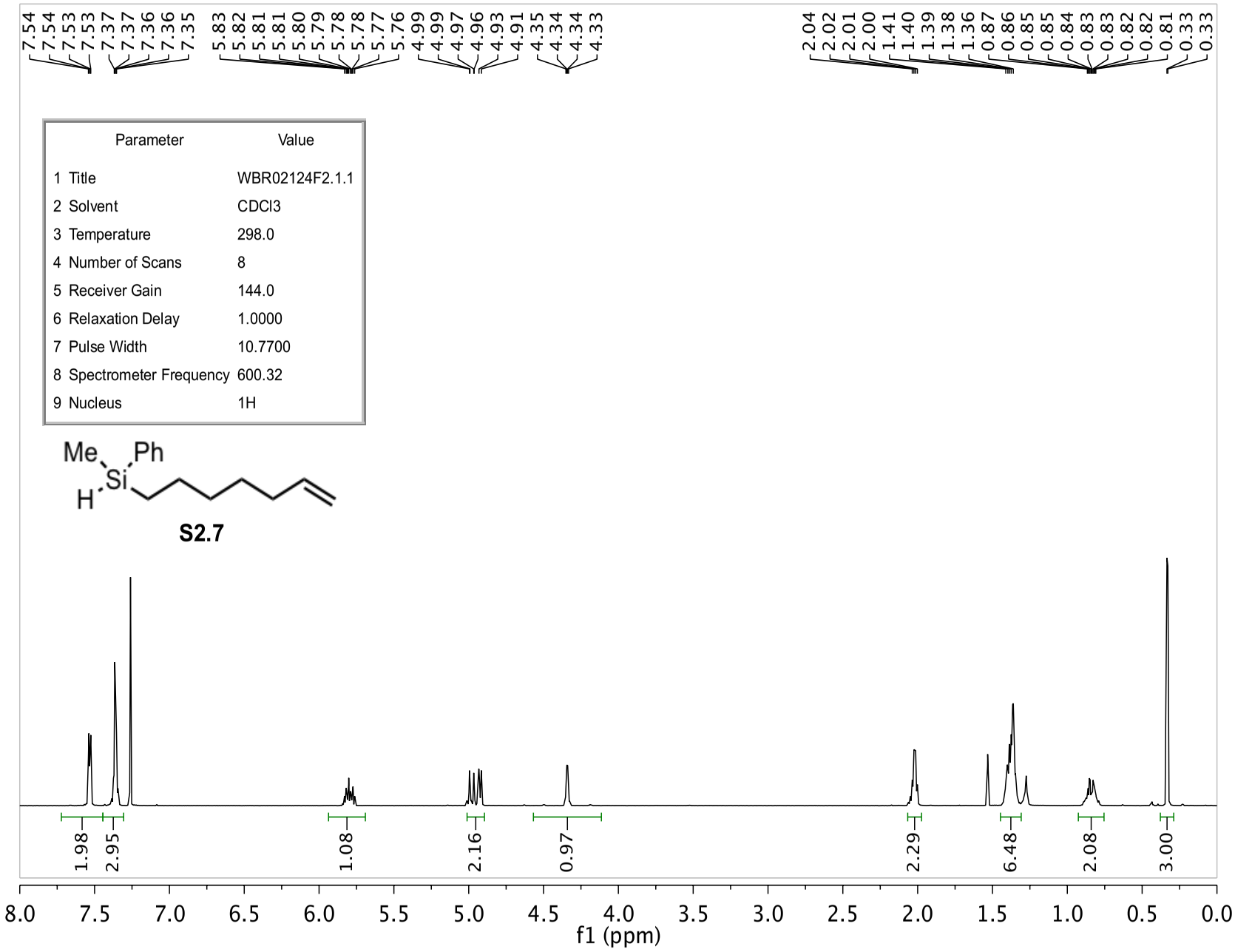
7.54 7.54 7.53 7.53 7.37 7.37 7.36 7.36 7.35
5.83 5.82 5.81 5.81 5.80 5.79 5.78 5.78 5.77 5.76
4.99 4.99 4.97 4.96 4.93 4.91
4.35 4.34 4.34 4.33
2.04 2.02 2.01 2.00 1.41 1.40 1.39 1.38 1.36 0.87 0.86 0.85 0.85 0.84 0.83 0.83 0.82 0.82 0.81 0.33 0.33
Parameter Value
1 Title WBR02124F2.1.1
2 Solvent CDCl3
3 Temperature 298.0
4 Number of Scans 8
5 Receiver Gain 144.0
6 Relaxation Delay 1.0000
7 Pulse Width 10.7700
8 Spectrometer Frequency 600.32
9 Nucleus 1H
Me
Ph
Si
H
S2.7
1.98
2.95
1.08
2.16
0.97
2.29
6.48
2.08
3.00
8.0 7.5 7.0 6.5 6.0 5.5 5.0 4.5 4.0 3.5 3.0 2.5 2.0 1.5 1.0 0.5 0.0
f1 (ppm)

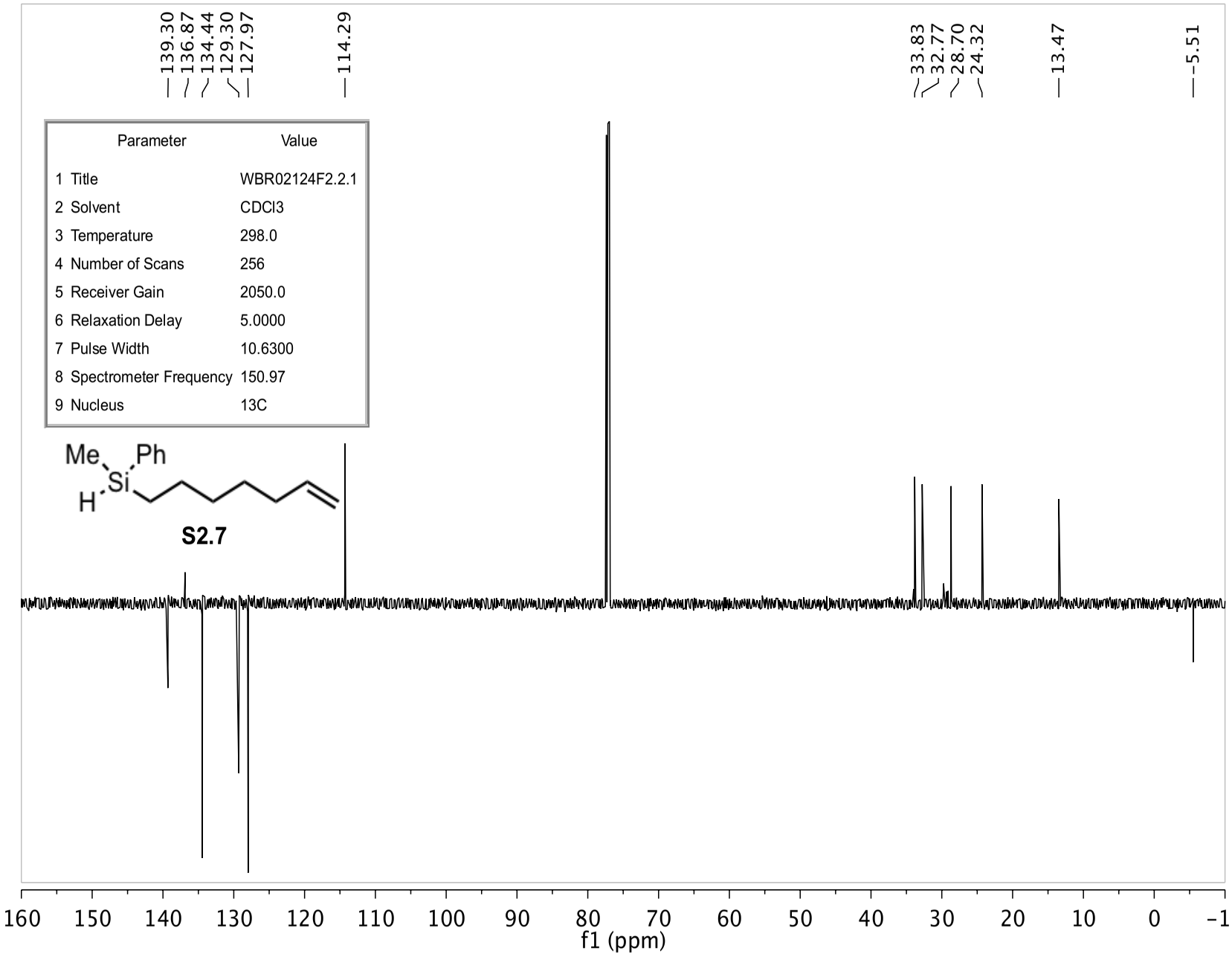
139.30
136.87
134.44
129.30
127.97
114.29
33.83
32.77
28.70
24.32
13.47
-5.51
Parameter Value
1 Title WBR02124F2.2.1
2 Solvent CDCl3
3 Temperature 298.0
4 Number of Scans 256
5 Receiver Gain 2050.0
6 Relaxation Delay 5.0000
7 Pulse Width 10.6300
8 Spectrometer Frequency 150.97
9 Nucleus 13C
Me
Ph
Si
H
S2.7
160 150 140 130 120 110 100 90 80 70 60 50 40 30 20 10 0 -10
f1 (ppm)

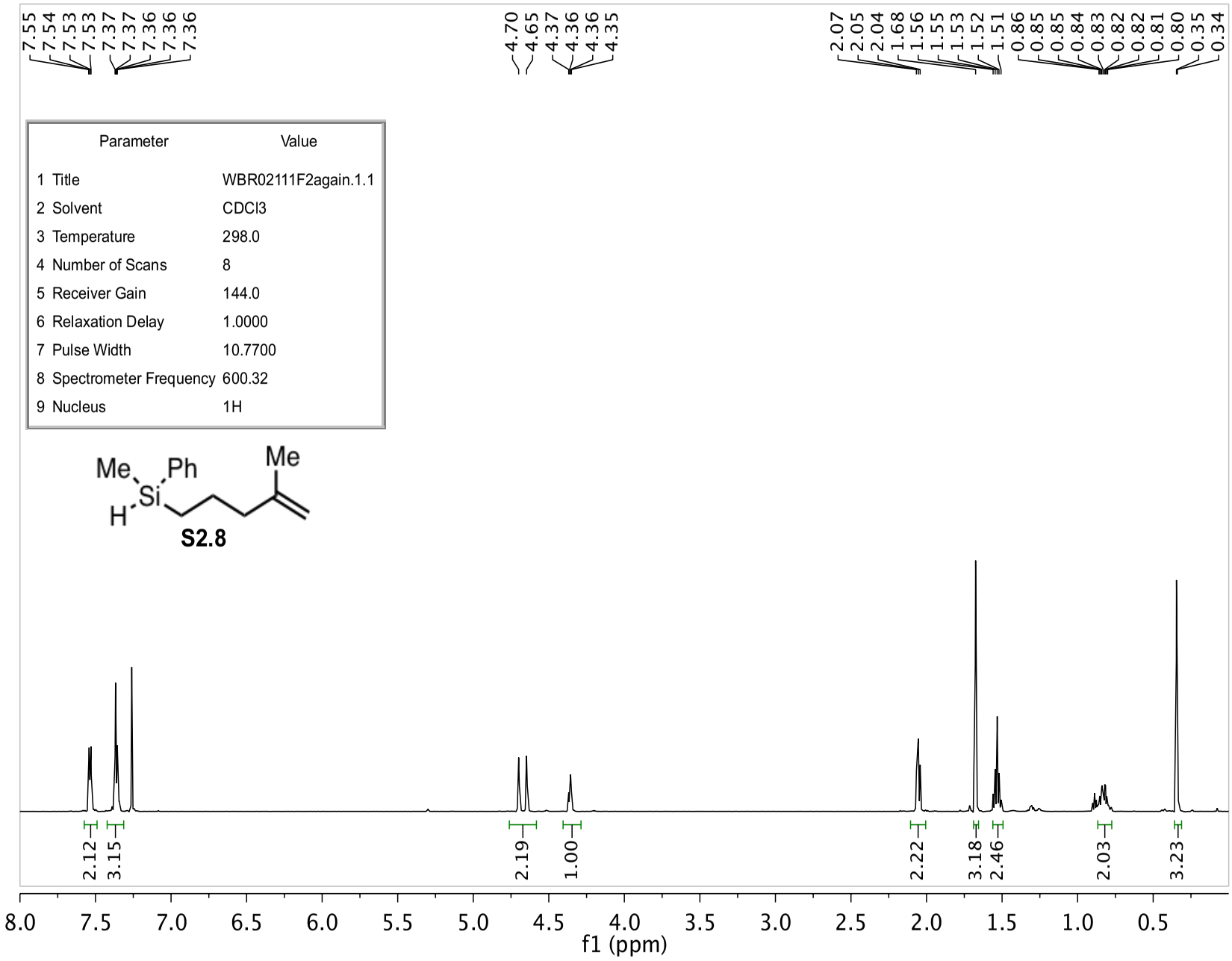
7.55
7.54
7.53
7.53
7.37
7.37
7.36
7.36
7.36
4.70
4.65
4.37
4.36
4.36
4.35
2.07
2.05
2.04
1.68
1.56
1.55
1.53
1.52
1.51
0.86
0.85
0.85
0.84
0.83
0.82
0.82
0.81
0.80
0.35
0.34
Parameter Value
1 Title WBR02111F2again.1.1
2 Solvent CDCl3
3 Temperature 298.0
4 Number of Scans 8
5 Receiver Gain 144.0
6 Relaxation Delay 1.0000
7 Pulse Width 10.7700
8 Spectrometer Frequency 600.32
9 Nucleus 1H
Me
Ph
Si
H
Me
S2.8
2.12
3.15
2.19
1.00
2.22
3.18
2.46
2.03
3.23
8.0
7.5
7.0
6.5
6.0
5.5
5.0
4.5
4.0
3.5
3.0
2.5
2.0
1.5
1.0
0.5
f1 (ppm)

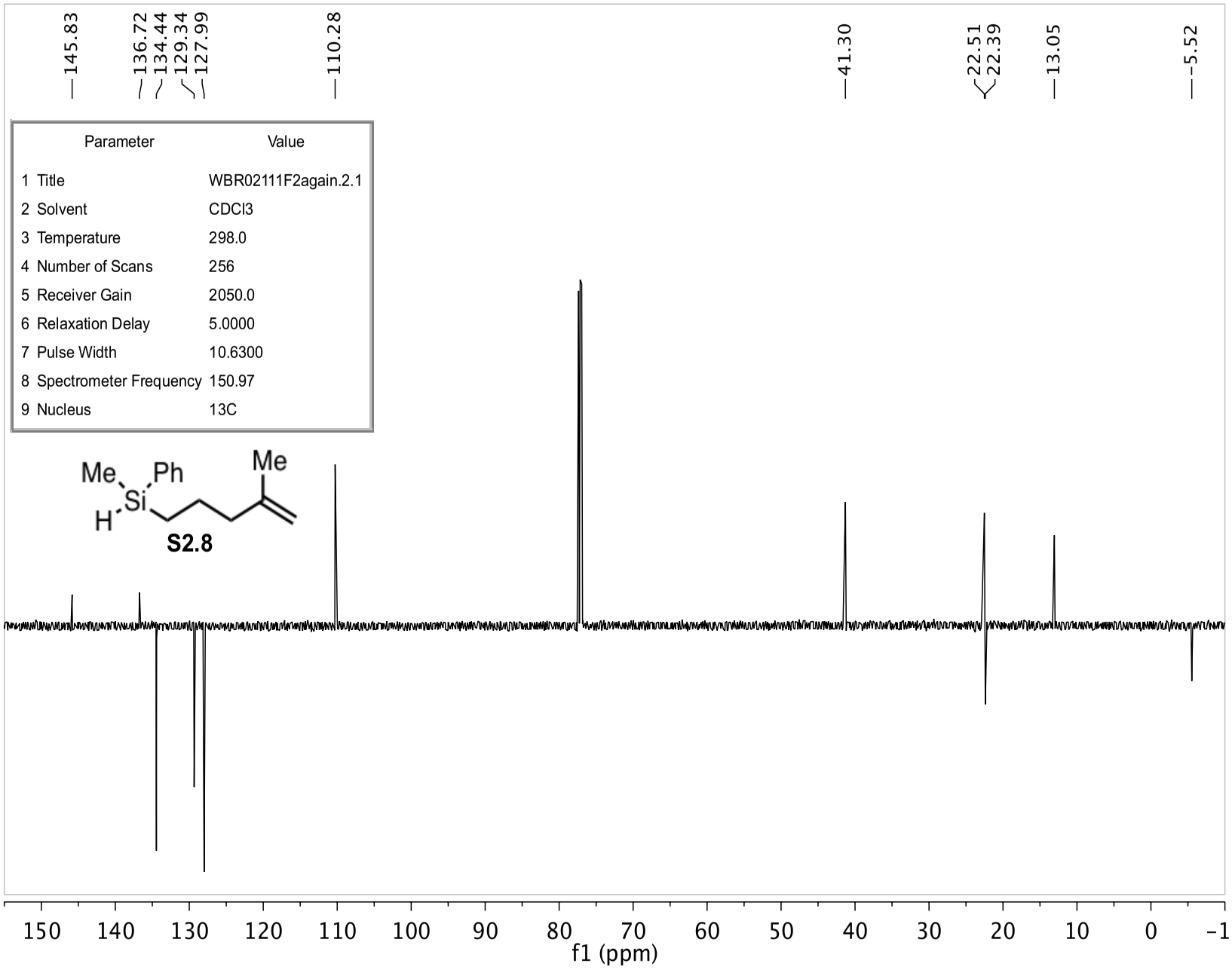
145.83
136.72
134.44
129.34
127.99
110.28
41.30
22.51
22.39
13.05
-5.52
Parameter Value
1 Title WBR02111F2again.2.1
2 Solvent CDCl3
3 Temperature 298.0
4 Number of Scans 256
5 Receiver Gain 2050.0
6 Relaxation Delay 5.0000
7 Pulse Width 10.6300
8 Spectrometer Frequency 150.97
9 Nucleus 13C
Me
Ph
Si
H
Me
S2.8
150 140 130 120 110 100 90 80 70 60 50 40 30 20 10 0 -10
f1 (ppm)

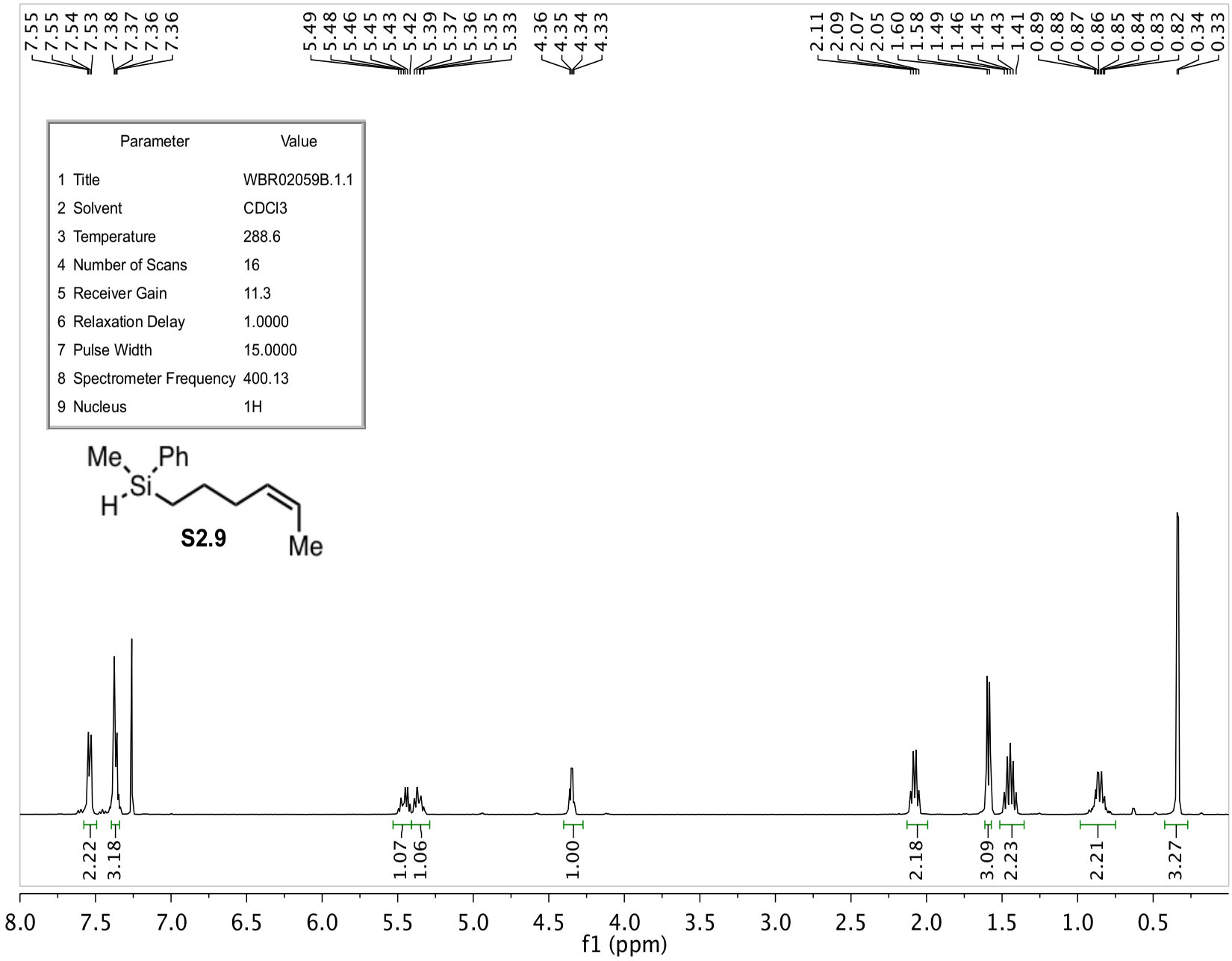
7.55 7.55 7.54 7.53 7.38 7.37 7.36 7.36
5.49 5.48 5.46 5.45 5.43 5.42 5.39 5.37 5.36 5.35 5.33
4.36 4.35 4.34 4.33
2.11 2.09 2.07 2.05 1.60 1.58 1.49 1.46 1.45 1.43 1.41
0.89 0.88 0.87 0.86 0.85 0.84 0.83 0.82 0.34 0.33
Parameter Value
1 Title WBR02059B.1.1
2 Solvent CDCl3
3 Temperature 288.6
4 Number of Scans 16
5 Receiver Gain 11.3
6 Relaxation Delay 1.0000
7 Pulse Width 15.0000
8 Spectrometer Frequency 400.13
9 Nucleus 1H
Me Ph Si H
S2.9
Me
2.22 3.18 1.07 1.06 1.00 2.18 3.09 2.23 2.21 3.27
8.0 7.5 7.0 6.5 6.0 5.5 5.0 4.5 4.0 3.5 3.0 2.5 2.0 1.5 1.0 0.5
f1 (ppm)

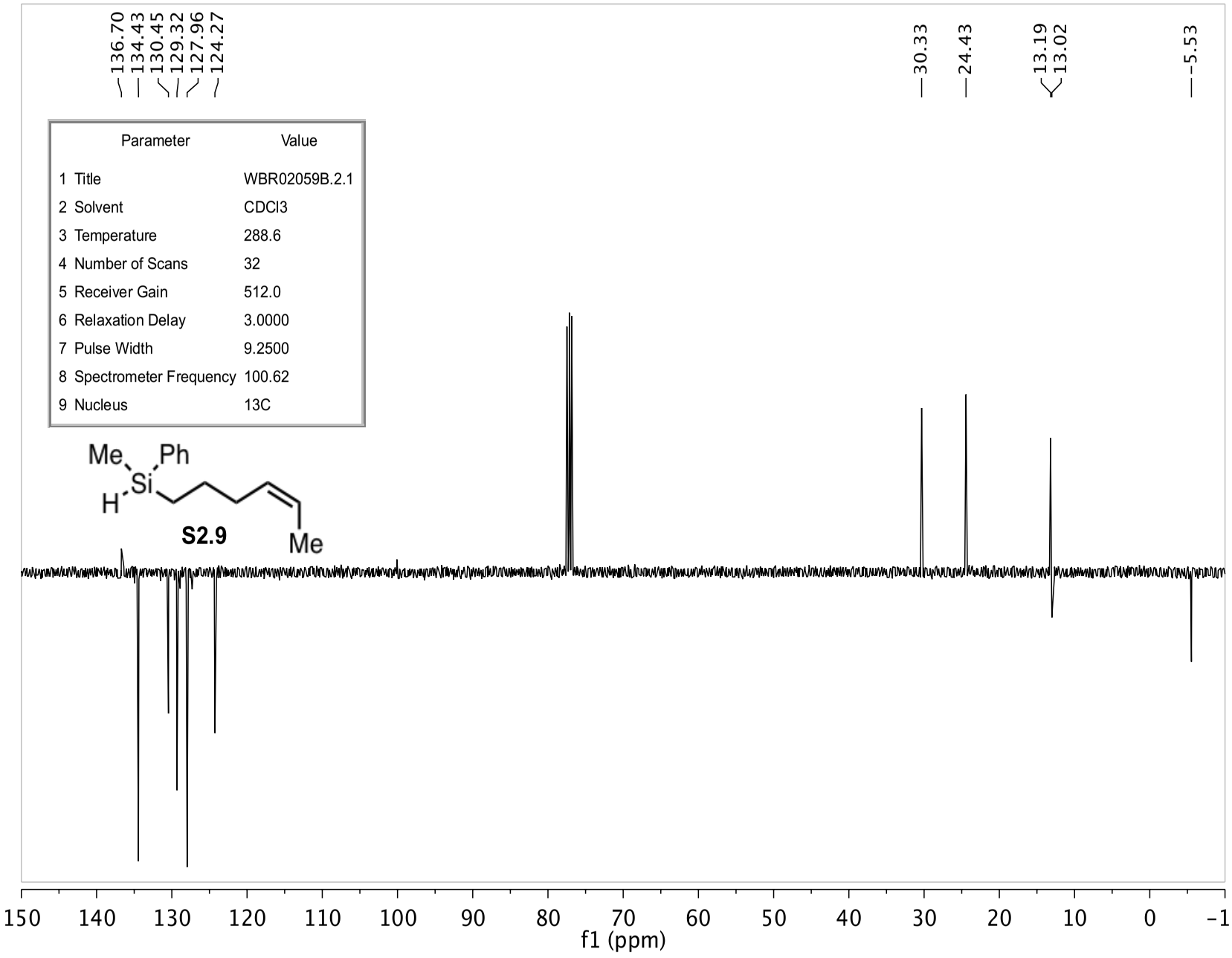
136.70
134.43
130.45
129.32
127.96
124.27
30.33
24.43
13.19
13.02
-5.53
Parameter Value
1 Title WBR02059B.2.1
2 Solvent CDCl3
3 Temperature 288.6
4 Number of Scans 32
5 Receiver Gain 512.0
6 Relaxation Delay 3.0000
7 Pulse Width 9.2500
8 Spectrometer Frequency 100.62
9 Nucleus 13C
Me
Ph
Si
H
S2.9
Me
150 140 130 120 110 100 90 80 70 60 50 40 30 20 10 0 -10
f1 (ppm)

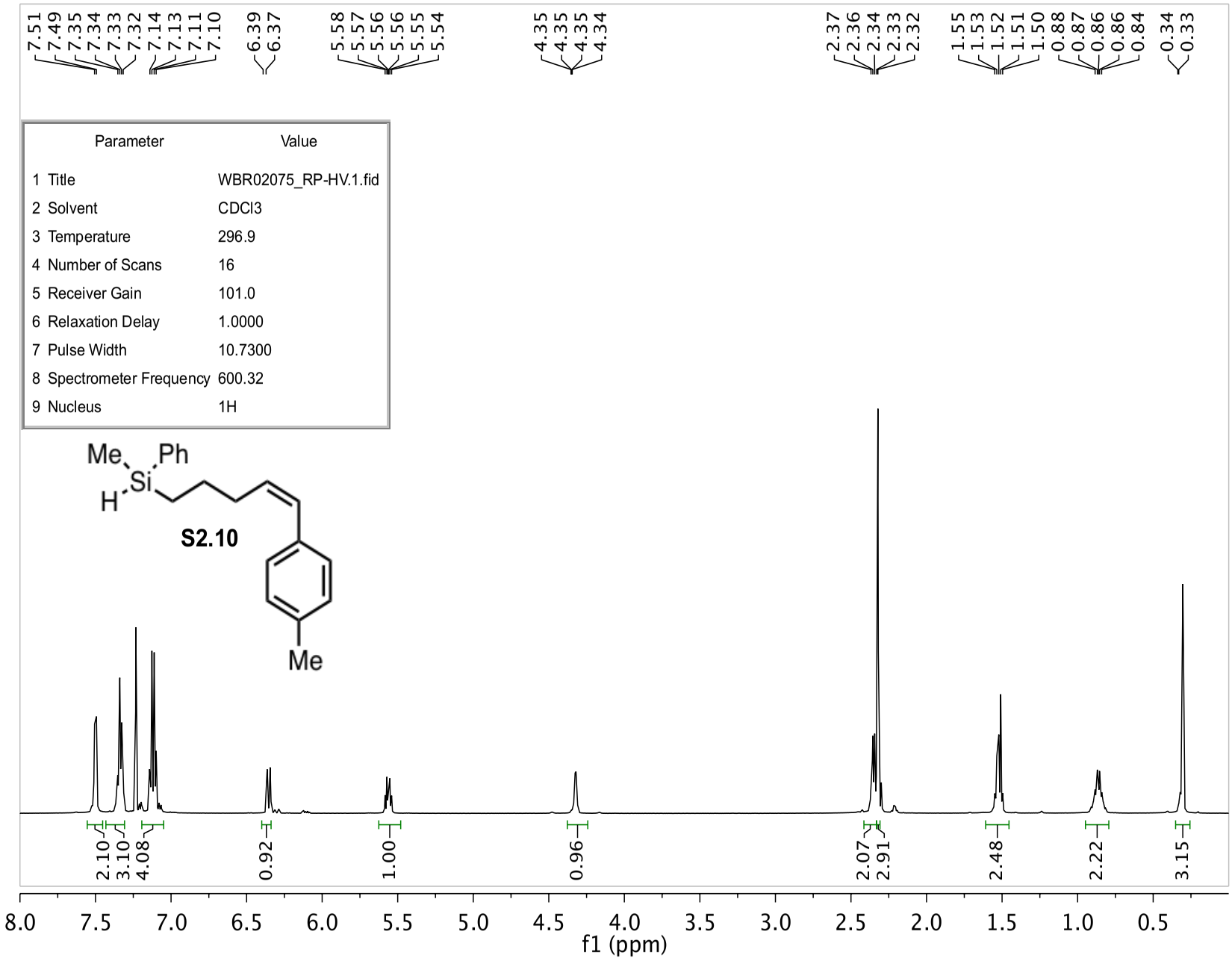
7.51 7.49 7.35 7.34 7.33 7.32 7.14 7.13 7.11 7.10 6.39 6.37 5.58 5.57 5.56 5.56 5.55 5.54 4.35 4.35 4.35 4.34 2.37 2.36 2.34 2.33 2.32 1.55 1.53 1.52 1.51 1.50 0.88 0.87 0.86 0.86 0.84 0.34 0.33
Parameter Value
1 Title WBR02075_RP-HV.1.fid
2 Solvent CDCl3
3 Temperature 296.9
4 Number of Scans 16
5 Receiver Gain 101.0
6 Relaxation Delay 1.0000
7 Pulse Width 10.7300
8 Spectrometer Frequency 600.32
9 Nucleus 1H
Me Ph H Si
S2.10
Me
2.10 3.10 4.08 0.92 1.00 0.96 2.07 2.91 2.48 2.22 3.15
8.0 7.5 7.0 6.5 6.0 5.5 5.0 4.5 4.0 3.5 3.0 2.5 2.0 1.5 1.0 0.5
f1 (ppm)

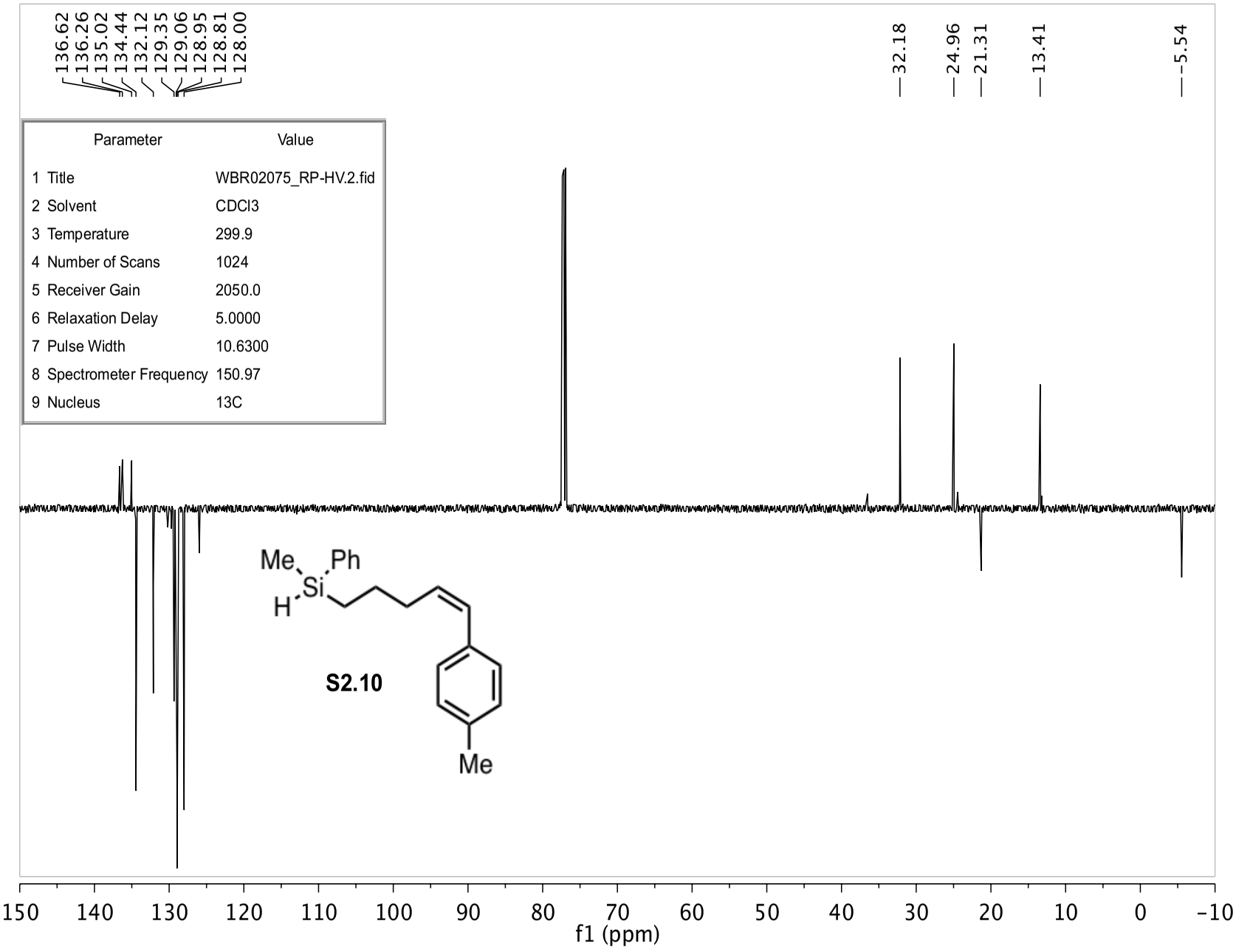
136.62
136.26
135.02
134.44
132.12
129.35
129.06
128.95
128.81
128.00
32.18
24.96
21.31
13.41
-5.54
Parameter Value
1 Title WBR02075_RP-HV.2.fid
2 Solvent CDCl3
3 Temperature 299.9
4 Number of Scans 1024
5 Receiver Gain 2050.0
6 Relaxation Delay 5.0000
7 Pulse Width 10.6300
8 Spectrometer Frequency 150.97
9 Nucleus 13C
Me
Ph
Si
H
S2.10
Me
150 140 130 120 110 100 90 80 70 60 50 40 30 20 10 0 -10
f1 (ppm)

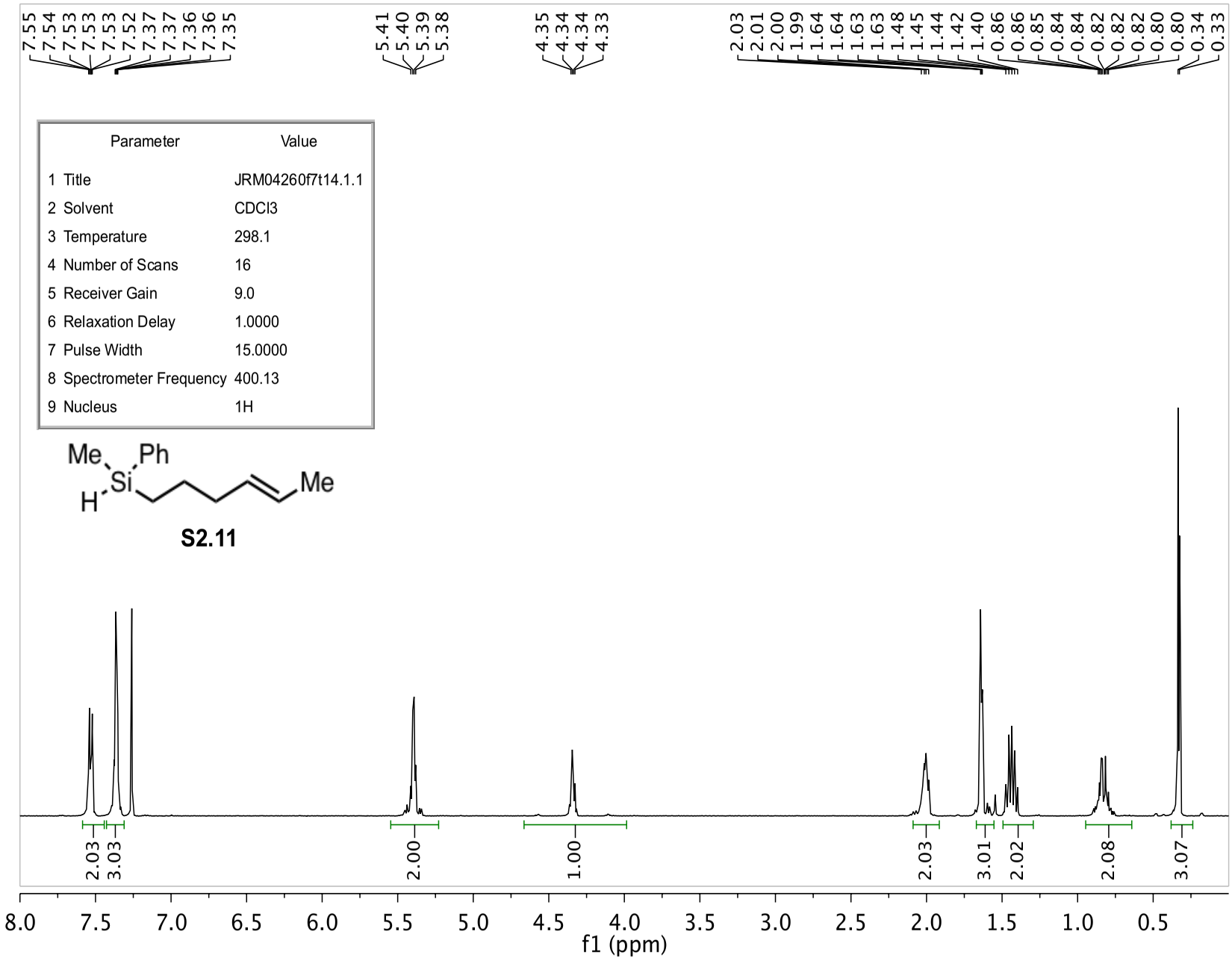
7.55 7.54 7.53 7.53 7.53 7.52 7.37 7.37 7.36 7.36 7.35
5.41 5.40 5.39 5.38
4.35 4.34 4.34 4.33
2.03 2.01 2.00 1.99 1.64 1.64 1.63 1.63 1.48 1.45 1.44 1.42 1.40 0.86 0.86 0.85 0.84 0.84 0.82 0.82 0.82 0.80 0.80 0.34 0.33
Parameter Value
1 Title JRM04260f7t14.1.1
2 Solvent CDCl3
3 Temperature 298.1
4 Number of Scans 16
5 Receiver Gain 9.0
6 Relaxation Delay 1.0000
7 Pulse Width 15.0000
8 Spectrometer Frequency 400.13
9 Nucleus 1H
Me Ph Si H Me
S2.11
2.03 3.03 2.00 1.00 2.03 3.01 2.02 2.08 3.07
8.0 7.5 7.0 6.5 6.0 5.5 5.0 4.5 4.0 3.5 3.0 2.5 2.0 1.5 1.0 0.5
f1 (ppm)

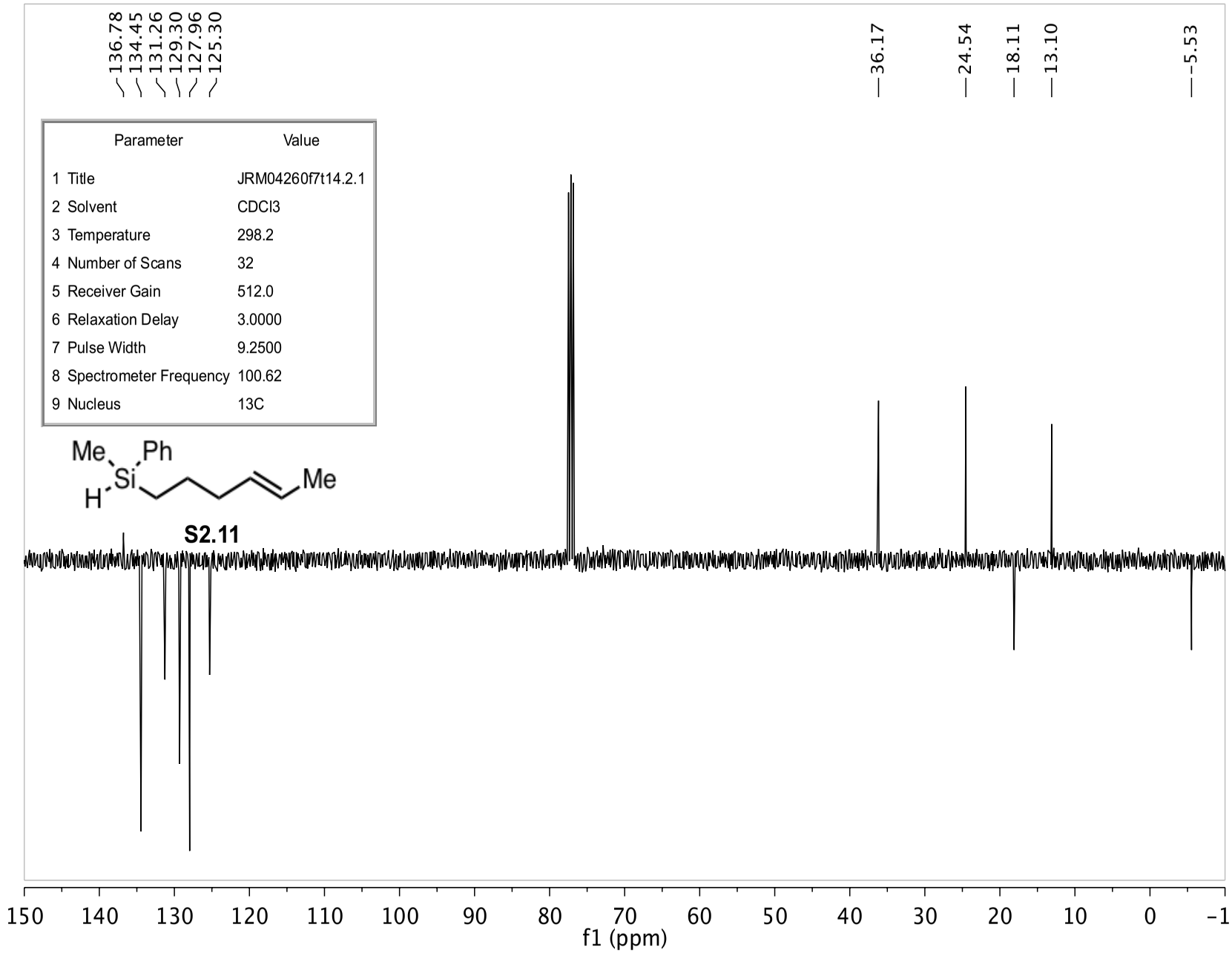
136.78
134.45
131.26
129.30
127.96
125.30
36.17
24.54
18.11
13.10
-5.53
Parameter Value
1 Title JRM04260f7t14.2.1
2 Solvent CDCl3
3 Temperature 298.2
4 Number of Scans 32
5 Receiver Gain 512.0
6 Relaxation Delay 3.0000
7 Pulse Width 9.2500
8 Spectrometer Frequency 100.62
9 Nucleus 13C
Me
Ph
Si
H
Me
S2.11
150 140 130 120 110 100 90 80 70 60 50 40 30 20 10 0 -10
f1 (ppm)

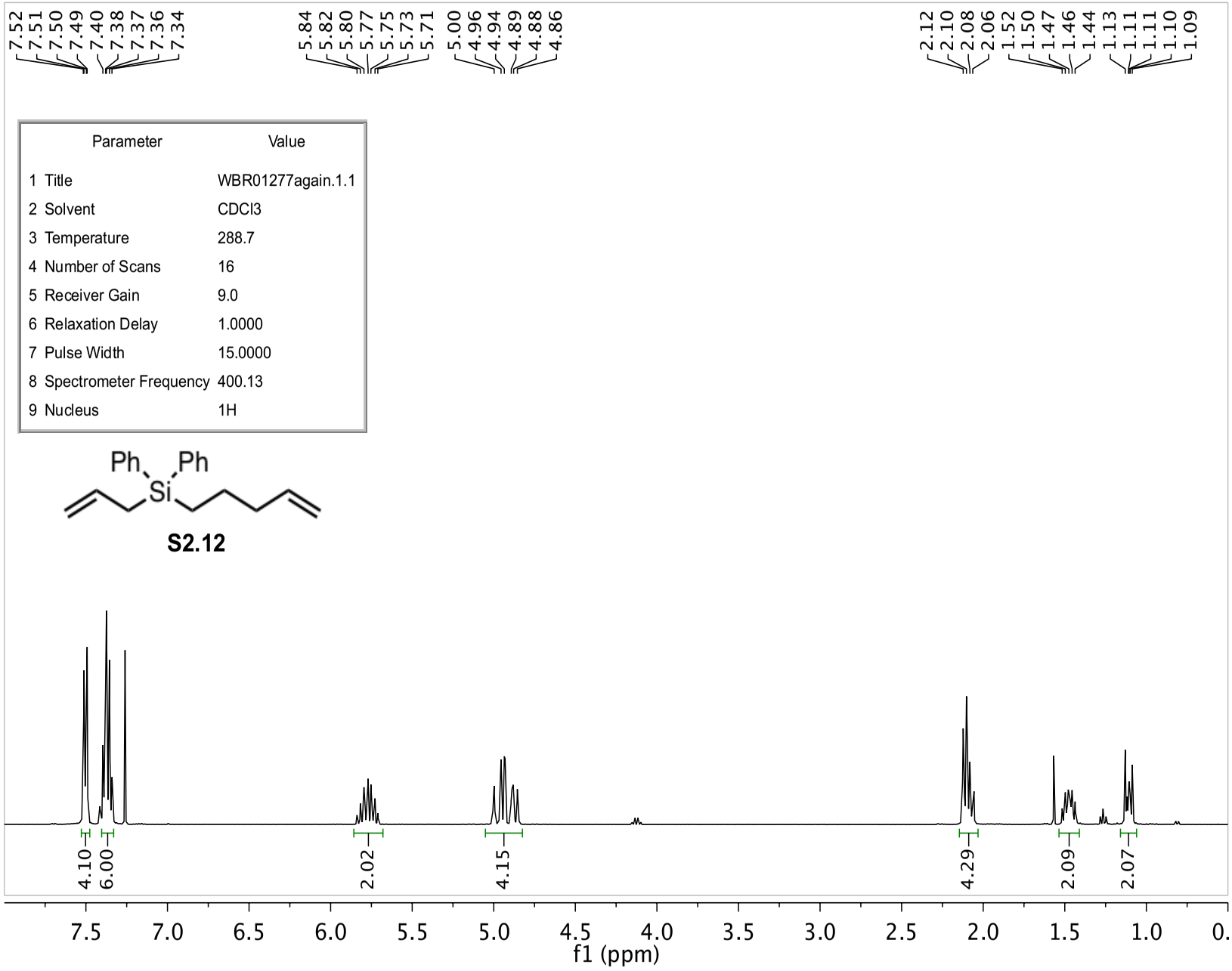
7.52
7.51
7.50
7.49
7.40
7.38
7.37
7.36
7.34
5.84
5.82
5.80
5.77
5.75
5.73
5.71
5.00
4.96
4.94
4.89
4.88
4.86
2.12
2.10
2.08
2.06
1.52
1.50
1.47
1.46
1.44
1.13
1.11
1.11
1.10
1.09
Parameter Value
1 Title WBR01277again.1.1
2 Solvent CDCl3
3 Temperature 288.7
4 Number of Scans 16
5 Receiver Gain 9.0
6 Relaxation Delay 1.0000
7 Pulse Width 15.0000
8 Spectrometer Frequency 400.13
9 Nucleus 1H
Ph
Ph
Si
S2.12
4.10
6.00
2.02
4.15
4.29
2.09
2.07
7.5
7.0
6.5
6.0
5.5
5.0
4.5
4.0
3.5
3.0
2.5
2.0
1.5
1.0
0.5
f1 (ppm)

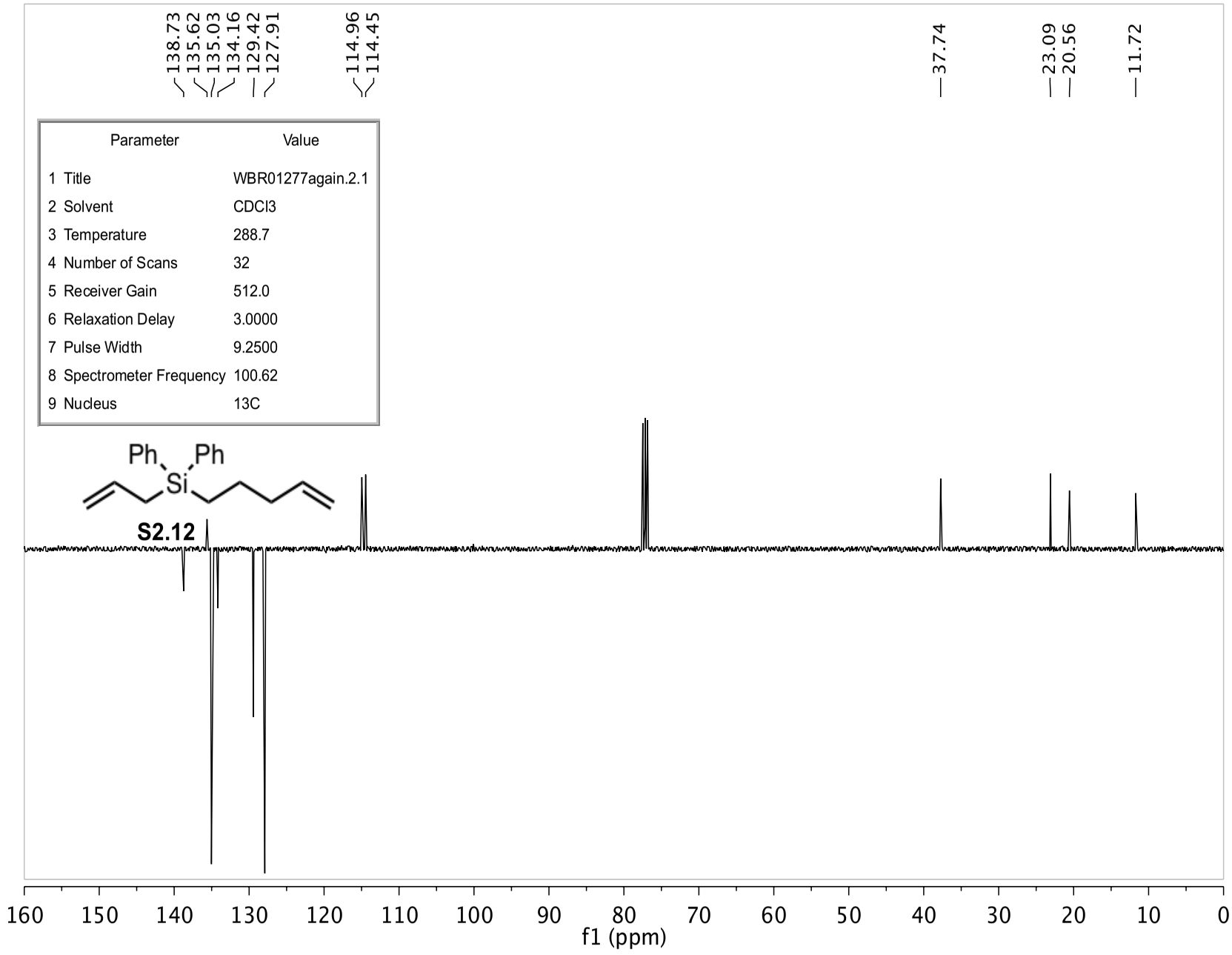
138.73
135.62
135.03
134.16
129.42
127.91
114.96
114.45
37.74
23.09
20.56
11.72
Parameter Value
1 Title WBR01277again.2.1
2 Solvent CDCl3
3 Temperature 288.7
4 Number of Scans 32
5 Receiver Gain 512.0
6 Relaxation Delay 3.0000
7 Pulse Width 9.2500
8 Spectrometer Frequency 100.62
9 Nucleus 13C
Ph
Ph
Si
S2.12
160 150 140 130 120 110 100 90 80 70 60 50 40 30 20 10 0
f1 (ppm)

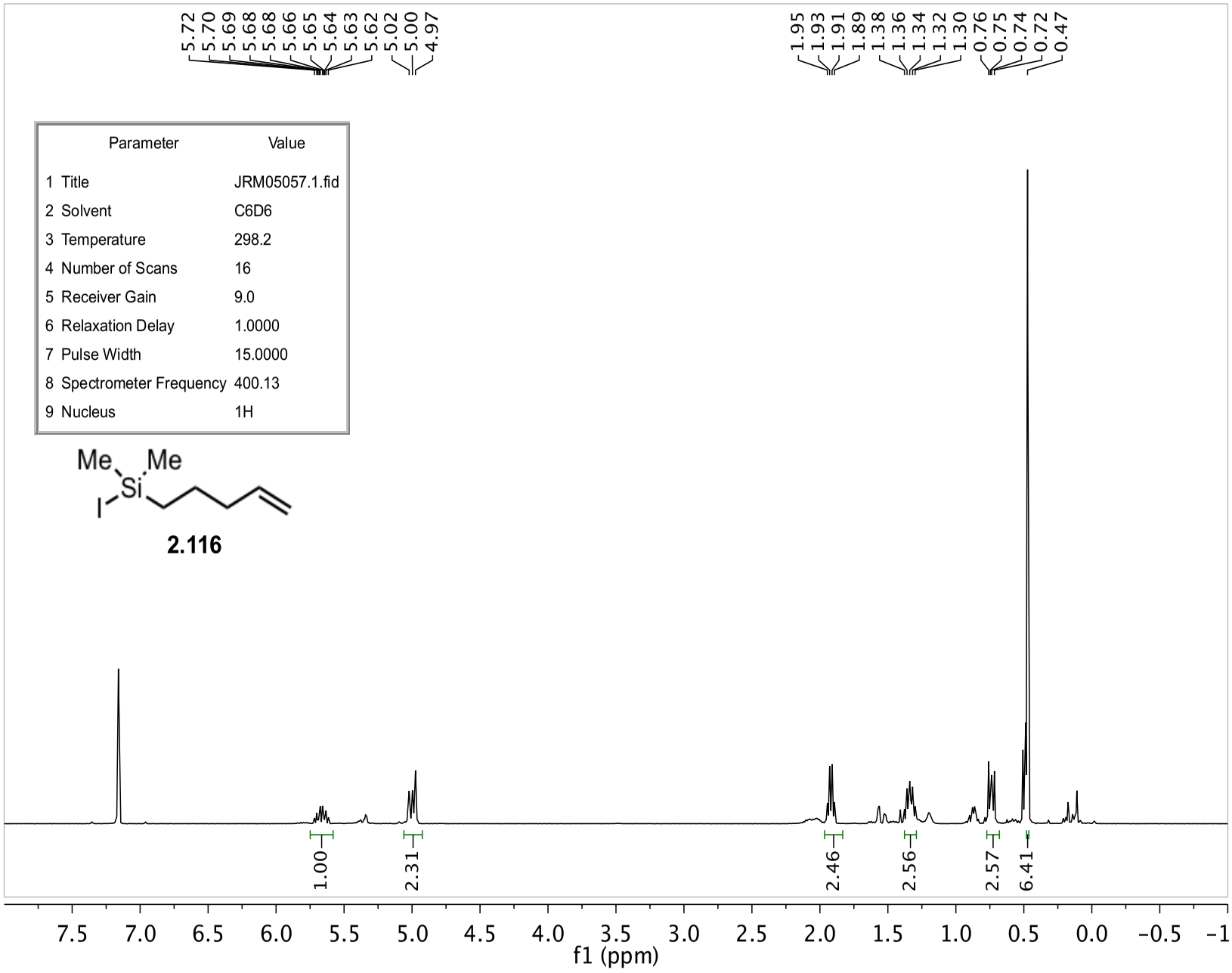
5.72
5.70
5.69
5.68
5.68
5.66
5.65
5.64
5.63
5.62
5.02
5.00
4.97
1.95
1.93
1.91
1.89
1.38
1.36
1.34
1.32
1.30
0.76
0.75
0.74
0.72
0.47
Parameter Value
1 Title JRM05057.1.fid
2 Solvent C6D6
3 Temperature 298.2
4 Number of Scans 16
5 Receiver Gain 9.0
6 Relaxation Delay 1.0000
7 Pulse Width 15.0000
8 Spectrometer Frequency 400.13
9 Nucleus 1H
Me
Me
Si
I
2.116
1.00
2.31
2.46
2.56
2.57
6.41
7.5
7.0
6.5
6.0
5.5
5.0
4.5
4.0
3.5
3.0
2.5
2.0
1.5
1.0
0.5
0.0
-0.5
-1.0
f1 (ppm)

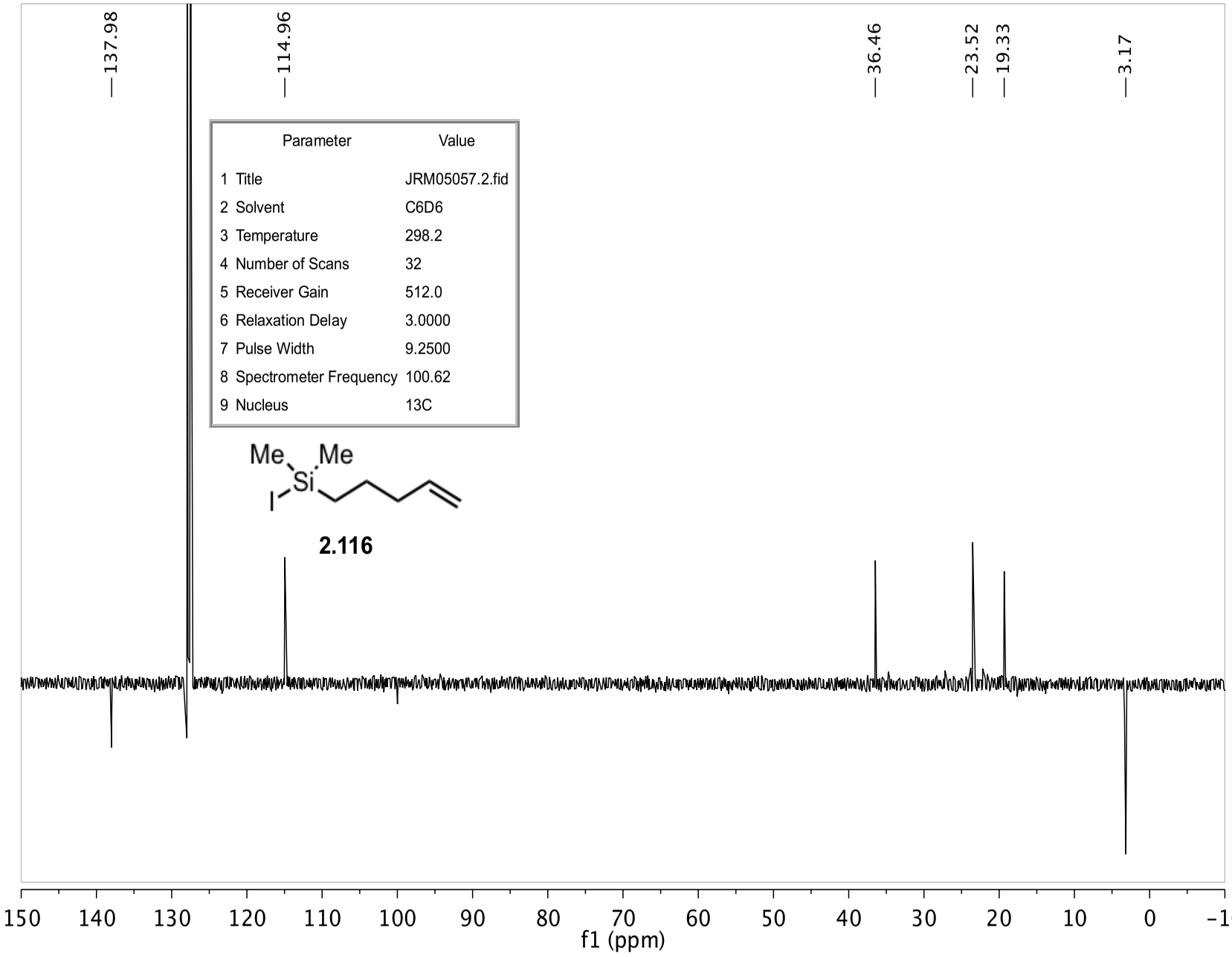
137.98
114.96
36.46
23.52
19.33
3.17
Parameter Value
1 Title JRM05057.2.fid
2 Solvent C6D6
3 Temperature 298.2
4 Number of Scans 32
5 Receiver Gain 512.0
6 Relaxation Delay 3.0000
7 Pulse Width 9.2500
8 Spectrometer Frequency 100.62
9 Nucleus 13C
Me
Me
Si
2.116
150 140 130 120 110 100 90 80 70 60 50 40 30 20 10 0 -10
f1 (ppm)

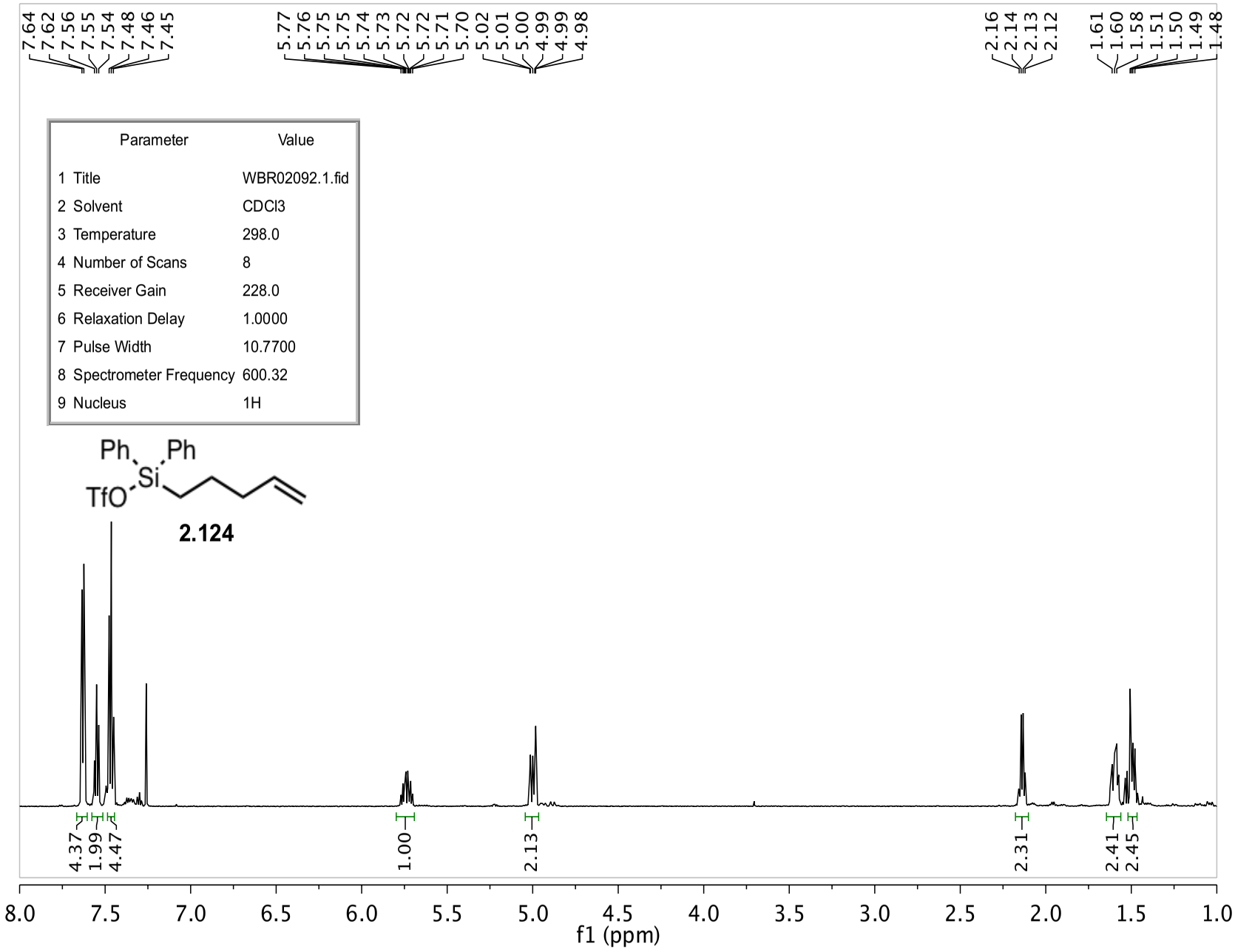
7.64 7.62 7.56 7.55 7.54 7.48 7.46 7.45
5.77 5.76 5.75 5.75 5.74 5.73 5.72 5.72 5.71 5.70 5.02 5.01 5.00 4.99 4.99 4.98
2.16 2.14 2.13 2.12
1.61 1.60 1.58 1.51 1.50 1.49 1.48
Parameter Value
1 Title WBR02092.1.fid
2 Solvent CDCl3
3 Temperature 298.0
4 Number of Scans 8
5 Receiver Gain 228.0
6 Relaxation Delay 1.0000
7 Pulse Width 10.7700
8 Spectrometer Frequency 600.32
9 Nucleus 1H
Ph
Ph
Si
TfO
2.124
4.37
1.99
4.47
1.00
2.13
2.31
2.41
2.45
8.0 7.5 7.0 6.5 6.0 5.5 5.0 4.5 4.0 3.5 3.0 2.5 2.0 1.5 1.0
f1 (ppm)

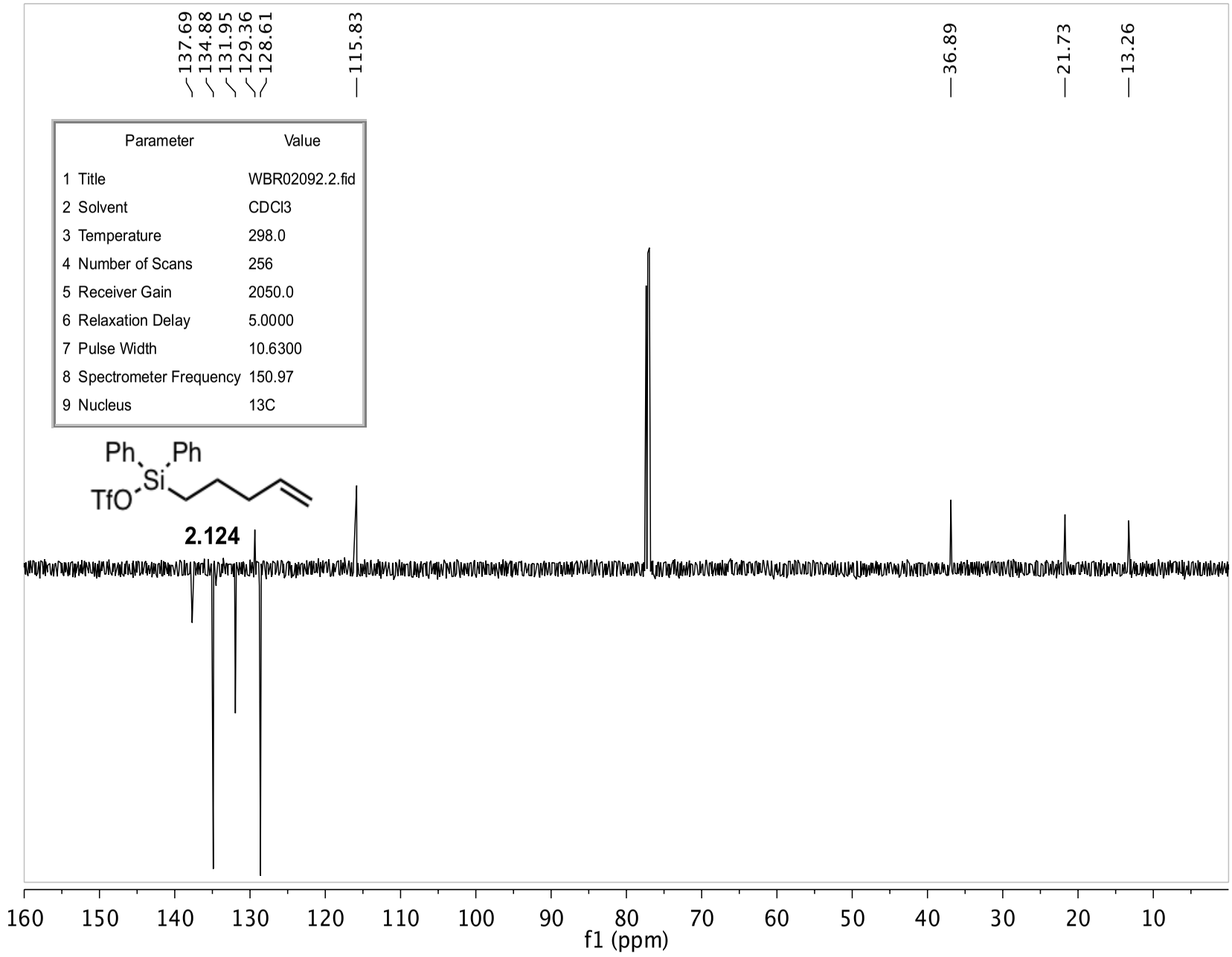
137.69
134.88
131.95
129.36
128.61
115.83
36.89
21.73
13.26
Parameter Value
1 Title WBR02092.2.fid
2 Solvent CDCl3
3 Temperature 298.0
4 Number of Scans 256
5 Receiver Gain 2050.0
6 Relaxation Delay 5.0000
7 Pulse Width 10.6300
8 Spectrometer Frequency 150.97
9 Nucleus 13C
Ph
Ph
Si
TfO
2.124
160 150 140 130 120 110 100 90 80 70 60 50 40 30 20 10
f1 (ppm)

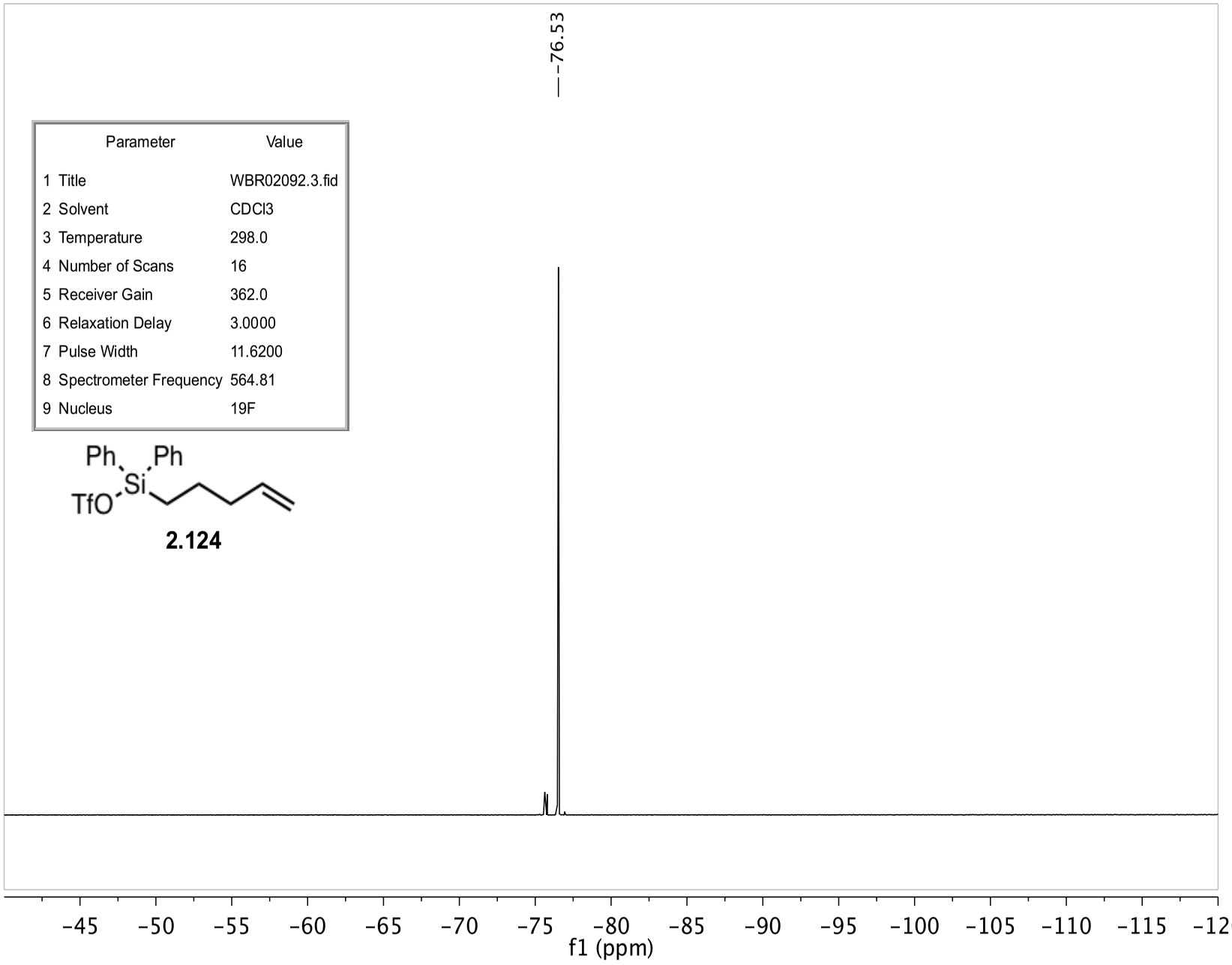
-76.53
Parameter Value
1 Title WBR02092.3.fid
2 Solvent CDCl3
3 Temperature 298.0
4 Number of Scans 16
5 Receiver Gain 362.0
6 Relaxation Delay 3.0000
7 Pulse Width 11.6200
8 Spectrometer Frequency 564.81
9 Nucleus 19F
Ph
Ph
Si
TfO
2.124
-45 -50 -55 -60 -65 -70 -75 -80 -85 -90 -95 -100 -105 -110 -115 -120
f1 (ppm)

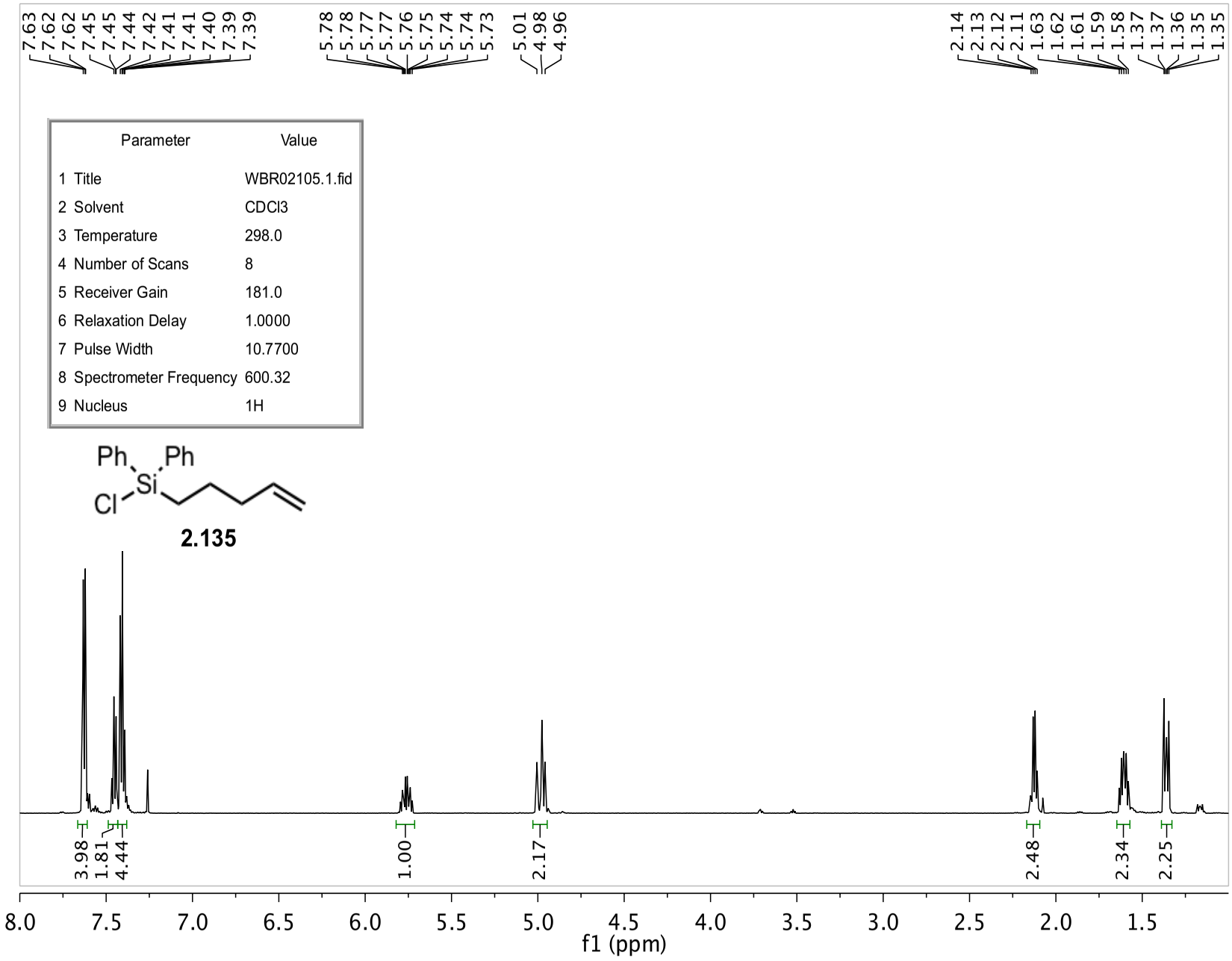
7.63 7.62 7.62 7.45 7.45 7.44 7.42 7.41 7.41 7.40 7.39 7.39
5.78 5.78 5.77 5.77 5.76 5.75 5.74 5.74 5.73
5.01 4.98 4.96
2.14 2.13 2.12 2.11 1.63 1.62 1.61 1.59 1.58 1.37 1.37 1.36 1.35 1.35
Parameter Value
1 Title WBR02105.1.fid
2 Solvent CDCl3
3 Temperature 298.0
4 Number of Scans 8
5 Receiver Gain 181.0
6 Relaxation Delay 1.0000
7 Pulse Width 10.7700
8 Spectrometer Frequency 600.32
9 Nucleus 1H
Ph
Ph
Si
Cl
2.135
3.98
1.81
4.44
1.00
2.17
2.48
2.34
2.25
8.0 7.5 7.0 6.5 6.0 5.5 5.0 4.5 4.0 3.5 3.0 2.5 2.0 1.5
f1 (ppm)

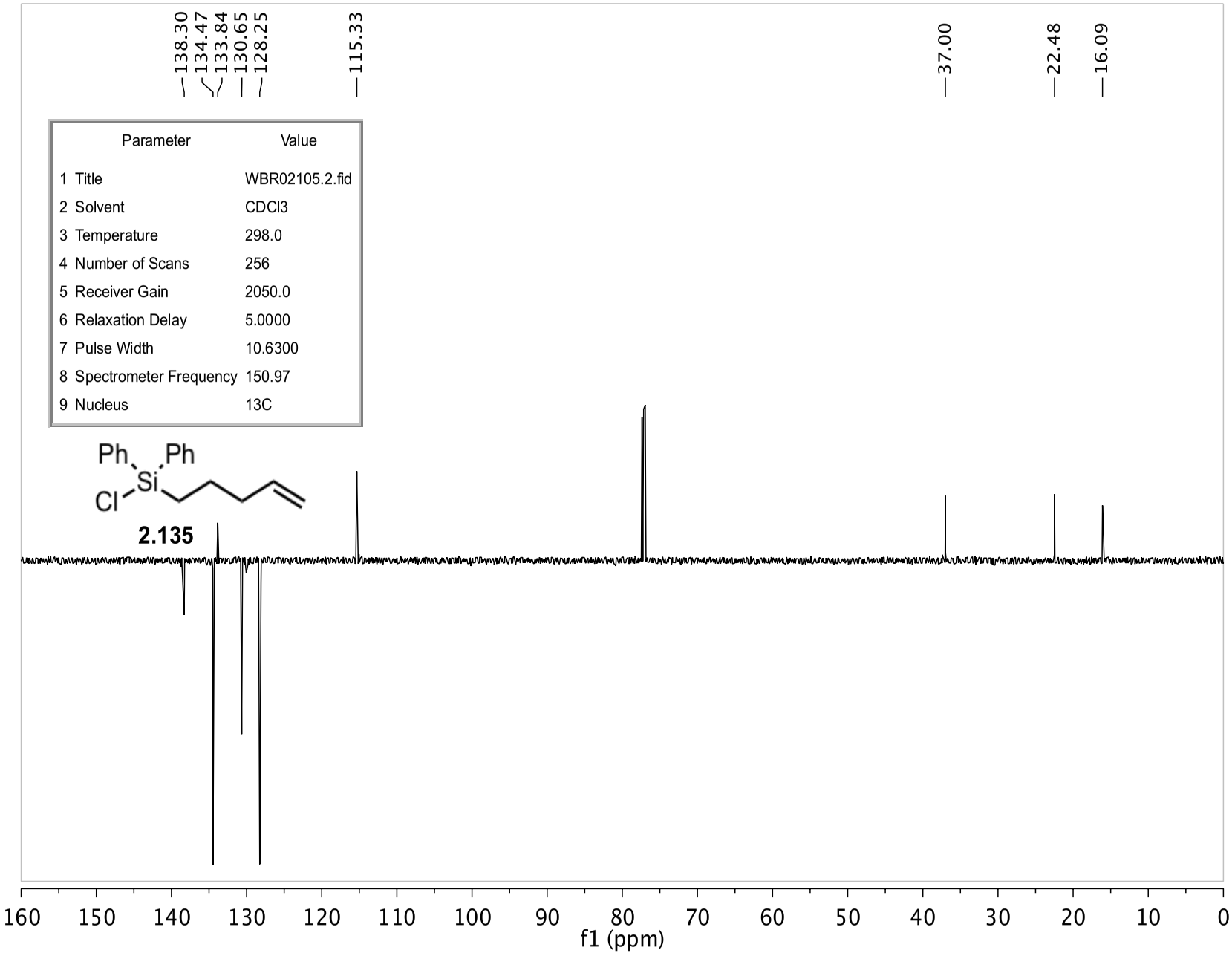
138.30
134.47
133.84
130.65
128.25
115.33
37.00
22.48
16.09
Parameter Value
1 Title WBR02105.2.fid
2 Solvent CDCl3
3 Temperature 298.0
4 Number of Scans 256
5 Receiver Gain 2050.0
6 Relaxation Delay 5.0000
7 Pulse Width 10.6300
8 Spectrometer Frequency 150.97
9 Nucleus 13C
Ph
Ph
Si
Cl
2.135
160 150 140 130 120 110 100 90 80 70 60 50 40 30 20 10 0
f1 (ppm)

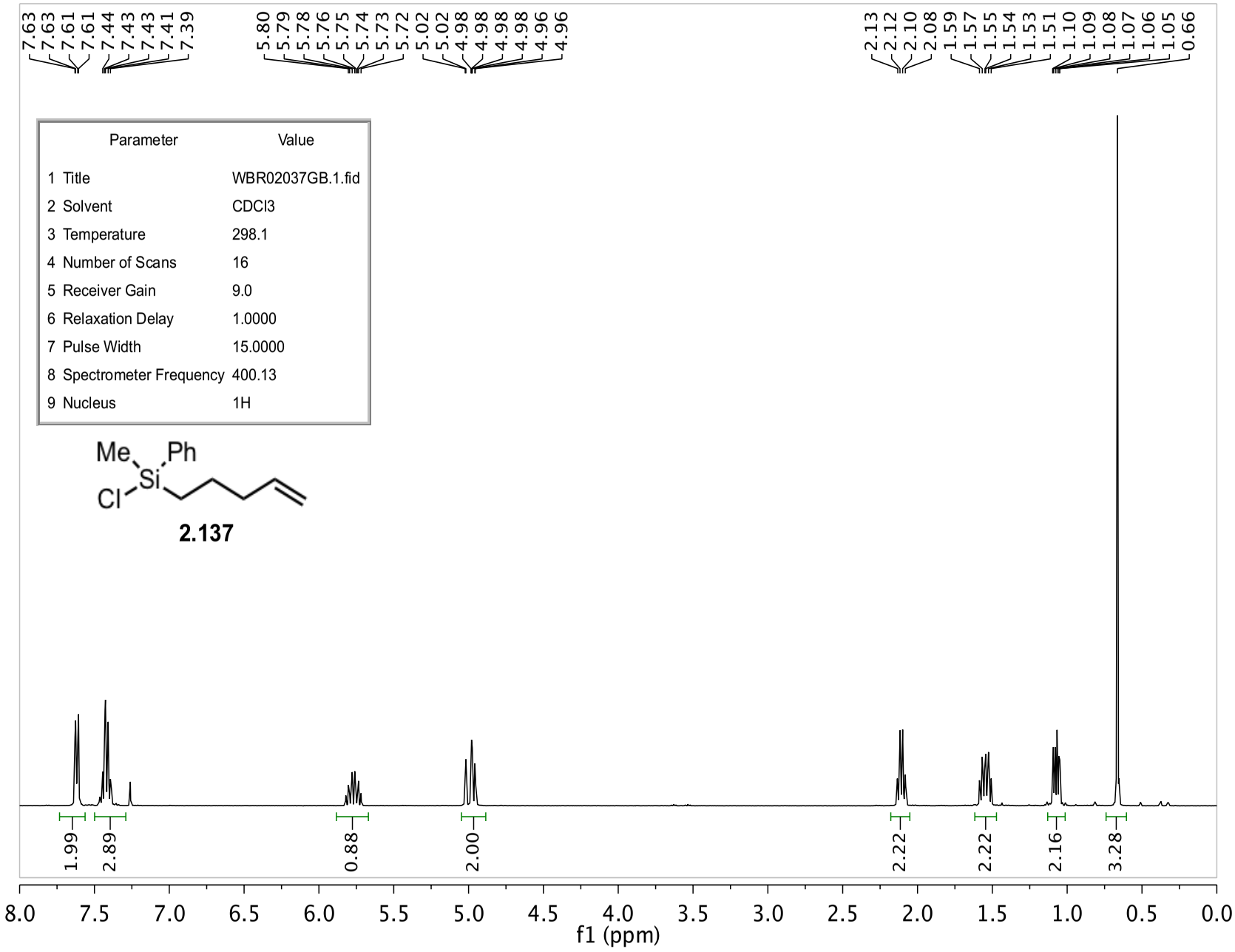
7.63 7.63 7.61 7.61 7.44 7.43 7.43 7.41 7.39
5.80 5.79 5.78 5.76 5.75 5.74 5.73 5.72 5.02 5.02 4.98 4.98 4.98 4.98 4.96 4.96
2.13 2.12 2.10 2.08 1.59 1.57 1.55 1.54 1.53 1.51 1.10 1.09 1.08 1.07 1.06 1.05 0.66
Parameter Value
1 Title WBR02037GB.1.fid
2 Solvent CDCl3
3 Temperature 298.1
4 Number of Scans 16
5 Receiver Gain 9.0
6 Relaxation Delay 1.0000
7 Pulse Width 15.0000
8 Spectrometer Frequency 400.13
9 Nucleus 1H
Me
Ph
Si
Cl
2.137
1.99 2.89 0.88 2.00 2.22 2.22 2.16 3.28
8.0 7.5 7.0 6.5 6.0 5.5 5.0 4.5 4.0 3.5 3.0 2.5 2.0 1.5 1.0 0.5 0.0
f1 (ppm)

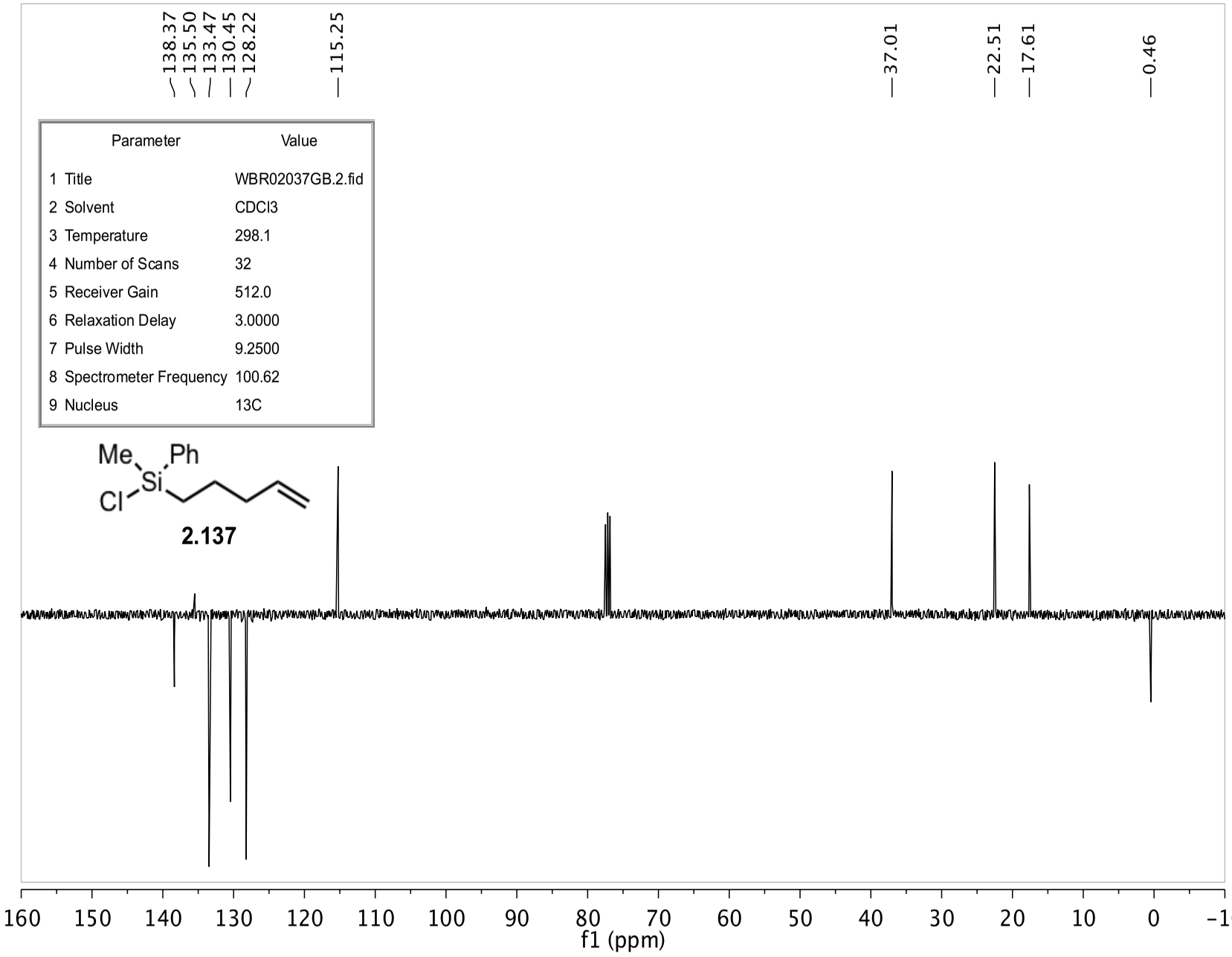
138.37
135.50
133.47
130.45
128.22
115.25
37.01
22.51
17.61
0.46
Parameter Value
1 Title WBR02037GB.2.fid
2 Solvent CDCl3
3 Temperature 298.1
4 Number of Scans 32
5 Receiver Gain 512.0
6 Relaxation Delay 3.0000
7 Pulse Width 9.2500
8 Spectrometer Frequency 100.62
9 Nucleus 13C
Me
Ph
Si
Cl
2.137
160 150 140 130 120 110 100 90 80 70 60 50 40 30 20 10 0 -10
f1 (ppm)

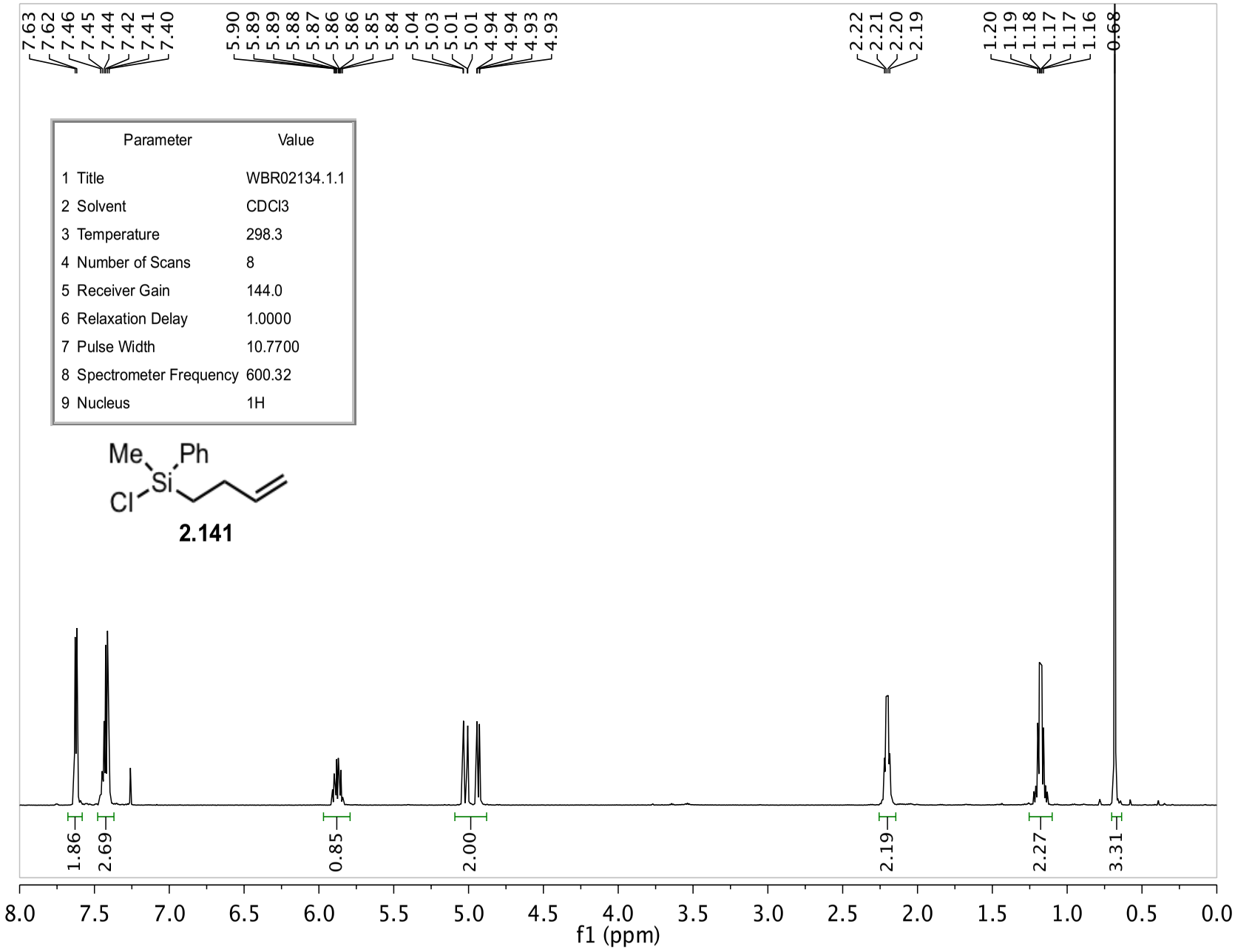
7.63 7.62 7.46 7.45 7.44 7.42 7.41 7.40
5.90 5.89 5.89 5.88 5.87 5.86 5.86 5.85 5.84
5.04 5.03 5.01 5.01 4.94 4.94 4.93 4.93
2.22 2.21 2.20 2.19
1.20 1.19 1.18 1.17 1.17 1.16
0.68
Parameter Value
1 Title WBR02134.1.1
2 Solvent CDCl3
3 Temperature 298.3
4 Number of Scans 8
5 Receiver Gain 144.0
6 Relaxation Delay 1.0000
7 Pulse Width 10.7700
8 Spectrometer Frequency 600.32
9 Nucleus 1H
Me
Ph
Si
Cl
2.141
1.86
2.69
0.85
2.00
2.19
2.27
3.31
8.0 7.5 7.0 6.5 6.0 5.5 5.0 4.5 4.0 3.5 3.0 2.5 2.0 1.5 1.0 0.5 0.0
f1 (ppm)

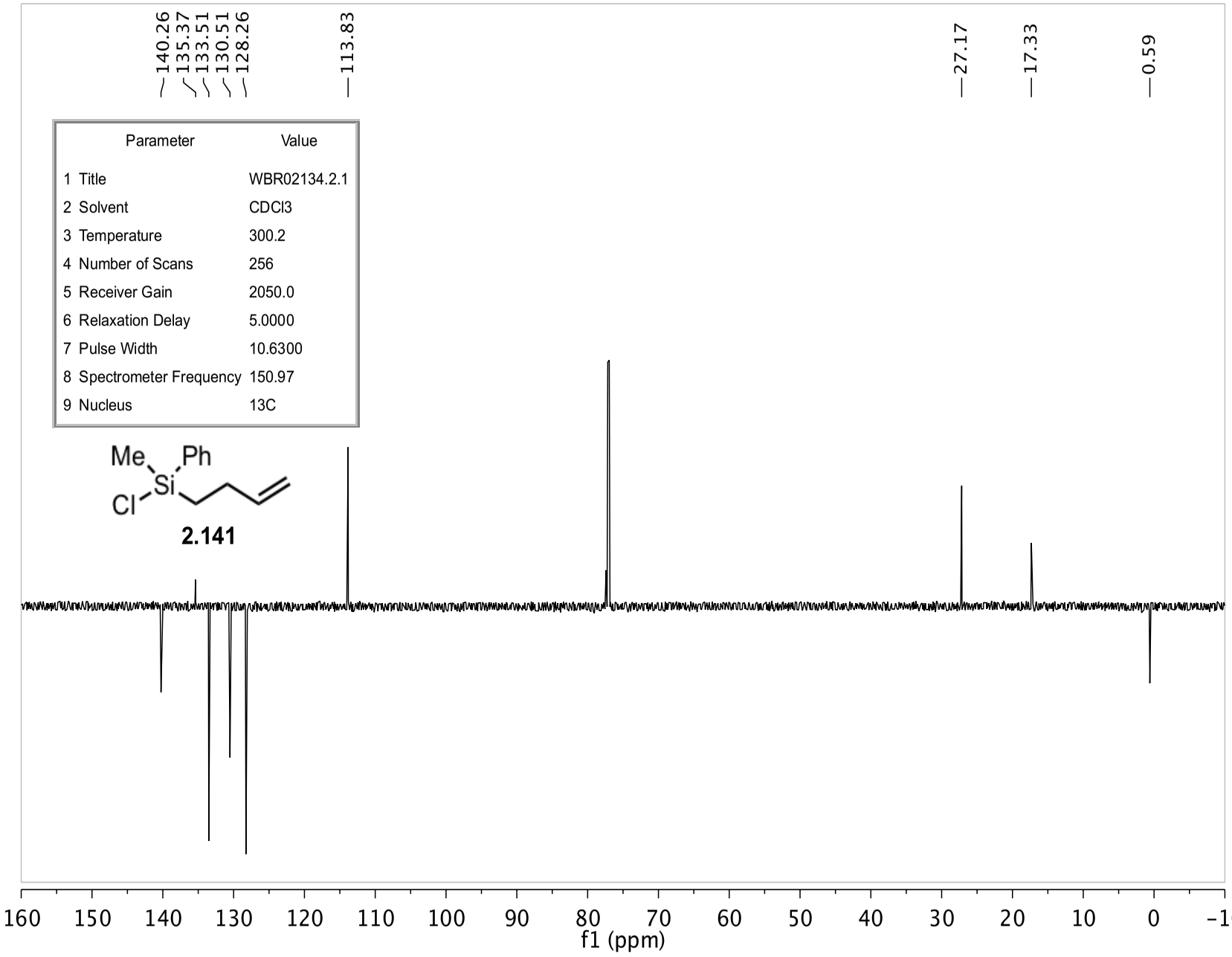
140.26
135.37
133.51
130.51
128.26
113.83
27.17
17.33
0.59
Parameter Value
1 Title WBR02134.2.1
2 Solvent CDCl3
3 Temperature 300.2
4 Number of Scans 256
5 Receiver Gain 2050.0
6 Relaxation Delay 5.0000
7 Pulse Width 10.6300
8 Spectrometer Frequency 150.97
9 Nucleus 13C
Me
Ph
Si
Cl
2.141
160 150 140 130 120 110 100 90 80 70 60 50 40 30 20 10 0 -10
f1 (ppm)

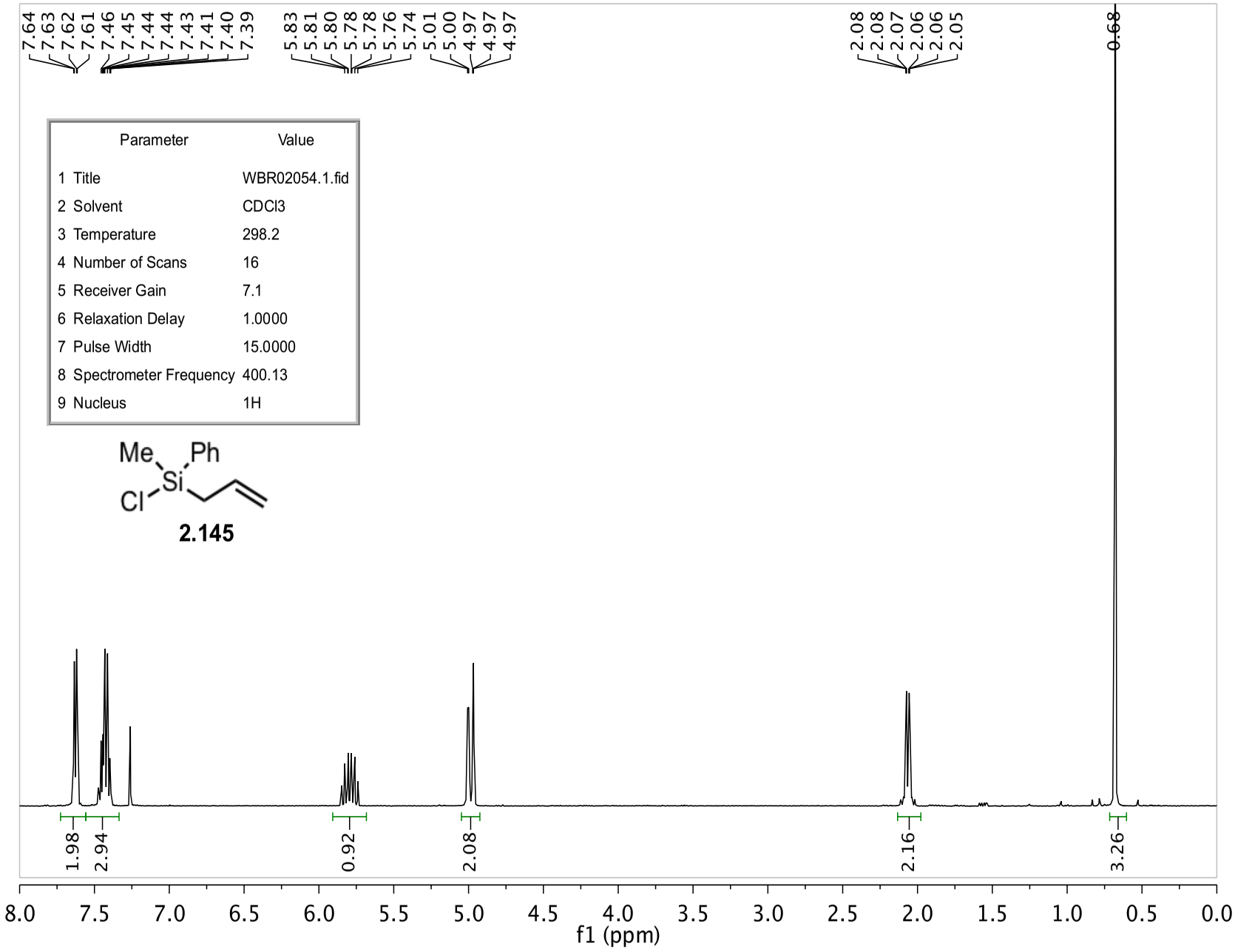
7.64 7.63 7.62 7.61 7.46 7.45 7.44 7.44 7.43 7.41 7.40 7.39
5.83 5.81 5.80 5.78 5.78 5.76 5.74 5.01 5.00 4.97 4.97 4.97
2.08 2.08 2.07 2.06 2.06 2.05
0.68
Parameter Value
1 Title WBR02054.1.fid
2 Solvent CDCl3
3 Temperature 298.2
4 Number of Scans 16
5 Receiver Gain 7.1
6 Relaxation Delay 1.0000
7 Pulse Width 15.0000
8 Spectrometer Frequency 400.13
9 Nucleus 1H
Me
Ph
Si
Cl
2.145
1.98
2.94
0.92
2.08
2.16
3.26
8.0 7.5 7.0 6.5 6.0 5.5 5.0 4.5 4.0 3.5 3.0 2.5 2.0 1.5 1.0 0.5 0.0
f1 (ppm)

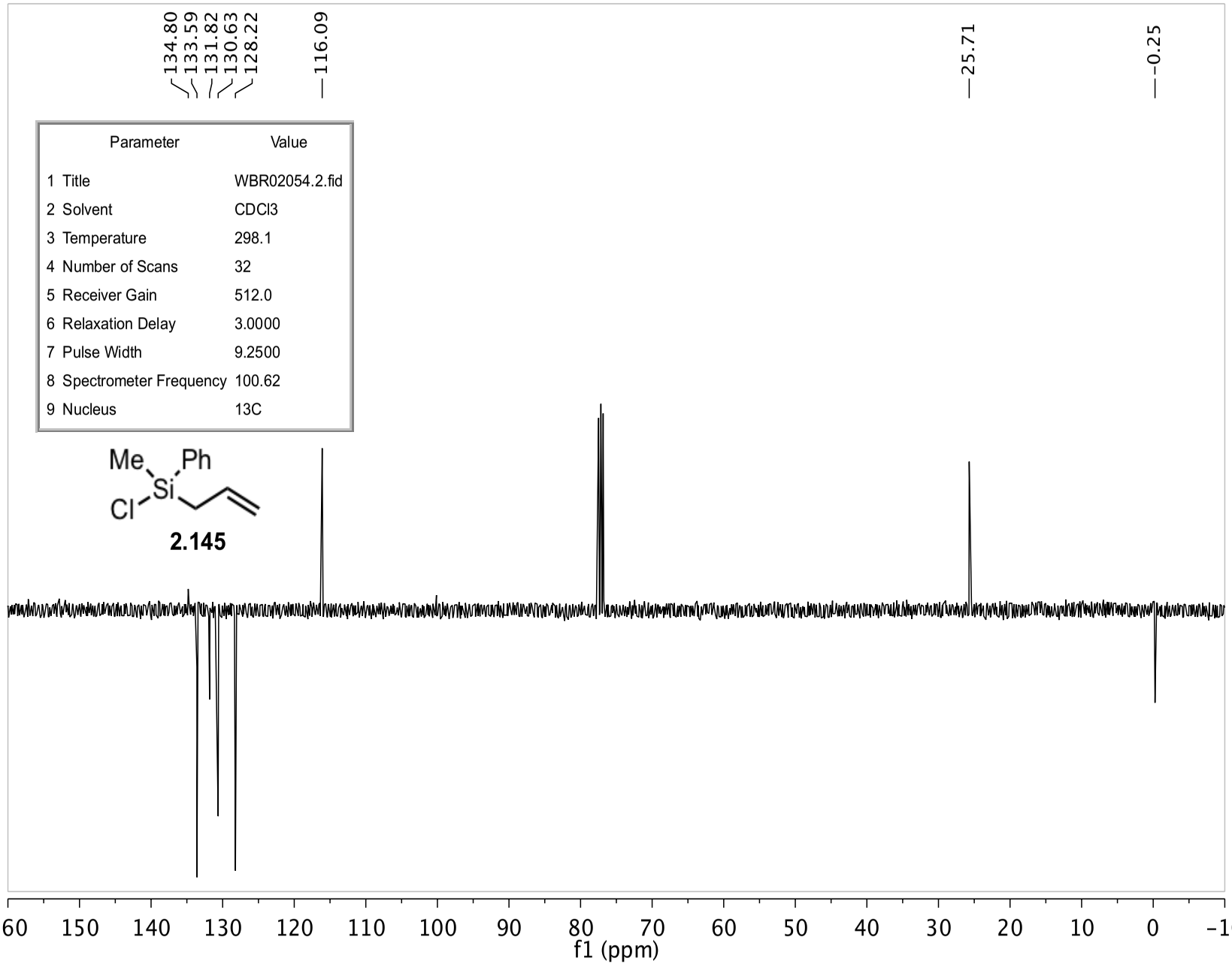
134.80
133.59
131.82
130.63
128.22
116.09
25.71
-0.25
Parameter Value
1 Title WBR02054.2.fid
2 Solvent CDCl3
3 Temperature 298.1
4 Number of Scans 32
5 Receiver Gain 512.0
6 Relaxation Delay 3.0000
7 Pulse Width 9.2500
8 Spectrometer Frequency 100.62
9 Nucleus 13C
Me
Ph
Si
Cl
2.145
160 150 140 130 120 110 100 90 80 70 60 50 40 30 20 10 0 -10
f1 (ppm)

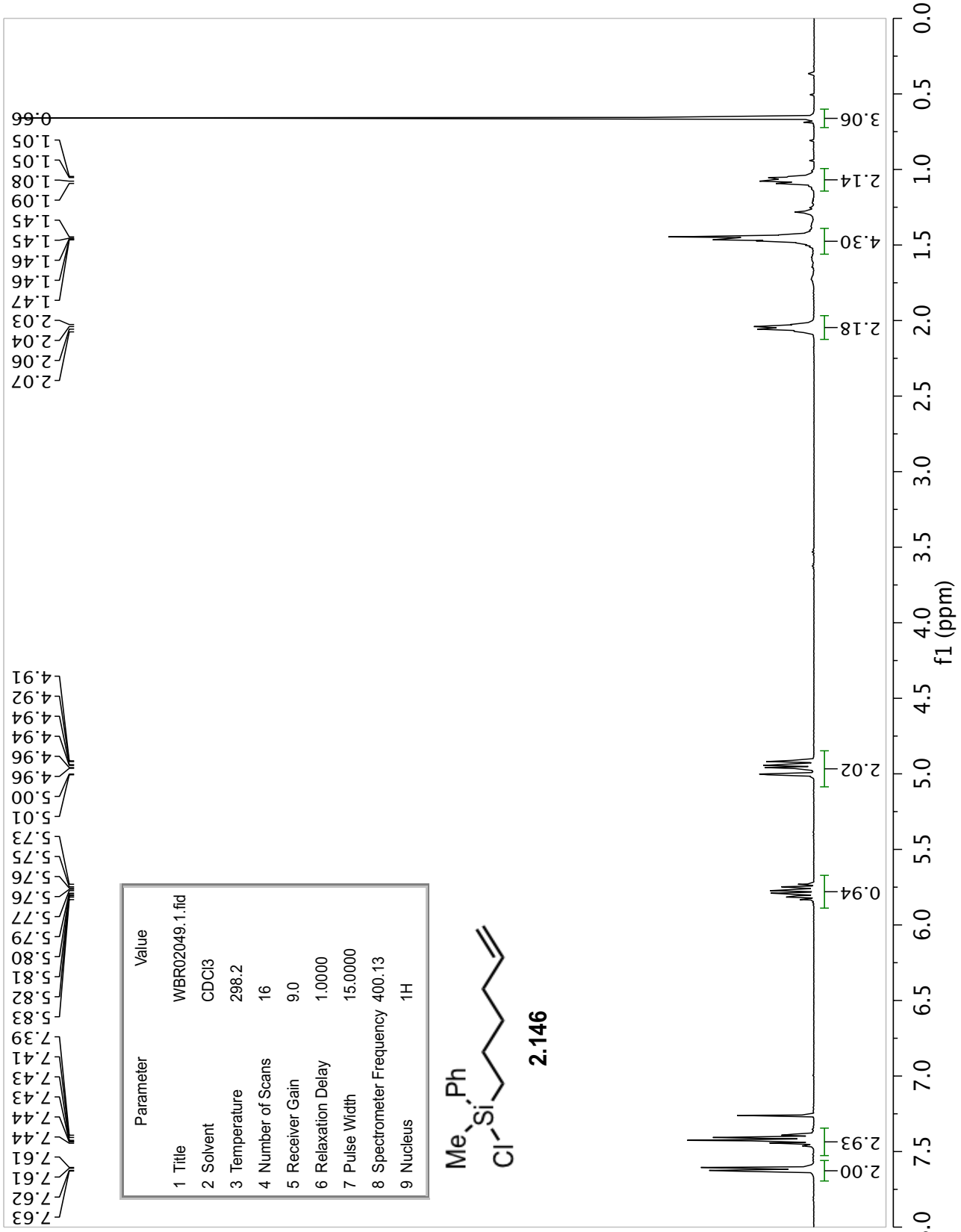
Parameter Value
1 Title WBR02049.1.fid
2 Solvent CDCl3
3 Temperature 298.2
4 Number of Scans 16
5 Receiver Gain 9.0
6 Relaxation Delay 1.0000
7 Pulse Width 15.0000
8 Spectrometer Frequency 400.13
9 Nucleus 1H
Me
Ph
Si
Cl
2.146
2.00
2.93
0.94
2.02
2.18
4.30
2.14
3.06
f1 (ppm)

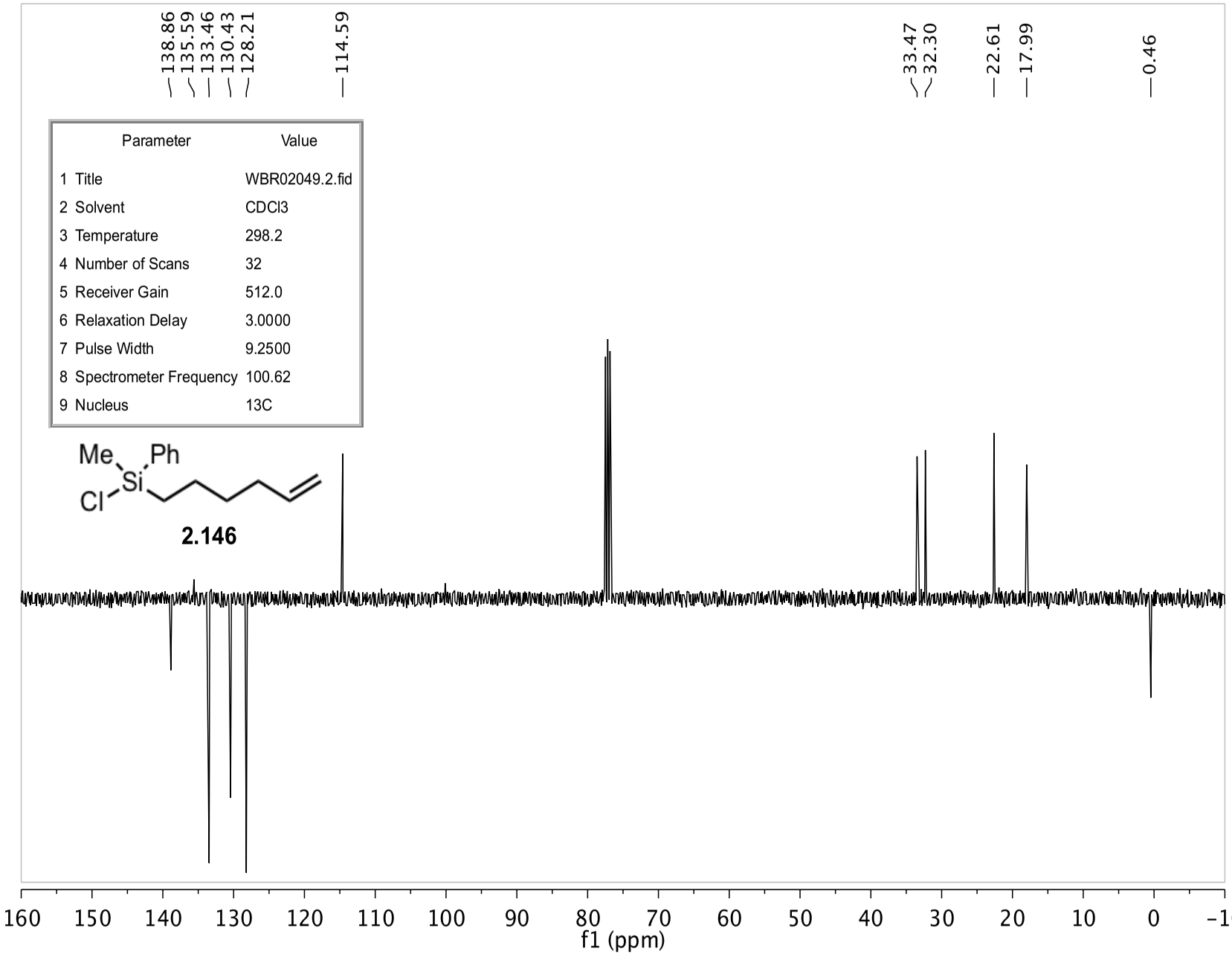
138.86
135.59
133.46
130.43
128.21
114.59
33.47
32.30
22.61
17.99
0.46
Parameter Value
1 Title WBR02049.2.fid
2 Solvent CDCl3
3 Temperature 298.2
4 Number of Scans 32
5 Receiver Gain 512.0
6 Relaxation Delay 3.0000
7 Pulse Width 9.2500
8 Spectrometer Frequency 100.62
9 Nucleus 13C
Me
Ph
Si
Cl
2.146
160 150 140 130 120 110 100 90 80 70 60 50 40 30 20 10 0 -10
f1 (ppm)

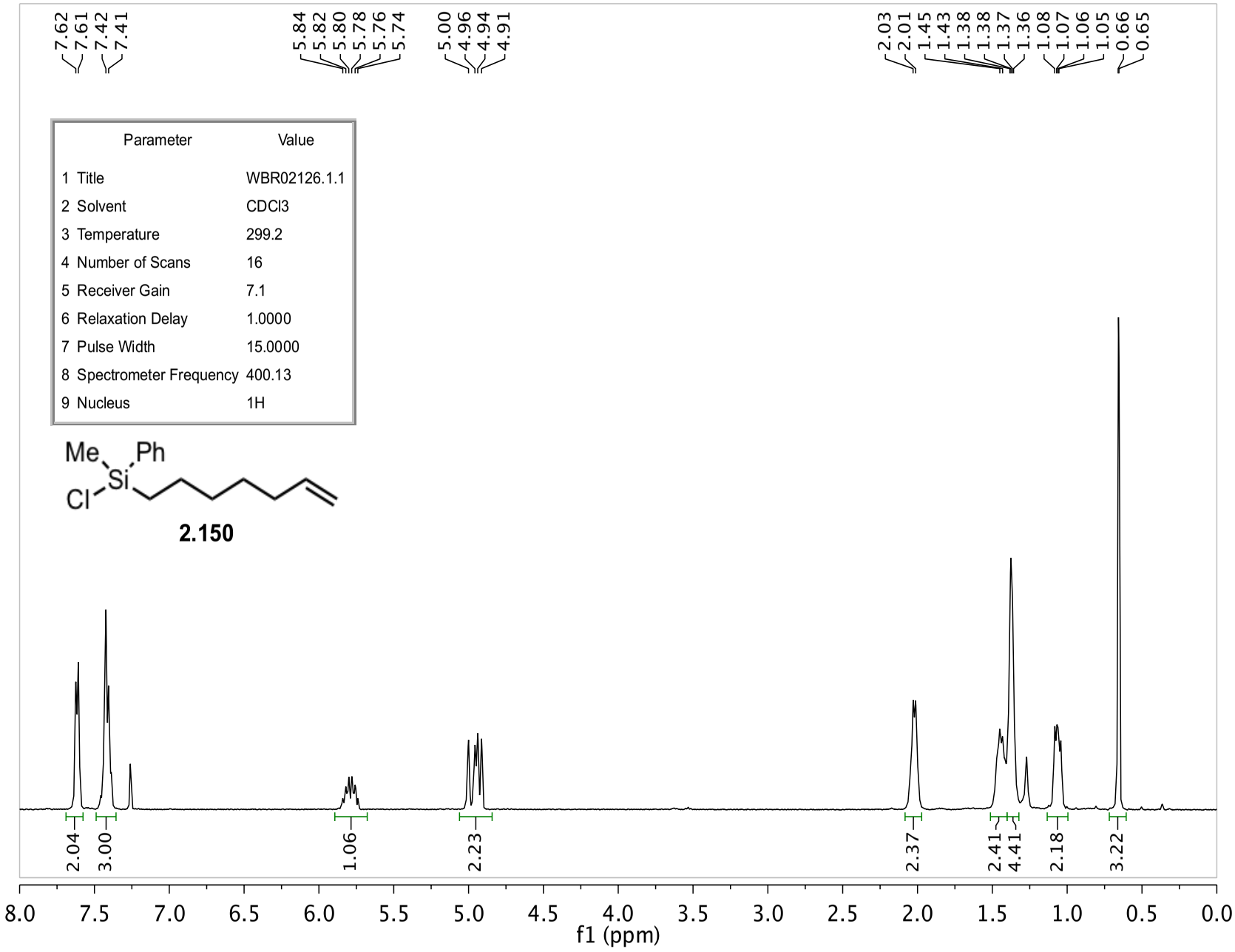
7.62
7.61
7.42
7.41
5.84
5.82
5.80
5.78
5.76
5.74
5.00
4.96
4.94
4.91
2.03
2.01
1.45
1.43
1.38
1.38
1.37
1.36
1.08
1.07
1.06
1.05
0.66
0.65
Parameter Value
1 Title WBR02126.1.1
2 Solvent CDCl3
3 Temperature 299.2
4 Number of Scans 16
5 Receiver Gain 7.1
6 Relaxation Delay 1.0000
7 Pulse Width 15.0000
8 Spectrometer Frequency 400.13
9 Nucleus 1H
Me
Ph
Si
Cl
2.150
2.04
3.00
1.06
2.23
2.37
2.41
4.41
2.18
3.22
8.0
7.5
7.0
6.5
6.0
5.5
5.0
4.5
4.0
3.5
3.0
2.5
2.0
1.5
1.0
0.5
0.0
f1 (ppm)

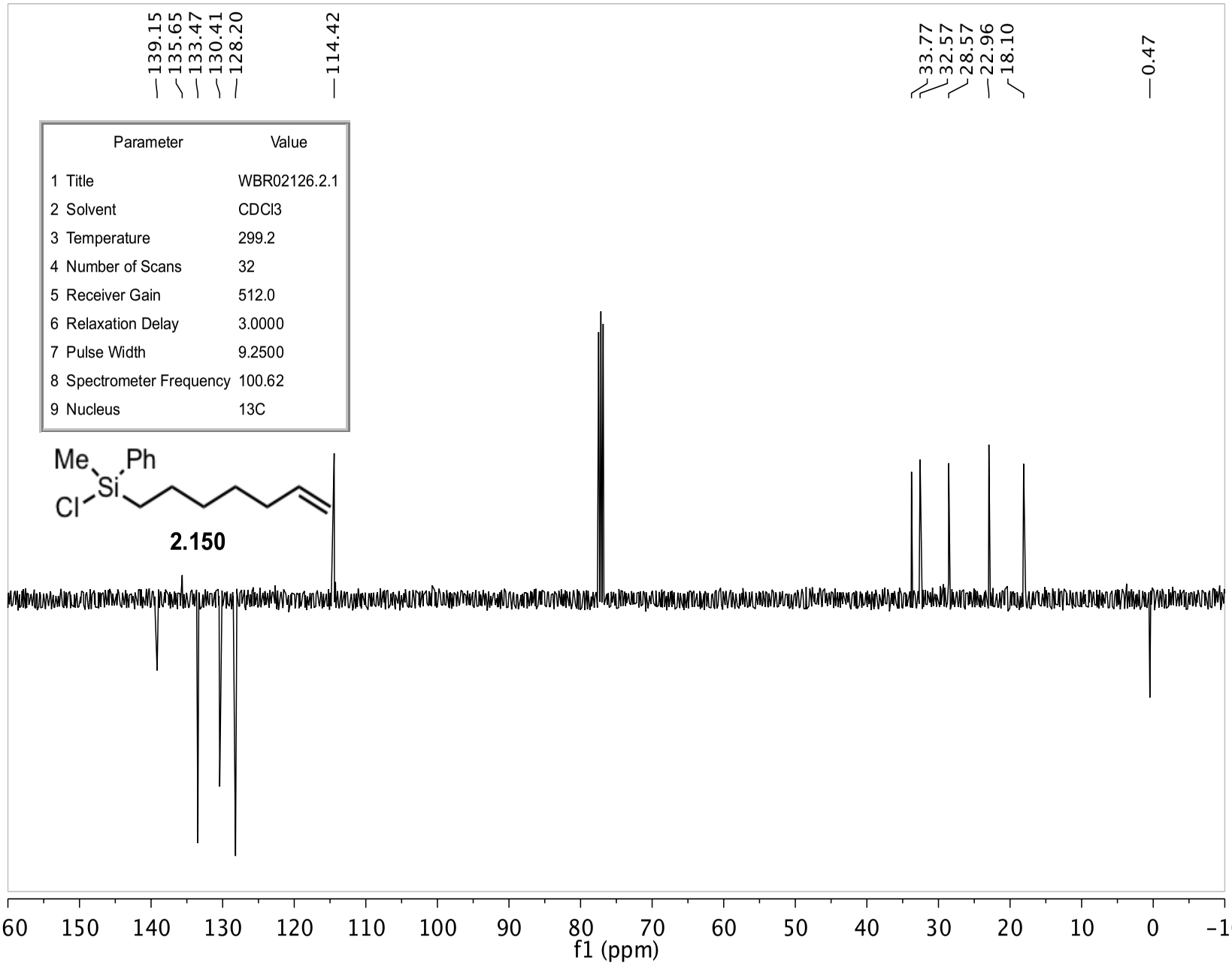
139.15
135.65
133.47
130.41
128.20
114.42
33.77
32.57
28.57
22.96
18.10
0.47
Parameter Value
1 Title WBR02126.2.1
2 Solvent CDCl3
3 Temperature 299.2
4 Number of Scans 32
5 Receiver Gain 512.0
6 Relaxation Delay 3.0000
7 Pulse Width 9.2500
8 Spectrometer Frequency 100.62
9 Nucleus 13C
Me
Ph
Si
Cl
2.150
160 150 140 130 120 110 100 90 80 70 60 50 40 30 20 10 0 -10
f1 (ppm)

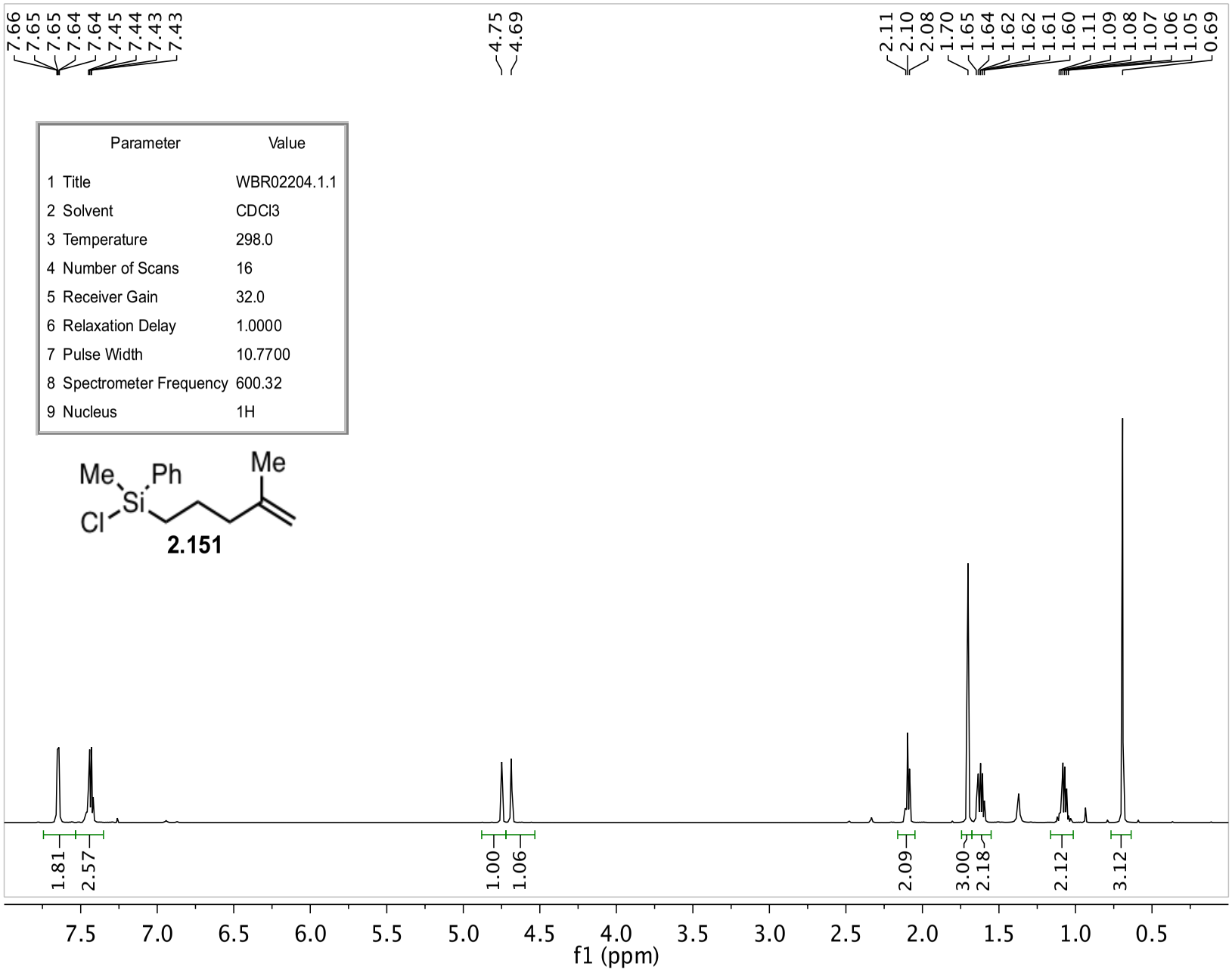
7.66
7.65
7.65
7.64
7.64
7.45
7.44
7.43
7.43
4.75
4.69
2.11
2.10
2.08
1.70
1.65
1.64
1.62
1.62
1.61
1.60
1.11
1.09
1.08
1.07
1.06
1.05
0.69
Parameter Value
1 Title WBR02204.1.1
2 Solvent CDCl3
3 Temperature 298.0
4 Number of Scans 16
5 Receiver Gain 32.0
6 Relaxation Delay 1.0000
7 Pulse Width 10.7700
8 Spectrometer Frequency 600.32
9 Nucleus 1H
Me
Ph
Me
Si
Cl
2.151
1.81
2.57
1.00
1.06
2.09
3.00
2.18
2.12
3.12
7.5
7.0
6.5
6.0
5.5
5.0
4.5
4.0
3.5
3.0
2.5
2.0
1.5
1.0
0.5
f1 (ppm)

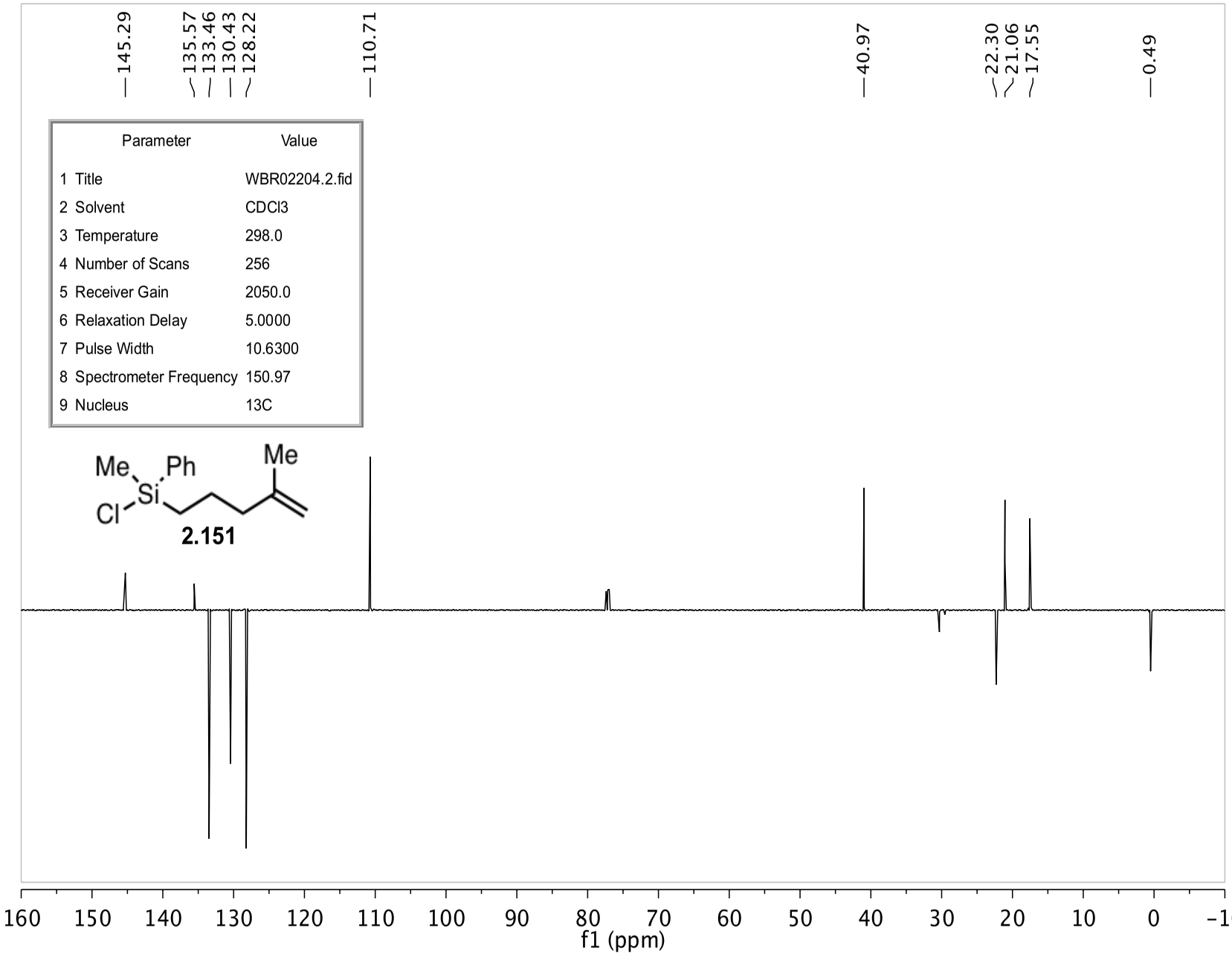
145.29
135.57
133.46
130.43
128.22
110.71
40.97
22.30
21.06
17.55
0.49
Parameter Value
1 Title WBR02204.2.fid
2 Solvent CDCl3
3 Temperature 298.0
4 Number of Scans 256
5 Receiver Gain 2050.0
6 Relaxation Delay 5.0000
7 Pulse Width 10.6300
8 Spectrometer Frequency 150.97
9 Nucleus 13C
Me
Ph
Si
Cl
Me
2.151
160 150 140 130 120 110 100 90 80 70 60 50 40 30 20 10 0 -10
f1 (ppm)

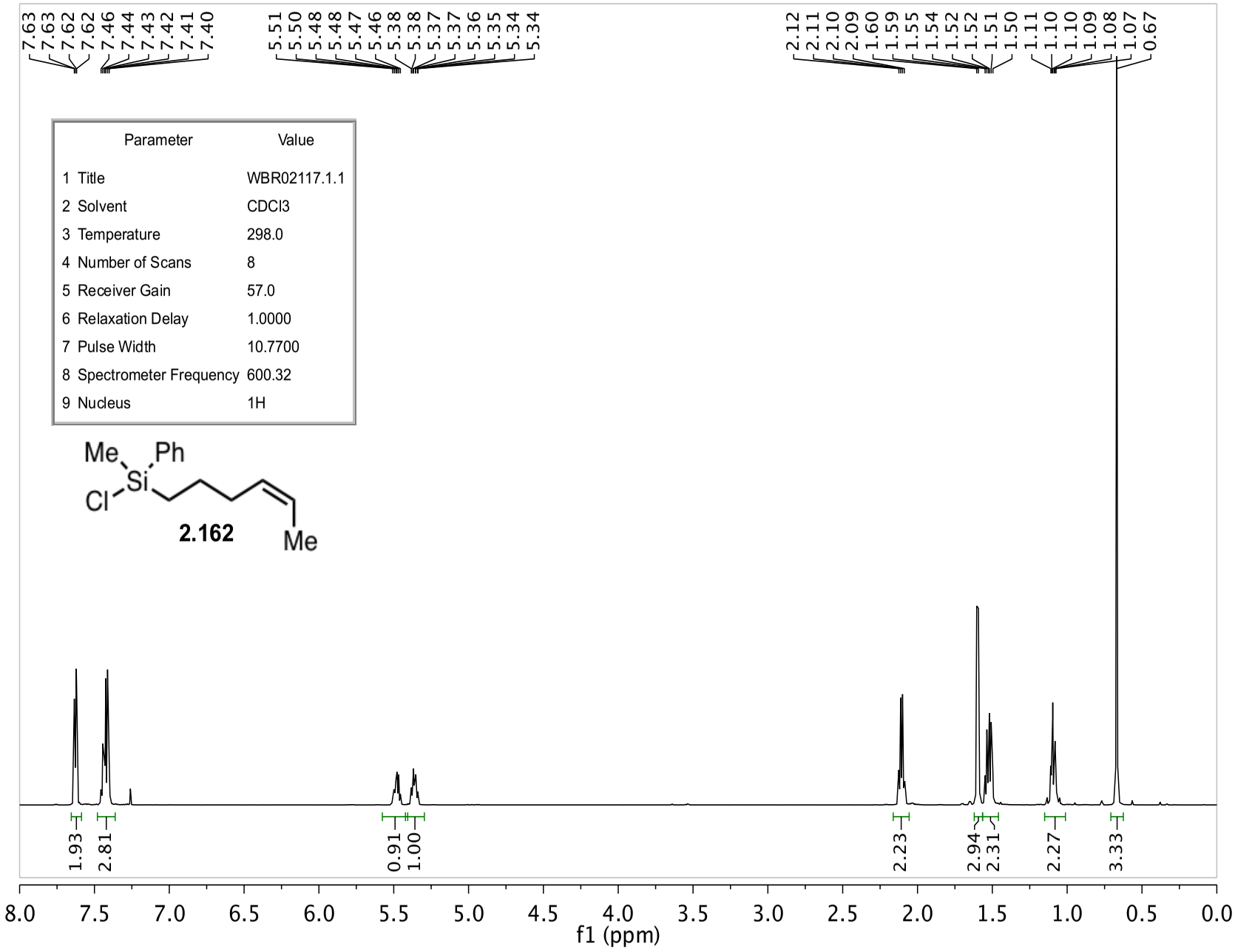
7.63 7.63 7.62 7.62 7.46 7.44 7.43 7.42 7.41 7.40
5.51 5.50 5.48 5.48 5.47 5.46 5.38 5.38 5.37 5.37 5.36 5.35 5.34 5.34
2.12 2.11 2.10 2.09 1.60 1.59 1.55 1.54 1.52 1.52 1.51 1.50 1.11 1.10 1.10 1.09 1.08 1.07 0.67
Parameter Value
1 Title WBR02117.1.1
2 Solvent CDCl3
3 Temperature 298.0
4 Number of Scans 8
5 Receiver Gain 57.0
6 Relaxation Delay 1.0000
7 Pulse Width 10.7700
8 Spectrometer Frequency 600.32
9 Nucleus 1H
Me Ph Si Cl Me
2.162
1.93 2.81 0.91 1.00 2.23 2.94 2.31 2.27 3.33
8.0 7.5 7.0 6.5 6.0 5.5 5.0 4.5 4.0 3.5 3.0 2.5 2.0 1.5 1.0 0.5 0.0
f1 (ppm)

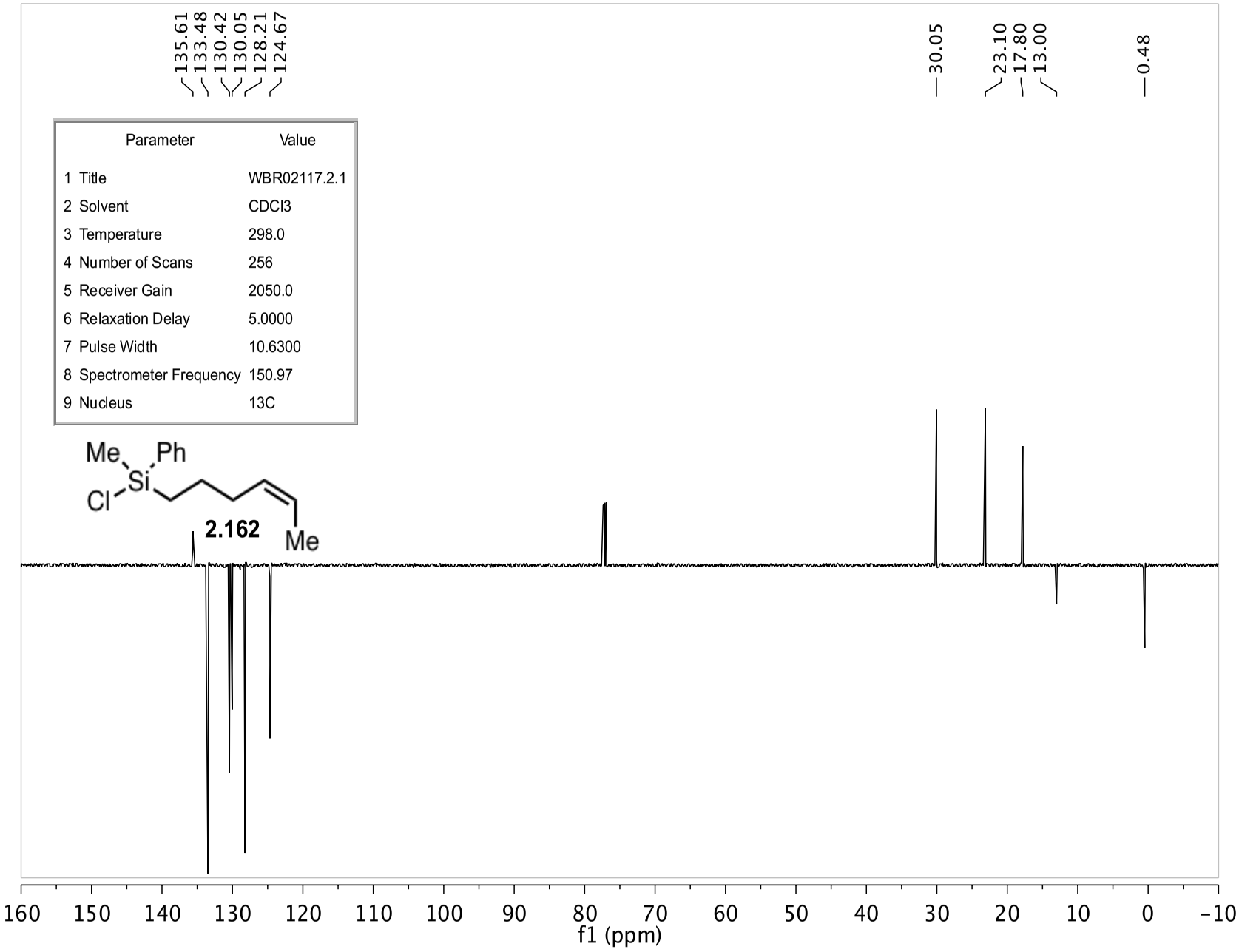
135.61
133.48
130.42
130.05
128.21
124.67
30.05
23.10
17.80
13.00
0.48
Parameter Value
1 Title WBR02117.2.1
2 Solvent CDCl3
3 Temperature 298.0
4 Number of Scans 256
5 Receiver Gain 2050.0
6 Relaxation Delay 5.0000
7 Pulse Width 10.6300
8 Spectrometer Frequency 150.97
9 Nucleus 13C
Me
Ph
Si
Cl
2.162
Me
160 150 140 130 120 110 100 90 80 70 60 50 40 30 20 10 0 -10
f1 (ppm)

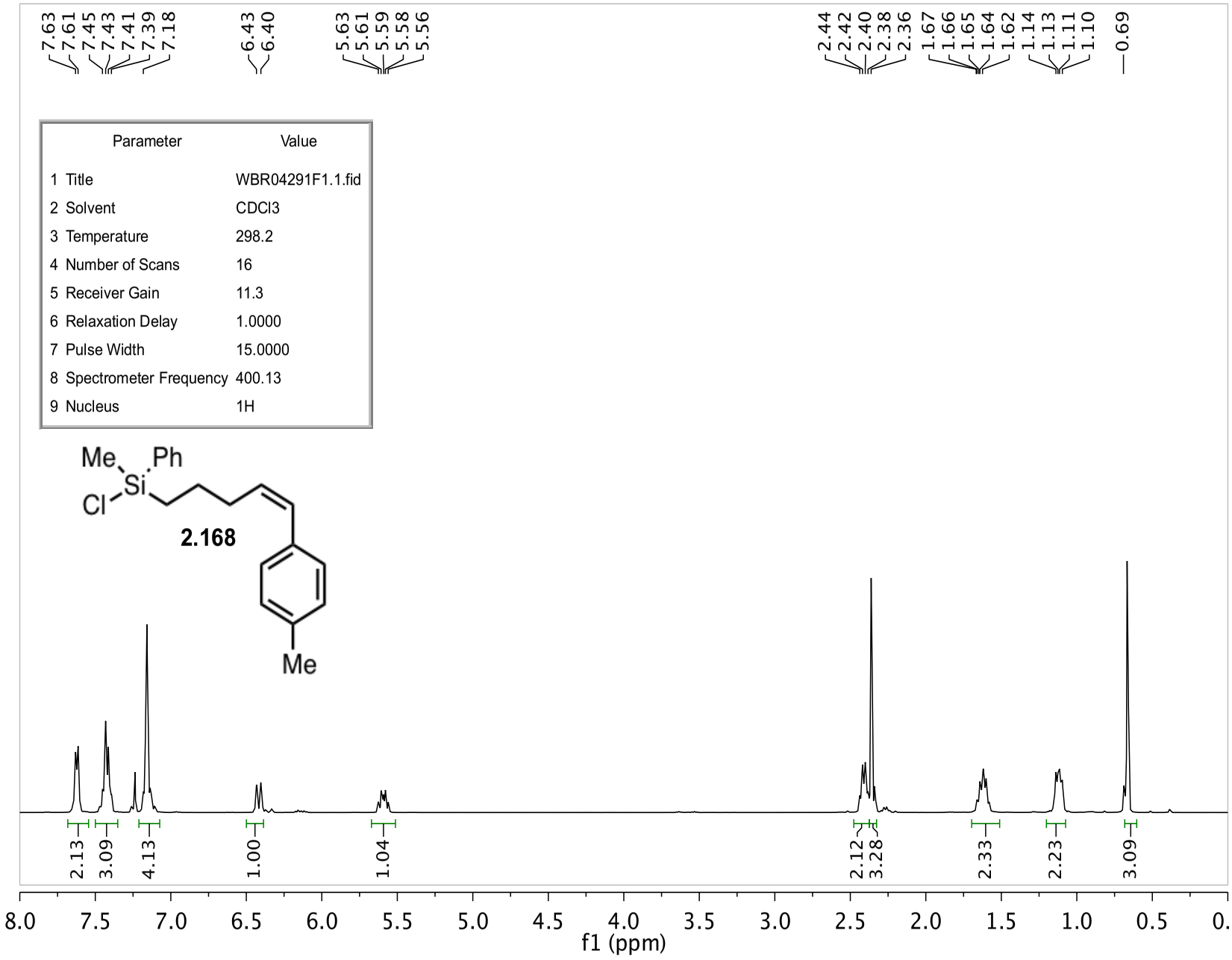
7.63
7.61
7.45
7.43
7.41
7.39
7.18
6.43
6.40
5.63
5.61
5.59
5.58
5.56
2.44
2.42
2.40
2.38
2.36
1.67
1.66
1.65
1.64
1.62
1.14
1.13
1.11
1.10
0.69
Parameter Value
1 Title WBR04291F1.1.fid
2 Solvent CDCl3
3 Temperature 298.2
4 Number of Scans 16
5 Receiver Gain 11.3
6 Relaxation Delay 1.0000
7 Pulse Width 15.0000
8 Spectrometer Frequency 400.13
9 Nucleus 1H
Me
Ph
Si
Cl
2.168
Me
2.13
3.09
4.13
1.00
1.04
2.12
3.28
2.33
2.23
3.09
8.0
7.5
7.0
6.5
6.0
5.5
5.0
4.5
4.0
3.5
3.0
2.5
2.0
1.5
1.0
0.5
0.0
f1 (ppm)

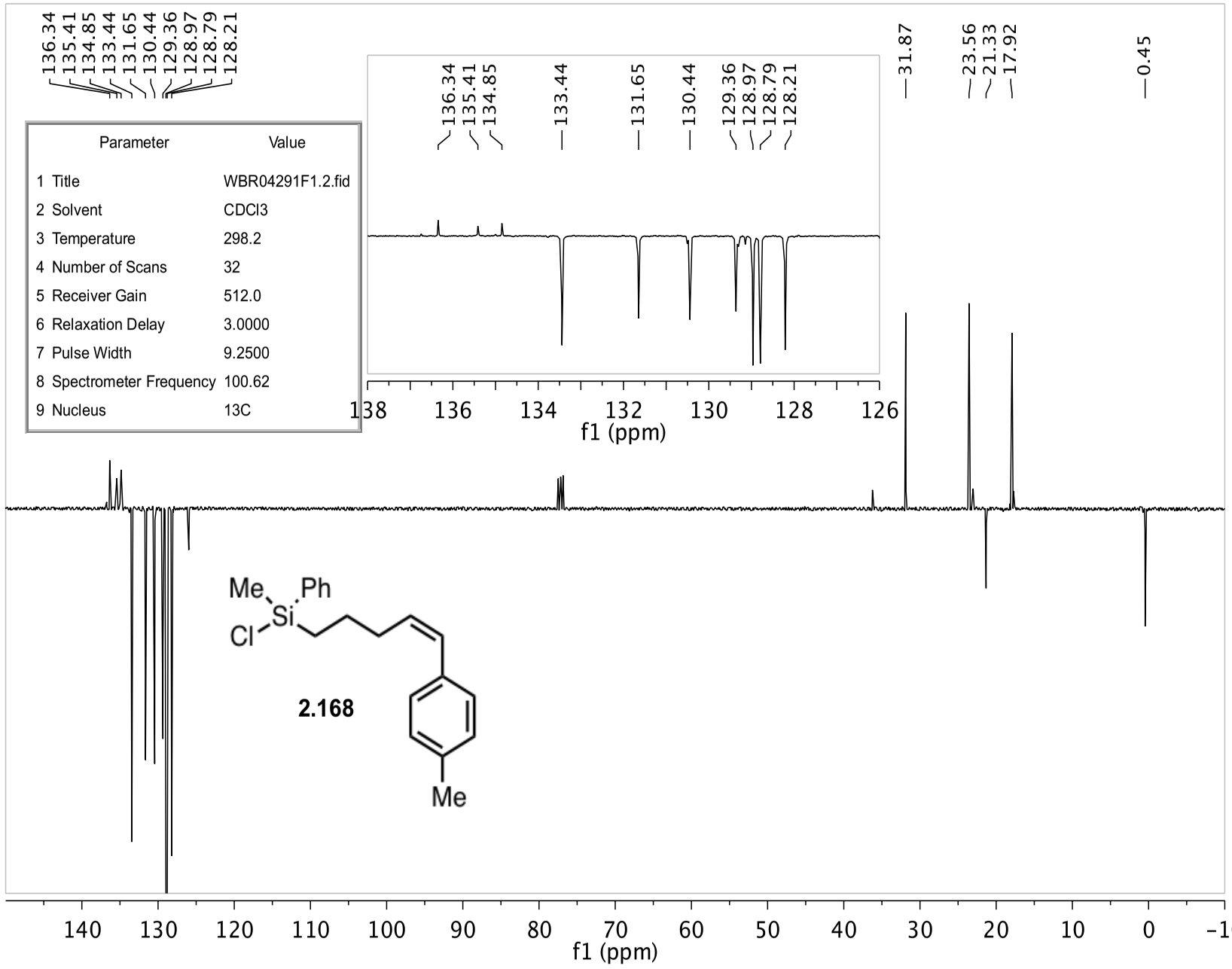
136.34
135.41
134.85
133.44
131.65
130.44
129.36
128.97
128.79
128.21
31.87
23.56
21.33
17.92
0.45
Parameter Value
1 Title WBR04291F1.2.fid
2 Solvent CDCl3
3 Temperature 298.2
4 Number of Scans 32
5 Receiver Gain 512.0
6 Relaxation Delay 3.0000
7 Pulse Width 9.2500
8 Spectrometer Frequency 100.62
9 Nucleus 13C
f1 (ppm)
Me
Ph
Si
Cl
2.168
Me

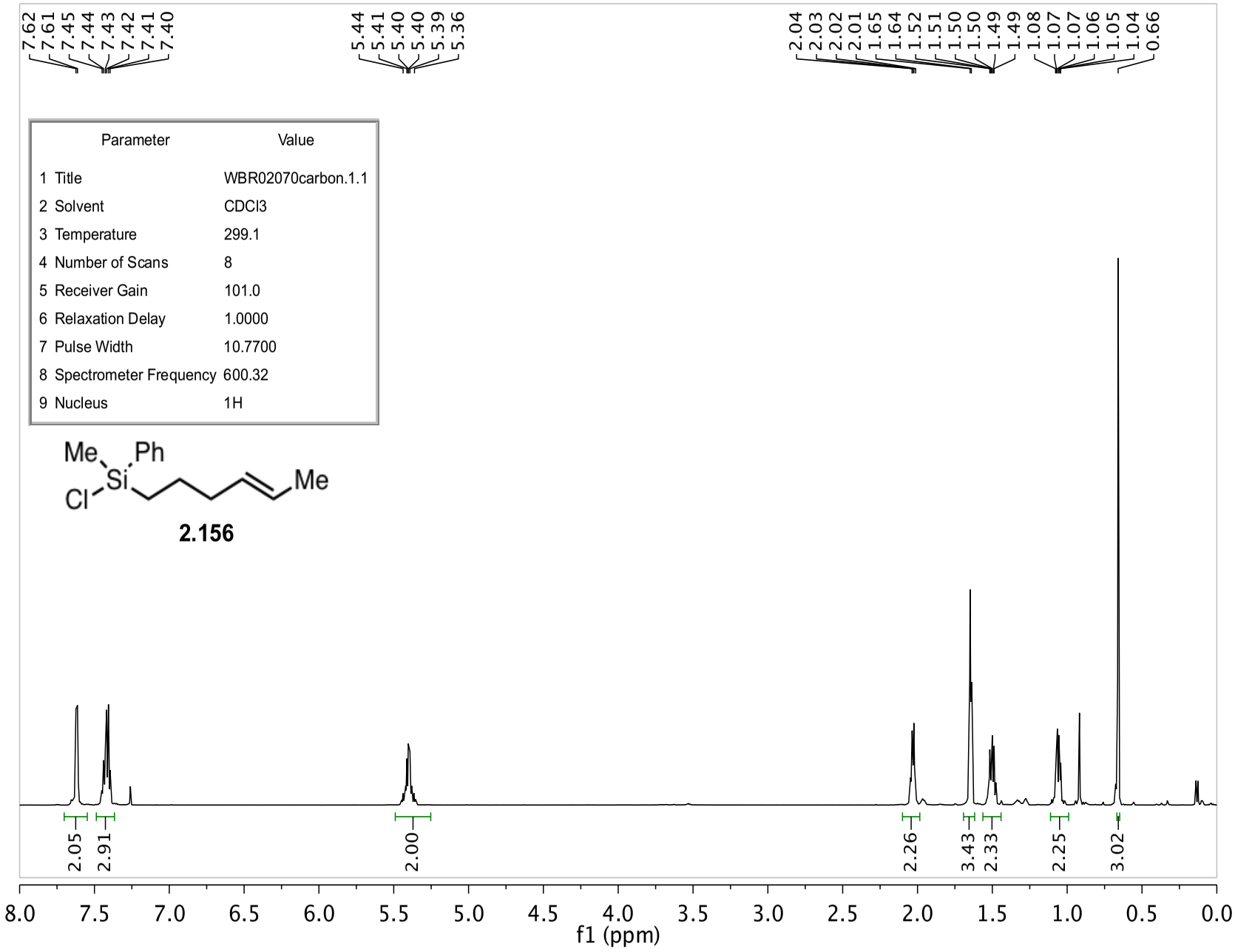
7.62
7.61
7.45
7.44
7.43
7.42
7.41
7.40
5.44
5.41
5.40
5.40
5.39
5.36
2.04
2.03
2.02
2.01
1.65
1.64
1.52
1.51
1.50
1.50
1.49
1.49
1.08
1.07
1.07
1.06
1.05
1.04
0.66
Parameter Value
1 Title WBR02070carbon.1.1
2 Solvent CDCl3
3 Temperature 299.1
4 Number of Scans 8
5 Receiver Gain 101.0
6 Relaxation Delay 1.0000
7 Pulse Width 10.7700
8 Spectrometer Frequency 600.32
9 Nucleus 1H
Me
Ph
Si
Cl
Me
2.156
2.05
2.91
2.00
2.26
3.43
2.33
2.25
3.02
8.0
7.5
7.0
6.5
6.0
5.5
5.0
4.5
4.0
3.5
3.0
2.5
2.0
1.5
1.0
0.5
0.0
f1 (ppm)

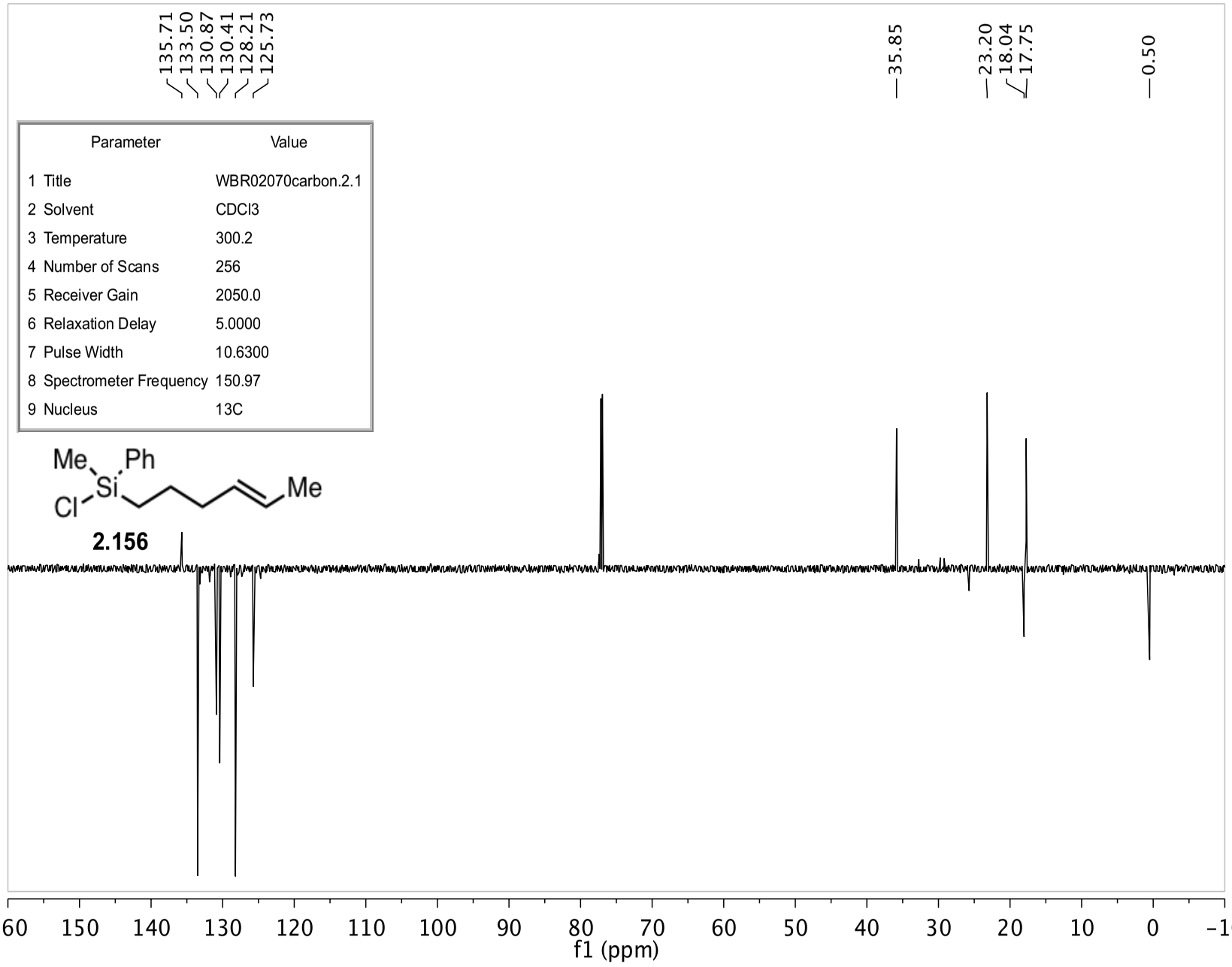
135.71
133.50
130.87
130.41
128.21
125.73
35.85
23.20
18.04
17.75
0.50
Parameter Value
1 Title WBR02070carbon.2.1
2 Solvent CDCl3
3 Temperature 300.2
4 Number of Scans 256
5 Receiver Gain 2050.0
6 Relaxation Delay 5.0000
7 Pulse Width 10.6300
8 Spectrometer Frequency 150.97
9 Nucleus 13C
Me
Ph
Si
Cl
Me
2.156
160 150 140 130 120 110 100 90 80 70 60 50 40 30 20 10 0 -10
f1 (ppm)

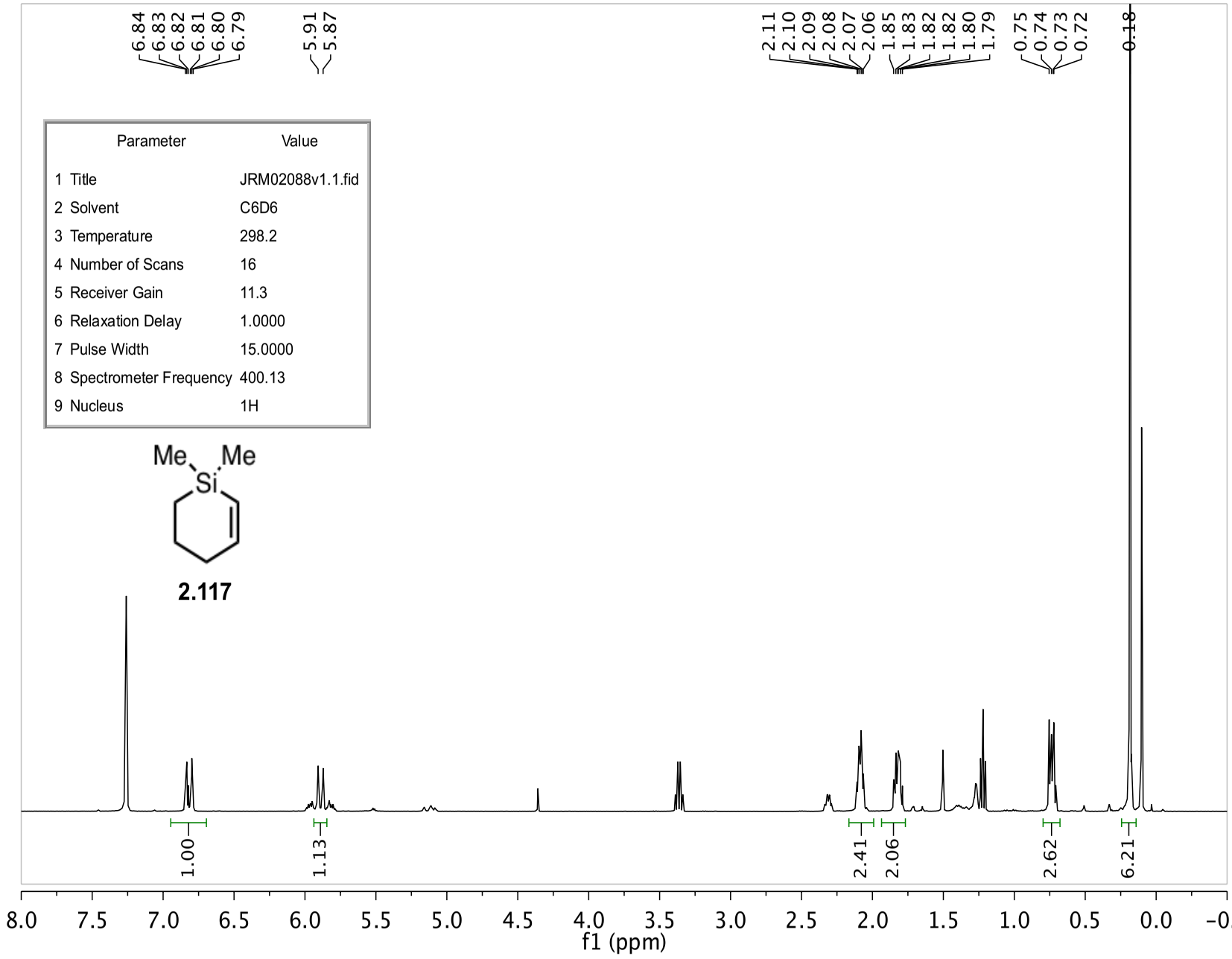
6.84
6.83
6.82
6.81
6.80
6.79
5.91
5.87
2.11
2.10
2.09
2.08
2.07
2.06
1.85
1.83
1.82
1.82
1.80
1.79
0.75
0.74
0.73
0.72
0.18
Parameter Value
1 Title JRM02088v1.1.fid
2 Solvent C6D6
3 Temperature 298.2
4 Number of Scans 16
5 Receiver Gain 11.3
6 Relaxation Delay 1.0000
7 Pulse Width 15.0000
8 Spectrometer Frequency 400.13
9 Nucleus 1H
Me
Me
Si
2.117
1.00
1.13
2.41
2.06
2.62
6.21
8.0
7.5
7.0
6.5
6.0
5.5
5.0
4.5
4.0
3.5
3.0
2.5
2.0
1.5
1.0
0.5
0.0
-0.5
f1 (ppm)

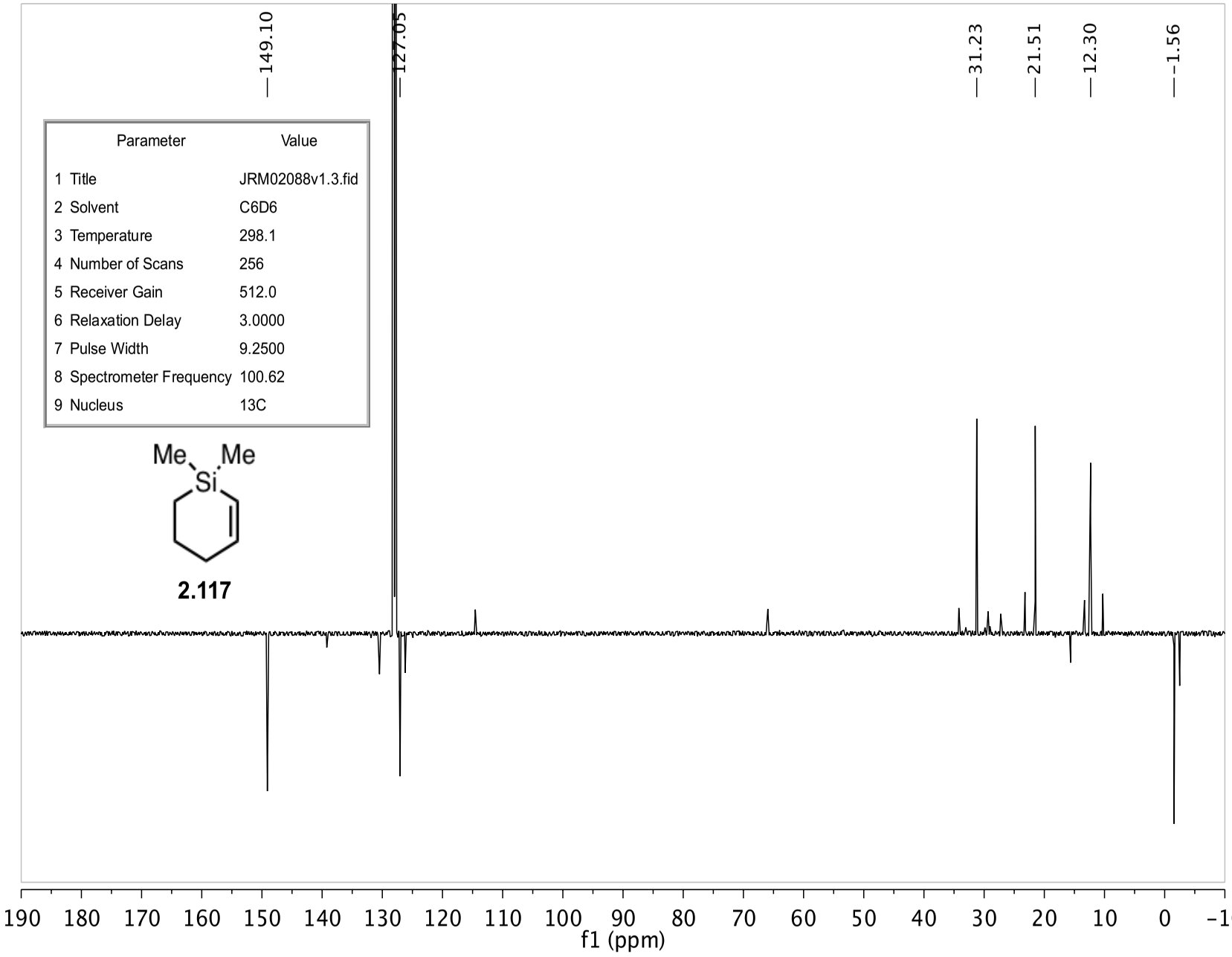
149.10
127.05
31.23
21.51
12.30
1.56
Parameter Value
1 Title JRM02088v1.3.fid
2 Solvent C6D6
3 Temperature 298.1
4 Number of Scans 256
5 Receiver Gain 512.0
6 Relaxation Delay 3.0000
7 Pulse Width 9.2500
8 Spectrometer Frequency 100.62
9 Nucleus 13C
Me
Me
Si
2.117
190 180 170 160 150 140 130 120 110 100 90 80 70 60 50 40 30 20 10 0 -10
f1 (ppm)

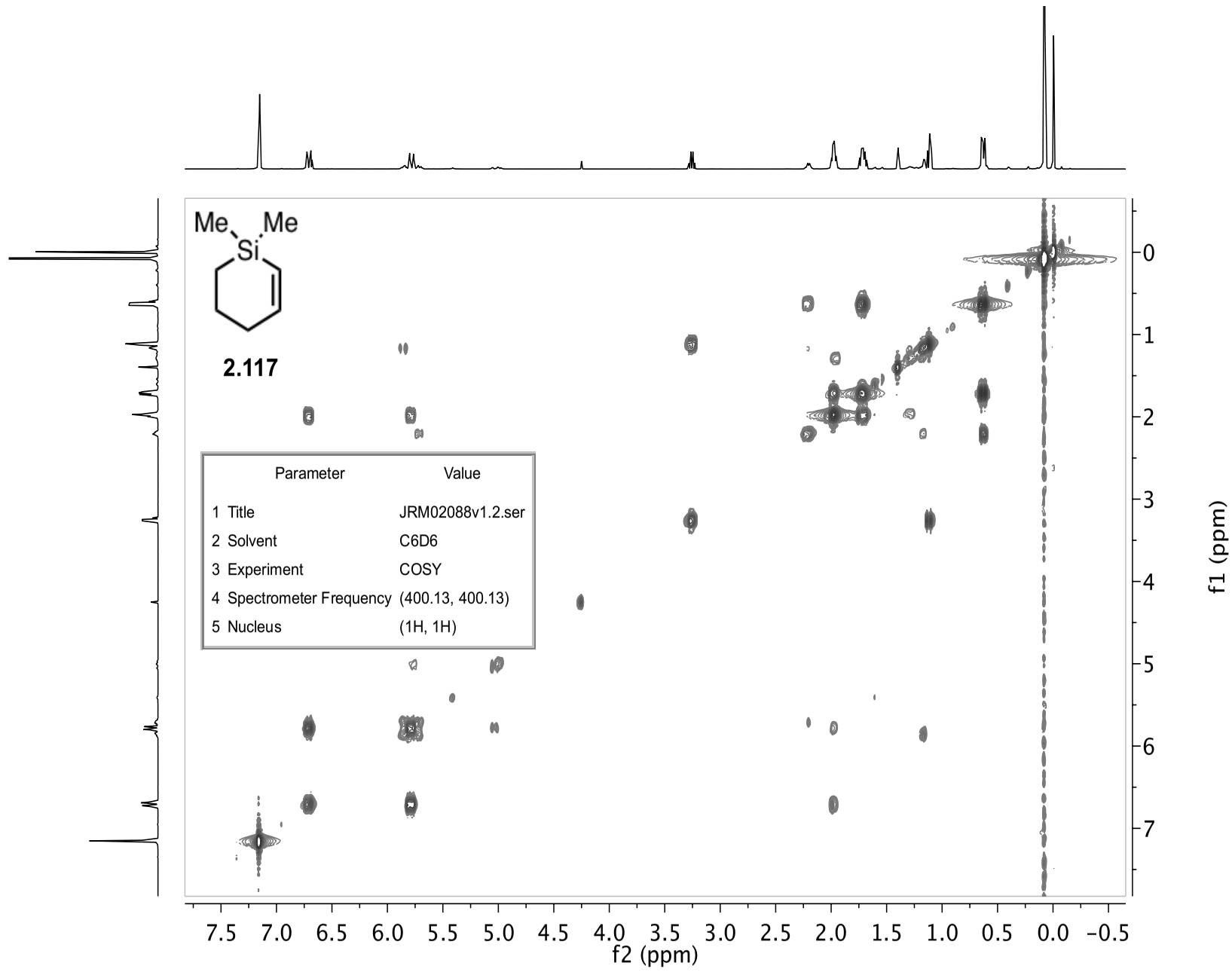
Me
Si
Me
2.117
Parameter Value
1 Title JRM02088v1.2.ser
2 Solvent C6D6
3 Experiment COSY
4 Spectrometer Frequency (400.13, 400.13)
5 Nucleus (1H, 1H)
f2 (ppm)
f1 (ppm)

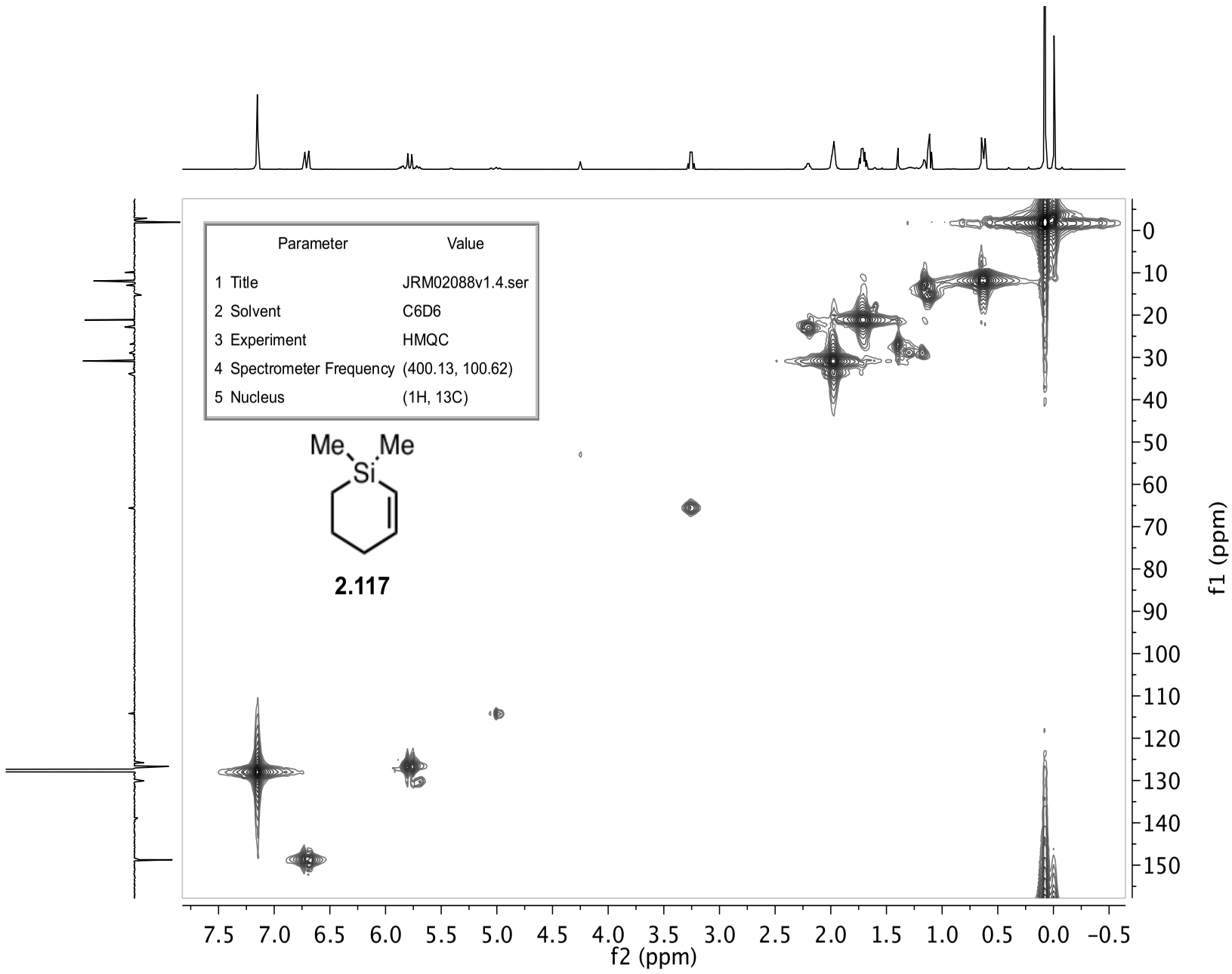
Parameter Value
1 Title JRM02088v1.4.ser
2 Solvent C6D6
3 Experiment HMQC
4 Spectrometer Frequency (400.13, 100.62)
5 Nucleus (1H, 13C)
Me
Me
Si
2.117
f2 (ppm)
f1 (ppm)

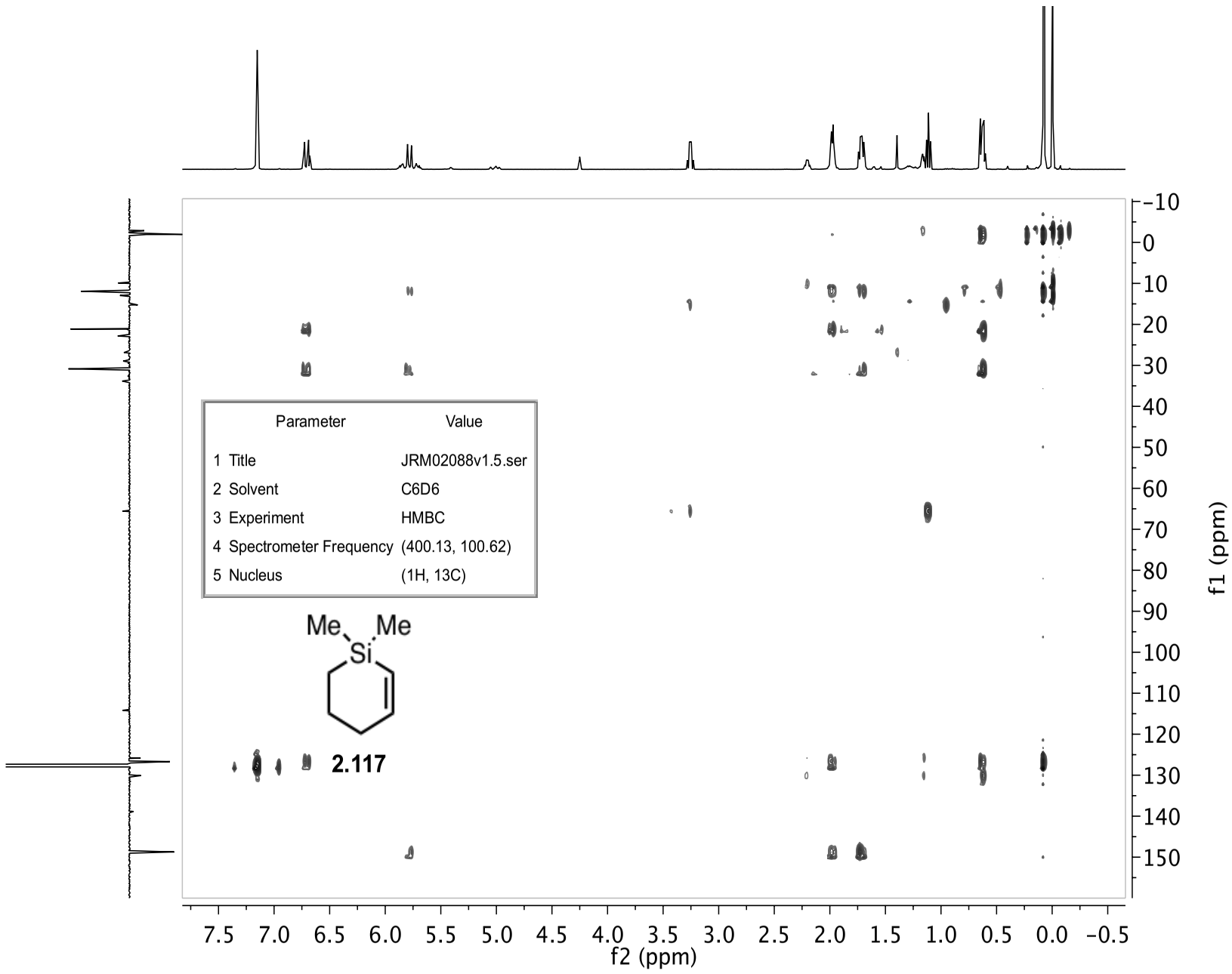
Parameter Value
1 Title JRM02088v1.5.ser
2 Solvent C6D6
3 Experiment HMBC
4 Spectrometer Frequency (400.13, 100.62)
5 Nucleus (1H, 13C)
Me
Me
Si
2.117
f2 (ppm)
f1 (ppm)

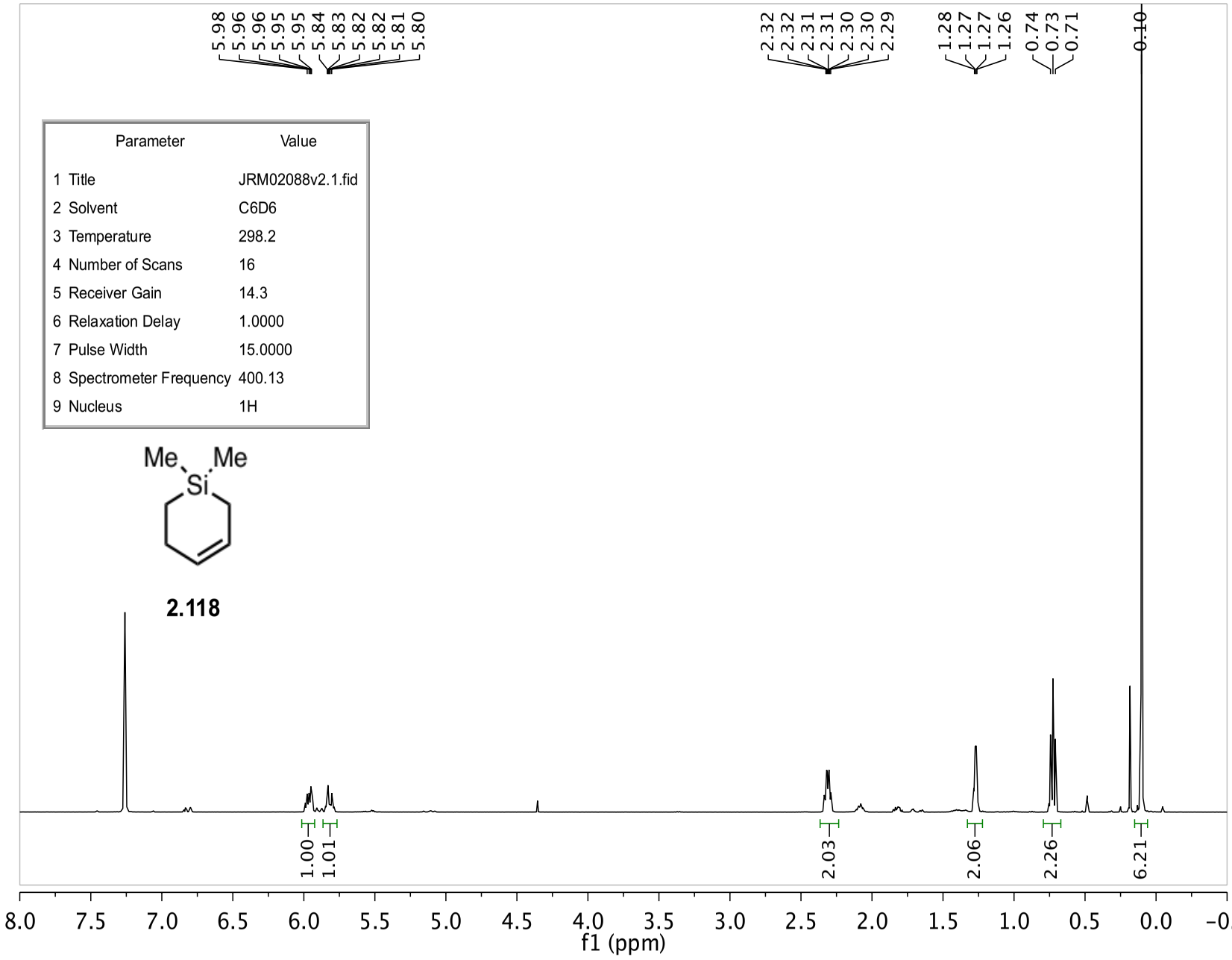
5.98
5.96
5.96
5.95
5.95
5.84
5.83
5.82
5.82
5.81
5.80
2.32
2.32
2.31
2.31
2.30
2.30
2.29
1.28
1.27
1.27
1.26
0.74
0.73
0.71
0.10
Parameter Value
1 Title JRM02088v2.1.fid
2 Solvent C6D6
3 Temperature 298.2
4 Number of Scans 16
5 Receiver Gain 14.3
6 Relaxation Delay 1.0000
7 Pulse Width 15.0000
8 Spectrometer Frequency 400.13
9 Nucleus 1H
Me
Me
Si
2.118
1.00
1.01
2.03
2.06
2.26
6.21
8.0
7.5
7.0
6.5
6.0
5.5
5.0
4.5
4.0
3.5
3.0
2.5
2.0
1.5
1.0
0.5
0.0
-0.5
f1 (ppm)

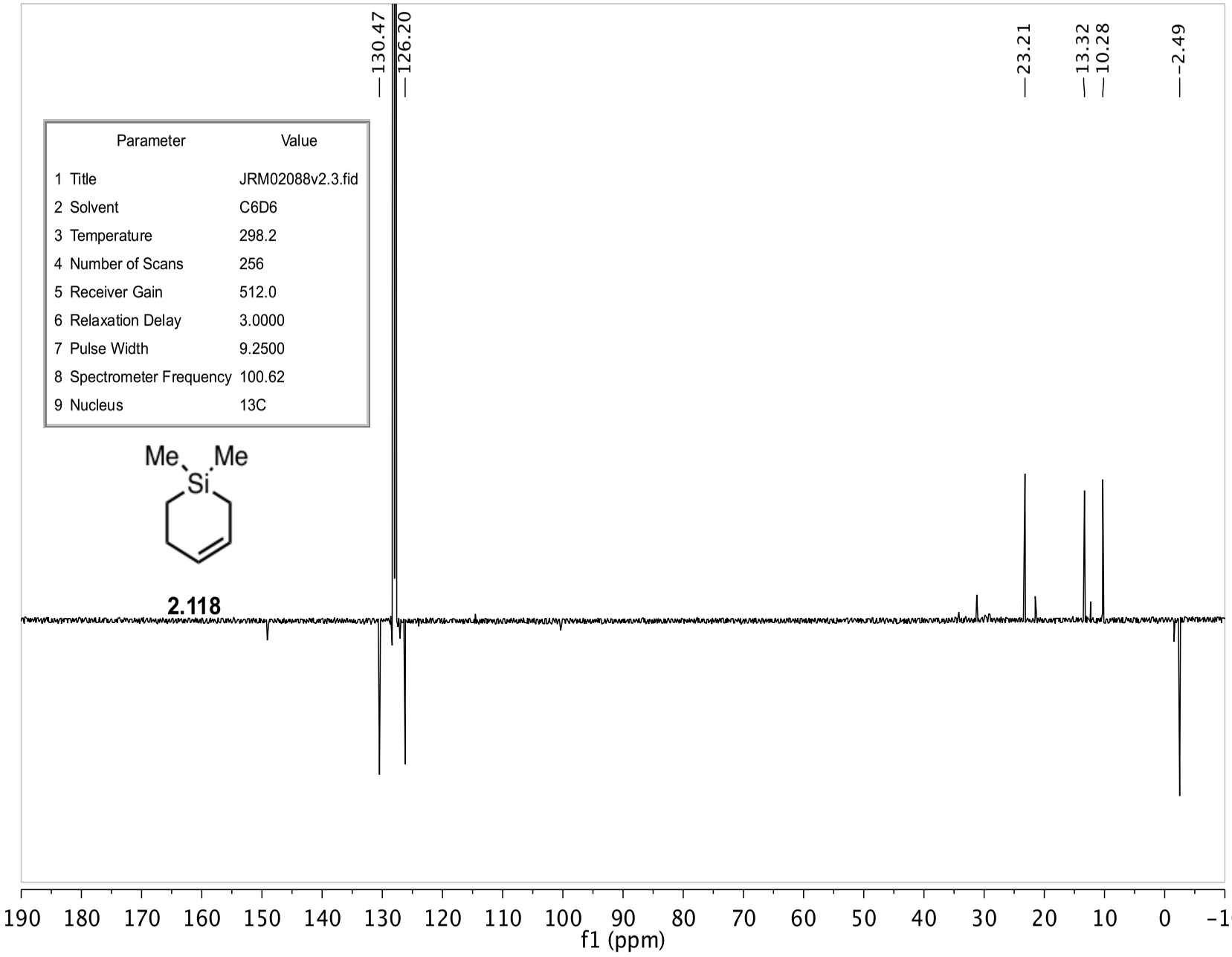
130.47
126.20
23.21
13.32
10.28
-2.49
Parameter Value
1 Title JRM02088v2.3.fid
2 Solvent C6D6
3 Temperature 298.2
4 Number of Scans 256
5 Receiver Gain 512.0
6 Relaxation Delay 3.0000
7 Pulse Width 9.2500
8 Spectrometer Frequency 100.62
9 Nucleus 13C
Me
Me
Si
2.118
190 180 170 160 150 140 130 120 110 100 90 80 70 60 50 40 30 20 10 0 -10
f1 (ppm)

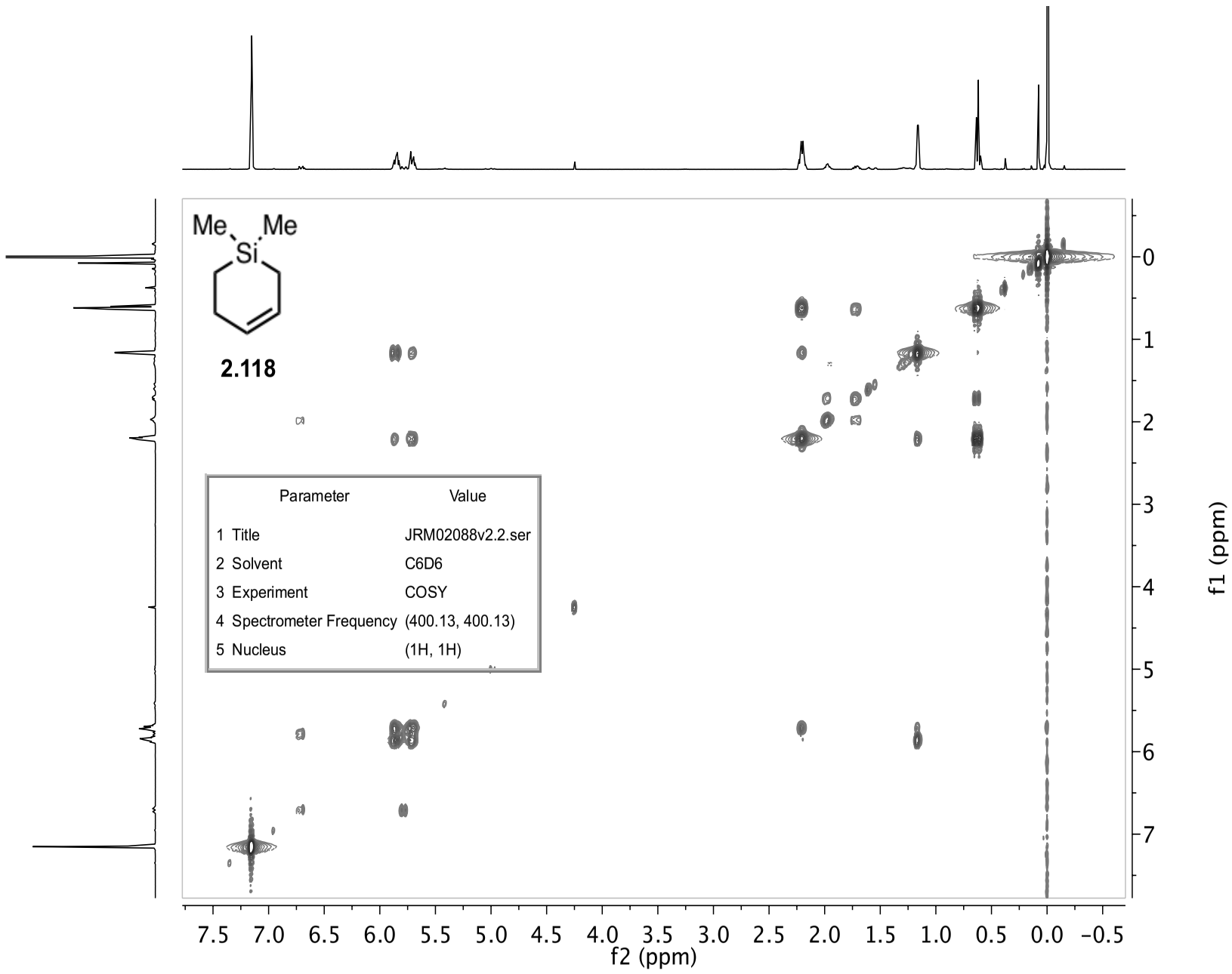
Me
Me
Si
2.118
Parameter Value
1 Title JRM02088v2.2.ser
2 Solvent C6D6
3 Experiment COSY
4 Spectrometer Frequency (400.13, 400.13)
5 Nucleus (1H, 1H)
7.5 7.0 6.5 6.0 5.5 5.0 4.5 4.0 3.5 3.0 2.5 2.0 1.5 1.0 0.5 0.0 -0.5
f2 (ppm)
0 1 2 3 4 5 6 7
f1 (ppm)

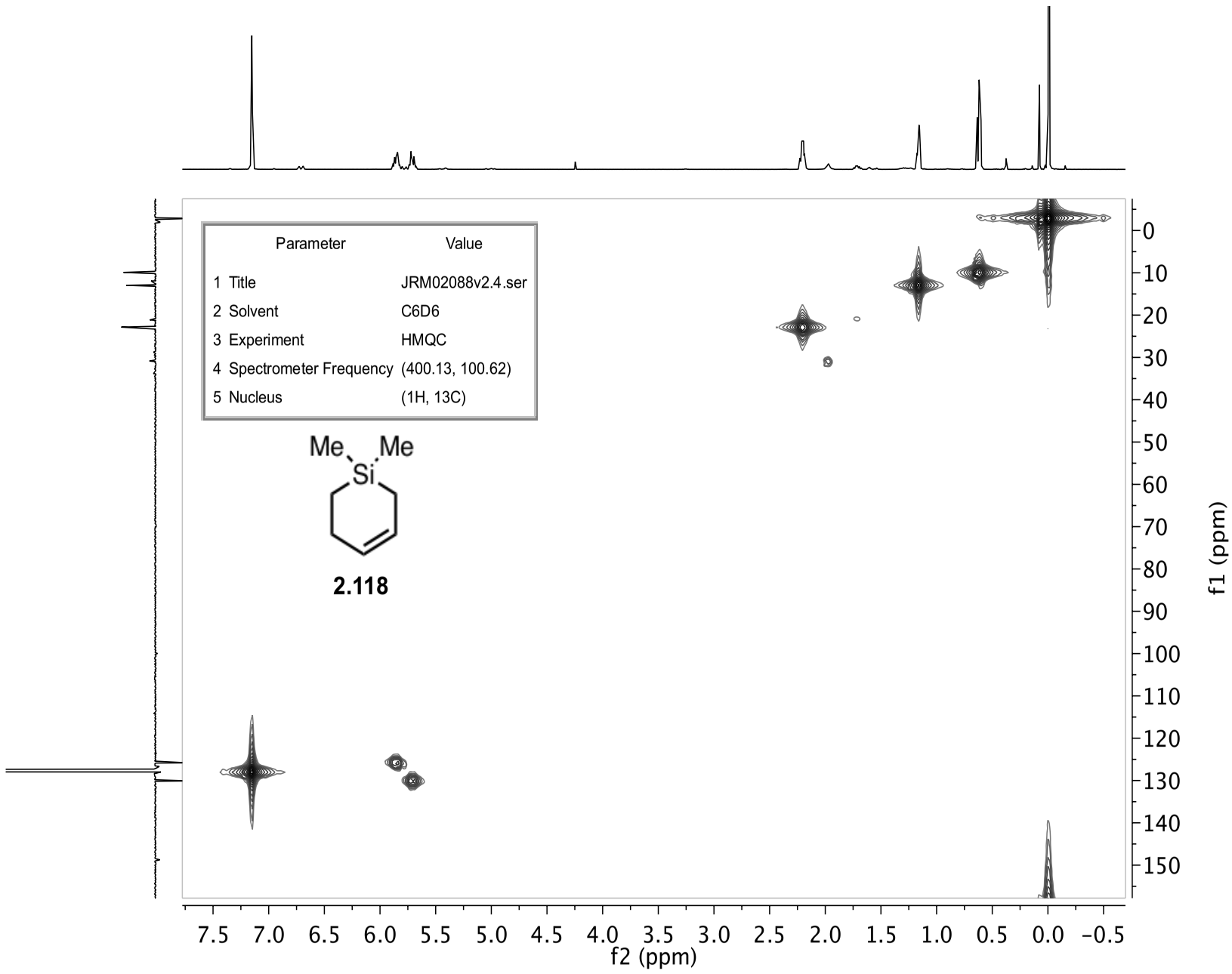
Parameter Value
1 Title JRM02088v2.4.ser
2 Solvent C6D6
3 Experiment HMQC
4 Spectrometer Frequency (400.13, 100.62)
5 Nucleus (1H, 13C)
Me
Me
Si
2.118
f2 (ppm)
f1 (ppm)

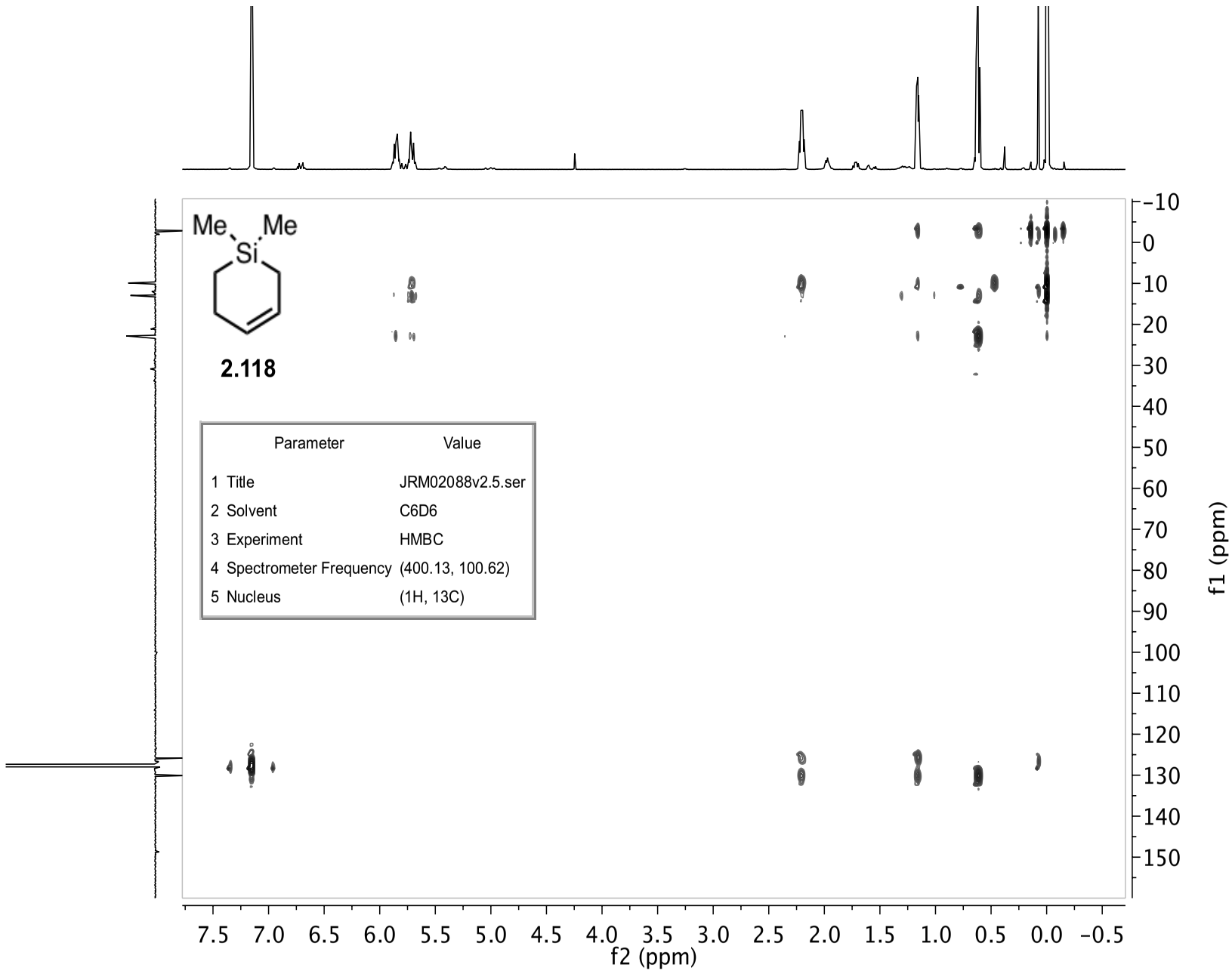
Me
Me
Si
2.118
Parameter Value
1 Title JRM02088v2.5.ser
2 Solvent C6D6
3 Experiment HMBC
4 Spectrometer Frequency (400.13, 100.62)
5 Nucleus (1H, 13C)
f2 (ppm)
f1 (ppm)

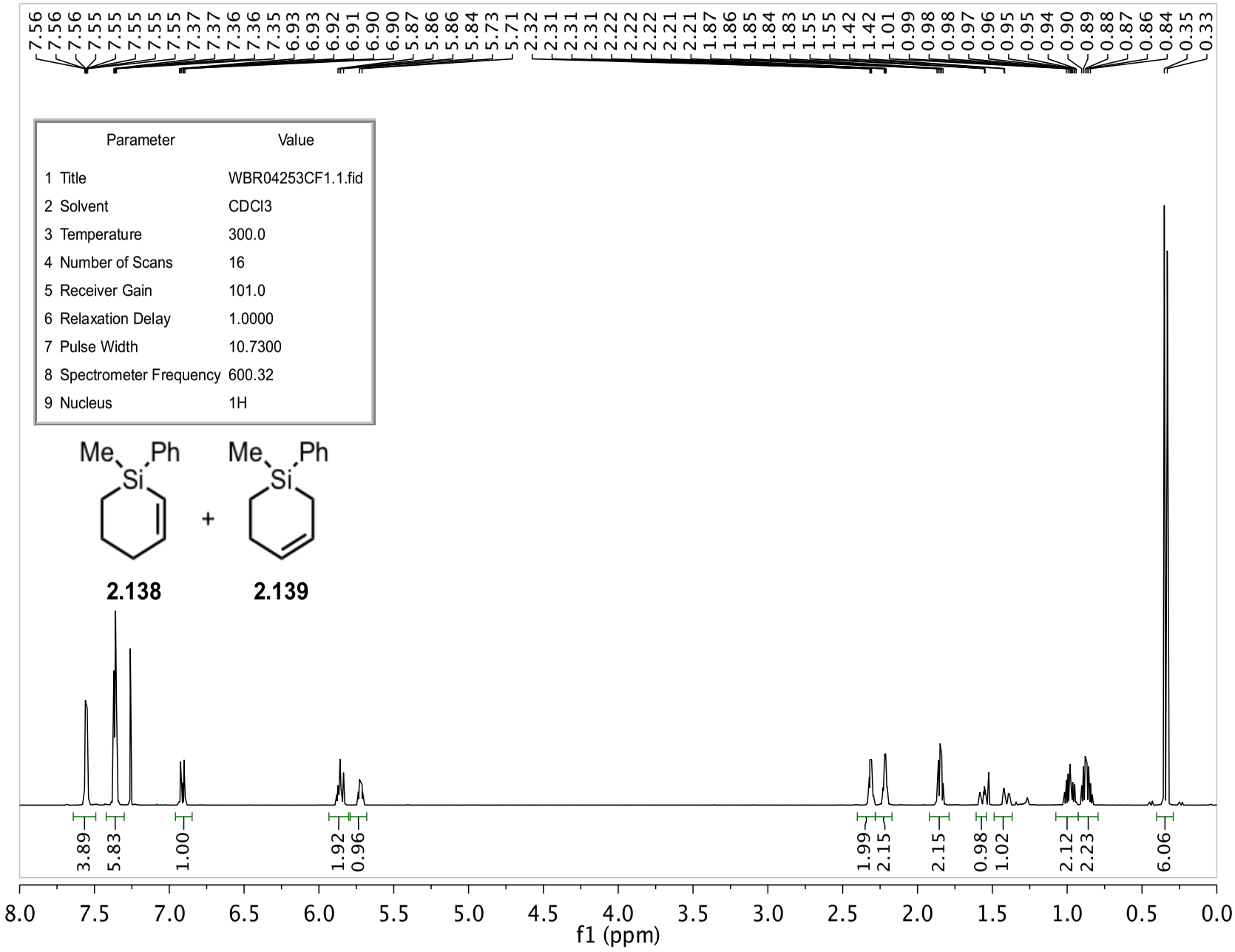
7.56 7.56 7.56 7.55 7.55 7.55 7.55 7.55 7.37 7.37 7.36 7.36 7.35 6.93 6.93 6.92 6.91 6.90 6.90 5.87 5.86 5.86 5.84 5.73 5.71 2.32 2.31 2.31 2.31 2.22 2.22 2.22 2.21 2.21 1.87 1.86 1.85 1.84 1.83 1.55 1.55 1.42 1.42 1.01 0.99 0.98 0.98 0.97 0.96 0.95 0.95 0.94 0.90 0.89 0.88 0.87 0.86 0.84 0.35 0.33
Parameter Value
1 Title WBR04253CF1.1.fid
2 Solvent CDCl3
3 Temperature 300.0
4 Number of Scans 16
5 Receiver Gain 101.0
6 Relaxation Delay 1.0000
7 Pulse Width 10.7300
8 Spectrometer Frequency 600.32
9 Nucleus 1H
Me Ph Si
+
Me Ph Si
2.138
2.139
3.89 5.83 1.00 1.92 0.96 1.99 2.15 2.15 0.98 1.02 2.12 2.23 6.06
8.0 7.5 7.0 6.5 6.0 5.5 5.0 4.5 4.0 3.5 3.0 2.5 2.0 1.5 1.0 0.5 0.0
f1 (ppm)

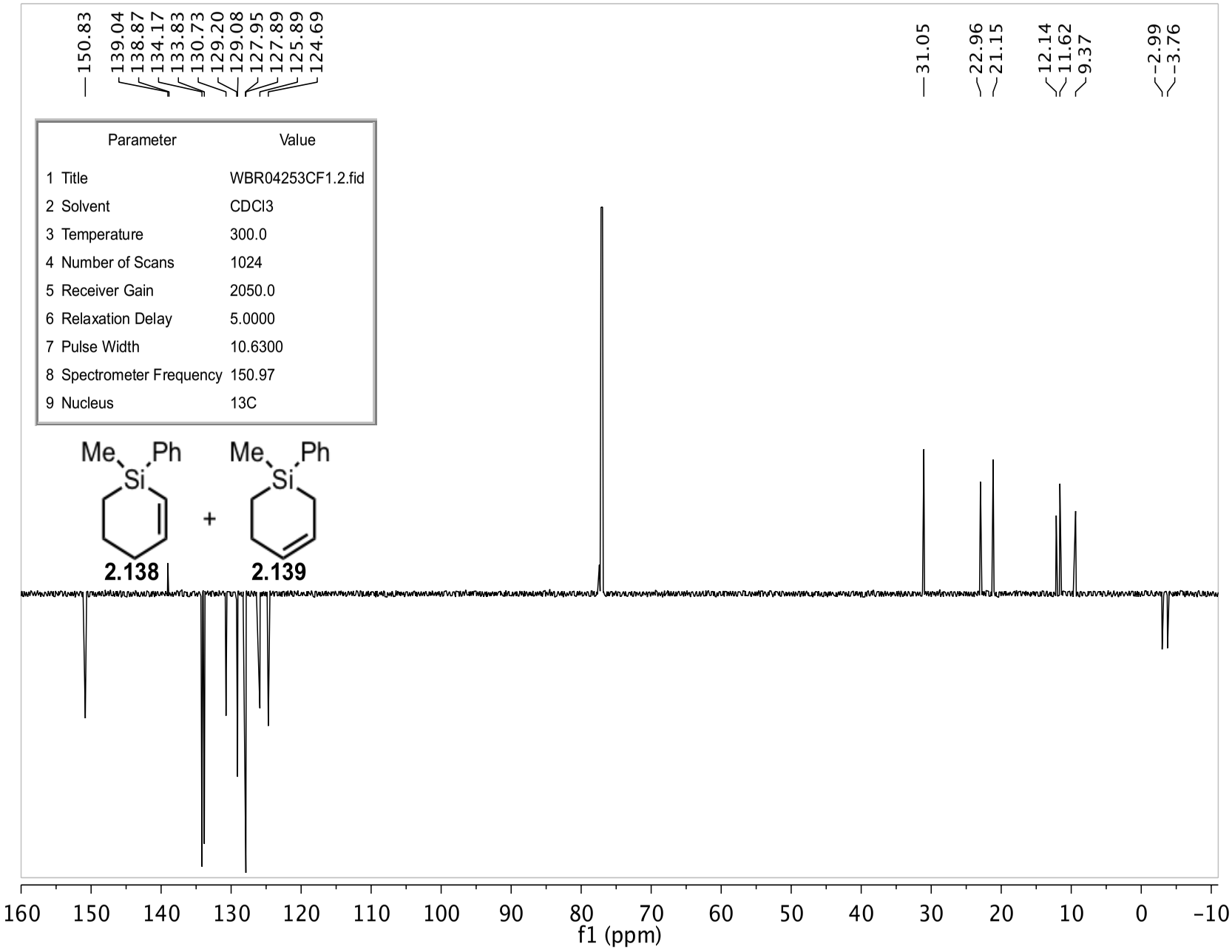
150.83
139.04
138.87
134.17
133.83
130.73
129.20
129.08
127.95
127.89
125.89
124.69
31.05
22.96
21.15
12.14
11.62
9.37
2.99
3.76
Parameter Value
1 Title WBR04253CF1.2.fid
2 Solvent CDCl3
3 Temperature 300.0
4 Number of Scans 1024
5 Receiver Gain 2050.0
6 Relaxation Delay 5.0000
7 Pulse Width 10.6300
8 Spectrometer Frequency 150.97
9 Nucleus 13C
Me Ph
Si
+
2.138
2.139
160 150 140 130 120 110 100 90 80 70 60 50 40 30 20 10 0 -10
f1 (ppm)

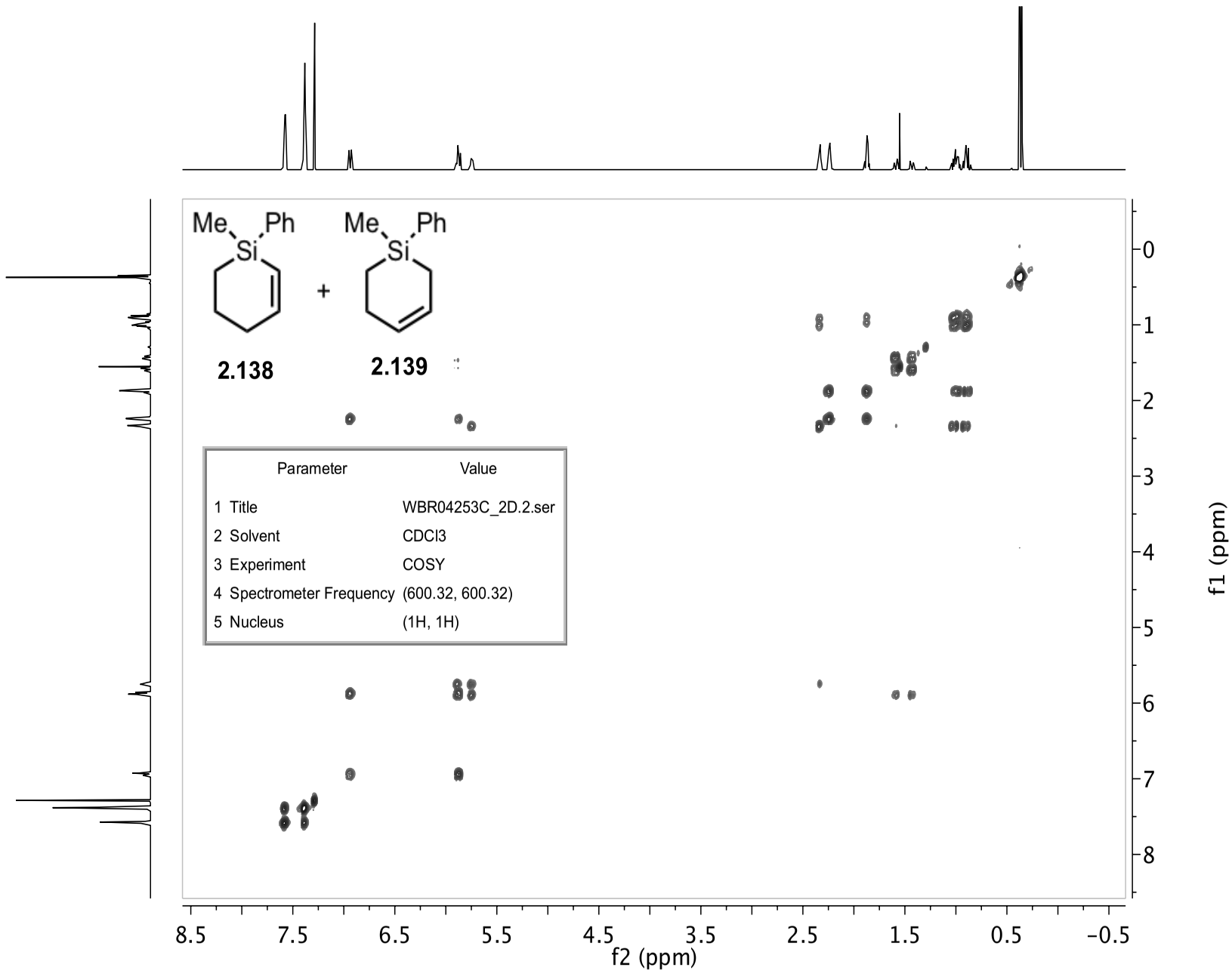
Me
Si
Ph
+
2.138
2.139
Parameter Value
1 Title WBR04253C_2D.2.ser
2 Solvent CDCl3
3 Experiment COSY
4 Spectrometer Frequency (600.32, 600.32)
5 Nucleus (1H, 1H)
8.5
7.5
6.5
5.5
4.5
3.5
2.5
1.5
0.5
-0.5
f2 (ppm)
f1 (ppm)
0
1
2
3
4
5
6
7
8

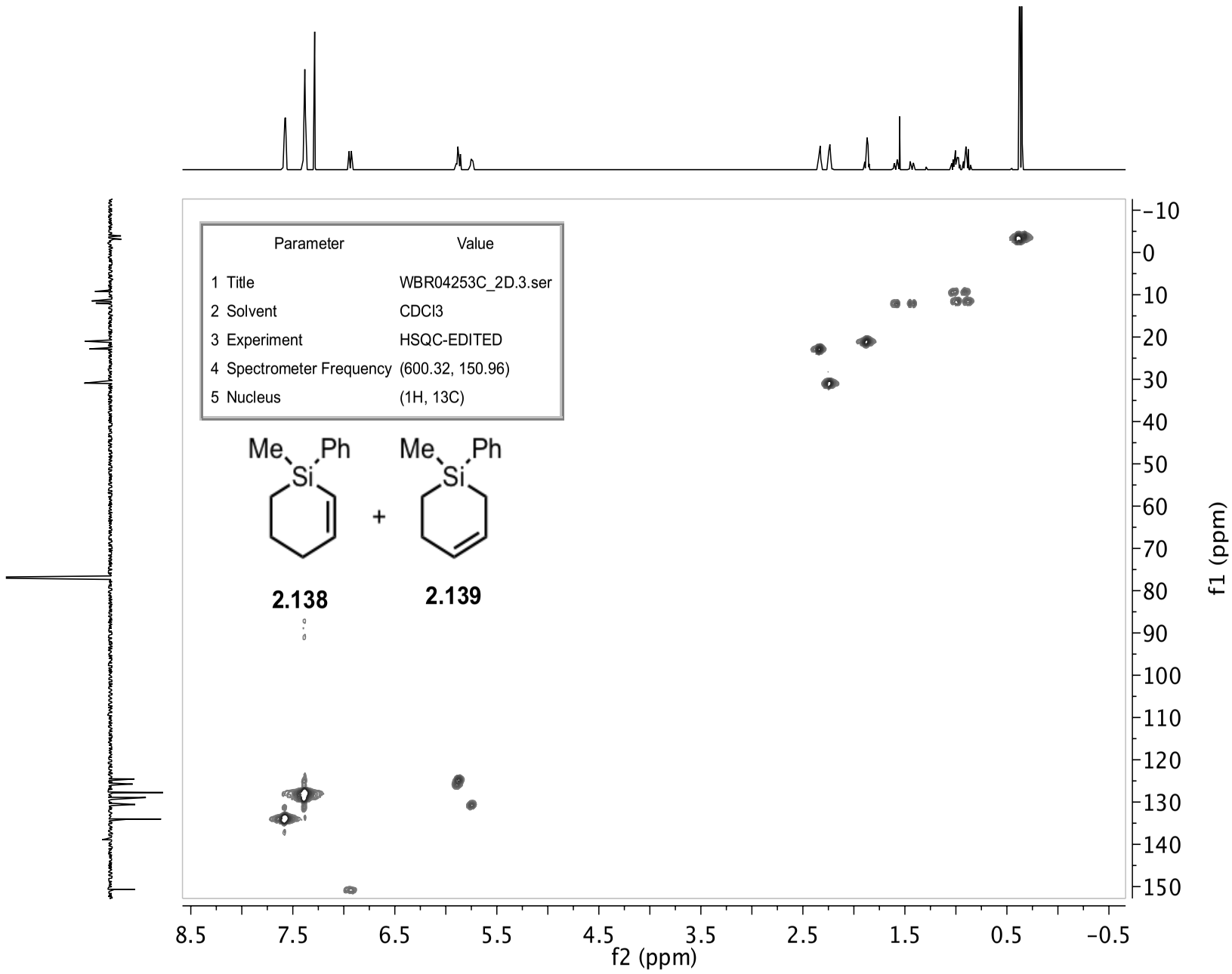
Parameter Value
1 Title WBR04253C_2D.3.ser
2 Solvent CDCl3
3 Experiment HSQC-EDITED
4 Spectrometer Frequency (600.32, 150.96)
5 Nucleus (1H, 13C)
Me Ph Si
+
Me Ph Si
2.138
2.139
8.5 7.5 6.5 5.5 4.5 3.5 2.5 1.5 0.5 -0.5
f2 (ppm)
-10 0 10 20 30 40 50 60 70 80 90 100 110 120 130 140 150
f1 (ppm)

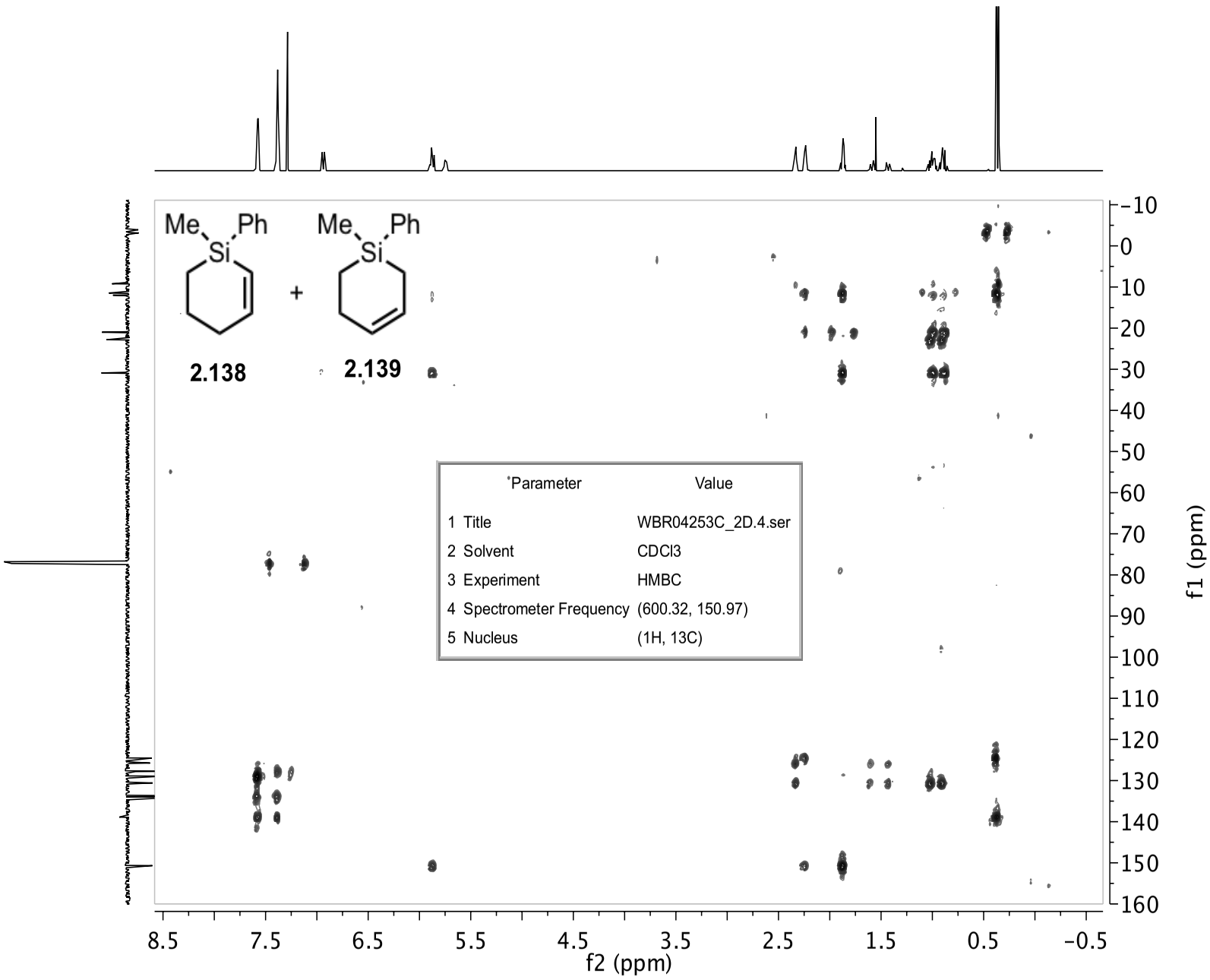
Me
Ph
Si
+
2.138
2.139
Parameter
Value
1 Title
WBR04253C_2D.4.ser
2 Solvent
CDCl3
3 Experiment
HMBC
4 Spectrometer Frequency
(600.32, 150.97)
5 Nucleus
(1H, 13C)
f2 (ppm)
f1 (ppm)

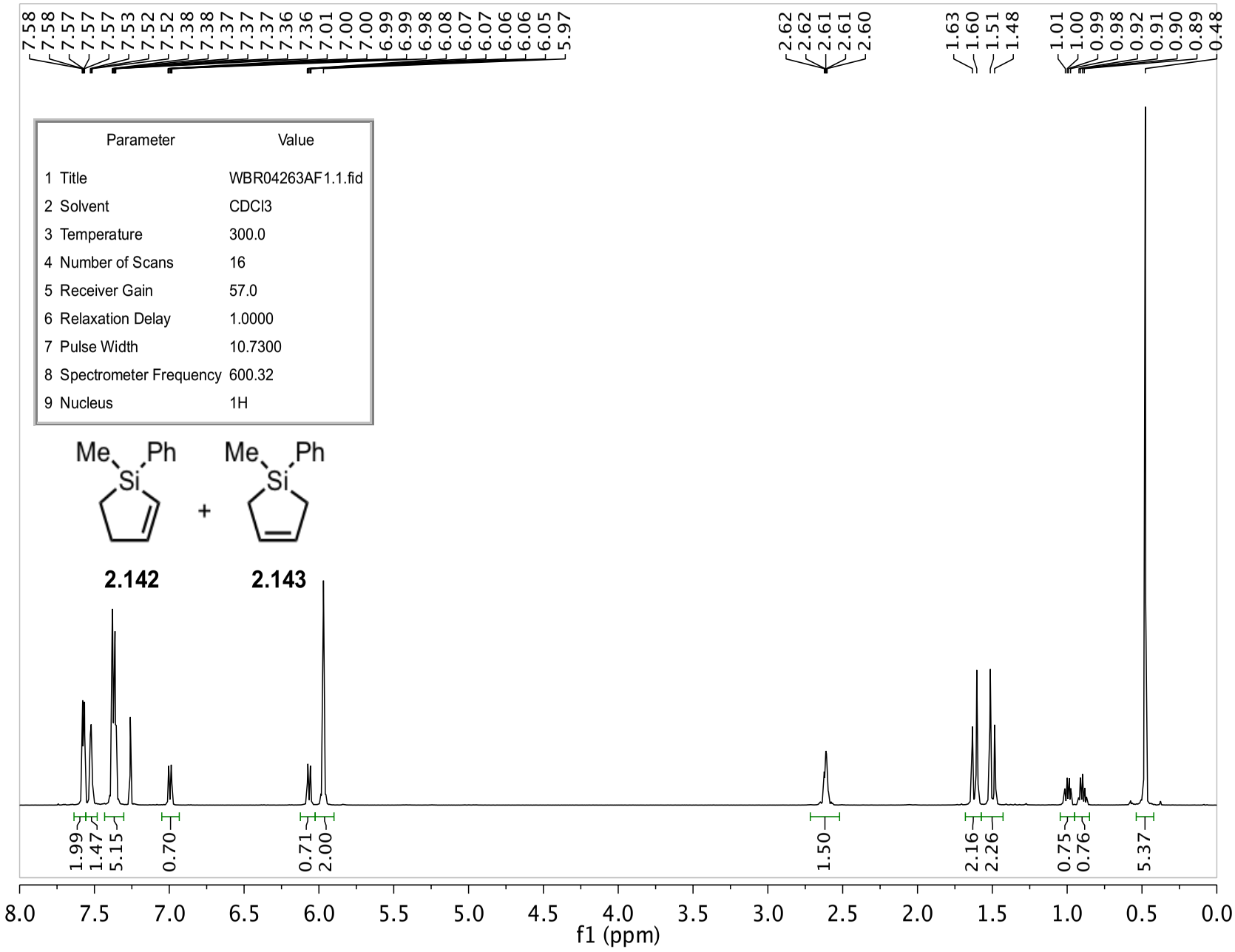
7.58 7.58 7.57 7.57 7.57 7.53 7.52 7.52 7.38 7.38 7.37 7.37 7.37 7.36 7.36 7.01 7.00 7.00 6.99 6.99 6.98 6.08 6.07 6.07 6.06 6.06 6.05 5.97
2.62 2.62 2.61 2.61 2.60
1.63 1.60 1.51 1.48
1.01 1.00 0.99 0.98 0.92 0.91 0.90 0.89 0.48
Parameter Value
1 Title WBR04263AF1.1.fid
2 Solvent CDCl3
3 Temperature 300.0
4 Number of Scans 16
5 Receiver Gain 57.0
6 Relaxation Delay 1.0000
7 Pulse Width 10.7300
8 Spectrometer Frequency 600.32
9 Nucleus 1H
Me Ph Si
+
Me Ph Si
2.142
2.143
1.99 1.47 5.15 0.70 0.71 2.00 1.50 2.16 2.26 0.75 0.76 5.37
8.0 7.5 7.0 6.5 6.0 5.5 5.0 4.5 4.0 3.5 3.0 2.5 2.0 1.5 1.0 0.5 0.0
f1 (ppm)

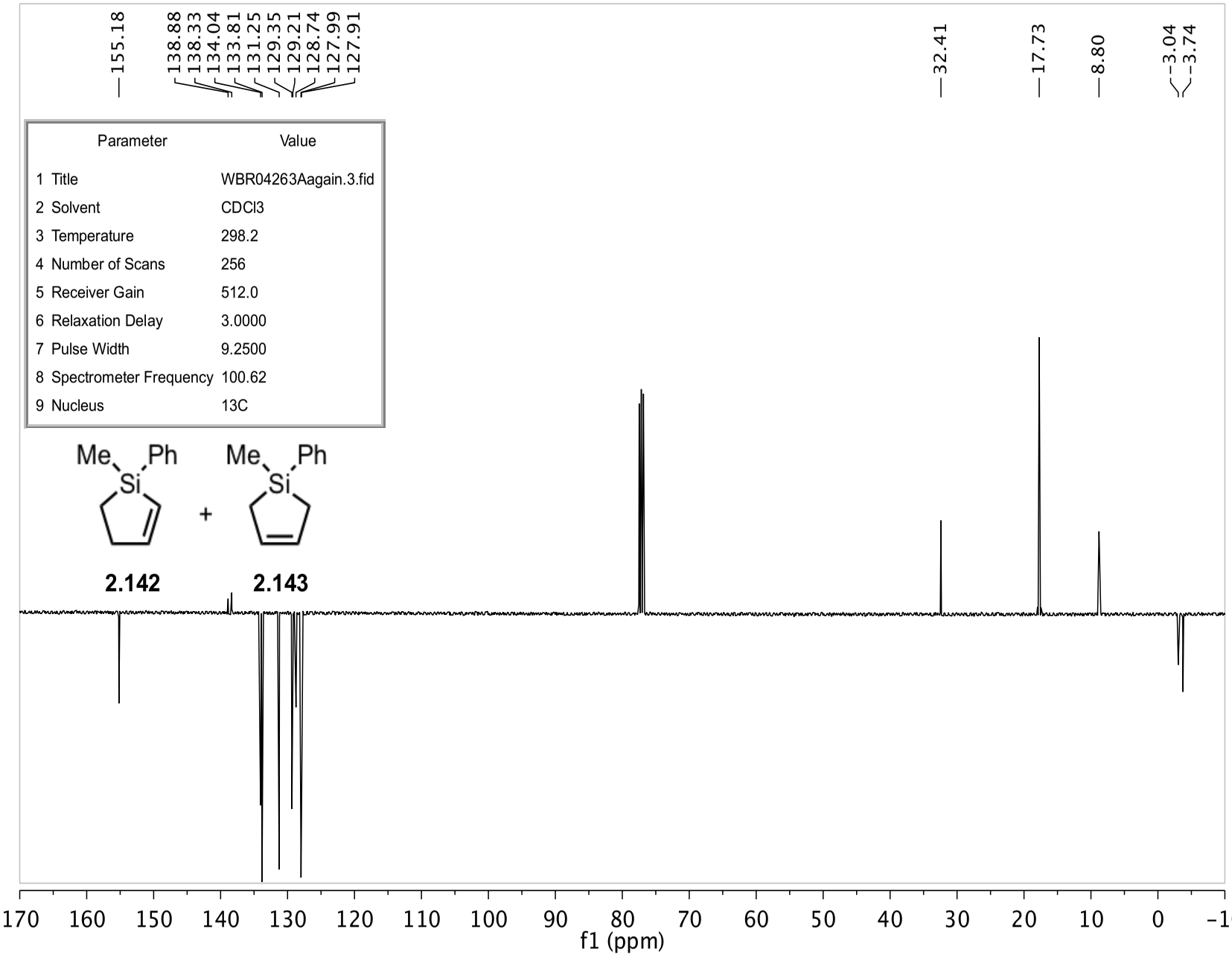
155.18
138.88
138.33
134.04
133.81
131.25
129.35
129.21
128.74
127.99
127.91
32.41
17.73
8.80
3.04
3.74
Parameter Value
1 Title WBR04263Aagain.3.fid
2 Solvent CDCl3
3 Temperature 298.2
4 Number of Scans 256
5 Receiver Gain 512.0
6 Relaxation Delay 3.0000
7 Pulse Width 9.2500
8 Spectrometer Frequency 100.62
9 Nucleus 13C
Me Ph Si
+
Me Ph Si
2.142
2.143
170 160 150 140 130 120 110 100 90 80 70 60 50 40 30 20 10 0 -10
f1 (ppm)

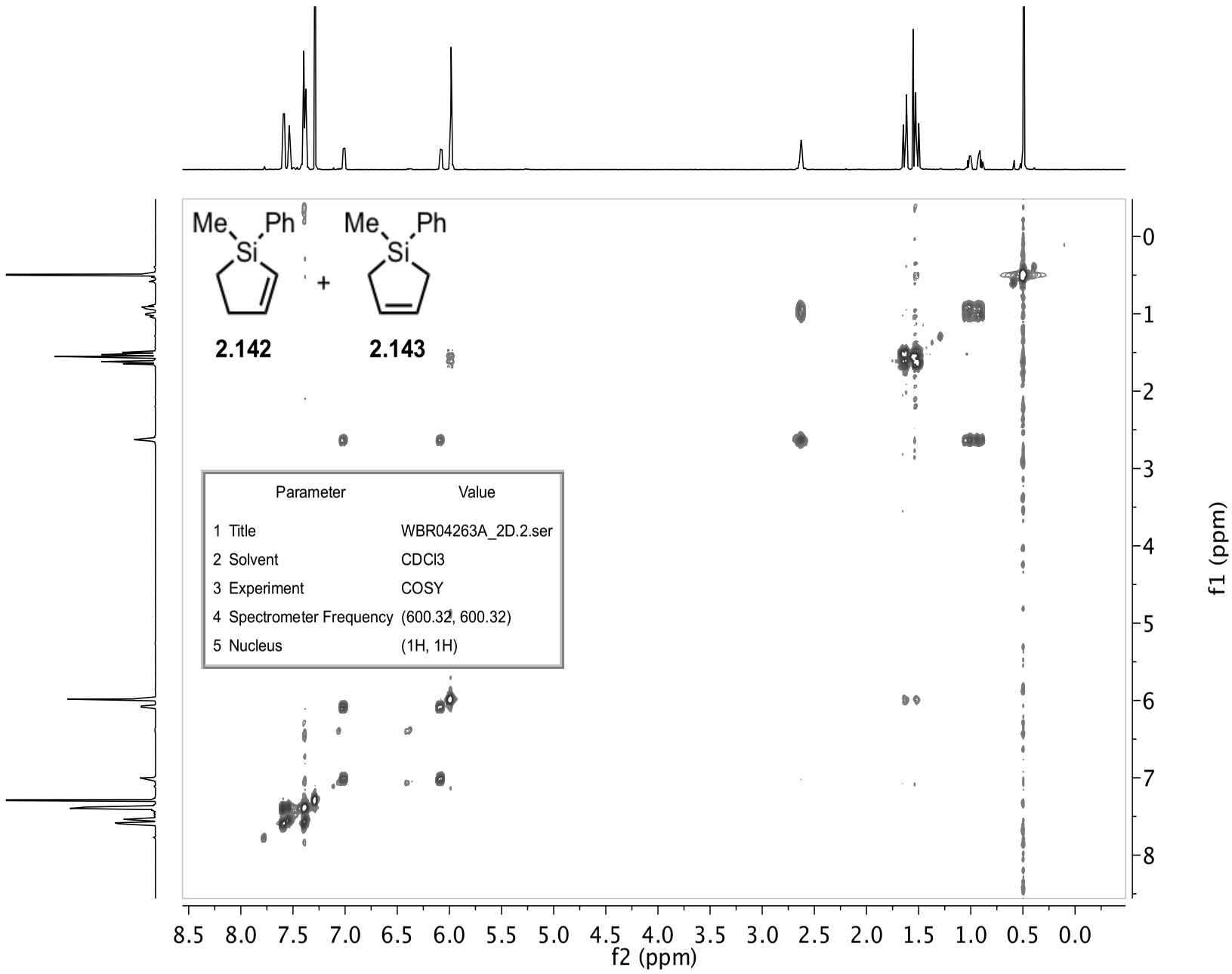
Me
Ph
Si
+
2.142
2.143
Parameter
Value
1 Title
WBR04263A_2D.2.ser
2 Solvent
CDCl3
3 Experiment
COSY
4 Spectrometer Frequency
(600.32, 600.32)
5 Nucleus
(1H, 1H)
f2 (ppm)
f1 (ppm)

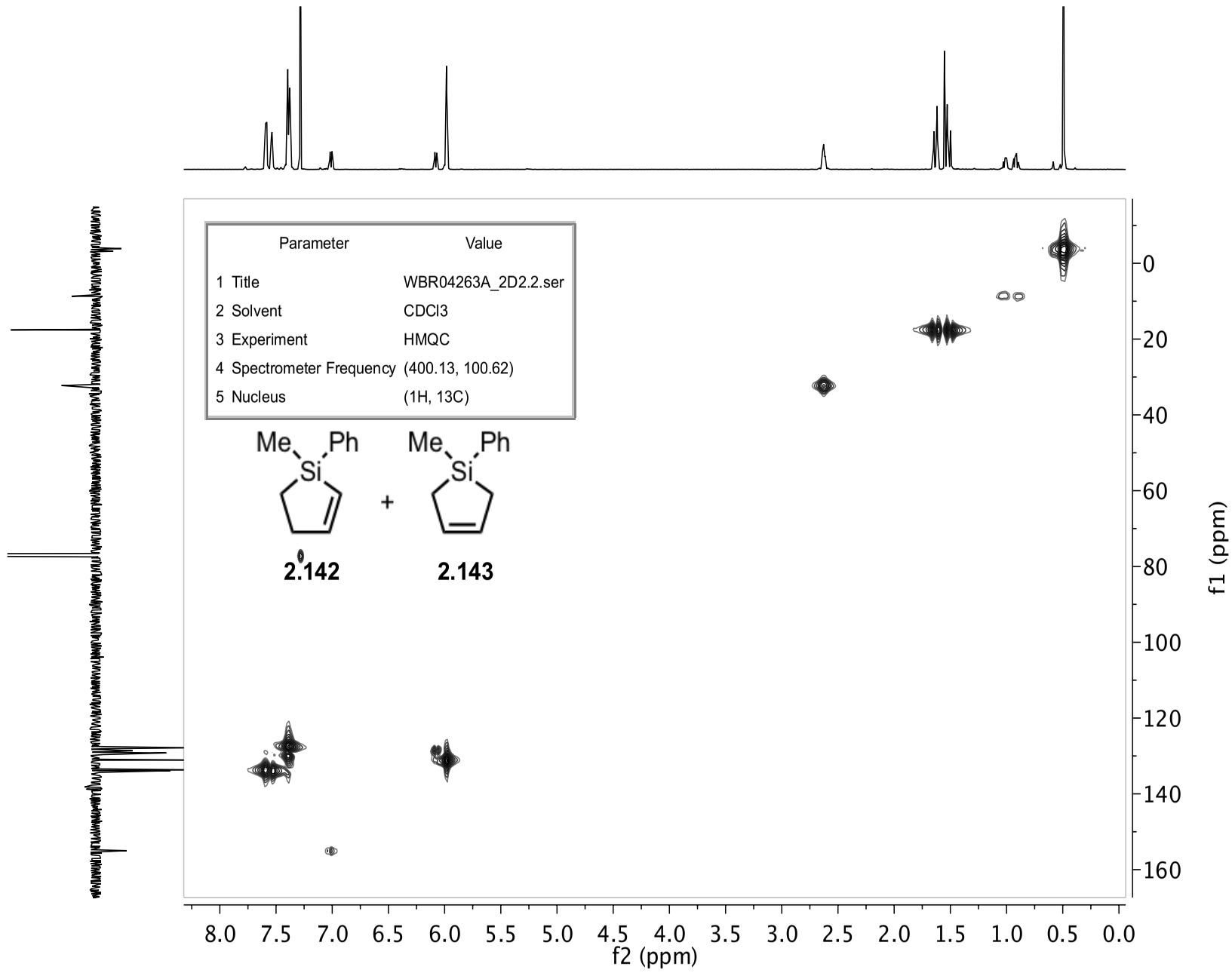
Parameter Value
1 Title WBR04263A_2D2.2.ser
2 Solvent CDCl3
3 Experiment HMQC
4 Spectrometer Frequency (400.13, 100.62)
5 Nucleus (1H, 13C)
Me Ph
Si
+
2.142
2.143
f2 (ppm)
f1 (ppm)

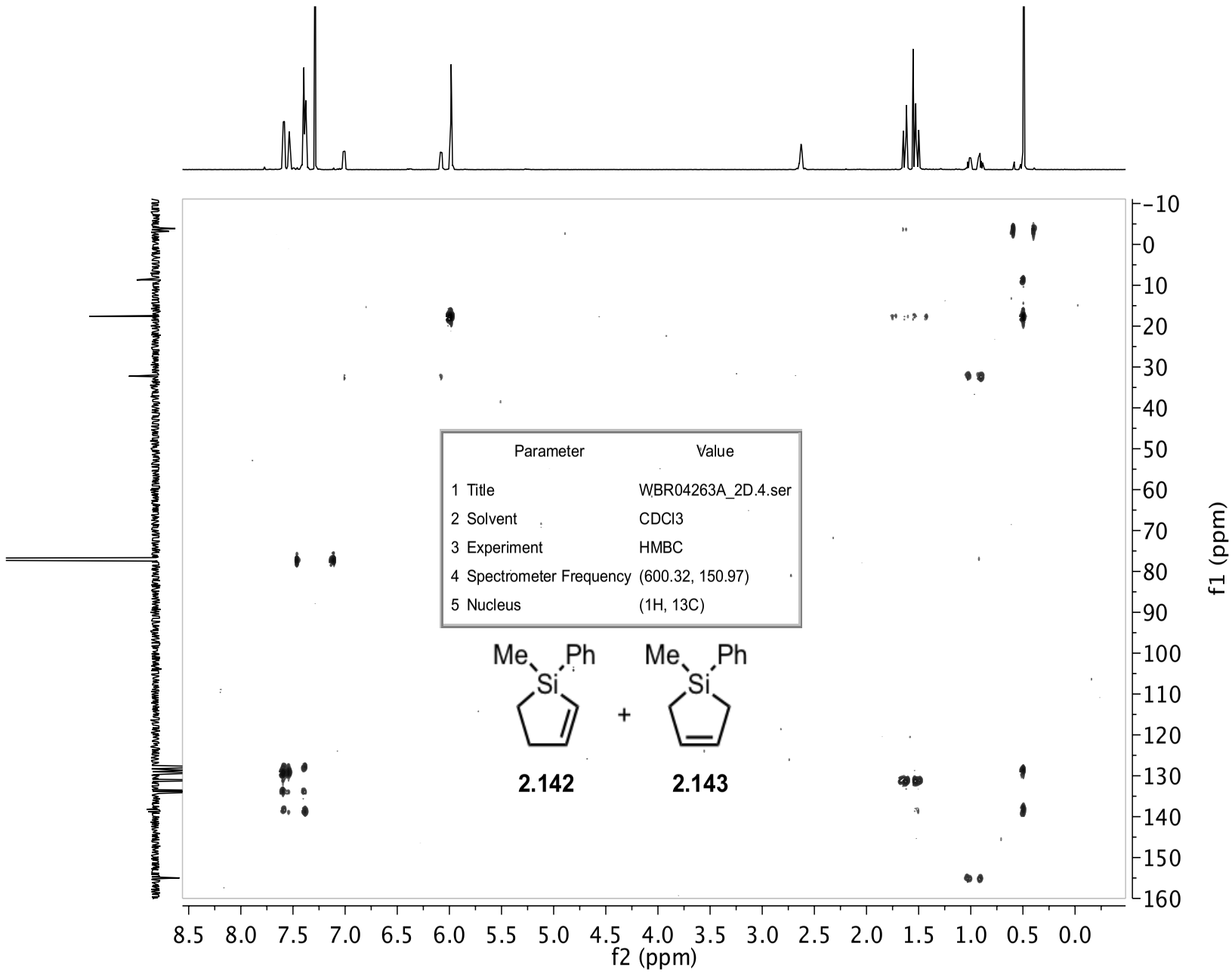
Parameter Value
1 Title WBR04263A_2D.4.ser
2 Solvent CDCl3
3 Experiment HMBC
4 Spectrometer Frequency (600.32, 150.97)
5 Nucleus (1H, 13C)
Me Ph
Si
+
Me Ph
Si
2.142
2.143
f2 (ppm)
f1 (ppm)

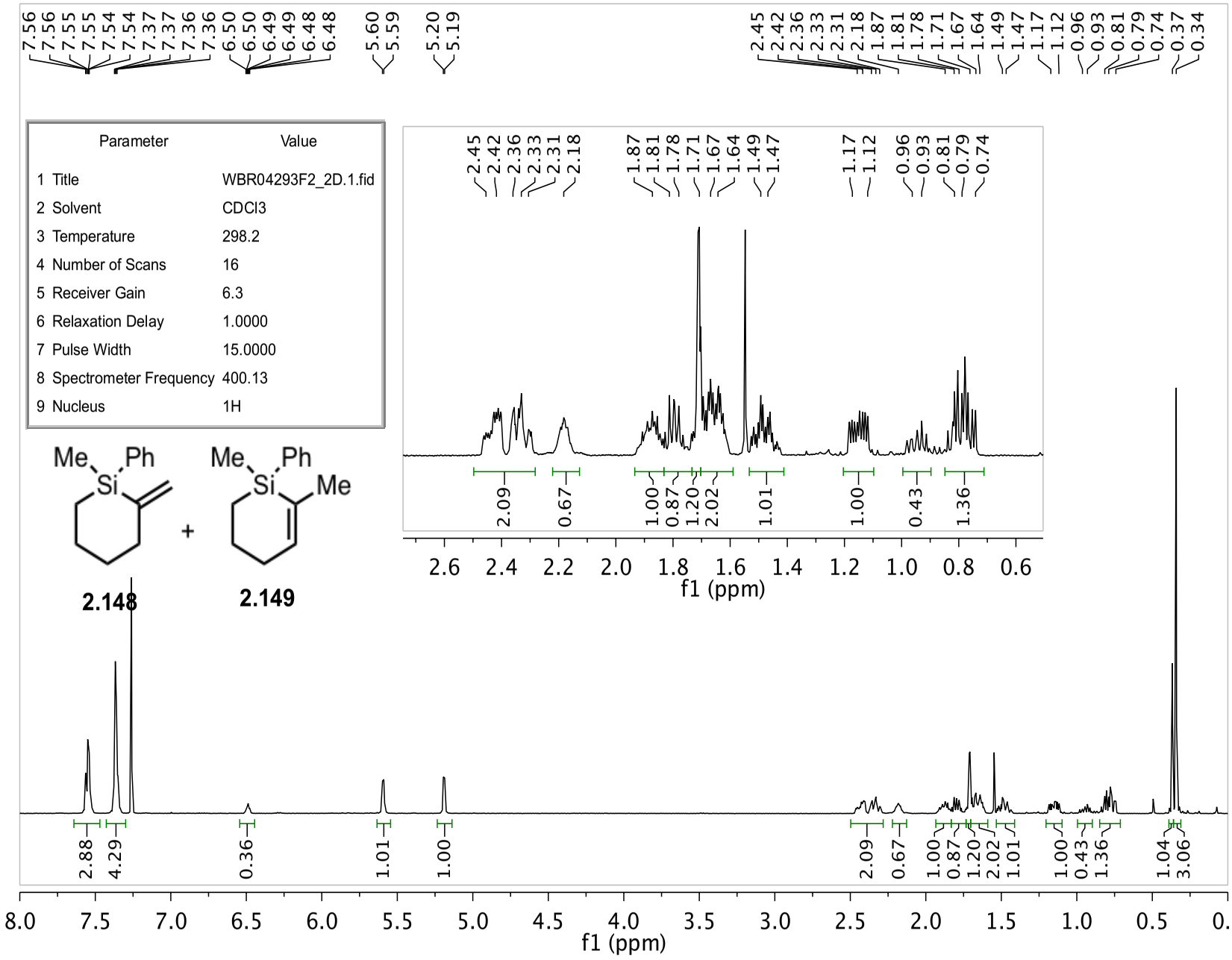
7.56 7.56 7.55 7.55 7.54 7.54 7.37 7.37 7.36 7.36 6.50 6.50 6.49 6.49 6.48 6.48 5.60 5.59 5.20 5.19
2.45 2.42 2.36 2.33 2.31 2.18 1.87 1.81 1.78 1.71 1.67 1.64 1.49 1.47 1.17 1.12 0.96 0.93 0.81 0.79 0.74 0.37 0.34
Parameter Value
1 Title WBR04293F2_2D.1.fid
2 Solvent CDCl3
3 Temperature 298.2
4 Number of Scans 16
5 Receiver Gain 6.3
6 Relaxation Delay 1.0000
7 Pulse Width 15.0000
8 Spectrometer Frequency 400.13
9 Nucleus 1H
Me Ph Si
Me Ph Si Me
+
2.148
2.149
2.09 0.67 1.00 0.87 1.20 2.02 1.01 1.00 0.43 1.36
2.6 2.4 2.2 2.0 1.8 1.6 1.4 1.2 1.0 0.8 0.6
f1 (ppm)
2.88 4.29 0.36 1.01 1.00 2.09 0.67 1.00 0.87 1.20 2.02 1.01 1.00 0.43 1.36 1.04 3.06
8.0 7.5 7.0 6.5 6.0 5.5 5.0 4.5 4.0 3.5 3.0 2.5 2.0 1.5 1.0 0.5 0.0
f1 (ppm)

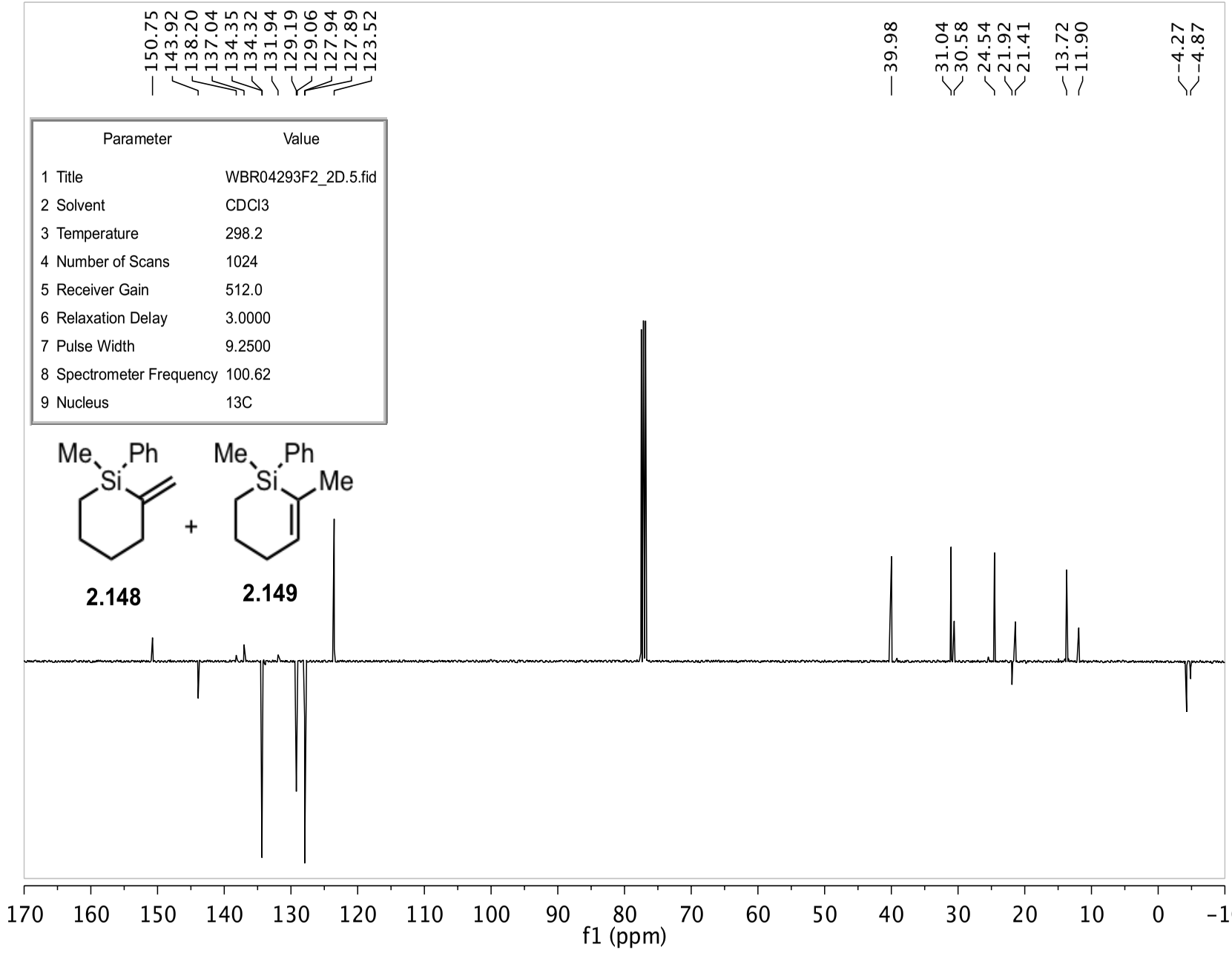
150.75
143.92
138.20
137.04
134.35
134.32
131.94
129.19
129.06
127.94
127.89
123.52
39.98
31.04
30.58
24.54
21.92
21.41
13.72
11.90
-4.27
-4.87
Parameter Value
1 Title WBR04293F2_2D.5.fid
2 Solvent CDCl3
3 Temperature 298.2
4 Number of Scans 1024
5 Receiver Gain 512.0
6 Relaxation Delay 3.0000
7 Pulse Width 9.2500
8 Spectrometer Frequency 100.62
9 Nucleus 13C
Me Ph Si
+
Me Ph Si Me
2.148
2.149
170 160 150 140 130 120 110 100 90 80 70 60 50 40 30 20 10 0 -10
f1 (ppm)

Me
Ph
Si
+
Me
Ph
Si
Me
2.148
2.149
Parameter
Value
1 Title
WBR04293F2_2D.2.ser
2 Solvent
CDCl3
3 Experiment
COSY
4 Spectrometer Frequency
(400.13, 400.13)
5 Nucleus
(1H, 1H)
f2 (ppm)
f1 (ppm)

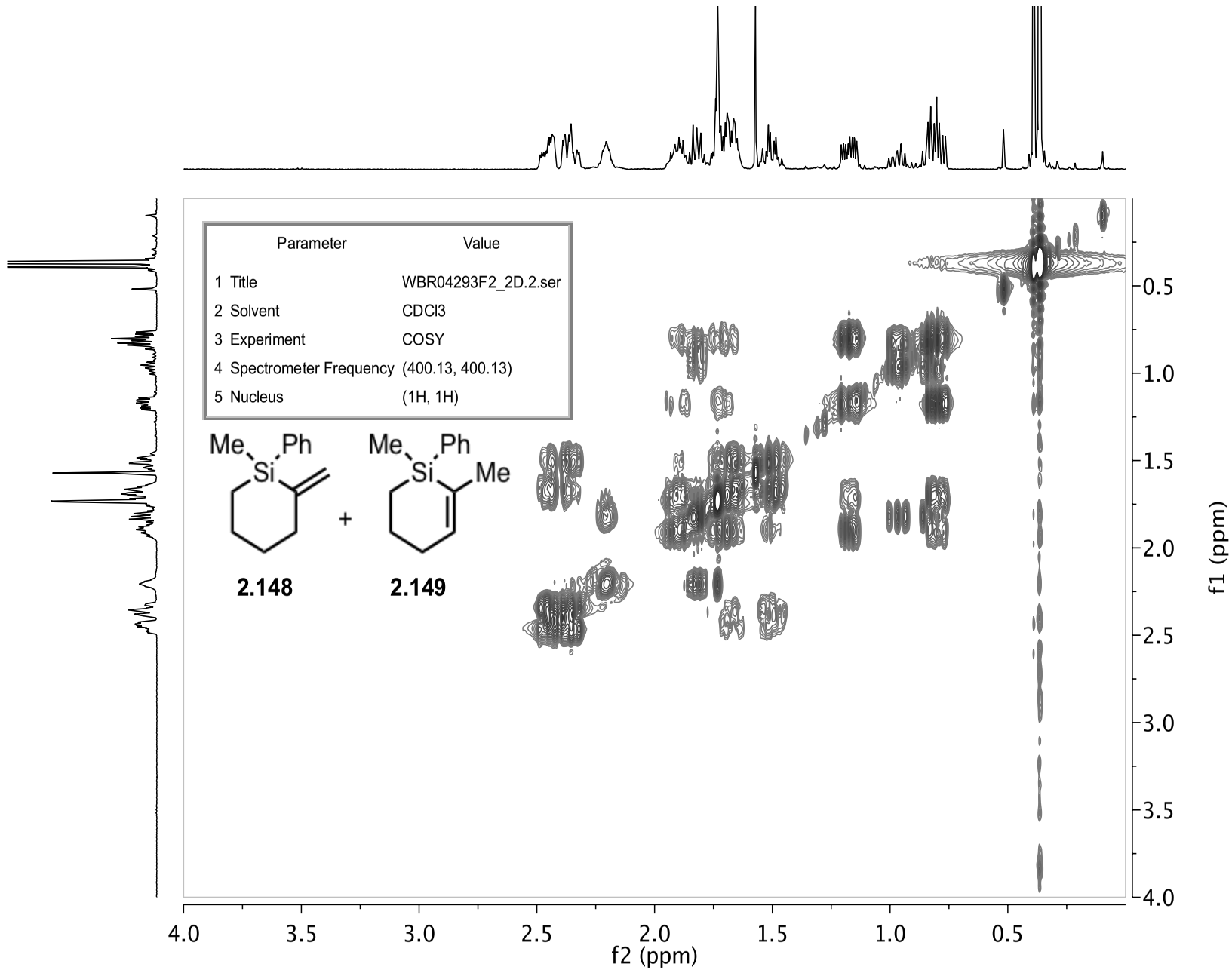
Parameter Value
1 Title WBR04293F2_2D.2.ser
2 Solvent CDCl3
3 Experiment COSY
4 Spectrometer Frequency (400.13, 400.13)
5 Nucleus (1H, 1H)
Me Ph Si
+
Me Ph Si Me
2.148
2.149
4.0 3.5 3.0 2.5 2.0 1.5 1.0 0.5
f2 (ppm)
0.5 1.0 1.5 2.0 2.5 3.0 3.5 4.0
f1 (ppm)

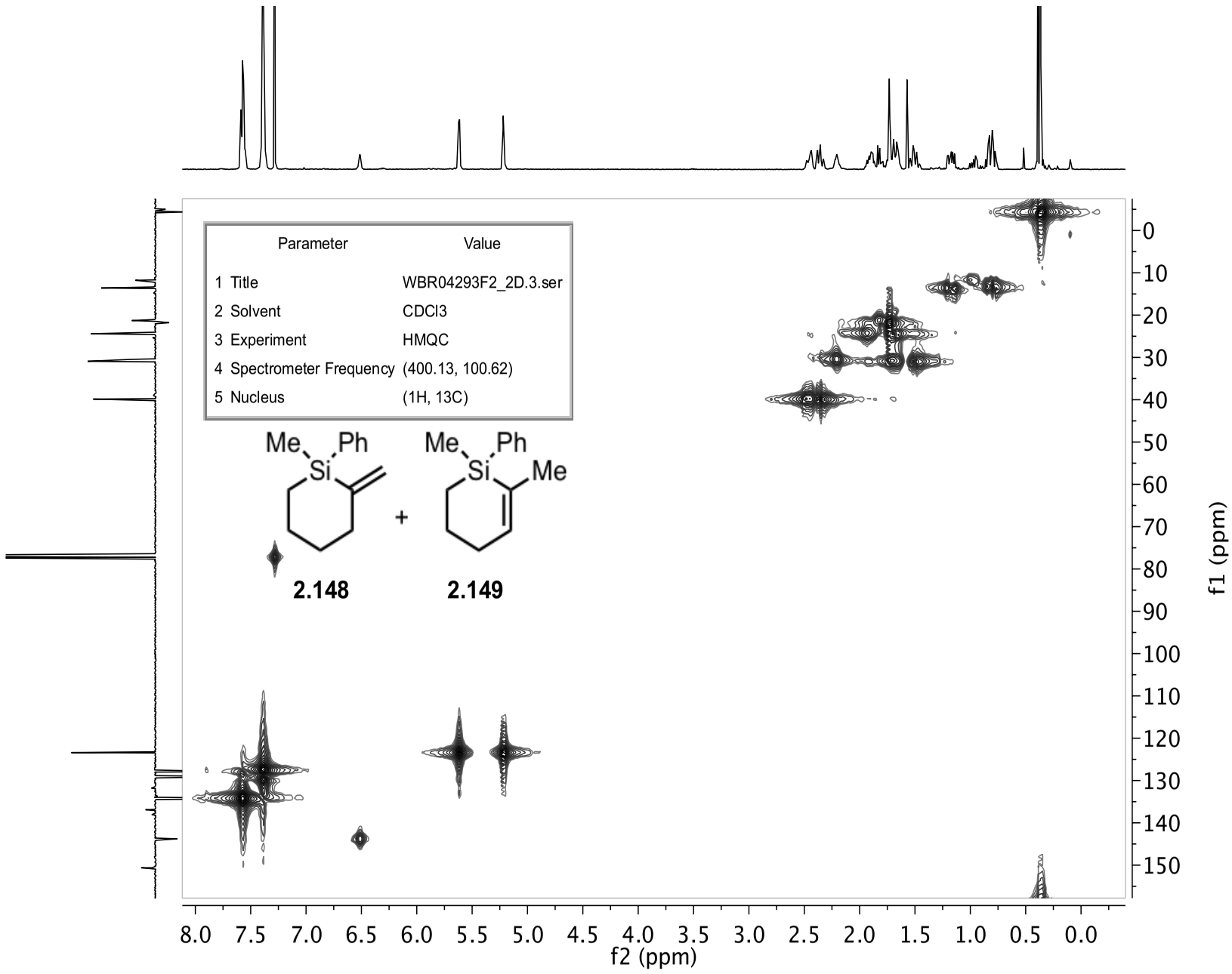
Parameter Value
1 Title WBR04293F2_2D.3.ser
2 Solvent CDCl3
3 Experiment HMQC
4 Spectrometer Frequency (400.13, 100.62)
5 Nucleus (1H, 13C)
Me Ph
Si
Me Ph
Si
Me
+
2.148
2.149
f2 (ppm)
f1 (ppm)

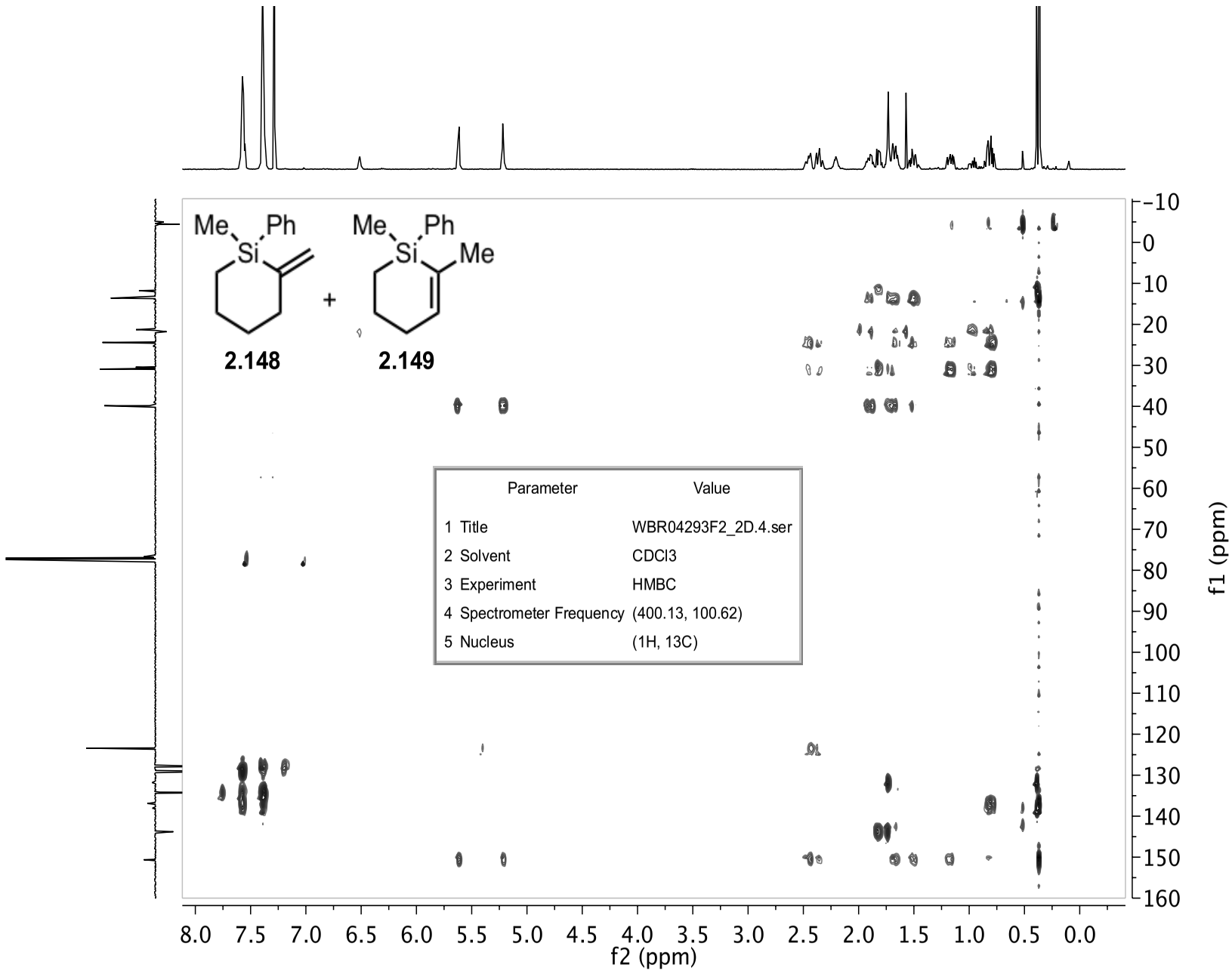
Me
Ph
Si
Me
Ph
Si
Me
+
2.148
2.149
Parameter
Value
1 Title
WBR04293F2_2D.4.ser
2 Solvent
CDCl3
3 Experiment
HMBC
4 Spectrometer Frequency
(400.13, 100.62)
5 Nucleus
(1H, 13C)
f2 (ppm)
f1 (ppm)

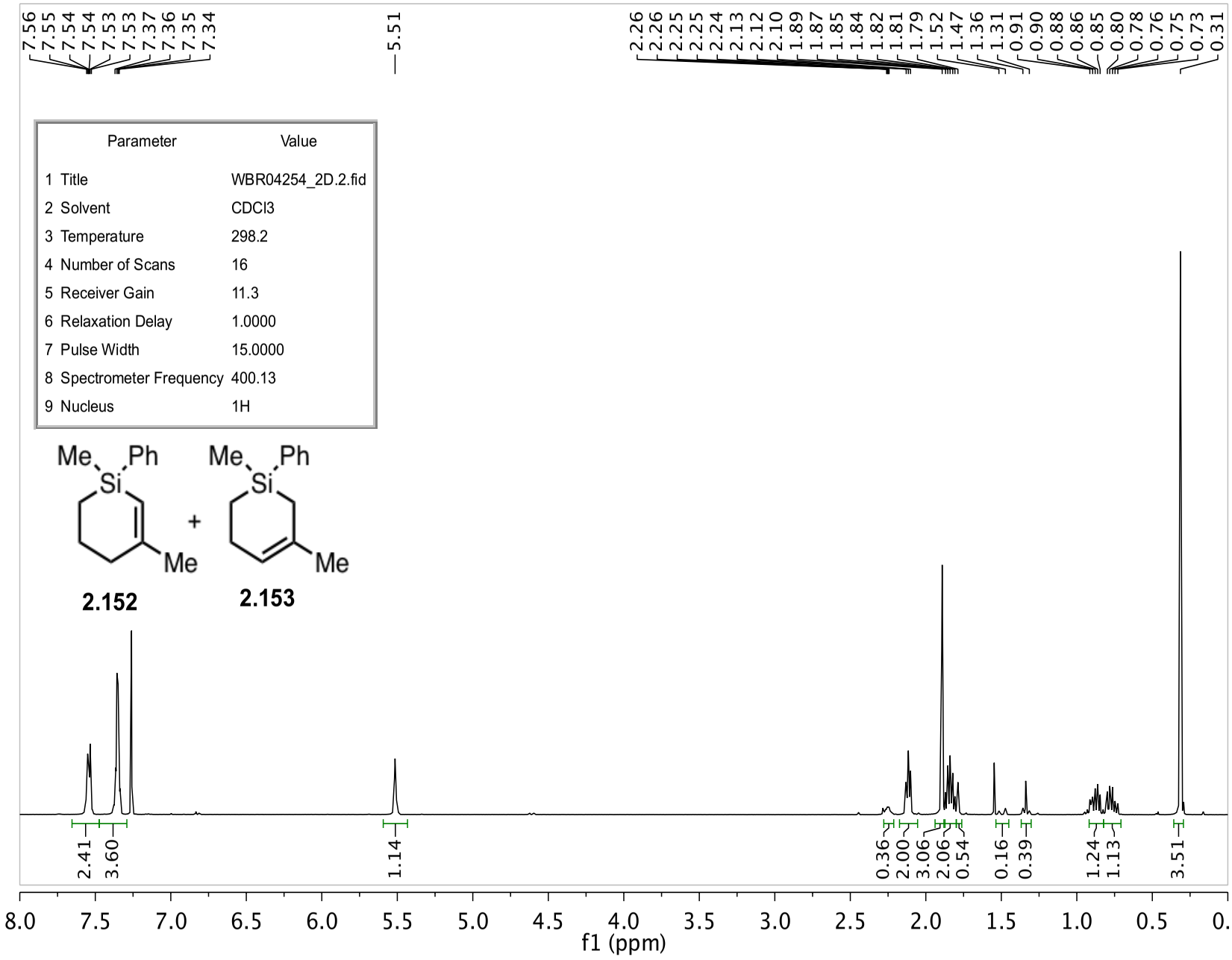
7.56 7.55 7.54 7.54 7.53 7.53 7.37 7.36 7.35 7.34
5.51
2.26 2.26 2.25 2.25 2.24 2.13 2.12 2.10 1.89 1.87 1.85 1.84 1.82 1.81 1.79 1.52 1.47 1.36 1.31 0.91 0.90 0.88 0.86 0.85 0.80 0.78 0.76 0.75 0.73 0.31
Parameter Value
1 Title WBR04254_2D.2.fid
2 Solvent CDCl3
3 Temperature 298.2
4 Number of Scans 16
5 Receiver Gain 11.3
6 Relaxation Delay 1.0000
7 Pulse Width 15.0000
8 Spectrometer Frequency 400.13
9 Nucleus 1H
Me Ph Si Me
+
Me Ph Si Me
2.152
2.153
2.41 3.60 1.14 0.36 2.00 3.06 2.06 0.54 0.16 0.39 1.24 1.13 3.51
8.0 7.5 7.0 6.5 6.0 5.5 5.0 4.5 4.0 3.5 3.0 2.5 2.0 1.5 1.0 0.5 0.0
f1 (ppm)

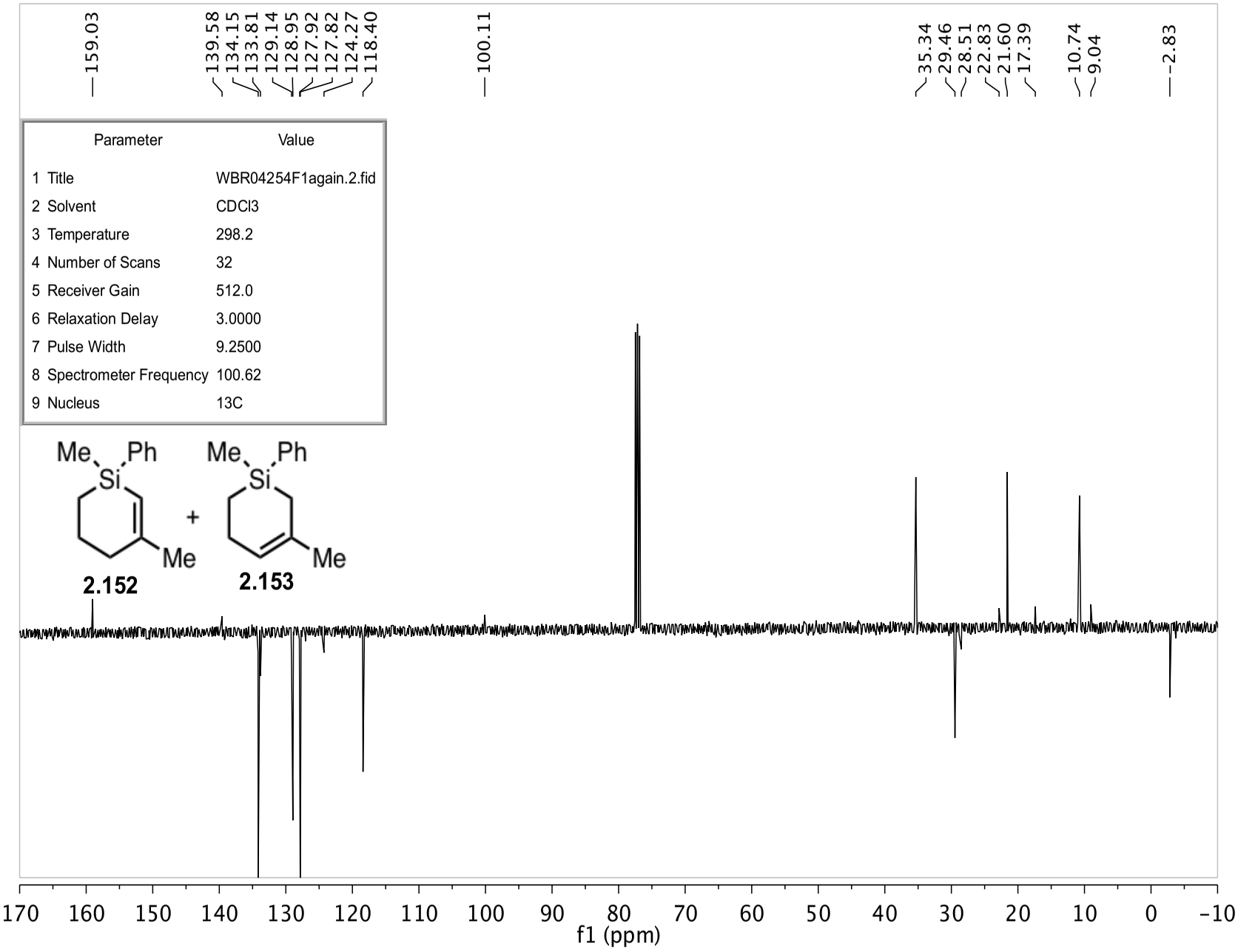
159.03
139.58
134.15
133.81
129.14
128.95
127.92
127.82
124.27
118.40
100.11
35.34
29.46
28.51
22.83
21.60
17.39
10.74
9.04
-2.83
Parameter Value
1 Title WBR04254F1again.2.fid
2 Solvent CDCl3
3 Temperature 298.2
4 Number of Scans 32
5 Receiver Gain 512.0
6 Relaxation Delay 3.0000
7 Pulse Width 9.2500
8 Spectrometer Frequency 100.62
9 Nucleus 13C
Me Ph Si Me
+
Me Ph Si Me
2.152
2.153
170 160 150 140 130 120 110 100 90 80 70 60 50 40 30 20 10 0 -10
f1 (ppm)

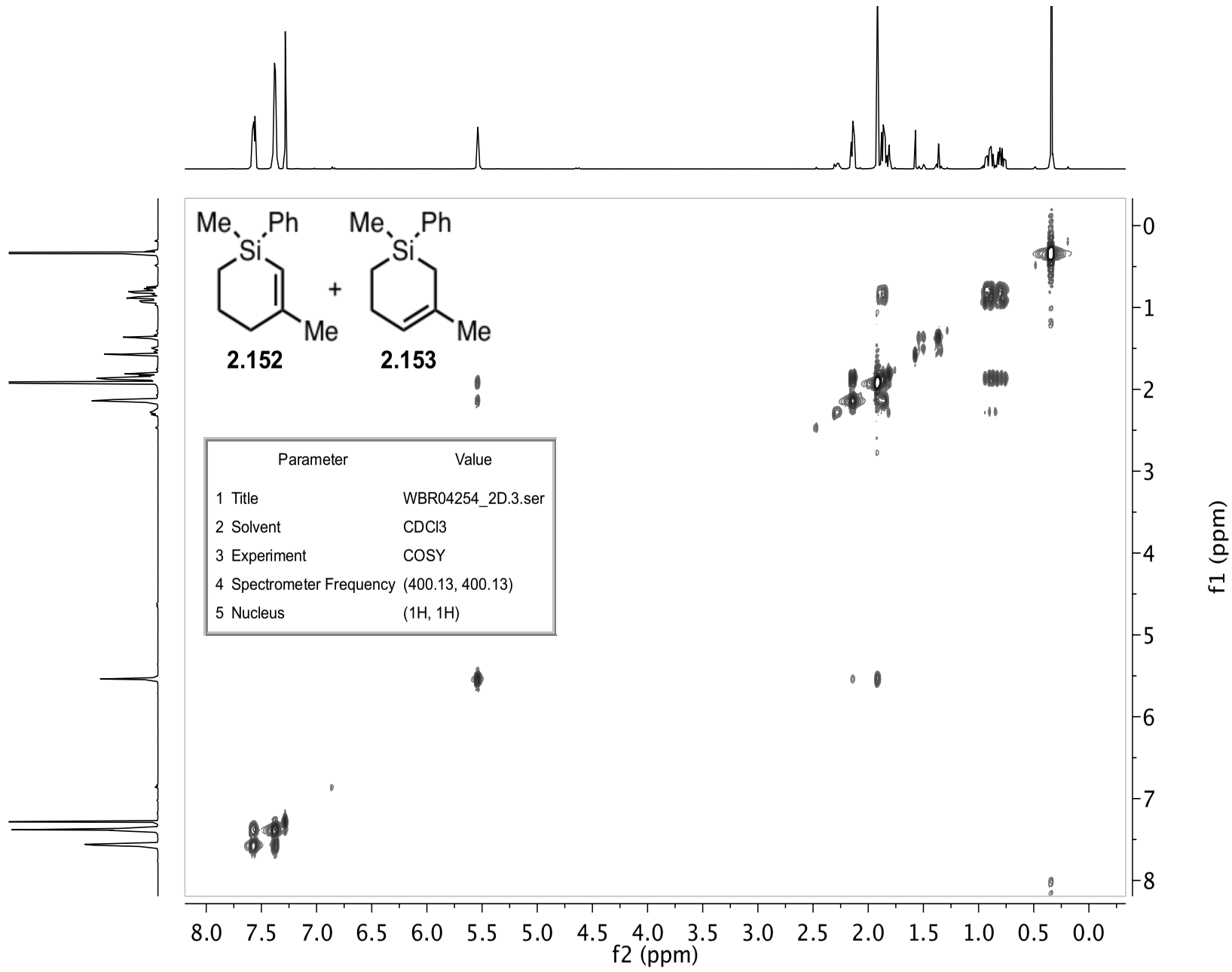
Me
Ph
Si
Me
+
Me
Ph
Si
Me
2.152
2.153
Parameter
Value
1 Title
WBR04254_2D.3.ser
2 Solvent
CDCl3
3 Experiment
COSY
4 Spectrometer Frequency
(400.13, 400.13)
5 Nucleus
(1H, 1H)
8.0
7.5
7.0
6.5
6.0
5.5
5.0
4.5
4.0
3.5
3.0
2.5
2.0
1.5
1.0
0.5
0.0
f2 (ppm)
0
1
2
3
4
5
6
7
8
f1 (ppm)

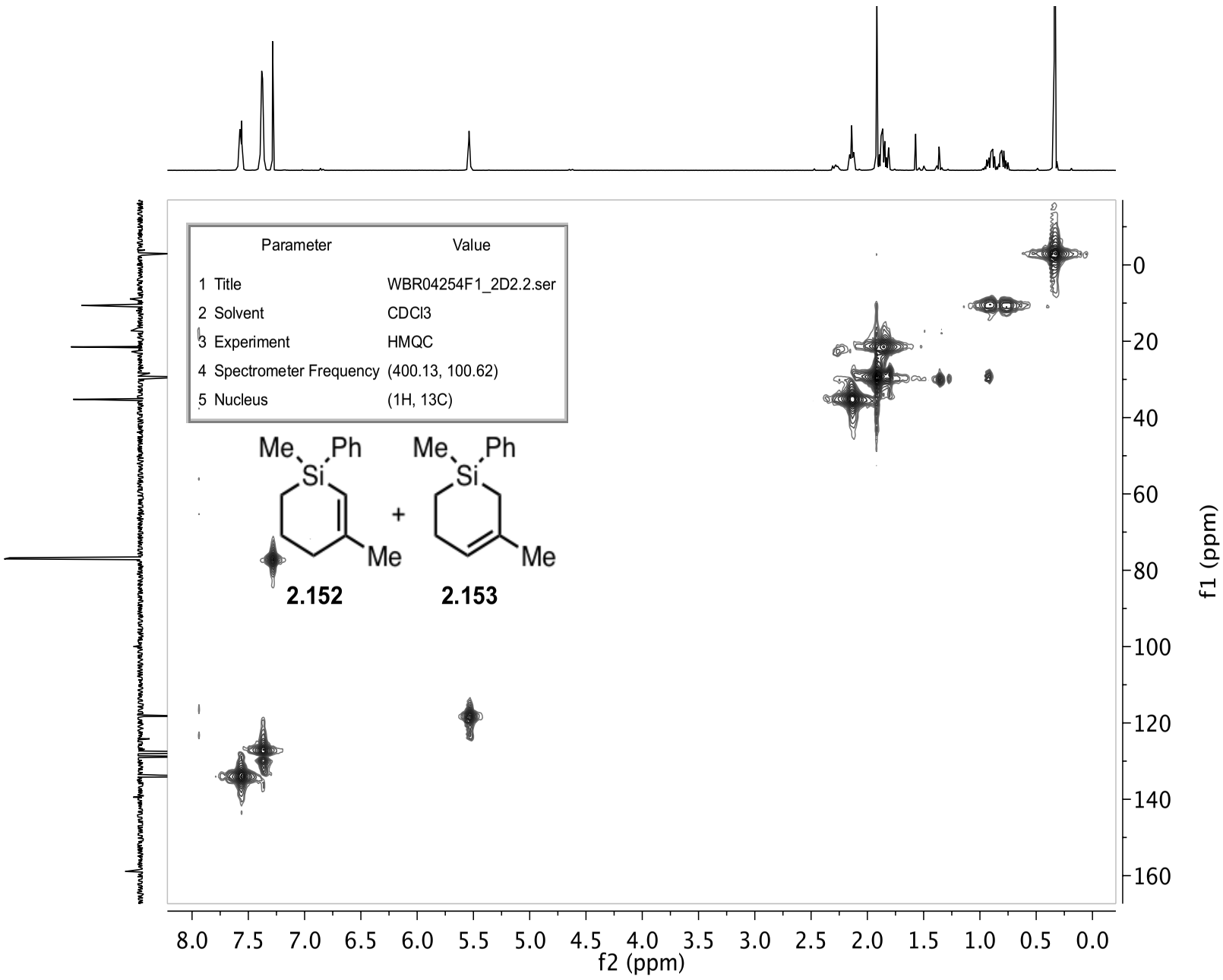
Parameter Value
1 Title WBR04254F1_2D2.2.ser
2 Solvent CDCl3
3 Experiment HMQC
4 Spectrometer Frequency (400.13, 100.62)
5 Nucleus (1H, 13C)
Me Ph
Si
Me
+
Me Ph
Si
Me
2.152
2.153
f2 (ppm)
f1 (ppm)

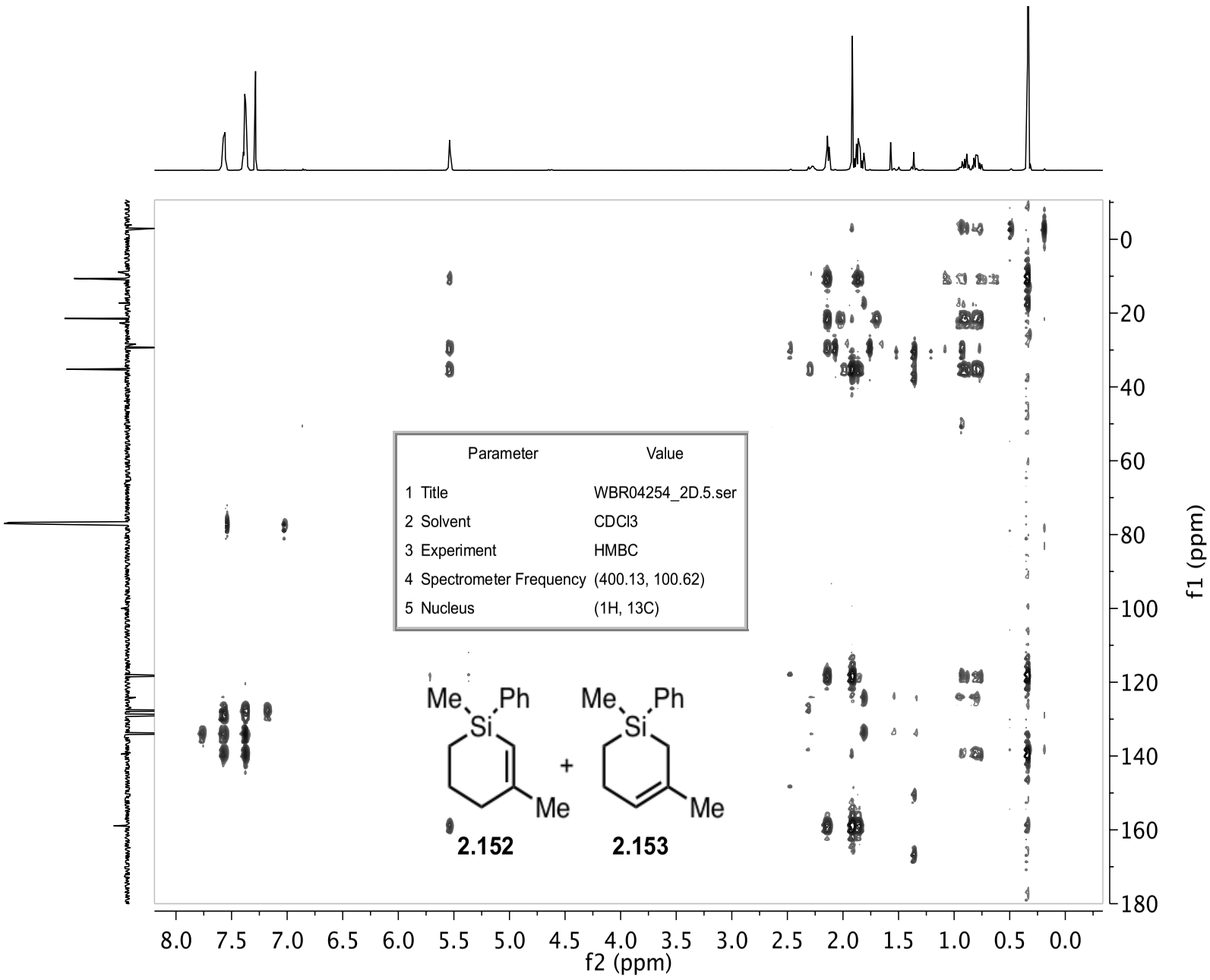
Parameter Value
1 Title WBR04254_2D.5.ser
2 Solvent CDCl3
3 Experiment HMBC
4 Spectrometer Frequency (400.13, 100.62)
5 Nucleus (1H, 13C)
Me Ph Si Me
2.152
Me Ph Si Me
2.153
f2 (ppm)
f1 (ppm)

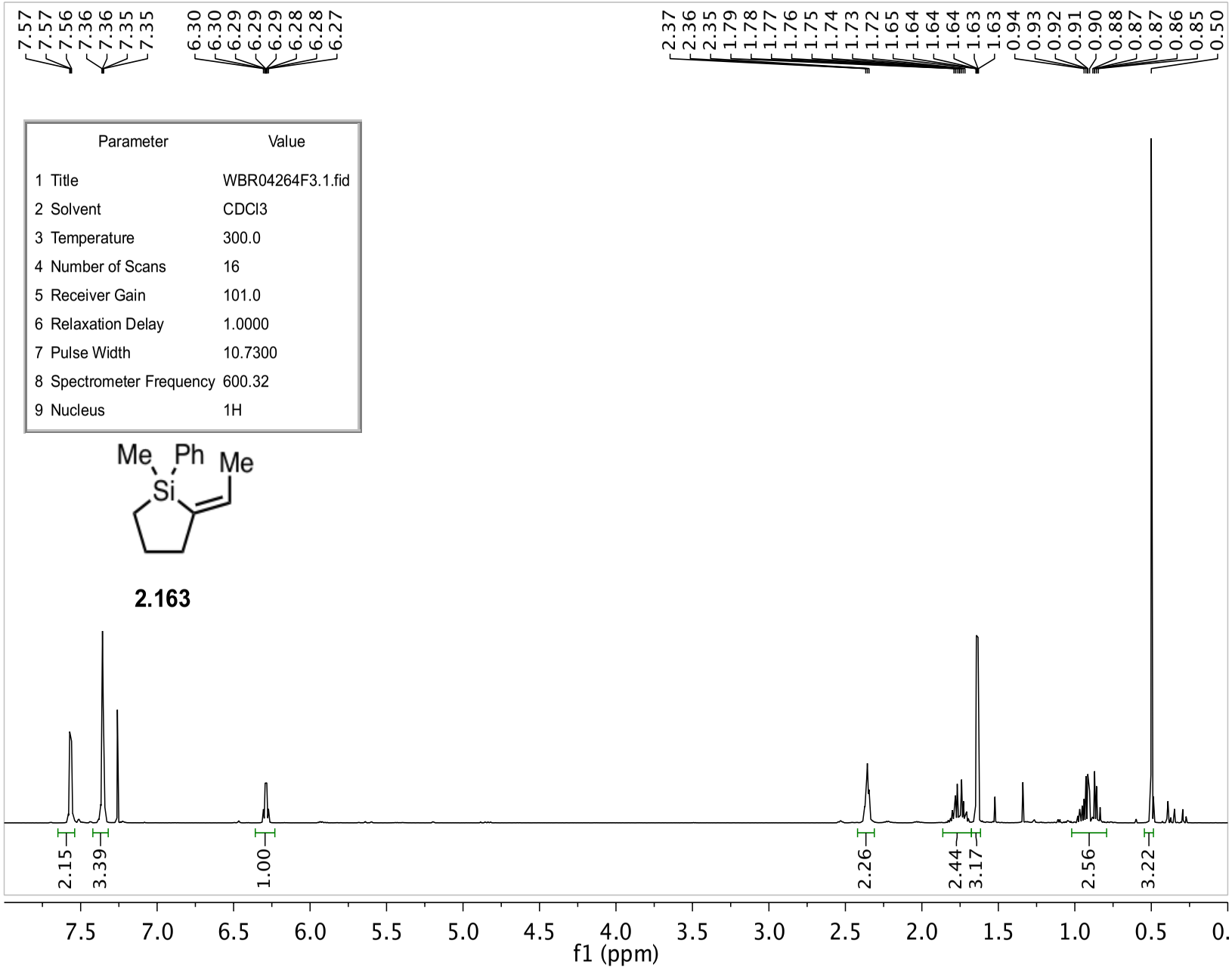
7.57 7.57 7.56 7.36 7.36 7.35 7.35
6.30 6.30 6.29 6.29 6.29 6.28 6.28 6.27
2.37 2.36 2.35 1.79 1.78 1.77 1.76 1.75 1.74 1.73 1.72 1.65 1.64 1.64 1.64 1.63 1.63 0.94 0.93 0.92 0.91 0.90 0.88 0.87 0.87 0.86 0.85 0.50
Parameter Value
1 Title WBR04264F3.1.fid
2 Solvent CDCl3
3 Temperature 300.0
4 Number of Scans 16
5 Receiver Gain 101.0
6 Relaxation Delay 1.0000
7 Pulse Width 10.7300
8 Spectrometer Frequency 600.32
9 Nucleus 1H
Me Ph Me
Si
2.163
2.15 3.39 1.00 2.26 2.44 3.17 2.56 3.22
7.5 7.0 6.5 6.0 5.5 5.0 4.5 4.0 3.5 3.0 2.5 2.0 1.5 1.0 0.5 0.0
f1 (ppm)

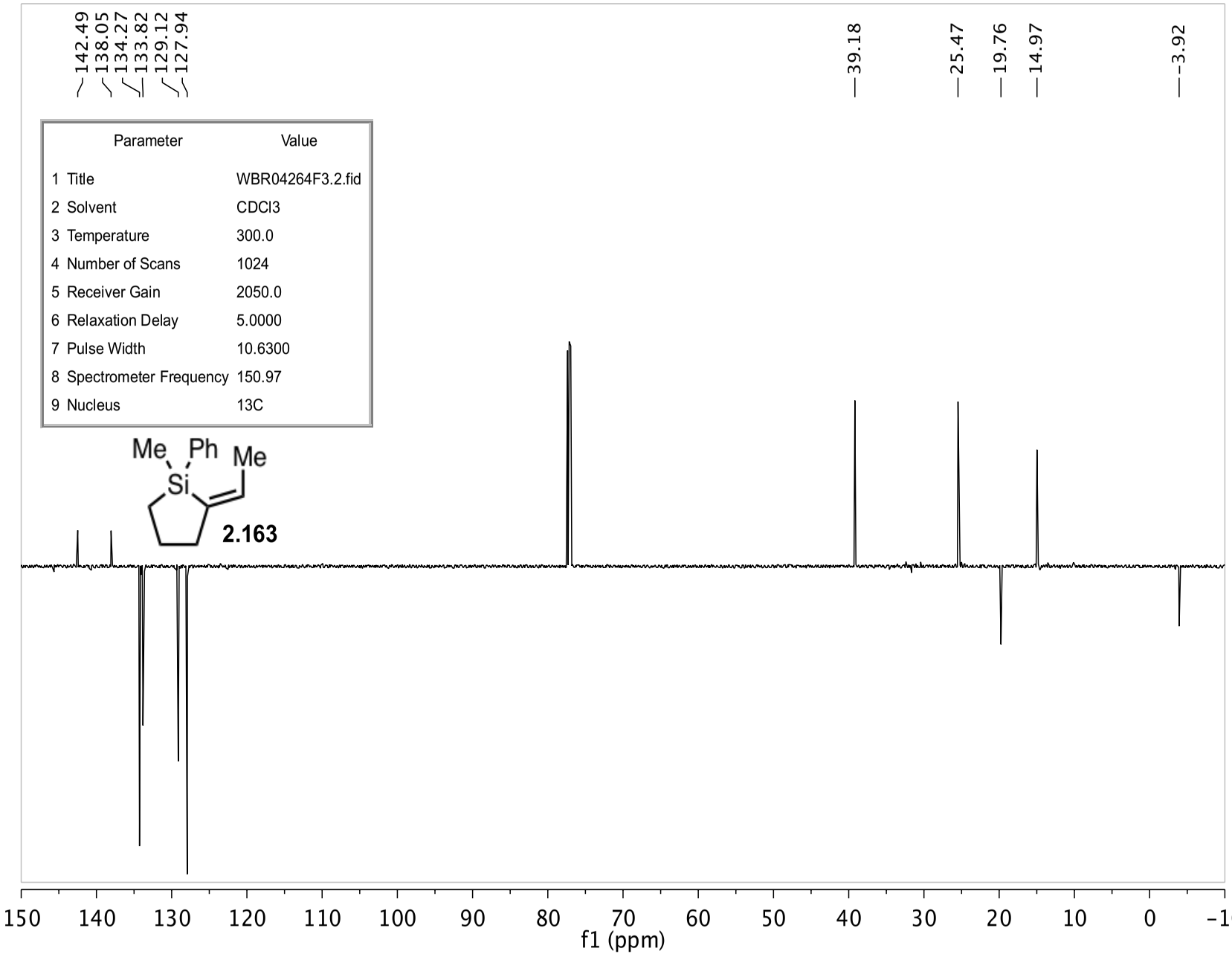
142.49
138.05
134.27
133.82
129.12
127.94
39.18
25.47
19.76
14.97
-3.92
Parameter Value
1 Title WBR04264F3.2.fid
2 Solvent CDCl3
3 Temperature 300.0
4 Number of Scans 1024
5 Receiver Gain 2050.0
6 Relaxation Delay 5.0000
7 Pulse Width 10.6300
8 Spectrometer Frequency 150.97
9 Nucleus 13C
Me
Ph
Me
Si
2.163
150 140 130 120 110 100 90 80 70 60 50 40 30 20 10 0 -10
f1 (ppm)

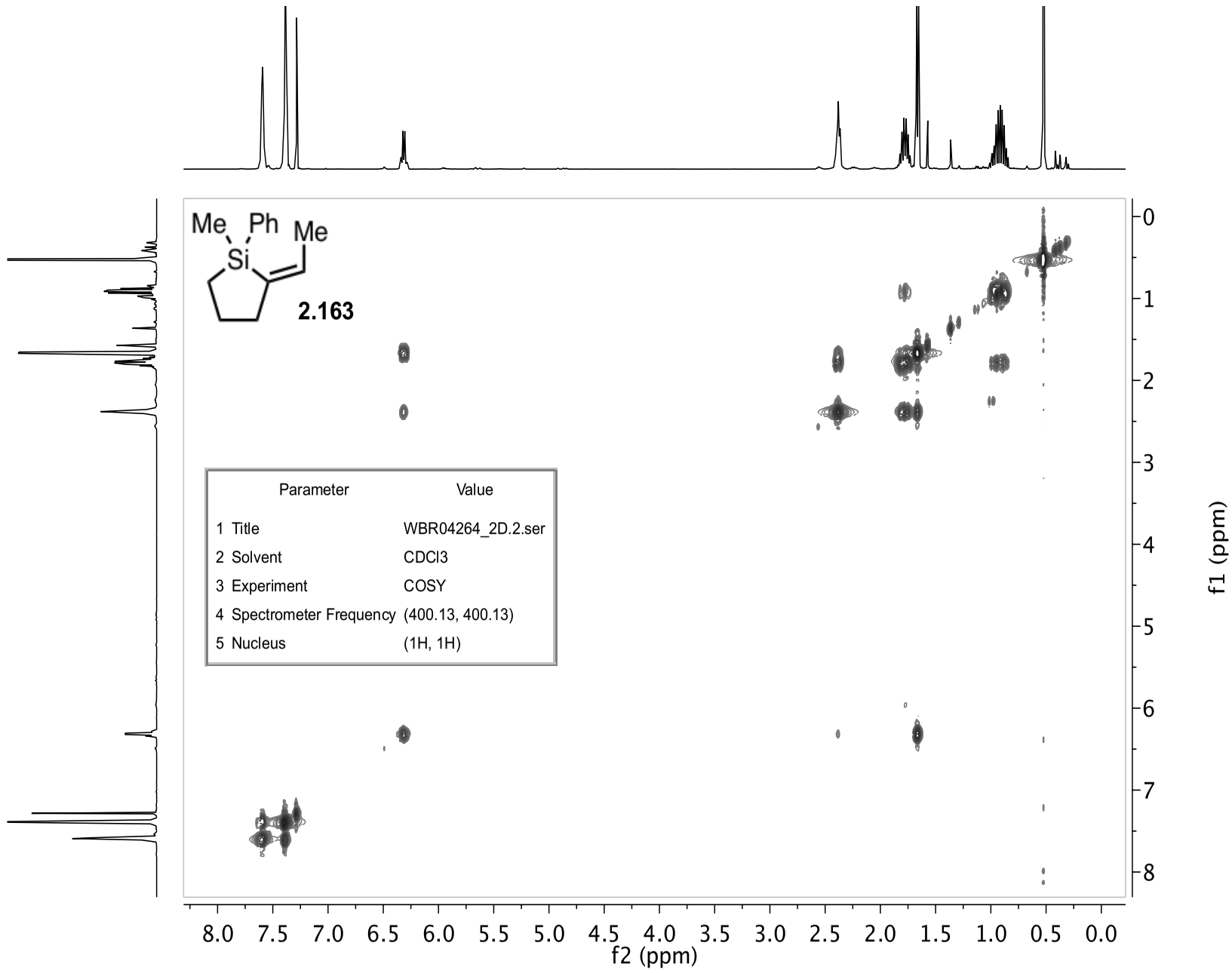
Me
Ph
Me
Si
2.163
Parameter
Value
1 Title
WBR04264_2D.2.ser
2 Solvent
CDCl3
3 Experiment
COSY
4 Spectrometer Frequency
(400.13, 400.13)
5 Nucleus
(1H, 1H)
f2 (ppm)
f1 (ppm)

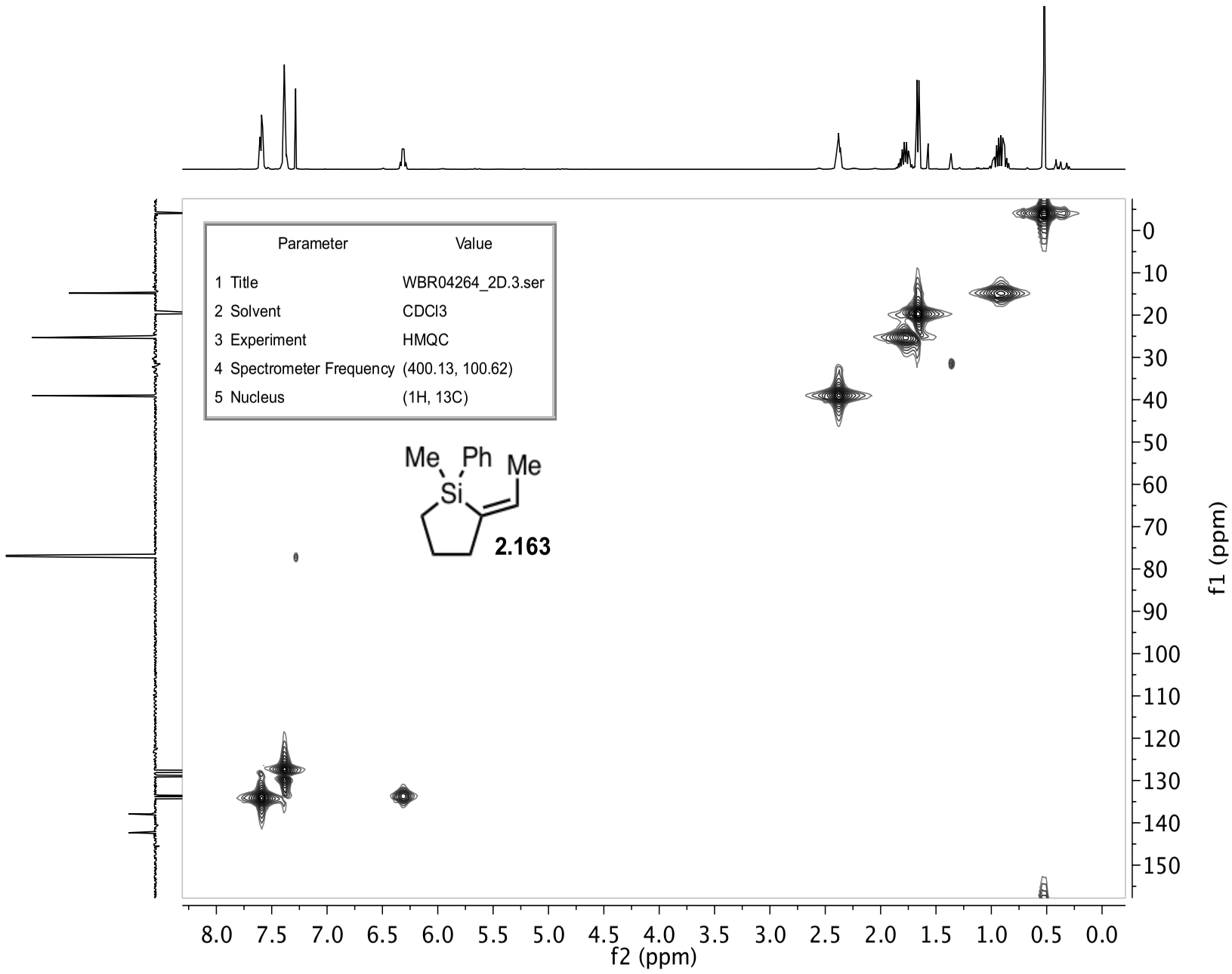
Parameter Value
1 Title WBR04264_2D.3.ser
2 Solvent CDCl3
3 Experiment HMQC
4 Spectrometer Frequency (400.13, 100.62)
5 Nucleus (1H, 13C)
Me Ph Me
Si
2.163
f2 (ppm)
f1 (ppm)

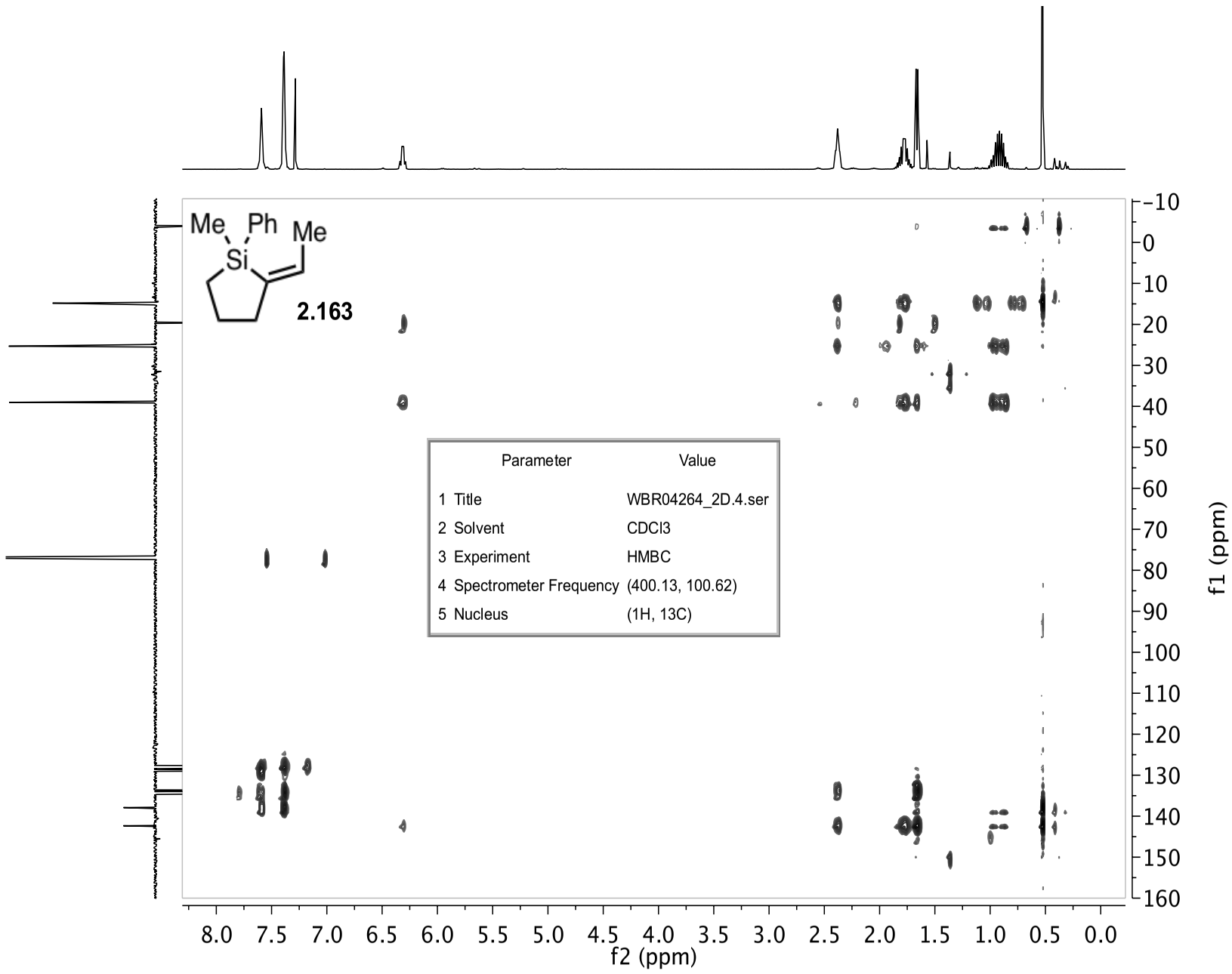
Me
Ph
Me
Si
2.163
Parameter Value
1 Title WBR04264_2D.4.ser
2 Solvent CDCl3
3 Experiment HMBC
4 Spectrometer Frequency (400.13, 100.62)
5 Nucleus (1H, 13C)
f2 (ppm)
f1 (ppm)

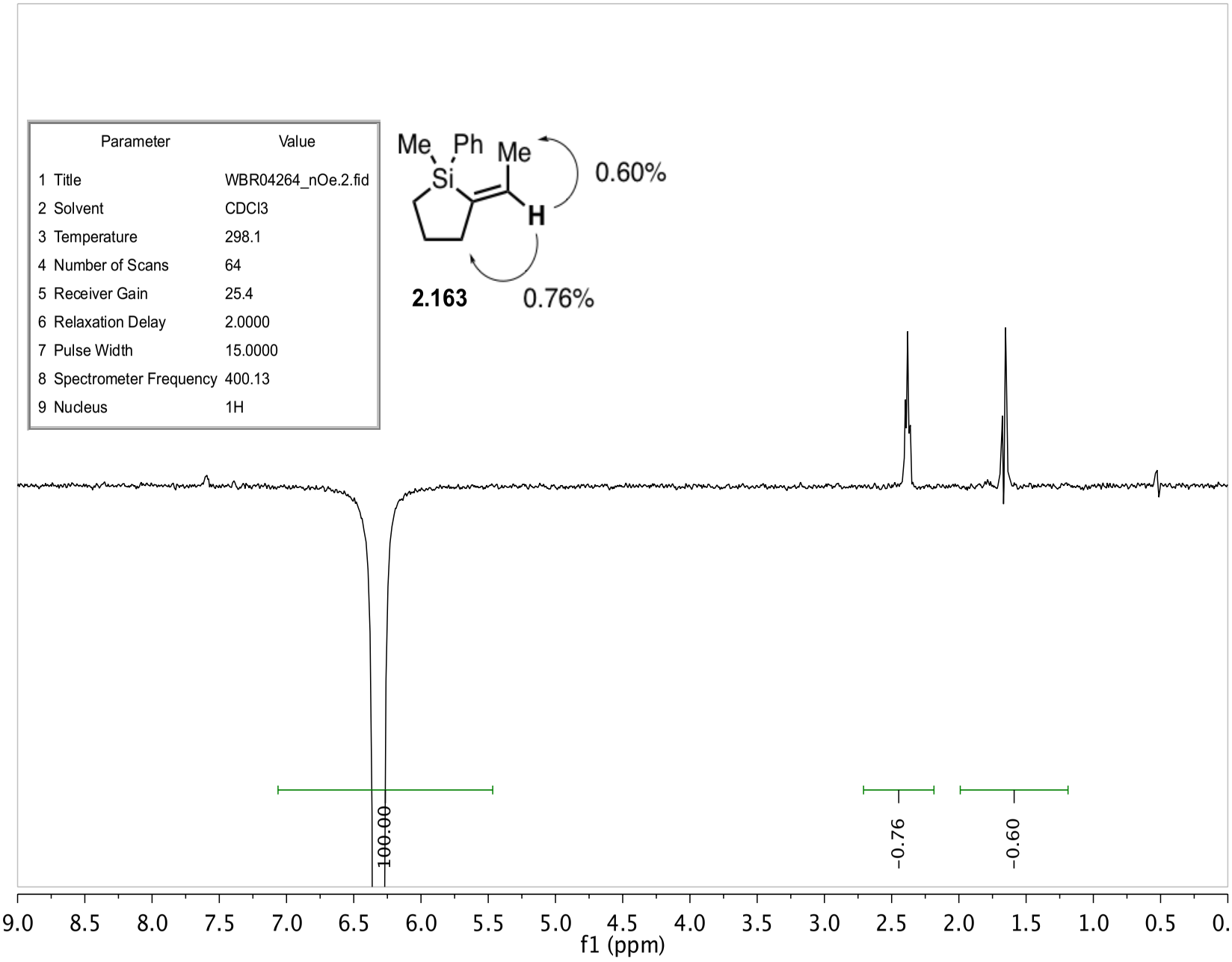
Parameter Value
1 Title WBR04264_nOe.2.fid
2 Solvent CDCl3
3 Temperature 298.1
4 Number of Scans 64
5 Receiver Gain 25.4
6 Relaxation Delay 2.0000
7 Pulse Width 15.0000
8 Spectrometer Frequency 400.13
9 Nucleus 1H
Me
Ph
Me
Si
H
0.60%
2.163
0.76%
100.00
-0.76
-0.60
9.0 8.5 8.0 7.5 7.0 6.5 6.0 5.5 5.0 4.5 4.0 3.5 3.0 2.5 2.0 1.5 1.0 0.5 0.0
f1 (ppm)

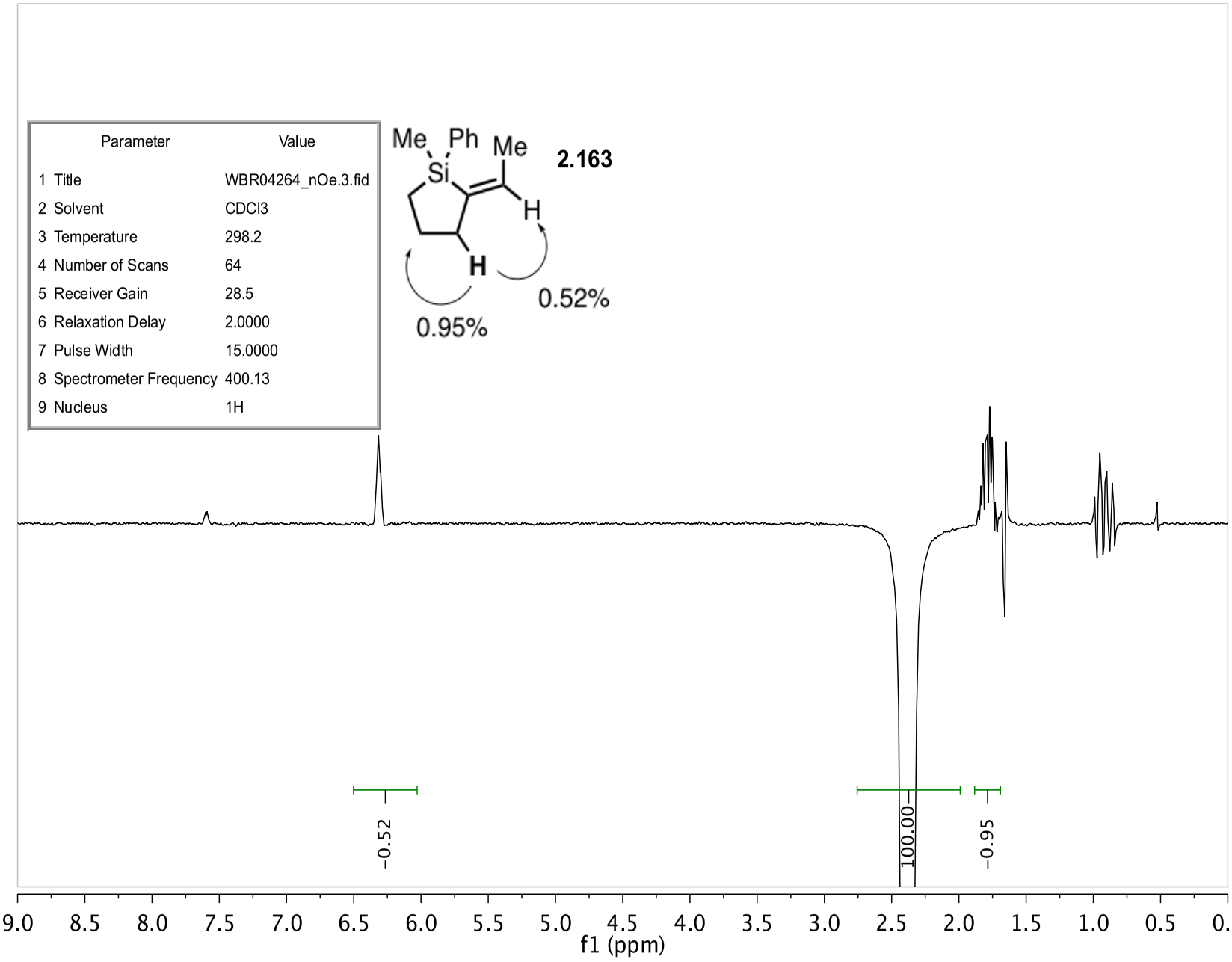
Parameter Value
1 Title WBR04264_nOe.3.fid
2 Solvent CDCl3
3 Temperature 298.2
4 Number of Scans 64
5 Receiver Gain 28.5
6 Relaxation Delay 2.0000
7 Pulse Width 15.0000
8 Spectrometer Frequency 400.13
9 Nucleus 1H
Me
Ph
Me
Si
H
H
2.163
0.52%
0.95%
0.52
100.00
0.95
9.0 8.5 8.0 7.5 7.0 6.5 6.0 5.5 5.0 4.5 4.0 3.5 3.0 2.5 2.0 1.5 1.0 0.5 0.0
f1 (ppm)

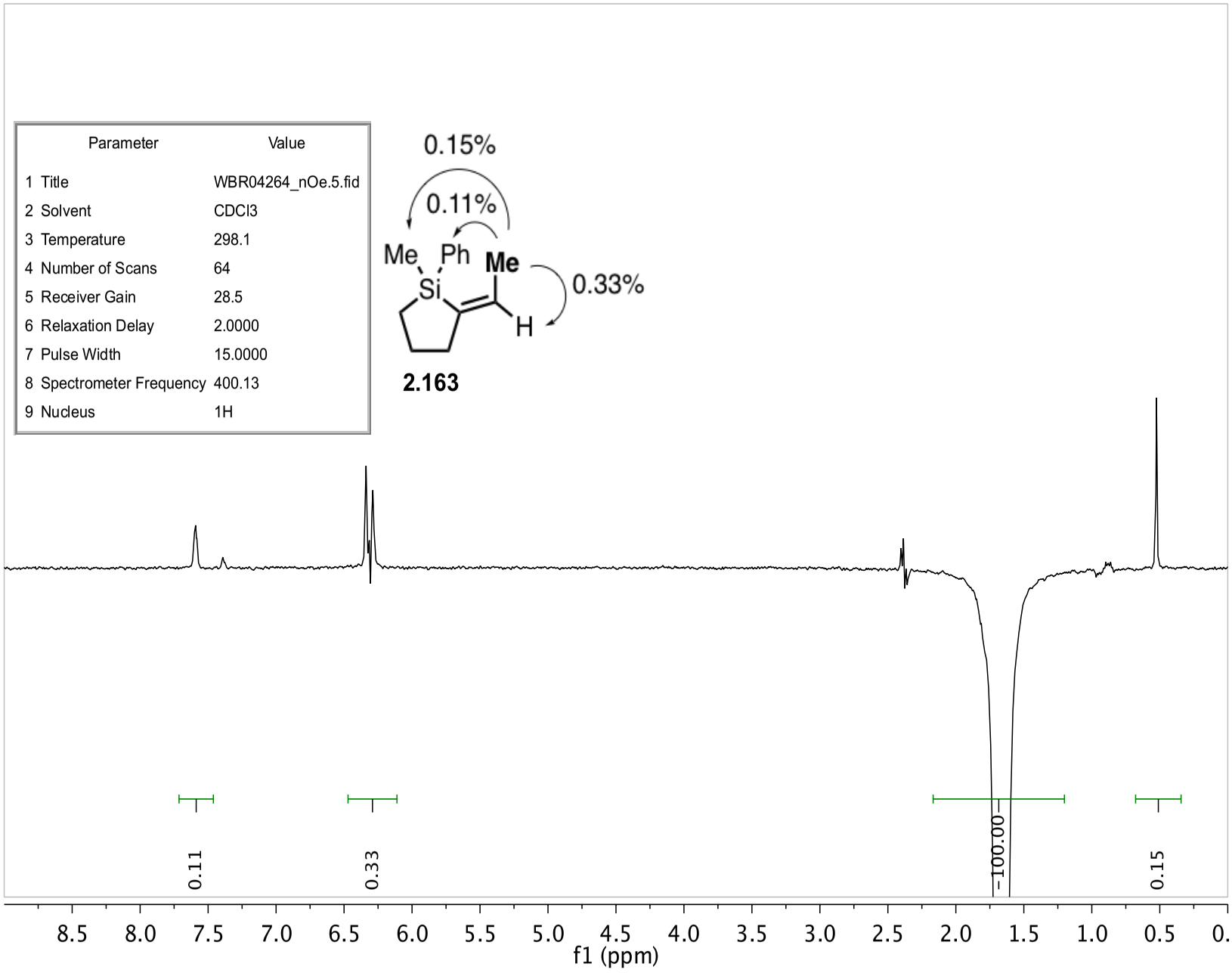
Parameter Value
1 Title WBR04264_nOe.5.fid
2 Solvent CDCl3
3 Temperature 298.1
4 Number of Scans 64
5 Receiver Gain 28.5
6 Relaxation Delay 2.0000
7 Pulse Width 15.0000
8 Spectrometer Frequency 400.13
9 Nucleus 1H
0.15%
0.11%
Me
Ph
Me
Si
0.33%
H
2.163
0.11
0.33
-100.00
0.15
8.5 8.0 7.5 7.0 6.5 6.0 5.5 5.0 4.5 4.0 3.5 3.0 2.5 2.0 1.5 1.0 0.5 0.0
f1 (ppm)

Parameter	Value
1 Title	WBR04264_nOe.7.fid
2 Solvent	CDCl3
3 Temperature	298.1
4 Number of Scans	64
5 Receiver Gain	28.5
6 Relaxation Delay	2.0000
7 Pulse Width	15.0000
8 Spectrometer Frequency	400.13
9 Nucleus	1H

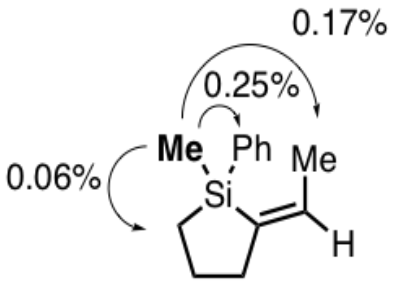

2.163

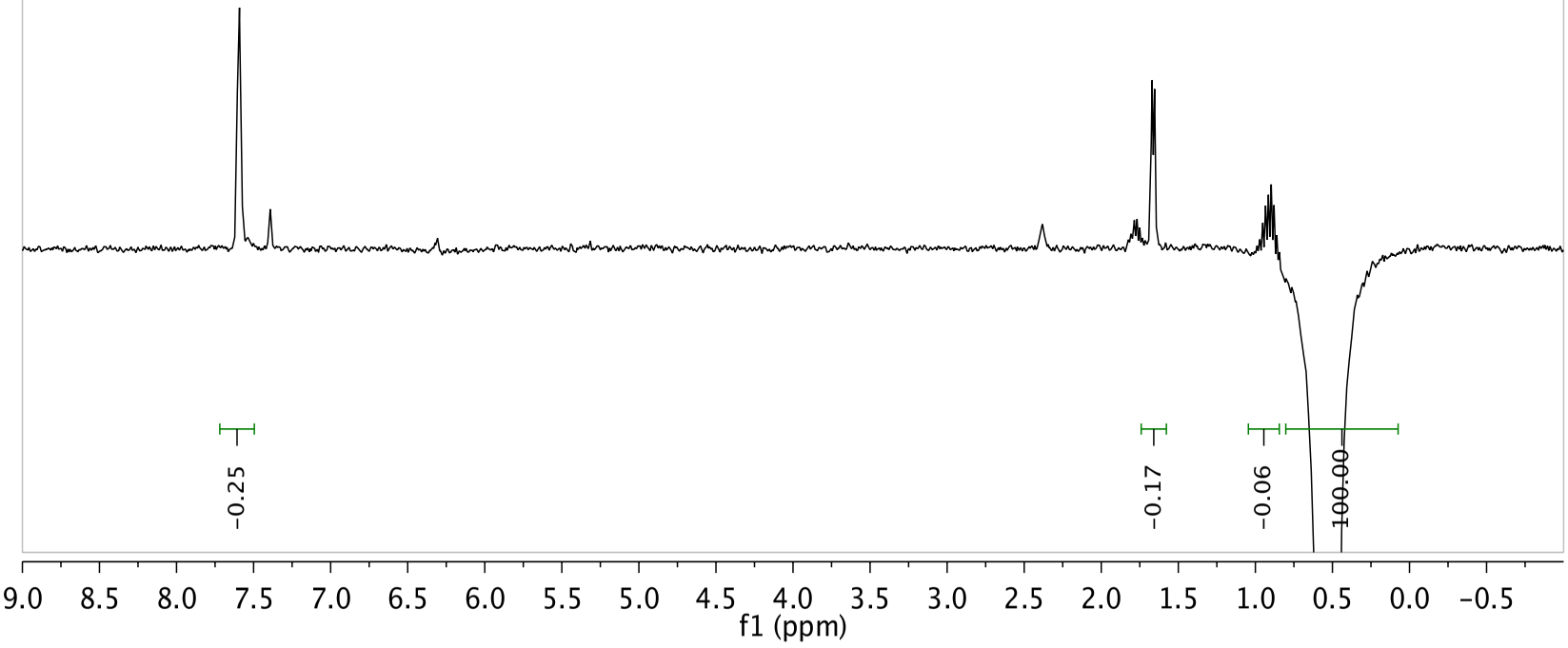

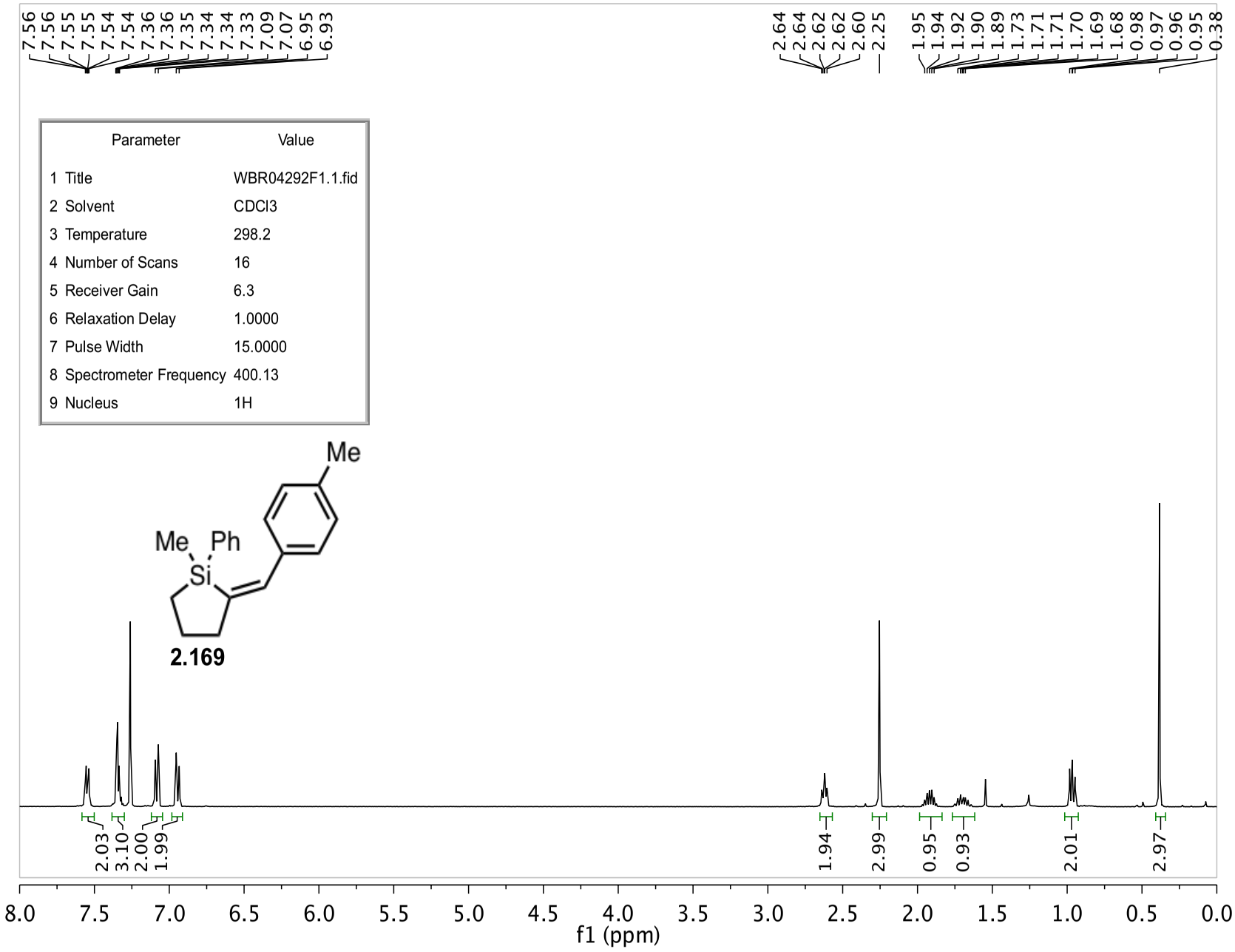
7.56
7.56
7.55
7.55
7.54
7.54
7.36
7.36
7.35
7.34
7.34
7.33
7.09
7.07
6.95
6.93
2.64
2.64
2.62
2.62
2.60
2.25
1.95
1.94
1.92
1.90
1.89
1.73
1.71
1.71
1.70
1.69
1.68
0.98
0.97
0.96
0.95
0.38
Parameter Value
1 Title WBR04292F1.1.fid
2 Solvent CDCl3
3 Temperature 298.2
4 Number of Scans 16
5 Receiver Gain 6.3
6 Relaxation Delay 1.0000
7 Pulse Width 15.0000
8 Spectrometer Frequency 400.13
9 Nucleus 1H
Me
Me
Ph
Si
2.169
2.03
3.10
2.00
1.99
1.94
2.99
0.95
0.93
2.01
2.97
8.0
7.5
7.0
6.5
6.0
5.5
5.0
4.5
4.0
3.5
3.0
2.5
2.0
1.5
1.0
0.5
0.0
f1 (ppm)

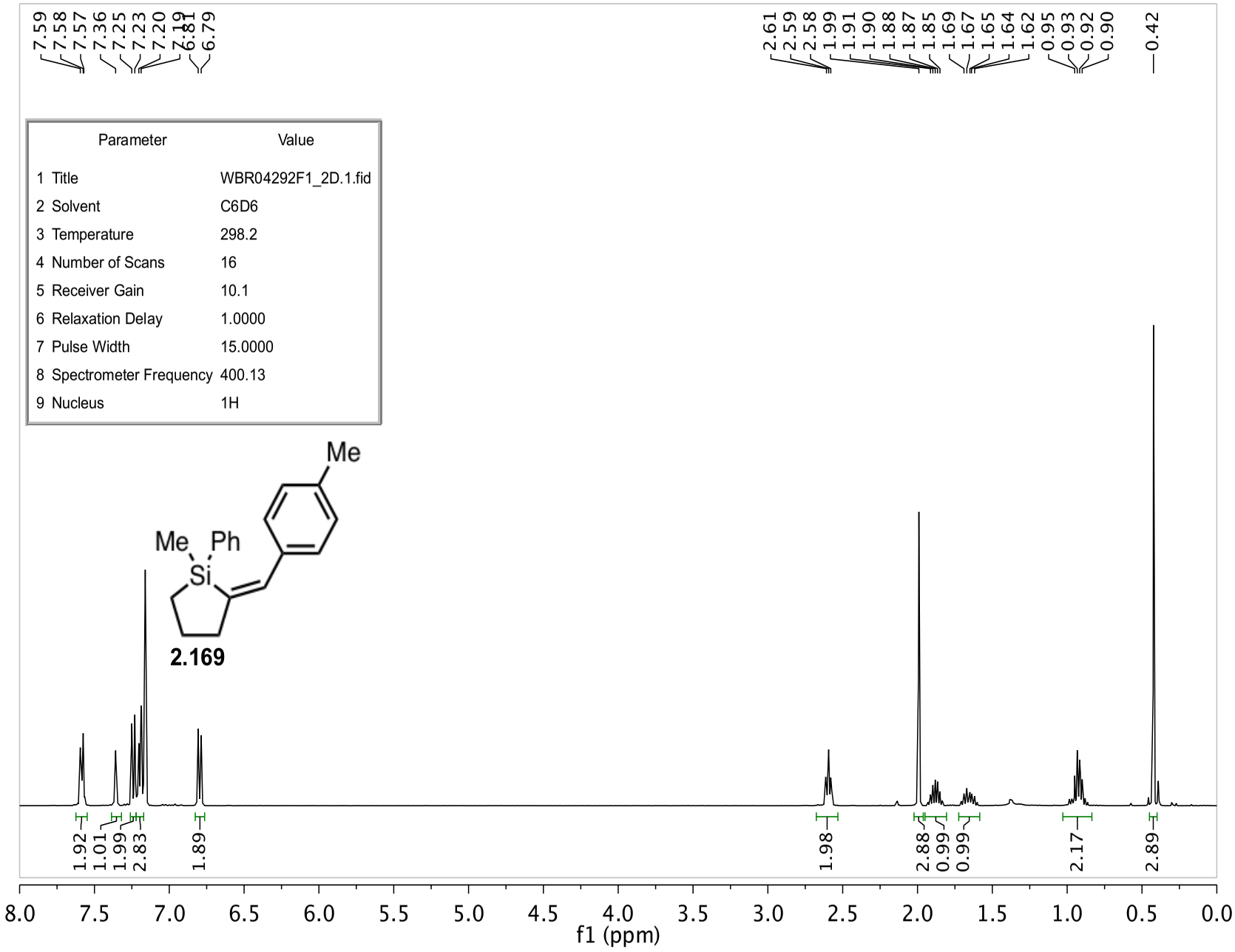
7.59
7.58
7.57
7.36
7.25
7.23
7.20
7.19
6.81
6.79
2.61
2.59
2.58
1.99
1.91
1.90
1.88
1.87
1.85
1.69
1.67
1.65
1.64
1.62
0.95
0.93
0.92
0.90
0.42
Parameter Value
1 Title WBR04292F1_2D.1.fid
2 Solvent C6D6
3 Temperature 298.2
4 Number of Scans 16
5 Receiver Gain 10.1
6 Relaxation Delay 1.0000
7 Pulse Width 15.0000
8 Spectrometer Frequency 400.13
9 Nucleus 1H
Me
Me Ph
Si
2.169
1.92
1.01
1.99
2.83
1.89
1.98
2.88
0.99
0.99
2.17
2.89
8.0 7.5 7.0 6.5 6.0 5.5 5.0 4.5 4.0 3.5 3.0 2.5 2.0 1.5 1.0 0.5 0.0
f1 (ppm)

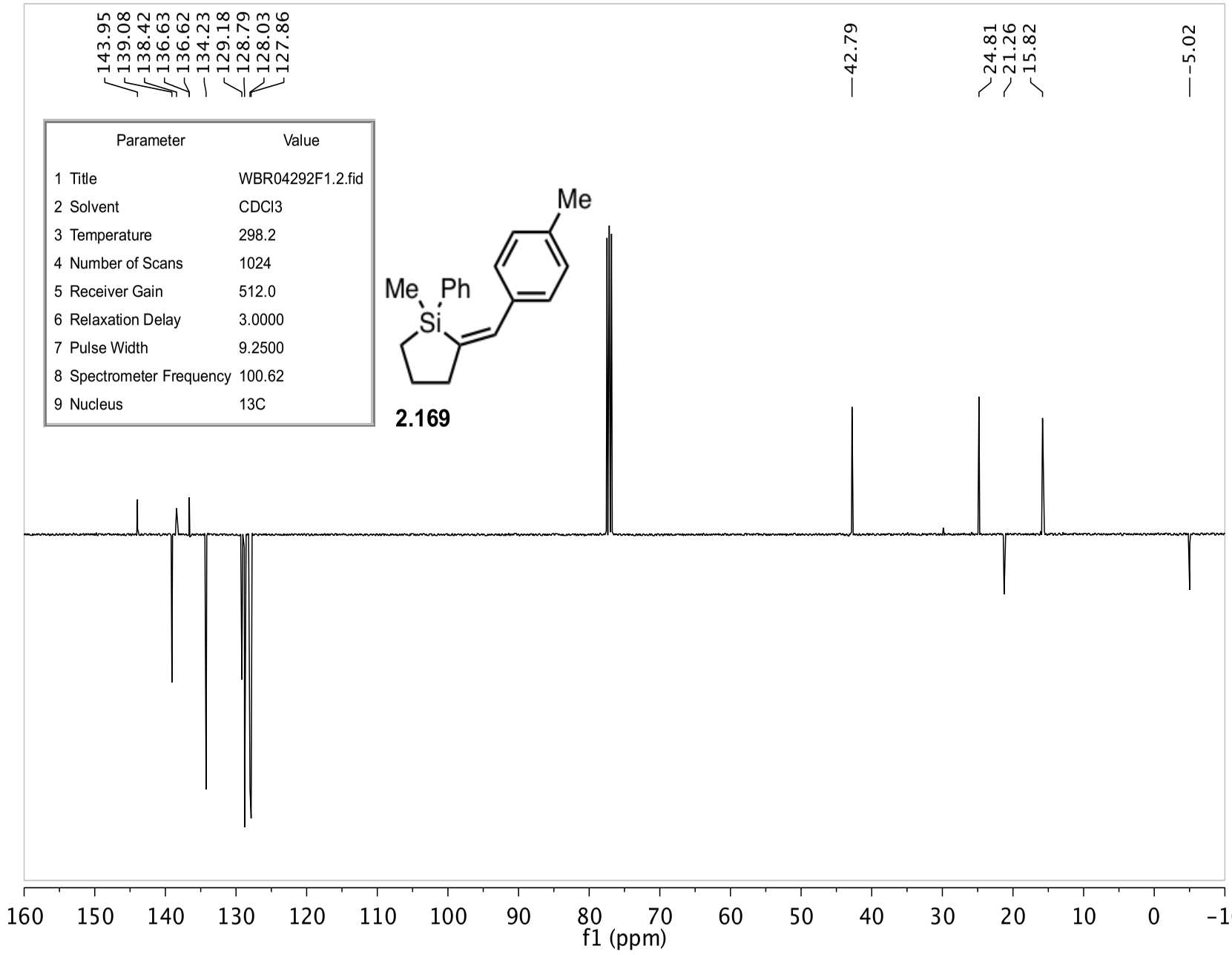
143.95
139.08
138.42
136.63
136.62
134.23
129.18
128.79
128.03
127.86
42.79
24.81
21.26
15.82
-5.02
Parameter Value
1 Title WBR04292F1.2.fid
2 Solvent CDCl3
3 Temperature 298.2
4 Number of Scans 1024
5 Receiver Gain 512.0
6 Relaxation Delay 3.0000
7 Pulse Width 9.2500
8 Spectrometer Frequency 100.62
9 Nucleus 13C
Me
Me
Ph
Si
2.169
160 150 140 130 120 110 100 90 80 70 60 50 40 30 20 10 0 -10
f1 (ppm)

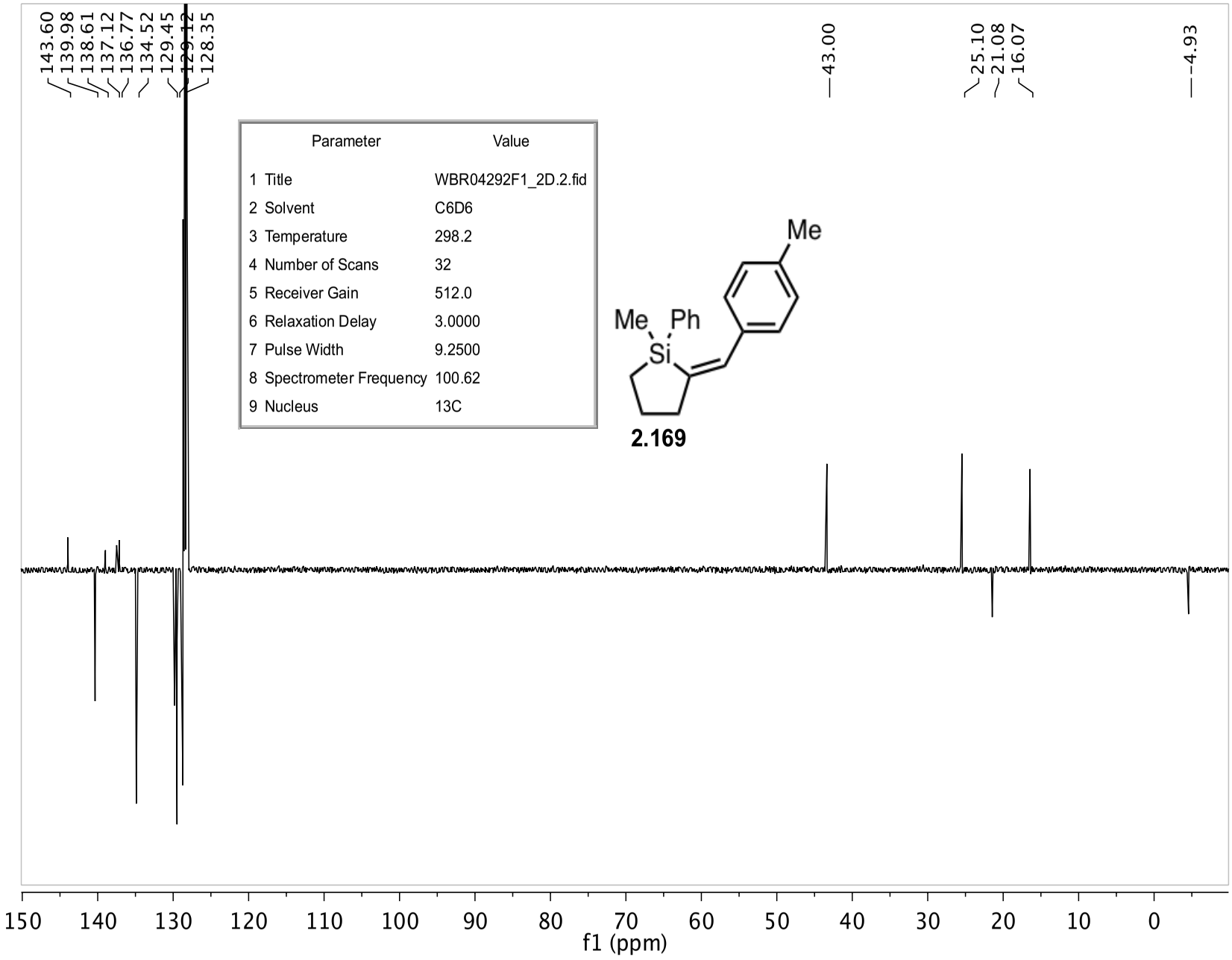
143.60
139.98
138.61
137.12
136.77
134.52
129.45
129.12
128.35
43.00
25.10
21.08
16.07
-4.93
Parameter Value
1 Title WBR04292F1_2D.2.fid
2 Solvent C6D6
3 Temperature 298.2
4 Number of Scans 32
5 Receiver Gain 512.0
6 Relaxation Delay 3.0000
7 Pulse Width 9.2500
8 Spectrometer Frequency 100.62
9 Nucleus 13C
Me
Me
Ph
Si
2.169
150 140 130 120 110 100 90 80 70 60 50 40 30 20 10 0
f1 (ppm)

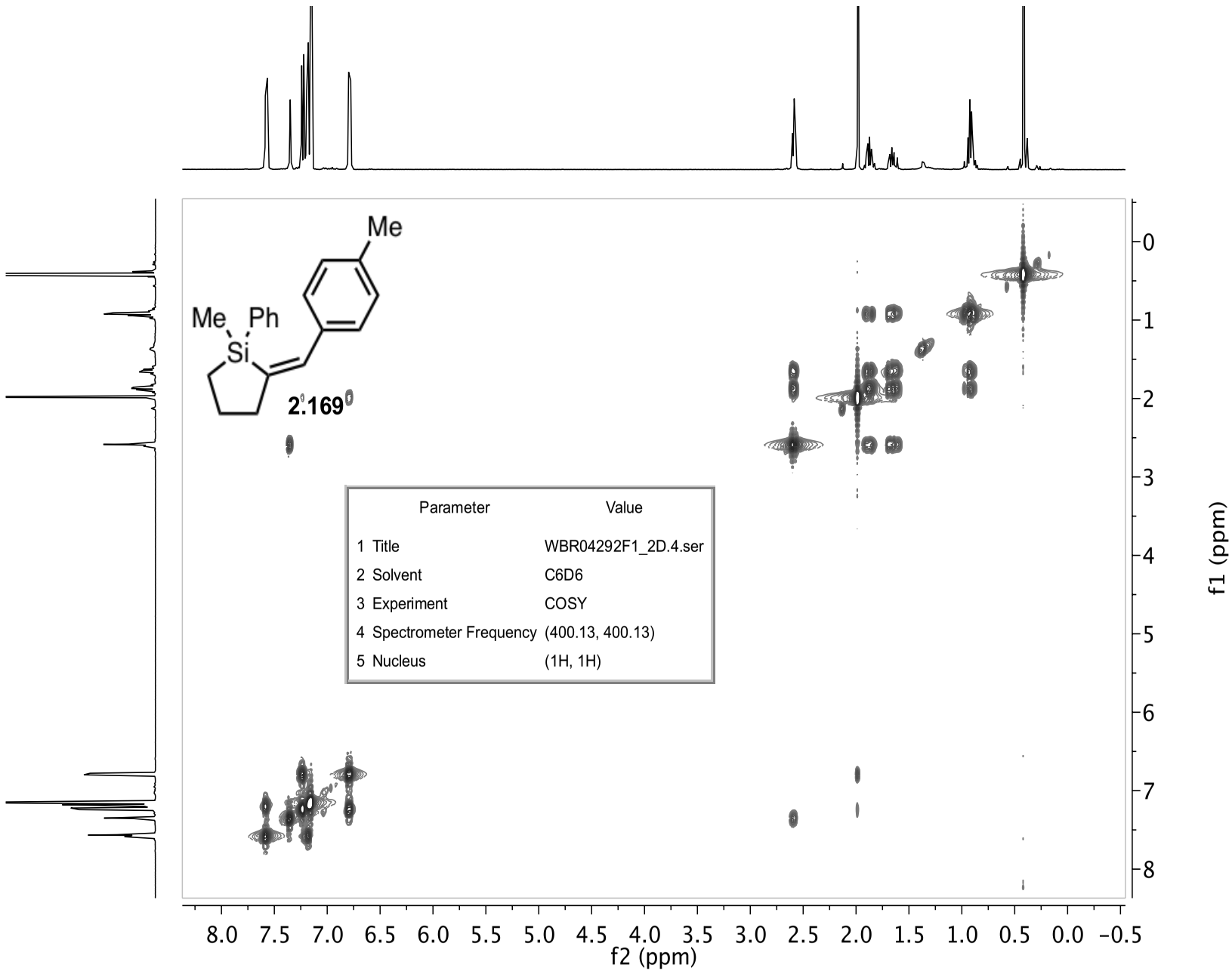
Me
Me
Ph
Si
2.169
Parameter Value
1 Title WBR04292F1_2D.4.ser
2 Solvent C6D6
3 Experiment COSY
4 Spectrometer Frequency (400.13, 400.13)
5 Nucleus (1H, 1H)
8.0 7.5 7.0 6.5 6.0 5.5 5.0 4.5 4.0 3.5 3.0 2.5 2.0 1.5 1.0 0.5 0.0 -0.5
f2 (ppm)
0 1 2 3 4 5 6 7 8
f1 (ppm)

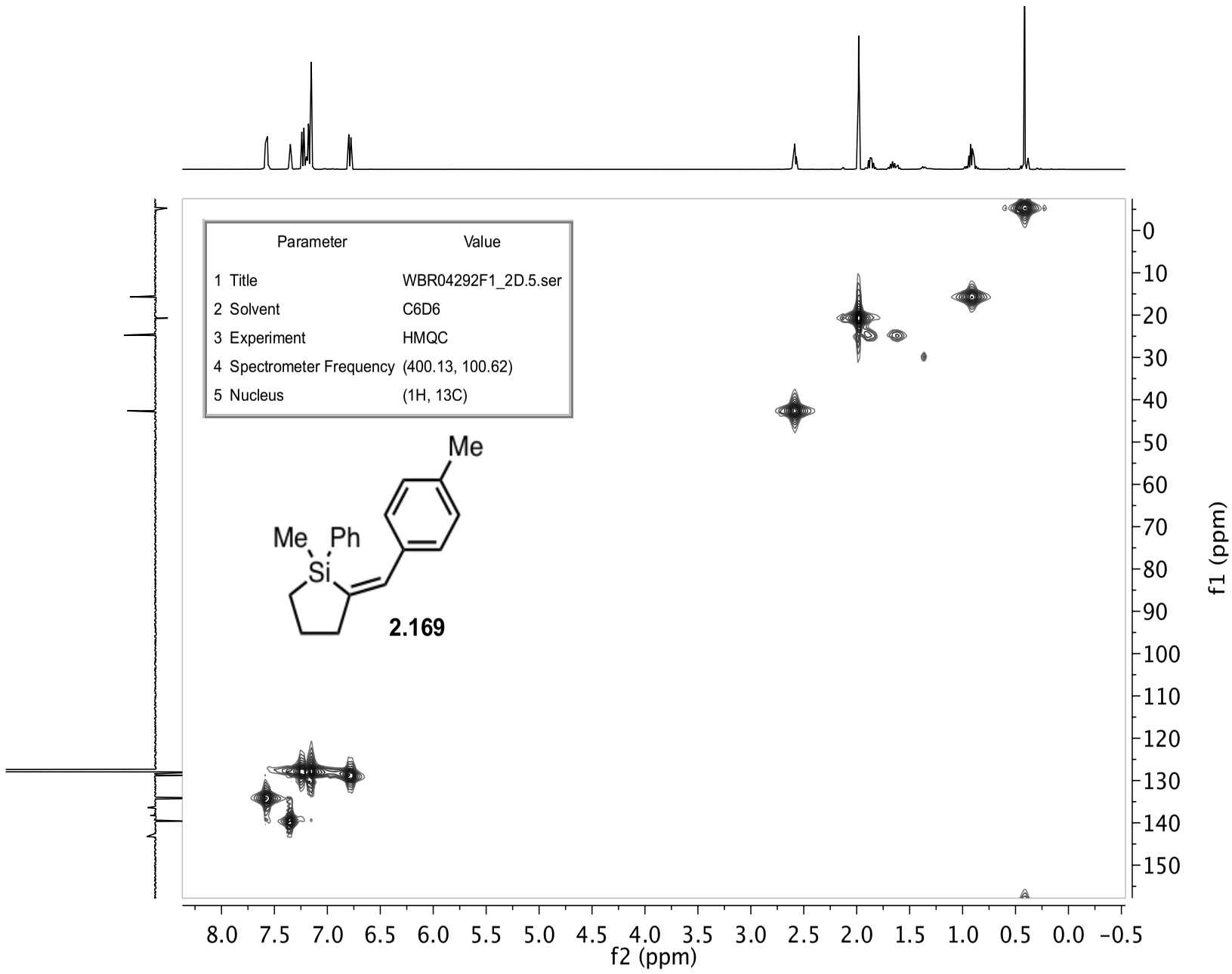
Parameter Value
1 Title WBR04292F1_2D.5.ser
2 Solvent C6D6
3 Experiment HMQC
4 Spectrometer Frequency (400.13, 100.62)
5 Nucleus (1H, 13C)
Me
Me Ph
Si
2.169
f2 (ppm)
f1 (ppm)

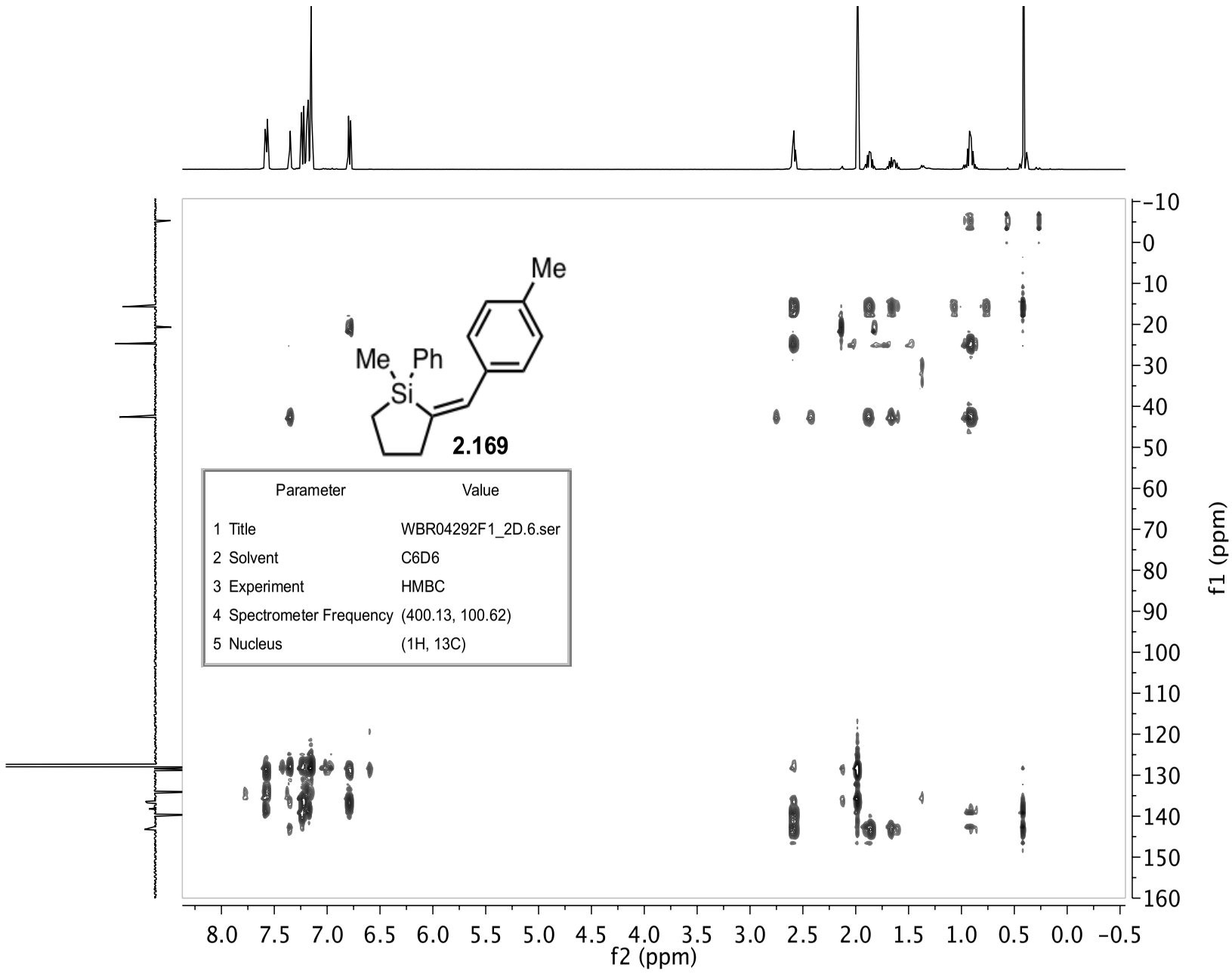
Me
Me
Ph
Si
2.169
Parameter Value
1 Title WBR04292F1_2D.6.ser
2 Solvent C6D6
3 Experiment HMBC
4 Spectrometer Frequency (400.13, 100.62)
5 Nucleus (1H, 13C)
f2 (ppm)
f1 (ppm)

Parameter	Value
1 Title	WBR04292F1_nOe.3.fid
2 Solvent	C6D6
3 Temperature	298.1
4 Number of Scans	64
5 Receiver Gain	18.0
6 Relaxation Delay	2.0000
7 Pulse Width	15.0000
8 Spectrometer Frequency	400.13
9 Nucleus	1H

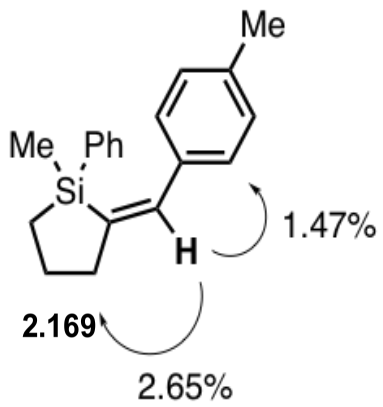

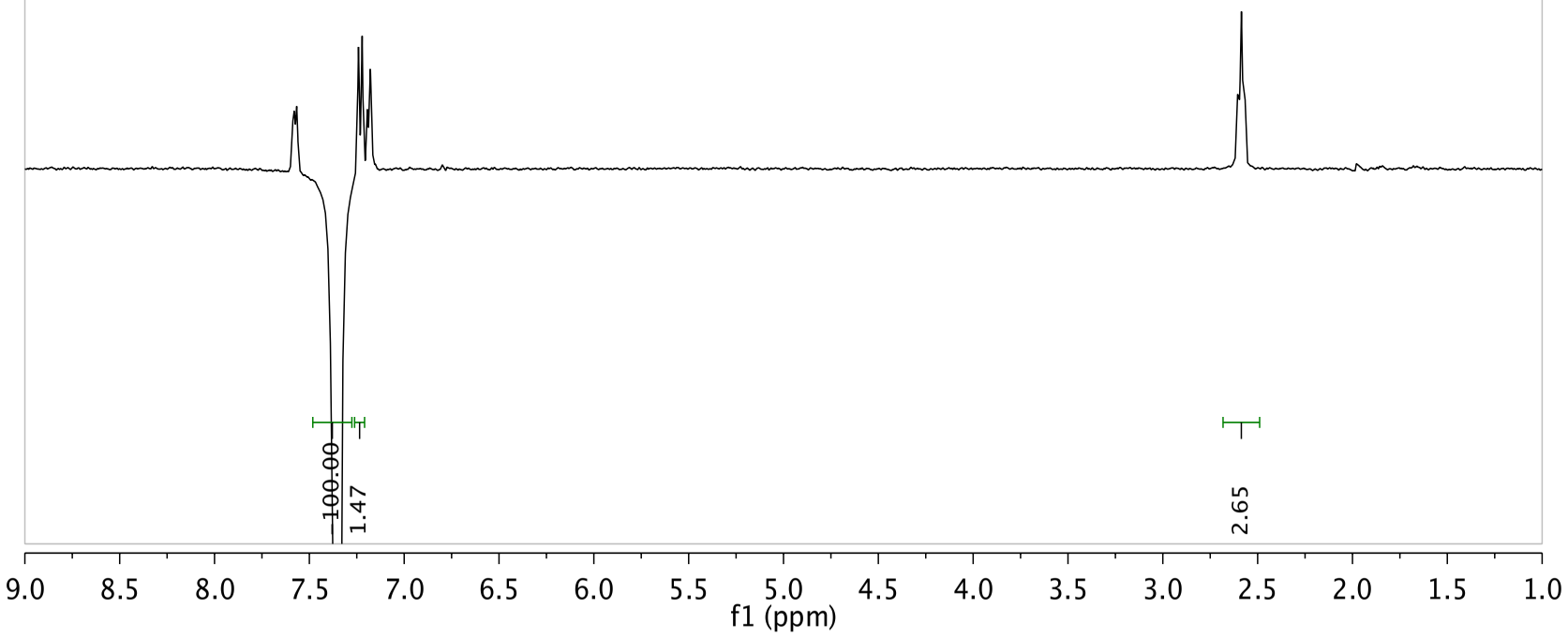

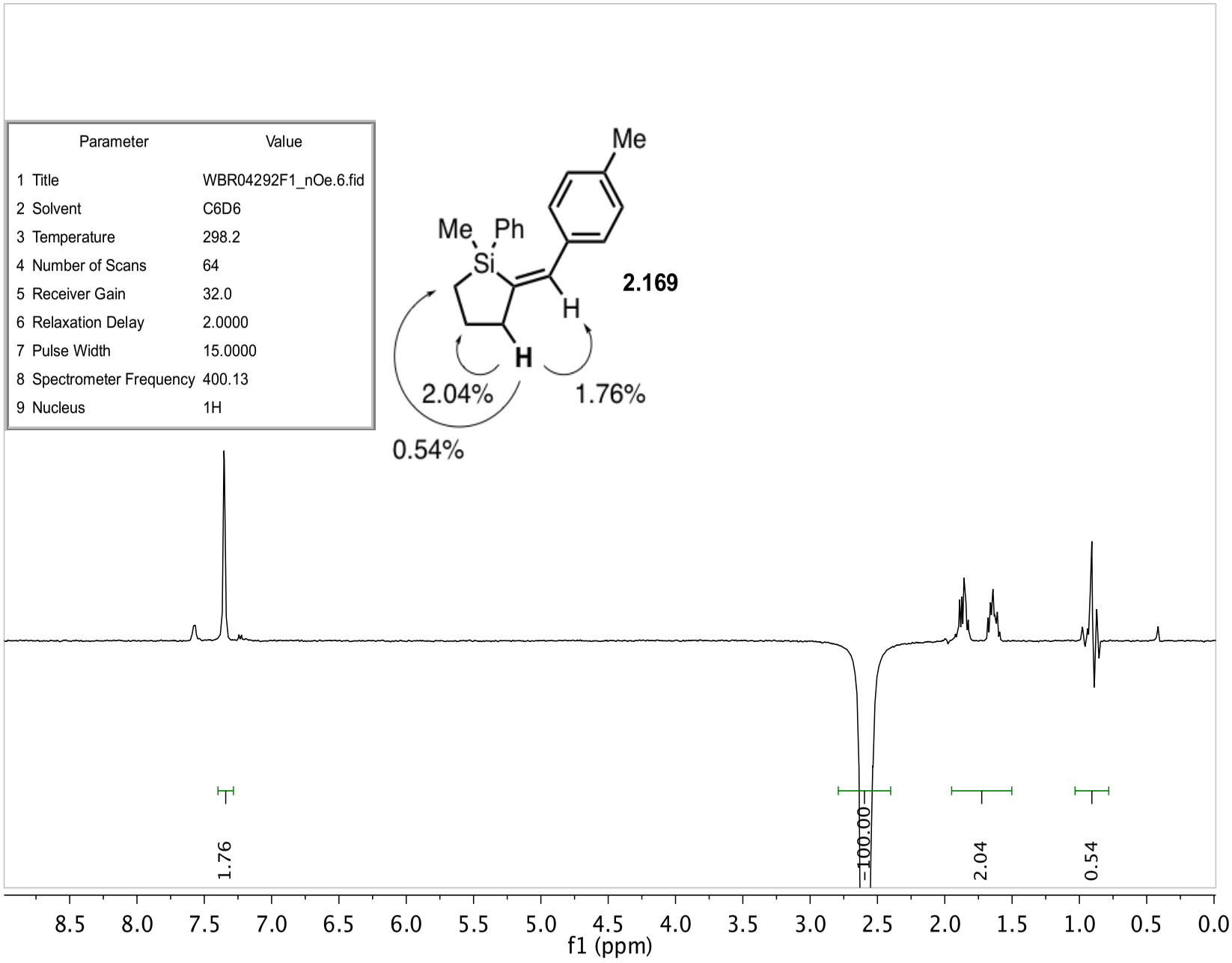
Parameter Value
1 Title WBR04292F1_nOe.6.fid
2 Solvent C6D6
3 Temperature 298.2
4 Number of Scans 64
5 Receiver Gain 32.0
6 Relaxation Delay 2.0000
7 Pulse Width 15.0000
8 Spectrometer Frequency 400.13
9 Nucleus 1H
Me
Me Ph
Si
H
H
2.169
2.04%
1.76%
0.54%
1.76
100.00
2.04
0.54
8.5 8.0 7.5 7.0 6.5 6.0 5.5 5.0 4.5 4.0 3.5 3.0 2.5 2.0 1.5 1.0 0.5 0.0
f1 (ppm)

Parameter	Value
1 Title	WBR04292F1_nOe.11.fid
2 Solvent	C6D6
3 Temperature	298.1
4 Number of Scans	64
5 Receiver Gain	28.5
6 Relaxation Delay	2.0000
7 Pulse Width	15.0000
8 Spectrometer Frequency	400.13
9 Nucleus	1H

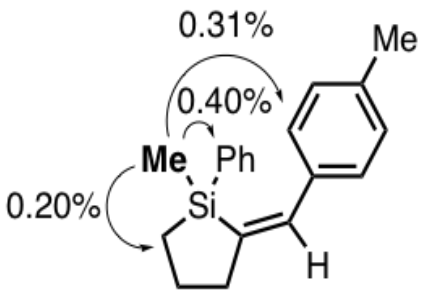

2.169

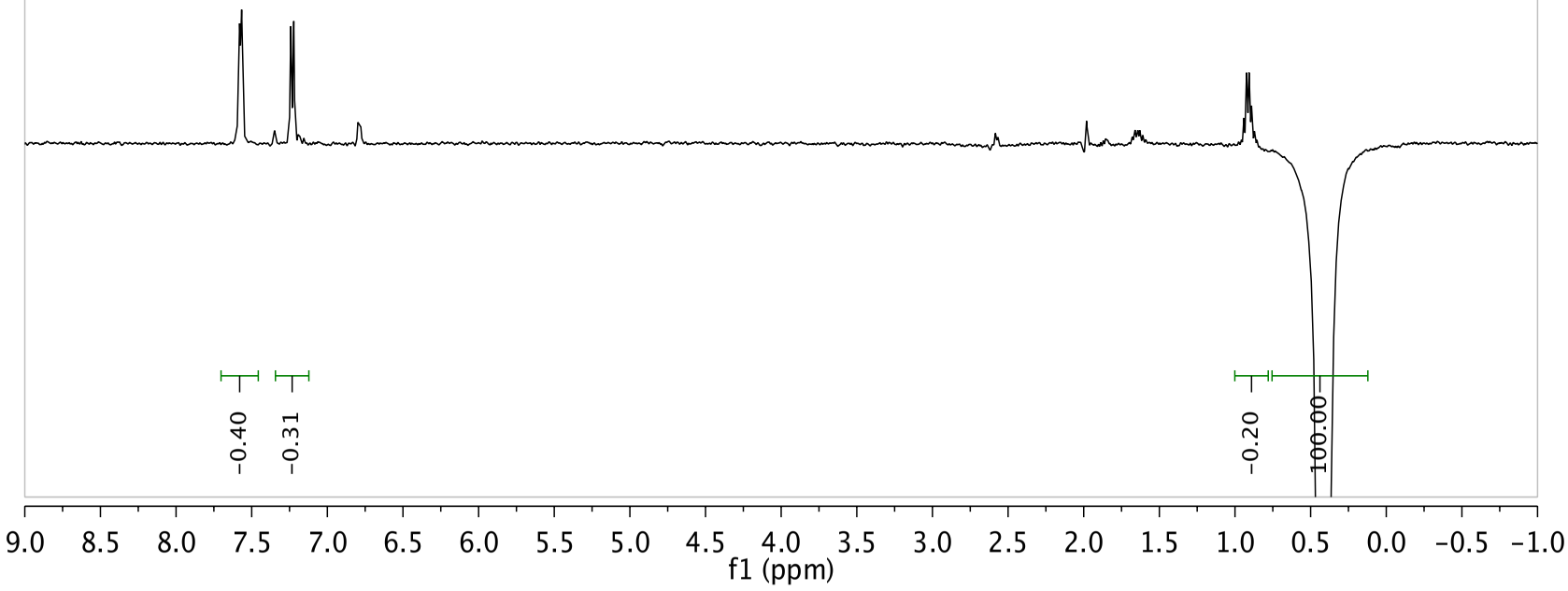

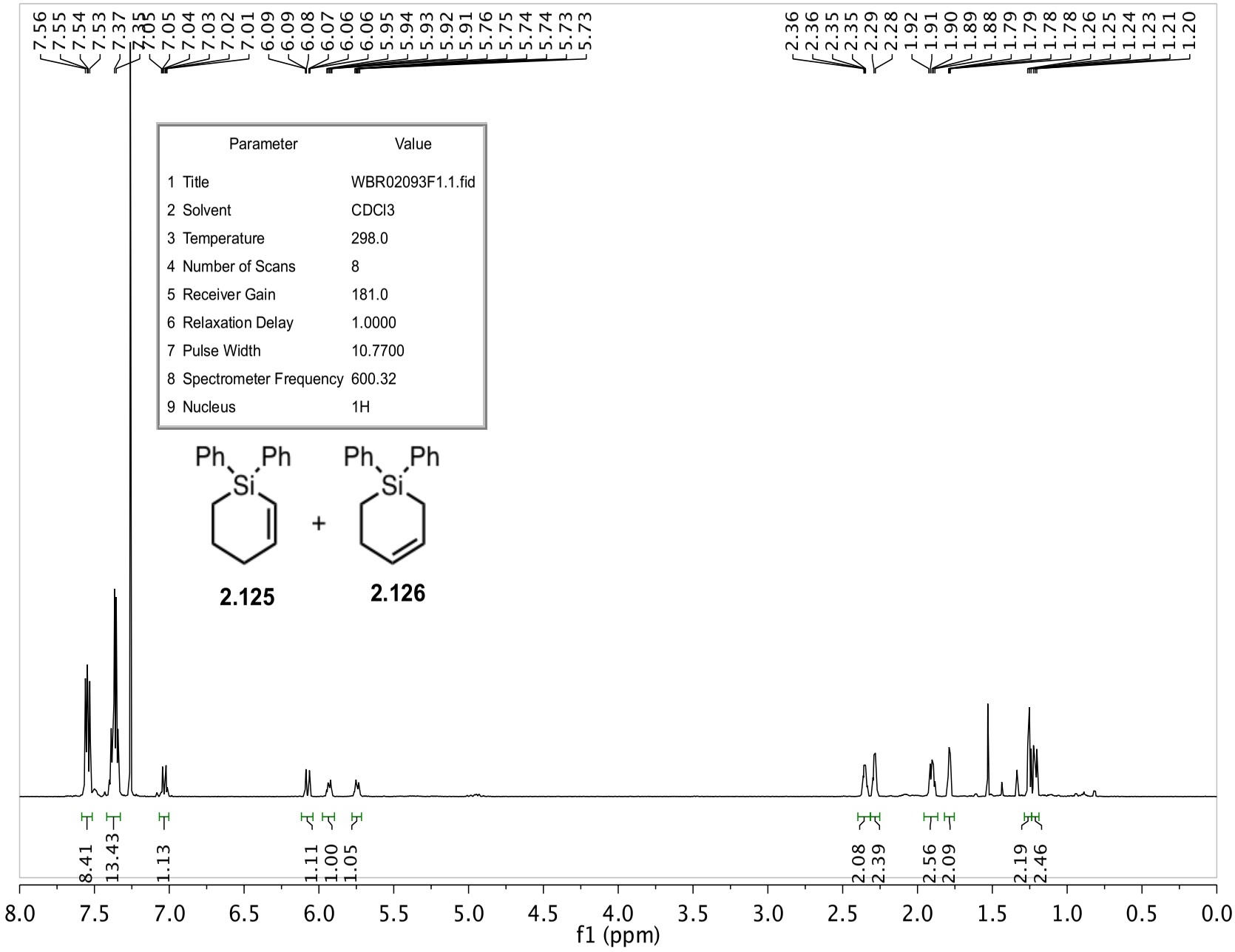
7.56 7.55 7.54 7.53 7.37 7.35 7.05 7.04 7.03 7.02 7.01 6.09 6.09 6.08 6.07 6.06 6.06 5.95 5.94 5.93 5.92 5.91 5.76 5.75 5.74 5.74 5.73 5.73
2.36 2.36 2.35 2.35 2.29 2.28 1.92 1.91 1.90 1.89 1.88 1.79 1.79 1.78 1.78 1.26 1.25 1.24 1.23 1.21 1.20
Parameter Value
1 Title WBR02093F1.1.fid
2 Solvent CDCl3
3 Temperature 298.0
4 Number of Scans 8
5 Receiver Gain 181.0
6 Relaxation Delay 1.0000
7 Pulse Width 10.7700
8 Spectrometer Frequency 600.32
9 Nucleus 1H
Ph Ph Si
+
2.125
2.126
8.41 13.43 1.13 1.11 1.00 1.05 2.08 2.39 2.56 2.09 2.19 2.46
8.0 7.5 7.0 6.5 6.0 5.5 5.0 4.5 4.0 3.5 3.0 2.5 2.0 1.5 1.0 0.5 0.0
f1 (ppm)

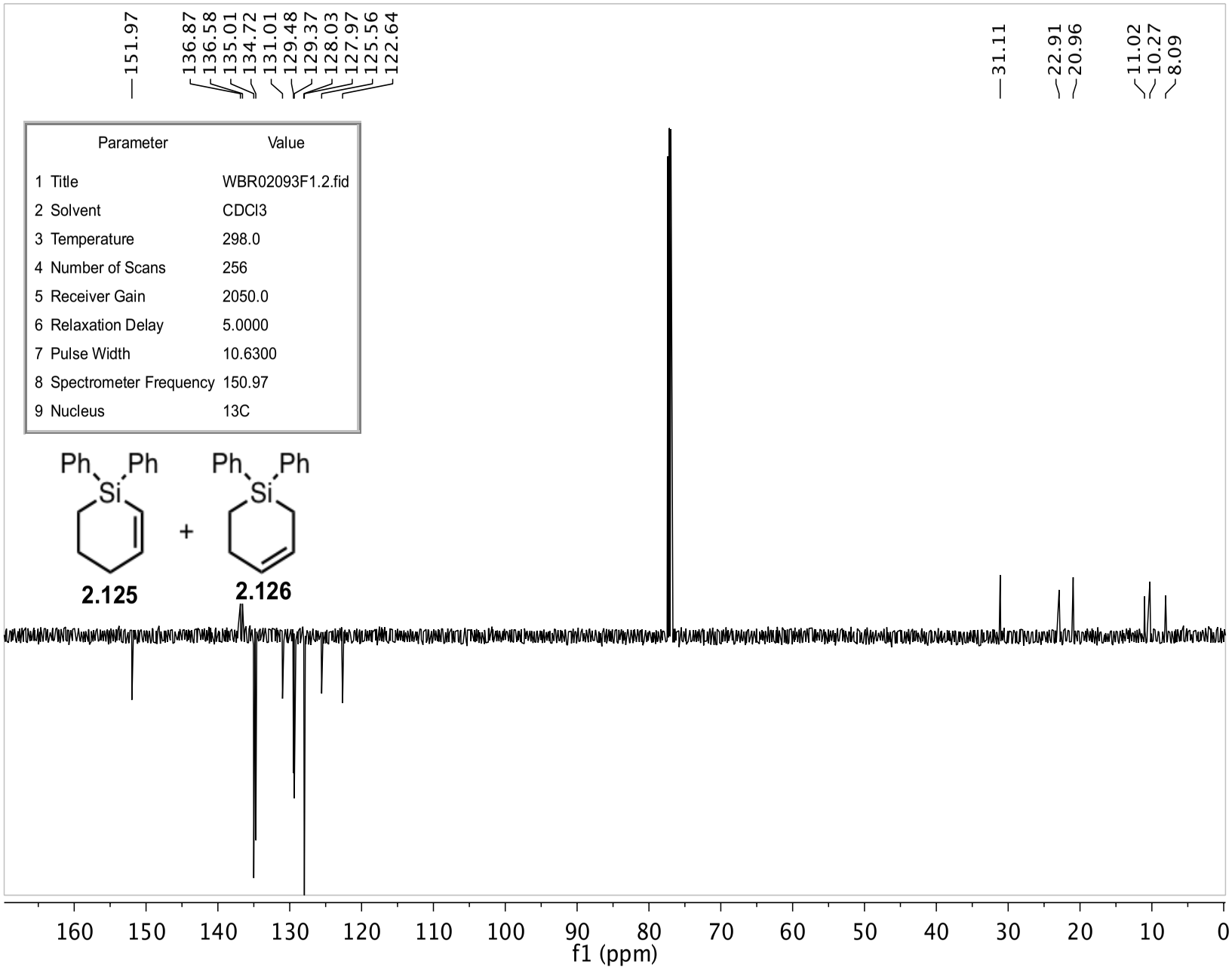
151.97
136.87
136.58
135.01
134.72
131.01
129.48
129.37
128.03
127.97
125.56
122.64
31.11
22.91
20.96
11.02
10.27
8.09
Parameter Value
1 Title WBR02093F1.2.fid
2 Solvent CDCl3
3 Temperature 298.0
4 Number of Scans 256
5 Receiver Gain 2050.0
6 Relaxation Delay 5.0000
7 Pulse Width 10.6300
8 Spectrometer Frequency 150.97
9 Nucleus 13C
Ph Ph
Si
+
2.125
2.126
160 150 140 130 120 110 100 90 80 70 60 50 40 30 20 10 0
f1 (ppm)

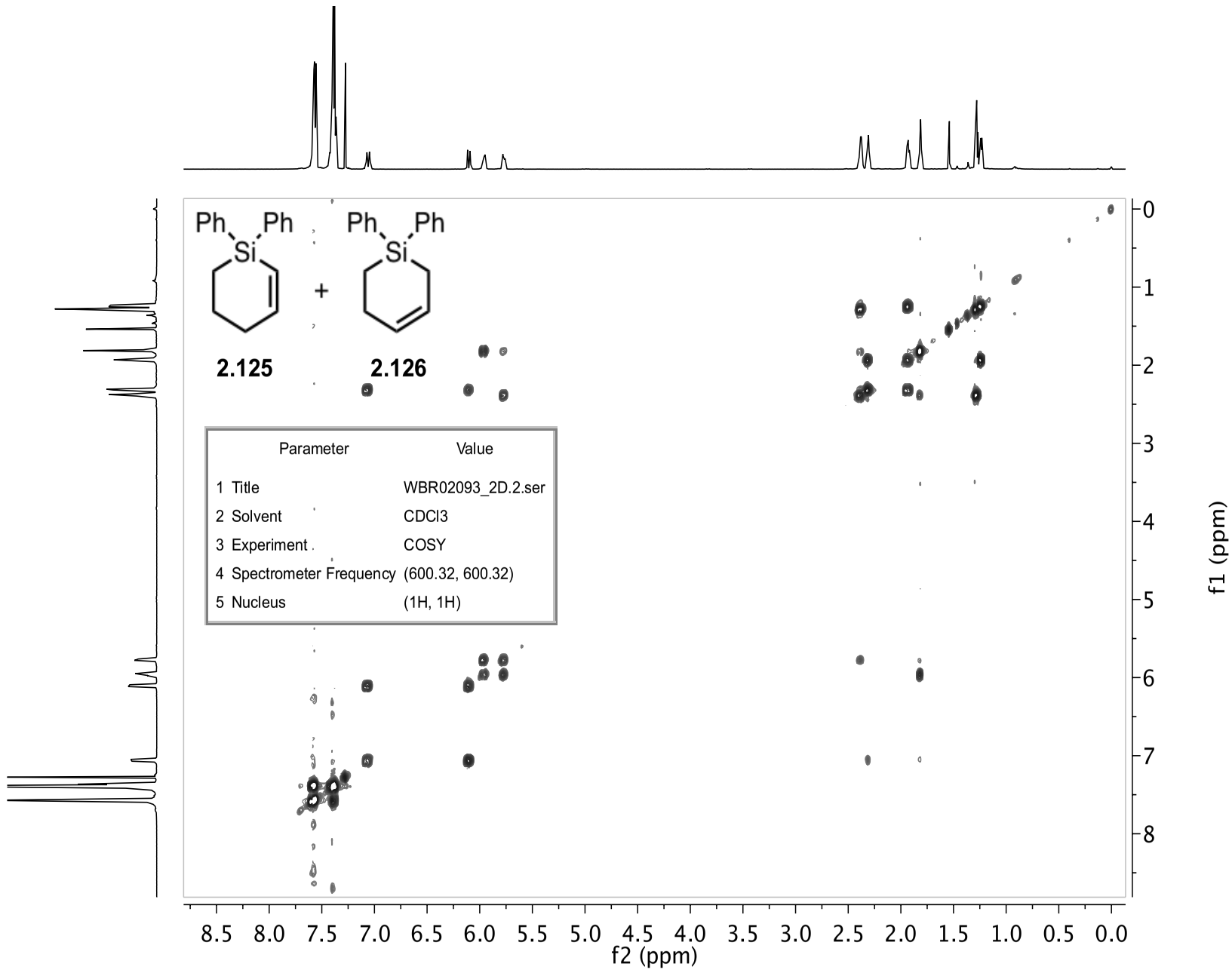
Ph Ph
Si
+
Ph Ph
Si
2.125
2.126
Parameter Value
1 Title WBR02093_2D.2.ser
2 Solvent CDCl3
3 Experiment COSY
4 Spectrometer Frequency (600.32, 600.32)
5 Nucleus (1H, 1H)
8.5 8.0 7.5 7.0 6.5 6.0 5.5 5.0 4.5 4.0 3.5 3.0 2.5 2.0 1.5 1.0 0.5 0.0
f2 (ppm)
0 1 2 3 4 5 6 7 8
f1 (ppm)

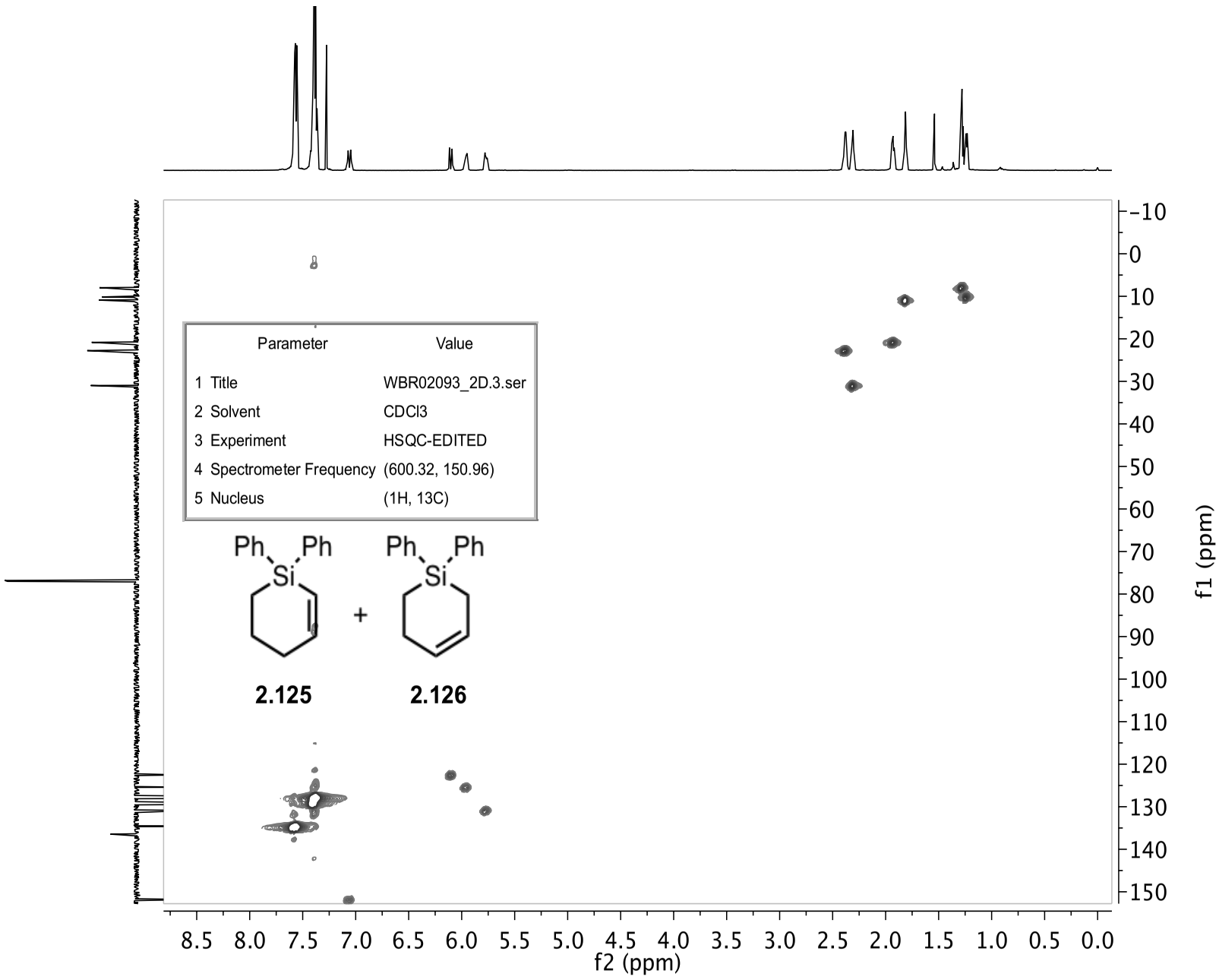
Parameter Value
1 Title WBR02093_2D.3.ser
2 Solvent CDCl3
3 Experiment HSQC-EDITED
4 Spectrometer Frequency (600.32, 150.96)
5 Nucleus (1H, 13C)
Ph Ph
Si
+
2.125
2.126
f2 (ppm)
f1 (ppm)

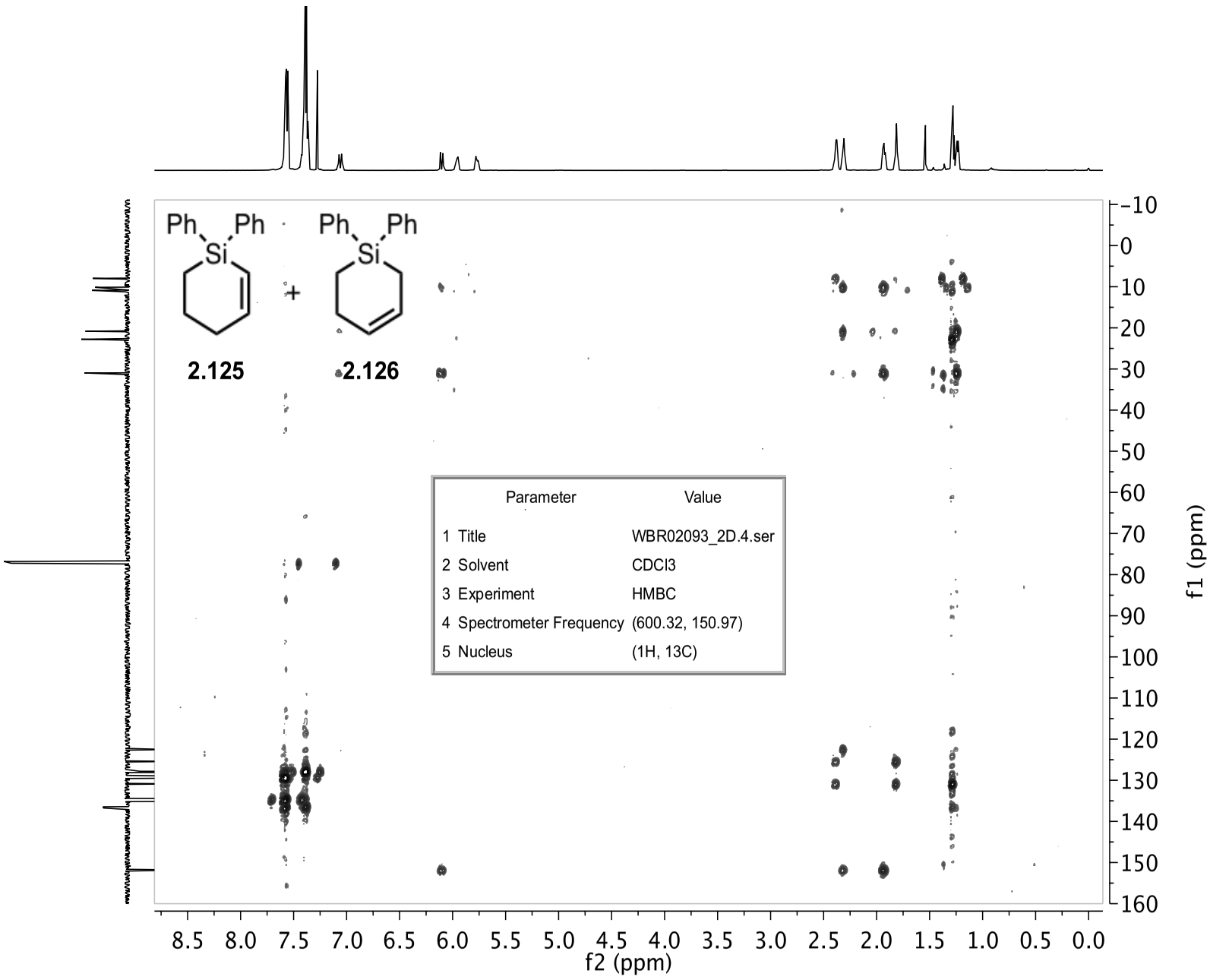
Ph
Ph
Si
+
2.125
2.126
Parameter
Value
1 Title
WBR02093_2D.4.ser
2 Solvent
CDCl3
3 Experiment
HMBC
4 Spectrometer Frequency
(600.32, 150.97)
5 Nucleus
(1H, 13C)
f2 (ppm)
f1 (ppm)

Appendix D

Spectral Data for Chapter 3

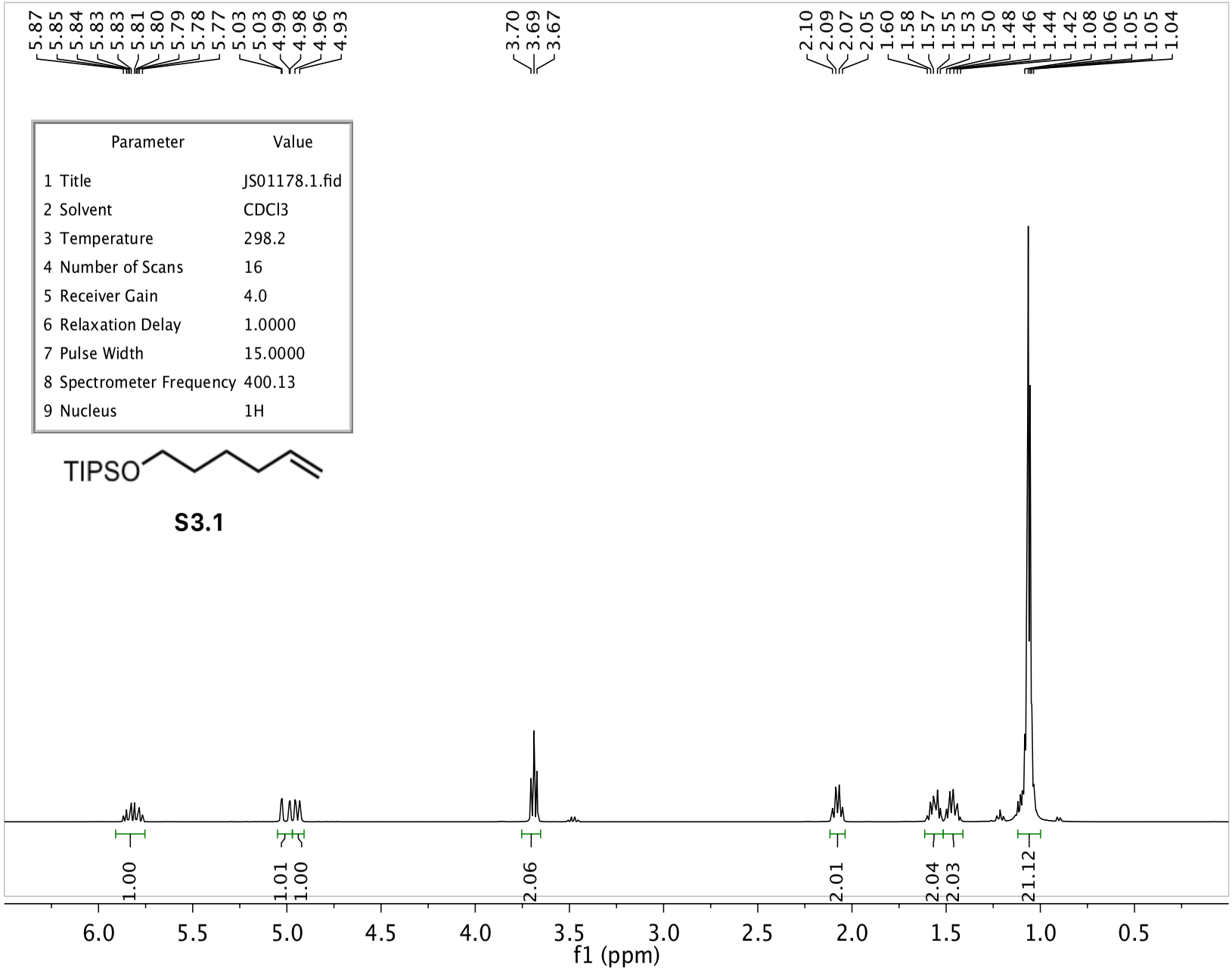
5.87
5.85
5.84
5.83
5.83
5.81
5.80
5.79
5.78
5.77
5.03
5.03
4.99
4.98
4.96
4.93
3.70
3.69
3.67
2.10
2.09
2.07
2.05
1.60
1.58
1.57
1.55
1.53
1.50
1.48
1.46
1.44
1.42
1.08
1.06
1.05
1.05
1.04
Parameter Value
1 Title JS01178.1.fid
2 Solvent CDCl3
3 Temperature 298.2
4 Number of Scans 16
5 Receiver Gain 4.0
6 Relaxation Delay 1.0000
7 Pulse Width 15.0000
8 Spectrometer Frequency 400.13
9 Nucleus 1H
TIPSO
S3.1
1.00
1.01
1.00
2.06
2.01
2.04
2.03
21.12
6.0
5.5
5.0
4.5
4.0
3.5
3.0
2.5
2.0
1.5
1.0
0.5
f1 (ppm)

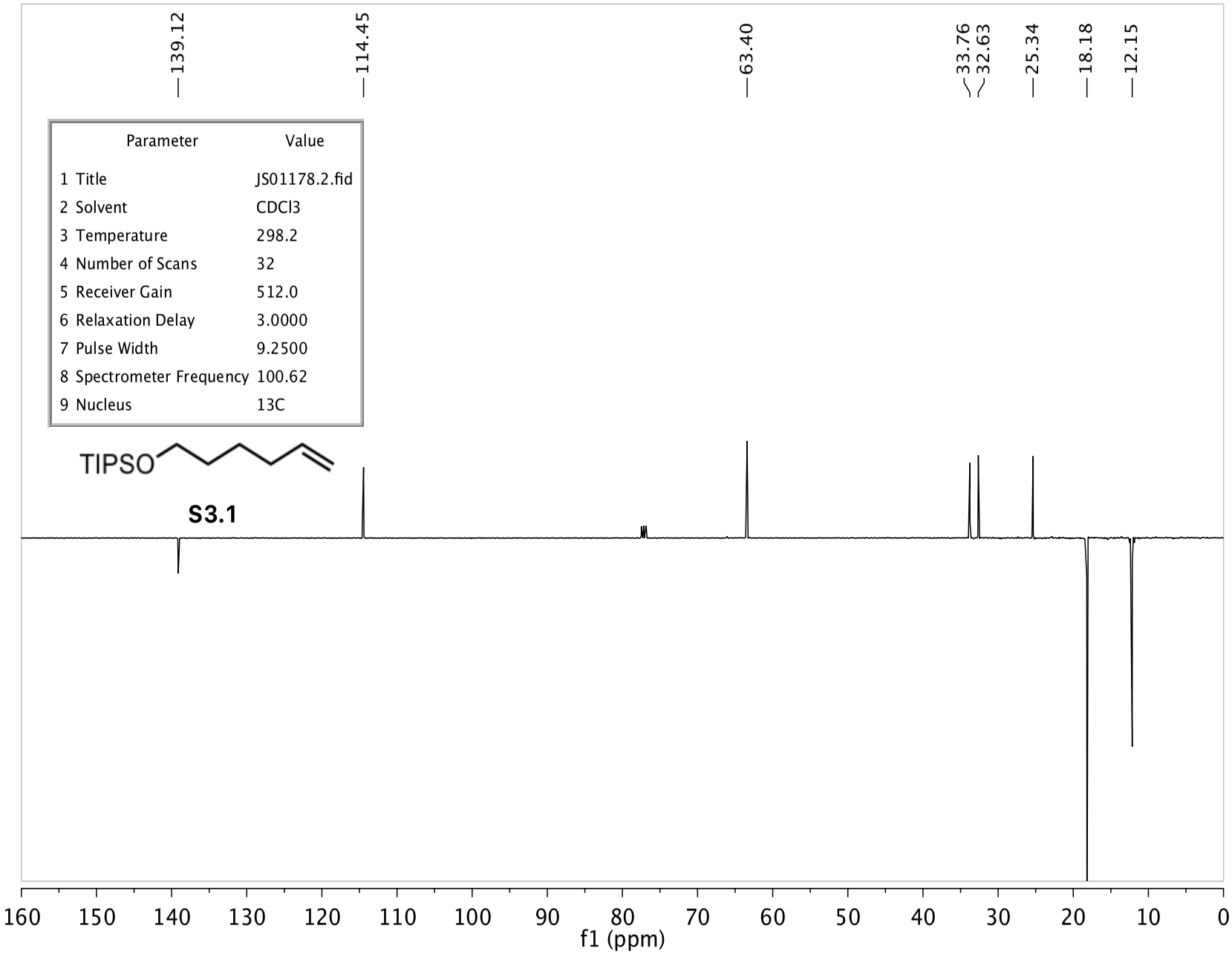
139.12
114.45
63.40
33.76
32.63
25.34
18.18
12.15
Parameter Value
1 Title JS01178.2.fid
2 Solvent CDCl3
3 Temperature 298.2
4 Number of Scans 32
5 Receiver Gain 512.0
6 Relaxation Delay 3.0000
7 Pulse Width 9.2500
8 Spectrometer Frequency 100.62
9 Nucleus 13C
TIPSO
S3.1
160 150 140 130 120 110 100 90 80 70 60 50 40 30 20 10 0
f1 (ppm)

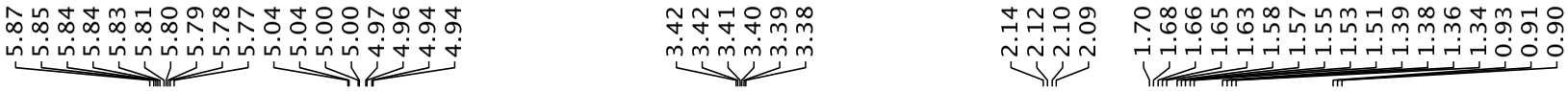

	Parameter	Value
1	Title	WBR03127F1.2.fid
2	Solvent	CDCl3
3	Temperature	298.1
4	Number of Scans	16
5	Receiver Gain	8.0
6	Relaxation Delay	1.0000
7	Pulse Width	15.0000
8	Spectrometer Frequency	400.13
9	Nucleus	1H

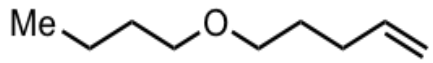

S3.2

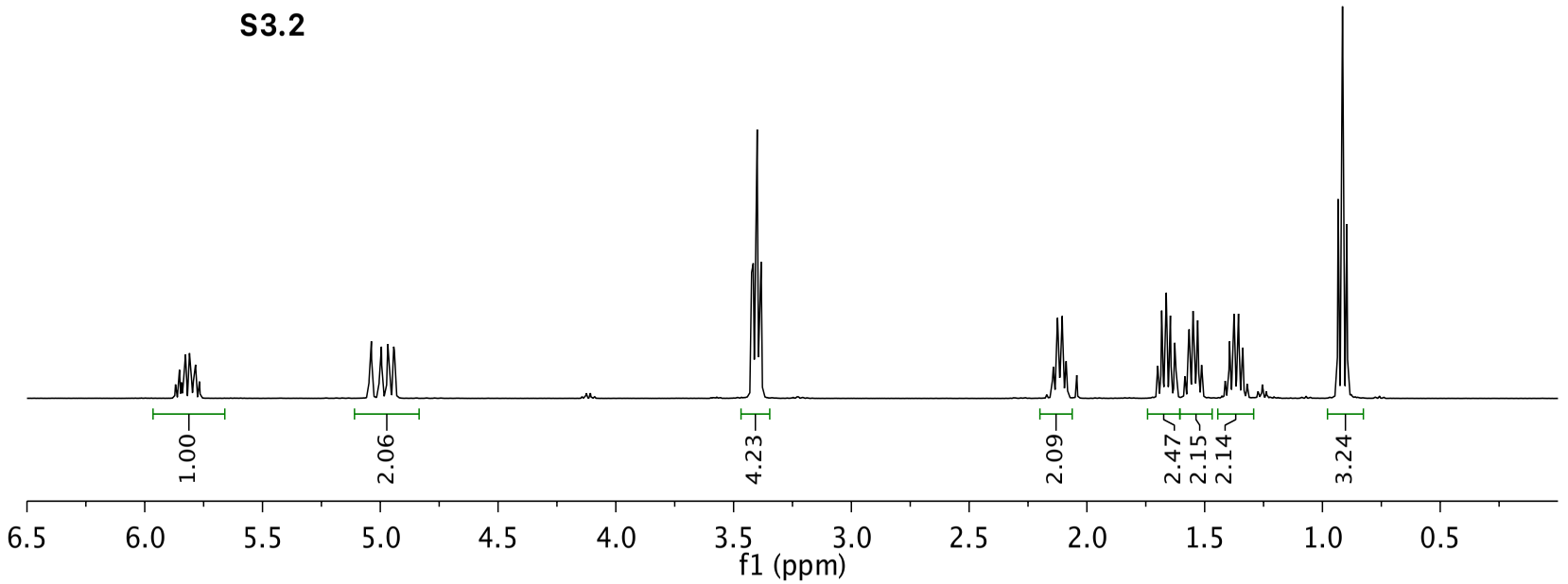

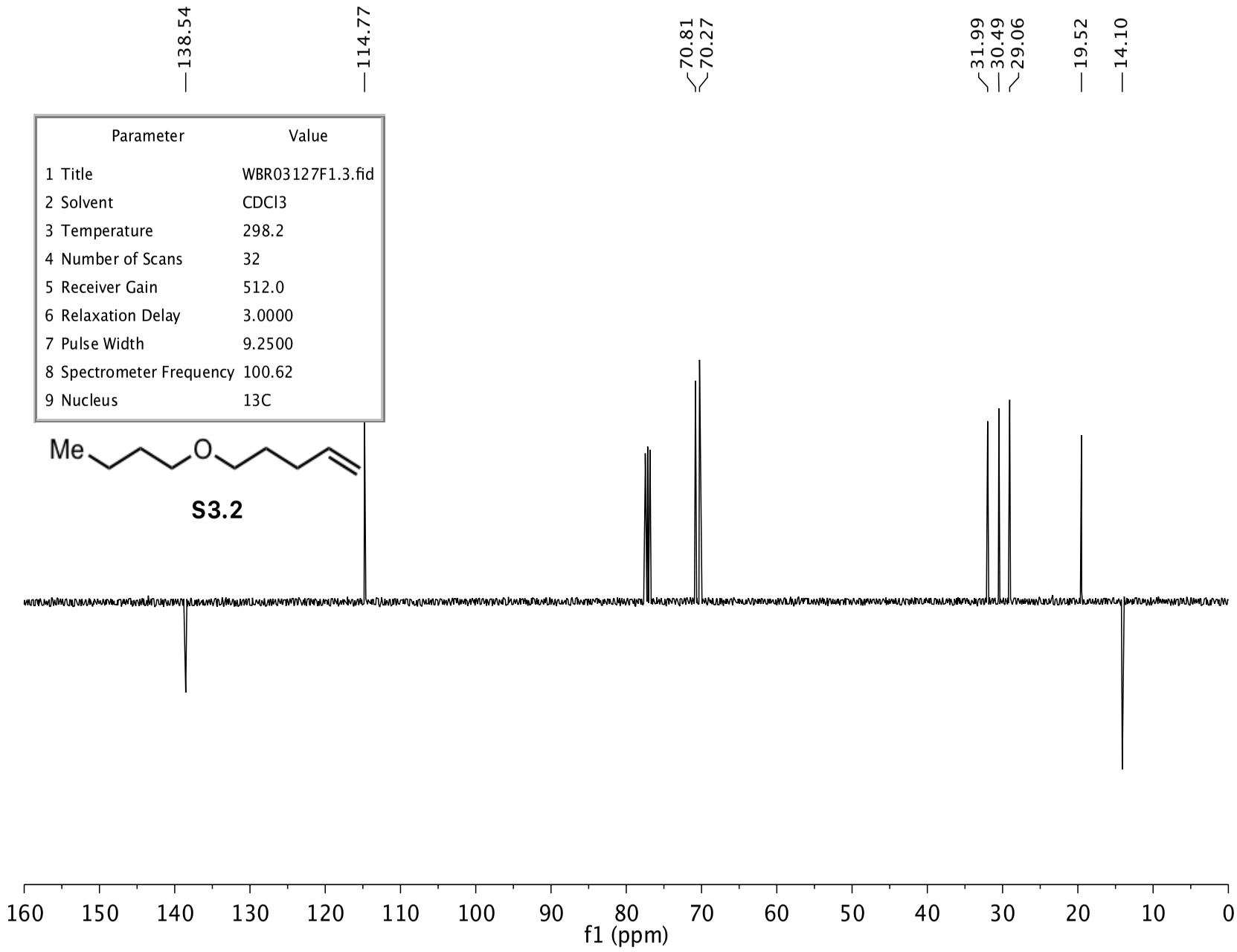
138.54
114.77
70.81
70.27
31.99
30.49
29.06
19.52
14.10
Parameter Value
1 Title WBR03127F1.3.fid
2 Solvent CDCl3
3 Temperature 298.2
4 Number of Scans 32
5 Receiver Gain 512.0
6 Relaxation Delay 3.0000
7 Pulse Width 9.2500
8 Spectrometer Frequency 100.62
9 Nucleus 13C
Me
O
S3.2
160 150 140 130 120 110 100 90 80 70 60 50 40 30 20 10 0
f1 (ppm)

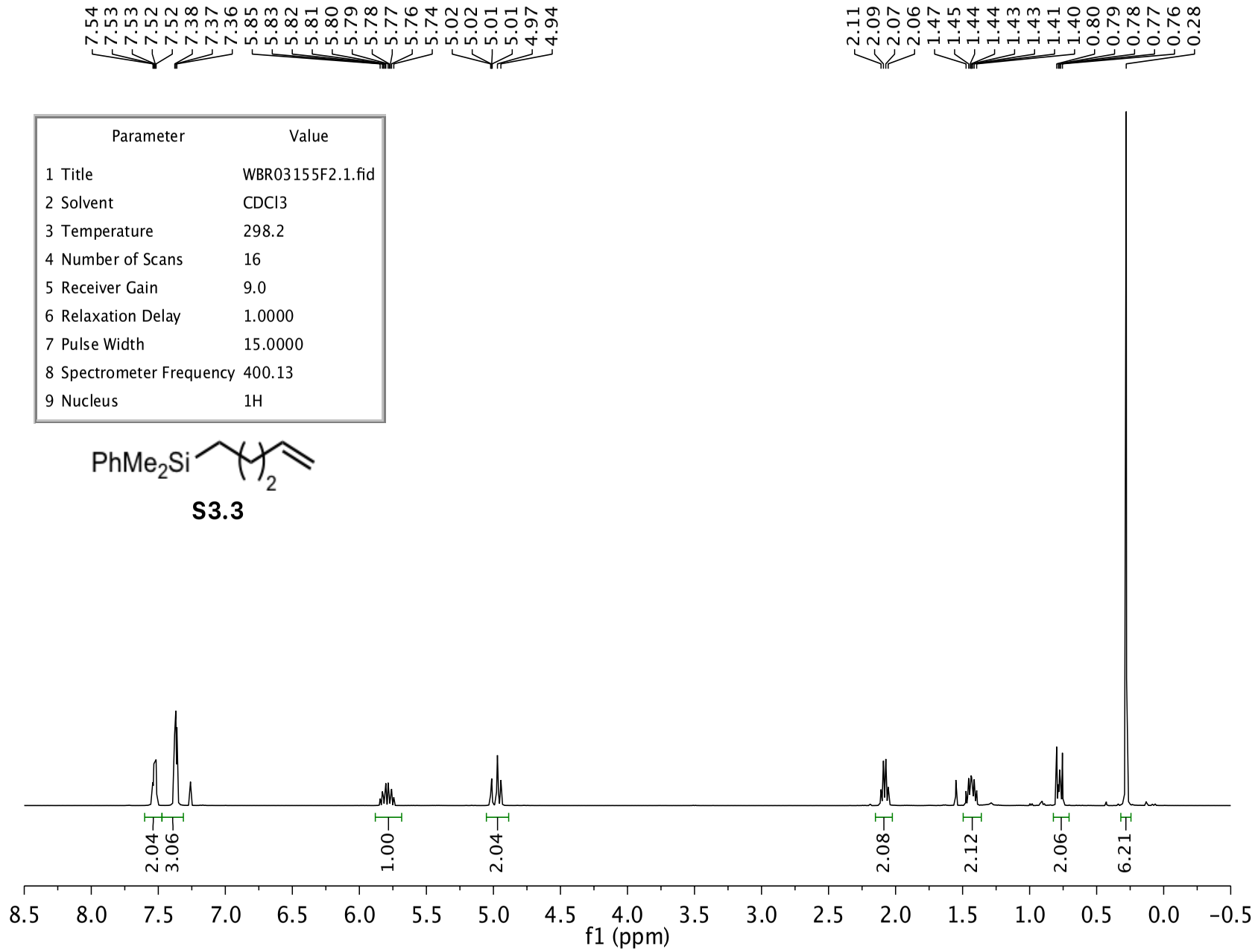
7.54 7.53 7.53 7.52 7.52 7.38 7.37 7.36 5.85 5.83 5.82 5.81 5.80 5.79 5.78 5.77 5.76 5.74 5.02 5.02 5.01 5.01 4.97 4.94
2.11 2.09 2.07 2.06 1.47 1.45 1.44 1.44 1.43 1.43 1.41 1.40 0.80 0.79 0.78 0.77 0.76 0.28
Parameter Value
1 Title WBR03155F2.1.fid
2 Solvent CDCl3
3 Temperature 298.2
4 Number of Scans 16
5 Receiver Gain 9.0
6 Relaxation Delay 1.0000
7 Pulse Width 15.0000
8 Spectrometer Frequency 400.13
9 Nucleus 1H
PhMe2Si
2
S3.3
2.04 3.06 1.00 2.04 2.08 2.12 2.06 6.21
8.5 8.0 7.5 7.0 6.5 6.0 5.5 5.0 4.5 4.0 3.5 3.0 2.5 2.0 1.5 1.0 0.5 0.0 -0.5
f1 (ppm)

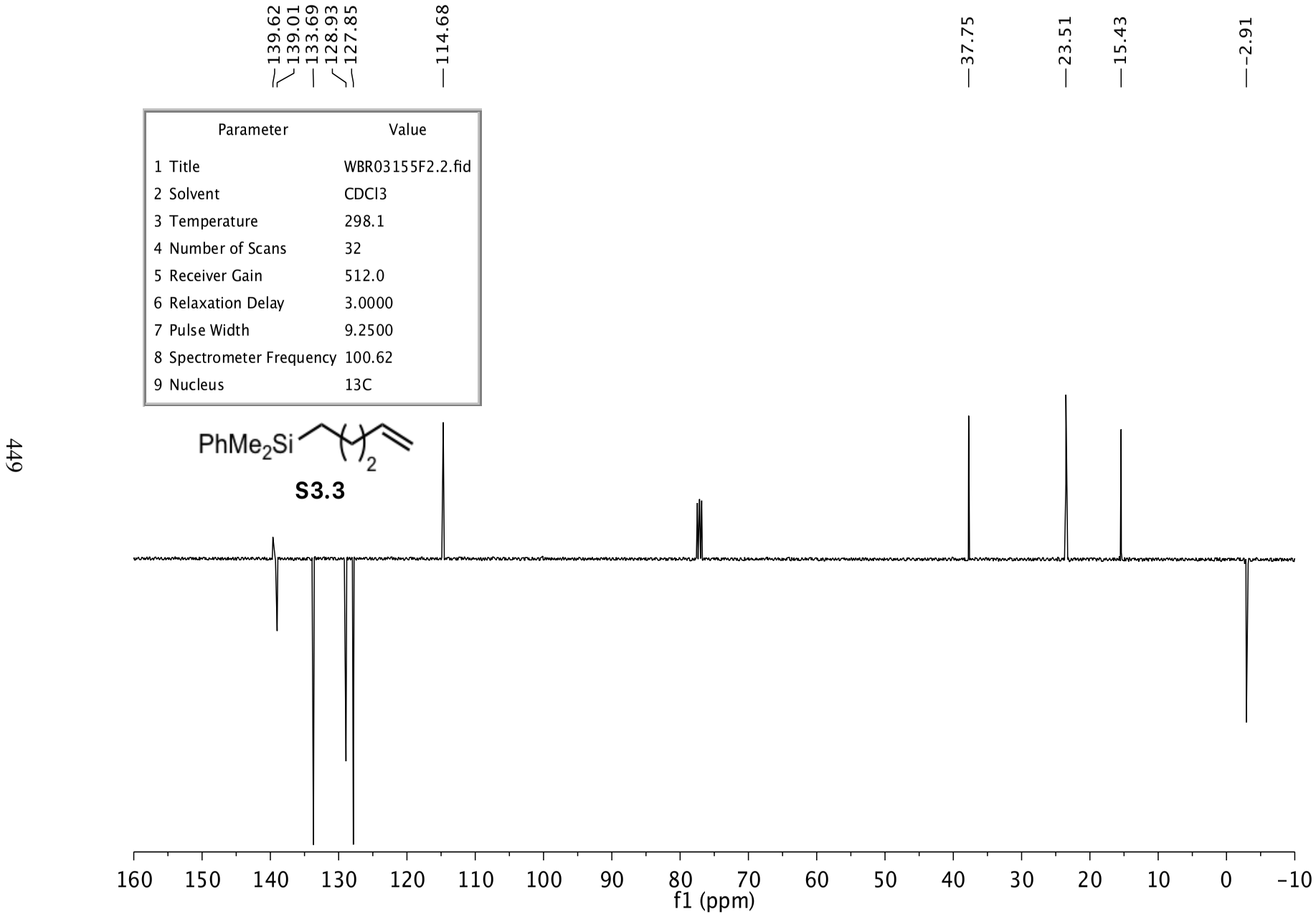
139.62
139.01
133.69
128.93
127.85
114.68
37.75
23.51
15.43
-2.91
Parameter Value
1 Title WBR03155F2.2.fid
2 Solvent CDCl3
3 Temperature 298.1
4 Number of Scans 32
5 Receiver Gain 512.0
6 Relaxation Delay 3.0000
7 Pulse Width 9.2500
8 Spectrometer Frequency 100.62
9 Nucleus 13C
PhMe2Si
2
S3.3
160 150 140 130 120 110 100 90 80 70 60 50 40 30 20 10 0 -10
f1 (ppm)

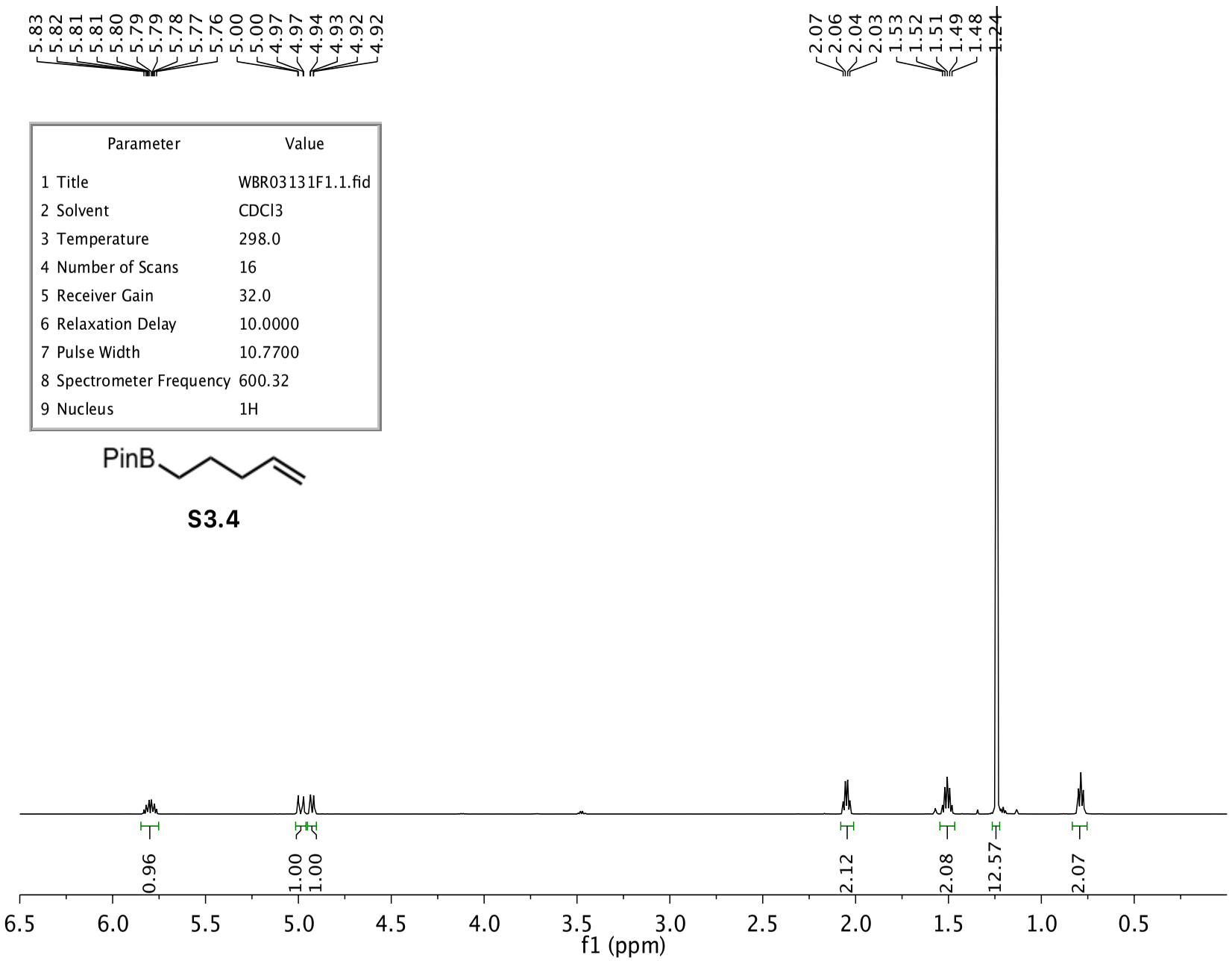
5.83
5.82
5.81
5.81
5.80
5.79
5.79
5.78
5.77
5.76
5.00
5.00
4.97
4.97
4.94
4.93
4.92
4.92
2.07
2.06
2.04
2.03
1.53
1.52
1.51
1.49
1.48
1.24
Parameter Value
1 Title WBR03131F1.1.fid
2 Solvent CDCl3
3 Temperature 298.0
4 Number of Scans 16
5 Receiver Gain 32.0
6 Relaxation Delay 10.0000
7 Pulse Width 10.7700
8 Spectrometer Frequency 600.32
9 Nucleus 1H
PinB
0.96
1.00
1.00
2.12
2.08
12.57
2.07
6.5
6.0
5.5
5.0
4.5
4.0
3.5
3.0
2.5
2.0
1.5
1.0
0.5
f1 (ppm)

S3.4

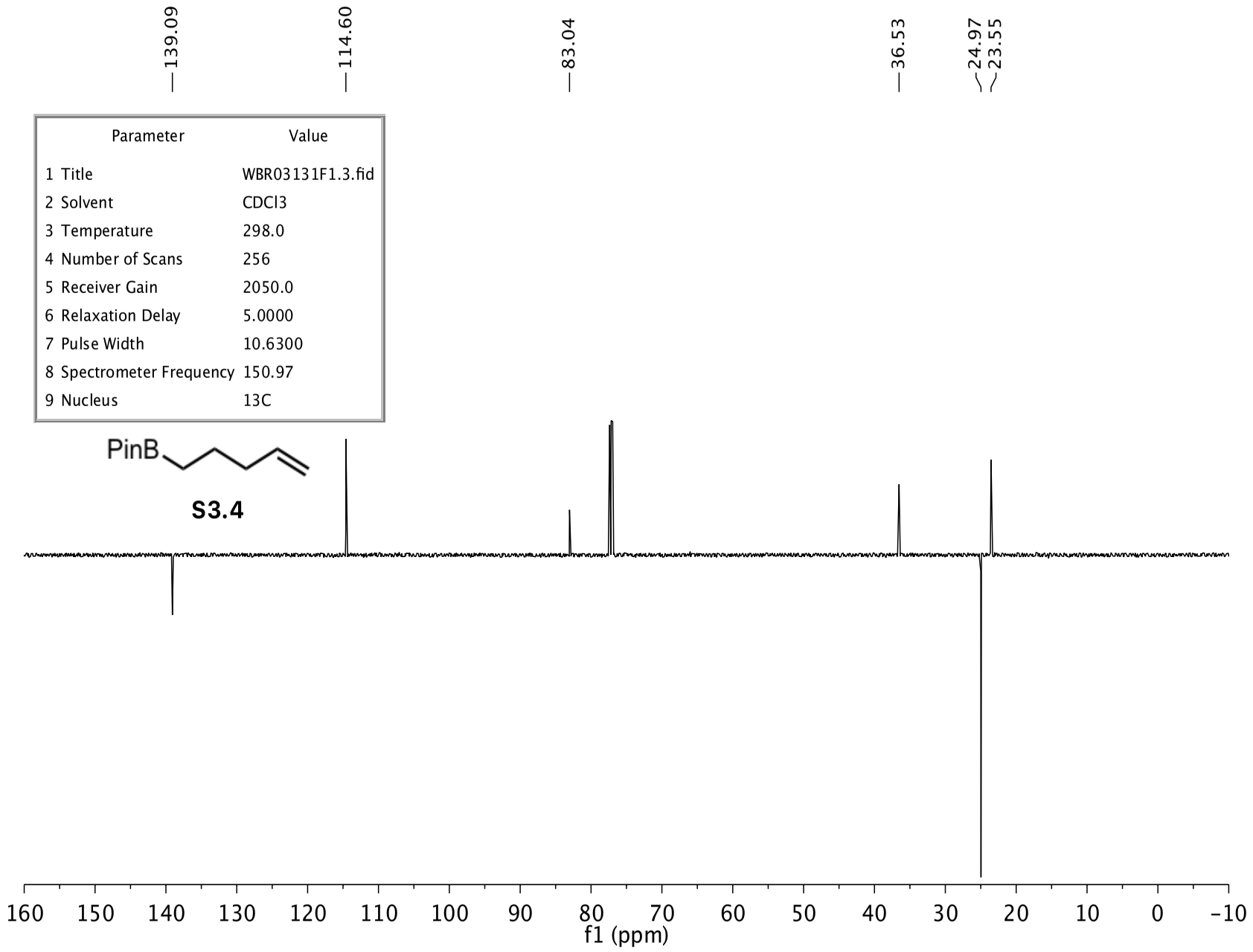
139.09
114.60
83.04
36.53
24.97
23.55
Parameter Value
1 Title WBR03131F1.3.fid
2 Solvent CDCl3
3 Temperature 298.0
4 Number of Scans 256
5 Receiver Gain 2050.0
6 Relaxation Delay 5.0000
7 Pulse Width 10.6300
8 Spectrometer Frequency 150.97
9 Nucleus 13C
PinB
S3.4
160 150 140 130 120 110 100 90 80 70 60 50 40 30 20 10 0 -10
f1 (ppm)

34.10

Parameter	Value
1 Title	WBR03131F1.2.fid
2 Solvent	CDCl3
3 Temperature	298.0
4 Number of Scans	128
5 Receiver Gain	322.0
6 Relaxation Delay	1.0000
7 Pulse Width	11.0000
8 Spectrometer Frequency	192.61
9 Nucleus	11B

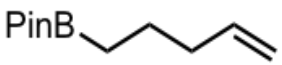

S3.4

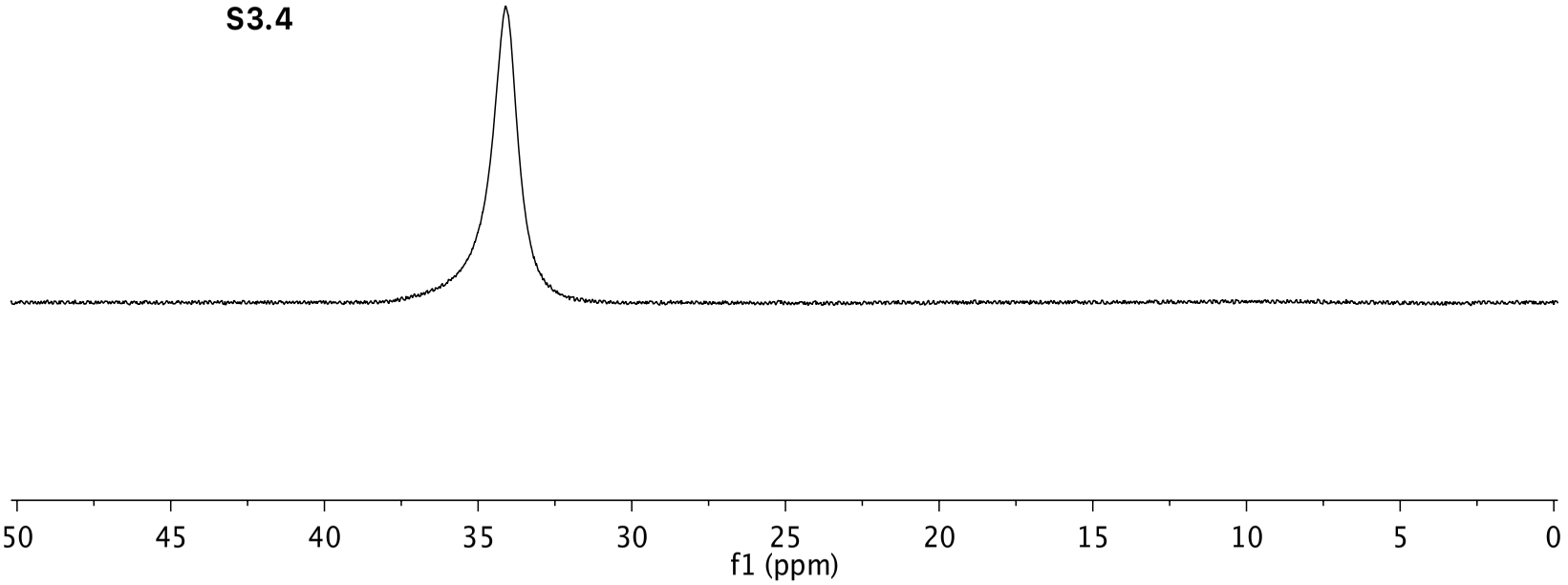

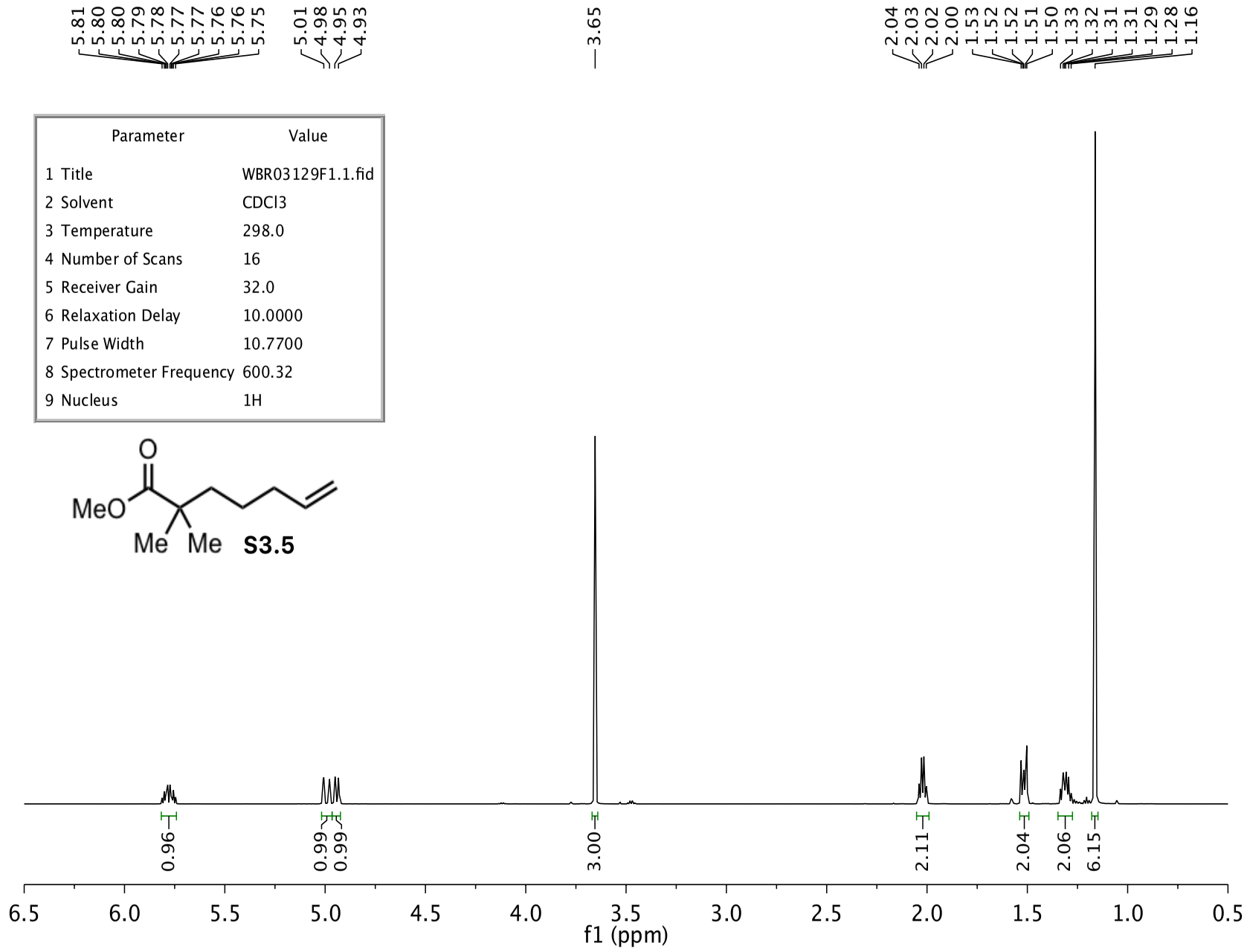
5.81
5.80
5.80
5.79
5.78
5.77
5.77
5.76
5.76
5.75
5.01
4.98
4.95
4.93
3.65
2.04
2.03
2.02
2.00
1.53
1.52
1.52
1.51
1.50
1.33
1.32
1.31
1.31
1.29
1.28
1.16
Parameter Value
1 Title WBR03129F1.1.fid
2 Solvent CDCl3
3 Temperature 298.0
4 Number of Scans 16
5 Receiver Gain 32.0
6 Relaxation Delay 10.0000
7 Pulse Width 10.7700
8 Spectrometer Frequency 600.32
9 Nucleus 1H
O
MeO
Me Me
S3.5
0.96
0.99
0.99
3.00
2.11
2.04
2.06
6.15
6.5
6.0
5.5
5.0
4.5
4.0
3.5
3.0
2.5
2.0
1.5
1.0
0.5
f1 (ppm)

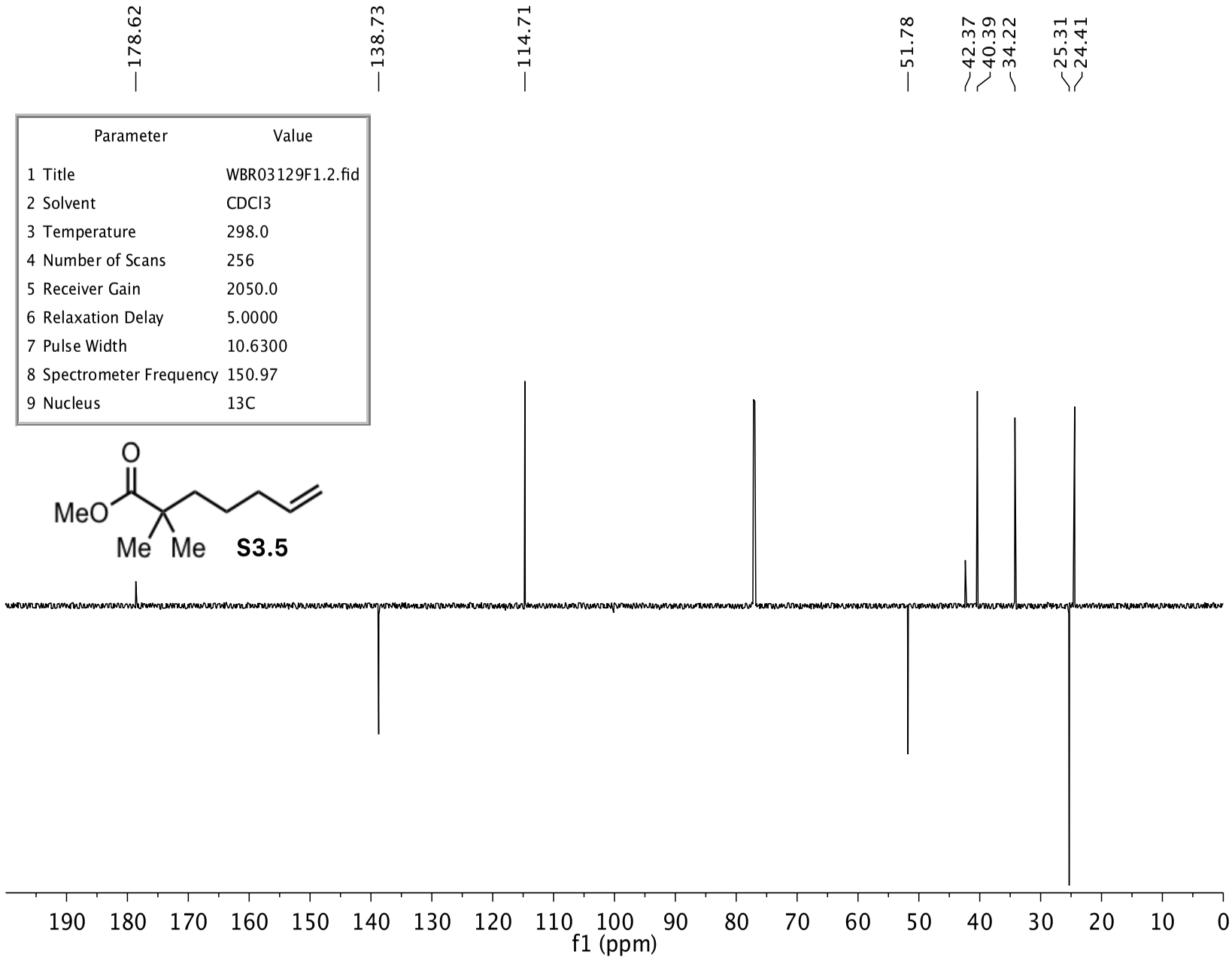
178.62
138.73
114.71
51.78
42.37
40.39
34.22
25.31
24.41
Parameter Value
1 Title WBR03129F1.2.fid
2 Solvent CDCl3
3 Temperature 298.0
4 Number of Scans 256
5 Receiver Gain 2050.0
6 Relaxation Delay 5.0000
7 Pulse Width 10.6300
8 Spectrometer Frequency 150.97
9 Nucleus 13C
O
MeO
Me Me
S3.5
190 180 170 160 150 140 130 120 110 100 90 80 70 60 50 40 30 20 10 0
f1 (ppm)

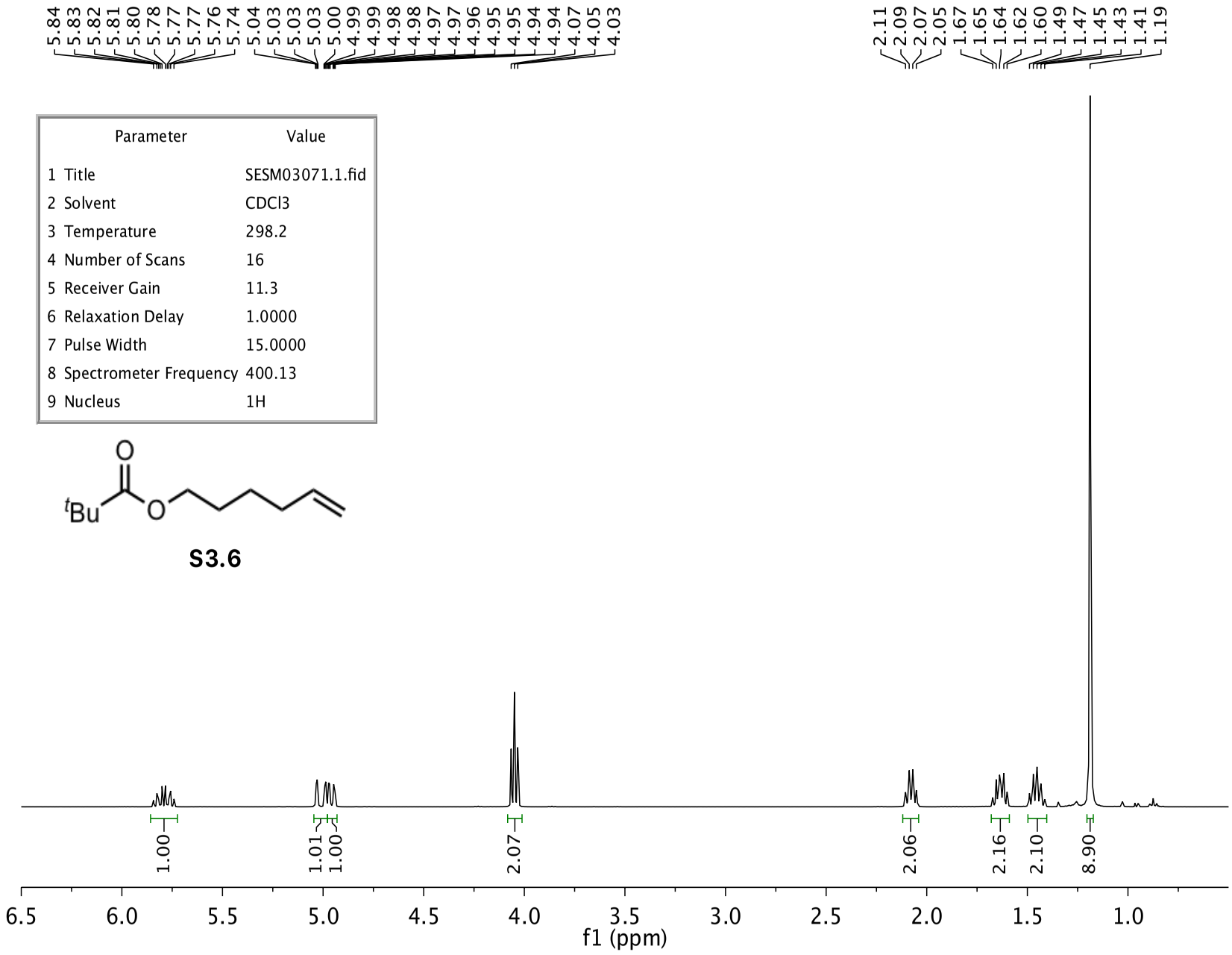
5.84 5.83 5.82 5.81 5.80 5.78 5.77 5.77 5.76 5.74
5.04 5.03 5.03 5.03 5.00 4.99 4.99 4.98 4.98 4.97 4.97 4.96 4.95 4.95 4.94 4.94 4.07 4.05 4.03
2.11 2.09 2.07 2.05 1.67 1.65 1.64 1.62 1.60 1.49 1.47 1.45 1.43 1.41 1.19
Parameter Value
1 Title SESM03071.1.fid
2 Solvent CDCl3
3 Temperature 298.2
4 Number of Scans 16
5 Receiver Gain 11.3
6 Relaxation Delay 1.0000
7 Pulse Width 15.0000
8 Spectrometer Frequency 400.13
9 Nucleus 1H
O
tBu
O
S3.6
1.00 1.01 1.00 2.07 2.06 2.16 2.10 8.90
6.5 6.0 5.5 5.0 4.5 4.0 3.5 3.0 2.5 2.0 1.5 1.0
f1 (ppm)

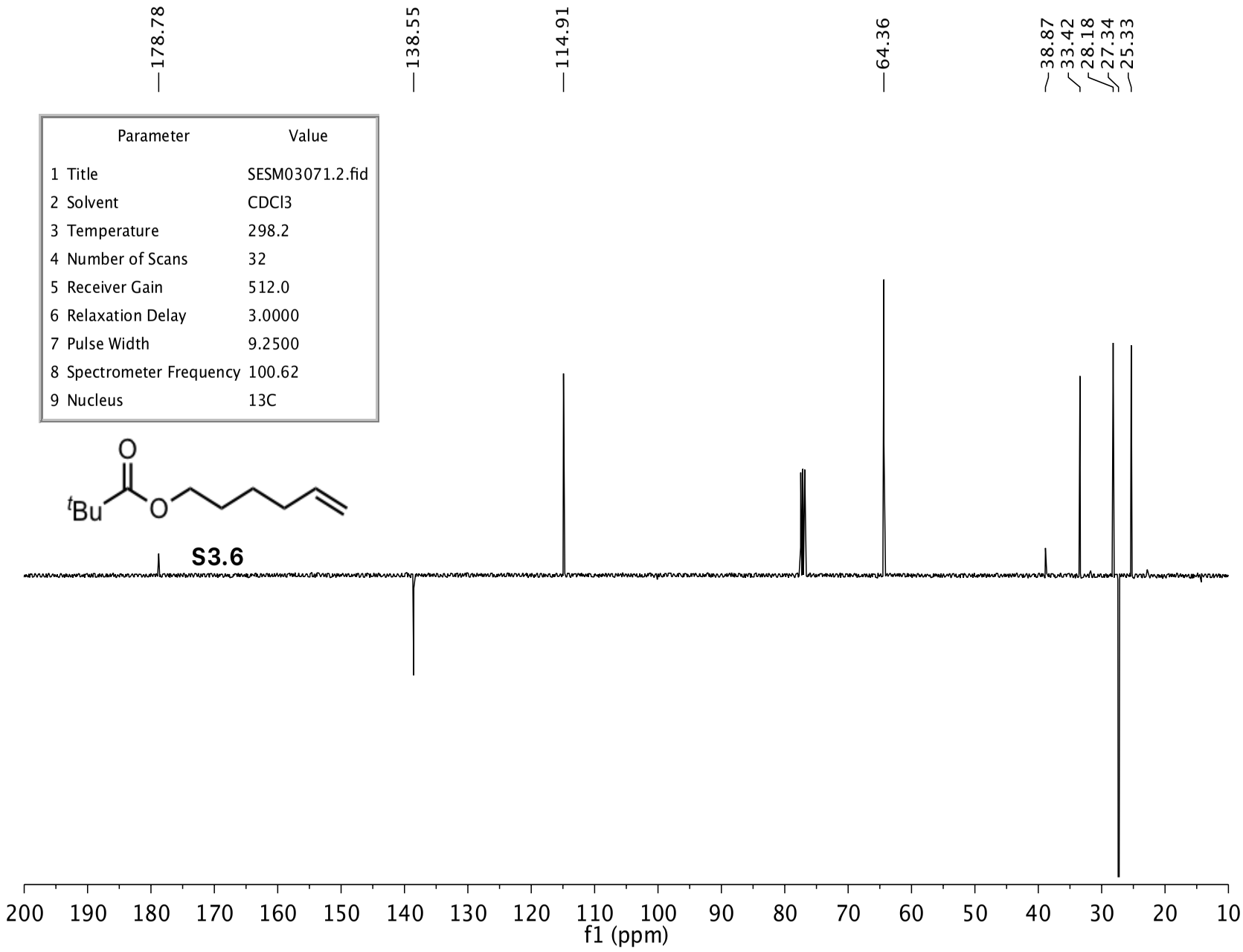
178.78
138.55
114.91
64.36
38.87
33.42
28.18
27.34
25.33
Parameter Value
1 Title SESM03071.2.fid
2 Solvent CDCl3
3 Temperature 298.2
4 Number of Scans 32
5 Receiver Gain 512.0
6 Relaxation Delay 3.0000
7 Pulse Width 9.2500
8 Spectrometer Frequency 100.62
9 Nucleus 13C
O
tBu
O
S3.6
200 190 180 170 160 150 140 130 120 110 100 90 80 70 60 50 40 30 20 10
f1 (ppm)

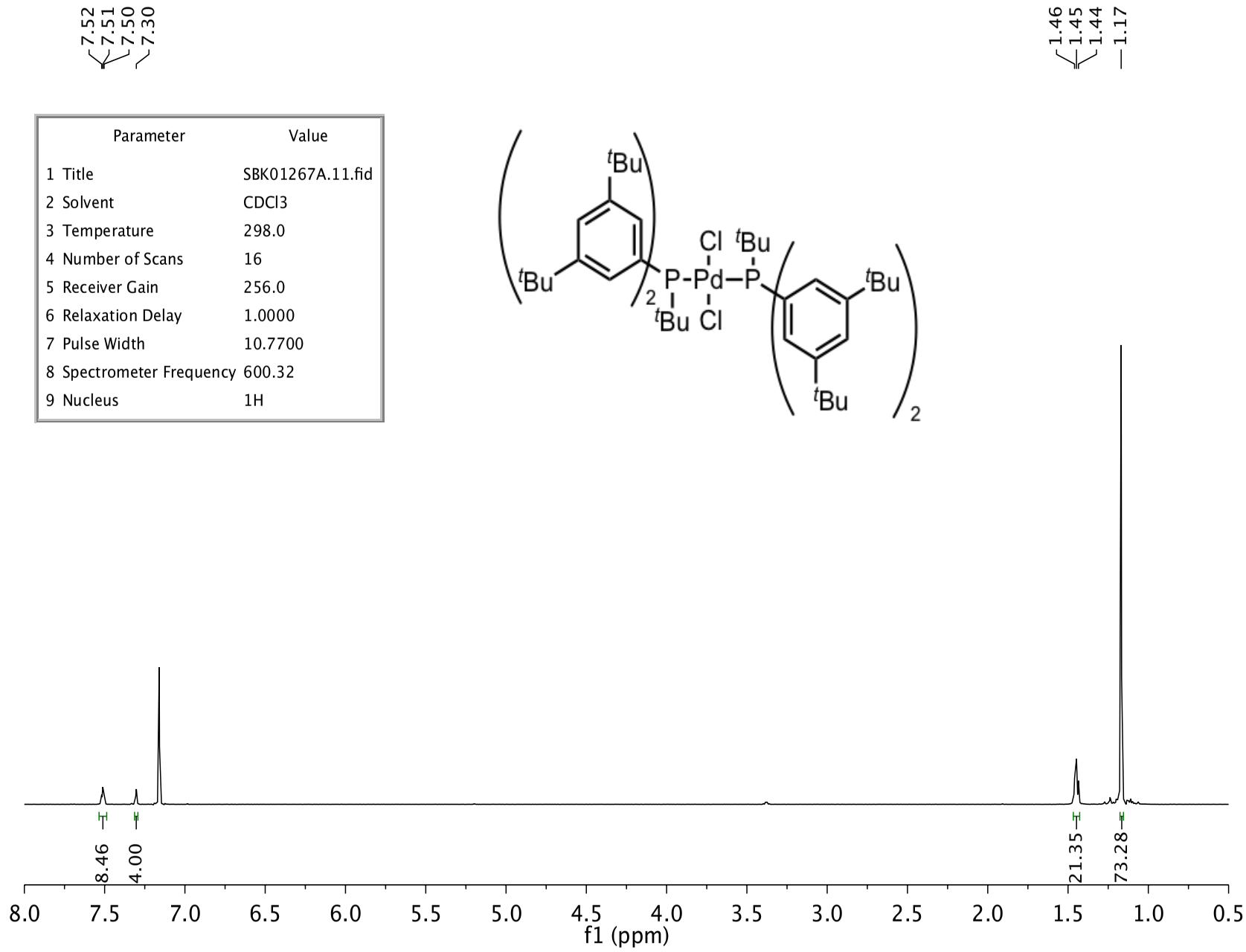
7.52
7.51
7.50
7.30
1.46
1.45
1.44
1.17
Parameter Value
1 Title SBK01267A.11.fid
2 Solvent CDCl3
3 Temperature 298.0
4 Number of Scans 16
5 Receiver Gain 256.0
6 Relaxation Delay 1.0000
7 Pulse Width 10.7700
8 Spectrometer Frequency 600.32
9 Nucleus 1H
tBu
Cl
P-Pd-P
8.46
4.00
21.35
73.28
f1 (ppm)

Parameter	Value
1 Title	SBK01280B.1.fid
2 Solvent	C6D6
3 Temperature	298.2
4 Number of Scans	16
5 Receiver Gain	5160.6
6 Relaxation Delay	2.0000
7 Pulse Width	9.2200
8 Spectrometer Frequency	161.97
9 Nucleus	31P

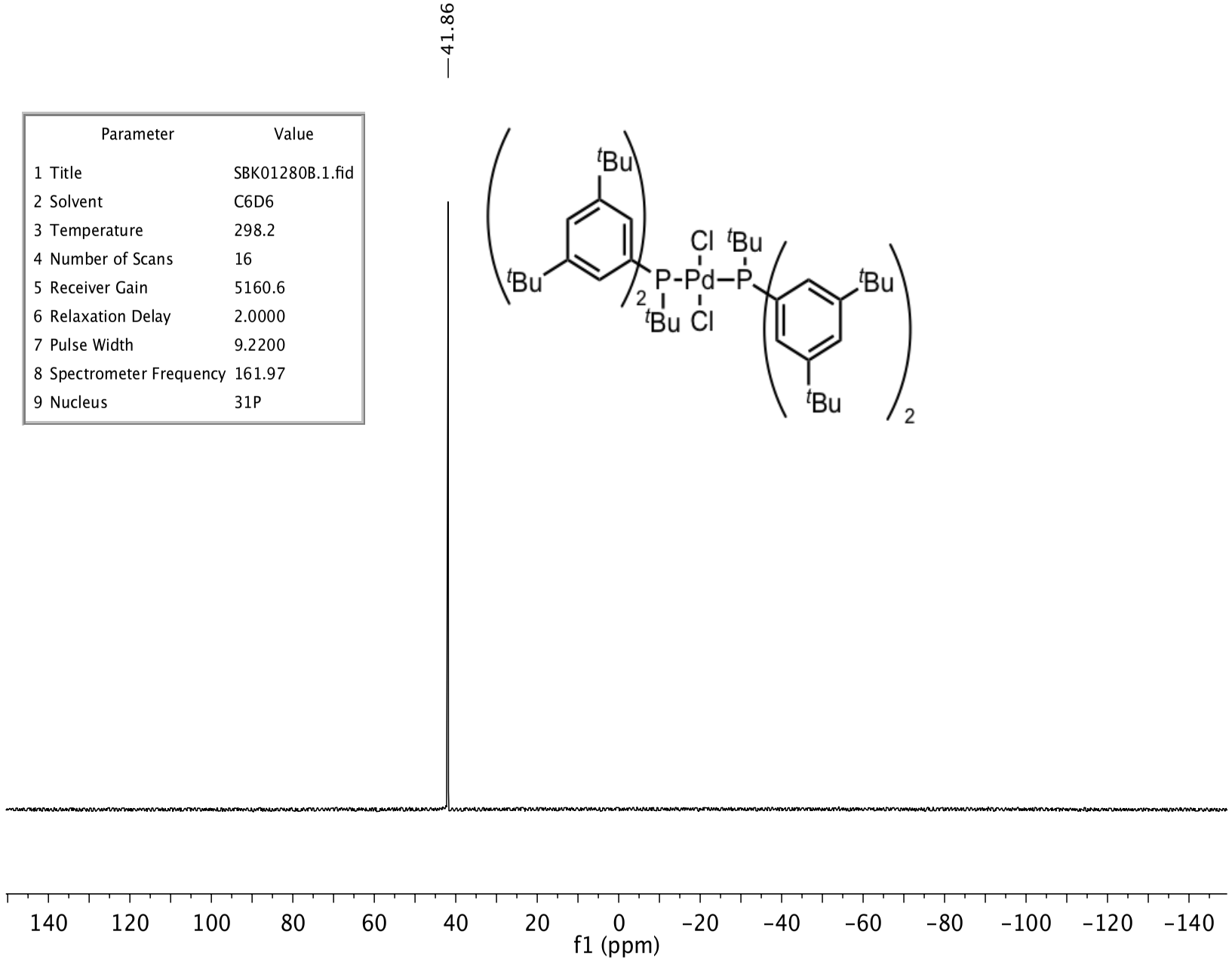

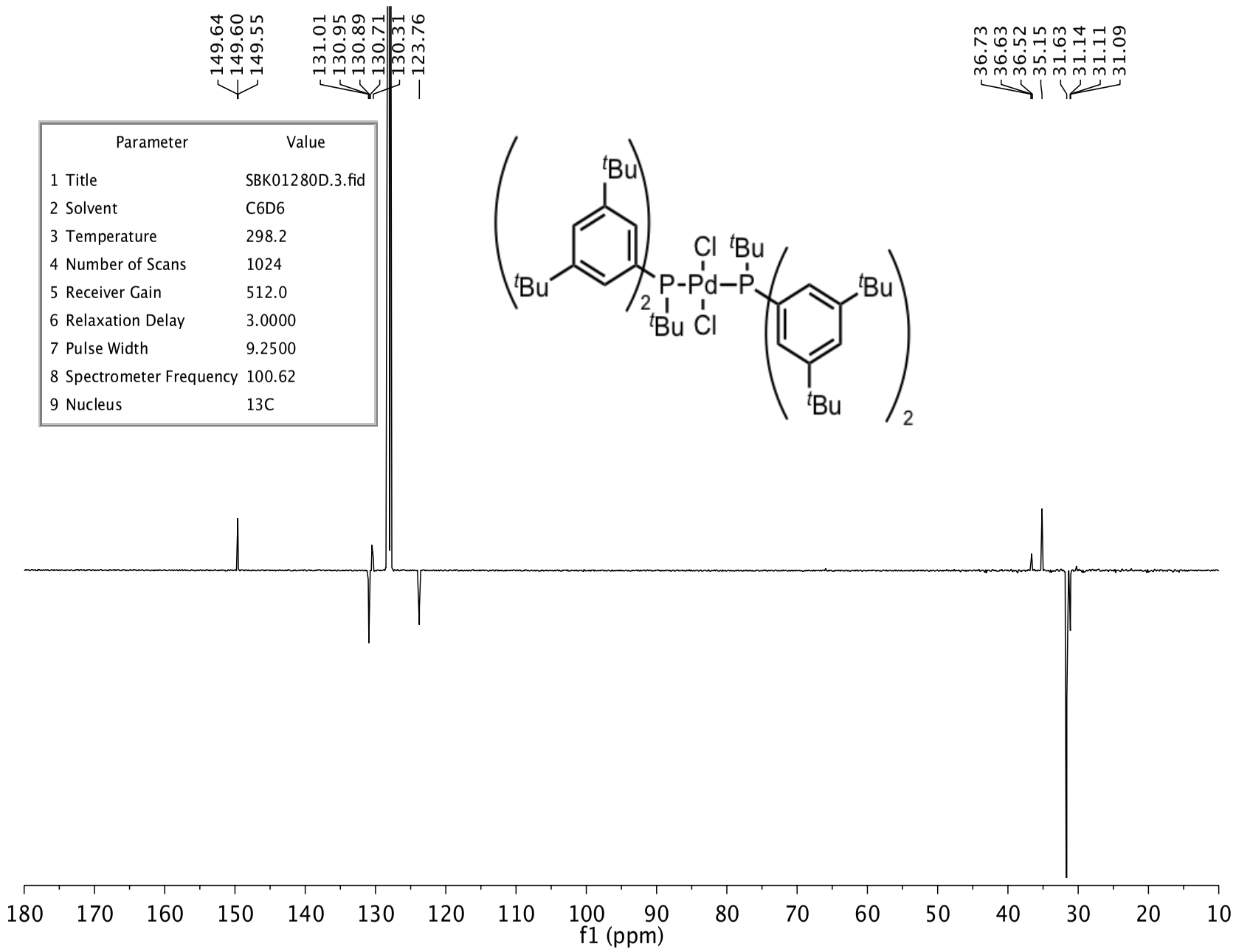
149.64
149.60
149.55
131.01
130.95
130.89
130.71
130.31
123.76
36.73
36.63
36.52
35.15
31.63
31.14
31.11
31.09
Parameter Value
1 Title SBK01280D.3.fid
2 Solvent C6D6
3 Temperature 298.2
4 Number of Scans 1024
5 Receiver Gain 512.0
6 Relaxation Delay 3.0000
7 Pulse Width 9.2500
8 Spectrometer Frequency 100.62
9 Nucleus 13C
tBu
Cl tBu
P-Pd-P
tBu Cl
2
2
180 170 160 150 140 130 120 110 100 90 80 70 60 50 40 30 20 10
f1 (ppm)

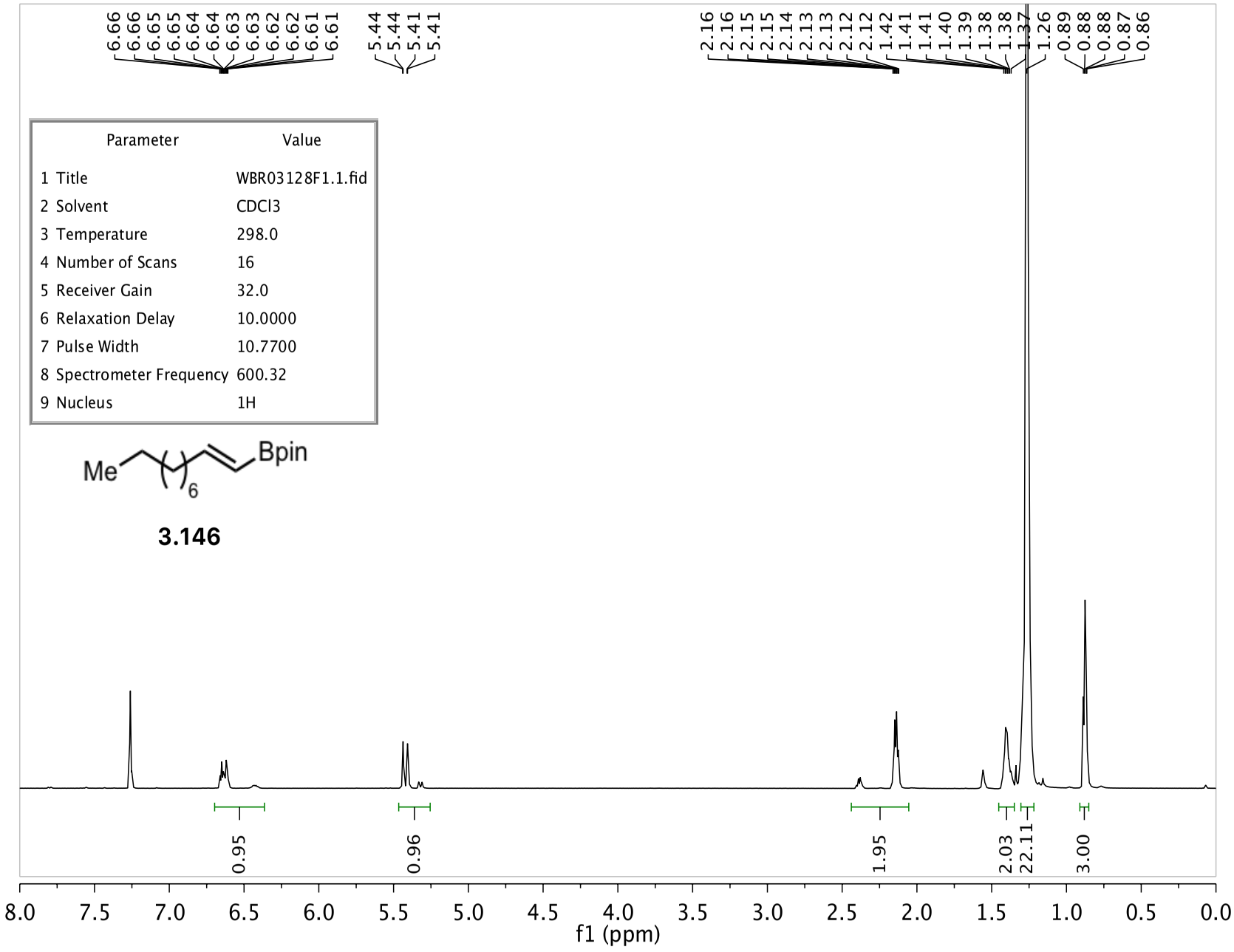
6.66 6.66 6.65 6.65 6.64 6.64 6.63 6.63 6.62 6.62 6.61 6.61
5.44 5.44 5.41 5.41
2.16 2.16 2.15 2.15 2.14 2.13 2.13 2.12 2.12 1.42 1.41 1.41 1.40 1.39 1.38 1.38 1.37 1.26 0.89 0.88 0.88 0.87 0.86
Parameter Value
1 Title WBR03128F1.1.fid
2 Solvent CDCl3
3 Temperature 298.0
4 Number of Scans 16
5 Receiver Gain 32.0
6 Relaxation Delay 10.0000
7 Pulse Width 10.7700
8 Spectrometer Frequency 600.32
9 Nucleus 1H
Me
6
Bpin
3.146
0.95
0.96
1.95
2.03
22.11
3.00
8.0 7.5 7.0 6.5 6.0 5.5 5.0 4.5 4.0 3.5 3.0 2.5 2.0 1.5 1.0 0.5 0.0
f1 (ppm)

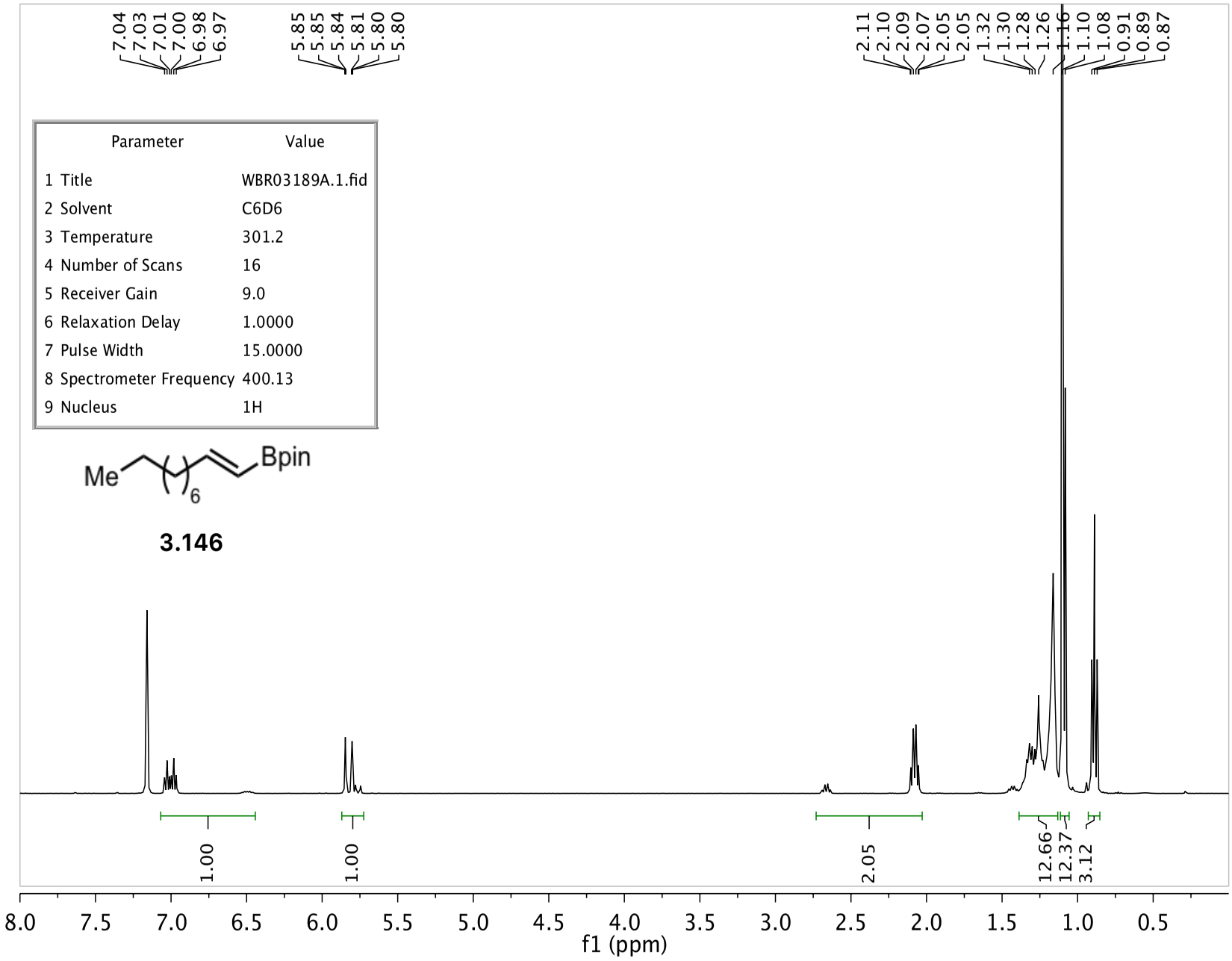
7.04
7.03
7.01
7.00
6.98
6.97
5.85
5.85
5.84
5.81
5.80
5.80
2.11
2.10
2.09
2.07
2.05
2.05
1.32
1.30
1.28
1.26
1.16
1.10
1.08
0.91
0.89
0.87
Parameter Value
1 Title WBR03189A.1.fid
2 Solvent C6D6
3 Temperature 301.2
4 Number of Scans 16
5 Receiver Gain 9.0
6 Relaxation Delay 1.0000
7 Pulse Width 15.0000
8 Spectrometer Frequency 400.13
9 Nucleus 1H
Me
Bpin
6
3.146
1.00
1.00
2.05
12.66
12.37
3.12
8.0
7.5
7.0
6.5
6.0
5.5
5.0
4.5
4.0
3.5
3.0
2.5
2.0
1.5
1.0
0.5
f1 (ppm)

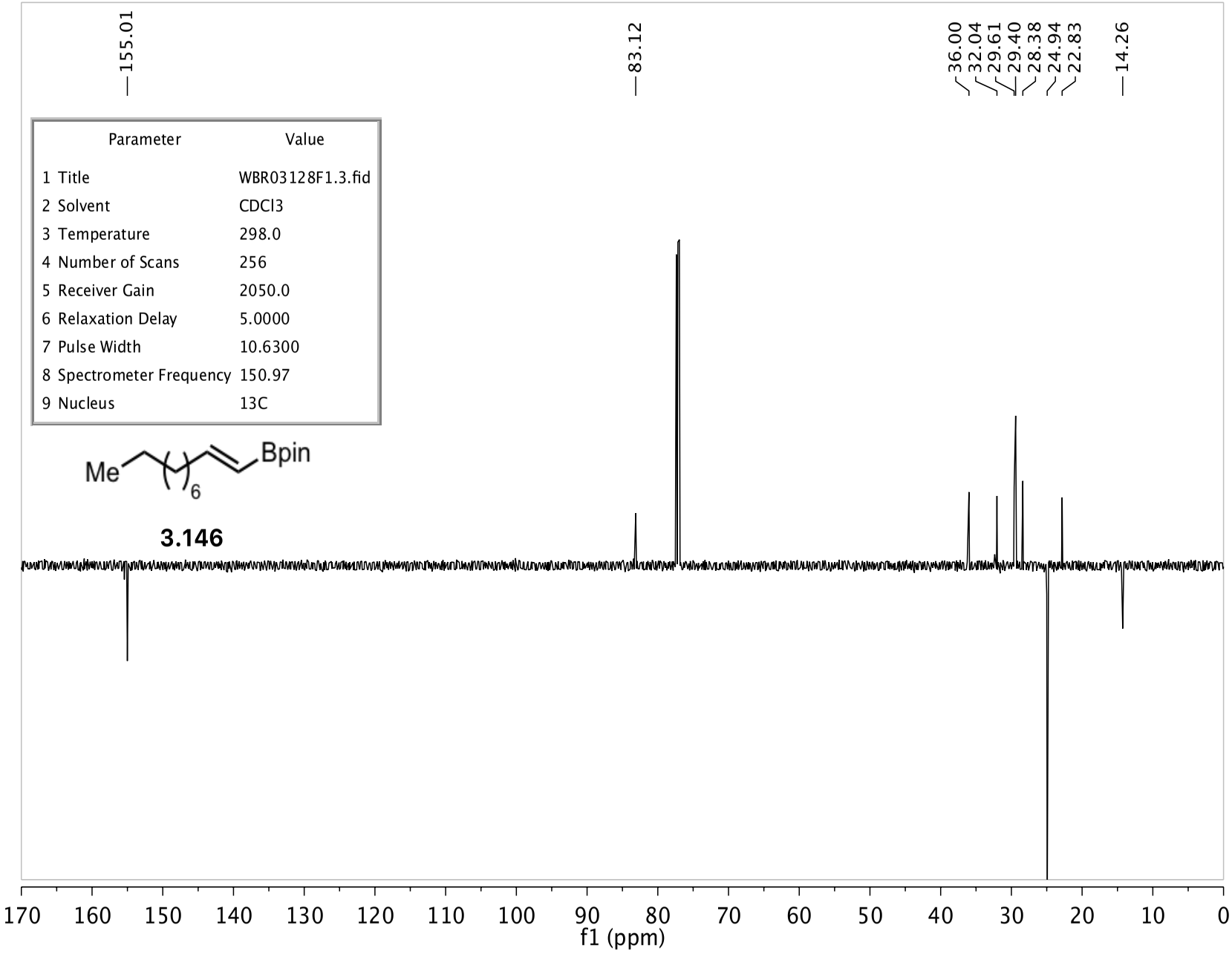
155.01
83.12
36.00
32.04
29.61
29.40
28.38
24.94
22.83
14.26
Parameter Value
1 Title WBR03128F1.3.fid
2 Solvent CDCl3
3 Temperature 298.0
4 Number of Scans 256
5 Receiver Gain 2050.0
6 Relaxation Delay 5.0000
7 Pulse Width 10.6300
8 Spectrometer Frequency 150.97
9 Nucleus 13C
Me
6
Bpin
3.146
170 160 150 140 130 120 110 100 90 80 70 60 50 40 30 20 10 0
f1 (ppm)

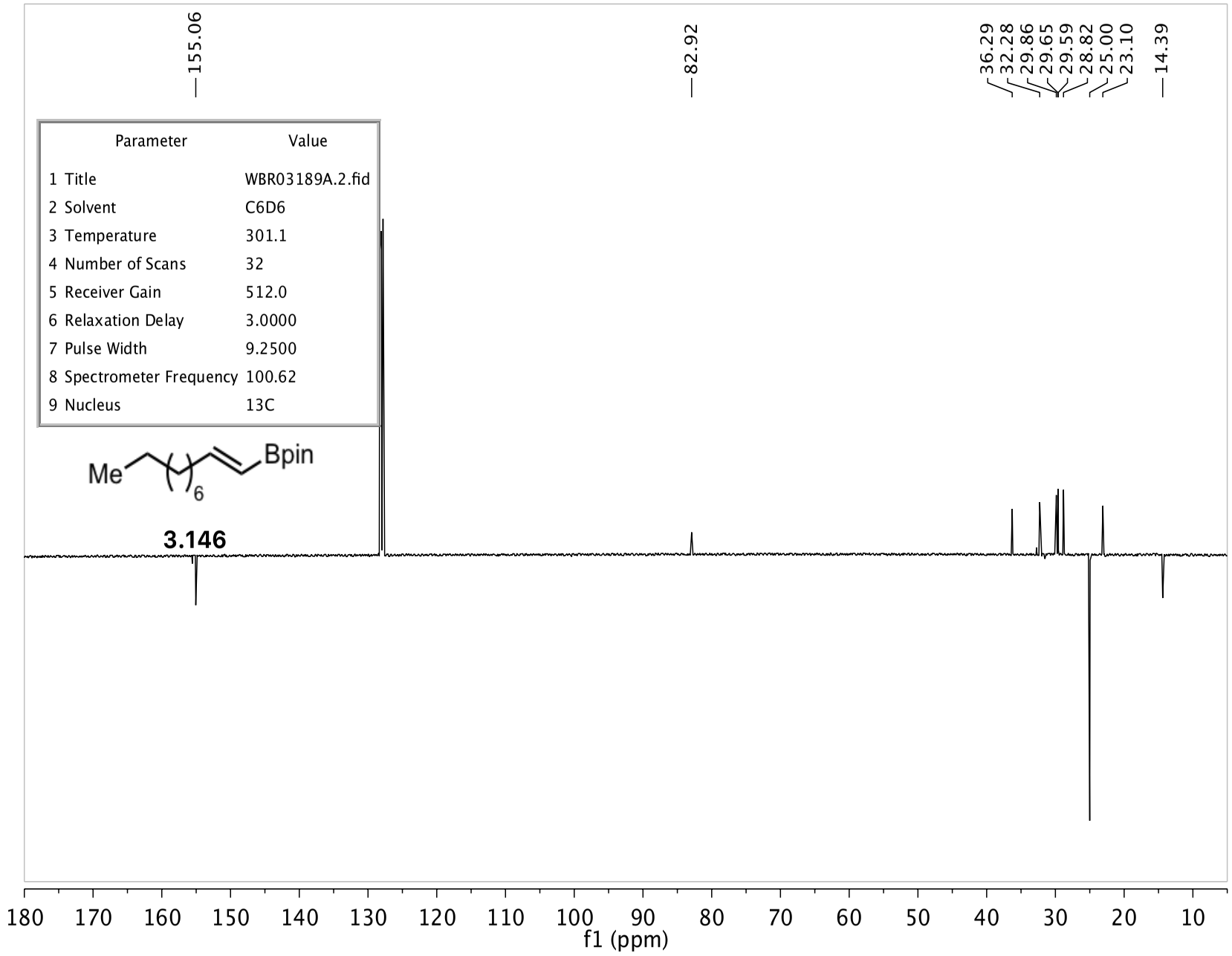
155.06
82.92
36.29
32.28
29.86
29.65
29.59
28.82
25.00
23.10
14.39
Parameter Value
1 Title WBR03189A.2.fid
2 Solvent C6D6
3 Temperature 301.1
4 Number of Scans 32
5 Receiver Gain 512.0
6 Relaxation Delay 3.0000
7 Pulse Width 9.2500
8 Spectrometer Frequency 100.62
9 Nucleus 13C
Me
6
Bpin
3.146
180 170 160 150 140 130 120 110 100 90 80 70 60 50 40 30 20 10
f1 (ppm)

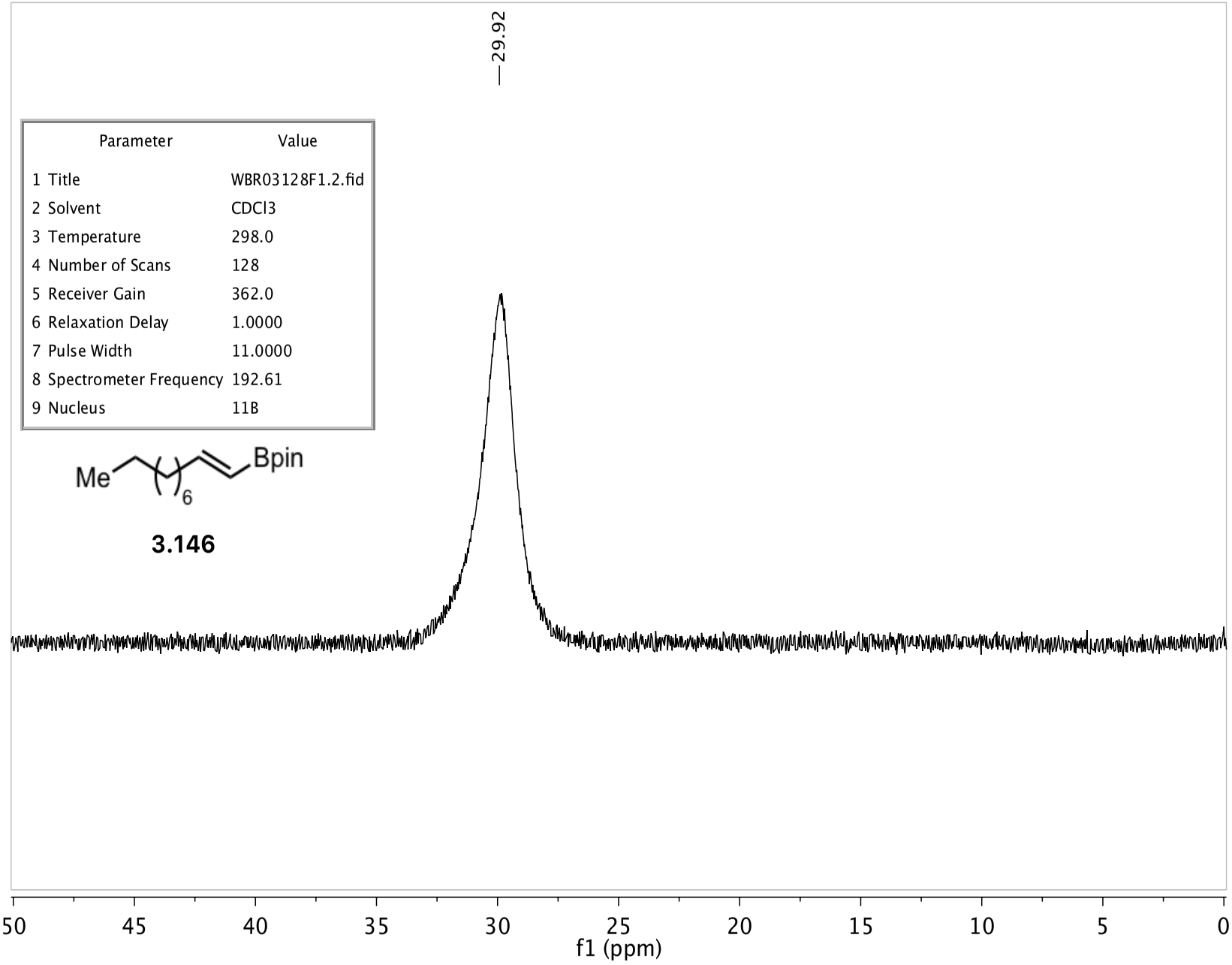
29.92
Parameter Value
1 Title WBR03128F1.2.fid
2 Solvent CDCl3
3 Temperature 298.0
4 Number of Scans 128
5 Receiver Gain 362.0
6 Relaxation Delay 1.0000
7 Pulse Width 11.0000
8 Spectrometer Frequency 192.61
9 Nucleus 11B
Me
6
Bpin
3.146
50 45 40 35 30 25 20 15 10 5 0
f1 (ppm)

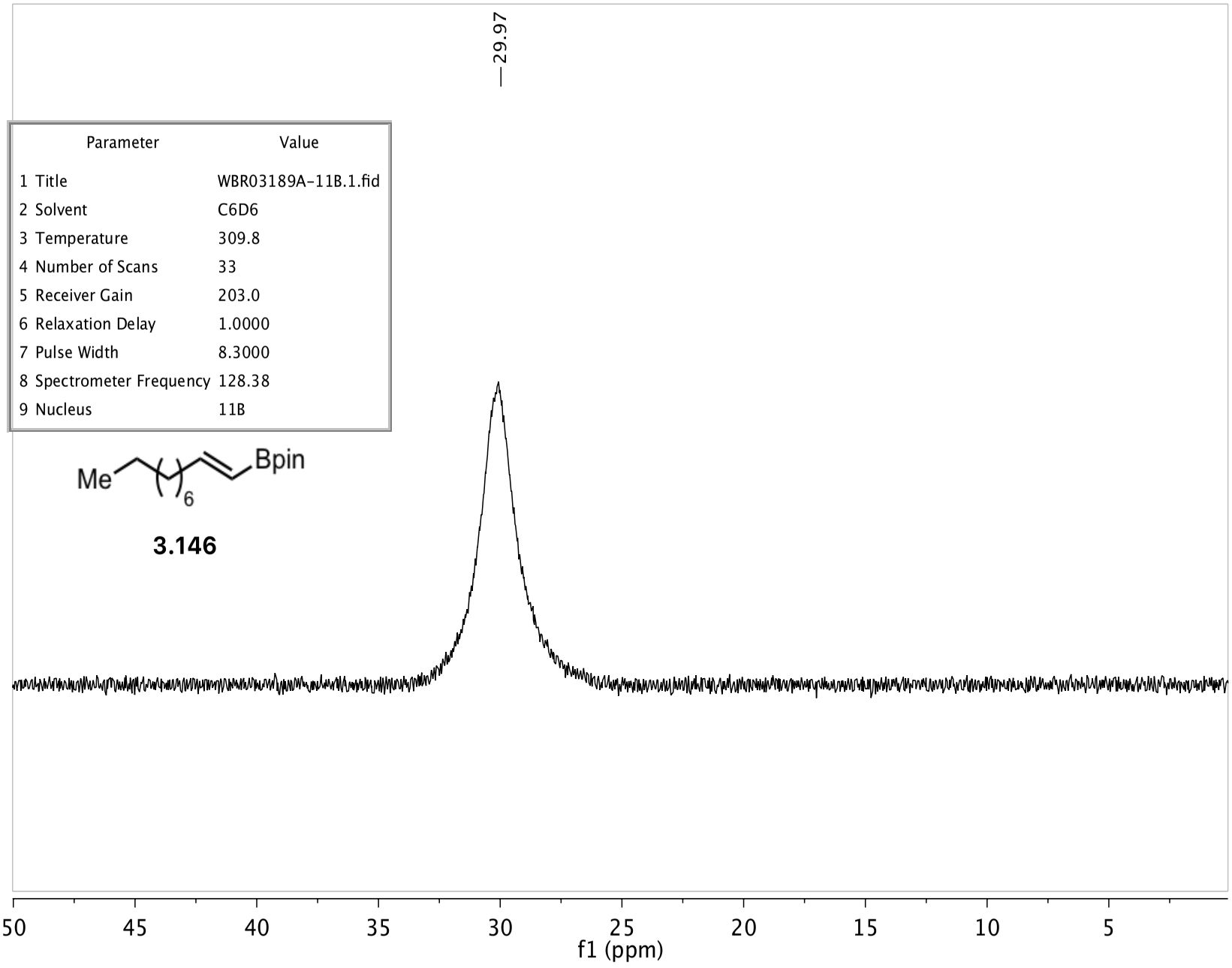
29.97
Parameter Value
1 Title WBR03189A-11B.1.fid
2 Solvent C6D6
3 Temperature 309.8
4 Number of Scans 33
5 Receiver Gain 203.0
6 Relaxation Delay 1.0000
7 Pulse Width 8.3000
8 Spectrometer Frequency 128.38
9 Nucleus 11B
Me
6
Bpin
3.146
50
45
40
35
30
25
20
15
10
5
f1 (ppm)

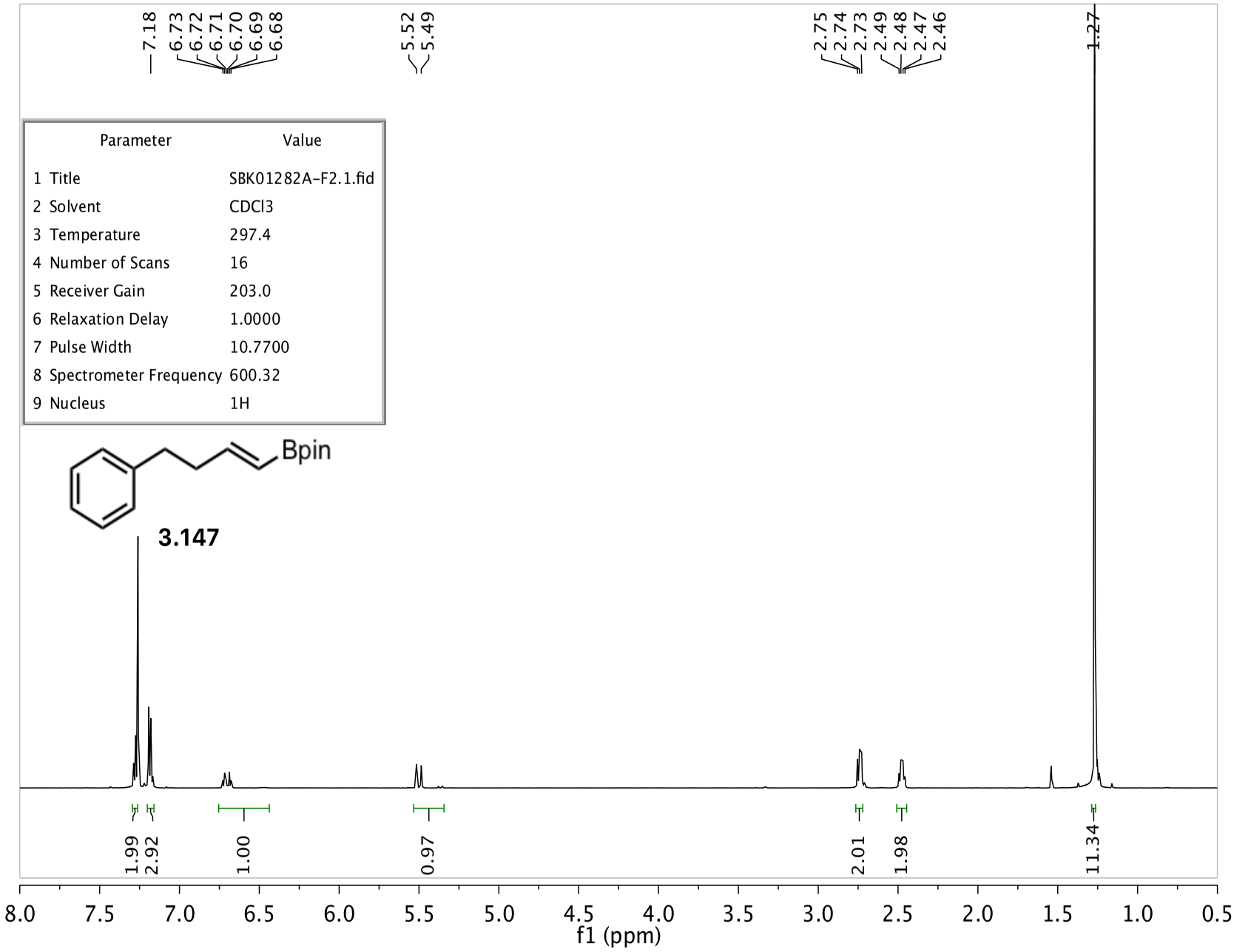
7.18
6.73
6.72
6.71
6.70
6.69
6.68
5.52
5.49
2.75
2.74
2.73
2.49
2.48
2.47
2.46
1.27
Parameter Value
1 Title SBK01282A-F2.1.fid
2 Solvent CDCl3
3 Temperature 297.4
4 Number of Scans 16
5 Receiver Gain 203.0
6 Relaxation Delay 1.0000
7 Pulse Width 10.7700
8 Spectrometer Frequency 600.32
9 Nucleus 1H
Bpin
3.147
1.99
2.92
1.00
0.97
2.01
1.98
11.34
8.0
7.5
7.0
6.5
6.0
5.5
5.0
4.5
4.0
3.5
3.0
2.5
2.0
1.5
1.0
0.5
f1 (ppm)

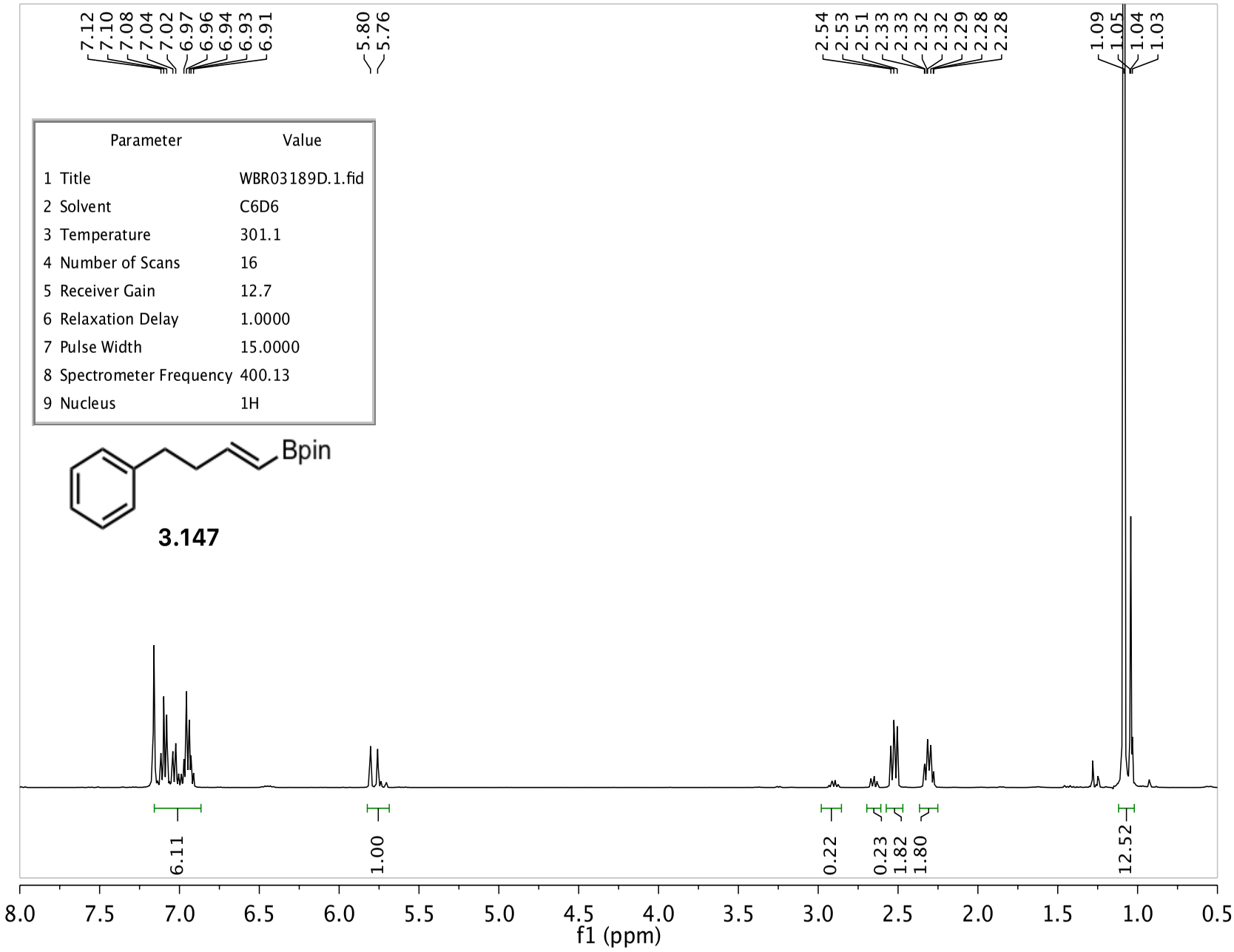
7.12
7.10
7.08
7.04
7.02
6.97
6.96
6.94
6.93
6.91
5.80
5.76
2.54
2.53
2.51
2.33
2.33
2.32
2.32
2.29
2.28
2.28
1.09
1.05
1.04
1.03
Parameter Value
1 Title WBR03189D.1.fid
2 Solvent C6D6
3 Temperature 301.1
4 Number of Scans 16
5 Receiver Gain 12.7
6 Relaxation Delay 1.0000
7 Pulse Width 15.0000
8 Spectrometer Frequency 400.13
9 Nucleus 1H
Bpin
3.147
6.11
1.00
0.22
0.23
1.82
1.80
12.52
8.0
7.5
7.0
6.5
6.0
5.5
5.0
4.5
4.0
3.5
3.0
2.5
2.0
1.5
1.0
0.5
f1 (ppm)

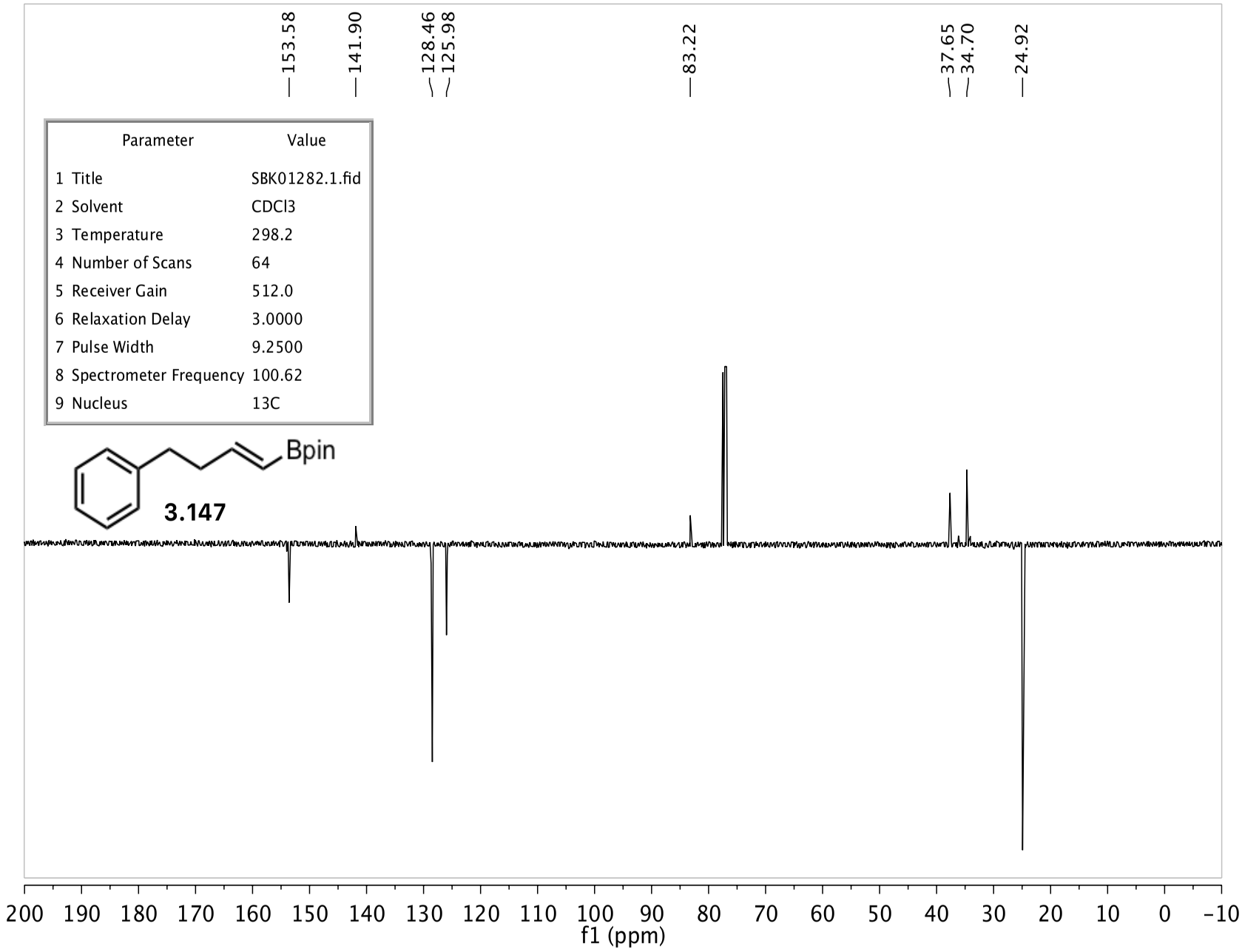
153.58
141.90
128.46
125.98
83.22
37.65
34.70
24.92
Parameter Value
1 Title SBK01282.1.fid
2 Solvent CDCl3
3 Temperature 298.2
4 Number of Scans 64
5 Receiver Gain 512.0
6 Relaxation Delay 3.0000
7 Pulse Width 9.2500
8 Spectrometer Frequency 100.62
9 Nucleus 13C
Bpin
3.147
200 190 180 170 160 150 140 130 120 110 100 90 80 70 60 50 40 30 20 10 0 -10
f1 (ppm)

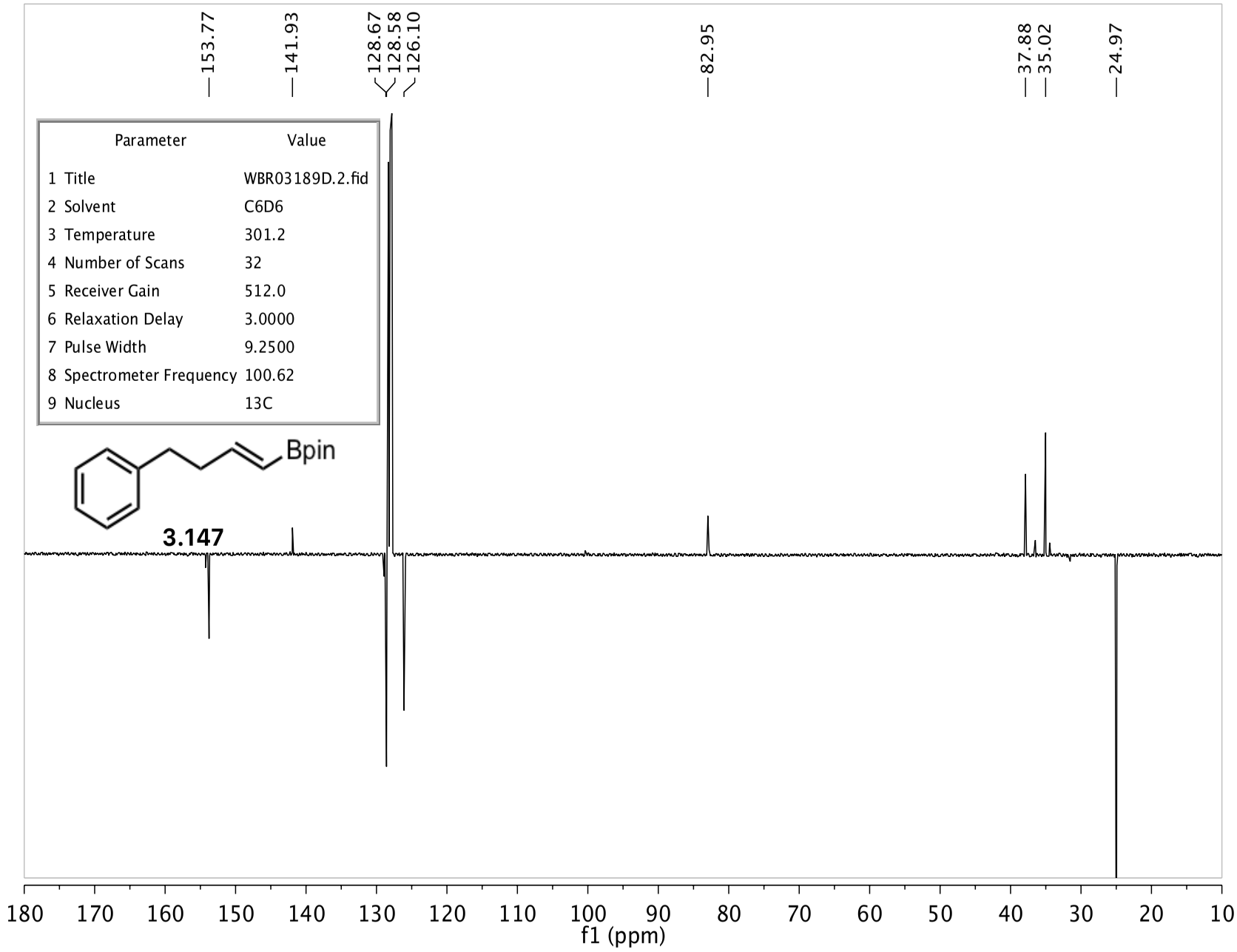
153.77
141.93
128.67
128.58
126.10
82.95
37.88
35.02
24.97
Parameter Value
1 Title WBR03189D.2.fid
2 Solvent C6D6
3 Temperature 301.2
4 Number of Scans 32
5 Receiver Gain 512.0
6 Relaxation Delay 3.0000
7 Pulse Width 9.2500
8 Spectrometer Frequency 100.62
9 Nucleus 13C
Bpin
3.147
180 170 160 150 140 130 120 110 100 90 80 70 60 50 40 30 20 10
f1 (ppm)

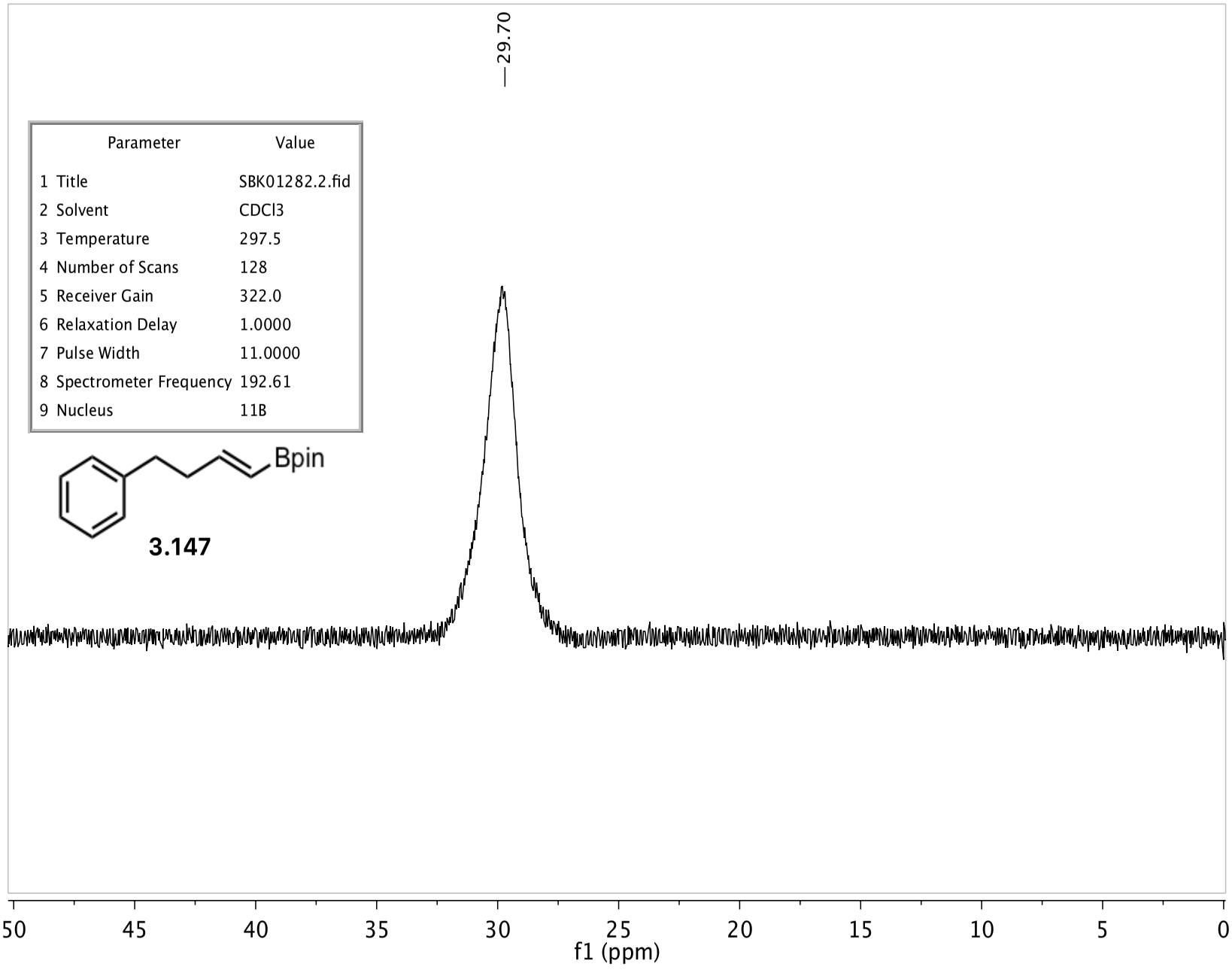
29.70
Parameter Value
1 Title SBK01282.2.fid
2 Solvent CDCl3
3 Temperature 297.5
4 Number of Scans 128
5 Receiver Gain 322.0
6 Relaxation Delay 1.0000
7 Pulse Width 11.0000
8 Spectrometer Frequency 192.61
9 Nucleus 11B
Bpin
3.147
50
45
40
35
30
25
20
15
10
5
0
f1 (ppm)

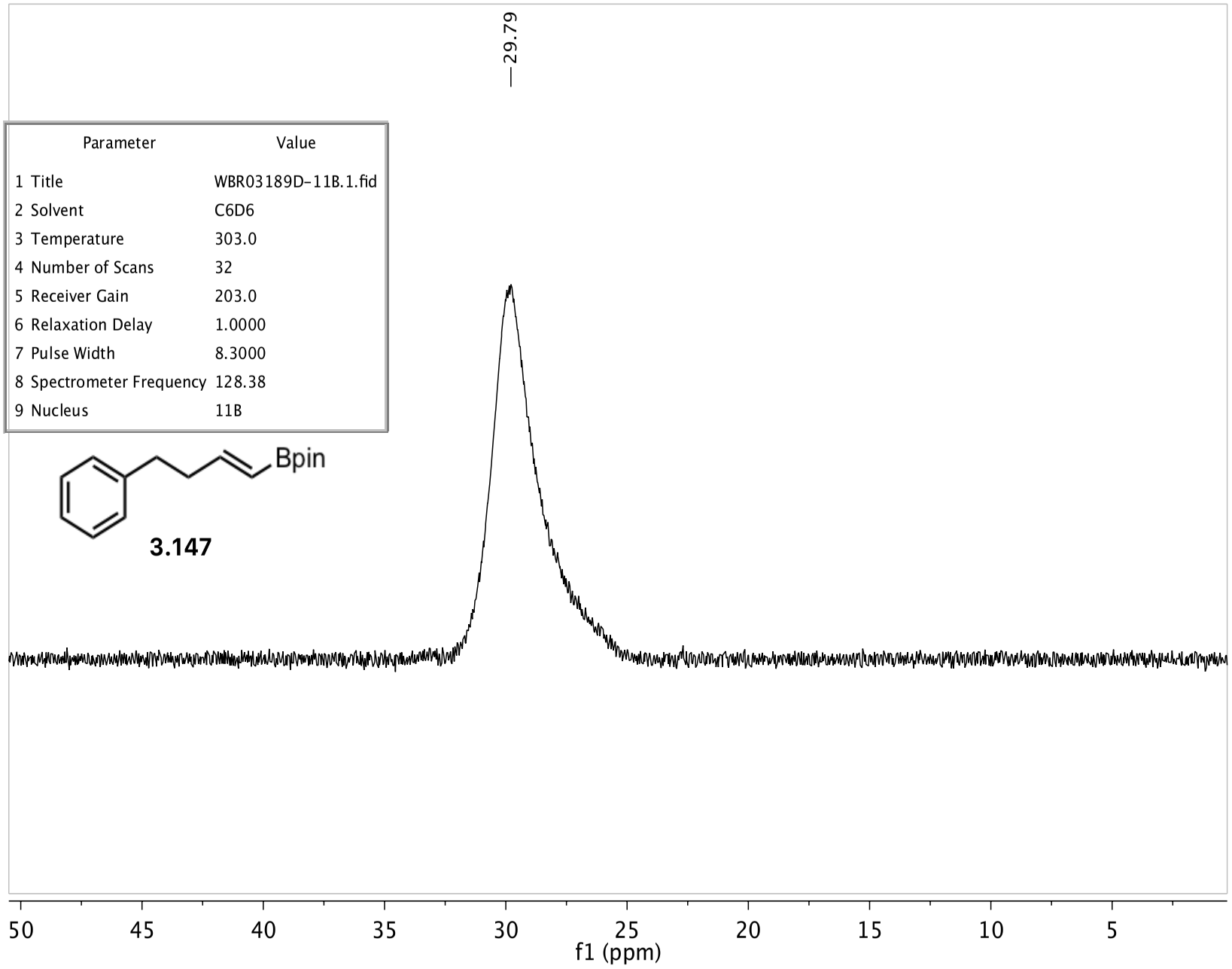
29.79
Parameter
Value
1 Title
WBR03189D-11B.1.fid
2 Solvent
C6D6
3 Temperature
303.0
4 Number of Scans
32
5 Receiver Gain
203.0
6 Relaxation Delay
1.0000
7 Pulse Width
8.3000
8 Spectrometer Frequency
128.38
9 Nucleus
11B
Bpin
3.147
50
45
40
35
30
25
20
15
10
5
f1 (ppm)

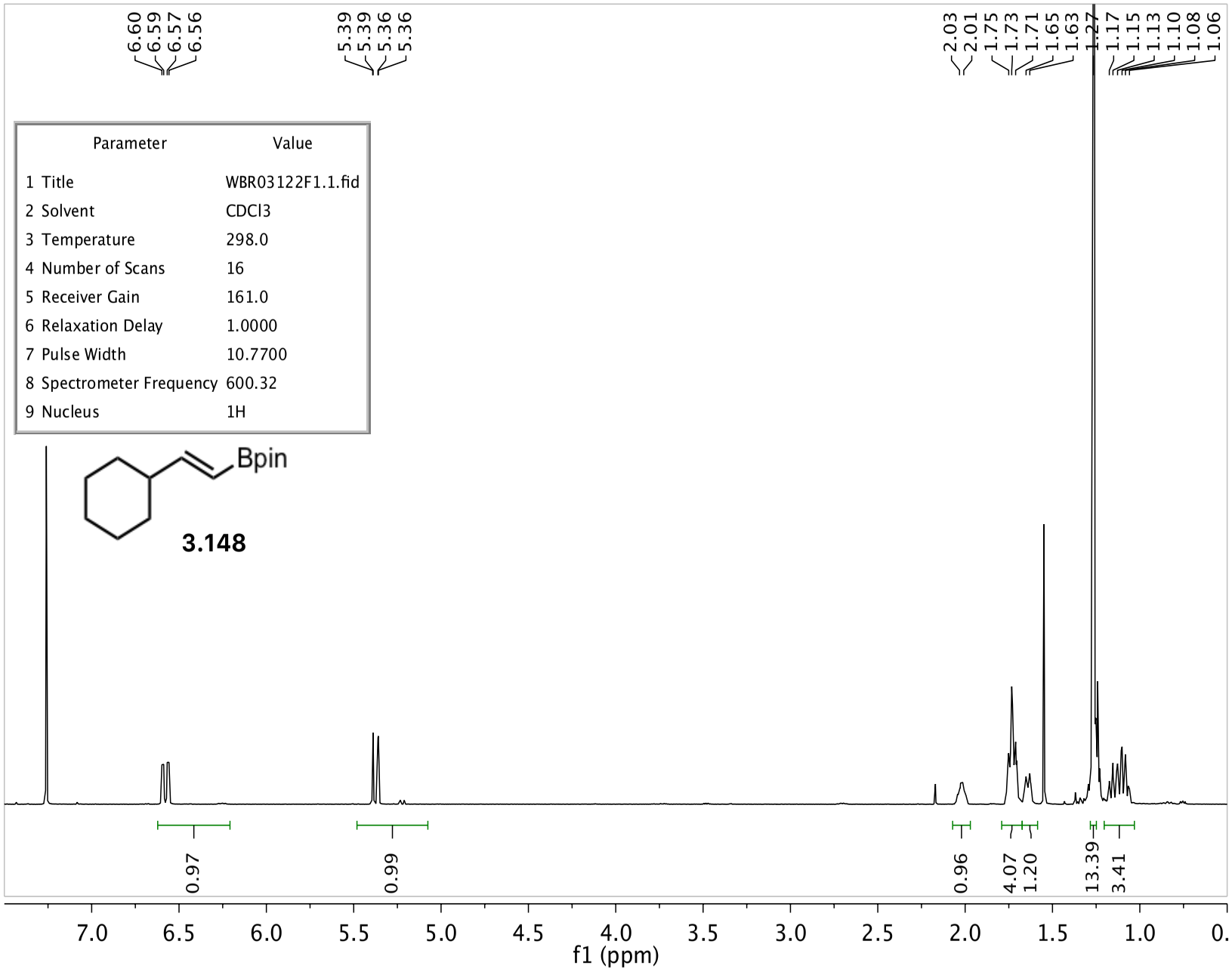
6.60
6.59
6.57
6.56
5.39
5.39
5.36
5.36
2.03
2.01
1.75
1.73
1.71
1.65
1.63
1.27
1.17
1.15
1.13
1.10
1.08
1.06
Parameter Value
1 Title WBR03122F1.1.fid
2 Solvent CDCl3
3 Temperature 298.0
4 Number of Scans 16
5 Receiver Gain 161.0
6 Relaxation Delay 1.0000
7 Pulse Width 10.7700
8 Spectrometer Frequency 600.32
9 Nucleus 1H
Bpin
3.148
0.97
0.99
0.96
4.07
1.20
13.39
3.41
7.0
6.5
6.0
5.5
5.0
4.5
4.0
3.5
3.0
2.5
2.0
1.5
1.0
0.5
f1 (ppm)

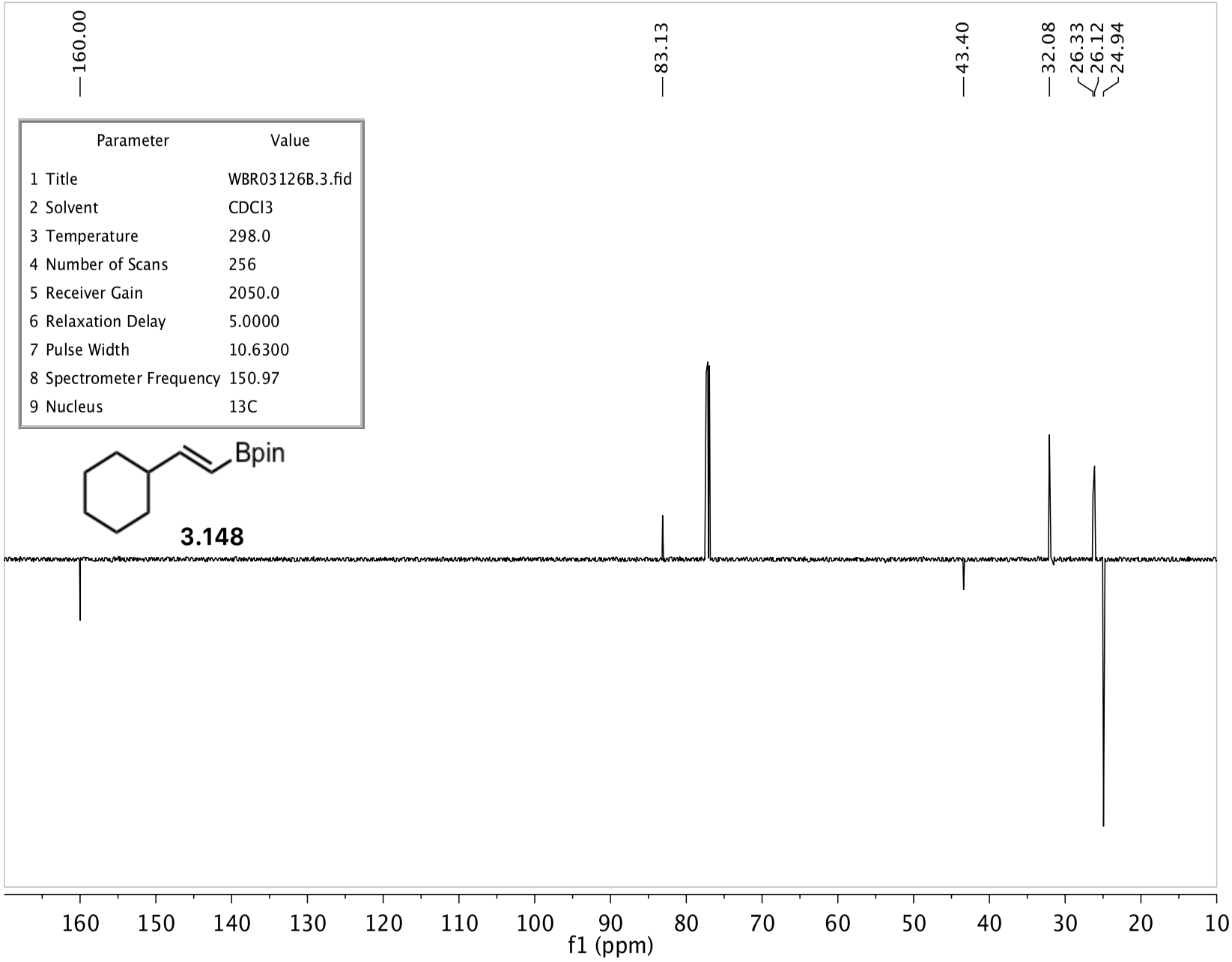
160.00
83.13
43.40
32.08
26.33
26.12
24.94
Parameter Value
1 Title WBR03126B.3.fid
2 Solvent CDCl3
3 Temperature 298.0
4 Number of Scans 256
5 Receiver Gain 2050.0
6 Relaxation Delay 5.0000
7 Pulse Width 10.6300
8 Spectrometer Frequency 150.97
9 Nucleus 13C
Bpin
3.148
160 150 140 130 120 110 100 90 80 70 60 50 40 30 20 10
f1 (ppm)

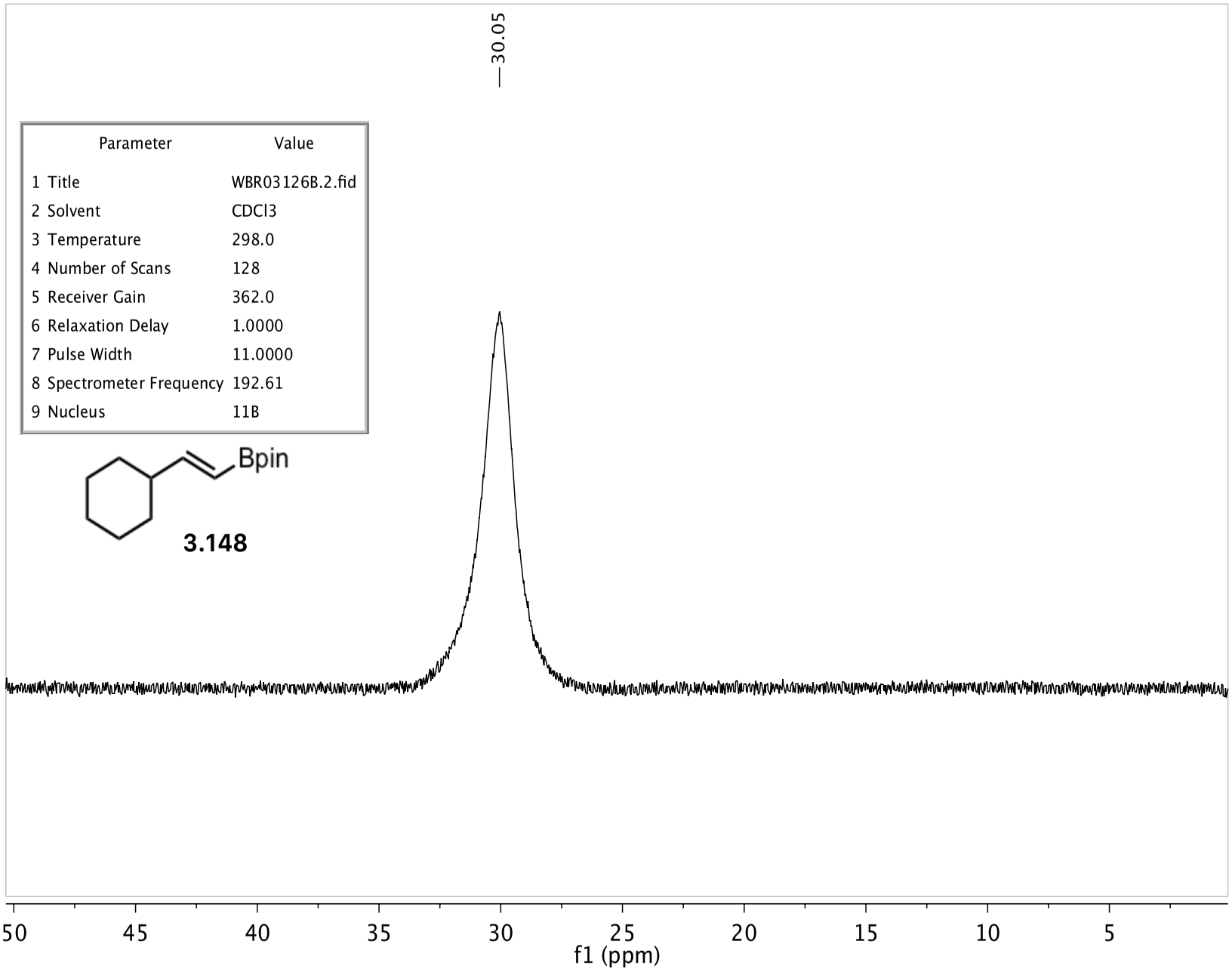
30.05
Parameter Value
1 Title WBR03126B.2.fid
2 Solvent CDCl3
3 Temperature 298.0
4 Number of Scans 128
5 Receiver Gain 362.0
6 Relaxation Delay 1.0000
7 Pulse Width 11.0000
8 Spectrometer Frequency 192.61
9 Nucleus 11B
Bpin
3.148
50
45
40
35
30
25
20
15
10
5
f1 (ppm)

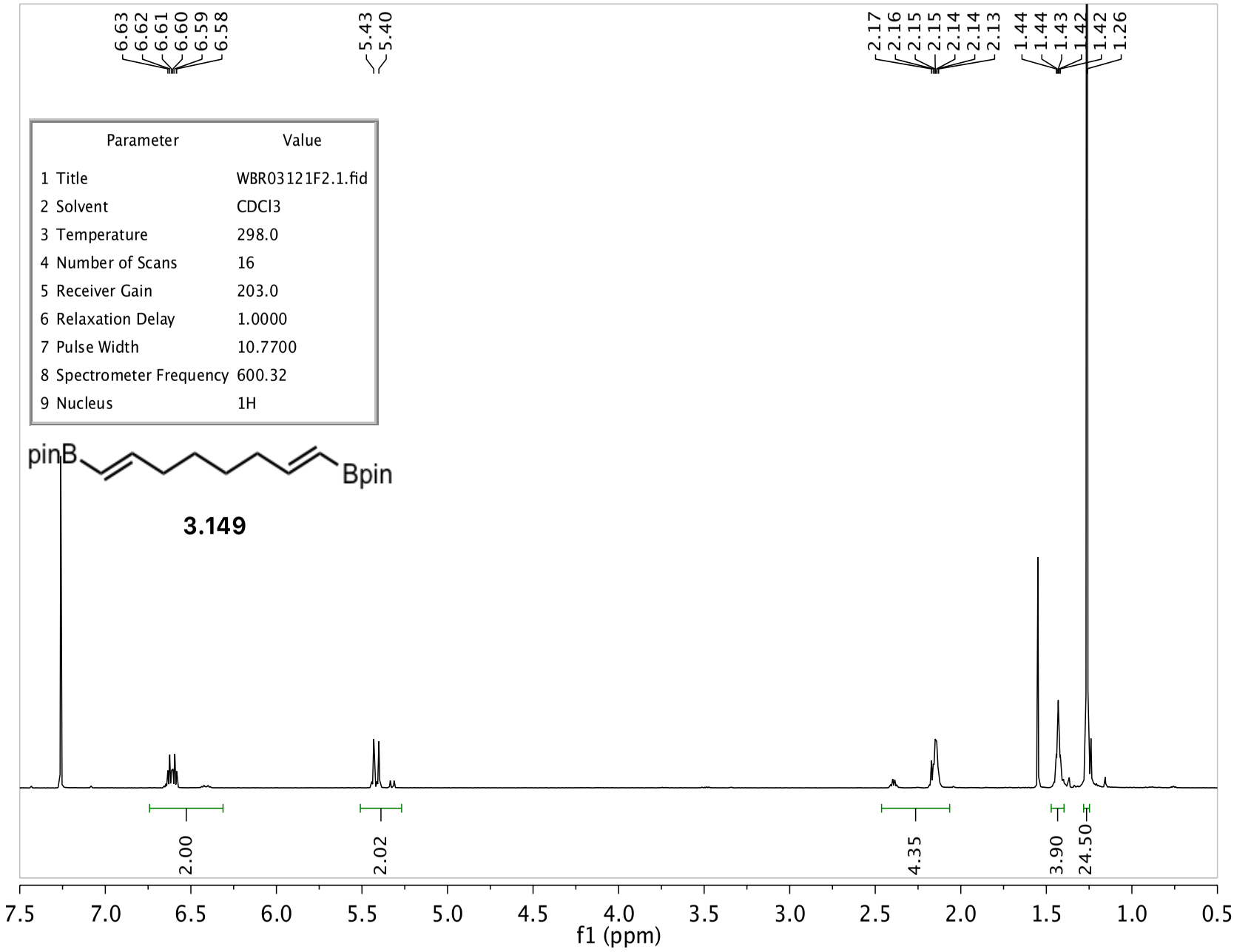
6.63
6.62
6.61
6.60
6.59
6.58
5.43
5.40
2.17
2.16
2.15
2.15
2.14
2.14
2.13
1.44
1.44
1.43
1.42
1.42
1.26
Parameter Value
1 Title WBR03121F2.1.fid
2 Solvent CDCl3
3 Temperature 298.0
4 Number of Scans 16
5 Receiver Gain 203.0
6 Relaxation Delay 1.0000
7 Pulse Width 10.7700
8 Spectrometer Frequency 600.32
9 Nucleus 1H
pinB
Bpin
3.149
2.00
2.02
4.35
3.90
24.50
7.5
7.0
6.5
6.0
5.5
5.0
4.5
4.0
3.5
3.0
2.5
2.0
1.5
1.0
0.5
f1 (ppm)

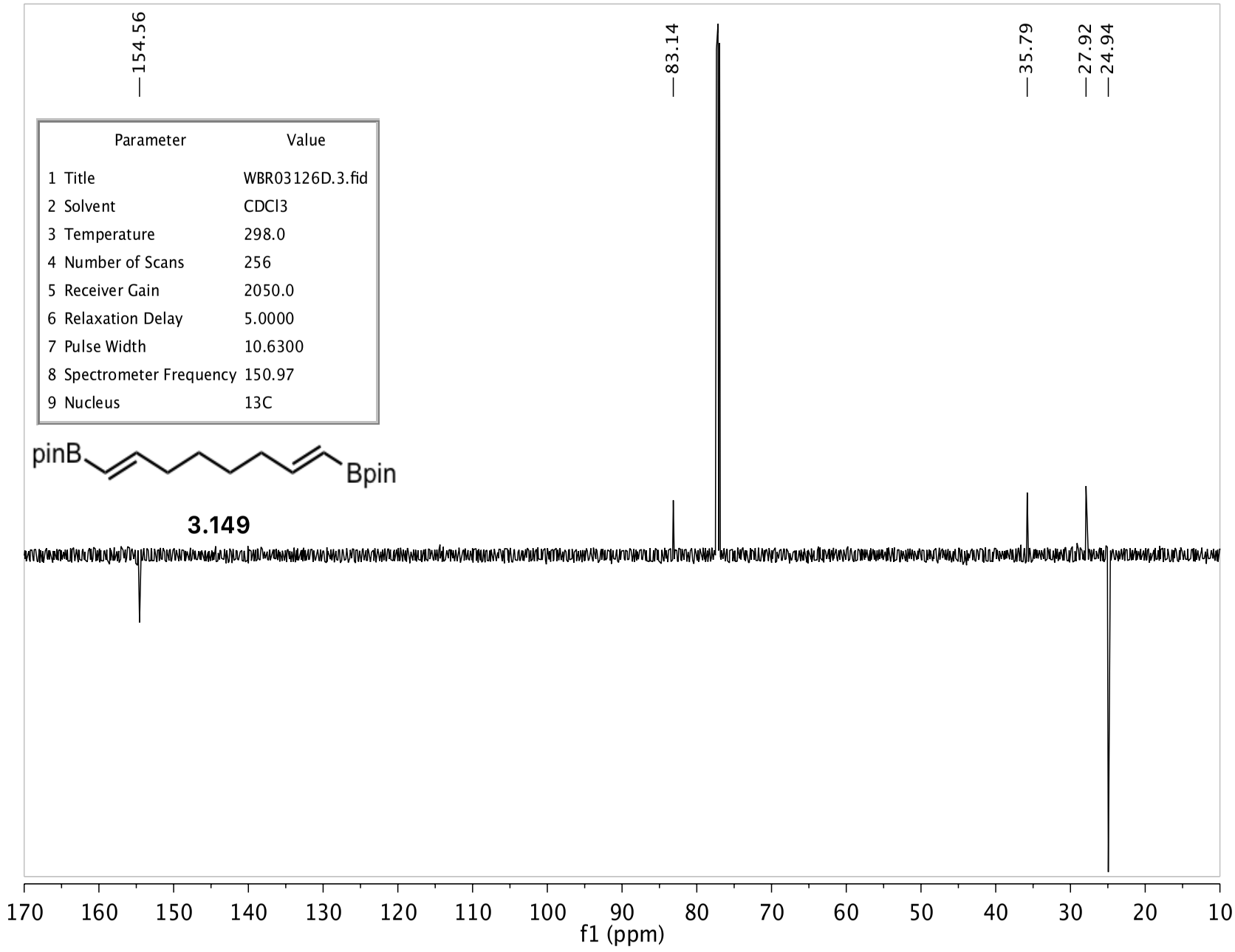
154.56
83.14
35.79
27.92
24.94
Parameter Value
1 Title WBR03126D.3.fid
2 Solvent CDCl3
3 Temperature 298.0
4 Number of Scans 256
5 Receiver Gain 2050.0
6 Relaxation Delay 5.0000
7 Pulse Width 10.6300
8 Spectrometer Frequency 150.97
9 Nucleus 13C
pinB
Bpin
3.149
170 160 150 140 130 120 110 100 90 80 70 60 50 40 30 20 10
f1 (ppm)

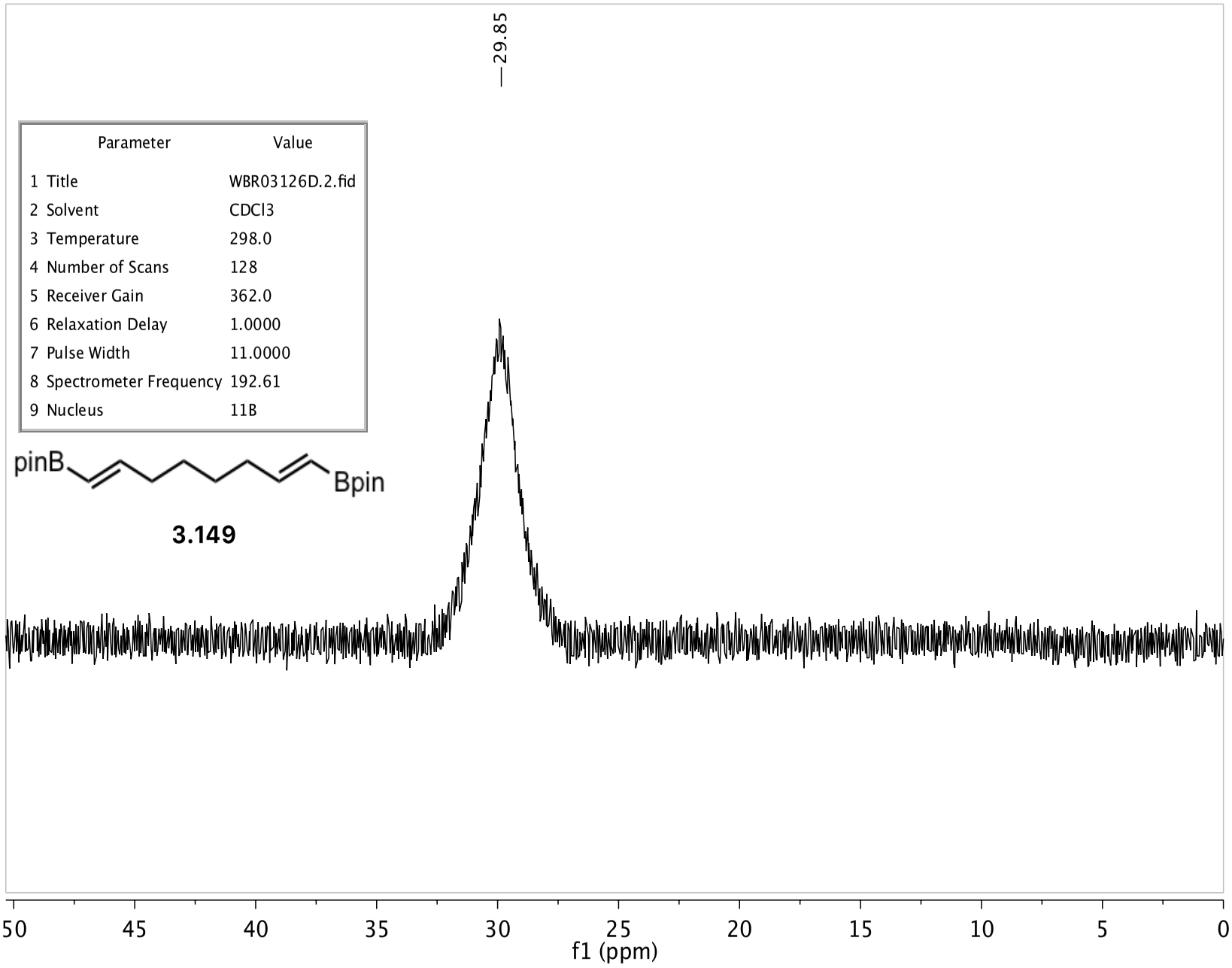
29.85
Parameter Value
1 Title WBR03126D.2.fid
2 Solvent CDCl3
3 Temperature 298.0
4 Number of Scans 128
5 Receiver Gain 362.0
6 Relaxation Delay 1.0000
7 Pulse Width 11.0000
8 Spectrometer Frequency 192.61
9 Nucleus 11B
pinB
Bpin
3.149
50 45 40 35 30 25 20 15 10 5 0
f1 (ppm)

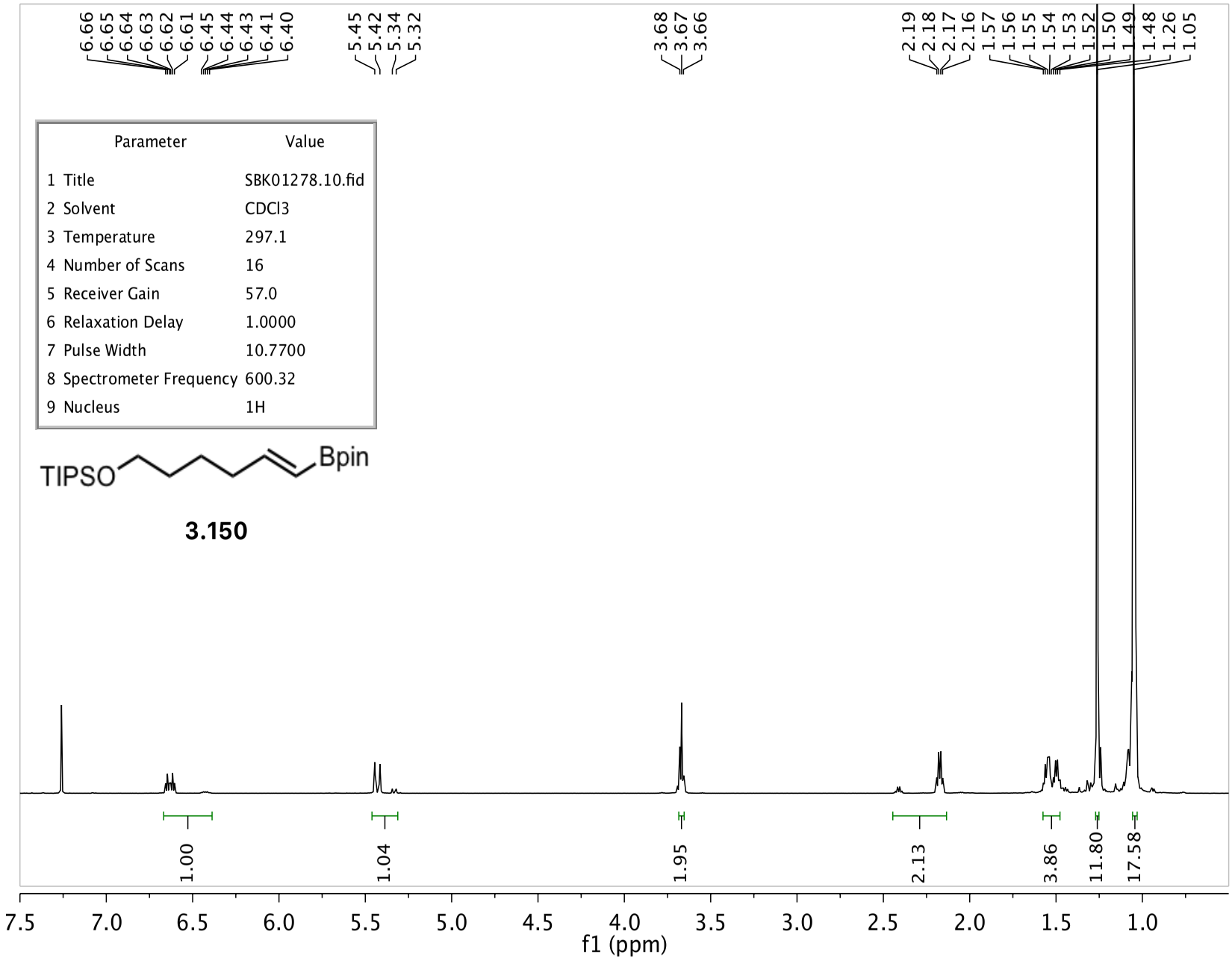
6.66 6.65 6.64 6.63 6.62 6.61 6.45 6.44 6.43 6.41 6.40
5.45 5.42 5.34 5.32
3.68 3.67 3.66
2.19 2.18 2.17 2.16 1.57 1.56 1.55 1.54 1.53 1.52 1.50 1.49 1.48 1.26 1.05
Parameter Value
1 Title SBK01278.10.fid
2 Solvent CDCl3
3 Temperature 297.1
4 Number of Scans 16
5 Receiver Gain 57.0
6 Relaxation Delay 1.0000
7 Pulse Width 10.7700
8 Spectrometer Frequency 600.32
9 Nucleus 1H
TIPSO
Bpin
3.150
1.00 1.04 1.95 2.13 3.86 11.80 17.58
7.5 7.0 6.5 6.0 5.5 5.0 4.5 4.0 3.5 3.0 2.5 2.0 1.5 1.0
f1 (ppm)

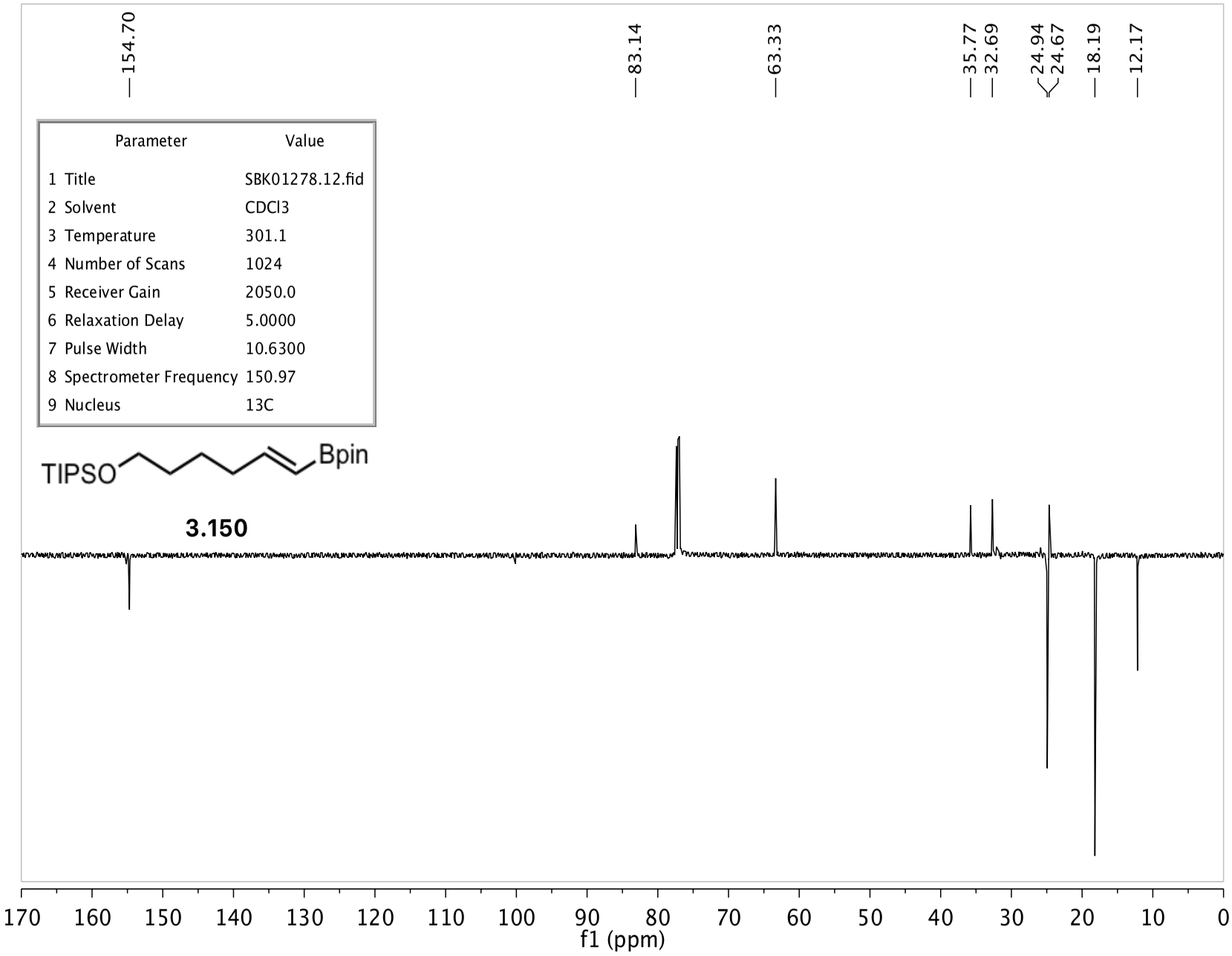
154.70
83.14
63.33
35.77
32.69
24.94
24.67
18.19
12.17
Parameter Value
1 Title SBK01278.12.fid
2 Solvent CDCl3
3 Temperature 301.1
4 Number of Scans 1024
5 Receiver Gain 2050.0
6 Relaxation Delay 5.0000
7 Pulse Width 10.6300
8 Spectrometer Frequency 150.97
9 Nucleus 13C
TIPSO
Bpin
3.150
170 160 150 140 130 120 110 100 90 80 70 60 50 40 30 20 10 0
f1 (ppm)

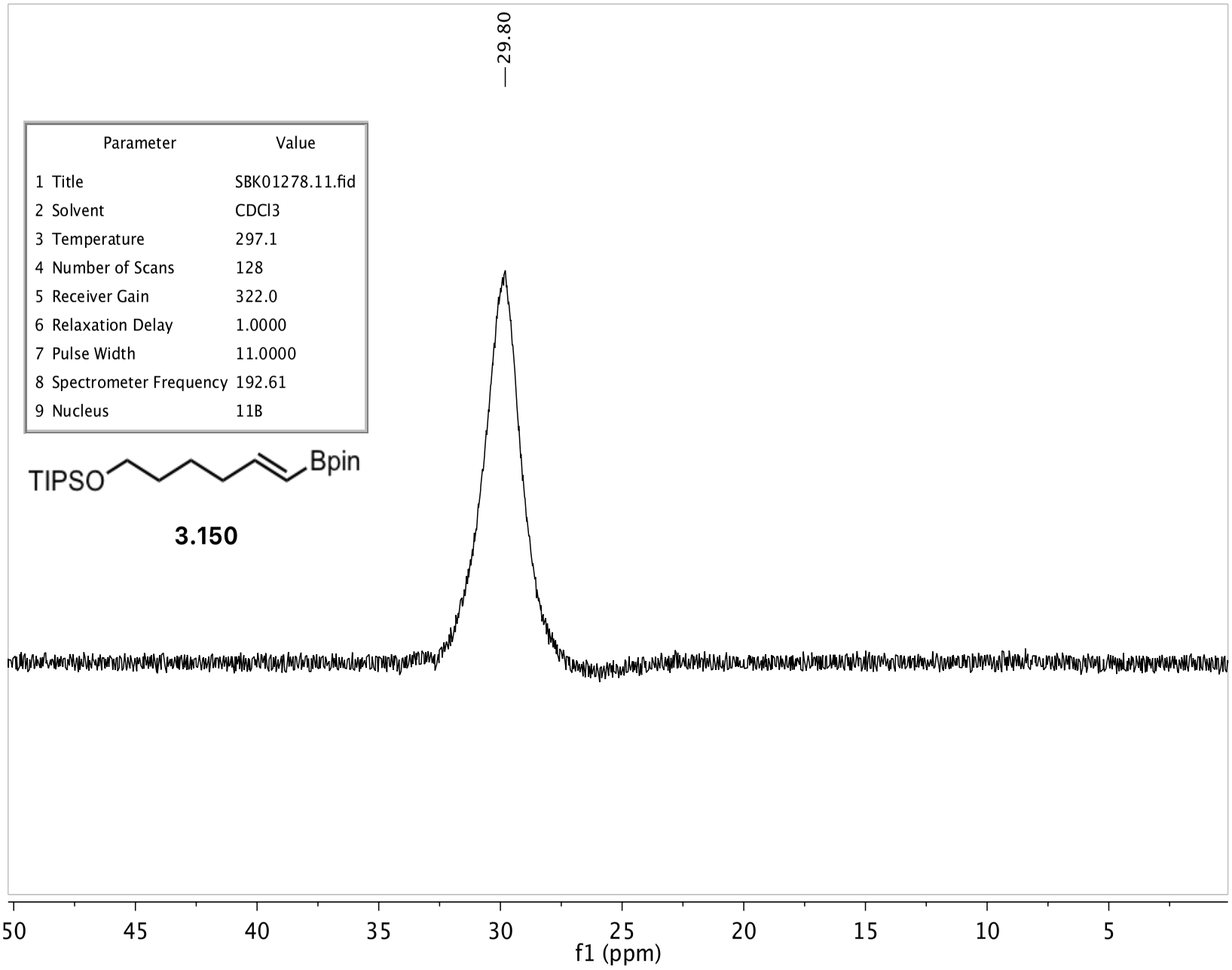
29.80
Parameter Value
1 Title SBK01278.11.fid
2 Solvent CDCl3
3 Temperature 297.1
4 Number of Scans 128
5 Receiver Gain 322.0
6 Relaxation Delay 1.0000
7 Pulse Width 11.0000
8 Spectrometer Frequency 192.61
9 Nucleus 11B
TIPSO
Bpin
3.150
50
45
40
35
30
25
20
15
10
5
f1 (ppm)

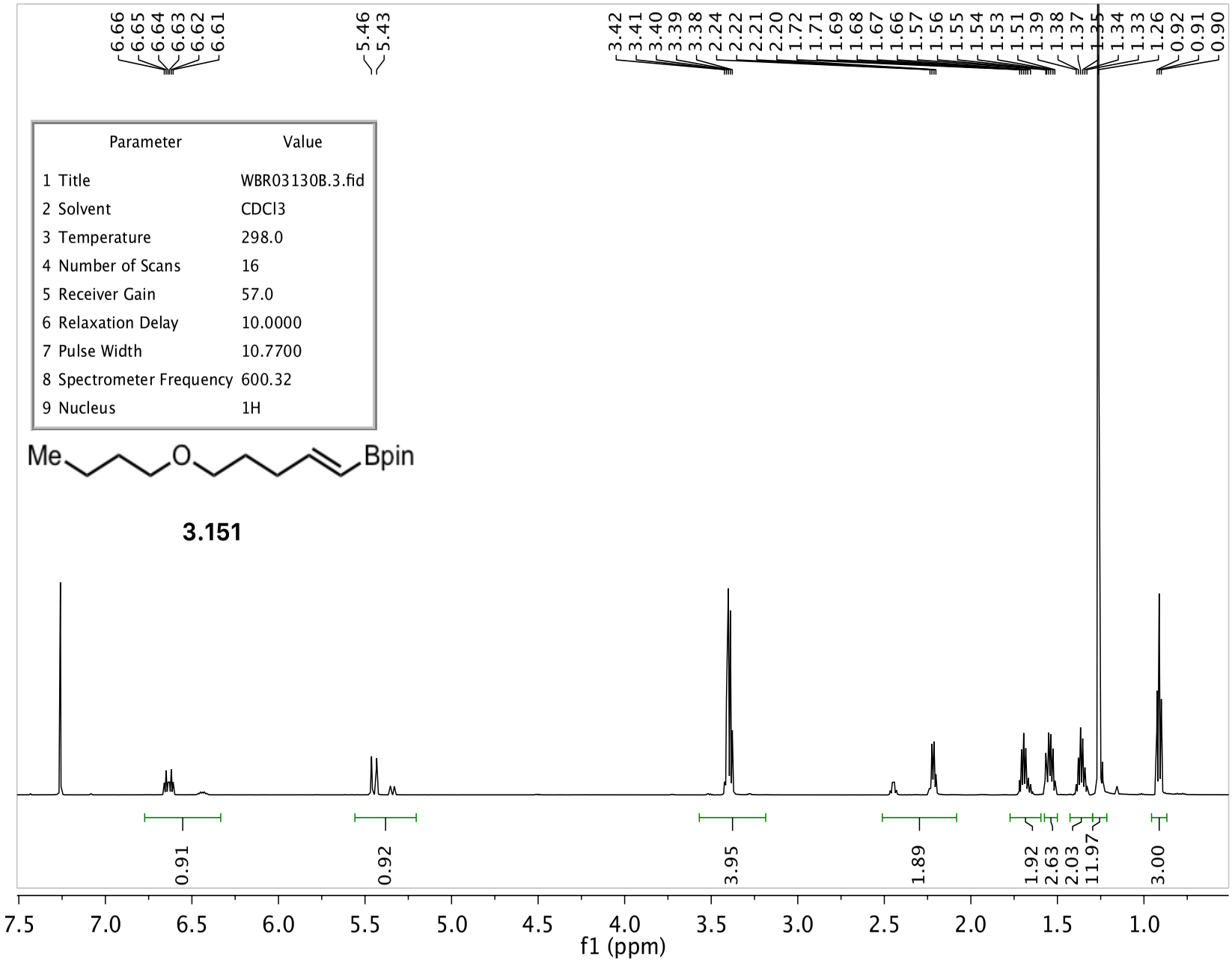
6.66 6.65 6.64 6.63 6.62 6.61
5.46 5.43
3.42 3.41 3.40 3.39 3.38 2.24 2.22 2.21 2.20 1.72 1.71 1.69 1.68 1.67 1.66 1.57 1.56 1.55 1.54 1.53 1.51 1.39 1.38 1.37 1.35 1.34 1.33 1.26 0.92 0.91 0.90
Parameter Value
1 Title WBR03130B.3.fid
2 Solvent CDCl3
3 Temperature 298.0
4 Number of Scans 16
5 Receiver Gain 57.0
6 Relaxation Delay 10.0000
7 Pulse Width 10.7700
8 Spectrometer Frequency 600.32
9 Nucleus 1H
Me O Bpin
3.151
0.91 0.92 3.95 1.89 1.92 2.63 2.03 11.97 3.00
7.5 7.0 6.5 6.0 5.5 5.0 4.5 4.0 3.5 3.0 2.5 2.0 1.5 1.0
f1 (ppm)

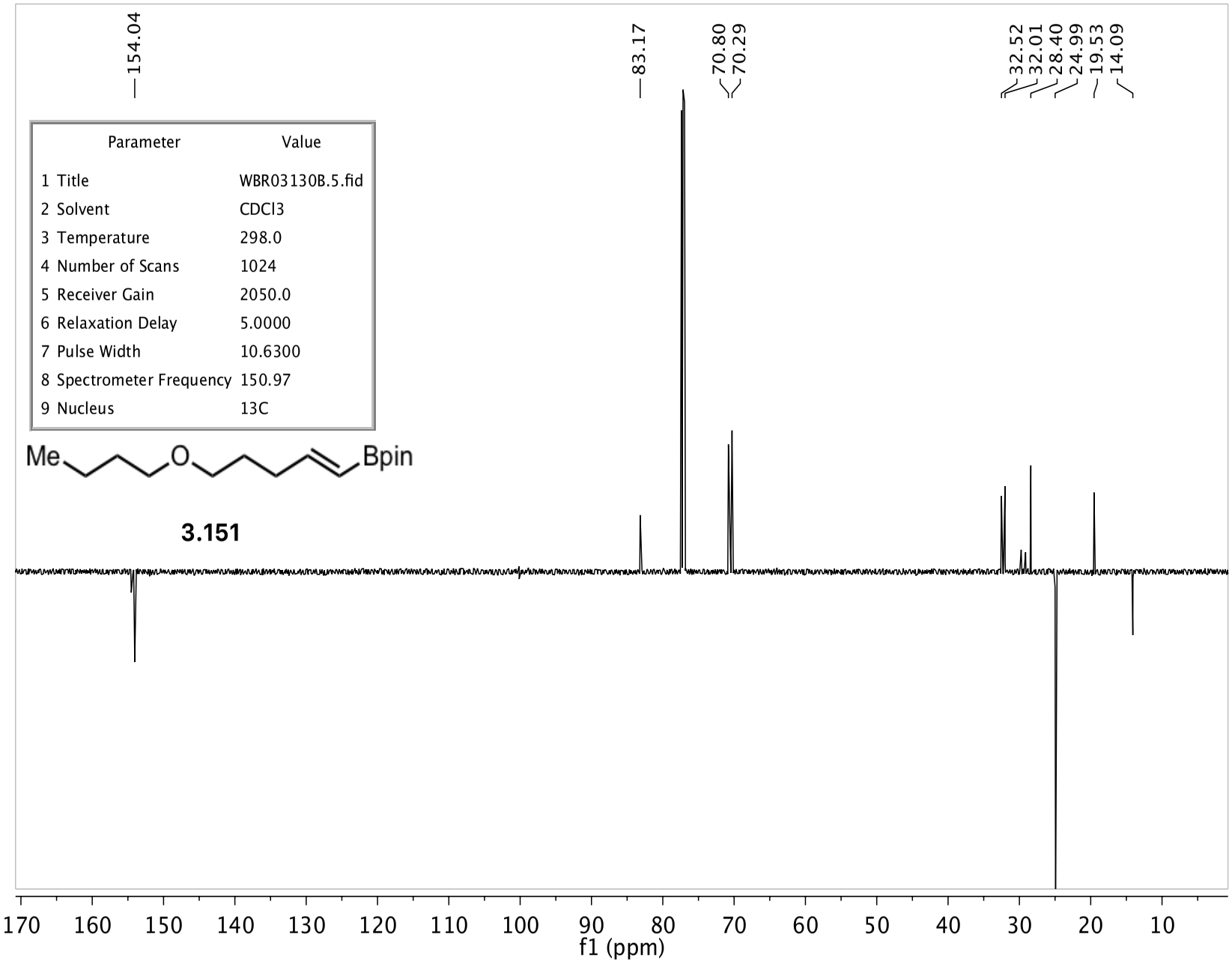
154.04
83.17
70.80
70.29
32.52
32.01
28.40
24.99
19.53
14.09
Parameter Value
1 Title WBR03130B.5.fid
2 Solvent CDCl3
3 Temperature 298.0
4 Number of Scans 1024
5 Receiver Gain 2050.0
6 Relaxation Delay 5.0000
7 Pulse Width 10.6300
8 Spectrometer Frequency 150.97
9 Nucleus 13C
Me
O
Bpin
3.151
170 160 150 140 130 120 110 100 90 80 70 60 50 40 30 20 10
f1 (ppm)

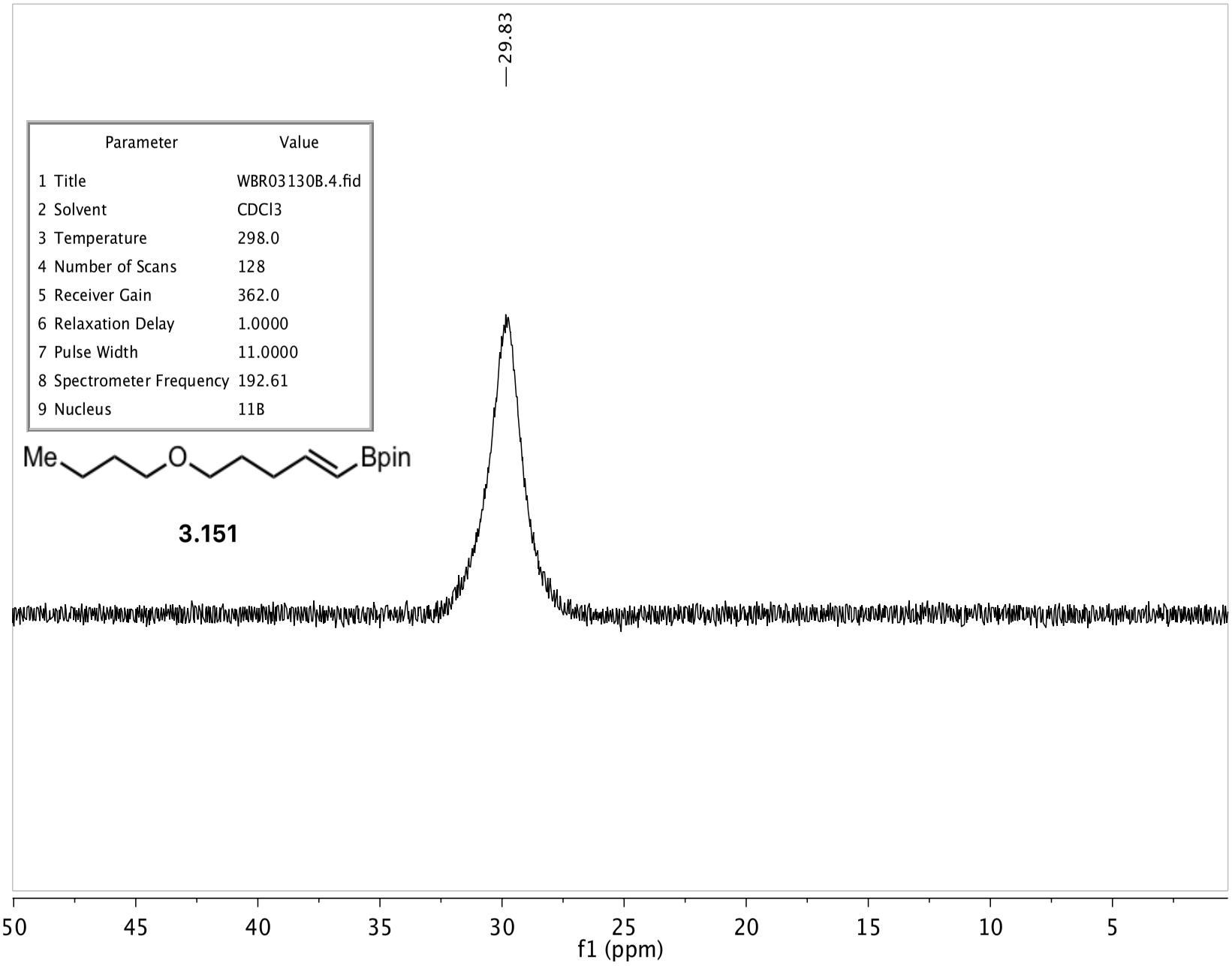
29.83
Parameter
Value
1 Title
WBR03130B.4.fid
2 Solvent
CDCl3
3 Temperature
298.0
4 Number of Scans
128
5 Receiver Gain
362.0
6 Relaxation Delay
1.0000
7 Pulse Width
11.0000
8 Spectrometer Frequency
192.61
9 Nucleus
11B
Me
O
Bpin
3.151
50
45
40
35
30
25
20
15
10
5
f1 (ppm)

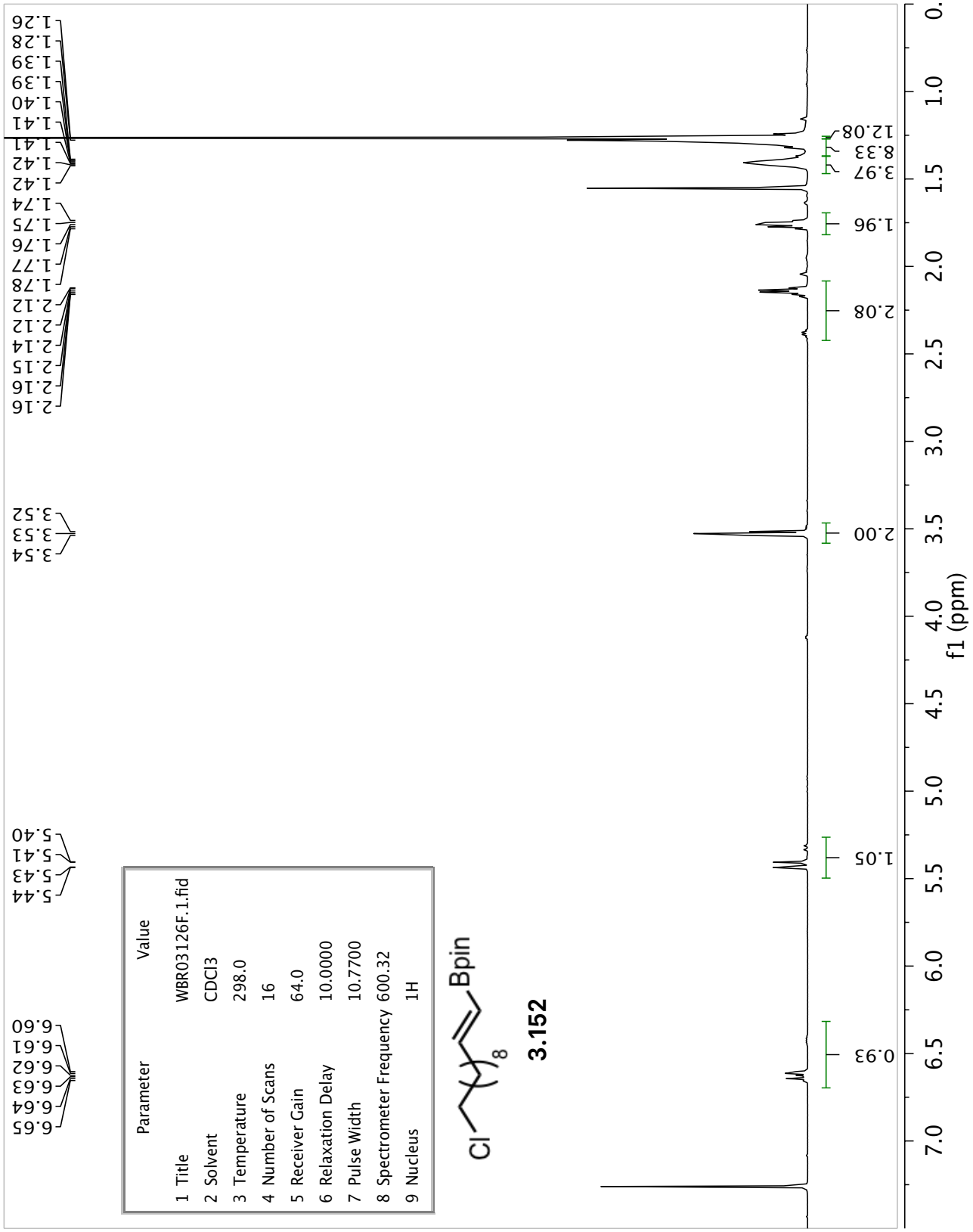
Parameter Value
1 Title WBR03126F.1.fid
2 Solvent CDCl3
3 Temperature 298.0
4 Number of Scans 16
5 Receiver Gain 64.0
6 Relaxation Delay 10.0000
7 Pulse Width 10.7700
8 Spectrometer Frequency 600.32
9 Nucleus 1H
Cl
8
Bpin
3.152
f1 (ppm)

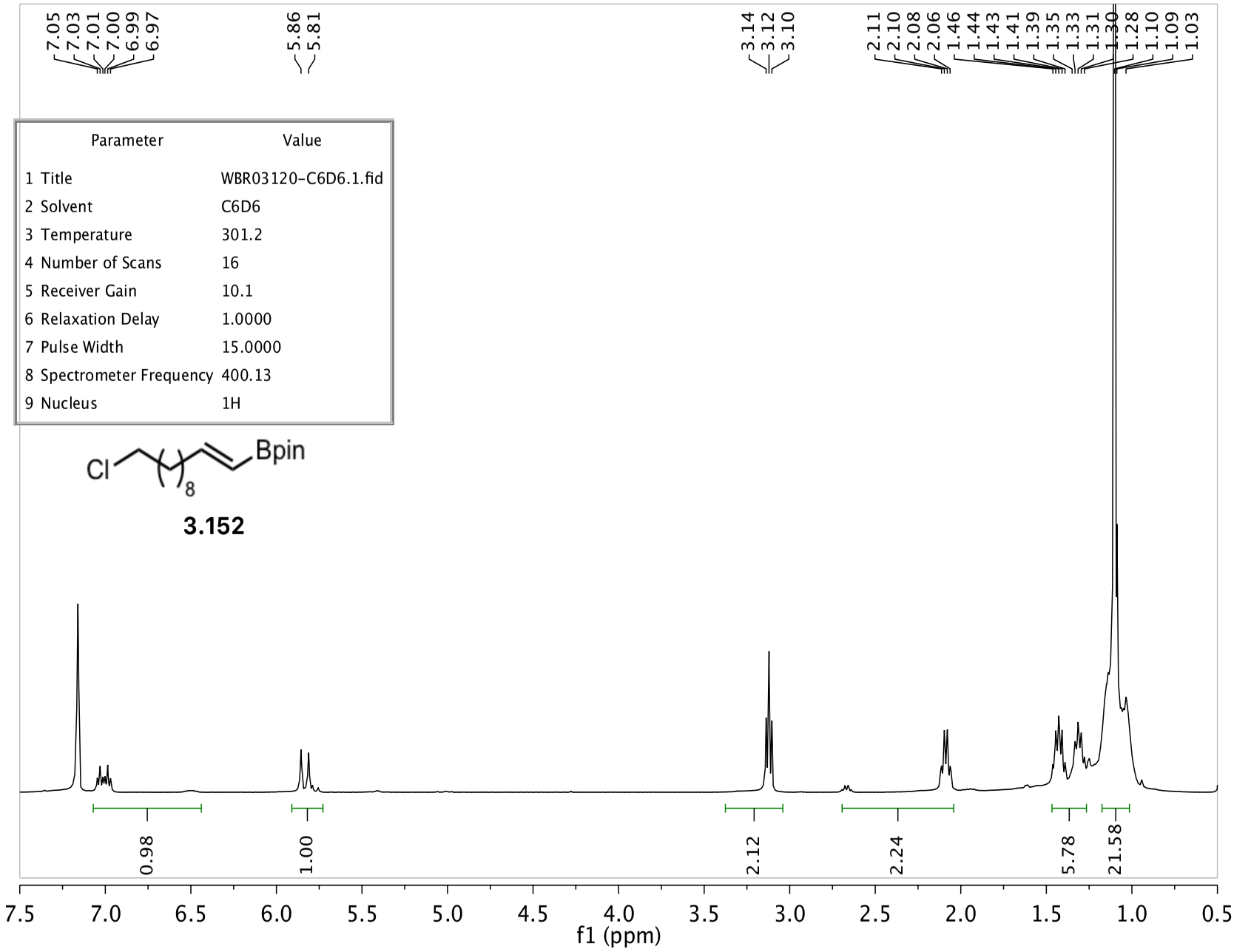
7.05
7.03
7.01
7.00
6.99
6.97
5.86
5.81
3.14
3.12
3.10
2.11
2.10
2.08
2.06
1.46
1.44
1.43
1.41
1.39
1.35
1.33
1.31
1.30
1.28
1.10
1.09
1.03
Parameter Value
1 Title WBR03120-C6D6.1.fid
2 Solvent C6D6
3 Temperature 301.2
4 Number of Scans 16
5 Receiver Gain 10.1
6 Relaxation Delay 1.0000
7 Pulse Width 15.0000
8 Spectrometer Frequency 400.13
9 Nucleus 1H
Cl
8
Bpin
3.152
0.98
1.00
2.12
2.24
5.78
21.58
7.5
7.0
6.5
6.0
5.5
5.0
4.5
4.0
3.5
3.0
2.5
2.0
1.5
1.0
0.5
f1 (ppm)

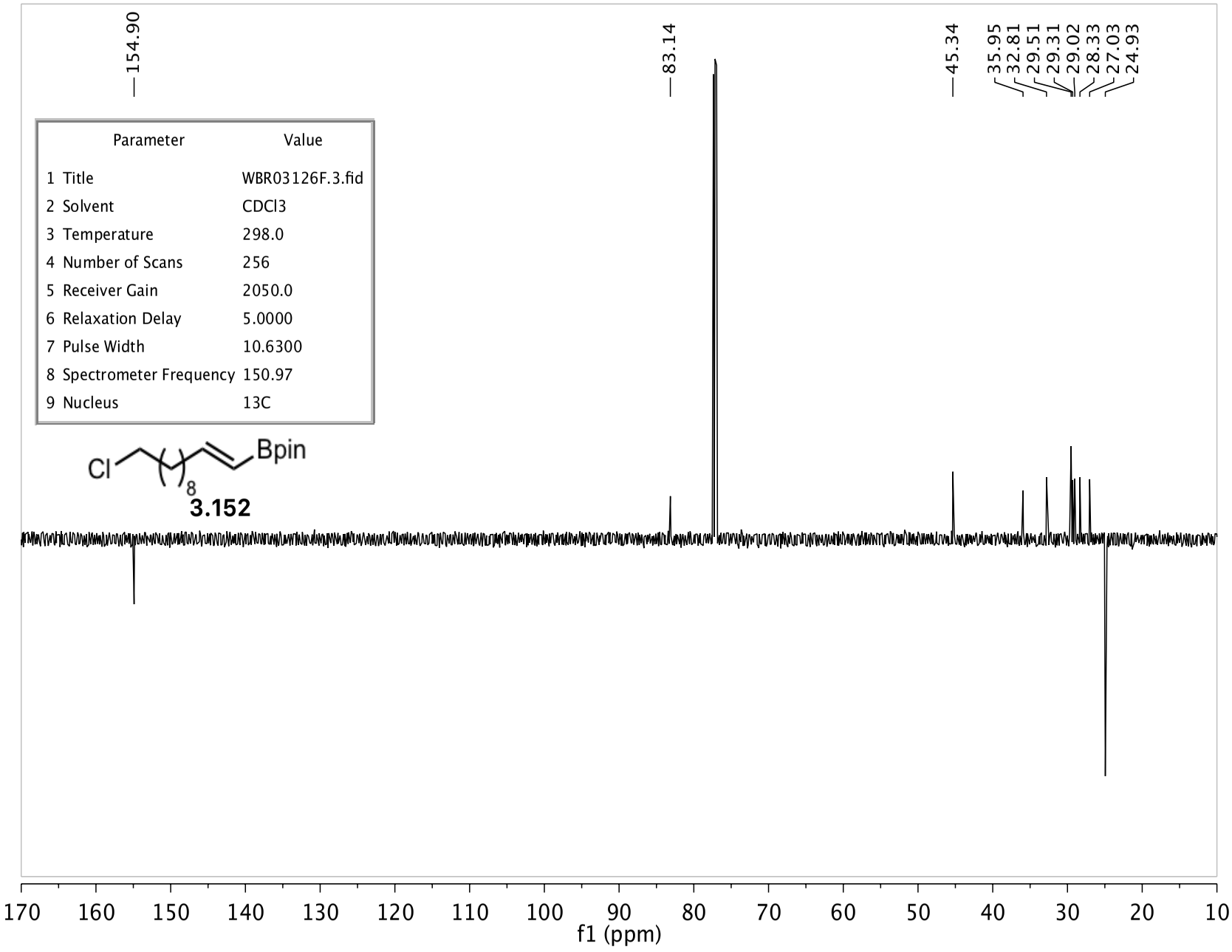
154.90
83.14
45.34
35.95
32.81
29.51
29.31
29.02
28.33
27.03
24.93
Parameter Value
1 Title WBR03126F.3.fid
2 Solvent CDCl3
3 Temperature 298.0
4 Number of Scans 256
5 Receiver Gain 2050.0
6 Relaxation Delay 5.0000
7 Pulse Width 10.6300
8 Spectrometer Frequency 150.97
9 Nucleus 13C
Cl
8
Bpin
3.152
170 160 150 140 130 120 110 100 90 80 70 60 50 40 30 20 10
f1 (ppm)

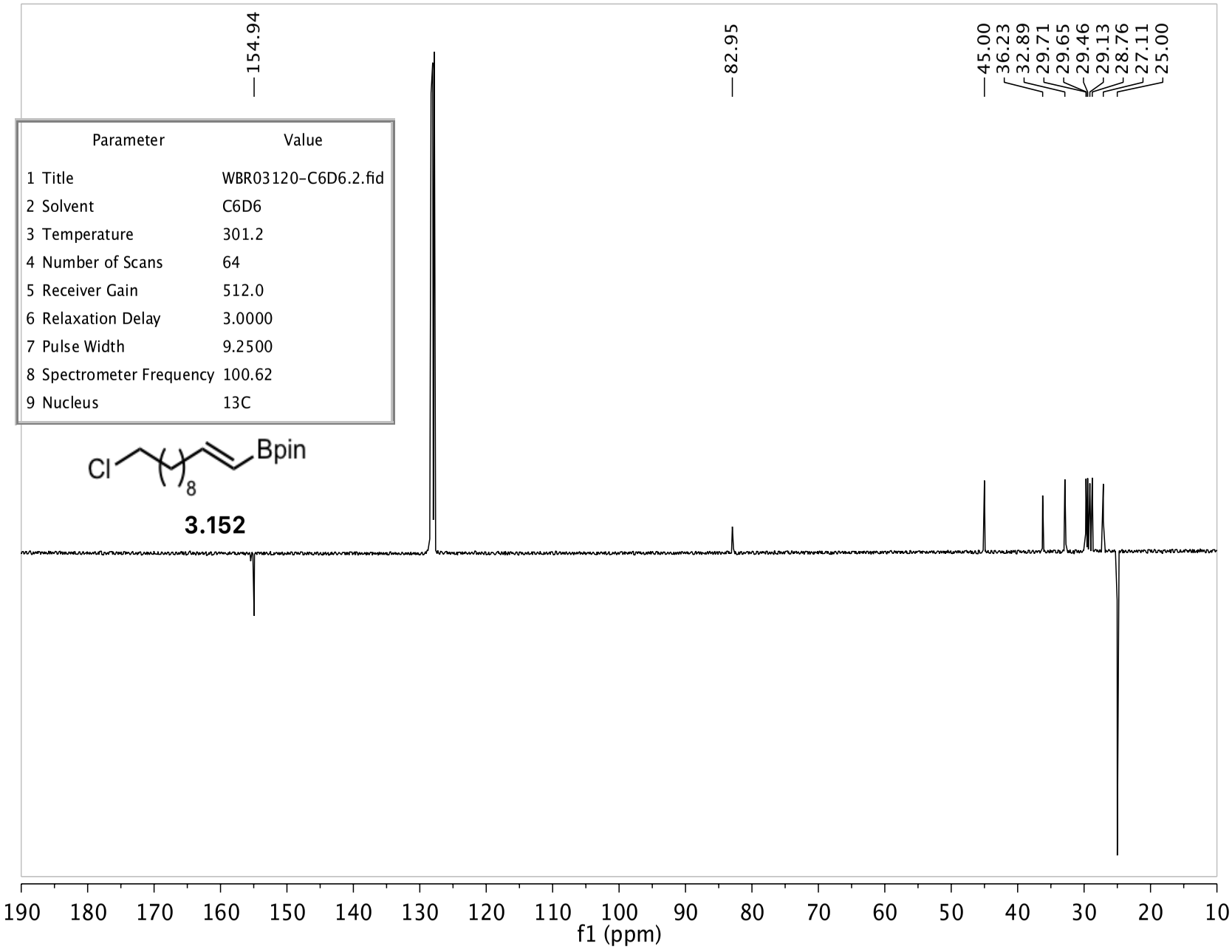
154.94
82.95
45.00
36.23
32.89
29.71
29.65
29.46
29.13
28.76
27.11
25.00
Parameter Value
1 Title WBR03120-C6D6.2.fid
2 Solvent C6D6
3 Temperature 301.2
4 Number of Scans 64
5 Receiver Gain 512.0
6 Relaxation Delay 3.0000
7 Pulse Width 9.2500
8 Spectrometer Frequency 100.62
9 Nucleus 13C
Cl
8
Bpin
3.152
190 180 170 160 150 140 130 120 110 100 90 80 70 60 50 40 30 20 10
f1 (ppm)

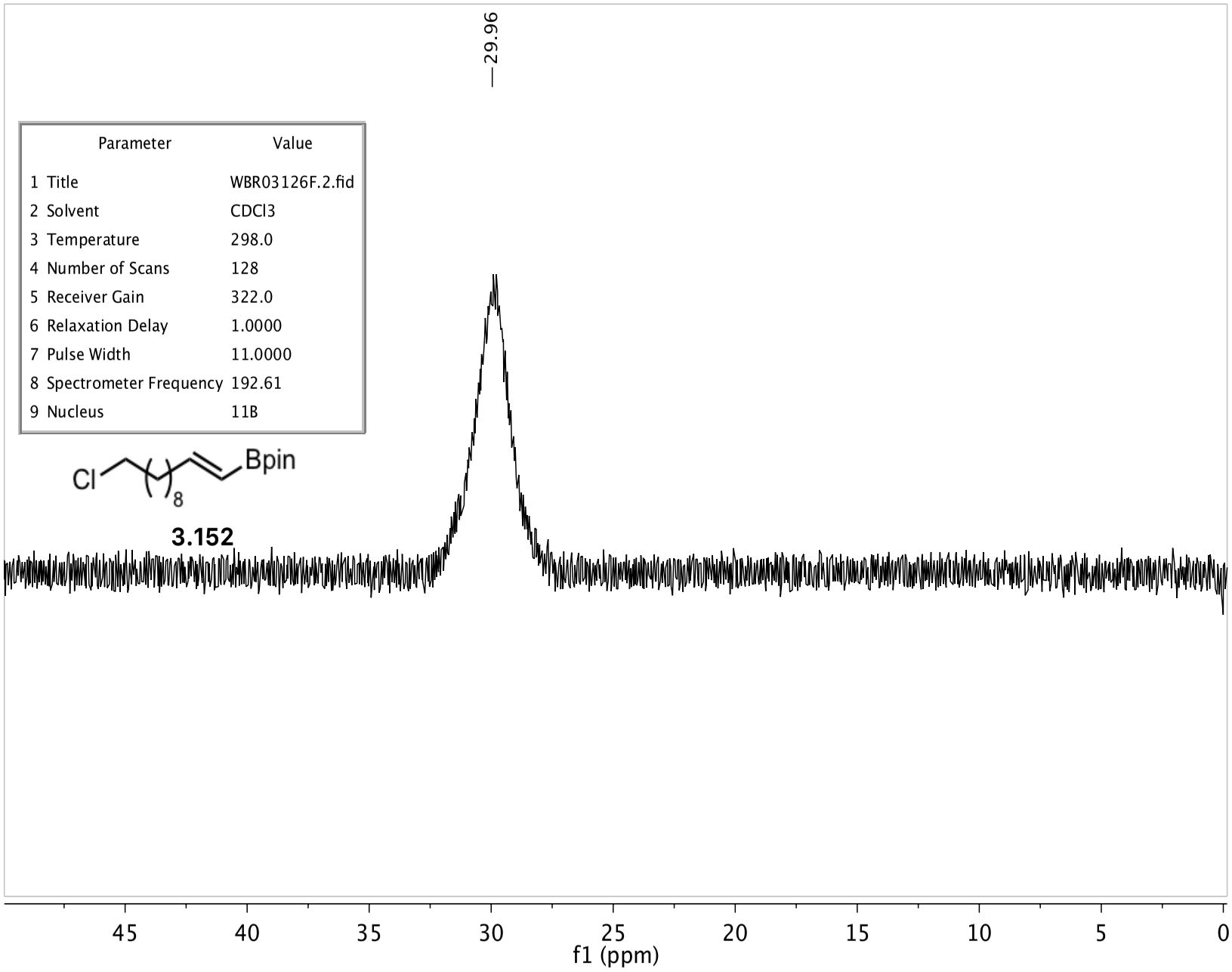
29.96
Parameter Value
1 Title WBR03126F.2.fid
2 Solvent CDCl3
3 Temperature 298.0
4 Number of Scans 128
5 Receiver Gain 322.0
6 Relaxation Delay 1.0000
7 Pulse Width 11.0000
8 Spectrometer Frequency 192.61
9 Nucleus 11B
Cl
8
Bpin
3.152
45
40
35
30
25
20
15
10
5
0
f1 (ppm)

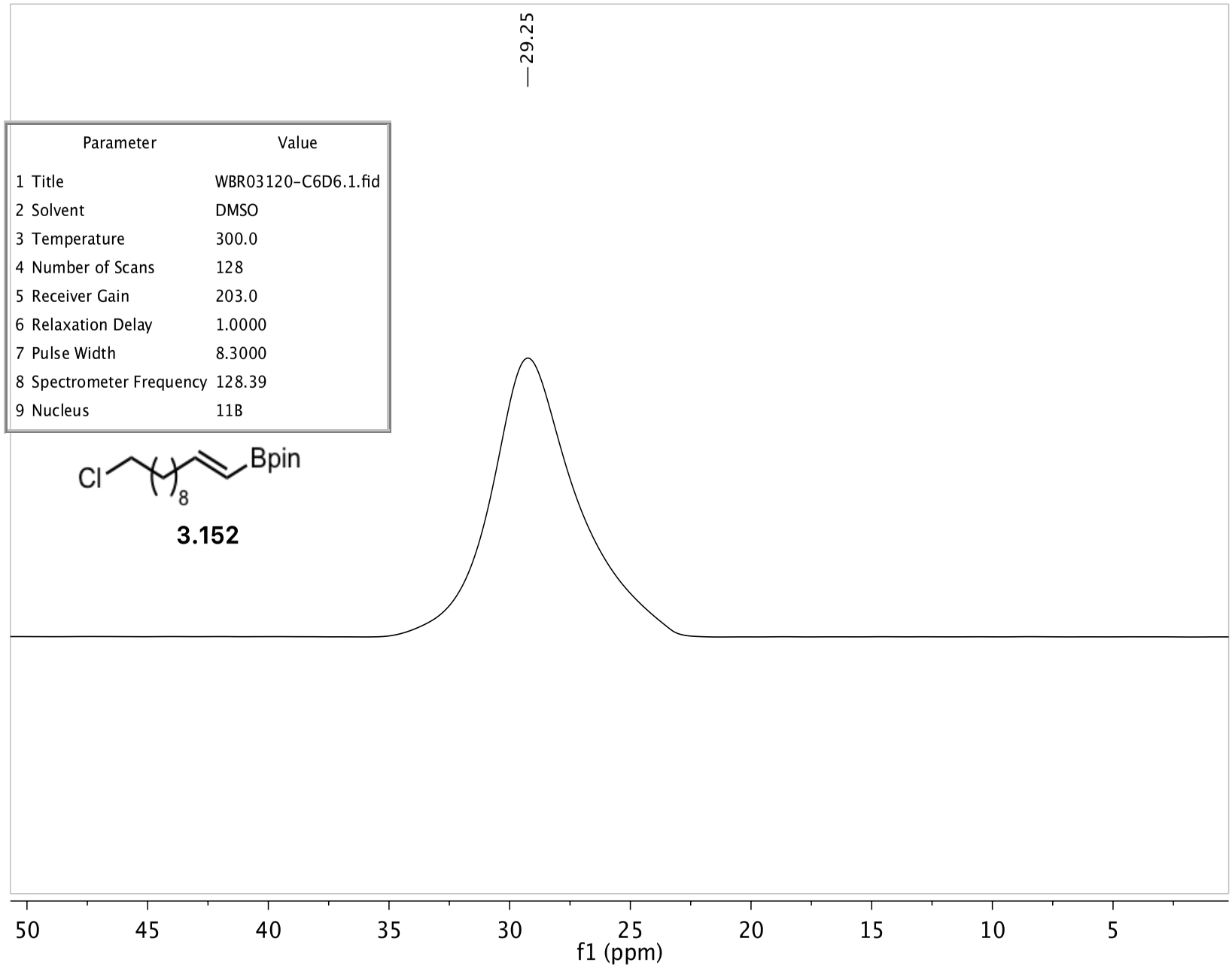
29.25
Parameter
Value
1 Title
WBR03120-C6D6.1.fid
2 Solvent
DMSO
3 Temperature
300.0
4 Number of Scans
128
5 Receiver Gain
203.0
6 Relaxation Delay
1.0000
7 Pulse Width
8.3000
8 Spectrometer Frequency
128.39
9 Nucleus
11B
Cl
8
Bpin
3.152
50
45
40
35
30
25
20
15
10
5
f1 (ppm)

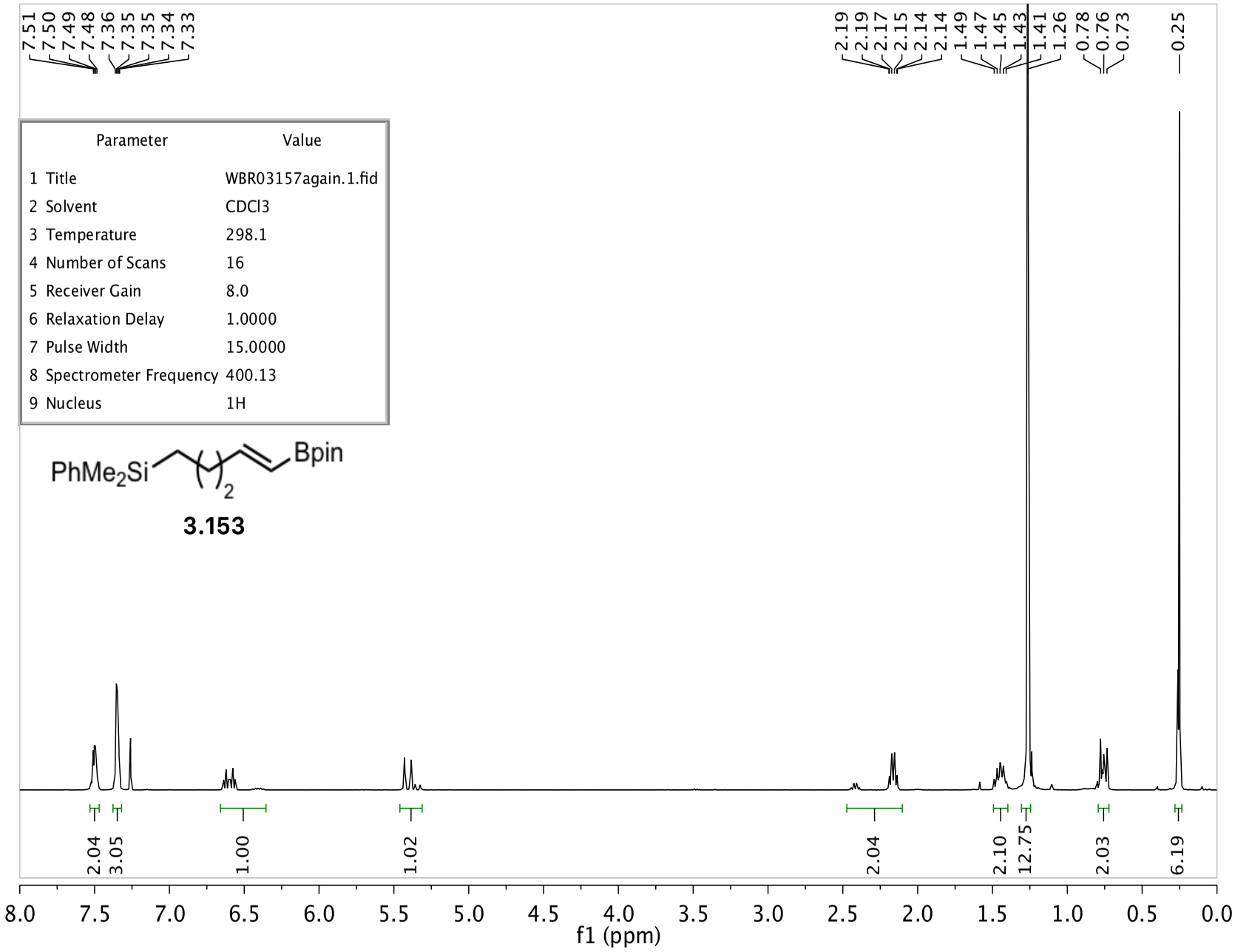
7.51
7.50
7.49
7.48
7.36
7.35
7.35
7.34
7.33
2.19
2.19
2.17
2.15
2.14
2.14
1.49
1.47
1.45
1.43
1.41
1.26
0.78
0.76
0.73
0.25
Parameter Value
1 Title WBR03157again.1.fid
2 Solvent CDCl3
3 Temperature 298.1
4 Number of Scans 16
5 Receiver Gain 8.0
6 Relaxation Delay 1.0000
7 Pulse Width 15.0000
8 Spectrometer Frequency 400.13
9 Nucleus 1H
PhMe2Si
Bpin
2
3.153
2.04
3.05
1.00
1.02
2.04
2.10
12.75
2.03
6.19
8.0
7.5
7.0
6.5
6.0
5.5
5.0
4.5
4.0
3.5
3.0
2.5
2.0
1.5
1.0
0.5
0.0
f1 (ppm)

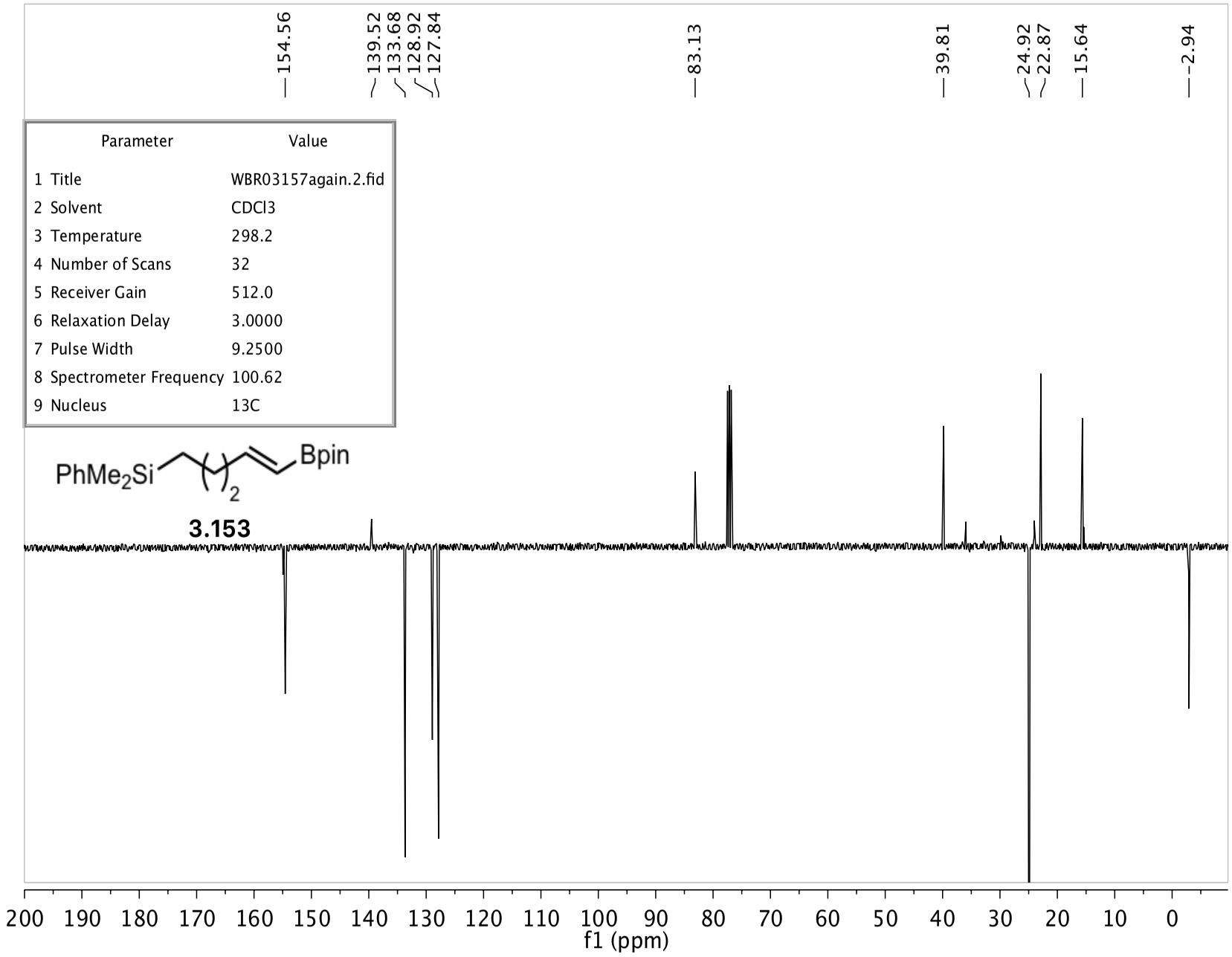
154.56
139.52
133.68
128.92
127.84
83.13
39.81
24.92
22.87
15.64
-2.94
Parameter Value
1 Title WBR03157again.2.fid
2 Solvent CDCl3
3 Temperature 298.2
4 Number of Scans 32
5 Receiver Gain 512.0
6 Relaxation Delay 3.0000
7 Pulse Width 9.2500
8 Spectrometer Frequency 100.62
9 Nucleus 13C
PhMe2Si
Bpin
2
3.153
200 190 180 170 160 150 140 130 120 110 100 90 80 70 60 50 40 30 20 10 0
f1 (ppm)

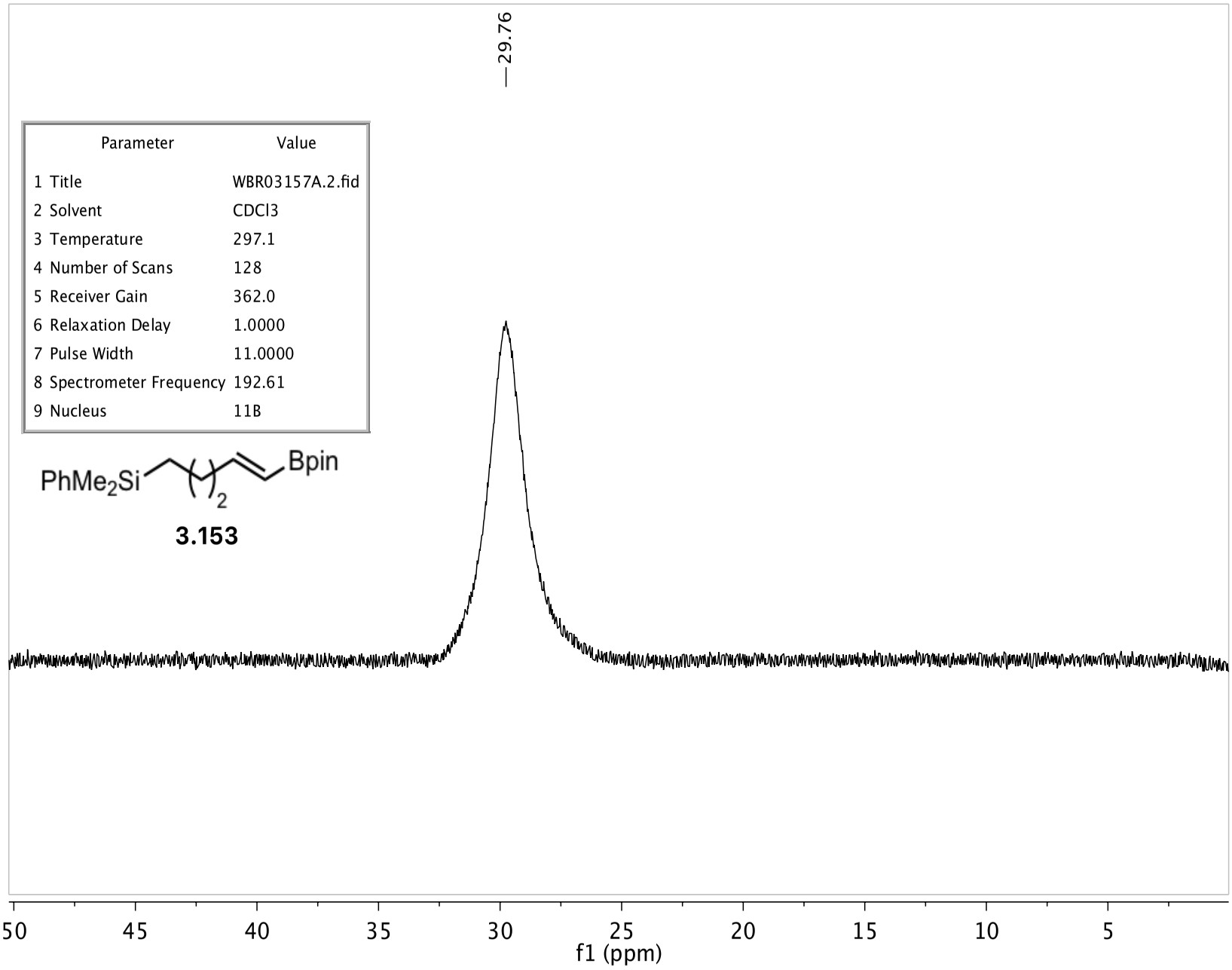
29.76
Parameter Value
1 Title WBR03157A.2.fid
2 Solvent CDCl3
3 Temperature 297.1
4 Number of Scans 128
5 Receiver Gain 362.0
6 Relaxation Delay 1.0000
7 Pulse Width 11.0000
8 Spectrometer Frequency 192.61
9 Nucleus 11B
PhMe2Si
Bpin
2
3.153
50
45
40
35
30
25
20
15
10
5
f1 (ppm)

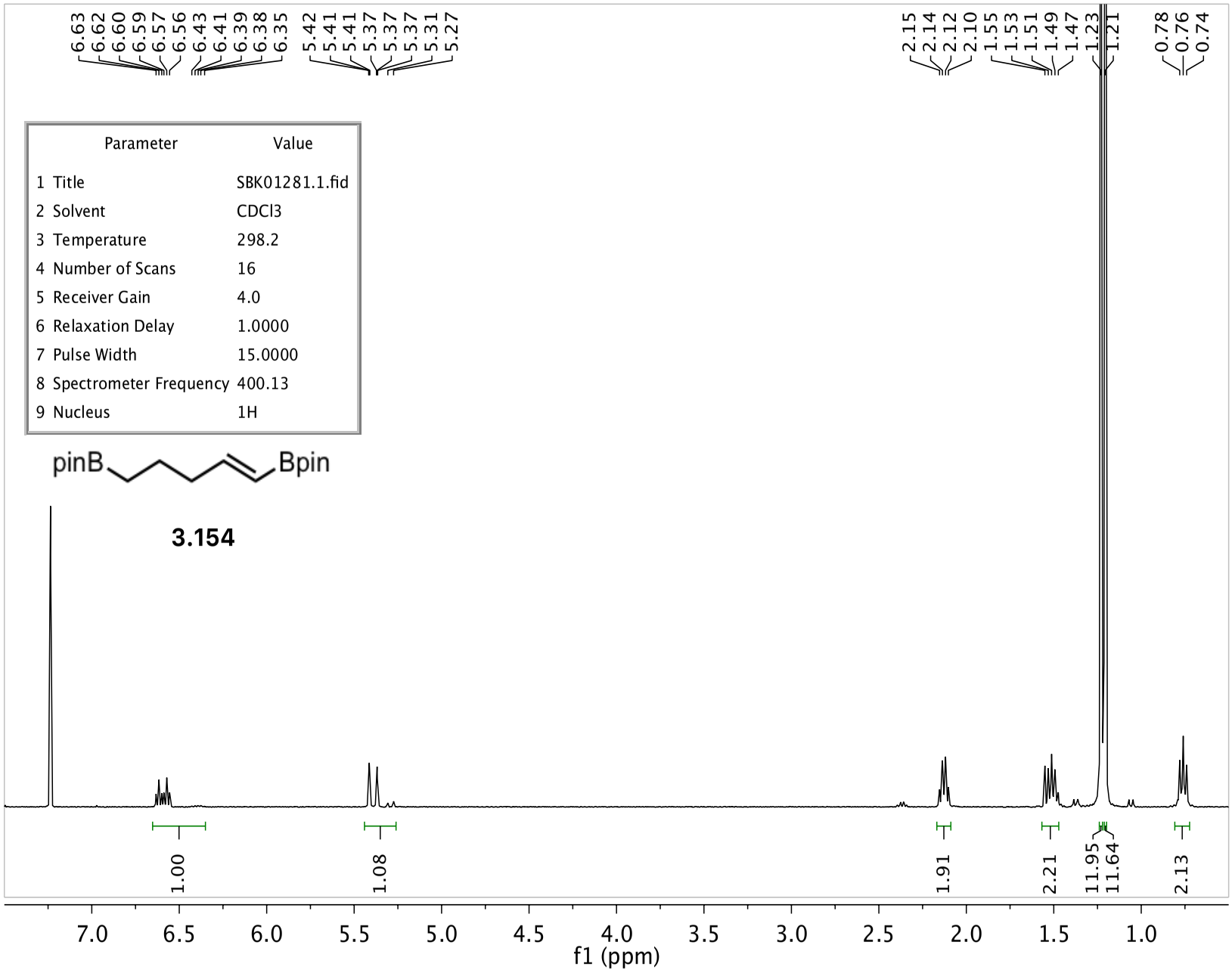
6.63
6.62
6.60
6.59
6.57
6.56
6.43
6.41
6.39
6.38
6.35
5.42
5.41
5.41
5.37
5.37
5.37
5.31
5.27
2.15
2.14
2.12
2.10
1.55
1.53
1.51
1.49
1.47
1.23
1.21
0.78
0.76
0.74
Parameter Value
1 Title SBK01281.1.fid
2 Solvent CDCl3
3 Temperature 298.2
4 Number of Scans 16
5 Receiver Gain 4.0
6 Relaxation Delay 1.0000
7 Pulse Width 15.0000
8 Spectrometer Frequency 400.13
9 Nucleus 1H
pinB
Bpin
3.154
1.00
1.08
1.91
2.21
11.95
11.64
2.13
7.0
6.5
6.0
5.5
5.0
4.5
4.0
3.5
3.0
2.5
2.0
1.5
1.0
f1 (ppm)

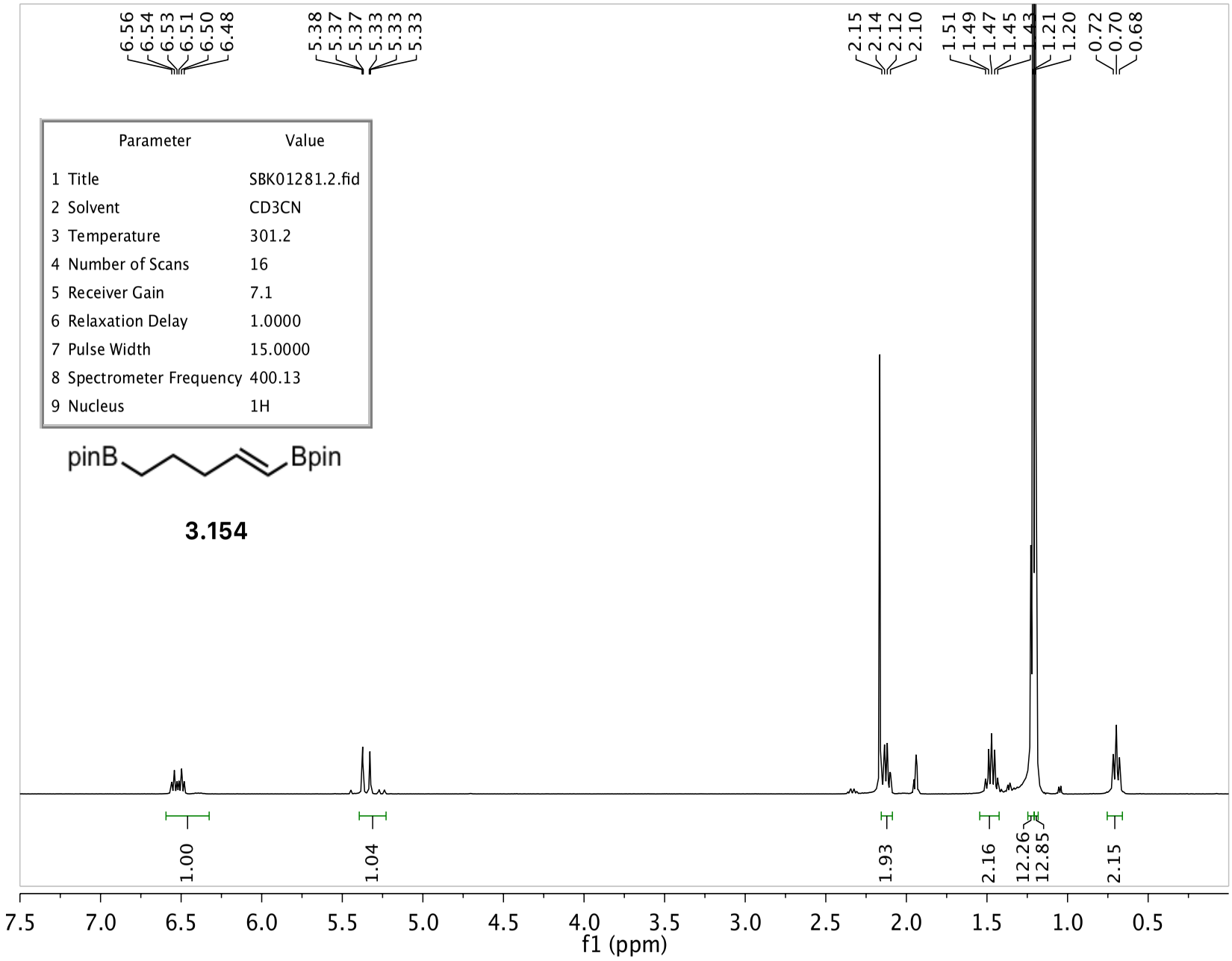
6.56
6.54
6.53
6.51
6.50
6.48
5.38
5.37
5.37
5.33
5.33
5.33
2.15
2.14
2.12
2.10
1.51
1.49
1.47
1.45
1.43
1.21
1.20
0.72
0.70
0.68
Parameter Value
1 Title SBK01281.2.fid
2 Solvent CD3CN
3 Temperature 301.2
4 Number of Scans 16
5 Receiver Gain 7.1
6 Relaxation Delay 1.0000
7 Pulse Width 15.0000
8 Spectrometer Frequency 400.13
9 Nucleus 1H
pinB
Bpin
3.154
1.00
1.04
1.93
2.16
12.26
12.85
2.15
7.5
7.0
6.5
6.0
5.5
5.0
4.5
4.0
3.5
3.0
2.5
2.0
1.5
1.0
0.5
f1 (ppm)

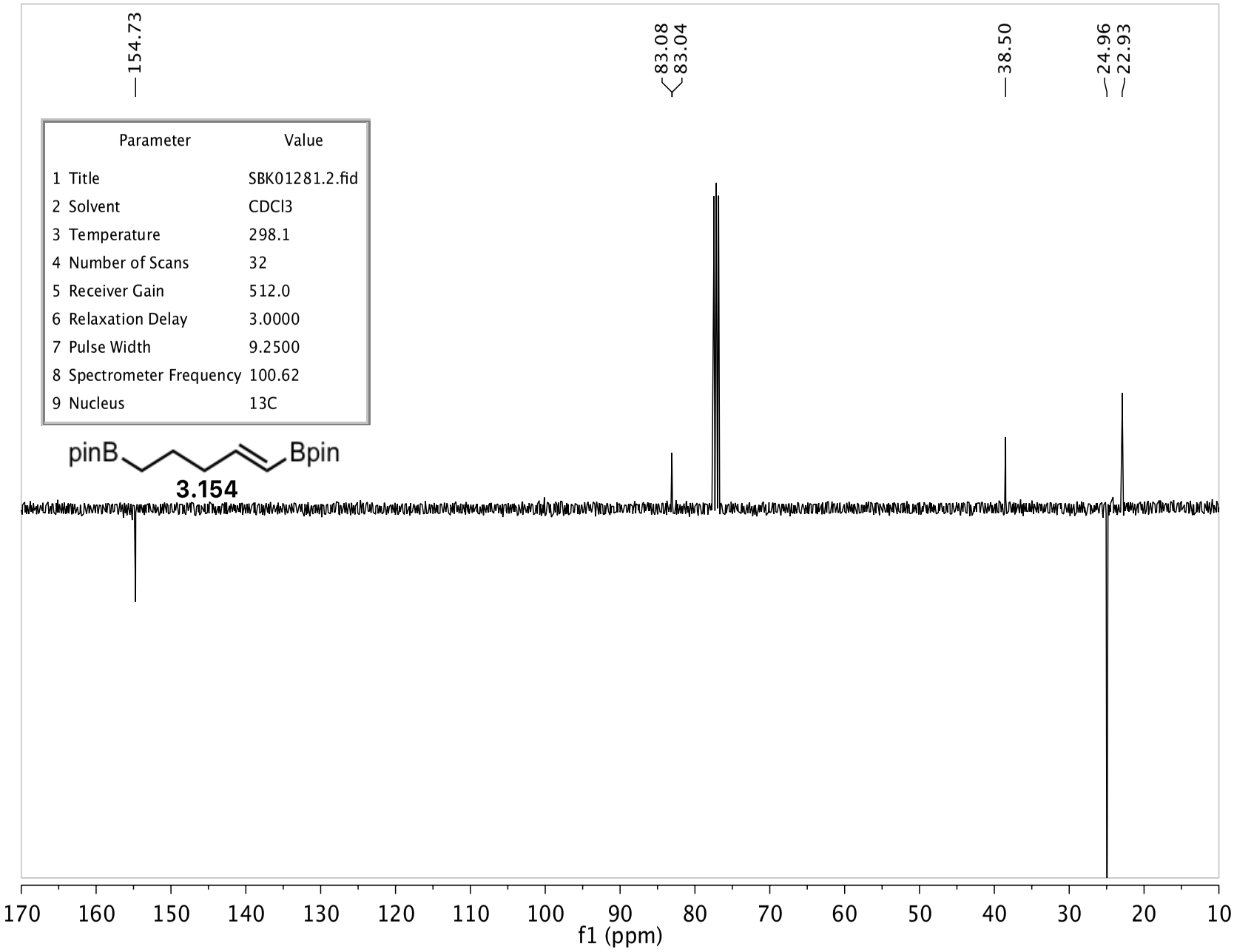
154.73
83.08
83.04
38.50
24.96
22.93
Parameter Value
1 Title SBK01281.2.fid
2 Solvent CDCl3
3 Temperature 298.1
4 Number of Scans 32
5 Receiver Gain 512.0
6 Relaxation Delay 3.0000
7 Pulse Width 9.2500
8 Spectrometer Frequency 100.62
9 Nucleus 13C
pinB
Bpin
3.154
170 160 150 140 130 120 110 100 90 80 70 60 50 40 30 20 10
f1 (ppm)

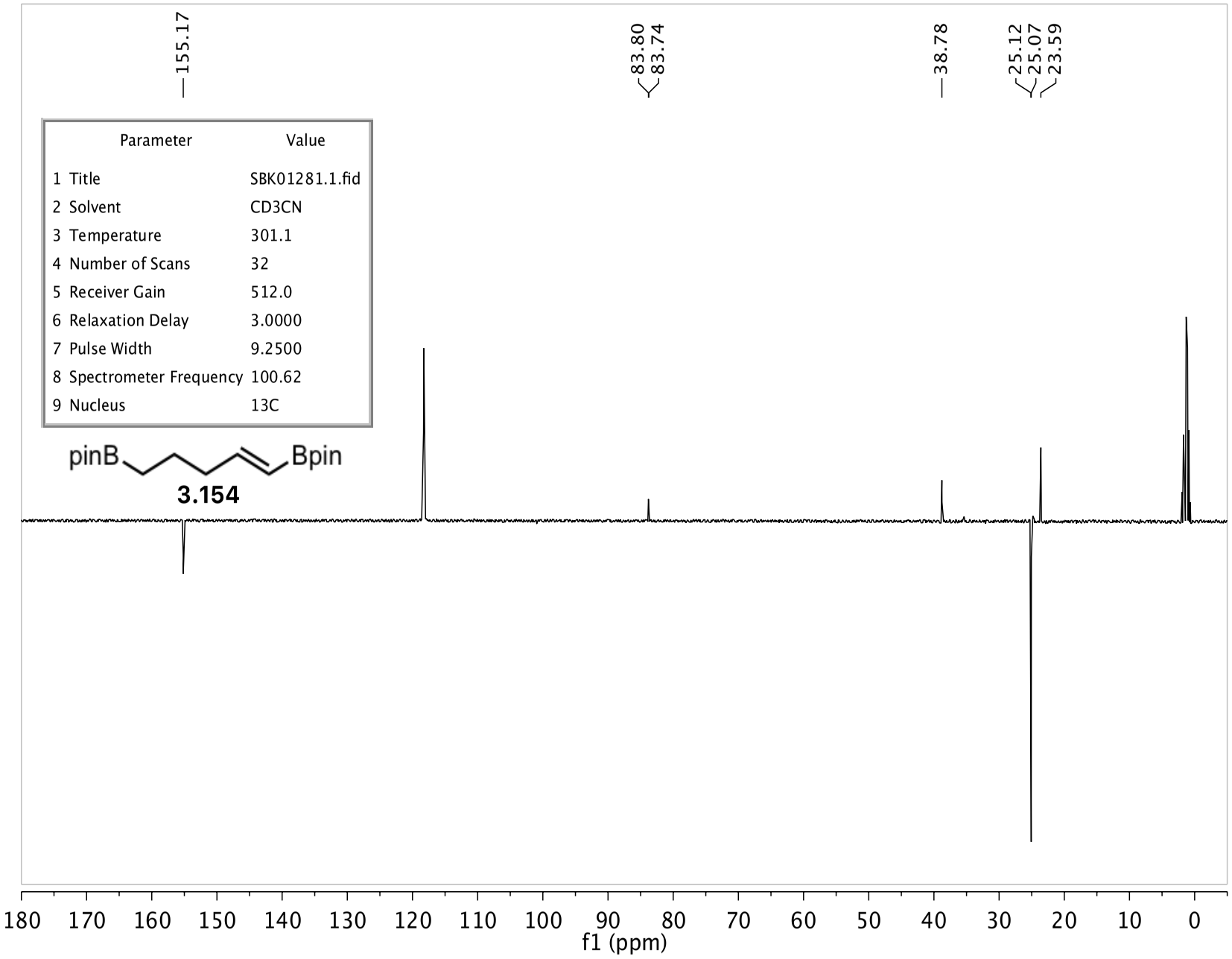
155.17
83.80
83.74
38.78
25.12
25.07
23.59
Parameter Value
1 Title SBK01281.1.fid
2 Solvent CD3CN
3 Temperature 301.1
4 Number of Scans 32
5 Receiver Gain 512.0
6 Relaxation Delay 3.0000
7 Pulse Width 9.2500
8 Spectrometer Frequency 100.62
9 Nucleus 13C
pinB
Bpin
3.154
180 170 160 150 140 130 120 110 100 90 80 70 60 50 40 30 20 10 0
f1 (ppm)

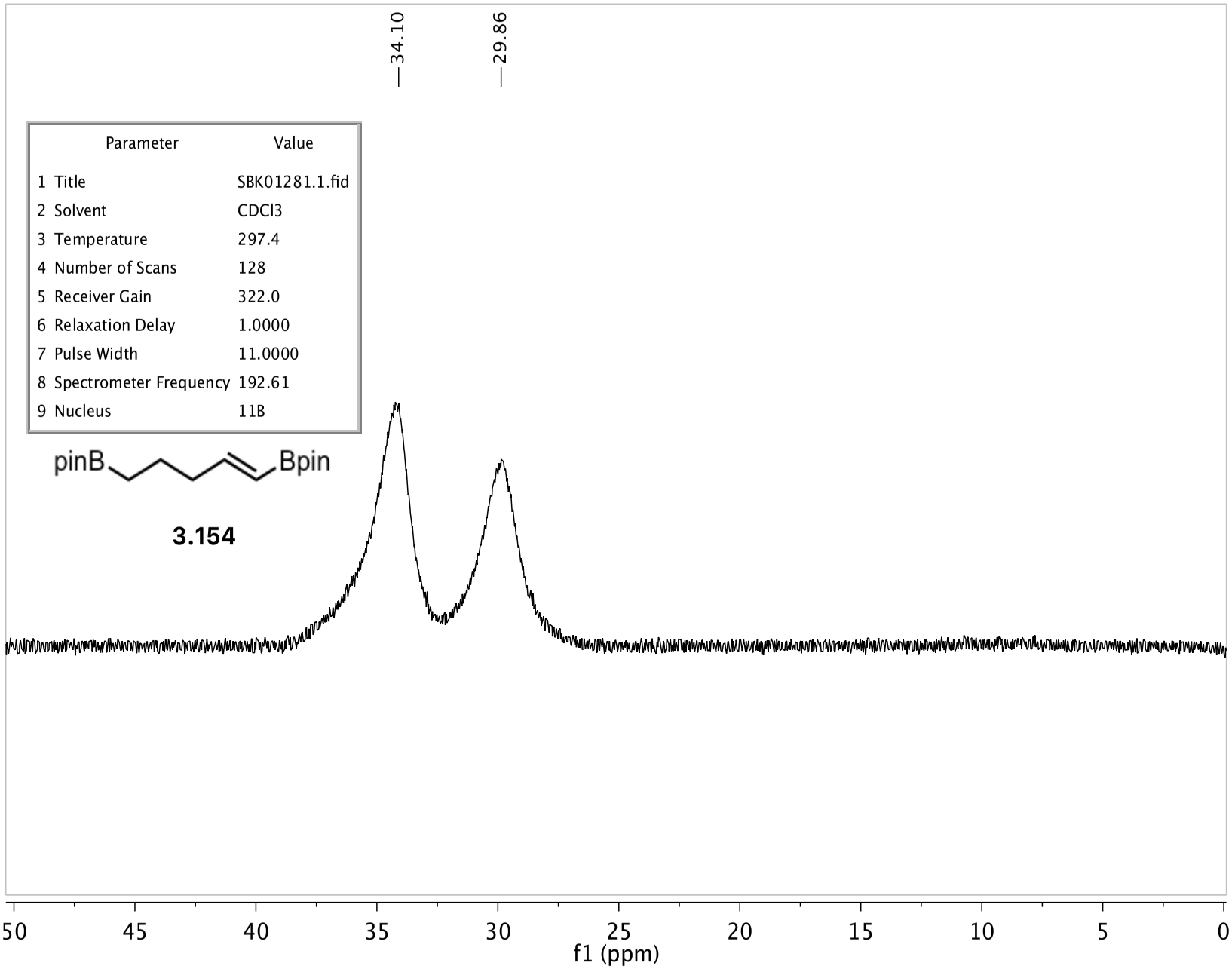
34.10
29.86
Parameter Value
1 Title SBK01281.1.fid
2 Solvent CDCl3
3 Temperature 297.4
4 Number of Scans 128
5 Receiver Gain 322.0
6 Relaxation Delay 1.0000
7 Pulse Width 11.0000
8 Spectrometer Frequency 192.61
9 Nucleus 11B
pinB
Bpin
3.154
50 45 40 35 30 25 20 15 10 5 0
f1 (ppm)

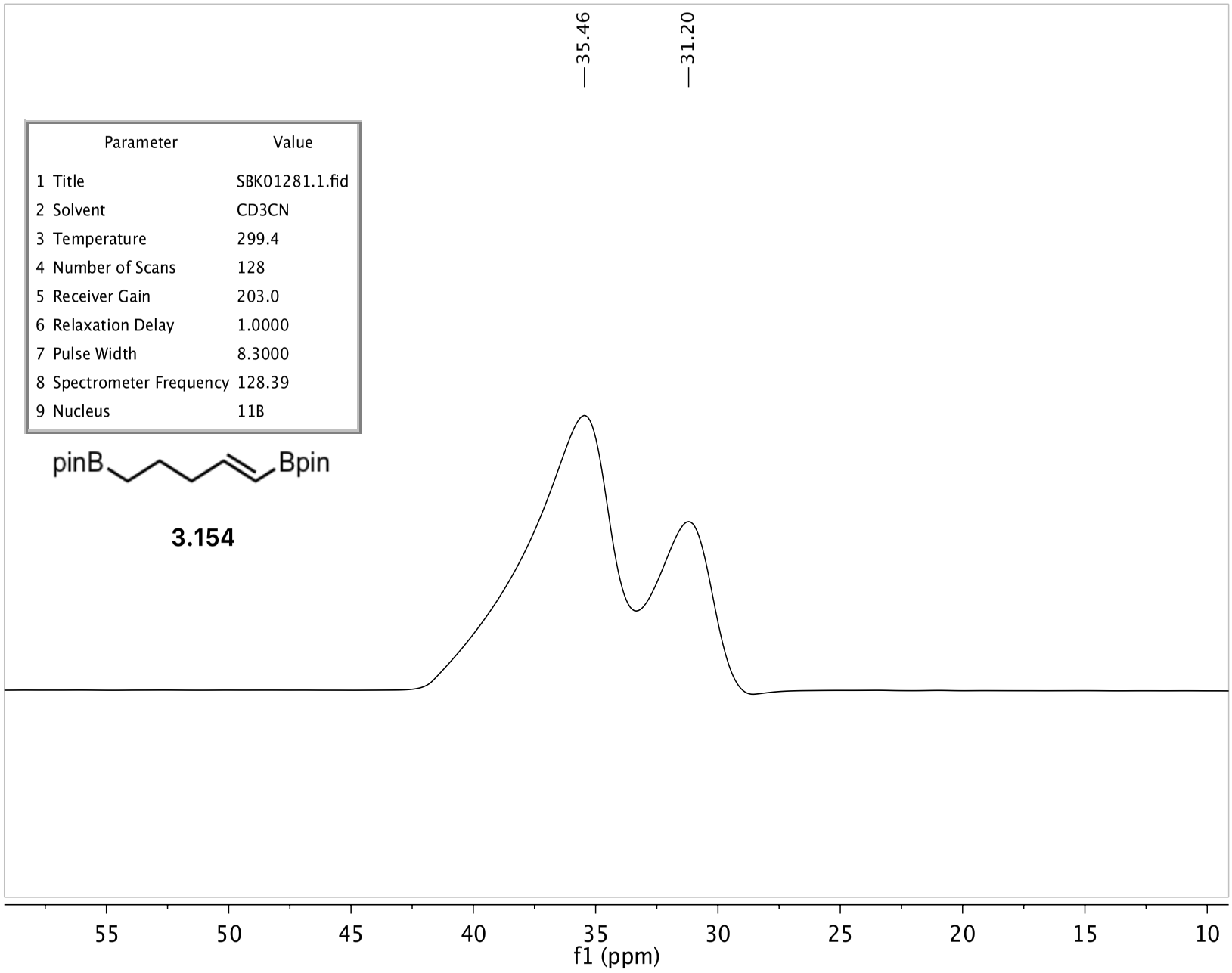
35.46
31.20
Parameter Value
1 Title SBK01281.1.fid
2 Solvent CD3CN
3 Temperature 299.4
4 Number of Scans 128
5 Receiver Gain 203.0
6 Relaxation Delay 1.0000
7 Pulse Width 8.3000
8 Spectrometer Frequency 128.39
9 Nucleus 11B
pinB
Bpin
3.154
55
50
45
40
35
30
25
20
15
10
f1 (ppm)

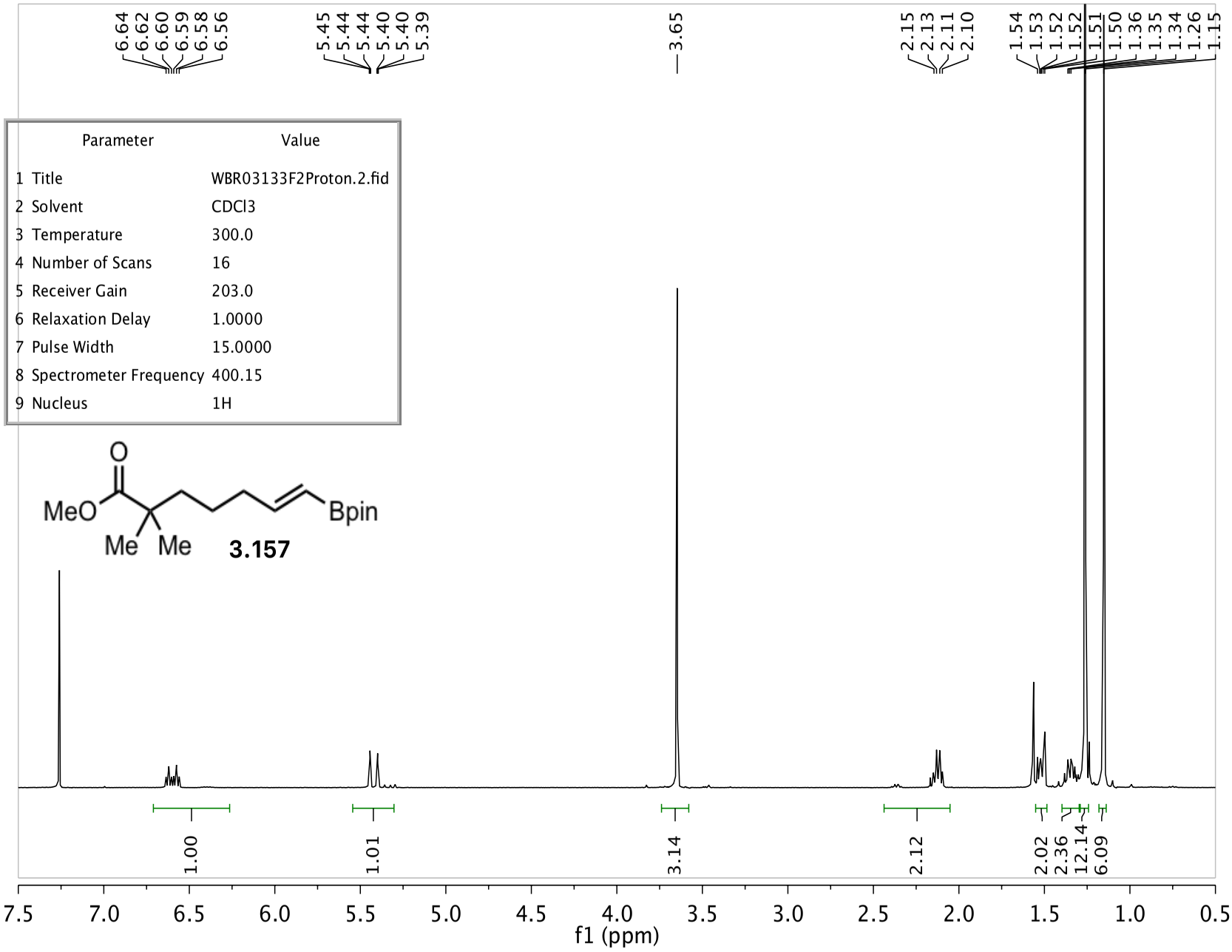
6.64
6.62
6.60
6.59
6.58
6.56
5.45
5.44
5.44
5.40
5.40
5.39
3.65
2.15
2.13
2.11
2.10
1.54
1.53
1.52
1.52
1.51
1.50
1.36
1.35
1.34
1.26
1.15
Parameter Value
1 Title WBR03133F2Proton.2.fid
2 Solvent CDCl3
3 Temperature 300.0
4 Number of Scans 16
5 Receiver Gain 203.0
6 Relaxation Delay 1.0000
7 Pulse Width 15.0000
8 Spectrometer Frequency 400.15
9 Nucleus 1H
MeO
Me Me
Bpin
3.157
1.00
1.01
3.14
2.12
2.02
2.36
12.14
6.09
7.5 7.0 6.5 6.0 5.5 5.0 4.5 4.0 3.5 3.0 2.5 2.0 1.5 1.0 0.5
f1 (ppm)

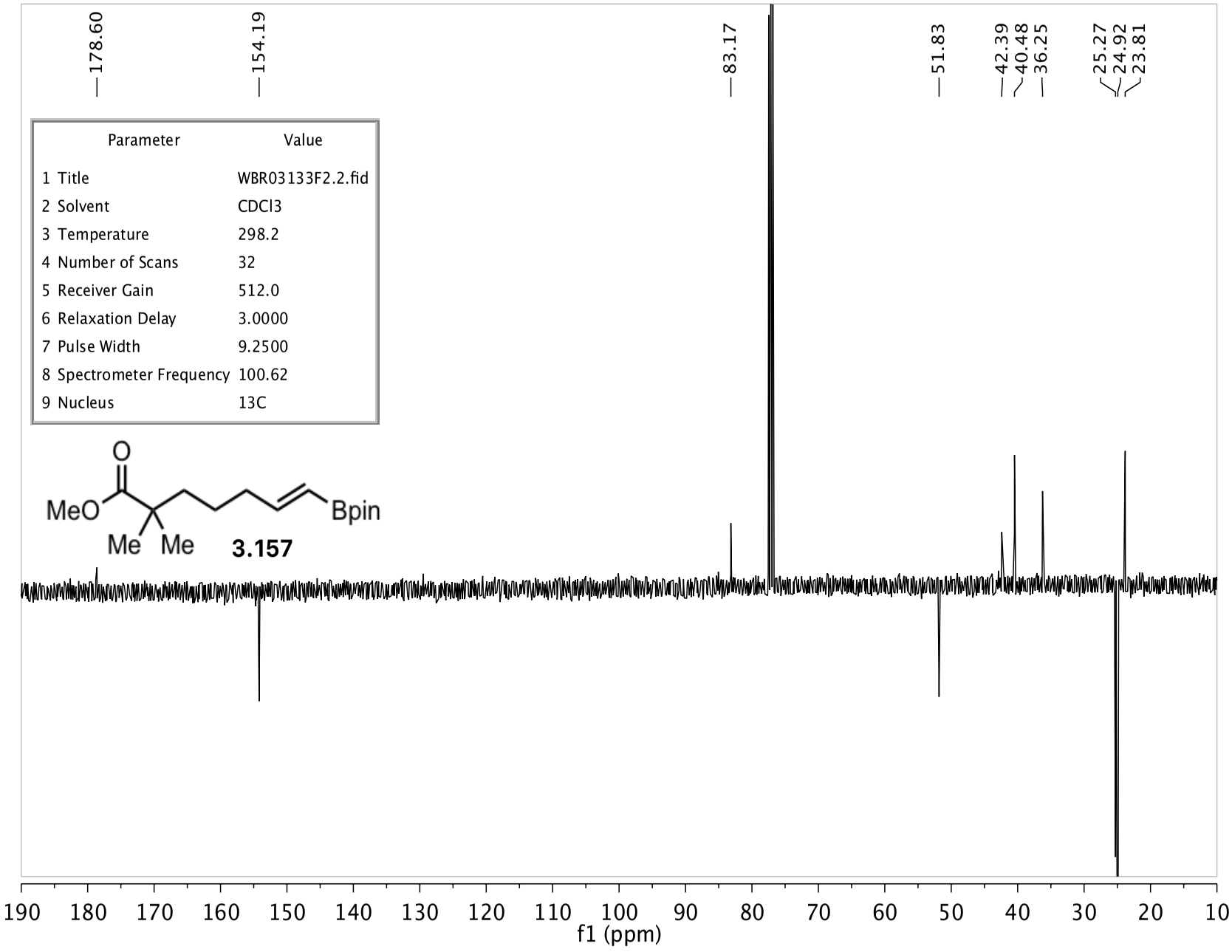
178.60
154.19
83.17
51.83
42.39
40.48
36.25
25.27
24.92
23.81
Parameter Value
1 Title WBR03133F2.2.fid
2 Solvent CDCl3
3 Temperature 298.2
4 Number of Scans 32
5 Receiver Gain 512.0
6 Relaxation Delay 3.0000
7 Pulse Width 9.2500
8 Spectrometer Frequency 100.62
9 Nucleus 13C
MeO
Me Me
Bpin
3.157
190 180 170 160 150 140 130 120 110 100 90 80 70 60 50 40 30 20 10
f1 (ppm)

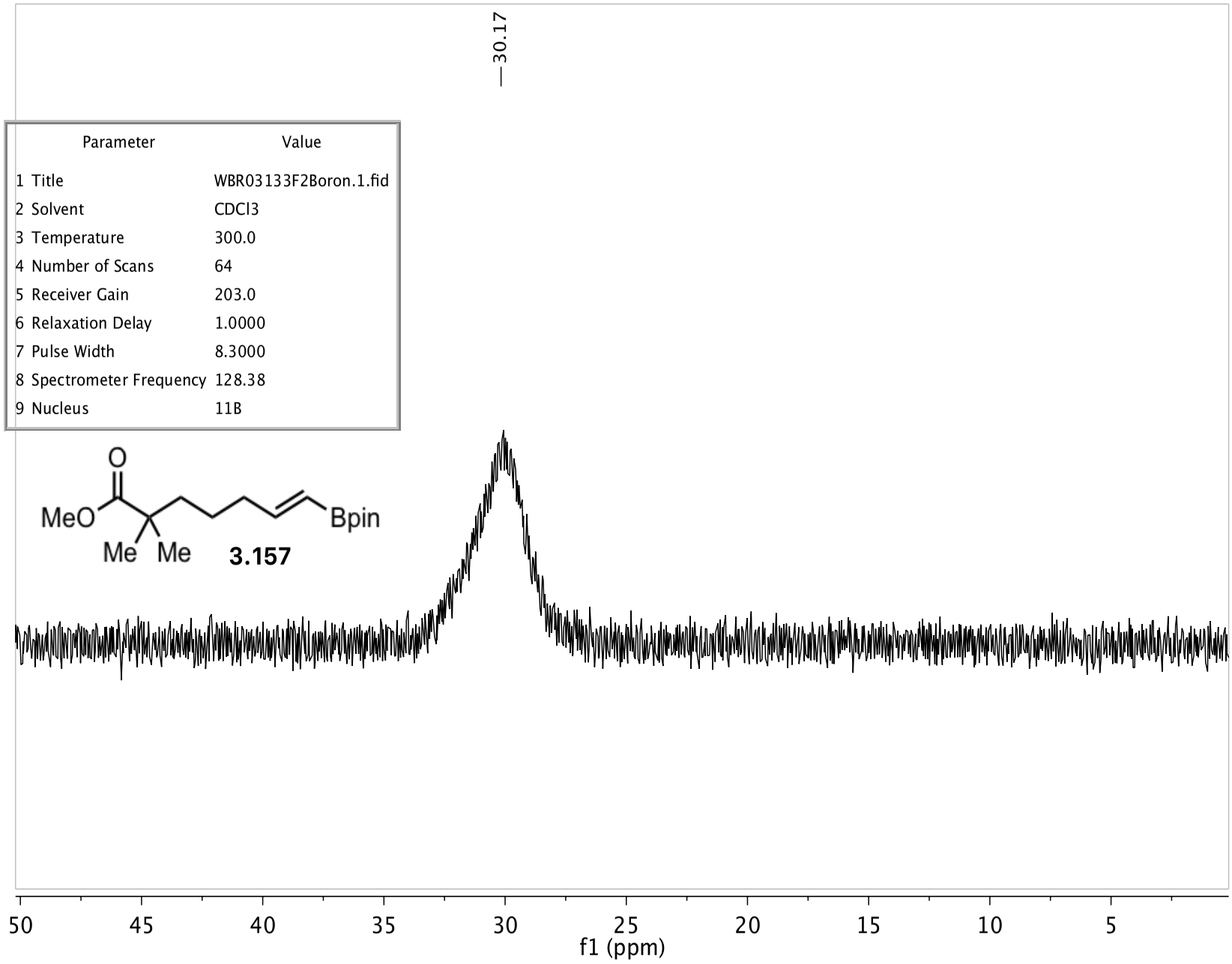
30.17
Parameter Value
1 Title WBR03133F2Boron.1.fid
2 Solvent CDCl3
3 Temperature 300.0
4 Number of Scans 64
5 Receiver Gain 203.0
6 Relaxation Delay 1.0000
7 Pulse Width 8.3000
8 Spectrometer Frequency 128.38
9 Nucleus 11B
O
MeO
Me Me
Bpin
3.157
50 45 40 35 30 25 20 15 10 5
f1 (ppm)

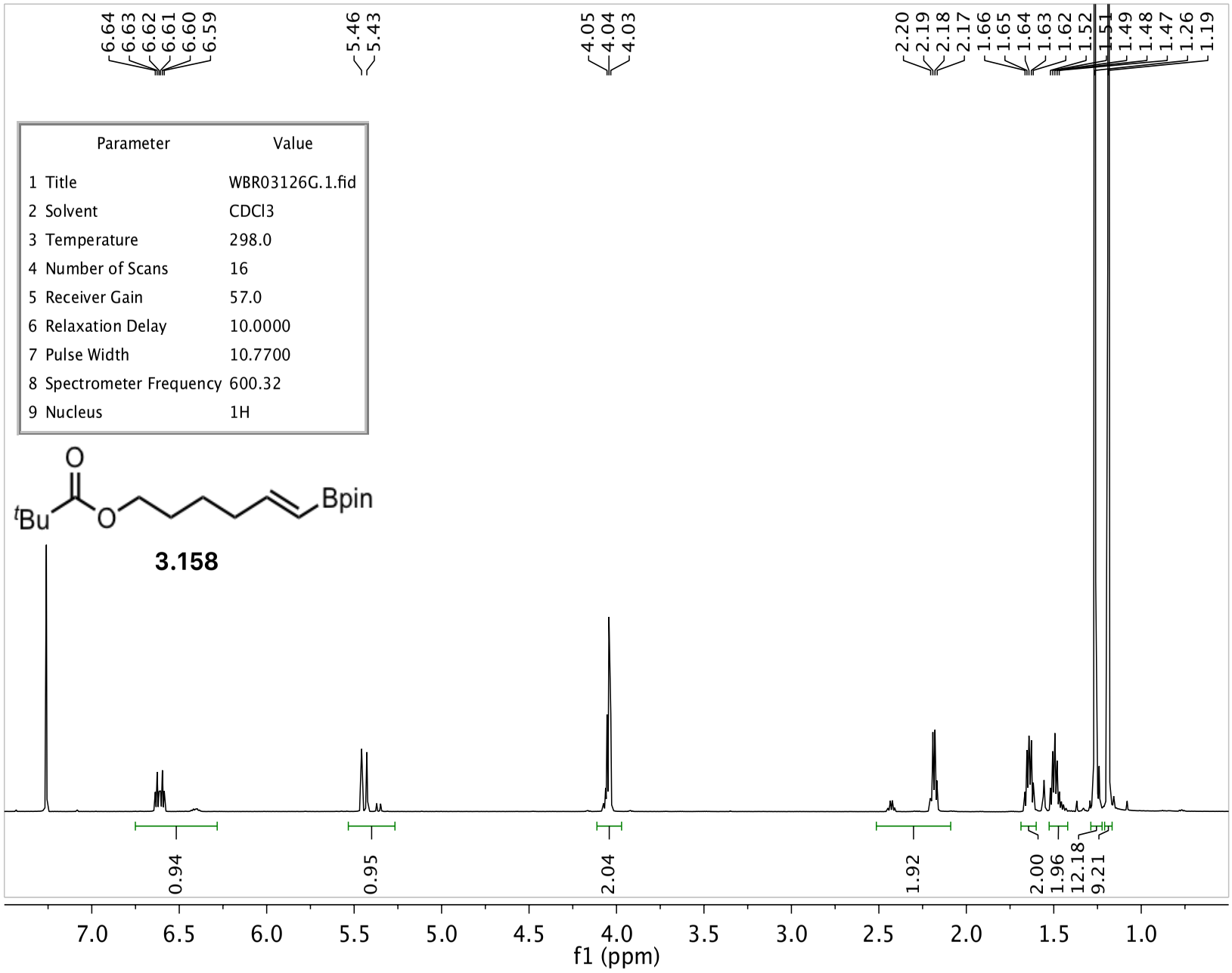
6.64
6.63
6.62
6.61
6.60
6.59
5.46
5.43
4.05
4.04
4.03
2.20
2.19
2.18
2.17
1.66
1.65
1.64
1.63
1.62
1.52
1.51
1.49
1.48
1.47
1.26
1.19
Parameter Value
1 Title WBR03126G.1.fid
2 Solvent CDCl3
3 Temperature 298.0
4 Number of Scans 16
5 Receiver Gain 57.0
6 Relaxation Delay 10.0000
7 Pulse Width 10.7700
8 Spectrometer Frequency 600.32
9 Nucleus 1H
tBu
O
O
Bpin
3.158
0.94
0.95
2.04
1.92
2.00
1.96
12.18
9.21
7.0
6.5
6.0
5.5
5.0
4.5
4.0
3.5
3.0
2.5
2.0
1.5
1.0
f1 (ppm)

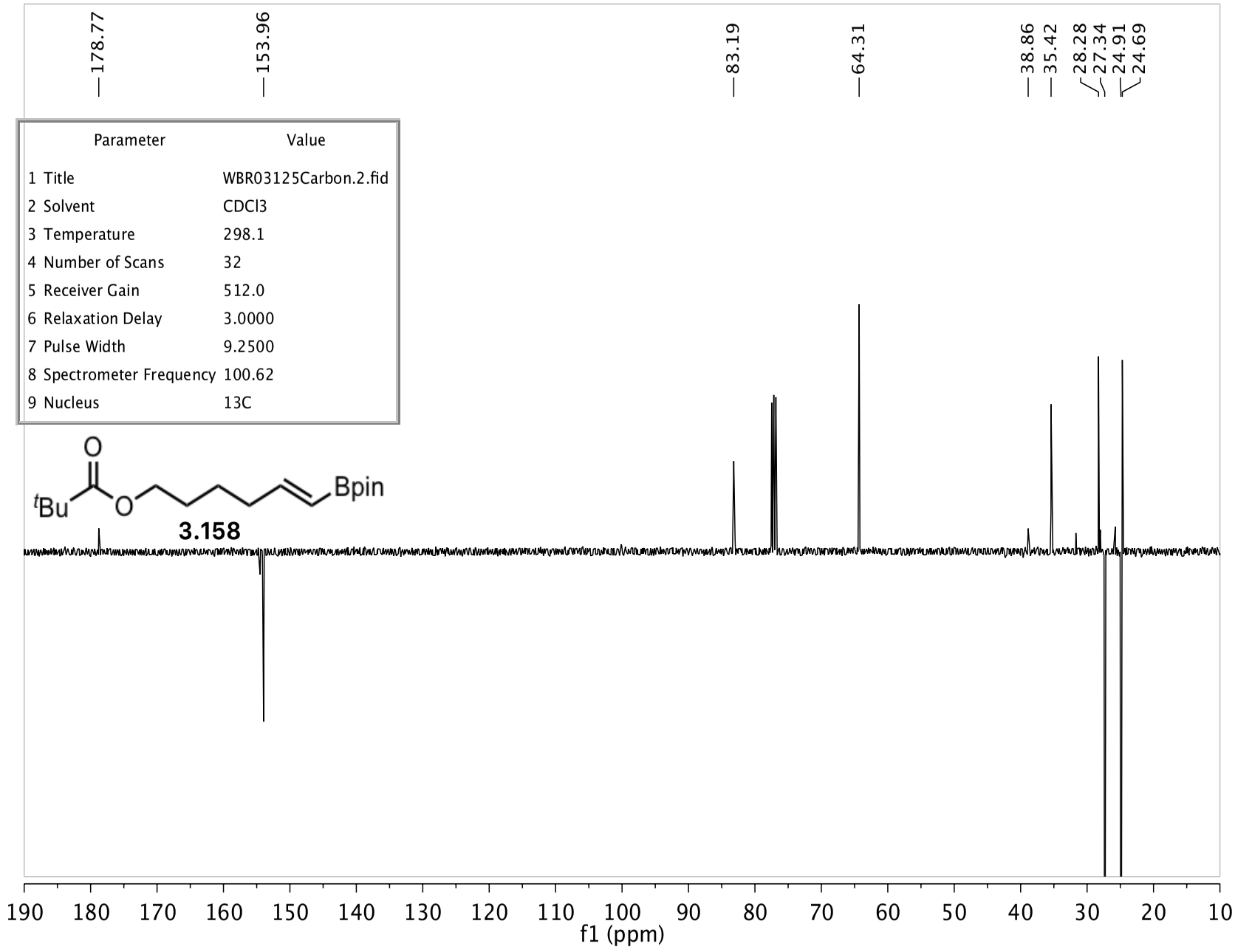
178.77
153.96
83.19
64.31
38.86
35.42
28.28
27.34
24.91
24.69
Parameter Value
1 Title WBR03125Carbon.2.fid
2 Solvent CDCl3
3 Temperature 298.1
4 Number of Scans 32
5 Receiver Gain 512.0
6 Relaxation Delay 3.0000
7 Pulse Width 9.2500
8 Spectrometer Frequency 100.62
9 Nucleus 13C
tBu
O
O
Bpin
3.158
190 180 170 160 150 140 130 120 110 100 90 80 70 60 50 40 30 20 10
f1 (ppm)

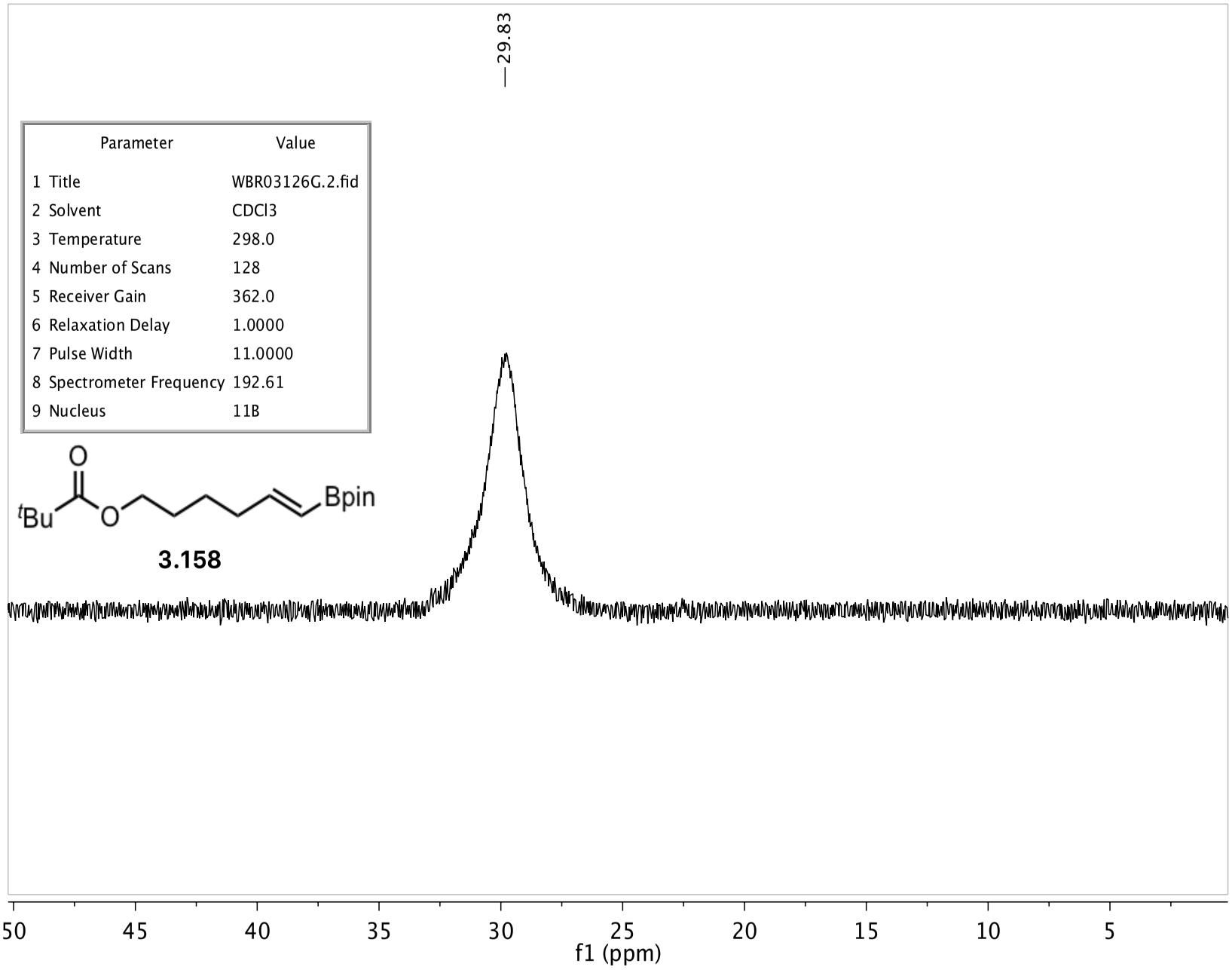
29.83
Parameter Value
1 Title WBR03126G.2.fid
2 Solvent CDCl3
3 Temperature 298.0
4 Number of Scans 128
5 Receiver Gain 362.0
6 Relaxation Delay 1.0000
7 Pulse Width 11.0000
8 Spectrometer Frequency 192.61
9 Nucleus 11B
O
tBu
O
Bpin
3.158
50
45
40
35
30
25
20
15
10
5
f1 (ppm)

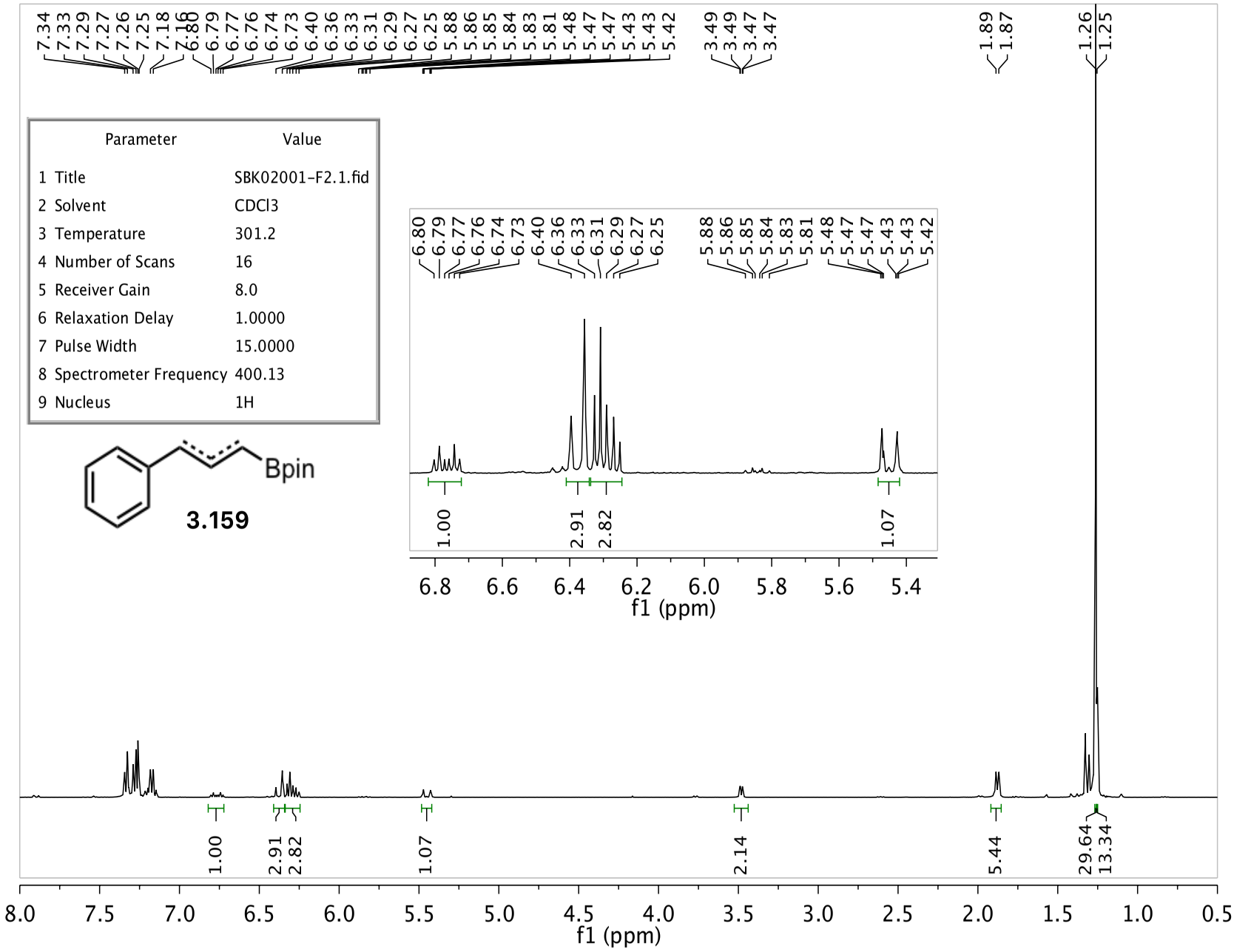
7.34 7.33 7.29 7.27 7.26 7.25 7.18 7.16 6.80 6.79 6.77 6.76 6.74 6.73 6.40 6.36 6.33 6.31 6.29 6.27 6.25 5.88 5.86 5.85 5.84 5.83 5.81 5.48 5.47 5.43 5.43 5.42
3.49 3.49 3.47 3.47
1.89 1.87
1.26 1.25
Parameter Value
1 Title SBK02001-F2.1.fid
2 Solvent CDCl3
3 Temperature 301.2
4 Number of Scans 16
5 Receiver Gain 8.0
6 Relaxation Delay 1.0000
7 Pulse Width 15.0000
8 Spectrometer Frequency 400.13
9 Nucleus 1H
Bpin
3.159
1.00 2.91 2.82 1.07
6.8 6.6 6.4 6.2 6.0 5.8 5.6 5.4
f1 (ppm)
1.00 2.91 2.82 1.07 2.14 5.44 29.64 13.34
8.0 7.5 7.0 6.5 6.0 5.5 5.0 4.5 4.0 3.5 3.0 2.5 2.0 1.5 1.0 0.5
f1 (ppm)

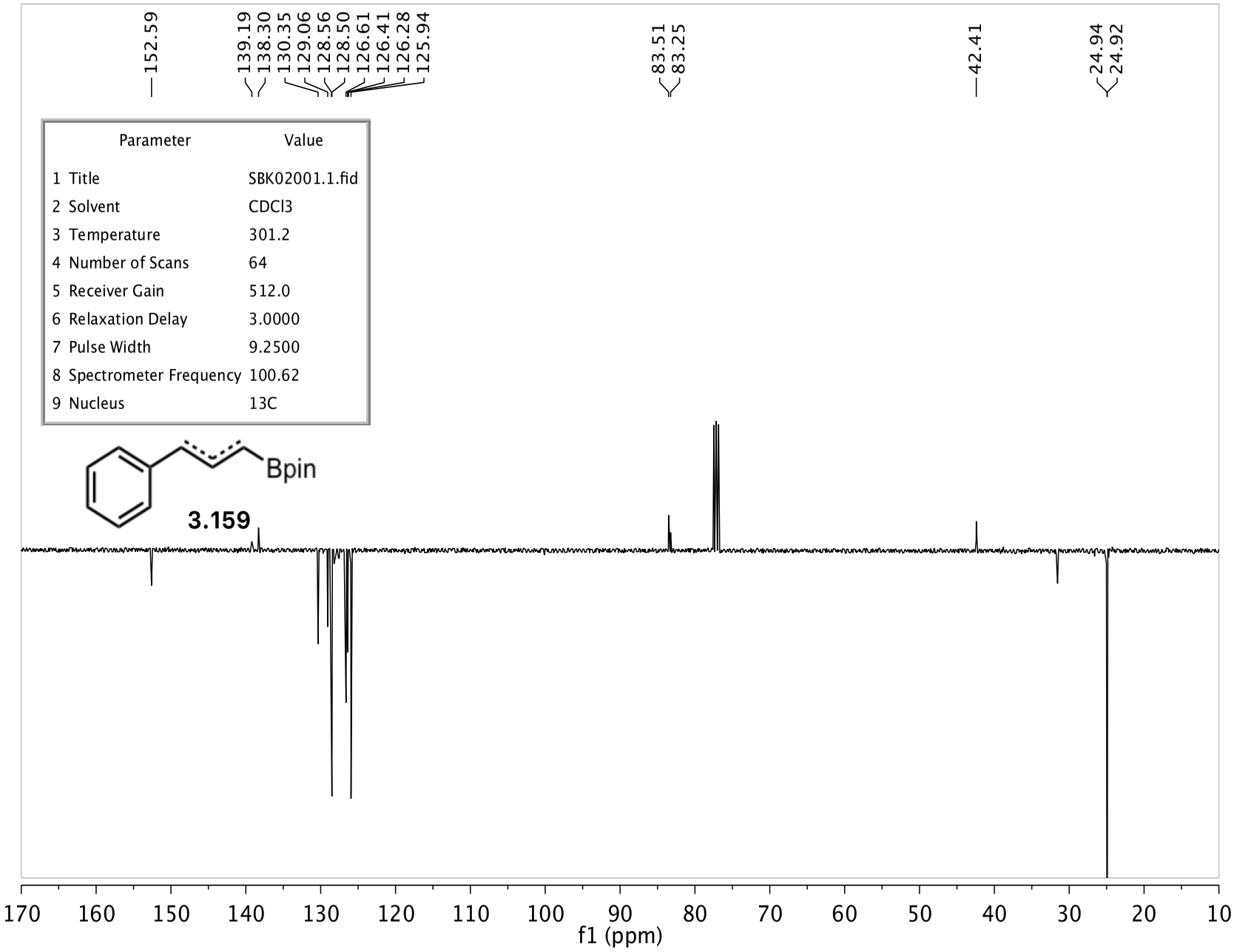
152.59
139.19
138.30
130.35
129.06
128.56
128.50
126.61
126.41
126.28
125.94
83.51
83.25
42.41
24.94
24.92
Parameter Value
1 Title SBK02001.1.fid
2 Solvent CDCl3
3 Temperature 301.2
4 Number of Scans 64
5 Receiver Gain 512.0
6 Relaxation Delay 3.0000
7 Pulse Width 9.2500
8 Spectrometer Frequency 100.62
9 Nucleus 13C
Bpin
3.159
170 160 150 140 130 120 110 100 90 80 70 60 50 40 30 20 10
f1 (ppm)

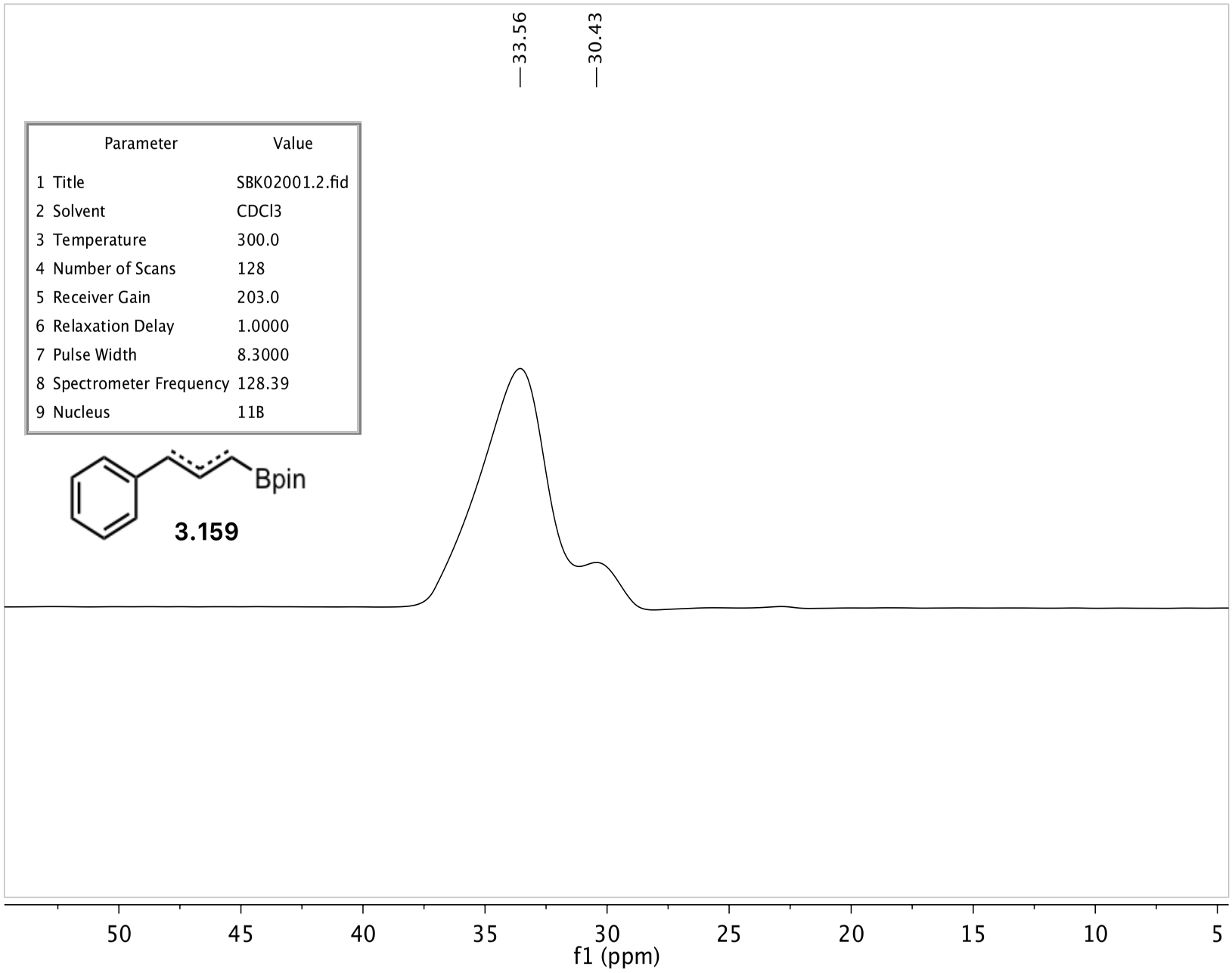
33.56
30.43
Parameter Value
1 Title SBK02001.2.fid
2 Solvent CDCl3
3 Temperature 300.0
4 Number of Scans 128
5 Receiver Gain 203.0
6 Relaxation Delay 1.0000
7 Pulse Width 8.3000
8 Spectrometer Frequency 128.39
9 Nucleus 11B
Bpin
3.159
50
45
40
35
30
25
20
15
10
5
f1 (ppm)

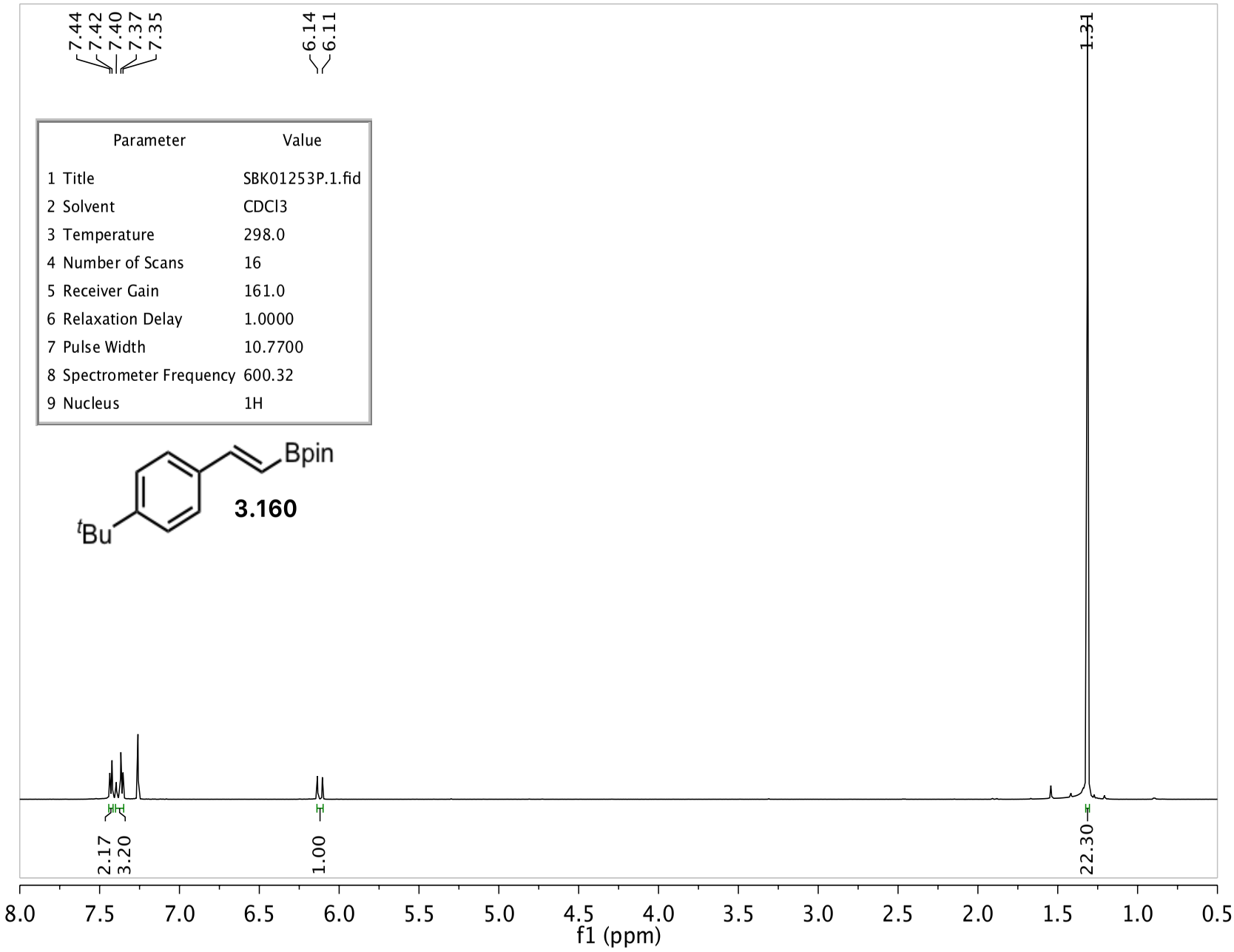
7.44
7.42
7.40
7.37
7.35
6.14
6.11
1.31
Parameter Value
1 Title SBK01253P.1.fid
2 Solvent CDCl3
3 Temperature 298.0
4 Number of Scans 16
5 Receiver Gain 161.0
6 Relaxation Delay 1.0000
7 Pulse Width 10.7700
8 Spectrometer Frequency 600.32
9 Nucleus 1H
Bpin
tBu
3.160
2.17
3.20
1.00
22.30
8.0 7.5 7.0 6.5 6.0 5.5 5.0 4.5 4.0 3.5 3.0 2.5 2.0 1.5 1.0 0.5
f1 (ppm)

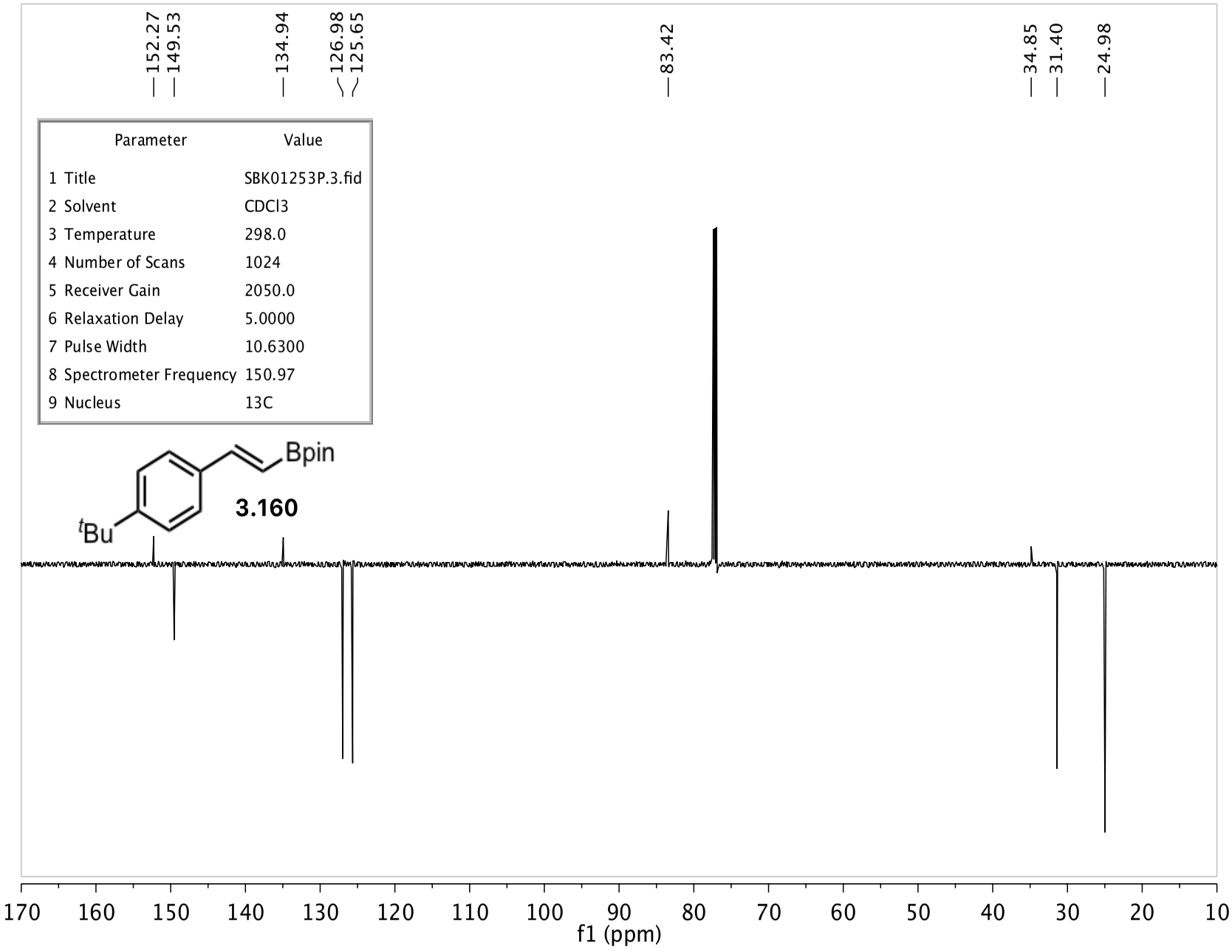
152.27
149.53
134.94
126.98
125.65
83.42
34.85
31.40
24.98
Parameter Value
1 Title SBK01253P.3.fid
2 Solvent CDCl3
3 Temperature 298.0
4 Number of Scans 1024
5 Receiver Gain 2050.0
6 Relaxation Delay 5.0000
7 Pulse Width 10.6300
8 Spectrometer Frequency 150.97
9 Nucleus 13C
Bpin
tBu
3.160
170 160 150 140 130 120 110 100 90 80 70 60 50 40 30 20 10
f1 (ppm)

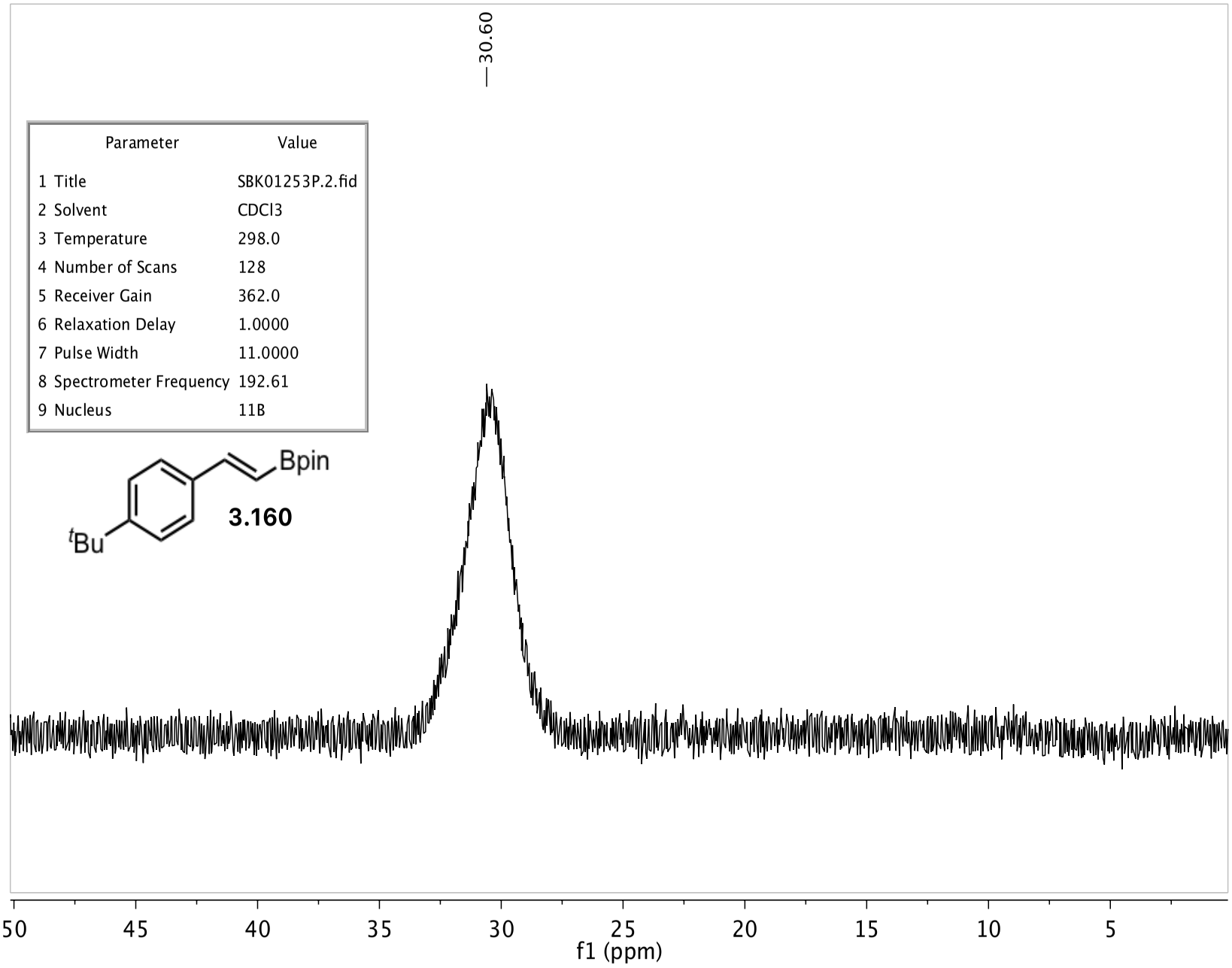
30.60
Parameter Value
1 Title SBK01253P.2.fid
2 Solvent CDCl3
3 Temperature 298.0
4 Number of Scans 128
5 Receiver Gain 362.0
6 Relaxation Delay 1.0000
7 Pulse Width 11.0000
8 Spectrometer Frequency 192.61
9 Nucleus 11B
Bpin
tBu
3.160
50
45
40
35
30
25
20
15
10
5
f1 (ppm)

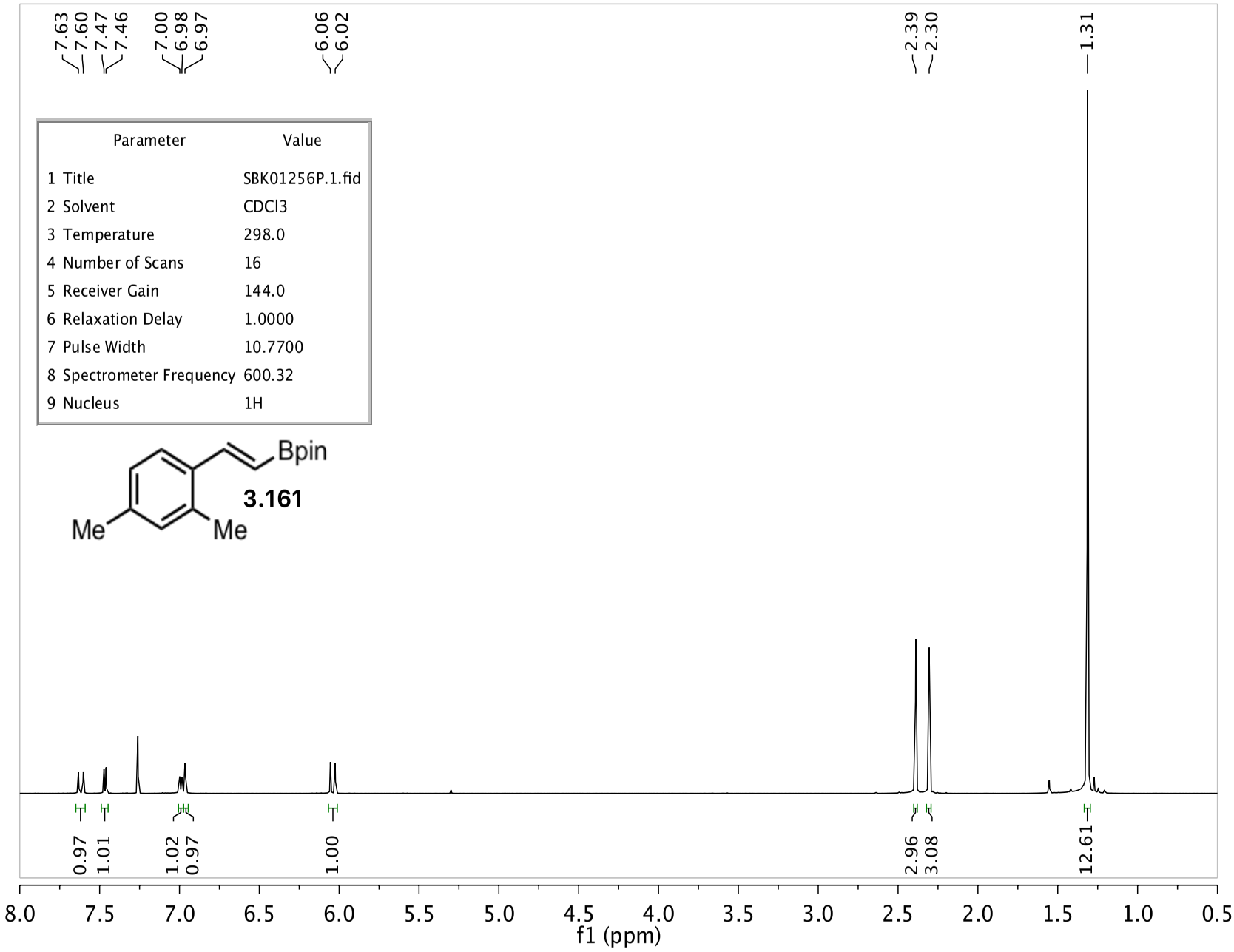
7.63
7.60
7.47
7.46
7.00
6.98
6.97
6.06
6.02
2.39
2.30
1.31
Parameter Value
1 Title SBK01256P.1.fid
2 Solvent CDCl3
3 Temperature 298.0
4 Number of Scans 16
5 Receiver Gain 144.0
6 Relaxation Delay 1.0000
7 Pulse Width 10.7700
8 Spectrometer Frequency 600.32
9 Nucleus 1H
Bpin
3.161
Me
Me
0.97
1.01
1.02
0.97
1.00
2.96
3.08
12.61
8.0
7.5
7.0
6.5
6.0
5.5
5.0
4.5
4.0
3.5
3.0
2.5
2.0
1.5
1.0
0.5
f1 (ppm)

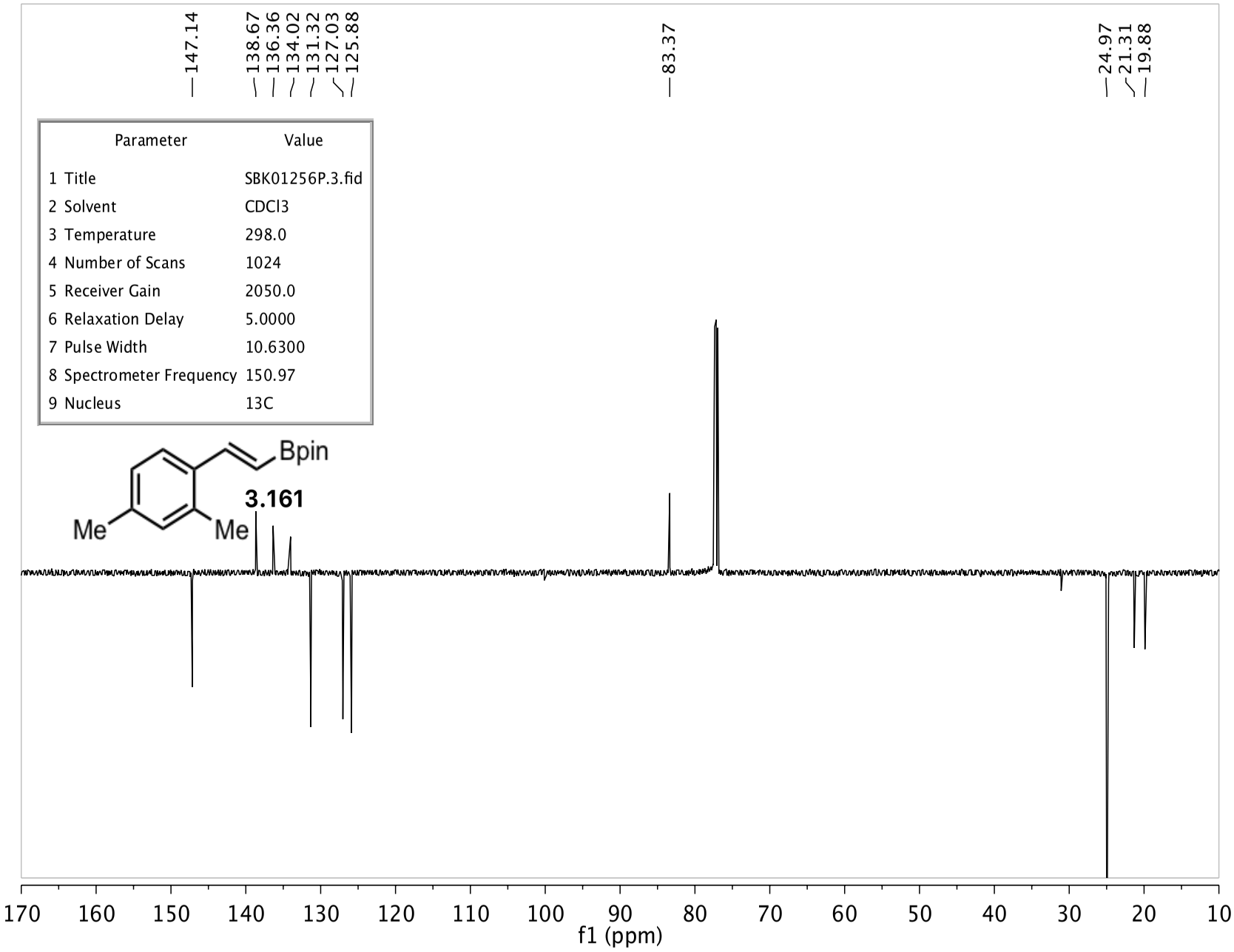
147.14
138.67
136.36
134.02
131.32
127.03
125.88
83.37
24.97
21.31
19.88
Parameter Value
1 Title SBK01256P.3.fid
2 Solvent CDCl3
3 Temperature 298.0
4 Number of Scans 1024
5 Receiver Gain 2050.0
6 Relaxation Delay 5.0000
7 Pulse Width 10.6300
8 Spectrometer Frequency 150.97
9 Nucleus 13C
Bpin
Me
Me
3.161
170 160 150 140 130 120 110 100 90 80 70 60 50 40 30 20 10
f1 (ppm)

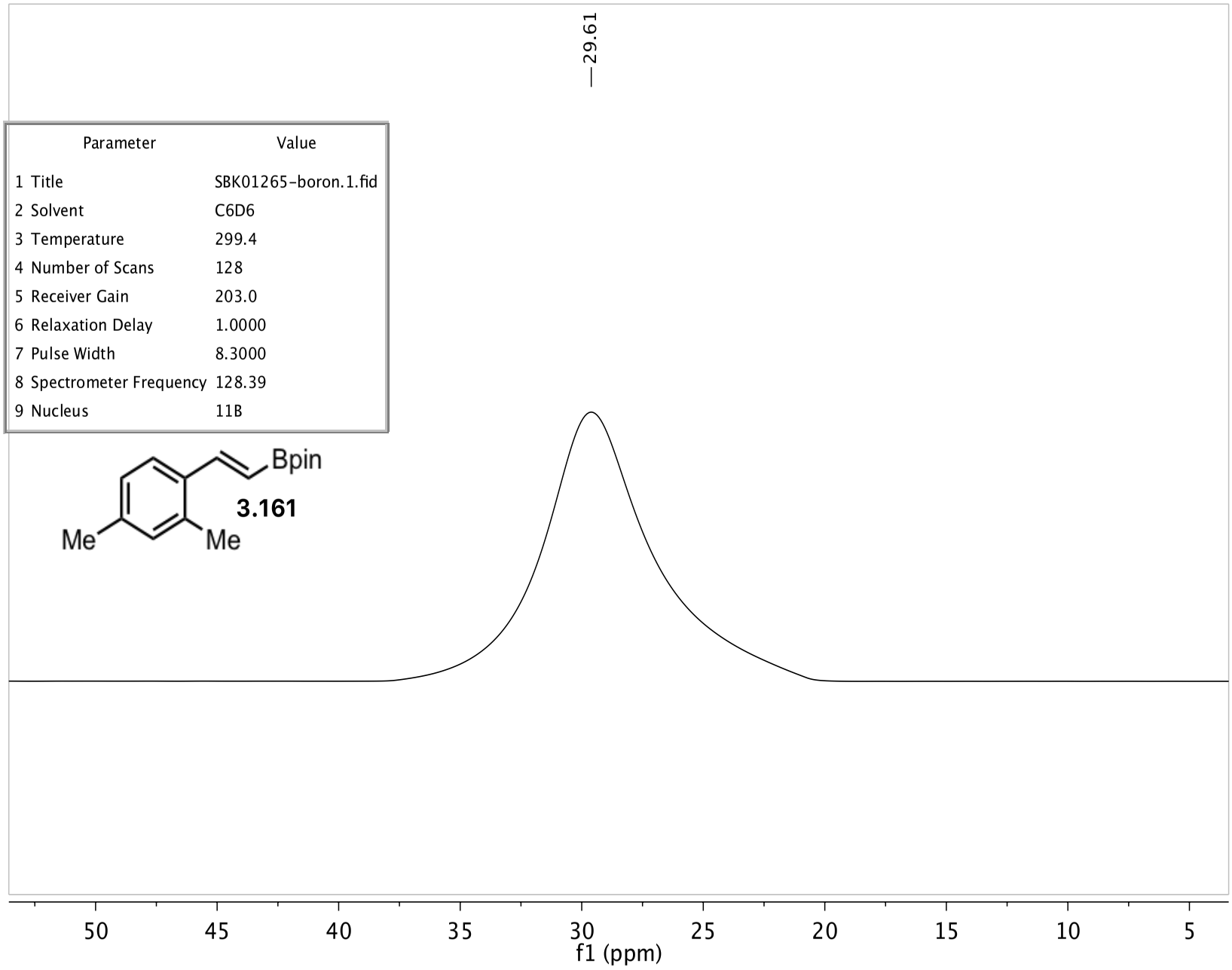
29.61
Parameter
Value
1 Title
SBK01265-boron.1.fid
2 Solvent
C6D6
3 Temperature
299.4
4 Number of Scans
128
5 Receiver Gain
203.0
6 Relaxation Delay
1.0000
7 Pulse Width
8.3000
8 Spectrometer Frequency
128.39
9 Nucleus
11B
Bpin
3.161
Me
Me
50
45
40
35
30
25
20
15
10
5
f1 (ppm)

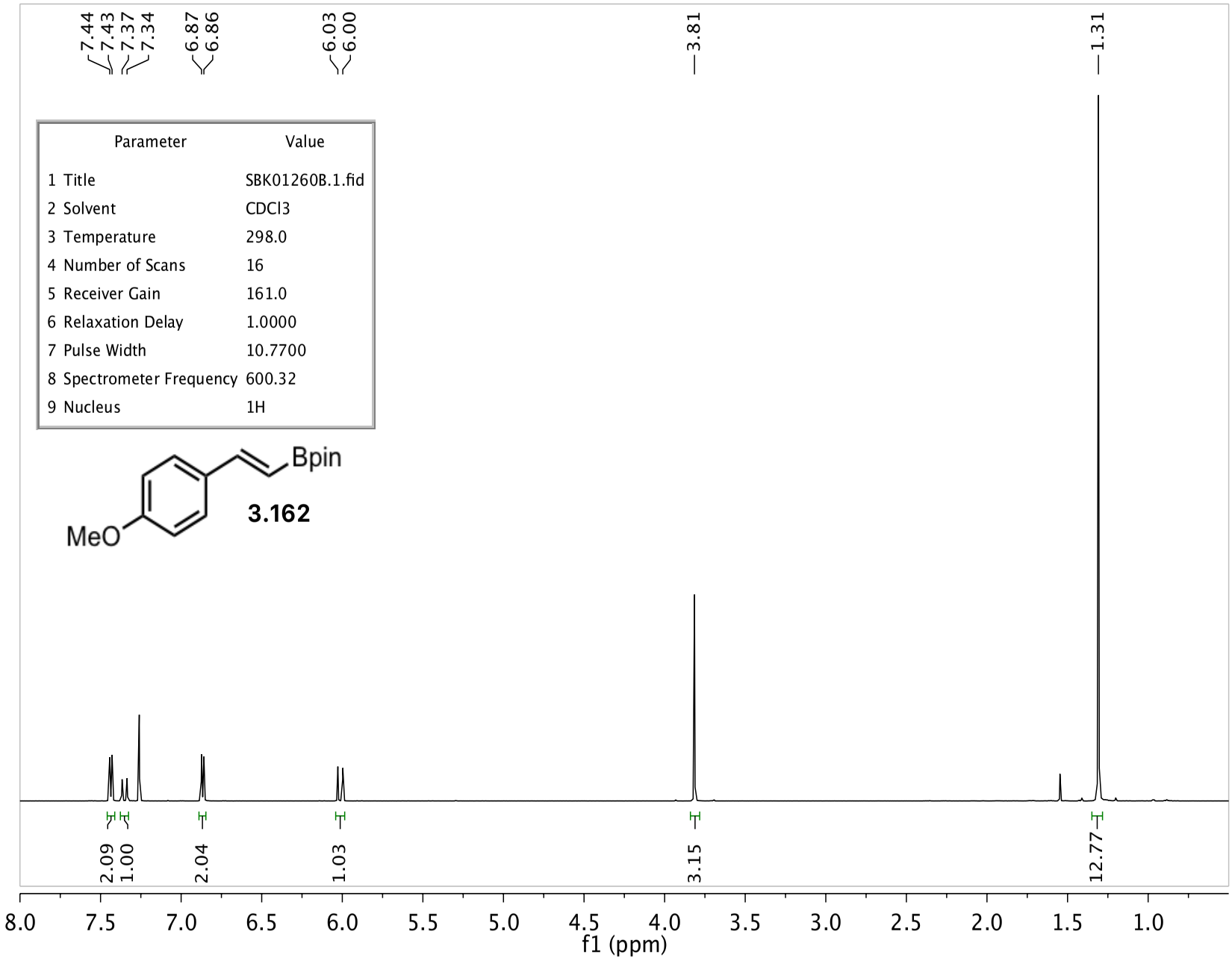
7.44
7.43
7.37
7.34
6.87
6.86
6.03
6.00
3.81
1.31
Parameter Value
1 Title SBK01260B.1.fid
2 Solvent CDCl3
3 Temperature 298.0
4 Number of Scans 16
5 Receiver Gain 161.0
6 Relaxation Delay 1.0000
7 Pulse Width 10.7700
8 Spectrometer Frequency 600.32
9 Nucleus 1H
Bpin
MeO
3.162
2.09
1.00
2.04
1.03
3.15
12.77
8.0 7.5 7.0 6.5 6.0 5.5 5.0 4.5 4.0 3.5 3.0 2.5 2.0 1.5 1.0
f1 (ppm)

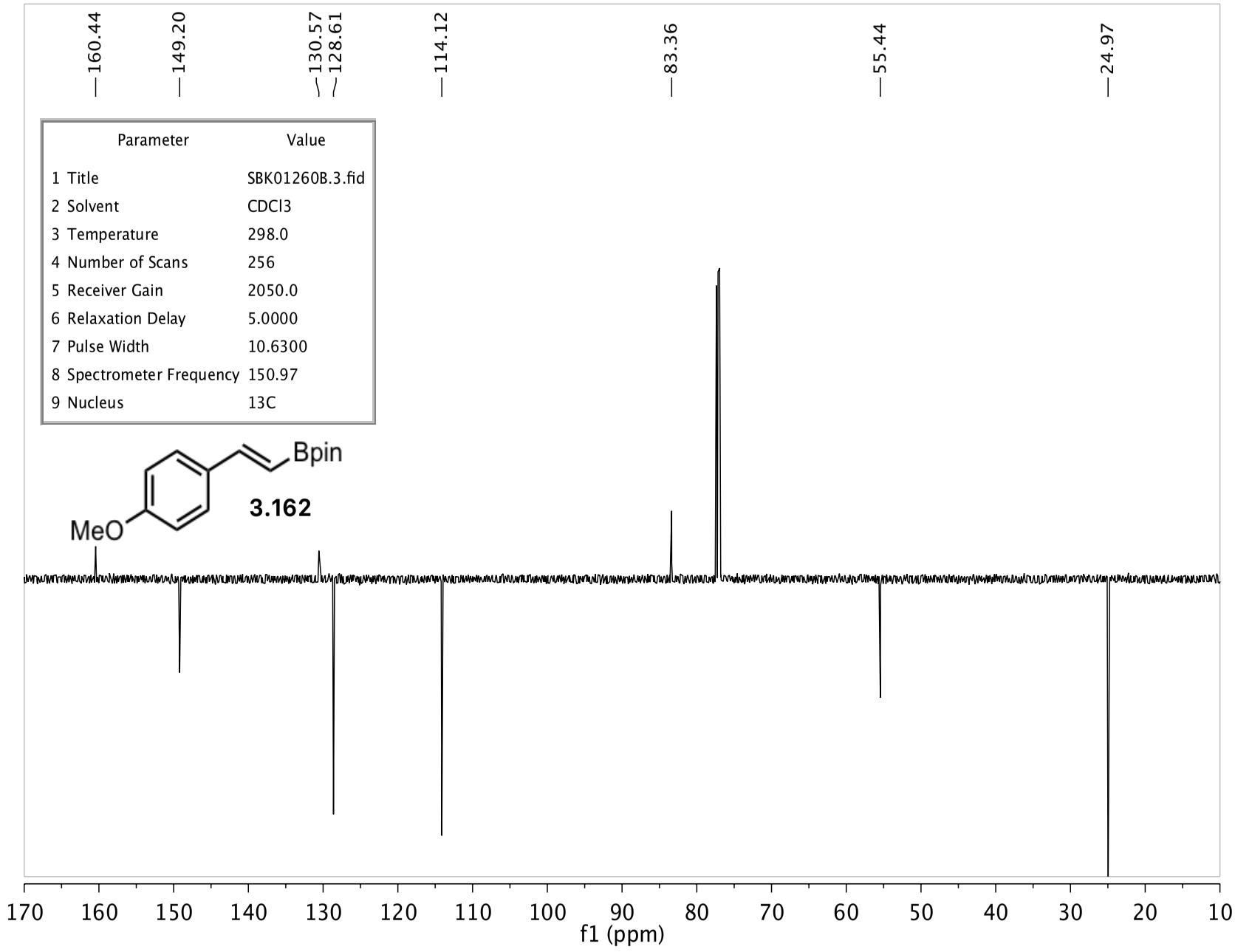
160.44
149.20
130.57
128.61
114.12
83.36
55.44
24.97
Parameter Value
1 Title SBK01260B.3.fid
2 Solvent CDCl3
3 Temperature 298.0
4 Number of Scans 256
5 Receiver Gain 2050.0
6 Relaxation Delay 5.0000
7 Pulse Width 10.6300
8 Spectrometer Frequency 150.97
9 Nucleus 13C
Bpin
MeO
3.162
170 160 150 140 130 120 110 100 90 80 70 60 50 40 30 20 10
f1 (ppm)

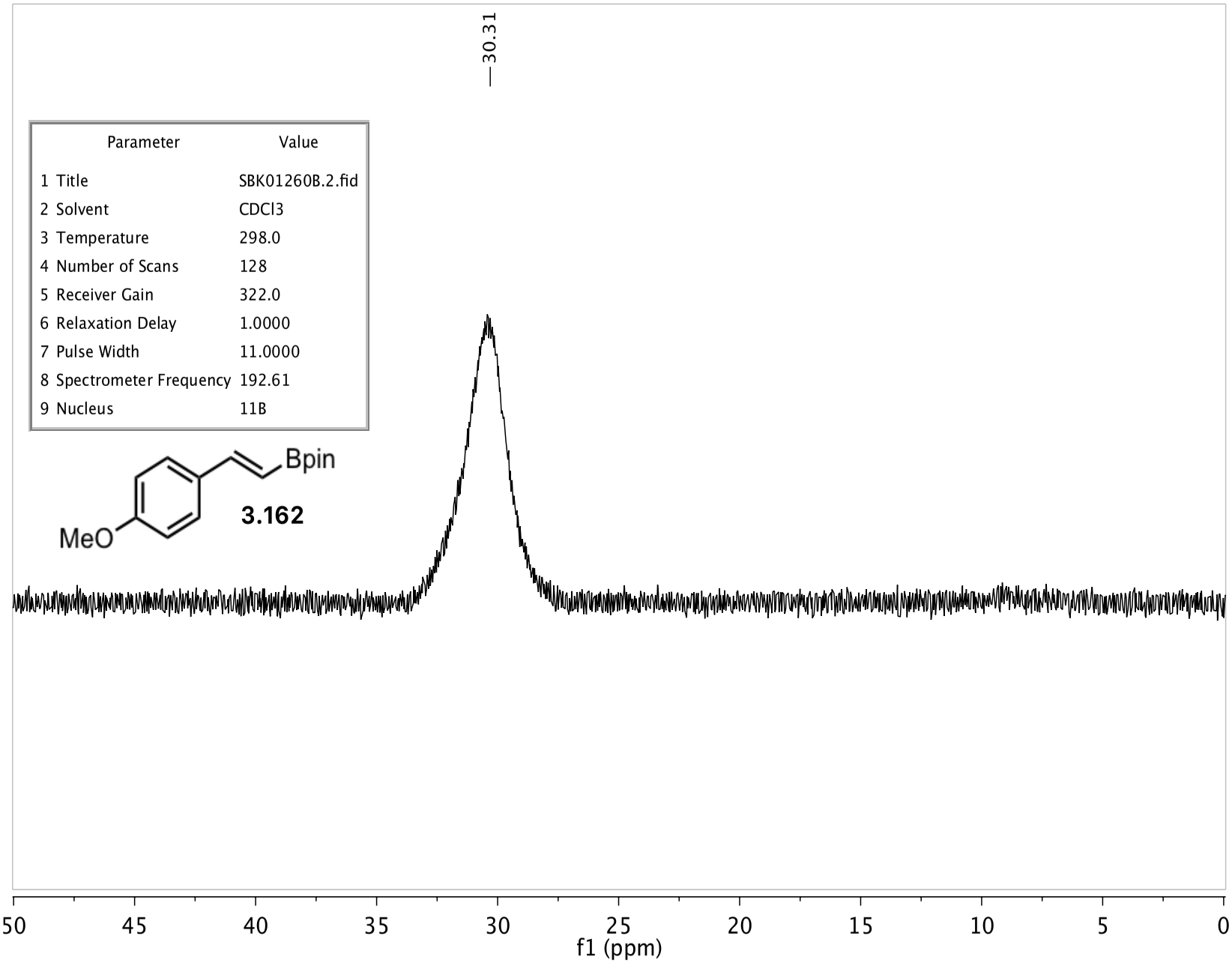
30.31
Parameter Value
1 Title SBK01260B.2.fid
2 Solvent CDCl3
3 Temperature 298.0
4 Number of Scans 128
5 Receiver Gain 322.0
6 Relaxation Delay 1.0000
7 Pulse Width 11.0000
8 Spectrometer Frequency 192.61
9 Nucleus 11B
Bpin
MeO
3.162
50
45
40
35
30
25
20
15
10
5
0
f1 (ppm)

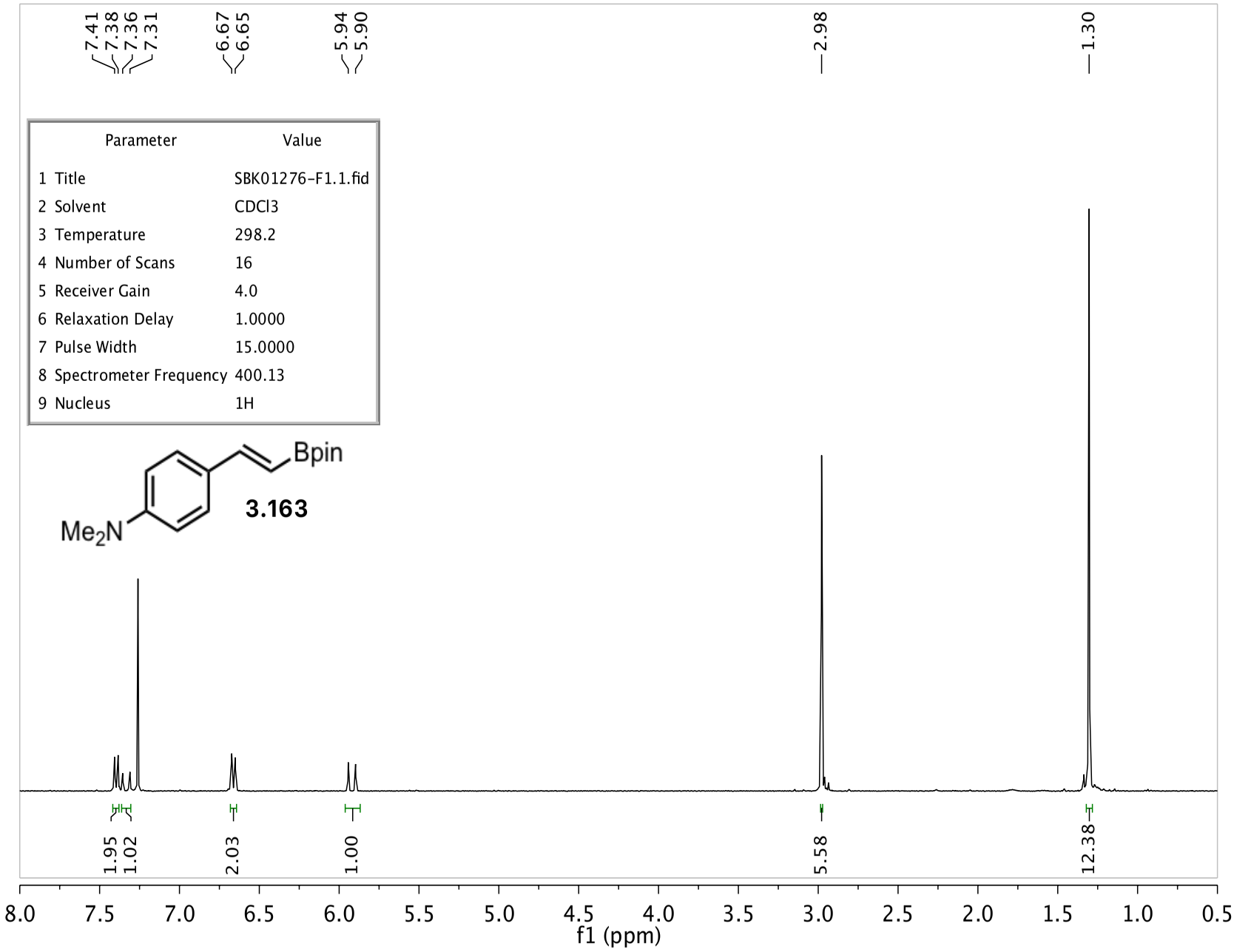
7.41
7.38
7.36
7.31
6.67
6.65
5.94
5.90
2.98
1.30
Parameter Value
1 Title SBK01276-F1.1.fid
2 Solvent CDCl3
3 Temperature 298.2
4 Number of Scans 16
5 Receiver Gain 4.0
6 Relaxation Delay 1.0000
7 Pulse Width 15.0000
8 Spectrometer Frequency 400.13
9 Nucleus 1H
Bpin
Me2N
3.163
1.95
1.02
2.03
1.00
5.58
12.38
8.0 7.5 7.0 6.5 6.0 5.5 5.0 4.5 4.0 3.5 3.0 2.5 2.0 1.5 1.0 0.5
f1 (ppm)

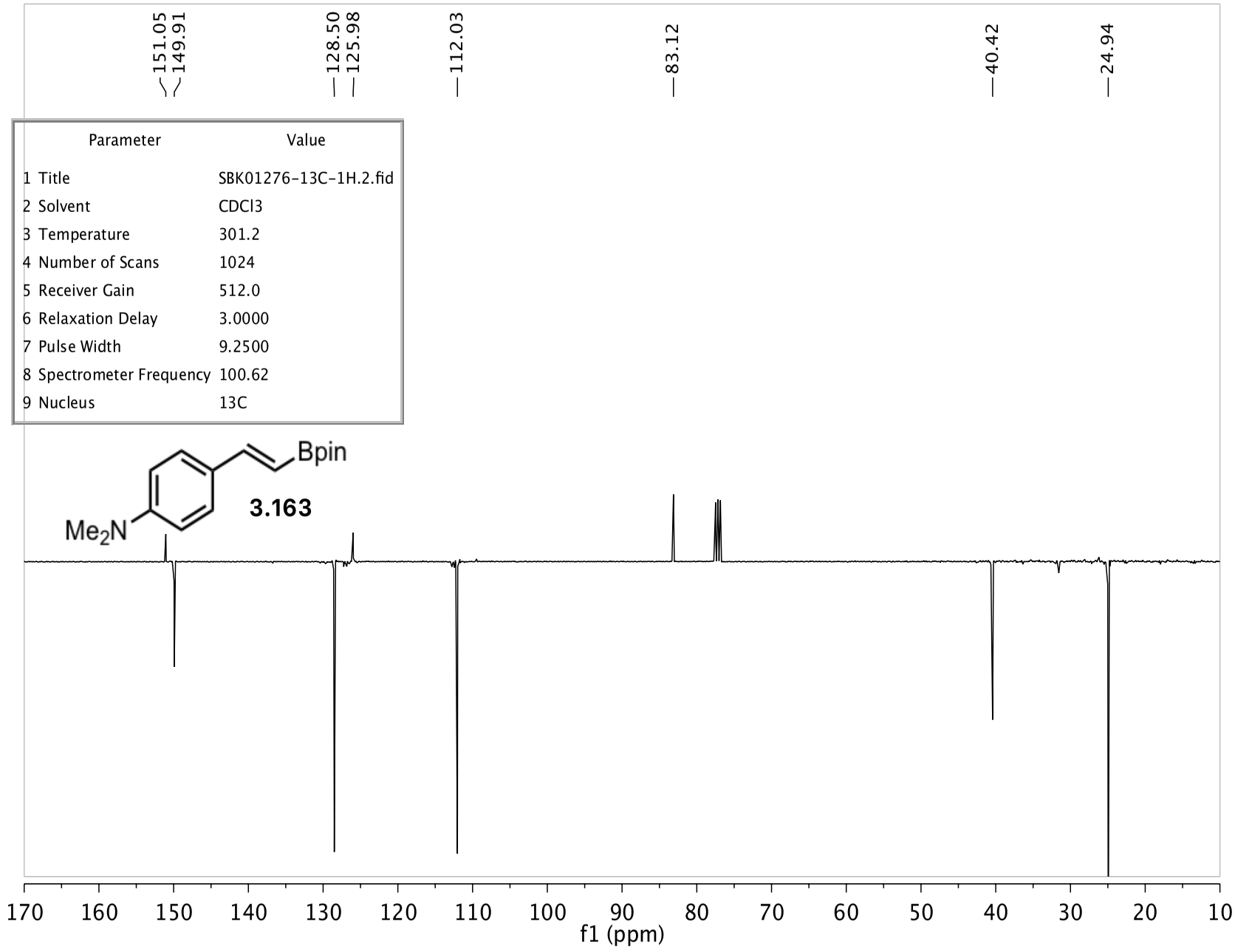
151.05
149.91
128.50
125.98
112.03
83.12
40.42
24.94
Parameter Value
1 Title SBK01276-13C-1H.2.fid
2 Solvent CDCl3
3 Temperature 301.2
4 Number of Scans 1024
5 Receiver Gain 512.0
6 Relaxation Delay 3.0000
7 Pulse Width 9.2500
8 Spectrometer Frequency 100.62
9 Nucleus 13C
Bpin
Me2N
3.163
170 160 150 140 130 120 110 100 90 80 70 60 50 40 30 20 10
f1 (ppm)

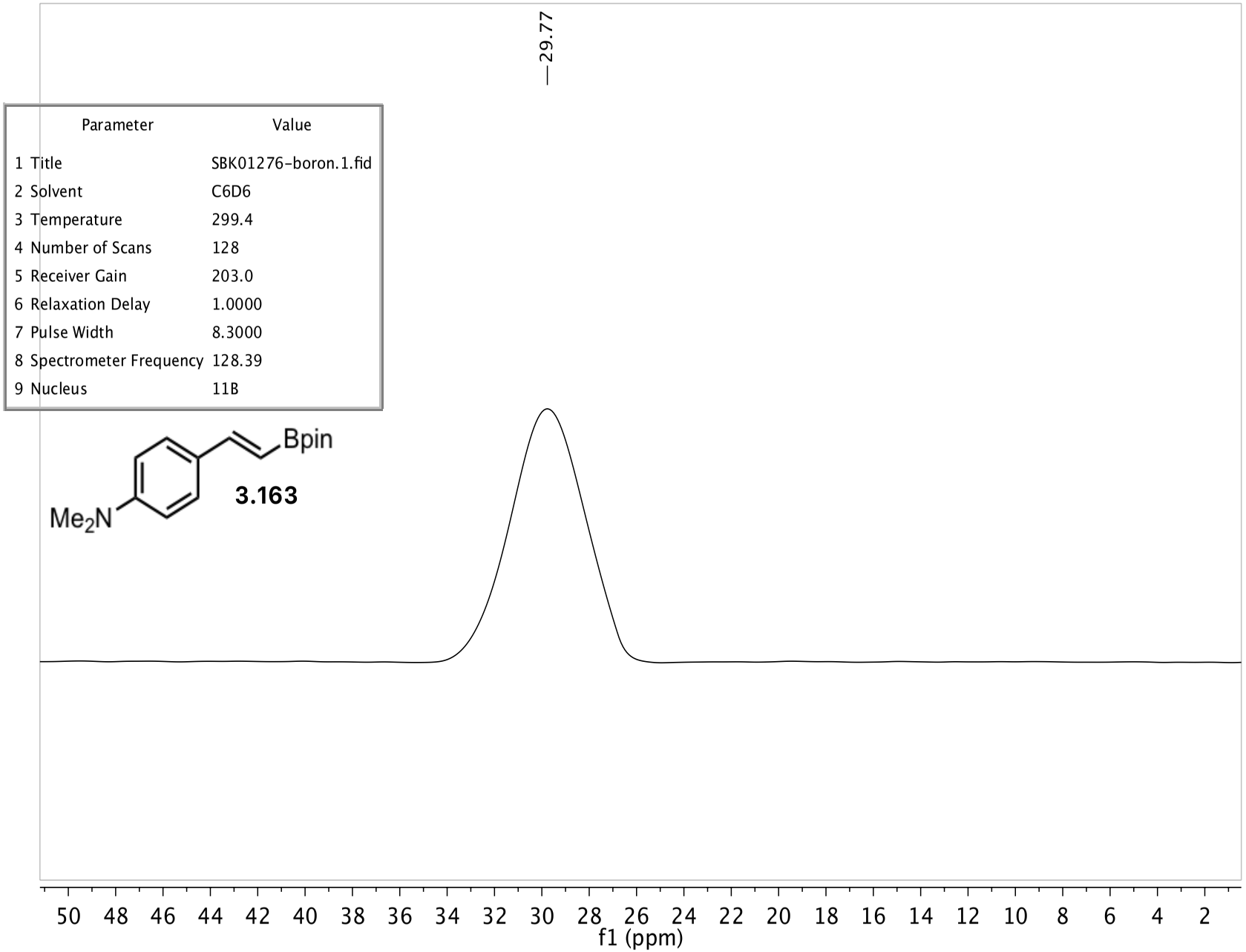
29.77
Parameter
Value
1 Title
SBK01276-boron.1.fid
2 Solvent
C6D6
3 Temperature
299.4
4 Number of Scans
128
5 Receiver Gain
203.0
6 Relaxation Delay
1.0000
7 Pulse Width
8.3000
8 Spectrometer Frequency
128.39
9 Nucleus
11B
Bpin
Me2N
3.163
50 48 46 44 42 40 38 36 34 32 30 28 26 24 22 20 18 16 14 12 10 8 6 4 2
f1 (ppm)

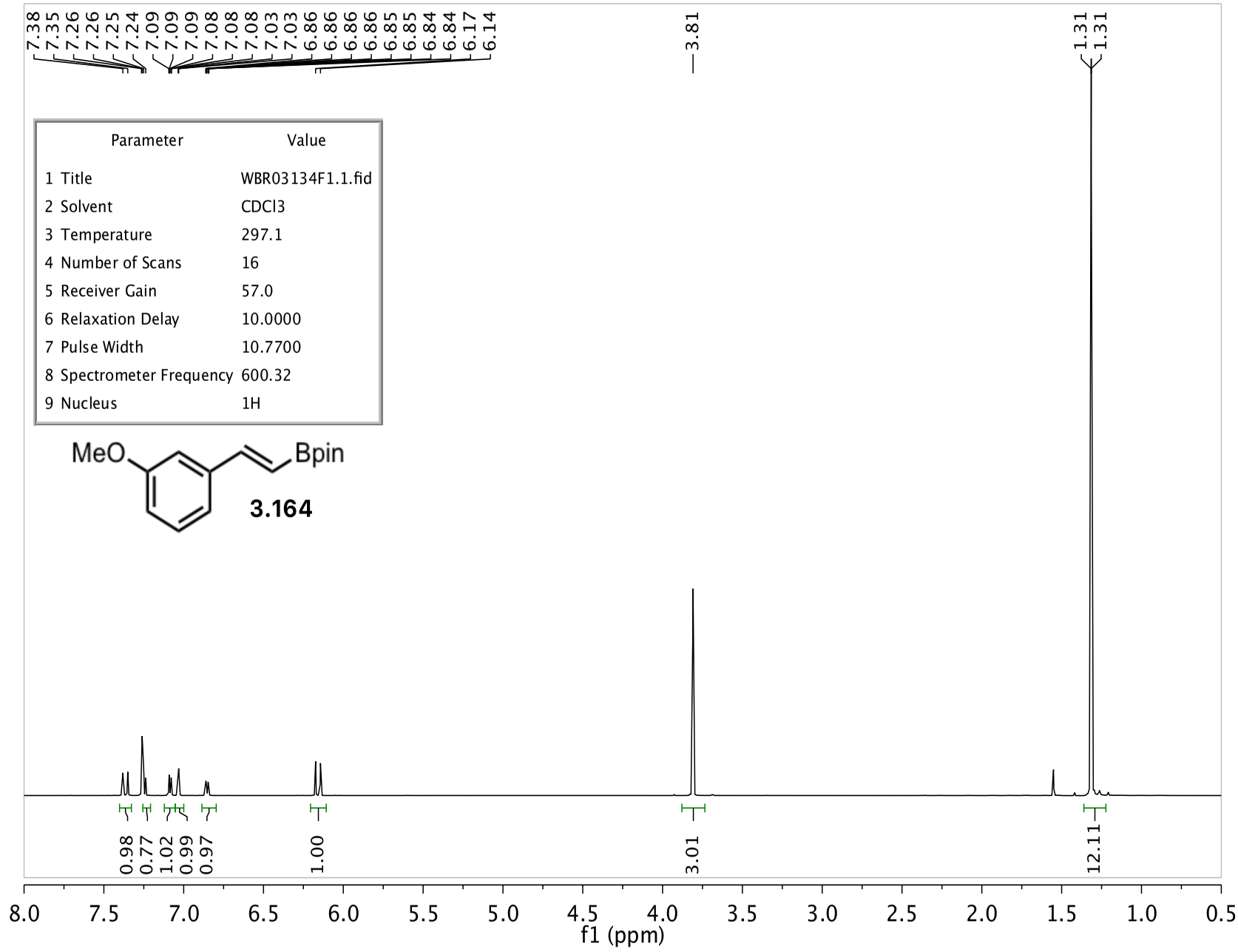
7.38
7.35
7.26
7.26
7.25
7.24
7.09
7.09
7.09
7.08
7.08
7.08
7.03
7.03
6.86
6.86
6.86
6.85
6.85
6.84
6.84
6.17
6.14
3.81
1.31
1.31
Parameter Value
1 Title WBR03134F1.1.fid
2 Solvent CDCl3
3 Temperature 297.1
4 Number of Scans 16
5 Receiver Gain 57.0
6 Relaxation Delay 10.0000
7 Pulse Width 10.7700
8 Spectrometer Frequency 600.32
9 Nucleus 1H
MeO
Bpin
3.164
0.98
0.77
1.02
0.99
0.97
1.00
3.01
12.11
8.0
7.5
7.0
6.5
6.0
5.5
5.0
4.5
4.0
3.5
3.0
2.5
2.0
1.5
1.0
0.5
f1 (ppm)

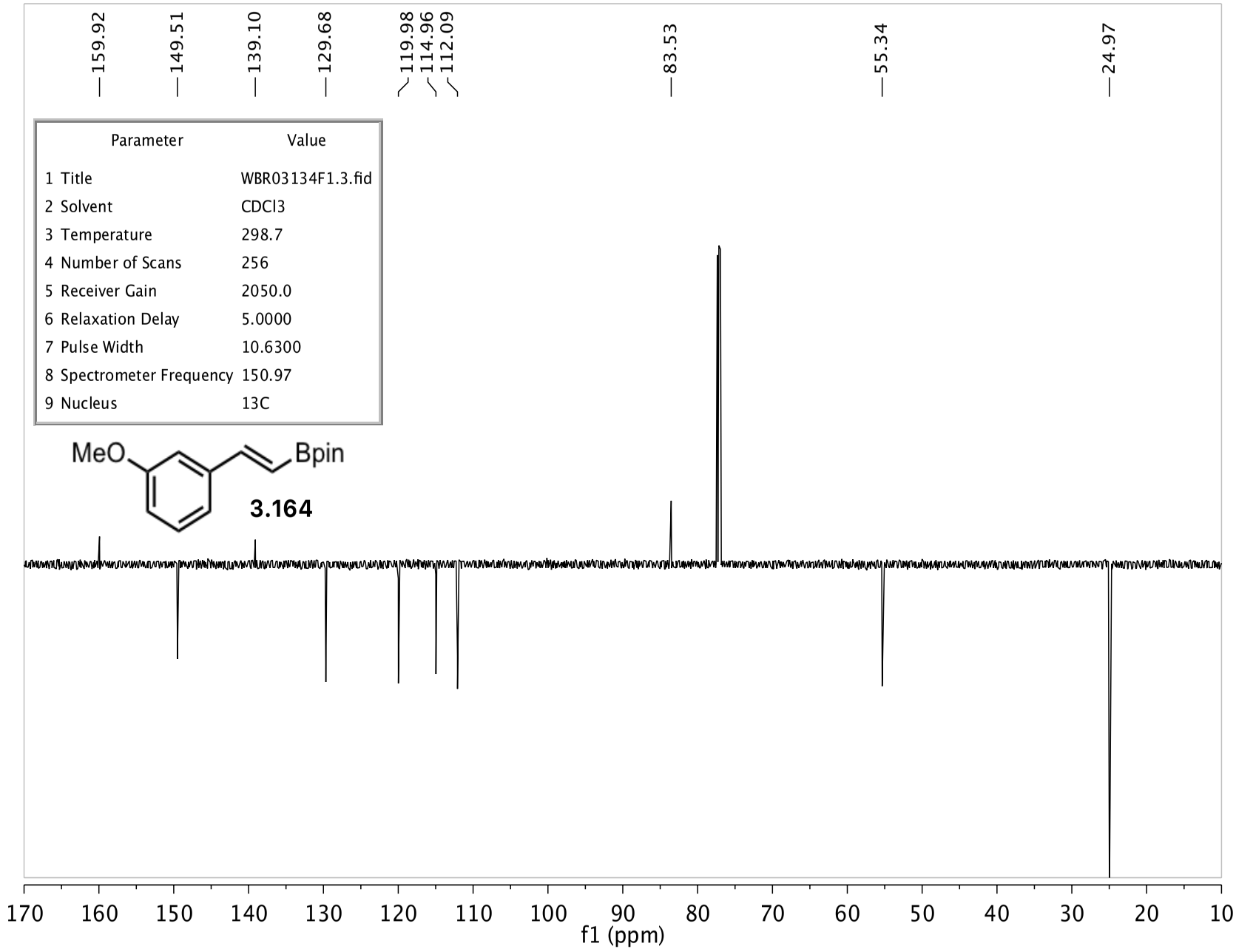
159.92
149.51
139.10
129.68
119.98
114.96
112.09
83.53
55.34
24.97
Parameter Value
1 Title WBR03134F1.3.fid
2 Solvent CDCl3
3 Temperature 298.7
4 Number of Scans 256
5 Receiver Gain 2050.0
6 Relaxation Delay 5.0000
7 Pulse Width 10.6300
8 Spectrometer Frequency 150.97
9 Nucleus 13C
MeO
Bpin
3.164
170 160 150 140 130 120 110 100 90 80 70 60 50 40 30 20 10
f1 (ppm)

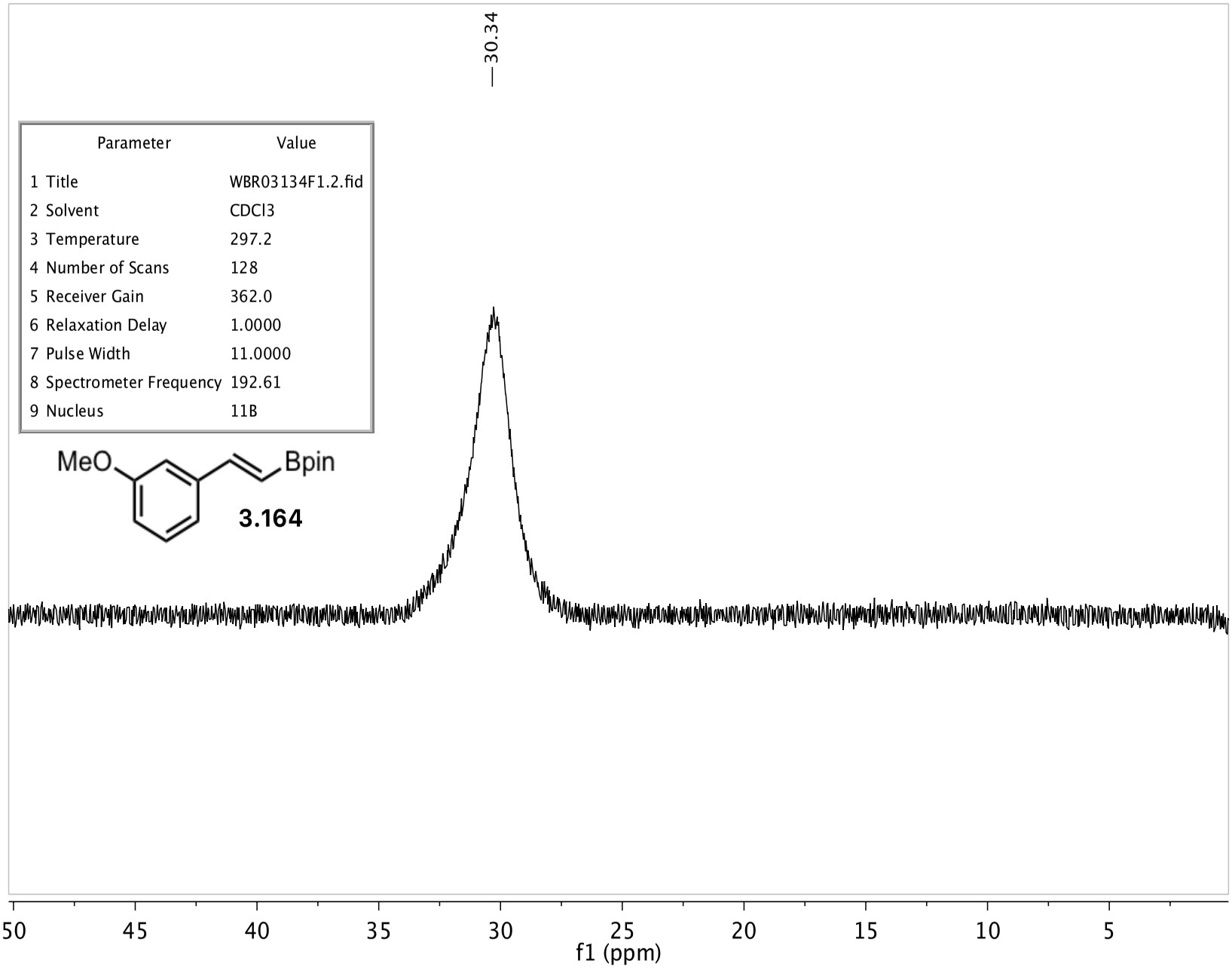
30.34
Parameter Value
1 Title WBR03134F1.2.fid
2 Solvent CDCl3
3 Temperature 297.2
4 Number of Scans 128
5 Receiver Gain 362.0
6 Relaxation Delay 1.0000
7 Pulse Width 11.0000
8 Spectrometer Frequency 192.61
9 Nucleus 11B
MeO
Bpin
3.164
50
45
40
35
30
25
20
15
10
5
f1 (ppm)

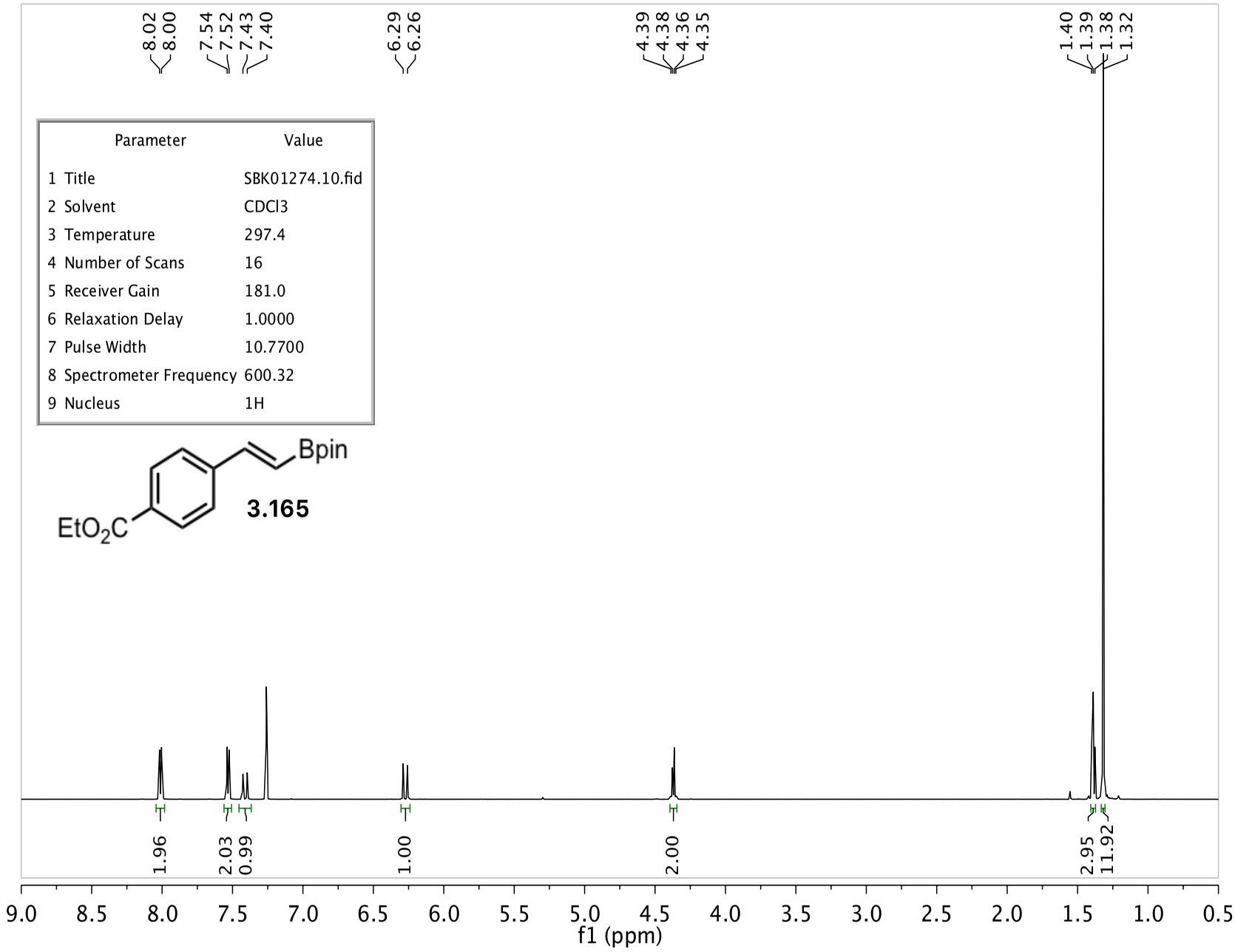
8.02
8.00
7.54
7.52
7.43
7.40
6.29
6.26
4.39
4.38
4.36
4.35
1.40
1.39
1.38
1.32
Parameter Value
1 Title SBK01274.10.fid
2 Solvent CDCl3
3 Temperature 297.4
4 Number of Scans 16
5 Receiver Gain 181.0
6 Relaxation Delay 1.0000
7 Pulse Width 10.7700
8 Spectrometer Frequency 600.32
9 Nucleus 1H
Bpin
EtO2C
3.165
1.96
2.03
0.99
1.00
2.00
2.95
11.92
9.0 8.5 8.0 7.5 7.0 6.5 6.0 5.5 5.0 4.5 4.0 3.5 3.0 2.5 2.0 1.5 1.0 0.5
f1 (ppm)

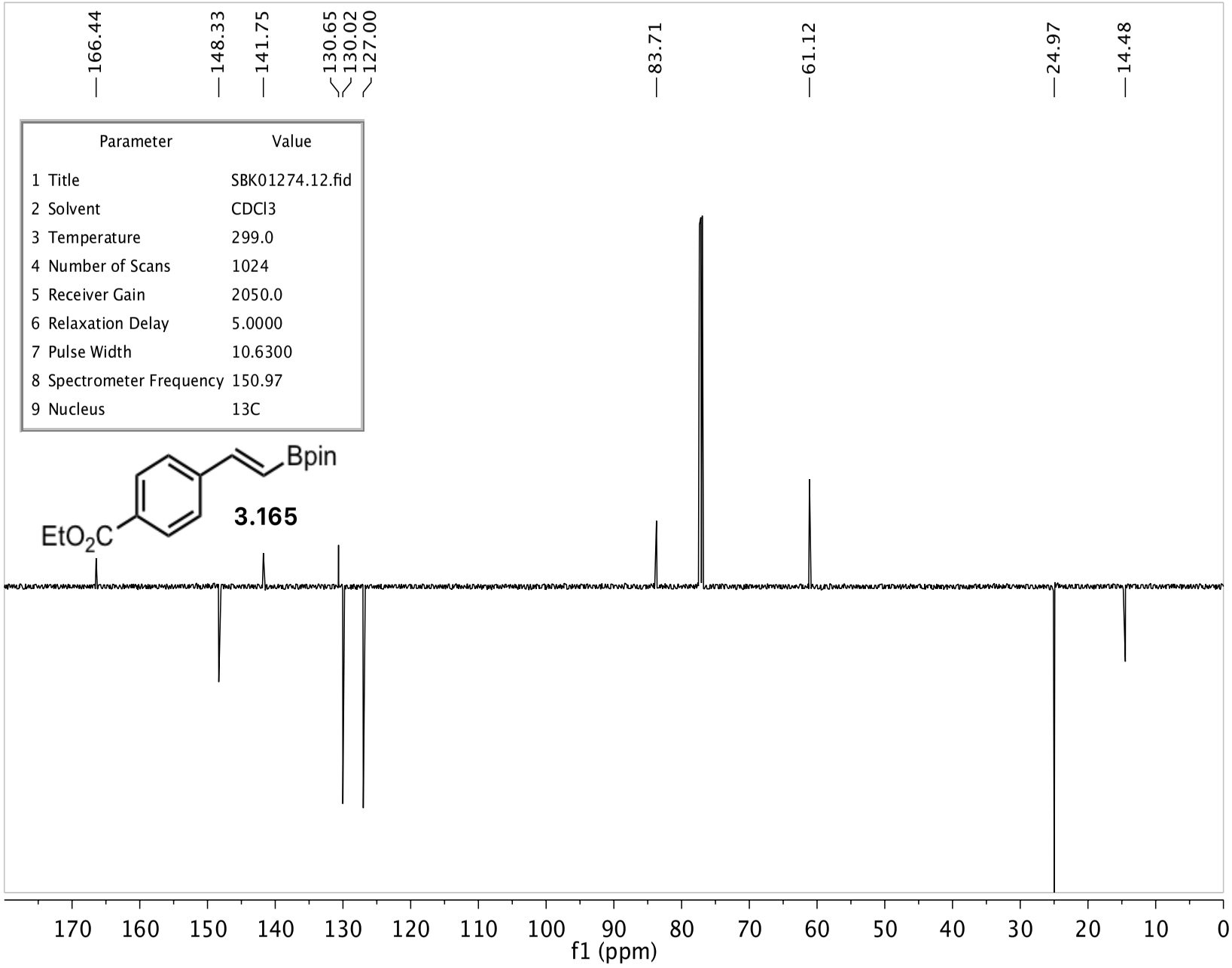
166.44
148.33
141.75
130.65
130.02
127.00
83.71
61.12
24.97
14.48
Parameter Value
1 Title SBK01274.12.fid
2 Solvent CDCl3
3 Temperature 299.0
4 Number of Scans 1024
5 Receiver Gain 2050.0
6 Relaxation Delay 5.0000
7 Pulse Width 10.6300
8 Spectrometer Frequency 150.97
9 Nucleus 13C
Bpin
EtO2C
3.165
170 160 150 140 130 120 110 100 90 80 70 60 50 40 30 20 10 0
f1 (ppm)

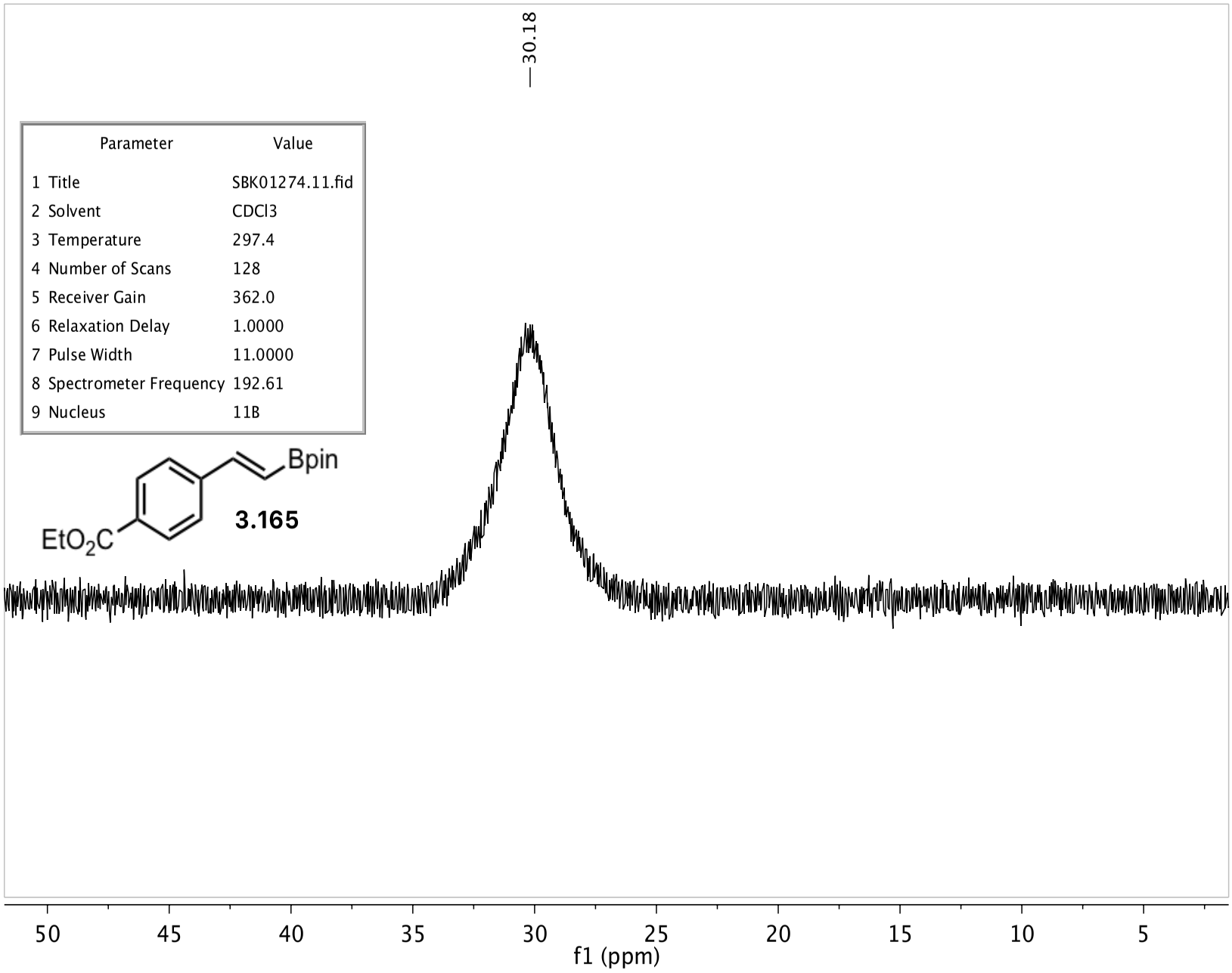
30.18
Parameter Value
1 Title SBK01274.11.fid
2 Solvent CDCl3
3 Temperature 297.4
4 Number of Scans 128
5 Receiver Gain 362.0
6 Relaxation Delay 1.0000
7 Pulse Width 11.0000
8 Spectrometer Frequency 192.61
9 Nucleus 11B
Bpin
EtO2C
3.165
50
45
40
35
30
25
20
15
10
5
f1 (ppm)

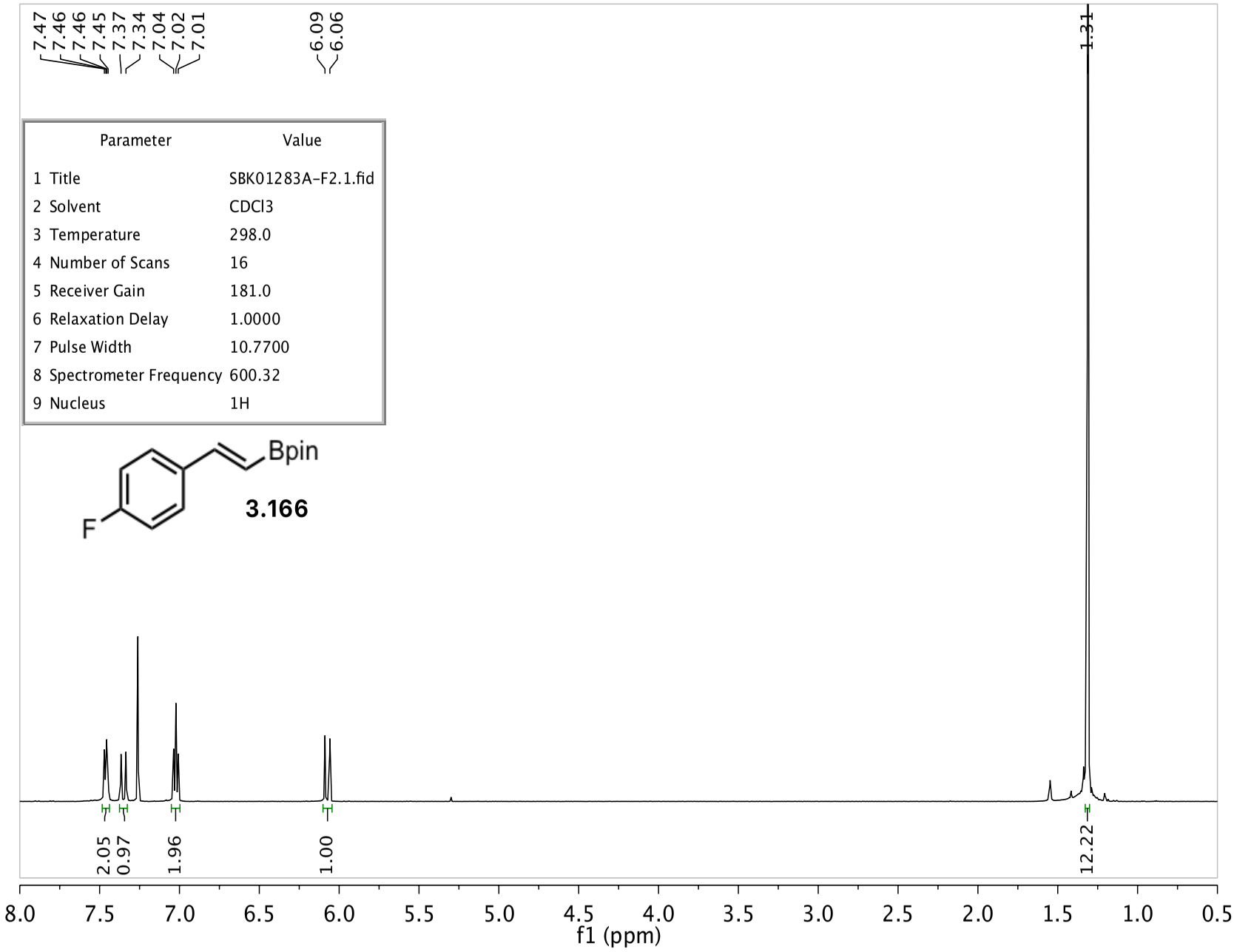
7.47
7.46
7.46
7.45
7.37
7.34
7.04
7.02
7.01
6.09
6.06
1.31
Parameter Value
1 Title SBK01283A-F2.1.fid
2 Solvent CDCl3
3 Temperature 298.0
4 Number of Scans 16
5 Receiver Gain 181.0
6 Relaxation Delay 1.0000
7 Pulse Width 10.7700
8 Spectrometer Frequency 600.32
9 Nucleus 1H
Bpin
F
3.166
2.05
0.97
1.96
1.00
12.22
8.0
7.5
7.0
6.5
6.0
5.5
5.0
4.5
4.0
3.5
3.0
2.5
2.0
1.5
1.0
0.5
f1 (ppm)

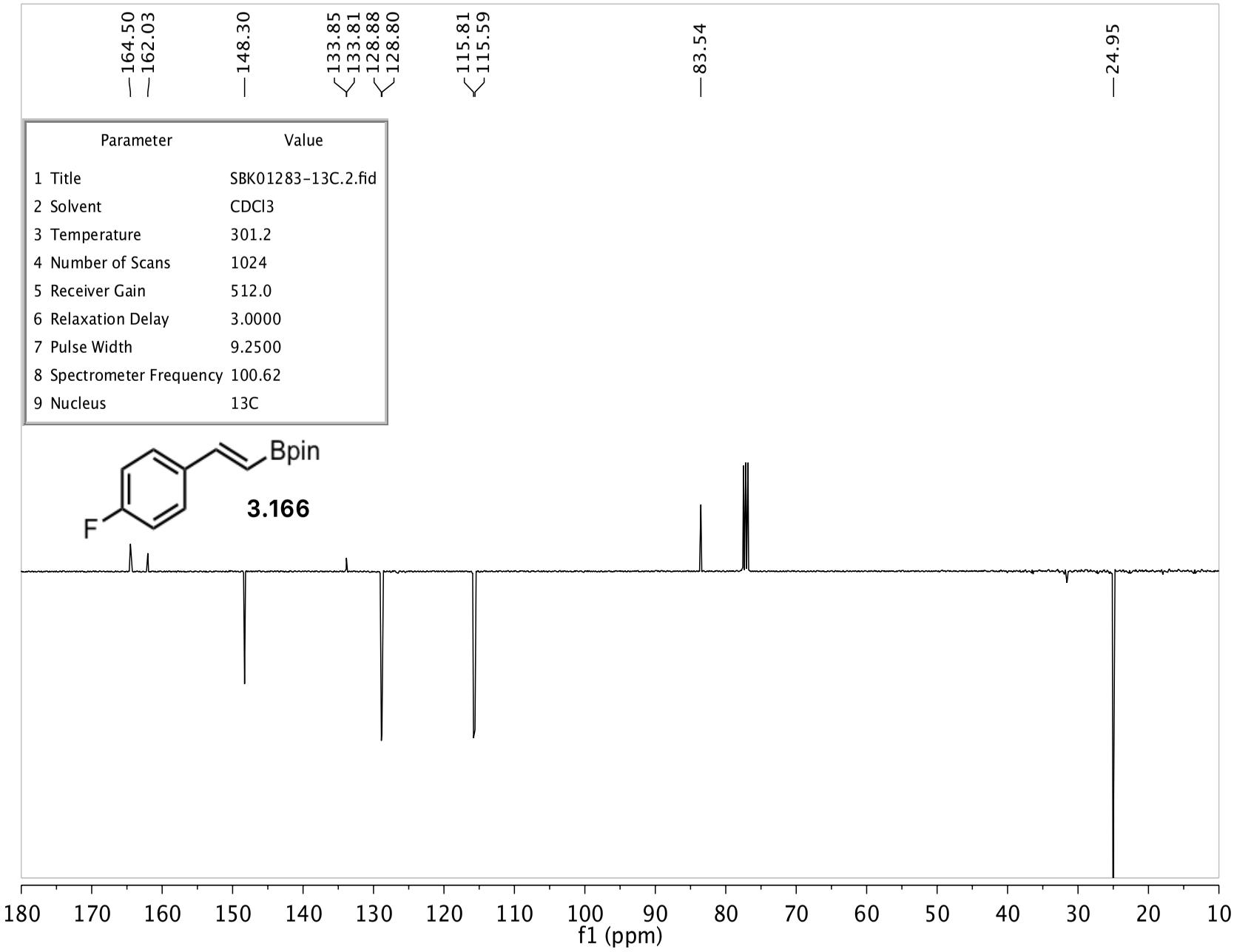
164.50
162.03
148.30
133.85
133.81
128.88
128.80
115.81
115.59
83.54
24.95
Parameter Value
1 Title SBK01283-13C.2.fid
2 Solvent CDCl3
3 Temperature 301.2
4 Number of Scans 1024
5 Receiver Gain 512.0
6 Relaxation Delay 3.0000
7 Pulse Width 9.2500
8 Spectrometer Frequency 100.62
9 Nucleus 13C
Bpin
F
3.166
180 170 160 150 140 130 120 110 100 90 80 70 60 50 40 30 20 10
f1 (ppm)

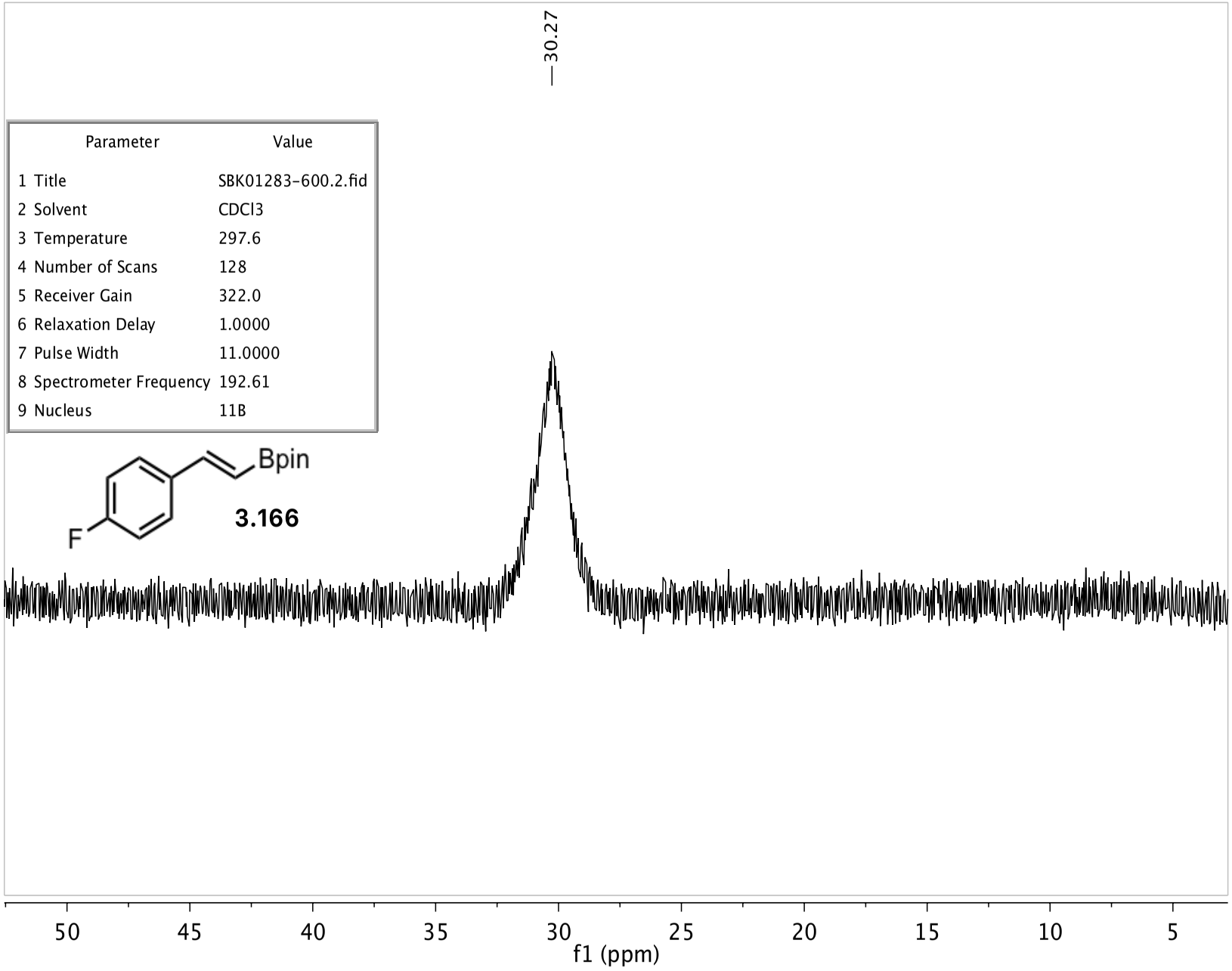
30.27
Parameter Value
1 Title SBK01283-600.2.fid
2 Solvent CDCl3
3 Temperature 297.6
4 Number of Scans 128
5 Receiver Gain 322.0
6 Relaxation Delay 1.0000
7 Pulse Width 11.0000
8 Spectrometer Frequency 192.61
9 Nucleus 11B
Bpin
F
3.166
50
45
40
35
30
25
20
15
10
5
f1 (ppm)

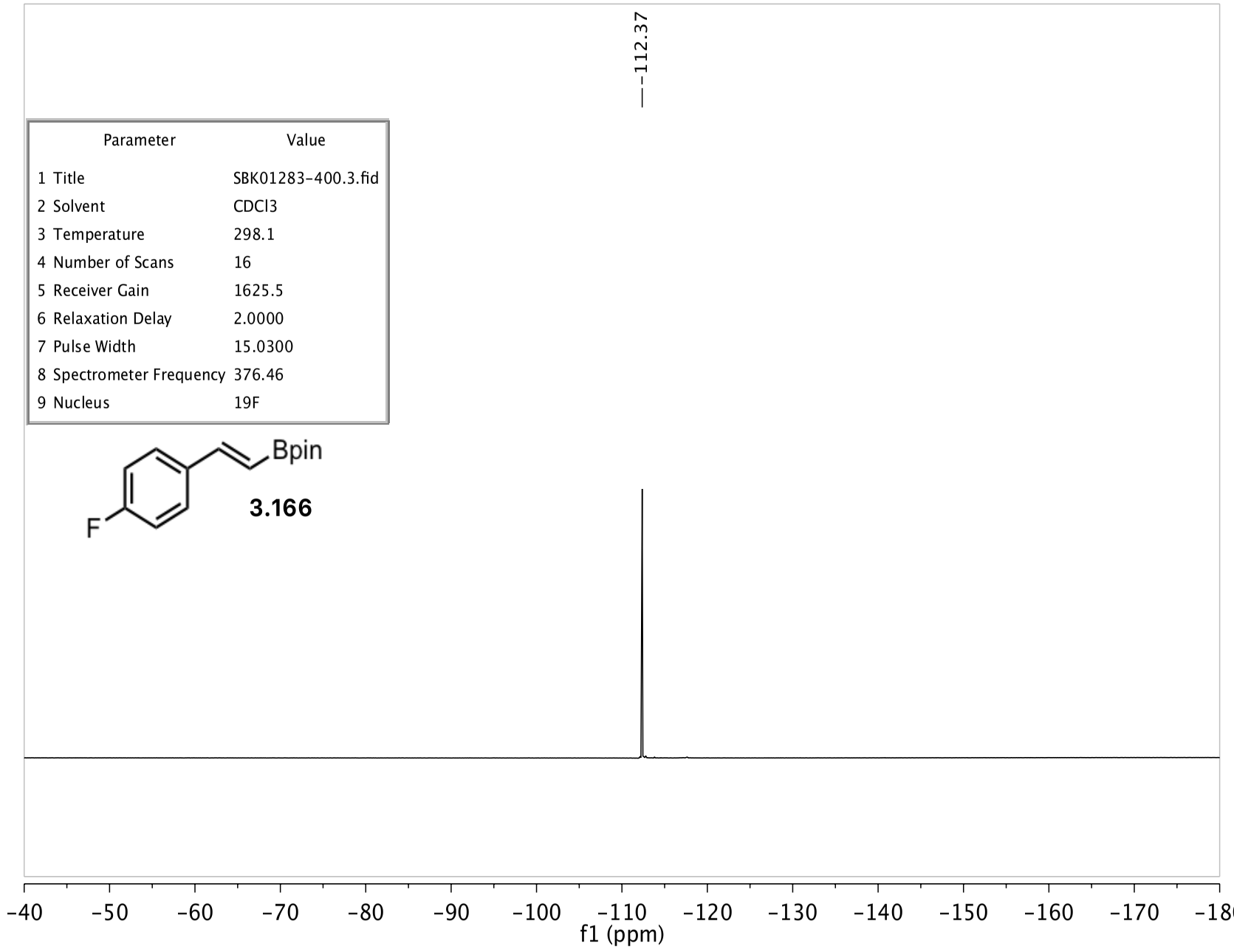
-112.37
Parameter Value
1 Title SBK01283-400.3.fid
2 Solvent CDCl3
3 Temperature 298.1
4 Number of Scans 16
5 Receiver Gain 1625.5
6 Relaxation Delay 2.0000
7 Pulse Width 15.0300
8 Spectrometer Frequency 376.46
9 Nucleus 19F
Bpin
F
3.166
-40 -50 -60 -70 -80 -90 -100 -110 -120 -130 -140 -150 -160 -170 -180
f1 (ppm)

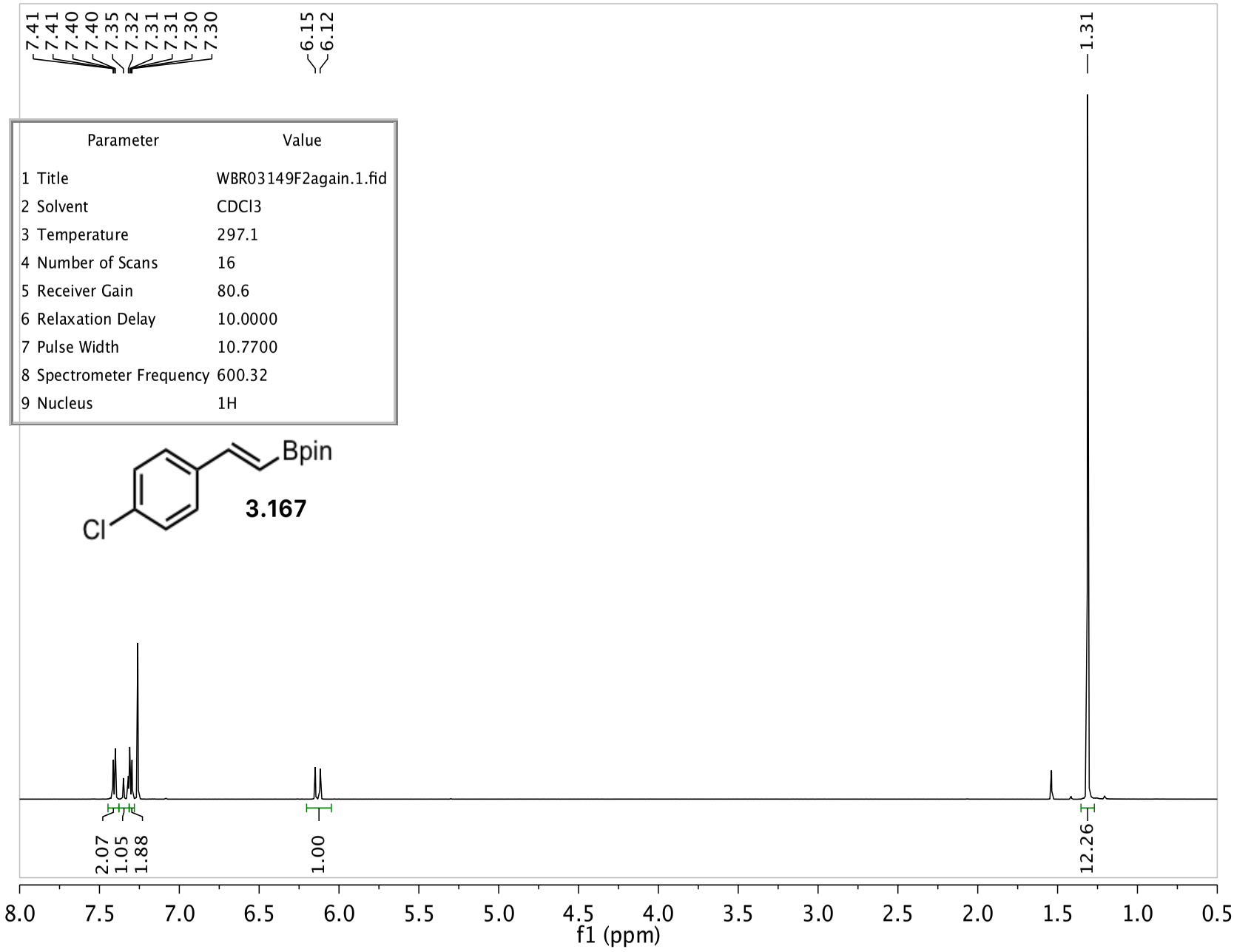
7.41
7.41
7.40
7.40
7.35
7.32
7.31
7.31
7.30
7.30
6.15
6.12
1.31
Parameter Value
1 Title WBR03149F2again.1.fid
2 Solvent CDCl3
3 Temperature 297.1
4 Number of Scans 16
5 Receiver Gain 80.6
6 Relaxation Delay 10.0000
7 Pulse Width 10.7700
8 Spectrometer Frequency 600.32
9 Nucleus 1H
Bpin
Cl
3.167
2.07
1.05
1.88
1.00
12.26
8.0
7.5
7.0
6.5
6.0
5.5
5.0
4.5
4.0
3.5
3.0
2.5
2.0
1.5
1.0
0.5
f1 (ppm)

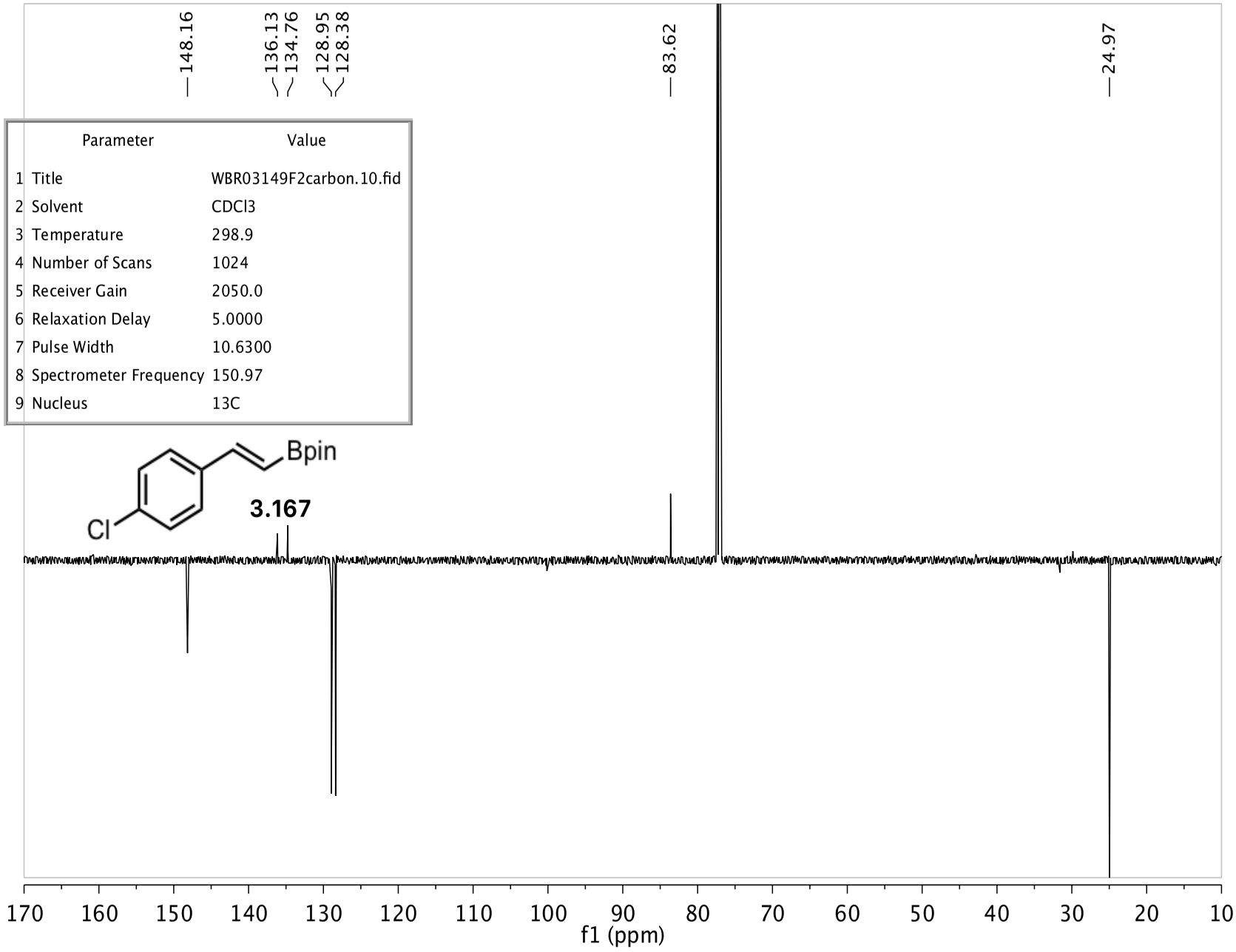
148.16
136.13
134.76
128.95
128.38
83.62
24.97
Parameter Value
1 Title WBR03149F2carbon.10.fid
2 Solvent CDCl3
3 Temperature 298.9
4 Number of Scans 1024
5 Receiver Gain 2050.0
6 Relaxation Delay 5.0000
7 Pulse Width 10.6300
8 Spectrometer Frequency 150.97
9 Nucleus 13C
Bpin
Cl
3.167
170 160 150 140 130 120 110 100 90 80 70 60 50 40 30 20 10
f1 (ppm)

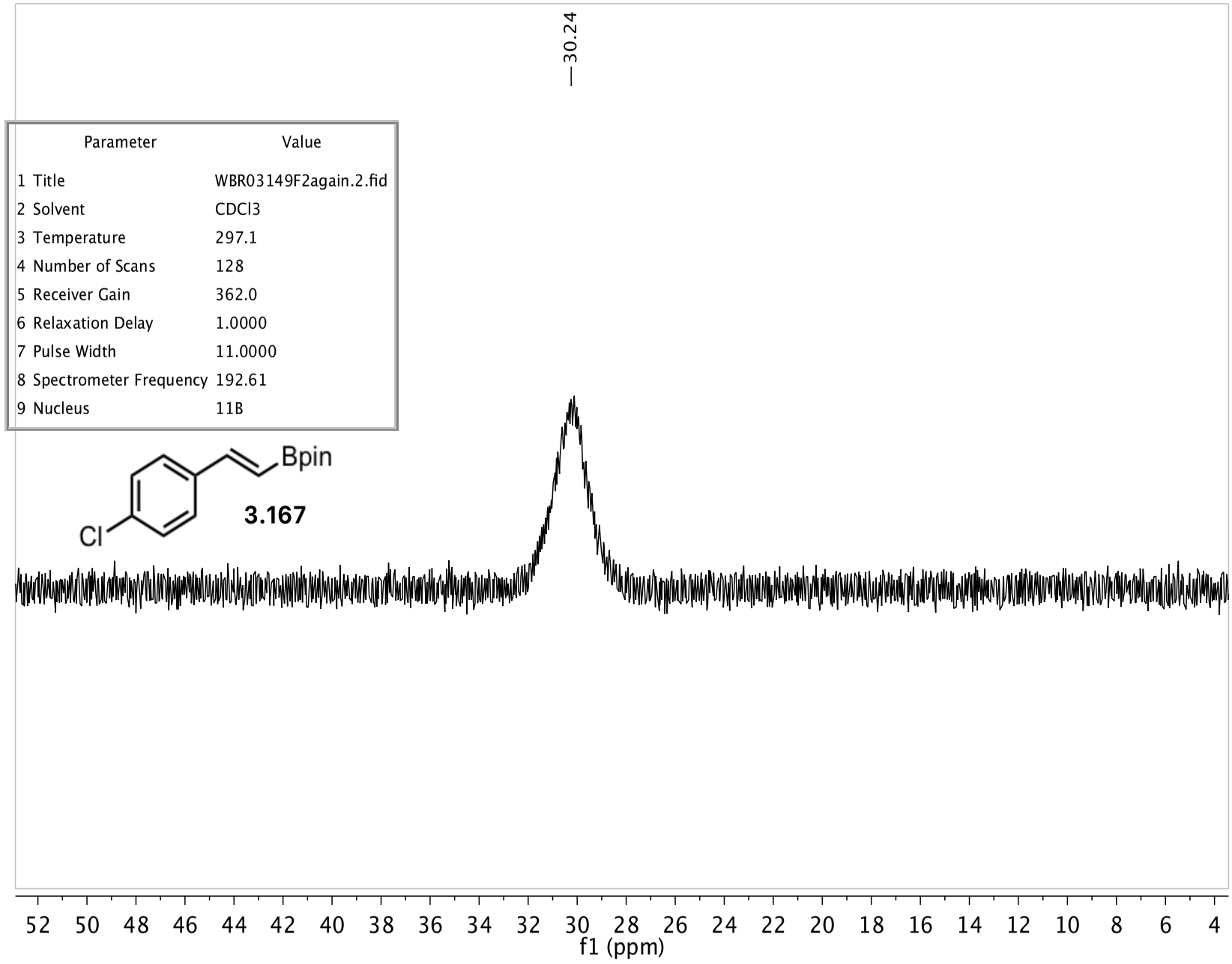
30.24
Parameter Value
1 Title WBR03149F2again.2.fid
2 Solvent CDCl3
3 Temperature 297.1
4 Number of Scans 128
5 Receiver Gain 362.0
6 Relaxation Delay 1.0000
7 Pulse Width 11.0000
8 Spectrometer Frequency 192.61
9 Nucleus 11B
Bpin
Cl
3.167
52 50 48 46 44 42 40 38 36 34 32 30 28 26 24 22 20 18 16 14 12 10 8 6 4
f1 (ppm)

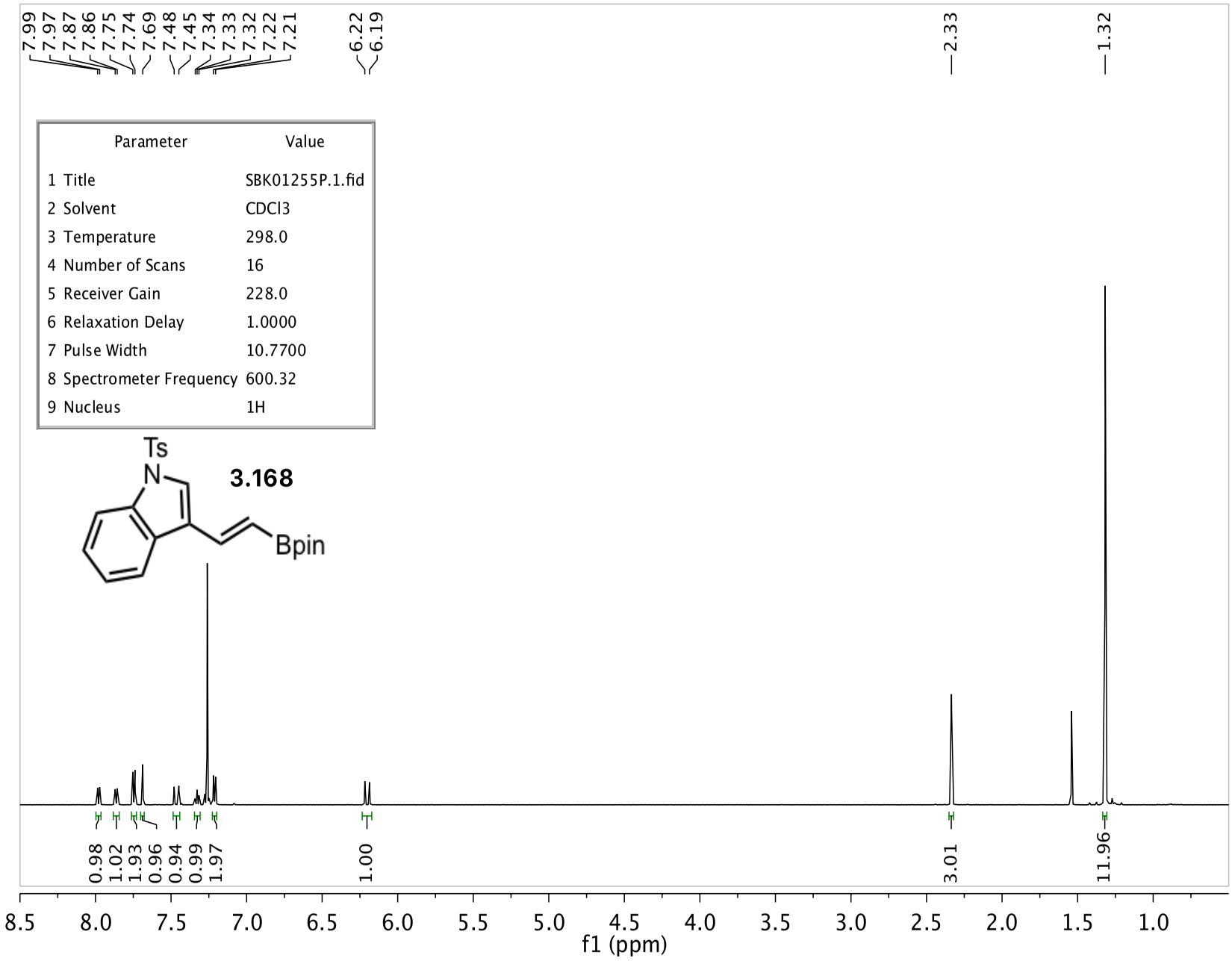
7.99
7.97
7.87
7.86
7.75
7.74
7.69
7.48
7.45
7.34
7.33
7.32
7.22
7.21
6.22
6.19
2.33
1.32
Parameter Value
1 Title SBK01255P.1.fid
2 Solvent CDCl3
3 Temperature 298.0
4 Number of Scans 16
5 Receiver Gain 228.0
6 Relaxation Delay 1.0000
7 Pulse Width 10.7700
8 Spectrometer Frequency 600.32
9 Nucleus 1H
Ts
N
3.168
Bpin
0.98
1.02
1.93
0.96
0.94
0.99
1.97
1.00
3.01
11.96
8.5
8.0
7.5
7.0
6.5
6.0
5.5
5.0
4.5
4.0
3.5
3.0
2.5
2.0
1.5
1.0
f1 (ppm)

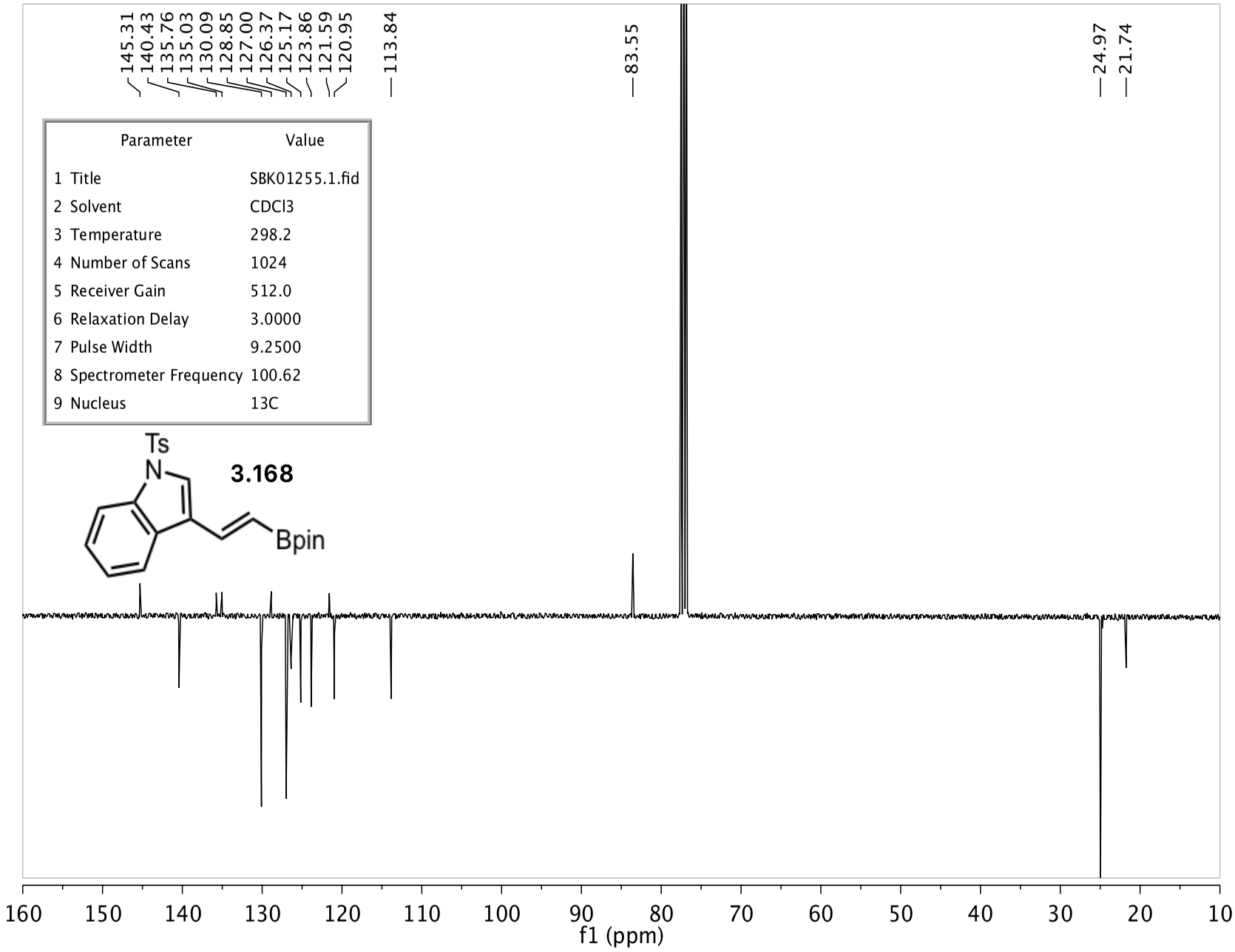
145.31
140.43
135.76
135.03
130.09
128.85
127.00
126.37
125.17
123.86
121.59
120.95
113.84
83.55
24.97
21.74
Parameter Value
1 Title SBK01255.1.fid
2 Solvent CDCl3
3 Temperature 298.2
4 Number of Scans 1024
5 Receiver Gain 512.0
6 Relaxation Delay 3.0000
7 Pulse Width 9.2500
8 Spectrometer Frequency 100.62
9 Nucleus 13C
Ts
N
3.168
Bpin
160 150 140 130 120 110 100 90 80 70 60 50 40 30 20 10
f1 (ppm)

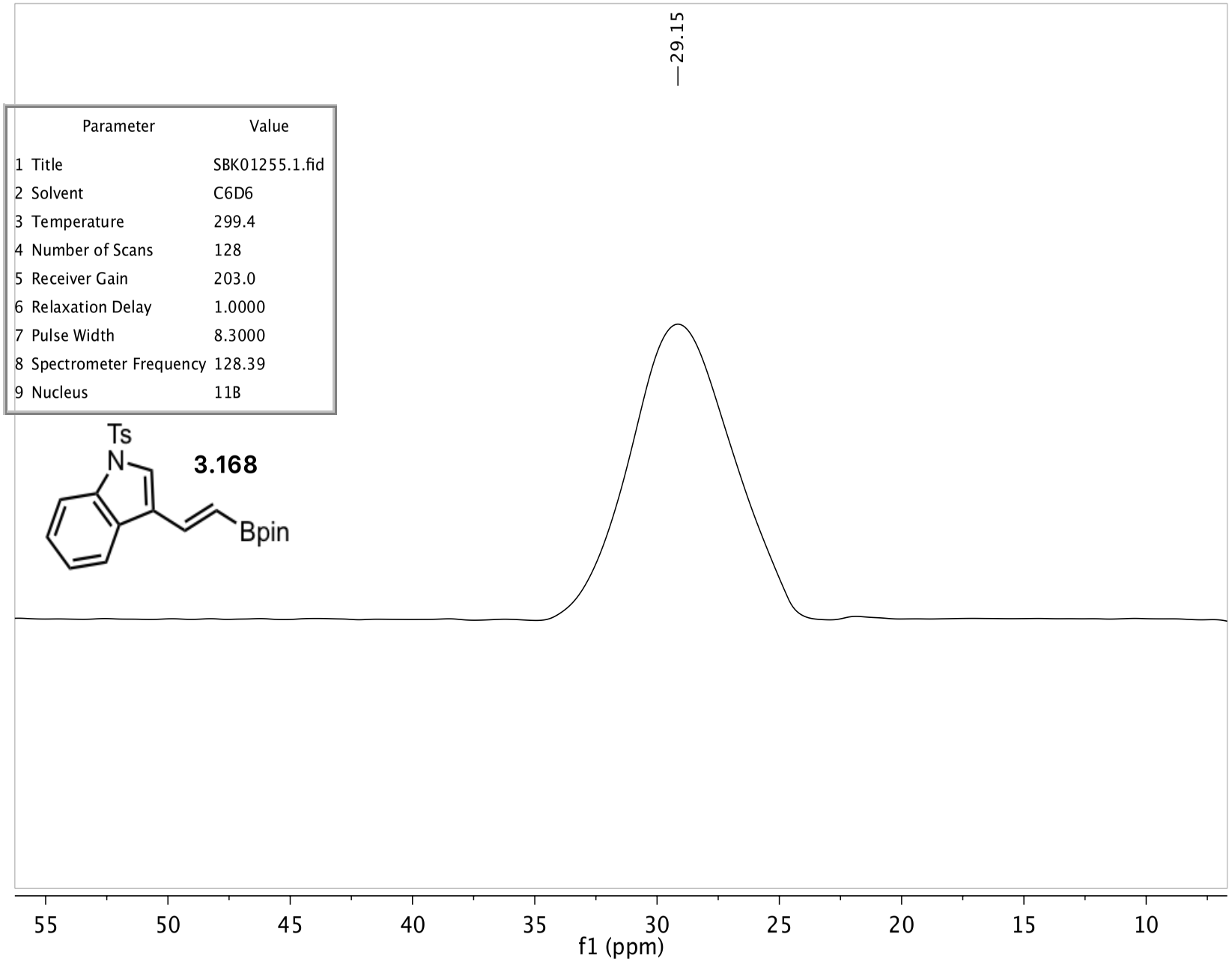
29.15
Parameter Value
1 Title SBK01255.1.fid
2 Solvent C6D6
3 Temperature 299.4
4 Number of Scans 128
5 Receiver Gain 203.0
6 Relaxation Delay 1.0000
7 Pulse Width 8.3000
8 Spectrometer Frequency 128.39
9 Nucleus 11B
Ts
N
3.168
Bpin
55
50
45
40
35
30
25
20
15
10
f1 (ppm)

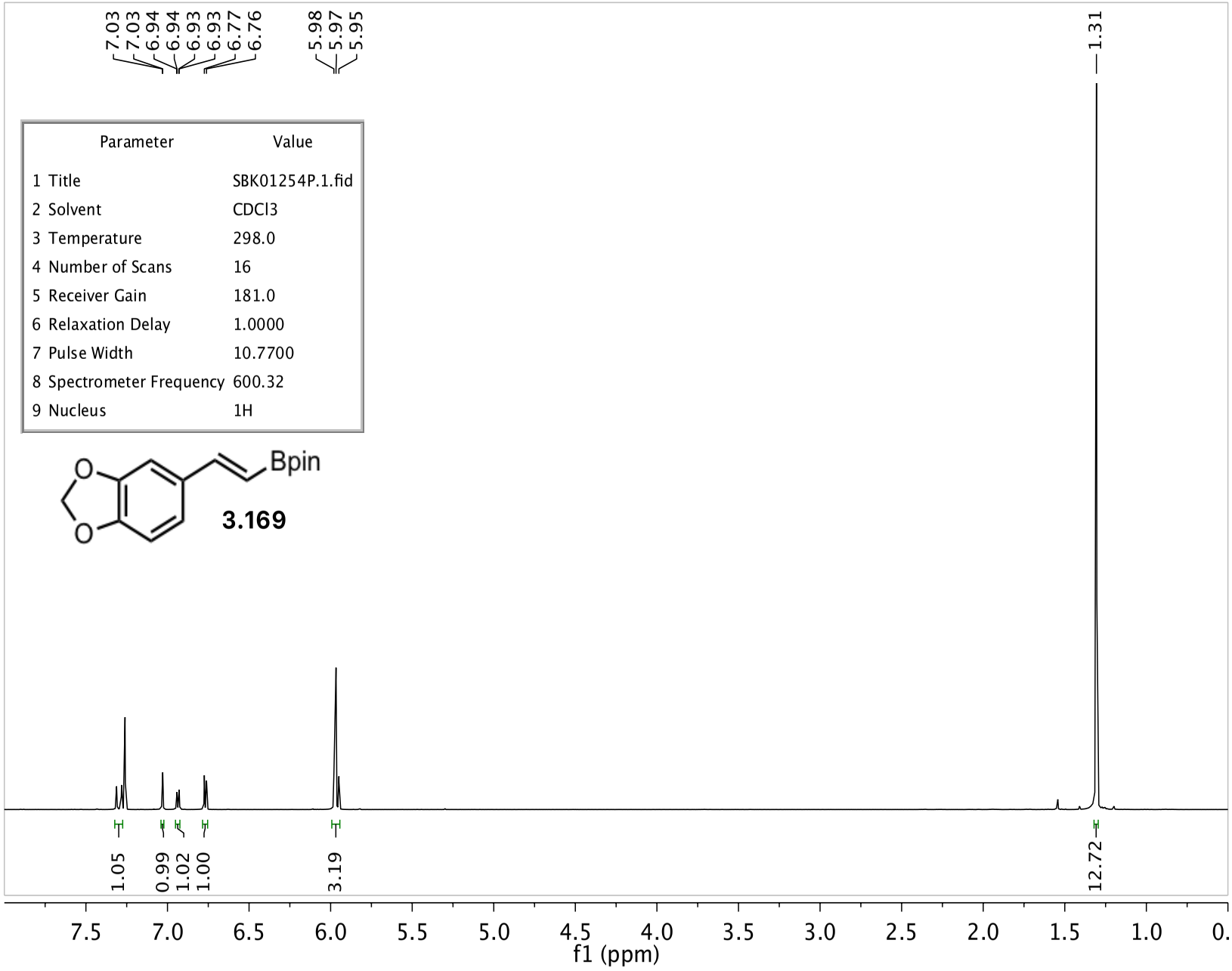
7.03
7.03
6.94
6.94
6.93
6.93
6.77
6.76
5.98
5.97
5.95
1.31
Parameter Value
1 Title SBK01254P.1.fid
2 Solvent CDCl3
3 Temperature 298.0
4 Number of Scans 16
5 Receiver Gain 181.0
6 Relaxation Delay 1.0000
7 Pulse Width 10.7700
8 Spectrometer Frequency 600.32
9 Nucleus 1H
Bpin
3.169
1.05
0.99
1.02
1.00
3.19
12.72
7.5
7.0
6.5
6.0
5.5
5.0
4.5
4.0
3.5
3.0
2.5
2.0
1.5
1.0
0.5
f1 (ppm)

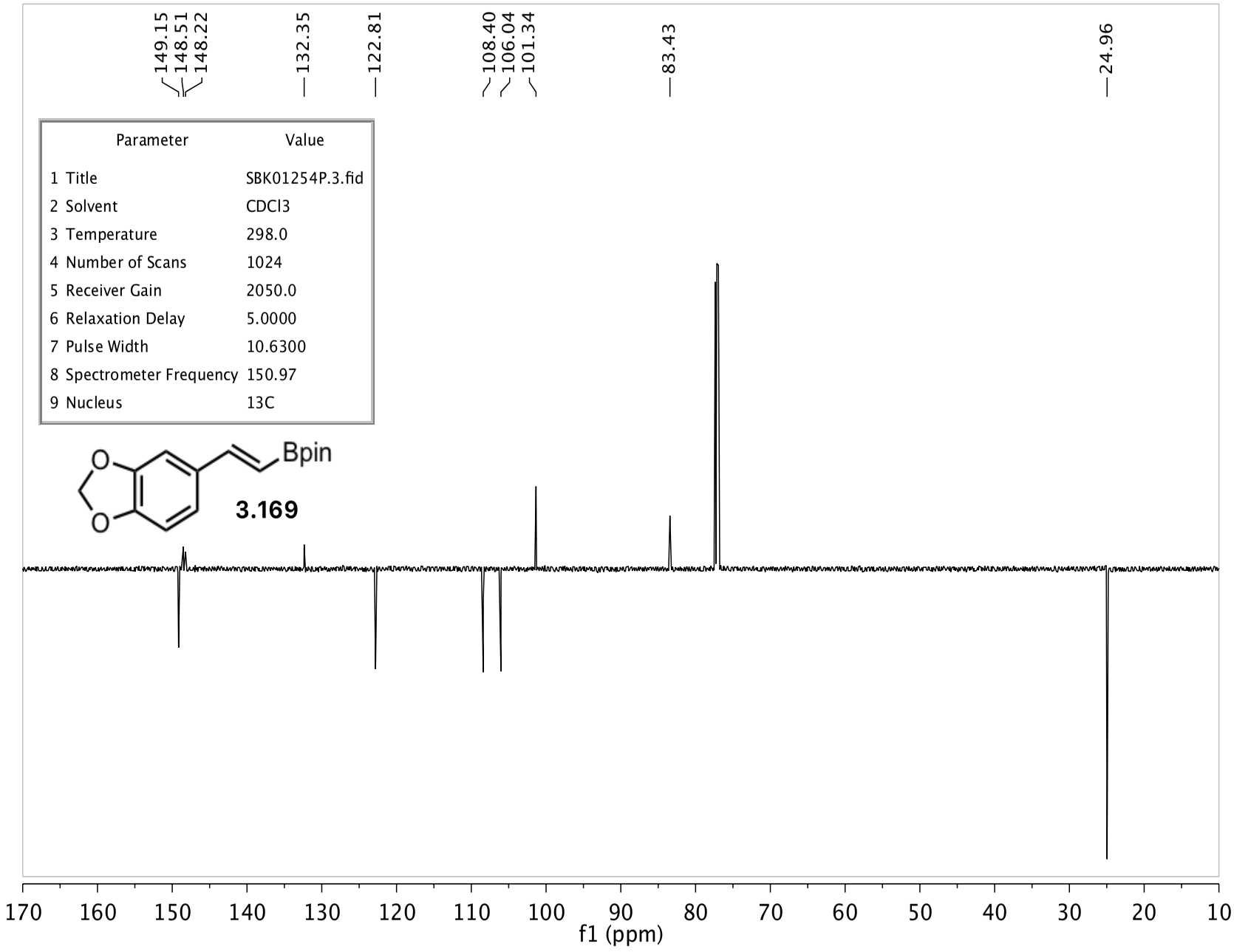
149.15
148.51
148.22
132.35
122.81
108.40
106.04
101.34
83.43
24.96
Parameter Value
1 Title SBK01254P.3.fid
2 Solvent CDCl3
3 Temperature 298.0
4 Number of Scans 1024
5 Receiver Gain 2050.0
6 Relaxation Delay 5.0000
7 Pulse Width 10.6300
8 Spectrometer Frequency 150.97
9 Nucleus 13C
Bpin
3.169
170 160 150 140 130 120 110 100 90 80 70 60 50 40 30 20 10
f1 (ppm)

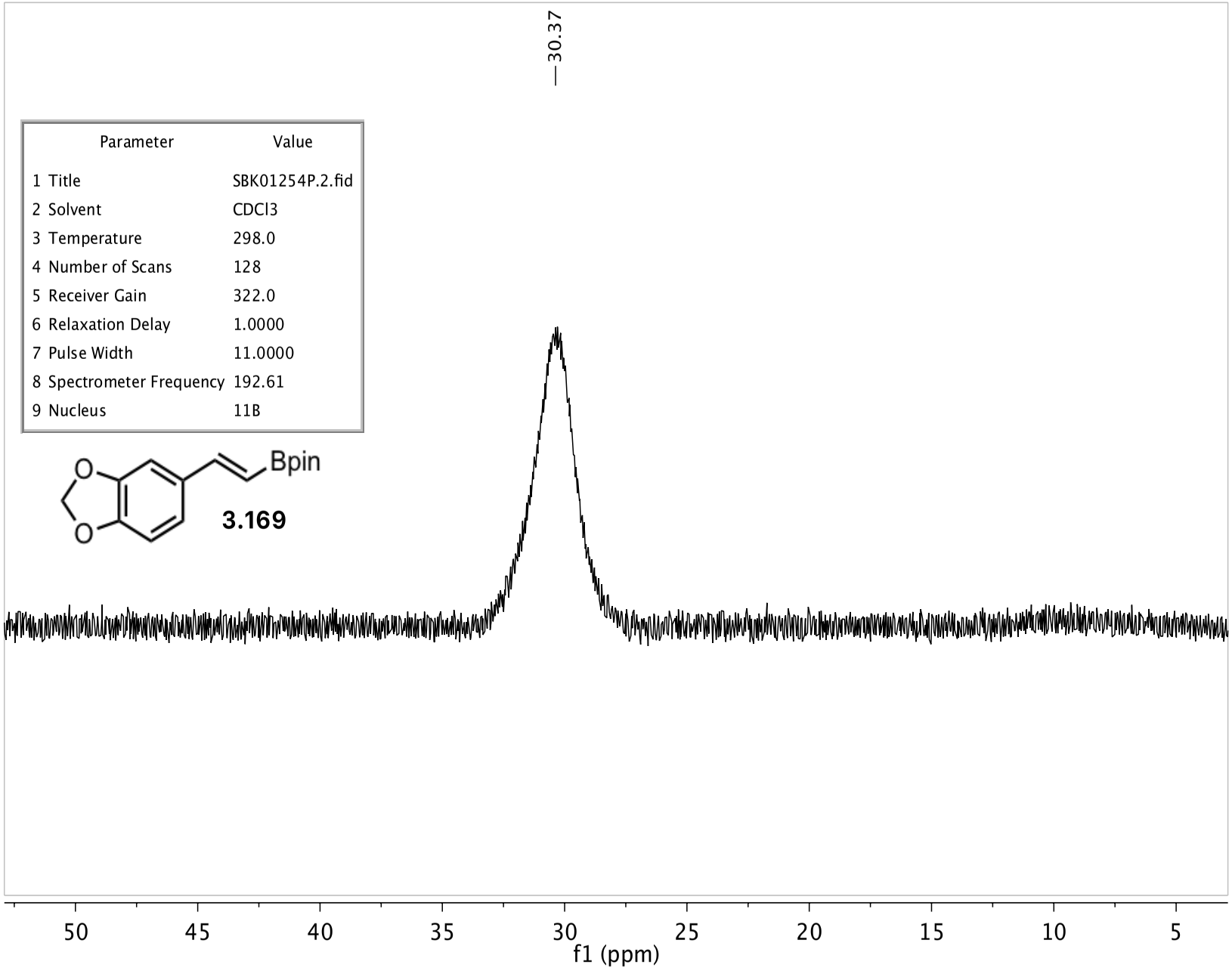
30.37
Parameter Value
1 Title SBK01254P.2.fid
2 Solvent CDCl3
3 Temperature 298.0
4 Number of Scans 128
5 Receiver Gain 322.0
6 Relaxation Delay 1.0000
7 Pulse Width 11.0000
8 Spectrometer Frequency 192.61
9 Nucleus 11B
Bpin
3.169
50
45
40
35
30
25
20
15
10
5
f1 (ppm)

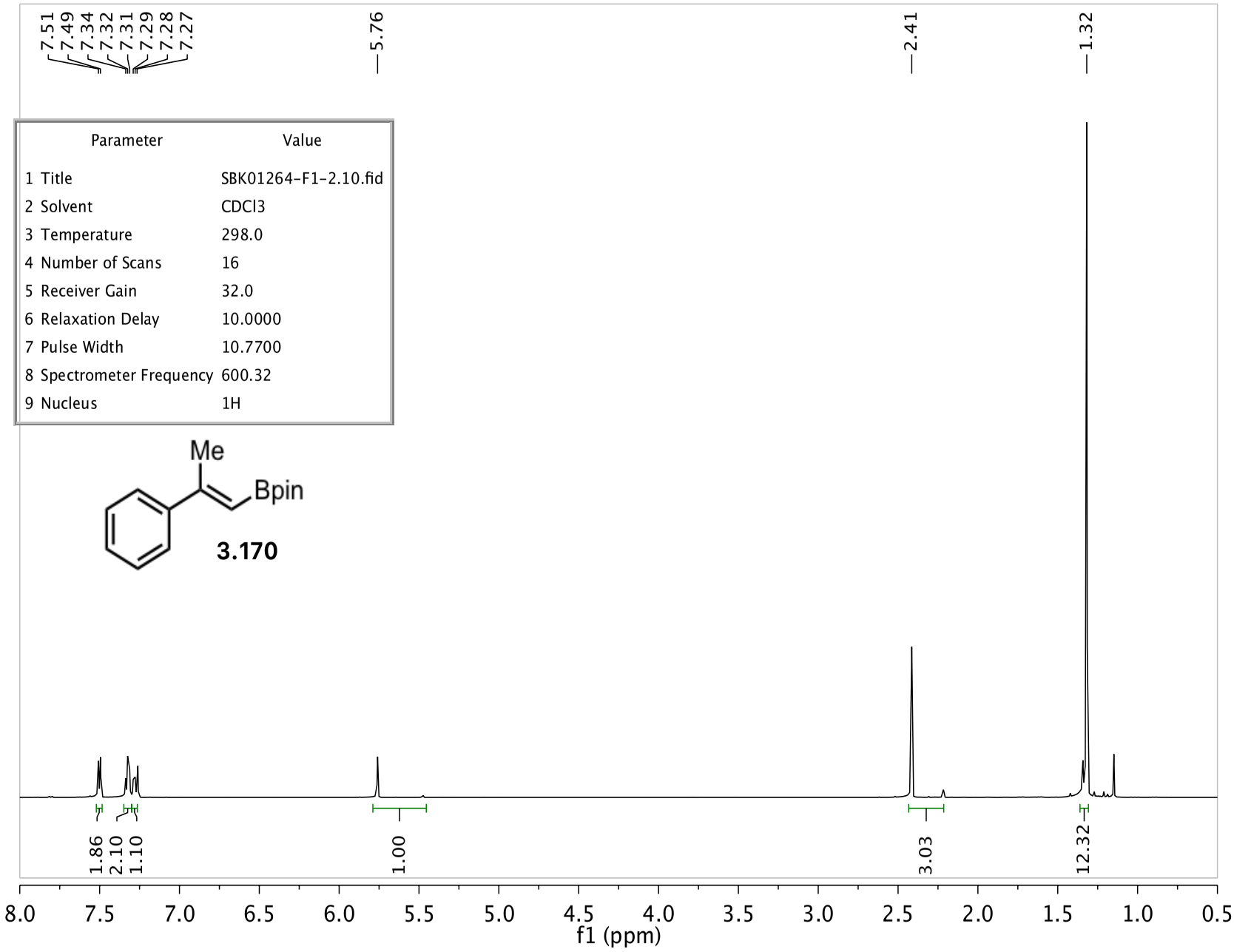
7.51
7.49
7.34
7.32
7.31
7.29
7.28
7.27
5.76
2.41
1.32
Parameter Value
1 Title SBK01264-F1-2.10.fid
2 Solvent CDCl3
3 Temperature 298.0
4 Number of Scans 16
5 Receiver Gain 32.0
6 Relaxation Delay 10.0000
7 Pulse Width 10.7700
8 Spectrometer Frequency 600.32
9 Nucleus 1H
Me
Bpin
3.170
1.86
2.10
1.10
1.00
3.03
12.32
8.0 7.5 7.0 6.5 6.0 5.5 5.0 4.5 4.0 3.5 3.0 2.5 2.0 1.5 1.0 0.5
f1 (ppm)

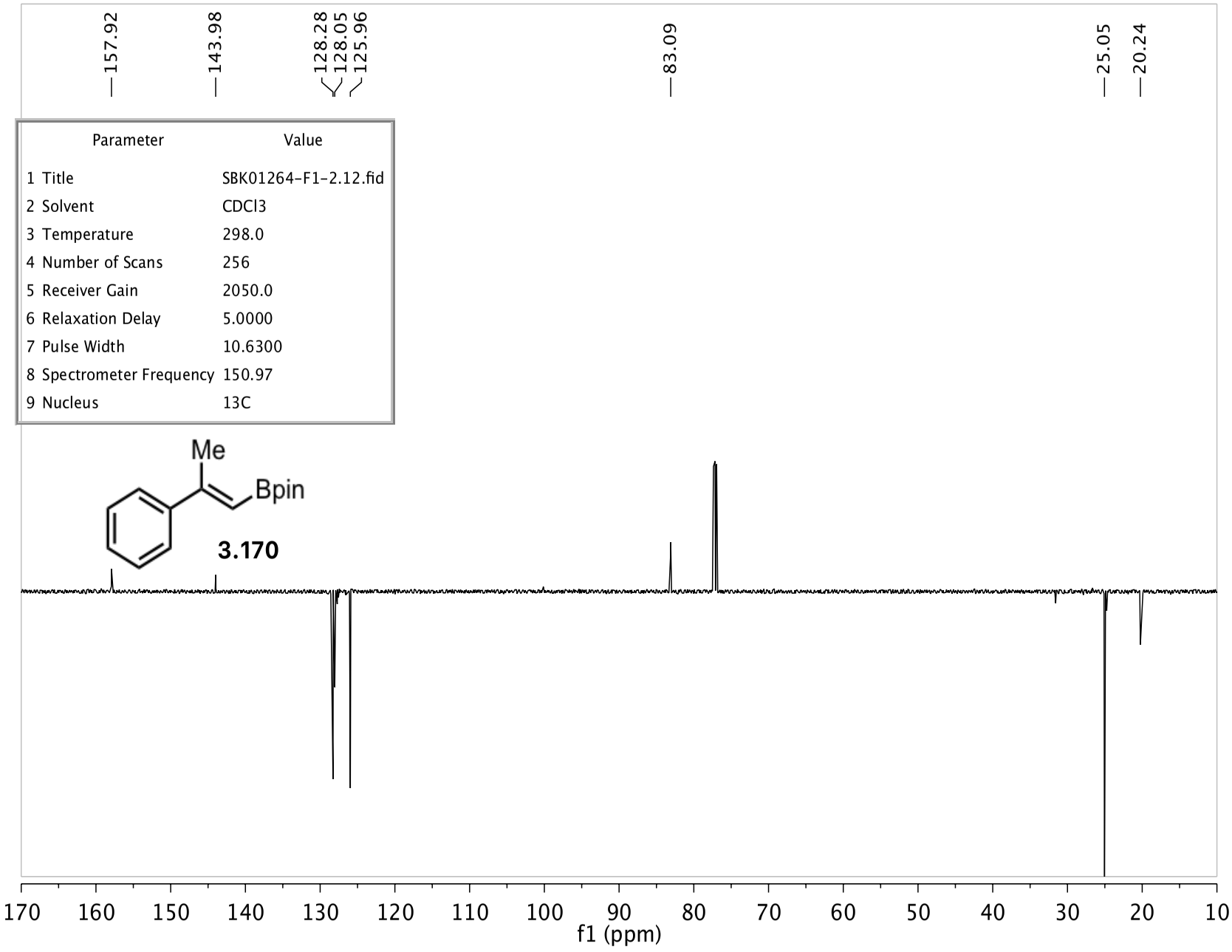
157.92
143.98
128.28
128.05
125.96
83.09
25.05
20.24
Parameter Value
1 Title SBK01264-F1-2.12.fid
2 Solvent CDCl3
3 Temperature 298.0
4 Number of Scans 256
5 Receiver Gain 2050.0
6 Relaxation Delay 5.0000
7 Pulse Width 10.6300
8 Spectrometer Frequency 150.97
9 Nucleus 13C
Me
Bpin
3.170
170 160 150 140 130 120 110 100 90 80 70 60 50 40 30 20 10
f1 (ppm)

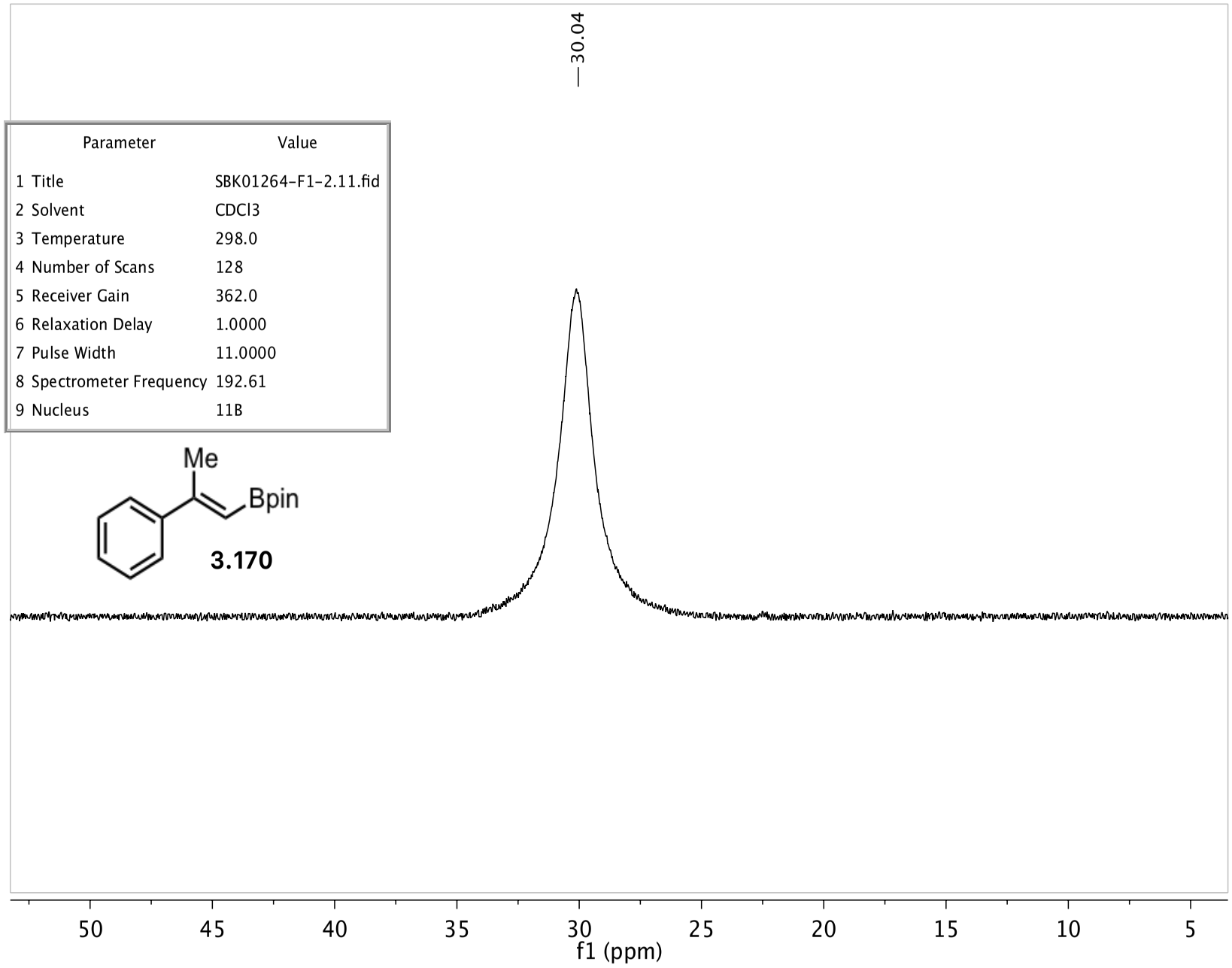
30.04
Parameter Value
1 Title SBK01264-F1-2.11.fid
2 Solvent CDCl3
3 Temperature 298.0
4 Number of Scans 128
5 Receiver Gain 362.0
6 Relaxation Delay 1.0000
7 Pulse Width 11.0000
8 Spectrometer Frequency 192.61
9 Nucleus 11B
Me
Bpin
3.170
50
45
40
35
30
25
20
15
10
5
f1 (ppm)

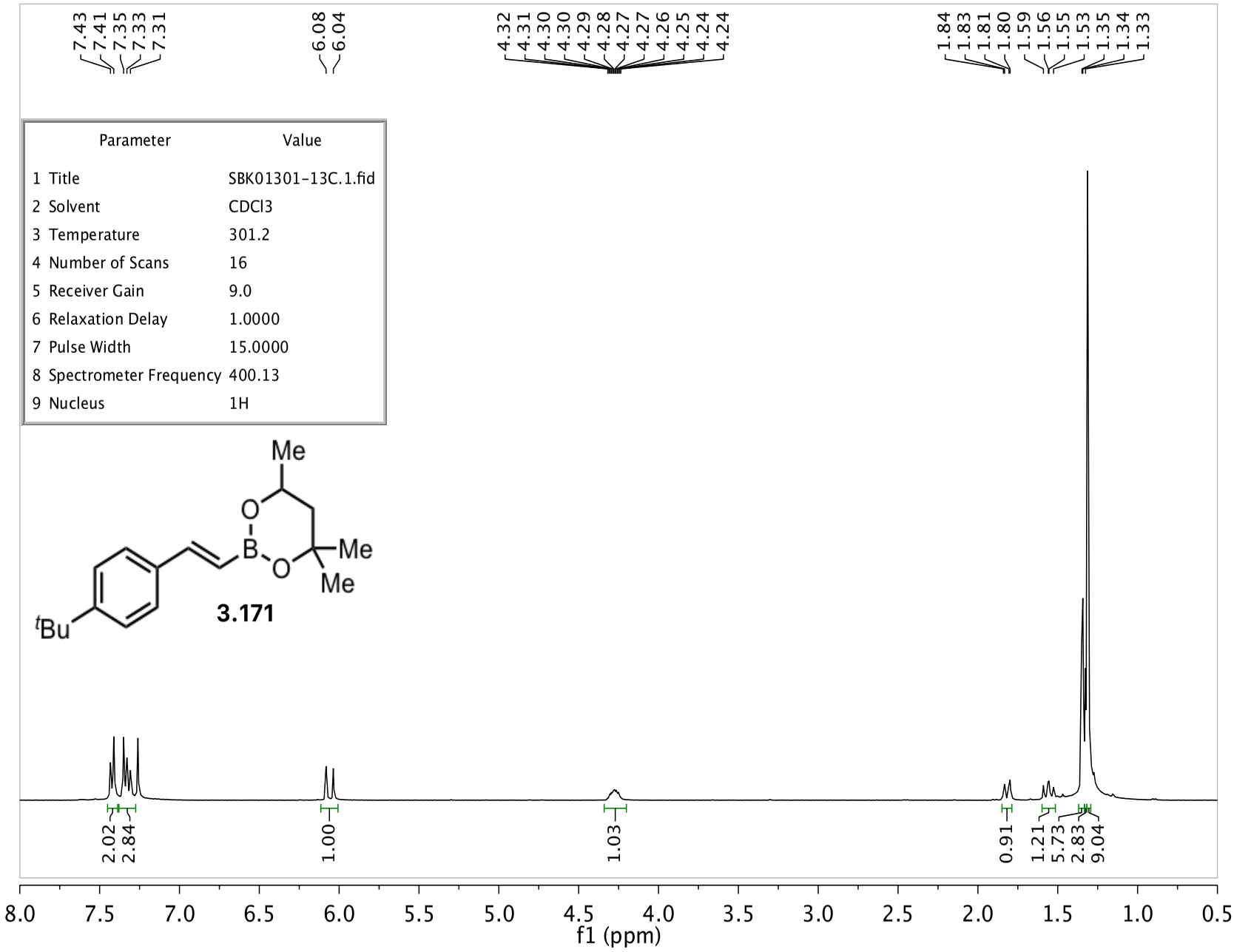
7.43
7.41
7.35
7.33
7.31
6.08
6.04
4.32
4.31
4.30
4.30
4.29
4.28
4.27
4.27
4.26
4.25
4.24
4.24
1.84
1.83
1.81
1.80
1.59
1.56
1.55
1.53
1.35
1.34
1.33
Parameter Value
1 Title SBK01301-13C.1.fid
2 Solvent CDCl3
3 Temperature 301.2
4 Number of Scans 16
5 Receiver Gain 9.0
6 Relaxation Delay 1.0000
7 Pulse Width 15.0000
8 Spectrometer Frequency 400.13
9 Nucleus 1H
Me
O
B
O
Me
Me
tBu
3.171
2.02
2.84
1.00
1.03
0.91
1.21
5.73
2.83
9.04
8.0
7.5
7.0
6.5
6.0
5.5
5.0
4.5
4.0
3.5
3.0
2.5
2.0
1.5
1.0
0.5
f1 (ppm)

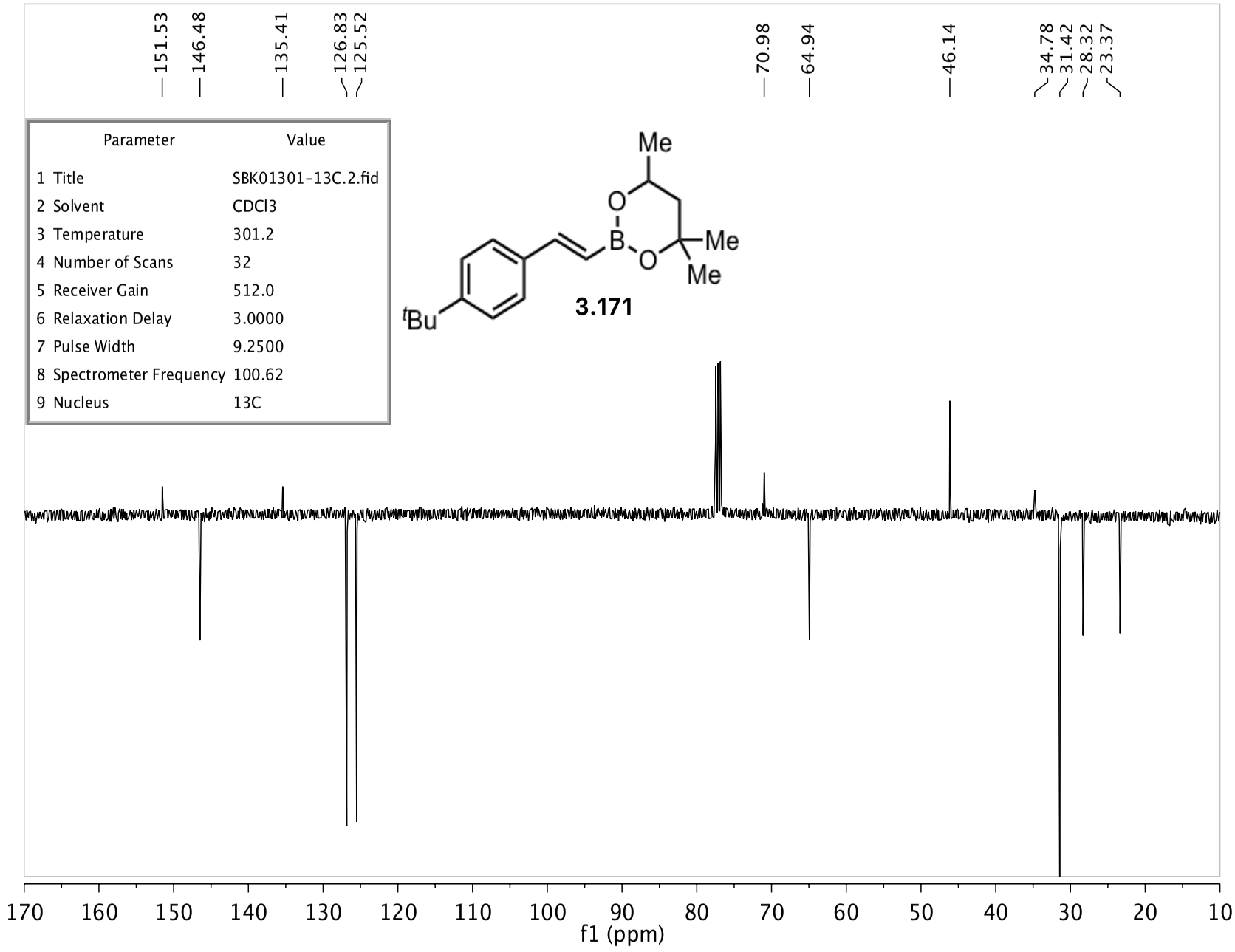
151.53
146.48
135.41
126.83
125.52
70.98
64.94
46.14
34.78
31.42
28.32
23.37
Parameter Value
1 Title SBK01301-13C.2.fid
2 Solvent CDCl3
3 Temperature 301.2
4 Number of Scans 32
5 Receiver Gain 512.0
6 Relaxation Delay 3.0000
7 Pulse Width 9.2500
8 Spectrometer Frequency 100.62
9 Nucleus 13C
Me
O
B
O
Me
Me
tBu
3.171
170 160 150 140 130 120 110 100 90 80 70 60 50 40 30 20 10
f1 (ppm)

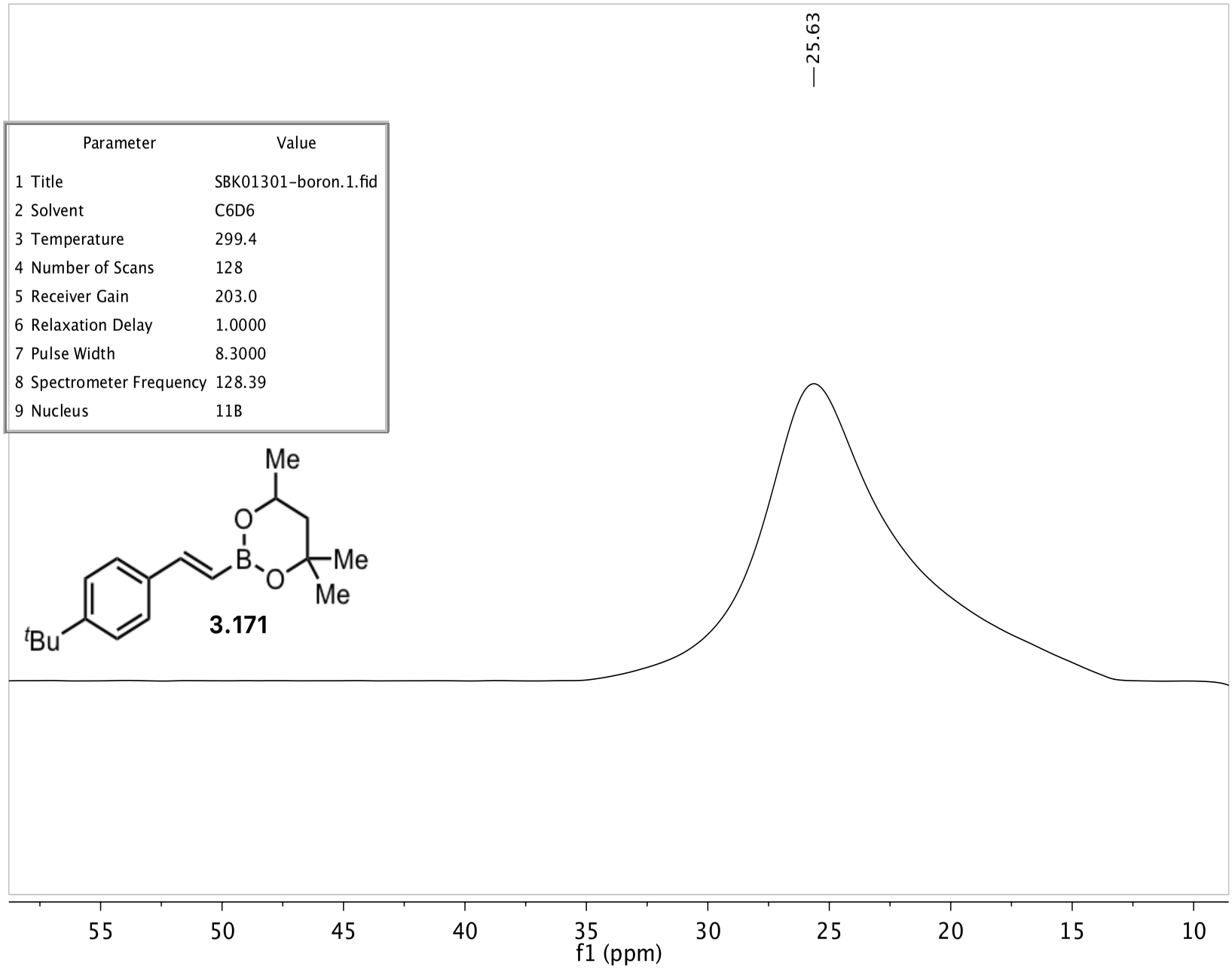
25.63
Parameter
Value
1 Title
SBK01301-boron.1.fid
2 Solvent
C6D6
3 Temperature
299.4
4 Number of Scans
128
5 Receiver Gain
203.0
6 Relaxation Delay
1.0000
7 Pulse Width
8.3000
8 Spectrometer Frequency
128.39
9 Nucleus
11B
Me
O
B
O
Me
Me
tBu
3.171
55
50
45
40
35
30
25
20
15
10
f1 (ppm)

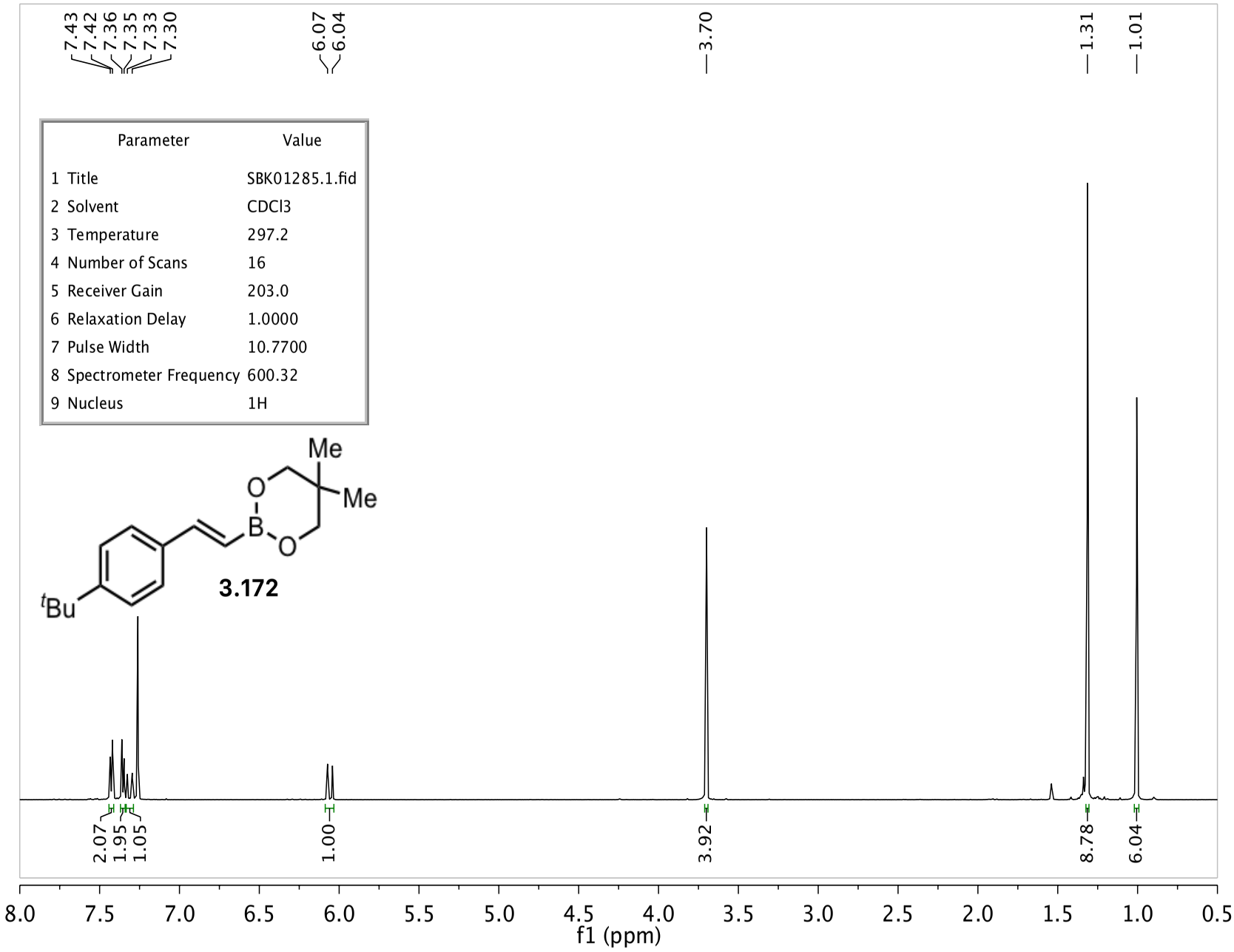
7.43
7.42
7.36
7.35
7.33
7.30
6.07
6.04
3.70
1.31
1.01
Parameter Value
1 Title SBK01285.1.fid
2 Solvent CDCl3
3 Temperature 297.2
4 Number of Scans 16
5 Receiver Gain 203.0
6 Relaxation Delay 1.0000
7 Pulse Width 10.7700
8 Spectrometer Frequency 600.32
9 Nucleus 1H
Me
Me
O
B
O
tBu
3.172
2.07
1.95
1.05
1.00
3.92
8.78
6.04
8.0
7.5
7.0
6.5
6.0
5.5
5.0
4.5
4.0
3.5
3.0
2.5
2.0
1.5
1.0
0.5
f1 (ppm)

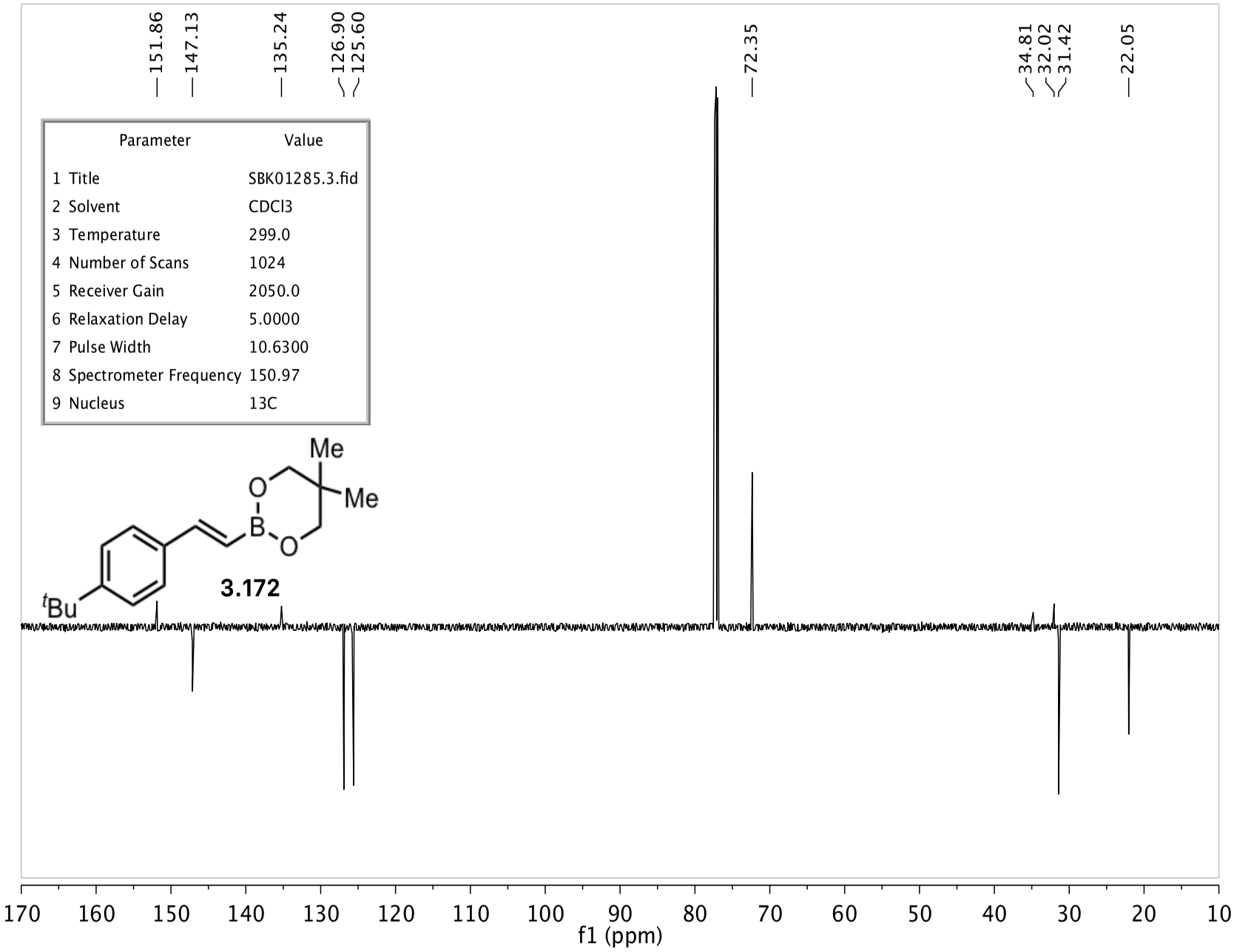
151.86
147.13
135.24
126.90
125.60
72.35
34.81
32.02
31.42
22.05
Parameter Value
1 Title SBK01285.3.fid
2 Solvent CDCl3
3 Temperature 299.0
4 Number of Scans 1024
5 Receiver Gain 2050.0
6 Relaxation Delay 5.0000
7 Pulse Width 10.6300
8 Spectrometer Frequency 150.97
9 Nucleus 13C
Me
Me
O
B
O
tBu
3.172
170 160 150 140 130 120 110 100 90 80 70 60 50 40 30 20 10
f1 (ppm)

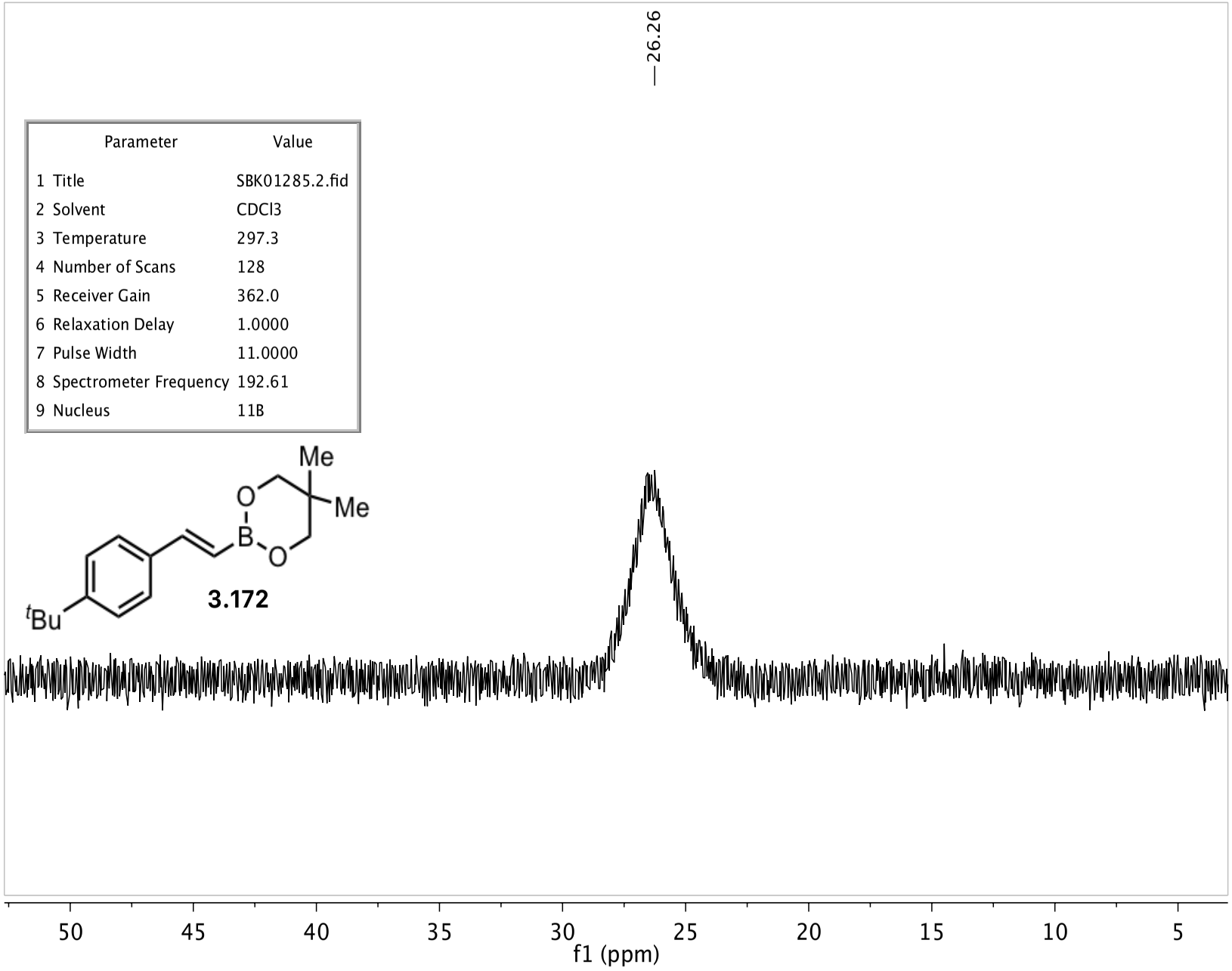
26.26
Parameter Value
1 Title SBK01285.2.fid
2 Solvent CDCl3
3 Temperature 297.3
4 Number of Scans 128
5 Receiver Gain 362.0
6 Relaxation Delay 1.0000
7 Pulse Width 11.0000
8 Spectrometer Frequency 192.61
9 Nucleus 11B
Me
Me
O
B
O
tBu
3.172
50
45
40
35
30
25
20
15
10
5
f1 (ppm)

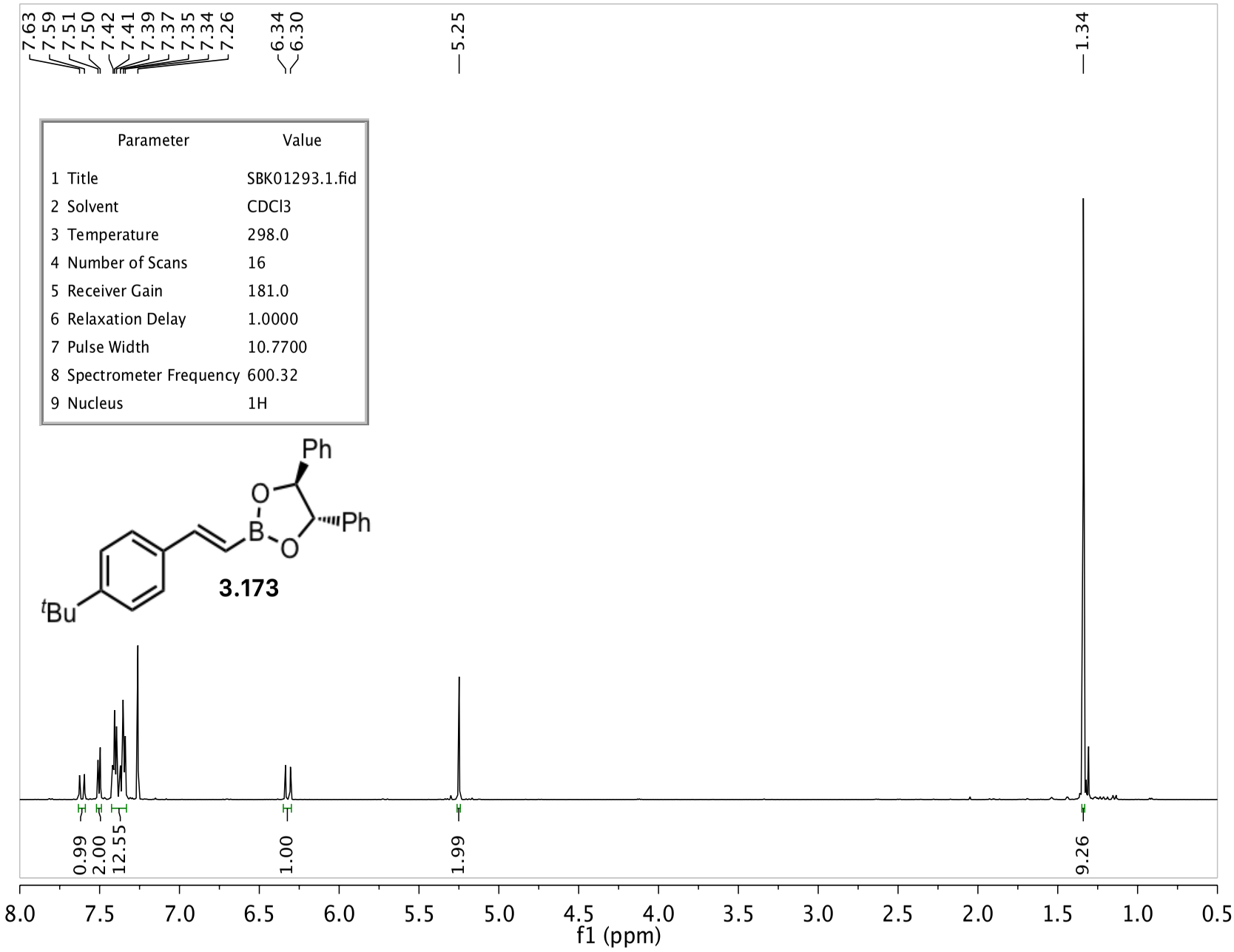
7.63
7.59
7.51
7.50
7.42
7.41
7.39
7.37
7.35
7.34
7.26
6.34
6.30
5.25
1.34
Parameter Value
1 Title SBK01293.1.fid
2 Solvent CDCl3
3 Temperature 298.0
4 Number of Scans 16
5 Receiver Gain 181.0
6 Relaxation Delay 1.0000
7 Pulse Width 10.7700
8 Spectrometer Frequency 600.32
9 Nucleus 1H
Ph
O
B
O
Ph
tBu
3.173
0.99
2.00
12.55
1.00
1.99
9.26
8.0
7.5
7.0
6.5
6.0
5.5
5.0
4.5
4.0
3.5
3.0
2.5
2.0
1.5
1.0
0.5
f1 (ppm)

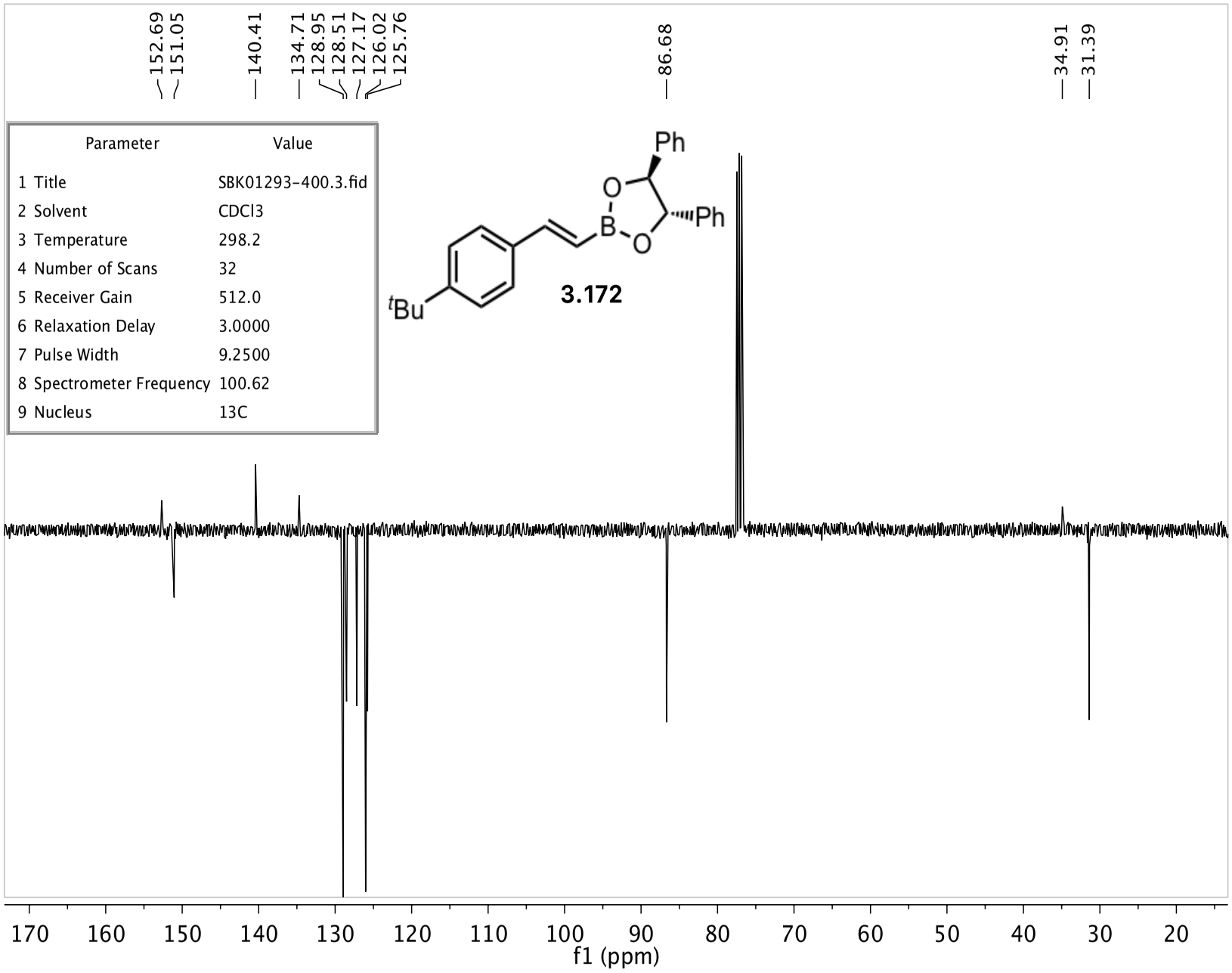
152.69
151.05
140.41
134.71
128.95
128.51
127.17
126.02
125.76
86.68
34.91
31.39
Parameter Value
1 Title SBK01293-400.3.fid
2 Solvent CDCl3
3 Temperature 298.2
4 Number of Scans 32
5 Receiver Gain 512.0
6 Relaxation Delay 3.0000
7 Pulse Width 9.2500
8 Spectrometer Frequency 100.62
9 Nucleus 13C
Ph
O
B
O
Ph
tBu
3.172
170 160 150 140 130 120 110 100 90 80 70 60 50 40 30 20
f1 (ppm)

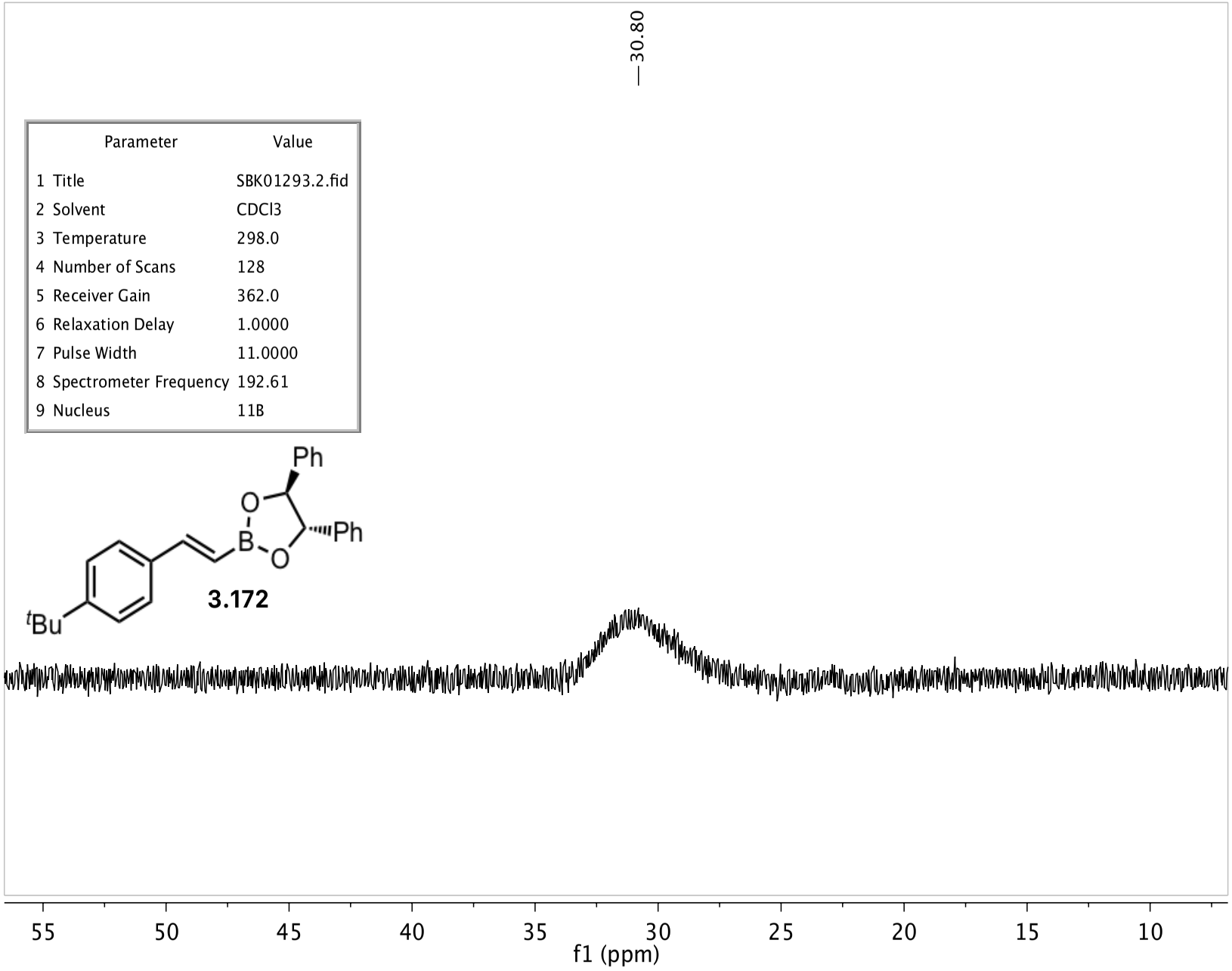
30.80
Parameter Value
1 Title SBK01293.2.fid
2 Solvent CDCl3
3 Temperature 298.0
4 Number of Scans 128
5 Receiver Gain 362.0
6 Relaxation Delay 1.0000
7 Pulse Width 11.0000
8 Spectrometer Frequency 192.61
9 Nucleus 11B
Ph
O
B
O
Ph
tBu
3.172
55
50
45
40
35
30
25
20
15
10
f1 (ppm)

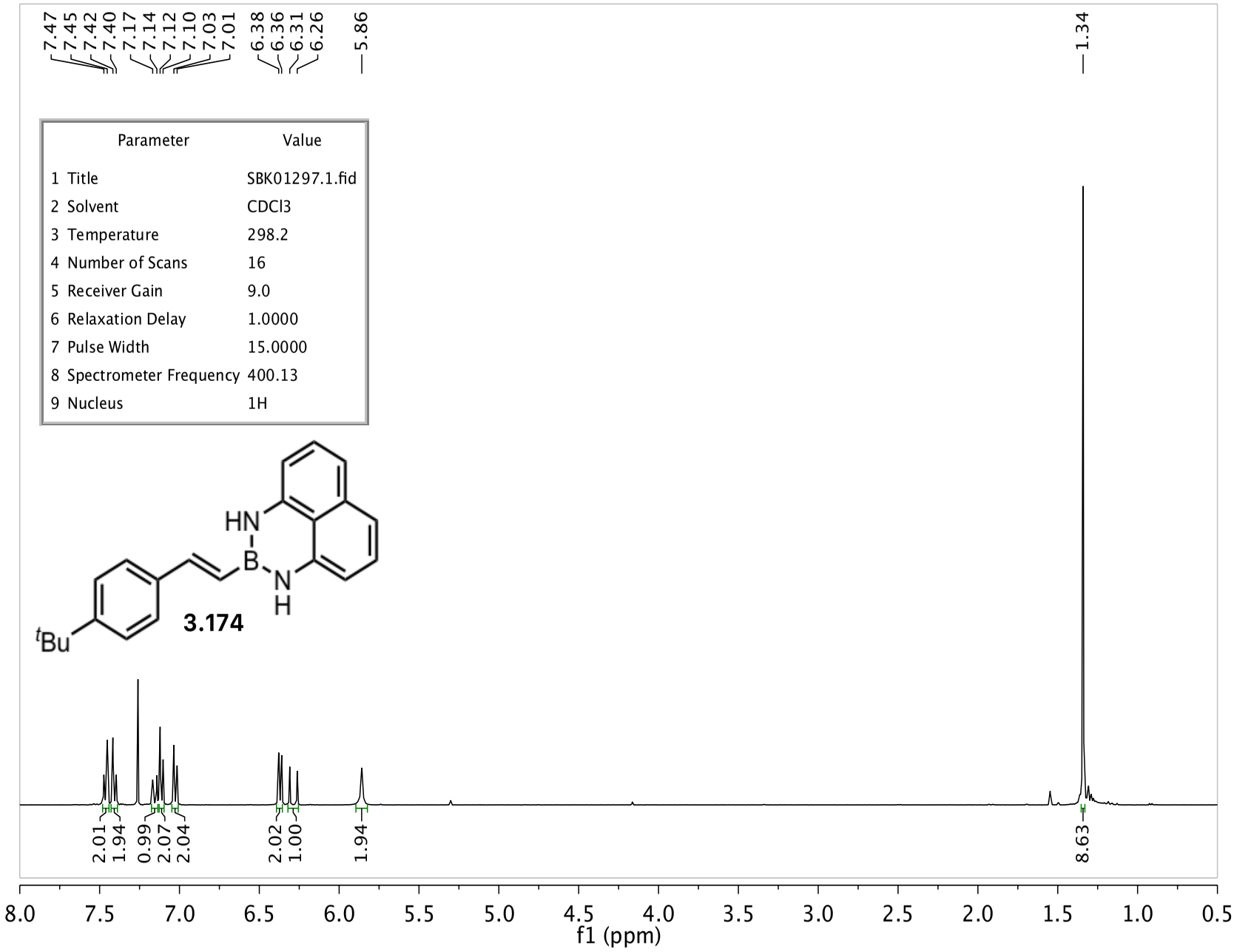
7.47
7.45
7.42
7.40
7.17
7.14
7.12
7.10
7.03
7.01
6.38
6.36
6.31
6.26
5.86
1.34
Parameter Value
1 Title SBK01297.1.fid
2 Solvent CDCl3
3 Temperature 298.2
4 Number of Scans 16
5 Receiver Gain 9.0
6 Relaxation Delay 1.0000
7 Pulse Width 15.0000
8 Spectrometer Frequency 400.13
9 Nucleus 1H
HN
B
N
H
tBu
3.174
2.01
1.94
0.99
2.07
2.04
2.02
1.00
1.94
8.63
8.0
7.5
7.0
6.5
6.0
5.5
5.0
4.5
4.0
3.5
3.0
2.5
2.0
1.5
1.0
0.5
f1 (ppm)

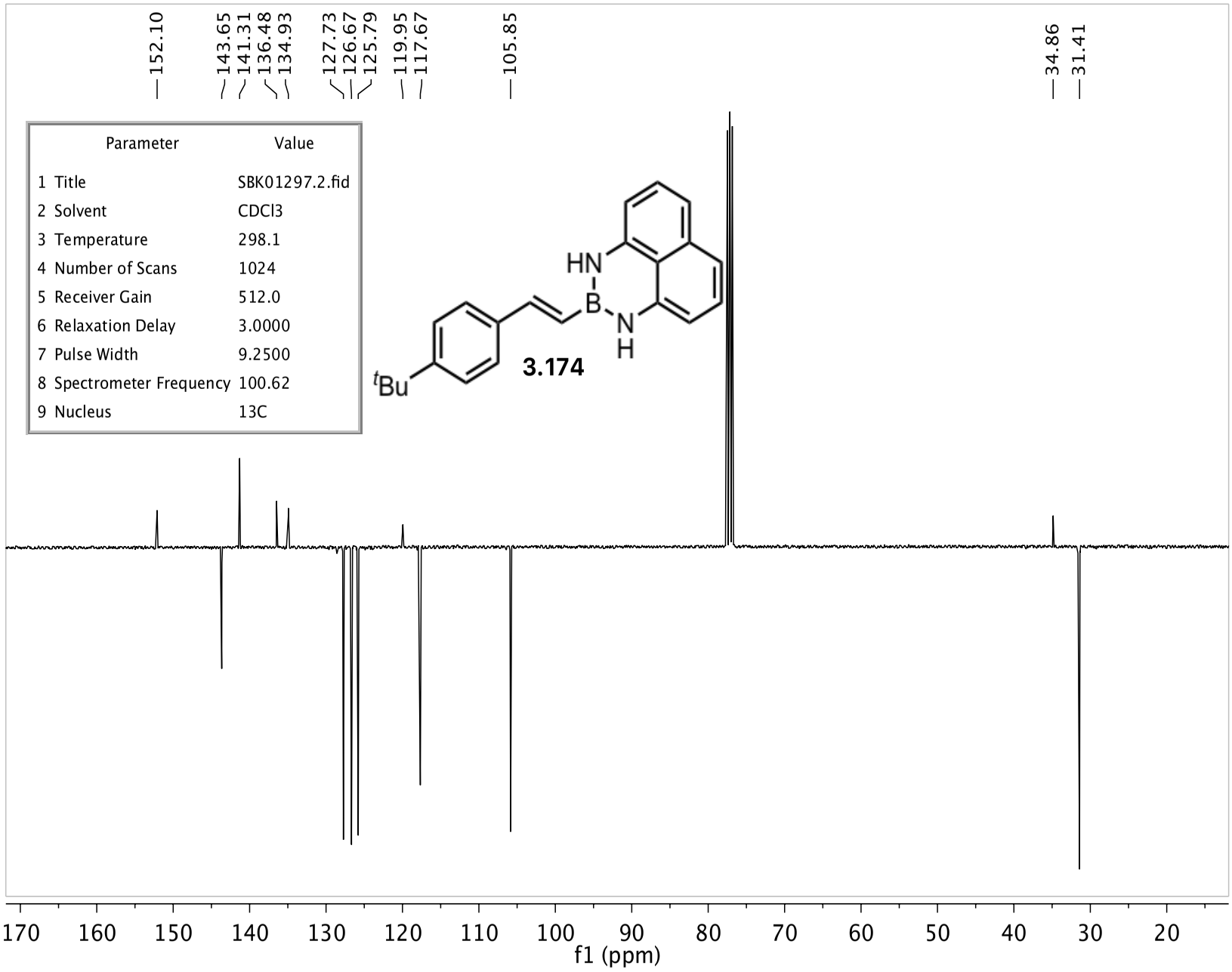
152.10
143.65
141.31
136.48
134.93
127.73
126.67
125.79
119.95
117.67
105.85
34.86
31.41
Parameter Value
1 Title SBK01297.2.fid
2 Solvent CDCl3
3 Temperature 298.1
4 Number of Scans 1024
5 Receiver Gain 512.0
6 Relaxation Delay 3.0000
7 Pulse Width 9.2500
8 Spectrometer Frequency 100.62
9 Nucleus 13C
HN
B
N
H
tBu
3.174
170 160 150 140 130 120 110 100 90 80 70 60 50 40 30 20
f1 (ppm)

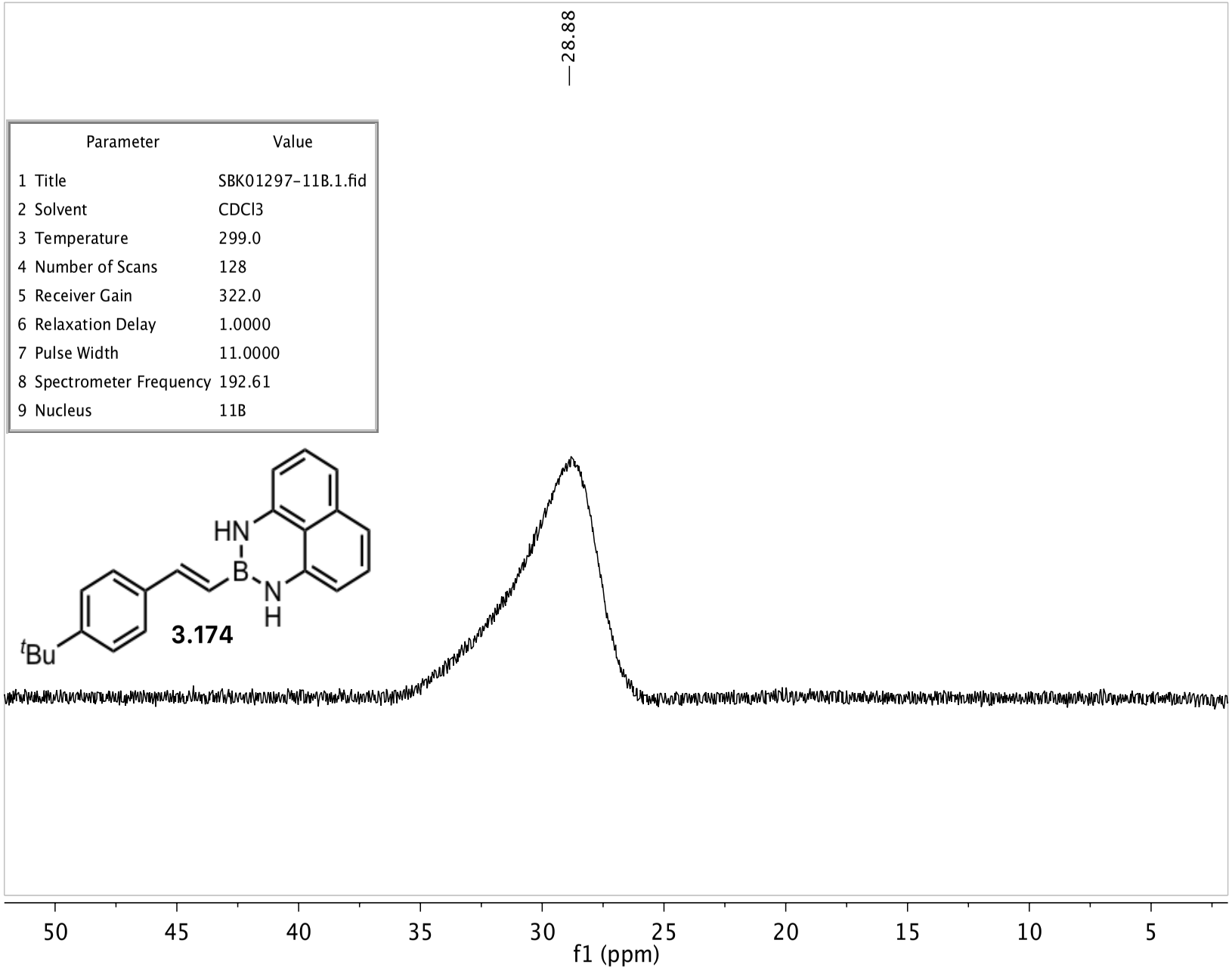
28.88
Parameter
Value
1 Title
SBK01297-11B.1.fid
2 Solvent
CDCl3
3 Temperature
299.0
4 Number of Scans
128
5 Receiver Gain
322.0
6 Relaxation Delay
1.0000
7 Pulse Width
11.0000
8 Spectrometer Frequency
192.61
9 Nucleus
11B
HN
B
N
H
tBu
3.174
50
45
40
35
30
25
20
15
10
5
f1 (ppm)

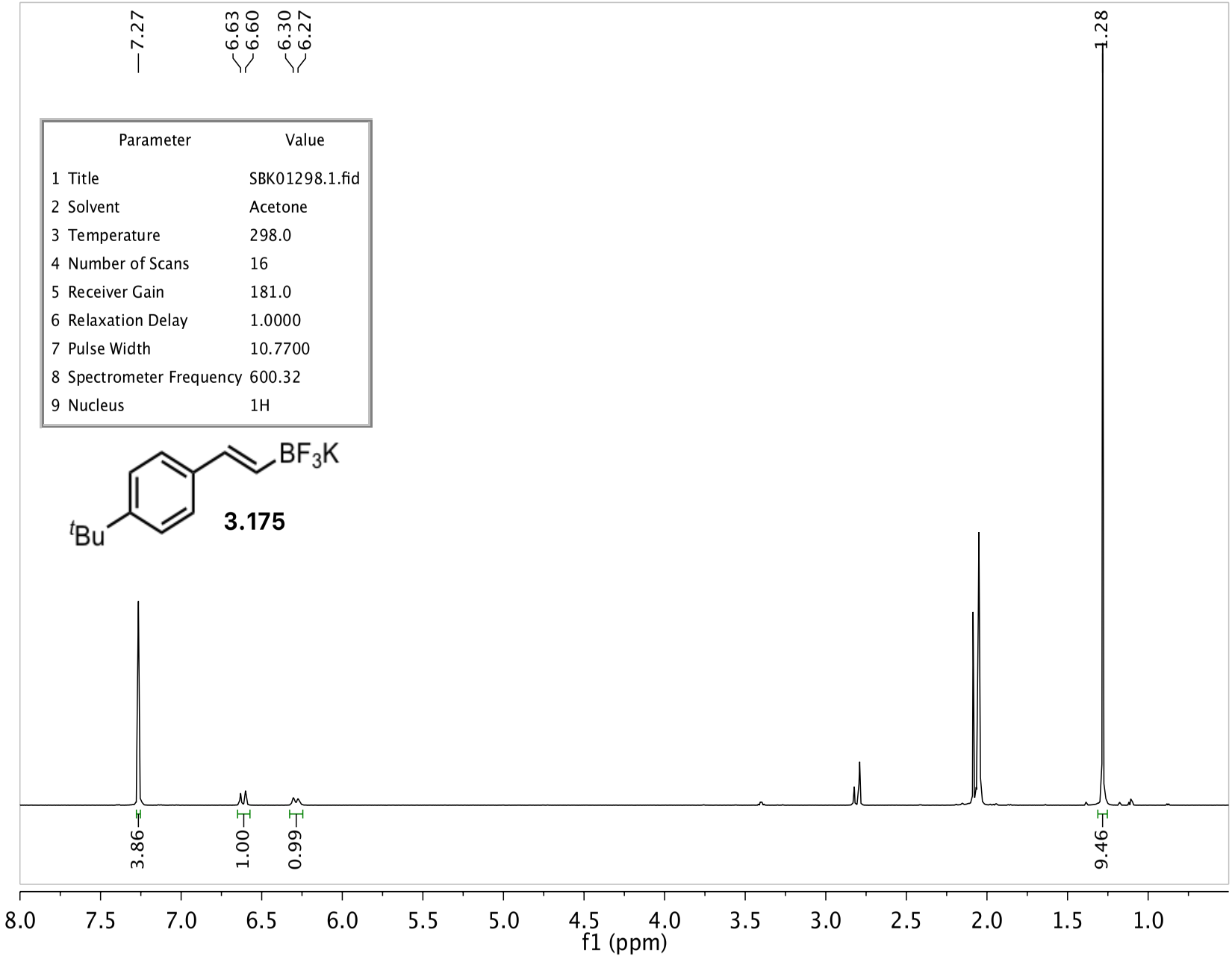
7.27
6.63
6.60
6.30
6.27
1.28
Parameter Value
1 Title SBK01298.1.fid
2 Solvent Acetone
3 Temperature 298.0
4 Number of Scans 16
5 Receiver Gain 181.0
6 Relaxation Delay 1.0000
7 Pulse Width 10.7700
8 Spectrometer Frequency 600.32
9 Nucleus 1H
BF3K
tBu
3.175
3.86
1.00
0.99
9.46
8.0 7.5 7.0 6.5 6.0 5.5 5.0 4.5 4.0 3.5 3.0 2.5 2.0 1.5 1.0
f1 (ppm)

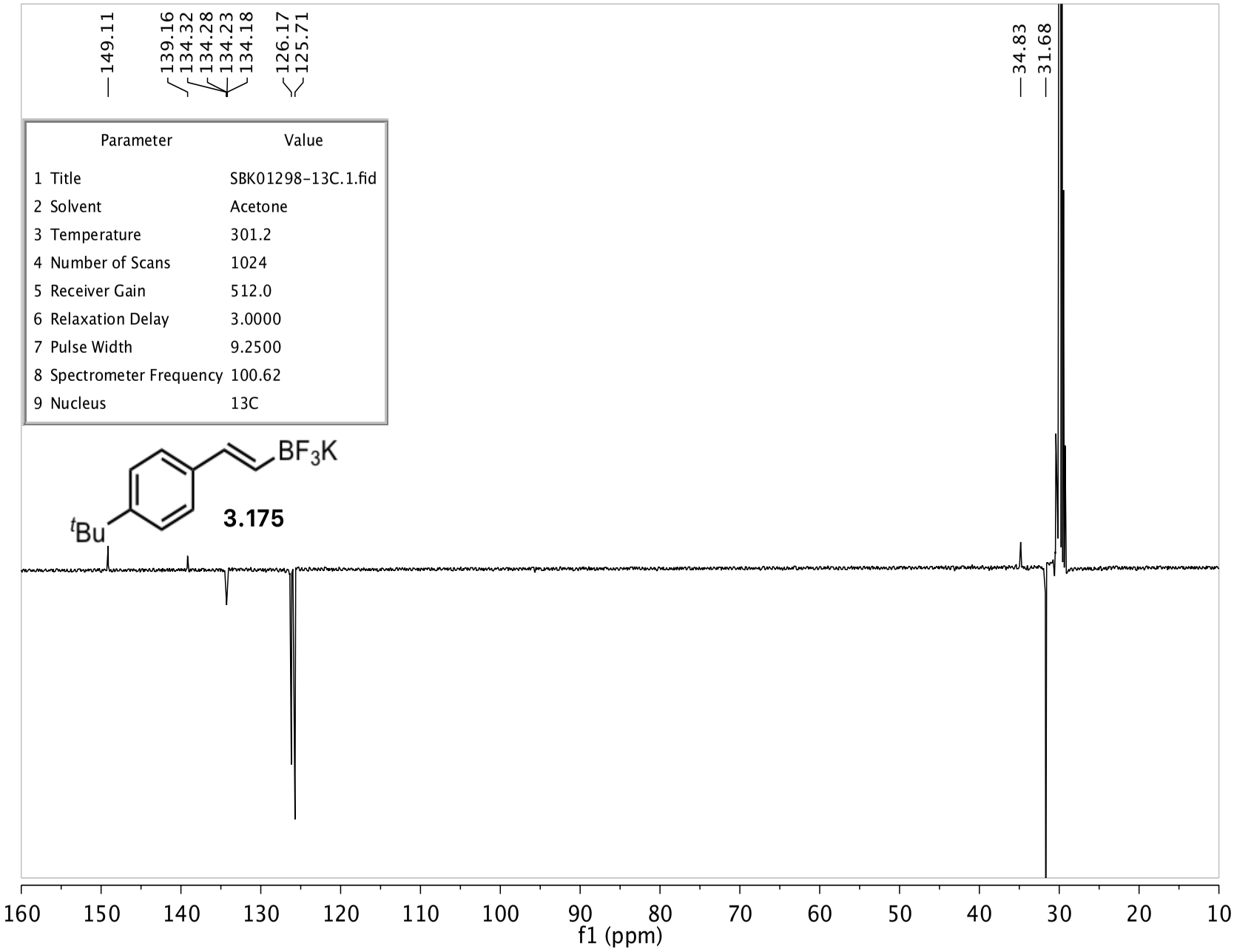
149.11
139.16
134.32
134.28
134.23
134.18
126.17
125.71
34.83
31.68
Parameter Value
1 Title SBK01298-13C.1.fid
2 Solvent Acetone
3 Temperature 301.2
4 Number of Scans 1024
5 Receiver Gain 512.0
6 Relaxation Delay 3.0000
7 Pulse Width 9.2500
8 Spectrometer Frequency 100.62
9 Nucleus 13C
BF3K
tBu
3.175
160 150 140 130 120 110 100 90 80 70 60 50 40 30 20 10
f1 (ppm)

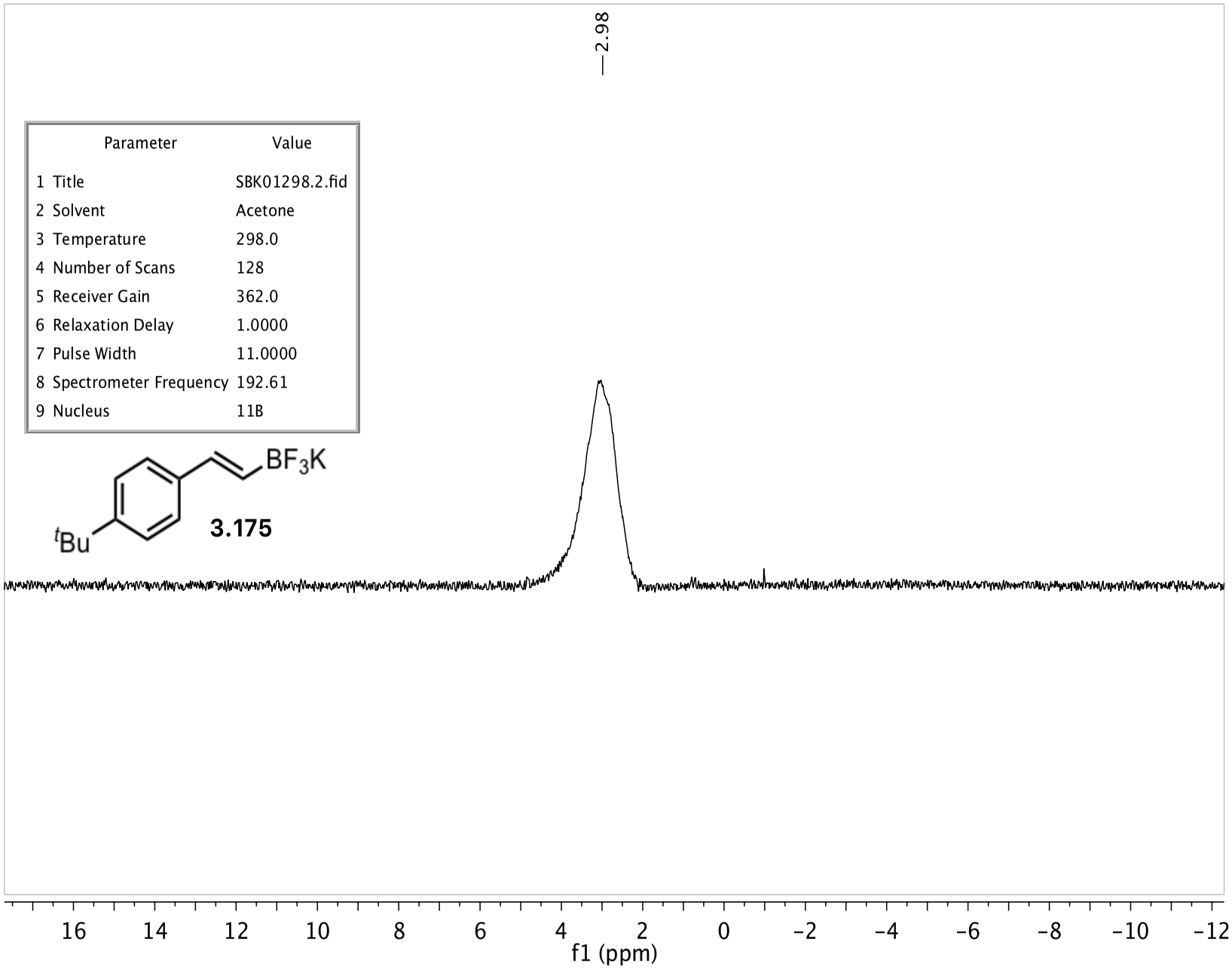
2.98
Parameter Value
1 Title SBK01298.2.fid
2 Solvent Acetone
3 Temperature 298.0
4 Number of Scans 128
5 Receiver Gain 362.0
6 Relaxation Delay 1.0000
7 Pulse Width 11.0000
8 Spectrometer Frequency 192.61
9 Nucleus 11B
BF3K
tBu
3.175
16 14 12 10 8 6 4 2 0 -2 -4 -6 -8 -10 -12
f1 (ppm)

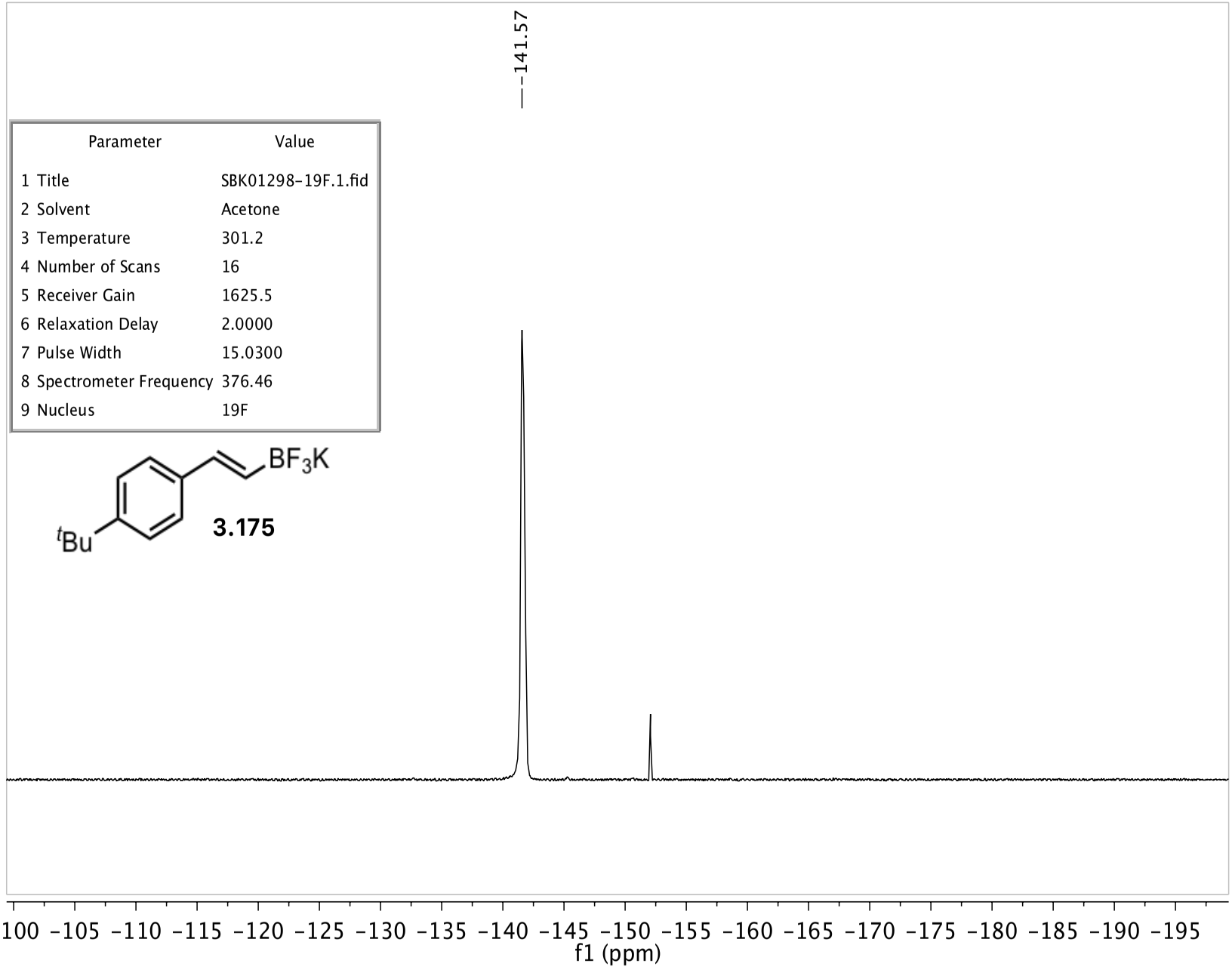
141.57
Parameter Value
1 Title SBK01298-19F.1.fid
2 Solvent Acetone
3 Temperature 301.2
4 Number of Scans 16
5 Receiver Gain 1625.5
6 Relaxation Delay 2.0000
7 Pulse Width 15.0300
8 Spectrometer Frequency 376.46
9 Nucleus 19F
BF3K
tBu
3.175
-100 -105 -110 -115 -120 -125 -130 -135 -140 -145 -150 -155 -160 -165 -170 -175 -180 -185 -190 -195
f1 (ppm)

Appendix E

Spectral Data for Chapter 4

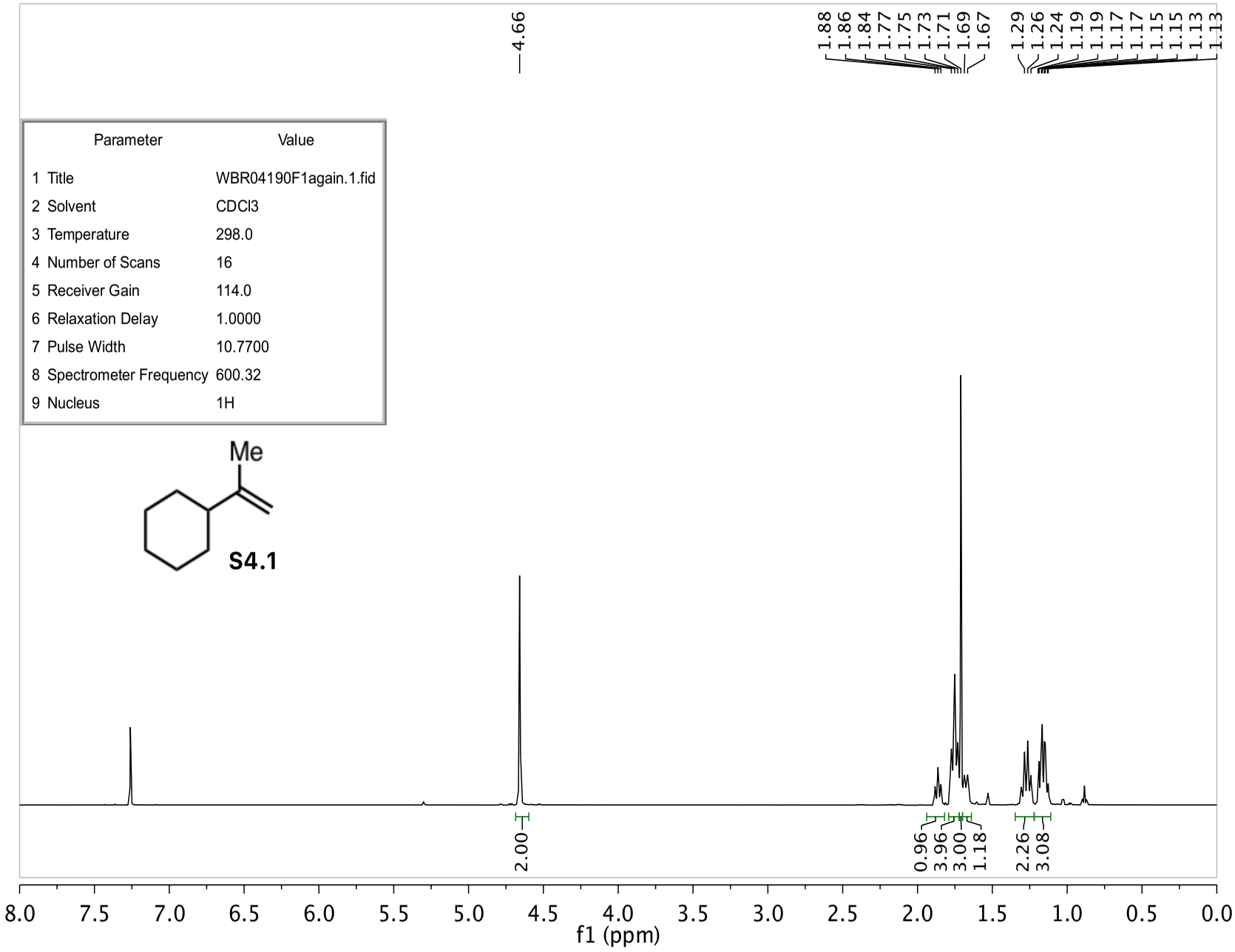
4.66
1.88
1.86
1.84
1.77
1.75
1.73
1.71
1.69
1.67
1.29
1.26
1.24
1.19
1.19
1.17
1.17
1.15
1.15
1.13
1.13
Parameter Value
1 Title WBR04190F1again.1.fid
2 Solvent CDCl3
3 Temperature 298.0
4 Number of Scans 16
5 Receiver Gain 114.0
6 Relaxation Delay 1.0000
7 Pulse Width 10.7700
8 Spectrometer Frequency 600.32
9 Nucleus 1H
Me
S4.1
2.00
0.96
3.96
3.00
1.18
2.26
3.08
8.0
7.5
7.0
6.5
6.0
5.5
5.0
4.5
4.0
3.5
3.0
2.5
2.0
1.5
1.0
0.5
0.0
f1 (ppm)

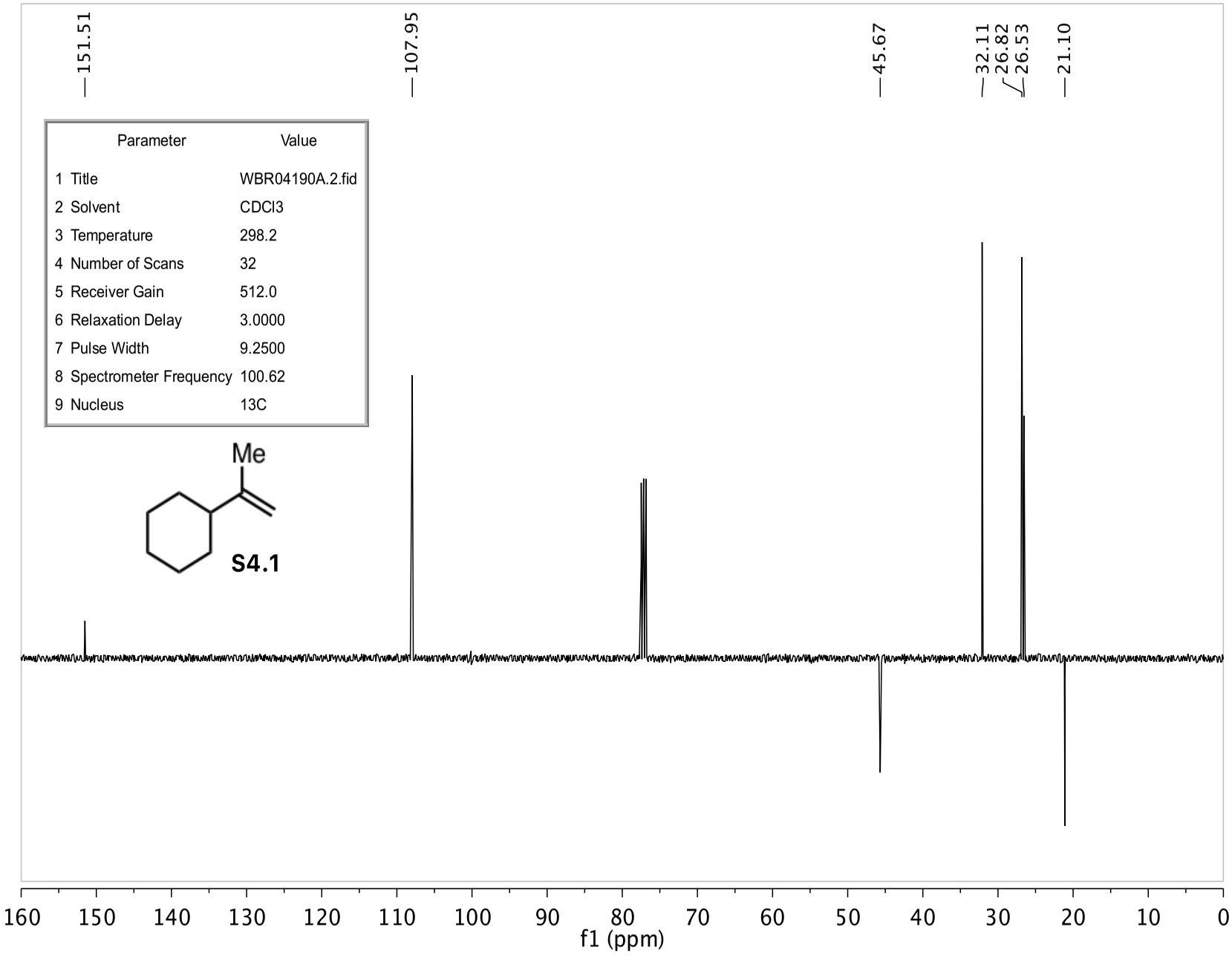
151.51
107.95
45.67
32.11
26.82
26.53
21.10
Parameter Value
1 Title WBR04190A.2.fid
2 Solvent CDCl3
3 Temperature 298.2
4 Number of Scans 32
5 Receiver Gain 512.0
6 Relaxation Delay 3.0000
7 Pulse Width 9.2500
8 Spectrometer Frequency 100.62
9 Nucleus 13C
Me
S4.1
160 150 140 130 120 110 100 90 80 70 60 50 40 30 20 10 0
f1 (ppm)

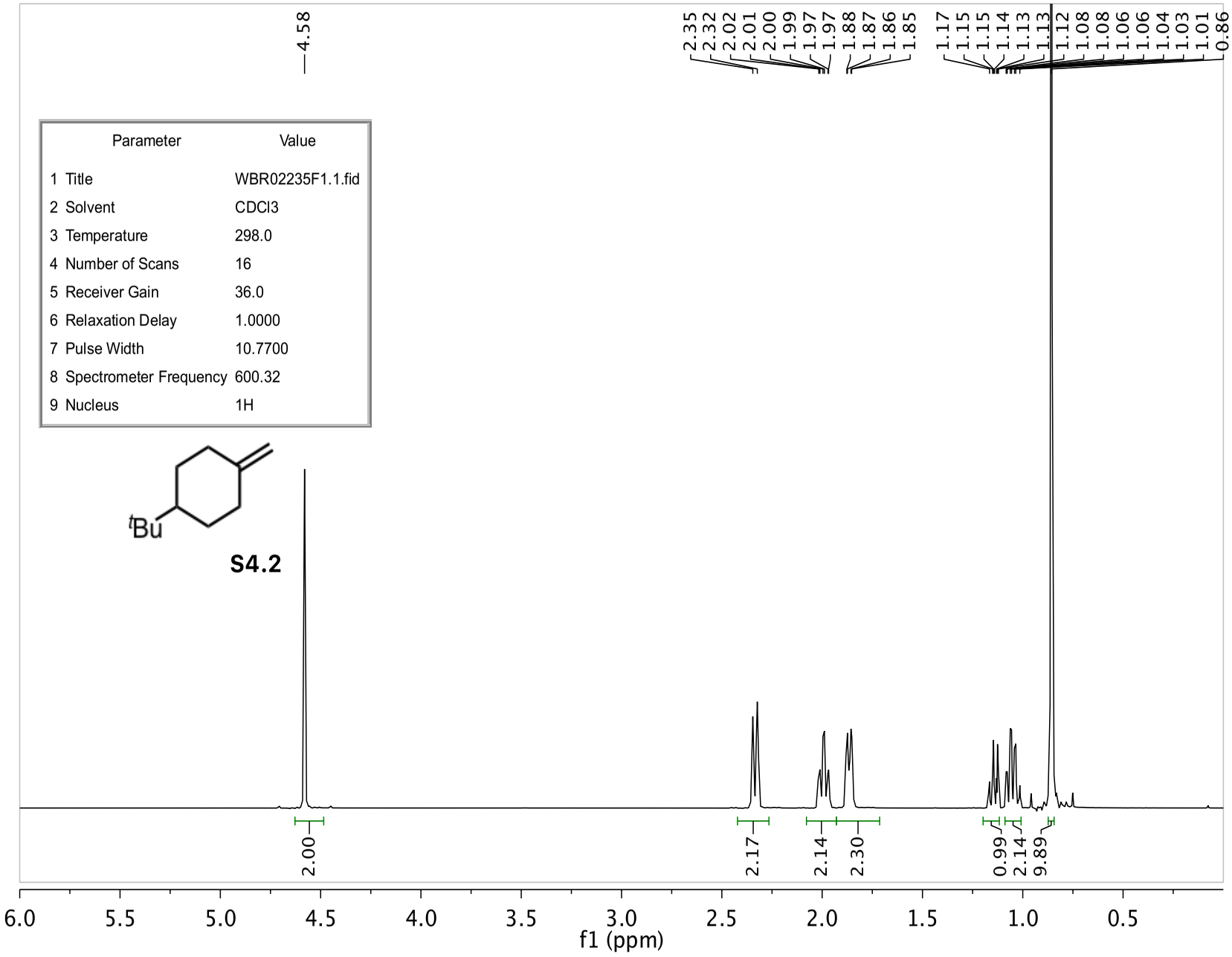
4.58
2.35
2.32
2.02
2.01
2.00
1.99
1.97
1.97
1.88
1.87
1.86
1.85
1.17
1.15
1.15
1.14
1.13
1.13
1.12
1.08
1.08
1.06
1.06
1.04
1.03
1.01
0.86
Parameter Value
1 Title WBR02235F1.1.fid
2 Solvent CDCl3
3 Temperature 298.0
4 Number of Scans 16
5 Receiver Gain 36.0
6 Relaxation Delay 1.0000
7 Pulse Width 10.7700
8 Spectrometer Frequency 600.32
9 Nucleus 1H
tBu
S4.2
2.00
2.17
2.14
2.30
0.99
2.14
9.89
6.0
5.5
5.0
4.5
4.0
3.5
3.0
2.5
2.0
1.5
1.0
0.5
f1 (ppm)

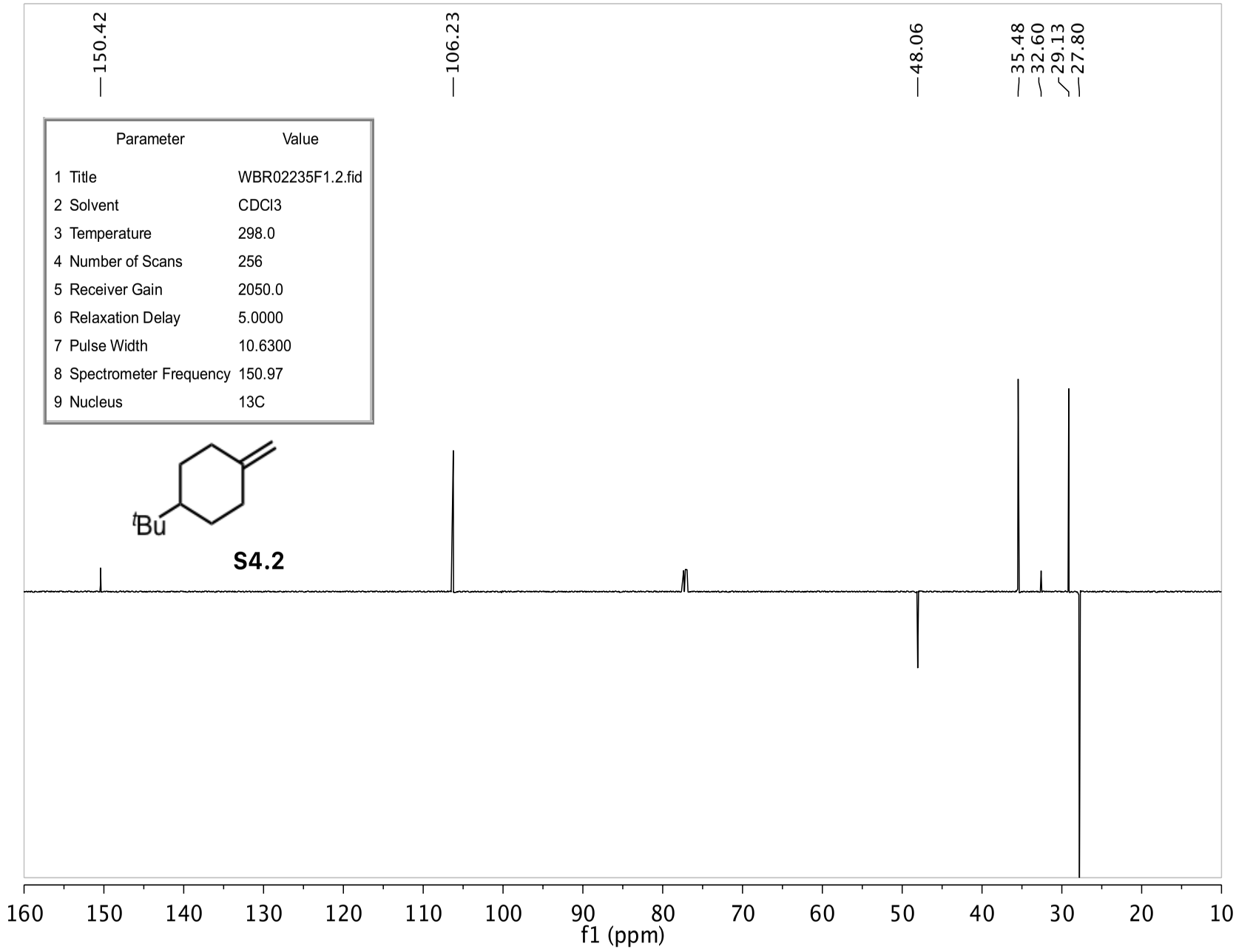
150.42
106.23
48.06
35.48
32.60
29.13
27.80
Parameter Value
1 Title WBR02235F1.2.fid
2 Solvent CDCl3
3 Temperature 298.0
4 Number of Scans 256
5 Receiver Gain 2050.0
6 Relaxation Delay 5.0000
7 Pulse Width 10.6300
8 Spectrometer Frequency 150.97
9 Nucleus 13C
tBu
S4.2
160 150 140 130 120 110 100 90 80 70 60 50 40 30 20 10
f1 (ppm)

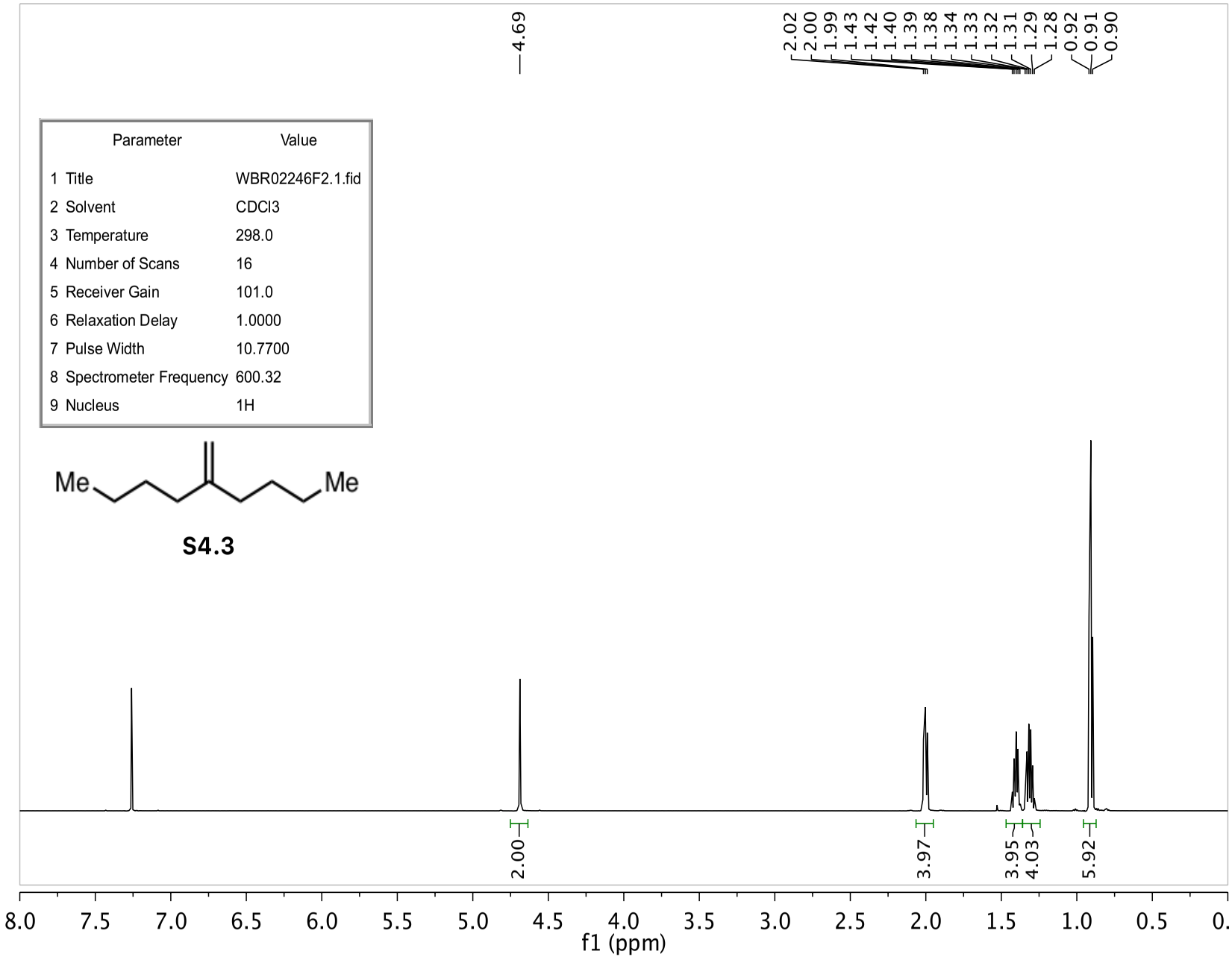
4.69
2.02
2.00
1.99
1.43
1.42
1.40
1.39
1.38
1.34
1.33
1.32
1.31
1.29
1.28
0.92
0.91
0.90
Parameter Value
1 Title WBR02246F2.1.fid
2 Solvent CDCl3
3 Temperature 298.0
4 Number of Scans 16
5 Receiver Gain 101.0
6 Relaxation Delay 1.0000
7 Pulse Width 10.7700
8 Spectrometer Frequency 600.32
9 Nucleus 1H
Me
Me
S4.3
2.00
3.97
3.95
4.03
5.92
8.0
7.5
7.0
6.5
6.0
5.5
5.0
4.5
4.0
3.5
3.0
2.5
2.0
1.5
1.0
0.5
0.0
f1 (ppm)

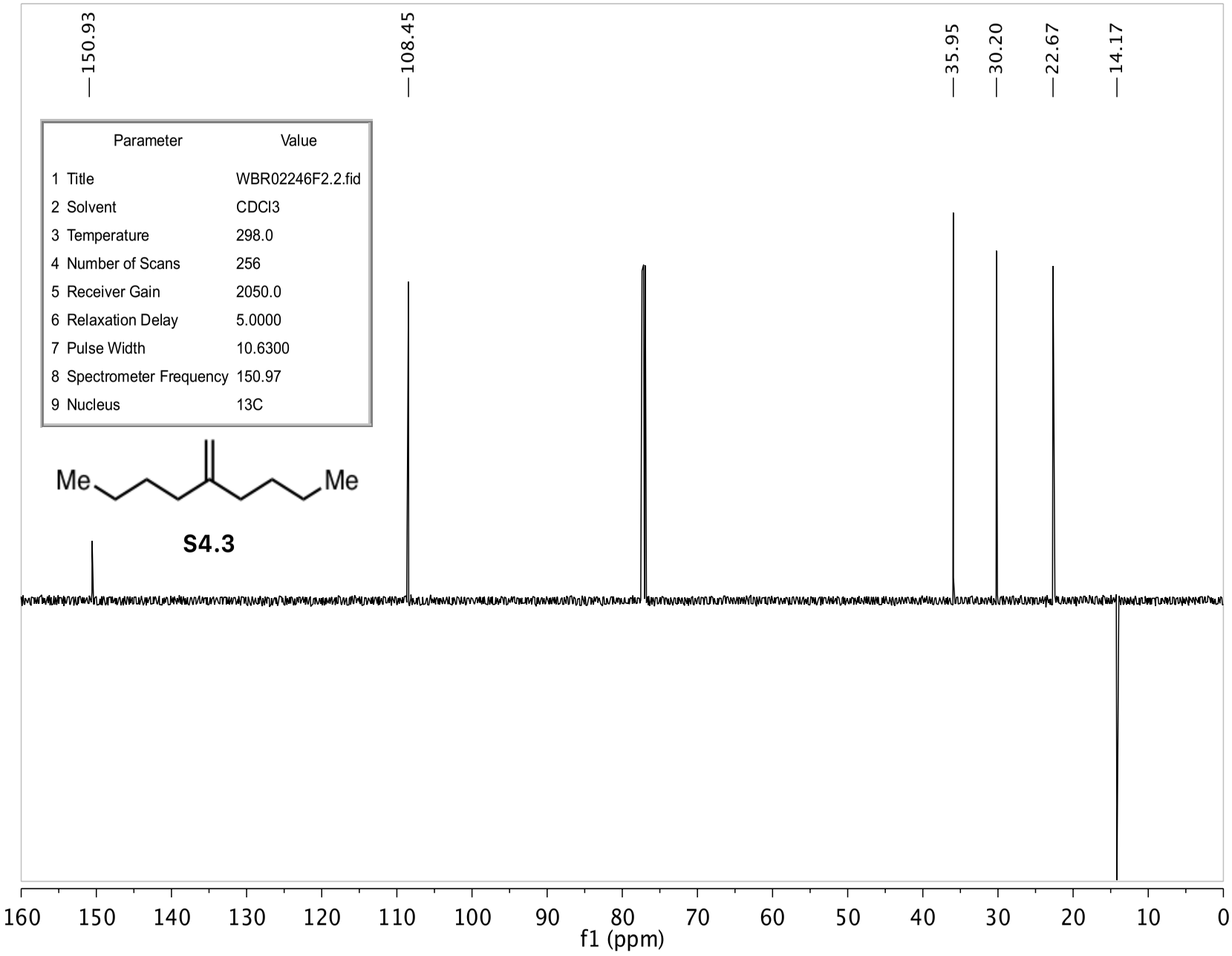
150.93
108.45
35.95
30.20
22.67
14.17
Parameter Value
1 Title WBR02246F2.2.fid
2 Solvent CDCl3
3 Temperature 298.0
4 Number of Scans 256
5 Receiver Gain 2050.0
6 Relaxation Delay 5.0000
7 Pulse Width 10.6300
8 Spectrometer Frequency 150.97
9 Nucleus 13C
Me
Me
S4.3
160 150 140 130 120 110 100 90 80 70 60 50 40 30 20 10 0
f1 (ppm)

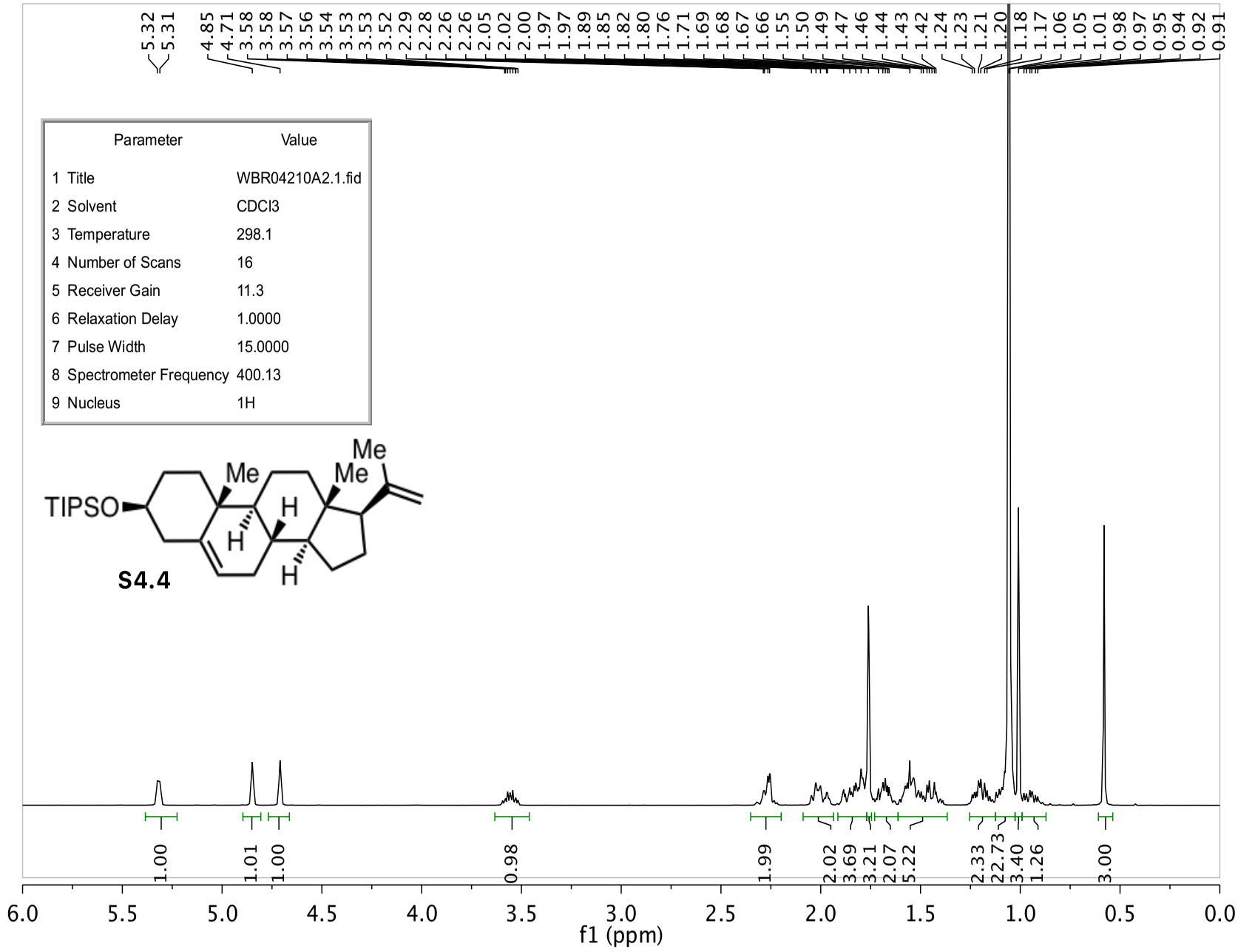
5.32 5.31 4.85 4.71 3.58 3.58 3.57 3.56 3.54 3.53 3.53 3.52 2.29 2.28 2.26 2.26 2.05 2.02 2.00 1.97 1.97 1.89 1.85 1.82 1.80 1.76 1.71 1.69 1.68 1.67 1.66 1.55 1.50 1.49 1.47 1.46 1.44 1.43 1.42 1.24 1.23 1.21 1.20 1.18 1.17 1.06 1.05 1.01 0.98 0.97 0.95 0.94 0.92 0.91
Parameter Value
1 Title WBR04210A2.1.fid
2 Solvent CDCl3
3 Temperature 298.1
4 Number of Scans 16
5 Receiver Gain 11.3
6 Relaxation Delay 1.0000
7 Pulse Width 15.0000
8 Spectrometer Frequency 400.13
9 Nucleus 1H
TIPSO
Me
Me
Me
H
H
H
S4.4
1.00 1.01 1.00 0.98 1.99 2.02 3.69 3.21 2.07 5.22 2.33 22.73 3.40 1.26 3.00
6.0 5.5 5.0 4.5 4.0 3.5 3.0 2.5 2.0 1.5 1.0 0.5 0.0
f1 (ppm)

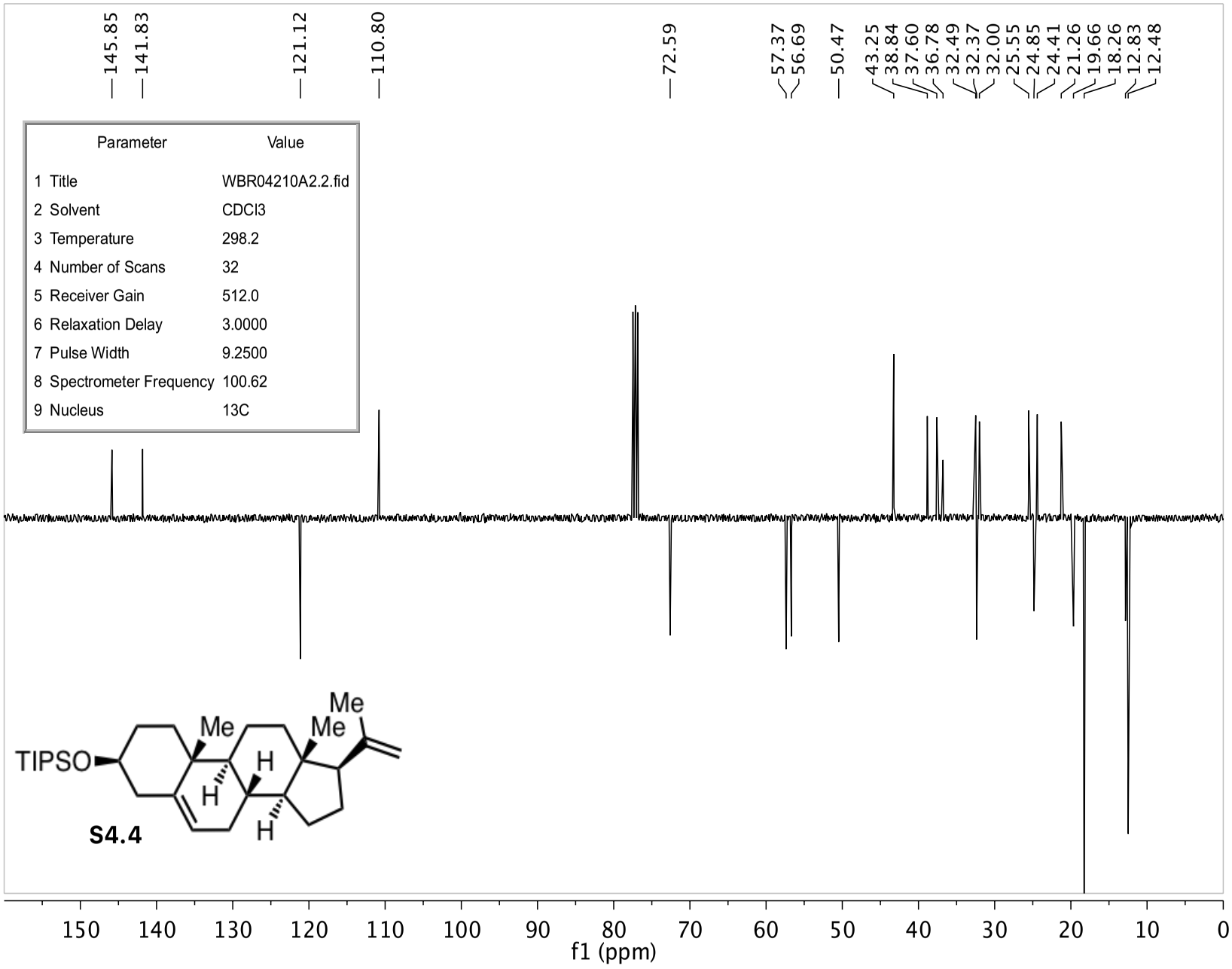
145.85
141.83
121.12
110.80
72.59
57.37
56.69
50.47
43.25
38.84
37.60
36.78
32.49
32.37
32.00
25.55
24.85
24.41
21.26
19.66
18.26
12.83
12.48
Parameter Value
1 Title WBR04210A2.2.fid
2 Solvent CDCl3
3 Temperature 298.2
4 Number of Scans 32
5 Receiver Gain 512.0
6 Relaxation Delay 3.0000
7 Pulse Width 9.2500
8 Spectrometer Frequency 100.62
9 Nucleus 13C
TIPSO
Me
Me
Me
H
H
H
S4.4
150 140 130 120 110 100 90 80 70 60 50 40 30 20 10 0
f1 (ppm)

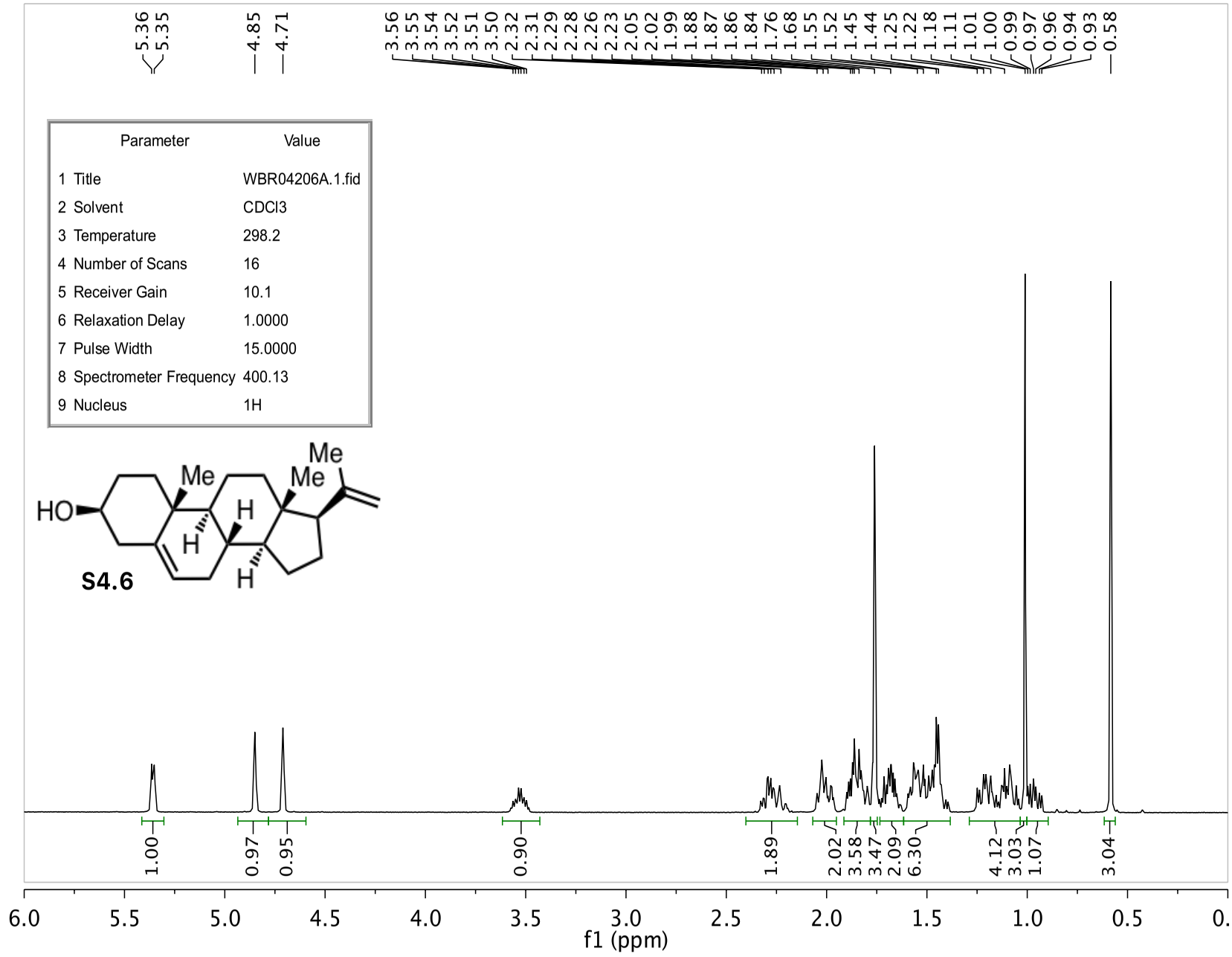
5.36
5.35
4.85
4.71
3.56
3.55
3.54
3.52
3.51
3.50
2.32
2.31
2.29
2.28
2.26
2.23
2.05
2.02
1.99
1.88
1.87
1.86
1.84
1.76
1.68
1.55
1.52
1.45
1.44
1.25
1.22
1.18
1.11
1.01
1.00
0.99
0.97
0.96
0.94
0.93
0.58
Parameter Value
1 Title WBR04206A.1.fid
2 Solvent CDCl3
3 Temperature 298.2
4 Number of Scans 16
5 Receiver Gain 10.1
6 Relaxation Delay 1.0000
7 Pulse Width 15.0000
8 Spectrometer Frequency 400.13
9 Nucleus 1H
HO
Me
Me
Me
H
H
H
S4.6
1.00
0.97
0.95
0.90
1.89
2.02
3.58
3.47
2.09
6.30
4.12
3.03
1.07
3.04
6.0
5.5
5.0
4.5
4.0
3.5
3.0
2.5
2.0
1.5
1.0
0.5
0.0
f1 (ppm)

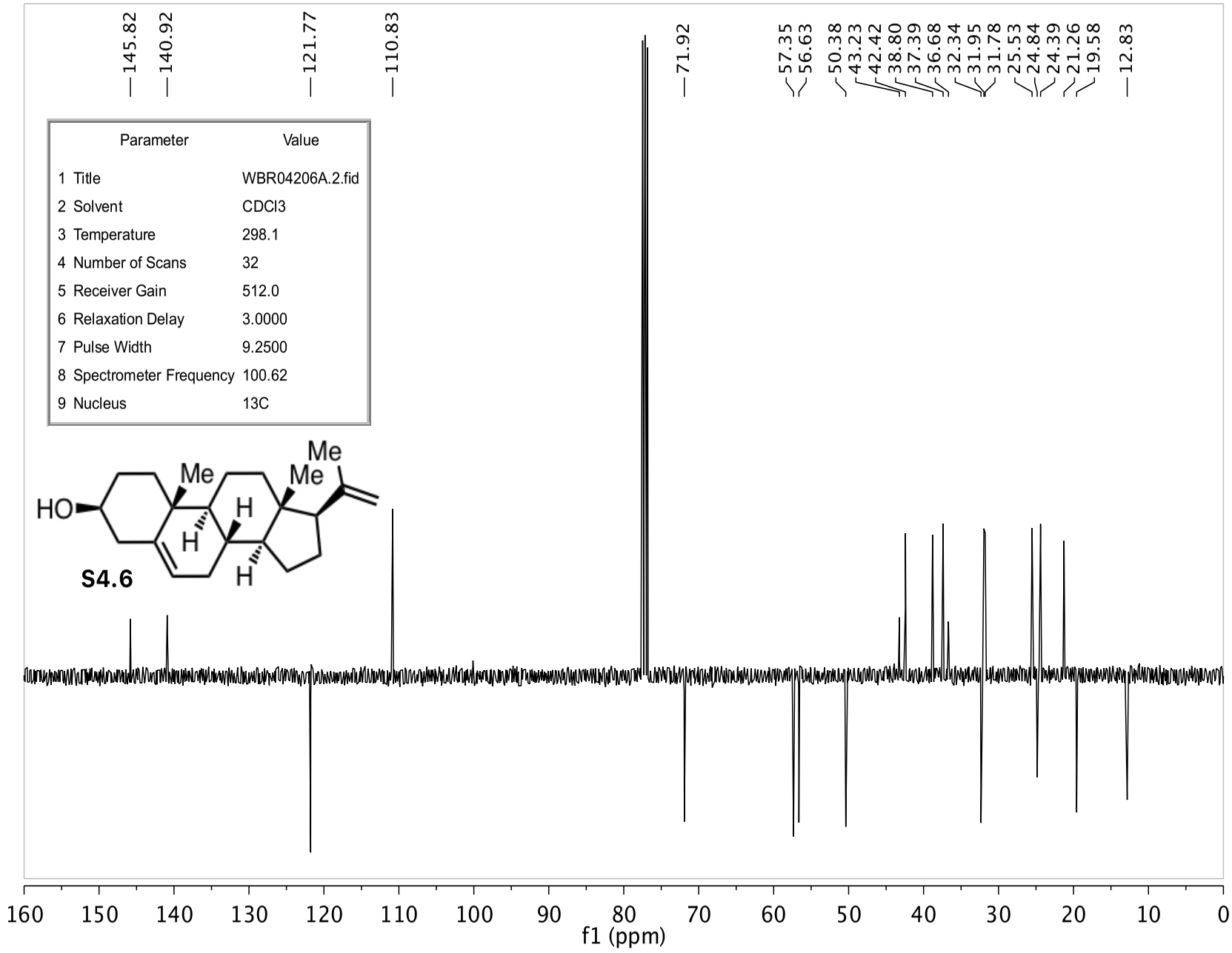
145.82
140.92
121.77
110.83
71.92
57.35
56.63
50.38
43.23
42.42
38.80
37.39
36.68
32.34
31.95
31.78
25.53
24.84
24.39
21.26
19.58
12.83
Parameter Value
1 Title WBR04206A.2.fid
2 Solvent CDCl3
3 Temperature 298.1
4 Number of Scans 32
5 Receiver Gain 512.0
6 Relaxation Delay 3.0000
7 Pulse Width 9.2500
8 Spectrometer Frequency 100.62
9 Nucleus 13C
HO
Me
Me
Me
H
H
H
S4.6
160 150 140 130 120 110 100 90 80 70 60 50 40 30 20 10 0
f1 (ppm)

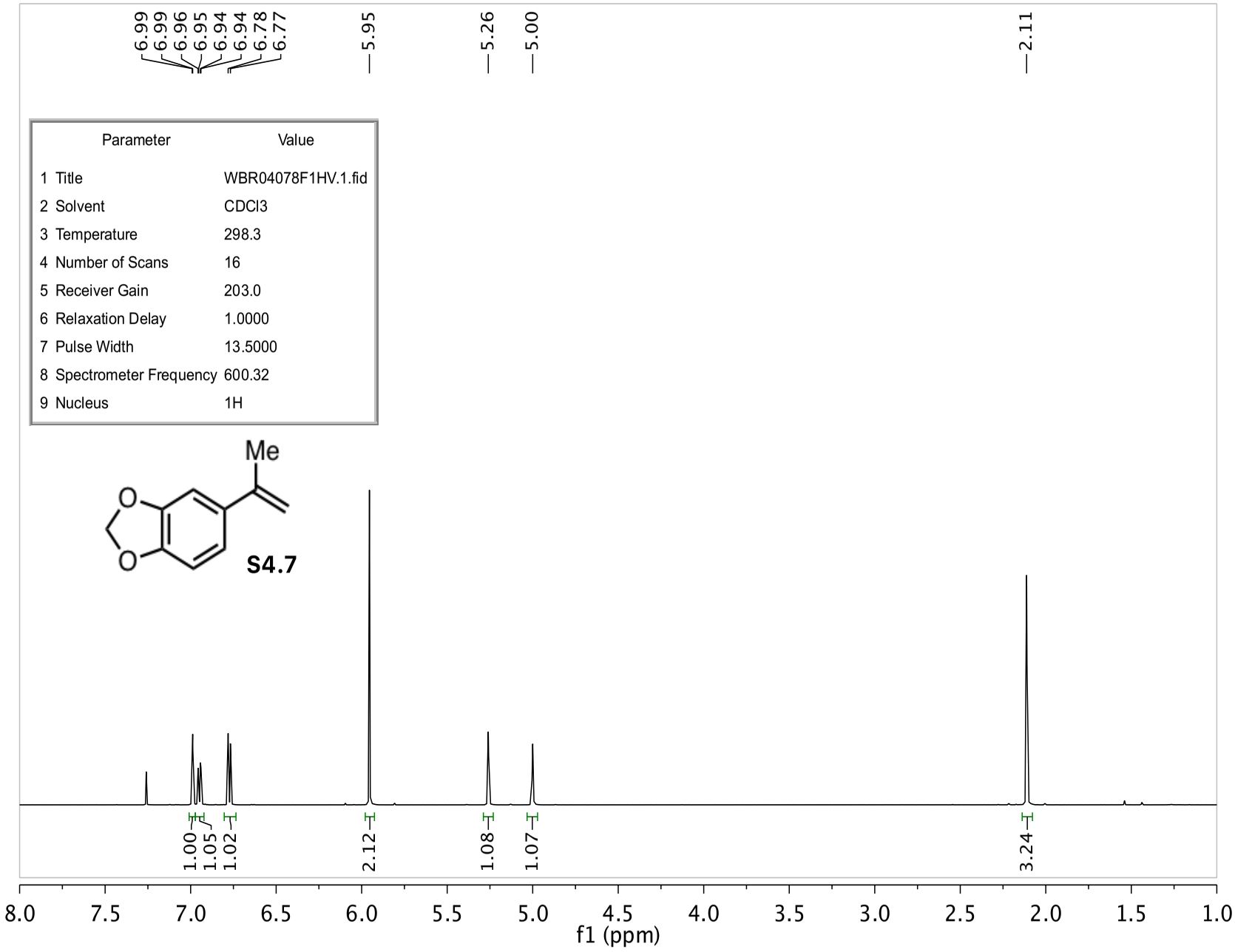
6.99
6.99
6.96
6.95
6.94
6.94
6.78
6.77
5.95
5.26
5.00
2.11
Parameter Value
1 Title WBR04078F1HV.1.fid
2 Solvent CDCl3
3 Temperature 298.3
4 Number of Scans 16
5 Receiver Gain 203.0
6 Relaxation Delay 1.0000
7 Pulse Width 13.5000
8 Spectrometer Frequency 600.32
9 Nucleus 1H
Me
O
O
S4.7
1.00
1.05
1.02
2.12
1.08
1.07
3.24
8.0
7.5
7.0
6.5
6.0
5.5
5.0
4.5
4.0
3.5
3.0
2.5
2.0
1.5
1.0
f1 (ppm)

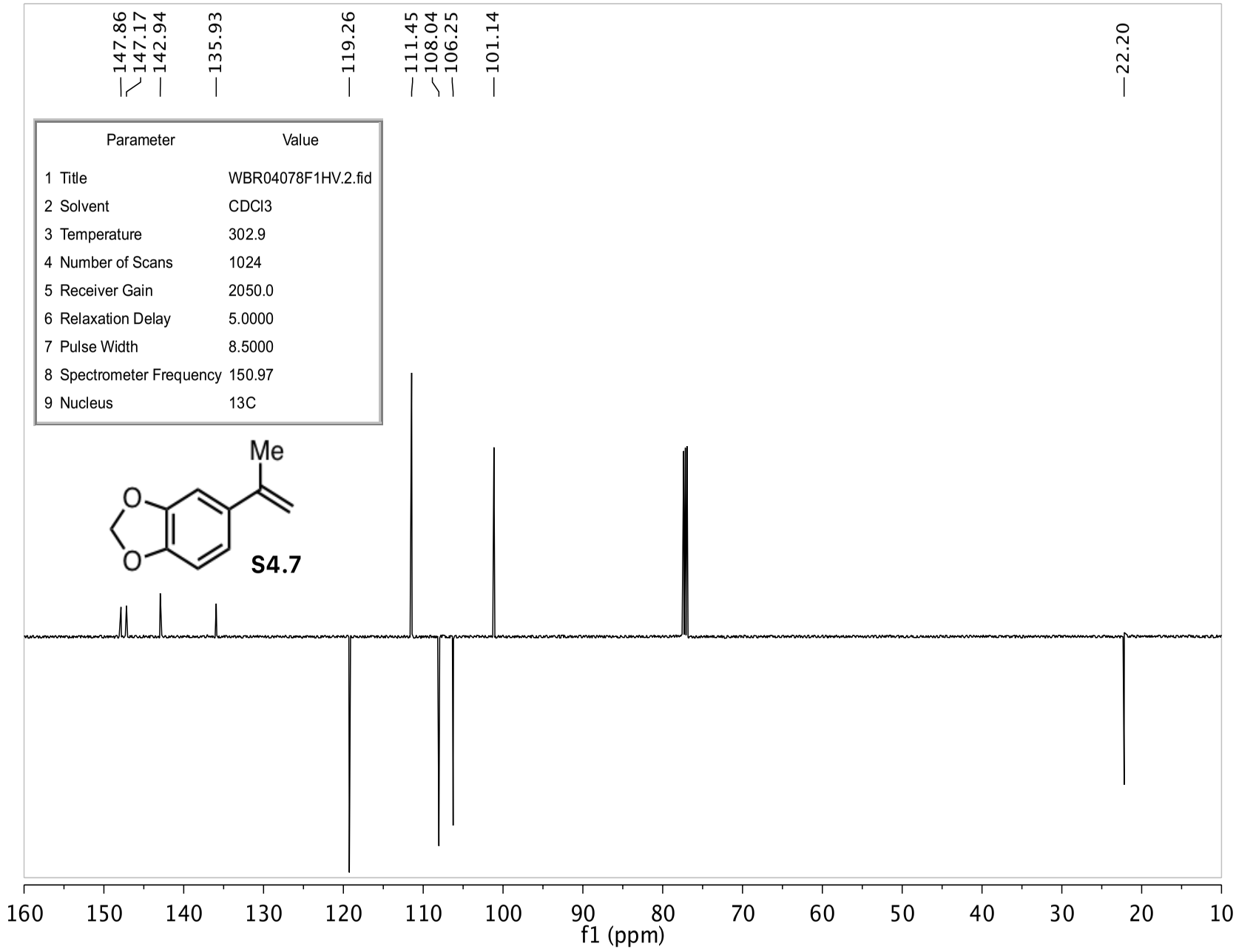
147.86
147.17
142.94
135.93
119.26
111.45
108.04
106.25
101.14
22.20
Parameter Value
1 Title WBR04078F1HV.2.fid
2 Solvent CDCl3
3 Temperature 302.9
4 Number of Scans 1024
5 Receiver Gain 2050.0
6 Relaxation Delay 5.0000
7 Pulse Width 8.5000
8 Spectrometer Frequency 150.97
9 Nucleus 13C
Me
O
O
S4.7
160 150 140 130 120 110 100 90 80 70 60 50 40 30 20 10
f1 (ppm)

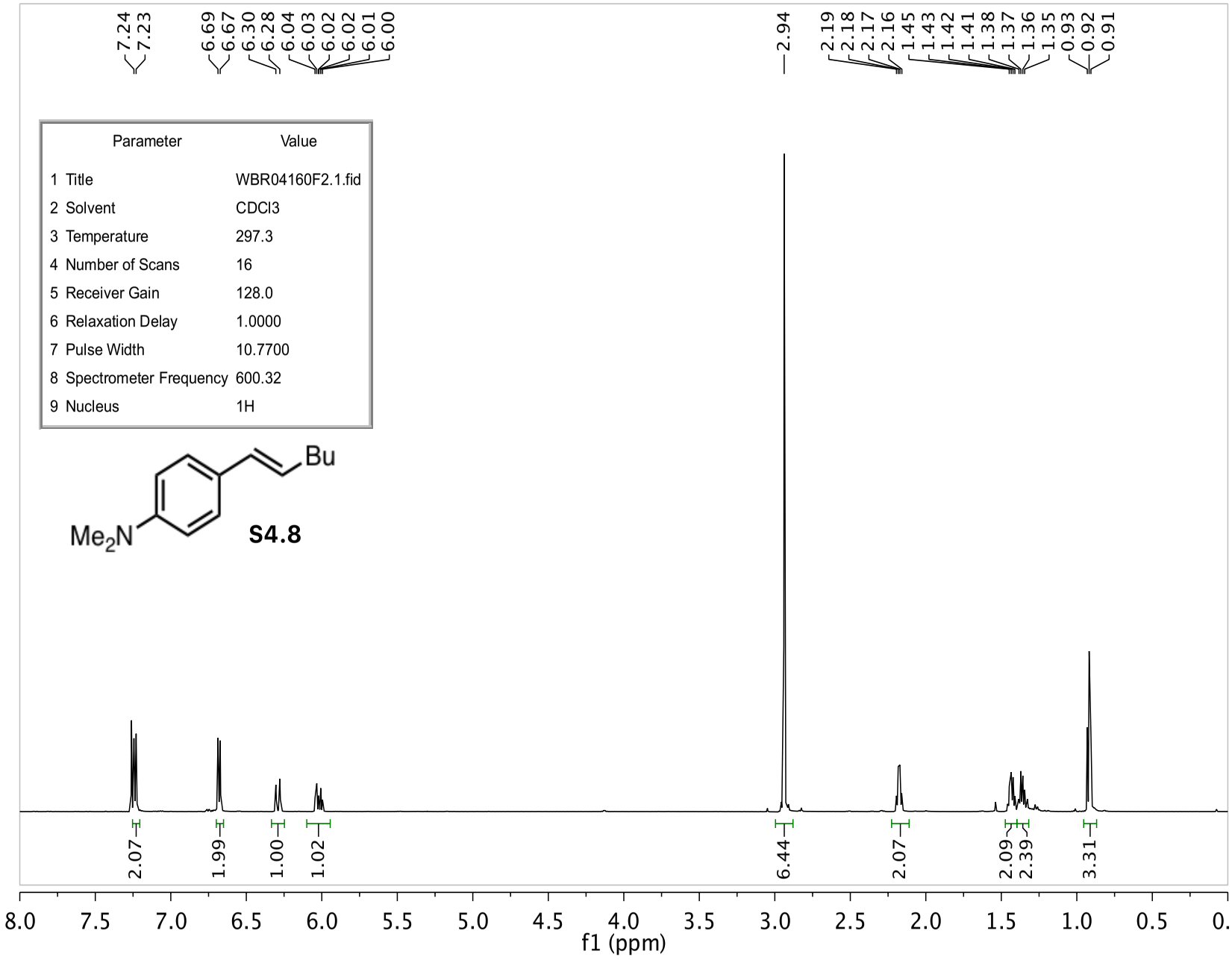
7.24
7.23
6.69
6.67
6.30
6.28
6.04
6.03
6.02
6.02
6.01
6.00
2.94
2.19
2.18
2.17
2.16
1.45
1.43
1.42
1.41
1.38
1.37
1.36
1.35
0.93
0.92
0.91
Parameter Value
1 Title WBR04160F2.1.fid
2 Solvent CDCl3
3 Temperature 297.3
4 Number of Scans 16
5 Receiver Gain 128.0
6 Relaxation Delay 1.0000
7 Pulse Width 10.7700
8 Spectrometer Frequency 600.32
9 Nucleus 1H
Bu
Me2N
S4.8
2.07
1.99
1.00
1.02
6.44
2.07
2.09
2.39
3.31
8.0
7.5
7.0
6.5
6.0
5.5
5.0
4.5
4.0
3.5
3.0
2.5
2.0
1.5
1.0
0.5
0.0
f1 (ppm)

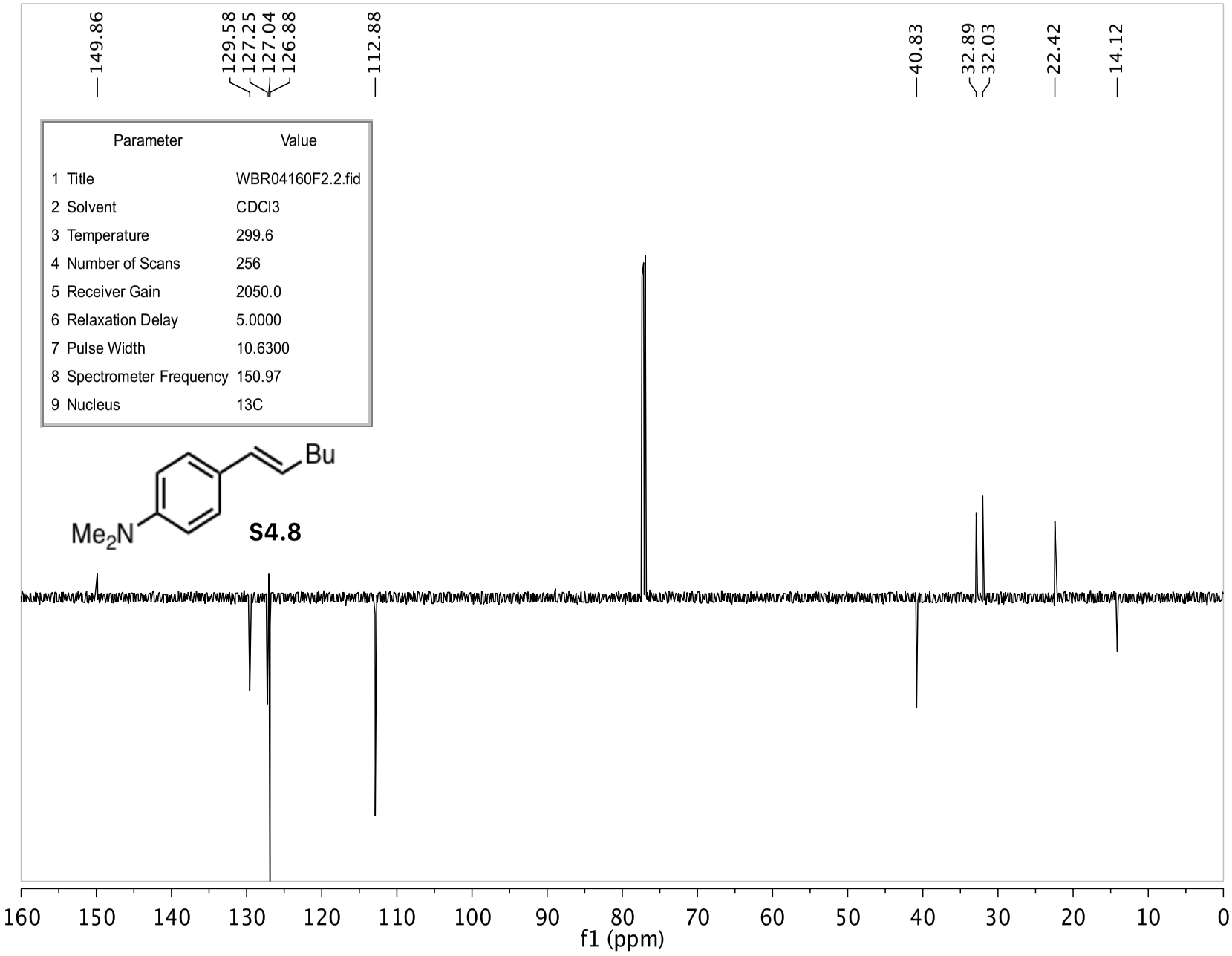
149.86
129.58
127.25
127.04
126.88
112.88
40.83
32.89
32.03
22.42
14.12
Parameter Value
1 Title WBR04160F2.2.fid
2 Solvent CDCl3
3 Temperature 299.6
4 Number of Scans 256
5 Receiver Gain 2050.0
6 Relaxation Delay 5.0000
7 Pulse Width 10.6300
8 Spectrometer Frequency 150.97
9 Nucleus 13C
Bu
Me2N
S4.8
160 150 140 130 120 110 100 90 80 70 60 50 40 30 20 10 0
f1 (ppm)

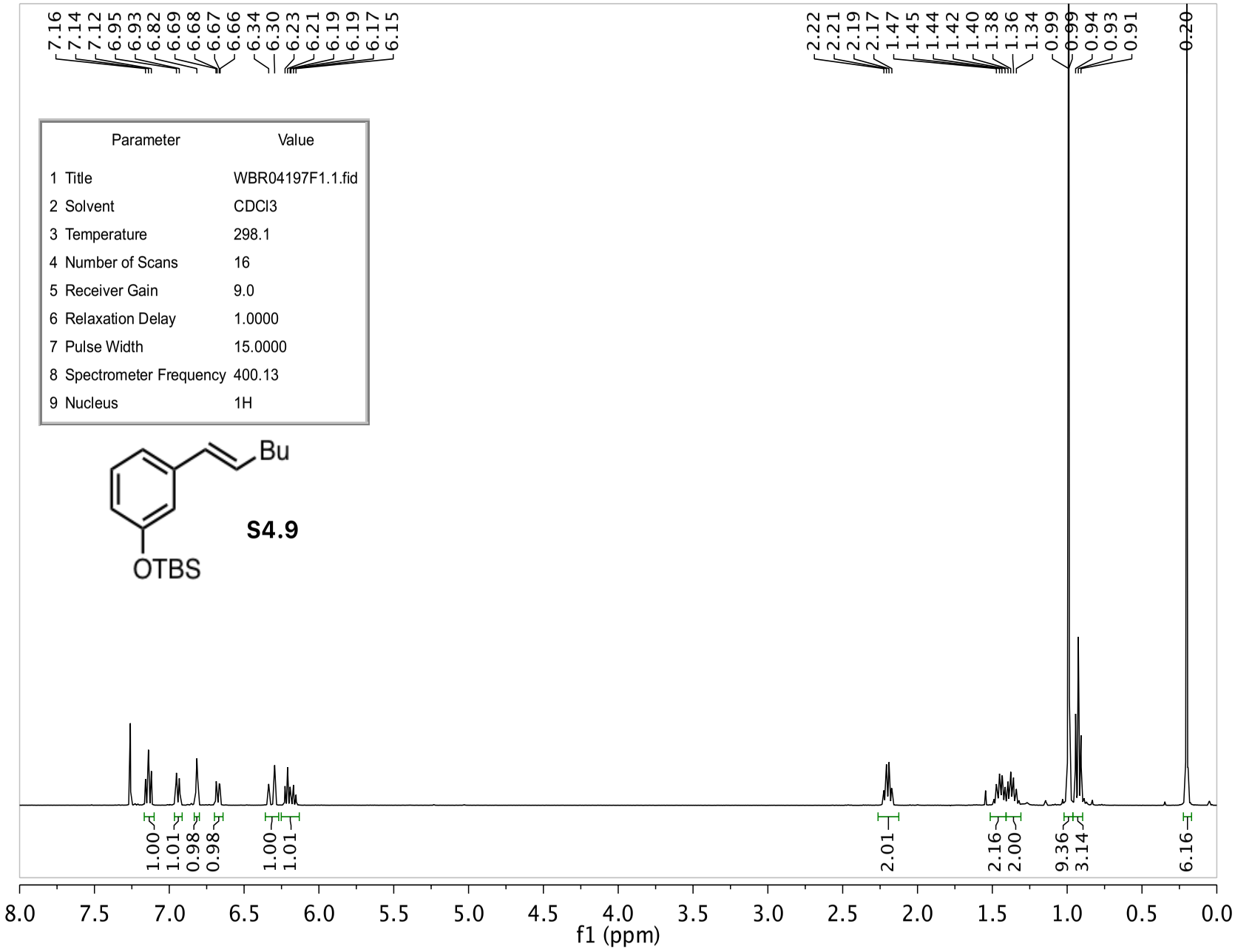
7.16
7.14
7.12
6.95
6.93
6.82
6.69
6.68
6.67
6.66
6.34
6.30
6.23
6.21
6.19
6.19
6.17
6.15
2.22
2.21
2.19
2.17
1.47
1.45
1.44
1.42
1.40
1.38
1.36
1.34
0.99
0.99
0.94
0.93
0.91
0.20
Parameter Value
1 Title WBR04197F1.1.fid
2 Solvent CDCl3
3 Temperature 298.1
4 Number of Scans 16
5 Receiver Gain 9.0
6 Relaxation Delay 1.0000
7 Pulse Width 15.0000
8 Spectrometer Frequency 400.13
9 Nucleus 1H
Bu
OTBS
S4.9
1.00
1.01
0.98
0.98
1.00
1.01
2.01
2.16
2.00
9.36
3.14
6.16
8.0
7.5
7.0
6.5
6.0
5.5
5.0
4.5
4.0
3.5
3.0
2.5
2.0
1.5
1.0
0.5
0.0
f1 (ppm)

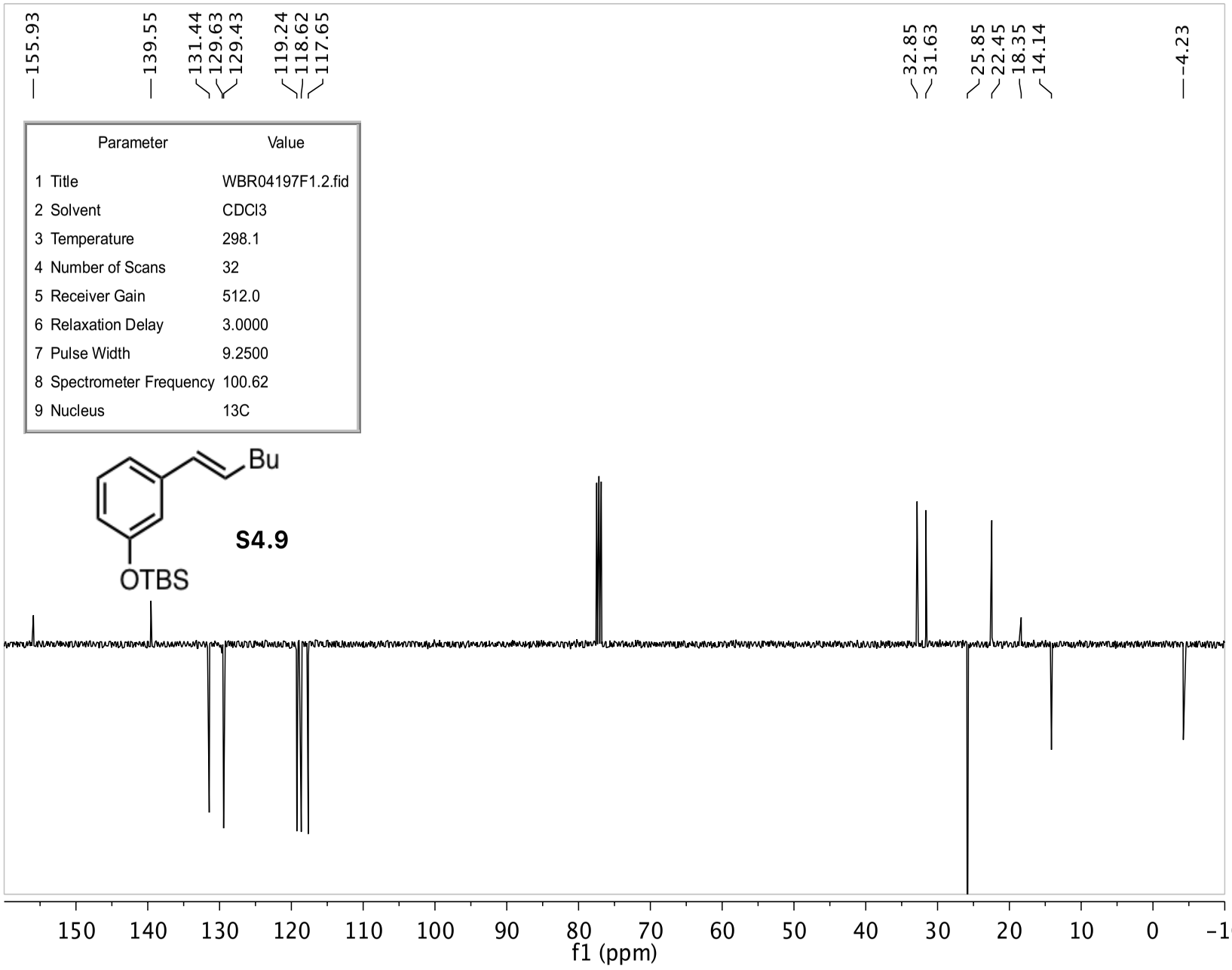
155.93
139.55
131.44
129.63
129.43
119.24
118.62
117.65
32.85
31.63
25.85
22.45
18.35
14.14
4.23
Parameter Value
1 Title WBR04197F1.2.fid
2 Solvent CDCl3
3 Temperature 298.1
4 Number of Scans 32
5 Receiver Gain 512.0
6 Relaxation Delay 3.0000
7 Pulse Width 9.2500
8 Spectrometer Frequency 100.62
9 Nucleus 13C
Bu
OTBS
S4.9
150 140 130 120 110 100 90 80 70 60 50 40 30 20 10 0 -10
f1 (ppm)

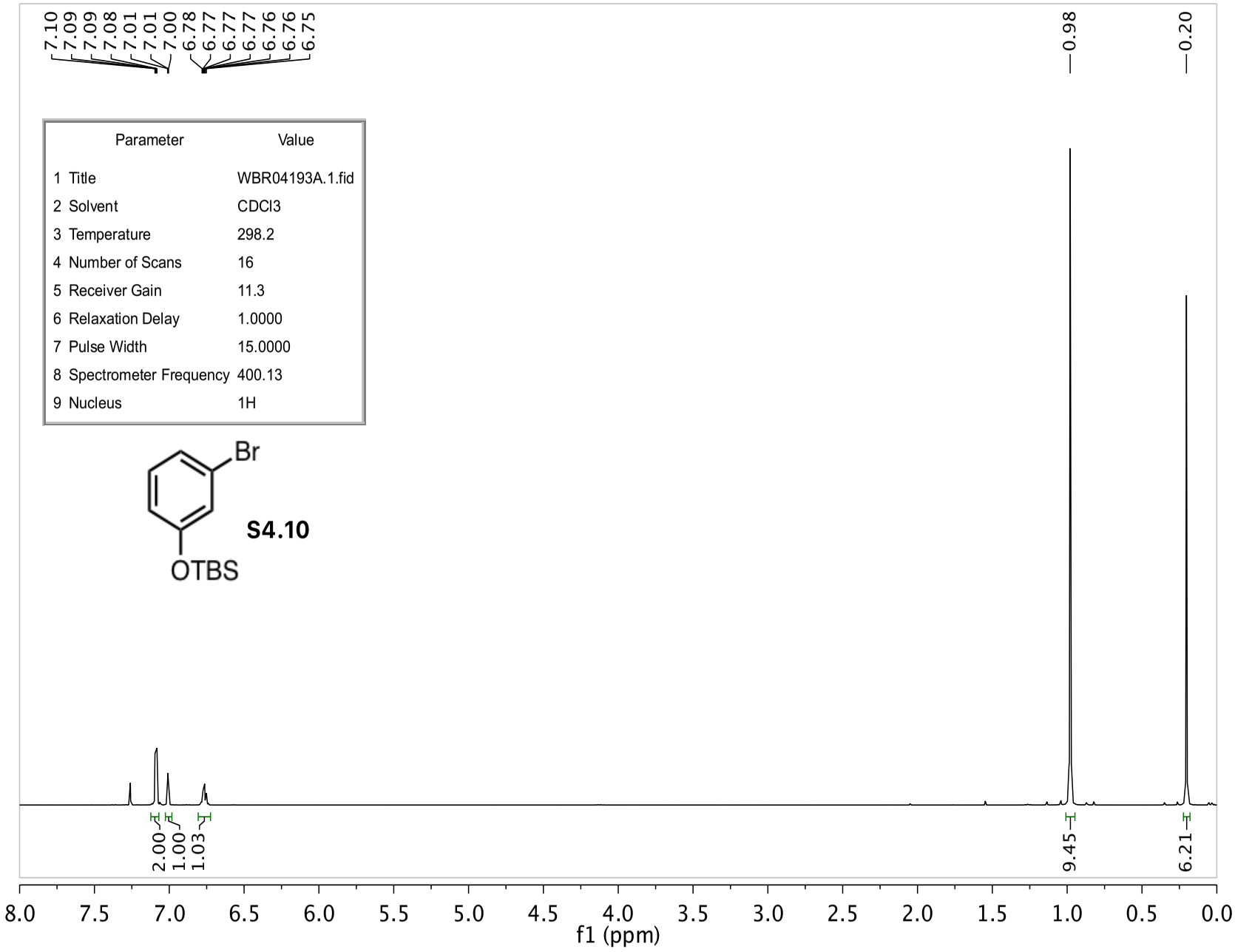
7.10
7.09
7.09
7.08
7.01
7.01
7.00
6.78
6.77
6.77
6.77
6.76
6.76
6.75
0.98
0.20
Parameter Value
1 Title WBR04193A.1.fid
2 Solvent CDCl3
3 Temperature 298.2
4 Number of Scans 16
5 Receiver Gain 11.3
6 Relaxation Delay 1.0000
7 Pulse Width 15.0000
8 Spectrometer Frequency 400.13
9 Nucleus 1H
Br
OTBS
S4.10
2.00
1.00
1.03
9.45
6.21
8.0 7.5 7.0 6.5 6.0 5.5 5.0 4.5 4.0 3.5 3.0 2.5 2.0 1.5 1.0 0.5 0.0
f1 (ppm)

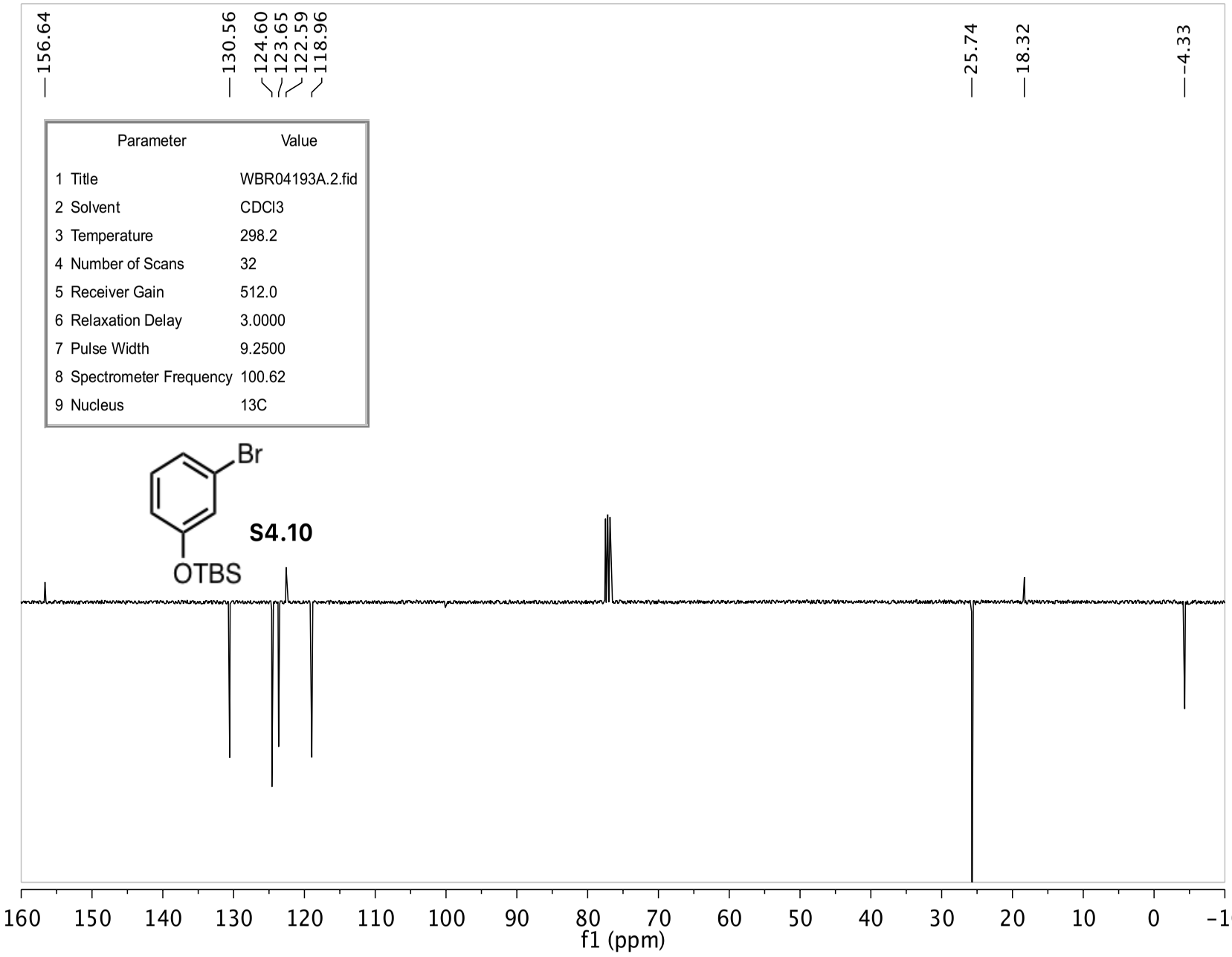
156.64
130.56
124.60
123.65
122.59
118.96
25.74
18.32
-4.33
Parameter Value
1 Title WBR04193A.2.fid
2 Solvent CDCl3
3 Temperature 298.2
4 Number of Scans 32
5 Receiver Gain 512.0
6 Relaxation Delay 3.0000
7 Pulse Width 9.2500
8 Spectrometer Frequency 100.62
9 Nucleus 13C
Br
OTBS
S4.10
160 150 140 130 120 110 100 90 80 70 60 50 40 30 20 10 0 -10
f1 (ppm)

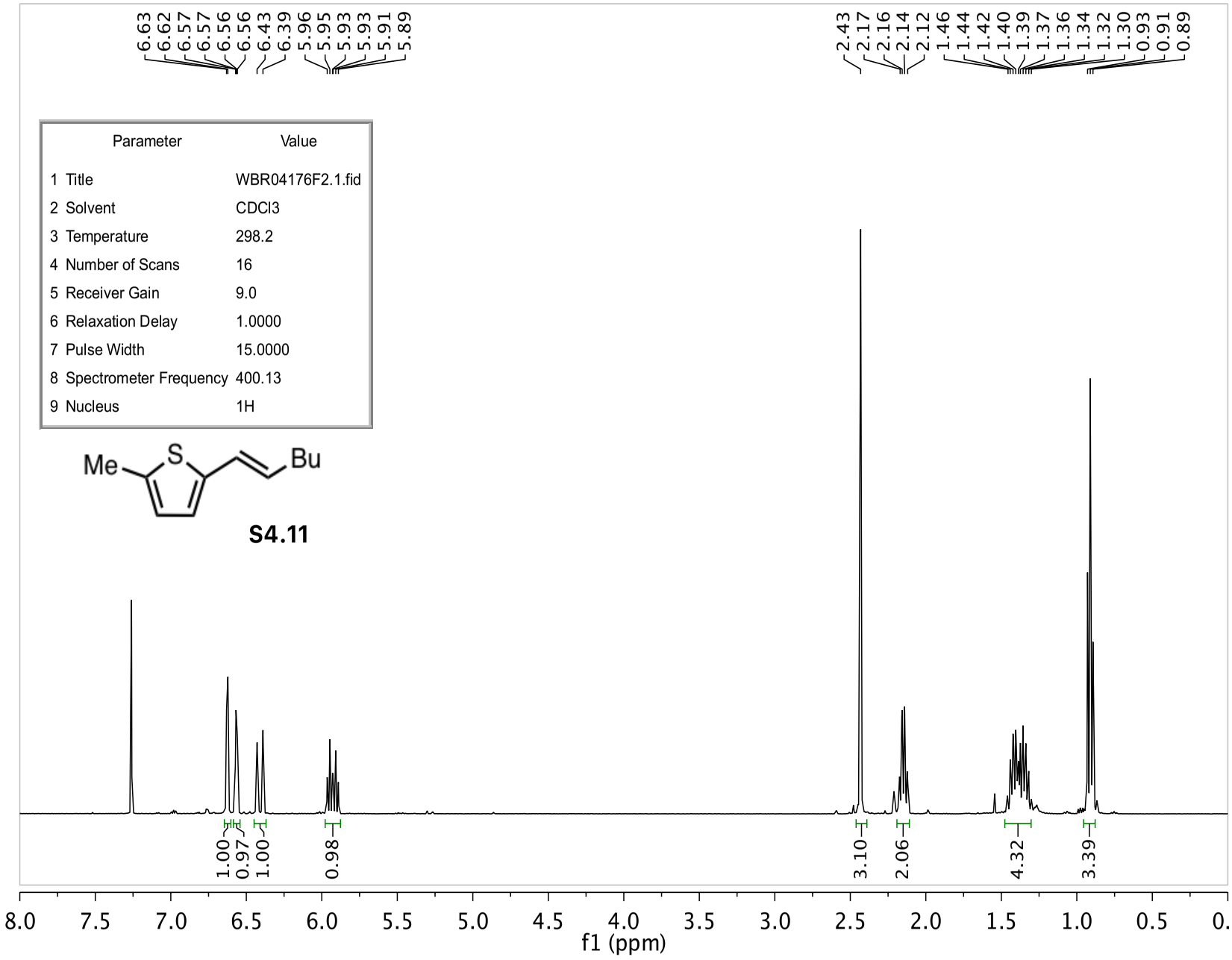
6.63
6.62
6.57
6.57
6.56
6.56
6.43
6.39
5.96
5.95
5.93
5.93
5.91
5.89
2.43
2.17
2.16
2.14
2.12
1.46
1.44
1.42
1.40
1.39
1.37
1.36
1.34
1.32
1.30
0.93
0.91
0.89
Parameter Value
1 Title WBR04176F2.1.fid
2 Solvent CDCl3
3 Temperature 298.2
4 Number of Scans 16
5 Receiver Gain 9.0
6 Relaxation Delay 1.0000
7 Pulse Width 15.0000
8 Spectrometer Frequency 400.13
9 Nucleus 1H
Me
S
Bu
S4.11
1.00
0.97
1.00
0.98
3.10
2.06
4.32
3.39
8.0
7.5
7.0
6.5
6.0
5.5
5.0
4.5
4.0
3.5
3.0
2.5
2.0
1.5
1.0
0.5
0.0
f1 (ppm)

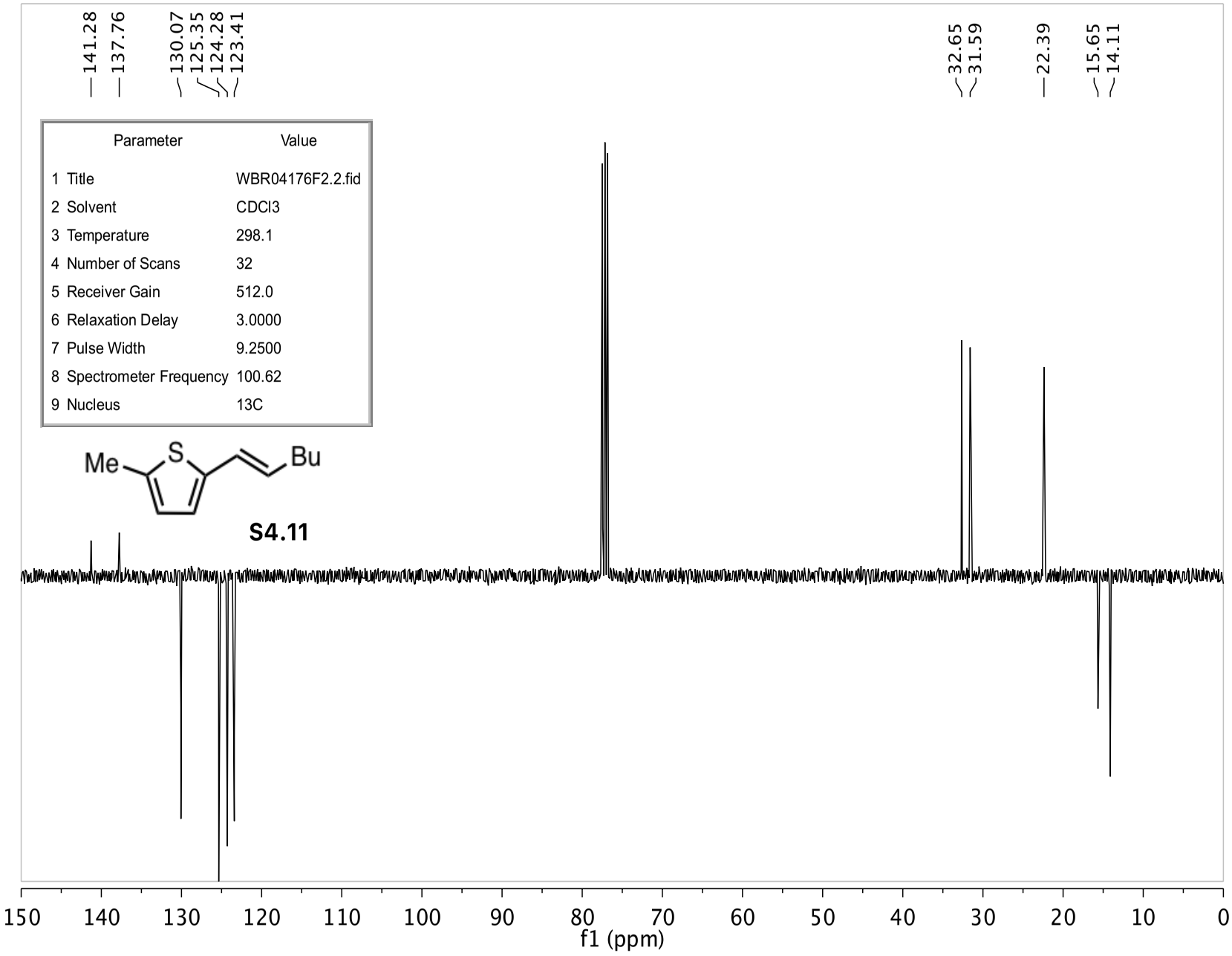
141.28
137.76
130.07
125.35
124.28
123.41
32.65
31.59
22.39
15.65
14.11
Parameter Value
1 Title WBR04176F2.2.fid
2 Solvent CDCl3
3 Temperature 298.1
4 Number of Scans 32
5 Receiver Gain 512.0
6 Relaxation Delay 3.0000
7 Pulse Width 9.2500
8 Spectrometer Frequency 100.62
9 Nucleus 13C
Me
S
Bu
S4.11
150 140 130 120 110 100 90 80 70 60 50 40 30 20 10 0
f1 (ppm)

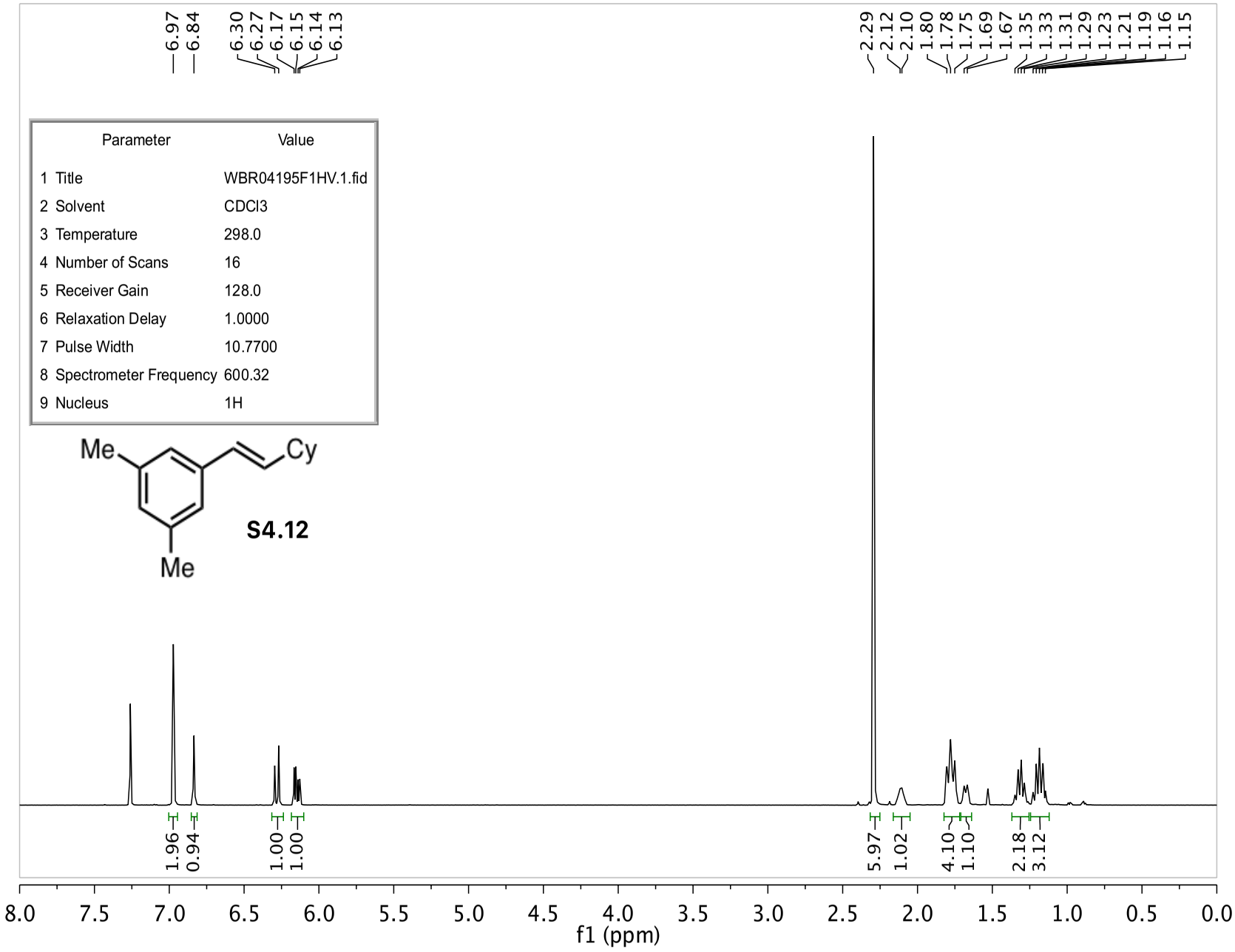
6.97
6.84
6.30
6.27
6.17
6.15
6.14
6.13
2.29
2.12
2.10
1.80
1.78
1.75
1.69
1.67
1.35
1.33
1.31
1.29
1.23
1.21
1.19
1.16
1.15
Parameter Value
1 Title WBR04195F1HV.1.fid
2 Solvent CDCl3
3 Temperature 298.0
4 Number of Scans 16
5 Receiver Gain 128.0
6 Relaxation Delay 1.0000
7 Pulse Width 10.7700
8 Spectrometer Frequency 600.32
9 Nucleus 1H
Me
Cy
Me
S4.12
1.96
0.94
1.00
1.00
5.97
1.02
4.10
1.10
2.18
3.12
8.0
7.5
7.0
6.5
6.0
5.5
5.0
4.5
4.0
3.5
3.0
2.5
2.0
1.5
1.0
0.5
0.0
f1 (ppm)

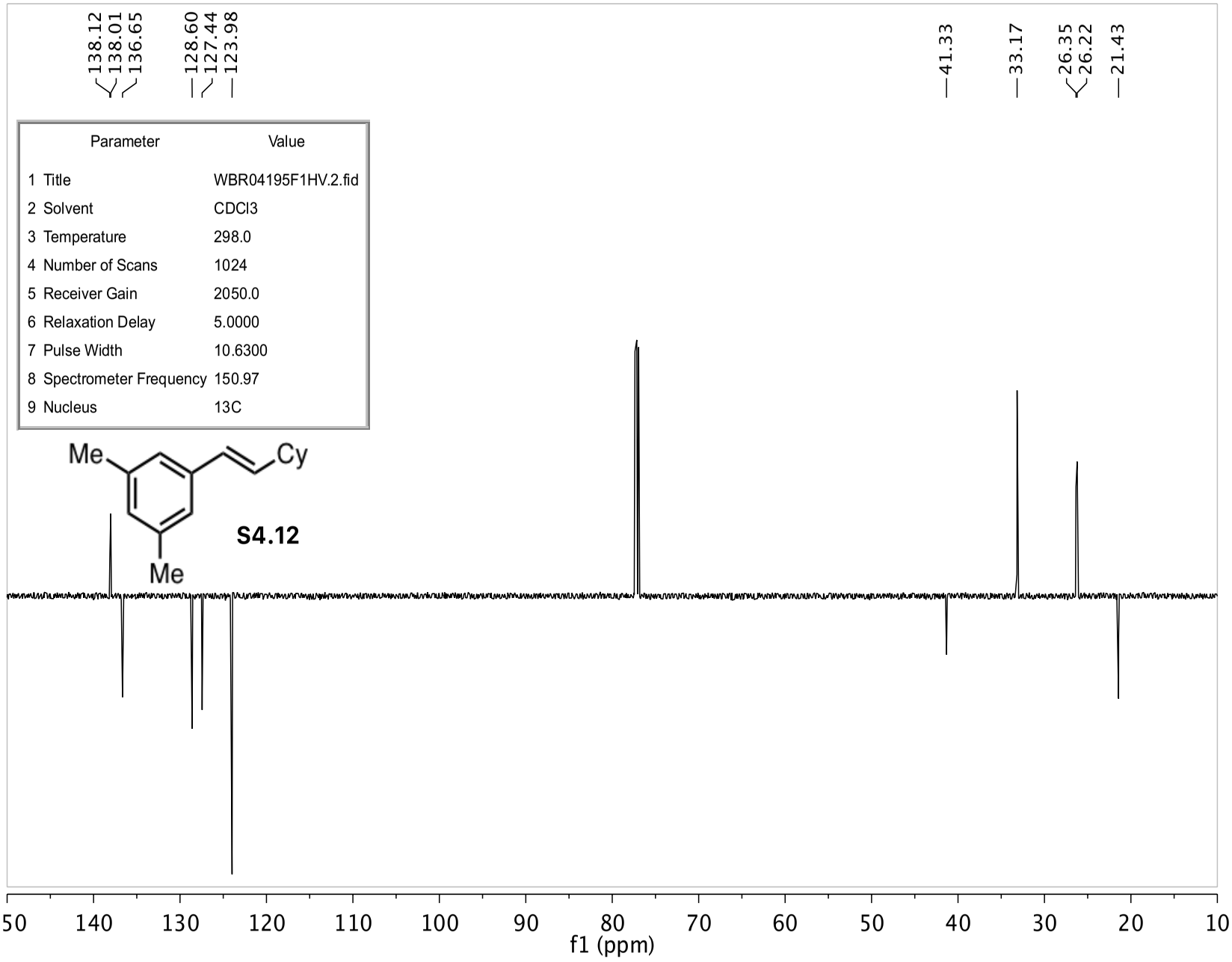
138.12
138.01
136.65
128.60
127.44
123.98
41.33
33.17
26.35
26.22
21.43
Parameter Value
1 Title WBR04195F1HV.2.fid
2 Solvent CDCl3
3 Temperature 298.0
4 Number of Scans 1024
5 Receiver Gain 2050.0
6 Relaxation Delay 5.0000
7 Pulse Width 10.6300
8 Spectrometer Frequency 150.97
9 Nucleus 13C
Me
Cy
Me
S4.12
150 140 130 120 110 100 90 80 70 60 50 40 30 20 10
f1 (ppm)

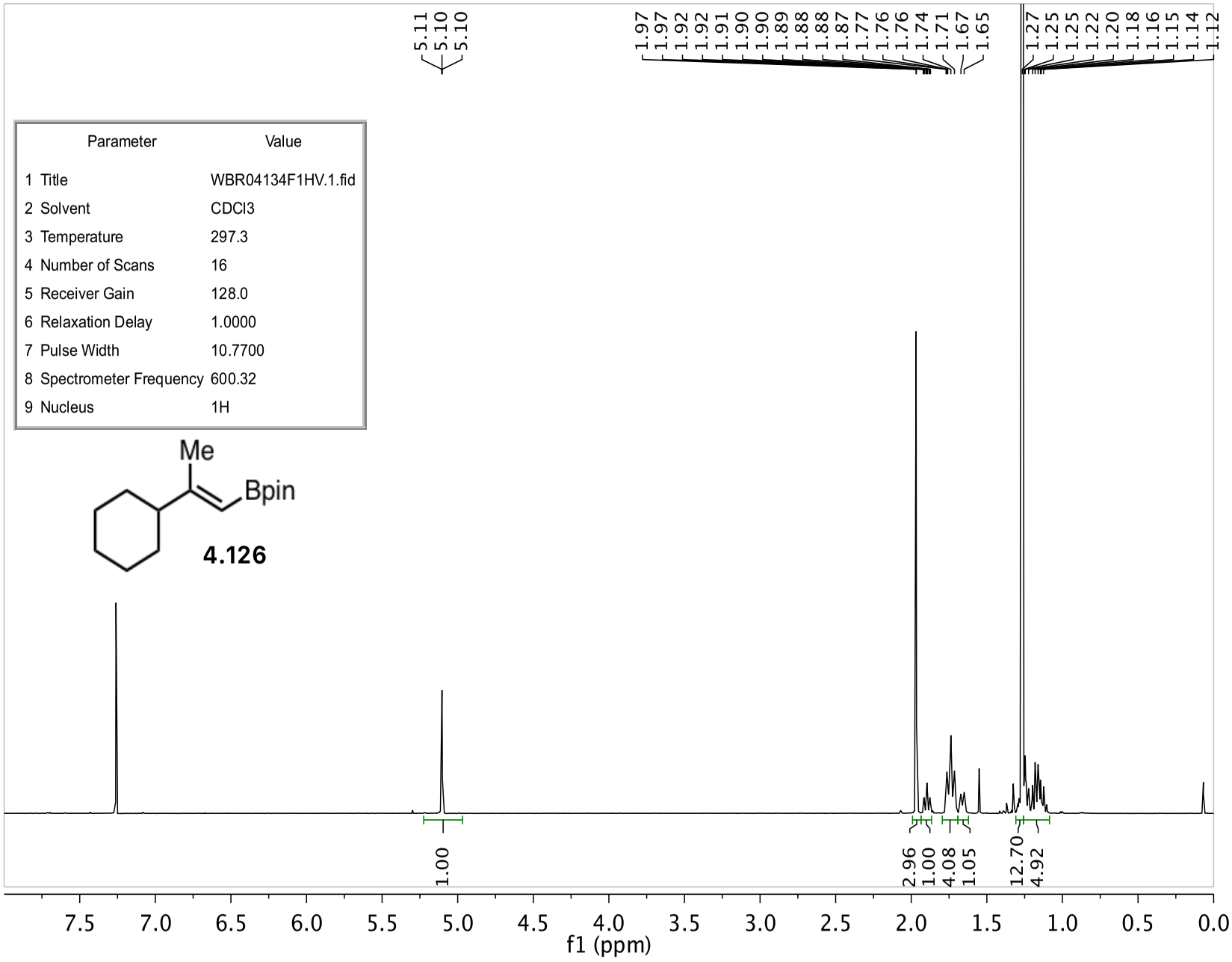
5.11
5.10
5.10
1.97
1.97
1.92
1.92
1.91
1.90
1.90
1.89
1.88
1.88
1.87
1.77
1.76
1.76
1.74
1.71
1.67
1.65
1.27
1.25
1.25
1.22
1.20
1.18
1.16
1.15
1.14
1.12
Parameter Value
1 Title WBR04134F1HV.1.fid
2 Solvent CDCl3
3 Temperature 297.3
4 Number of Scans 16
5 Receiver Gain 128.0
6 Relaxation Delay 1.0000
7 Pulse Width 10.7700
8 Spectrometer Frequency 600.32
9 Nucleus 1H
Me
Bpin
4.126
1.00
2.96
1.00
4.08
1.05
12.70
4.92
7.5
7.0
6.5
6.0
5.5
5.0
4.5
4.0
3.5
3.0
2.5
2.0
1.5
1.0
0.5
0.0
f1 (ppm)

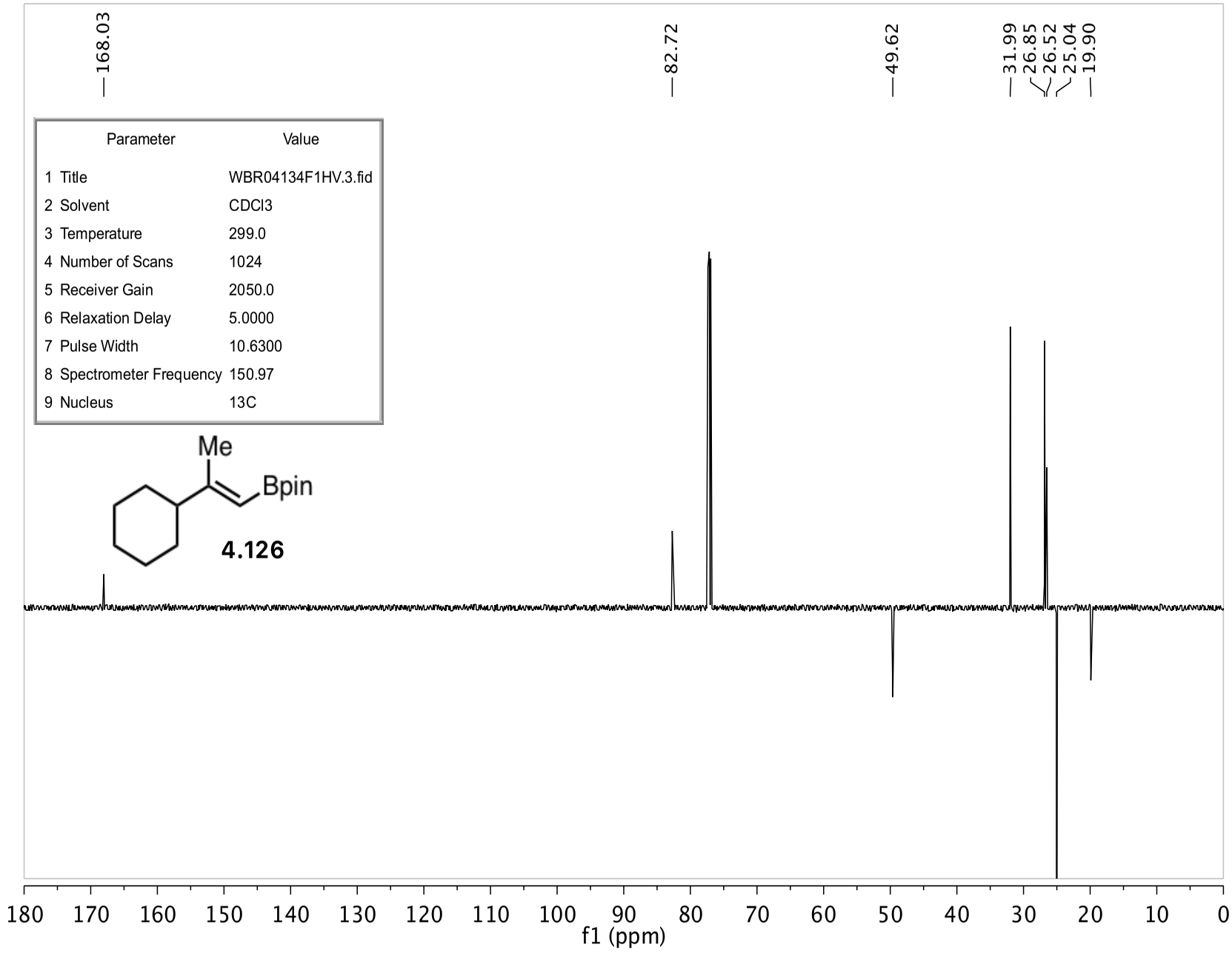
168.03
82.72
49.62
31.99
26.85
26.52
25.04
19.90
Parameter Value
1 Title WBR04134F1HV.3.fid
2 Solvent CDCl3
3 Temperature 299.0
4 Number of Scans 1024
5 Receiver Gain 2050.0
6 Relaxation Delay 5.0000
7 Pulse Width 10.6300
8 Spectrometer Frequency 150.97
9 Nucleus 13C
Me
Bpin
4.126
180 170 160 150 140 130 120 110 100 90 80 70 60 50 40 30 20 10 0
f1 (ppm)

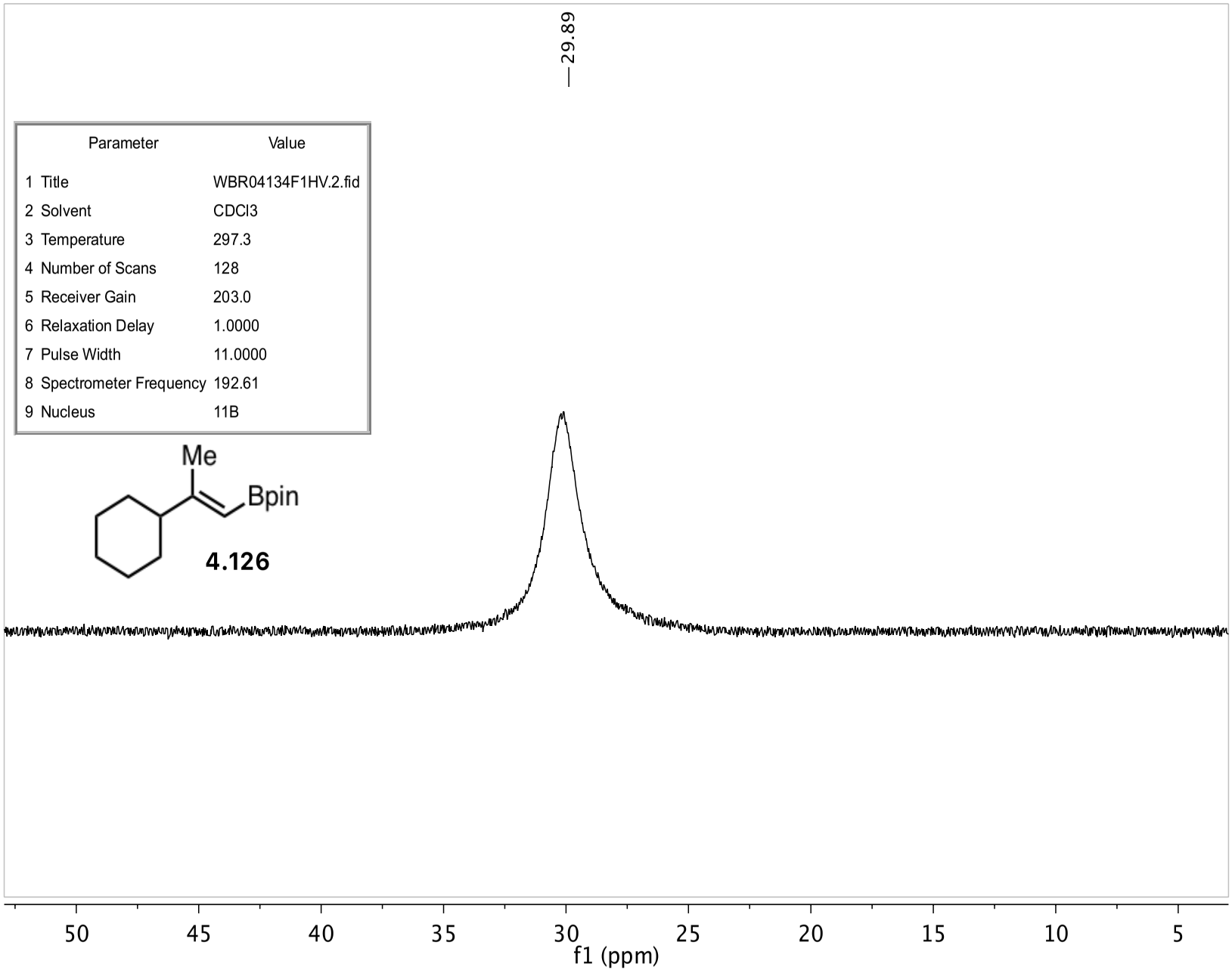
29.89
Parameter Value
1 Title WBR04134F1HV.2.fid
2 Solvent CDCl3
3 Temperature 297.3
4 Number of Scans 128
5 Receiver Gain 203.0
6 Relaxation Delay 1.0000
7 Pulse Width 11.0000
8 Spectrometer Frequency 192.61
9 Nucleus 11B
Me
Bpin
4.126
50
45
40
35
30
25
20
15
10
5
f1 (ppm)

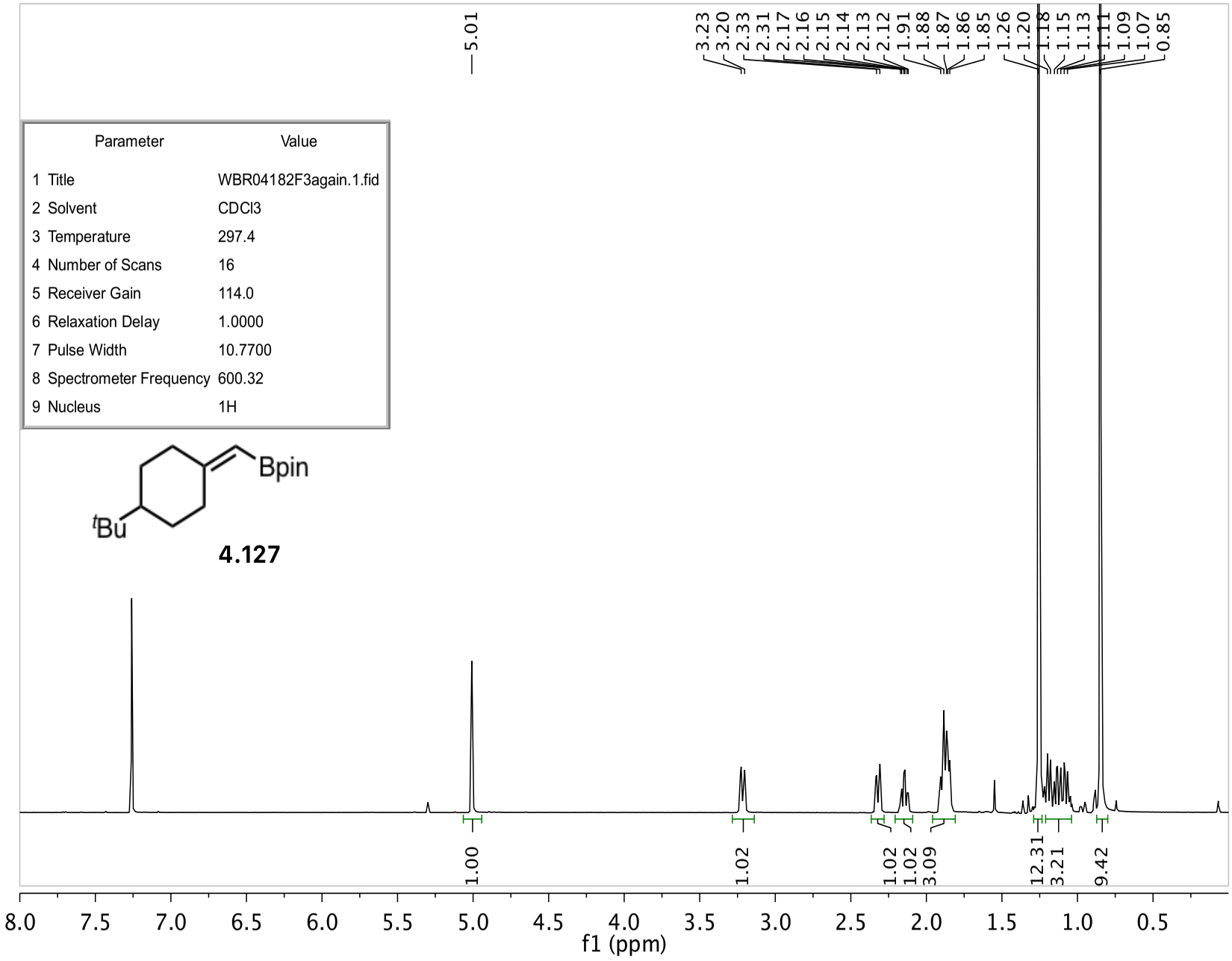
5.01
3.23
3.20
2.33
2.31
2.17
2.16
2.15
2.14
2.13
2.12
1.91
1.88
1.87
1.86
1.85
1.26
1.20
1.18
1.15
1.13
1.11
1.09
1.07
0.85
Parameter Value
1 Title WBR04182F3again.1.fid
2 Solvent CDCl3
3 Temperature 297.4
4 Number of Scans 16
5 Receiver Gain 114.0
6 Relaxation Delay 1.0000
7 Pulse Width 10.7700
8 Spectrometer Frequency 600.32
9 Nucleus 1H
Bpin
tBu
4.127
1.00
1.02
1.02
1.02
3.09
12.31
3.21
9.42
8.0
7.5
7.0
6.5
6.0
5.5
5.0
4.5
4.0
3.5
3.0
2.5
2.0
1.5
1.0
0.5
f1 (ppm)

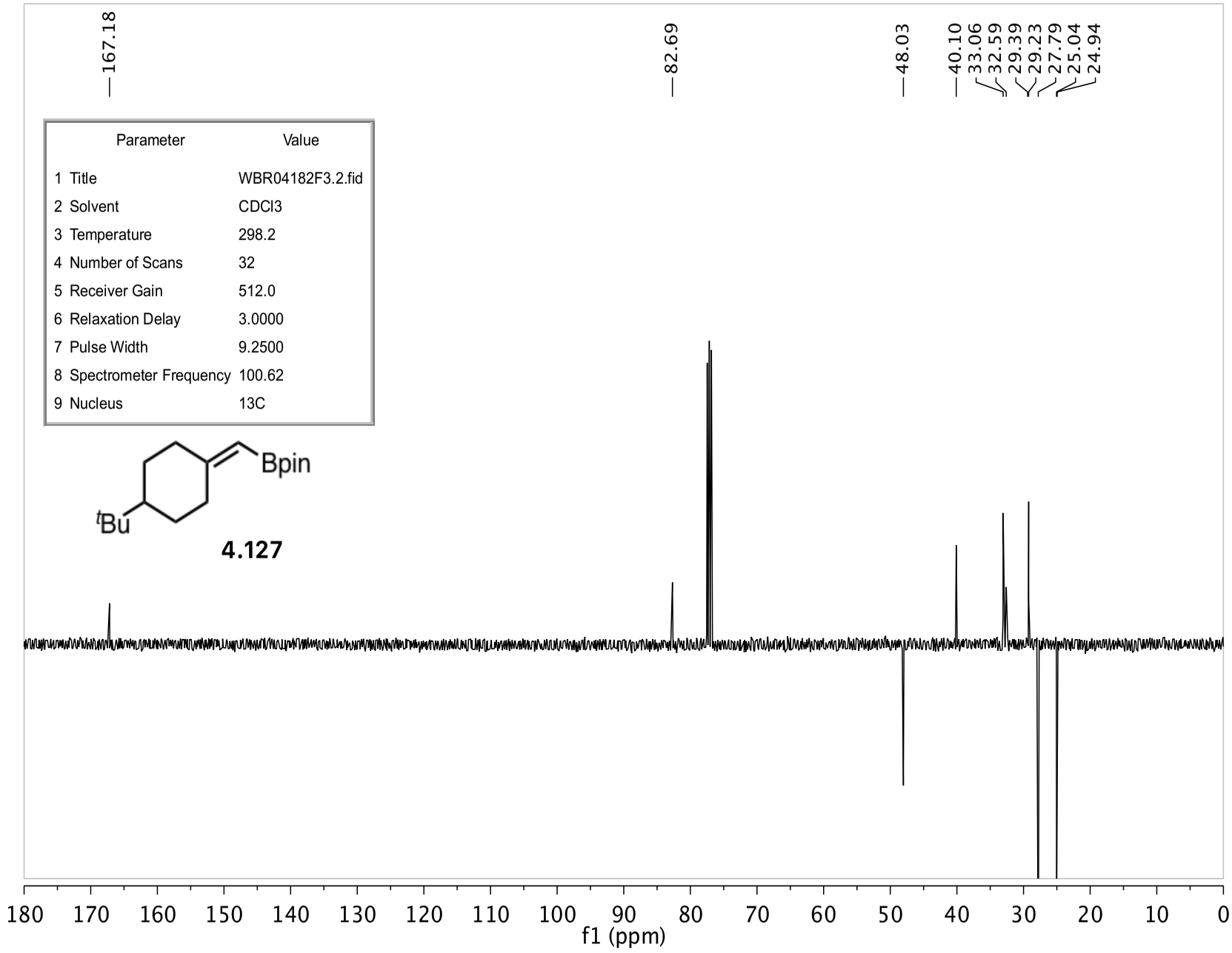
167.18
82.69
48.03
40.10
33.06
32.59
29.39
29.23
27.79
25.04
24.94
Parameter Value
1 Title WBR04182F3.2.fid
2 Solvent CDCl3
3 Temperature 298.2
4 Number of Scans 32
5 Receiver Gain 512.0
6 Relaxation Delay 3.0000
7 Pulse Width 9.2500
8 Spectrometer Frequency 100.62
9 Nucleus 13C
Bpin
tBu
4.127
180 170 160 150 140 130 120 110 100 90 80 70 60 50 40 30 20 10 0
f1 (ppm)

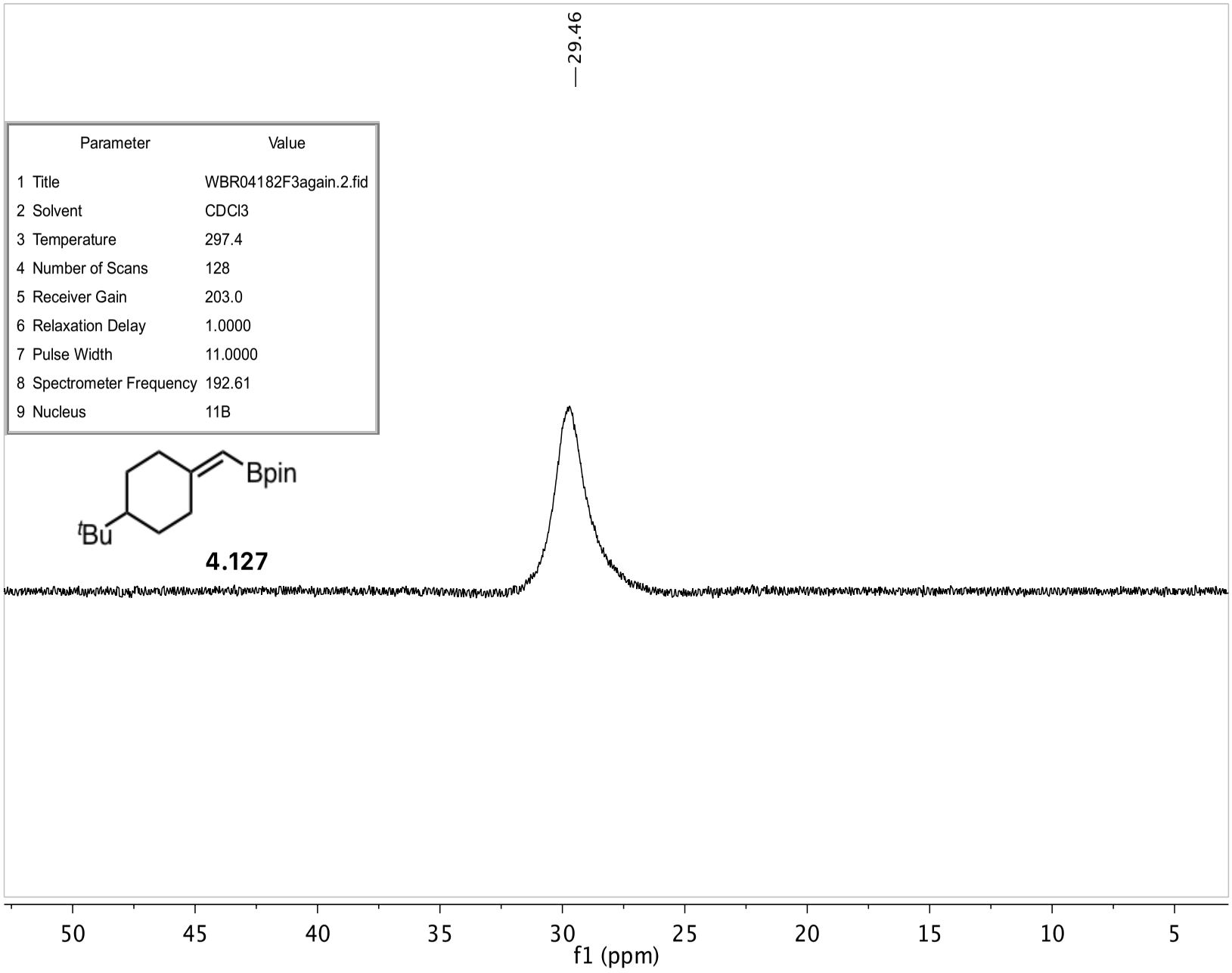
29.46
Parameter
Value
1 Title
WBR04182F3again.2.fid
2 Solvent
CDCl3
3 Temperature
297.4
4 Number of Scans
128
5 Receiver Gain
203.0
6 Relaxation Delay
1.0000
7 Pulse Width
11.0000
8 Spectrometer Frequency
192.61
9 Nucleus
11B
Bpin
tBu
4.127
50
45
40
35
30
25
20
15
10
5
f1 (ppm)

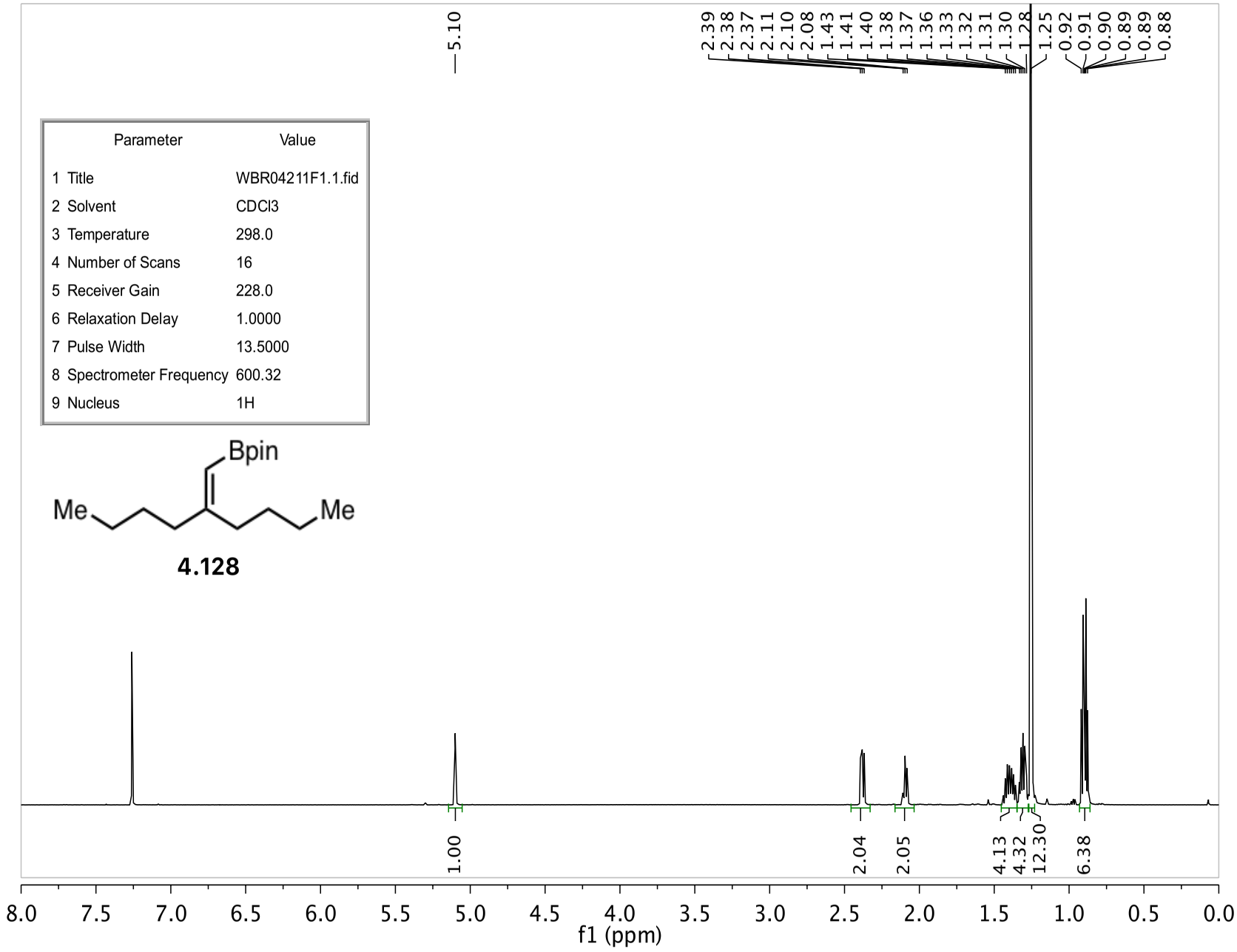
5.10
2.39
2.38
2.37
2.11
2.10
2.08
1.43
1.41
1.40
1.38
1.37
1.36
1.33
1.32
1.31
1.30
1.28
1.25
0.92
0.91
0.90
0.89
0.89
0.88
Parameter Value
1 Title WBR04211F1.1.fid
2 Solvent CDCl3
3 Temperature 298.0
4 Number of Scans 16
5 Receiver Gain 228.0
6 Relaxation Delay 1.0000
7 Pulse Width 13.5000
8 Spectrometer Frequency 600.32
9 Nucleus 1H
Bpin
Me
Me
4.128
1.00
2.04
2.05
4.13
4.32
12.30
6.38
8.0
7.5
7.0
6.5
6.0
5.5
5.0
4.5
4.0
3.5
3.0
2.5
2.0
1.5
1.0
0.5
0.0
f1 (ppm)

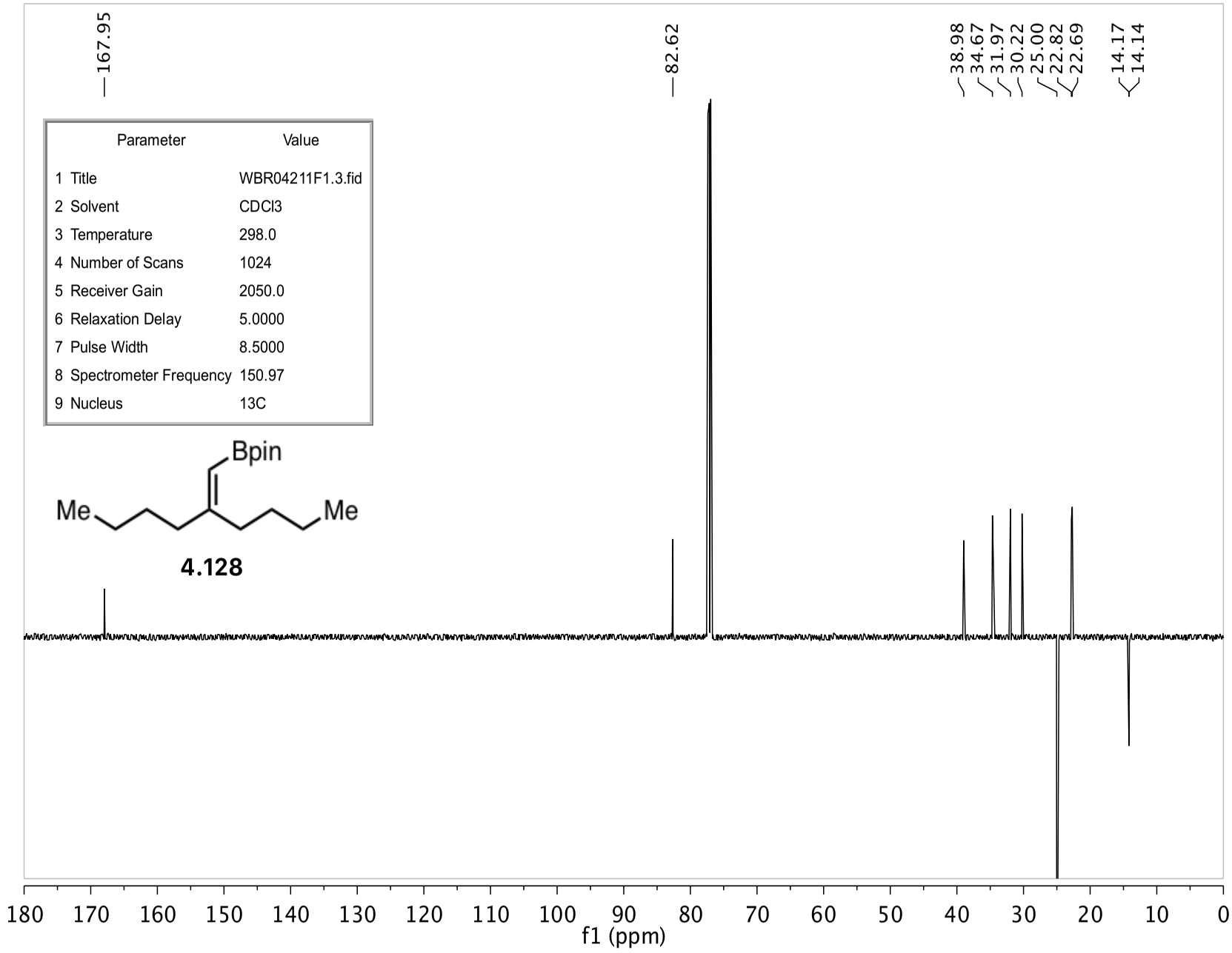
167.95
82.62
38.98
34.67
31.97
30.22
25.00
22.82
22.69
14.17
14.14
Parameter Value
1 Title WBR04211F1.3.fid
2 Solvent CDCl3
3 Temperature 298.0
4 Number of Scans 1024
5 Receiver Gain 2050.0
6 Relaxation Delay 5.0000
7 Pulse Width 8.5000
8 Spectrometer Frequency 150.97
9 Nucleus 13C
Bpin
Me
Me
4.128
180 170 160 150 140 130 120 110 100 90 80 70 60 50 40 30 20 10 0
f1 (ppm)

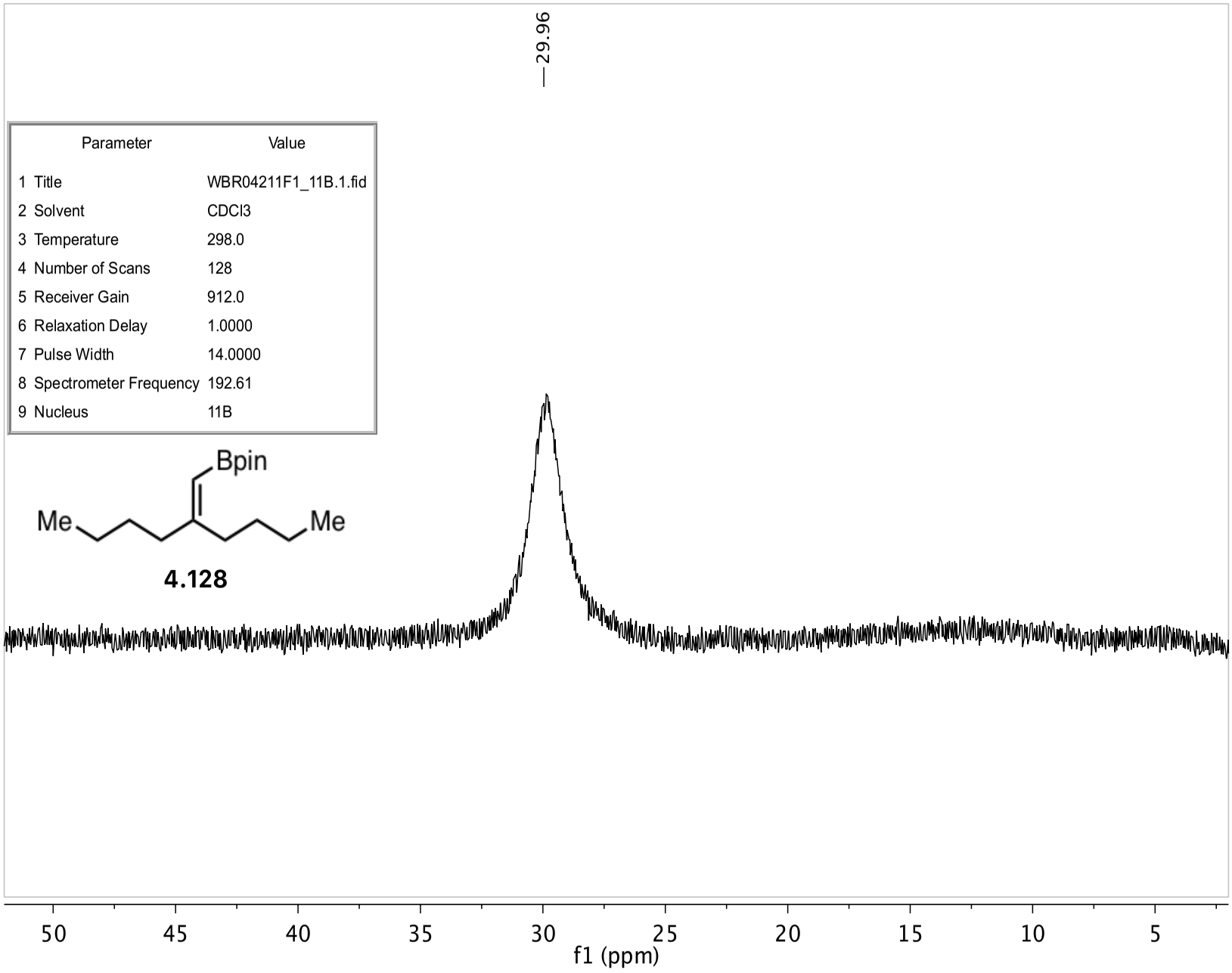
29.96
Parameter
Value
1 Title
WBR04211F1_11B.1.fid
2 Solvent
CDCl3
3 Temperature
298.0
4 Number of Scans
128
5 Receiver Gain
912.0
6 Relaxation Delay
1.0000
7 Pulse Width
14.0000
8 Spectrometer Frequency
192.61
9 Nucleus
11B
Bpin
Me
Me
4.128
50
45
40
35
30
25
20
15
10
5
f1 (ppm)

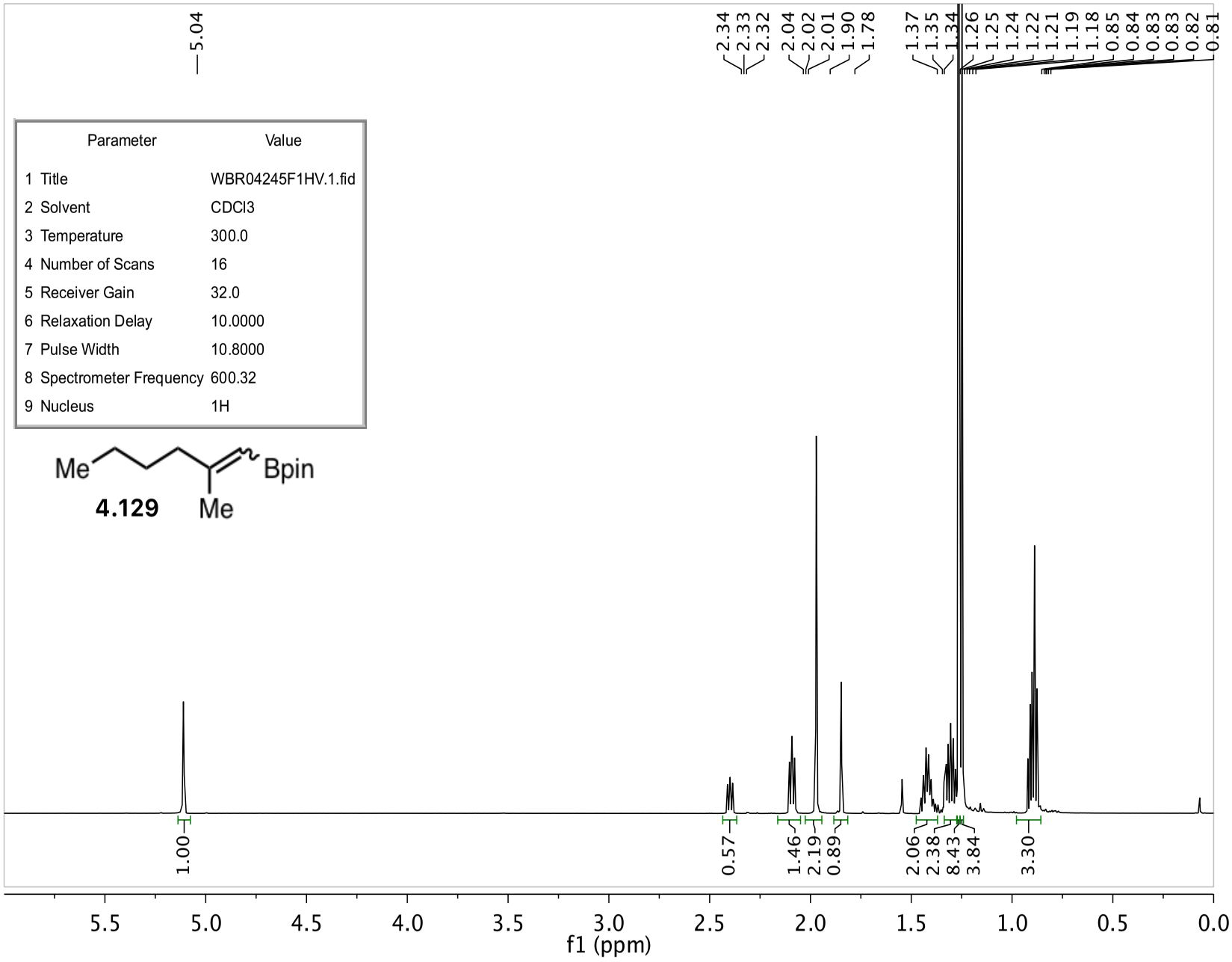
5.04
2.34
2.33
2.32
2.04
2.02
2.01
1.90
1.78
1.37
1.35
1.34
1.26
1.25
1.24
1.22
1.21
1.19
1.18
0.85
0.84
0.83
0.83
0.82
0.81
Parameter Value
1 Title WBR04245F1HV.1.fid
2 Solvent CDCl3
3 Temperature 300.0
4 Number of Scans 16
5 Receiver Gain 32.0
6 Relaxation Delay 10.0000
7 Pulse Width 10.8000
8 Spectrometer Frequency 600.32
9 Nucleus 1H
Me
Bpin
4.129
Me
1.00
0.57
1.46
2.19
0.89
2.06
2.38
8.43
3.84
3.30
5.5
5.0
4.5
4.0
3.5
3.0
2.5
2.0
1.5
1.0
0.5
0.0
f1 (ppm)

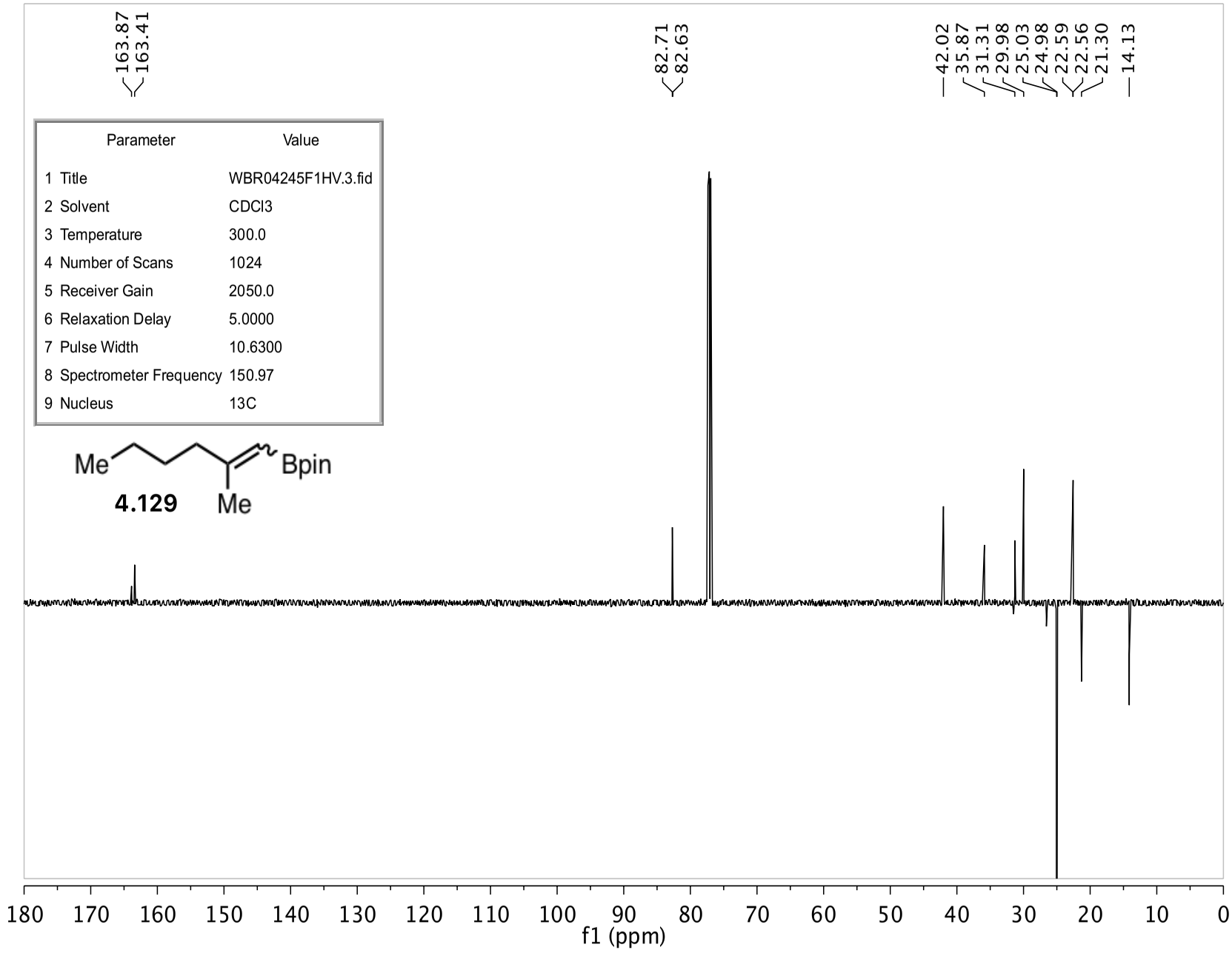
163.87
163.41
82.71
82.63
42.02
35.87
31.31
29.98
25.03
24.98
22.59
22.56
21.30
14.13
Parameter Value
1 Title WBR04245F1HV.3.fid
2 Solvent CDCl3
3 Temperature 300.0
4 Number of Scans 1024
5 Receiver Gain 2050.0
6 Relaxation Delay 5.0000
7 Pulse Width 10.6300
8 Spectrometer Frequency 150.97
9 Nucleus 13C
Me
Bpin
4.129
Me
180 170 160 150 140 130 120 110 100 90 80 70 60 50 40 30 20 10 0
f1 (ppm)

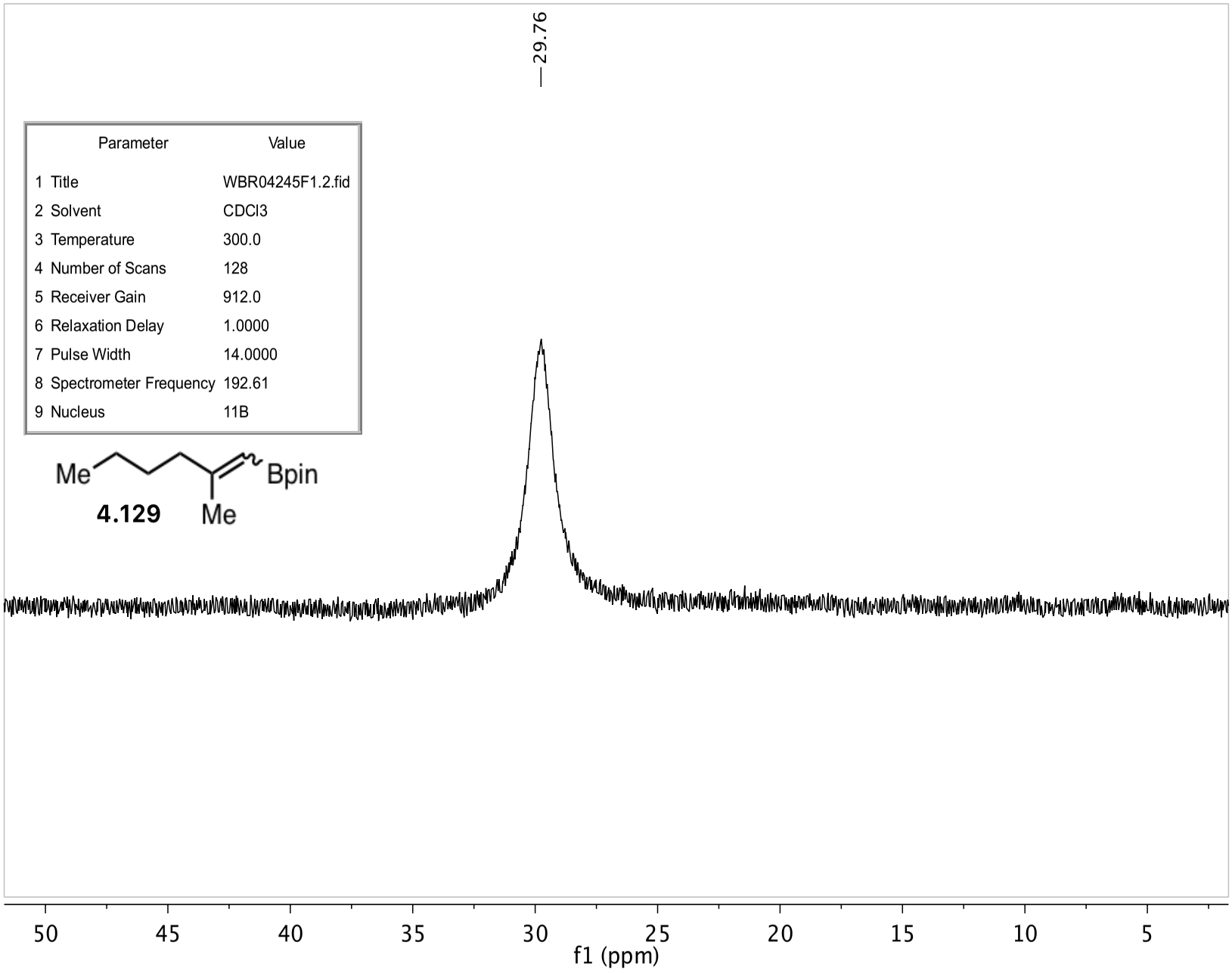
29.76
Parameter Value
1 Title WBR04245F1.2.fid
2 Solvent CDCl3
3 Temperature 300.0
4 Number of Scans 128
5 Receiver Gain 912.0
6 Relaxation Delay 1.0000
7 Pulse Width 14.0000
8 Spectrometer Frequency 192.61
9 Nucleus 11B
Me
Bpin
4.129
Me
50
45
40
35
30
25
20
15
10
5
f1 (ppm)

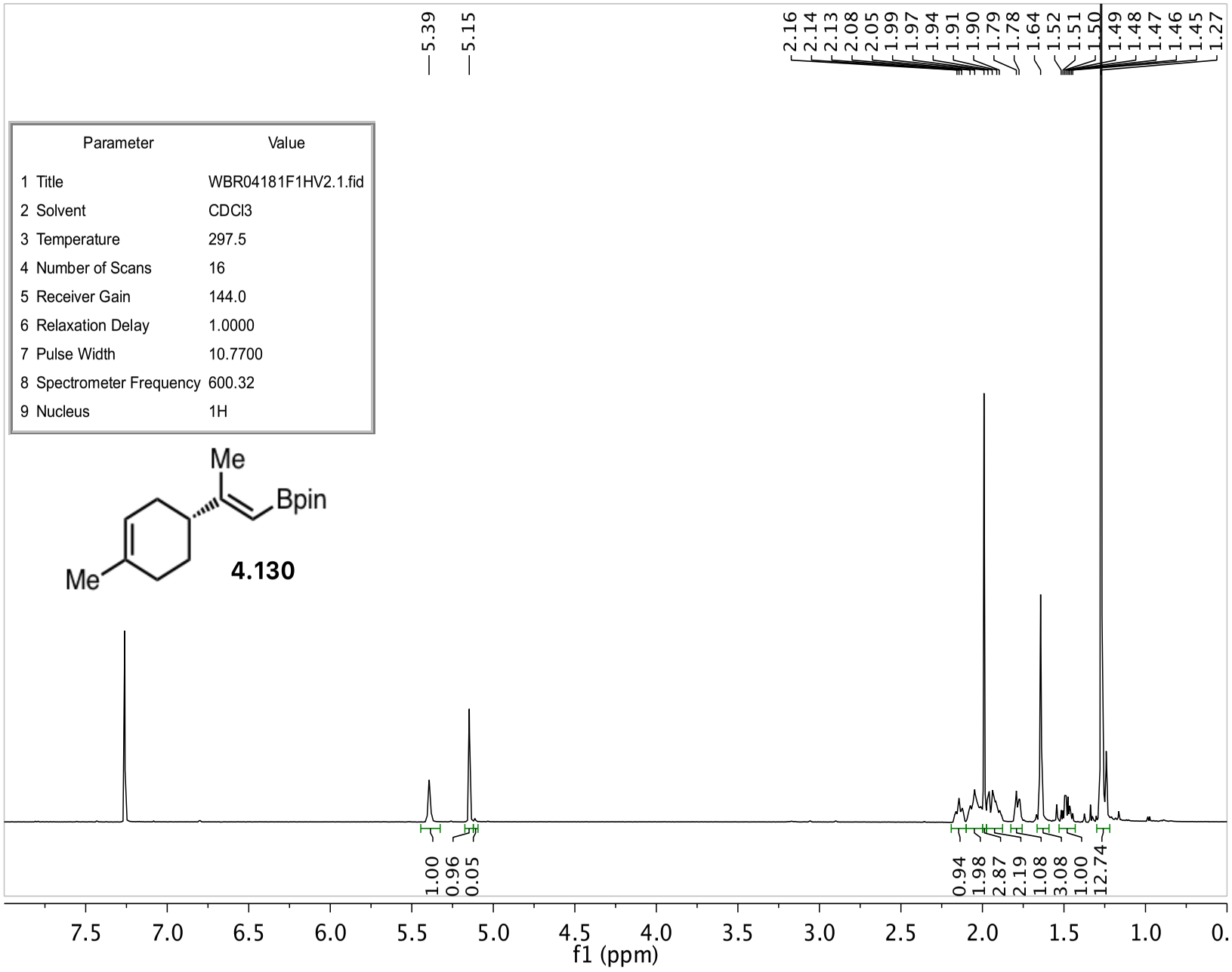
5.39
5.15
2.16
2.14
2.13
2.08
2.05
1.99
1.97
1.94
1.91
1.90
1.79
1.78
1.64
1.52
1.51
1.50
1.49
1.48
1.47
1.46
1.45
1.27
Parameter Value
1 Title WBR04181F1HV2.1.fid
2 Solvent CDCl3
3 Temperature 297.5
4 Number of Scans 16
5 Receiver Gain 144.0
6 Relaxation Delay 1.0000
7 Pulse Width 10.7700
8 Spectrometer Frequency 600.32
9 Nucleus 1H
Me
Bpin
Me
4.130
1.00
0.96
0.05
0.94
1.98
2.87
2.19
1.08
3.08
1.00
12.74
7.5
7.0
6.5
6.0
5.5
5.0
4.5
4.0
3.5
3.0
2.5
2.0
1.5
1.0
0.5
f1 (ppm)

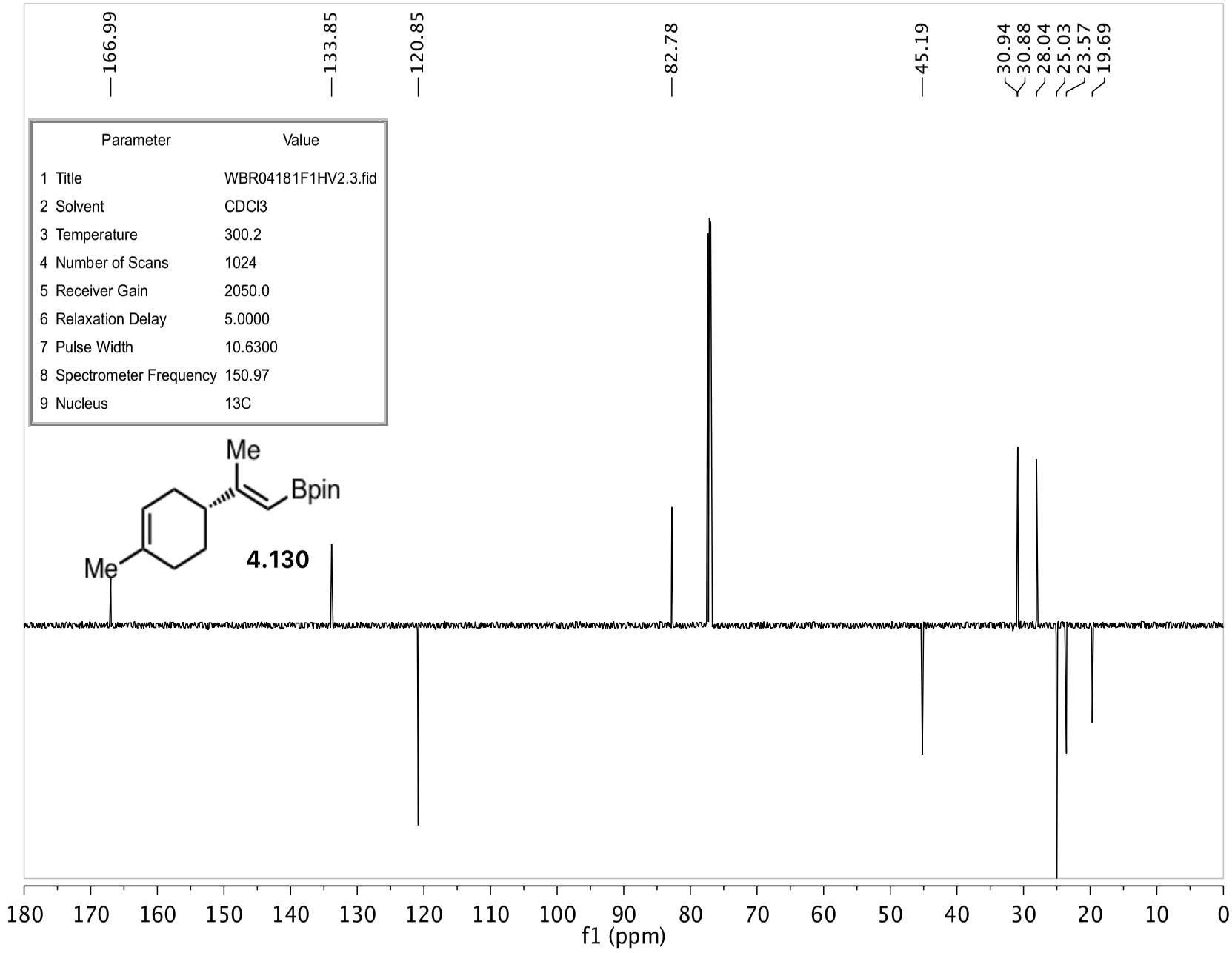
166.99
133.85
120.85
82.78
45.19
30.94
30.88
28.04
25.03
23.57
19.69
Parameter Value
1 Title WBR04181F1HV2.3.fid
2 Solvent CDCl3
3 Temperature 300.2
4 Number of Scans 1024
5 Receiver Gain 2050.0
6 Relaxation Delay 5.0000
7 Pulse Width 10.6300
8 Spectrometer Frequency 150.97
9 Nucleus 13C
Me
Bpin
Me
4.130
180 170 160 150 140 130 120 110 100 90 80 70 60 50 40 30 20 10 0
f1 (ppm)

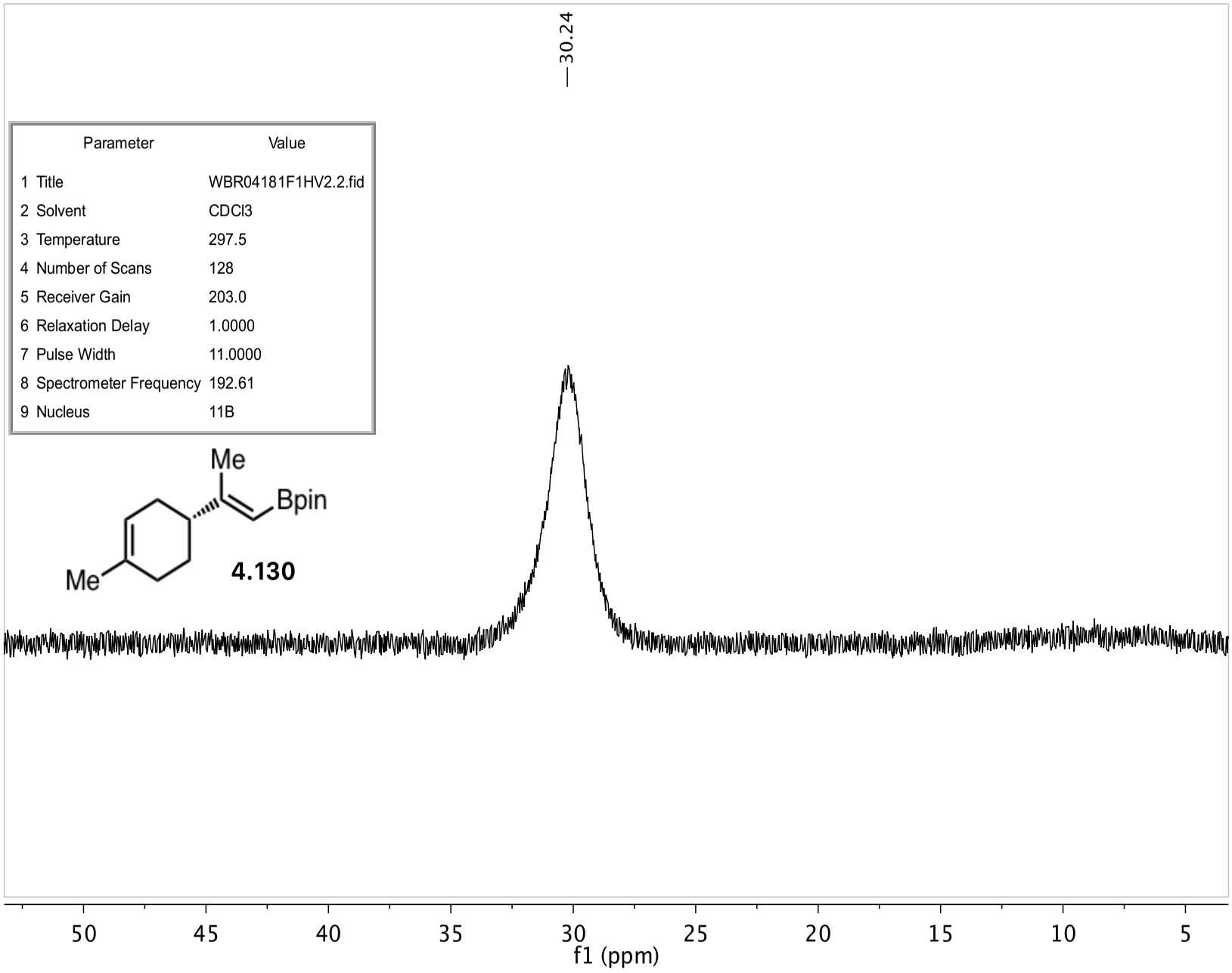
30.24
Parameter
Value
1 Title
WBR04181F1HV2.2.fid
2 Solvent
CDCl3
3 Temperature
297.5
4 Number of Scans
128
5 Receiver Gain
203.0
6 Relaxation Delay
1.0000
7 Pulse Width
11.0000
8 Spectrometer Frequency
192.61
9 Nucleus
11B
Me
Bpin
Me
4.130
50
45
40
35
30
25
20
15
10
5
f1 (ppm)

Parameter	Value
1 Title	WBR05080B_600.63.fid
2 Solvent	CDCl3
3 Temperature	300.0
4 Number of Scans	32
5 Receiver Gain	144.0
6 Relaxation Delay	2.0000
7 Pulse Width	10.8000
8 Spectrometer Frequency	600.32
9 Nucleus	1H

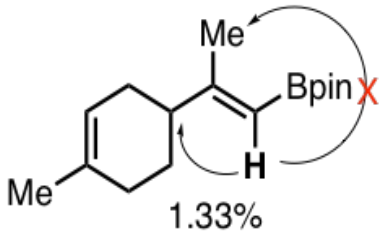

4.130

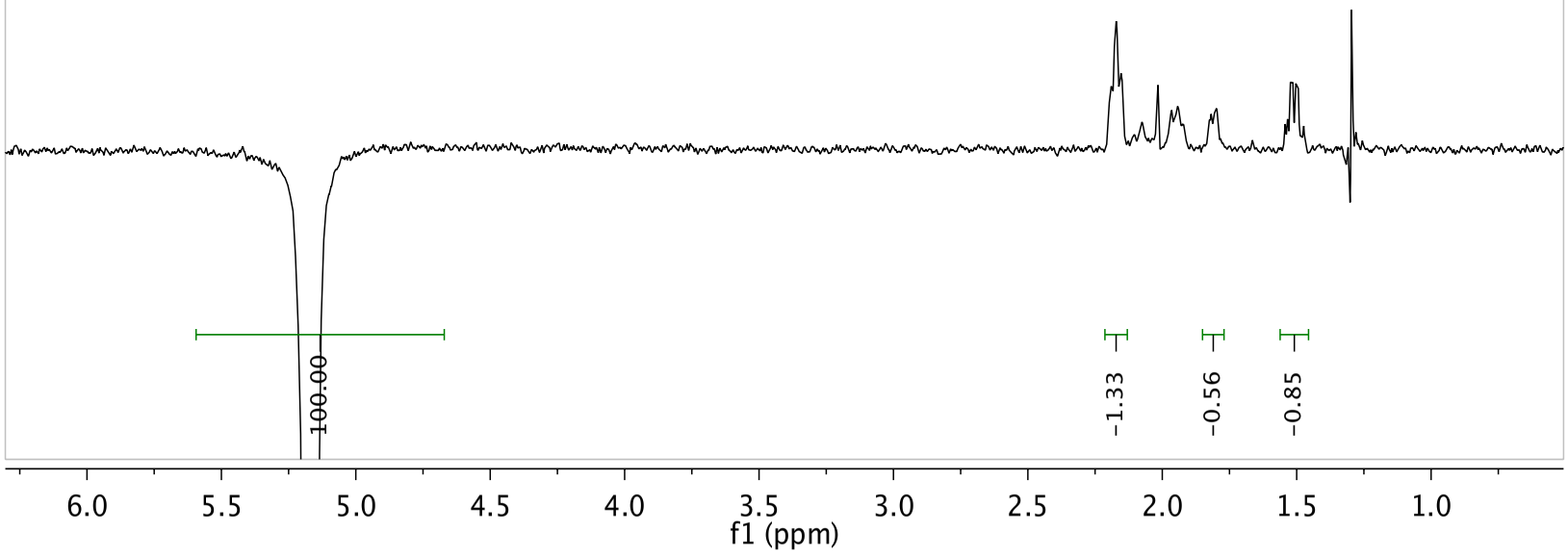

Parameter	Value
1 Title	WBR05080B_600.68.fid
2 Solvent	CDCl3
3 Temperature	300.0
4 Number of Scans	32
5 Receiver Gain	114.0
6 Relaxation Delay	2.0000
7 Pulse Width	10.8000
8 Spectrometer Frequency	600.32
9 Nucleus	1H

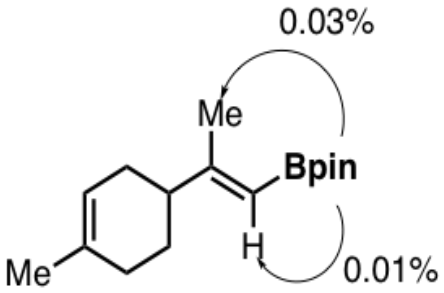

4.130

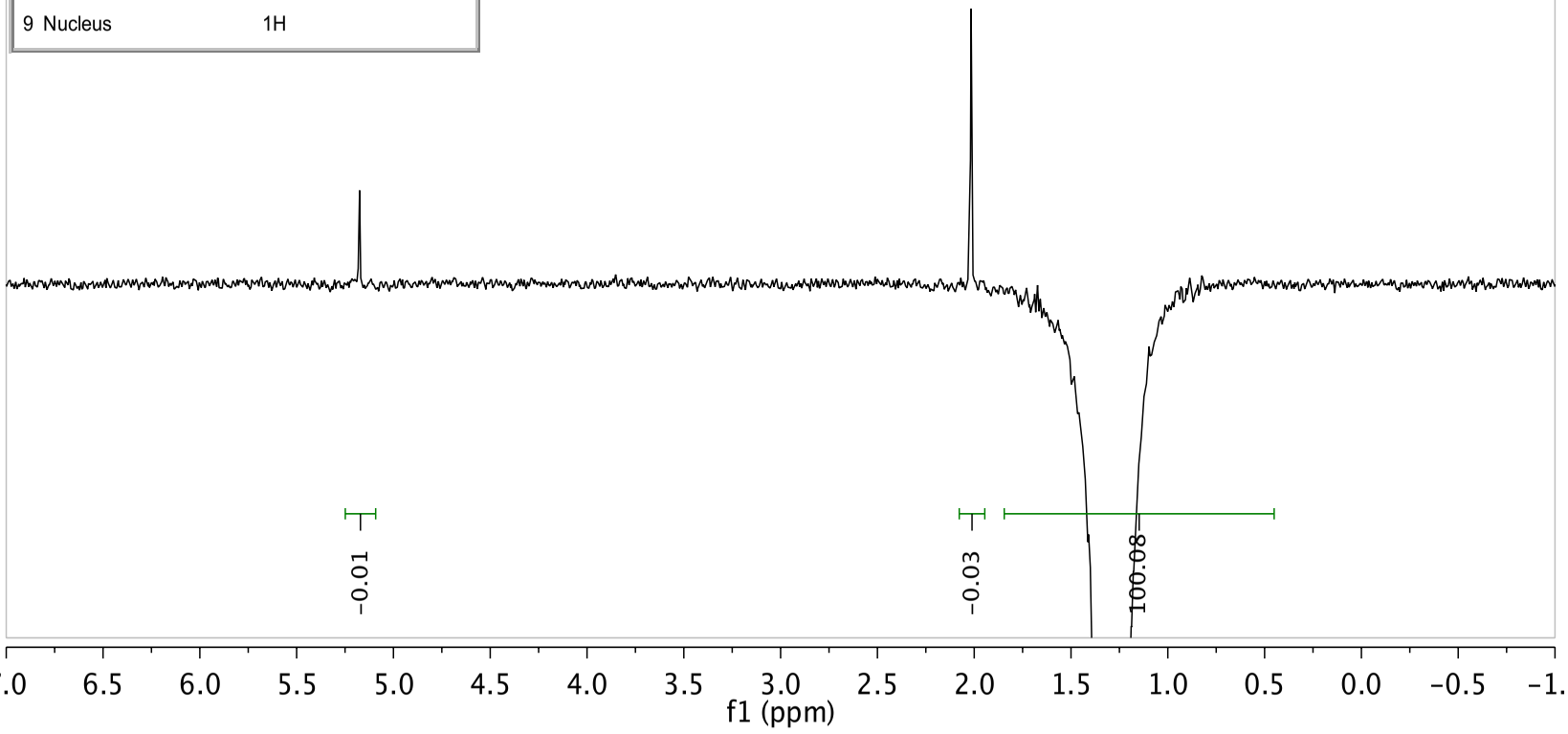

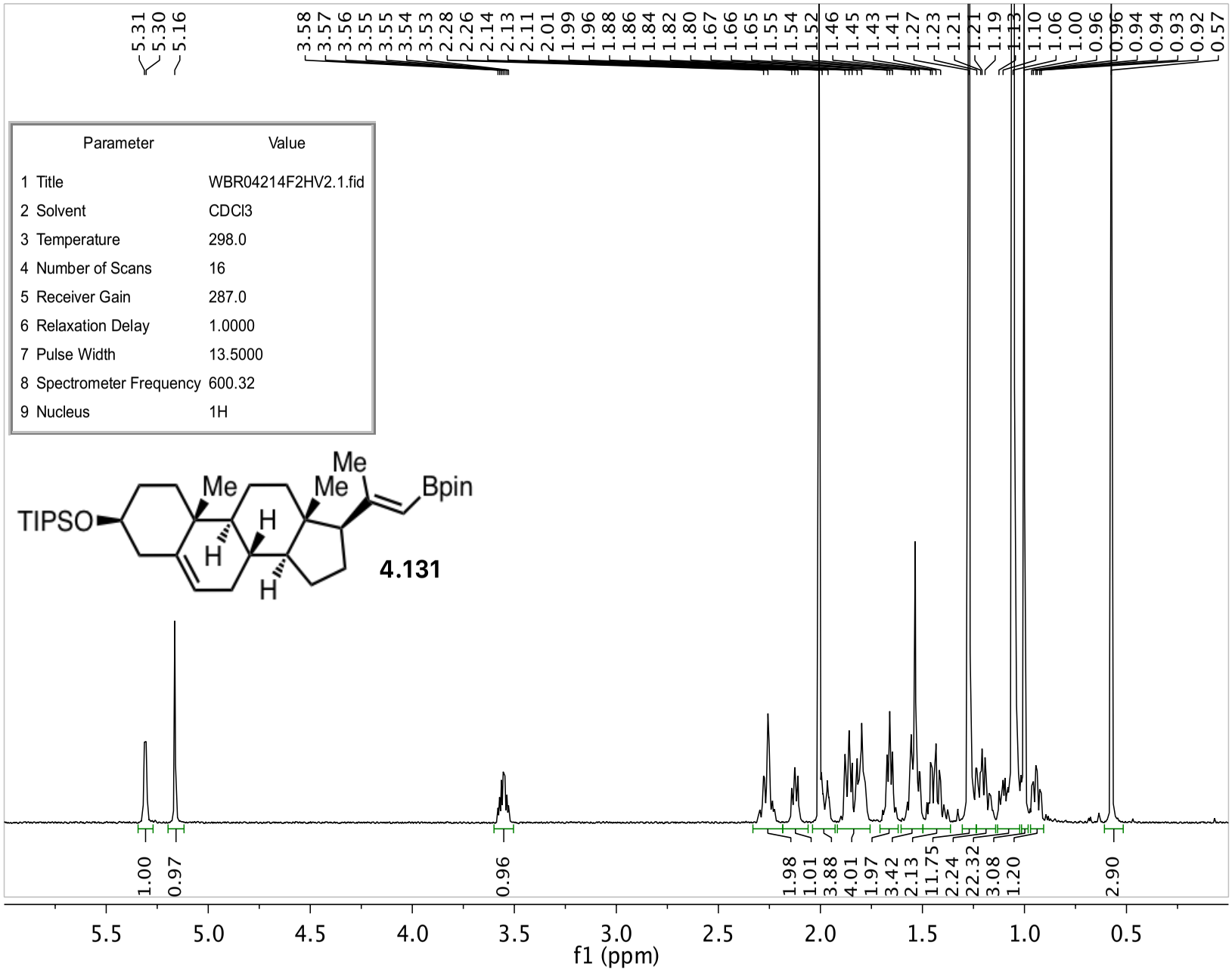
5.31
5.30
5.16
3.58
3.57
3.56
3.55
3.55
3.54
3.53
2.28
2.26
2.14
2.13
2.11
2.01
1.99
1.96
1.88
1.86
1.84
1.82
1.80
1.67
1.66
1.65
1.55
1.54
1.52
1.46
1.45
1.43
1.41
1.27
1.23
1.21
1.21
1.19
1.13
1.10
1.06
1.00
0.96
0.96
0.94
0.94
0.93
0.92
0.57
Parameter Value
1 Title WBR04214F2HV2.1.fid
2 Solvent CDCl3
3 Temperature 298.0
4 Number of Scans 16
5 Receiver Gain 287.0
6 Relaxation Delay 1.0000
7 Pulse Width 13.5000
8 Spectrometer Frequency 600.32
9 Nucleus 1H
TIPSO
Me
Me
Me
Bpin
H
H
H
4.131
1.00
0.97
0.96
1.98
1.01
3.88
4.01
1.97
3.42
2.13
11.75
2.24
22.32
3.08
1.20
2.90
5.5
5.0
4.5
4.0
3.5
3.0
2.5
2.0
1.5
1.0
0.5
f1 (ppm)

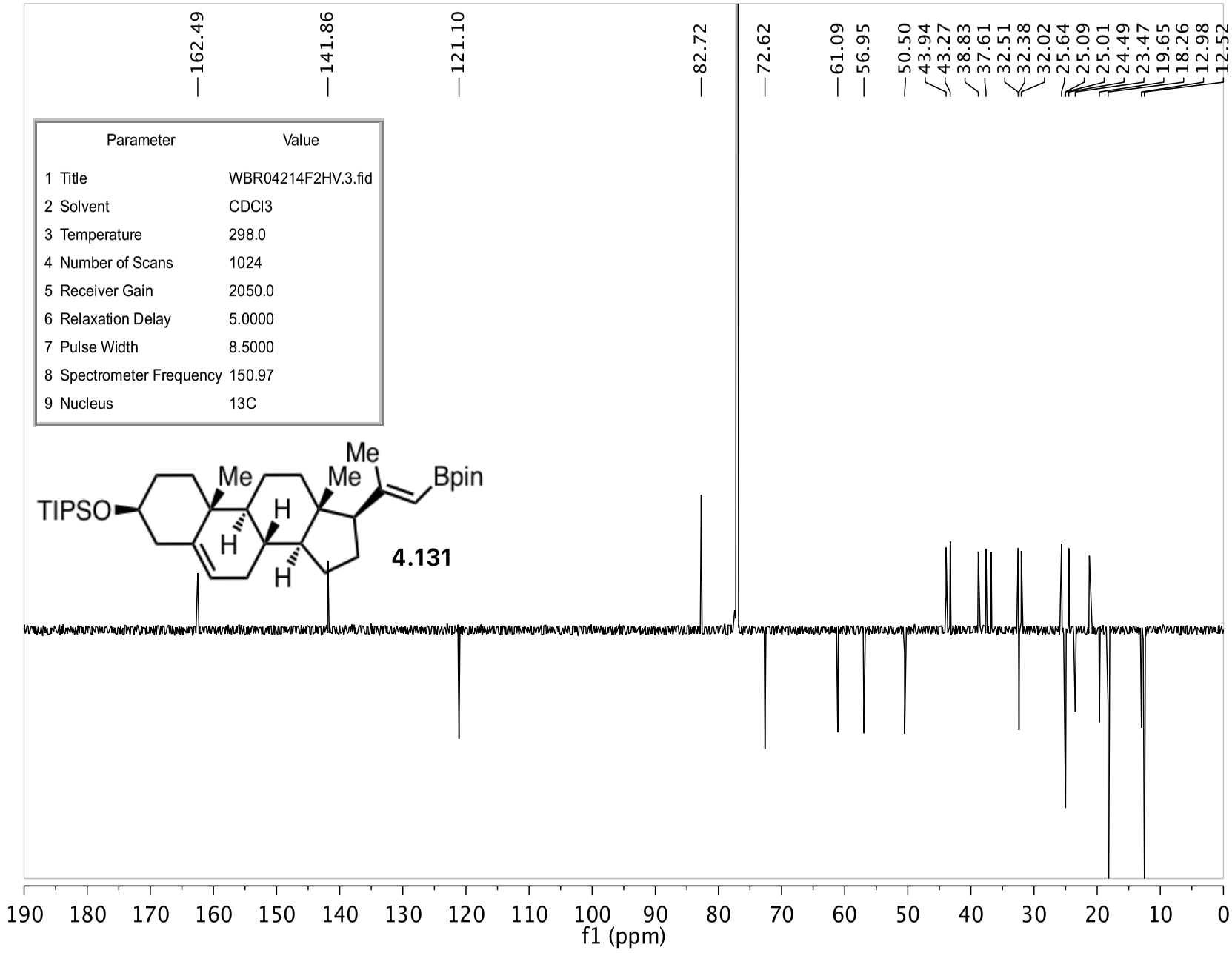
162.49
141.86
121.10
82.72
72.62
61.09
56.95
50.50
43.94
43.27
38.83
37.61
32.51
32.38
32.02
25.64
25.09
25.01
24.49
23.47
19.65
18.26
12.98
12.52
Parameter Value
1 Title WBR04214F2HV.3.fid
2 Solvent CDCl3
3 Temperature 298.0
4 Number of Scans 1024
5 Receiver Gain 2050.0
6 Relaxation Delay 5.0000
7 Pulse Width 8.5000
8 Spectrometer Frequency 150.97
9 Nucleus 13C
TIPSO
Me
Me
Me
Bpin
H
H
H
4.131
190 180 170 160 150 140 130 120 110 100 90 80 70 60 50 40 30 20 10 0
f1 (ppm)

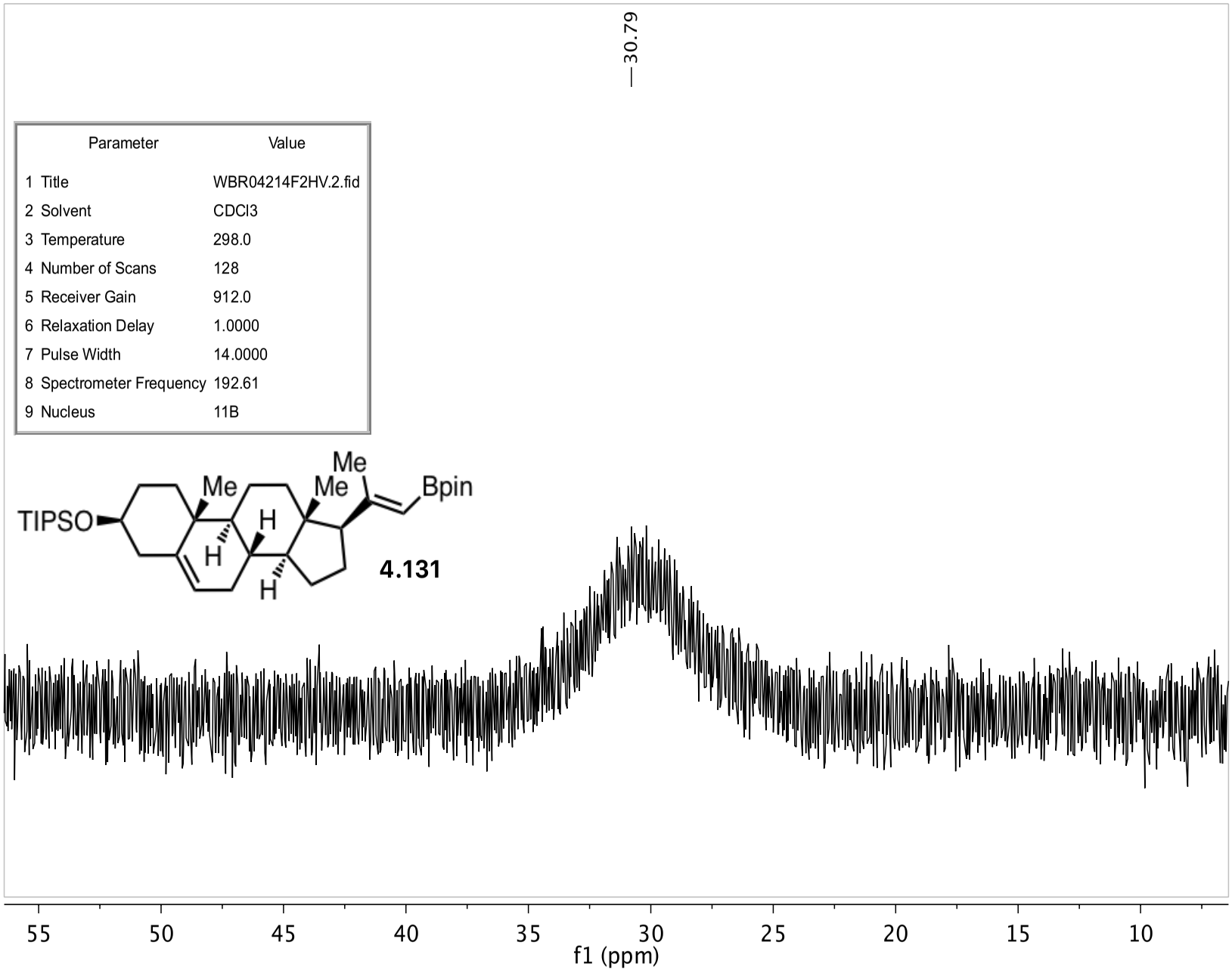
30.79
Parameter
Value
1 Title
WBR04214F2HV.2.fid
2 Solvent
CDCl3
3 Temperature
298.0
4 Number of Scans
128
5 Receiver Gain
912.0
6 Relaxation Delay
1.0000
7 Pulse Width
14.0000
8 Spectrometer Frequency
192.61
9 Nucleus
11B
TIPSO
Me
Me
Me
Bpin
H
H
H
4.131
55
50
45
40
35
30
25
20
15
10
f1 (ppm)

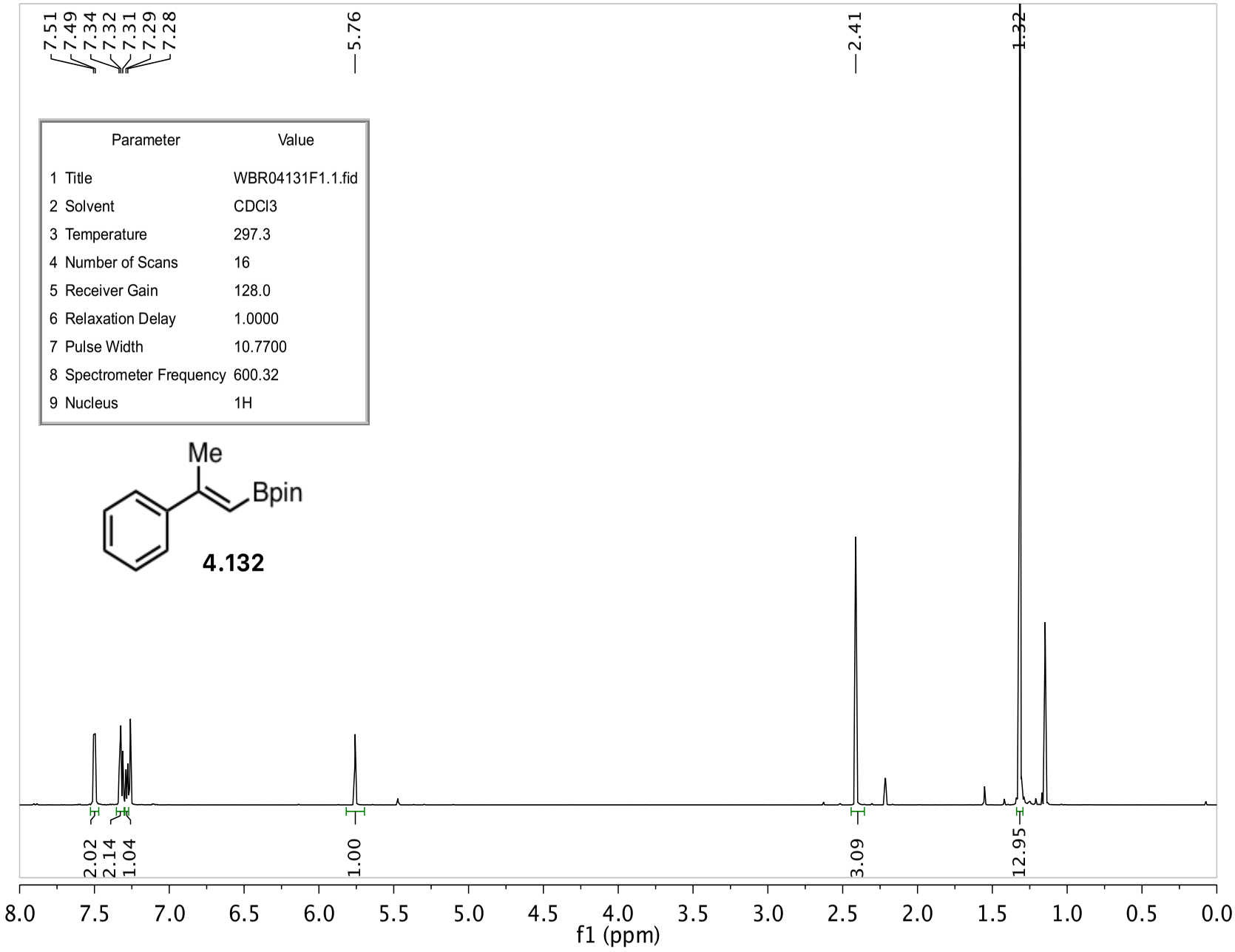
7.51
7.49
7.34
7.32
7.31
7.29
7.28
5.76
2.41
1.32
Parameter Value
1 Title WBR04131F1.1.fid
2 Solvent CDCl3
3 Temperature 297.3
4 Number of Scans 16
5 Receiver Gain 128.0
6 Relaxation Delay 1.0000
7 Pulse Width 10.7700
8 Spectrometer Frequency 600.32
9 Nucleus 1H
Me
Bpin
4.132
2.02
2.14
1.04
1.00
3.09
12.95
8.0 7.5 7.0 6.5 6.0 5.5 5.0 4.5 4.0 3.5 3.0 2.5 2.0 1.5 1.0 0.5 0.0
f1 (ppm)

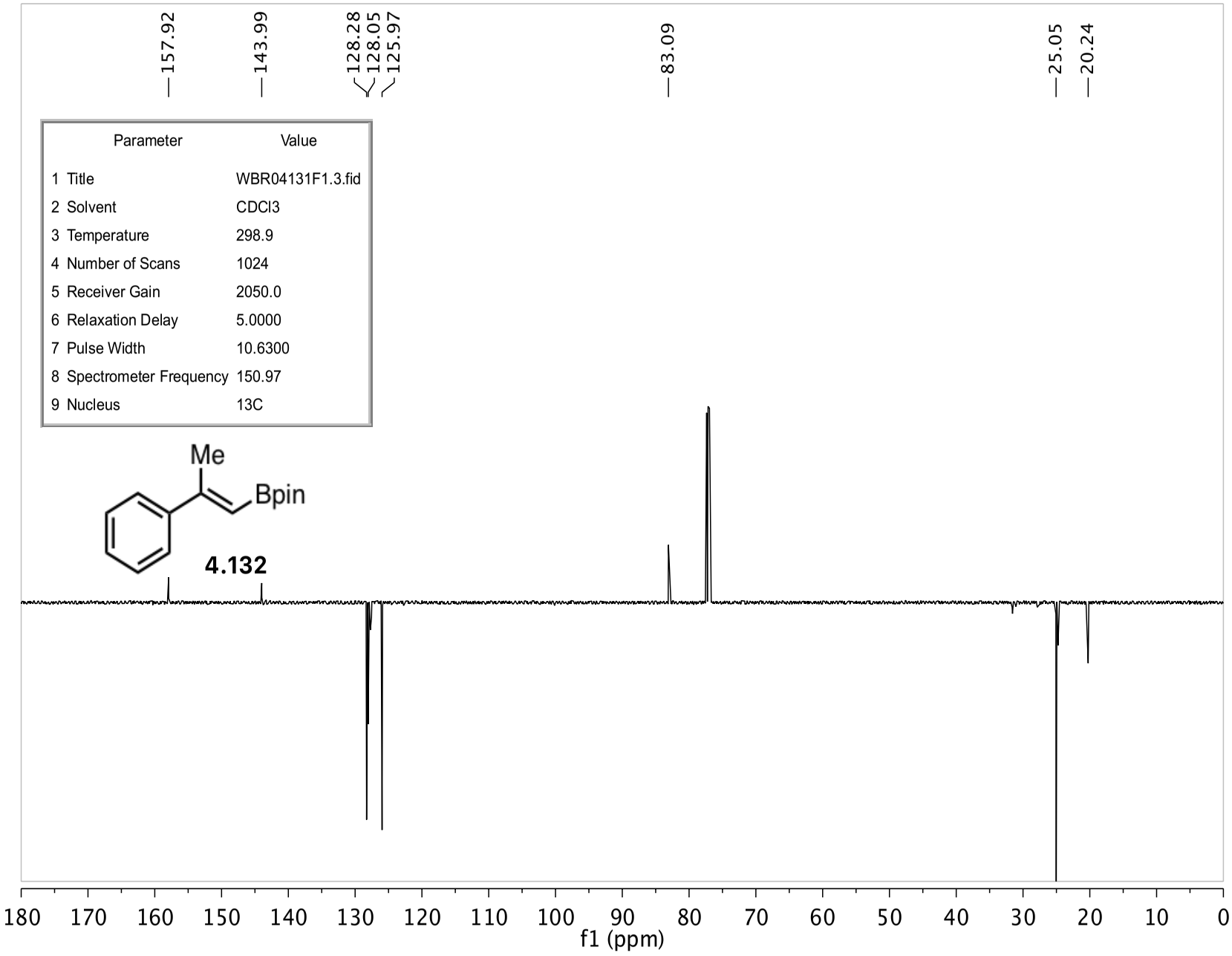
157.92
143.99
128.28
128.05
125.97
83.09
25.05
20.24
Parameter Value
1 Title WBR04131F1.3.fid
2 Solvent CDCl3
3 Temperature 298.9
4 Number of Scans 1024
5 Receiver Gain 2050.0
6 Relaxation Delay 5.0000
7 Pulse Width 10.6300
8 Spectrometer Frequency 150.97
9 Nucleus 13C
Me
Bpin
4.132
180 170 160 150 140 130 120 110 100 90 80 70 60 50 40 30 20 10 0
f1 (ppm)

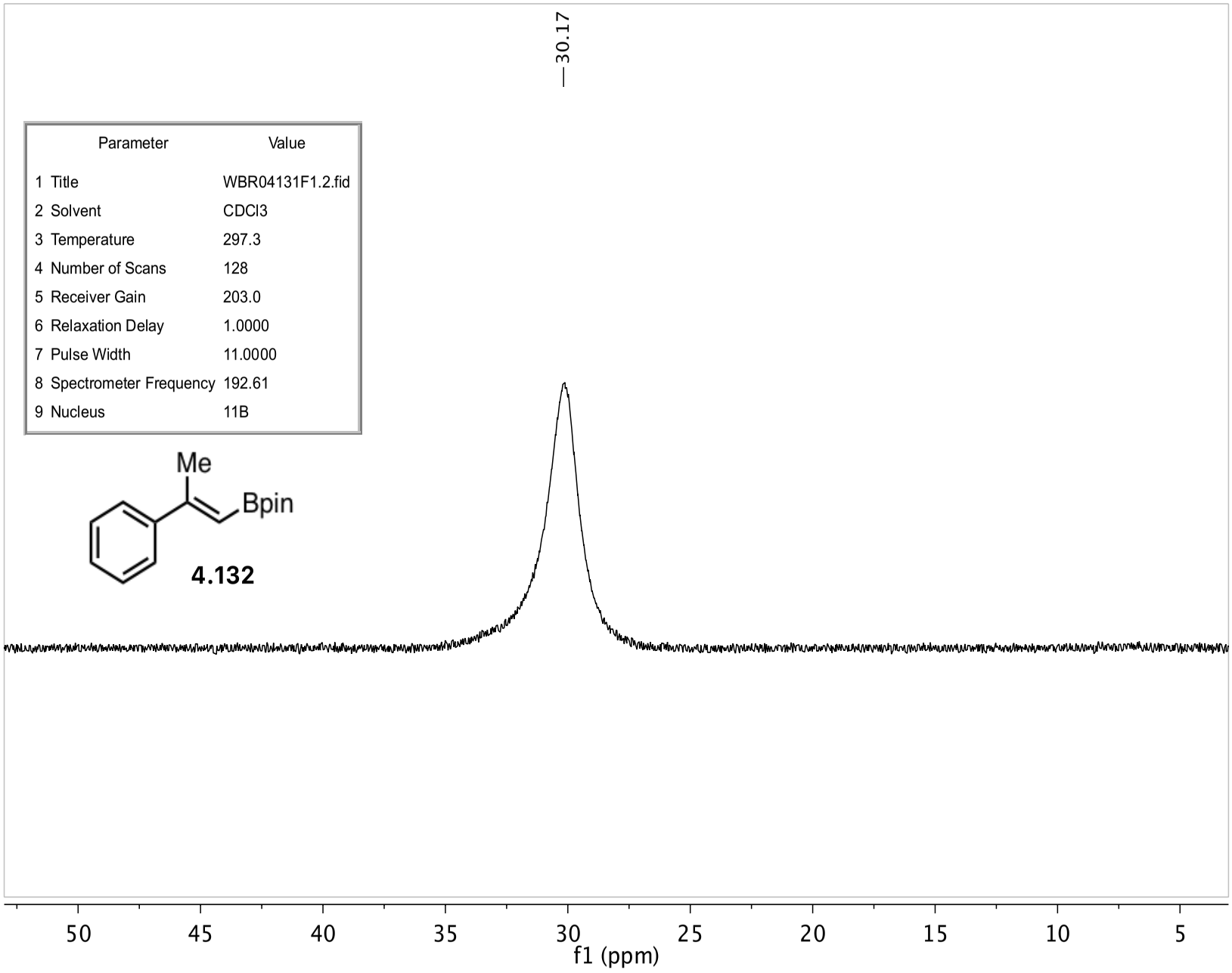
30.17
Parameter Value
1 Title WBR04131F1.2.fid
2 Solvent CDCl3
3 Temperature 297.3
4 Number of Scans 128
5 Receiver Gain 203.0
6 Relaxation Delay 1.0000
7 Pulse Width 11.0000
8 Spectrometer Frequency 192.61
9 Nucleus 11B
Me
Bpin
4.132
50 45 40 35 30 25 20 15 10 5
f1 (ppm)

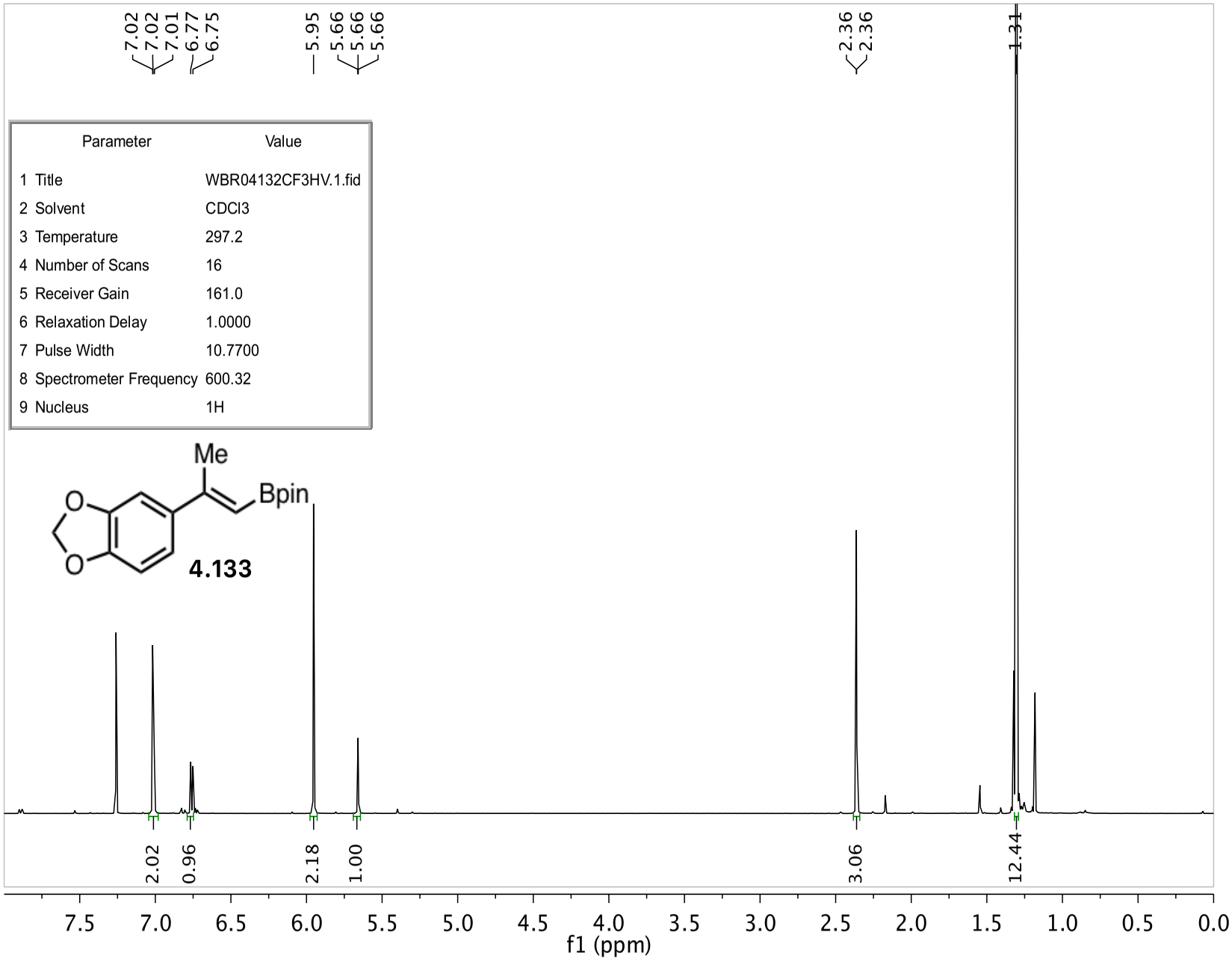
7.02
7.02
7.01
6.77
6.75
5.95
5.66
5.66
5.66
2.36
2.36
1.31
Parameter Value
1 Title WBR04132CF3HV.1.fid
2 Solvent CDCl3
3 Temperature 297.2
4 Number of Scans 16
5 Receiver Gain 161.0
6 Relaxation Delay 1.0000
7 Pulse Width 10.7700
8 Spectrometer Frequency 600.32
9 Nucleus 1H
Me
Bpin
O
O
4.133
2.02
0.96
2.18
1.00
3.06
12.44
7.5 7.0 6.5 6.0 5.5 5.0 4.5 4.0 3.5 3.0 2.5 2.0 1.5 1.0 0.5 0.0
f1 (ppm)

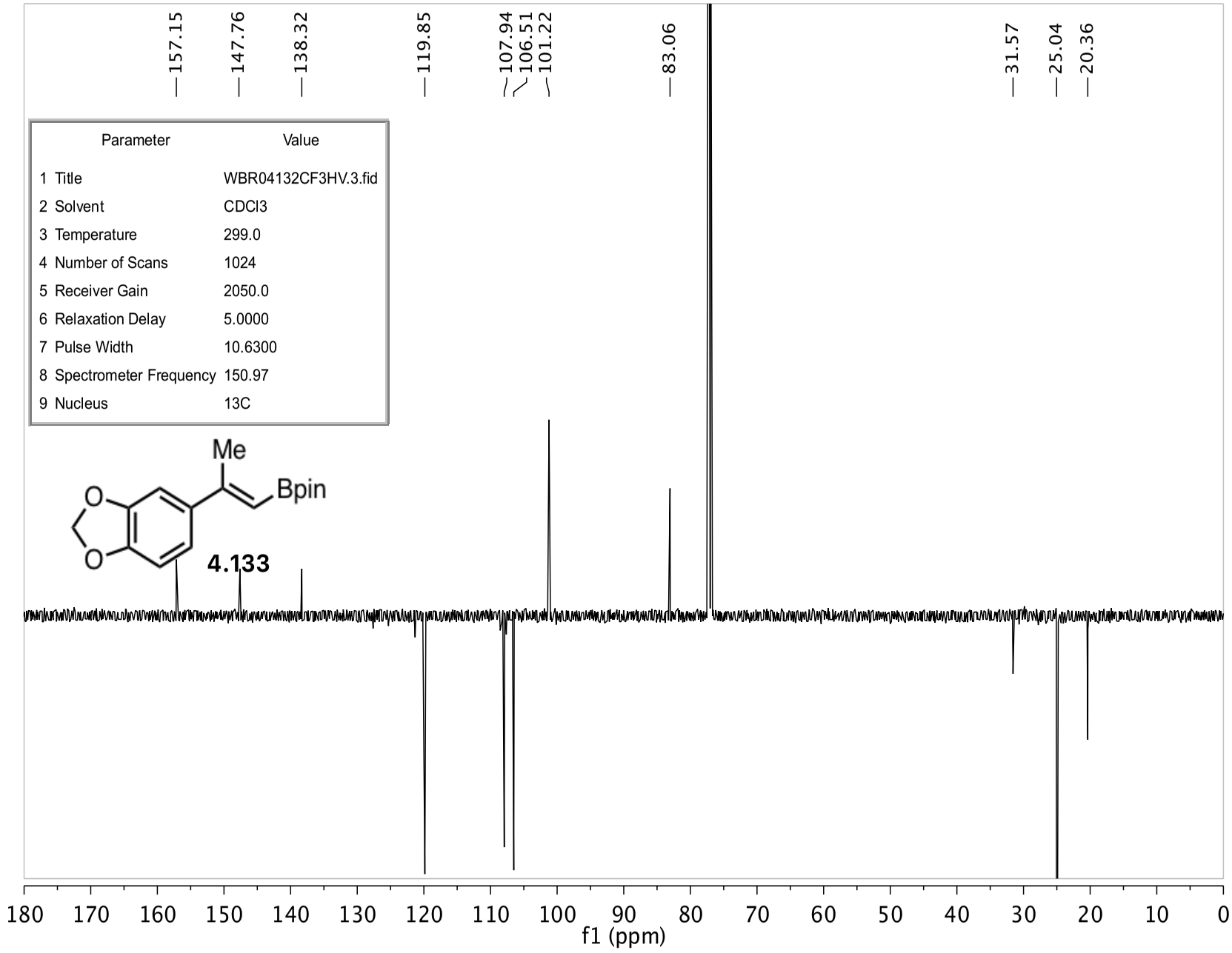
157.15
147.76
138.32
119.85
107.94
106.51
101.22
83.06
31.57
25.04
20.36
Parameter Value
1 Title WBR04132CF3HV.3.fid
2 Solvent CDCl3
3 Temperature 299.0
4 Number of Scans 1024
5 Receiver Gain 2050.0
6 Relaxation Delay 5.0000
7 Pulse Width 10.6300
8 Spectrometer Frequency 150.97
9 Nucleus 13C
Me
Bpin
O
O
4.133
180 170 160 150 140 130 120 110 100 90 80 70 60 50 40 30 20 10 0
f1 (ppm)

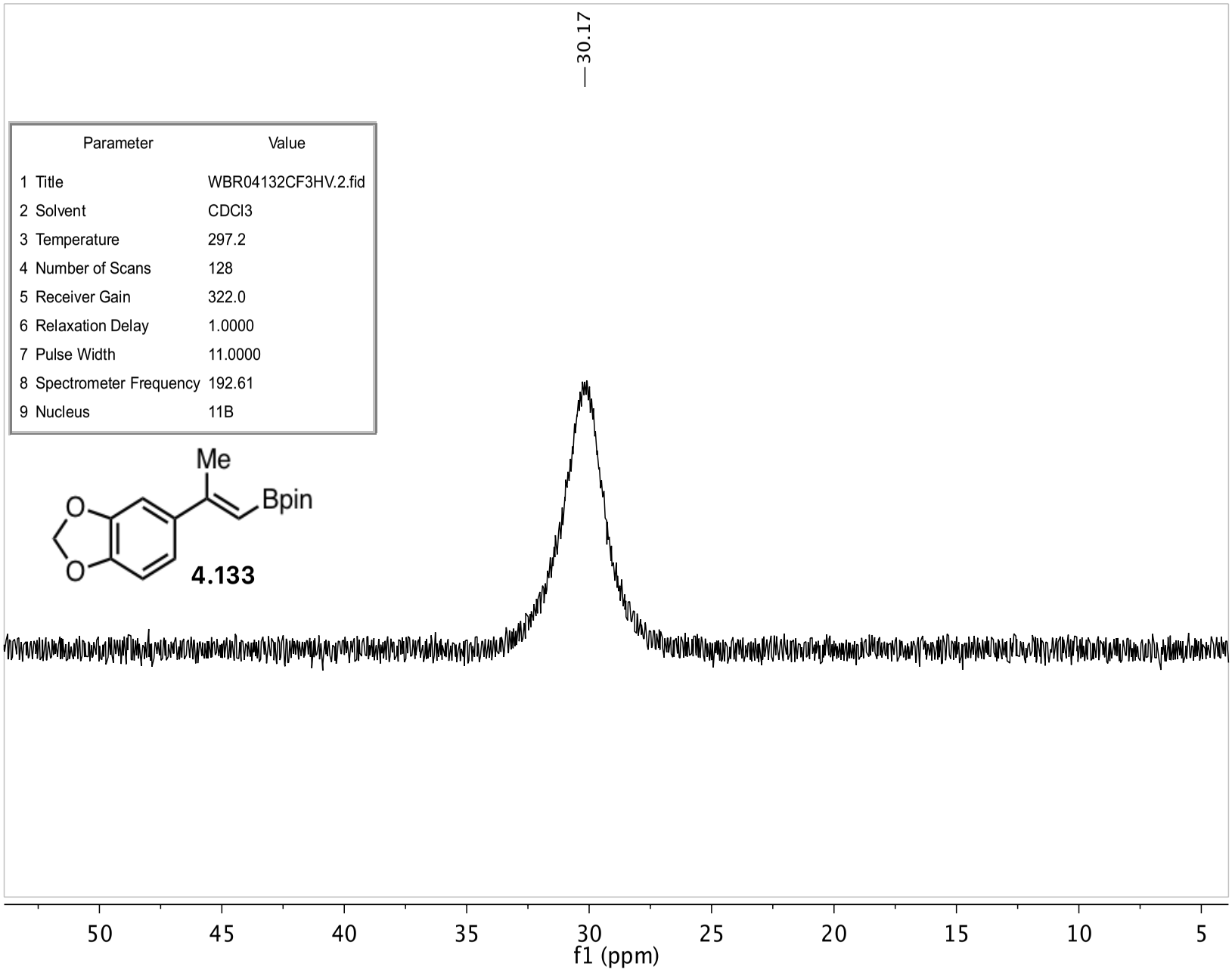
30.17
Parameter Value
1 Title WBR04132CF3HV.2.fid
2 Solvent CDCl3
3 Temperature 297.2
4 Number of Scans 128
5 Receiver Gain 322.0
6 Relaxation Delay 1.0000
7 Pulse Width 11.0000
8 Spectrometer Frequency 192.61
9 Nucleus 11B
Me
Bpin
O
O
4.133
50
45
40
35
30
25
20
15
10
5
f1 (ppm)

Parameter	Value
1 Title	WBR05080A 2.5.fid
2 Solvent	CDCl3
3 Temperature	300.0
4 Number of Scans	64
5 Receiver Gain	203.0
6 Relaxation Delay	2.0000
7 Pulse Width	13.8000
8 Spectrometer Frequency	400.15
9 Nucleus	1H

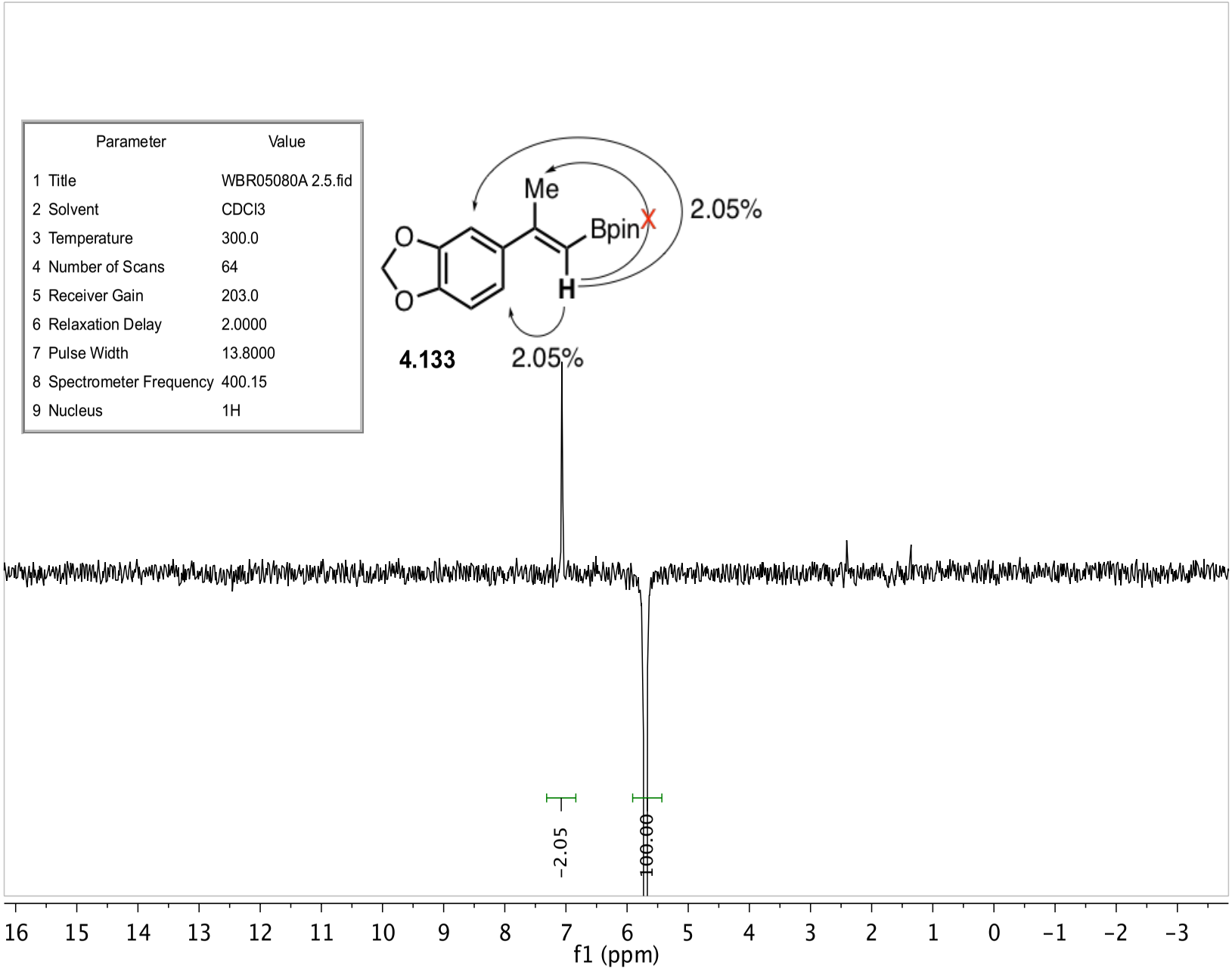

Parameter	Value
1 Title	WBR05080A 1.3.fid
2 Solvent	CDCl3
3 Temperature	300.0
4 Number of Scans	32
5 Receiver Gain	203.0
6 Relaxation Delay	2.0000
7 Pulse Width	13.8000
8 Spectrometer Frequency	400.15
9 Nucleus	1H

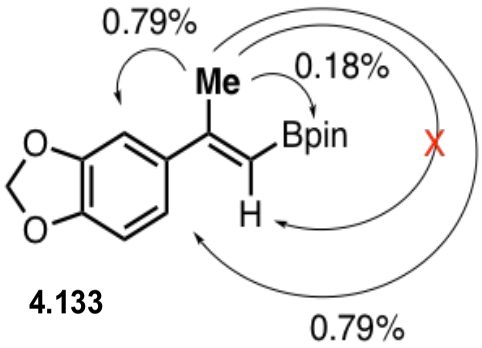

4.133

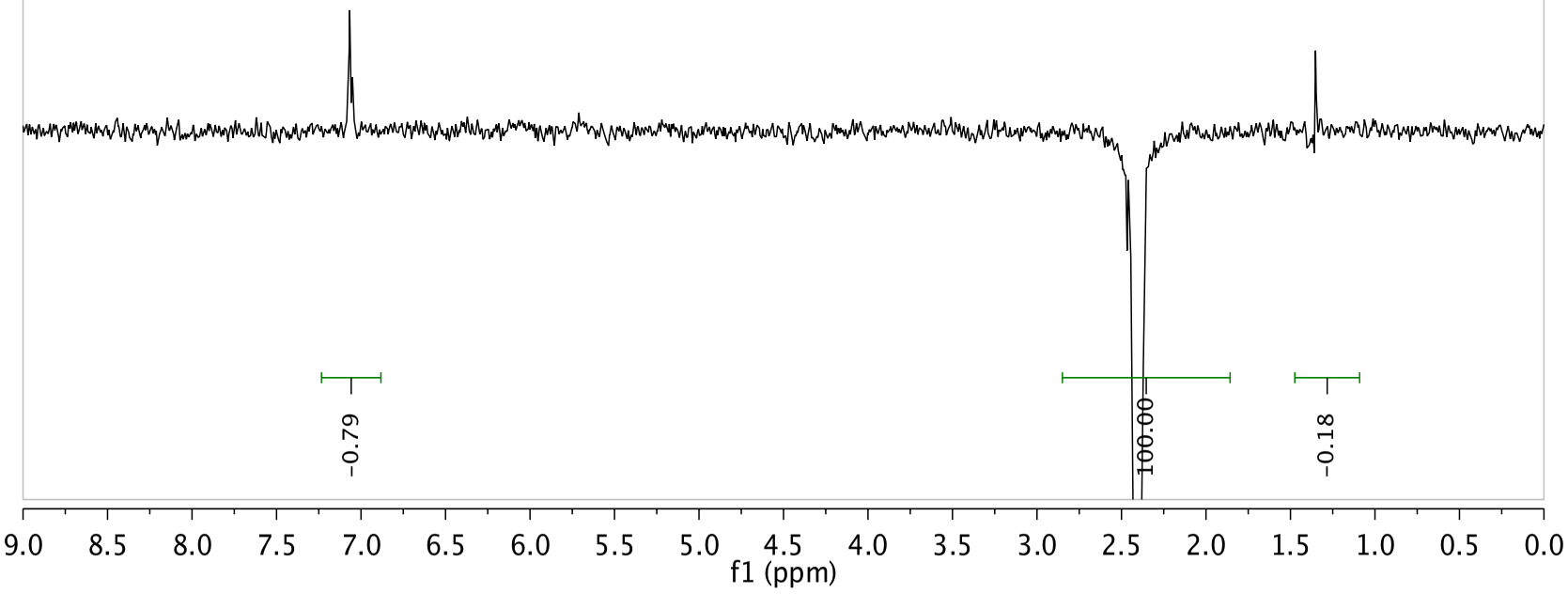

Parameter	Value
1 Title	WBR05080A 1.4.fid
2 Solvent	CDCl3
3 Temperature	300.0
4 Number of Scans	32
5 Receiver Gain	203.0
6 Relaxation Delay	2.0000
7 Pulse Width	13.8000
8 Spectrometer Frequency	400.15
9 Nucleus	1H

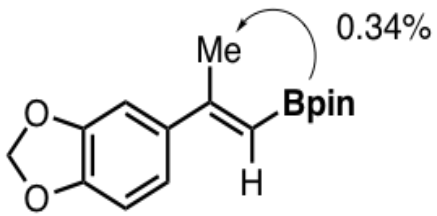

4.133

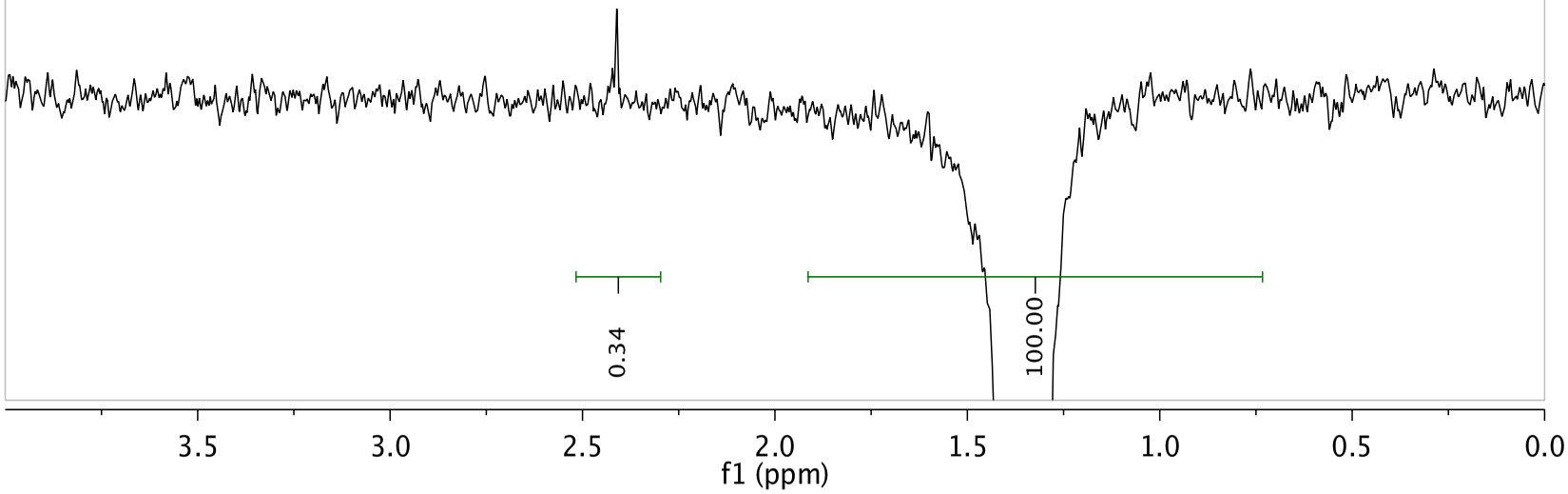

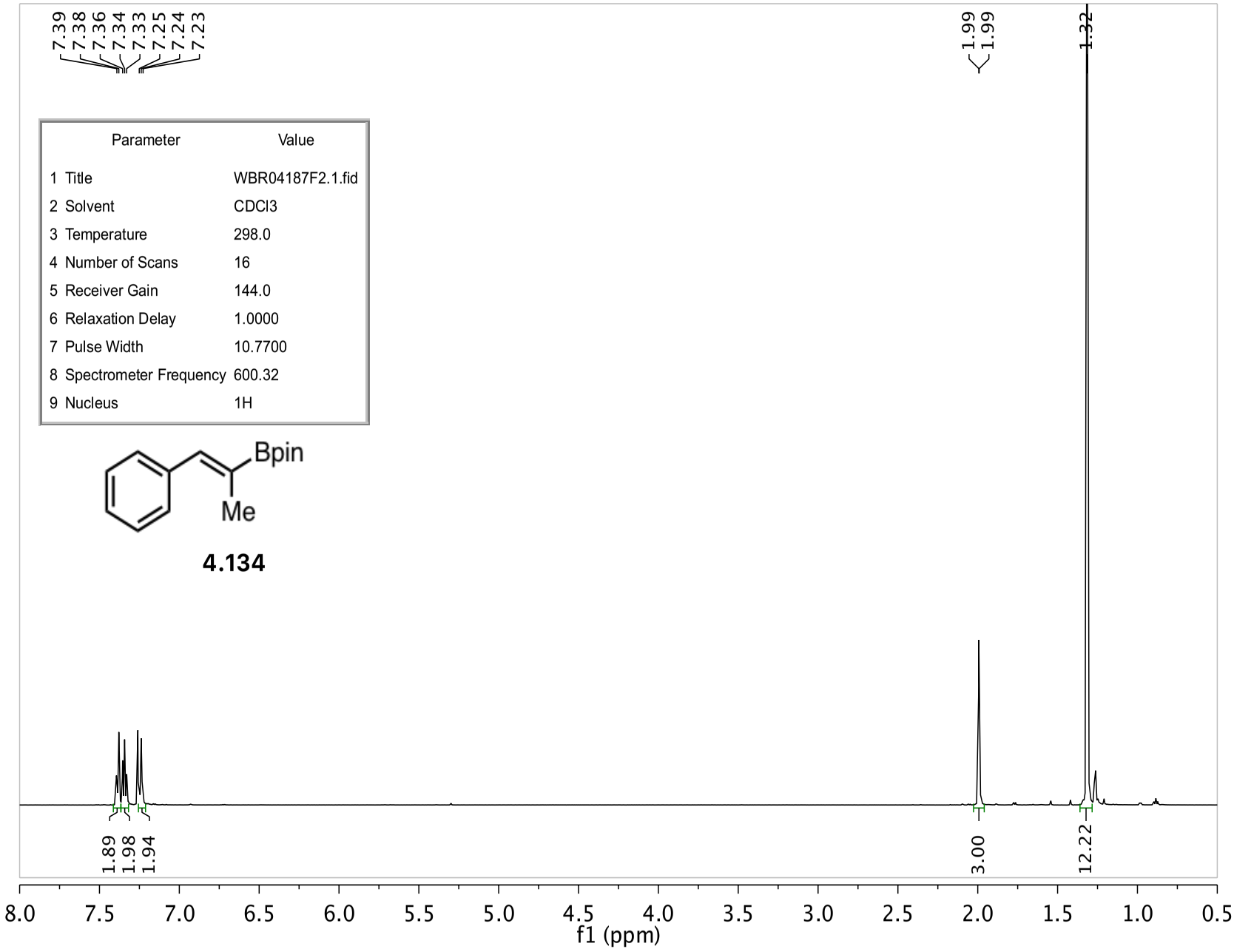
7.39
7.38
7.36
7.34
7.33
7.25
7.24
7.23
1.99
1.99
1.32
Parameter Value
1 Title WBR04187F2.1.fid
2 Solvent CDCl3
3 Temperature 298.0
4 Number of Scans 16
5 Receiver Gain 144.0
6 Relaxation Delay 1.0000
7 Pulse Width 10.7700
8 Spectrometer Frequency 600.32
9 Nucleus 1H
Bpin
Me
4.134
1.89
1.98
1.94
3.00
12.22
8.0
7.5
7.0
6.5
6.0
5.5
5.0
4.5
4.0
3.5
3.0
2.5
2.0
1.5
1.0
0.5
f1 (ppm)

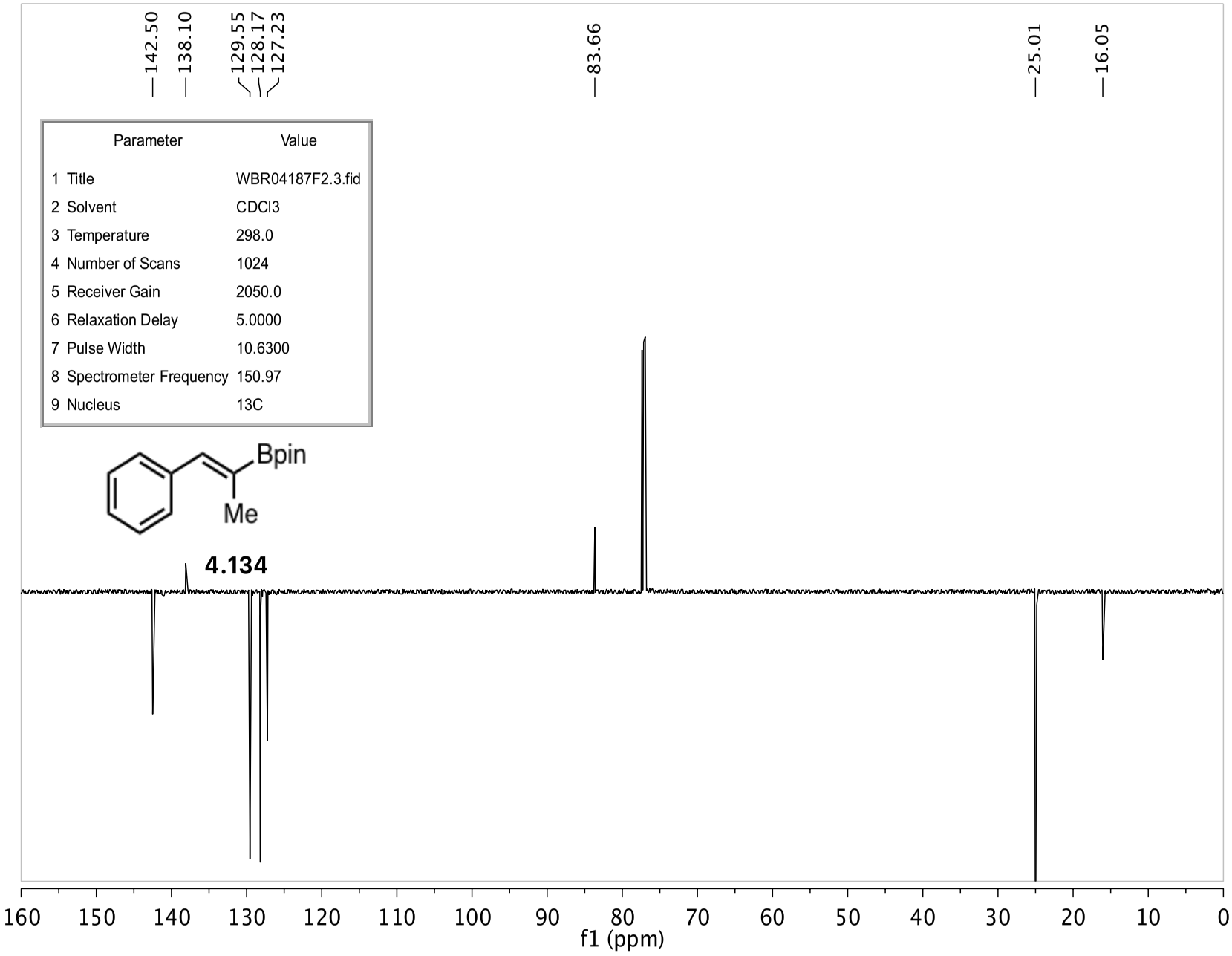
142.50
138.10
129.55
128.17
127.23
83.66
25.01
16.05
Parameter Value
1 Title WBR04187F2.3.fid
2 Solvent CDCl3
3 Temperature 298.0
4 Number of Scans 1024
5 Receiver Gain 2050.0
6 Relaxation Delay 5.0000
7 Pulse Width 10.6300
8 Spectrometer Frequency 150.97
9 Nucleus 13C
Bpin
Me
4.134
160 150 140 130 120 110 100 90 80 70 60 50 40 30 20 10 0
f1 (ppm)

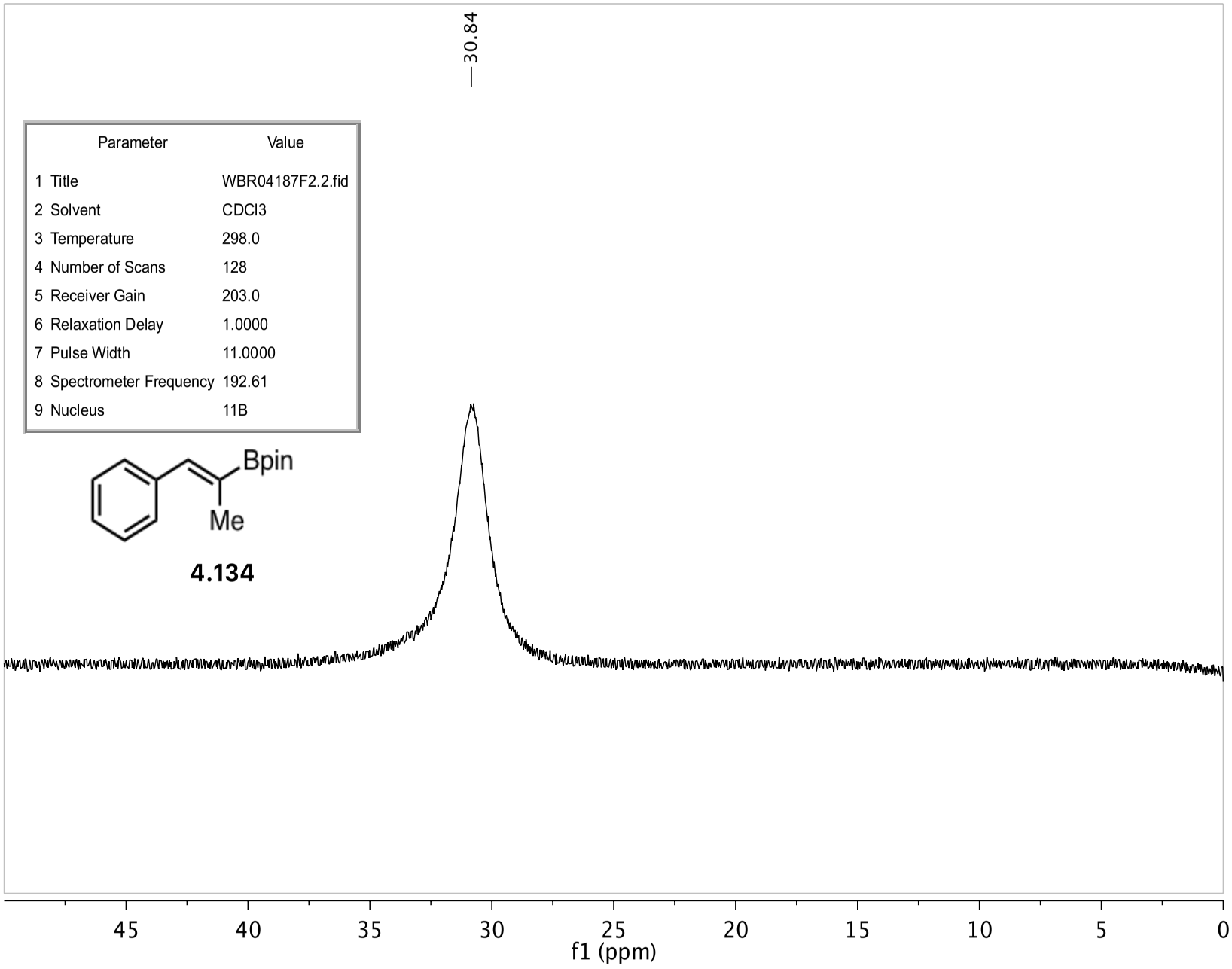
30.84
Parameter Value
1 Title WBR04187F2.2.fid
2 Solvent CDCl3
3 Temperature 298.0
4 Number of Scans 128
5 Receiver Gain 203.0
6 Relaxation Delay 1.0000
7 Pulse Width 11.0000
8 Spectrometer Frequency 192.61
9 Nucleus 11B
Bpin
Me
4.134
45
40
35
30
25
20
15
10
5
0
f1 (ppm)

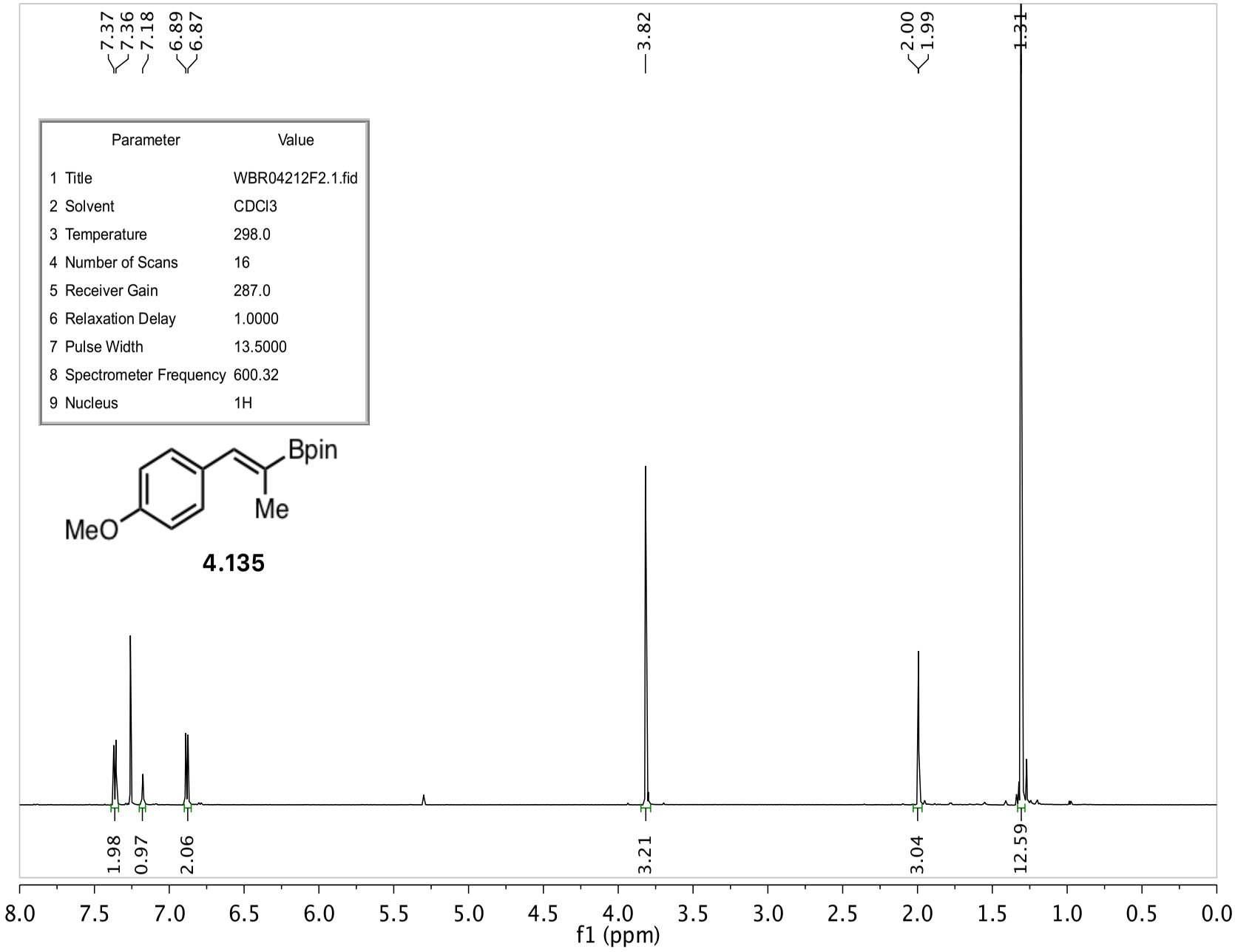
7.37
7.36
7.18
6.89
6.87
3.82
2.00
1.99
1.31
Parameter Value
1 Title WBR04212F2.1.fid
2 Solvent CDCl3
3 Temperature 298.0
4 Number of Scans 16
5 Receiver Gain 287.0
6 Relaxation Delay 1.0000
7 Pulse Width 13.5000
8 Spectrometer Frequency 600.32
9 Nucleus 1H
Bpin
Me
MeO
4.135
1.98
0.97
2.06
3.21
3.04
12.59
8.0 7.5 7.0 6.5 6.0 5.5 5.0 4.5 4.0 3.5 3.0 2.5 2.0 1.5 1.0 0.5 0.0
f1 (ppm)

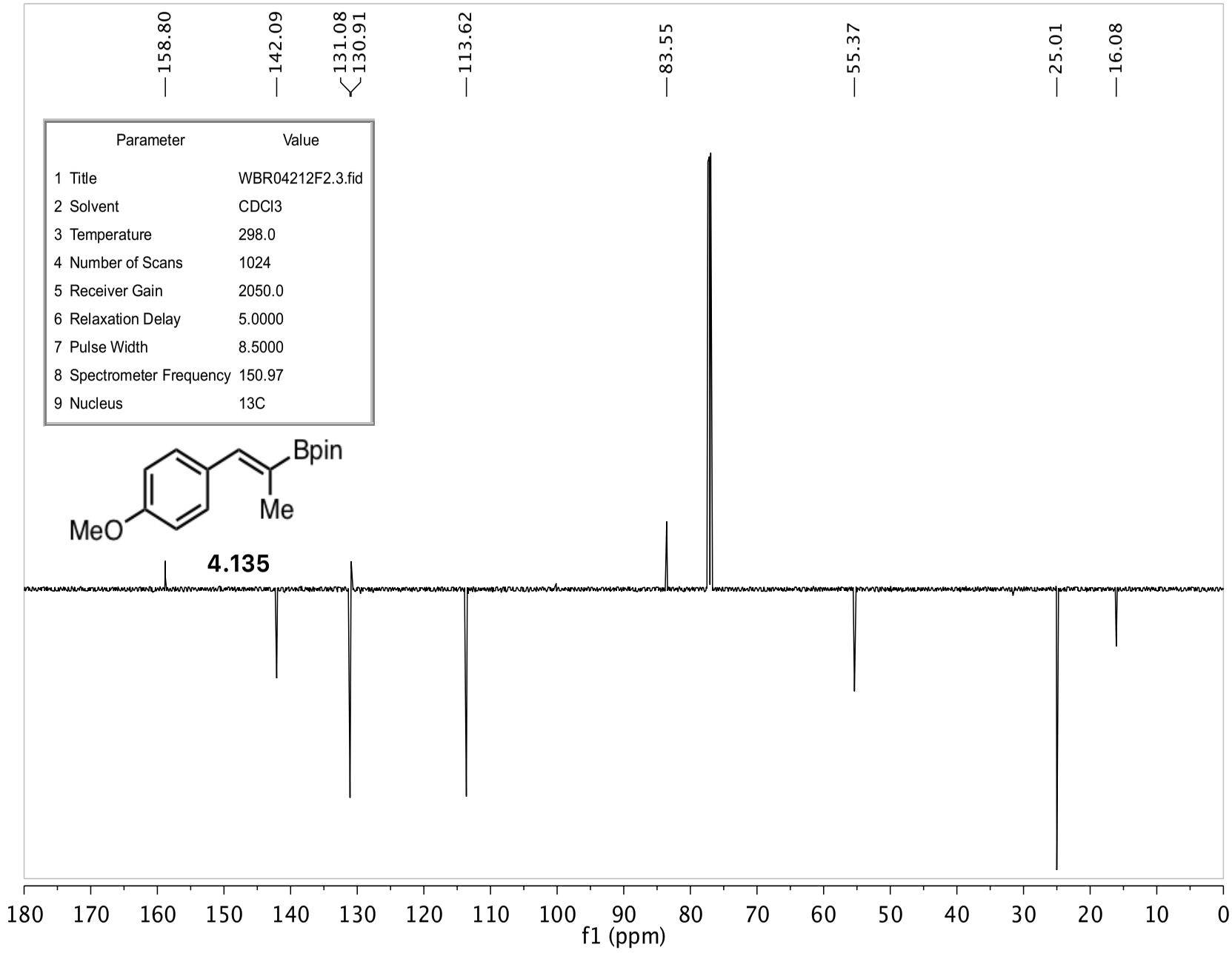
158.80
142.09
131.08
130.91
113.62
83.55
55.37
25.01
16.08
Parameter Value
1 Title WBR04212F2.3.fid
2 Solvent CDCl3
3 Temperature 298.0
4 Number of Scans 1024
5 Receiver Gain 2050.0
6 Relaxation Delay 5.0000
7 Pulse Width 8.5000
8 Spectrometer Frequency 150.97
9 Nucleus 13C
Bpin
Me
MeO
4.135
180 170 160 150 140 130 120 110 100 90 80 70 60 50 40 30 20 10 0
f1 (ppm)

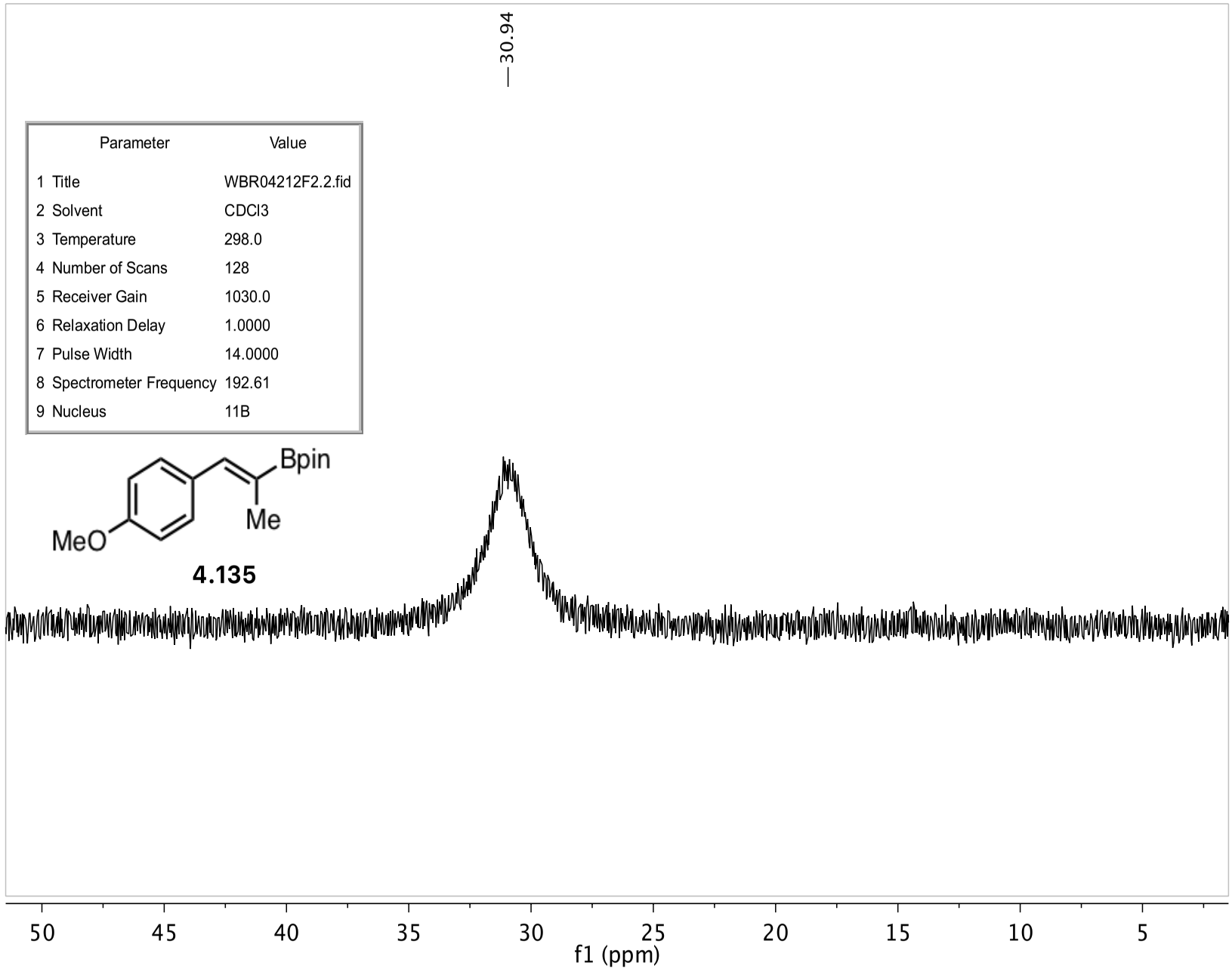
30.94
Parameter Value
1 Title WBR04212F2.2.fid
2 Solvent CDCl3
3 Temperature 298.0
4 Number of Scans 128
5 Receiver Gain 1030.0
6 Relaxation Delay 1.0000
7 Pulse Width 14.0000
8 Spectrometer Frequency 192.61
9 Nucleus 11B
Bpin
Me
MeO
4.135
50 45 40 35 30 25 20 15 10 5
f1 (ppm)

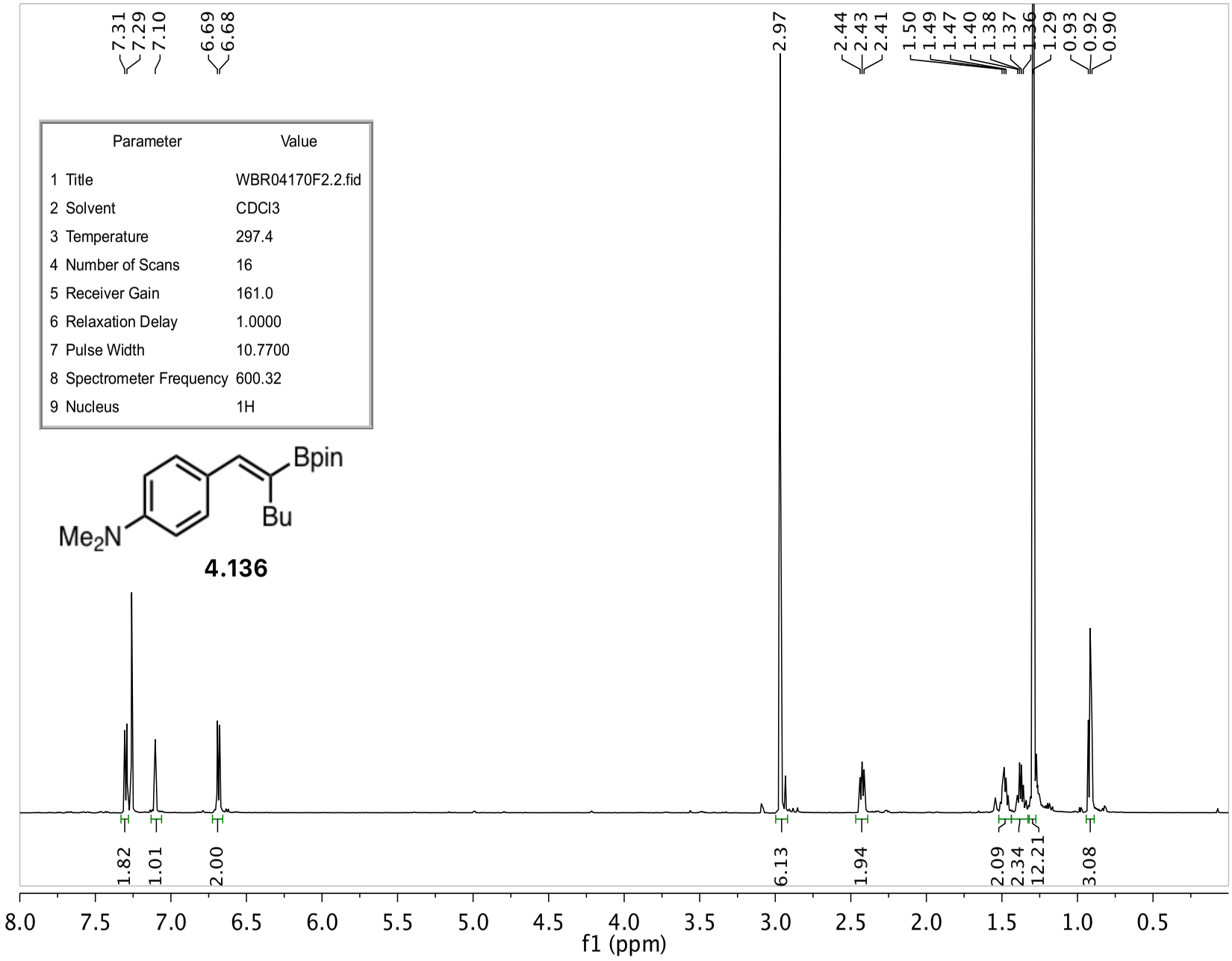
7.31
7.29
7.10
6.69
6.68
2.97
2.44
2.43
2.41
1.50
1.49
1.47
1.40
1.38
1.37
1.36
1.29
0.93
0.92
0.90
Parameter Value
1 Title WBR04170F2.2.fid
2 Solvent CDCl3
3 Temperature 297.4
4 Number of Scans 16
5 Receiver Gain 161.0
6 Relaxation Delay 1.0000
7 Pulse Width 10.7700
8 Spectrometer Frequency 600.32
9 Nucleus 1H
Bpin
Bu
Me2N
4.136
1.82
1.01
2.00
6.13
1.94
2.09
2.34
12.21
3.08
8.0
7.5
7.0
6.5
6.0
5.5
5.0
4.5
4.0
3.5
3.0
2.5
2.0
1.5
1.0
0.5
f1 (ppm)

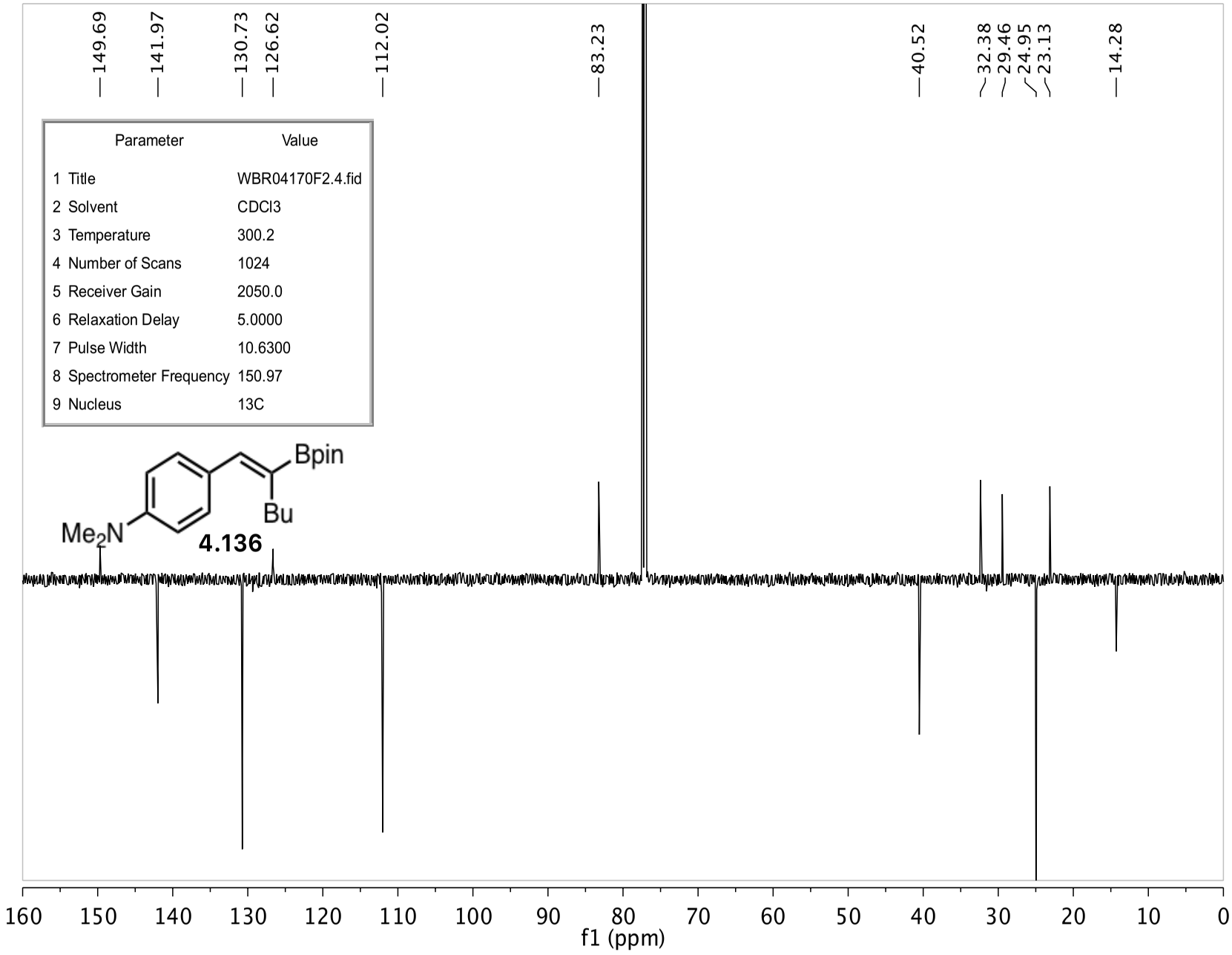
149.69
141.97
130.73
126.62
112.02
83.23
40.52
32.38
29.46
24.95
23.13
14.28
Parameter Value
1 Title WBR04170F2.4.fid
2 Solvent CDCl3
3 Temperature 300.2
4 Number of Scans 1024
5 Receiver Gain 2050.0
6 Relaxation Delay 5.0000
7 Pulse Width 10.6300
8 Spectrometer Frequency 150.97
9 Nucleus 13C
Bpin
Bu
Me2N
4.136
160 150 140 130 120 110 100 90 80 70 60 50 40 30 20 10 0
f1 (ppm)

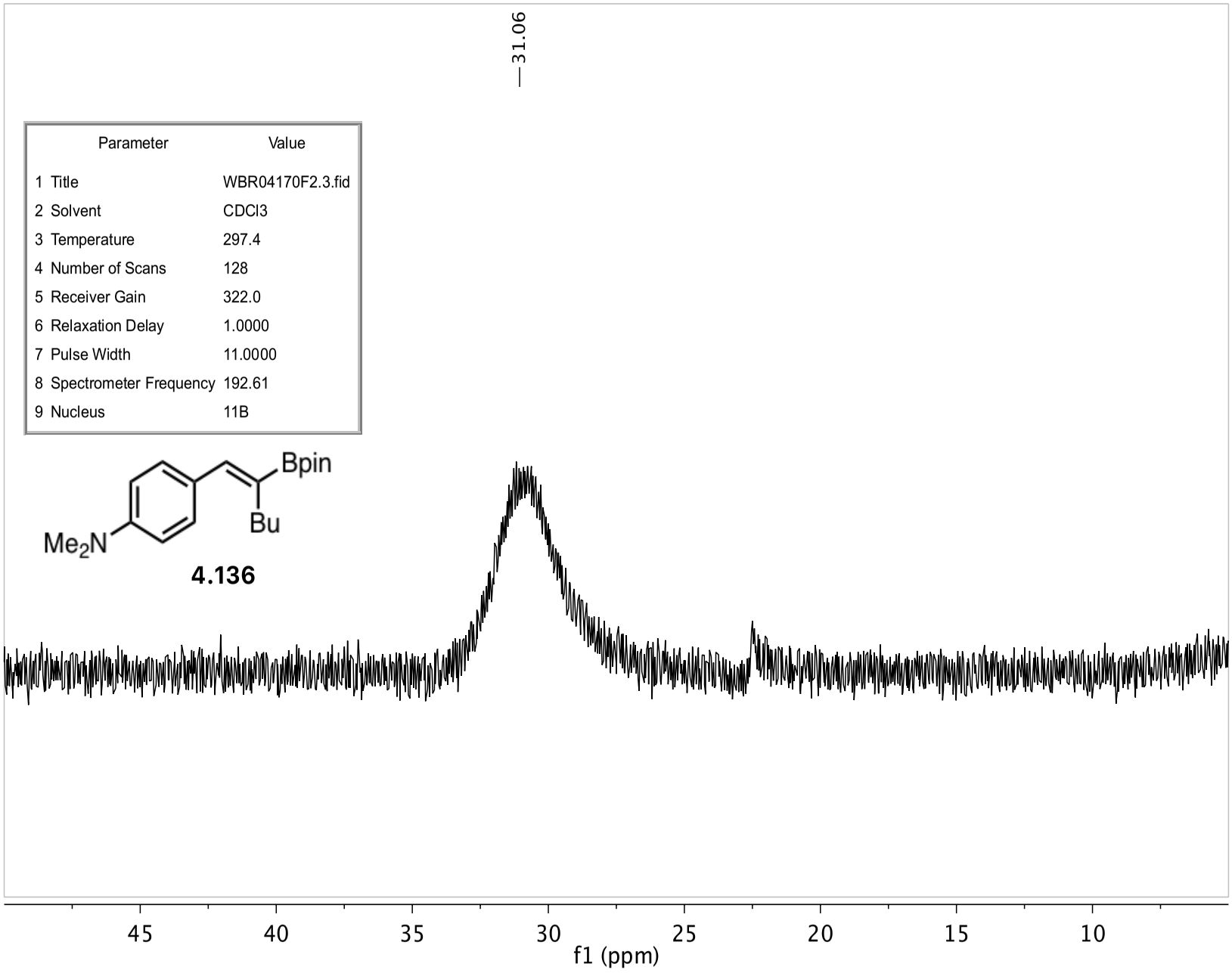
31.06
Parameter Value
1 Title WBR04170F2.3.fid
2 Solvent CDCl3
3 Temperature 297.4
4 Number of Scans 128
5 Receiver Gain 322.0
6 Relaxation Delay 1.0000
7 Pulse Width 11.0000
8 Spectrometer Frequency 192.61
9 Nucleus 11B
Bpin
Bu
Me2N
4.136
45
40
35
30
25
20
15
10
f1 (ppm)

Parameter	Value
1 Title	WBR05080D_2D.3.fid
2 Solvent	CDCl3
3 Temperature	299.4
4 Number of Scans	32
5 Receiver Gain	203.0
6 Relaxation Delay	2.0000
7 Pulse Width	15.9700
8 Spectrometer Frequency	400.15
9 Nucleus	1H

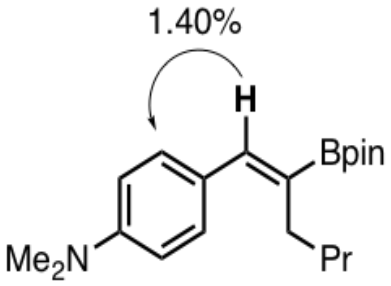

4.136

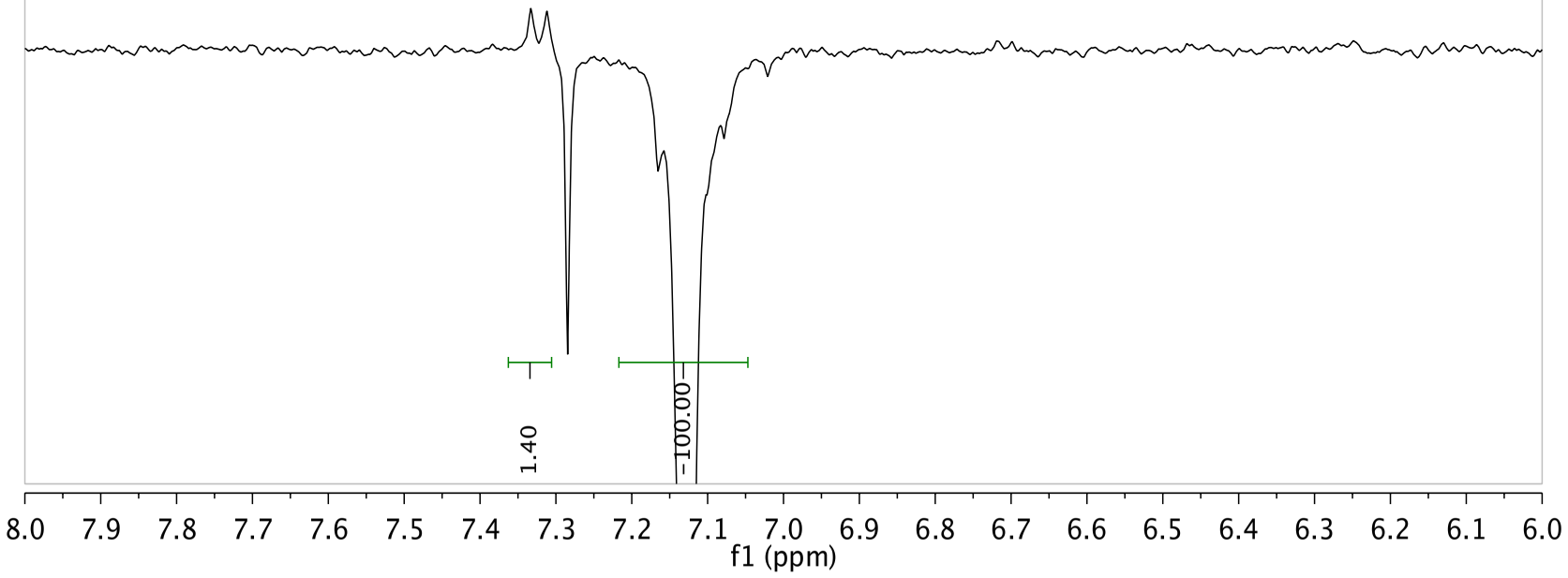

Parameter	Value
1 Title	WBR05080D_2D.6.fid
2 Solvent	CDCl3
3 Temperature	299.4
4 Number of Scans	32
5 Receiver Gain	203.0
6 Relaxation Delay	2.0000
7 Pulse Width	15.9700
8 Spectrometer Frequency	400.15
9 Nucleus	1H

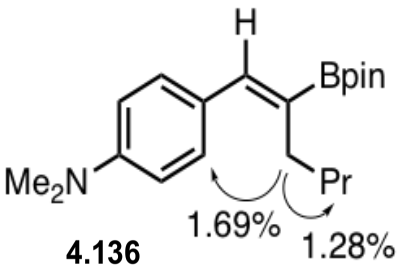

4.136

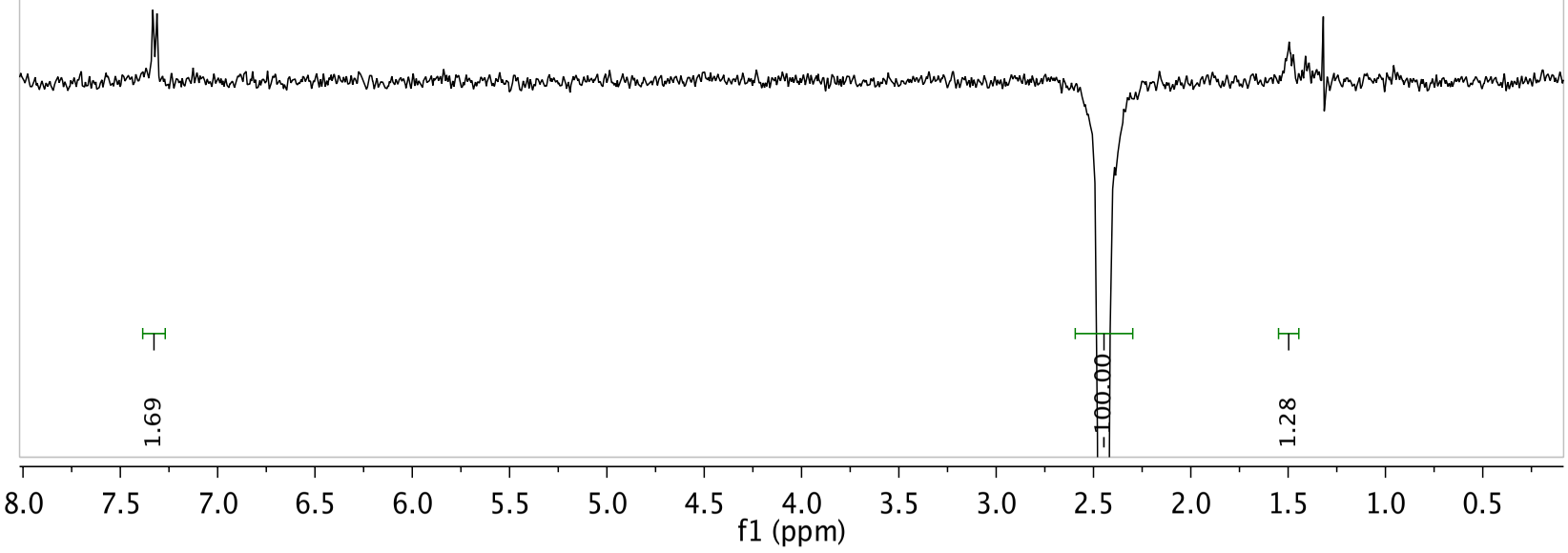

Parameter	Value
1 Title	WBR05080D_2D.9.fid
2 Solvent	CDCl3
3 Temperature	299.4
4 Number of Scans	32
5 Receiver Gain	203.0
6 Relaxation Delay	2.0000
7 Pulse Width	15.9700
8 Spectrometer Frequency	400.15
9 Nucleus	1H

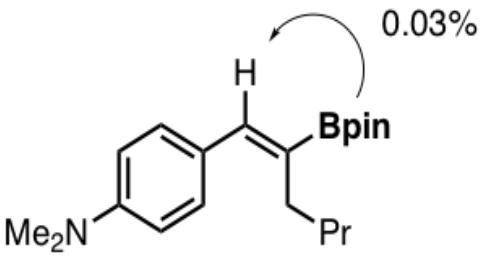

4.136

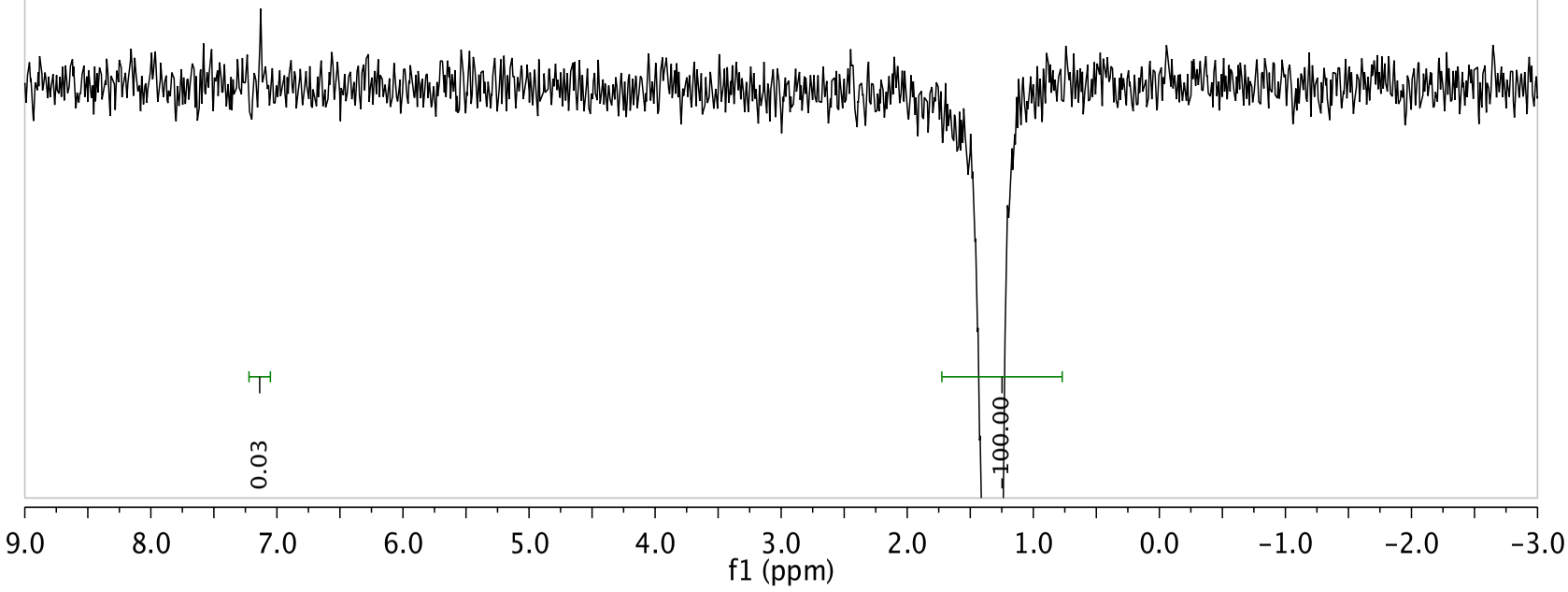

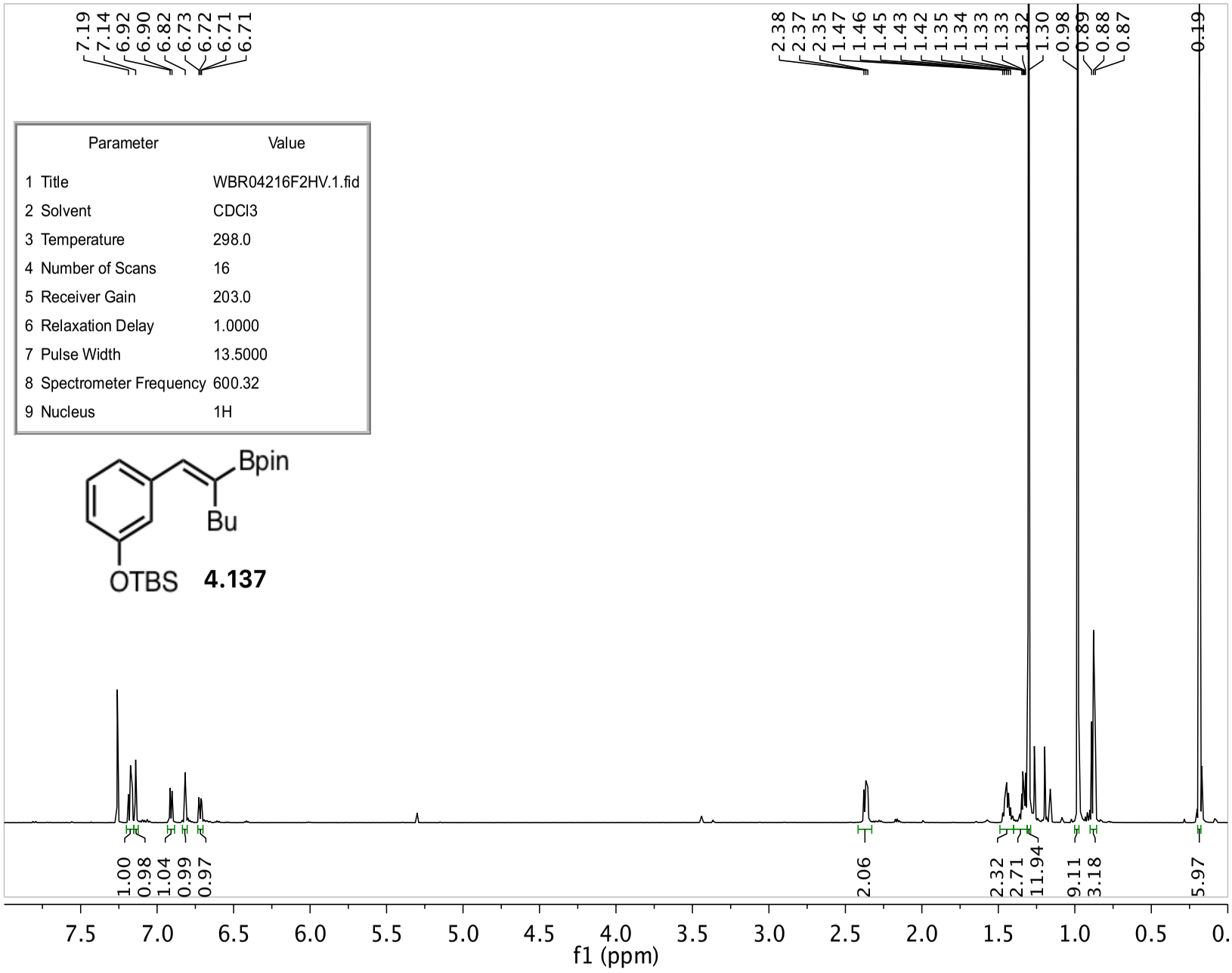
7.19
7.14
6.92
6.90
6.82
6.73
6.72
6.71
6.71
2.38
2.37
2.35
1.47
1.46
1.45
1.43
1.42
1.35
1.34
1.33
1.33
1.32
1.30
0.98
0.89
0.88
0.87
0.19
Parameter Value
1 Title WBR04216F2HV.1.fid
2 Solvent CDCl3
3 Temperature 298.0
4 Number of Scans 16
5 Receiver Gain 203.0
6 Relaxation Delay 1.0000
7 Pulse Width 13.5000
8 Spectrometer Frequency 600.32
9 Nucleus 1H
Bpin
Bu
OTBS
4.137
1.00
0.98
1.04
0.99
0.97
2.06
2.32
2.71
11.94
9.11
3.18
5.97
7.5
7.0
6.5
6.0
5.5
5.0
4.5
4.0
3.5
3.0
2.5
2.0
1.5
1.0
0.5
0.0
f1 (ppm)

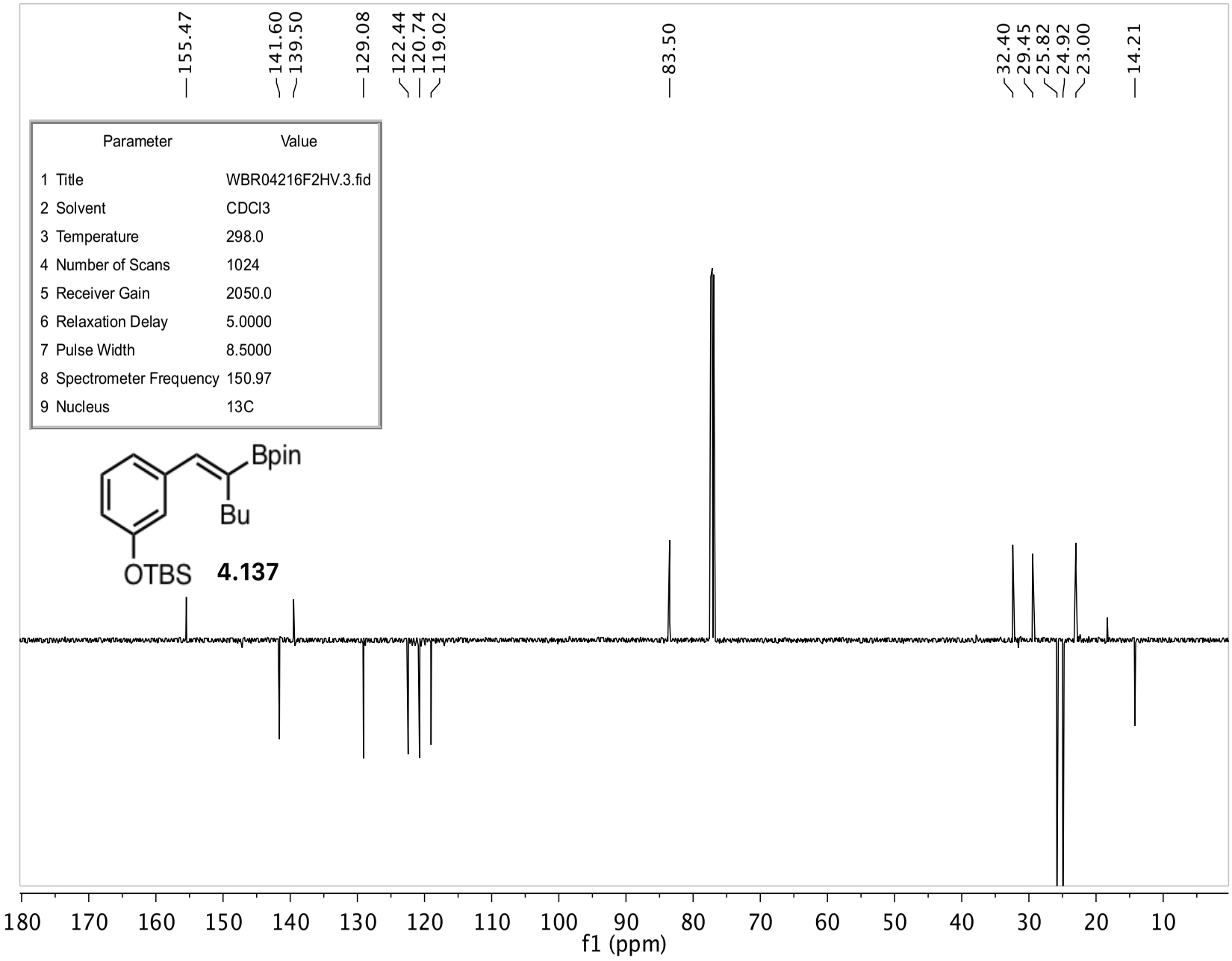
155.47
141.60
139.50
129.08
122.44
120.74
119.02
83.50
32.40
29.45
25.82
24.92
23.00
14.21
Parameter Value
1 Title WBR04216F2HV.3.fid
2 Solvent CDCl3
3 Temperature 298.0
4 Number of Scans 1024
5 Receiver Gain 2050.0
6 Relaxation Delay 5.0000
7 Pulse Width 8.5000
8 Spectrometer Frequency 150.97
9 Nucleus 13C
Bpin
Bu
OTBS
4.137
180 170 160 150 140 130 120 110 100 90 80 70 60 50 40 30 20 10
f1 (ppm)

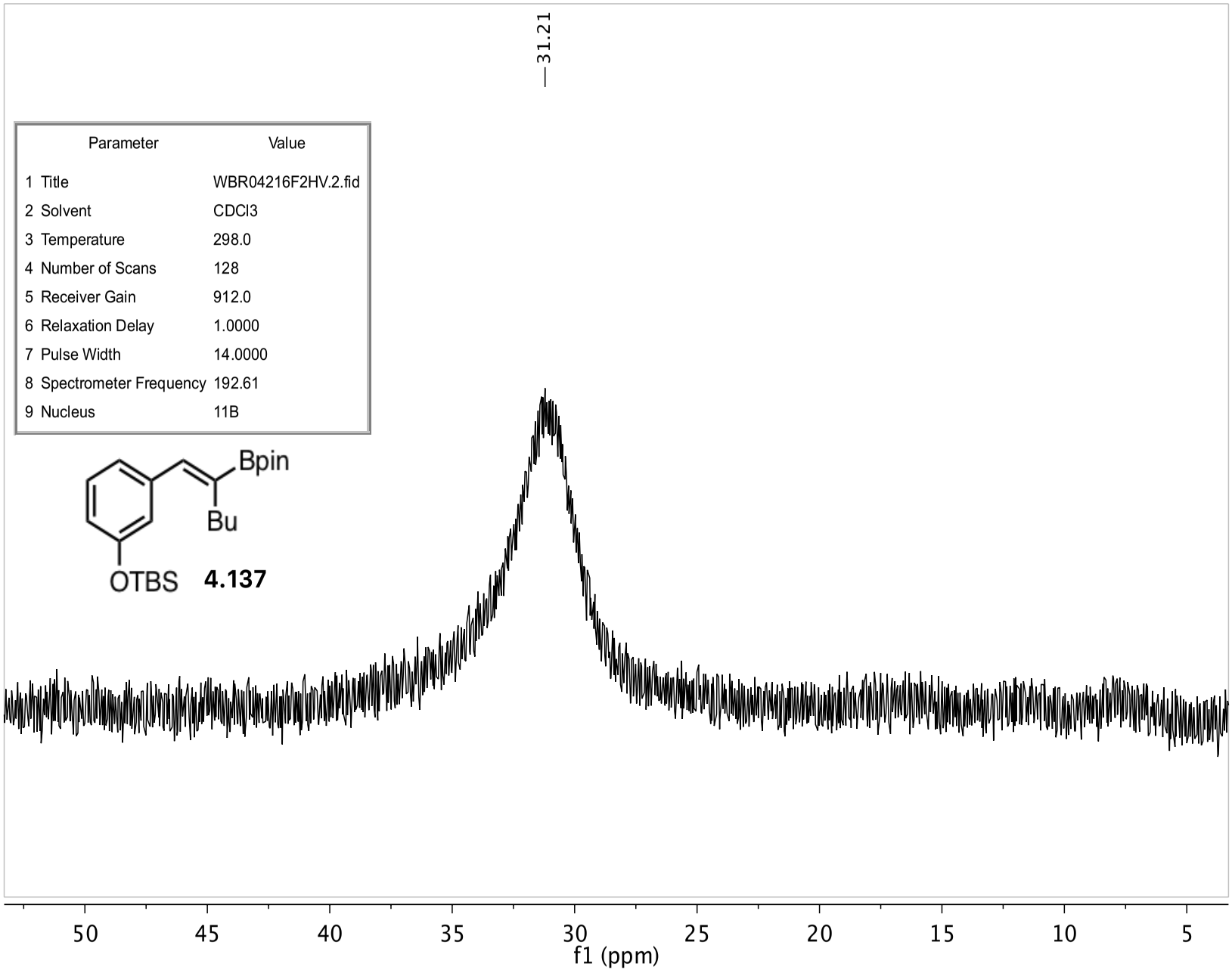
31.21
Parameter Value
1 Title WBR04216F2HV.2.fid
2 Solvent CDCl3
3 Temperature 298.0
4 Number of Scans 128
5 Receiver Gain 912.0
6 Relaxation Delay 1.0000
7 Pulse Width 14.0000
8 Spectrometer Frequency 192.61
9 Nucleus 11B
Bpin
Bu
OTBS
4.137
50
45
40
35
30
25
20
15
10
5
f1 (ppm)

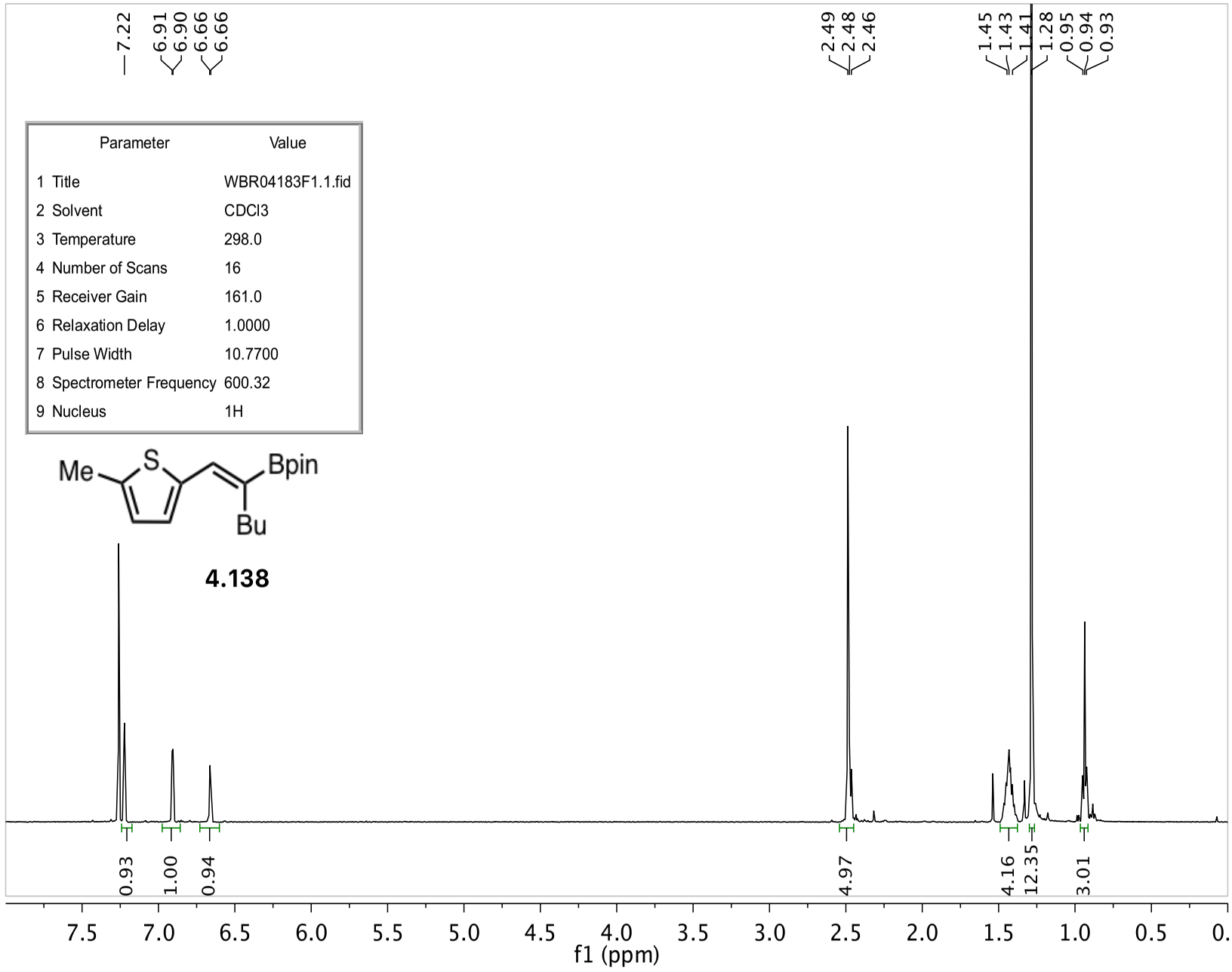
7.22
6.91
6.90
6.66
6.66
2.49
2.48
2.46
1.45
1.43
1.41
1.28
0.95
0.94
0.93
Parameter Value
1 Title WBR04183F1.1.fid
2 Solvent CDCl3
3 Temperature 298.0
4 Number of Scans 16
5 Receiver Gain 161.0
6 Relaxation Delay 1.0000
7 Pulse Width 10.7700
8 Spectrometer Frequency 600.32
9 Nucleus 1H
Me
S
Bpin
Bu
4.138
0.93
1.00
0.94
4.97
4.16
12.35
3.01
7.5
7.0
6.5
6.0
5.5
5.0
4.5
4.0
3.5
3.0
2.5
2.0
1.5
1.0
0.5
0.0
f1 (ppm)

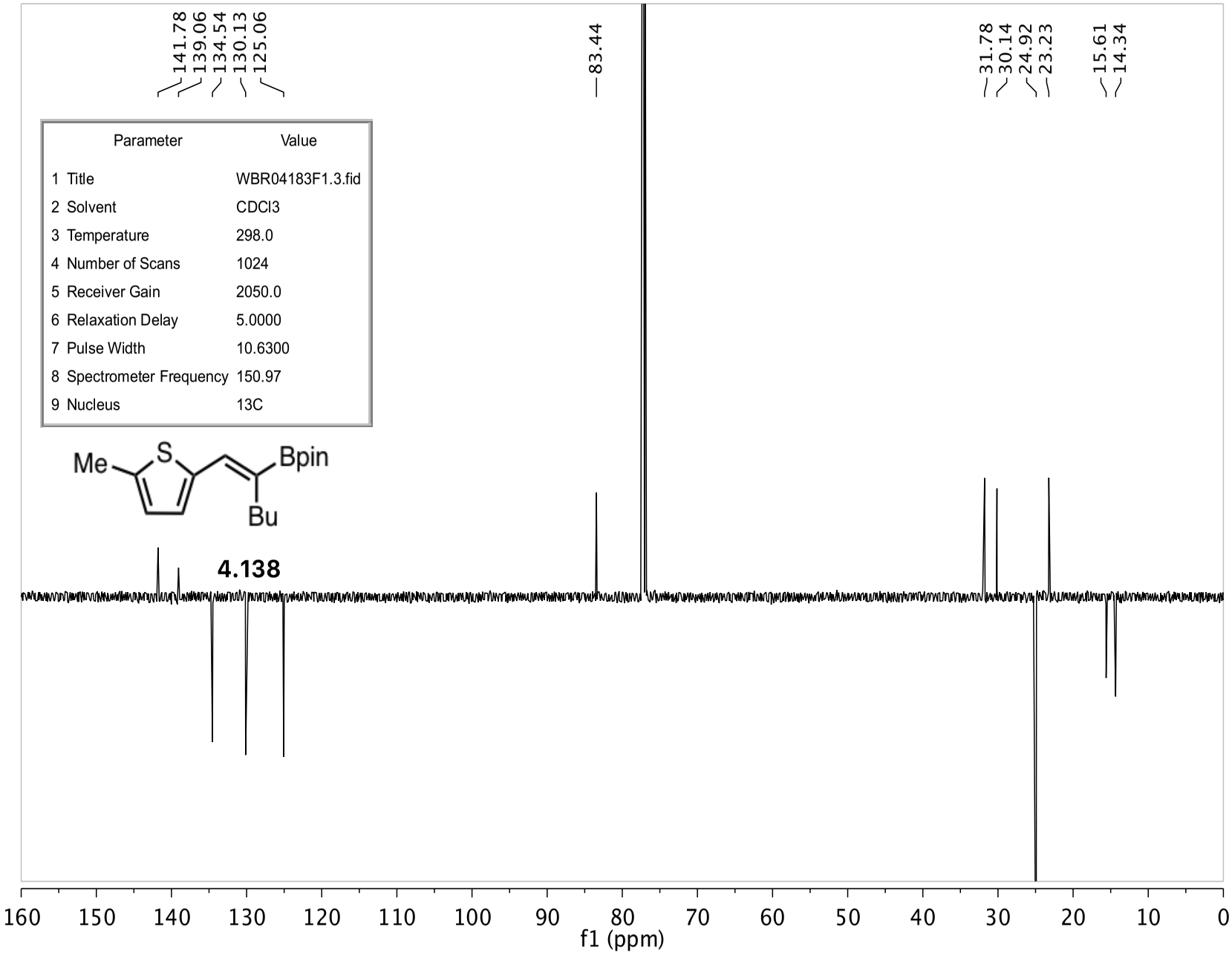
141.78
139.06
134.54
130.13
125.06
83.44
31.78
30.14
24.92
23.23
15.61
14.34
Parameter Value
1 Title WBR04183F1.3.fid
2 Solvent CDCl3
3 Temperature 298.0
4 Number of Scans 1024
5 Receiver Gain 2050.0
6 Relaxation Delay 5.0000
7 Pulse Width 10.6300
8 Spectrometer Frequency 150.97
9 Nucleus 13C
Me
S
Bpin
Bu
4.138
160 150 140 130 120 110 100 90 80 70 60 50 40 30 20 10 0
f1 (ppm)

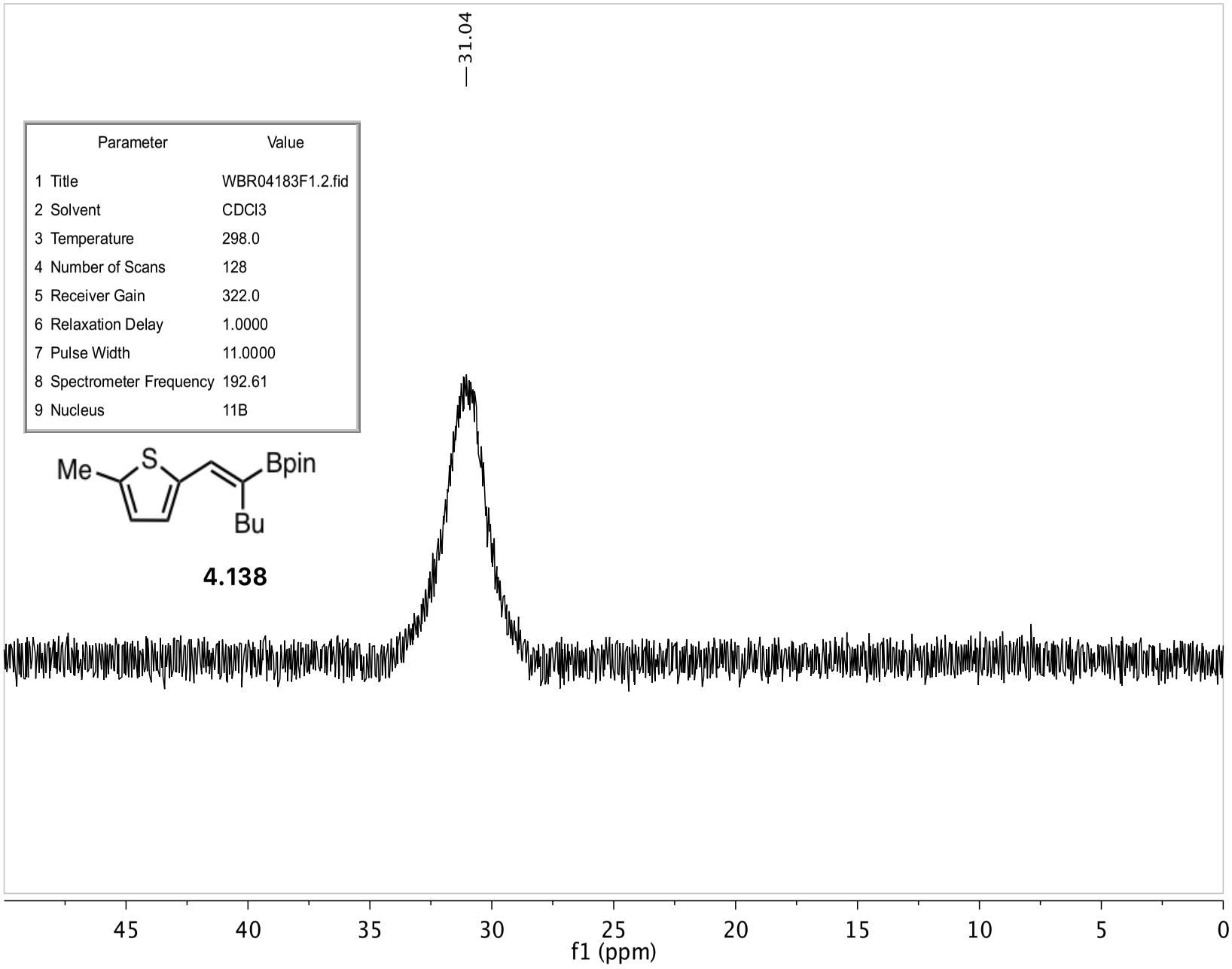
31.04
Parameter Value
1 Title WBR04183F1.2.fid
2 Solvent CDCl3
3 Temperature 298.0
4 Number of Scans 128
5 Receiver Gain 322.0
6 Relaxation Delay 1.0000
7 Pulse Width 11.0000
8 Spectrometer Frequency 192.61
9 Nucleus 11B
Me
S
Bpin
Bu
4.138
45
40
35
30
25
20
15
10
5
0
f1 (ppm)

Parameter	Value
1 Title	WBR05080@_2D.9.fid
2 Solvent	CDCl3
3 Temperature	299.4
4 Number of Scans	32
5 Receiver Gain	203.0
6 Relaxation Delay	2.0000
7 Pulse Width	15.9700
8 Spectrometer Frequency	400.15
9 Nucleus	1H

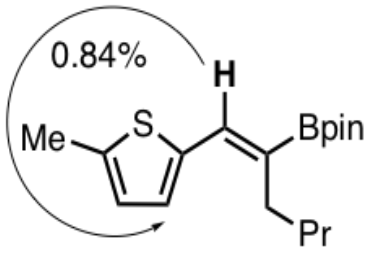

4.138

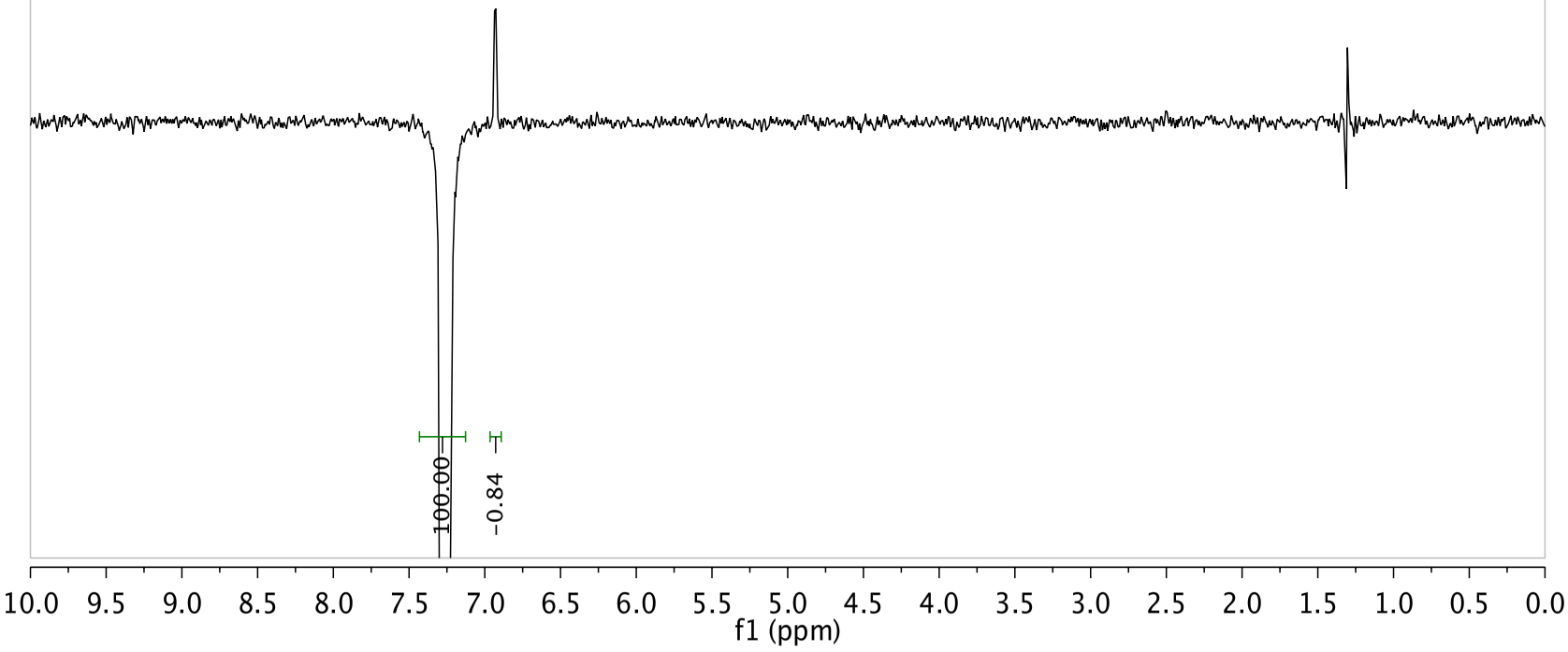

Parameter	Value
1 Title	WBR05080@_2D.10.fid
2 Solvent	CDCl3
3 Temperature	299.4
4 Number of Scans	32
5 Receiver Gain	203.0
6 Relaxation Delay	2.0000
7 Pulse Width	15.9700
8 Spectrometer Frequency	400.15
9 Nucleus	1H

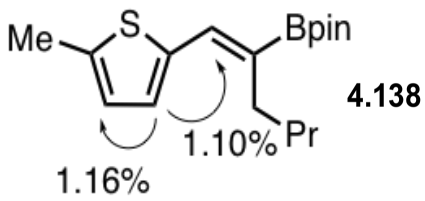

4.138

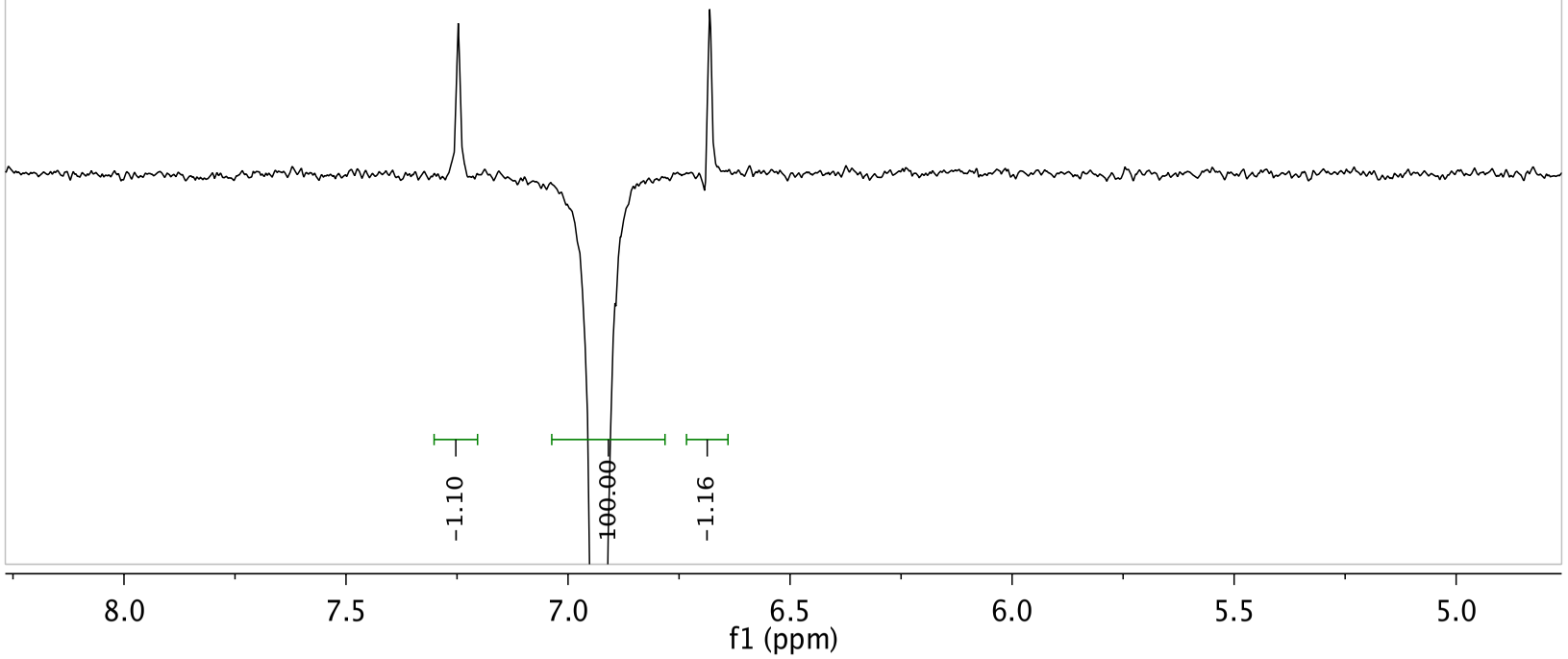

Parameter	Value
1 Title	WBR05080@_2D.13.fid
2 Solvent	CDCl3
3 Temperature	299.4
4 Number of Scans	32
5 Receiver Gain	203.0
6 Relaxation Delay	2.0000
7 Pulse Width	15.9700
8 Spectrometer Frequency	400.15
9 Nucleus	1H

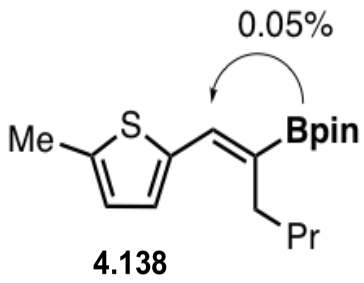

4.138

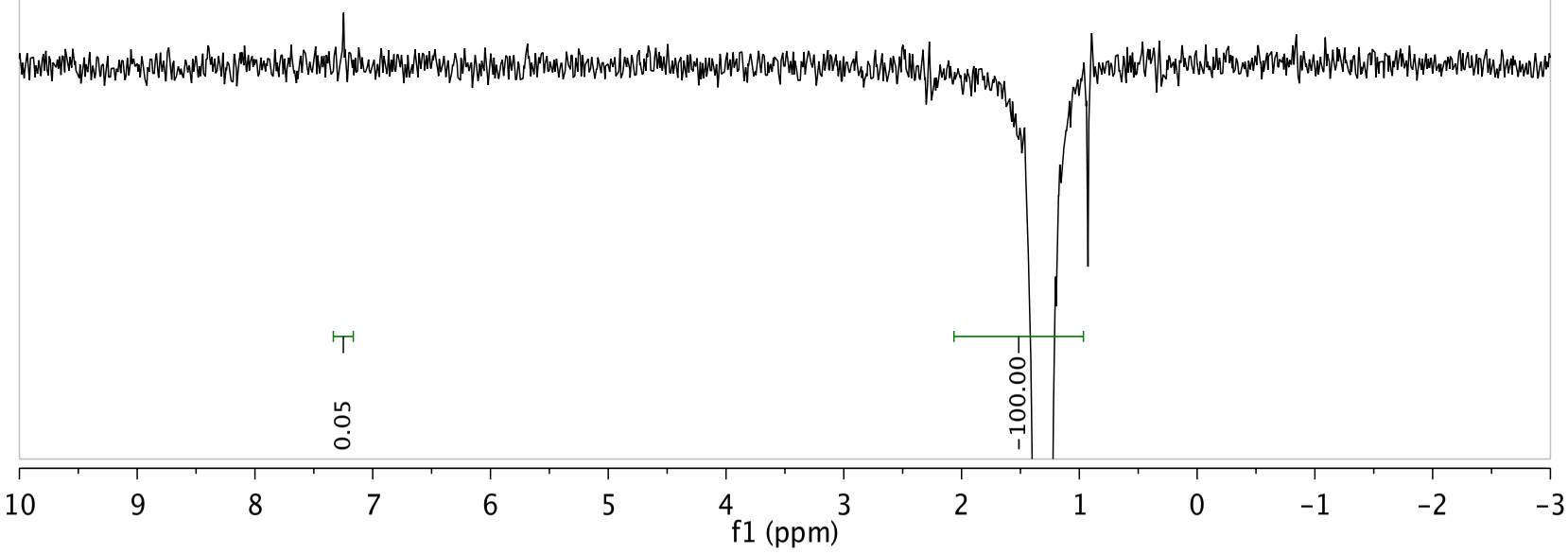

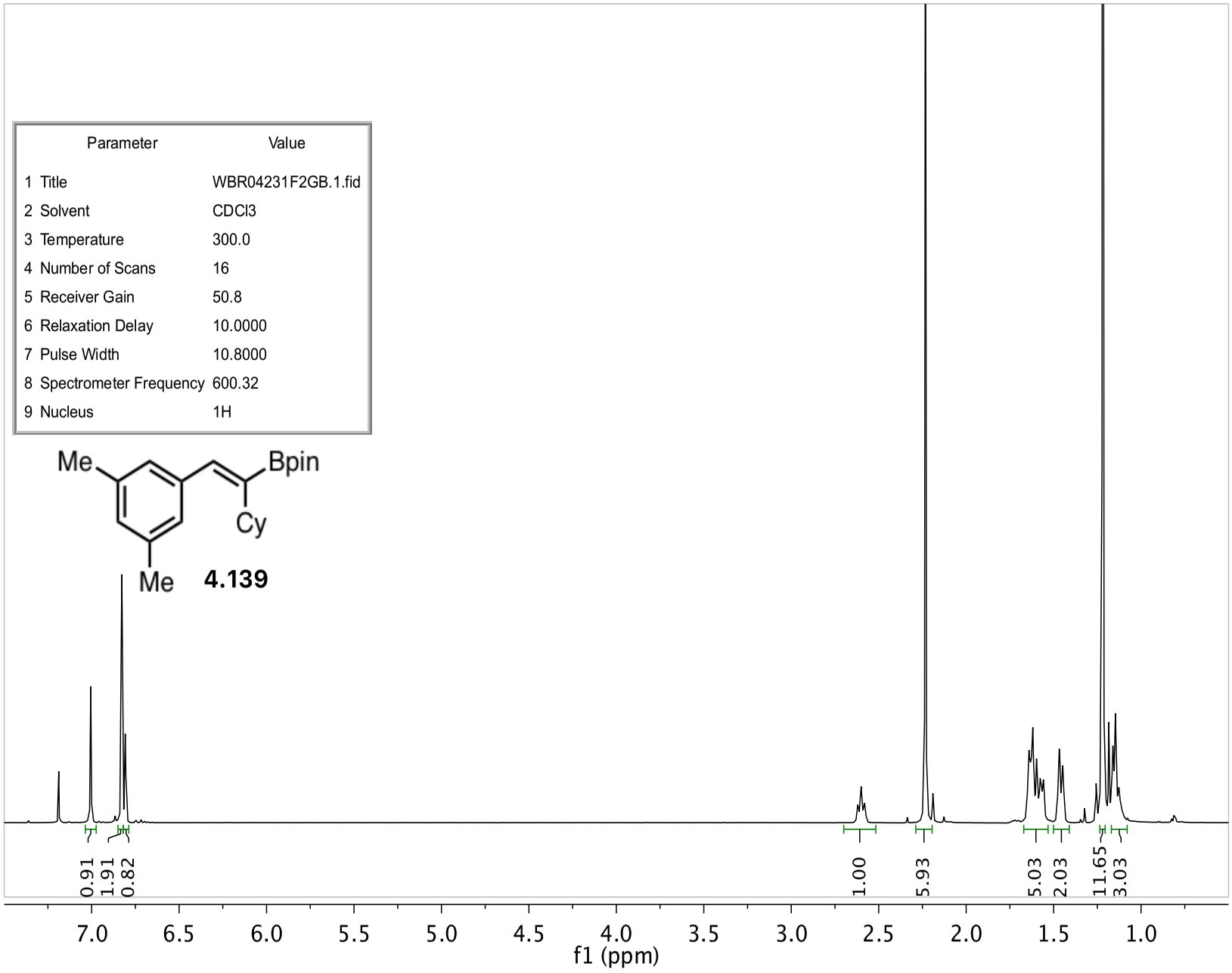
Parameter Value
1 Title WBR04231F2GB.1.fid
2 Solvent CDCl3
3 Temperature 300.0
4 Number of Scans 16
5 Receiver Gain 50.8
6 Relaxation Delay 10.0000
7 Pulse Width 10.8000
8 Spectrometer Frequency 600.32
9 Nucleus 1H
Me
Bpin
Cy
Me
4.139
0.91
1.91
0.82
1.00
5.93
5.03
2.03
11.65
3.03
7.0
6.5
6.0
5.5
5.0
4.5
4.0
3.5
3.0
2.5
2.0
1.5
1.0
f1 (ppm)

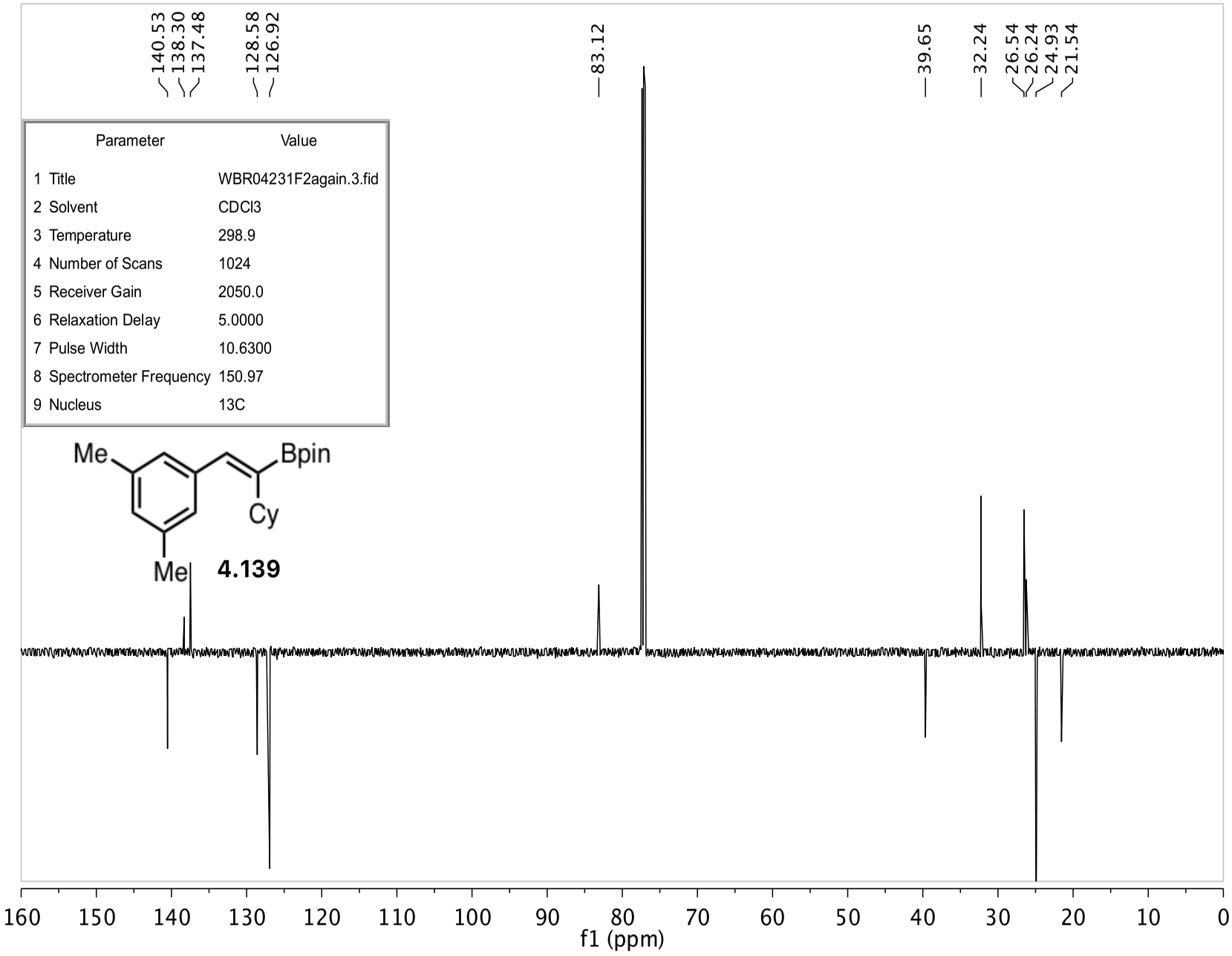
140.53
138.30
137.48
128.58
126.92
83.12
39.65
32.24
26.54
26.24
24.93
21.54
Parameter Value
1 Title WBR04231F2again.3.fid
2 Solvent CDCl3
3 Temperature 298.9
4 Number of Scans 1024
5 Receiver Gain 2050.0
6 Relaxation Delay 5.0000
7 Pulse Width 10.6300
8 Spectrometer Frequency 150.97
9 Nucleus 13C
Me
Bpin
Cy
Me
4.139
160 150 140 130 120 110 100 90 80 70 60 50 40 30 20 10 0
f1 (ppm)

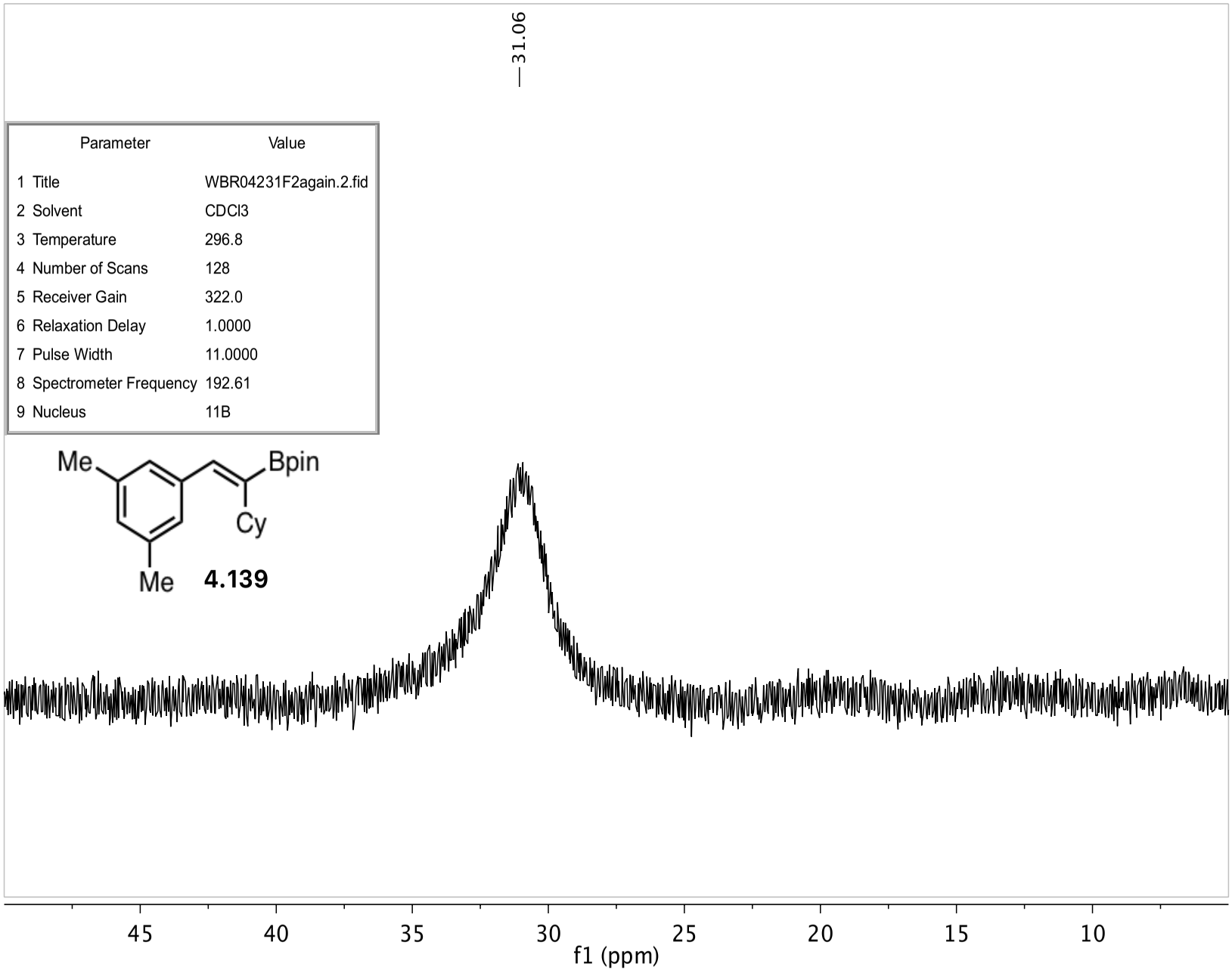
31.06
Parameter Value
1 Title WBR04231F2again.2.fid
2 Solvent CDCl3
3 Temperature 296.8
4 Number of Scans 128
5 Receiver Gain 322.0
6 Relaxation Delay 1.0000
7 Pulse Width 11.0000
8 Spectrometer Frequency 192.61
9 Nucleus 11B
Me
Bpin
Cy
Me
4.139
45
40
35
30
25
20
15
10
f1 (ppm)

Parameter	Value
1 Title	WBR05080G_2D.2.fid
2 Solvent	CDCl3
3 Temperature	299.4
4 Number of Scans	32
5 Receiver Gain	203.0
6 Relaxation Delay	2.0000
7 Pulse Width	15.9700
8 Spectrometer Frequency	400.15
9 Nucleus	1H

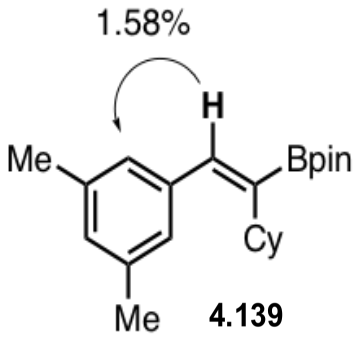

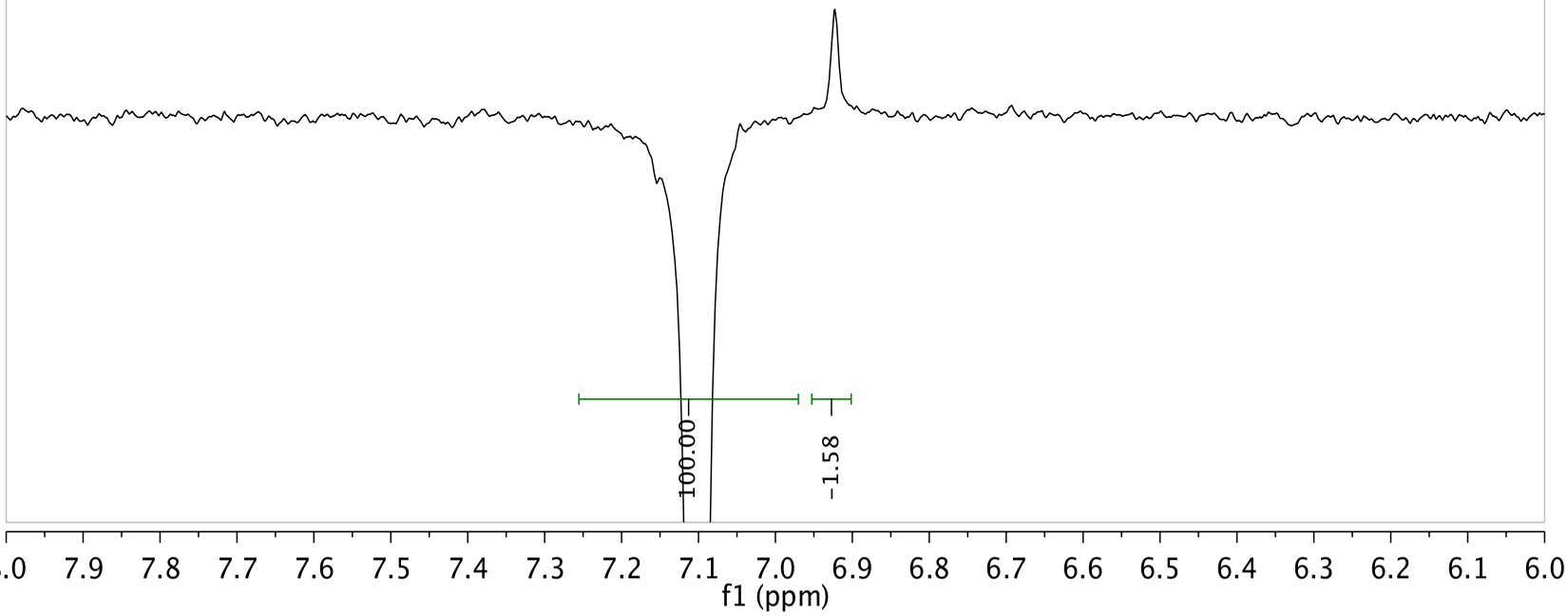

Parameter	Value
1 Title	WBR05080G_2D.5.fid
2 Solvent	CDCl3
3 Temperature	299.4
4 Number of Scans	32
5 Receiver Gain	203.0
6 Relaxation Delay	2.0000
7 Pulse Width	15.9700
8 Spectrometer Frequency	400.15
9 Nucleus	1H

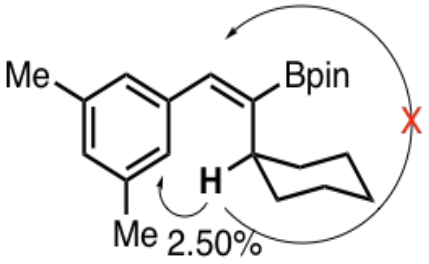

4.139

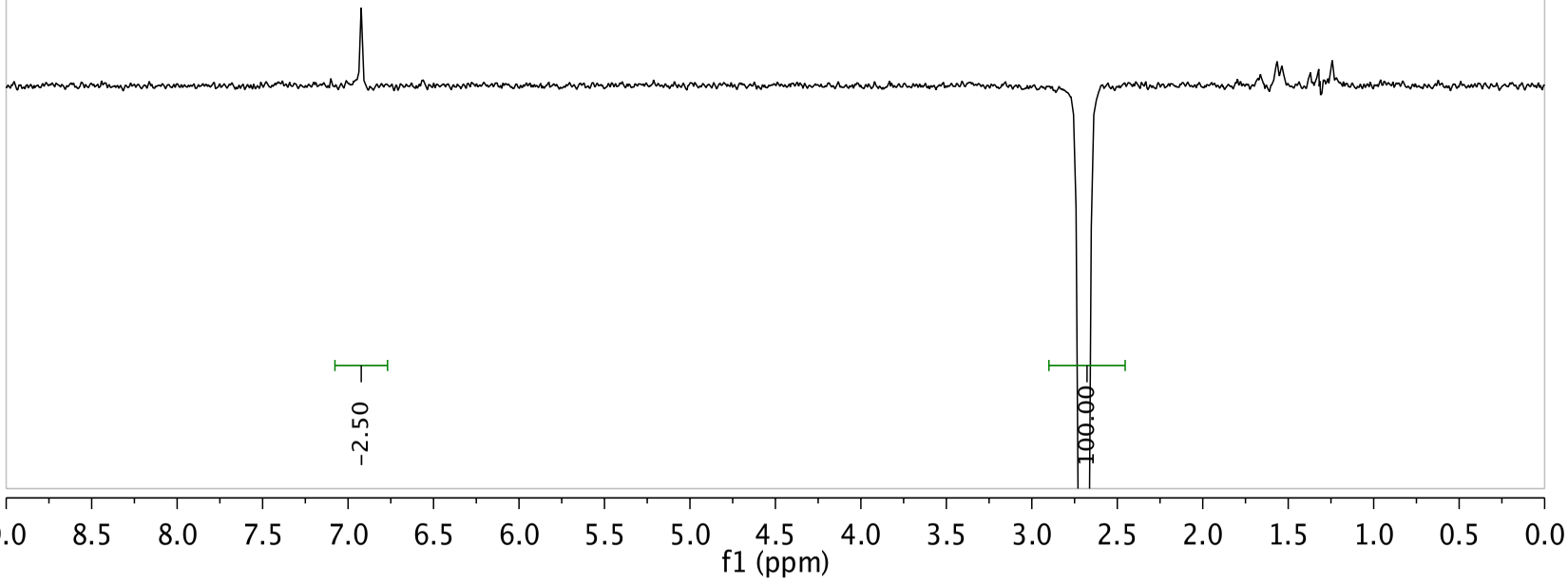

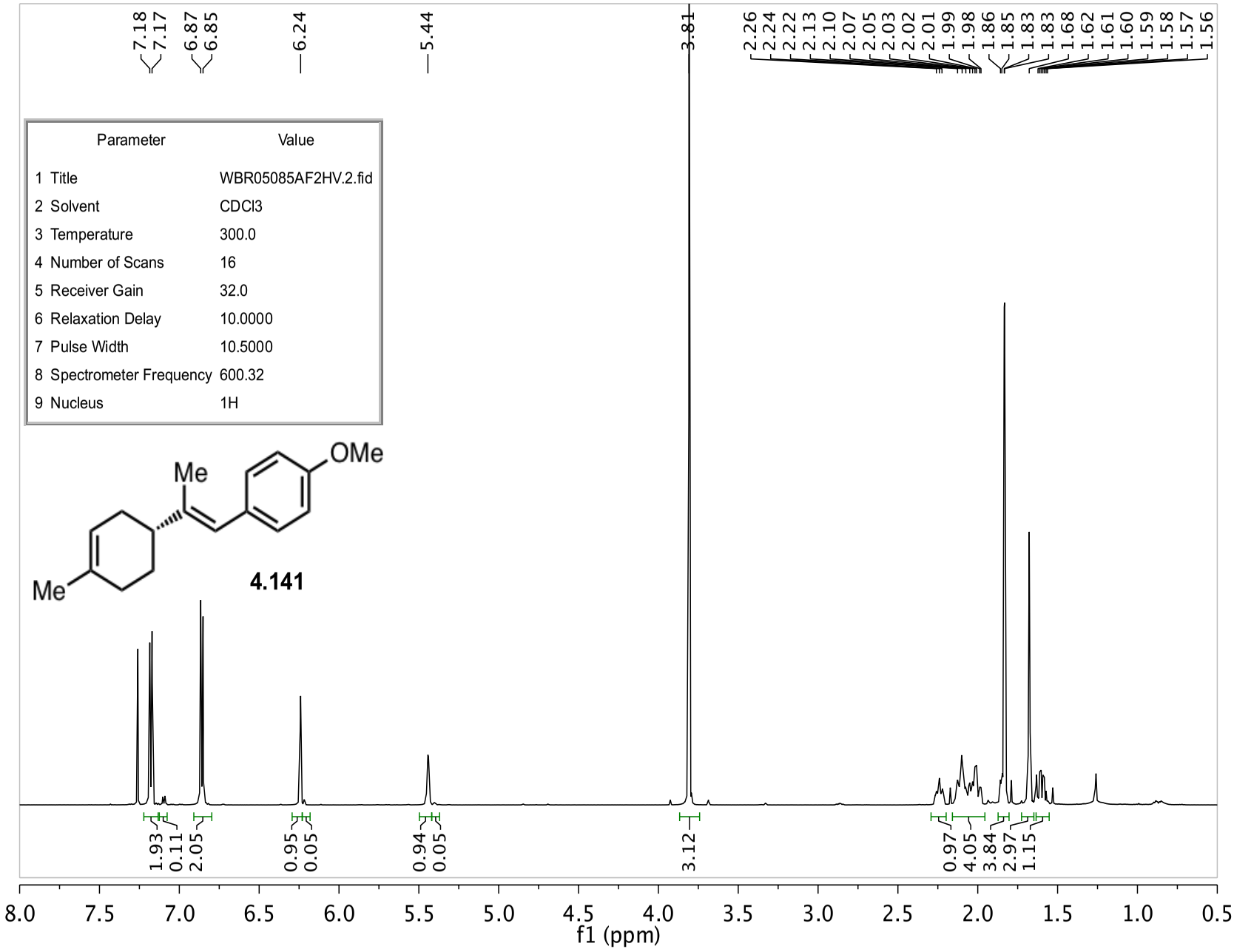
7.18
7.17
6.87
6.85
6.24
5.44
3.81
2.26
2.24
2.22
2.13
2.10
2.07
2.05
2.03
2.02
2.01
1.99
1.98
1.86
1.85
1.83
1.83
1.68
1.62
1.61
1.60
1.59
1.58
1.57
1.56
Parameter Value
1 Title WBR05085AF2HV.2.fid
2 Solvent CDCl3
3 Temperature 300.0
4 Number of Scans 16
5 Receiver Gain 32.0
6 Relaxation Delay 10.0000
7 Pulse Width 10.5000
8 Spectrometer Frequency 600.32
9 Nucleus 1H
Me
OMe
Me
4.141
1.93
0.11
2.05
0.95
0.05
0.94
0.05
3.12
0.97
4.05
3.84
2.97
1.15
8.0
7.5
7.0
6.5
6.0
5.5
5.0
4.5
4.0
3.5
3.0
2.5
2.0
1.5
1.0
0.5
f1 (ppm)

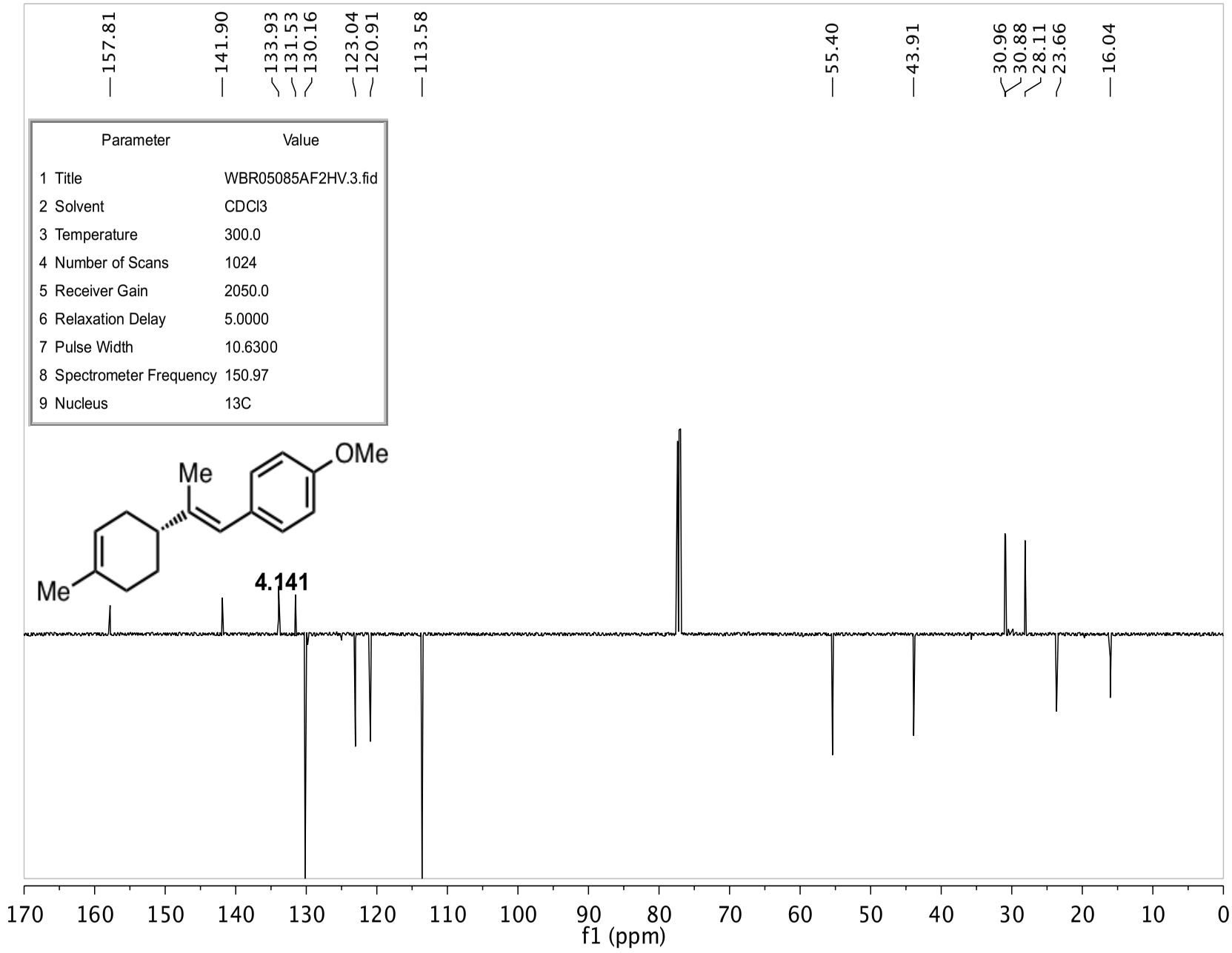
157.81
141.90
133.93
131.53
130.16
123.04
120.91
113.58
55.40
43.91
30.96
30.88
28.11
23.66
16.04
Parameter Value
1 Title WBR05085AF2HV.3.fid
2 Solvent CDCl3
3 Temperature 300.0
4 Number of Scans 1024
5 Receiver Gain 2050.0
6 Relaxation Delay 5.0000
7 Pulse Width 10.6300
8 Spectrometer Frequency 150.97
9 Nucleus 13C
Me
OMe
Me
4.141
170 160 150 140 130 120 110 100 90 80 70 60 50 40 30 20 10 0
f1 (ppm)

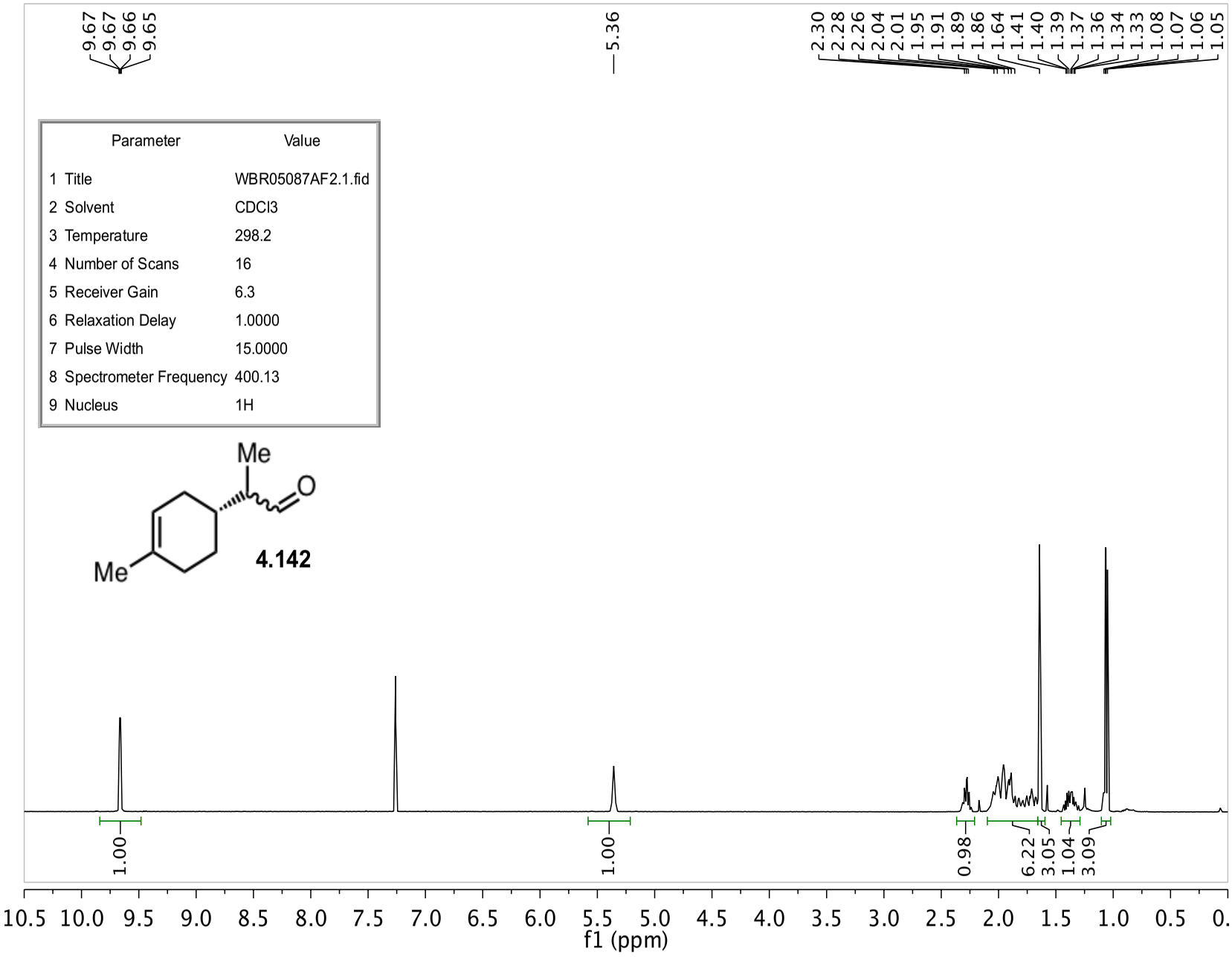
9.67
9.67
9.66
9.65
5.36
2.30
2.28
2.26
2.04
2.01
1.95
1.91
1.89
1.86
1.64
1.41
1.40
1.39
1.37
1.36
1.34
1.33
1.08
1.07
1.06
1.05
Parameter Value
1 Title WBR05087AF2.1.fid
2 Solvent CDCl3
3 Temperature 298.2
4 Number of Scans 16
5 Receiver Gain 6.3
6 Relaxation Delay 1.0000
7 Pulse Width 15.0000
8 Spectrometer Frequency 400.13
9 Nucleus 1H
Me
O
Me
4.142
1.00
1.00
0.98
6.22
3.05
1.04
3.09
10.5 10.0 9.5 9.0 8.5 8.0 7.5 7.0 6.5 6.0 5.5 5.0 4.5 4.0 3.5 3.0 2.5 2.0 1.5 1.0 0.5 0.0
f1 (ppm)

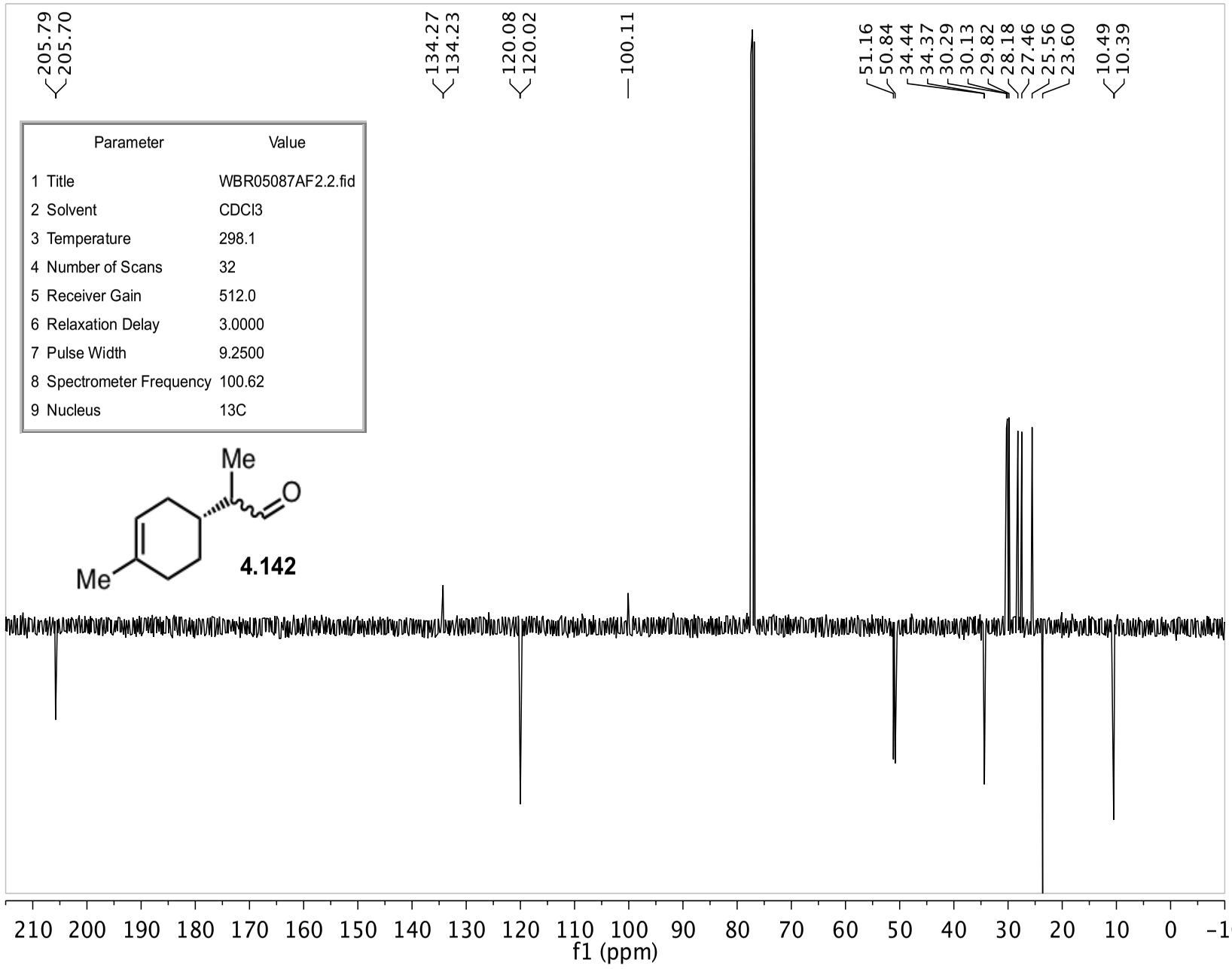
205.79
205.70
134.27
134.23
120.08
120.02
100.11
51.16
50.84
34.44
34.37
30.29
30.13
29.82
28.18
27.46
25.56
23.60
10.49
10.39
Parameter Value
1 Title WBR05087AF2.2.fid
2 Solvent CDCl3
3 Temperature 298.1
4 Number of Scans 32
5 Receiver Gain 512.0
6 Relaxation Delay 3.0000
7 Pulse Width 9.2500
8 Spectrometer Frequency 100.62
9 Nucleus 13C
Me
O
Me
4.142
210 200 190 180 170 160 150 140 130 120 110 100 90 80 70 60 50 40 30 20 10 0 -10
f1 (ppm)

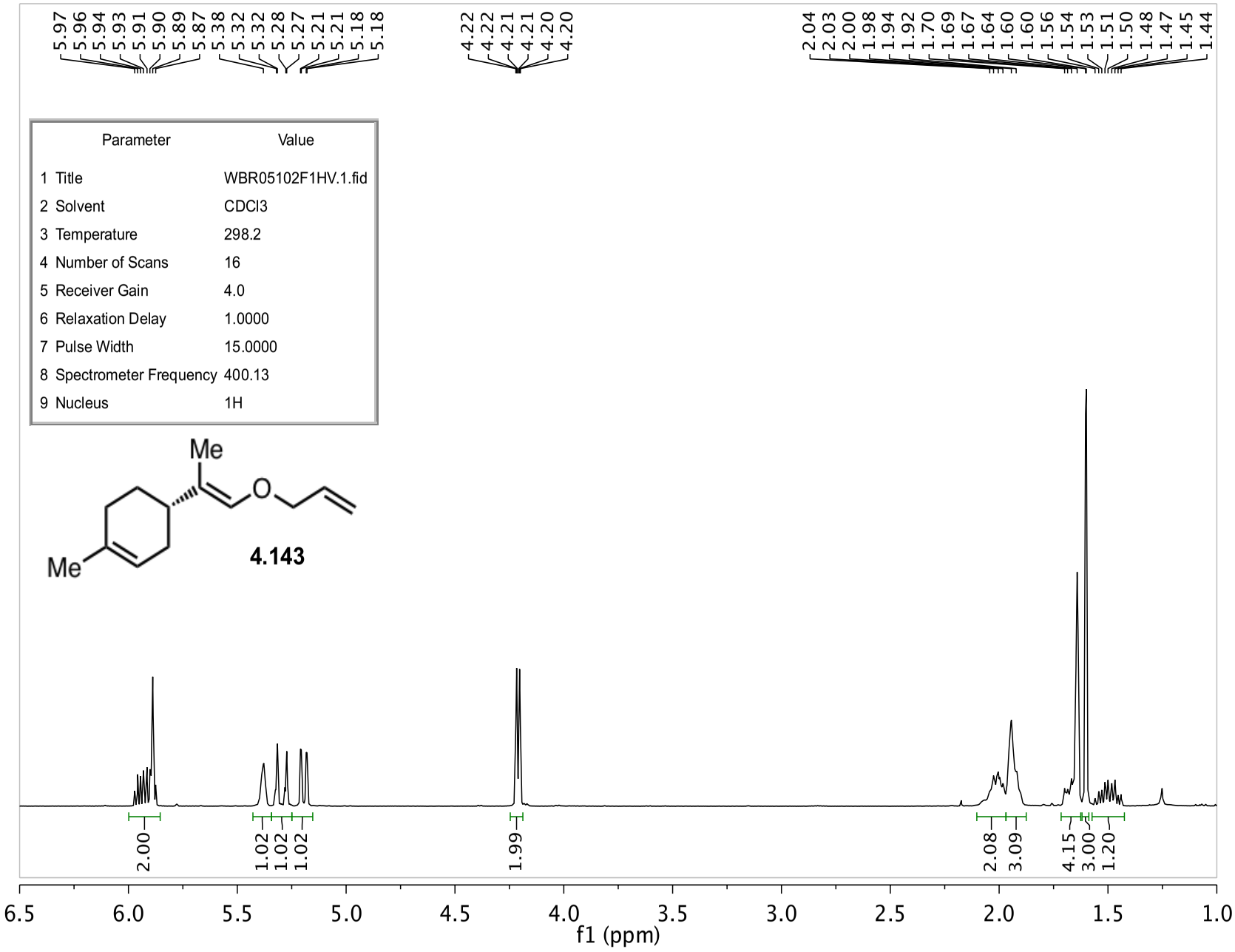
5.97
5.96
5.94
5.93
5.91
5.90
5.89
5.87
5.38
5.32
5.32
5.28
5.27
5.21
5.21
5.18
5.18
4.22
4.22
4.21
4.21
4.20
4.20
2.04
2.03
2.00
1.98
1.94
1.92
1.70
1.69
1.67
1.64
1.60
1.60
1.56
1.54
1.53
1.51
1.50
1.48
1.47
1.45
1.44
Parameter Value
1 Title WBR05102F1HV.1.fid
2 Solvent CDCl3
3 Temperature 298.2
4 Number of Scans 16
5 Receiver Gain 4.0
6 Relaxation Delay 1.0000
7 Pulse Width 15.0000
8 Spectrometer Frequency 400.13
9 Nucleus 1H
Me
O
Me
4.143
2.00
1.02
1.02
1.02
1.99
2.08
3.09
4.15
3.00
1.20
6.5
6.0
5.5
5.0
4.5
4.0
3.5
3.0
2.5
2.0
1.5
1.0
f1 (ppm)

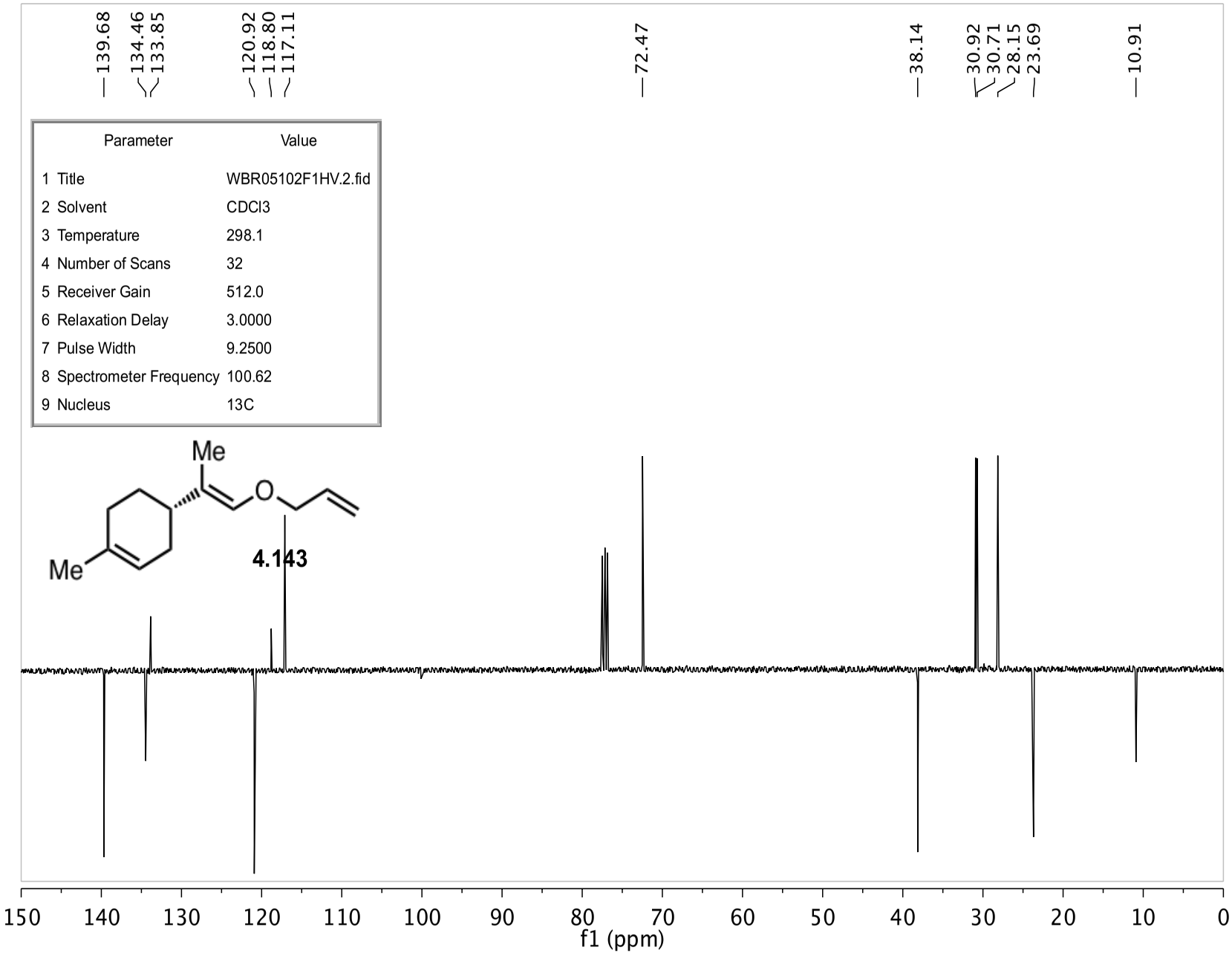
139.68
134.46
133.85
120.92
118.80
117.11
72.47
38.14
30.92
30.71
28.15
23.69
10.91
Parameter Value
1 Title WBR05102F1HV.2.fid
2 Solvent CDCl3
3 Temperature 298.1
4 Number of Scans 32
5 Receiver Gain 512.0
6 Relaxation Delay 3.0000
7 Pulse Width 9.2500
8 Spectrometer Frequency 100.62
9 Nucleus 13C
Me
O
Me
4.143
150 140 130 120 110 100 90 80 70 60 50 40 30 20 10 0
f1 (ppm)

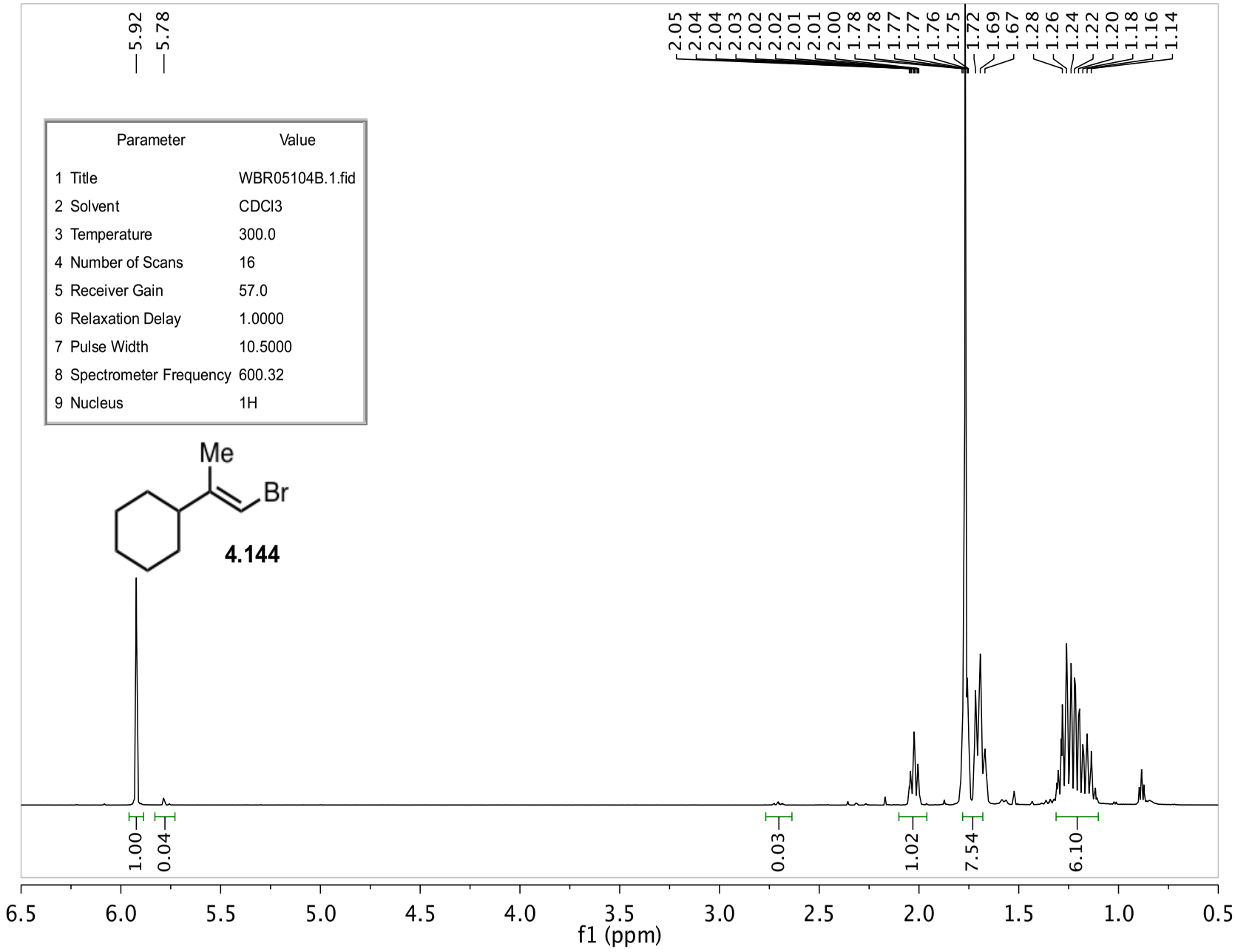
5.92
5.78
2.05
2.04
2.04
2.03
2.02
2.02
2.01
2.01
2.00
1.78
1.78
1.77
1.77
1.76
1.75
1.72
1.69
1.67
1.28
1.26
1.24
1.22
1.20
1.18
1.16
1.14
Parameter Value
1 Title WBR05104B.1.fid
2 Solvent CDCl3
3 Temperature 300.0
4 Number of Scans 16
5 Receiver Gain 57.0
6 Relaxation Delay 1.0000
7 Pulse Width 10.5000
8 Spectrometer Frequency 600.32
9 Nucleus 1H
Me
Br
4.144
1.00
0.04
0.03
1.02
7.54
6.10
6.5
6.0
5.5
5.0
4.5
4.0
3.5
3.0
2.5
2.0
1.5
1.0
0.5
f1 (ppm)

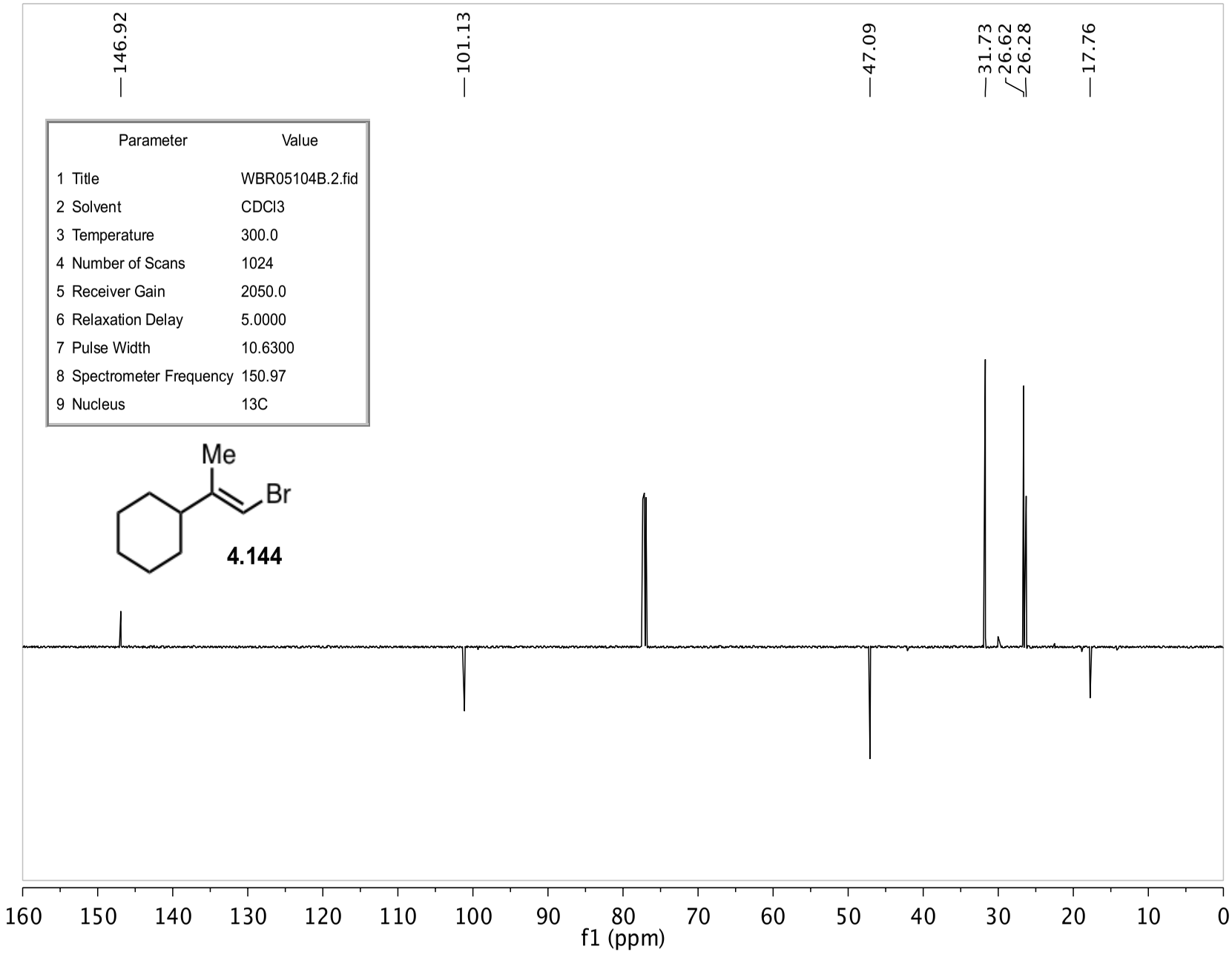
146.92
101.13
47.09
31.73
26.62
26.28
17.76
Parameter Value
1 Title WBR05104B.2.fid
2 Solvent CDCl3
3 Temperature 300.0
4 Number of Scans 1024
5 Receiver Gain 2050.0
6 Relaxation Delay 5.0000
7 Pulse Width 10.6300
8 Spectrometer Frequency 150.97
9 Nucleus 13C
Me
Br
4.144
160 150 140 130 120 110 100 90 80 70 60 50 40 30 20 10 0
f1 (ppm)